ANNEX 1

Let's grow up together

The project is co-funded by the European Union,
Instrument for Pre-Accession Assistance

Annex 1:

1.1. Report: Climate and climate change data for Italy
1.2. Report: Climate and climate change data for Friuli Venezia Giulia Region (Italy)
1.3. Report: Climate and climate change data for Marche Region (Italy)
1.4. Report: Climate and climate change data for Apulia Region (Italy)
1.5. Report: Climate and climate change data for Slovenia
1.6. Report: Climate and climate change data for Croatia
1.7. Report: Climate and climate change data for Bosnia and Herzegovina
1.8. Report: Climate and climate change data for Montenegro
1.9. Report: Climate and climate change data for Serbia
1.10. Report: Climate and climate change data for Albania
1.11. Report: Climate and climate change data for Greece

Report:

Climate and climate change data on national level - Italy

Water Research Institute –
National Research Council

(FB3)

Bari, September 2014.

Let's grow up together

DRINK ADRIA

Adriatic IPA
Cross Border Cooperation 2007-2013

The project is co-funded by the European Union,
Instrument for Pre-Accession Assistance

Climate and climate change characteristics based on observed data

The Italian monthly temperature (mean, maximum and minimum) and precipitation secular data set was updated and completely revised by Brunetti et al. (2006[1]). Station density and metadata availability were greatly improved compared to previous studies and the series were subjected to a detailed quality control and homogenisation procedure. The bias affecting original data is quantified by studying the temporal evolution of the mean adjustments applied to the series and examined in the light of the stations history. The results stress the importance of homogenisation in climate change studies. The final data set was clustered into climatically homogeneous regions by means of a Principal Component Analysis and allowed to achieve the following results in terms of observed climatic trends.

Yearly and seasonal trend analyses were performed both on regional average series and on the mean Italian series. Quite a uniform temperature trend was observed in the different regions, with a trend of 1 K per century all over Italy on a yearly basis. Also on a seasonal basis the situation is quite uniform and no significant differences are evident, either for the different regions or for the different seasons. The trend is generally higher for minimum temperature than for maximum temperature for all the seasons and the year, the only exception being the Pianura Padana region, whose trend is always higher for maximum temperature.

Precipitation trend analysis showed a decreasing tendency, even if the decreases are very low and rarely significant. Considering the average all over Italy, there is a 5% decrease per century in the annual precipitation amount, mainly due to the spring season (−9% per century).

A progressive trend analysis revealed that, both for temperature and precipitation, the significance and the slope of the trends strictly depended on the selected period. In particular, for minimum and maximum temperatures, a turning in the relative behavior was highlighted, minimum temperature trend over the whole series length being higher than that of maximum temperature, and lower if the last 50 years are considered. This suggested that we investigate DTR progressive trends too. The results showed that, considering the whole series length 1865–2003, there was a significant negative trend in the DTR that, in the last 50 years, became positive and significant, the only exception being autumn.

Climate and climate change simulations for future

As far as concern the future climate projections, the Italy as part of the Mediterranean region is expected to undergo particularly negative climate change impacts over the next decades, which, combined with the effects of anthropogenic stress on natural resources, make this region one of the most vulnerable areas in Europe. The anticipated negative impacts are mainly related to possible extraordinary heat spells (especially in summer), increased frequency of extreme weather events (heat waves, droughts and severe rainfalls) and reduced annual precipitation and river flow.

Most of the climate-related threats reported here are taken from the "Sixth National Communication under the UN Framework Convention on Climate Change" developed by the Italian Ministry for the Environment, Land and Sea in December 2013. In this context,

[1] Brunetti M., Maugeri M., Monti F. and Nanni T. Temperature and precipitation variability in italy in the last two centuries from homogenised instrumental time series. Int. J. Climatol.26: 345–381 (2006).

Italy may undergo some expected climate change impacts that would critically affect the following national circumstances, including:

- water resources and areas at risk of desertification;
- coastal areas prone to erosion and flooding and susceptible to alterations of marine ecosystems;
- Alpine regions and mountain ecosystems experiencing glacial loss and snow cover loss;
- Areas prone to flood and landslide risk (i.e. hydro-geological risks including the risk of flash floods,flash mud/debris flows, rock falls and other mass movements related to soil and land management) and, in particular, the hydrographical basin of the Po River.

Climate change is likely to magnify the regional differences in terms of quality and availability of natural resources and ecosystems in Europe and also in Italy.

Water resources (in terms of annual precipitation and river discharge) are projected to decrease over Southern Europe, and this regional pattern could intensify in the last decades of this century. The existing conditions of high stress on water resources and of hydro-geologic disturbance in some Italian regions could be exacerbated by projected climate change including: reduced water availability and quality, increases in frequency and intensity of droughts especially in summer, increases in frequency and severity of river summer flows reductions and annual river flow decline and limited groundwater recharge.

Water quantity/availability and quality in Italy could be particularly affected by:

- reduced water availability, especially in summer;
- increased water stress;
- severe negative impacts in the South, where vegetation and territory are already experiencing a marginal water supply regime;
- increased seasonal water deficit due to significant pressures of summer tourism peaks in small Italian islands;
- potential increased conflicts among multiple uses of water resources.

Report:

Climate and climate change data for Friuli Venezia Giulia Region (Italy)

by AcegasApsAmga and DMG-UNITS (LP)

Trieste, 2014

Let's grow up together

DRINK ADRIA

Adriatic IPA
Cross Border Cooperation 2007-2013

The project is co-funded by the European Union, Instrument for Pre-Accession Assistance

CONTENT:

1. INTRODUCTION

1. INTRODUCTION

Last century measurements show a significant, rapid and accelerating global warming. According to the IPCC (Intergovernmental Panel on Climate Change) statements, "most of the observed increase in globally averaged temperatures since the mid-20th century is very likely due to the observed increase in anthropogenic greenhouse gas concentrations". Although there are significant differences in estimations whether mentioned observed recent climate change can be attributed to global climate change or just periodic climate variations. Previous projections and manifestations show the need to take into account the possible continuation and even increase of those negative climate change trends in water resource management, regardless if those are irreversible changes or normal climate variations. Contemporary approaches to water resource management seek the elaboration of different scenarios of possible long-term changes, to identify risks on time and prepare and optimize protective control measures. This is the aim of the DRINKADRIA project. This is especially evident because of the relationship of globally present flow decrease trends, observed especially in the Mediterranean, where at the same time water use increased significantly. According to the most commonly cited reports of IPCC, it is predicted that the ocean level could rise between 9 and 88 cm until 2100, where the mean value is 48 cm. Such changes, even with less intensity of changes, will certainly result in the need to protect and optimize the use of water resources, where special meaning for the population have water resources for water supply. For analyzed regional area, different scenarios of climate change impact assessment, are made also for sea level rise, and ways of slowing down unwanted processes are discussed, as well as adjustment to such changes. In that sense, several previous documents and recent research projects results considered regional manifestations of climate change/variations, different scenarios of possible further changes, as well as possible strategy for responding to them.
As reference climate period, the range 1961-1990 was considered, for this reason, also for the Friuli Venezia Giulia Region, we took into account the data falling within the chosen reference period.
The present report focuses on the variations of temperatures and precipitations in the Friuli Venezia Giulia Region. For this area, existing as well as estimated analyses for some of the most likely climate change scenarios were determined by the application of several standard methodological referenced procedures.

2. EXISTING CLIMATE FEATURES IN FRIULI VENEZIA GIULIA

According to Koppen classification the pilot area belongs to the climate type ***Cfa***, a warm temperate rainy (humid mesothermal), humid all year round, with very hot summer.

Figure 2-1 Köppen classification for pilot area. Cfa climate is: warm temperate rainy (humid mesothermal), humid all year round, with very hot summer. The Soca/Isonzo river basin have Cfb climate, warm temperate rainy (humid mesothermal), humid all year round, with hot summer.

The region has a great variety of climates and landscapes: 42.5% of its surface is made up of mountains, 19.3% of hills and the remaining 38.2% of the plains located in the central areas and along the coast.
Friuli Venezia Giulia has a humid, temperate climate which varies considerably from one area to another. The Alpine System protects the Region from the direct impact of the rigid northerly winds. The opening toward the Po Valley influences the general circulation of air masses from the west to the east. Along this direction, the low pressure canters develop and move, bringing with them thunderstorms and hailstorms, especially in the summer times. Being open to the Adriatic Sea, the territory also receives Sirocco winds, that brings with him heavy rainfalls.
For a first assessing of possible climate change effects in the last decades at regional level, OSMER (ARPA FVG Department) started to collect historical data series on temperatures and precipitations. The longest historical termometric and pluviometric series in Friuli-Venezia Giulia belong to the former National Hydrographic and Mareographic Service stations (now inherited by the Hydrographic Operational Unit of the Friuli-Venezia Giulia Region). The

collected data allow defining the evolution through the years of the precipitations and temperatures in the FVG Region.
The Meteorological Regional Observatory (OSMER) ARPA FVG, in 2013, proposes an evaluation of the anomalies found in the historical series and meteorological data, which can be interpreted as potential or preliminary signals of climate changes.
From a general point of view, the Assessment Report realized by IPCC (2007a, b, c), reports that the global warming is unequivocal. There has been an increasing in the temperatures of 0,74°C in the period between 1906-2005 with an important acceleration within the last fifty years (0,13°C/10 years).
In the Alpine region, the ZAMG (Austrian Meteorological Service), in the framework of CLIVALP and HISTALP projects (2006 and 2011), elaborated and homogenized the historical temperatures time series. In particular, in the sub-region of the southern east Alps, which also includes the Friuli Venezia Giulia, is noticed a temperature increase of about 1 ° C in the last thirty years.
Analyzing more in details the results of the European HISTALP project elaborated by ZAMG for the stations of Udine and Trieste, emerges an increase in the temperatures (Cicogna et al., 2012).
The present report, based on data collected and available at the web site www.meteofvg.it, focused on the analyses of the historical dataset, part of the climate atlas of the entire FVG Region, containing daily rainfalls and temperatures data validated and elaborated by OSMER for the period in the range 1961 and 2000. From these data, at regional level, a series of elaborated tables and maps were later obtained.

Friuli Venezia Giulia Region is famous to be a rainy place, at least when compared to other Italian and European regions. The city of Udine contends, with a few other provincial capitals, the scepter of the rainiest with over 1450 mm of rain per year. To reinforce the image of very "wet", we must always remember that, about 25 km in the NE of Udine, on the Julian Pre-Alps (Mt. Canin area), the average annual rainfall exceeds 3 meters, a value which is among the highest registered in Europe.
In the collective imagination while thinking to another city in the region, Trieste, the first weather element that comes to mind is the bora wind and not the rain. In fact, with its 1000 mm of annual rainfall (which, however, at least in Italy, are few) the town has certainly not the reputation of being a rainy city.
If we add to these considerations the fact that going from Trieste to Tarvisio, the alpine town located further to the NE of the Region, the average rainfall per year, after having raised till the record values of the Julian Pre-Alps, go back down to levels that almost coincide with those of Udine. So one realizes that precipitation in Friuli Venezia Giulia are actually quite complex. To understand better this phenomenon, it is first necessary to answer to specific questions.
The rain in the Friuli Venezia Giulia Region is due mainly to:
1) Fronts/depressions; 2) the orographic interactions-wet flows: Stau/Foehn; 3) the instability/storms.
These mechanisms interact with the geographic position and with the site-specific orography of the Region that influence a lot, at local scale, the precipitations.

In the Northern emisphere, at 46°N of Lat, where FVG Region is, blow the westerly, wide air masses that guided by the polar front, move from west to east. In them are sited the fronts causing rainfalls and snowfalls. Indeed, is at higher Latitudes (between 50 and 60°N) that the perturbed belt reaches their maximum. Usually also the zones between 40° and 50° parallel are affected by perturbations. To this main „weather engine“ are added depressions that

originate over Mediterranean, especially during winter times, and that are concentrated on the Genova Gulf or on the middle Adriatic sea.

Regarding the geography and the orography of the study area, is necessary to remember that the Region is located between the Adriatic sea and the Alps in a S-N direction, while at W, there is the Po Plain and the Dolomites; to the E instead, some alpine reliefs and the first Balcans. It is important to note as the main range of the Eastern Alps are the Tauri, in Austria, while the Carnian and the Julian Alps are of lesser height and vastness. This implies a complete protection of the Region by the cold airflows and usually humid, coming from N-W and N-E. Conversely, the exposure of the Region is to the southern flows between E and W. At the exception of eastern flows, less humid, but during wintertime, particularly cold, from the other sectors arrive high humid and quite warm air masses coming from the Mediterranean basin. The regional orography, with the pre-Alps before and the Alps after (Carnian and Julian) amplify the effects of the Mediterranean humid flows while uplifting them during the southern blowing winds (Stau). In the summertime, the Adriatic Sea as the Po plain are warm and humid. Here the Alps are not enough high comparing with the western sector (4000 m), so often, cold air, at high altitude (since 3000 m) can take over the region and provoke thunderstorms.

All these elements explain why the Region is quite rainy not only as frequency, but also as quantity, why the most rainy area is the Prealps, in particular the Julian ones, while close to the sea and in the northern alpine zones the rain decrease, and finally why during summertime, thunderstorms are quite frequent (1 event every 2nd day).

To answer instead to when, how and where precipitations occur, the following maps will widely explain the situation. All the maps and graphs were elaborated or downloaded using data available at the OSMER web site, validated and elaborated by OSMER itself. All the data refers to the analysis of the historical series from 1961 to 2000.

In the Friuli Venezia Giulia Region, several meteorological stations are active; some of them are recording since tens of years. Within the times, several have been the Authorities that managed the existing network.

- Il Magistrato alle acque di Venezia,
- La Regione autonoma Friuli Venezia Giulia,
- L'Osservatorio Meteorologico Regionale,
- L'Agenzia Regionale Per l'Ambiente,
- Il Consiglio Nazionale delle Ricerche,
- La Protezione Civile del FVG.

Nowadays, at the website http://www.osmer.fvg.it/ is possible to find all the information, data, weather forecasts, publications, updated and free.

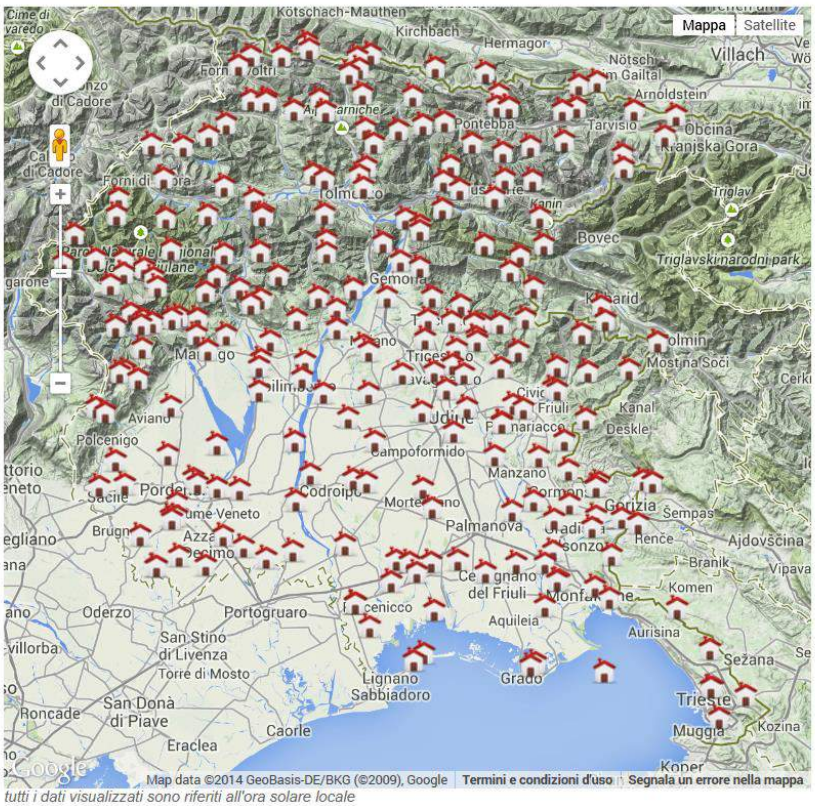

Figure 1 Spatial distribution of the hydro-meteorological monitoring stations in FVG Region (www.protezionecivile.fvg.it).

stazione	Bacino Idrografico	Altitudine (m. s.l.m.)	lat (N)	lon (E)
ALESSO	Tagliamento	197	46°19'	13°03'
AMPEZZO	Tagliamento	560	46°25'	12°48'
ARIIS	Pianura fra Isonzo e Tagliamento	12	45°52'	13°05'
ATTIMIS	Isonzo	196	46°10'	13°19'
AVIANO	Livenza	159	46°04'	12°36'
AVOSACCO	Tagliamento	473	46°29'	13°01'
BARCIS	Livenza	409	46°11'	12°35'
BASALDELLA	Livenza	142	46°05'	12°47'
BASOVIZZA	Bacini minori dal Confine di Stato all' Isonzo	372	45°39'	13°53'
BONIFICA VITTORIA	Pianura fra Isonzo e Tagliamento	1	45°44'	13°08'
CAMPONE	Livenza	450	46°16'	12°50'
CASTIONS DI STRADA	Pianura fra Isonzo e Tagliamento	23	45°55'	13°11'
CAVE DEL PREDIL	Drava	906	46°26'	13°34'
CERGNEU SUPERIORE	Isonzo	280	46°13'	13°19'
CERVIGNANO	Pianura fra Isonzo e Tagliamento	7	45°49'	13°20'
CHIALINA (OVARO)	Tagliamento	492	46°29'	12°52'
CHIEVOLIS	Livenza	342	46°15'	12°44'
CHIUSAFORTE	Tagliamento	394	46°25'	13°19'
CISERIIS	Isonzo	264	46°14'	13°14'
CIVIDALE	Isonzo	135	46°06'	13°25'
CLAUT	Livenza	613	46°16'	12°31'
CLAUZETTO	Tagliamento	553	46°14'	12°55'
CLODIG	Isonzo	248	46°09'	13°36'
CODROIPO	Pianura fra Isonzo e Tagliamento	43	45°58'	12°59'
CORMONS	Pianura fra Isonzo e Tagliamento	59	45°57'	13°28'
DIGA CELLINA	Livenza	350	46°11'	12°36'
FORNI AVOLTRI	Tagliamento	888	46°36'	12°46'
GEMONA	Tagliamento	215	46°15'	13°07'
GORGAZZO	Livenza	53	46°02'	12°30'
GORIZIA	Isonzo	86	45°56'	13°36'
GRADISCA	Pianura fra Isonzo e Tagliamento	32	45°53'	13°30'
GRADO	Pianura fra Isonzo e Tagliamento	1	45°41'	13°24'
LATISANA	Pianura fra Isonzo e Tagliamento	7	45°46'	13°01'
MALBORGHETTO	Tagliamento	721	46°30'	13°26'
MANIAGO	Livenza	283	46°11'	12°44'
MOGGIO UDINESE	Tagliamento	337	46°25'	13°12'
MONFALCONE	Bacini minori dal Confine di Stato all' Isonzo	6	45°49'	13°32'
MONTEMAGGIORE	Isonzo	954	46°12'	13°32'
MORUZZO	Pianura fra Isonzo e Tagliamento	262	46°07'	13°07'
MUSI	Isonzo	635	46°19'	13°16'
OPICINA	Bacini minori dal Confine di Stato all' Isonzo	320	45°41'	13°48'
OSEACCO	Tagliamento	490	46°22'	13°18'
PALMANOVA	Pianura fra Isonzo e Tagliamento	28	45°55'	13°18'
PALUZZA	Tagliamento	602	46°32'	13°01'
PASSO MAURIA	Tagliamento	1298	46°27'	12°31'
PAULARO	Tagliamento	648	46°32'	13°07'
PESARIIS	Tagliamento	758	46°31'	12°47'
PINZANO	Tagliamento	201	46°12'	12°57'
POFFABRO	Livenza	510	46°13'	12°43'
PONTE DELLA DELIZIA	Tagliamento	52	45°58'	12°53'
PONTEBBA	Tagliamento	568	46°31'	13°18'
PORDENONE	Pianura fra Tagliamento e Piave	23	45°58'	12°40'
PULFERO	Isonzo	184	46°10'	13°29'
RESIA	Tagliamento	380	46°23'	13°17'
RIVAROTTA	Pianura fra Isonzo e Tagliamento	11	45°49'	13°05'
S. DANIELE	Tagliamento	252	46°09'	13°00'
S. FRANCESCO	Tagliamento	378	46°19'	12°56'
S. GIORGIO DI NOGARO	Pianura fra Isonzo e Tagliamento	7	45°50'	13°13'
S. MARTINO AL TAGLIAMENTO	Tagliamento	71	46°02'	12°52'
S. QUIRINO	Livenza	116	46°01'	12°38'
S. VITO AL TAGLIAMENTO	Pianura fra Tagliamento e Piave	31	45°55'	12°51'
SACILE	Livenza	25	45°58'	12°31'
SALETTO DI RACCOLANA	Tagliamento	517	46°24'	13°23'
SAURIS	Tagliamento	1212	46°28'	12°43'
SESTO AL REGHENA	Pianura fra Tagliamento e Piave	13	45°51'	12°49'
SPILIMBERGO	Tagliamento	132	46°07'	12°53'
TARVISIO	Drava	751	46°30'	13°34'
TIMAU	Tagliamento	821	46°35'	13°00'
TOLMEZZO	Tagliamento	323	46°24'	13°01'
TRAMONTI DI SOPRA	Livenza	420	46°19'	12°47'
TRAVESIO	Tagliamento	218	46°12'	12°51'
TRIESTE	Bacini minori dal Confine di Stato all' Isonzo	11	45°39'	13°47'
UCCEA	Isonzo	645	46°18'	13°24'
UDINE	Pianura fra Isonzo e Tagliamento	106	46°04'	13°15'
VEDRONZA	Isonzo	325	46°16'	13°15'
VENZONE	Tagliamento	230	46°20'	13°08'

Figure 2: 76 meteorological stations actually working and available in the Friuli Venezia Giulia Region.

3. PRECIPITATIONS

The longest historical time-series in the FVG Region are the ones of the ex-Servizio Idrografico e Mareografico Nazionale (now Unità Operativa Idrografica del FVG).

To compute the map presented in Figure 3, were used the daily data recorded in the period ranging within 1971-2008 in 109 rainfall stations and in 46 temperature stations, all of them managed by the Unità Idrografica Regionale and by OSMER. Missing data were updated using linear regression techniques Stepwise or multiregressions), already used in the updating of the Climatic Atlas of the Friuli Venezia Giulia Region (Osmer, 2008). Rainfalls and temperatures daily data were spatialized over a 500 m grid overlapped to the Digital Elevation Model (DEM) having a kernel of 40 m. Natural Neighbor algorithm allowed to elaborate precipitation maps. For the temperatures instead, were used the altimetric experimental gradients obtained through the correlation between the temperature daily data and the elevation of each single station. In the mountain basins, the snow process has been described as follow: all the precipitations fallen at low temperature were considered snow.

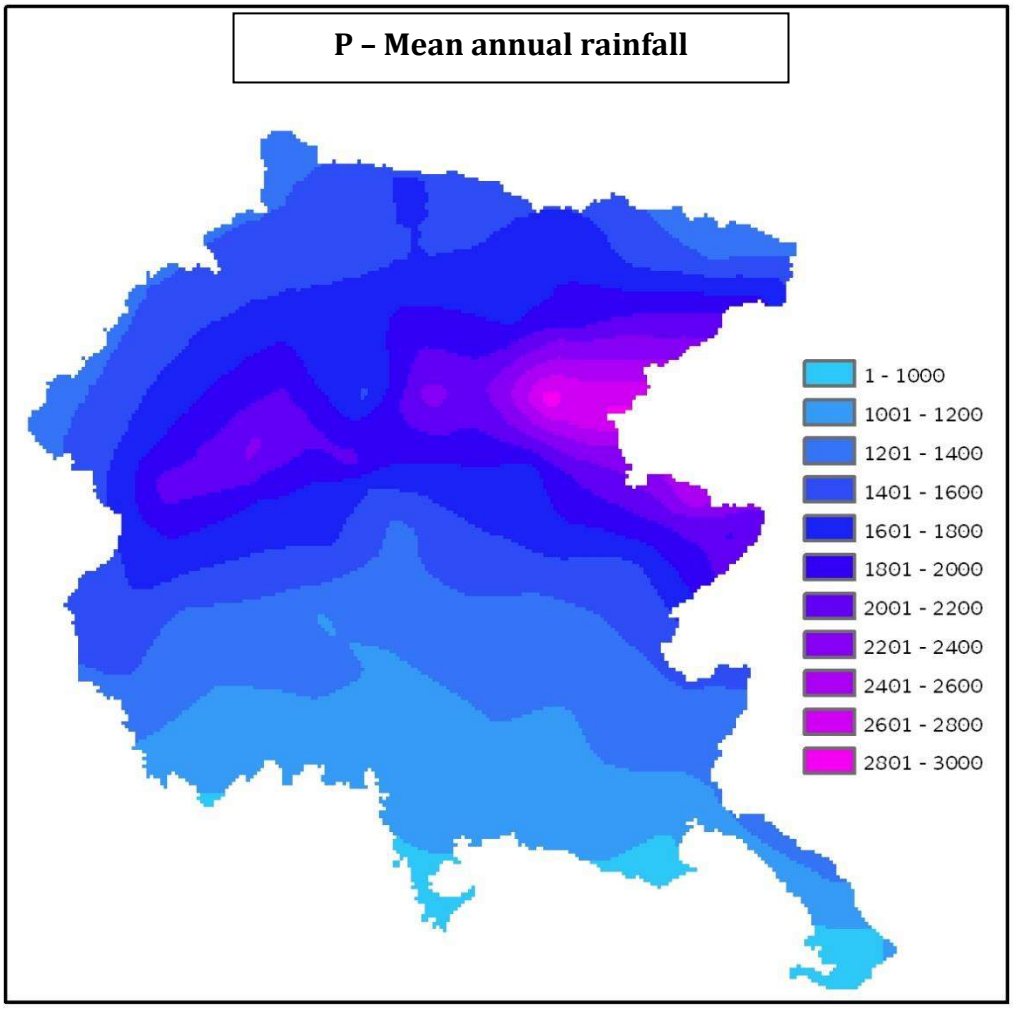

Figure 3: Mean annual rainfall of the FVG Region calculated over the period 1971 – 2008. Data are expressed in mm/y (Zini et al., 2011).

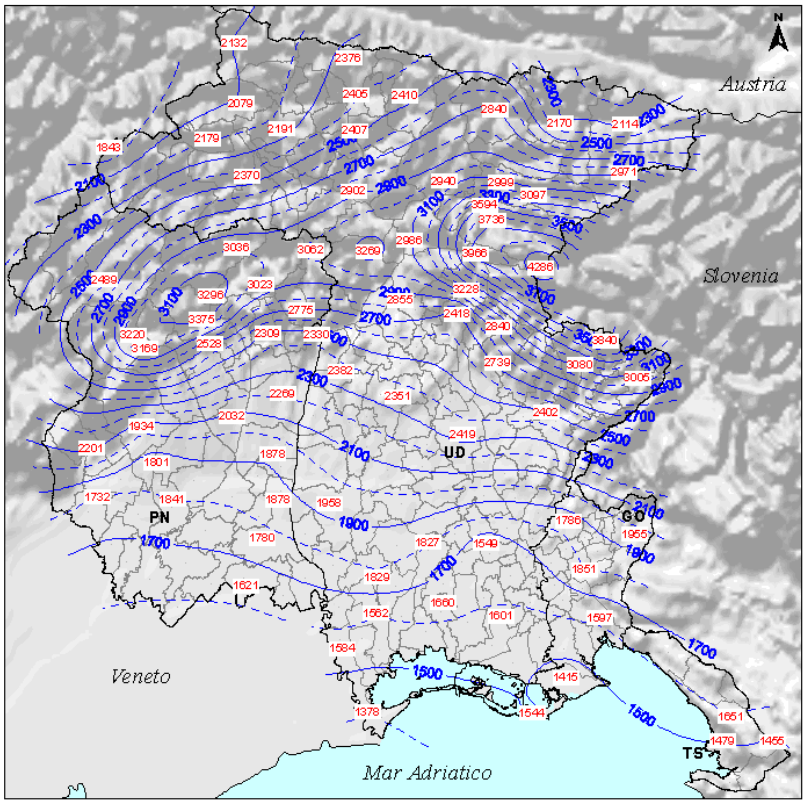

Figure 4: Cumulative rainfall, annual maximum over the period 1961-2000 (www.osmer.fvg.it).

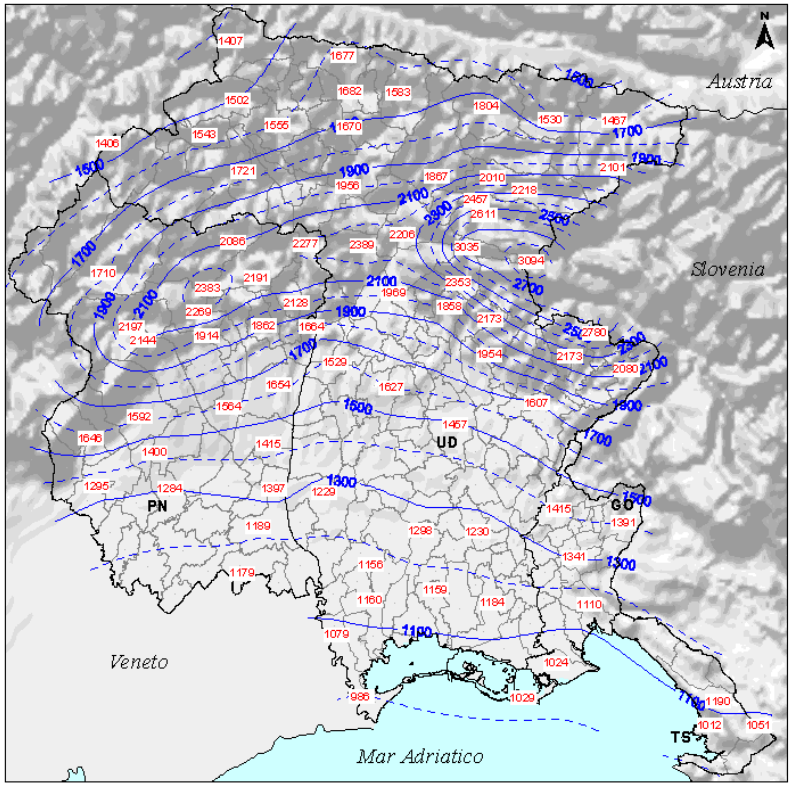

Figure 5: Cumulative rainfall, annual medium over the period 1961-2000 (www.osmer.fvg.it).

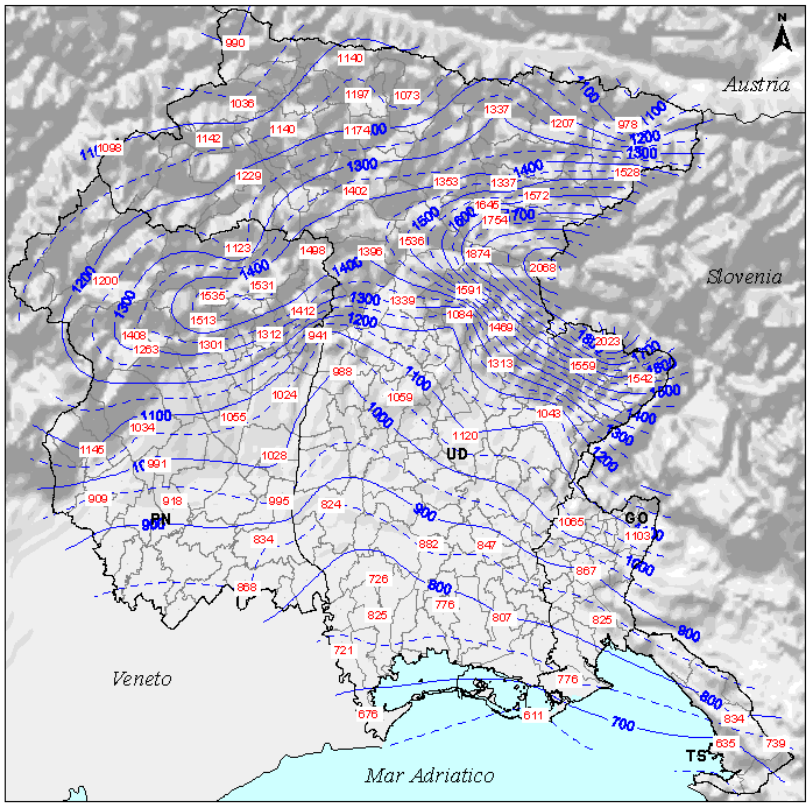

Figure 6: Cumulative rainfall, annual minimum over the period 1961-2000 (www.osmer.fvg.it).

The general precipitation map showed in Figure 3, is just an overview of the entire area. On the same data, but using a wider dataset (1961-2000), researchers of the OSMER, prepared a series of maps available on the web site (www.osmer.fvg.it). Among the others, there are the ones presented in the previous figures, concerning the maximum, mean and minimum values, expressed in mm, computed on the precipitation cumulative values and later interpolated. From the maps analysis emerges, that the lower mean annual precipitations occur along the coastal area where rain about 1000 mm. In the plain area, the mean values oscillates between 1000 mm in the Low Plain and 1500 mm in the High Plain or in the pedimont zone. Between the pedimont and the pre-alpine belt, the mean annual rainfall value increase up to 1500-2000 mm. Over the Pre-Alps, it reaches values that exceeds 2000 mm with peaks of 2400 mm in the Carnian Pre-Alps and 3100 mm in the Julian Pre-Alps. In the Carnian Alps mountain range, and in the area around Tarvisio, rainfall values can reach 1500-1700 mm. Analyzing the percentiles, every 10 years, in the less rainy year, can fall from 750-800 mm of rain on the coast and 2500-2600 mm over the Pre-Alps. In the rainier year, instead, precipitations can vary from 1200 mm over the coast until 3600-3700 over the Pre-Alps (Mt. Canin area). Within the period 1961-2000, the highest recorded values of rain has been of 4256 mm in the 1965 and 6100 mm in 1960 at Uccea, in Val Resia (UD), close to the Slovenian border.

If we consider the rainy days, that mean the days during which rained at least 1 mm, at year level, the value vary from 90 for the coast are until 120 of the pedimont and mountain areas. With a return time of approximately 10 years, these values rise reaching 100-110 days over the coast and 140 days on the pedimont and mountain. During the dryer years instead, over the coast there can be only 70-80 rainy days and 100-110 over the mountains. In the analyzed period, during 1966, at Uccea was recorded a value of 146 rainy days. In the winter times (DJF), the average number of rainy days is almost the same on the whole region with a value of 6-7. During March, November and October, this value increase with differences over the

areas. The inhomogeneity is maxima during June when on the coast there can be 9 days of rain, while over the mountain these count could reach the value of 15.

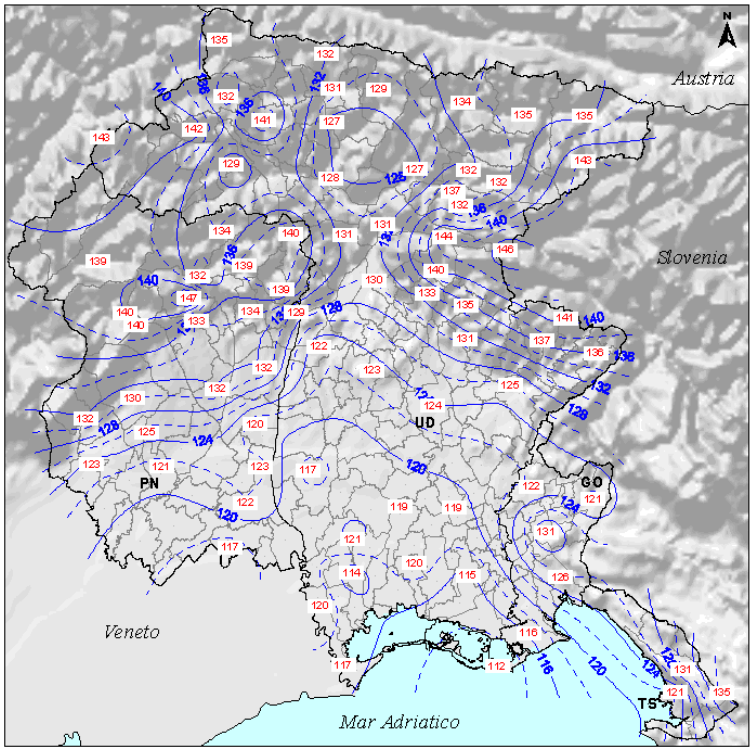

Figure 7: Days of rain, maximum over the year (1961-2000)(www.osmer.fvg.it).

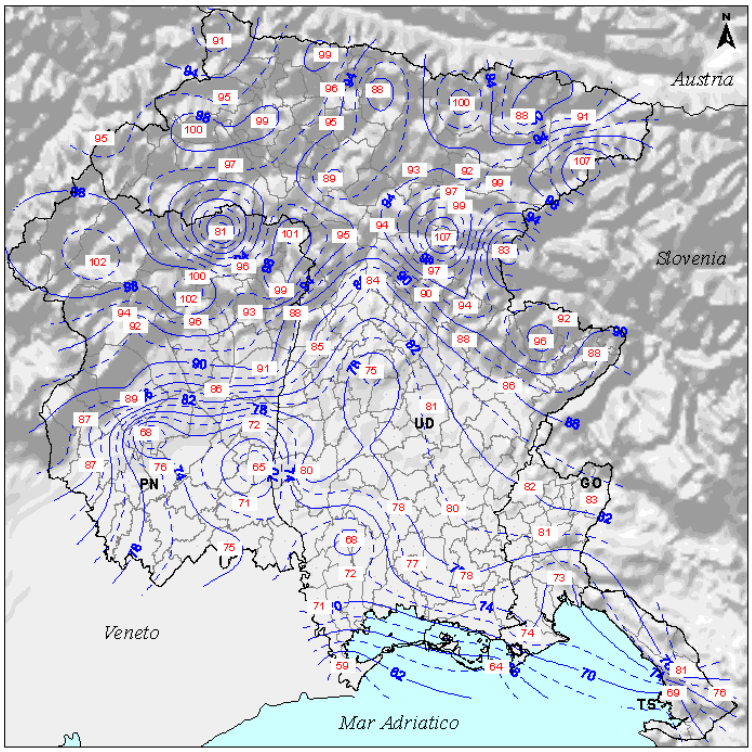

Figure 8: Days of rain, minimum over the year (1961-2000) (www.osmer.fvg.it).

4. TEMPERATURES

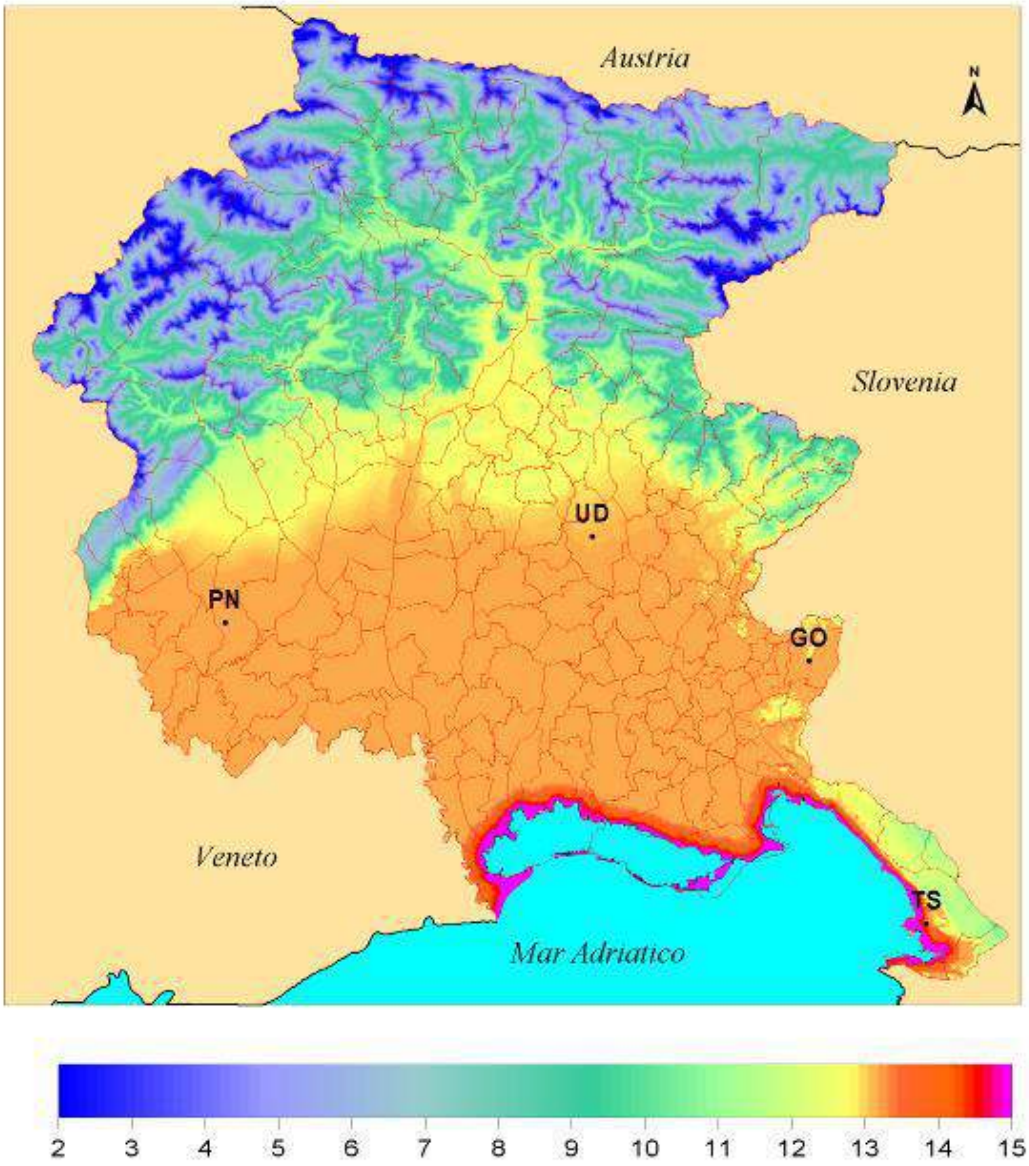

Figure 9: Mean annual temperatures expressed in °C (Micheletti, 2014).

As for the precipitations, the Authors analyzed also the temperatures. Analyzed data come from 47 meteorological stations within the period 1993-2012. We used data to create annual and monthly maps. The spatialization was done taking into account the elevation (if required), the plain effect, the coast and the mountain areas. The rasterization has been realized on a kernel of 500 m.

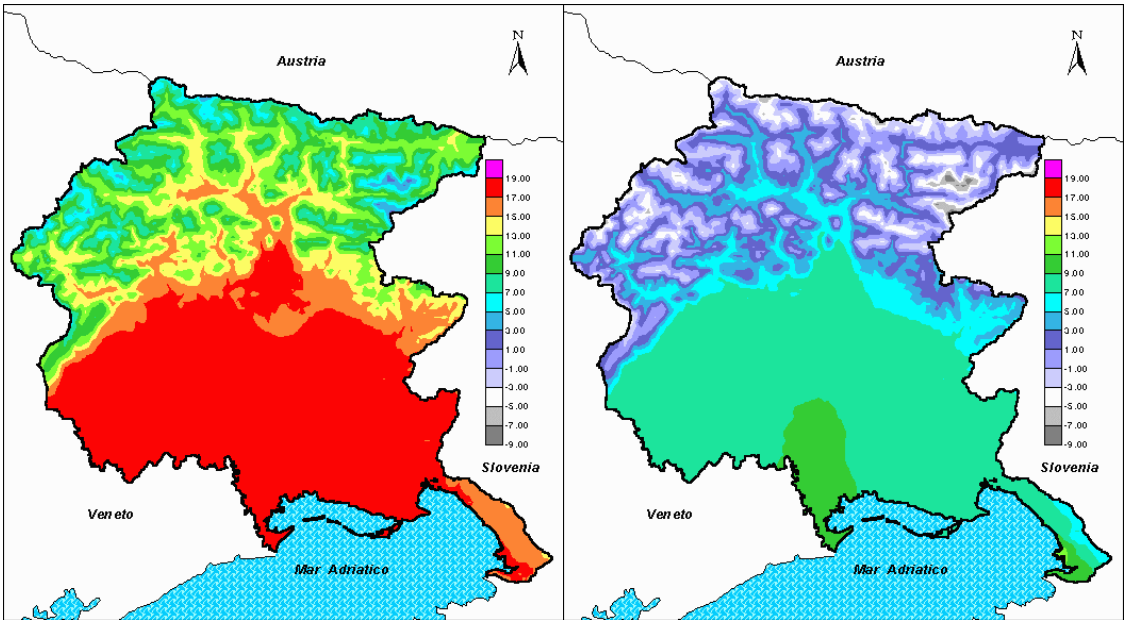

Figure 10: Max and min temperature computed for the period 1991-2010 for the whole FVG region (Micheletti, 2013).

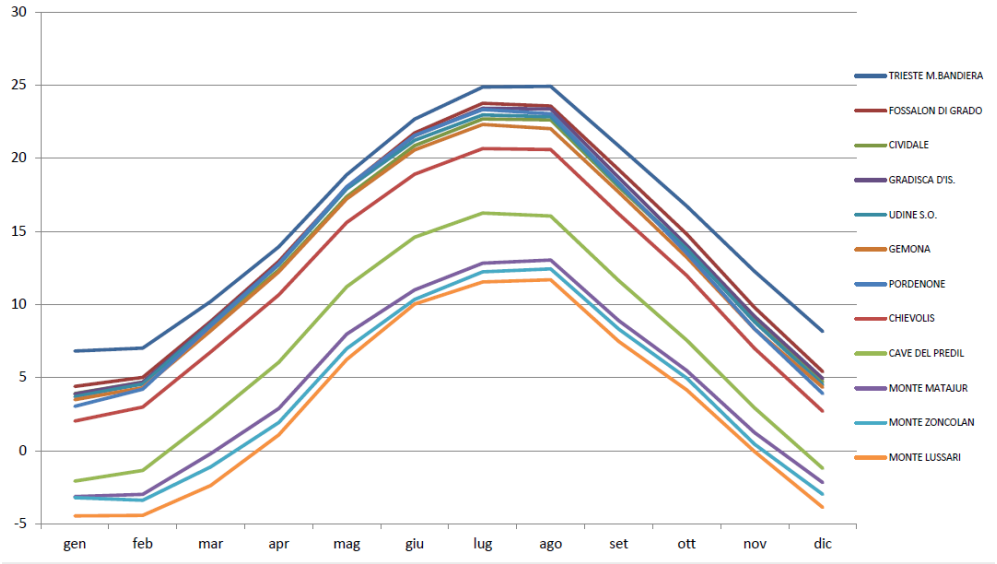

Figure 11: Mean monthly trend, in different places/stations of the Region within the period 1991-2010 (Micheletti, 2013).

Some stations in the region are historical, as the one in Trieste and the other in Udine. This means that they hold long time-series, more than 30 years.

To highlight better the annual variations, OSMER evaluated the differences from the mean annual temperatures in four different meteorological stations having the data availability since 1961. Using data made available by the Friuli Venezia Giulia Region - Direzione centrale ambiente, energia e politiche per la montagna - Servizio idraulica, it has been possible to extend the time series within the period 1961-2010(Antolini and Tomei, 2006). The data analysis highlighted that during the last 20 years, mean annual temperatures increased with years having more often values higher than 13°C. In the past two decades has been calculated an average increase of temperature of 0.7°C (Cicogna et al., 2012). In particular, two stations were analyzed: Trieste and Udine.

The time series of the mean annual temperatures at Trieste station (data available from 1840 to 2005 granted by HISTALP archive as result of different European projects) show an

uncertain trend (Auer at al., 2007). Analyzing the mobile mean temperatures over a period of 10 years, the value clearly attests around 13,5°C till the 1920. After that date, it increases reaching the 14°C, value that was overcome for the first time in the 1940. During the last 20 years, a rapid increase took the temperature to reach average values of 15°C (after the 2000).

If we observe Udine's dataset, also obtained from the historical series of the HISTALP database, the trend is similar to the one from Trieste. The mobile mean is oscillating between 12 and 13°C for all nineteenth century. In the first half of the 20th century, the temperature values starts to rise reaching the 13° in the 1940. It slightly decrease a little bit and remain constant until the 1985. Finally, it increases again going permanently over the 13° C.

If we analyze all the other available stations, 22 has 50-years series. Among these, the mean minimum temperatures remained almost stable in the period between 1950 and 1985, while during the second half of the 80s, they started to increase fairly gradually and steadily. The overall increase, in a 20-year period, varies between a few tenths of a degree and 2°C.

For the maximum temperatures, also in this case, after 30 years of stability, is possible to note an abrupt jump upwards in the 1985 followed by 10 years of increasing temperatures. During the last ten years, the trend seems to have a lower growth.

Overall, the increase, during the last 20 years varies between 0.5 °C and 2.5°C.

From the same archive (the HISTALP database) were obtained the deviations of the min and max temperatures from the mean seasonal values on the standard period 1961-1990. Analyzing the data, in wintertime, most for maximum than for minimum temperatures, the values showed a meaningful and rapid increase in the second half of the 80s, reaching the maximum values over 50-years period as had happened during a peak in the mid-70s. Over the past 20 years, the situation seems to be stabilized at these high values (roughly about 1°C over the historical mean). In springtime, after a stable 30-year period, with a sharp deviation from the mid-80s, temperatures have risen steadily, reaching values between 1°C and 3°C above the historical average (less than the min). During summer times, the temperatures increase started already from the early 70s for the maximum values and from the 1980 from the minimum ones. They reached 1°C to 3°C in the max and 0.5°C and 2°C in the min. In autumn, the mean maximum temperatures, while periodically oscillating, do not show clear signs of changes.

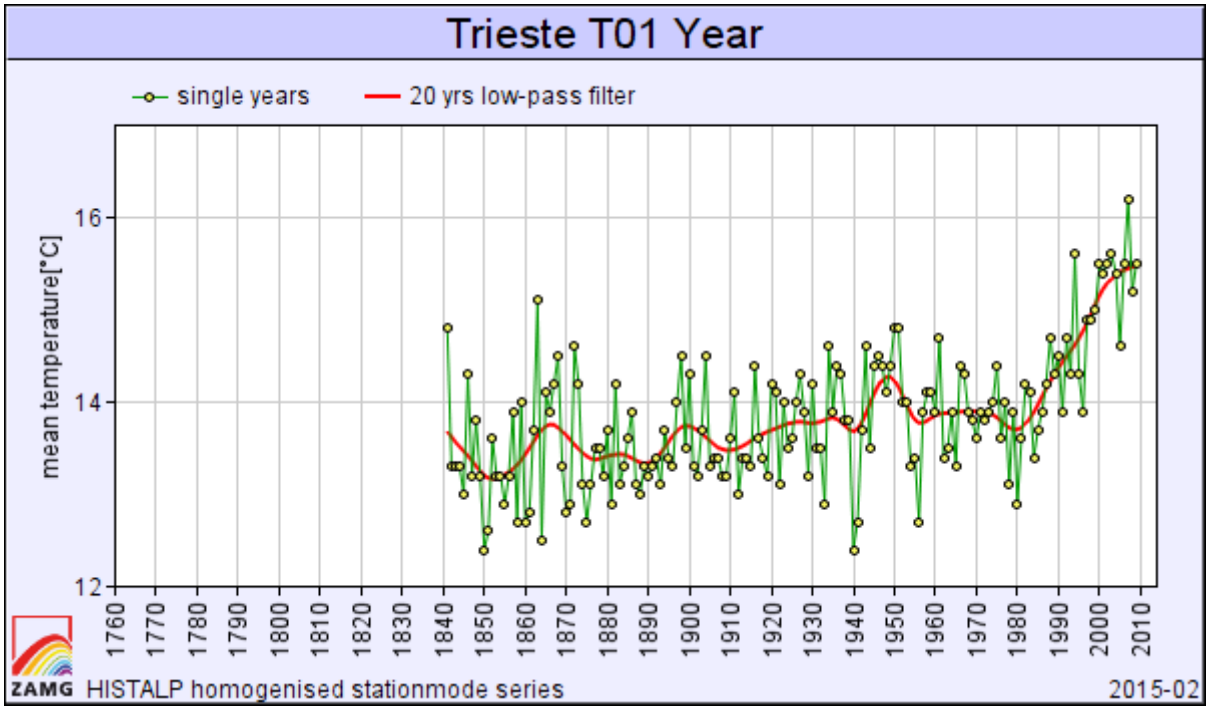

Figure 12: Mean annual temperature for the Trieste station [°C]. All the data are exportable from HISTALP dataset (http://www.zamg.ac.at/histalp/dataset/station/csv.php).

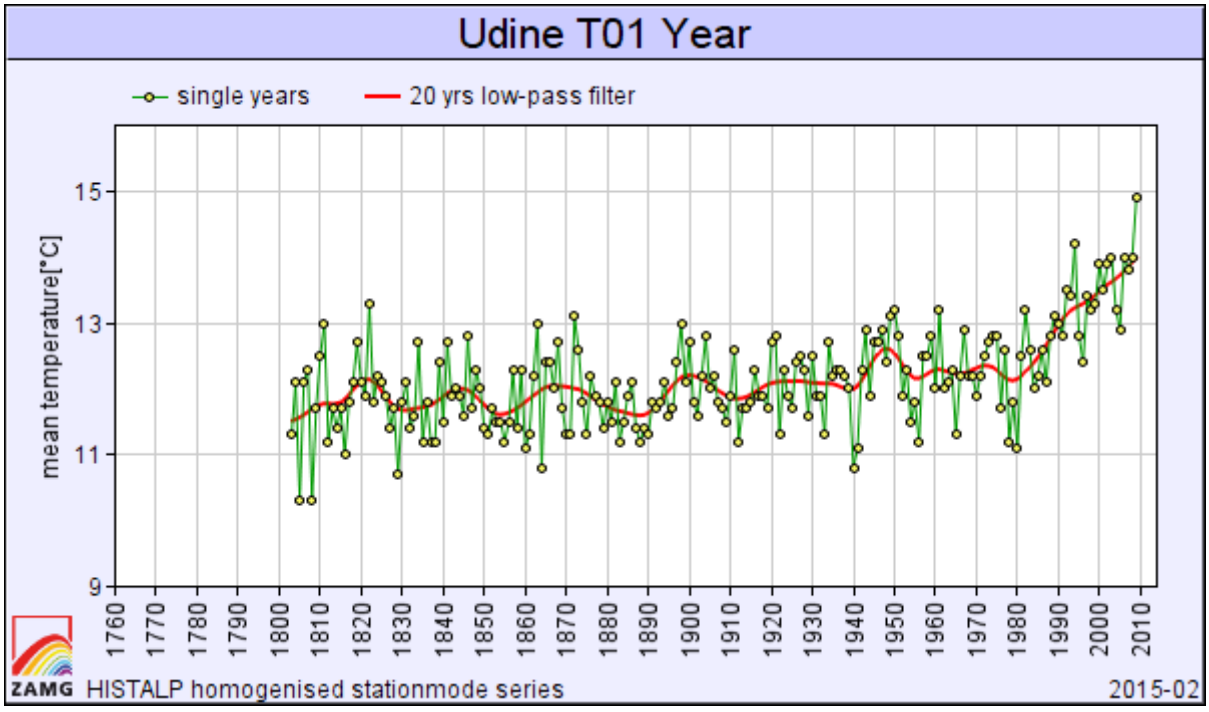

Figure 13: Mean annual temperature for the Udine station [°C]. All the data are exportable from HISTALP dataset (http://www.zamg.ac.at/histalp/dataset/station/csv.php).

5. CONCLUSIONS

In a nutshell, despite all the uncertainties, in the Friuli Venezia Giulia Region, the temperatures during the last 20 years seems to be highly increased almost everywhere, in tune and even more with what is happening in the rest of the world, especially concerning the maximum spring and summer values. Seems very likely that the values recorded in recent years are the highest for many decades, if not centuries. All the analysis indicates a rapid

increase in the temperatures of about 2/4°C within 2100 with a more pronounced increase during the summer season.
Regarding precipitations, on yearly basis, it is difficult to draw conclusions on possible increasing or decreasing trends, beyond some temporary or local signs. For some stations there is a trend indicating a decreasing in the precipitations of about 20% in correspondence of the summer seasons. During the winter times instead, it is expected a slight increase in the precipitation amount taking to a year almost unchanged balance (Fig. 14).

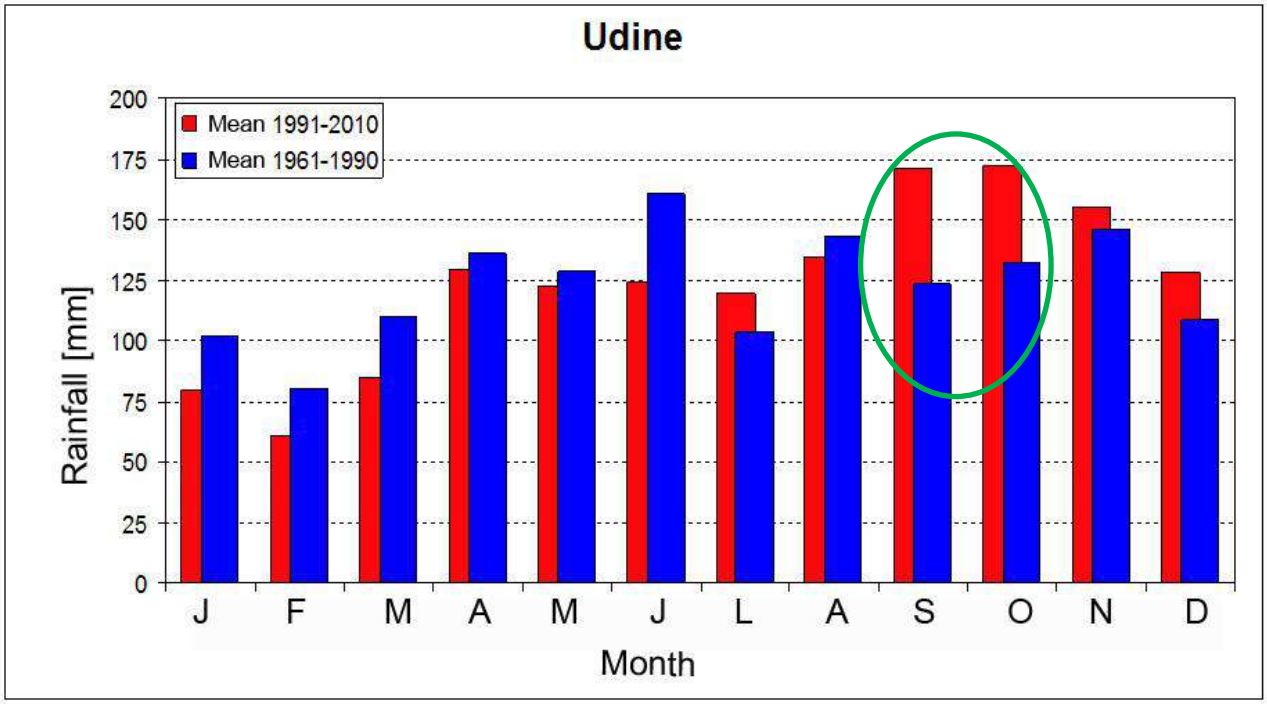

Figure 14: Mean precipitation computed for the Udine station (modified after OSMER, 2010).

Unlike the case of temperatures, the wide and frequent oscillations of the pluviometric regime mean that a lot depends from the length of the considered time series.
The results obtained by the different projects over the period 1961-1990 show clear signals even if sometimes conflicting, of climate changes. This can only lead us to apply the principle of caution and to continue the painstaking and relentless work of collecting meteorological data, always of the highest quality, day after day, year after year, in order to avoid future doubts about the validity of the time series used for the analysis allowing, in the future, a better knowledge of the reality in which we live.

4. REFERENCES

[1] Antolini G., Tomei F. (2006) PRAGA - Programma di Analisi e Gestione di dati Agrometeorologici, Atti del convegno AIAM 'Agrometeorologia e gestione delle colture agrarie, Torino, 6-8 giugno 2006.
[2] Arpa-Osmer (2008): Atlante climatico del Friuli Venezia Giulia: 1.Precipitazioni, pp.42, on line published on www.meteo.fvg.it
[3] Auer I., Bohm R., Jurkovic A., Lipa W., Orlik A., Potzmann R., Schoner W., Ungersbock M., Matulla C., Briffa K., Jones P., Efthymiadis D., Brunetti M., Nanni T., Maugeri M., Mercalli L., Mestre O., Moisselin J.-M., Begert M., Muller-Westermeier G., Kveton V., Bochnicek O., Stastny P., Lapin M., Szalai S., Szentimrey T., Cegnar T., Dolinar M., Gajic-Capka M., Zaninovic K.,

Majstorovic Z., Nieplova E. (2007) HISTALP – historical instrumental climatological surface time series of the Greater Alpine Region. Int. J. Climatol., 27: 17 – 46. DOI: 10.1002/joc.1377.
[4] Bolle H. J. (2003) Mediteran climate: variability and trends. Springer Verlag, Berlin (GER), pp. 320.
[5] Bradley R. S., Jones P. D. (1995) Climate since A.D. 1500, Routledge, London & New York, pp. 706.
[6] Cicogna A., Giani M., Micheletti S. (2012) Cambiamenti climatici, Rapporto Sullo Stato dell'Ambiente, ARPA FVG, Forum Editrice Universitaria, Udine.
[7] HISTALP (2014) Historical Instrumental Climatological Surface Time Series of the Greater Alpine Region. http://www.zamg.ac.at/histalp/ , last access 10.08.2014.
[8] IPCC (2007) Summary for Policymakers. In: Climate Change 2007: The Physical Science Basis. Contribution of Working Group I to the Fourth Assessment Report of the Intergovernmental Panel on Climate Change (ed. by S. Solomon, D. Qin, M. Manning, Z. Chen, M. Marquis, K. B. Averyt, M. Tignor & H. L. Miller), 1–18. Cambridge University Press, UK and New York, NY, USA
(*http://www.ipcc.ch/pdf/assessment-report/ar4/wg1/ar4-wg1-spm.pdf*).
[9] Isotta F.A., Frei C., Weilguni V., Tadic M., Lassegues P., Rudolf B., Pavan V., Cacciamani C., Antolini G., Ratto S., Munari M., Micheletti S., Bonati V., Lussana C., Ronchi C., Panettieri E., Marigo G., Vertacnik G. (2013) The climate of daily precipitations in the Alps: development and analysis of a high-resolution grid dataset from pan-Alpine rain-gauge data. Int. J. Climatol. doi: 10.1002/joc.3794.
[10] Leroux M. (2005) Global Warming: Myth or Reality? The Erring Ways of Climatology. Chichester (UK) Springer (Eds.). ISBN 3-540-23909-X.
[11] Lionello P., Malanotte-Rizzoli P., Boscolo R. (2006) Mediterranean climate variability. Amsterdam (The Nederlands) Elsevier (Eds.).
[12] Micheletti S. (2014) Climatologia recente del Friuli. Unpubblished presentation in the framework of GEP european project. Gorizia, sala consiglio comunale, 27.06.2014.
[13] Zini L., Calligaris C., Treu F., Iervolino D., Lippi F. (2011) Risorse idriche sotterranee del Friuli Venezia Giulia: sostenibilità dell'attuale utilizzo. EUT (Eds.), ISBN 978-88-8303-314-8.

5. VISITED WEB SITES

http://www.zamg.ac.at/histalp/

http://www.osmer.fvg.it/

http://www.gepgis.eu/it/category/dogodki/

http://astis.ung.si/it

http://www.hydrokarst-project.eu/it/pubblicazioni

Let's grow up together

DRINK ADRIA

Adriatic IPA
Cross Border Cooperation 2007-2013

The project is co-funded by the European Union,
Instrument for Pre-Accession Assistance

WP4 / ACT. 4.1: Regional characteristics of climate and climate change

Existing Climate and Climate Change Data on Local Level: Marche Region (ITALY)

Lead Author/s	Daniele Nardi
Lead Authors Coordinator	
Contributor/s	
Date last release	30/04/2014
State of document	Final

Let's grow up together

DRINK ADRIA

Adriatic IPA
Cross Border Cooperation 2007-2013

The project is co-funded by the European Union,
Instrument for Pre-Accession Assistance

Introduction

In this report you'll find a summary of the results of the research activity implemented by A.ATO 3 Organization in order to contribute to the DRINKADRIA Project objective to develop a review of existing climate and climate change data and elaborate a database concerning the available hydrological data for Adriatic region.

Such a database will be useful to develop a common platform to exchange and compare data related to water resources availability and use in trans-boundary context. Harmonized concept of current trends and future scenarios in precipitation, runoff and water storage will represent a starting point and useful basis for the harmonization of more complex issues relating water availability and its use in transboundary and cross-border (regional) context.

According to international and national studies and publications the Mediterranean region is expected to undergo particularly negative climate change impacts over the next decades, which, combined with the effects of anthropogenic stress of natural resources, make this region one of the most vulnerableareas in Europe. The anticipated negative impacts are mainly related to possible extraordinary heat spells (especially in summer), increased frequency of extreme weather events (heat waves, droughts and severe rainfalls) and reduced annual precipitation and river flow. In this context, Italy may undergo some expected climate change impacts that would critically affect the following national circumstances, including:

- water resources and areas at risk of desertification;
- coastal areas prone to erosion and flooding and susceptible to alterations of marine ecosystems;
- Alpine regions and mountain ecosystems experiencing glacial loss and snow cover loss;
- areas prone to flood and landslide risk (i.e. hydro-geological risks including the risk of flash floods, flash mud/debris flows, rock falls and other mass movements related to soil and land management) and, in particular, the hydrographical basin of the Po river.

Climate change is likely to magnify the regional differences in terms of quality and availability of natural resources and ecosystems in Europe and also in Italy. It can threat Italian biodiversity at the level of species and habitats especially in the mountain environments. Therefore, Italy is expected to face an extremely high risk of biodiversity and natural ecosystems loss under future climate change.
Water resources (in terms of annual precipitation and river discharge) are projected to decrease over Southern Europe, and this regional pattern could intensify in the last decades of this century. The existing conditions of high stress on water resources and of hydro-geologic disturbance in some Italian regions could be exacerbated by projected climate change including: reduced water availability and quality, increases in frequency and intensity of droughts especially in summer, increases in frequency and severity of river summer flows reductions and annual river flow decline and limited groundwater recharge.

Water quantity/availability and quality in Italy could be affected by:

- reduced water availability, especially in summer;
- increased water stress;
- severe negative impacts in the South, where vegetation and territory are already experiencing a marginal water supply regime;
- increased seasonal water deficit due to significant pressures of summer tourism peaks in small Italian islands;
- potential increased conflicts among multiple uses of water resources.

A mapping of the hydrological risk in Italy (2006) showed that:

- 5.2% of the Italian territory is exposed to the risk of landslides;
- 4.1% is under risk of flooding and 0.5% is prone to avalanches.

According to a more recent (2008) assessment 9.8% of the Italian territory is characterized by the highest level of hydro-geological criticality (that represents the states of "high" and "very high" risk and danger), of which 6.8% include areas with exposed properties (urban centres, infrastructures, industrial areas, etc.).

Climate change impacts on the Italian hydro-geological system include:

- variations in the hydrologic regime related to e.g.:
    - progressive melting of the glaciers and reduction of seasonal snow cover in Alpine catchments, due to rising temperatures and changing precipitation patterns;
    - increase in the aridity of soils and in the frequency of drought events in the plain areas;
    - changes in groundwater resources, related to SLR resulting in increased saltwater intrusion in coastal aquifers, accompanied by limited capacity of beach nourishment due to the lower river sediment transport (induced by reduced rivers medium ratings because of decreased precipitation but also by man-made dam works and withdrawals);
- higher risk of inland flooding, due to increased events of river flood heights in relation to heavy precipitation events;
- increased winter run-off by 90% and decreased summer run-off by 45% in central Europe Alpine rivers, with consequent greater risk of flooding and drought respectively;
- significant changes in the hydrologic balance (and water quality) of some river basins with an estimated reduction in annual discharge as well as nutrients and sediments transport in the next decades;
- increased risk of flash mud/debris flows, due to a potential increase of extreme weather events;
- increased risk of landslides in the Alps, due to temperature warming and ice melting;
- risk of rock falls in the Apennines, because of possible more frequent and sudden temperature changes, especially in winter;
- risk of flash floods in both areas, due to severe precipitation events.

The areas most exposed to the hydro-geological risk include: the hydrographical basin of the Po River, subject to increased flood risk, and the Alpine and Apennine areas, subject to increased flash flood risk.

It is therefore evident that analysis of the available climate and climate change data, relating to Marche Region is a crucial aspect to be taken into account when studying the effects of climate change on water resources in the Adriatic region, also useful for comparison of current trends and future scenario in different locations of the same Adriatic region.

Input data (T2m, precipitations...., period of time)

As far as concerns Marche Region, a Report edited by Macerata Ecology and Climatology Center, on behalf of the Local Civil Protection Department, concerning "Marche Region climatology: average mean temperature for the period 1950-2000", shows a characterization of the region through the analysis of temperature series. To carry out the study the following parameters were statistically processed: average monthly temperature, monthly mean value of daily absolute maximum temperature and monthly mean value of daily absolute minimum temperature of 24 measuring stations of the regional meteo-climatic monitoring network, for the period 1950 to 2000.

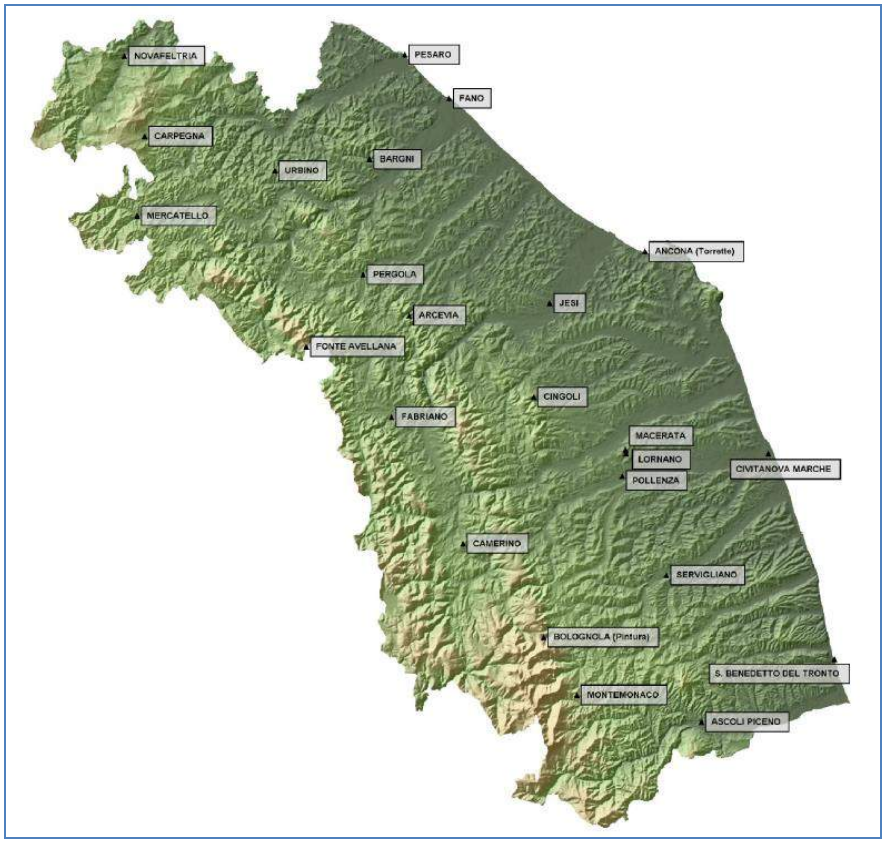

Fig. 1 – Geographical distribution of thermometric stations (24) in Marche Region

According to recommendations given by the World Meteorological Organization (WMO), the period considered for the conventional climatological analysis and comparison is the period 1961-1990 (thirty years).

Another study, concerning "average precipitation for the period 1950-2000 on Marche Region" was also carried out (2002) by the same Ecology and Climatology Center, after collecting and statistically processing monthly rainfall data relating to 102 gauging stations for the period 1950-1989, based on the available data and continuity of the series. For each station the probability distribution of the monthly precipitation has been determined, as a valuable tool to calculate the probability of occurrence of a precipitation less than or equal to a critical value (or greater). The trend of annual precipitation at each location has also been analyzed and expressed as a percentage of the variation in precipitation compared to the mean value. Specific climatological maps concerning calculated annual and seasonal average precipitation, for the period 1950-1989 , were finally drawn using the output data of previous statistical analyses.

Fig. 2 – Geographical distribution of rainfall gauging stations (102) in Marche Region

Obtainment of meteorological data, in order to implement a specific hydrogeological data set, is quite easy, as most of the data are published and available on the web. Particularly interesting are the websites listed below:

- www.meteo.marche.it (ASSAM meteorological data networ)
- www.acq.isprambiente.it/annalipdf (collection of historical Annual hydrogeological records, period 1961-1990, in .gif format)
- protezionecivile.regione.marche.it (Annual hydrological Records, period 1990-2012)
- clima.meteoam.it (Studies, Publications, etc.)

Concerning drinking water quality, especially referring to those parameters analysed in accordance with D.Lgs. 31/2001 (Dir. 98/83/CE) the Regional Environmental Protection Agency of Marche Region (www.arpa.marche.it) also published (2003) a white paper on potable water for each of the 4 Provinces.

Used methodology (explained in short)

Concerning temperatures, sound statistical analysis were carried out on investigated variables, aiming to develop a reliable investigation, integrating those information already available in the scientific literature about the thermal characteristics of Marche Region. Basic data were then processed and GIS (Geographic Information System) used to show them in form of maps.

Finally, the available time series have been examined, with the objective of determining a possible trend in the progress of temperatures in Marche Region.

For short discontinuity in the data set (1 to 3 years missing), interpolation of available data from the same station has been employed, considering at least 30 year long data records series. For longer periods (over 3 years), the used methodology consists in calculating the Pearson linear correlation coefficient among all the pairs of stations for each parameter for each month of the year in the range 1961-1990. Reconstruction of missing data occurred then through the simple linear regression relationship between the target station and the nearest one (in terms of observations), by using the method of least squares standard approach.

Following *cluster analysis*, temperature variability was investigated using multivariate statistical analysis, analysis and *Empirical Orthogonal Functions* (EOFs), with the purpose to reduce the large data set to a reduced number of data, chosen so that they can represent a large fraction of the variability in the original set.

Very often, in Scientific literature you find relations between temperature and geographical features. As far as concerns Marche Region a specific correlation between temperature, elevation, distance from the sea and latitude was investigated, by applying a multiple linear regression model. Because of regional morphology and short distances, by using the forward selection criterion, it comes out that elevation is the only variable to take into account in relation to temperature variations in space, according to the following relation:

$$T = aH + c$$

where the parameters *a* and *c* have been determined for each month with statistical analysis of monthly average temperatures.

Average temperature gradient mean value for Marche Region can be expressed as:

$$\Delta T/\Delta H = (-0{,}44 +/- 0{,}05)\ °C/100m$$

Similar relation, valid for whole Europe is as follow:

$$\Delta T = 0{,}55 + 0{,}15\ sin(m + 300) + 0{,}05\ sin(2m + 360)\ °C$$

where *m* is the time, in the form of an angle, starting from the beginning of the year (1st of January is 0°) and setting 360° as end of the year. Average value is 0,55 °C per 100 m elevation.

Average annual and monthly (January, July) temperature maps where drawn, on regional scale, also using a Digital Elevation Model (DEM) and GIS elaboration.

In order to obtain the necessary data for the preparation of average annual and seasonal (spring, summer, autumn and winter) precipitation maps, the total yearly and seasonal rainfall values and their mean values in mm has been calculated for the period 1950-1989.

The amount of monthly precipitation, although it is calculated from measurements rounded to discrete values, can be classified as a continuous random variable, since it can assume any value in a predetermined range when the number of observations is large enough. To determine the probability of occurrence of monthly precipitation amount less than or equal to a certain treshold (or greater) the probability distribution of the data of monthly precipitation for each location has been studied. That is well represented by the *Gamma* continuous probability distribution.

The reduction - as a percentage- of annual precipitation compared to the mean value in the period 1950 - 1989 for the stations with significant trend, has been quantified by approximation of the precipitation values through linear regression, and the variation in mm of water of rainfall in the studied time interval has been assessed comparing it to the mean value.

For further details on the used methodology, please refer to the documents listed in References.

Results (differences/trends in T2m, precipitations, ...)

According to the results shown in the following graphs it is clear that temperatures in Marche Region are increasing. The observed trend is characterized by increases ranging between 0,5 and 1,3 °C every 50 year, in maximum temperature series, according to the data recorded in the period 1950 - 2000. Concerning the

minimum temperature series the annual trend is similar, although higher (between 0,8 and 1,7 °C/50 years).

Ancona (Torrette)

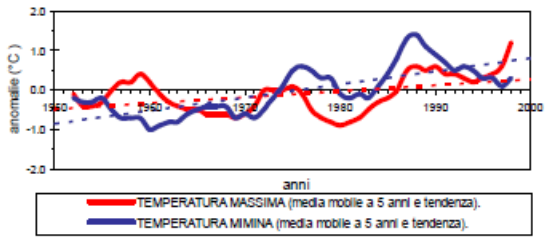

Arcevia

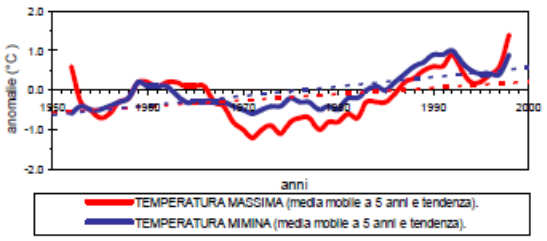

Ascoli Piceno

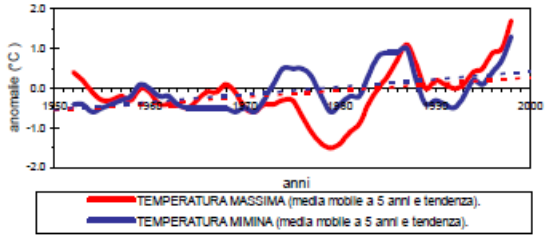

Bargni

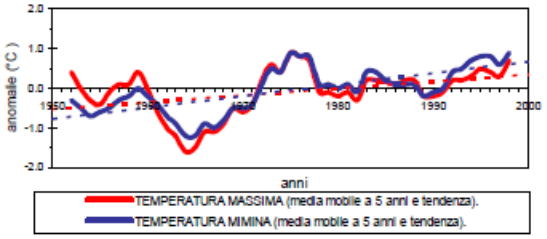

Bolognola (Pintura)

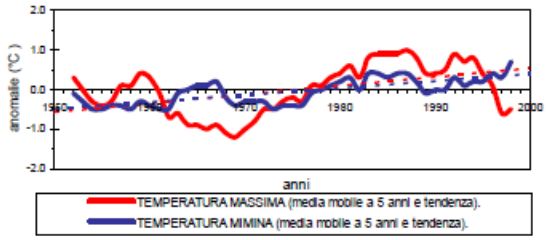

Camerino

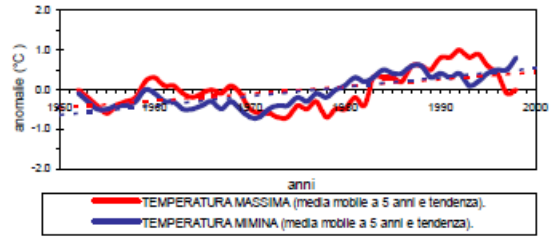

Carpegna

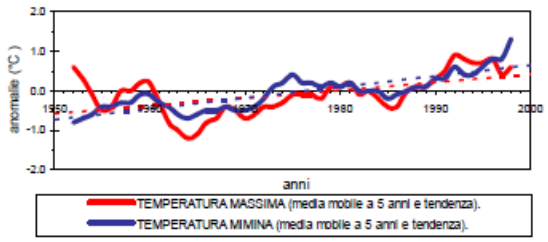

Cingoli

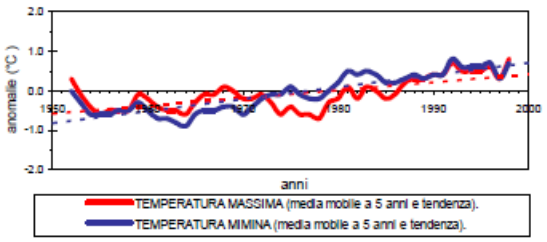

Civitanova Marche

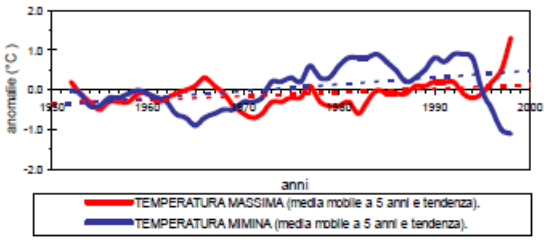

Fabriano

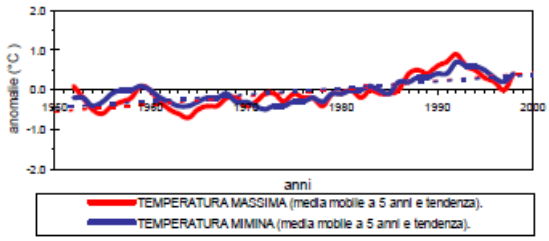

Fano

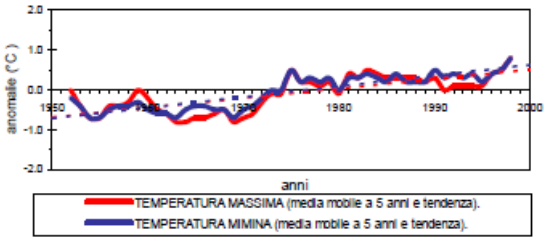

Fonte Avellana

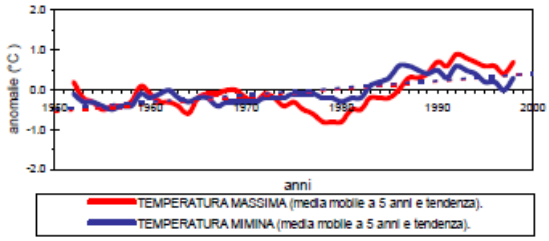

Jesi

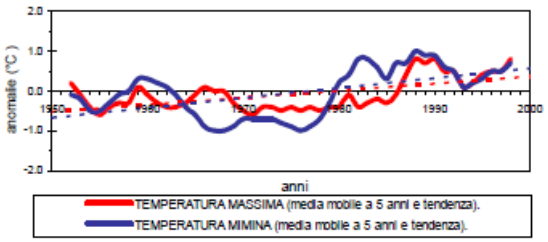

Lornano

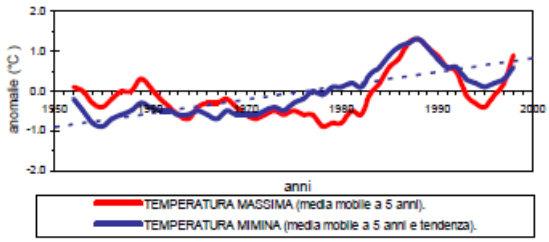

Macerata

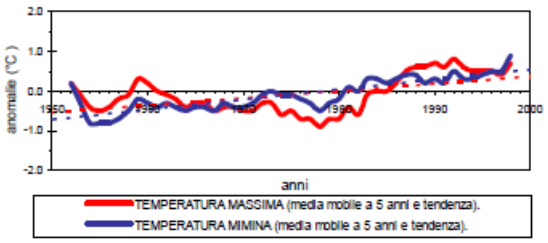

Mercatello

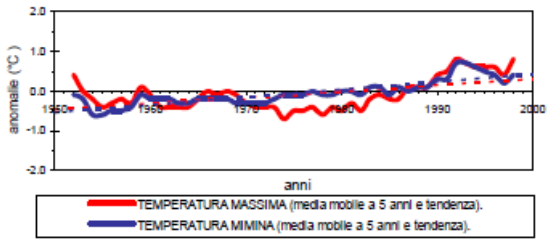

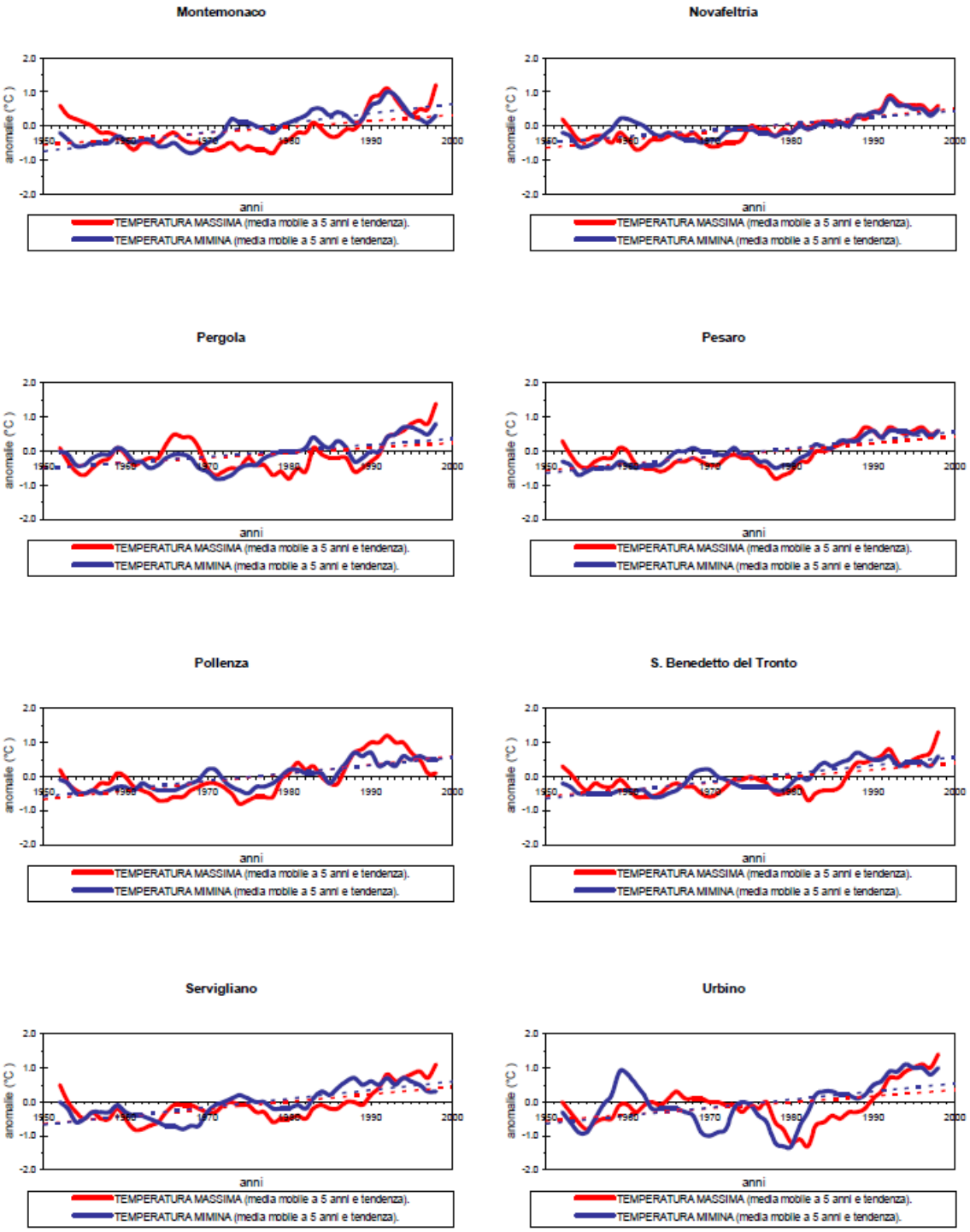

Fig. 3 - Temporal trends of annual maximum and minimum mean temperature values.

Analysing the graphs reported above, you can see that, in most cases, the minimum temperature shows a increasing trend more pronounced compared to that of the maximum temperature. To better quantify this phenomenon, the increase in temperature has been reported as percentage calculated in relation to the corresponding average values for the period under study.

Monthy values of average decreasing temperature per 100 m elevation have also been calculated, as shown in the following Table:

Tab. 1 – Monthly average decrease in temperature per 100 m elevation, in Marche Region.

JAN	FEB	MAR	APR	MAY	JUN	JUL	AUG	SEP	OCT	NOV	DEC
0,39	0,47	0,46	0,47	0,45	0,43	0,37	0,38	0,46	0,48	0,50	0,43

As far as concerns rainfall, 5 different maps have been edited, concerning average annual and seasonal (spring, summer, autumn and winter) precipitation. Annual average precipitation data for each gauging station were calculated using arithmetic mean of the total annual precipitation recorded in each station, referring to the period 1950 to 1989. Similarly, seasonal rainfall mean values were also calculated for the same period. Notice that for the calculation of winter mean values the data taken into account refers to the month of December of the previous year and the months of January and February of the year in question.

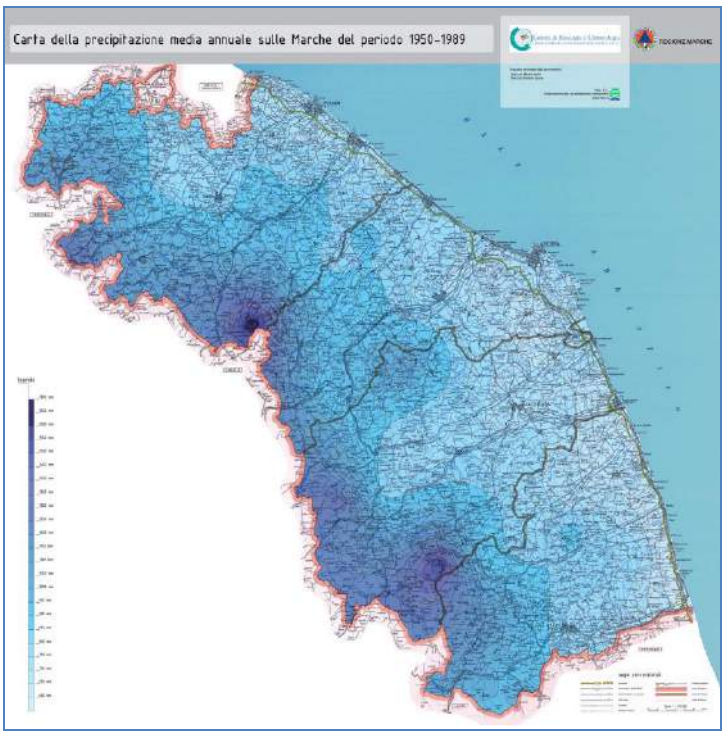

Fig. 4 – Average annual precipitation on Marche Region 1950-1989

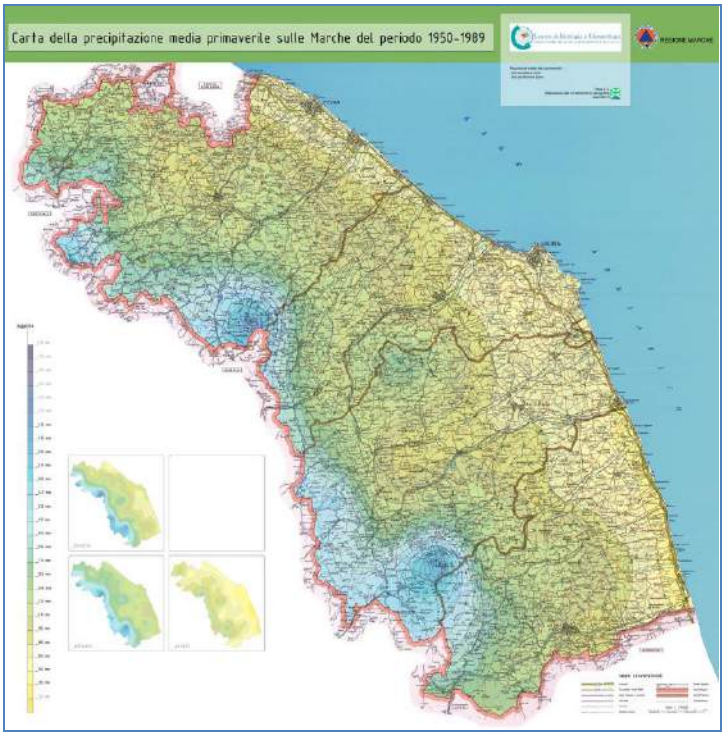

Fig. 5 – Average Spring precipitation on Marche Region 1950-1989

Fig. 6 – Average Summer precipitation on Marche Region 1950-1989

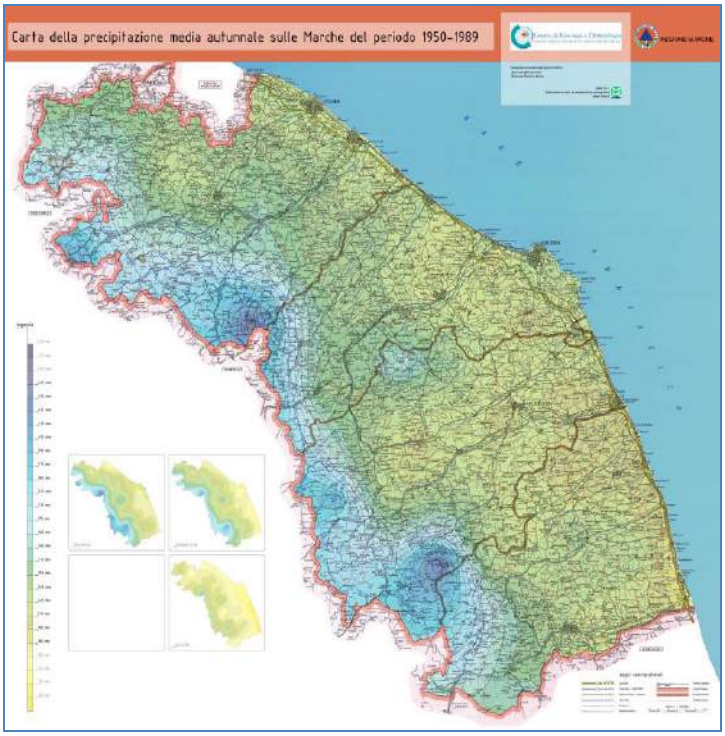

Fig. 7 – Average Autumn precipitation on Marche Region 1950-1989

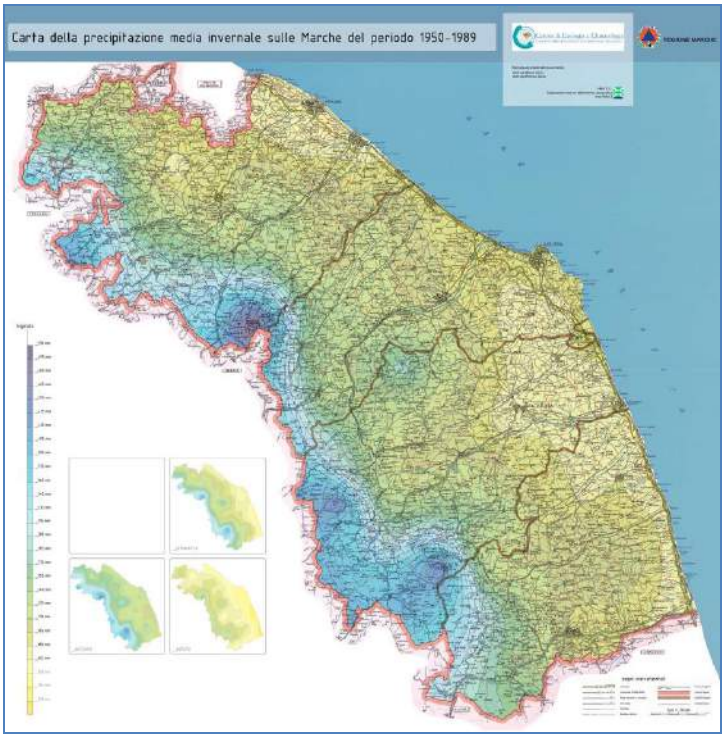

Fig. 8 – Average Winter precipitation on Marche Region 1950-1989

Being affected by both atmospheric flow and local orography, rainfall is not in direct relationship with soil elevation.

Observing the maps reported above you can see that Marche Region can be divided into 3 bands: coastal zone with rainfall values ranging between 600 and 850 mm, medium-low hill area with values in the range 850 to 1100 mm and mountains area with values above 1100 mm.

The wettest area is the Appennines, with maximum annual rainfall value (1550-1700 mm) on Monte Catria (1701 m asl), followed by other significant high values in the area of Monti Sibillini (1500-1550 mm), Monte Pennino (1570 m asl – 1350-1400 mm) and Monte San Vicino (1050-1100 mm).

Regarding average seasonal precipitation, Marche Region can be divided in the same areas as above, with average waterfall in the range shown in the following table:

Tab. 2 – Annual and seasonal total rainfall in the different zones

Zone ***Period***	*Coastal*	*Medium-low hill*	*High-hill/mountains*
Spring	120-195 mm	195-270 mm	270-435 mm
Summer	105-165 mm	165-195 mm	195-285 mm
Autumn	165-225 mm	225-315 mm	315-480 mm
Winter	150-210 mm	210-300 mm	300-525 mm
Year	600-850 mm	850-1100 mm	1100-1750 mm

It should be noted that autumn is the wettest season, except for a wider range of winter rainfall for the high hill/mountains area, with the upper limit higher than the corresponding autumn one.

Another interesting map is the one showing the average annual rainfall on Marche Region River Basins, which can be considered a very important parameter when talking about Water Resources availability and Climate Change effect on it.

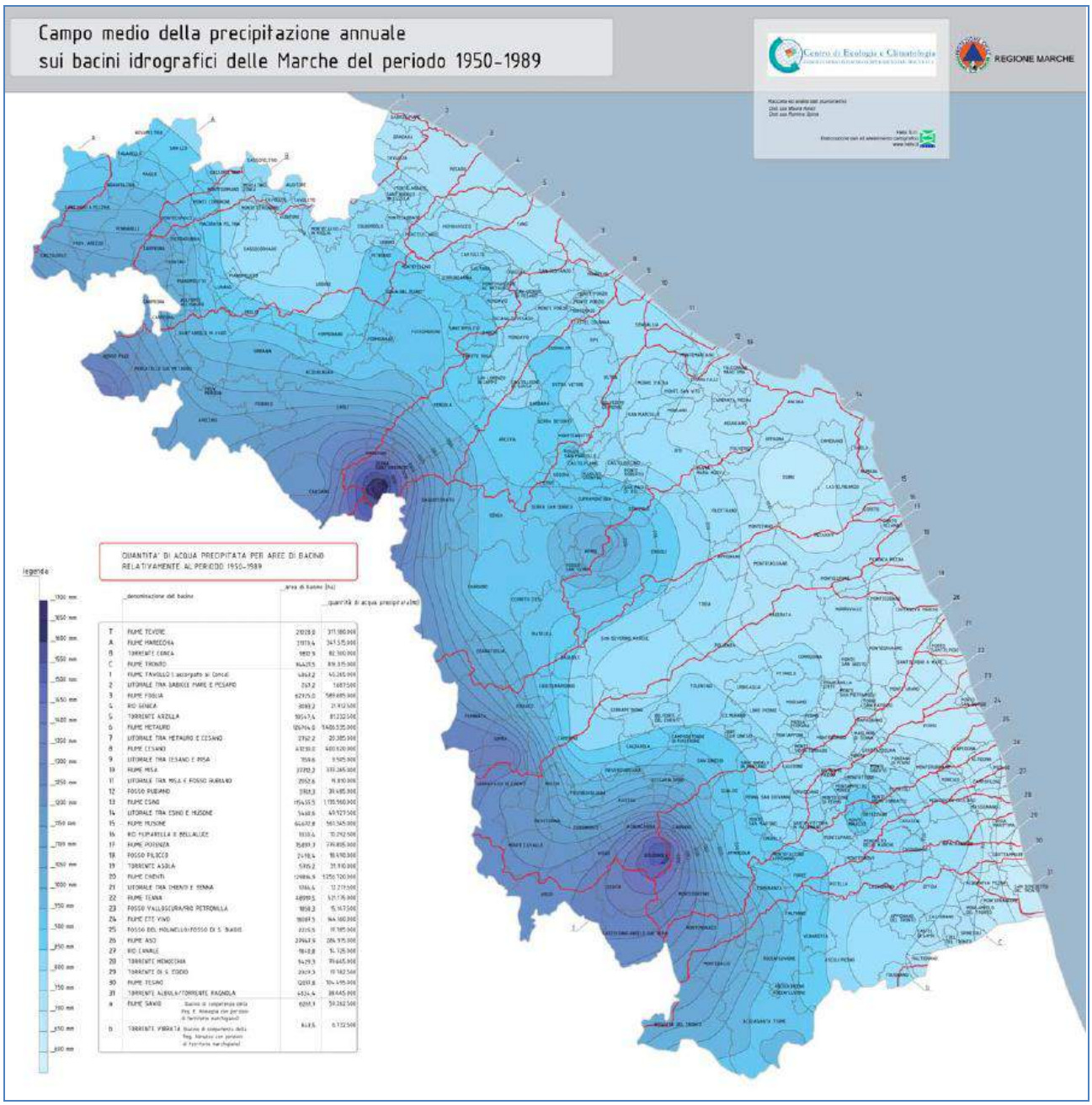

Fig. 9 – Average annual precipitation on Marche Region River Basins 1950-1989

Five extra maps referring to average annual and seasonal precipitation in the period 1950-2000 were also drawn, limited to a portion of Marche Region, taking into account records concerning 28 stations belonging to Macerata and Ancona Provinces, with available data up to year 2000.

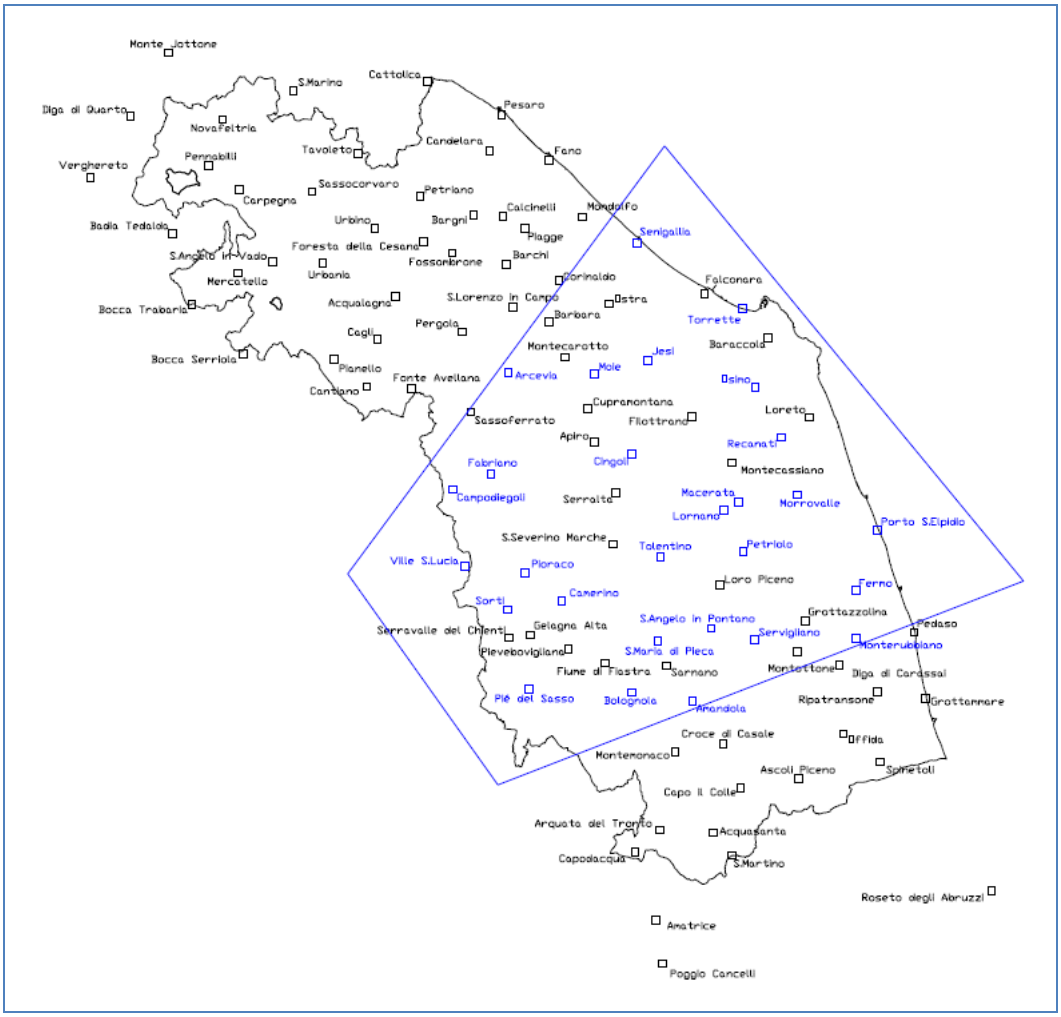

Fig. 10 – Geographical distribution of rainfall gauging stations updated until 2000

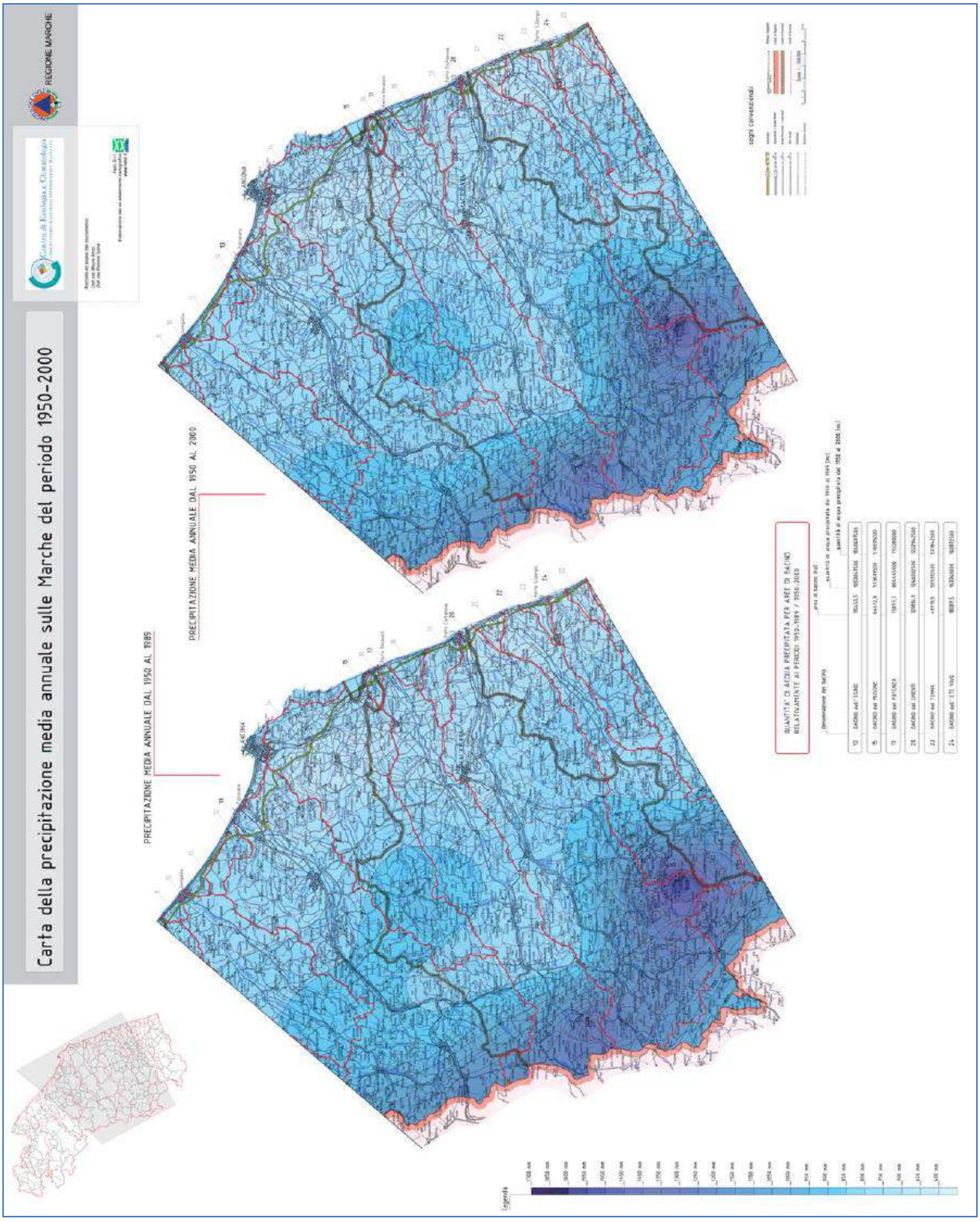

Fig. 11 – Average annual precipitation on Marche Region 1950-2000

Comments on results

Concerning temperatures, annual increase has been observed in most of the stations over the whole period. Such increase is around 5-6% for the maximum temperature values and 10-12% for the minimum values. The increase is evident in all seasons for minimum temperature, with average growth of 1,1 °C every 50 years in Spring, 1,4 °C in Summer, 1,0 °C in Autumn, 1,3 °C in Winter in the period under study. Positive trend (growth) in maximum temperature is especially evident in spring and winter (1,1 °C and 1,2 °C/50 years, respectively). Screening in elevation bands suggests that temperature is increasing with greater intensity in mountain and high hills areas, rather than in coastal zones and lower hills.

Results concerning rainfall analyses reveal a significant decreasing trend in annual precipitation in the period 1950 to 1989 for 59 stations. Maps referred to those stations whose data are updated until 2000 show a decline of rainfall compared to the 40 year long data set for the same area, except for autumn, when there is an increase in precipitation.

Further researches and studies about the probability distribution of monthly precipitation and trend in annual precipitation should update the data set to be taken into account up to present days. If the trend of annual precipitation would prove negative, as shown in the present work, it would be important studying the intensity of rainfall considering the trend of the number of rainy days in the month: if the latter showed a significant negative trend, steeper than the one corresponding to the quantity of rainfall, this would result in a growing intensity trend. Monitoring of the precipitation intensity parameter, correlated to other factors, it is of utmost importance in the prevention of disasters, such as flooding , flash floods, etc.

The results of the investigation on the variability of typical weather indicators, such as precipitation and air temperature near the ground (T2m), made in the recent years in order to study potential climate change on a regional basis, can be summarized as follows:

- detection of a decreasing trend of annual precipitation, even with its natural oscillations, and determination of a reduction, for the most part of the cases, more than 10% and less than or equal to 30%, compared to the average value of the period from 1950 to 1989, which means a reduction of the average annual rainfall of about 5 mm per year, during the time interval in the study;

- determination of a growing trend in the mean maximum and mean minimum temperature. More precisely, based on the analysis of the annual maximum temperature, a positive trend of 0.5 to 1.3 °C every 50 years is evident, to be compared to a different trend of 0.8 to 1.7 °C every 50 years for the minimum, referring to the range from 1950 to 2000.

These results outline a framework of possible climate change on Marche Region, identifiable in a decrease in total annual rainfall and increase in temperatures.

References (existing analyses, national reports, papers, etc.)

1. IMELS (Italian Ministry of Environment, Land and Sea) - "Sixth National Communication under the UN Framework Convention on Climate Change", December 2013
2. IPCC (2007) – Parry M.L., O.F. Canziani, J.P. Palutikof, P.J. van der Linden and C.E. Hanson, Eds., 2007, Climate Change 2007: Impacts, Adaptation and Vulnerability. Contribution of Working Group II to the Fourth Assessment Report of the Intergovernmental Panel on Climate Change, Cambridge University Press, Cambridge, UK, 982pp.
3. EEA (European Environment Agency) (2012b) "Climate change, impacts and vulnerability in Europe, An indicator-based report". EEA Report No 12/2012. Copenhagen: EEA.
4. Portoghese I., Vurro M. and Mariotti A. (2009) "Impatti sul ciclo idrologico e risorse idriche". In Castellari S. and Artale V. (2009). Bononia University Press.
5. Funari E., Martinelli A., Blasi M. F., Carere M., Della Bella V., Mancini L., Marcheggiani S., Mattera F. and Stefanelli M. (2007) "3.1 Water". In Menne B. and Wolf T., 2007. Rome, WHO-APAT.
6. Funari E., Blasi M. F., Carere M., Della Bella V., Mancini L., Marcheggiani S., Mattera F. and Stefanelli M. (2007) "4.3 Flooding and health. In Menne B. and Wolf T., 2007. Rome, WHO-APAT.
7. Bigano A. and Pauli F. (2007) "Dimensioni socio-economiche, costi dell'inazione e strategie di adattamento per l'impatto del cambiamento climatico sul sistema idrogeologico italiano" in Carraro C., 2008. Società editrice il Mulino.
8. IMELS (Italian Ministry of Environment Land and Sea) - Direzione Generale per difesa del suolo (2008) "Il rischio idrogeologico in Italia". Rome: IMELS.
9. Beniston M. (2006) "Climatic change in the Alps: Perspectives and impacts". Proceedings of the "Wengen 2006 Workshop – Adaptation to the Impacts of Climate Change in the European Alps". Organisation for Economic Co-operation and Development (OECD).
10. Lo Porto A. et al. (2007) "Influenza dei cambiamenti climatici sul regime idrologico di due bacini idrografici in ambiente mediterraneo". In Carli B., Cavarretta G., Colacino M., Fuzzi S. (eds) "Clima e Cambiamenti Climatici: Le attività di ricerca del CNR", 577-580. CNR.
11. Macerata Ecology and Climatology Center – Experimental Geophisic Observatory (2002) "Caratterizzazione climatologica della Regione Marche: campo medio della temperatura per il perodo 1950-2000".
12. Macerata Ecology and Climatology Center (2002) "Campo medio della precipitazione annuale e stagionale sulle Marche per il perodo 1950-2000".

Climate and CC on local level – Macerata 30.04.2014

Let's grow up together

DRINK ADRIA

Adriatic IPA
Cross Border Cooperation 2007-2013

The project is co-funded by the European Union,
Instrument for Pre-Accession Assistance

Report:

Climate and climate change change data for the Apulia region (Italy)

Water Research Institute –
National Research Council

(FB3)

Bari, 2014

Let's grow up together

DRINK ADRIA

Adriatic IPA
Cross Border Cooperation 2007-2013

The project is co-funded by the European Union,
Instrument for Pre-Accession Assistance

CONTENT

(This report is prepared by the Water Research Institute of the Italian National Research Council, CNR-IRSA and is partly based on the Sixth National Communication under the UN Framework Convention on Climate Change and the reported references, and partly on other published materials, for which we are grateful)

1. INTRODUCTION

According to international and national studies and publications [1] the Mediterranean region is expected to undergo particularly negative climate change impacts over the next decades, which, combined with the effects of anthropogenic stress on natural resources, make this region one of the most vulnerable areas in Europe. The anticipated negative impacts are mainly related to possible extraordinary heat spells (especially in summer), increased frequency of extreme weather events (heat waves, droughts and severe rainfalls) and reduced annual precipitation and river flow. [2], [3]

Most of the climate-related threats reported here are taken from the ''Sixth National Communication under the UN Framework Convention on Climate Change'' developed by the Italian Ministry for the Environment, Land and Sea in December 2013. In this context, Italy may undergo some expected climate change impacts that would critically affect the following national circumstances, including:

- water resources and areas at risk of desertification;
- coastal areas prone to erosion and flooding and susceptible to alterations of marine
- ecosystems;
- Alpine regions and mountain ecosystems experiencing glacial loss and snow cover loss;
- Areas prone to flood and landslide risk (i.e. hydro-geological risks including the risk of flash floods,flash mud/debris flows, rock falls and other mass movements related to soil and land management) and, in particular, the hydrographical basin of the Po River.

Climate change is likely to magnify the regional differences in terms of quality and availability of natural resources and ecosystems in Europe and also in Italy.

Water resources (in terms of annual precipitation and river discharge) are projected to decrease over Southern Europe, and this regional pattern could intensify in the last decades of this century. The existing conditions of high stress on water resources and of hydro-geologic disturbance in some Italian regions could be exacerbated by projected climate change including: reduced water availability and quality, increases in frequency and intensity of droughts especially in summer, increases in frequency and severity of river summer flows reductions and annual river flow decline and limited groundwater recharge [4].

Hydrogeologic systems

A mapping of the hydrological risk in Italy showed that in 2006: 5.2% of the Italian territory is exposed to the risk of landslides; 4.1% is under risk of flooding and 0.5% is prone to avalanches. [5] According to a more recent (dated 2008) assessment [6] 9.8% of the Italian territory is characterized by the highest level of hydro-geological criticality (that represents the states of “high” and “very high” risk and danger), of which 6.8% include areas with exposed properties (urban centres, infrastructures, industrial areas, etc.).

Climate change impacts on the Italian hydro-geological system include:

- variations in the hydrologic regime related to e.g.: progressive melting of the glaciers and reduction of seasonal snow cover in Alpine catchments, due to rising temperatures and changing precipitation patterns;
- increase in the aridity of soils and in the frequency of drought events in the plain areas;
- changes in groundwater resources, related to SLR resulting in increased saltwater intrusion in coastal aquifers, accompanied by limited capacity of beach nourishment due to the lower river sediment transport (induced by reduced rivers medium ratings because of decreased precipitation but also by man-made dam works and withdrawals);
- higher risk of inland flooding, due to increased events of river flood heights in relation to heavy precipitation events; [3]
- increased winter run-off by 90% and decreased summer run-off by 45% in central Europe Alpine rivers, [7] with consequent greater risk of flooding and drought respectively;
- significant changes in the hydrologic balance (and water quality) of some studied river basins (Rio Mulargia in Sardegna and Alento river in Campania), [8] with an estimated reduction in annual discharge as well as nutrients and sediments transport in the next decades;
- increased risk of flash mud/debris flows, due to a potential increase of extreme weather events;
- increased risk of landslides in the Alps, due to temperature warming and ice melting; risk of rock falls in the Apennines, because of possible more frequent and sudden temperature changes, especially in winter; risk of flash floods in both areas, due to severe precipitation events.

The areas most exposed to the hydro-geological risk include: the hydrographical basin of the Po River, subject to increased flood risk, the Alpine and Apennine areas, subject to increased flash flood risk.

Drought and desertification

About one third of the country is vulnerable to varying degrees to the processes of land degradation. A classification of the vulnerability of the Italian territory to land degradation and desertification, based on the Environmentally Sensitive Area Index (ESAI) showed that (in 2000) Sicilia was affected by a regional medium-high degree of environmental vulnerability (sensitive areas represented about 70% of the regional territory), followed by Molise (58%), Apulia (57%) and Basilicata (55%). Six regions (Sardegna, Marche, Emilia-Romagna, Umbria, Abruzzo and Campania) had similar conditions (between 30% and 50%); for seven other regions (Calabria, Toscana, Friuli-Venezia-Giulia, Lazio, Lombardia, Veneto and Piemonte) sensitive areas represented between 10% and 25%, while in three regions (Liguria, Valle d'Aosta and Trentino Alto Adige) the percentages were fairly small (2% - 6%).

More recent studies show the sensitivity to desertification and drought of the Italian territory based on the Sensitivity to Desertification Index (SDI), which considers soil quality, climate and vegetation parameters. The gradual worsening of desertification trends, already observed

in the whole country, can be accelerated from climate change by increasing the actions of erosion, salinization, loss of organic matter and drying up of soil.85 About 30% of the Italian territory can be considered at risk of desertification, with the key vulnerabilities located in the South. Furthermore, especially vulnerable areas are farmlands with intensive and marginal production, areas at risk of accelerated erosion (e.g. coastal areas), areas damaged by contamination, pollution and fires, and fallow and abandoned lands.

Severe indirect socio-economic impacts of this desertification process may follow, including: decline in agriculture and tourism productivity, growing unemployment in rural areas with consequent migration, conflicts over water uses, harm to properties and people, due to increased frequency of fires, overall biodiversity loss. [9], [10]

Water quantity and quality

Water quantity/availability and quality in Italy could be affected by [4], [11]:

- reduced water availability, especially in summer;
- increased water stress;
- severe negative impacts in the South, where vegetation and territory are already experiencing a marginal water supply regime;
- increased seasonal water deficit due to significant pressures of summer tourism peaks in small Italian islands;
- potential increased conflicts among multiple uses of water resources.

2. ADOPTED METHODOLOGY FOR CLIMATE CHANGE EVALUATION AND IMPACT ASSESSMENT

One of the goals of achieved within the CIRCE FP6 Research Project (No. 036961) was to define a methodology for the use of climate change information in water resources evaluations suitable for Mediterranean environments. In particular, this topic was developed by the IRSA-CNR and was focused on the Apulia region, a semi-arid region of Southern Italy, with regard to its water resources.

When considering the impacts of global climate change on fresh water the focus is primarily on environmental responses at the local and regional scale, taking into account the roles of the mesoscale features, orography, land–sea interaction and regional mechanisms characterizing local climate (Fig. 1).

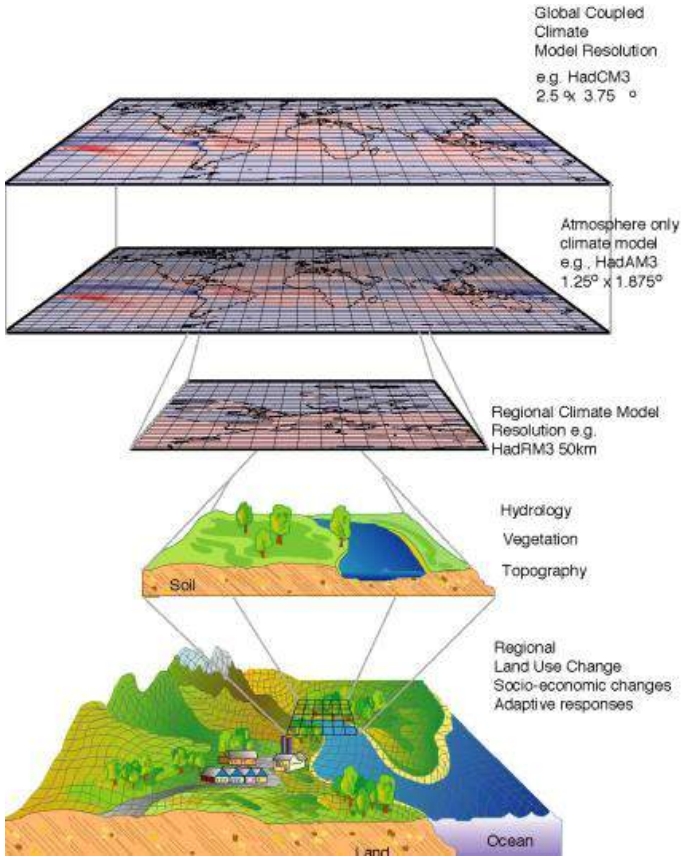

Figure 0 Scales of investigation in the model's chain (from MetOffice).

The study of global climate change effects on hydrological system requires climate scenarios as input to impact models. The projection of future climate depends partly on the assumptions made about future population or economic growth based on the future development paths in various sectors such as energy [12] and on the estimate of greenhouse gases emissions. Currently, climate projections for the 21th century are based on simulations from coupled atmospheric-ocean general circulation model (AOGCM) of the global climate system as response to changes in anthropogenic forcing [13], [14]. However, outputs from GCMs are generally not sufficient enough to feed impact models because of the limited representation of mesoscale atmospheric processes, topography and land-sea distribution in GCMs [15], [16]. While the climate evolution at synoptic-scale (10^4-10^6 km^2) is well reproduced by most GCMs, the climate change experiments are not adequate to asses the effects of climate alterations on land-surface processes at regional and local scale. In particular for the precipitation fields, the gap between GCM scale (grid-point area) and that usually needed in impact studies, leads to inconsistencies in frequency statistics, such as the exceedance of a threshold for heavy precipitation [17], and to insufficient reproduction of observed spatial patterns [18] and daily variability [19]. So that, the sub-grid scale processes are treated in GCMs by using empirical parameterizations, which describe processes (i.e. precipitation) as functions of the state variables (temperature and relative humidity) using semi-empirical equations [20].

A more realistic representation of sub-grid weather system is obtained by introducing regional climate models (RCMs) in the climate modelling chain. This procedure of regionalization, well known as dynamical downscaling [21], [22] allows to obtain high-resolution models (in order of tens kilometres) able to describe sub-grid detail such as topography, land cover patterns or coastline. Despite RCMs have improved climate

information, these models do not yet provide climate scenarios directly usable in impacts models. In fact, it is well known that RCMs simulations are affected by errors due both to their own dynamics and to those of the global model that provide the boundary conditions and only increasing the resolution itself does not ensure more realistic regional climate scenarios [23]. Further, considerable uncertainty is due to the variability in internal parameterizations [24]. Particularly, the precipitation estimates still not replicate observed precipitation amounts from rain-gauges stations, and larger errors are found in daily precipitation statistics, such as wet-day frequency, precipitation intensity, and quantiles of the frequency distribution. In particular, the simulation of too dry summer conditions represent a problem for the climate models in Mediterranean region as pointed out by Frei et al. [25].

Climate change impact on hydrological system can be evaluated using the following equation as the difference between the outputs of a hydrological model (Out) under climate change conditions S (from climate model) and under current climate conditions R (from observations or control run simulations of climate models):

$$Impact = Out(S) - Out(R)$$

In the most general terms, the impact assessment of climate change on water resources involves the following stages, as in Arnell and co-authors [26]:

1. To define a hydrological model which converts climatic inputs into hydrological response, and calibrate under the current climatic conditions;
2. To create a 'perturbed' climatic time series, representing the climate under the defined scenario;
3. To run the model with the perturbed climate inputs, and compare hydrological outputs under the perturbed climate with those under the current climate.

Depending on the investigation scale, different hydrologic impact approaches of climate change are identified in literature as reviewed by Xu and Singh [27]. These include the use of direct GCM-derived hydrological output, the method of coupling GCMs and macroscale hydrologic models (MHMs), the use of dynamic downscaling, the use of statistical downscaling and the use of hypothetical scenarios as input to hydrological models.

To simulate the flow regime of small to median sized catchments a statistical downscaling method [28], [29] to link GCM raw output to hydrological models is required. The main purpose of these techniques is to solve the mismatch between GCM performance and the needs of regional or local scale impact assessment. So that, an integrated approach in hydrological impact assessment of climate change at regional and local scale includes the uses of:

- climate models which simulate climatic effects of increasing atmospheric concentration of greenhouse gases;
- hydrological models at basin scale which simulate hydrological impacts of changing climate;
- statistical downscaling techniques which link climate models and application-scale hydrological models.

The methodology developed in the CIRCE Project, based on the approach proposed by Frederick and Gleick [30], includes the followiong steps:

1. Using GCM to simulate future climate conditions on a global scale;
2. Using RCM to simulate future climate conditions on a regional scale;
3. Re-scaling regional climate simulations down to a local scale (downscaling approach);
4. Develop hydrologic model applications adopting downscaled RCM data to simulate hydrological processes under altered climate conditions.

In particular, the methodology was applied on a semi-arid region of Southern Italy (Apulia) which is exposed to frequent and prolonged drought events. The analysis of climate change effects was performed focusing on the water balance of the main hydrological systems of the region. In this report, the analysis of climate change data developed by the IRSA-CNR in the Circe Project [31] is presented in short.

2. CLIMATE CHANGE ANALYSIS

In this section, results on local assessment and bias correction of climate simulations obtained from a state of the art RCM against ground based observation of climate variables are presented with regad to the Apulia region. The methodology for the local projection of RCM control simulations and scenarios is based on a quantile variable correction supported by an incremental assessment. This methodology was applied to both dynamical (temperature) and non-dynamical fields (precipitation) of climatic variables supplied by the PROTHEUS RCM [32] adopting a spatial scale which is consistent with that of a mesoscale hydrological basin (of the order of 10^3 km^2). Monthly point observations from 1951 to 2001 are used as reference data set.

The distribution of temperature and precipitation in a pair of RCM PROTHEUS simulations covering the end of 20th (past scenario) and first half of the 21st (future scenario) centuries were examined. A control dataset was then necessary so that the statistical downscaling of the output of a high resolution climate model will preserve the space-time dynamics of the GCM projections. In fact, as the stationarity hypothesis will fail due to substantial change in Earth's climate affecting meteorological variables both in term of mean and distribution, a direct statistical downscaling of future scenario based on station observations has to be avoided. Oppositely, a RCM simulation obtained with more realistic boundary conditions (as the ERA-40 reanalysis) combined with a long term time series of local observation used as reference (truth), can be used to characterise and isolate the RCM systematic bias. Such a bias can be filtered out with statistical methods based on probability of occurrences (as the quantiles comparison) though preserving time-space dynamics of future climate scenarios [33].

From the RCM simulation 37 nodes were selected as representative of the entire region (Fig. 2). These nodes and the corresponding regions of interest were associated by proximity rules

to the corresponding weather stations scattered throughout the study area. Monthly means of daily maximum and minimum temperature as well as monthly rainfall totals were considered from a sub-set of the available gauge stations characterized by a low amount of missing data. Concerning the reference period corresponding to the second half of the 20th Century, 82 temperature stations and 111 rainfall gauge stations were selected in the available data set. The data coverage was slightly different between the chosen atmospheric variables with maximum and minimum temperature covering the period 1951-1994 while rainfall records were considered for the period 1951-2001. The location map of temperature and precipitation sampling station are referred with black stars in Fig. 2, while the RCM nodes are referred with grey circles.

Monthly observations are used here to determine month-by-month quantiles of the reference period. In study case, all weather stations with less than 20% of missing data were retained. An undoubted advantage of the quantile method is that some missing data do not affect the overall estimation.

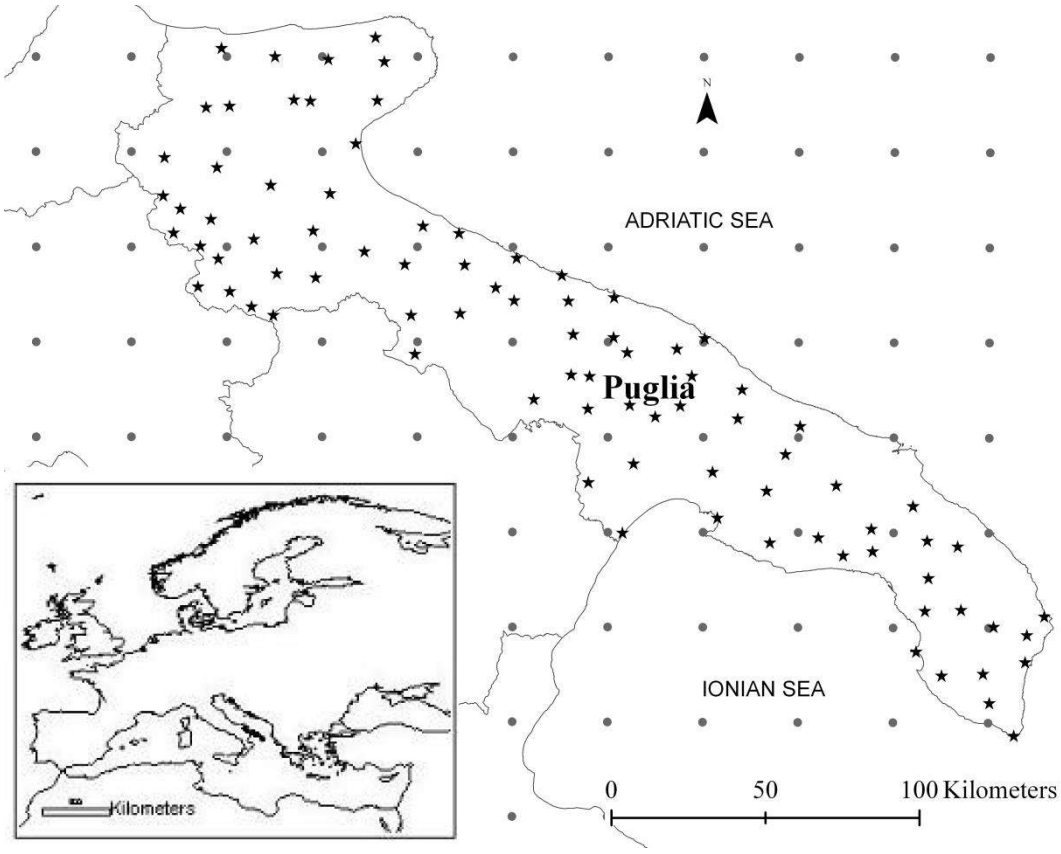

Figure 2. The Apulia case study with precipitation and temperature land measurement network (black stars) and RCM nodes (grey circles).

Focusing on physical phenomena, the hydrological regimes characterizing both surface and groundwater resources are the outcome of the complex interactions between climate, landscape geo-morphology, and soil-vegetation continuum, controlling the hydrological response across scales (from the hill slope to the regional scale). An overview of the case

study landscape pattern complexity at the RCM node scale is present in Fig. 3 through the topography and land use intra-node variability of the PROTHEUS nodes in the Apulia region.

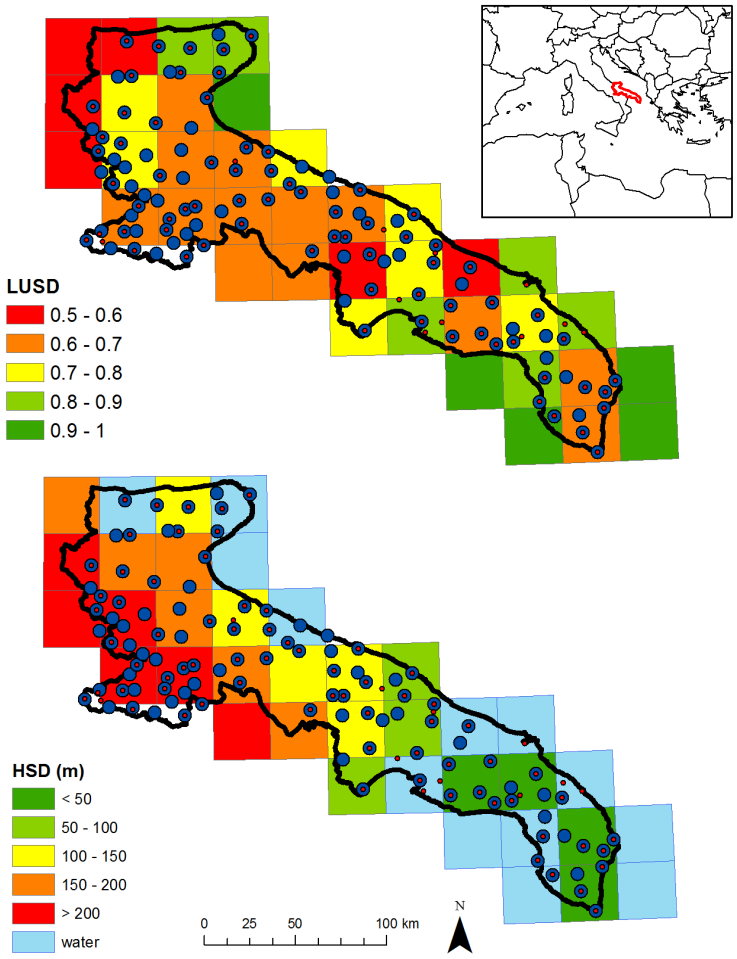

Figure 3. Land use (LUSD) and topography (HSD) intra-node variability for PROTEHUS RCM nodes in the Apulia region; Blue and Red full circle presenting respectively precipitation and temperature land measurement network.

The intra-node variability of topography represents the standard deviation of altitudes (HSD) between each model node can be used as index to know the altitudinal changes across a region. To monitor the spatial heterogeneity we define the land use intra-node variability (LUSD) at RCM scale as the ratio of the cumulated surface of most representative land use and the total surface inside the node Region Of Interest (ROI). Differences in LUSD can have an impact on relative humidity and evapotranspiration due to presence of water, soil moisture and vegetation cover, also impacting parametric variables such as precipitation and cloud cover [34]. The HSD was created from a high resolution Digital Elevation Model scale. The LUSD has been computed using the ratio of the surface of most representative land use classes of Corine Land Cover 2000 level 3 and the total surface inside the node region of interest. Figure 3 shows a high orographic complexity in the north-west of the region decreasing towards south-east. Further complexity is due to the substantial lack of measurements regarding the hydrological processes in the region. Only about 15 % of its extent has been regularly monitored for the stream flow, while in the rest of the region groundwater table measurements are discontinuous in space and time.

The assessment of the statistical downscaling is presented both in terms of time series (averaging the spatial heterogeneity distribution) and maps integrating the dynamic of monthly variability of rainfall at spatial scales of the RCM and the REF observations. Similarly, the assessment of the impact of DSC on the atmospheric variables is presented both in terms of time series averaging the spatial heterogeneity distribution and maps presenting the impact of statistical downscaling on scenario's trends. Finally, in order to illustrate result of the applied methodology, the monthly mean differences of temperature and precipitation between future and past scenarios after DSC at the available observation station grid scale were presented.

The statistical downscaling was done through the comparison of land control measurements (REF) and dynamical downscaled control simulations (PROTHEUS RCM forced by the ERA-40). To assess the performance of downscaling procedure a further comparison of REF and RCM after the DSC (RCM-DSC). Figure 4, 5 and 6 present the yearly mean of daily minimum, maximum temperature and cumulated precipitation for the overall Apulia, respectively. In order to underling the variance connected with the spatial heterogeneity, the 5^{th}, 25^{th}, 75^{th} and 95^{th} percentile was associated to the relevant mean values (50^{th} percentile) both REF and control simulations (RCM and RCM-DSC).

As regards the daily minimum temperature (Fig. 4b) the DSC allows correcting the mean bias (defined as the mean signed difference) over the whole case study between control simulation and observation from -0.4°C to 0.06 °C and reducing associated the Root Mean Square Error (RMSE) from 0.47°C to 0.35°C. Moreover, the fit of the 25^{th} and 75^{th} percentile was significantly improved both in terms of mean biases (corrected from -0.61°C to 0.37°C and from -0.80°C to -0.19°C, respectively) and RMES (corrected from 0.63°C to 0.44°C and from 0.81°C to 0.42°C, respectively), demonstrating a better fit to the case study spatial heterogeneity. The fit of extreme values of the yearly means spatial distribution, illustrated by the 5^{th} and 95^{th} percentile remain slightly unchanged: the upper limit mean bias is reduced from 1.07°C to -0.61°C and for associated RMSE from 1.08°C to 0.76°C; the lower limit present similar improvements in terms of both mean biases (from 0.58°C to 0.36°C) and associated RMSE. (from 0.63°C to 0.48°C).

With regard to the daily maximum temperature (Fig. 5), the mean bias remains unchanged due to the high performance of the PROTHEUS RCM for this variable (from -0.04 °C to 0.06 °C), while the RMSE is reduced from 0.52°C to 0.39°C. Moreover, the estimation of the spatial heterogeneity is improved considering the 5^{th}, 75^{th} and 95^{th} percentile distribution both in terms of mean (from 2.17°C, -0.35°C and -0.95°C to 0.46°C, -0.17°C and -0.75°C respectively) and RMSE (from 2.17°C, 0.71°C and 1.08°C to 0.71°C, 0.54°C and -0.86°C respectively).

Finally, for annual precipitation (Fig. 6a) a general overestimation of *RCM* as regards REF of 25 mm y^{-1} was observed, after the DSC the mean bias is reduced at 0.7 mm y^{-1} (Fig. 6b). Meanwhile the associated RMSE has been slightly reduced from 92.7 to 84.2 mm y^{-1}, while the whole spatial heterogeneity has been considerably improved even for the extreme values. In fact the 5^{th}, 25^{th}, 75^{th} and 95^{th} percentile associated mean biases were reduced from 39.5, 68.3, 20.0 and -99.3 mm y^{-1} to 12.5, 7.3, 2.5 and -21.6 mm y^{-1}. The reduction of the associated

RMSE was significant only for 25th and 95th percentile (from 101.3 and 155.2 to 75.1 and 131.7 mm y^{-1}, respectively) while unchanged for 5th and 75th percentile (from 74.4 and 100.8 to 72.4 and 97.8 mm y^{-1}, respectively).

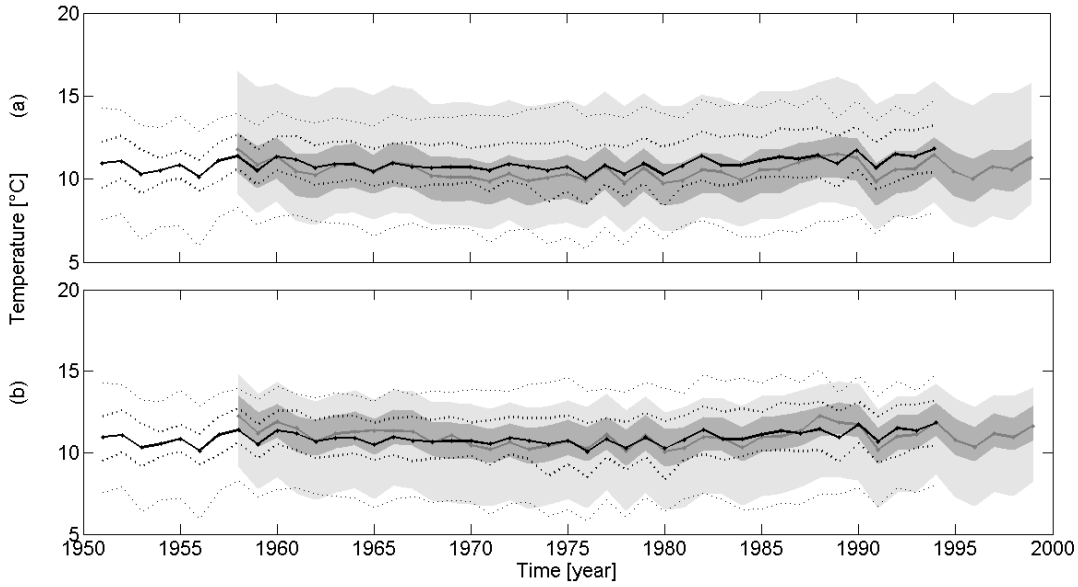

Figure 4 Yearly mean of daily minimum temperature for the overall Apulia before (a) and after (b) the statistical downscaling (DSC). In both graphs the black full line represents the reference series (REF) (land control measurements) and associated percentile at 5th and 95th, and 25th and 75th are indicated with a black dot lines. The grey full lines show the control simulations e.g. RCM (a) and RCM-DSC (b), while associated percentile at 5th and 95th, 25th and 75th are indicated with grey areas (lighter and darker, respectively).

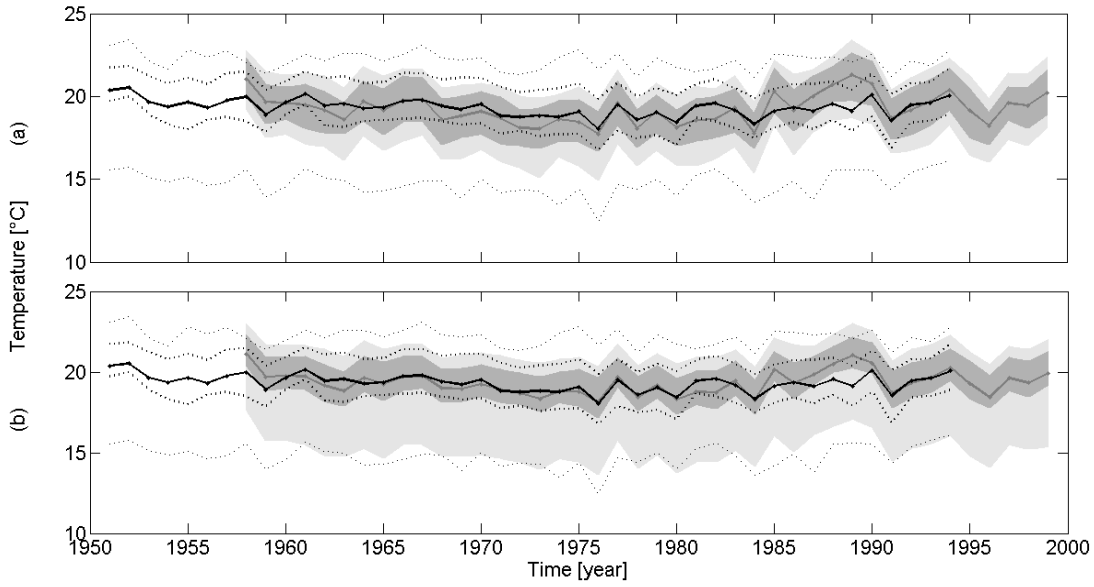

Figure 5 Yearly mean of daily maximum temperature for the overall Apulia Region before (a) and after (b) the statistical downscaling (DSC). Further details are provided in Fig. 4.23

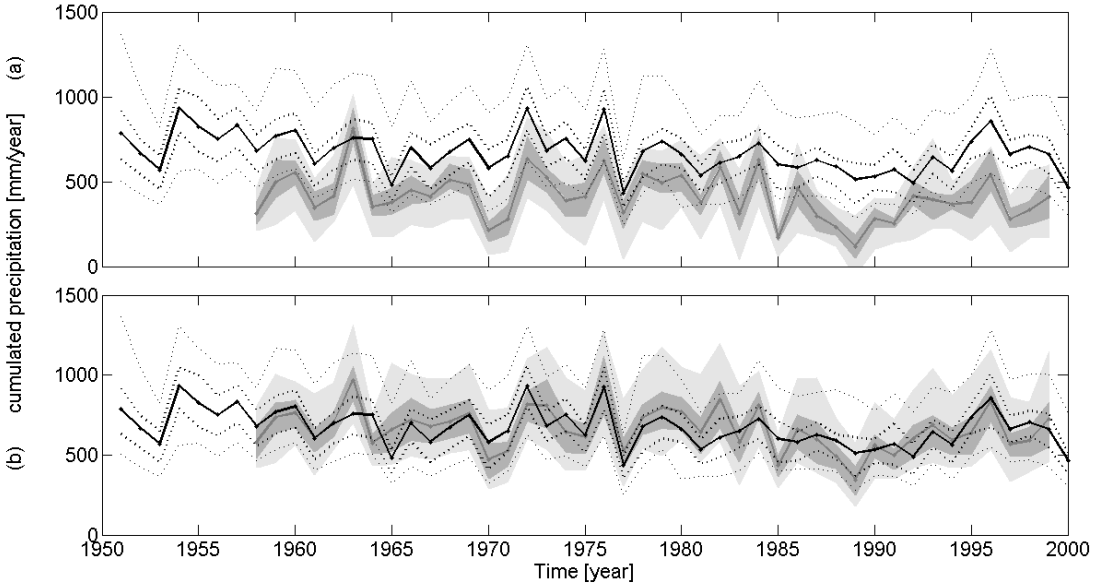

Figure 6 Yearly mean of precipitation for the overall Apulia Region before (a) and after (b) the statistical downscaling (DSC). Further details are provided in Fig. 4.23.

Figures 7 and 8 aim to examine the benefits of the DSC as regards as the spatial and temporal scale suitable to feed hydrological models applied to impact studies. In particular these figures show the comparison, at monthly scale, between REF and control simulations according to the RCM resolution output (Fig. 7) and according to the Thiessen polygons of the land control measurements (RCM-DSC) (Fig. 8). This analysis was performed for all variables considered previously, but here only the results for precipitation are shown because of their larger relevance in impact studies and a more complex dynamic. As a misfit indicator of the monthly mean dynamic over the last 50 years, monthly standard deviation (STD) differences between control simulations and REF was used. In Table 1 monthly reference and control simulations mean values of over the whole case study are shown. Figure 7 presents a large spatial variation of the STD differences across different months.

From July to January, the monthly variability is generally underestimated by the RCM, meanwhile the spring one (April, May and June) is mainly overestimated. The Apulia Region does not present a spatial homogeneity across different months, even if the central part of the case study is better represented. On the contrary Figure 8 presents a larger spatial coherence, together with a whole better fit after DSC. May is the unique month presenting a general overestimation, while during the summer an underestimation was evaluated.

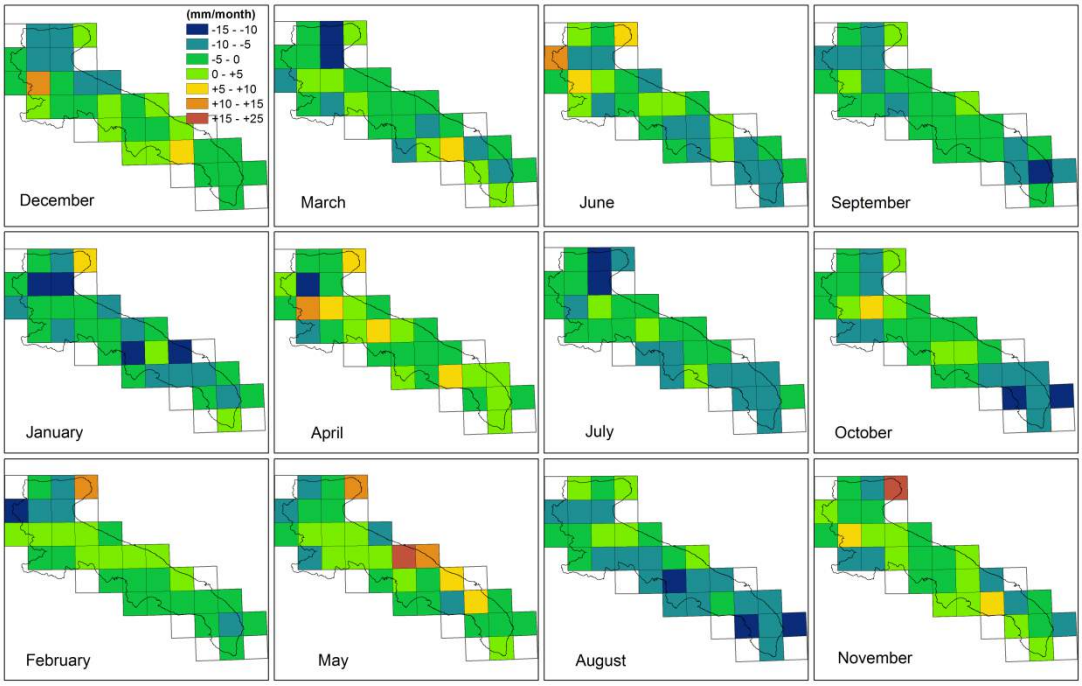

Figure 7 Monthly standard deviation (STD) differences (1958-1999) between control simulation and reference (REF) according to the RCM resolution output.

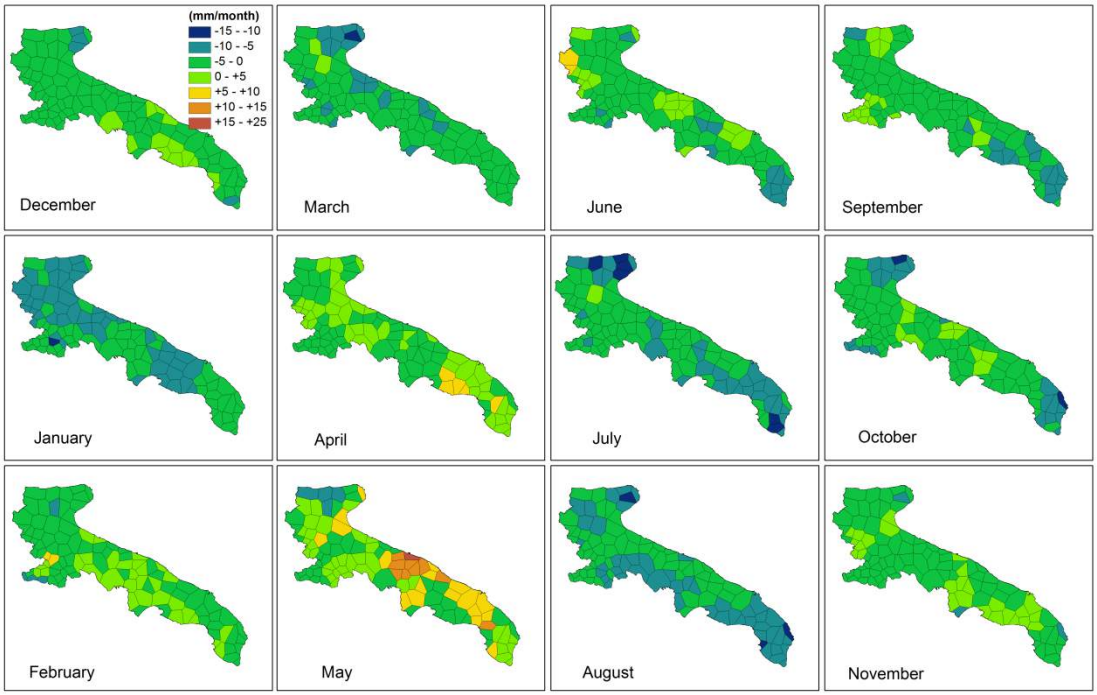

Figure 8 Monthly standard deviation (STD) differences (1958-1999) between control simulation (RCM-DSC) and reference (REF) according to the Thiessen polygons of the land control measurements.

According to the proposed methodological framework, impact study can be done through the comparison between future and past scenarios at each step of the data flow. Impact study performances become more accurate according to the improvement of scenarios performances along the downscaling process, reaching temporal and spatial scales more and more detailed.

Figure 9, 10 and 11 present the comparison between reference (REF) and the scenario simulations integrating the bias introduced by the GCM. The aim of this step is to point out the benefit produced by the DSC on the impact study comparing the goodness of fit between (GCM-RCM*)* vs REF and (*GCM-RCM-DSC)* vs *REF*. Past and future scenarios in term of annual mean of daily minimum and maximum temperature and precipitation are presented. Similarly to figure 4, 5 and 6, the spatial heterogeneity is evaluated through the 5th, 25th, 75th and 95th associated percentile.

Figure 9 shows goodness of fit for the daily minimum temperature. The overall mean bias along all analysed period between REF and (*GCM-RCM)* is -0.36 °C (Fig. 9a), after the *DSC* has been cancelled (-0.02 °C) (Fig. 9b), meanwhile the associated RMSE remains unchanged (from 0.59°C to 0.56 °C). Similar results are obtained for the 5th, 25th, 75th and 95th percentile, with a significant reduction of mean biases (from 0.60, -0.61, -0.63 and 0.98°C to 0.32, 0.29, -0.22 and -0.56 °C, respectively), and a relatively low impact on the associated RMSE (from 0.76, 0.84, 0.72 and 1.06°C to 0.73, 0.67, 0.54 and 0.78 °C, respectively).

By analysing daily maximum temperature similar results were found (Fig. 10). The atmospheric parameters obtained from the GCM-RCM are characterized by a general underestimation of the spatial heterogeneity. After the DSC the mean bias was almost removed (from -0.27 to 0.03°C) and the associated RMSE reduced from 0.92 to 0.77°C. Even the 25th and 75th percentile were better represented after DSC both in terms of mean bias (reduced from -0.44 and -0.59°C to 0.25 and -0.30°C, respectively) and the RMSE (reduced from 1.01 and 1.01°C to 0.85 and 0.74°C, respectively). However the major bias reductions was obtained on the 5th and 95th percentile (reduced from 1.91 and -1.34°C to 0.36 and -0.80°C, respectively) combined with a significant improvement of RMSE (reduced from 1.99 and 1.44°C to 0.96 and 1.00°C, respectively)

Finally, the mean bias of the annual precipitation for the GCM-RCM shows an overestimation (23 mm y^{-1}) (Fig. 11a), after the *DSC* the mean bias was reduced to -1.6 mm y^{-1}(Fig. 11b), meanwhile the associated RMSE remains unchanged (from 144.7 to 140.3 mm y^{-1}, respectively). The limits of the DSC in adjusting the (*GCM-RCM*) time dynamic was confirmed by the low reduction of the RMSE for the 5th, 25th, 75th and 95th percentile (reduced from 121.1, 148.7, 164.6 and 199.8 mm y^{-1}to 120.4, 128.2, 151.7 and 176.1 mm y^{-1}, respectively) even if the associated mean biases were significantly reduced (from 59.3, 66.6, 12.7 and -89.5 mm y^{-1}to 16.0, 7.1, -4.1 and -8.3 mm y^{-1}, respectively).

For the all three considered variables (Figures 9, 10 and 11), the impact of the DSC on the future scenario is similar to the impact on the past simulation both in terms of mean values and spatial heterogeneity. The daily minimum and maximum temperature was increased on average over the whole case study and the spatial range of values was slightly reduced for both 25th and 75th percentile. In the case of daily minima, the lowest percentile of the distribution (5th percentile) was extended by the DSC meanwhile the highest percentile (95th percentile) was significantly reduced (Fig. 9b). Concerning the daily maxima, both the upper and lower percentiles was extended, with a marked offset impact on the 5th percentile (Fig. 10b). Finally, the cumulated precipitation was slightly reduced over the whole case study,

with an increased spatial variability, mainly concerning the upper limit of the percentile distribution (95th percentile) (Fig. 11b).

Additional statistics about monthly mean values for both precipitation and temperature (regarding reference data sets, past simulation and future scenario) were summarized in Table 1 for the whole case study before and after the DSC application.

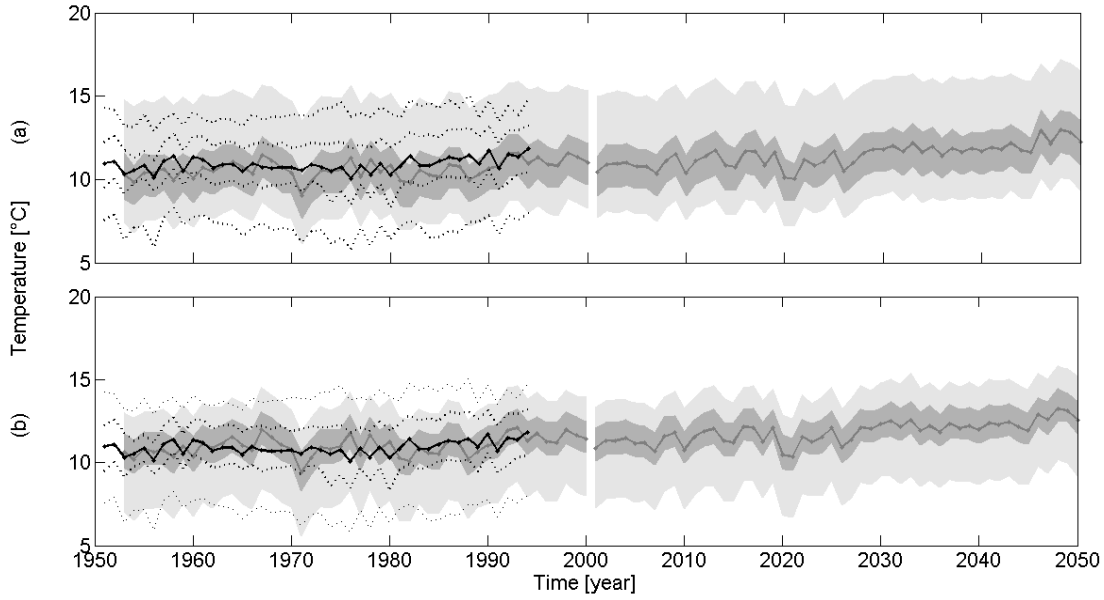

Figure 9 Yearly mean of daily minimum temperature in past and future scenarios for the overall Apulia Region before (a) and after (b) the statistical downscaling (DSC). In both graphs the black full line represents the reference series (REF) (land control measurements) and associated percentile at 5th and 95th, and 25th and 75th are indicated with a black dot lines. The grey full lines show the control simulations e.g. GCM-RCM (a) and GCM-RCM-DSC (b), while associated percentile at 5th and 95th, 25th and 75th are indicated with grey areas (lighter and darker, respectively).

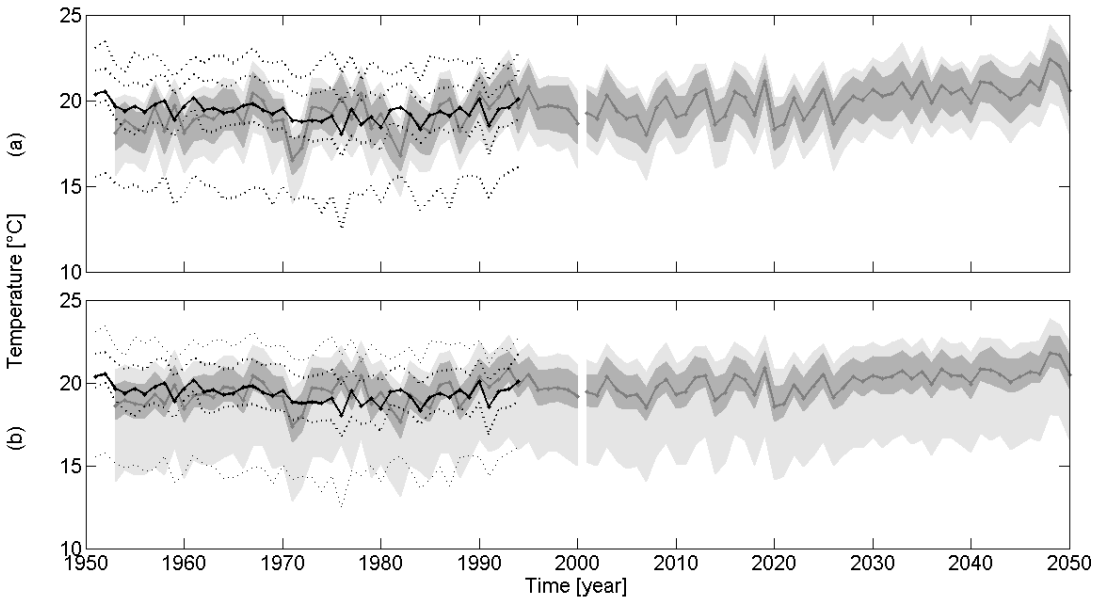

Figure 10 Yearly mean of daily maximum temperature for the overall Apulia Region before (a) and after (b) the statistical downscaling (DSC). Further details are provided in Fig. 9.

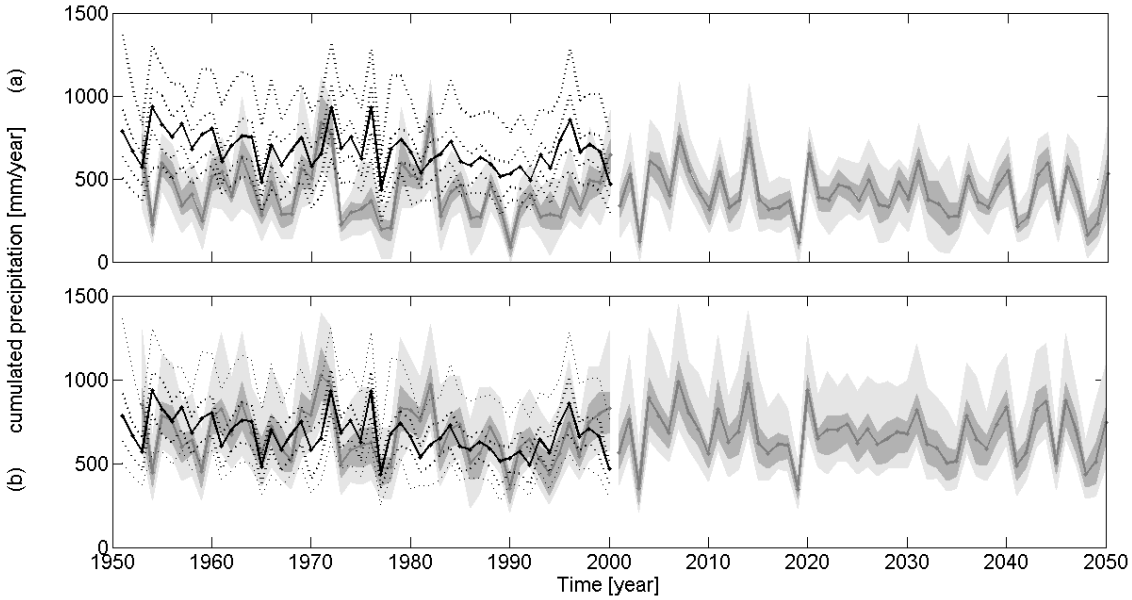

Figure 11 Yearly mean of precipitation for the overall Apulia Region before (a) and after (b) the statistical downscaling (DSC). Further details are provided in Fig. 9.

The impact of the statistical downscaling on the scenario spatial heterogeneity was detailed. In Figure 12 trend differences (or acceleration) between future and past scenarios, for daily minimum and maximum temperature and for cumulated precipitation, before and after DSC were shown. As highlighted by the results in Figure 9 and 10, the spatial variation of both daily minimum and maximum temperature was enhanced by the statistical downscaling. Focusing on daily minimum temperature acceleration, the whole case study present a relative homogeneity before DSC (Fig. 12a), with trend differences ranged between 0 and -0.01 °C/yr. This result indicates that increase of minimum temperature on the 2001-2050 period slows down homogeneously in comparison with 1970-2000 period. In Table 1 absolute trends values of both scenarios before and after DSC were shown. After DSC (Fig. 12b), the daily minimum temperature trend differences was globally higher (in absolute value) and was presented an higher heterogeneity, with trends ranged between 0 and -0.015 °C/yr. Oppositely, the daily maximum temperature presents trends differences globally lower (in absolute value) after DSC (Fig. 12b) than before (Fig. 12c) together with a higher spatial variability but a lower range of values. Note that the RCM nodes (Fig. 12a and 12c) or stations (Fig. 12b and 12d) presenting the highest acceleration are not systematically the same between daily minimum and maximum temperature.

The annual cumulated precipitation trends present a better spatial correlation between GCM-RCM results (Fig. 12e) and *GCM-RCM-DSC* results (Fig. 12f). Moreover, the range of values remains mostly unchanged. Precipitation decrease slows down in most of the case study at rate ranged between 0 and 0.4 mm/yr, similar or higher than absolute trends. In Table 1 the absolute trend values of both scenarios before and after DSC were shown. The tendency is inversed far from the cost with a decreasing in the precipitation acceleration.

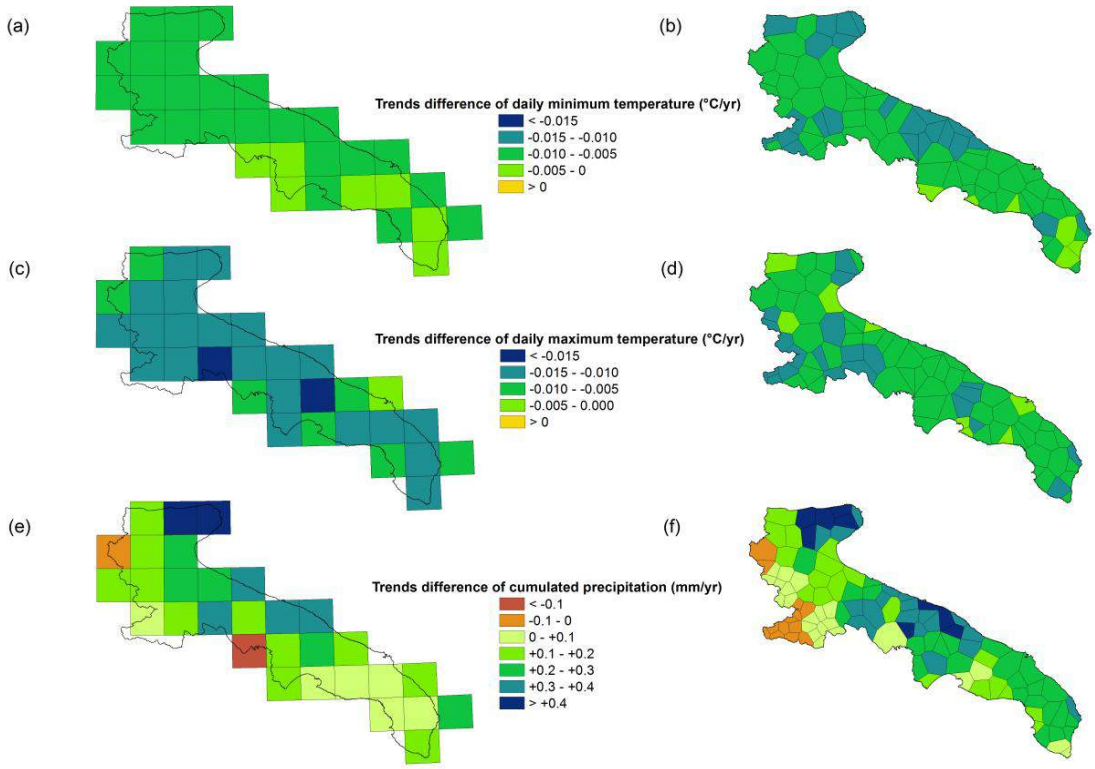

Figure 12 Acceleration between future and past scenarios before and after DSC for daily minimum temperature (respectively (a) and (b)), daily maximum temperature (respectively (c) and (d)) and cumulated precipitation (respectively (e) and (f))

As a result of the downscaling processes, differences between future and past scenarios of the daily minimum and maximum temperature monthly means (Fig. 13 and 14, respectively), and the means of monthly cumulated precipitation (Fig. 15) were presented. This study is supported by the previous assessment of *RCM*, *RES-DSC* system, *GCM-RCM* system and *GCM-RCM-DSC* system.

In Figure 13 results of daily minimum temperature were shown. Differences of monthly means between future and past scenarios over the whole period (1953-2000 and 2001-2050, respectively) were considered. Temperature increasing concerned mostly the period ranged between early spring and late autumn (from April to October) with a maximum in October. The maximum of spatial heterogeneity was found on the same period, with value ranging from 0.5 to 2.6°C. From November to March, a homogeneous increasing (below 1°C) of minimum temperature over the whole region were resulted.

Similar results for monthly means of daily maximum temperature (Fig. 14) were found. A temperature increasing concerned mostly the period comprise between early spring and late autumn (from April to November) with a maximum in September. The maximum of spatial heterogeneity occurs on the same period, with value ranging from 0.5 to 2.1°C (maximum in August). From December to March, an homogeneous increasing (below 1°C) of minimum temperature over the whole region was found.

Finally, in Figure 15 the mean differences of the monthly cumulated precipitation were shown. Precipitation presents heterogeneity globally higher than temperature. Contrarily to minimum and maximum temperature which globally continues to increase during the future scenario (Fig. 13, 14) even if associated trends globally decrease (Fig. 12), the global trend of decreasing precipitation is not confirmed over the whole case study. In fact, in October, precipitation increases between 10 and 20 mm/month at the south of the region and between 5 and 10 mm/month at north, meanwhile oppositely in December maximum increase is concentrated at the north of the region with a maximum of 36 mm/month. During January, February, March, May June and August precipitation are stable in confront with the past scenario, with value ranging between -5 and + 5 mm/month over mostly the whole case study. In January, March and June, a minority of stations present a major decreases, with value ranging from -5 to -10 mm/month. Finally, April, July and September at north and November at south presents a global decrease of precipitation, with a maximum of -21 mm/month in July.

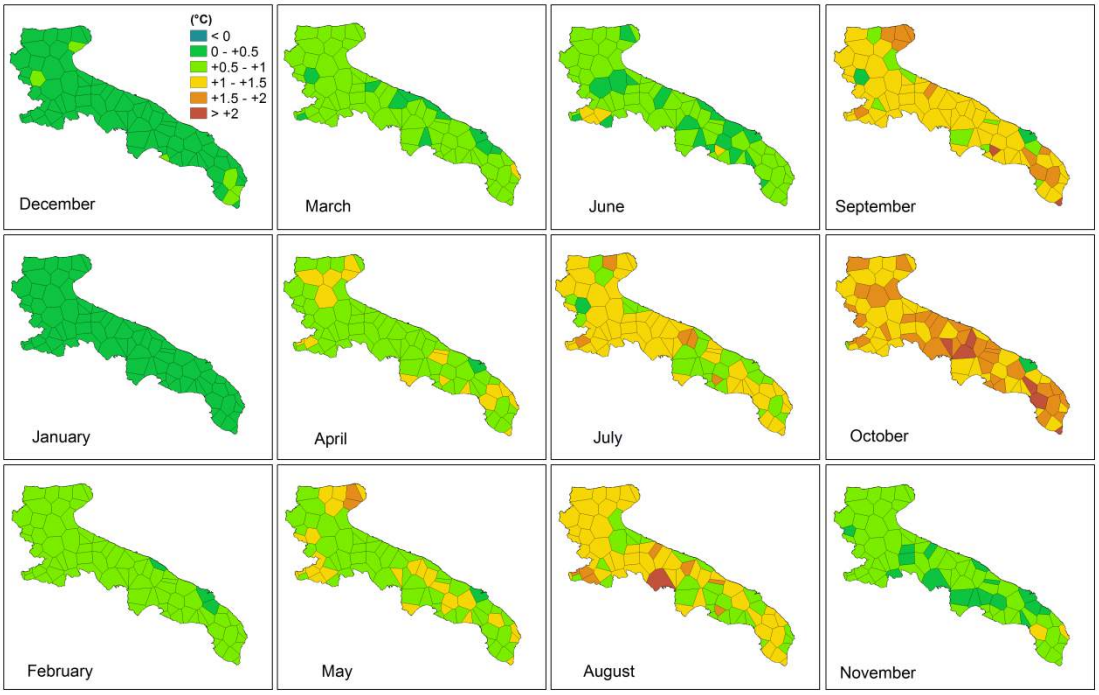

Figure 13 Daily minimum temperature difference between future and past scenarios after both dynamical (RCM) and statistical (DSC) downscaling. Results are presented for monthly means over the whole period (respectively 1953-2000 e 2001-2050)

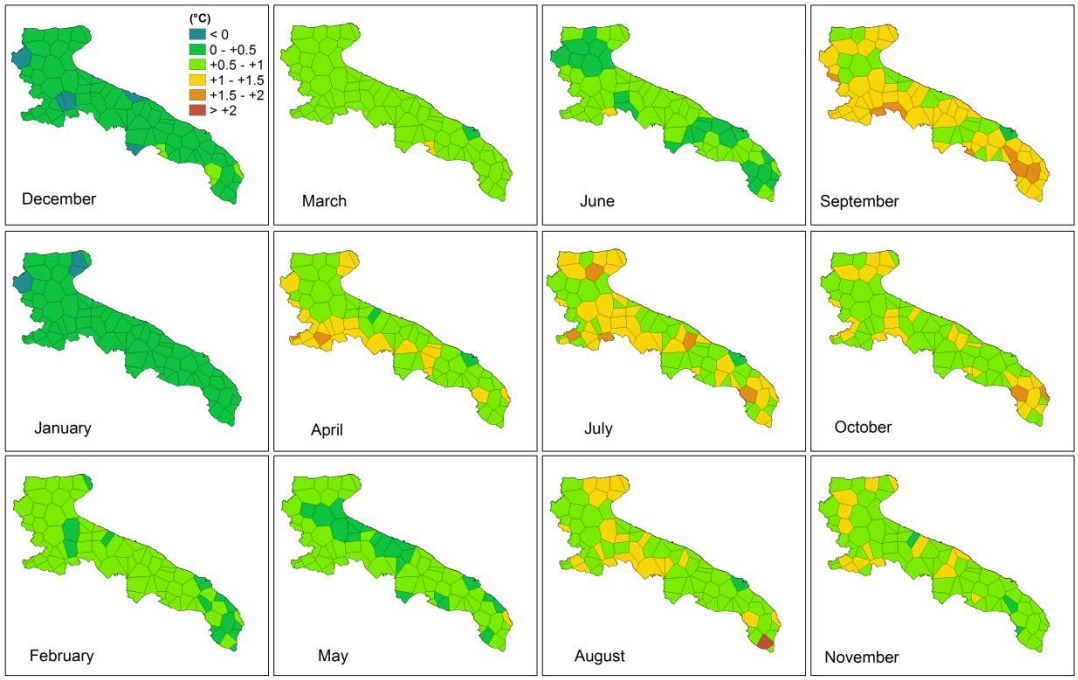

Figure 14 Daily maximum temperature difference between future and past scenarios after both dynamical (RCM) and statistical (DSC) downscaling. Further details are provided in Fig. 13.

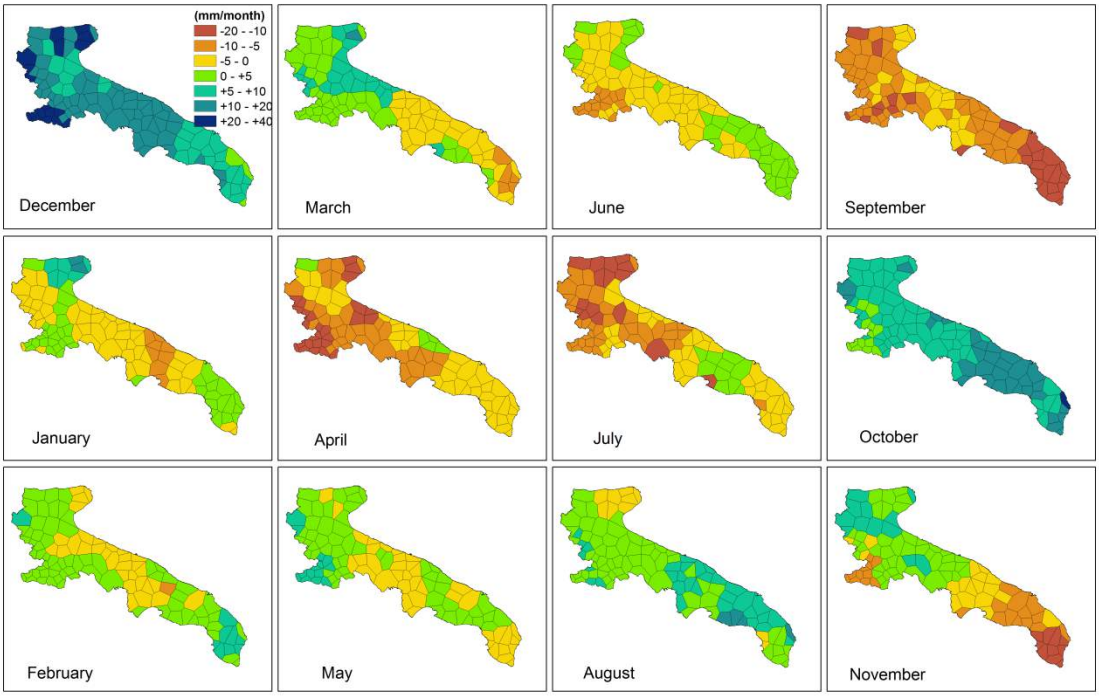

Figure 15 Total precipitation difference between future and past scenarios after both dynamical (RCM) and statistical (DSC) downscaling. Results are presented for monthly cumulated means over the whole period (respectively 1953-2000 e 2001-2050).

Table 1 Monthly cumulated mean values over space (whole case study) and time (period of considered time series) and trends of precipitation and daily minimum and maximum temperature of each simulation (control and scenarios) and reference. Trends are computed from 1970 for control simulation, reference and past scenarios and from 2001 to 2050 for future scenario. Control, Scen-20th, Scen-21th and reference stand for control simulation, past scenario, future scenario, observation. DSC indicated results of DSC.

	Daily minimum temperature (°C)												**°C/yr**
	Jan	**Feb**	**Mar**	**Apr**	**May**	**Jun**	**Jul**	**Aug**	**Sep**	**Oct**	**Nov**	**Dec**	**trend**
Control	3.7	3.9	5.6	8.2	12.4	16.1	19.1	19.7	16.0	11.8	7.6	5.0	**+0.039**
Scen-20th	5.1	5.0	6.5	8.7	12.1	16.0	18.3	18.1	15.3	11.5	8.3	5.7	**+0.043**
Scen-21th	5.3	5.7	7.1	9.4	12.9	16.7	19.7	19.3	16.5	12.8	9.0	6.1	**+0.037**
Reference	4.1	4.3	6.0	8.4	12.3	16.0	18.5	18.8	16.0	12.3	8.4	5.5	**+0.055**
Control-DSC	4.4	4.3	5.9	8.5	12.4	16.1	18.8	19.0	16.0	12.4	8.5	5.6	**+0.041**
Sc-20th-DSC	5.5	5.2	6.8	8.9	12.0	16.0	18.0	17.4	15.1	11.7	9.0	6.1	**+0.043**
Sc-21th-DSC	5.7	5.9	7.4	9.7	12.9	16.7	19.1	18.6	16.3	13.3	9.6	6.5	**+0.035**
	Daily maximum temperature (°C)												**°C/yr**
	Jan	**Feb**	**Mar**	**Apr**	**May**	**Jun**	**Jul**	**Aug**	**Sep**	**Oct**	**Nov**	**Dec**	**trend**
Control	9.4	10.1	12.5	15.8	21.6	27.1	31.8	32.4	26.3	19.6	13.8	10.5	**+0.062**
Scen-20th	10.7	11.0	12.9	16.0	21.3	27.3	30.2	29.6	24.8	19.0	14.1	11.3	**+0.054**
Scen-21th	10.8	11.6	13.6	16.9	22.0	28.2	31.9	30.9	26.3	20.0	14.8	11.4	**+0.044**
Reference	10.4	11.9	13.7	17.0	22.0	26.1	29.1	29.1	25.3	20.2	15.3	11.7	**+0.047**
Control-DSC	10.5	11.2	13.6	17.0	22.1	26.4	29.3	29.4	25.2	20.3	15.1	11.7	**+0.046**
Sc-20th-DSC	11.7	12.1	14.7	17.3	21.9	26.6	28.4	27.5	24.2	19.7	15.6	12.5	**+0.042**
Sc-21th-DSC	11.8	12.6	14.8	18.1	22.5	27.2	29.4	28.4	25.2	20.6	16.3	12.6	**+0.034**
	Cumulated precipitation (mm/month)												**mm/yr**
	Jan	**Feb**	**Mar**	**Aprl**	**May**	**Jun**	**Jul**	**Aug**	**Sep**	**Oct**	**Nov**	**Dec**	**trend**
Control	63.1	63.9	59.2	68.5	62.6	41.1	16.1	16.3	42.7	57.8	68.5	67.5	**-0.291**
Scen-20th	64.8	66.7	72.9	70.3	53.0	25.8	28.0	26.6	54.3	51.4	72.7	55.8	**-0.292**
Scen-21th	64.9	68.8	74.8	65.5	53.3	26.0	20.1	26.6	40.9	59.5	70.6	66.1	**-0.148**
Reference	66.5	59.5	62.1	53.2	39.8	32.3	25.5	30.7	51.5	70.6	85.0	77.1	**-0.277**
Control-DSC	66.0	60.4	62.8	53.4	41.2	32.1	25.3	30.6	52.6	71.0	86.2	78.5	**-0.207**
Sc-20th-DSC	68.7	63.4	76.6	53.6	32.5	21.2	35.0	39.2	58.2	63.9	90.6	63.9	**-0.295**
Sc-21th-DSC	68.3	64.6	78.3	47.4	33.6	19.4	29.6	43.4	49.4	72.9	88.5	77.6	**-0.097**

Yearly mean values of daily minimum and maximum temperature were assessed at each step of the model coupling approach (Fig. 4, 5, 9), with typical mean bias for both RCM and GCM of 0.5°C before the statistical downscaling and 0.05°C after. The statistical downscaling also able to correct the time dynamical misfit, illustrated by the reduction of the RMSE of yearly means, typically 0.5°C for RCM assessment, and almost 1°C for GCM-RCM assessment, reduce to 0.3 and 0.6°C respectively after DSC. Moreover, the spatial distribution is better represented after DSC, as illustrated by the 5^{th}, 25^{th}, 75^{th} and 95^{th} percentile comparison. At higher frequencies, the monthly mean value over the whole simulations period and over the whole case study (Table 1) present similar results, with a typical misfit of 1°C after dynamical downscaling, reduce to 0.1°C on the control simulation, and 0.8°C integrating GCM. Finally, the DSC effect on the GCM dynamic mostly in term of spatial distribution keeping almost unchanged the range of the differences between future and past scenario (Fig 12). Similarly, the yearly cumulated precipitation presents (Fig. 11) a typical bias for both RCM and GCM of 25 mm/yr, with an associated RMSE of 100 mm/yr and 150 mm/yr respectively. After the statistical downscaling, the mean bias is reduced to less than 1mm/yr, with a typical RMSE of 80mm/yr for the control simulation, and 120 mm/yr for the scenario. At higher frequencies, the monthly mean value over the whole simulations period and over the whole case study (Table 1) present similar results, with a typical misfit of 10 mm/month after dynamical downscaling, reduce to less than 1mm/month on the control simulation, and 8mm/month integrating GCM. Moreover, at a monthly time scale, the spatial distributions as well as the time dynamic are significantly improved through the DSC, as illustrated by the assessment of monthly precipitation standard deviation done at both RCM and available observation station grid after DSC (Fig. 7 and 8). As for temperature, the DSC did not impact the GCM dynamic, keeping unchanged the range of trend differences between future and past scenario (Fig 12).

The adopted downscaling methodology is therefore able to supply HM with a realistic meteorological forcing at monthly time scale, and typical kilometers scales thanks to the high quantity and quality of available observation stations. In fact, if the spatial resolution of the DSC directly depends on the observation station density, the quality of the associated time series is critical for the DSC performances. For the obtained local projection of climate scenarios, homogeneous long time series of observation should be made available. This is a critical point, since both instrumentations and stations availability change over decades. Homogenisation of meteorological time series requires meta-data describing the stations, instrumentation, implementation and exploitation, which are often not available. This is particularly critical before the advent of reading automation for weather instrumentation, since the quality, frequency and time coherence of time series highly depends on the acquisition modes.

Moreover, if the assessment done through the control simulation insure realistic forcing both in term of mean bias and time-space dynamic, same assessment done on scenarios significantly decrease performances, mostly in term of time-space dynamic, as revealed by RMSE computed over the spatial distribution of annual mean values. In fact, the presented methodology uses the RCM forecast capabilities and the historical cumulated distribution function to provide a complex local statistical filter but did not directly correct GCM

prediction, in order to preserve scenarios from hypothesis of statistical stationarity. Therefore, due to persistent uncertainty which is due, by a relevant amount, to the bias inherited from the GCM providing the lateral boundary conditions to the RCM, the evaluation of impacts should be preferably undertaken trough a comparative model simulation using past and future scenarios conditions which are both generated from the global model, leading to a robust impact study of meteorological boundary condition. If such a methodology results in a limited impact study as GCM simulations is not used as one would use a weather forecast, they can provide valuable insight to the range of potential climate change. In the present case study for example, application of the describe methodology on the monthly mean values (Fig. 13, 14 and 15) leads to the conclusion that during the next 50 years, temperature increase will be limited to about 1°C from December to June but may exceed 2° C from July to October, that minimum temperature may be more affect than maximum temperature, and that precipitation may decrease in April, July and September while increase in October and December, which are critical information for HM studies.

Nevertheless, performances of the methodology present in this section, aiming to provide realistic meteorological forcing in local climate change impact studies, will depends finally on the GCM performances. First because the nonlinearities and thresholds present in HMs may generate bias in the further HM scenarios comparison in case the GCM introduce important biases and secondly because the greatest uncertainty lies in the assumptions that must be made with regard to social and economic development, leading to the scenarios of climate evolution over the coming decades. Therefore, the capacity of the methodology to allow for the assessment of HM impacts using realistic patterns of altered climate highly depends of the capacity of GCM to present limited biases over the region under study as well as global realistic scenarios.

4. LITERATURE:

[1] IMELS (Italian Ministry for the Environment, Land and Sea) (2013) “Sixth National Communication under the UN Framework Convention on Climate Change”. Rome: IMELS.

[2] IPCC (2007) – Parry M.L., O.F. Canziani, J.P. Palutikof, P.J. van der Linden and C.E. Hanson, Eds., 2007, Climate Change 2007: Impacts, Adaptation and Vulnerability. Contribution of Working Group II to the Fourth Assessment Report of the Intergovernmental Panel on Climate Change, Cambridge University Press, Cambridge, UK, 982pp.

[3] EEA (European Environment Agency) (2012b) “Climate change, impacts and vulnerability in Europe, An indicator-based report”. EEA Report No 12/2012. Copenhagen: EEA.

[4] Portoghese I., Vurro M. and Mariotti A. (2009) “Impatti sul ciclo idrologico e risorse idriche”. In Castellari S. and Artale V. (2009). Bononia University Press.

[5] Bigano A. and Pauli F. (2007) "Dimensioni socio-economiche, costi dell'inazione e strategie di adattamento per l'impatto del cambiamento climatico sul sistema idrogeologico italiano" in Carraro C., 2008. Società editrice il Mulino.

[6] IMELS (Italian Ministry of Environment Land and Sea) - Direzione Generale per difesa del suolo (2008) "Il rischio idrogeologico in Italia". Rome: IMELS.

[7] Beniston M. (2006) "Climatic change in the Alps: Perspectives and impacts". Proceedings of the "Wengen 2006 Workshop - Adaptation to the Impacts of Climate Change in the European Alps". Organisation for Economic Co-operation and Development (OECD).

[8] Lo Porto A. et al. (2007) "Influenza dei cambiamenti climatici sul regime idrologico di due bacini idrografici in ambiente mediterraneo". In Carli B., Cavarretta G., Colacino M., Fuzzi S. (eds) "Clima e Cambiamenti Climatici: Le attività di ricerca del CNR", 577-580. CNR.

[9] Perini L., Salvati L., Ceccarelli T., Sorrenti S. and Zitti M. (2008) "La desertificazione in Italia. Processi, indicatori, vulnerabilità del territorio". Acireale – Roma: Bonanno Editore.

[10] Sciortino M., Luise A. and Genesio L. (2009) "La desertificazione e il degrado del territorio". In Castellari S. and Artale V. (2009). Bononia University Press.

[11] Funari E., Blasi M. F., Carere M., Della Bella V., Mancini L., Marcheggiani S., Mattera F. and Stefanelli M. (2007) "4.3 Flooding and health. In Menne B. and Wolf T., 2007. Rome, WHO-APAT.

[12] Houghton, Ding, Griggs, Noguer, Van der Linder, Dai, Maskell, Johnson (Eds). Climate Change (2001). The scientific basis. Contribution of Working Group I to the third assessment report of the IPCC. Cambridge University Press, Cambridge, UK.

[13] Kattenberg, A., F. Giorgi, H. Grassl, G. A. Meehl, J. F. B. Mitchell, R. J. Stouffer, T. Tokioka, A. J. Weaver, and T. M.L. Wigley (1996). Climate models - projections of future climate. In Climate Change 1995: The Science of Climate Change, 285-357, (Eds J. T. Houghton, L. G. M. Filho, B. A. Callander, N. Harris, A. Kattenberg, and K. Maskell) Cambridge University Press, Cambridge, UK.

[14] Cubasch, U., Meehl, G. A., Boer, G. J., Stouffer, R. J., Dix, M., Noda, A., Senior, C. A., Raper, S., Yap, K. S. (2001). Projections of future climate change. In IPCC, 2001: Climate Change 2001: The Scientific Basis. CUP, Cambridge, UK.

[15] Cohen, S. J. (1990). Bringing the global warming issue close to home: the challenge of regional impact studies. Bull. Amer. Meteor. Soc., 71, 520-526.

[16] von Storch, H., (1995). Inconsistencies at the interface of climate impact studies and global climate research. Meteor. Z., 4, 72–80.

[17] Schmidli, J., C.M. Goodess, C. Frei, M.R. Haylock, Y. Hundecha, J. Ribalaygua, T. Schmidth, (2007). Statistical and dynamical downscaling of precipitation: An evaluation and comparison of scenarios for the European Alps. J. Geophys. Res.-Atmos., 112 (D4), Art No D04105.

[18] Salathé EP. (2003). Comparison of various precipitation downscaling methods for the simulation of streamflow in a rainshadow river basin. International Journal of Climatology 23: 887–901.

[19] Burger G. and Chen Y. (2005). Regression-based downscaling of spatial variability for hydrologic applications. Journal of Hydrology 311: 299–317.

[20] Van Den Hurk B. (2008). Cap.6 Land surface scheme and climate models in " Climate and the hydrological cycle" book. IAHS special publication 8.

[21] Giorgi, F. and Mearns, L.O., (1999). Regional climate modelling revisited. An introduction to the special issue. J. Geophys. Res. 104, 6335-6352.

[22] Giorgi, F., Hewitson B., J. Christensen, C. Fu, R. Jones, M. Hulme, L. Mearns, H. Von Storch, and P. Whetton (2001), Regional climate information | evaluation and projections, in Climate Change 2001: The scientificc basis, p. 944pp, J. T. Houghton et al. Eds., Cambridge University Press.

[23] Lionello, P., Malanotte-Rizzoli, P., Boscolo, R. (2006). Mediterranean Climate Variability. - (Developments in earth & environmental sciences ; 4) 1. Mediterranean climate 2. Climatic changes - Mediterranean Region. British Library Cataloguing in Publication Data

[24] Fowler, H. J., Blenkinsop, S., and Tebaldi, C. (2007). Review Linking climate change modeling to impacts studies: recent advances in downscaling techniques for hydrological modeling. Int. J. Climatol. 27: 1547–1578.

[25] Frei, C., Christensen, J.H., Déqué, M., Jacob, D., Jones, R.G., and Vidale, P.L. (2003). Daily precipitation statistics in regional climate models: Evaluation and intercomparison for the European Alps. Journal of Geophysical Research, 108(D3), 4124-4143.

[26] Arnell, N. W. and Reynard, N. S. (1989). Estimating the impacts of climatic change on river flows: Some examples from Britain. Proc. Conference on Climate and Water, Helsinki, 1, pp. 413–425.

[27] Xu C.Y., and Singh, (2004). Review on Regional Water Resources Assessment Models under Stationary and Changing Climate Water Resources Management 18: 591–612, 2004.

[28] von Storch, H., E. Zorita, and U. Cubasch (1993). Downscaling of global climate change estimates to regional scales: An application to Iberian rainfall in wintertime, J. Climate, 6, 1161-1171.

[29] Wilby RL, Charles SP, Zorita E, Timbal B, Whetton P, Mearns LO. (2004). Guidelines for use of climate scenarios developed from statistical downscaling methods, Supporting material of the Intergovernmental Panel on Climate Change, available from the DDC of IPCC TGCIA, 27.

[30] Frederick, K.D., and P.H. Gleick, (1999): Water and Global Climate Change: Potential Impacts on U.S. Water Resources. Pew Center on Global Climate Change, Arlington, VA.

[31] Guyennon, N., Romano, E., Portoghese, I., Salerno, F., Calmanti, S., Petrangeli, A.B., Tartari, G., and Copetti, D., (2013). Benefits from using combined dynamical-statistical downscaling

approaches – lessons from a case study in the Mediterranean region, Hydrol. Earth Syst. Sci., 17, 705–720.

[32] Artale V., Calmanti S., Carillo A., Dell'Aquila A., Herrmann M., Pisacane G., Ruti P.M., Sannino G., Struglia M.V., Giorgi F., Bi X., Pal J.S., Rauscher S.(2009). An Atmosphere-Ocean Regional Climate Model for the Mediterranean area: Assessment of a Present Climate Simulation, Climate Dynamics, DOI 10.1007/s00382-009-0691-8.

[33] Wood A.W., Leung L.R., Sridhar V., and Lettenmaier D.P. (2004) Hydrologic Implications of Dynamical and Statistical Approaches to Downscaling Climate Model Outputs, Climatic Change 62, 189-216.

[34] Anav A., Ruti P.M., Artale V., Valentini R (2010): Modelling the effects of land-cover changes on surface climate in the Mediterranean region. Clim Res 41:91-104.

Report about existing climate and climate change data on national level Republic of Slovenia

Faculty of Natural Sciences and Engineering
University of Ljubljana
(FB5)

Ljubljana, 2014

Lead Author/s	Petra Žvab Rožič, Barbara Čenčur Curk
Lead Authors Coordinator	Name and Surname
Contributor/s	Name and Surname
Date last release	31.6.2014
State of document	Final

Let's grow up together

DRINK ADRIA

Adriatic IPA
Cross Border Cooperation 2007-2013

The project is co-funded by the European Union,
Instrument for Pre-Accession Assistance

Table of content

1 Introduction

In the last two decades climate change are extended research topics, which are often used as a tool and comparison with other changes in nature. According to numerous studies, noticeable changes in climate are increasingly common, and the consequences are evident mainly as more frequent and intense natural disasters. Causes of climate change may be different, but in addition to natural climate variability increasing role for changes attributable to human activities. In the latter a major role plays greenhouse gas emissions (CO_2, CH_4, N_xO, O_3 etc.) and aerosols, which alter the atmospheric composition.

In this report the existing climate characteristics as well as predicted climate change scenarios for the current century of Republic of Slovenia are presented. Based on measured meteorological parameters (temperature, precipitation) general trend of rising temperatures across the country as well as more frequent warm years in last two decades are observed. Changes in precipitation are especially seasonal noticeable with general peak of rainfall in autumn and less rainfall in spring and especially in summer.

World Meteorological Organization shows climate conditions using a 30-year period in order to avoid misinterpretation of climatic conditions due to the effects of various cyclical changes. On the basis of such long periods in describing the climate characteristics, significant climate fluctuations are captures due to external factors and characteristic climate variability are estimated as a result of such fluctuations. Therefore, the climatic conditions in Slovenia are presented for this period. Although world organisations as a 30-year average used the period 1961-1990, in Slovenia comparative period 1971-2000 were applied due to more complete meteorological data for this period. In determining the long-term trends in climate variables in some cases also a longer period is covered (ARSO, 2006).

2 Existing climate features in Slovenia

The climate of Slovenia is determined by numerous factors such as geographic location, relief diversity, orientation of mountain ridges and proximity to the sea. Consequently, diversity and combinations and of number of factors are reflected in a very diverse climate. There are three dominant types of climate, but in certain areas their effects are intertwined: the east Slovenia has a temperate continental climate, in central Slovenia subalpine climate (in mountain alpine climate), and in west of Alpine-Dinaric barrier sub-Mediterranean climate. Climatic diversity of Slovenia is reflected in the differences between the values climate variables and their daily, seasonal and multi-annual variability.

2.1 Temperature

Temperature characteristics in Slovenia are heavily dependent on the type of climate and relief in a given area. The most obvious is the dependence of the temperature conditions of the altitude, where the temperature usually decreases with heght. The average annual temperature in Slovenia decreases for 5.3 °C every 1000 m. Besides the altitude, also exposure has a significant impact on the temperature conditions. For example, in closed valleys temperature inversion may occur (ARSO, 2006).

The spatial distribution of mean annual temperature is in accordance with relief of Slovenia (Figure 1). The warmest is on the coast and some other valleys on the west, where the average annual temperature exceeds 12 °C. Temperatures between 10 and 12 °C are also found in the rest of the Primorska region (west Slovenia) and in the lowlands of eastern Slovenia, while in the lower parts of central Slovenia the average annual temperatures are between 8 and 10 °C. Lower temperatures are characteristic for mountains, where on the highest peaks average annual temperatures not exceed 0 °C (ARSO, 2006).

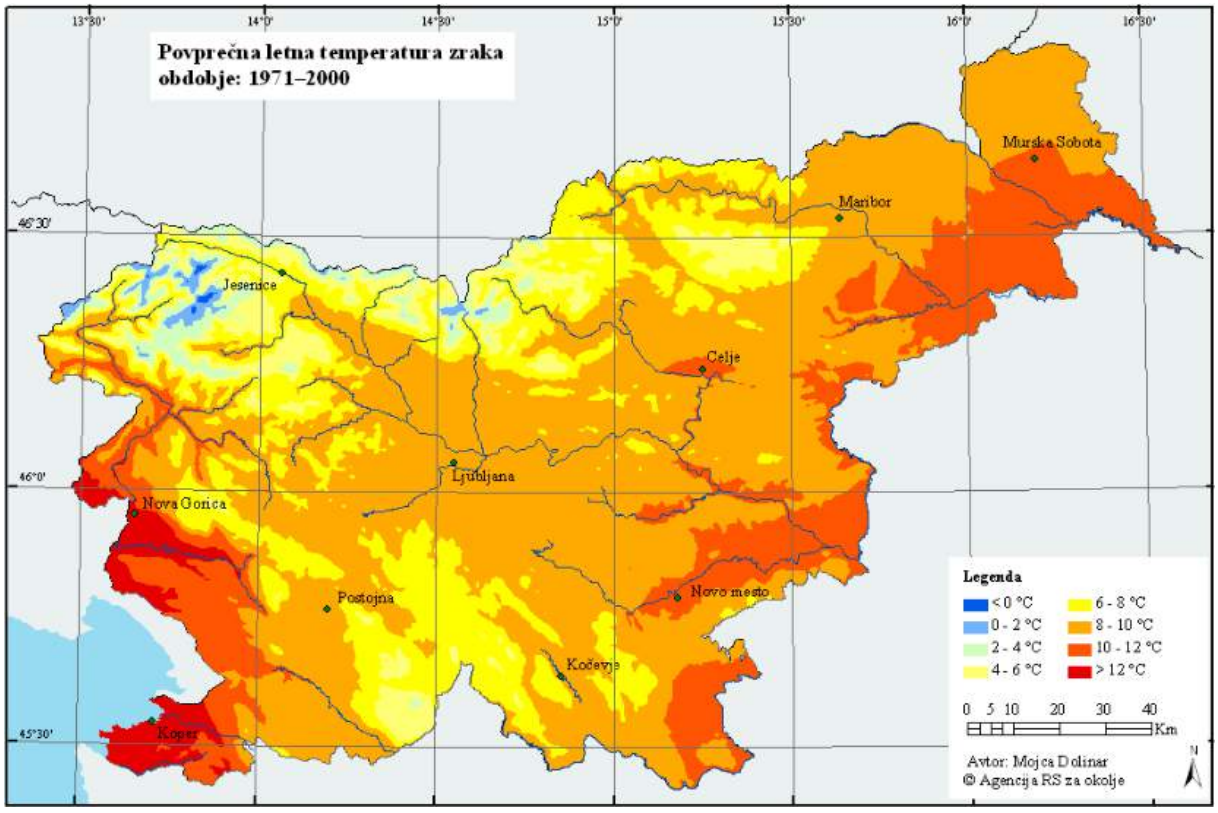

Figure 1: The average annual air temperature for the period 1971-2000 (ARSO, 2006).

For temperature in Slovenia daily and seasonal variations are characterized. Maximum daily temperatures are usually recorded at about 2 pm and the lowest just before sunrise. The warmest month is usually July and August in the mountains while the coldest month everywhere is January (Figure 2). The highest daily and seasonally fluctuations in temperatures are typical for areas with continental climate (eastern Slovenia). On the contrary, the lowest differences are characterized in Primorska region (western Slovenia) due to influence of the sea as well as in the mountains due to open atmosphere.

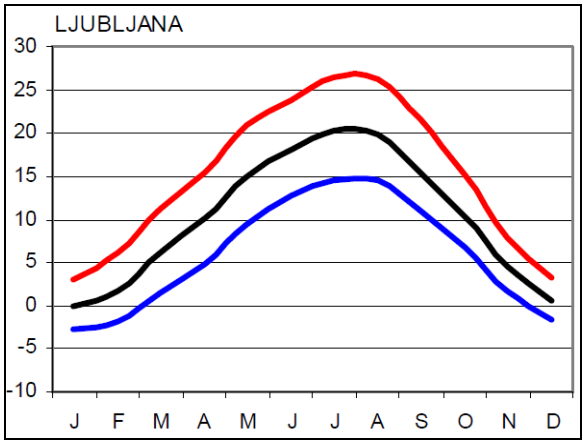

Figure 2: Average (black), maximum (red) and minimum (blue) monthly air temperatures for the period 1971-2000 (example for Ljubljana observation location) (ARSO, 2006).

Temperature conditions during the reference period 1971-2000 show on average increasing across the whole country. In average the coldest temperatures were determined at the beginning of period and the warmest in last years of the period (Figure 3) (ARSO, 2006).

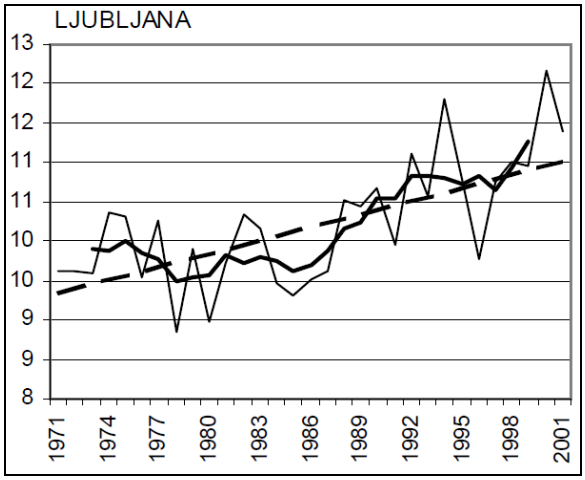

Figure 3: The annual average temperature for the period 1971-2001 (bold full curve indicates the 5-year average, dashed curve a statistically significant trend) (ARSO, 2006).

The temperature increasing was also observed positive deviations of annual average temperature during the last 50 years (Figure 4). The results show that positive deviations of temparture (warmer than the reference period) increase with decades, while negative deviation decrease. In 60's and 70's three positive and seven negative deviations were observed. The following decades show siginifcantly more warmer years with higher temperatures, such as five in 80's, eight in 90's and nine in the last decade. Besides, the last three years show also highly positive deviations.

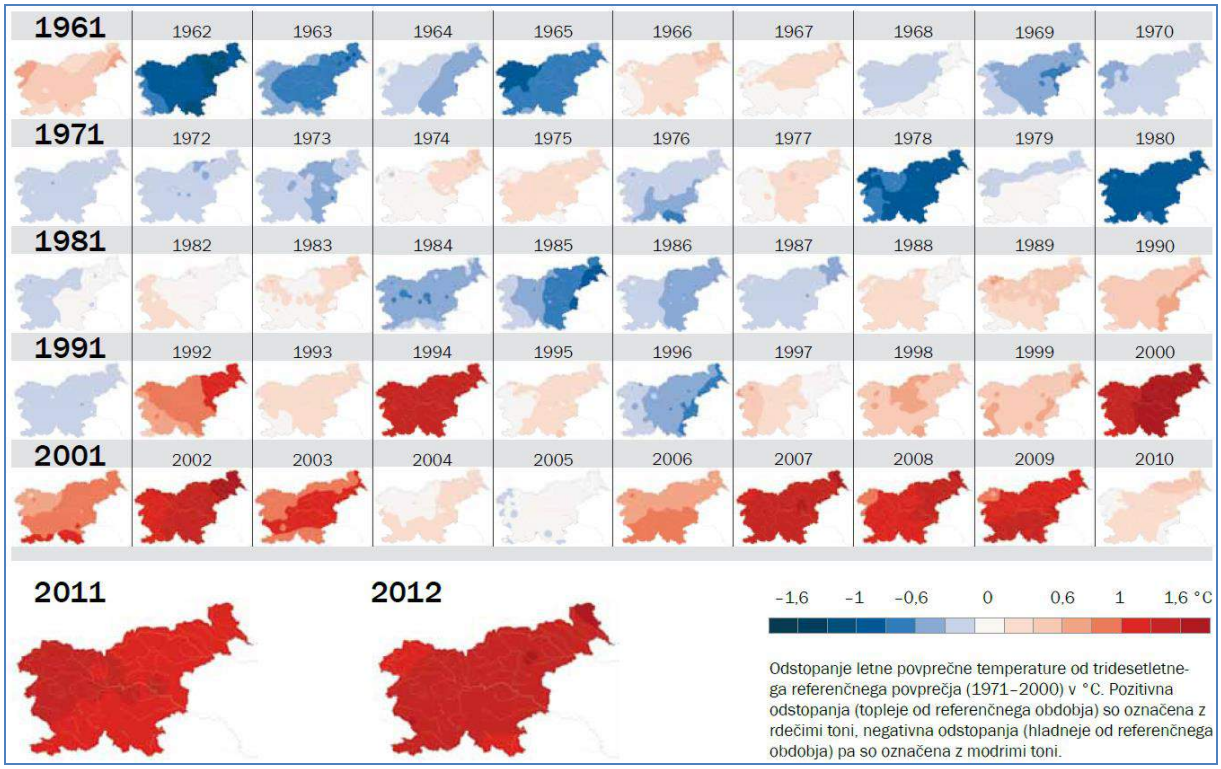

Figure 4: Deviation of annual average temperature of thirty years reference average (1971-2000) in °C. Positive deviations (warmer than the reference period) are marked with red, negative deviations (cooler than reference period) are marked with blue (Vertačnik et al, 2013).

2.2 Precipitation

The spatial distribution of precipitation in Slovenia (Figure 5) is strongly associated with its relief diversity. Due to the orographic effect the rainfall (amount of precipitation) increases with the distances from the sea towards the interior of Slovenia and reaches its maximum at the Dinaric-Alpine barrier. Slightly lower, but noticeable maximum rainfall also occurs in the Kamnik-Savinian Alps due to the effect of rising of air masses. On the other side of the Dinaric barrier to the northeast the rainfall rapidly decreases. The northeast of the country has a strong influence of the continental climate and the annual rainfall does not exceed 900 mm. Along the coastline the annual rainfall ranges between 1100 and 1200 mm. Such spatial distribution of rainfall is due to the fact that in Slovenia the most precipitation falls in the weather situations when moist and relatively warm air mass are moving across the country with south-westerly wind. The direction of air masses movement is perpendicular to orographic barrier, causing the rising of air masses, cooling of the air and consequently, the formation of precipitation. Therefore, the maximum of annual precipitation is in the Julian Alps, where falls annually over 3200 mm of precipitation. This area also belongs to the wetter areas in the Alps and in Europe (ARSO, 2006).

Precipitation regime determines the distribution of rainfall throughout the year. In Slovenia, dry or wet part of the year is not evident, but significant differences are observed during the months and seasons. The annual precipitation cycle is dependent on main climate type of certain region. For the sub-Mediterranean climate two precipitation maxima are characterized: the first occurs at the end of spring and the second in autumn. Alpine climate is characterized by main precipitation maximum in autumn and slightly less pronounced maximum in late spring and early summer. East part of the country, where the effect of continental climate occurs, is characterised by most precipitation during the summer showers and thunderstorms, while the winter months are the driest (ARSO, 2006).

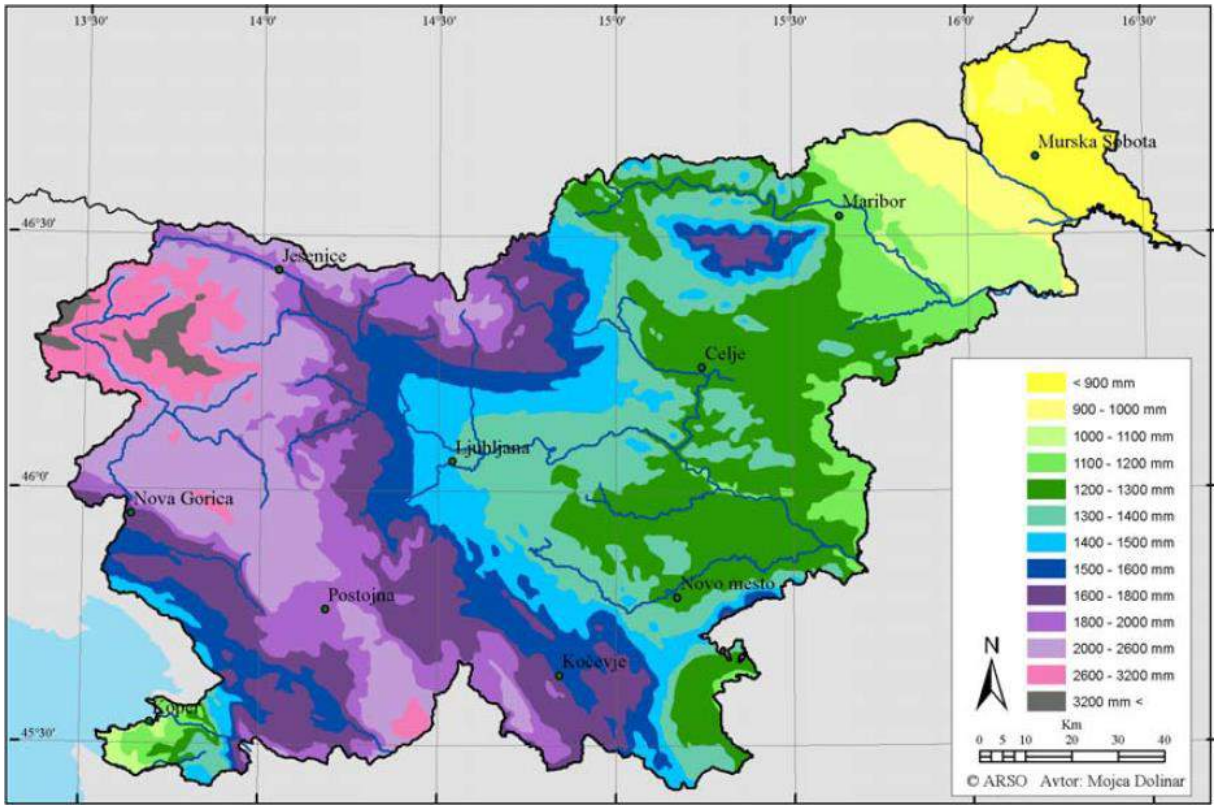

Figure 5: The average annual amount of corrected precipitation for the period 1971-2000 (ARSO, 2006).

Although the global climate changes foresee changes in precipitation, on an annual basis not significant trends are observed in the past (Figure 6). But more obvious variability is shown within individual seasons. The autumn rainfall increases almost across the all country with just some exception of small areas. During the winter the amount of precipitation is decreasing across western Slovenia, while in eastern Slovenia no changes are observed. In spring fairly uniform trend of decreasing rainfall throughout the country is observed with the exception in eastern Slovenia. In summer the situation is different with less precipitation practically everywhere except in higher elevations of the Alps (ARSO, 2006).

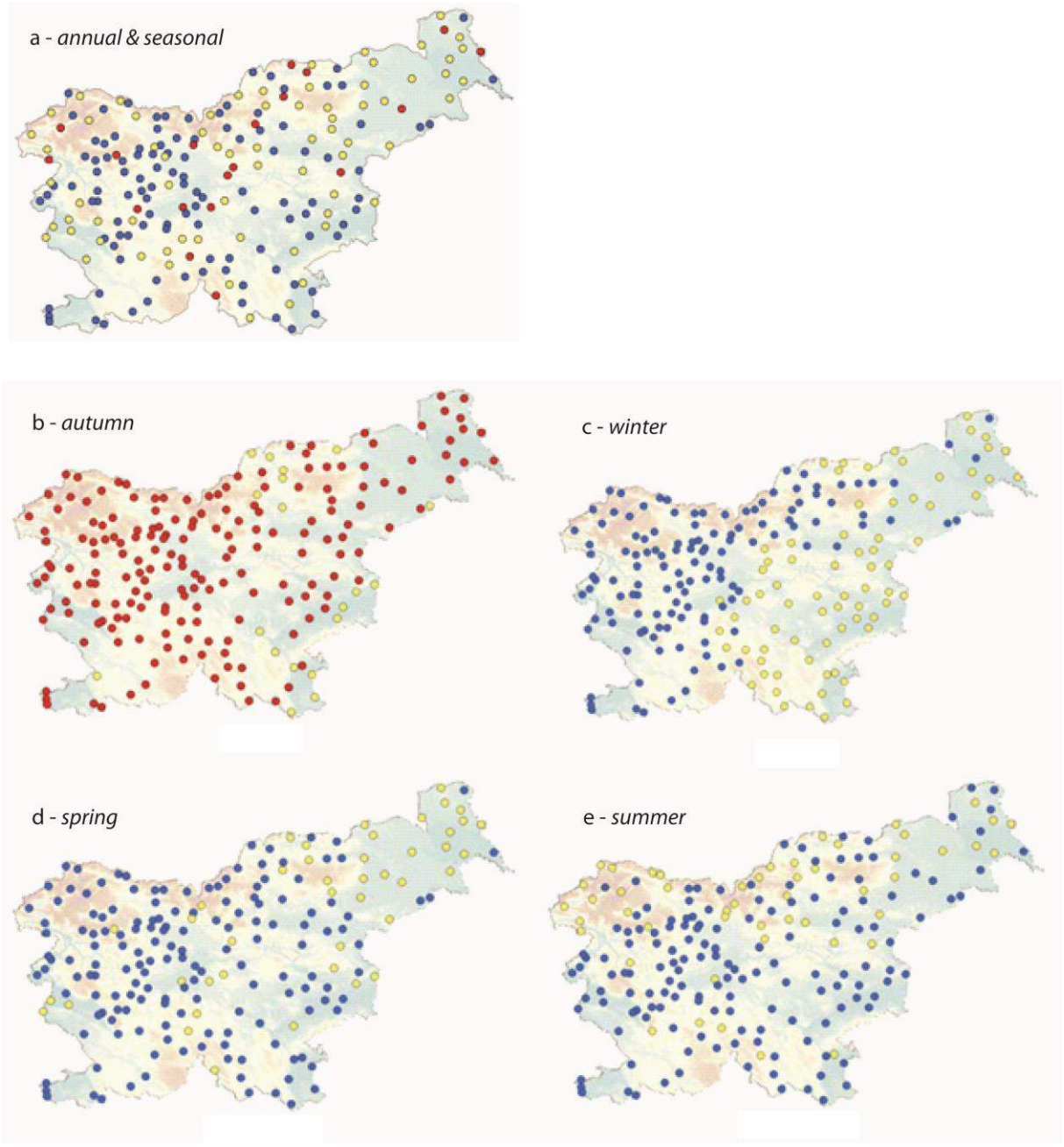

Figure 6: Statistically significant trends in (a) annual and seasonal precipitation [(b) autumn, (c) winter, (d) spring, and (e) summer] for the period 1971-2005. Red sign means a statistically significant increase in annual/seasonal precipitation, blue sign a statistically significant decline in annual/seasonal quantities precipitation, and yellow sign means that the trend is not statistically significant (ARSO, 2006).

On the basis of the cumulative meteorological water balance the distribution and intensity of agriculture droughts in 10 selected locations in Slovenia has been studied (Figure 7). It was found out that during the summer period (June to end of August) in the last fifty years (1963-2013) water deficit for agricultural plants 17-times caused problems with agricultural drought. Drought on national scale has emerged 7-times (red bars) since 1990, 5-times since 2000. All of these droughts have reached the dimensions of a natural disaster (Sušnik, 2014).

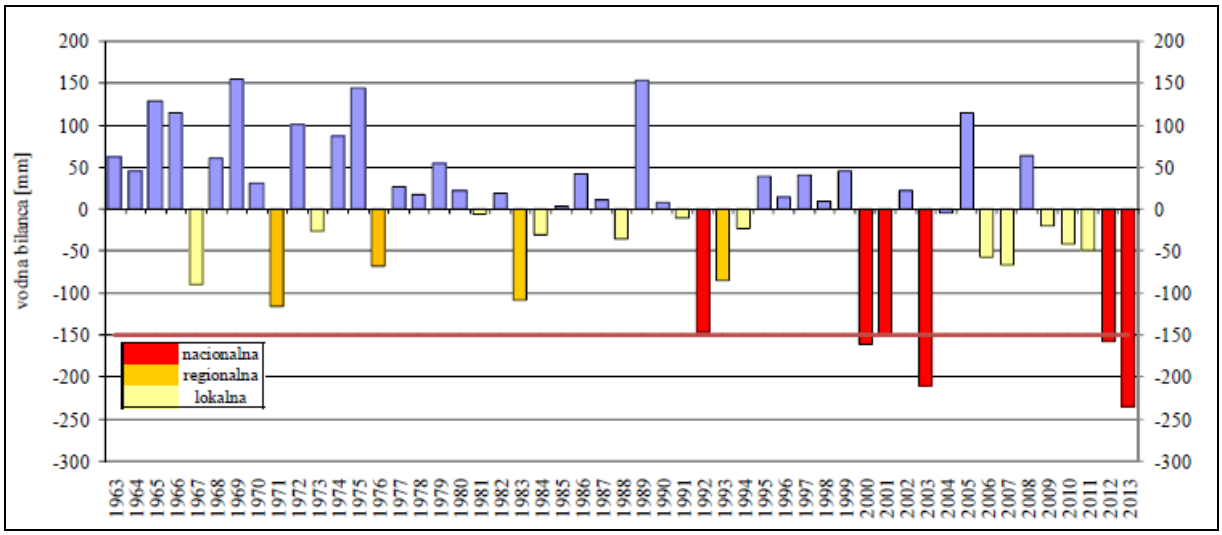

Figure 7: The average cumulative SUMMER hydro-meteorological period 1963-2013 (the red line represents the 75th percentile - drought) for 10 meteorological stations in Slovenia. The extent of the drought has been classified as: national drought (more than 5 regions), regional drought (3 or 4 regions) and local drought (in 1 or 2 regions) (Sušnik, 2014).

3 Climate change scenarious

Whereas changes in climate are very irregular, climatic conditions in the future cannot be accurately predicted (Lorentz, 1967). Therefore, several different climate models have been developed to assess the forecasting climate changes in the future. The most commonly used tool for studying the response of the climate system to changes in atmospheric composition are general circulation models (GCM) (Storch et al., 1993; Zorita & Storch, 1997; Rummukainen, 1997; Schubert, 1998; Zorita & Storch, 1999; Houghton et al., 2001). The results of these models present the basis for climate change scenarios. The Intergovernmental Panel on Climate Change (IPCC) suggests the use of different emission scenarios grouped under the acronym SRES (Second Report on Emission Scenarios) (Nakićenović et al, 2000; Swart et al. 2001), the implementation of which in the future is equally likely. Scenarios based on different assumptions of socio-economic development in the future and can be divided into four groups (A1, A2, B1 and B2) (Nakićenović et al, 2000; Houghton et al., 2001).

General circulation models constitute a good basis for assessing the impact and prepare adaptation strategies climate change in Slovenia by individual regions. According to the IPCC maps (Figure 8), which represents the synthesis of the results of many models of general circulation by the end of this century (IPCC, 2007), Slovenia and its wider surroundings is expected to have warmer summers more than winters. In winter we can expect a slightly more precipitation and in summer less.

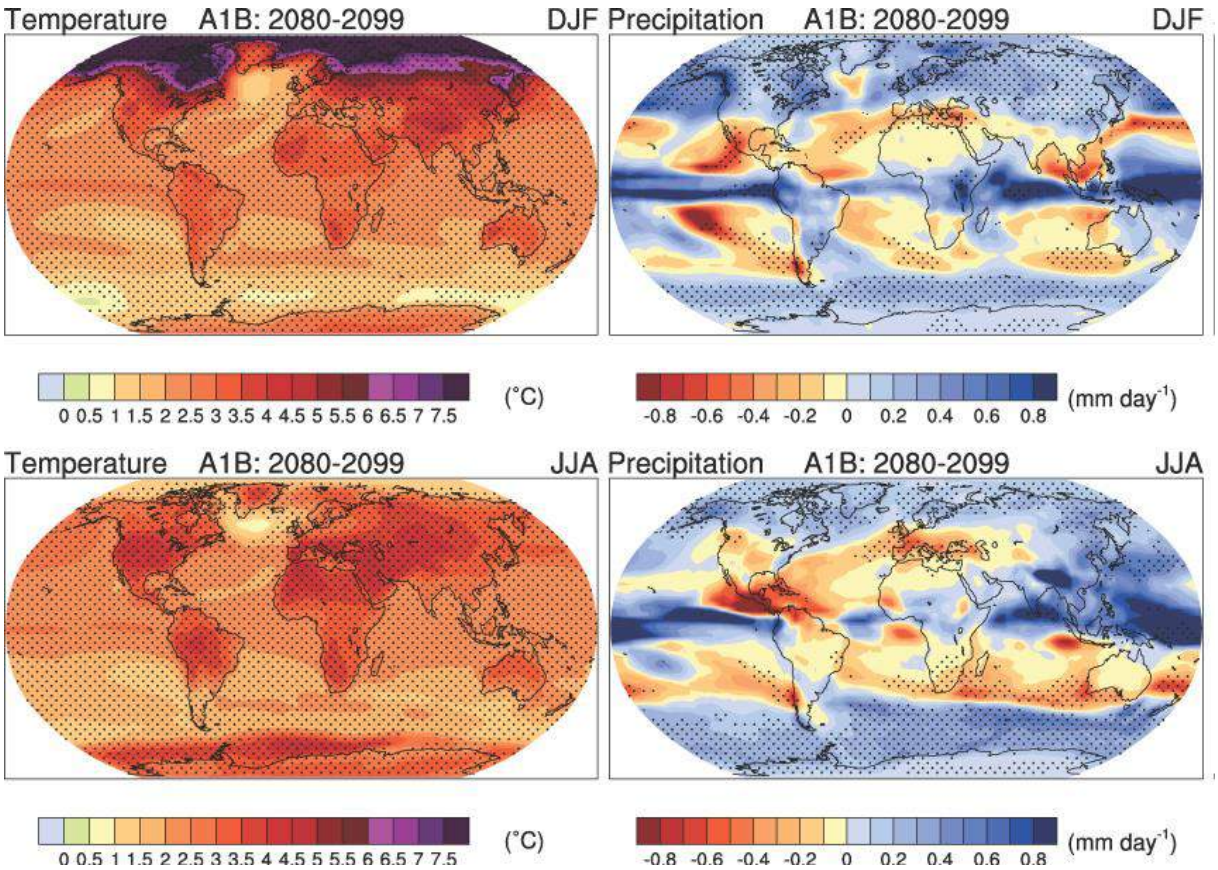

Figure 8: The modeled mean changes in air temperature (in ° C, left) and precipitation (mm/day, right) for winter (DJF, top) and summer (JJA, bottom) according SRES scenario A1B for the periods 2080-2099 (IPCC, 2007).

For the assessment of climate change in Slovenia in the future, the simulation results with 4 MSC methods with incorporated SRES emissions scenarios were used. Changes are shown in relation to the comparative period 1961-1990 as a 30-year average with a step of 10 years.

The results show that the temperature of the air will increase in the entire area Slovenia (Figure 9) with no significant differences between areas of Slovenia were observed. Size of the projected changes in temperature is largely dependent on the selected emission scenarios. In the period from 2001 to 2030 air temperature is expected to rise by 0.5 °C to 2.5 °C, over a period of 2031 to 2060 ° C from 1 to 3.5 °C, and in the period 2061 to 2090 for 1.5 °C to 6.5 °C (Bergant et al., 2004; Bergant & Kajfež Bogataj, 2004).

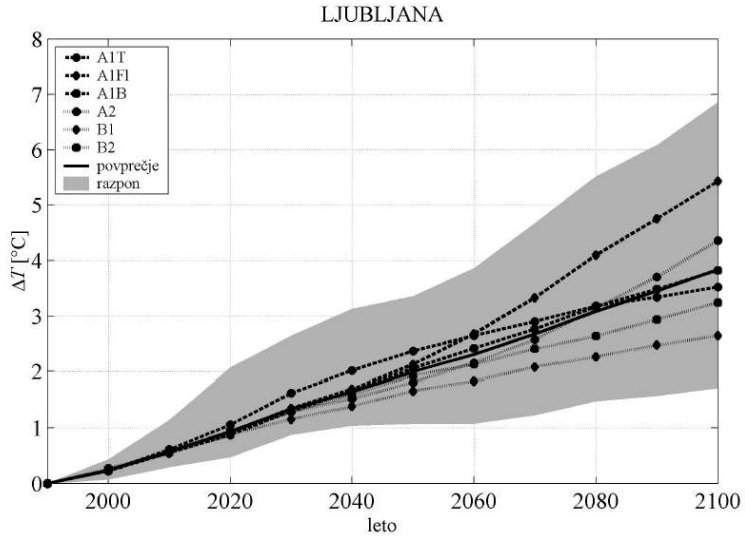

Figure 9: Estimated increase in air temperature (in ° C), an example for Ljubljana (Bergant & Kajfež Bogataj, 2004).

The predictions of changes in annual precipitation in Slovenia are less reliable and the quality of models is usable for most meteorological stations only for the months of cold half year. One of the reasons is diversity of climate conditions on a small area that locally impact on precipitation variables, especially in the warm half of the year. Therefore the empirical models for assessing precipitation variables produce no high-quality results. Some projections (as a predictor used air pressure at sea level as a temperature of the air) (Figure 10) show the trend towards less rainfall, while the others (as a predictor used only air pressure at sea level as a temperature of the air) the trend to a reduction in precipitation projections of results is not observed. Therefore, projections of changes in precipitation are used only as a rough estimate in the elaboration of climate change scenarios (Bergant et al., 2004; Bergant & Kajfež Bogataj, 2004).

The projected changes in annual precipitation in the future range from +10% to -30%. The precipitation in summer is likely lowered up to 20% (Bergant et al, 2004).

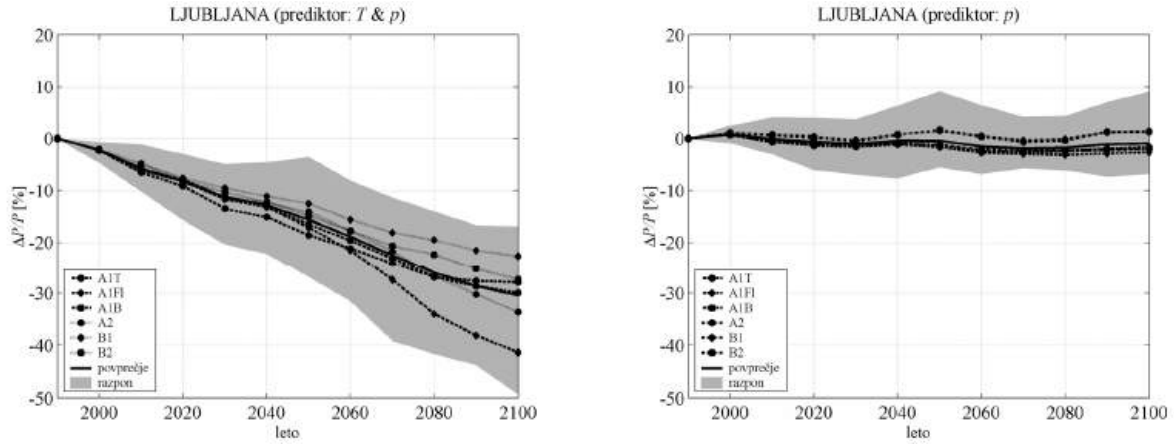

Figure 10: Projected changes in precipitation (ΔP/P in %), example for Ljubljana. The left side shows the results of the projections, which were empirical models designed using air temperature (T) and the air pressure at sea level (p) and on the right side the results of the projection, which was only used as a predictor p (Bergant & Kajfež Bogataj, 2004).

Climate change characteristics of South East Europe with a higher spatial resolution were observed within CC-WaterS project. The main focus was on the climate variables of temperature and precipitation. The dynamical downscaling and statistical downscaling were applied to obtain high-resolution climate change scenarios. Dynamical downscaling leads to Regional Climate Models (RCMs), which are limited to a smaller modeling domain, but resolved at a higher spatial resolution. With statistical downscaling models (SDMs), GCM variables (predictors) are linked with local and regional variables (predictands) (CC-WaterS, 2010b).

Three selected RCMs were used to simulate the future climate: RCM Aladin driven by GCM ARPEGE (run by the Centre Nationale de Recherches Météorologique, CNRM), RCM PROMES driven by GCM HadCM3Q0 (Universidad de Castilla-La Mancha, UCLM) and RCM RegCM driven by GCM ECHAM5-r3 (International Centre for Theoretical Physics, ICTP). Besides, regarding the green house emission scenario, the A1B scenario was selected as the common scenario for all analyses. Three meteorologcal stations with different altitudes were included in calculation (CC-WaterS, 2010b).

For Slovenia analysis was performed for three meteorological stations: Kredarica in the Apls, Ljubljana (the capital) and Murska Sobota (in SE Panonian basin flat area).

RCMs were bias corrected with EOBS data base. By comparing observation data (OBS) to EOBS data sets we came to conclusion that EOBS is a good approximation for locations with flat relief, but not for the high alpine terrain due to underestimation of altitude, which results in underestimation of both air temperature as well as precipitation. Also, there is aconsiderable difference between OBS and EOBS distributions of rainfall amounts, since EOBS underestimates the frequency of rain events with less than 5 mm rainfall amount as well as the frequency of events with 25 mm or more rainfall. Similarly to EOBS, model data significantly overestimates air temperature in high alpine terrain. Apart from the high

altitude location of Kredarica the model to model differences are slim in case of temperature. On the other hand, the precipitation differences among models have a high level of dissimilarity.

By applying statistical downscaling (quantile method approach) temperature biases can be successfully removed from RCMcorr data. Also, this approach adjusts the distribution of rainfall amounts.

The future model simulations showed the increase in air temperature on average more han 3 °C at all observed locations. The strongest increase was identified in the warm part of the year, particularly in the summer, and least strong in the cold par of the year (Figure 11) (CC-WaterS, 2010a).

Precipitation data manifests a high degree of ambiguity in the future periods, but the model simulations agree on a general trend pointing to less precipitation in the summer. All models predict an increase of percipitation in autumn (Figure 12). Model data also indicates trends in the direction of longer duration of dry spell and greater maximum daily rainfall (Figure 13) (CC-WaterS, 2010a).

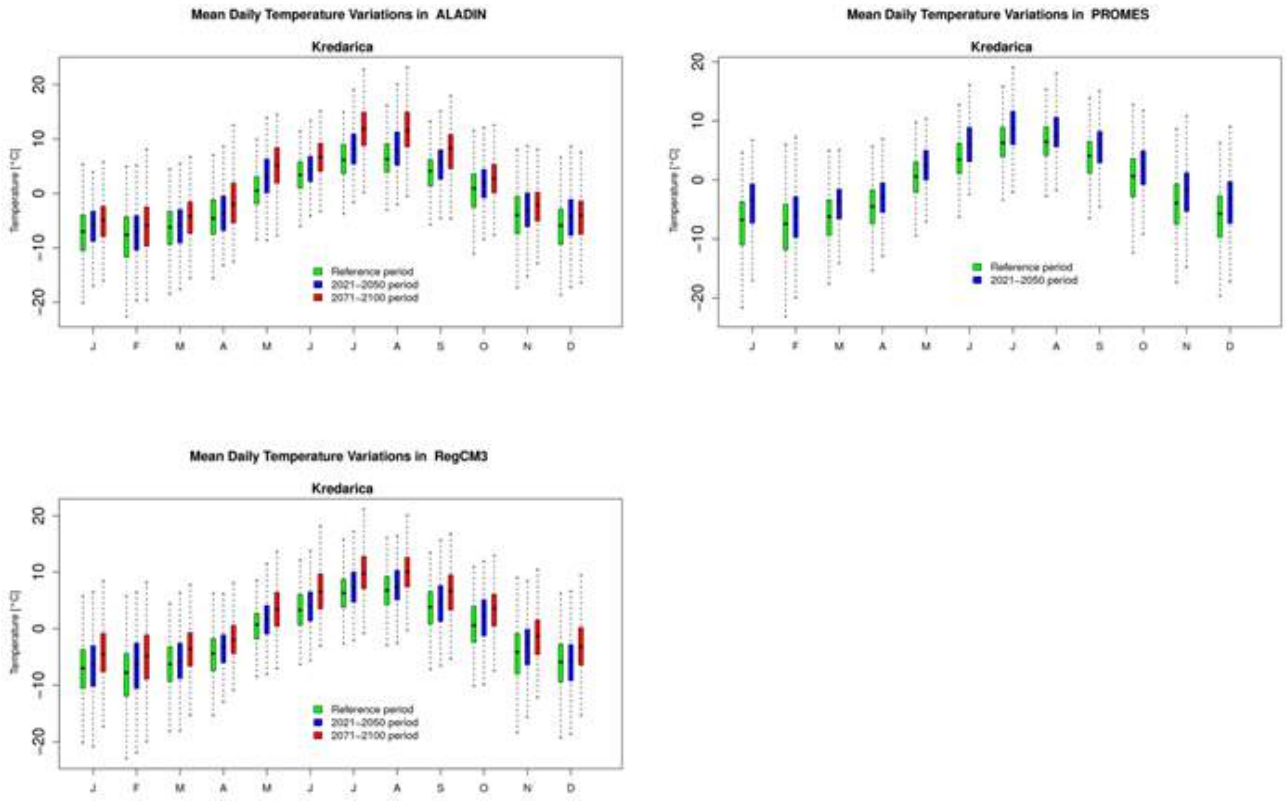

Figure 11: Trends in the mean temperature and seasonality at selected location (Kredarica) using three scenarious models (ALADIN, PROMES and RegCM3) (CC-WaterS, 2010a).

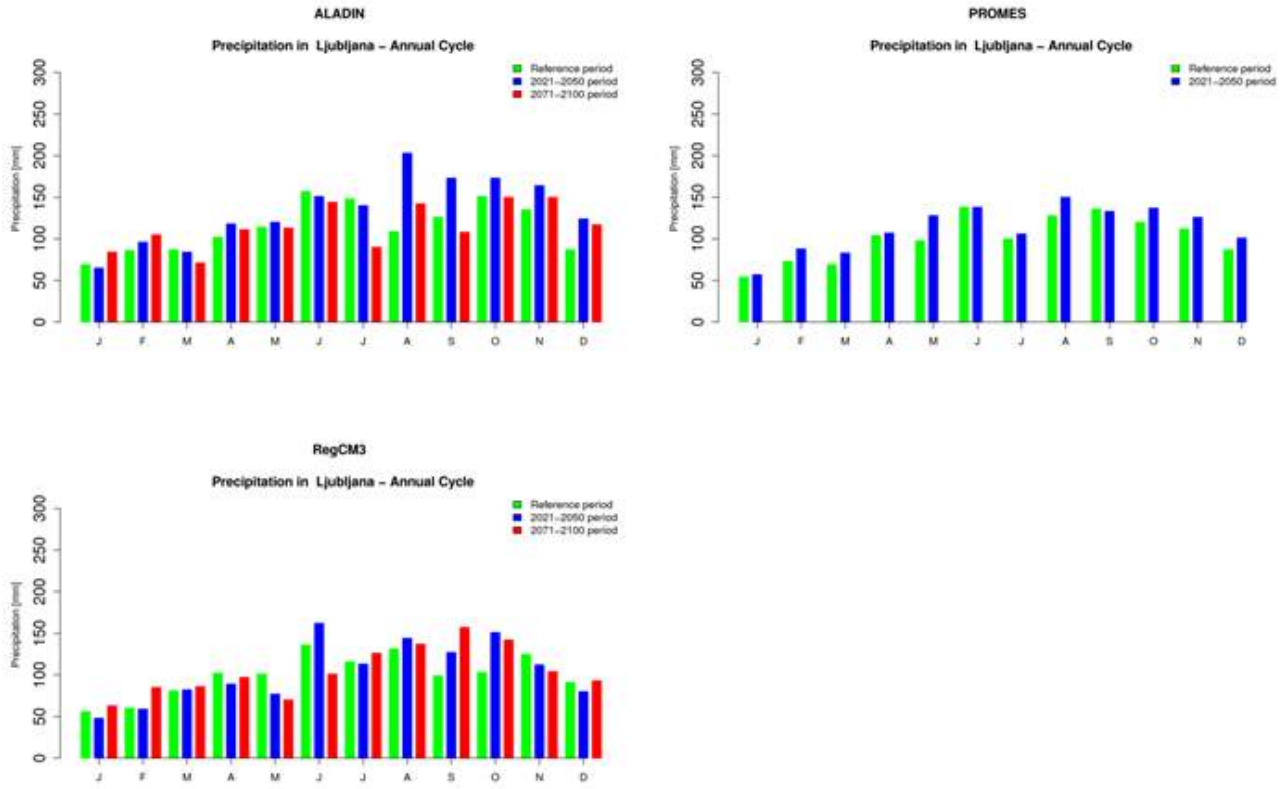

Figure 12: Trends in the mean monthly percipitation at selected location (Ljubljana) using three scenarious models (ALADIN, PROMES and RegCM3) (CC-WaterS, 2010a).

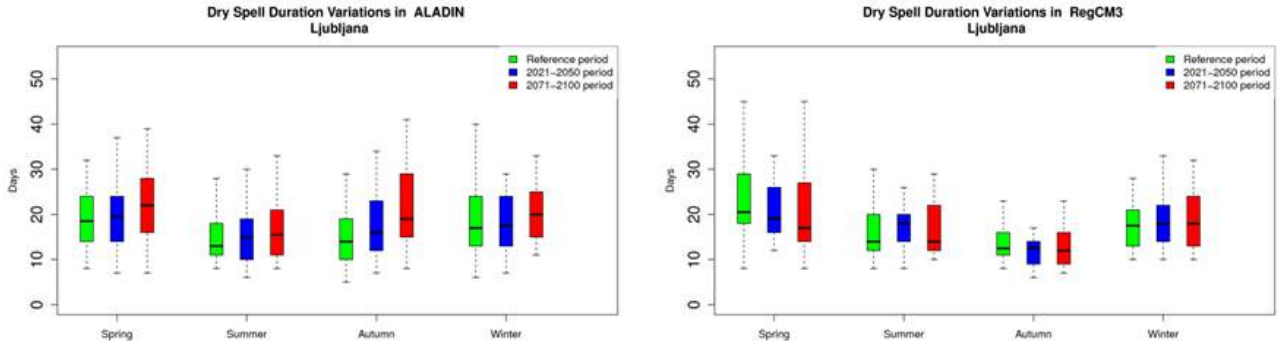

Figure 13: Trends of dry spell duration at selected location (Ljubljana) simulated by ALADIN and RegCM3 models (CC-WaterS, 2010a).

By studying future model simulations we observe the increase in air temperature is the strongest in the warm part of the year, particularly in the summer. Precipitation data manifests a high degree of ambiguity in the future periods, but the model simulations agree on a general trend pointing to less precipitation in the summer. Model data also indicates trends in the direction of longer duration of dry spell and greater maximum daily rainfall.

4 References

ARSO (Agencija Republike Slovenije za Okolje), 2006. Podnebne razmere v Sloveniji (obdobje 1971-2000). Ljubljana. Dostopno (5.6.2014): http://meteo.arso.gov.si/uploads/probase/www/climate/text/sl/publications/podnebne_razmere_v_sloveniji_71_00.pdf

Bergant K., Kajfež Bogataj L., Sušnik A., Cegnar T., Črepinšek Z., Kurnik B., Dolinar M., Gregorič G., Rogelj D., Žust A., Matajc I., Zupančič B., Pčenko A., 2004. Spremembe podnebja in kmetjistvo v Sloveniji. Agencija Republike Slovenije za okolje,

Bergant K., Kajfež Bogataj L., 2004. Nekatere metode za pripravo regionalnih scenarijev podnebnih sprememb. Acta agriculturae slovenica, 83/2, 273 – 287.

CC-WaterS, 2010a. Climate Change and Impacts on Water Supply (CC-WaterS) - WP3 report: Climate Change – Applications to project test areas (Slovene test areas). 39 pp.

CC-WaterS, 2010b. Climate Change and Impacts on Water Supply (CC-WaterS) - WP3 Climate Change - Executive summary. 17 pp.

Houghton J. T., Ding Y., Griggs D. J., Noguer M., van der Linden P. J., Dai X., Maskell K., Johnson C. A., 2001. *Climate change 2001: The scientific basis.* Cambridge, Cambridge University Press: 752 str. URL = http://www.grida.no/climate/ipcc_tar/wg1/index.htm

IPCC, 2007. Climate Change 2007: The Physical Science Basis. Contribution of Working Group I to the Fourth Assessment. [Solomon, S., D. Qin, M. Manning, Z. Chen, M. Marquis, K.B. Averyt, M. Tignor in H.L. Miller (ur.)]. Cambridge University Press, Cambridge, United Kingdom and New York, NY, USA, 996 str.

Lorenz E., 1967. The nature and theory of general circulation of the atmosphere. WMO Publication 218, 59-96.

Nakićenović N., Davidson O, Davis G., Grübler A., Kram T., Rovere E. L. L., Metz B., Morita T., Pepper W., Pitcher H., Sankovski A., Shukla P., Swart R., Watson R., Dadi Z., 2000. *Emissions scenarios – summary for policymakers.* A special report of WG III, Intergovernmental Panel on Climate Change, Cambridge, Cambridge University Press: 21 str.

Rummukainen M., 1997. *Methods for statistical downscaling of GCM simulations.* Tehnično poročilo 80, Norrkoping, Rossby Centrem SMHI: 33 str.

Schubert S., 1998. Downscaling local extreme temperature changes in south-eastern Australia from CSIRO MARK2 GCM. *International Journal of Climatology*, 18:1419-1438.

Storch von H., Zorita E., Cubasch U., 1993. Downscaling of global climate change estimates to regional scales: an application to Iberian rainfall in wintertime. *Journal of Climate*, 6: 1161-1171.

Sušnik A., 2014. Zasnove kazalcev spreminjanja suše na kmetjiskih površinah (Scheme of indicators for drought monitoring on agricultural land). Doctoral dissertation, Ljubljana.

Vertačnik, G., Dolinar, M., Bertalanič, R., Klančar, M., Dvoršek, D., Nadbath, M., 2013. Podnebna spremenljivost Slovenije; Glavne značilnosti gibanja temperature zraka v obdobju 1961–2011. Ministrstvo za kmetijstvo in okolje, Agencija RS za okolje (ARSO). Dostopno (5.6.2014): http://meteo.arso.gov.si/uploads/probase/www/climate/text/sl/publications/PSS-Glavne-znacilnosti-gibanja-temperature-zraka-1961-2011.pdf

Zorita E., Storch von H., 1997. *A survey of statistical downscaling techniques*. Tehnično poročilo, Geesthacht, Institute of Hydrophysics, GKSS Forshungszentrum: 42 str.

Zorita E., Storch von H,. 1999. The analog method as a simple statistical downscaling technique: comparison with more complicated methods. *Journal of Climate*, 12:2474-2489.

Report about existing climate and climate change data on national level Republic of Slovenia - Ljubljana, June 2014

Let's grow up together

DRINK ADRIA

Adriatic IPA
Cross Border Cooperation 2007-2013

The project is co-funded by the European Union,
Instrument for Pre-Accession Assistance

Report:

Climate and climate change data for Croatia

Faculty of Civil Engineering
University of Rijeka
(FB8)

Rijeka, 2014

Lead Author/s	Josip Rubinić, Čedo Branković
Lead Authors Coordinator	Barbara Karleuša
Contributor/s	Ivana Radman
Date last release	15.09.2014.
State of document	FINAL

Let's grow up together

DRINK ADRIA

Adriatic IPA
Cross Border Cooperation 2007-2013

The project is co-funded by the European Union,
Instrument for Pre-Accession Assistance

CONTENT:

1. INTRODUCTION

Occurrence of long dry periods, which is becoming more prominent and frequent on the wider regional area covered by DRINK ADRIA project, coincides with the observed global temperature increase on Earth over the past decades. Although there are significant differences in estimations whether mentioned observed recent climate change can be attributed to global climate change or just periodic climate variations, previous projections and manifestations of such possible changes *[1], [2], [3], [4], [5], [6], [7]* show the need to take into account the possible continuation and even increase of those negative climate change trends in water resource management, regardless if those are irreversible changes or normal climate variations. Contemporary approaches to water resource management seek the elaboration of different scenarios of possible long-term changes, to identify risks on time and prepare and optimize protective control measures. This is especially evident because of the relationship of globally present flow decrease trends *[8]*, which are observed especially in the Mediterranean, where at the same time water use increased significantly *[9]*. According to the most commonly cited reports of IPCC (Intergovemmental Panel on Climate Change) which is advocate of global climate change presence, it is predicted that the ocean level could rise between 9 and 88 cm until 2100, where the mean value is 48 cm *[10]*. Such changes, even with less intensity of changes, will certainly result in the need to protect and optimize the use of water resources, where special meaning for the population have water resources for water supply.

For analyzed regional area different scenarios of climate change impact assesment are made also for sea level rise, and ways of slowing down unwanted processes are discussed, as well as adjustment to such changes. In that sense, Croatia took over the obligations of the United Nations Framework Convention on Climate Change in 1996, and brought *First national communication of the Republic of Croatia to the United Nations Framework Convention on Climate Change (UNFCCC), 2001 [11]*. Since then, several revisions of such national report were brought, in accordance with the general knowledge about possible global climate change scenarios. Therefore, this report is based on the last, the *Sixth National Communication and First Biennial Report of the Republic of Croatia under the United Nations Framework Convention on Climate Change (UNFCCC), 2014* (in further text referenced as *Sixth National Communication, 2014 [12]*) as well as several previous documents and recent research projects results which considered regional manifestations of climate change/variations in Croatia, different scenarios of possible further changes, as well as possible strategy for responding to them. A part of the report enhasizes the climate and climate change data only for the Adriatic part.

As reference climate period in most of those documents period 1961-1990 was taken. The focus of this report are temperature and precipitation data for the Republic of Croatia, existing as well as estimated for some of the most likely climate change scenarios, which are determined by the application of several standard methodological procedures, which are referenced. Figure 1-1 shows the Republic of Croatia map with marked pilot areas of project DRINK ADRIA.

Figure 1-1. Republic of Croatia map with pilot areas of project DRINK ADRIA [13]

2. EXISTING CLIMATE FEATURES IN CROATIA

According to Köppen classification for a standard period 1961-1990, the largest part of Croatia belongs to the climate type C, a moderately warm rainy climate. The southernmost part of the island of Lošinj, the Dalmatian coast and islands have the Mediterranean climate with dry and hot summers (Csa), whereas the coastal areas of Istria, the Kvarner littoral and the Dalmatia's interior have a moderately warm and humid climate with hot summers (Cfa). The moderately warm and humid climate with warm summers (Cfb) prevails in the major part of Croatia, in the continental Pannonian region and the interior of Istria. Only the regions of Gorski kotar, Lika and the Dinaric Alps above altitude of 1200 m belong to the climate type D, subtype Df, a humid snowy forest climate *[12]*.

The annual mean air temperature in the lowland area of northern Croatia is 10-12 ºC, at altitudes above 400 m it is under 10 ºC and in the mountains it is 3-4 ºC. In the coastal area it is 12-17 ºC. January is the coldest month on average, with the temperature in the Pannonian region ranging from 0 to -2 ºC. Along the Adriatic coast winters are milder;

January temperatures are 4- 6 ºC. In the north and east of Croatia average July temperatures are 20-22 ºC and on the Adriatic coast 23-26 ºC. The absolute minimum temperature of -35.5 ºC was measured in Čakovec on 3 February 1929 and the absolute maximum of 42.8 ºC in Ploče on 5 August 1981 *[12]*.

The least precipitation in Croatia is recorded in the open part of the central Adriatic (Palagruža, 304 mm) and in the eastern Slavonia and Baranja (Osijek, 650 mm). Central Croatia and the coastal zone have annual precipitation between 800 and 1,200 mm. The amount of precipitation in the Pannonian region decreases from the west towards the east. From the coast towards the inland the precipitation increases. Most of the precipitation is recorded on the coastal slopes and peaks of the Dinarides (Risnjak, 3,470 m), from Gorski Kotar in the northwest to the southern Velebit in the southeast *[12]*.
Spatial distribution of selected climate parameters is shown in Figure 2-1.

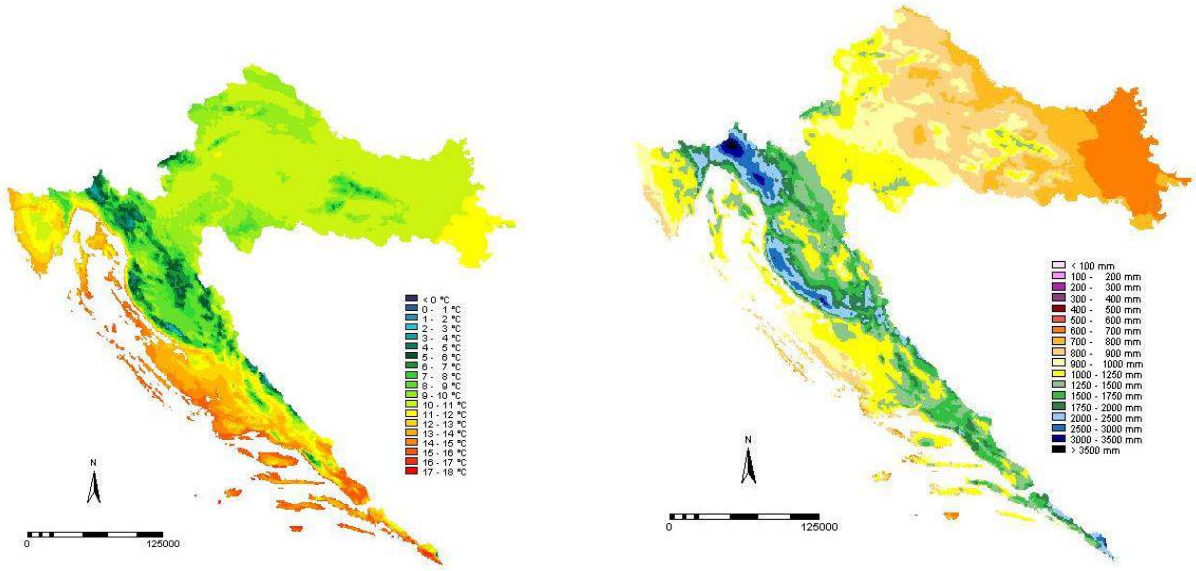

Figure 2-1. Spatial distribution of selected climate parameters for reference climate period 1961-1990. Left: mean annual air temperature; right: mean annual precipitation amount [14]

Climate change in Croatia over the period 1961-2010 has been determined by trends in annual and seasonal mean air temperature, mean minimum and mean maximum temperature; and in indices of temperature extremes; then in precipitation amounts and precipitation indices, as well as in dry and wet spells.
Temperature trends were calculated for the temperature deviations from the associated 1961-1990 means, and expressed in ºC per decade, while trends in indices of temperature extremes are expressed by number of days per decade. Trends in air temperature (mean, mean minimum and mean maximum temperature) in the last 50 years (1961-2010) show warming all over Croatia (Figure 2-2). Annual temperature trends are positive and significant, and the changes are higher on the mainland than at the **coast** and the **Dalmatian hinterland**. The maximum temperature values were exposed to the greatest

changes (Figure 2-2) with the highest frequency of trends in the class of 0.3-0.4 ºC per decade, while trends in the mean and the mean minimum air temperatures mostly range between 0.2 and 0.3 ºC per decade. The overall positive trend in the annual air temperatures comes are mainly caused by the significant positive summer trends, while the trends for the winter and spring gave almost equal contribution to the increasing trends of mean maximum temperature. Autumn temperatures are subjected to small changes and they are mostly positive. Observed warming can be seen in all indices of temperature extremes, with positive trends of warm temperature indices (warm days and nights as well as warm spell duration index) and with the negative trends of cold temperature indices (cold days and nights and cold spell duration index) (Fig. 2-3). At most stations, the increase of the number of SU ranges between 2 and 8 days per decade. Increase in the number of warm days (Tx90) most often accounted 6-10 days and warm nights (Tn90) even 8-12 days per decade. The duration of warm spells at most stations has increased for 4-6 days. Cold days and cold nights (Tx10 and Tn10) have the most significant trends, and their number at most stations is reduced for up to 4 days per decade *[12]*.

Table 2-1. List of the selected indices of temperature extremes and precipitation and their definition. The abbreviations and definitions are according to standardisation of WMO-CCL/CLIVAR working group for climate change [12]

Indices of cold temperature extremes		
FD	Frost days (absoulte treshold)	Number of days with minimum temperature below 0°C
TN10%	Cold nights (percentile treshold)	Number of days with minimum temperature (TN) below the 10th percentile from the 1961-1990 baseline period
TX10%	Cold days (percentile treshold)	Number of days with maximum temperature (TX) below the 10th percentile from the 1961-1990 baseline period
CSDI	Cold spell duration index	Number of days in periods with at least 6 consecutive days with minimum temperature below TN10%
Indices of warm temperature extremes		
TN90%	Warm nights (percentile treshold)	Number of days with minimum temperature (TN) above the 90th percentile from the 1961-1990 baseline period
TX90%	Warm days (percentile treshold)	Number of days with maximum temperature (TX) above the 90th percentile from the 1961-1990 baseline period
WSDI	Warm spell duration index	Number of days in periods with at least 6 consecutive days with minimum temperature above TX90%
SU	Summer days (absolute treshold)	Number of days with maximum temperature 25°C
List of the percipitation indices and their definitions		
Indices	Unit	Definition
DD	days	Dry days (absolute extreme) *(Number of days with daily precipitation amount Rd<1.0 mm)*
SDII	Mm/days	Simple daily intensity index (absolute extreme) *(annual precipitation amount / annual number of wet days (Rd≥1.0 mm)*
R75	days	Moderate wet days (percentible treshold) *(Number of days with precipitation Rd>R75%, where R75% is the 75th percentile of the distribution of daily precipitation amounts at days with 1 mm or more precipitation in the 1961-1990 baseline period)*
R95	days	Very wet days (percentile treshold) *(Number of days with precipitation Rd>R95%, where R95% is the 95th percentile of the distribution of daily precipitation amounts at days with 1 mm or more precipitation in the 1961-1990 baseline period)*
R25T	%	Precipitation fraction due to days with Rd<R25% (percentile threshold) *(Fraction of annual total precipitation ΣRd/Rt, where ΣRd indicatest he sum of daily precipitation less than the 25th percentile of precipitation at days with R25% in the 1961-1990 baseline period. ARt is the total annual precipitation amount.)*
R25-75T	%	Precipitation fraction due to days with R25%≤Rd≤R75% (percentile threshold) *(Fraction of annual total precipitation ΣRd/Rt, where ΣRd indicates the sum of daily precipitation equal to or exceeding the 25th percentile of precipitation at days with R25% and equal to or less than the 75th percentile of precipitation at days with R75% in the 1961-1990 baseline period. Rt is the total annual precipitation amount.)*
R75-95T	%	Precipitation fraction due to days with R75%<Rd≤R95% (percentile threshold) *(Fraction of annual total precipitation ΣRd/Rt, where ΣRd indicates the sum of daily precipitation exceeding the 75th percentile of precipitation at days with R75% and equal to or less than the 95th percentile of precipitation at days with R95% in the 1961-1990 baseline period. Rt is the total annual precipitation amount.)*
R95T	%	Percipitation fraction due to very wet days (percentile treshold) *(Fraction of annual total precipitation ΣRd/Rt, where ΣRd indicates the sum of daily precipitation exceeding the 95th percentile of precipitation at very wet days R95% in the 1961-1990 baseline period)*
Rx1d	mm	Highest 1-day percipitation amount (absolute extreme) *(Maximum precipitation sums for 1-day intervals)*
Rx5d	mm	Highest 5-day percipitation amount (absolute extreme) *(Maximum precipitation sums for 5-day intervals)*

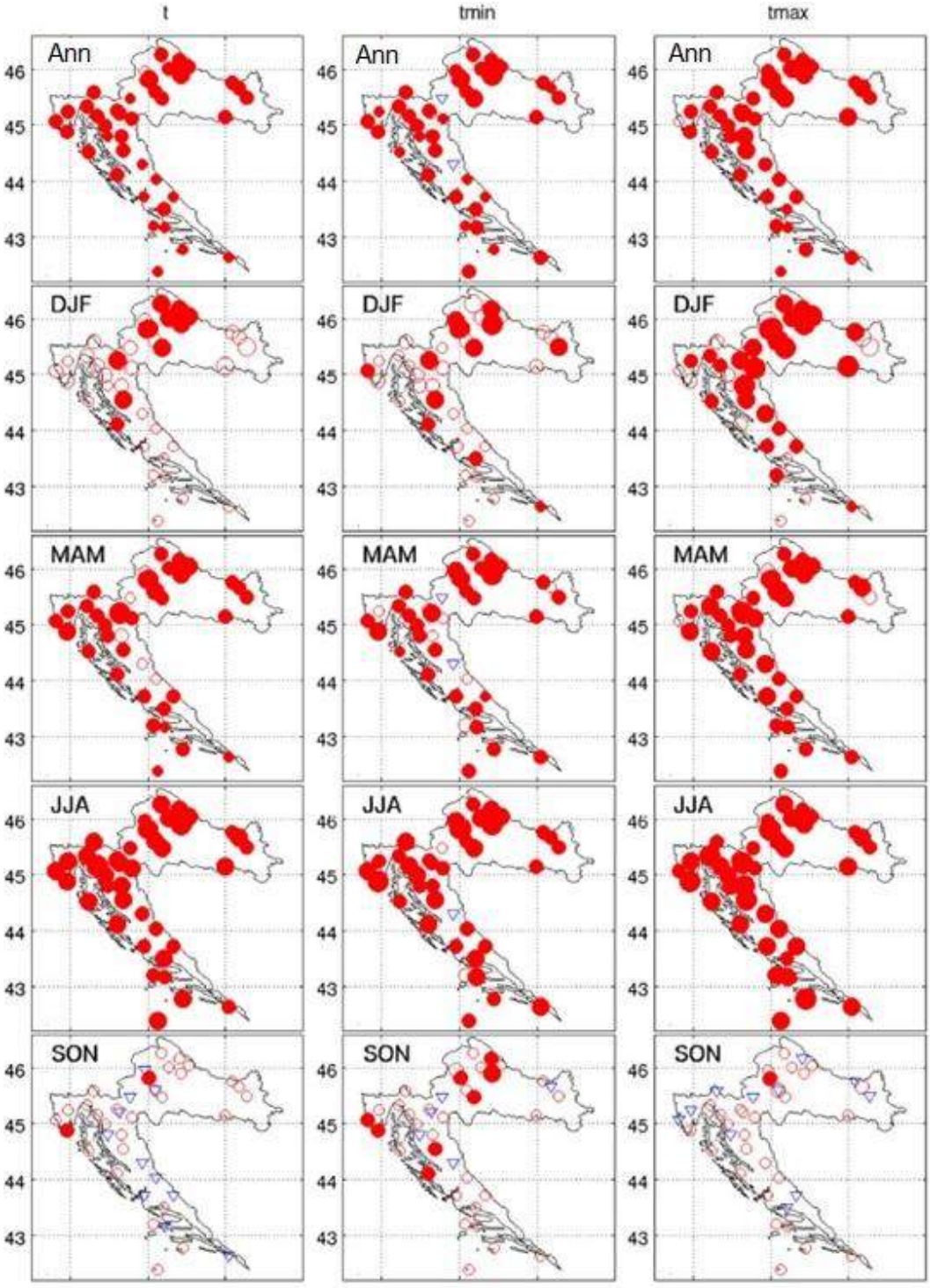

Figure 2-2. Decadal trends (ºC/10yrs) in annual and seasonal (DJF-winter, MAM-spring, JJA-summer, SON-autumn) mean (t), mean minimum (tmin) and mean maximum temperature (tmax) values in the 1961-2010 period. Circles denote positive trends, triangles the negative one, whereas filling means statistically significant trend. Four sizes of symbols are proportional to the absolute value of change (in ºC) per decade relative to the respective average from the period 1961-1990: <0.2, 0.2-0.4, 0.4-0.6 and >0.6, respectively [12]

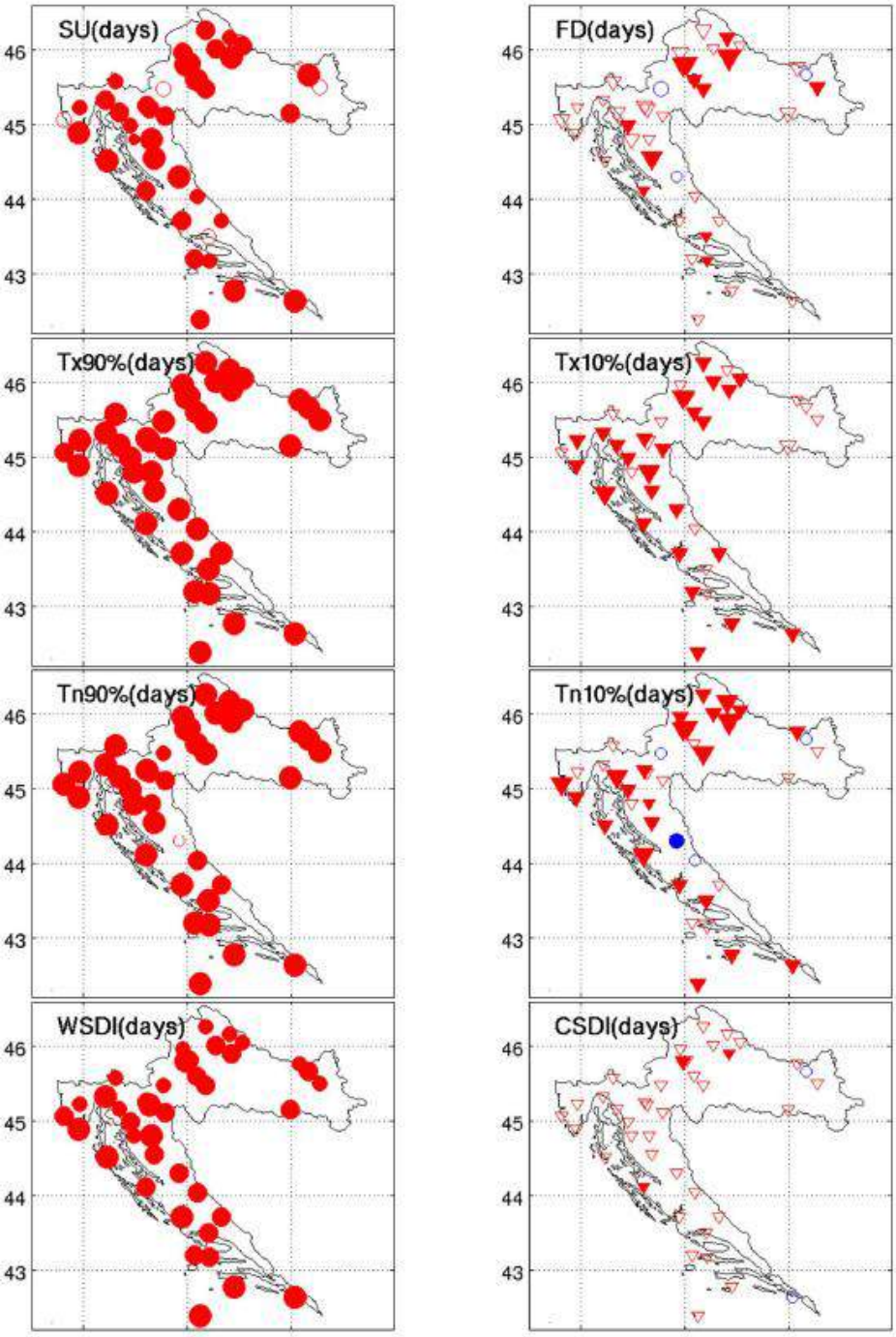

Figure 2-3. Decadal trends (days/10yrs) in annual extreme temperature indices in the 1961-2010 period. Circles denote positive trends, triangles the negative one, whereas filling means statistically significant trend. Four sizes of symbols are proportional to the absolute value of change (in days) per decade relative to the respective average from the period 1961-1990: <2, 2-4, 4-6 and >6, respectively [12]

The positive temperature trends in the continental part of Croatia is mostly due to winter trends (+0.06 °C/10 years in Osijek, +0.13 °C/10 years in Zagreb and Gospić), while on the **Adriatic** to summer trends (+0.13 °C/10 years in **Crikvenica** and +0.07 °C/10 years in **Hvar**), Table 2-2.
In Table 2-2 it is shown that annual amounts of precipitation showed a downward trend in five parts of Croatia. It is more expressed over the **Adriatic** (**Crikvenica**: -1.8% in 10 years, statistically significant and **Hvar**: -1.2% in 10 years), than in the inland (mountainous hinterland– Gospić: -0.8% in 10 years, eastern Slavonija, Osijek: -1.3% in 10 years, north-western Croatia, Zagreb-Grič: -0.3% in 10 years), *[15]*.

Table 2-2: Trends in mean annual and seasonal air temperature (°C/10 years); trends in annual and seasonal precipitation amounts. Trends significant at the 5% level are bolded. [15]

	Osijek	**Zagreb-Grič**	**Gospić**	**Crikvenica**	**Hvar**
Mean air temperature trend 1901-2008 (°C/10 years)					
WINTER	+0.06	+0.13	+0.13	+0.08	+0.04
SPRING	+0.05	**+0.11**	+0.05	+0.04	**+0.05**
SUMMER	+0.06	**+0.09**	+0.04	**+0.13**	**+0.07**
AUTUMN	+0.03	+0.07	+0.03	**+0.09**	+0.05
YEAR	+0.05	**+0.10**	**+0.06**	**+0.09**	**+0.06**
Percipitation amount trend 1901-2000 (% /10 years)					
WINTER	+0.6	-0.3	-2.7	-1.8	-2.9
SPRING	**-4.1**	-1.1	-2.0	-2.2	-2.0
SUMMER	+0.7	+1.2	+0.9	-2.7	+2.8
AUTUMN	-3.0	-1.4	+0.1	-0.9	-0.4
YEAR	-1.3	-0.3	-0.8	**-1.8**	-1.2

During the recent 50-year period (1961-2010) the annual precipitation amounts (*R*) experienced prevailing insignificant trends that are increasing in the eastern lowland and decreasing elsewhere (Fig.2-4. (a)). The statistically significant decreases (filled symbols) are found for the stations in the mountainous region of Gorski kotar and in the **Istria peninsula** (**northern Adriatic**) as well as in the **southern coastal** region. Expressed per decade as percentages of the respective average values, these decreases range between -7% and -2%. Annual negative trends are mainly caused by decreasing trends in summer amounts (*RJJA*), which are found to be statistically significant at most stations in the mountainous region and at some stations along the **Adriatic and its hinterland** (Fig. 2-4. (b)). The statistical significance of the annual negative trend in **Istria** and Gorski kotar is also influenced by spring negative tendencies (from -8% to -5%; Fig. 2-4. (c)). Positive (circles) annual trends in eastern lowland are primarily caused by the significant increasing trends in autumn (Fig. 2-4 (d)) and to a less extent in spring and summer.

Summer precipitation shows a clear prominence of negative trend estimates all over the country and there is a number of stations for which this decrease is statistically significant, with the relative change between -11% and -6% per decade. In autumn, the trends are weak and mixed in sign, except in the eastern lowland where some locations show significant increasing trend in precipitation (8% to 11%). In spring results suggest no signal in the southern and eastern part of the country, while a negative tendency seems to affect the rest of the country, significantly only in **Istria** and Gorski kotar (-5% to -7%). During winter season (Fig.2-4. (e)), precipitation trends are not significant and they range between -11% and 8%. They are mostly negative at the southern and eastern parts as well as at **Istria** peninsula *[12]*.

Regional distribution of trends in precipitation indices, that define magnitude and frequency of precipitation extremes, shows complex structure. Spatial distribution of trends in frequency of dry and wet precipitation extremes as indicated by number of dry days (*DD*), moderate wet days (*R75*) and very wet days (*R95*) are presented in Fig.2-4. (f, g, h). The trends in *DD* are predominantly weak, but statistically significant positive trends (1% to 2%) appear at some stations in the mountainous region of Gorski kotar, **Istria** peninsula and in the **southern coastal** region. The trend pattern of *R75* is spatially very similar to the annual precipitation one. The regional distribution of *R95* trends shows no signal over the majority of the country. Statistically significant changes are present at few stations; positive over the northern lowlands and negative in the highlands of Gorski kotar as well as at the **very southern coast** *[12]*.

Trends in the intensity of precipitation for wet days (Fig.2-4 (i)), as measured by the simple daily intensity index (*SDII*), reflect changes of trend magnitudes in two variables, annual amounts and annual number of wet days. For example, for two stations in different regions (indicated by two arrows in Fig.2-4. (i)), the same change in frequency of *Rd* (in these cases significant decrease, see Fig.2-4. (f)) but different changes in *R*, resulted in the similar significant increase in *SDII* at both stations. It implies that *SDII* is not suitable for explaining the causes of changes in *R*. Because of this fact, this index and its trends should be used with caution in application studies *[12]*.

Characteristic trends of mean annual temperatures and annual precipitation amounts for selected stations on the Croatian coastal area (station Crikvenica for the northern Adriatic and Hvar for the southern Adriatic) are shown in Figure 2-5.

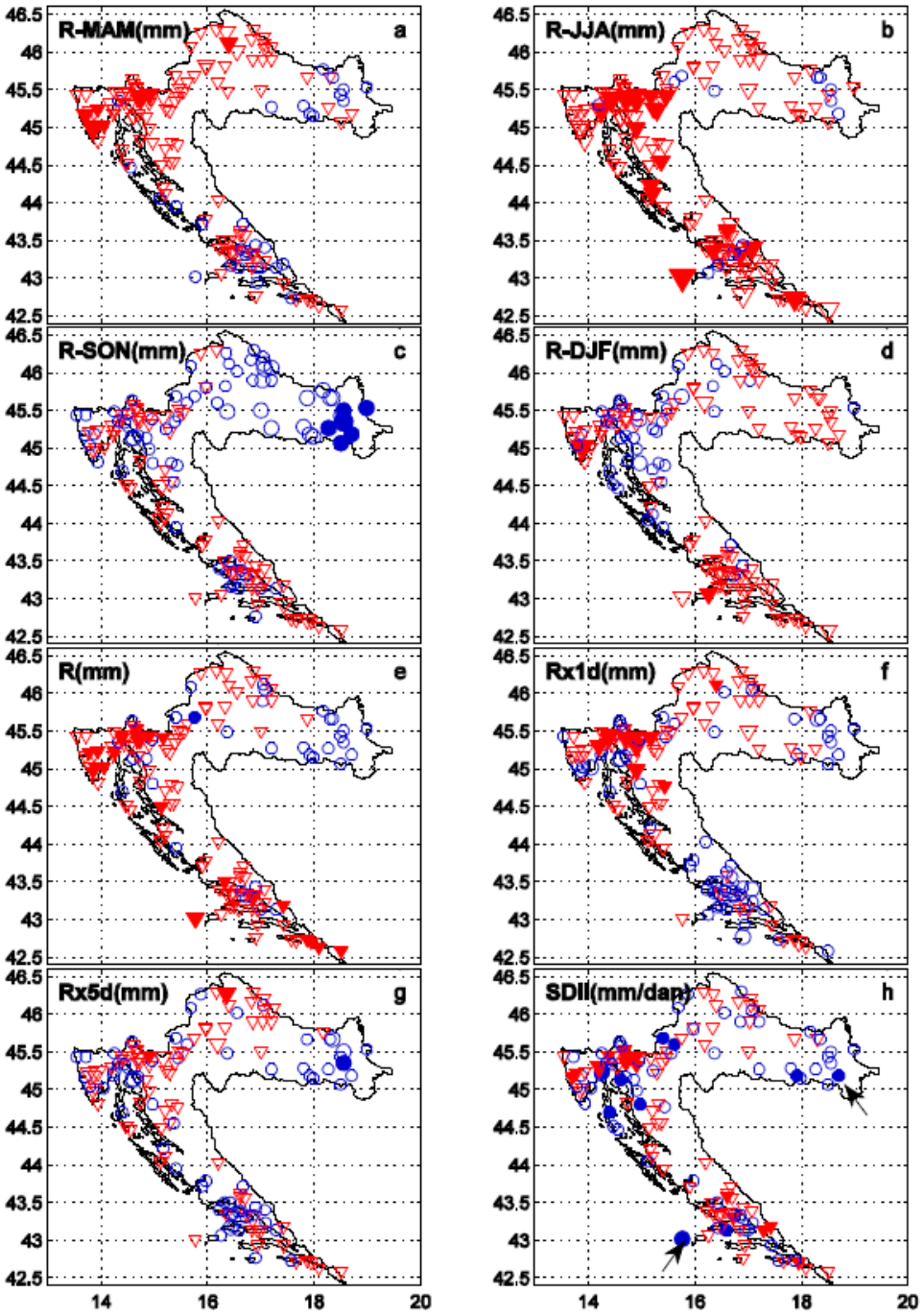

Figure 2-4. Decadal trends (%/10yrs) in seasonal and annual precipitation (R-MAM, R-JJA, R-SON. R-DJF, R) and precipitation indices (Rx1d, Rx5d, SDII, R75, R95, R25T, R25-50T, R50-75T, R75-95T, R95T and DD) in the 1961-2010 period. Circles denote positive trends, triangles the negative one, whereas filling means statistically significant trend. Four sizes of symbols are proportional to the absolute value of change per decade relative to the respective average from the period 1961-1990: <5%, 5-10%, 10-15% and >15%, respectively [12]

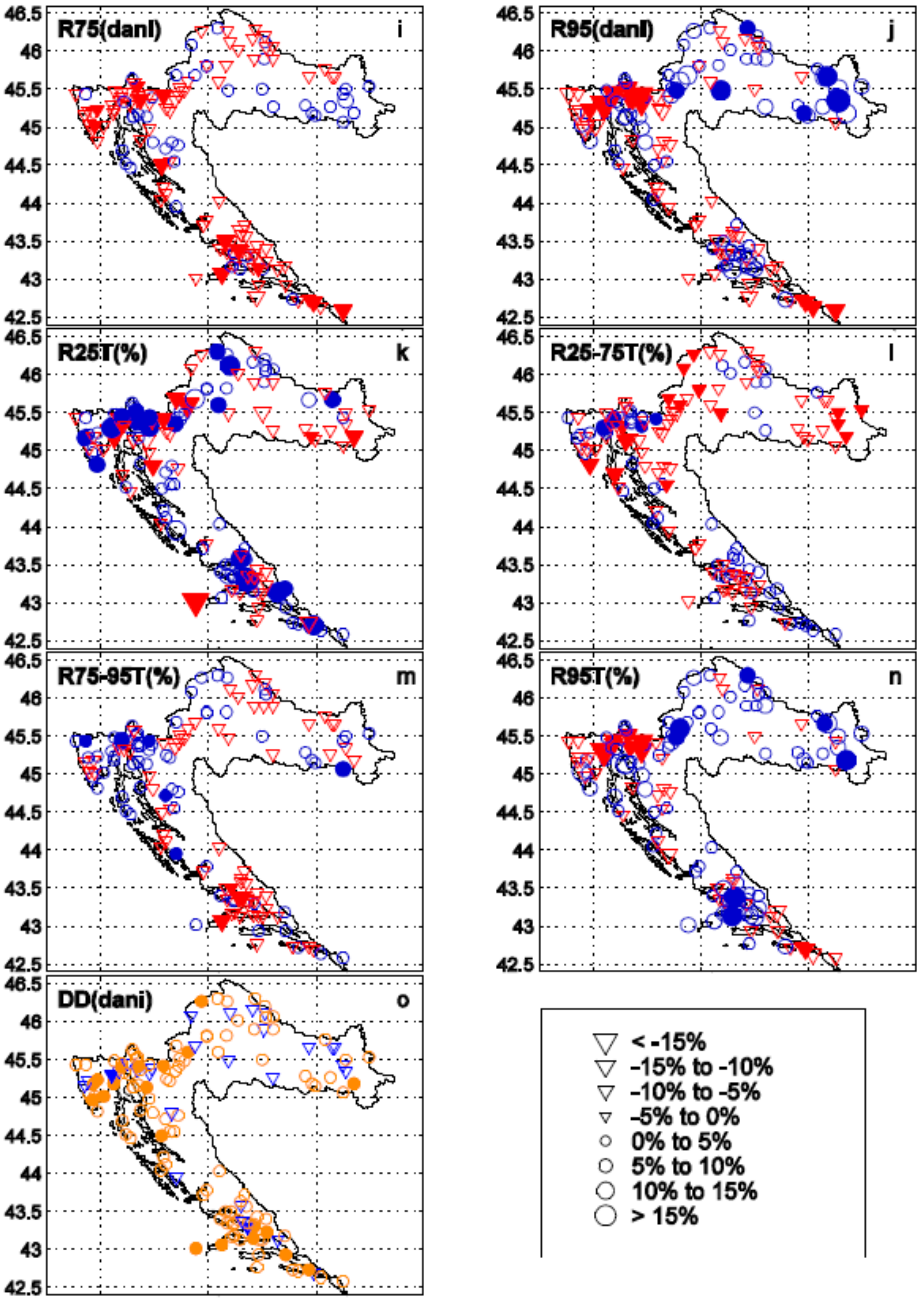

Figure2-4. cont. [12]

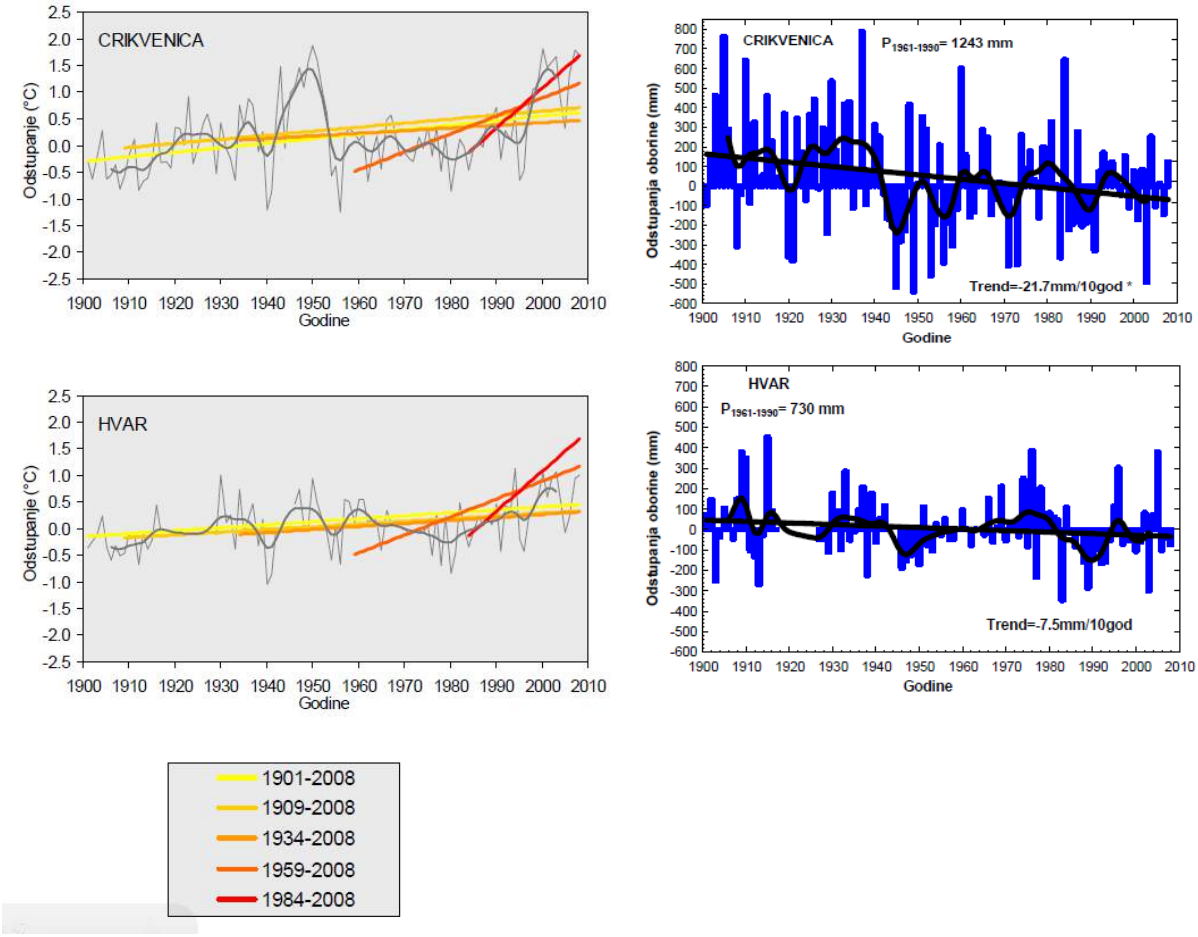

Figure 2-5. Time series of deviations from the mean (1961-1990) for stations Crikvenica and Hvar: left - mean annual air temperatures; right - annual precipitation amounts [16]

3. CLIMATE CHANGE SCENARIOS

On the Croatian area for the assessment of climate change several climate models are used. The most common is climate model RegCM, developed in *International Centre for Theoretical Physics* in Trieste *[17]*, which was used for climate predictions for the period 2011-2040 within the *Sixth National Communication, 2014 [12].* It is a regional climate model which, for climate change simulations, takes initial and boundary conditions from joint global climate model ECHAM5/MPI-OM *[18], [19]*. For climate change assessment for the period up to the year 2100 in the framework of project CCWaterS *[20]*, with mentioned RegCM, model Aladin was also used *[21]*, and model Promes *[22]* where climate change projections are made until the year 2050.

In (for Croatia) reference *Sixth National Communication, 2014*, the results of the future climate change in a broader region of Croatia are discussed for temperature at 2 m (T2m) and precipitation. The results for each parameter are obtained from the two data sources:

a) from dynamical downscaling by the RegCM RCM made at the Croatian Meteorological and Hydrological Service (DHMZ) for the IPCC A2 scenario (Nakićenović et al., 2000) and
b) from dynamical downscaling of various RCMs that participated in the European project ENSEMBLES (van der Linden and Mitchell 2009, Christensen et al. 2010) for the IPCC A1B scenario *[12]*.

Climate changes in Croatia were analyzed with model RegCM for two 30-year periods:

1. Period from year 2011 to 2040 represents the near future, and is of greatest interest for the users of climate information in long-term planning of climate change adaptation.
2. Period from year 2041 to 2070 represents the middle of the 21st century in which, by the A2 scenario, further increase of the carbon dioxide concentration (CO_2) in the atmosphere is predicted, and the signal of climate change is stronger *[23]*.

In the first period of future climate (2011-2040) in Croatia (Figure 3-1) during winter a temperature increase of 0.6 °C is expected, and 1°C during summer *[23].*

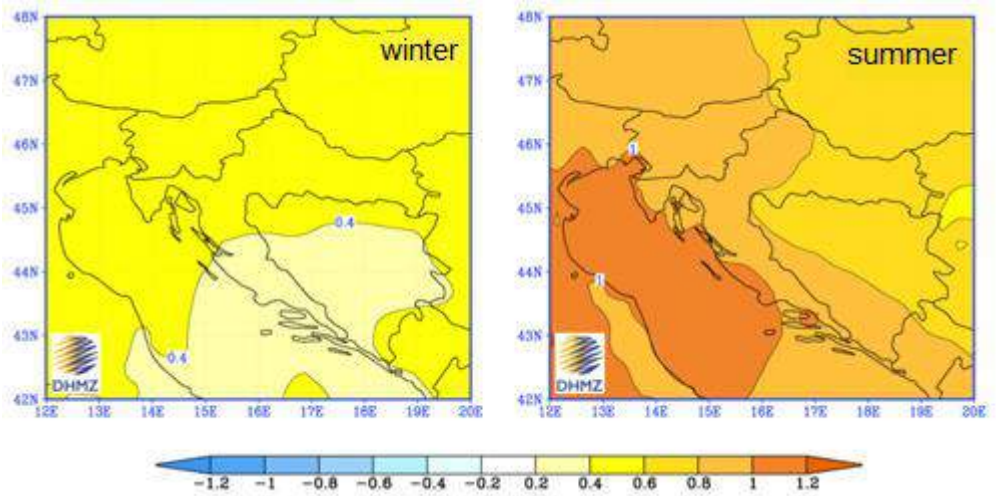

Figure 3-1. Change in ground air temperature (in °C) in Croatia in the period 2011-2040 in respect of the period 1961-1990 according to the results of the ensemble mean of regional climate model RegCM for the A2 scenario of greenhouse gas emissions for winter (left) and summer (right) [23]

In the second period of future climate (2041-2070) the expected increase amplitude in Croatia (Figure 3-2) during winter is up to 2 °C in continental part and up to 1.6 °C in the south, and during summer up to 2.4 °C in the continental Croatia, and up to 3 °C in the coastal zone *[23]*.

Changes in precipitation amounts **in the near future** (2011-2040) are very small and limited to smaller areas, and they vary in the sign depending of the season (Figure 3-3). The biggest change in precipitation, according to A2 scenario, can be expected in the Adriatic in autumn when RegCM indicates a decrease of precipitation with a maximum of approximately 45-50 mm in the southern Adriatic. However, this reduction of autumn precipitation amount is not statistically significant *[23]*.

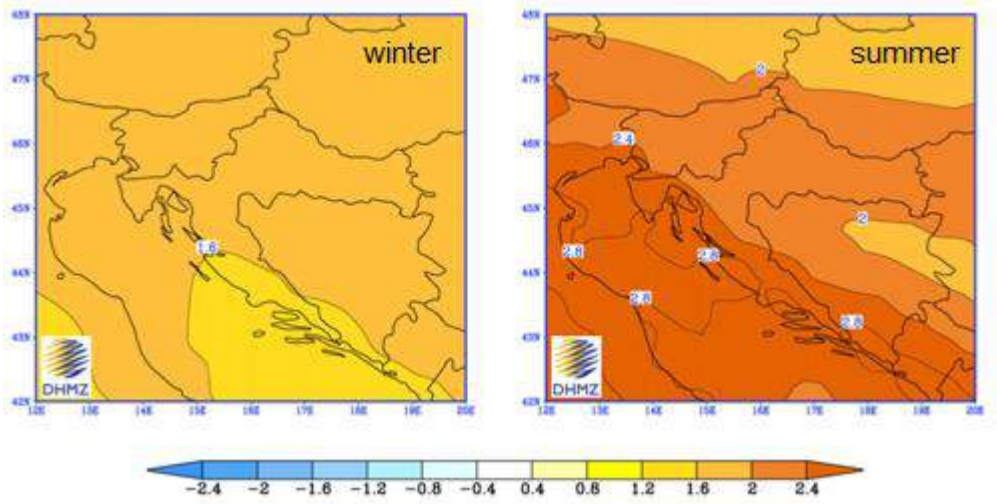

Figure 3-2. Change in ground air temperature (in °C) in Croatia in the period 2041-2070 in respect of the period 1961-1990 according to the results of the ensemble mean of regional climate model RegCM for the A2 scenario of greenhouse gas emissions for winter (left) and summer (right) [23]

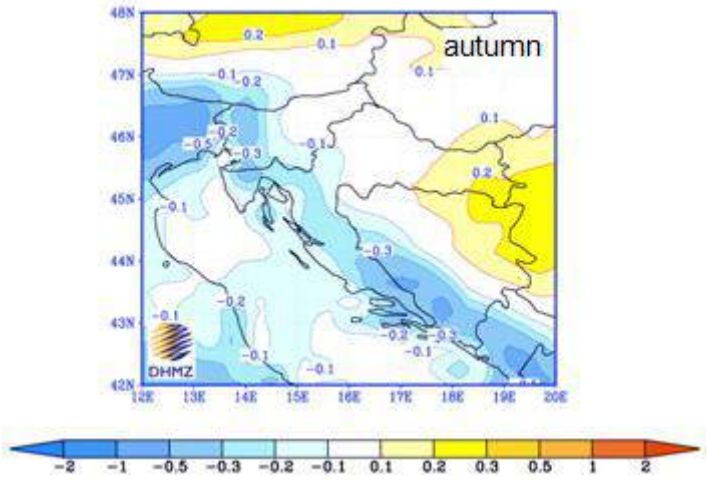

Figure 3-3. Change in precipitation in Croatia (in mm/day) in the period 2011-2040 in respect of the period 1961-1990 according to the results of the ensemble mean of regional climate model RegCM for the A2 scenario of greenhouse gas emissions for autumn [23]

In the second period of future climate (2041-2070) precipitation changes in Croatia are somewhat more expressed (Figure 3-4). During summer in the mountainous Croatia and in the coastal area a decrease in precipitation is expected. Reductions reach value of 45-50 mm and they are statistically significant. During winter an increase in precipitation in north-western Croatia and on the Adriatic can be expected, however that increase is not statistically significant *[23]*.

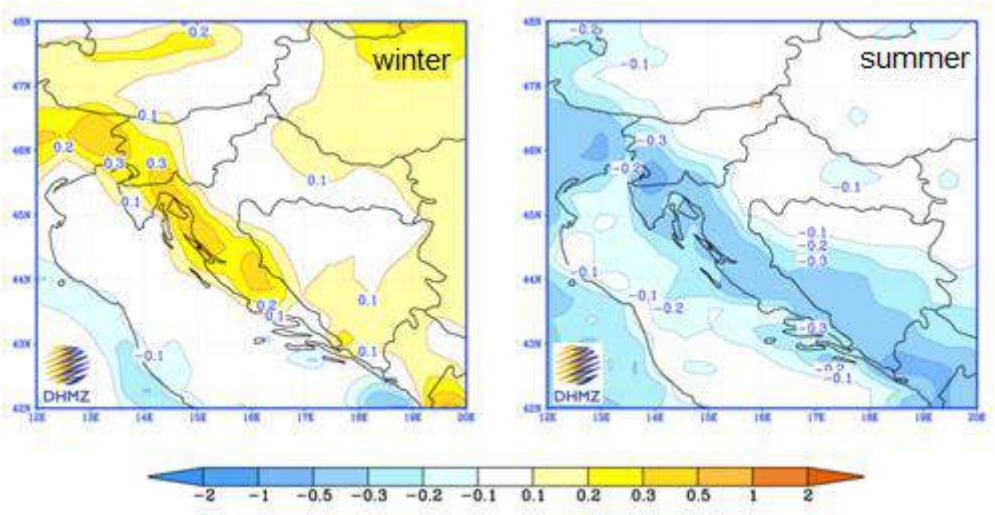

Figure 3-4. Change in precipitation in Croatia (in mm/day) in the period 2041-2070 in respect of the period 1961-1990 according to the results of the ensemble mean of regional climate model RegCM for the A2 scenario of greenhouse gas emissions for winter (left) and summer (right) [23]

For the purpose of project CCWaterS *[20]* realisation on pilot areas in Croatia, DHMZ (2010) made estimates of climate conditions for three pilot areas in Croatia, which were represented by selected climatological stations Cres (North Adriatic), Zadar (Middle Adriatic) and Vela Luka on the island of Korčula (South Adriatic). For illustration, the results of conducted climate change predictions in the temperature (Figure 3-5) and precipitation regime (Figure 3-6) are chosen on station Vela Luka, given that within the project DRINK ADRIA continuation of activities in pilot area Blato on the island of Korčula is predicted (activities started in project CCWaterS). P0 indicates reference 30-year period 1961-1990, P1 (2021-2050), and P2 (2071-2100) *[24], [25]*.

According to the *Sixth National Communication, 2014*, although the Republic of Croatia belongs to a group of countries for which water issues are not a limiting factor of development, climate changes will cause problems in water supply and meeting the evergrowing drinking water requirements. Research show that water resources in Croatia are already under challenge of climate change, as certain impacts and changes occur in regard to water flow, evapotranspiration, groundwater inflow, water level in rivers and lakes, water temperature, etc. Change in precipitation form will influence not only the discharge, but the intensity, time period and frequency of floods and droughts as well. Some sources estimate that discharges in the largest watercourses of the Republic of Croatia will be decreased by 10% to 20%, although in eastern part of the country such

change could be less than 10%. This issue requires research, since results of global and regional models of climate change indicate changes in precipitation in Croatia. Moreover, evapotranspiration increase due to temperature rise could also make an impact. The Government of the Republic of Croatia adopted the River Basin Management Plan (OG No. 82/2013) and Croatian Waters prepare the Flood Risk Management Plan. In their measure programmes, documents contain adaptation measures to climate change consequences *[12]*.

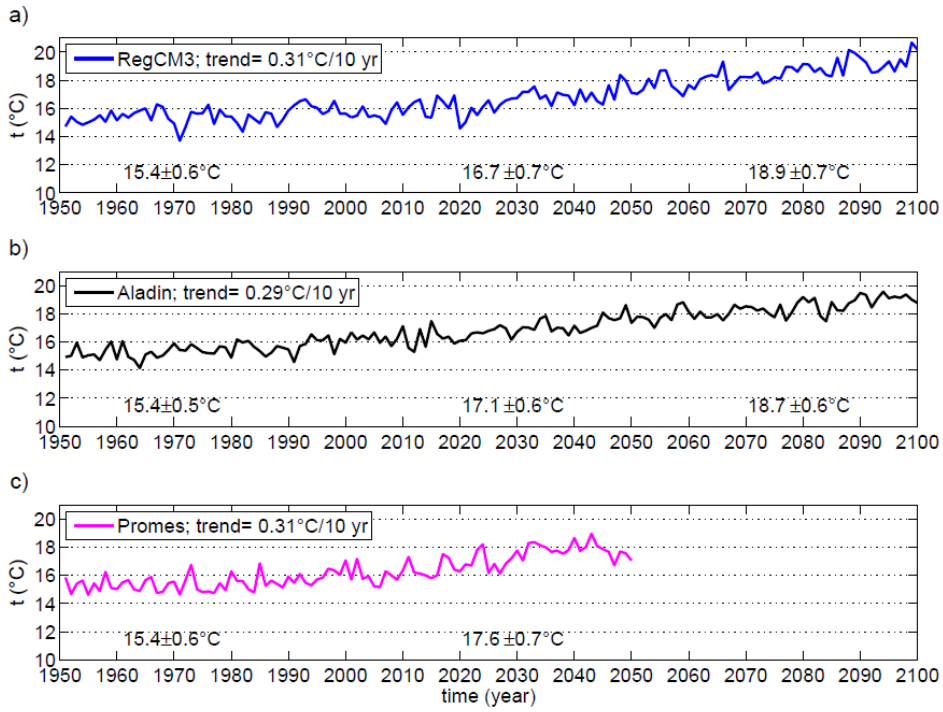

Figure 3-5. The Blato catchment: annual mean temperatures a) RegCM3 b) Aladin c) Promes. In each panel decadal trend based on entire available time series is shown. Additional numbers at the bottom of each panel are mean values and standard deviations during P0, P1 and P2. [24]

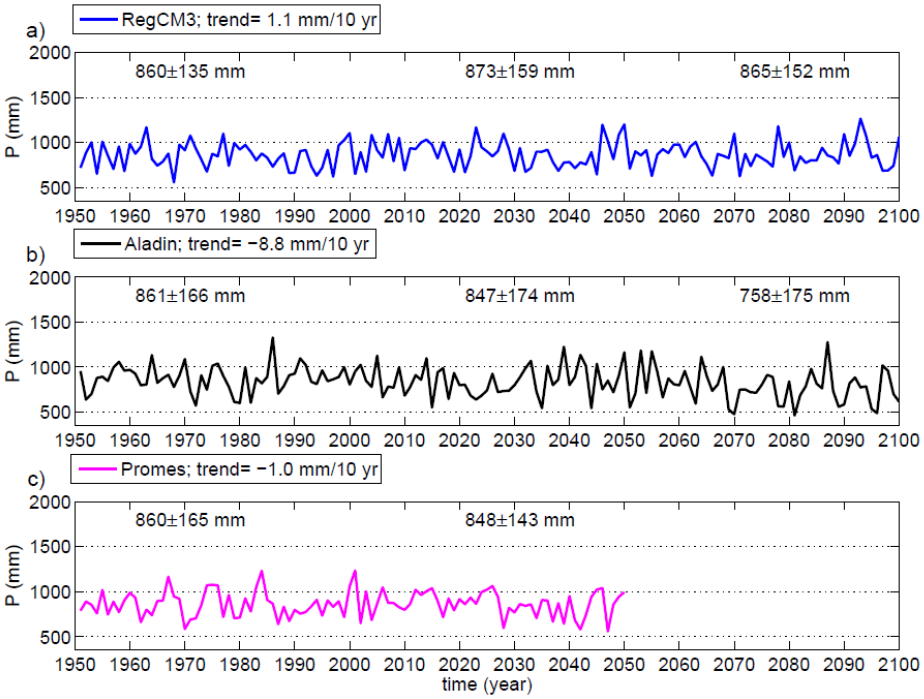

Figure 3-6. The Blato catchment: annual precipitation amounts a) RegCM3 b) Aladin c) Promes. In each panel decadal trend based on entire available time series is shown. Additional numbers at the bottom of each panel are mean values and standard deviations during P0, P1 and P2. [24]

4. CLIMATE AND CLIMATE CHANGE OVER THE CROATIAN ADRIATIC

Following content is extracted from the report *[26]* in order to highlight the features of the Adriatic part of Croatia.

4.1. Introduction

Climate of the two meteorological parameters, 2m air temperature (*T2m*) and total precipitation (*R*), over the Croatian Adriatic region for the reference period 1961-1990 and the projection of the near-future climate in the 21st century will be described in the following text. These two climatological parameters will be analysed in detail for the two Croatian pilot areas: Mirna River and Prud wellspring catchments within the DRINKADRIA project. The future climate projections for the Croatian Adriatic are based on the downscaling simulations of regional climate models (RCMs). Owing to their relatively high horizontal resolution (between 10 and 50 km), RCMs are normally used to study regional climate and climate change. They are more appropriate than global climate models (GCMs) for describing climate at relatively small spatial scales where local topography and the land-sea distribution are important. However, in the process of dynamical downscaling the RCM results strongly depend on the quality of the boundary conditions which are typically provided either by GCMs or by reanalysis data (e.g. *[27]*; *[28]*). In this report, the analysed projections of the 21st century air temperature and precipitation are obtained from various RCMs that participated in the EU FP6 project ENSEMBLES (*[29]*, *[30]*) using the IPCC[1] A1B scenario of the greenhouse gases concentrations *[31]*. More details are given in the *Sixth National Communication, 2014 [12]*[2].

4.2. Data and methodology

The average climate conditions shown and discussed here for the Croatian Adriatic in the reference climate period 1961-1990 are based on the data from the Climate Atlas of Croatia *[14]* and on an analysis of the climate conditions over the Adriatic catchments regions *[32]*. In this overview the average annual cycle of air temperature and precipitation is discussed and their seasonality, that would be used to calculate the water balance components, is emphasised. The data series are obtained from the Croatian Meteorological and Hydrological Service (DHMZ), where a routine operational quality control recommended by WMO (*[33]*, *[14]*), is carried out. The long-term changes in the observed annual and seasonal air temperature and precipitation are analysed for the 1961-2010 period. Most results presented and discussed here are described in *[12]* and in *[34]*. Trends are estimated by the Kendall's tau method and the non-parametric Mann-Kendall test was applied to determine statistical significance of trends at the 95% confidence level *[35]*.
From the ENSEMBLES database, 18 combinations of various RCMs, all available at a 25-km horizontal resolution, and forced by various GCMs are analysed (Table 4.2-1). The RCMs results of the future climate are discussed only for the period 2011-2040 (denoted as P1). For other future periods of the 21st century the results are presented in *[12]*. The climate change in the future period is computed as the differences between the 30-year

[1] Intergovernmental Panel on Climate Change (http://www.ipcc.ch)

[2] Available from http://unfccc.int/national_reports/annex_i_natcom/submitted_natcom/items/7742.php

means of the P1 and P0 periods. Additionally, the agreement in the sign of the projected changes among different RCMs is determined.

Table 4.2-1: Analysed regional climate models (RCMs), organisations which performed the simulations and the sources of the boundary conditions (see [12] for more details) [

	Regional climate model	Organisation	Global climate model providing the boundary conditions
1.	RCA3	C4I	HadCM3Q16
2.	RM5.1	CNRM	HadCM3Q1
3.	HIRHAM5	DMI	ARPEGE
4.	HIRHAM5	DMI	ECHAM5
5.	HIRHAM5	DMI	BCM
6.	CLM	ETHZ	HadCM3Q0
7.	RegCM3	ICTP	ECHAM5
8.	RACMO2	KNMI	ECHAM5
9.	HadRM3Q0	MetoHC	HadCM3Q0
10.	HadRM3Q16	MetoHC	HadCM3Q16
11.	HadRM3Q3	MetoHC	HadCM3Q3
12.	REMO	MPI-M	ECHAM5
13.	RCA3	SMHI	BCM
14.	RCA3	SMHI	ECHAM5
15.	RCA3	SMHI	HadCM3Q3
16.	HIRHAM	Met.No	BCM
17.	HIRHAM	Met.No	HadCM3Q0
18.	PROMES	UCLM	HadCM3Q0

4.3. Croatian Adriatic climate in the reference period

Climate of the Croatian Adriatic is primarily determined by circulation of the northern mid-latitudes weather systems with frequent and often intense changes of the local weather during the most part of the year *[14]*. In the summer, this area is influenced by the ridge of the Azorean high with prevailing dry and warm weather and with regular daily wind circulation from the sea and the night circulation down the hill slopes towards the sea. Local factors - the land/sea contrast and high and steep orography of the Dinarides - together with the north-Adriatic cyclogenetic effect, strongly affect climate of the Croatian Adriatic. In calm weather, which normally prevails during the cold part of the year and at night, the local geophysical conditions are dominant and relatively large differences in the values of meteorological parameters can occur even at nearby stations. Cyclonic activity, typical for winter, early spring and late autumn, affects cloudiness and precipitation regime of both coastal areas and the hinterland.

The Croatian Adriatic river catchments (Figure 4.4-1) cover the coastal area and its hinterland, including the mountainous regions of Gorski kotar and Lika, where the mountainous climate is present. Over the Croatian Adriatic catchments, July is the hottest and January is the coldest month in the annual cycle of the mean monthly air temperature (see Figures 2a and 2b in *[32]*). Such annual cycle is under a strong influence of the sea and has typically maritime characteristics with the autumn season (SON) being warmer than the spring (MAM). The effect of the sea on the climate of the Adriatic islands and in a wider coastal zone of Istria is manifested as a moderation of the minimum air temperature. However, in the mountainous areas of the coastal basin, due to strong winter radiative cooling, the minimum temperatures attain their lowest values, especially at the Lika plateau (-28.9ºC in Gospić) as well as in the interior of the Istrian peninsula (-18.7ºC in Pazin). The influence of the sea is also manifested in a reduction of the amplitude of the extreme temperatures on the Dalmatian islands (Lastovo: tmax=36.2ºC, tmin=-6.8ºC) and at the coast (Zadar: tmax=35.7ºC, tmin=-9.1ºC). Away from the coast, in the karst fields of the Dalmatian hinterland, the impacts of winter cooling and of summer warming are, on the other hand, enhanced, resulting in higher absolute maxima and lower absolute minima (e.g. Sinj: tmax=39.3ºC, tmin=-22.2ºC) than at the coast.

The entire area has a maritime precipitation regime with larger amounts of precipitation in the cold (October to March) than in the warm part (April to September) of the year, and with the minimum in summer (see Figures 3a and 3b in *[32]*).

The maximum in the precipitation annual cycle occurs in November (on the Dalmatian islands in December), but with different amplitudes at different locations (Pazin: 134 mm, Rijeka: 175 mm, Gospić: 179 mm, Cres: 136 mm, Split–Marjan: 108 mm, Knin: 122 mm, Opuzen: 180 mm, Hvar: 91 mm). The monthly minimum appears in July (Pazin: 72 mm, Rijeka: 81 mm, Gospić: 66 mm, Cres: 53 mm, Split-Marjan: 28 mm, Knin: 46 mm, Opuzen: 36 mm, Hvar: 25 mm). Interannual variability of monthly amounts is largest in October in Primorje-Istrian basin (70-90% of the total precipitation for that month) and in the Dalmatian hinterland (about 80%), and in July in the southern part of the Croatian Adriatic - on the Dalmatian islands and in the Neretva River valley (120%) and in the Dubrovnik area (100%). The least variable (most stable) on the year-to-year basis are the precipitation amounts in April (31-62%) over the whole area of the Adriatic catchments.

The annual precipitation totals are highest in the Primorje-Istrian catchment: in Gorski Kotar (Parg 1849 mm) and Lika (Zavižan 1899 mm and Gospić 1369 mm) and over a broader area of Rijeka (Rijeka 1561 mm). The amounts decrease from the coast towards the outer islands (Cres 1053 mm), and from the interior of the Istrian Peninsula (Pazin 1167 mm) to the coast (Pula 847 mm). Over the Dalmatian basin, the largest annual amounts are found in the hinterland and increasing from the northwest (Knin 1074 mm) to the southeast (Opuzen 1308 mm). The lowest amounts are at the Dalmatian islands and they increase from the outer islands towards the coast (Lastovo 691 mm, Hvar 730 mm, Split-Marjan 825 mm). Interannual variability of the annual precipitation amounts is smaller than that for monthly amounts (c_v is from 10% to 24%).

4.4. Observed trends

Observed trends in the annual and seasonal quantities of climate parameters indicate their temporal change over the area of interest. Temperature trends are calculated for deviations (anomalies) of air temperature from the 1961-1990 mean and expressed in °C per decade. In three seasons, JJA, MAM and DJF, trends in the mean air temperature show warming all over Croatian Adriatic while trends in SON are of the mixed sign (Figure 4.4-2). The annual temperature trends are all positive and significant, and they range mostly between 0.2°C and 0.3°C per decade.

During the recent 50-year period (1961-2010) the prevailing trends in the annual precipitation amounts indicate a decrease in precipitation which, at most stations, is statistically insignificant (Figure 4.4-3). The trend values go down to the 7% of the respective climate means. Generally, when negative trends are observed for the whole year, they are mainly caused by decreasing trends (drying) in the summer; the summer trends, in turn, are found to be statistically significant at most stations in the mountainous region and at some stations along the Adriatic and its hinterland.

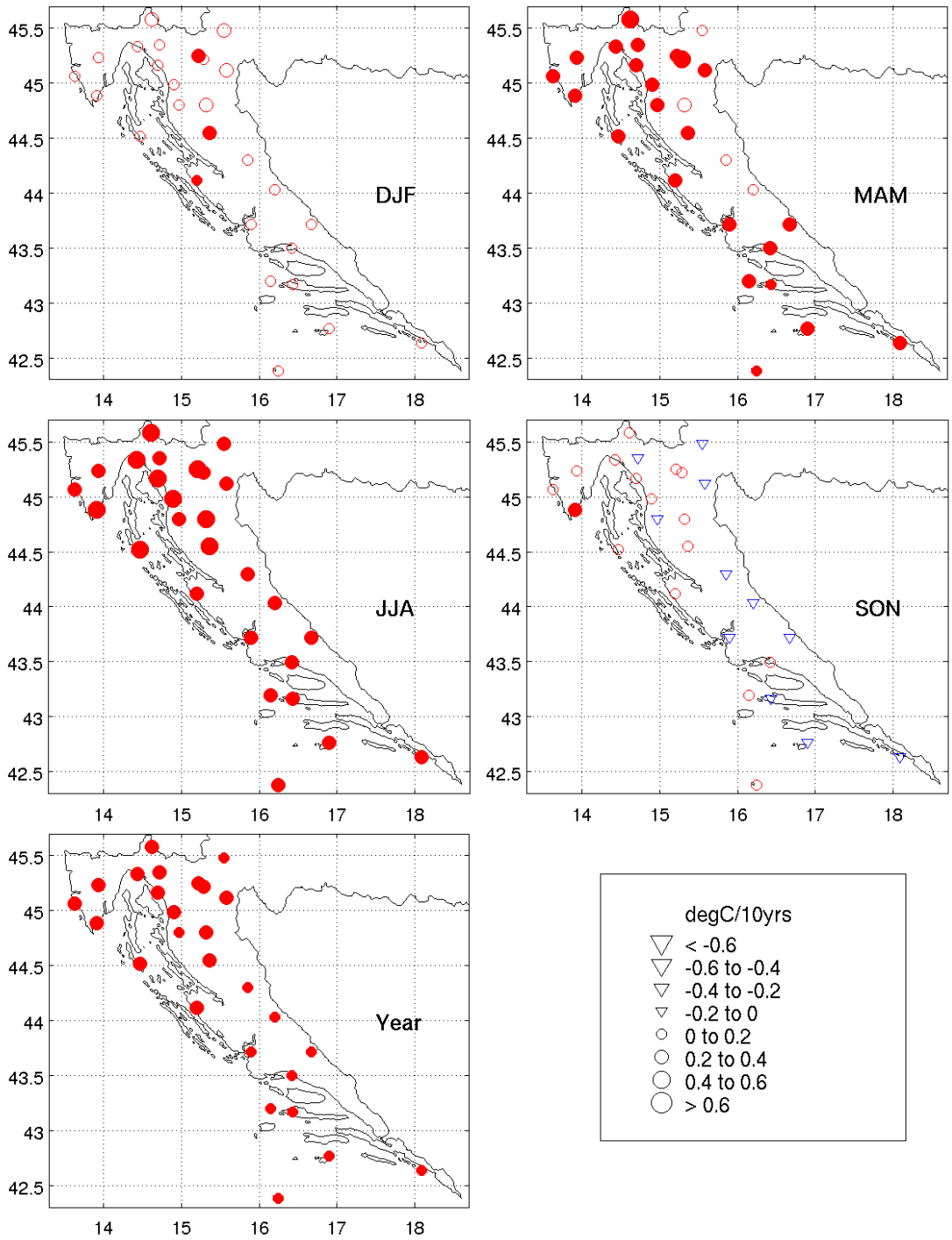

Figure 4.4-2. Decadal trends (°C/decade) in the annual and seasonal (DJF-winter, MAM-spring, JJA-summer, SON-autumn) mean air temperature in the 1961-2010 period. Circles denote positive trends, triangles the negative ones; solid symbols indicate statistically significant trend at the 5% confidence level. The symbol size is proportional to the magnitude of change (in °C) per decade. [26]

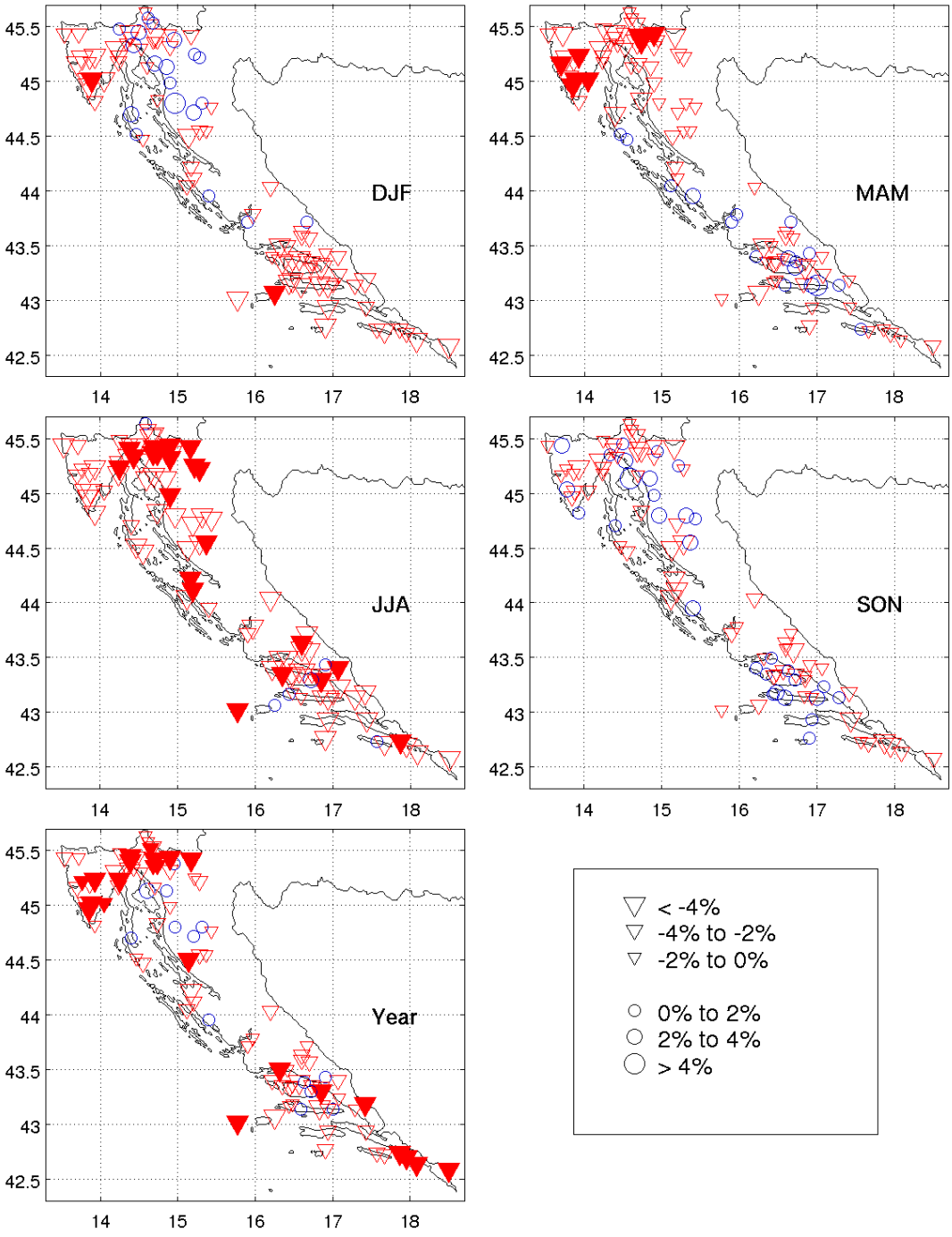

Figure 4.4-3. Decadal trends (%/10yrs) in annual (R) and seasonal precipitation (R-MAM, R-JJA, R-SON, R-DJF) in the 1961-2010 period. Circles denote positive trends, triangles the negative one, whereas filling means statistically significant trend at 5% level. Three sizes of symbols are proportional to the absolute value of change per decade relative to the respective average from the period 1961-1990: <2%, 2-4%, and >4%, respectively. [26]

Annual and seasonal long-term precipitation trends for the period 1961-2010, expressed as absolute changes (in mm/decade), are calculated for five regions which belong to the Croatian Adriatic catchments (Table 4.4-1). During the recent 50-year period, trends in the annual precipitation amounts are negative (indicating a reduction in precipitation) in all regions; only in Gorski kotar this trend is statistically significant (-50.6 mm/10yrs). In spring and summer, drying occurred in all regions, but it is statistically significant only during summer in three regions. In other seasons a decreasing trend prevails but it is not statistically significant *[36]*.

Table 4.4-1: Decadal trends in annual and seasonal precipitation amounts for five sub-regions in the Croatian Adriatic catchments in the period 1961-2010. Statistically significant trends at the 95% confidence level are in bold. [36]

Regions	MAM	JJA	SON	DJF	YEAR
Lika and Dalmatian hinterland	-3.6	**-16.0**	-3.6	-6.0	-24.6
Gorski kotar	-12.5	**-21.0**	-15.5	-7.9	**-50.6**
Littoral of Kvarner bay	-4.0	**-22.6**	4.0	2.9	-7.7
Istria and Northern coastal region	-7.9	-10.8	-7.9	-5.9	-24.7
Central and Southern coastal region	-1.4	-7.1	-1.7	-15.9	-28.9

4.5. Simulated climate change

Projected differences between P1 and P0 periods according to ENSEMBLES simulations are presented in this section. Additionally, agreement in the sign of the projected changes is determined by evaluating if the same sign of simulated climate change as in the difference between the entire ensemble means is simulated by the two thirds of all ENSEMBLES RCMs considered here.

The RCM simulations from the ENSEMBLES project indicate for the P1 period an increase of 2m air temperature (*T2m*) in all seasons with the amplitude typically between 1°C and 1.5°C (Fig. 4.5-1). A somewhat higher warming, between 1.5°C and 1.75°C, is projected over central and southern Dalmatia during the summer (Fig. 4.5-1 c). For the P1 period, more than the two-thirds of all ENSEMBLES models agree in the sign of projected changes (warming) when compared to the P0 period. A weak decrease of the mean *T2m* amounting to -0.5°C may be possible in some months during P1, mostly as the consequence of internal variability of the climate system. However, in the rest of the 21st century and for the IPCC A1B scenario all ENSEMBLES simulations indicate only warming, on both seasonal and monthly timescales (e.g. *[38]*; *[12]*).

In the first part of the 21st century (P1), the total precipitation amount *R* during winter is projected to increase over parts of the Kvarner region with the amplitude between approximately 5% and 15% relative to the reference period P0, 1961-1990 (Fig. 4.5-2 a). The sign of these changes agrees in at least the two thirds of all models.

For the summer season in the same period P1, *R* is projected to decrease from approximately -5% down to -15% over large parts of the Dalmatian hinterland, the mountainous region of Gorski kotar and the Lika highlands (Fig. 4.5-2 c). This decrease in precipitation is also found in at least the two-thirds of the models. A reduction of precipitation of the same amplitude is projected for the southern Croatia during spring (Fig. 4.5-2 b), while during autumn the projected changes are almost negligible, between approximately -5% and +5% (Fig. 4.5-2 d). For more details and similar analysis of the later periods of the 21st century see *[12]*.

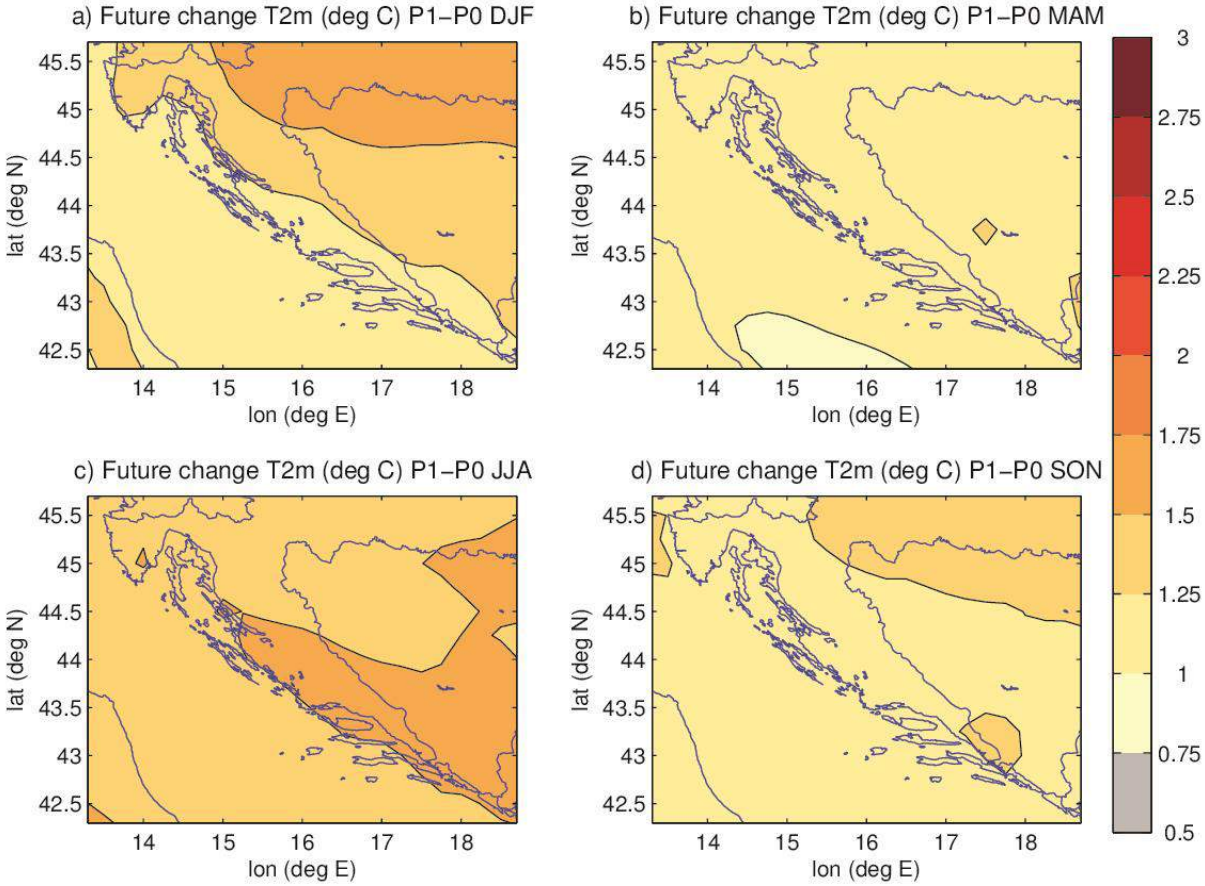

Figure 4.5-1. The air temperature ensemble-mean difference between the periods P1 (2011-2040) and P0 (1961-1990): a) winter (DJF), b) spring (MAM), c) summer (JJA) and d) autumn (SON). Units are °C. In all grid points, the sign of change in at least the two-thirds of the models agrees with the sign of change in the ensemble mean.[26]

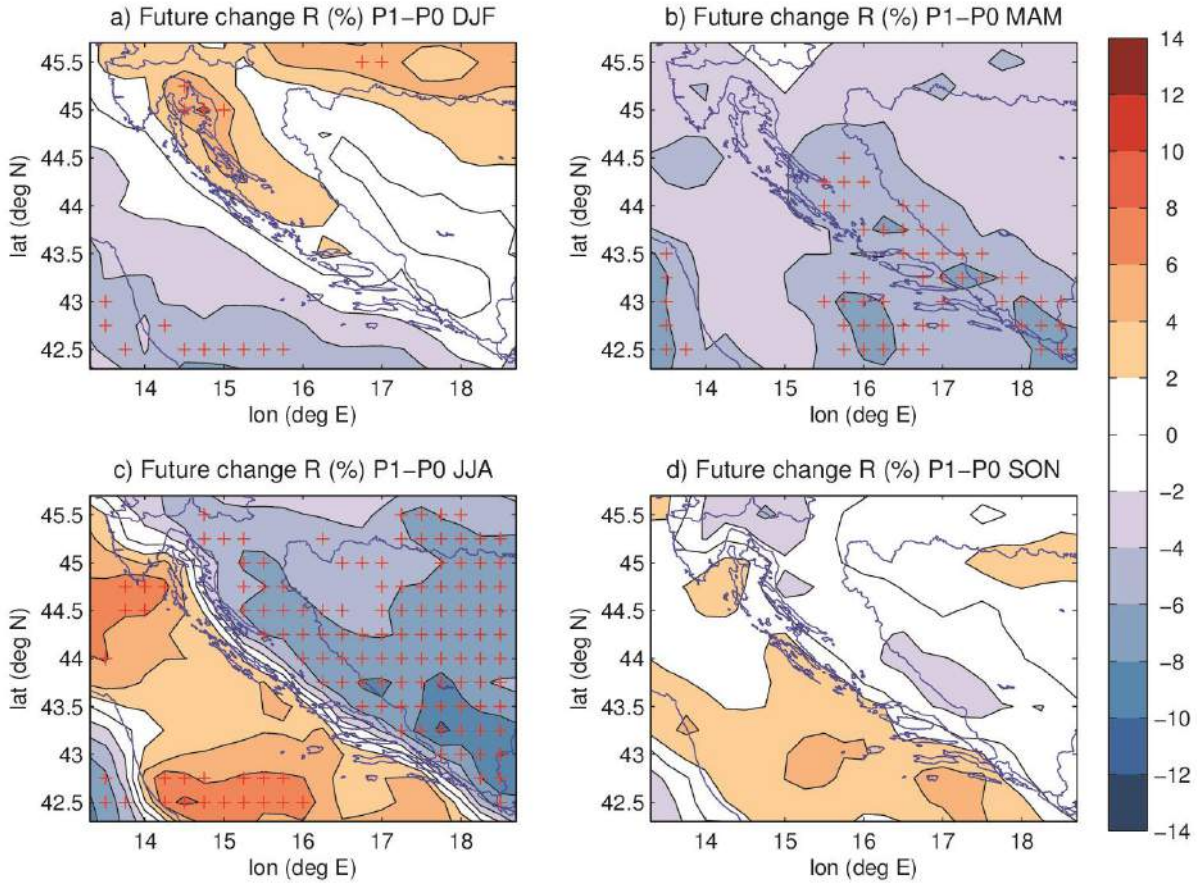

Figure 4.5-2. Ensemble-mean relative difference (in %) of the total precipitation between the periods P1 and P0 in: a) winter (DJF), b) spring (MAM), c) summer (JJA) and d) autumn (SON). The + marker denotes grid points where the sign of change in at least the two-thirds of the models agrees with the sign of change of the ensemble mean difference and when the relative difference of ensemble means is outside the interval ±5%.

5. LITERATURE

[1] Bradley, R. S., Jones, P. D. (1995): Climate since A.D. 1500, Routledge, London & New York, pp 706.

[2] Bolle, H. J. (2003): Mediteran climate - variability and trends. Springer Verlag, Berlin, pp 320.

[3] Leroux, M. (2005): Global Warming - Myth or Reality? - The Erring Ways of Climatology. Chichester: Springer.

[4] Lionello, P., Malanotte-Rizzoli, P., Boscolo, R., eds., (2006): Mediterranean Climate Variability. Amsterdam: Elsevier, pp 422.

[5] IPCC (2007): Summary for Policymakers. In: Climate Change 2007: The Physical Science Basis. Contribution of Working Group I to the Fourth Assessment Report of the Intergovernmental Panel on Climate Change (ed. by S. Solomon, D. Qin, M. Manning, Z. Chen, M. Marquis, K. B. Averyt, M. Tignor & H. L. Miller), 1–18. Cambridge University Press, UK and New York, NY, USA (http://www.ipcc.ch/pdf/assessment-report/ar4/wg1/ar4-wg1-spm.pdf)

[6] Kundzewicz, Z. W., Mata, L.J., Arnell, N.W., Döll, P., Kabat, P., Jiménez, B., Miller, K. A., Oki, T., Sen, Z., Shiklomanov, I.A. (2007): Freshwater resources and their management. Climate Change 2007: Impacts, Adaptation and Vulnerability. Contribution of Working Group II to the Fourth Assessment Report of the Intergovernmental Panel on Climate Change, M.L. Parry, O.F. Canziani, J.P. Palutikof, P.J. van der Linden and C.E. Hanson, Eds., Cambridge University Press, Cambridge, UK, 173-210.
[7] Kundzewicz, Z.W., Mata, L.J., Arnell, N.W., Döll, P., Kabat, P., Jiménez, B., Miller, K.A., Oki, T., Sen, Z., Shiklomanov, I. A. (2008): The implications of projected climate change for freshwater resources and their management. Hydrological Sciences Journal, 53:1, 3-10.
[8] Svensson, C., Kundzewicz, Z.W., Maurer, T. (2004): Trends in flood and low flow hydrological time series. Report to the World Meteorological Organization (WMO), World Climate Programme-Water. World Climate Programme Applications and Services Report WCASP–66, WMO/TD no. 1241. WMO, Geneva. Also published by the Global Runoff Data Centre (GRDC) under the title “Trends in flood and low flow series” in the GRDC (Report no. 33), GRDC, Koblenz.
[9] Cudennec, C., Leduc, C., Koutsoyiannis, D. (2007): Dryland hydrology in Mediterranean regions - a review. Hydrological Sciences Journal, 52(6), pp 1077-87.
[10] IPCC (2001): Climate Change 2001: The scientific Basis. Contribution of Working Group I to the Third Assessment Report of the Intergovernmental Panel on Climate Change. Houghton, J.T. et al. (eds.). Cambridge University Press, Cambridge, UK and New York, NY, USA, pp 881.
[11] First national communication of the Republic of Croatia to the United Nations Framework Convention on Climate Change (UNFCCC), Republic of Croatia, Ministry of Environmental Protection and Physical Planning, 2001.
[12] MZOIP (2014): Sixth National Communication and First Biennial Report of the Republic of Croatia under the United Nations Framework Convention on Climate Change (UNFCCC), Republic of Croatia, Ministry of Environmental and Nature Protection (MZOIP), 2014.
[13] http://croaticum.ffzg.unizg.hr/hrv/hrvatska.html
[14] Zaninović, K., Gajić-Čapka, M., Perčec Tadić, M., Vučetić, M. et all. (2008): Klimatsaki atlas Hrvatske / Climate atlas of Croatia 1961−1990, 1971−2000. Državni hidrometeorološki zavod (DHMZ), Zagreb.
[15] Fifth National Communication of the Republic of Croatia under the United Nation Framework Convention on the Climate Change, Republic of Croatia, Ministry of Environmental Protection, Physical Planning and Construction, 2010.
[16] DHMZ (2009): Peto nacionalno izvješće Republike Hrvatske prema Okvirnoj konvenciji Ujedinjenih naroda o promjeni klime (UNFCCC) - Izabrana poglavlja, Zagreb, pp 47.
[17] Pal, J.S. et all. (2007): The ICTP RegCM3 and RegCNET: Regional climate modeling for the developing world, Bull. Amer. Meteor. Soc., 88, 1395–1409.
[18] Roeckner, E., Bäuml, G., Bonaventura, L., Brokopf, R., Esch, M., Giorgetta, M., Hagemann, S., Kirchner, I., Kornblueh, L., Manzini, E., Rhodin, A., Schlese, U., Schulzweida, U., Tompkins, A. (2003): The atmospheric general circulation model

ECHAM5. Part I: model description. Max-Planck Institute for Meteorology Rep. 349, Hamburg, pp 127.
[19] Marsland, G.A., Haak, H., Jungclaus, J.H., Latif, M., Röske, F. (2003): The Max Planck Institute global/sea-ice model with orthogonal curvilinear coordinates. Ocean Model 5, 91-127.
[20] http://www.ccwaters.eu/
[21] Bubnová, R., Hello, G., Bénard, P., Geleyn, J.F. (1995): Integration of the Fully Elastic Equations Cast in the Hydrostatic Pressure Terrain-Following Coordinate in the Framework of the ARPEGE/Aladin NWP System, Mon. Wea. Rev., 123(2), 515–535.
[22] Castro, M., Fernandez, C., Gaertner, M.A. (1993): Description of a mesoscale atmospheric numerical model, Mathematics, Climate, and Environment, Rech. Math. Appl. Ser., vol. 27, Masson, Paris. 230– 253.
[23] http://klima.hr/klima.php?id=klimatske_promjene (DHMZ)
[24] DHMZ (2010): Contribution to CC-WaterS project: a study of climate and climate change for three test bed sin Croatia. Zagreb, pp 59, nepublicirano.
[25] Gajić-Čapka, M., Güttler, I., Branković, Č. (2011): Climate and climate change analyses for CCwaterS project. Pocc. 5th Croatian water conference Croatian waters facing the challenge of climate changes. Croatian waters, Zagreb, 109-118.
[26] Branković, Č. (2014) Report: Analysis and interpretation of the observed and simulated climate over the Adriatic coast, Zagreb.
[27] Giorgi F., Mearns L. O. (1991) Approaches to the simulation of regional climate change: A review. Reviews of Geophysics, 29(2), 191-216
[28] Rummukainen M. (2010) State-of-the-art with regional climate models. WIREs: Clim. Change, 1(1), 82-96
[29] van der Linden P, J.F.B. Mitchell (eds.), (2009) ENSEMBLES: climate change and its impacts: summary of research and results from the ENSEMBLES project. Met Office Hadley Centre, FitzRoy Road, Exeter EX1 3 PB, UK, pp 160
[30] Christensen J. H., Kjellström E., Giorgi F., Lenderink G., Rummukainen M. (2010) Weight assignment in regional climate models. Clim. Res., 44,179-194
[31] Nakićenović N. et al. (2000) Special report on emission scenarios. A special report of Working Group III of the IPCC. Cambridge University Press, Cambridge, pp 599
[32] Zaninović, K., Gajić-Čapka, M. (2005) Klimatske prilike jadranskih slivova (Climate conditions over Adriatic catchment), Hrvatske vode, 13(50), 1-14
[33] WMO (Climate conditions over Adriatic) Guidelines on the quality control of Surface Climatological Data (Prepared by Abbott PF, UK as Rapporteur in the WMO Commission for Climatology). Technical Document No. 111. Series: WCP-85
[34] Gajić Čapka M., Cindrić K. (2011) Secular trends in indices of precipitation extremes in Croatia, 1901–2008. Geofizika, 28(2), 293-312
[35] Gilbert, R.O. (1987) Statistical methods for environmental pollution monitoring. John Wiley & Sons, Inc., New York
[36] Gajić Čapka M., Cindrić K., Pasarić Z. (2014) Trends in precipitation indices in Croatia, 1961-2010. Theor Appl Climatol (conditionally accepted)
[37] Branković Č., Güttler I., Gajić-Čapka M. (2013) Evaluating climate change at the Croatian Adriatic from observations and regional climate models' simulations. Clim. Dyn., doi:10.1007_s00382-012-1646-z

Climate and climate change data for Croatia – Rijeka 15.09.2014.

Let's grow up together

DRINK ADRIA

Adriatic IPA
Cross Border Cooperation 2007-2013

The project is co-funded by the European Union,
Instrument for Pre-Accession Assistance

CLIMATE CHANGE

Climate and climate change data on national level - Bosnia and Herzegovina

Lead Author/s	Željko Majstorović
Lead Authors Coordinator	Sabina Hadžiahmetović
Contributor/s	Sabina Hadžiahmetović
Date last release	October, 20th 2014
State of document	Final

Let's grow up together

DRINK ADRIA

Adriatic IPA
Cross Border Cooperation 2007-2013

The project is co-funded by the European Union, Instrument for Pre-Accession Assistance

CONTENT:

1. INTRODUCTION

Bosnia and Herzegovina has a total surface area of 51,209.2 km², composed of 51,197 km² of land and 12.2 km² of sea. Of the total land area, 5% is lowlands, 24% hills, 42% mountains, and 29% karst region. According to its geographical position on the Balkan Peninsula, it belongs to the Adriatic basin and the Black Sea basin *[1]*.

Recent drastical climate changes showed some extreem weather conditions in teritory of Bosnia and Herzegovina. These conditions were mostly extreme dry periods and extreme periods of flooding. Extreme dry periods were recorded mostly in southern part of the Bosnia and Herzegovina where the pilot areas of project DRINKADRIA are situated (Figure 1-1).

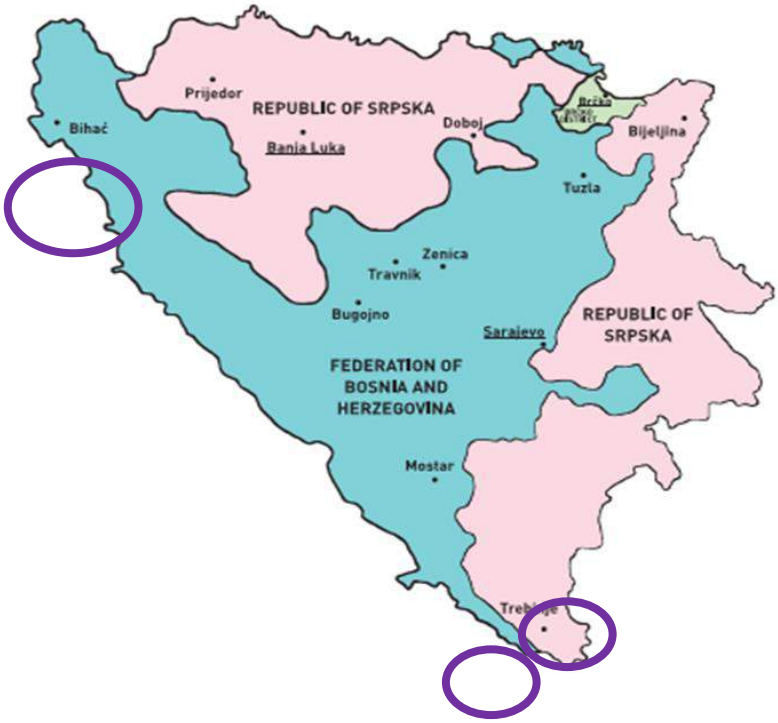

Figure 1-1. Map of Bosnia and Herzegovina with pilot areas of project DRINK ADRIA

Developing countries, including Bosnia and Herzegovina, are among the most susceptible to the adverse effects of global climate change as confirmed by many previous studies. Estimates show that BiH will be exposed to climate change impacts that could have consequences for its entire society. Opportunities to protect against such impacts at the local level are quite limited, but there are still numerous options for climate change adaptation. Global climate change and its impacts will require the introduction of new environmental models and development strategies.

The extensive climate changes observed in rapid temperature growing and negative precipitation are visible in the whole Balkan area but most visible in the Mediterranean area of Balkan countries where the project DRINKADRIA pilot areas are situated. Since this areas are known as dryest area of BiH it is important to approach to new water management not only for the sucesufful and long term drinking water supply of BiH population but as well as population of Republic of Croatia. Population of southern Croatia (Dalmatia) have a intensive summer tourist season and this part of Republic of Coatia is the most populated part of the country during summer months (driest). For the future number of tourist is tending to increase making cros-border water issues more and more important for both countries.

Data collected in this report are collected from the Second National Communication of Bosnia and Herzegovina under the United Nations Framework Convention on Climate Change. Bosnia and Herzegovina ha san obligation following the United Nations Framework Convention of Climate Changes and it made First and Second National Communication of Bosnia and Herzegovina under the United Nations Framework Convention on Climate Change *[2]*. *[3]*.In this document most data were gathered from the period from 1961-1990 with focus on temperature and precipitation data from different meteorological stations in whole territory of Bosnia and Herzegovina *[4]*. *[5]*.

2. EXISTING CLIMATE FEATURES IN B&H

Bosnia and Herzegovina has several climate types: the temperate continental climate type, which is represented mostly in the northern and central parts of BiH; the sub-mountainous and mountainous type (over 1000 m); and the Adriatic (Mediterranean) and modified Adriatic climate type, which represented in coastal area of Neum and includes the Herzegovinian lowlands. The climate of Bosnia and Herzegovina therefore varies from a temperate continental climate in the northern Pannonia lowlands along the Sava River and in the foothill zone, to an alpine climate in the mountain regions, and a Mediterranean climate in the coastal and lowland areas of the Herzegovina region in the south and southeast. In the northern part of the country, air temperature generally ranges between -1 and -2°C in January and between 18 and 20°C in July. In highlands with the altitude above 1000 m, the average temperature ranges from -4 to -7°C in January to 9 to to 14°C in July. On the Adriatic coast and in the lowland regions of Herzegovina, air temperature ranges from 3 to 9°C in January to 22 to 25°C in July (for the period 1961-1990). Extremes of -41.8°C (low) and 42.2°C (high) have been recorded *[5]*.

The lowland area of northern BiH has a mean annual temperature of between 10°C and 12°C, and in areas above 500 m the temperature is below 10°C. Mean annual air temperature in the coastal area ranges between 12°C and 17°C. In the period 1981-2010, an increase in air temperature was recorded in the entire territory of Bosnia and Herzegovina. The highest increase of approximately 1°C is recorded during summer and winter period *[5]*.

Annual precipitation amounts range from 800 mm in the north along the Sava River to 2000 mm in the central and south-eastern mountainous regions of the country (period 1961-1990).

In the continental part of BiH belonging to the Danube River catchment area, a major part of annual precipitation occurs in the warmer half of the year, reaching its maximum in June. The central and southern part of the country with numerous mountains and narrow coastal regions is characterized by a maritime pluviometric regime under the influence of the Mediterranean Sea, so the monthly maximum amounts of precipitation are reached in late autumn and at the beginning of the winter, mostly in November and December. During the period 1981-2010, major parts of the Herzegovinian lowlands saw a decrease in annual precipitation, whereas the majority of mountainous meteorological stations recorded an increase in precipitation. Compared to 1961-1990, this period had a more uneven distribution of precipitation throughout, which was one of the main factors causing more frequent droughts and flooding *[5]*.

The duration of sunshine decreases from the sea towards the mainland and at higher altitudes. Annual duration of sunshine in the central mountainous area is 1700-1900 hours, as a consequence of the above average cloudiest conditions (60-70%). Due to frequent fogs during the cold part of the year, solar irradiation inland is lower than at the same altitudes in the coastal area.
In southern regions, there are 1900-2300 hours of sunshine (Mostar = 2285 hours). In northern Bosnia and Herzegovina, there are 1800-2000 hours of sunshine, more in the eastern part than in the western part. Cloudiness declines from the west to the east *[5]*.

Average annual precipitation in BiH is about 1,250 mm, which given that the surface area of BiH is 51,209 km2 amounts to 64 x 109 m3of water, or 2,030 m3/s. The outflow from the territory of BiH is 1,155 m3/s, or 57% of total precipitation. However, these volumes of water are not evenly distributed, either spatially or temporally. For example, the average annual outflow from the Sava River basin, which has a surface area of 38,719 km2(75.7%) in BiH, amounts to 722 m3/s, or 62.5%, while the outflow from the Adriatic Sea basin, which has a surface area of 12,410 km2(24.3%) in BiH, is 433 m3/s, or 37.5% *[4] [5]*.

Observed climate changes in Second National Communication of Bosnia and Herzegovina under the United Nations Framework Convention on Climate Change was estimated by analyses of available data from Hydrometorogical Institute of FBiH and Republic Hydrometeorogical Institute of RS. The data was colected from 22 difrent meteorological stations from period 1961-1990 and 1981-2010 *[5]*.

Studies of temperature change for the period 1961-2010 indicate that temperatures have increased in all areas of the country. A comparative seasonal analysis for 1981-2010 and 1961- 1990 showed that the largest increases in average temperature during the summer months were observed in southern (1.2°C) and in central areas (0.8°C), while the largest increase in spring and winter temperatures was recorded in north-central areas (0.7°C). The lowest increase in autumn temperatures ranges from 0.1 to 0.3°C (Figure 2-1). The increase in annual air temperature ranges from 0.4 to 0.8°C, while the increase in air temperature during the growing season (April – September) even reaches 1.0°C. However, increases in air temperature during the last decade are even more pronounced (Figure 2-2; Figure 2-3; Figure 2-4).

Spatial distribution of selected climate parameters is shown in Figure 2-1.

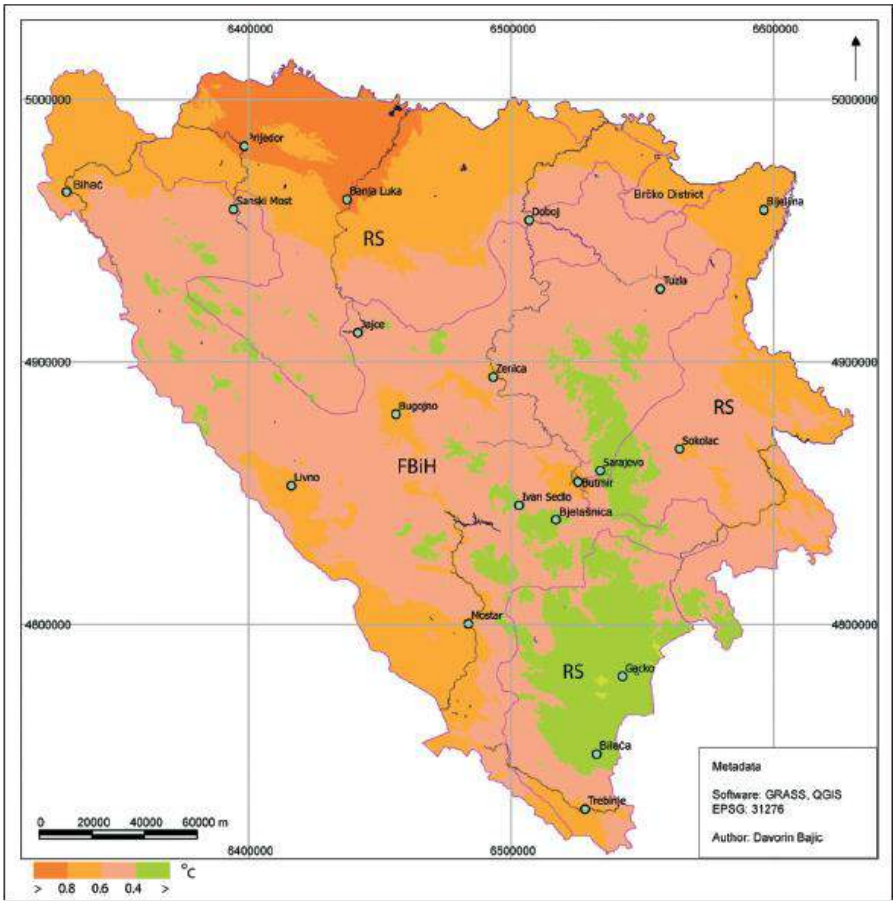

Figure 2-1. Changes in annual air temperature in Bosnia and Herzegovina (during 1981-2010 compared with 1961-1990) [5]

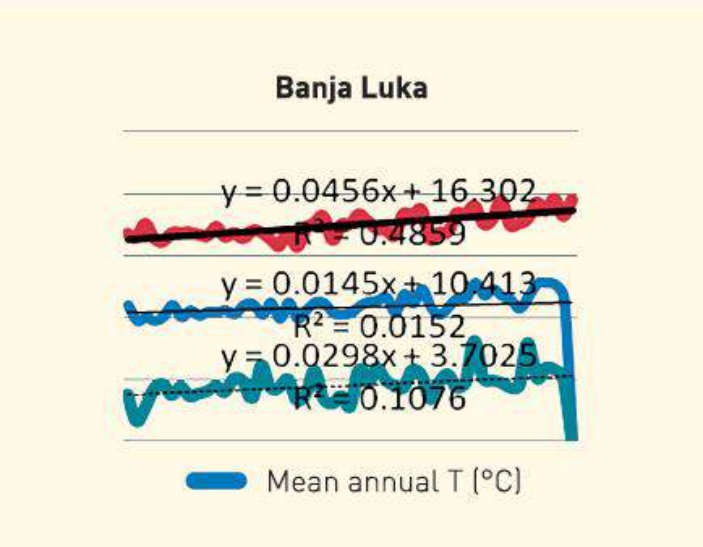

Figure 2-2. Changes in temperature in northern (Banja Luka) part of BiH [5]

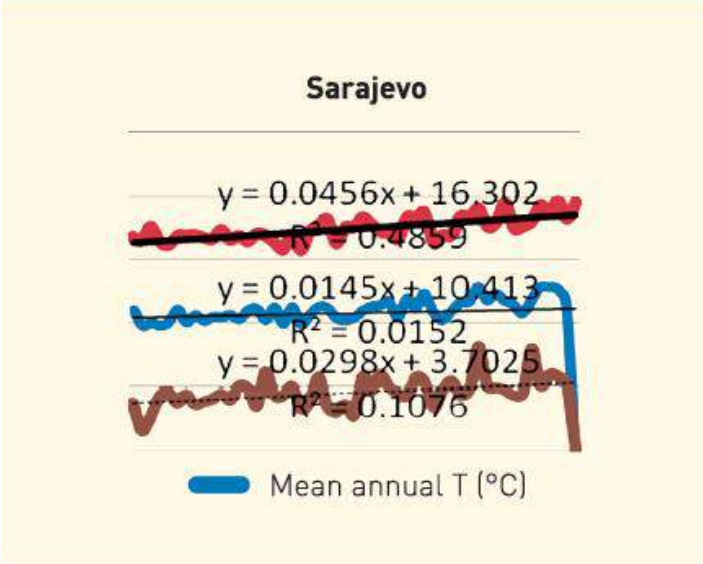

Figure 2-3. Changes in temperature in central (Sarajevo) part of BiH [5]

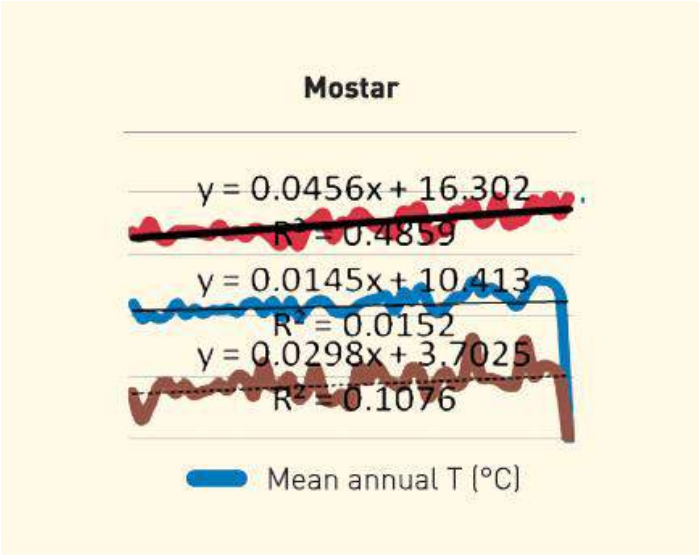

Figure 2-4. Changes in temperature in southern (Mostar) part of BiH [5]

During 1961–2010, much of the territory of Bosnia and Herzegovina showed a slightly increasing trend in annual precipitation. The largest increase in annual precipitation occurred in the central mountain areas (Bjelašnica and Sokolac) and near Doboj, while the largest deficit was recorded in the south (Mostar and Bileća). The largest decrease in precipitation was during the spring and summer seasons, in the region of Herzegovina (up to 20%). The autumn season saw the largest increase in precipitation, particularly in northern and central areas. Although the level of annual precipitation has not significantly changed, the pluviometric regime, i.e. annual distribution, has been greatly altered. The number of days with rainfall above 1 mm decreased across the entire country, while the percentage of annual precipitation due to rainfall above 95th percentile during 1961-2010 was increasing. In other words, although the level of annual precipitation has not significantly changed, a decrease in number of days with rainfall above 1.0 mm and an increase in the number of days with intense rain events has significantly distorted the pluviometric regime. Pronounced variability in the annual rainfall regime and temperature increases are key factors in the occurrence of more frequent and intense droughts in Bosnia and Herzegovina (Figure 2-5; Figure 2-6). *[5]*

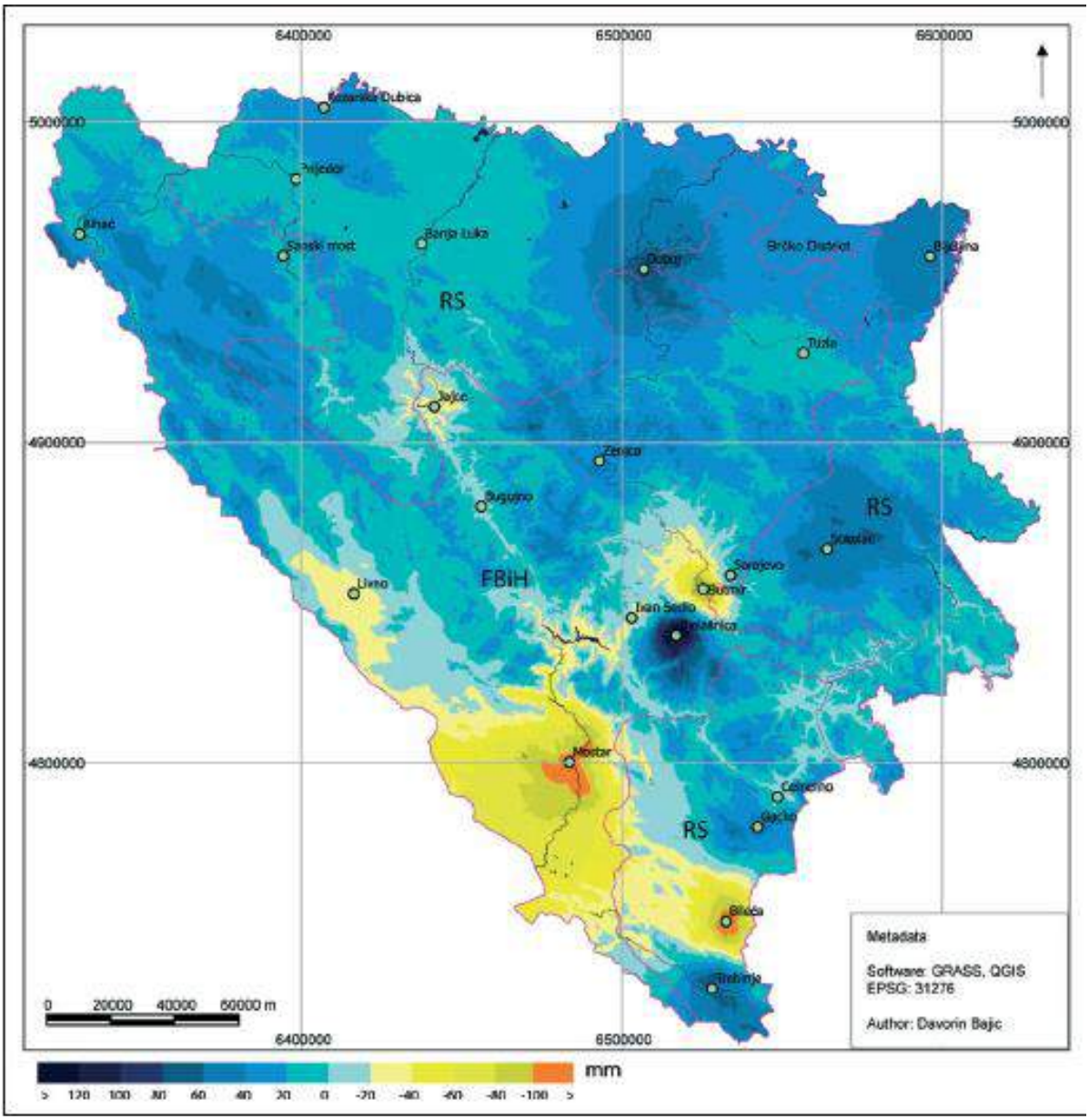

Figure 2-5. Changes in annual precipitation in Bosnia and Herzegovina (1981-2010 compared with 1961-1990) [5]

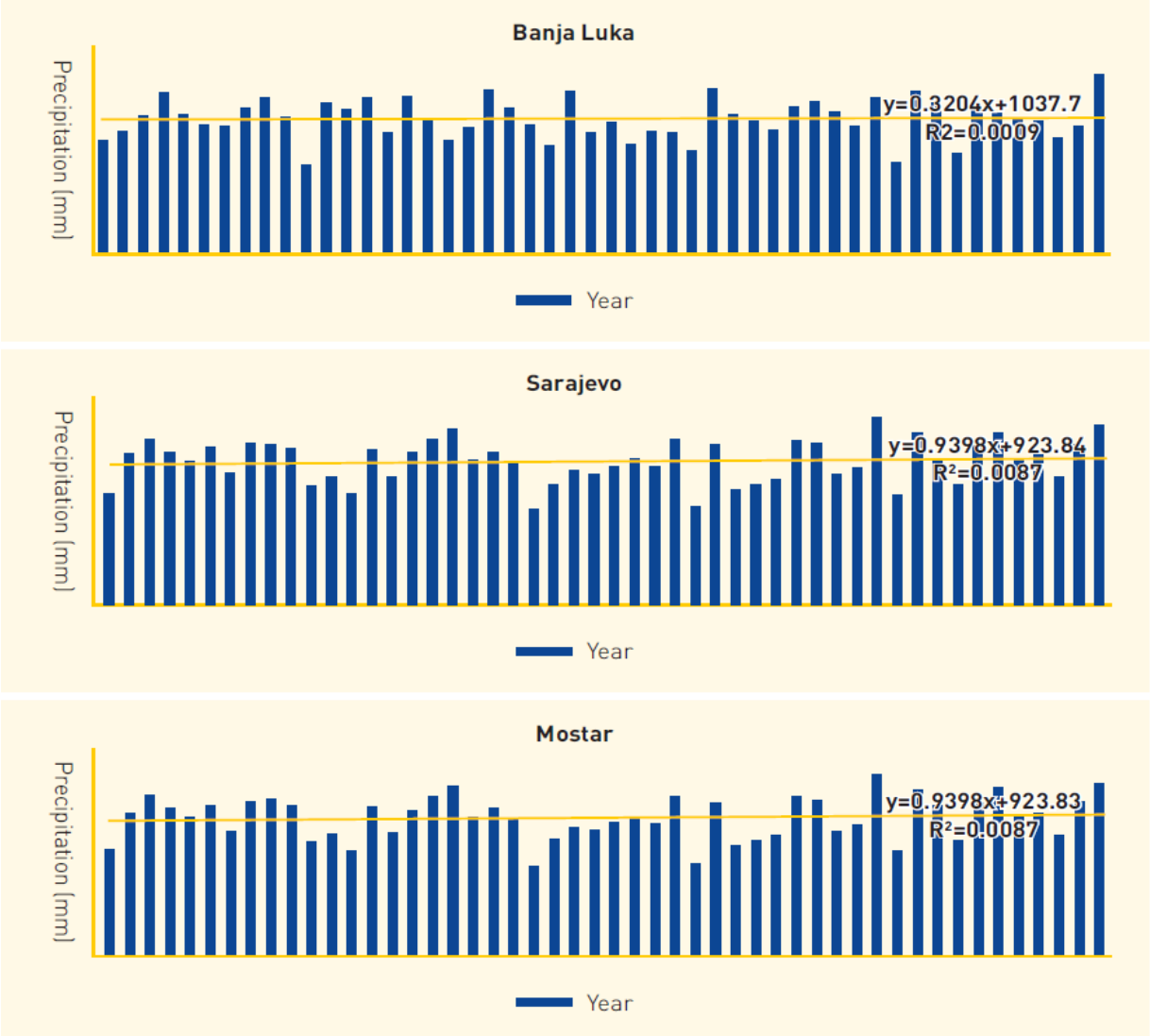

Figure 2-6. Changes in precipitations in northern (Banja Luka), central (Sarajevo) and southern part (Mostar) of BiH [5]

There is an evident increasing trend in number of "hot" days (tropical days with a maximum daily air temperature above 30°C) across almost the entire territory (Figure 2-7).Most of these days are recorded in the north (Posavina), central parts and in Podrinje (Višegrad). In the lowland area of the Herzegovina region (Mostar), there is a slight increase of a number of tropical days. However, during the last 5 years (2007 – 2012), there is an increased occurrence of extremely high temperatures (over 40 °C). In other words, although there is no significant increase in number of tropical days, there is an increased number of days with temperatures over 40 °C (Federal hydrometeorological institute FBIH) *[5]*.

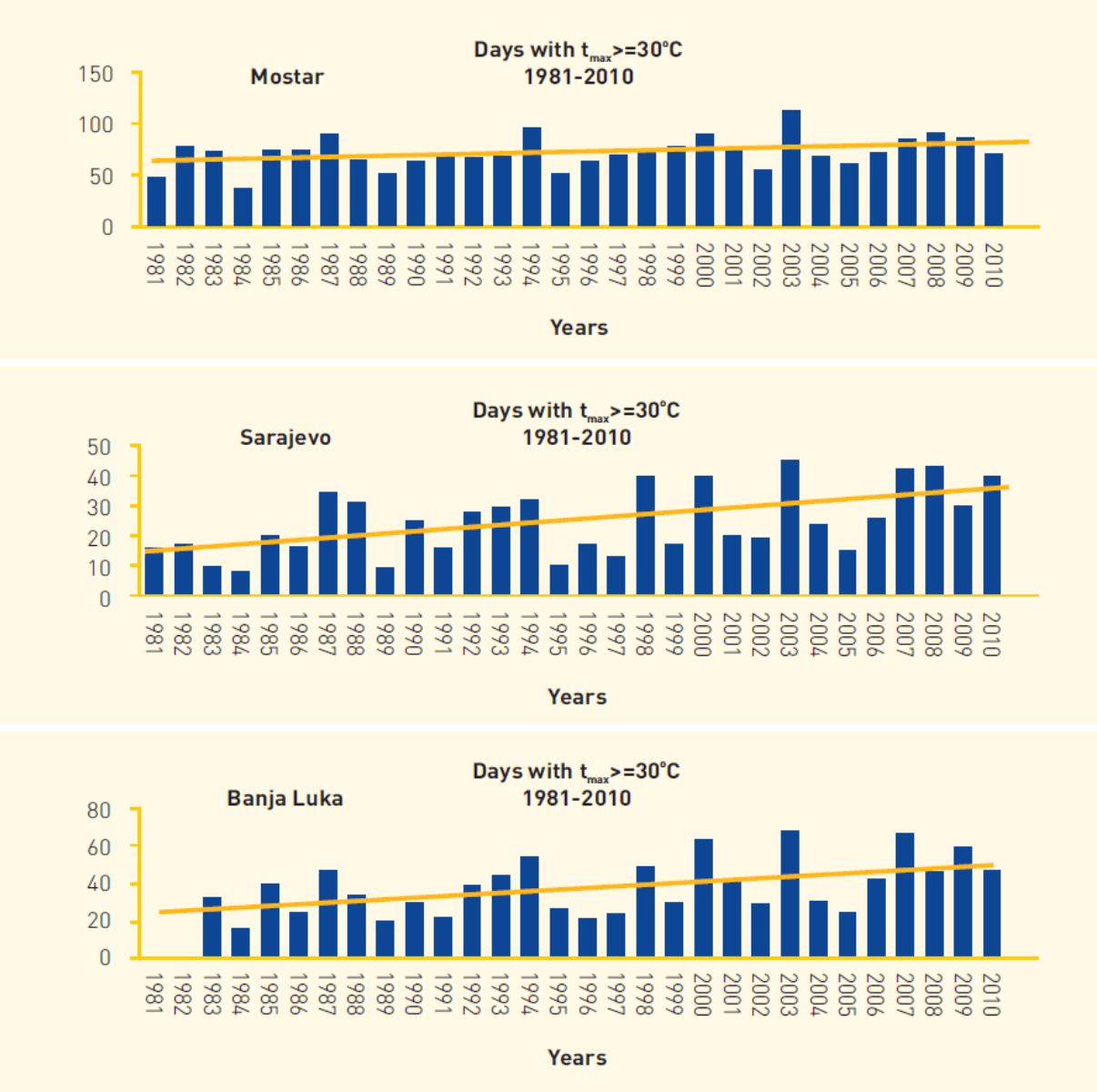

Figure 2-7. Average number of tropic days (tmax>30°C) [5]

Maximum daily precipitation during 1961-2011 was as follows: Banja Luka - 156 mm, Mostar 127 mm, and Sarajevo - 118 mm. Average maximum precipitation for the same period was: Banja Luka - 54 mm, Mostar - 79 mm, and Sarajevo - 50 mm. The return period for these values is approximately 1000 years. Even though the probability of increasing the absolute maximum daily precipitation is low, the increase in the number of days with rainfall above 10.0 mm speaks to the seriousness of the problem (Figure 2-8). *[5]*

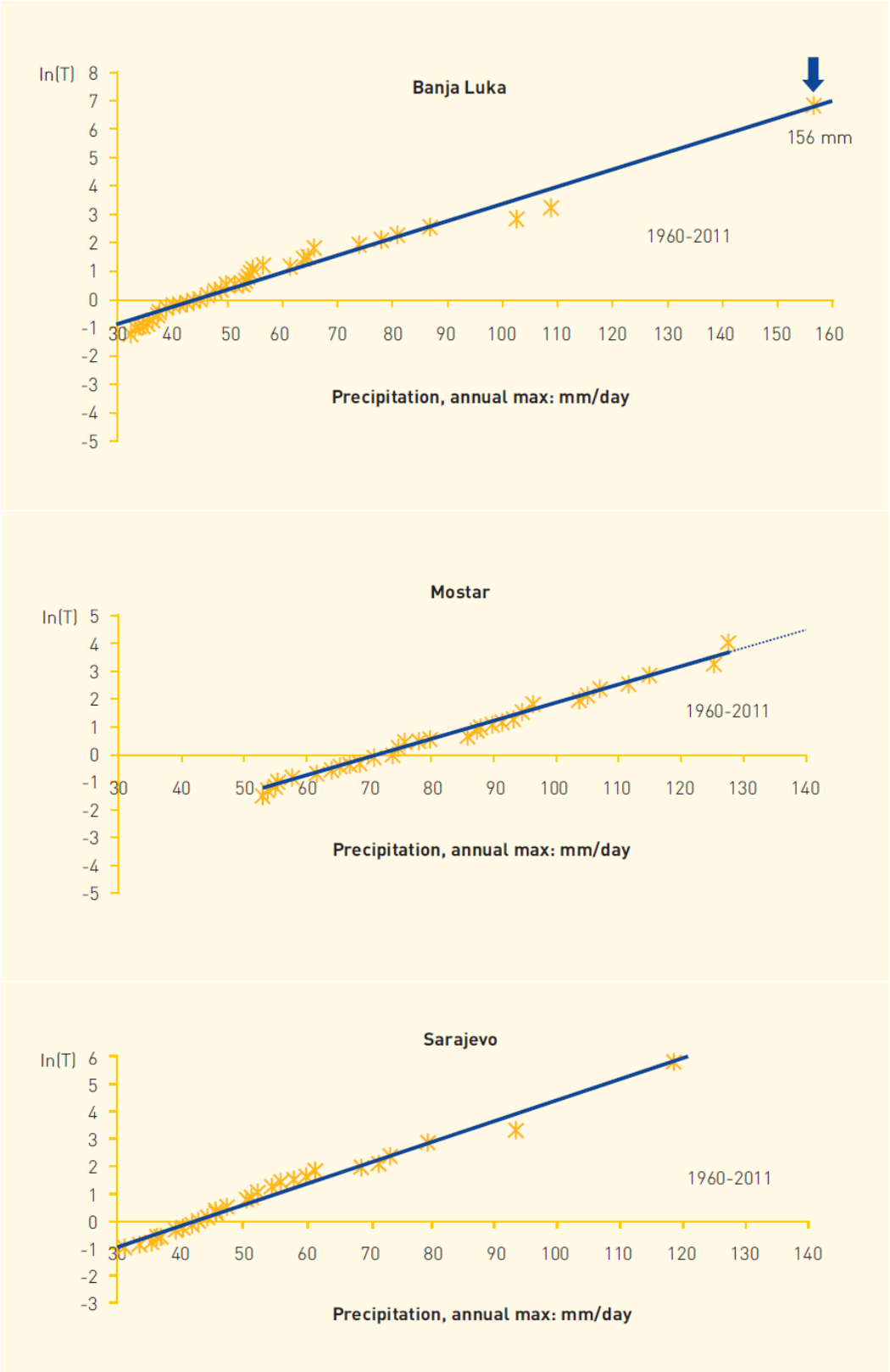

Figure 2-8. Empirical function – distribution of maximum daily precipitation in Banja Luka, Mostar and Sarajevo, 1961-2011) [5]

3. CLIMATE CHANGE SCENARIOS

Bosnia and Herzegovina developmed a climate models and a selection of adequate future climate change scenarios. Results of the coupled regional climate was made in model EBU-POM from future climate change experiments, received by the method of dynamic downscaling of results from two global climate change models of atmosphere and ocean, SINTEX-G and ECHAM5. The focus was on results from two IPCC scenarios on climate change: the SRES A1 B and A2 scenarios. A1B is characterized as a “medium” scenario and A2 as a “high” scenario according to the projected levels of greenhouse gases in the atmosphere. In the A1B scenario, the value of the atmospheric concentration of carbon dioxide (CO2), one of the greenhouse gases is approximately 690 parts per million (ppm) at the end of 21st century, and in the A2 scenario it is approximately 850 ppm. Model results were analyzed for the time series 2001- 2030 and 2071-2100. This section focuses on two basic ground meteorological parameters: air temperature at 2 meters and accumulated precipitation. Changes in these parameters are shown with reference to mean values from the so-called base (standard) period of 1961-1990 *[5]*.

A1 B Scenario (2001-2030)

According to climate model results, the mean seasonal temperature changes for the thirty-year period is expected to range from +0,6 to +1,4 °C. This depends from the region of BiH and the biggest temperature changes during summer months will be +1,4 °C in northern parts and +1,1 °C in souther parts of BiH where the project pilot areas are situated. During the spring months temperatures will rise for approximettly +0,8 to +0,9 °C, during the autumn months range of average temperatures will rise from +0,6 to +0,9 °C. (Table 3-1). *[5]*
Increasing of temperatures will affect the precipitation changes for wich model showed positive and negative variations. Positive changes of precipitations will be seen during spring months from +5% and during summer months even up to +15%. This is just for the north-east part of the BiH while in the other parts of the BiH with ephasis on southern parts where the project pilot areas is situated showed the biggest deficit in precipitation raging even up to -20% (Figure 3-1; Table 3-2). *[5]*

Table 3-1: Temperature change (in °C) in SINTEX – 5 and ECHAM5 model [5]

Model	**SINTEX – 5**	**ECHAM5**
Scenario	**A1 B Scenario (2001-2030)**	
Winter seison	0,6-0,9	0,2-0,5
Spring seison	0,8-0,9	<0,2
Summer seison	1,1-1,4	0,5-0,8
Autumn seison	0,5-0,9	0,9-1,1
Year	0,8-1,0	0,4-0,6

Table 3-2: Precipitation change (in %) in SINTEX – 5 and ECHAM5 model [5]

Model	SINTEX – 5	ECHAM5
Scenario	**A1 B Scenario (2001-2030)**	
Winter seison	-15 – -5	0 – 10
Spring seison	-10 – 5	0 – 15
Summer seison	-5 – 15	-10 – 10
Autumn seison	-10 – 20	-10 – 5
Year	-20 – 10	-5 – 10

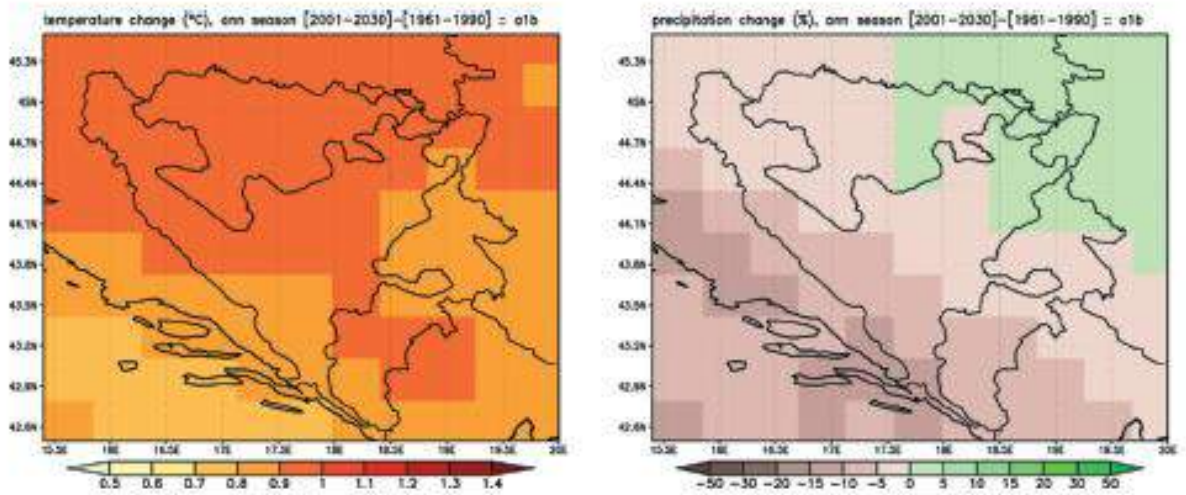

Figure 3-1. Average annual temperature change in °C (left) and precipitation change in % (right) [5]

A1 B Scenario (2071-2100)

Results in A1 B scenario during the period from 2071 to 2100 showed that distribution of temperature parameter remains the same as in observed period 2001-2030 but with greater magnitudes in changes. Temperature changes in this period ranges from + 1,8 to +3,6 °C with biggest walues in summer months. During the winter and autumn months temperature will rise up to + 2,4 °C and during the spring months up to +2,6 °C (Table 3-3). *[5]*

Increasing of temperatures will take affect the precipitation changes in this period which will be characterized in positive percipitation anomaly. Larger negative anomalies are perdict in winter and autumn months with changes from -10% to – 50%. Spring months are characterized with value up to -10% while the precipitation defficit in summer months will be greather in southern parts of the country raging up to – 30% (Figure 3-2; Table 3-4). *[5]*

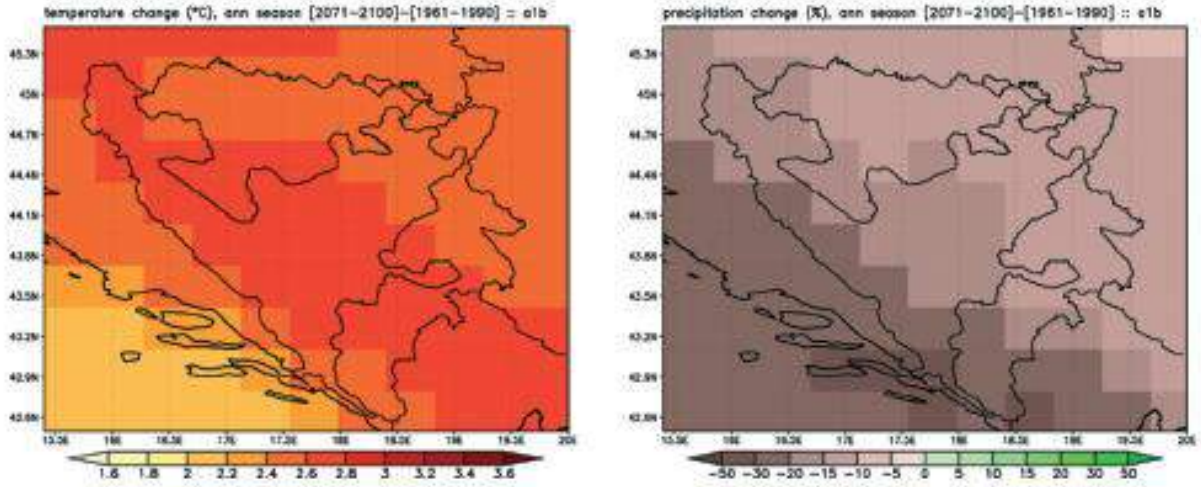

Figure 3-2. Average annual temperature change in °C (left) and precipitation change in % (right) [5]

Table 3-3: Temperature change (in °C) in SINTEX – 5 and ECHAM5 model [5]

Model	SINTEX – 5	ECHAM5
Scenario	**A1 B Scenario (2071-2100)**	
Winter seison	1,8 – 2,4	3 – 3,8
Spring seison	2,4 – 2,6	2,2 – 2,6
Summer seison	3,4 – 3,6	4 – 4,2
Autumn seison	2,0 – 2,4	3,4 – 3,8
Year	2,4 – 2,8	3,2 – 3,6

Table 3-4: Precipitation change (in %) in SINTEX – 5 and ECHAM5 model [5]

Model	SINTEX – 5	ECHAM5
Scenario	**A1 B Scenario (2071-2100)**	
Winter seison	-50 – 10	-15 – 5
Spring seison	-15 – 0	-5 – 15
Summer seison	-30 – 0	-50 – -20
Autumn seison	-50 – 15	-30 – -5
Year	-30 – -10	-15 – -5

A2 Scenario (2071-2100)

In the A2 scenario for the period 2071-2100, the expected increase in temperature in the entire territory of BiH ranges from +2.4 to +4.8°C. The biggest increase will be during the summer months with values above +4.8°C. During the winter months, the maximum predicted change is approximately +3.6°C. For the spring months period it is predicted values ranging from +3.4 to +3.6°C while during the autumn months the changes are again bigger in the western part of the country, ranging from +2.8 to +3°C (Table 3-5) *[5]*

The A2 scenario has a negative anomaly in terms of accumulated precipitation across the entire territory, with the exception of the southeastern regions, the winter months seison has a positive anomaly across almost the entire territory, ranging from 0 to +30%. The biggest changes in this scenario are predicted during the summer season, with values of -50%. During the spring and autumn seison, anomalies range from -30 to 0% (Figure 3-4; Table 3-6). *[5]*

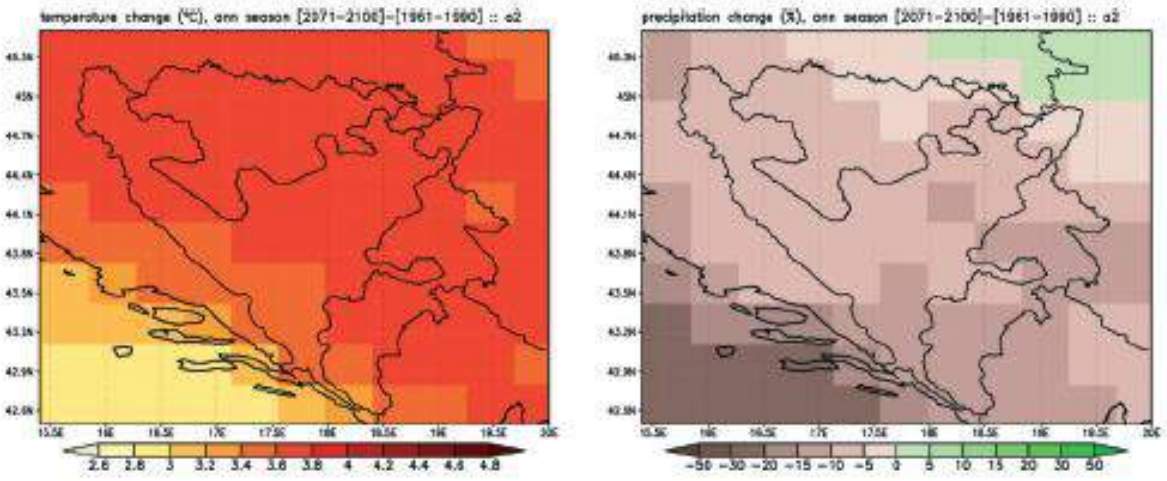

Figure 3-4. Average annual temperature change in °C (left) and precipitation change in % (right) [5]

Table 3-5: Temperature change (in °C) in SINTEX – 5 and ECHAM5 model [5]

Model	**SINTEX – 5**	**ECHAM5**
Scenario	**A2 Scenario (2071-2100)**	
Winter seison	2,4 – 3,6	3,2 – 4
Spring seison	3,4 – 3,8	2,6 – 3,2
Summer seison	4,6 - >4,8	4,4 – 4,8
Autumn seison	2,8 – 3,2	3,8 – 4,2
Year	3,4 – 3,8	3,6 – 4,0

Table 3-6: Precipitation change (in %) in SINTEX – 5 and ECHAM5 model [5]

Model	**SINTEX – 5**	**ECHAM5**
Scenario	**A2 Scenario (2071-2100)**	
Winter seison	-5 – 30	-30 – 15
Spring seison	-30 – 0	-10 – 10
Summer seison	-50 – 0	-50 – 20
Autumn seison	-30 – 0	-20 – 0
Year	-15 – 0	-20 – 5

The climate change modells show that mean seisonal temperature increasing averaging +1°C by 2030 compared to the period of 1961-1990 over the whole territory of BiH. Largest temperature rising will take up to +1,4 °C during summer seison. A2 scenario showed rapid temperature increasing up to +4°C yearly with maximum during summer seison +4,8°C. Model show unequal precipitation changes but negative precipitation are expected in whole territory of BiH even up to 50% comparing to the period from 1961 to 1990 during summer seison.

4. LITERATURE

[1] 1) BiH Country Review – Environmental Protection. UN Economic Commission for Europe. 2004. www. unece.org/env/epr/countriesreviewed.htm.
[2] 2) Kyoto Protocol to the United Nations Framework Convention on Climate Change http://unfccc.int/ resource/docs/convkp/kpeng.pdf.
[3] 3) Ministry of Urban Planning, Civil Engineering and Ecology of the Republic of Srpska: 2001 the Round Table on subject “Framework UN Convention on Climate Change and Kyoto Protocol - Rights and obligations of Bosnia and Herzegovina as a member of the Convention”: Proceedings, Institute for Urbanism of the Republic of Srpska, 2001, Bosnia and Herzegovina.
[4] 4) UNDP BiH First National Communication of Bosnia and Herzegovina under the United Nations Framework Convention on Climate Change, Banja Luka, 2009.
[5] 5) UNDP BiH Second National Communication of Bosnia and Herzegovina under the United Nations Framework Convention on Climate Change, Sarajevo, 2013

Hydro – Engineering Institute Sarajevo – Sarajevo 18.05.2014

Let's grow up together

DRINK ADRIA

Adriatic IPA
Cross Border Cooperation 2007-2013

The project is co-funded by the European Union,
Instrument for Pre-Accession Assistance

Report on existing climate and climate change data on the national level of the sate of Montenegro

Public Utility" Vodovod i kanalizacija" - Niksic
(FB14)

Lead Author/s	Bozovic Olivera
Lead Authors Coordinator	Bozovic Olivera
Contributor/s	Papovic Mira
Date last release	2014. year
State of document	FINAL

Let's grow up together

DRINK ADRIA

Adriatic IPA
Cross Border Cooperation 2007-2013

The project is co-funded by the European Union,
Instrument for Pre-Accession Assistance

I INTRODUCTION

This document was prepared by the Public Utility Vodovod i kanalizacija Nikšić i.e. by its working team that have been implementing DRINKADRIA project within IPA ADRIATIC program. WP4 has been implemented within DRINKADRIA project and these data will be used within this work package.

During the preparation of this document, the data were taken from:

- The Initial National Communication on Climate Change of Montenegro according to The *United Nations Framework Convention* on *Climate Change* (UNFCCC) - 2010 - Ministry for Spatial Planning and environment
- Draft of the Second National Communication on Climate Change of Montenegro according to The *United Nations Framework Convention* on *Climate Change* (UNFCCC)- 2014 -Ministry of Sustainable development and Tourism
- Study on Climate Change Vulerability- 2012- The *South East European Forum* on *Climate Change* Adaptation (SEEFCCA)

2. CLIMATE CHARACTERISTICS OF MONTENEGRO

2.1 . Current climate characteristics

Besides latitude and altitude, the climate in Montenegro is determined by the presence of large bodies of water (the Adriatic Sea, Lake Skadar), the sea entering deeply into the land (the Bay of Kotor), moderately high mountainous hinterland near the coast (Orjen, Lovćen, Rumija), Ulcinj field in the far southeast and the mountainous massif of Durmitor, Bjelasica and Prokletije.

Montenegro is located in the central part of the warm temperate zone of the northern latitudes. Large bodies of water, height and direction of the coastal mountains and the relief influence both locally and regionally on the climate, creating at a small space big differences

between coastal climate and climate of high mountainous region with numerous transitional forms of local climate.

The southern part of Montenegro and Zeta-Bjelopavlići plain have Mediterranean climate with long, hot and dry summers and relatively mild and rainy winters. The central and northern parts of Montenegro have some characteristics of mountain climate, but the influence of the Mediterranean Sea is also evident. The far north of Montenegro has a continental climate characterized by low annual precipitation evenly distributed over all months. In the mountainous areas in the north summers are relatively cool and humid, and winters are with low temperatures, which rapidly decrease with elevation. Characteristic winds of Montenegro are the bora and sirocco.

`

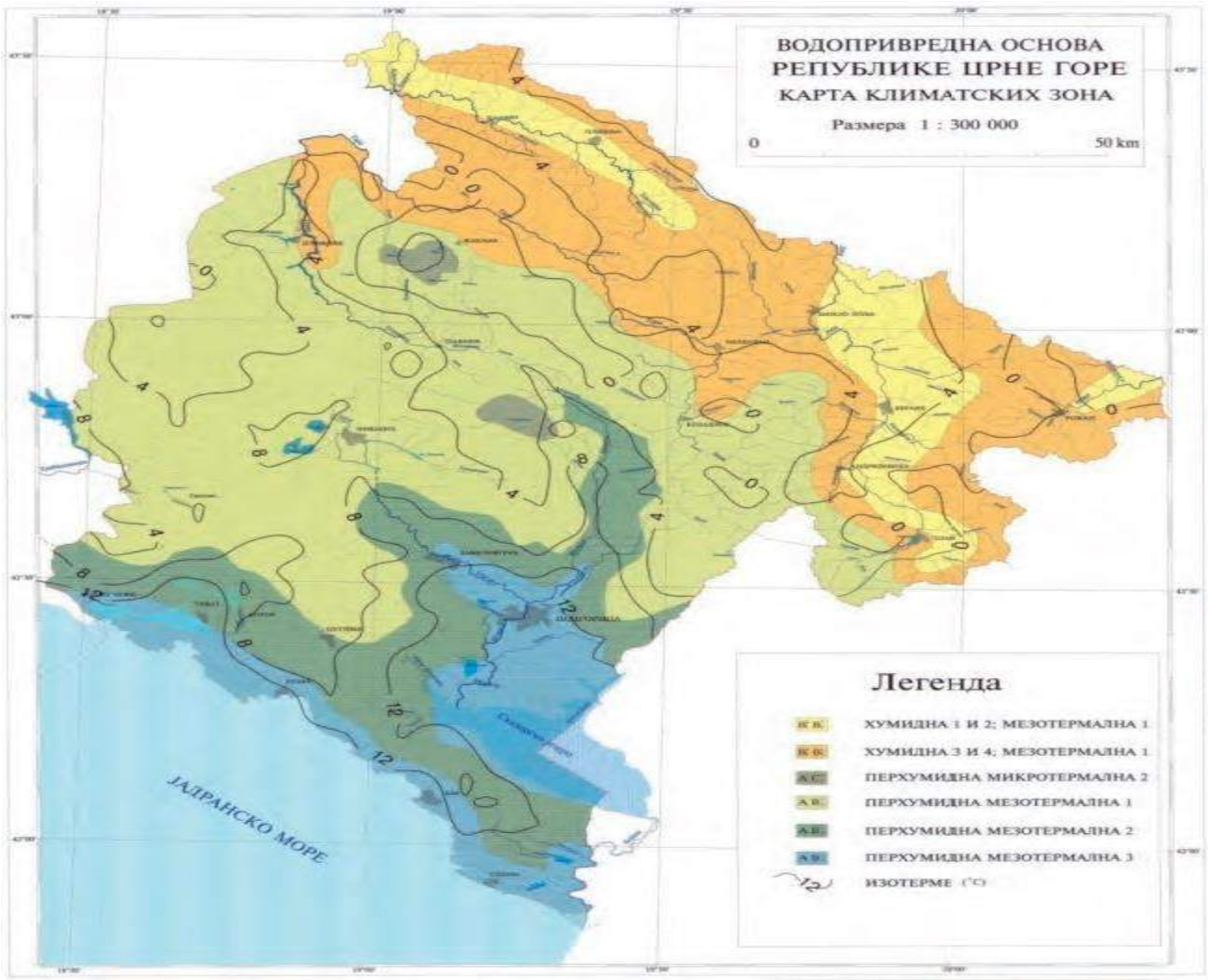

Map of climate zones of Montenegro (Source: Water Management Master Plan of Montenegro)

2.1.1. Temperature

The last decade of the twentieth century was warmer in relation to a multi-year series of measurements (since 1949 until the present day). The average annual air temperature ranges from 4.6 ^{0}C in the north (Žabljak) to 15.8^0 C in the south.

The year 2003 was the warmest year in Montenegro, when a tropical period of 100 tropical days (with maximum daily temperature greater than or equal to 30^{0}C) was recorded in Podgorica. The highest daily temperature of 44.8^{0}C was recorded in August 2007 in Podgorica, while the lowest daily temperature of -32^{0}C was measured in Rožaje, in the eastern part of Montenegro, in January 1985.

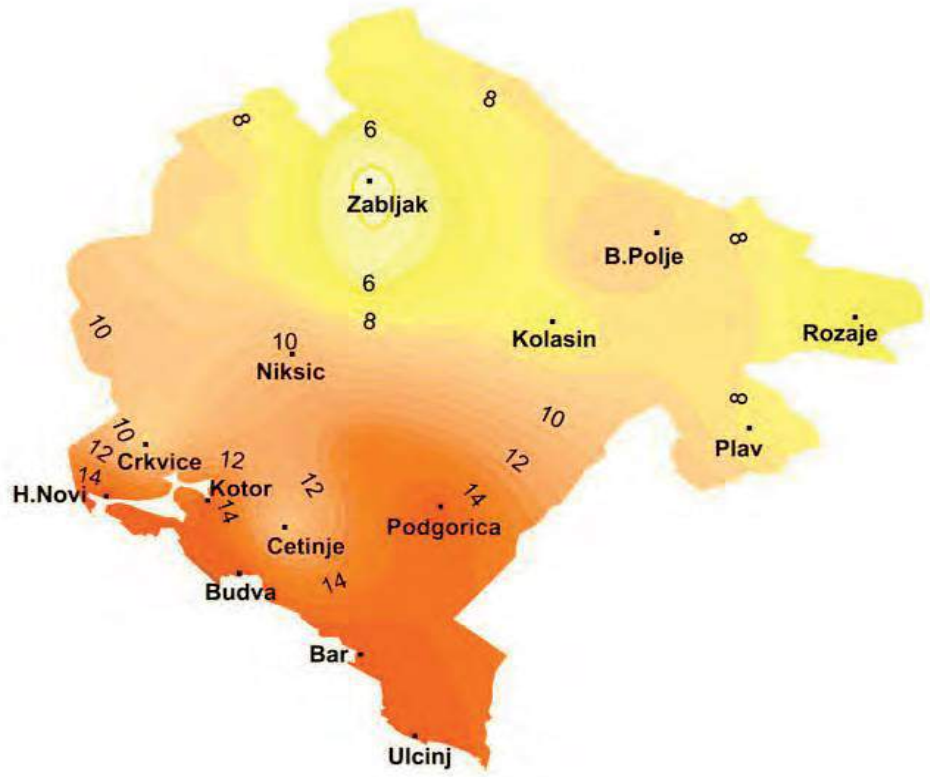

Annual distribution of air temperature (°C) for the averaging period of 1961-1990 (Source HMZ)

2.1.2. Precipitation

Average, annual number of days with precipitation is about 115-130 on the coast or up to 172 in the north. The rainiest months on average have 13-17 days, and the driest ones 4-10 rainy days. The number of days with more abundant daily rainfall (over 10 mm) ranges from 25 (Pljevlja) to 59 (Kolašin). However, the largest number of days with heavy precipitation is recorded in Cetinje – 74 days. On the slopes Orjen, in the village Crkvice precipitation may even reach 7,000 mm in record years, which makes it the rainiest place in Europe.

The snow cover is formed at the altitudes above 400 meters. A snow cover deeper than 30 cm can be found at the altitudes above 600 m, and even deeper than 50 cm at those above 800 m. An average number of days with a snow cover deeper than 50 cm is 76 days (Žabljak).

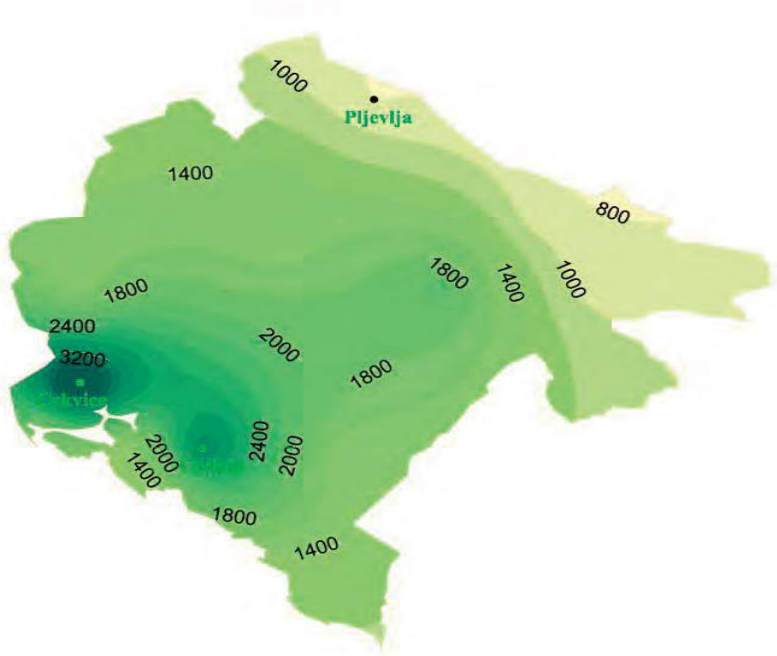

Annual distribution of rainfall (mm) for the averaging period 1961-1990 (Source HMZ)

3. WATER RESOURCES OF MONTENEGRO

In Montenegro, there are significant differences in the distribution and abundance of water resources - starting with arid karst areas to those that are rich in both surface and groundwater. Generally speaking, with an average annual runoff of 624 m^3/s (i.e. the volume of 19.67 billion m^3), the territory of Montenegro falls among the areas rich in water. An average specific runoff is about 43 $l/s/km^2$. Of the total runoff, about 95% are inland waters, while the remaining 5% are transit waters.

3.1. Surface water

The rivers flow into two basins: the Black Sea, with a total area of 7,260 km^2 (or 52.5% of the territory) and the Adriatic Sea with about 6,560 km^2 (or 47.5%). The major rivers of the Black Sea basin are the Lim (the longest river, 220 km long), the Tara (146 km), the Ćehotina (125 km) and the Piva (78 km). The main rivers of the Adriatic Sea basin are the Morača (99 km), the Zeta (65 km) and the Bojana (40 km).

Natural lakes are also an important water resource and the most significant ones are Biogradsko (area of 0.23 km^2), Plav (1.99 km^2), Black (0.52 km^2), Šasko (3.6 km^2) and Skadar Lake. The surface area of Skadar Lake, depending on the water level, varies from about 360 to over 500 km^2, while the volume of the lake ranges from 1.7 to 4.0 km^3. The total catchment area of Skadar Lake is approximately 5,500 km^2 (4,470 km^2 in Montenegro and 1,030 km^2 in Albania). Natural lakes are located at elevations ranging from 1.4 m (Šasko Lake) to 1,418 m (Black Lake), and three of them - Biogradsko, Black, and Skadar - are a part of national parks. The largest artificial reservoir is Piva Lake with a total accumulation capacity of 880 x $106m^3$. Other significant accumulations include lakes of Slano, Krupac and Vrtac (225 x 106 m^3) and the accumulation of Otilovići (18 x $106m^3$).

3.2. Ground water

Groundwater in Montenegro is present in rocks of different ages from Paleozoic to Quaternary. It is a very important resource which is practically a sole source of water supply of the population. In addition to the water supply of the population, groundwater is used in part for the industry, as well as for agriculture.

75 water sources are used for public water supply of 40 urban settlements, including 21 municipal centers, as well as a large number of suburban areas. Out of the total number of sources, on 64 of them water is abstracted from karsts aquifers and on 11 sources ground

water is abstracted from intergranular aquifers. Over 3.3 m^3 /s of groundwater is abstracted for total water supply for the population on the territory of Montenegro - from karsts aquifer around 2.5 m3/s and from intergranular aquifers about 0.8 m^3 /s.

4. WATER USE IN MONTENEGRO

4.1. The use of water for water supply

Industry and population are the biggest water users. Statistics show that from 2005 to 2011 the quantity of water abstracted for public water supply increased from 101.8 million m^3 in 2005 to 109.5 million m^3 in 2011 i.e. for 7.4%. In 2011 49.67 million m^3 of the total abstracted water was delivered to the public water supply system, which is in comparison with 2005 (53.67 million m^3) lower by 7.4%. In 2001, households were delivered 35 million m^3 of water, i.e. 70.4% out of the total water supplied, commercial enterprises 9.6 million m^3, i.e. 19.3%, and other users were delivered 5.1 million m^3 of water. In the researched period 2005-2011 water losses increased from 48.19 million m^3 in 2005 to 59.77 million m^3 in 2011 i.e. from 24% m^3 to 10.3%.

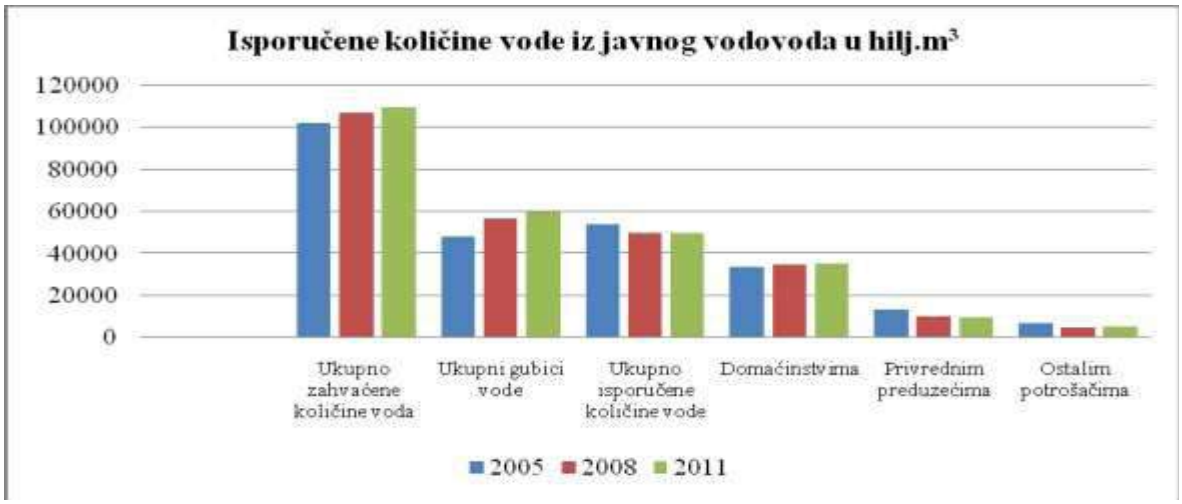

Water quantities delivered from the public water supply system 2007-2011

4.2. The use of water in industry

Water consumption in the industry also increased in the period from 2007 to 2011. Industry is supplied with water partly from the public water supply (in 2011 only 1.2 million m3 of water, i.e. 0.04% of the total amount of water used), while it is largely supplied from their own water supplies, surface water and groundwater (in 2011 3197.8 million m3, i.e. 99.96%). Water consumption in the industry for the period 2007 - 2011 is shown in the chart. Out of the total used water in industry 99.27% of water is used in the sector of power supply, for gas, steam and air conditioning, while 0.73% is water used in the sectors of mining and manufacturing industries.

The use of water for industry in the thousands of m3, 2007-2011

4.3. The use of water in agriculture

The use of water for irrigation for the reference period 2007-2011 is shown in the chart. Ground water sources are mainly used for irrigation (96.6% in 2011) while the surface water sources are used very little (3.4% in 2011).

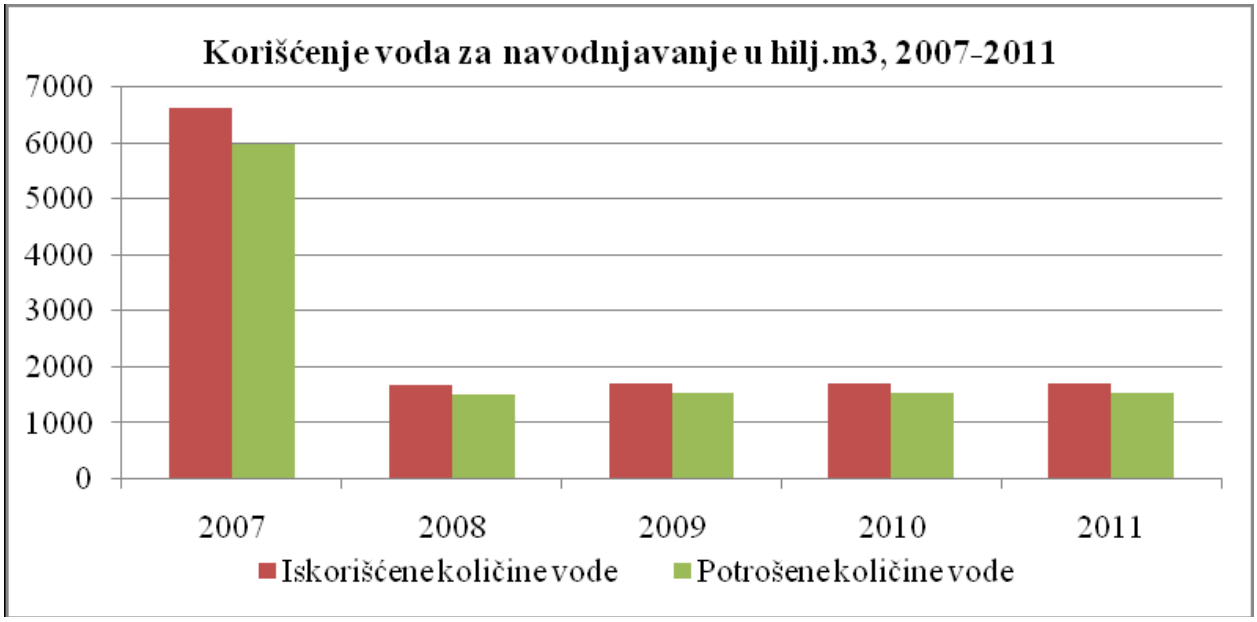

The use of water for irrigation in the thousands of m3, 2007-2011

5. CHANGE OF CLIMATE PARAMETRES - TRENDS

5.1 Temperature

Monitoring and evaluation of climate shows that the climate is changing in Montenegro as a result of global climate changes as well as variability. The clearest indicators are: a significant increase in air temperature, an increase in sea surface temperature and medium sea level, changes in extreme weather and climate events. Given that climate changes are related to long-term sequential changes (increase or decrease) in mean state of the atmosphere, that is one of the clearest signals of climate change changes in air temperature:

- Changes in annual temperatures from 1951 to 2012;
- mean decade values of annual air temperature
- mean values for the period 1961-1990
- Decade deviation (Δ) of climate normal.

On the basis of belonging to a certain type of climate, four representative municipalities in Montenegro (Žabljak, Pljevlja, Podgorica and Bar) were chosen also taking into consideration the quality of the data.

The mean annual air temperature for four municipalities - representatives of climate types

	Climate normal	DECADE						
REGIONS	61-90	51-60	61-70	71-80	81-90	91-00	01-10	Δ
Municipality Žabljak	4.6	5.1	4.7	4.5	4.7	5.4	6.0	+1.4
Municipality Pljevlja	8.1	8.6	8.1	7.9	8.2	8.8	9.1	+1.0
Municipality Podgorica	15.3	15.5	15.4	15.0	15.4	15.8	16.3	+1.0
Municipality Bar	15.5	15.7	15.7	15.3	15.6	15.9	16.8	+1.3

(Δ - Deviation of decadal 2001-2010 annual temperature of climate normal)

The results of the table indicate:

- Slightly colder weather during the decade of '71-'80;
- Changes to the warmer climate of the 90s (especially pronounced in the northern mountain region);
- 2001-2010 the warmest decade since the measurements began ('49 / '51)
- The biggest changes in the northern mountainous region of +1.4 ^{0}C and coastal region of +1.3 ^{0}C in period 2001-2010.

This part of the northern mountainous region at an altitude of about 1450 meters above sea level was interesting for the selection and overview of climate change due to major changes in annual temperature and the existence of Debeli namet i.e. a glacier located in Durmitor National Park whose research as a possible endangered system has been in the course. In the picture it can be seen that the variability has been more pronounced since the beginning of the 90s, while a positive slope trend line (i.e. its upward flow) indicates climate changes. For visual effects, deviations of the mean annual air temperature in Žabljak from 1958 to 2012 are graphically shown including the explanation of variability and climate changes.

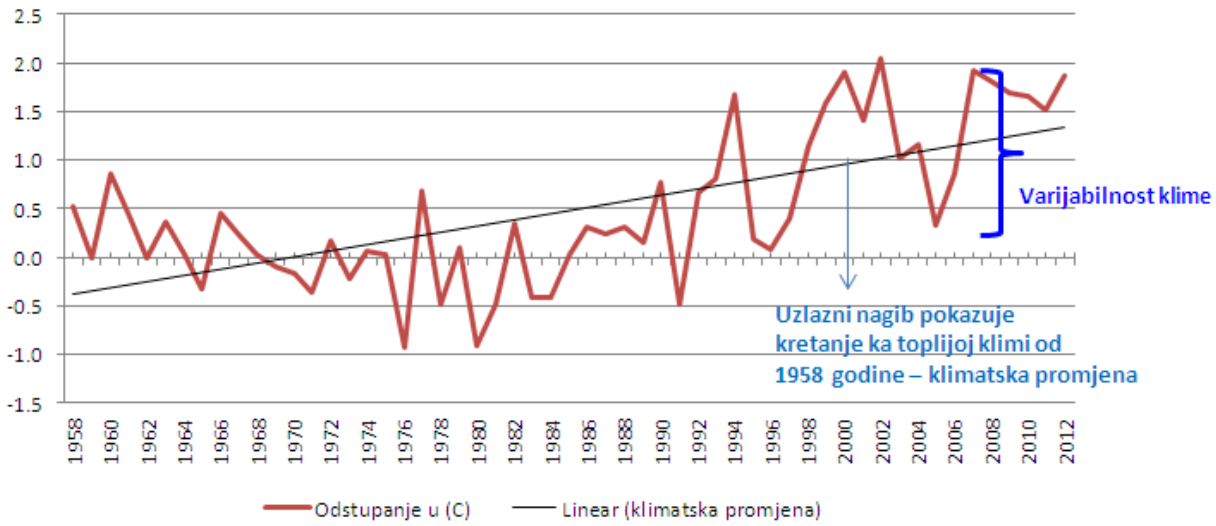

Deviations of the mean annual air temperature in Žabljak in relation to the climate normal

5.2. Precipitation

In the period 1991-2005, there was a statistically significant increase in mean precipitation in September compared to the climate normal (Podgorica, Kolašin). Exceptions are the mountainous areas above 1,000 m, where there is a weak trend of precipitation (Žabljak).

Generally, these changes indicate a change in precipitation regime that takes extreme character:

- decade 2001-2010 was at a record one by mean annual amount of rainfall after twenty years of continuous deficits;
- slightly higher amounts of rainfall were registered in 1971-1980 in the north mountainous region up to 1000 m above sea level and in the coastal region;
- 2010 was a record year by an annual amount of precipitation in the northern mountainous region of over 1000 meters above sea level and Zeta-Bjelopavlici region.

Decadal annual precipitation (mm)

	Climate normal	DECADE						
REGIONS	61-90	51-60	61-70	71-80	81-90	91-00	01-10	Δ
Municipality Žabljak	1455.4	-	1514.2	1564.4	1287.5	1370.1	1610.6	+155.2
Municipality Pljevlja	796.50	735.7	783.8	865.4	740.4	733	839.86	+43.4
Municipality Podgorica	1657.90	1632.1	1756.7	1695.2	1521.7	1593.7	1781.6	+123.7
Municipality Bar	1390.90	1414.1	1473.2	1480.5	1218.9	1241.9	1463.90	+73

(Δ - Deviation of decadal 2001-2010 annual precipitation of climate normal)

The annual amount of precipitation fluctuates around the normal and generally shows no tendency to increase or decrease. Exceptions are the north-eastern regions of Montenegro (Bijelo Polje) and the coast. In the northeast of the state, precipitation has been increased since 1949 (the correlation is good), while on the coast there is a trend of slight reductions in precipitation (correlation is small, i.e. 0.3).

CLIMATE CHANGE SCENARIO

The scenario of climate change for the area of Montenegro was made with the assistance of the EBU-POM (Eta Belgrade University – The Princeton Ocean Model) climate models. It is a linked regional climate model, which is a system of two regional models, one for the atmosphere and one of the oceans.

The results of the regional climate model EBU-POM from the experiments of future climate change for Montenegrin territory are focused on the results of scenario A1B for the period 2001-2030 and 2071-2100 and scenario A2 for the period 2071-2010. The values of CO_2 concentration at

the end of the twenty-first century for the A1B scenario are around 690 ppm, and for A2 scenario about 850 ppm, which represents approximately twice, i.e. 2.2 times higher value compared to the current observed value of 385 ppm.

The A1B scenario assumes a well-balanced mix of technology and utilization of basic resources, and technological development that allows avoiding the use of only one source of energy. The implications of such possible development of society in the future will be reflected on the emissions of greenhouse gases, ranging from very intense carbon emissions to possible decarbonization of emissions, at least as much as it is the variability of other conditioning factors relevant to this SRES scenario.

The A2 scenario assumes a heterogeneous society. In the background of this society are the requirements for reliance on local resources and preserving the identity of local communities. Due to a very slow increase of material goods and their proper allocation by regions, a more significant increase of the population would be expected. Economic development is primarily regionally oriented and technological exchanges would be much slower and more locally oriented compared to other scenarios (Nakicenovic and Swart, 2000).

The report focuses on two fundamental changes: surface meteorological parameters, temperature at 2 meters and accumulated rainfall. Changes in these parameters are shown in comparison to the average baseline period 1961-1990.

A model with four defined seasons (DJF - December, January, February, MAM - March, April, May, JJA June, July, August, and SON - September, October, November) was made for the SRES A1B scenario for the change in temperature at 2 meters above the ground and accumulated precipitation. Mean anomalies were calculated for the period 2001-2030.

According to the results of the model seasonal changes in mean temperature during the observed period, 2001-2030, are moving in the range of 0.600 C to 1.3°C, depending on the season and the area of Montenegro. Except for the SON season, it is evident that the temperature changes are significantly greater in the northern, mountainous part of Montenegro, compared with smaller changes in the area near the Adriatic Sea. The biggest change is during the season JJA, with values of 1.3°C in the north and 1° C in coastal areas. For the season DJF changes in the coastal part are about 0.5°C, while in the northern part the temperature increases by 0.9°C. For the season MAM, changes are a bit larger than in DJF with a value of 0.8°C in the south to 1.1°C in the north. The SON season was characterized by almost the absence of differences in temperature change, going from south to north, with more or less steady change in the entire territory of about 0.7°C.

Model results show negative and positive changes in precipitation, depending on the part of Montenegro and the season. Positive changes in precipitation and their increase can be seen for the season JJA, for the central area of Montenegro, and for the MAM season in parts bordering Bosnia and Herzegovina. These positive changes are very small, ranging up to 5%, compared to the

value of the baseline period, 1961-1990. In other areas of Montenegro during the two seasons, DJF and MAM, model results show a decrease in precipitation from -10% to 0%. The MAM season is characterized by deficient rainfall and the highest values of -20%, almost over the whole territory of Montenegro.

Results for scenario A1B for the period 2071-2100 for the past 30 years of the twenty-first century show that the spatial structure of changes of relevant parameters has been similar to the previously observed period 2001-2030, but with a greater magnitude of change. Again, the area along the Adriatic Sea has minor temperature changes compared to those in the northern mountainous region. This time temperature changes 2 meters above the ground range between 1.6°C and 3.4°C. The biggest changes are again recorded in the season JJA. Along the coastal area the temperature has increased by approximately 2.4°C, and in the northern mountainous region of the country these values are 3.4 °C. During the winter season (DJF), there is a noticeable gradient from the south towards the north of the country, with a temperature increase of 1.6°C in the coastal area, and 2.6°C in the north. For the MAM season, these changes vary from 1.6°C to 2.6°C, though the area with a change of 2.6° is much wider than in the previous period. Finally, for the SON season changes in the coastal region are about 1.6°C, and 2.4°C in the northern area along the border with Serbia.

During this period there is no season or area in Montenegro which is characterized by a positive anomaly of precipitation. For the DJF season in the central parts of Montenegro there is a negative anomaly of precipitation of -30%, while the northern and coastal parts have also a negative change but with values of up to -30%. The MAM season was characterized by a far more uniform deficit and values of about -10% in the whole territory. A significant deficit during the season JJA is evident in coastal areas, while in the central and northern parts negative anomalies are in the range of -20 to -15%. For the season SON, model results also show a significant decrease in precipitation from -30 to -50%.

The most significant changes in temperature according to the applied model were recorded for A2 scenario for the period 2071-2100, for the northern part of the country during summer period and they are 4.8°C. The greatest increase is during the JJA season in the mountainous region in the north, with values over 4.8° C. For this season, an increase in temperature of 3.4°C is foreseen in the coastal area. For the DJF season, temperature increase along the Adriatic coast is about 2.6°C, while this value in the northern parts is about 3.4°C. These values are a little higher during the MAM season, from 2.8°C to 3.6°C. Spatial distribution of changes is far more uniform during the SON season, in relation to other seasons, in the range of 2.6°C to 3°C.

For this scenario, the south-north gradient in the amplitude of temperature change is again present.

During all seasons, except for DJF, a negative anomaly of accumulated rainfall over the entire territory of Montenegro is predicted for the A2 scenario. A positive anomaly in the range 5-10% will be recorded only in the north-western parts during the season DJF, while during the same

season changes in other parts of the country will vary from -5% to -10%. The biggest changes according to this scenario are along the coast and during the JJA season, with a value of -50%. During this season an anomaly of -10% will occur in the northern parts. During the seasons of MAM and SON, the spatial distribution of anomalies is more uniform with a mean value of -20%.

The effect of a long-term climate changes was considered for the sensitive sectors such as: water resources, coastal areas, agriculture, forestry, biodiversity and public health. Predictions are made on the basis of climate scenarios A1B and A2 for Montenegro.

The analyses have shown that at about 90% of the country there is a deficit-reduction of annual precipitation that ranges up to 20% in certain areas. As water resources have a high degree of correlation with rainfall volumes and regime, the decrease in precipitation will generate changes in water resources. Changes in water resources are reflected in the significant amplitude and fluctuations, reduced capacity, a sudden increase in flood waters, and longer periods with reduced capacity.

According to the model of correlation between rainfall and the amount of flow, during the climate period 2071-2100, the trend of change in flow quantity on the example of the water resource of the Morača River through Podgorica will be reduced by 31% compared to the climatic normal for the period 1961-1990.

Considering the scenario for the changes in precipitation and temperature, a strong disturbance in the balance of water resources is expected to occur until 2100. Given that there is a high degree of correlation among the rainfall, flow volumes and yield, and in accordance with the expected climate scenarios envisaging different percentages of reduction in rainfall, ranging even up to 50% in some periods (scenario A2 for the period 2071-2100), it can be expected that an overall water balance (water potential) in certain areas will be reduced by as much as 50%. The changes in water resources will be determined by climate change, especially in the regime of precipitation, as follows: first, a reduction of overall water balance and secondly an increase in the amplitude of the hydrological cycles.

Accordingly, in years with low overall water balance and with pronounced oscillations there will also be periods of severe deficits and those with an intensive surplus in rainfall. In this new situation, there will be pronounced dry and rainy periods. Flood waves will become more frequent due to an increased intensity of rainfall (not of the volumes, since for example the volumes shall remain within average monthly limits but the number of rainy days will be lower than it is normally the case) and a change in the type of precipitation. Specifically, during the cold months of the year, when precipitation is the largest in major river upper flows (which are mostly mountainous), rainfall usually occurs in the form of snow. Over the past twenty years, due to global warming and higher temperatures, there has been an absence of snow and rainfall, so that it happens that with the same volume of precipitation there is a lot more water in the lower courses of rivers, and an increased risk of flooding, only because a part of this

water used to be deposited in the form of snow with a delayed discharge over a longer period of time, which is no longer the case. In accordance with the scenario A1B and a little more pessimistic scenario A2, which envisage an increase in temperature, it can be expected that the lack of snow, and thus the flood waves as well, will be more frequent and stronger.

THE EFFECT OF CLIMATE CHANGES ON WATER RESOURCES

Climate changes will certainly affect the condition of water resources, so that those will be generally reduced, consequently resulting in the reduction of reliability of their exploitation. According to the IPCC, the strongest losses of water resources will be in the Mediterranean and southern Europe.

Due to rising sea level, salt water will intrude into coastal aquifers, thereby endangering drinking water. According to INC, the trend of change in flow of the Morača River water resource through Podgorica will be reduced by 31% compared to the climate normal for the period 1961-1990. ECC study predicts significant vulnerability of drinking water sources to climate change. The findings of the project DMCSEE show that due to climate change, the available water resources for water supply have reduced capacities.

The *Law on water* and the *Law on financing water management* were adopted. Water has to become an economic category so that the policy of social development is in line with the policy of protection of aquatic ecosystems. There are no strategy or adaptation measures and estimates of the expected mechanisms of self-adaptation in the water sector.

In order to better monitor the status of aquatic ecosystems, it is important to continue the harmonization of national legislation with European (especially with Water Framework Directive 2000/60/EC) and Marine Strategy Framework Directive 2008/56/EC. National objectives should be in line with European and international ones regarding these types of aquatic ecosystems, good ecological status of surface waters and the sea; it is necessary to establish a set of characteristics, as well as a list of indicators with parameters (physical-chemical features, habitat types)

Current issues in the water sector:

- Lack of transparency of environmental data
- Significant overlapping of the competencies of institutions
- Insufficient use of land reclamation measures
- Small accumulation space of water management, uneven regime and unregulated level of high water
- Lack of systematic monitoring of water quantity and quality
- Inadequate regulation and protection of river beds
- Low level of waste water and rainwater treatment
- Lack of a register of polluters
- Lack of pre-treatment of industrial wastewater discharged into the public sewer systems
- Low level of population connected to the sewage systems

Measures for adaptation to climate change with reference to the water sector

- To establish a uniform water monitoring
- To establish a cadastre and measures to protect water supply sources
- To reduce losses in water supply networks and reduce / rationalize consumption
- To increase the production of table carbo-acidic mineral water
- To intensify the use of bottled drinking water and thus take advantage of unexploited healthy mineral water
- To provide sufficient quantities of drinking water (desalination, rainwater tanks)
- To build rural water pipelines
- To provide adequate drainage and wastewater treatment
- To achieve and maintain "good ecological and chemical status" of water
- To build modern land reclamation systems
- To build accumulations in accordance with the requirements of the environment
- To increase the overall capacity of reservoirs and also to se this reservoirs for different purposes
- To use boundary water resources (Skadar Lake, the Bojana River, Bilećko lake, The Piva River, etc.) through cross-border cooperation
- To regulate the water level of Skadar Lake
- To manage water according to the principle of river basins
- To define measures against degradation of river beds
- To conduct ongoing protection against flooding and erosion
- To coordinate the approach for each of river basins, according to the EU directives
- To raise public awareness of the need to save and protect water
- To provide water infrastructure.

Hanc ego cum tene sententiam – Trieste 22.04.2014

Let's grow up together

DRINK ADRIA

Adriatic IPA
Cross Border Cooperation 2007-2013

The project is co-funded by the European Union,
Instrument for Pre-Accession Assistance

Report:

Climate and climate change data on national level

Republic of Serbia

Institute for Development of Water Resources

“Jaroslav Černi”

(FB10)

Belgrade, 2014

Let’s grow up together

DRINK ADRIA

Adriatic IPA Cross Border Cooperation 2007-2013

The project is co-funded by the European Union, Instrument for Pre-Accession Assistance

Report about existing climate and climate change data on national level Republic of Serbia

This draft is prepared by DRINKADRIA project team at the Institute for water resources development "Jaroslav Cerni", Belgrade Serbia as a contribution to DRINKADRIA project implementation activities relevant for WP4

Belgrade, 2014.

Table of Content

1. INTRODUCTION

In this report, the selected general data for Republic of Serbia are presented. Since there is no pilot location in republic of Serbia, all data and information presented in this report apply to the whole territory. Climatic characteristics are exhibited based on data included in the official National Water Management Master Plan and include overall synthesis on precipitation and temperature as the most important climatological parameters of relevance for water management. Moreover, the short, general characteristics and specificities of surface and ground waters are presented.

Although different methodologies are applied in the climate change assessments and studies, from paleoclimate analysis, satellite observations the most frequent approaches are application of different methodologies, e.g., trend analyses, on the observed data and regional climatological models .

All global and regional climate models (RCMs) predict an increase in temperature and a decrease in precipitation in Serbia, with expected range from 2°C to 6°C/100 years, largely depending on the selected scenario and to a much lesser extent on the analyst (IPCC 2007; SINTA 2008; SEECOF 2010; CC-Waters 2011).

Annual precipitation predictions range from current levels (trend=0) to -25%/100 years. However, only a few of these models offer spatial (within Serbia) and temporal (yearlong) distributions. Each prediction is sensitive to assumption uncertainties and calculation imperfections. The quality of a prediction grows with increasing validation by recorded long-term trends.

Although the climatic models are widely used, the comprehensive analyses of the trend in the historical data sets are of the great significance. Given that, analyses of Climate parameters presented in this report are based on available data for observed Temperature and Precipitation, on the annual, seasonal and monthly level. Moreover,, some remarks are given for daily data.

All trend charts presented in this report are generated by application of the Surfer software, based on data recorded at analyzed temperature/precipitation or hydrological stations, removing the stochastic component by regional averaging.

2. EXISTING CLIMATE FEATURES IN SERBIA

2.1 Characteristic of present Climate

Serbia is landlocked country with diverse topography. The climate of Serbia is under the influences of the landmass of Eurasia and Atlantic Ocean and Mediterranean Sea. With mean January temperatures around 0 °C, and mean July temperatures around 22 °C In the northern part of the country, the climate is more continental, with cold winters, and hot, humid summers. In the south, summers and autumns are drier, and winters are relatively cold, with heavy inland snowfall in the mountains. Differences in elevation, proximity to the Adriatic Sea and large river basins, as well as exposure to the winds results in climate variations. Southern Serbia is subject to Mediterranean influences. However, the Dinaric Alps and other mountain ranges contribute to the cooling of most of the warm air masses. Winters are quite harsh in the Pešter plateau, because of the mountains, which encircle it. One of the climatic features of Serbia is Košava, a cold and very squally southeastern wind which starts in the Carpathian Mountains and follows the Danube northwest through the Iron Gate where it gains a jet effect and continues to Belgrade and can spread as far south as Niš. Generally speaking, mean annual air temperatures are more uniform than mean temperatures in singular months. Annual mean air temperatures in the North part of the Republic vary between 10 and 11.8 ^{o}C, in lower areas in the Central and South parts between 10 and 12 ^{o}C. Lower temperatures occur in hilly and mountainous regions. Mean annual temperatures linearly decline with increase of terrain elevation. Mean annual temperatures for the Republic are approximately as follows: on elevation of 300 m 11,4 ^{0}C; on 1000 m 7.3 ^{0}C and on 1700 m 3.3 ^{0}C. Therefore, vertical mean temperature gradient is approximately –0.6 ^{0}C / 100 m.

Precipitation is one of the most important climatological components. Average depth of precipitation on the territory of Republic of Serbia is 734 mm/year. Precipitation regime is very heterogeneous with respect to time and space due to the atmospheric processes and topographic characteristics. The Southwest parts of Kosovo belong to the Maritime precipitation regime (precipitation that occurs during cold half of a year (October-March) presents more than 50% of total annual rainfall). Other parts of the Republic have Continental regime (more that 50% of total annual rainfall occurs in warmer half of a year). Central and Eastern part of Kosovo and Metohija belong to the transition zone that is characterized with influence of both mentioned regimes.

Total annual precipitation in the River Beli Drim watershed and particularly in its right tributaries (Pećka Bistrica, Erenik and others) is 1500 mm/year. Something smaller but also substantial precipitations occur in the watersheds of upper Ibar River, Plavska River and Lepenica River (more than 900 mm/year). In the central part of the Republic, total annual precipitation depths vary from 1000 mm/year (in mountainous regions) to 600 mm/year. There is a tendency toward decreasing of precipitation depths from the West to the East in the plain areas.

Table 1: average monthly and annual precipitation (mm)at the selected localities in Serbia.

Station	Month												Year
	1	2	3	4	5	6	7	8	9	10	11	12	
Sombor	35,4	33,5	33,0	48,7	60,0	76,3	60,9	48,8	35,8	40,6	53,4	44,7	571
Kikinda	33,5	34,7	32,3	44,8	53,0	74,1	52,9	50,2	36,4	35,1	48,0	46,3	541
Zrenjanin	35,2	36,3	36,1	45,7	62,4	83,9	58,8	47,7	36,0	35,1	47,8	47,3	571
Novi Sad	43,6	43,4	43,8	52,0	62,5	85,9	67,5	54,0	38,4	41,6	54,4	56,6	643
S. Mitrovica	40,8	39,7	40,3	49,6	60,9	84,5	65,1	52,0	39,5	44,0	54,0	53,1	623
Beograd	48,3	44,1	48,9	55,3	73,6	95,8	66,2	50,0	47,6	44,9	57,8	57,5	690
Šabac	47,7	43,9	46,1	54,8	65,4	84,6	65,4	55,7	47,6	47,6	60,3	60,0	678
Valjevo	50,1	45,5	52,1	62,7	86,7	98,8	75,9	69,4	54,5	54,0	62,7	57,8	770
S. Palanka	44,9	38,5	44,7	49,7	66,9	88,4	59,1	47,3	42,6	45,3	54,4	49,0	631
Rudnik	71,3	72,1	72,2	80,2	105,2	121,3	90,9	74,8	66,2	61,7	74,6	75,8	966
Negotin	51,8	47,7	46,8	55,7	82,3	91,0	68,3	56,4	50,5	45,8	56,1	60,2	713
Kragujevac	42,6	38,5	43,9	50,6	74,2	82,5	67,8	48,8	42,5	39,4	48,8	49,1	629
Požega	50,3	45,5	47,3	54,9	82,6	83,8	79,1	57,9	56,9	55,2	63,5	52,7	729
Zlatibor	62,0	58,6	58,0	72,7	100,8	103,0	90,0	76,3	77,5	73,1	84,7	67,9	924

Sjenica	45,5	40,4	37,8	47,7	73,6	80,2	65,3	61,6	55,0	60,8	74,0	53,0	695
Dimitrovgr.	39,2	39,2	43,7	52,4	79,2	85,8	55,5	43,5	39,1	43,3	58,9	48,8	629
Niš	38,6	38,3	39,8	51,6	64,5	63,4	43,3	41,8	41,0	40,0	57,8	51,6	571
Vranje	40,0	41,5	42,6	50,3	65,5	70,1	49,2	38,2	45,8	52,2	66,1	52,8	614
Priština	35,8	38,3	38,6	51,4	69,7	62,0	48,3	44,7	43,2	50,0	65,0	53,2	600
Prizren	67,8	54,5	57,9	58,2	69,1	65,2	54,5	44,4	56,5	60,5	84,1	72,3	744

The majority of surface water in Serbia originates out of its territory, approximately 92% (162, 5 billion m^3 / year) entering the country from the upstream countries. Domicile surface water resources are approximately 16 billion m^3 /year, e.g., 8%. In the table bellow, average, maximum and low flows are presented for selected localities for the largest rivers.

Table 2: Flows at the largest rivers in Serbia

River	Station	Q (m^3/s)		
		Q_{av}	$Q_{min\ 95\%}$	$Q_{max\ 1\%}$
Dunav	Bezdan	2267	952	7017
	Pančevo	5264	1976	15311
Tisa	Senta	794	134	3914
Sava	Sr. Mit.	1535	272	6379
Morava	LJ. Most	234	35	2396
Drina	Radalj	362	69	4940

Groundwater is significant source for drinking water supply in Serbia, more precisely; over 70% of population and industry use it. More than half of groundwater is from alluvial aquifers, with **80-90%** being infiltrated river water.

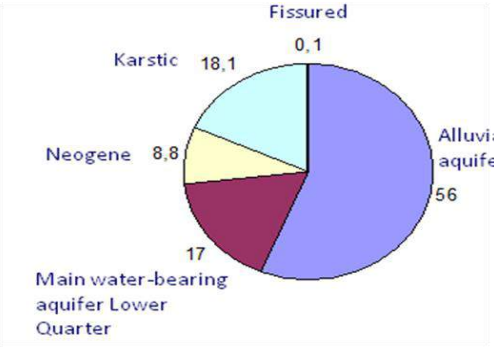

Figure 1: aquifers types in Republic of Serbia

2.2 Observed Climate changes in Serbia

The period selected for observed data analysis in this report is from 1949 to 2006. This period is convenient because it is relatively long (58 years), data are available from numerous monitoring stations, and they exhibit a close similarity to estimated long term temperature and precipitation trends (JČI 2011; HMSS 2011).

Temperature

To assess past temperature trend, 26 temperature stations were selected (JČI 2011). They are presented in the table 3

Table 3: Monthly and yearly temperature trends for period 1949 – 2006 (°C/100yrs)

	Temper. station	Jan	Feb	Mar	Apr	May	Jun	Jul	Aug	Sep	Okt	Nov	Dec	Annual
1	TS Sombor	2.9	1.4	2.6	-0.2	2.3	1.6	1.7	2.0	-0.6	0.9	-1.3	-1.8	**1.0**
2	TS S.Mitrovica	1.7	1.3	2.4	-0.4	2.2	0.5	0.3	1.2	-1.0	1.6	-1.3	-1.8	**0.6**
3	TS Senta	3.2	2.6	3.2	0.9	3.0	2.3	2.3	2.1	-0.2	1.9	-0.9	-1.6	**1.6**
4	TS Beograd	2.5	2.5	4.0	0.6	2.8	1.7	1.8	1.9	-0.9	1.4	-0.7	-1.5	**1.3**

5	TS Zlatibor	2.9	1.6	2.8	0.0	2.2	1.5	1.6	0.6	-2.1	1.8	-1.4	-2.3	**0.8**
6	TS Kruševac	1.8	1.5	3.4	0.0	1.7	1.0	1.0	0.7	-1.6	0.9	-2.0	-2.9	**0.5**
7	TS Niš	1.2	0.8	3.0	-0.3	1.1	0.4	1.0	0.5	-2.0	1.0	-2.2	-2.7	**0.1**
8	TS Požega	1.8	1.6	4.1	1.6	3.3	2.7	2.3	1.4	-0.5	1.5	-2.4	-2.9	**1.2**
9	TS Pirot	2.1	1.6	4.3	1.3	2.6	2.2	2.2	1.8	0.1	2.0	-1.6	-1.4	**1.4**
10	TS Vranje	0.5	0.1	2.5	-0.6	0.9	0.7	0.6	-0.1	-2.3	0.3	-2.6	-3.1	**-0.3**
11	TS Zaječar	2.9	2.1	4.5	0.1	1.9	2.0	1.8	1.2	-1.1	0.8	-2.1	-1.9	**1.0**
12	TS Knjaževac	1.9	0.6	3.1	-0.8	1.2	0.8	0.4	-0.3	-2.4	0.0	-3.1	-2.4	**-0.1**
13	TS V. Gradište	1.3	1.0	2.2	-0.7	1.1	0.5	0.6	0.5	-2.1	0.0	-1.8	-2.9	**0.0**
14	TS Aleksandrovac	1.1	1.4	2.6	-1.9	-0.7	-1.0	-0.6	0.0	-2.1	1.0	-2.2	-3.4	**-0.5**
15	TS Leskovac	0.6	-0.4	2.2	-1.1	0.4	0.2	0.0	-0.9	-3.4	-0.8	-3.6	-3.2	**-0.8**
16	TS Prokuplje	0.4	0.2	2.3	-1.8	-0.3	-0.8	-0.2	-0.6	-2.5	0.4	-2.9	-3.2	**-0.7**
17	TS Ćuprija	1.2	0.4	2.2	-1.1	0.7	-0.2	0.1	-0.1	-2.4	0.0	-2.4	-3.1	**-0.4**
18	TS Čačak	2.1	1.0	2.8	0.2	2.1	1.2	1.5	1.1	-1.0	1.1	-2.6	-1.9	**0.6**
19	TS Novi Pazar	4.4	4.2	5.8	2.1	3.6	3.4	3.6	2.5	1.3	3.4	-0.6	-0.3	**2.8**
20	TS Sjenica	2.9	1.4	2.8	-0.2	1.3	1.4	2.1	0.9	-1.1	2.0	-2.1	-1.0	**0.9**
21	TS Ivanjica	3.4	2.8	4.6	1.4	3.0	2.4	2.3	1.1	-0.5	2.2	-1.5	-0.8	**1.7**
22	TS Jagodina	1.1	1.6	3.8	-0.4	2.4	1.3	1.6	1.3	-0.9	1.2	-1.8	-2.7	**0.7**
23	TS Čumić	2.3	2.0	3.0	-1.0	1.0	0.0	0.4	1.1	-0.8	2.3	-1.2	-1.9	**0.6**
24	TS Valjevo	2.1	1.2	2.9	0.2	2.6	1.4	1.7	2.0	-0.5	1.6	-1.8	-2.1	**0.9**
25	TS Dragaš	0.6	-0.4	2.5	-0.9	-0.5	-0.9	-1.6	-1.9	-4.3	0.7	-1.9	-3.3	**-1.0**
26	TS Bujanovac	1.8	0.6	3.4	0.1	1.8	1.4	1.0	0.0	-0.6	2.4	-1.3	-1.9	**0.7**
	Average	**1.9**	**1.3**	**3.2**	**-0.1**	**1.7**	**1.1**	**1.1**	**0.8**	**-1.4**	**1.2**	**-1.9**	**-2.2**	**0.6**

It is observed based on analyses that the annual average temperature trend in Serbia was found to be about 0.6°C/100 years. The spatial distribution is shown in Figure 2 .

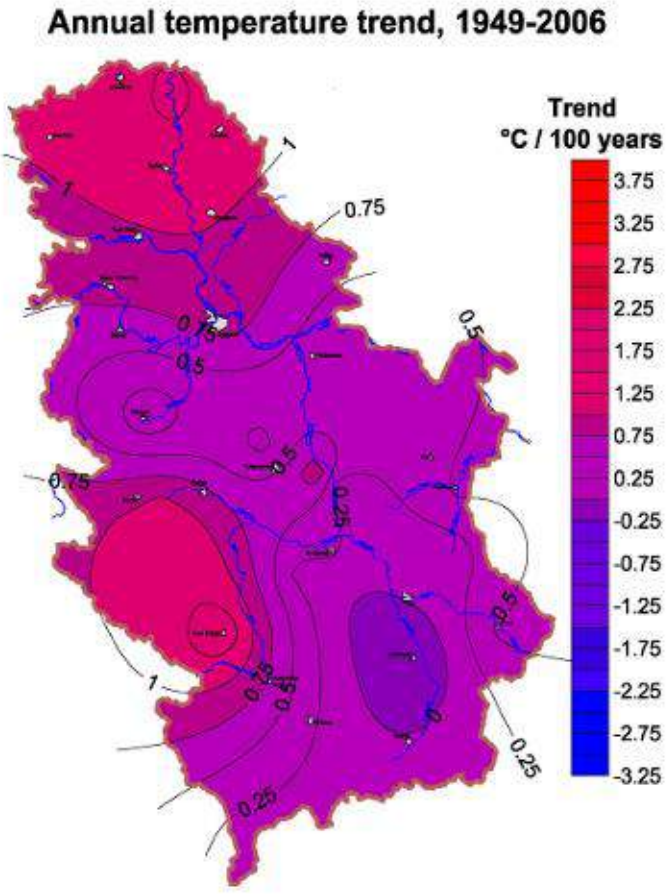

Figure 2: Temperature trends in annual data series in Republic of Serbia (Dimkic et al, 2011)

The greatest increase was noted in mountainous regions and in the north of the country, and the smallest increase in the southeast of the country.

The greatest increase has been recorded in the **spring** (some 1.5°C/100yrs), followed by the **summer** (1.0°C/100yrs) and **winter** (0.5°C/100yrs), while the **autumn** exhibited a negative trend of about -0.7°C/100yrs .

If the seasons were assessed by calendar instead of groups of three months, the claim about the greatest T increase over the summer months would become quite questionable in Serbia.

Short remarks regarding Temperature daily data: While all stations reported a significant temperature increase (trend) for daily maxima, the daily minima exhibited from no distinct trend to a negative trend in the southeastern part of the country (consistent with annual trends); in the remainder of the country it was positive but much lower than that of the daily maxima. Nearly all stations recorded a downward stochastic trend, indicating relative consistency of the described temperature trends.

Precipitation

To assess past precipitation trend, 34 precipitation stations were selected (JČI 2011). They are presented in the table 4.

Table 4 Monthly and yearly precipitation trends for period 1949 – 2006 (%/100yrs)

	Precip. station	Jan	Feb	Mar	Apr	May	Jun	Jul	Aug	Sep	Okt	Nov	Dec	Annual
1	PS Bezdan	-4.3	-60.1	2.0	-21.1	-48.2	-6.9	15.7	43.8	97.5	49.8	-32.9	-43.7	**-1.7**
2	PS Šid	62.3	-7.8	23.8	35.2	6.5	42.9	50.8	16.7	99.2	110.3	12.2	-47.8	**33.2**
3	PS Horgoš	-2.6	-8.8	30.3	35.2	-63.6	-7.7	63.8	25.1	116.6	39.6	-76.4	-31.1	**7.2**
4	PS Jaša Tomić	-35.3	-76.9	-1.3	68.3	-9.3	21.7	25.5	50.4	121.0	36.7	-76.5	-37.0	**9.4**
5	PS Prijepolje	-7.6	34.2	9.6	90.7	6.3	-26.1	4.7	86.8	97.6	23.5	22.9	42.2	**30.4**
6	PS Kuršumlija	-11.7	-35.0	-38.0	44.1	-18.5	-42.5	60.4	22.7	68.4	-92.0	-42.8	-1.9	**-7.4**
7	PS Leskovac	-9.5	-3.8	-37.0	65.7	-9.4	-4.5	40.0	31.9	90.7	13.9	-38.5	13.9	**11.9**
8	PS Beoce	-49.7	16.4	45.8	85.4	-5.0	-5.4	77.6	75.6	113.5	12.0	-20.3	20.8	**30.9**
9	PS Pirot	12.6	-47.0	4.1	37.3	-19.4	-6.4	-26.8	110.9	34.4	-4.4	-90.3	-6.8	**-2.4**
10	PS Vranje	-49.8	-32.4	-51.1	12.0	-27.6	15.1	-27.7	66.1	-4.1	-32.1	-117.4	-52.2	**-25.9**
11	PS Knjaževac	-5.4	-25.0	-11.1	63.1	-23.2	-8.2	-55.8	45.3	79.7	22.9	-80.6	-52.4	**-6.2**
12	PS Svrljig	24.0	-13.9	2.1	47.4	-58.0	2.4	17.8	115.2	46.7	-19.4	-51.6	-30.8	**3.6**
13	PS Voluja	-22.9	-70.1	9.2	58.2	-54.8	-76.7	-76.6	21.8	7.0	13.1	-93.0	-45.5	**-31.0**
14	PS Aleksandrovac	-54.2	-33.4	-68.0	26.7	-96.0	-12.3	14.4	36.9	28.9	-78.7	-51.1	-6.2	**-24.2**
15	PS Vučje	22.2	64.1	-4.1	-9.0	-87.7	-28.2	34.1	26.3	55.4	8.7	-46.2	3.9	**-2.1**

16	PS Trećak	-28.8	-78.1	-43.1	23.4	-90.9	-39.1	-15.9	-30.3	-13.7	-107.6	-47.6	-37.3	**-43.0**
17	PS Ćuprija	-1.1	10.3	16.8	69.0	-64.1	10.3	-6.4	39.9	64.4	25.3	-39.3	-4.2	**7.4**
18	PS Kosjerić	-5.2	27.6	-23.9	15.9	-54.9	-4.1	-9.0	3.2	54.6	7.1	-15.4	-6.8	**-2.9**
19	PS Novi Pazar	-40.6	6.2	5.5	68.7	-43.7	-29.1	57.5	50.3	102.1	-11.3	-7.7	9.8	**13.7**
20	PS Brodarevo	-26.2	17.8	-34.8	66.2	-30.5	-1.2	-17.2	21.7	122.5	-45.9	11.9	0.4	**7.2**
21	PS Ivanjica	-75.3	-5.6	-57.9	13.7	-60.8	-31.1	5.3	28.4	92.1	-13.1	38.0	-3.5	**-5.9**
22	PS Vranovina	-30.1	4.1	-36.7	66.7	-20.8	-1.2	59.3	81.8	102.9	0.0	-10.5	36.9	**22.5**
23	PS Rekovac	-20.2	-19.1	4.4	33.1	-71.7	9.5	1.3	69.5	93.7	-4.4	-56.2	-28.5	**-0.7**
24	PS D. Šatornja	-55.2	-38.2	-49.3	20.7	-68.0	55.1	32.8	49.5	71.9	28.4	17.4	7.9	**8.8**
25	PS Osečina	-11.8	-14.3	3.1	39.5	-27.9	79.1	50.4	55.9	86.2	59.7	11.0	-8.1	**29.3**
26	PS Dragaš	46.2	46.4	59.2	37.7	-46.2	-55.6	-16.6	39.7	4.8	-11.2	-32.6	54.5	**7.4**
27	PS Bujanovac	-55.9	-16.2	-38.6	45.7	-65.7	22.4	2.7	7.3	13.1	-24.2	-110.2	7.4	**-18.8**
28	PS Jajinci	-8.4	-17.2	-16.6	41.9	-75.8	-14.7	-6.4	63.0	73.4	64.0	-38.0	-10.3	**1.5**
29	PS Senta	-24.9	-61.2	2.9	34.4	-43.7	-5.5	35.3	10.0	131.0	37.2	-59.2	-30.0	**1.0**
30	PS S. Mitrovica	-26.0	-84.4	-9.9	1.3	-52.9	-8.4	2.3	70.5	74.6	87.2	-38.2	-112.5	**-8.1**
31	PS K. Reka-Brus	13.0	-18.3	-52.8	40.5	-42.7	-19.4	-5.2	42.1	100.3	-49.5	-63.9	-23.1	**-7.7**
32	PS Martinci	-15.0	-59.1	3.3	9.9	-45.4	-6.7	10.9	77.5	91.2	86.7	-11.5	-70.9	**4.1**
33	PS Krupac	-27.1	-93.3	-61.9	-20.6	-55.5	-38.1	-61.0	-18.3	26.1	-74.2	-132.2	-40.8	**-50.3**
34	PS Bogojevo	-17.9	-44.3	-6.6	-33.1	-16.4	-2.4	53.2	27.7	65.4	57.8	-39.8	-75.9	**-2.2**
	Average	**-16.0**	**-21.7**	**-12.4**	**35.7**	**-43.7**	**-6.6**	**11.5**	**43.1**	**70.9**	**6.3**	**-41.4**	**-17.9**	**-0.3**

The annual average precipitation trend in Serbia was found to be slightly negative. The spatial distribution is shown on Figure 3 (JČI 2011, period 1949-2006; Smailagić 2009, period 1950-2004).

The change in magnitude of precipitation is of great interest among the scientific community since it is important input in water management policies and infrastructure development. Diverse methodologies are applied in the assessment and modeling (trend analysis, climate models). With respect to spatial scale, projections of the future precipitation magnitude refer

to local, regional, continental and global scale. According to the available literature precipitation amount, magnitude, and temporal distribution are changing. Observed and detected changes and associated influence on hydrological cycle affect water management and human society in many ways.

It is noteworthy to mention that understanding of data sets, methodology applied, and associated constrains are prerequisite for the reasonable findings.

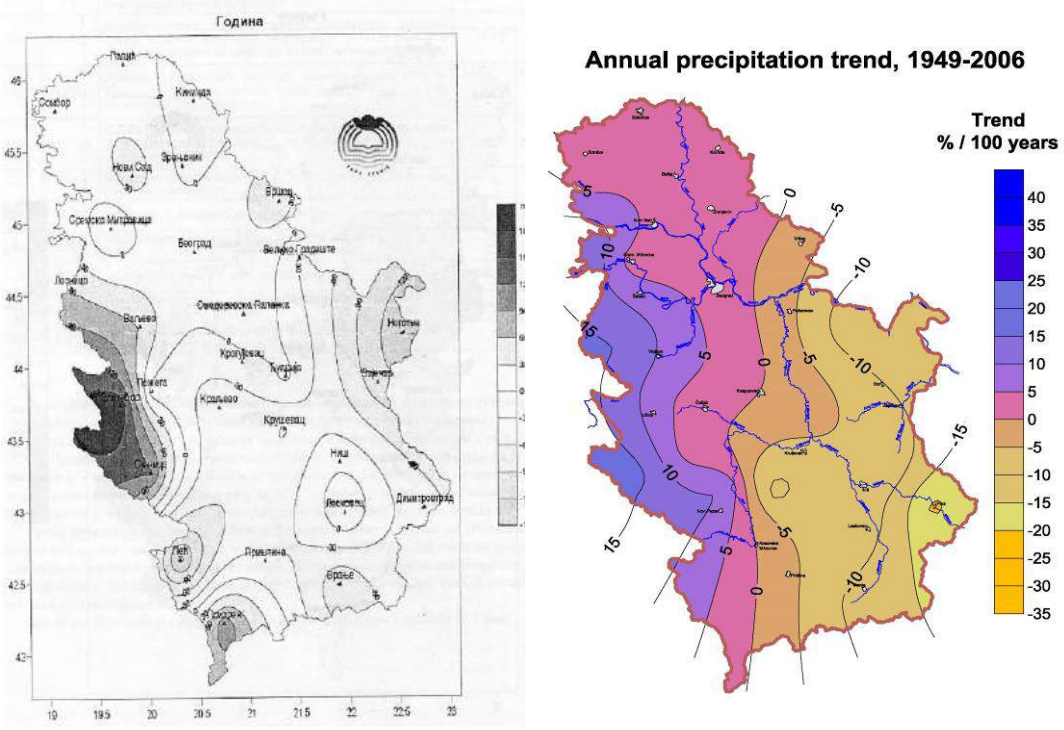

Figure 3 Observed precipitation data annual trends evaluation in Serbia by Smailagic (left Figure, in mm/55 yrs) and Dimkic (right Figure, in %/100 yrs) Source: Smailagic (2009) and Dimkic et.al. (2012).

Despite that results depicted in Figure 3 origin from different methodologies applied for trend assessment in individual studies they exhibit similarities with respect to trends in observed precipitation data across the Serbia. Furthermore, the findings from majority of GCM and RCM demonstrate decrease in average precipitation in Serbia, with more significant trend in eastern part of the country. According to results of trend evaluation in average precipitation data by Dimkic et.al.(2012) the lowest negative trend is from -5% to 0% /100 yrs in Central Serbia with gradual trend decrease in average precipitation in Eastern Serbia. These trend

projections agree very well with observed data. The summary results for monthly data are exhibited in figure 4.

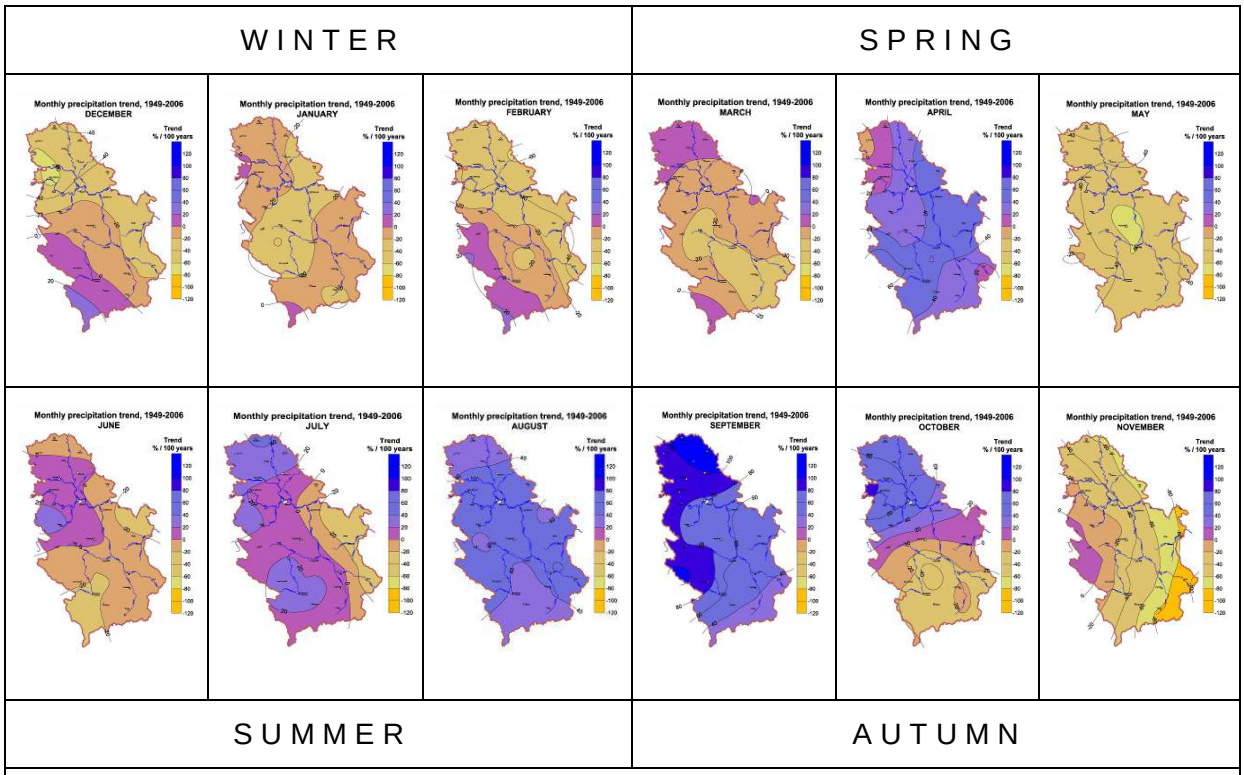

Figure 4. Spatial precipitation trend distribution by month(%/100yrs).

Short remarks regarding precipitation daily data: To a large extent in line with the annual distribution of the precipitation trend, daily maxima exhibited an upward trend in the western and northern parts of the country (albeit with an upward stochastic trend, suggesting increasing unpredictability), while there was a downward trend of daily maxima in the southeastern part of the country, in parallel with a declining stochastic component.

3. CLIMATE CHANGE SCENARIOS

Since the first GCM the improvement of resolution is significant by the development of Regional Climate Models (RCM). Different RCM models are developed in Serbia (SINTA 2008; SEECOF 2010; CC-Waters 2011, etc)

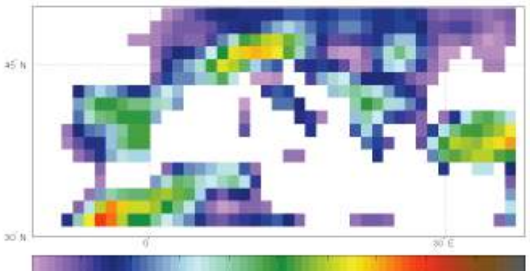

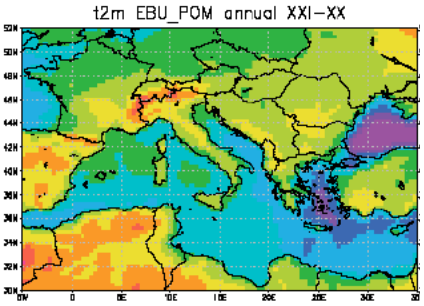

Figure 5a: Echam4 model; world scale 1,125° - 2° Fig. 5b : Ebu-Pom model; med scale 0,2° - 0,25°

The most significant improvement is accomplished in last years within the Climate change centre of Hydrometeorological Service of Serbia in cooperation with the faculty of Physics at the University of Belgrade. Figures bellow present climate change predictions developed by this centre, based on scenario A1B i A2 (Djurdjevic, 2012).

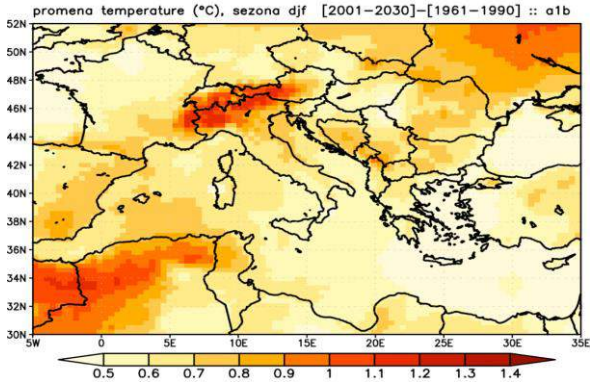

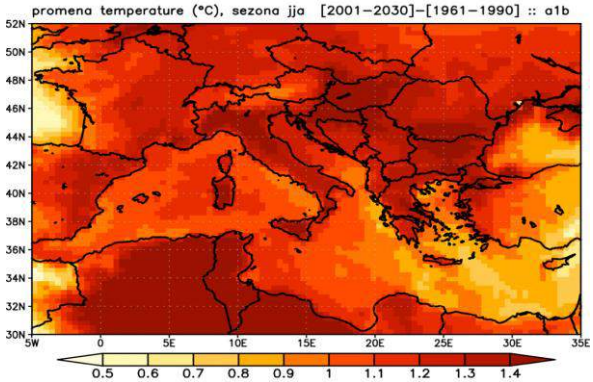

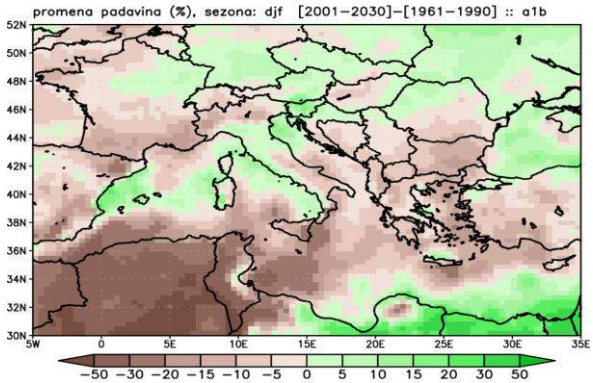

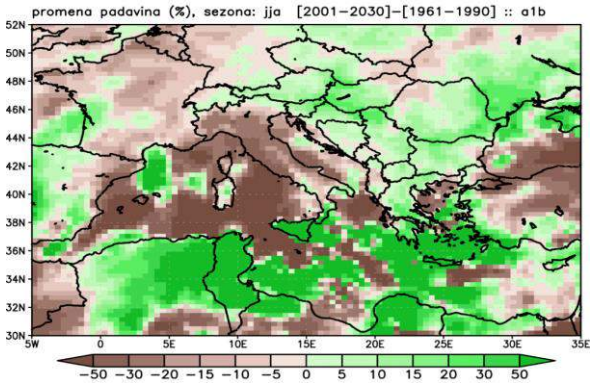

Since for the near future, the difference between two scenarios are unsignificant, results based on scenario A1B are presented .

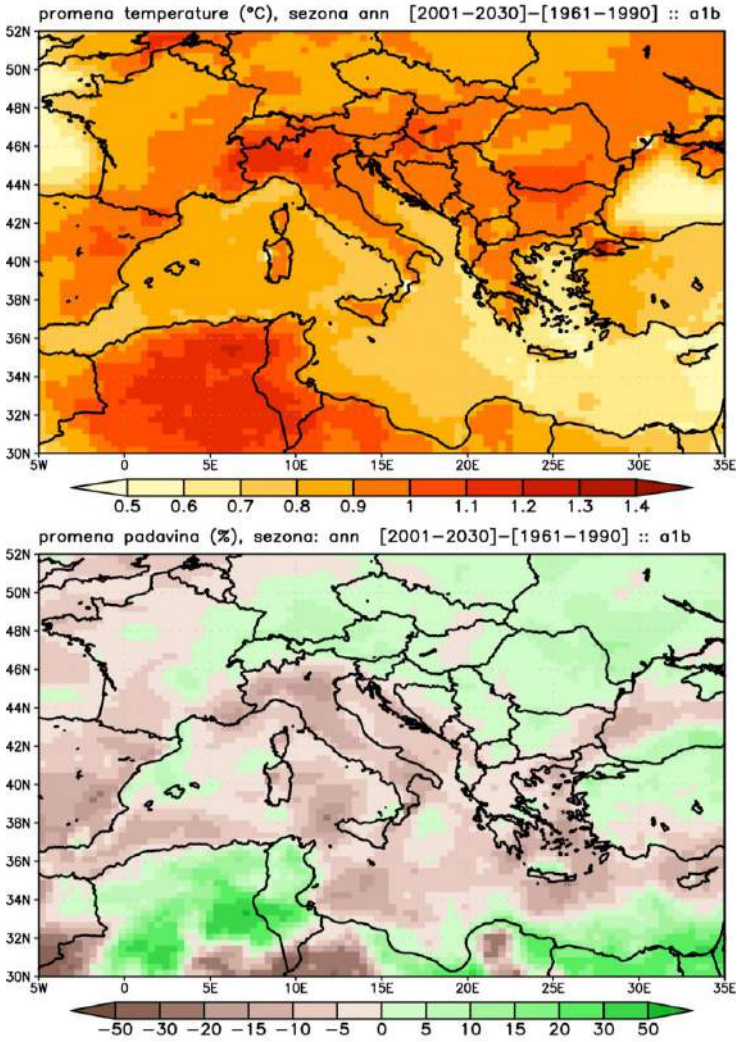

Figure 8: change in precipitation and temperature based on scenario A1B

Based on the figures, the average temperature change an the annual basis is around +1°C, e.g., while change in precipitation are between - 5% to ±5%.

For the long term predictions, the results based on both scenarios (A1B and A2) are presented in this report. Based on data exhibited in Figure 9 (a and b).

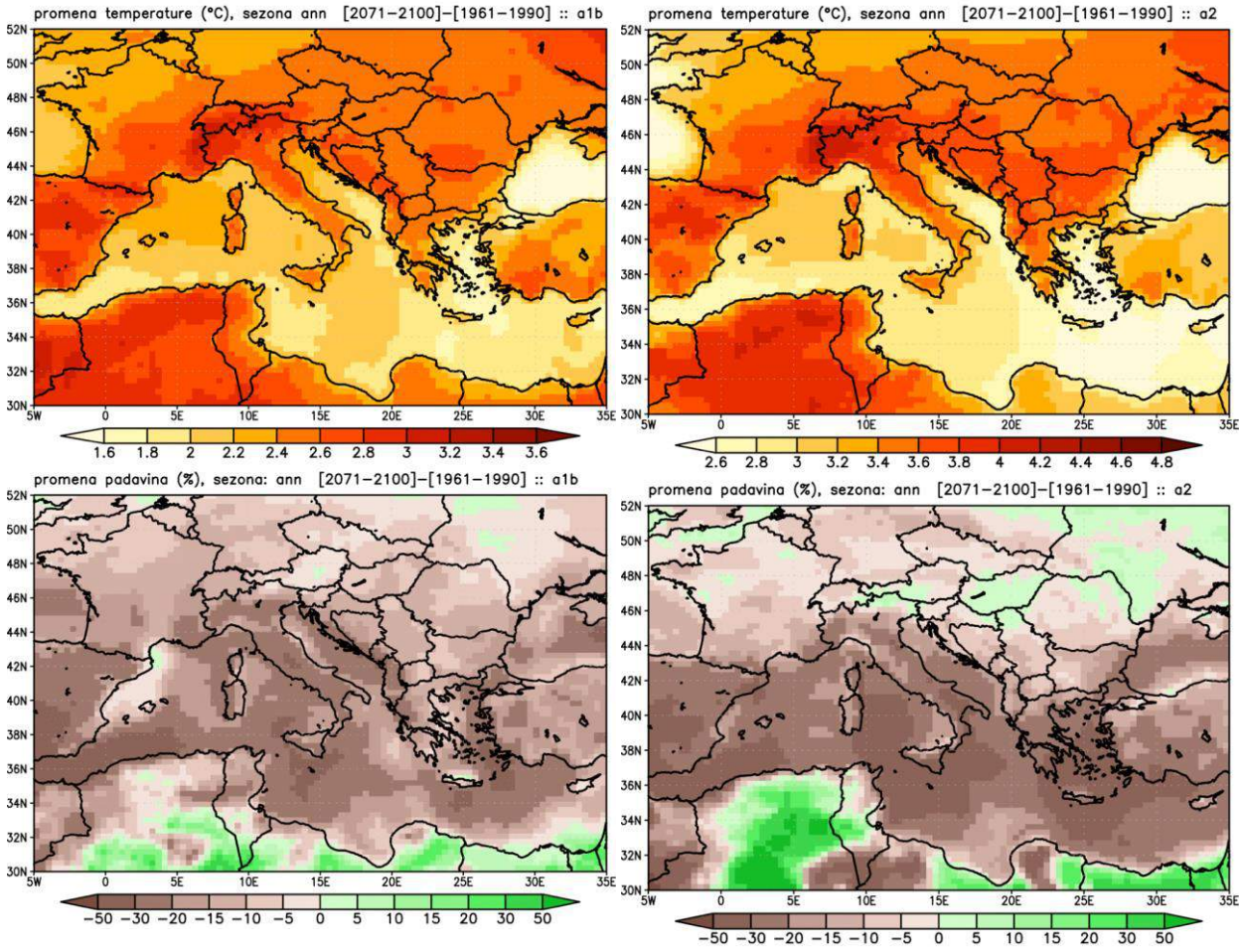

Figure 9 : Changes in precipitation and temperature based on scenarios A2 and A1B

According to this two scenarios, by the end of 21 century change in the annual average precipitation values are expected to be approximately -15%, while for the temperatures there are difference in the predicted changes in average temperatures +2.5°C and +3.7°C, for A1B and A2 , respectively.

4. UNCERTAINITIES

When we think about prediction of future changes in climate and especially water sector, we must consider the probability and reliability of such events. Two reasons exist why is especially important to underline uncertainties in any forecast or projection. First, because ordinary people often accept any projection as one claim, and they are often confused seeing quite (sometimes totally) opposite results in several different projections. Second, because uncertainties is not the same for different issues. There are many sources of uncertainty, e.g., length of time series used for assessment, spatial resolution, selected scenarios, data quality, etc.

Two approaches for the degree of certainty are proposed by the IPCC (IPCC 2013, Summary for Policymakers):

• Qualitative Confidence according to type, amount, quality, and consistency of evidence (e.g., mechanistic understanding, theory, data, models, expert judgment) and the degree of agreement.

• Quantified measures of uncertainty in a finding expressed probabilistically (based on statistical analysis of observations or model results, or expert judgment).

When it comes to variables and phenomena that impact water resources management, the Strategy on adaptation to climate change for the Danube River Basin (DRB), (ICPDR, 2013), Figure 10, weighty uncertainties for the CC impacts in the DRB are attributed to floods, sedimentation and contamination, etc. The medium certainty is assigned to the great number of variables/ events, e.g., droughts, runoff, water availability, low flow, etc. High and very high certainties are assigned to the average precipitation and temperature projections, respectfully. Figure 8 depicts graphically level of certainty associated with different impacts on Danube River Basin. Our opinion is that this figure is very illustrative and representative for Serbia: the most certainty forecast is related to temperature increasing, after that to snow regime, than to precipitation, runoff and drought forecasts, and the most uncertainty field (regarding the main issues and from the water point of view) are floods. That's because generally decrease of precipitation on annual level is expecting in Serbia, but also likely increase of extreme rainfall, particularly on hours scale.

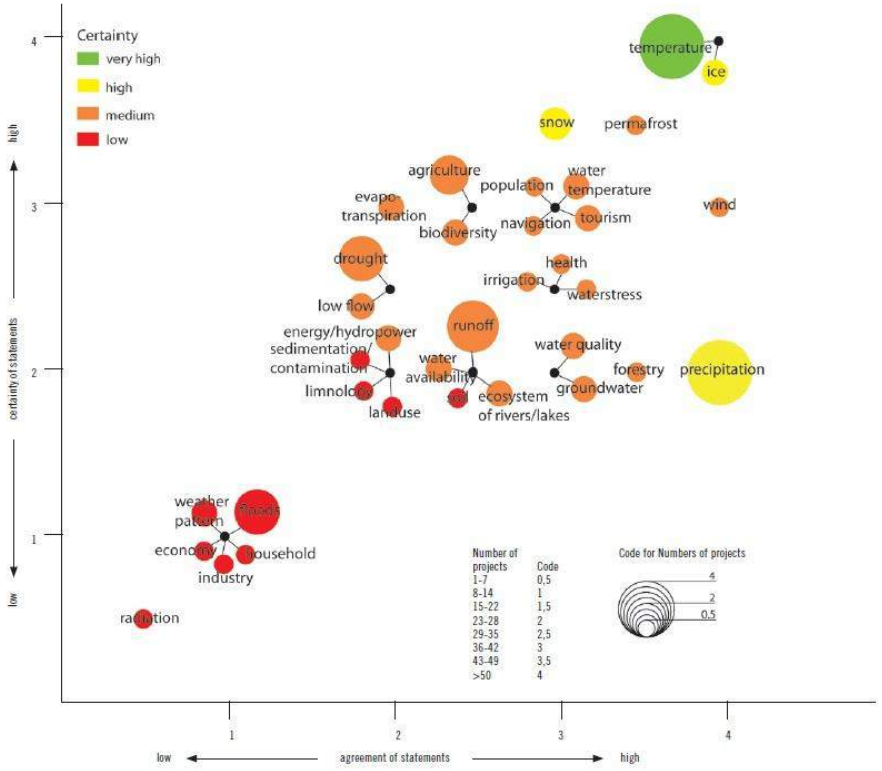

Figure 10: Certainty for the impacts in the Danube River Basin due to projected climate changes (ICPDR, 2013)

Even exist, the lowest uncertainties exist for observed changes. Measured data with relevant long period of observation increase certainty not just regarding observed changes, but also with respect to future prediction results and conclusions.

Uncertainty is inherent in any prediction and as the distance in the future increases, so does the degree of uncertainty (i.e. the range of possible developments expands while the probability of occurrence of each one of them decreases).

5. REFERENCES

Climate Change and Impacts on Water Supply (CC-WaterS) - International Study for SE Europe, 18 Institutions from SE Europe, May 2009 – May 2012, [Available online at http://www.ccwaters.eu/index.php?option=com_content&view=article&id=48&Itemid=54&56b00064c3e6beb26da3b96d1578b92a=caac98a9a4248cd115a194c70c97a142].

Dimkić, D. and J. Despotović, 167-180, Climate Change - Anthology, Inferences from Paleoclimate and Regional Aspects, 2012, (Eds.) A. Berger, F. Mesinger, Dj. Šijački, ISBN 978-3-7091-0972-4

Dimkić, D., D. Ljubisavljevic and M. Milovanović, Observed and future climate and hydrological trends in Serbia, 2012, Hydropredict Conference, Vienna, Austria

Djurdjević, V., 2012: Zoning of climate scenarios in South East Europe using a dynamic climate model (in Serbian); Presentation at the Militin Milanković Association, Belgrade, September 2012, www.milutinmilankovic.rs

ICPDR Strategy on Adaptation to Climate Change (2013), ICPDR – International Commission for the Protection of the Danube River

IPCC, 2007: Climate Change 2007: Synthesis Report. Contribution of Working Groups I, II and III to the Fourth Assessment Report of the Intergovernmental Panel on Climate Change. Core Writing Team, Pachauri, R. K. and Reisinger, A. (Eds.) IPCC, Geneva, Switzerland. 104 pp. [Available online at http://www.ipcc.ch/publications_and_data/publications_ipcc_fourth_assessment_report_synthesis_report.htm.]

Jaroslav Černi Institute for the Development of Water Resources (JCI), 2010-2012, Climate Change Impacts on River Hydrology in Serbia – National Study (in Serbian).

Arnell, N. W., 2003: Effects of IPCC SRES emissions scenarios on river runoff: A global perspective. *Hydrol. Earth Syst. Sci*., **7**, 619–641.

Fowler, H. J., C. G. Kilsby, and J. Stunell, 2007: Modelling the impacts of projected future climate change on water resources in north-west England. *Hydrol. Earth Syst. Sci*., **11**, 1115–1126.

Fujihara, Y., K. Tanaka, T. Watanabe, T. Nagano, and T. Kojiri, 2008: Assessing the impacts of climate change on the water resources of the Seyhan River Basin in Turkey: Use of dynamically downscaled data for hydrologic simulations. *J. Hydrol*., **353**, 33–48.

Hydro-Meteorological Service of Serbia (HMSS), 2011, [Available online at http://www.hidmet.gov.rs].

International project SINTA (Mediterranean project, participants: Euro-Mediterranean Center for Climate Change from Bologna, University of Belgrade Institute of Meteorology, and the Hydro-Meteorological Service of Serbia), 2007-2008, [Available online at http://www.earth-prints.org/handle/2122/4675].

Juckem, P. F., R. J. Hunt, M. P. Anderson, and D. M. Robertson, 2008: Effects of climate and land management change on stream flow in the driftless area of Wisconsin. *J. Hydrol*., **355**, 123– 130.

Ma, Z., S. Kang, L. Zhang, L. Tong, and X. Su, 2008: Analysis of impacts of climate variability and human activity on stream flow for a river basin in arid region of northwest China. *J. Hydrol*., **352**, 239–249.

Novotny, E. V., and H. G. Stefan, 2007: Stream flow in Minnesota: Indicator of climate change. *J. Hydrol.,* **334**, 319–333.

Smailagić, J., Climate change in Serbia, Monograph: In Memory of Milutin Milanković, 2009, ISBN 978-86-910313-1-2.

South East Europe Climate Outlook Forums (SEECOFs), 2008-2010., [Available online at http://www.google.rs/search?hl=sr&source=hp&q=climate+change+seecof&btnG=Google+%D0%BF%D1%80%D0%B5%D1%82%D1%80%D0%B0%D0%B3%D0%B0&meta=&gbv=2&oq=climate+change+seecof&aq=f&aqi=&aql=&gs_sm=s&gs_upl=1280l13231l0l17334l23l23l1l5l3l0l297l3464l0.9.8l17l0].

Janjic ZI (1990) Physical package for step-mountain, Eta coordinate model. Mon Weather Rev 118: 1429–1443

Janjic ZI (1996) The surface layer parameterization in NCEP Eta model. CAS/C WGNE 4.16–4.17, WMO, Geneva

Xue Y, Vasic R, Janjic Z, Mesinger F, Mitchell KE (2007) Assessment of dynamic downscaling of the continental U.S. regional climate using the Eta/SSiB Regional Climate

Model. J Clim 20: 4172–4193. doi: 10.1175/ JCLI4239.1

Mesinger F, Janjic ZI, Nickovic S, Gavrilov D, Daven D (1988) The step mountain coordinate: model description and performance for cases of alpine lee cyclogenesis and for a case of an Appalachian redevelopment. Mon Weather Rev 116: 1493–1518

Rajkovic B. and Djurdjevic V., 2009: Examples from the "SINTA" project: Dynamical downscaling for the Mediterranean region, Stvaralstvo Milutina Milankovica, SANU.

Vasiljević B., Dimkić D., Đurđević V.: Historical Overview and Different Methodologies Applied in Climate Change Studies, International Conference Climate Change Impacts on Water Resources, 17-18 October 2013, Belgrade, Serbia, Publisher: Jaroslav Černi Institute for the Development of Water Resources, ISBN 978-86-82565-41-3, pp. 183-194, 2013

Zavatarelli, M., and Pinardi, N. 2003: The Adriatic sea modeling system: A nested approach, Ann. Geophys., 21, 345–364, http://www.ann-geophys.net/21/345/2003/.

Let's grow up together

DRINK ADRIA

Adriatic IPA
Cross Border Cooperation 2007-2013

The project is co-funded by the European Union,
Instrument for Pre-Accession Assistance

Report:

Climate and climate change data for Albania

SHUKALB: Water Supply and Sewerage Utility of Albania (FB11)

Tirane, 2014

Lead Author/s	Alban Kuriqi
Lead Authors Coordinator	Arlinda Ibrahimllari
Contributor/s	Anisa Aliaj
Date last release	8.10.2014
State of document	Final Report

Let's grow up together

DRINK ADRIA

Adriatic IPA Cross Border Cooperation 2007-2013

DRINK ADRIA

The project is co-funded by the European Union, Instrument for Pre-Accession Assistance

CONTENT

1. INTRODUCTION

The republic of albania is located in southeastern europe, in the western part of balkan peninsula facing the adriatic sea and the ionian sea. Albania has a surface area of 28,745 km2. Its terrain is mountainous, where hilly and mountainous areas represent 77% of the country's territory. Climate of albania is typically mediterranean. It is characterized by mild winters with abundant precipitation and hot summers. Temperature values vary from 7° c over the highest zones up to 15° c on the coastal zone; in the south- west the temperatures even reach up to 16° c. Annual mean maximum of the temperature varies from 11.3 °c in the mountainous areas up to 21.8 °c in the low and coastal zones while annual mean minimum temperature various from 0.1°c - 14.6 °c.

The mean annual precipitation total over albania is about 1485 mm/year. The highest precipitation is recorded in the albanian alps with the value of 2800-3000 mm/year, while the southeast part has lower precipitation about 1000 mm/year. Since the country produces majority of the electricity from hydropower's the precipitation is an important factor in national electricity production and agriculture. Precipitation changes, increase of the temperature, and increases in the frequency and severity of natural disasters are forcing people to address the impacts in new and innovative ways and begin adapting to a climate changes.

Because of the high percentage of the electricity that is produced by hydropower and the industrial productivity that has continued to fall the levels of the greenhouse gas emissions in albania are about four to five times lower than average international levels. In a regional context albania is considered as one of the most risky countries in east europe and central asia this because of the high exposure to extreme weather, high sensitivity combined with low adaptive capacity[1].the albanian government became part of the united nations framework convention on climate change in 1995. Recently, approved the kyoto protocol.also, has just started the third national communication to united nation framework convention on climate changes with united nation development program and global environmental facilities [2].

2. EXISTING CLIMATE FEATURES IN ALBANIA

Albania is located in southeastern europe, in the western part of balkan peninsula facing the adriatic sea and the ionian sea. Generally speaking, the climate regime of albania is typical mediterranean, characterized by mild winters with abundant precipitation and hot, dry summers. Considering the complexity of the different physical and geographical factors, the country is divided in four main climate areas as shown in the picture below.

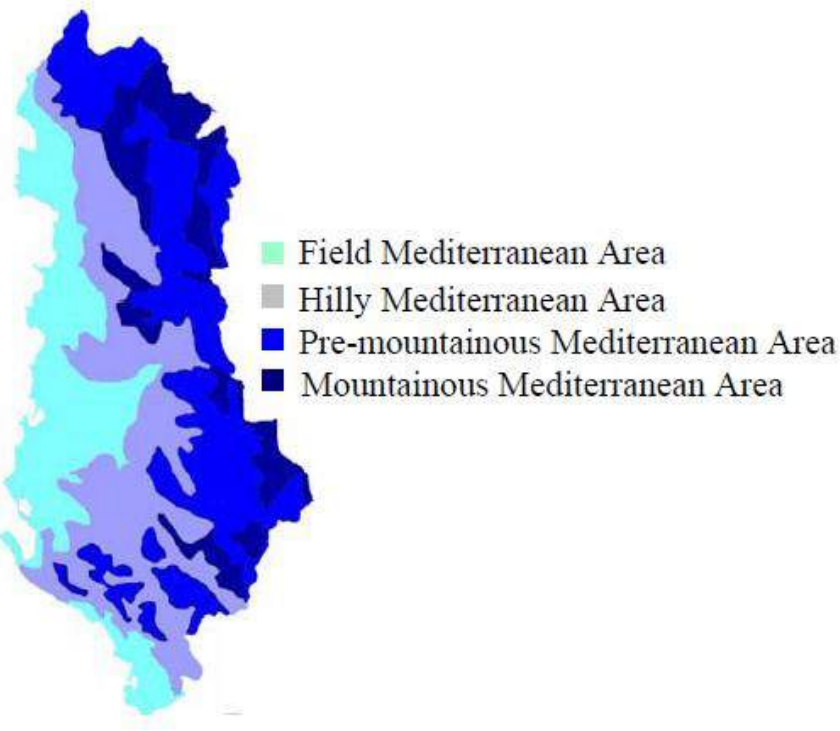

Figure 1. Climate areas in albania [3]

The field mediterranean area which is divided further in three subareas, northern, central, and southern, is characterized by mild winters, and a typical mediterranean climate. Due to the closeness to the sea, and the low elevation, the precipitation in this part of the country is mostly in the form of rainfall. The hilly mediterranean area, is located parallel to the coastal area, and extends to the inner of the country. Due to the extension of this area from north to the south, and the diversity of the elevation features, the climate can vary significantly in different parts of this part of the country. The hilly mediterranean area includes four climate subareas: northern, central, south-eastern, and south-western. The pre-mountainous mediterranean area is divided in two subareas: pre-mountainous northern mediterranean and the pre-mountainous southern mediterranean. The valley nature and the high elevation are the two main factors that drive the climate in this area. The mountainous mediterranean area represents the high elevations, above 1000-1300 m above sea level. It is divided in four subareas: northern mountainous mediterranean, eastern mountainous mediterranean, southeastern mountainous mediterranean, and the southern mountainous mediterranean [4].

The mean annual precipitation total over albania is about 1485 mm/year. However, the spatial distribution of precipitation varies a lot, depending on the physical and geographical features of the area. The alps and the north-western part of the country are the areas that receive more precipitation compared to other parts of the country, and in the same time they represent one of the areas with high precipitation in europe. The mean annual precipitation in the alps is roughly 2000 mm/year, and due to the high altitude, a major part of precipitation in this area is in the form of snow. The alps have recorded also the highest precipitation total with the annual values reach up to 3000 mm/year [5].

The southeast mountainous zone is also one of the areas with high precipitation, where the annual values reach up to 2200 mm.the north-eastern part of the territory is characterized by low precipitation due to the continental climate. The average annual precipitation in the area is between 700 and 900 mm. The eastern part of the central region represents one of the regions with the least amount of precipitation, and the annual average values of precipitation range between 600 and 700 mm. The southeast part of thecountry receives the smaller amount of precipitation with the annual value up to 600 mm.

The temperature values for the country range between 7°c in the highest altitudes up to 15°c in the coastal zone. The albanian alps together with the eastern central mountainous area represent one of the coldest zones. The mean annual temperature in this area is around 7°c. Annual mean maximum air temperature varies from 11.3 °c in the mountainous areas up to 21.8 °c in the low and coastal zones. The annual mean minimum varies from –0.1°c in the mountainous areas up to 14.6°c in the low and coastal zones. The central mountainous area is influenced by the cold continental air masses coming from the east as well as the cold air masses coming from the sea. As a result, the highest temperatures in this area are in the river valley of shkumbin (14-15°c), mat (12-14°c), drini i bardhe (12-13°c), drini i zi (11-12°c), etc. In the southern mountainous area, the warm air masses coming from the mediterranean bring high annual temperatures. The ionian coastal zone of this region is characterized generally speaking by high annual temperatures, varying from 7 to 18°c.

The lowland coastal zone, is under the direct effect of the warm air masses coming from the sea, and in the same time is influenced by the latitude of albania. As a result, despite of the high average annual temperature, the temperature varies a lot from 17°c in the south, up to 14°c in the north. The same temperature regime is present in the north-eastern part of the country, with the only difference that this area is affected also by the mountainous features of the area [6].the air temperature records measured in the meteorological stations of shkoder and tirana for the period 1931 - 2000 show an increase in the temperature by 1°c during the end of the first half of the 20th century. The third quarter of the 20th century is characterized by cooling of 0.6°c, while the rest of that period up to today, the climate has demonstrated an increase in temperature by 1.2°c, figure 2 and figure 3 demonstrate these variations in temperature for the above mentioned period, for some of the stations in albania.

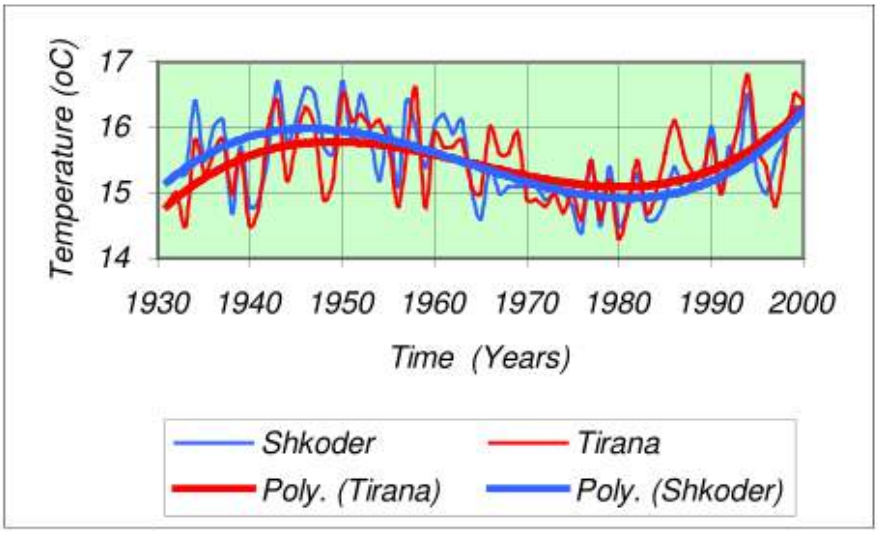

Figure 2. The mean annual air temperature variation in the meteorological stations of Tirana and Shkoder for teh period 1931 - 2000 [7]

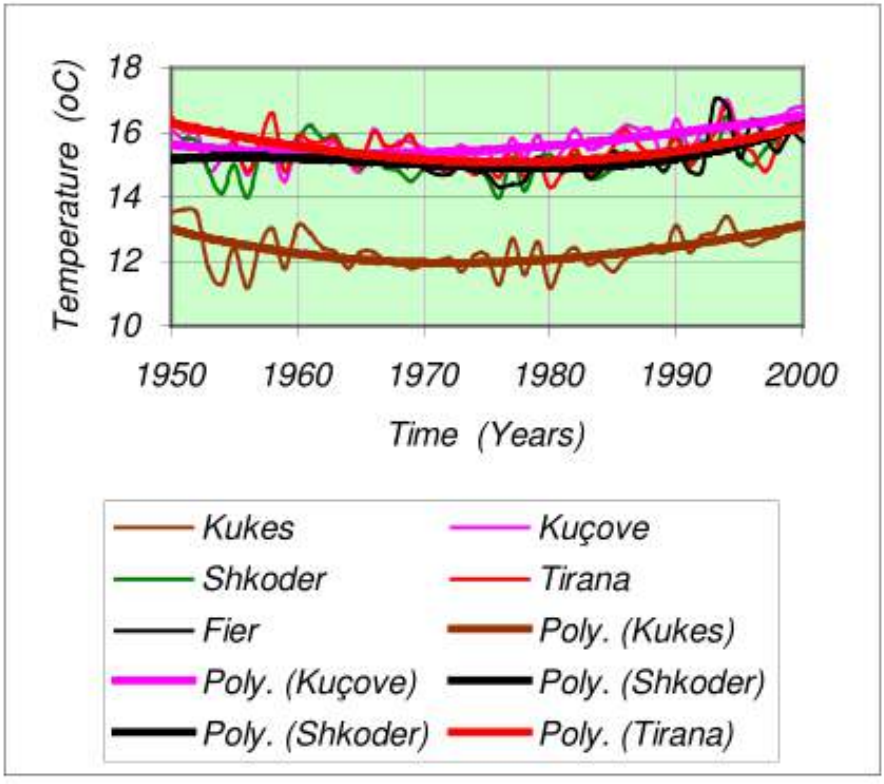

Figure 2.The mean annual air temperature variation in the meteorological stations of Tirana, Shkoder, Kukes, Kucova, and Fier [8]

The changes in the air temperature are associated with changes in the amount of precipitation as well as shown in the figure below. Temperature (^{0}c)

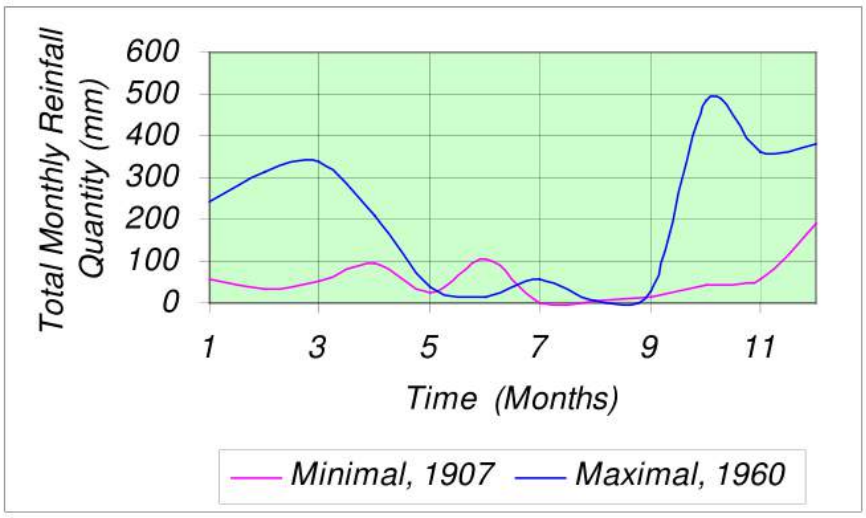

Figure 3.The total annual precipitation in the driest (1907) and wettest (1960) years, measured in the meteorological station of Shkoder [9]

This variability of climate can be also noticed in the below study area (drini river basin) from the report prepared on albania's second national communication on climate changefigure 4.

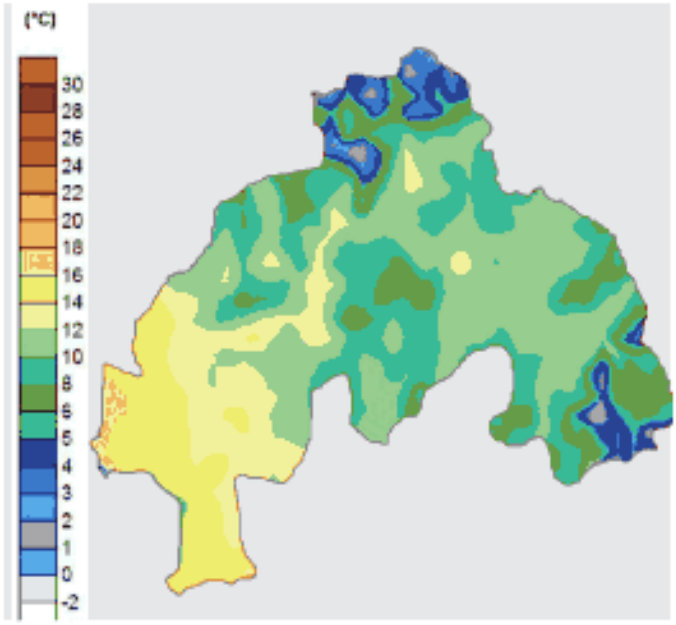

Figure 4.Yearly mean air temperature[10]

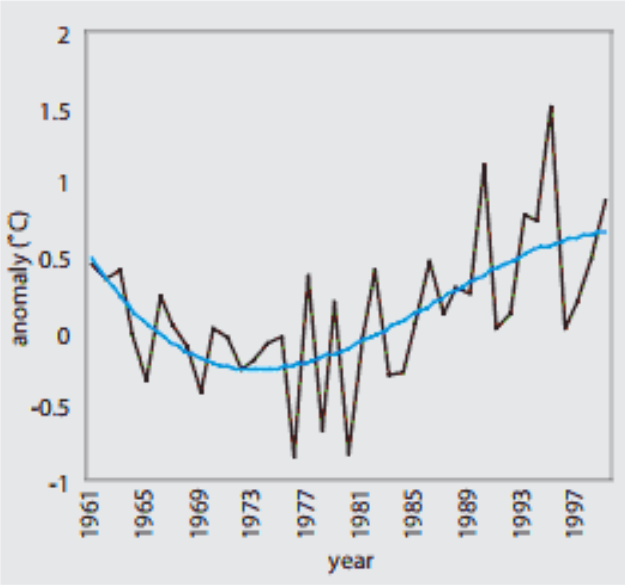

Figure 5.Yearly anomaly and the trend of airtemperature (Shkoder) [11]

From the graph in figure 5 it can be noticed that that in general the annual mean temperature has increased by approximately 1.0°c for the entirezone.

The precipitation in the drini river basin varies widely also from 910 mm in the eastern part (kukës) to 2260 mm in iballe, and the average precipitation is 1634mm per year as shown in figure 6.

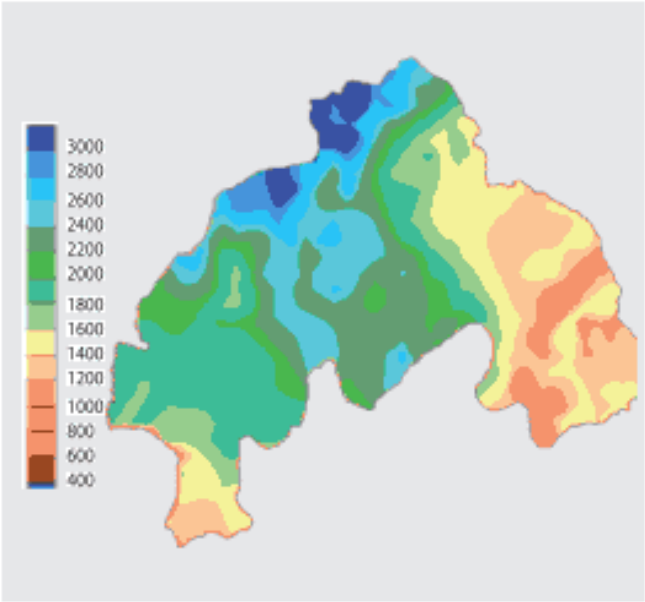

Figure 6. Distribution of annual precipitationtotal (1961–90)[12]

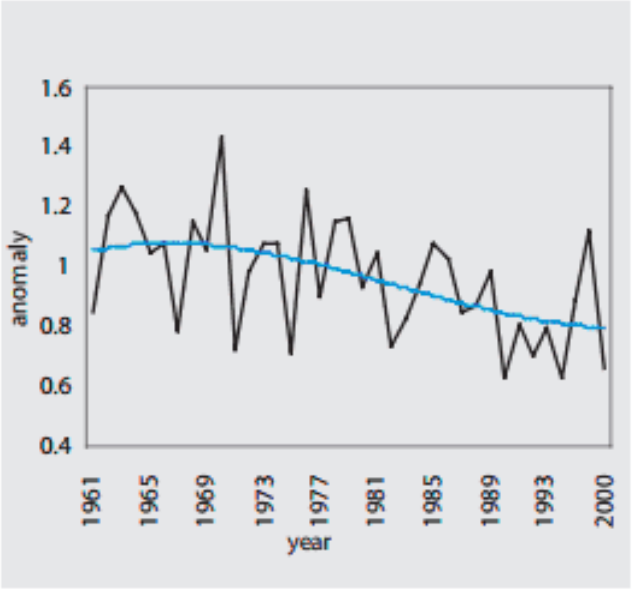

Figure 7.The annual precipitation anomaly andtrend (kukës)[13]

The data on precipitation for the period 1961-2000 show a slightly decreasing trend in the total precipitation. The highest amount of precipitation (66 % of the total), is recorded during the cold months (october-march). The wettest months are november–december, and the driest are july-august[14]

3. CLIMATE CHANGE SCENARIOS

According to the climate scenarios for albania, developed within the 2nd nc, milder winters, warmer springs, hotter and drier summers and drier autumns are likely to be expected. A dramatic increase in temperature (+4.0°c to +7.3°c) is projected for summer according to *the high-resolution regional climate projections sres a2 scenarios were provided by the hadley centre, uk for the project "climate change projection for south eastern europe", wb.* Within the south east european climate change framework action plan for adaptation report. The projections show a decrease in annual precipitation and a drastic decrease in summer precipitation (~40%). Sea level rise of between 30–45 cm is projected by 2100 for the adriatic sea.

According to the 2nd nc the projected change in climate extremes show more hot days and heat waves are very likely in almost the entire territory of albania. There are likely to be more frequent and severe droughts with greater fire risk. An increase in the wind speed is expected for the 2080s. A decreased number of frost days (temperatures ≤–5°c) in high altitudes is likely to occur. Owing to higher average temperatures in winter more precipitation is likely to fall in the form of rain rather than snow, and this will increase both soil moisture and run-off. Although total precipitation is expected to decrease, the number of days with heavy precipitation is likely to increase resulting in greater risks of soil erosion and landslides [15].

In albania reference *second national communication, 2009*, the results of the future climate change in a broader region of albania are discussed for temperature at 2 m (t2m) and precipitation.

Likely changes in temperature and precipitation in albania (including the study area) are presented in table 1. Temperature is expected to increase and precipitation to decrease, giving milder winters, warmer springs, hotter and drier summer and drier autumn, while figure 1, 2 illustrates likely annual changes for the study area.

Scanarios for albania		Time horizon		
		2025	2050	2100
Annual	Temperature (^{0}c)	0.8 to 1.1	1.7 to 2.3	2.9 to 5.3
	Precipitation (%)	-3.4 to -2.6	-6.9 to -5.3	-16.2 to -8.8
Winter	Temperature (^{0}c)	0.7 to 0.9	1.5 to 1.9	2.4 to 4.5
	Precipitation (%)	-1.8 to -1.3	-3.6 to -2.8	-8.4 to -4.6
Spring	Temperature (^{0}c)	0.7 to 0.9	1.4 to 1.8	2.3 to 4.2
	Precipitation (%)	-1.2 to -0.9	-2.5 to -1.9	-5.8 to -3.2
Summer	Temperature (^{0}c)	-11.5 to -8.7	-23.2 to -17.8	-54.1 to -29.5
	Precipitation (%)	1.2 to 1.5	2.4 to 3.1	4.0 to 7.3
Autumn	Temperature (^{0}c)	0.8 to 1.1	1.7 to 2.2	2.9 to 5.2
	Precipitation (%)	-3.0 to -2.3	-6.1 to -4.7	-14.2 to -7.7

Table 1. Predicted scenarios for climate changes [16]

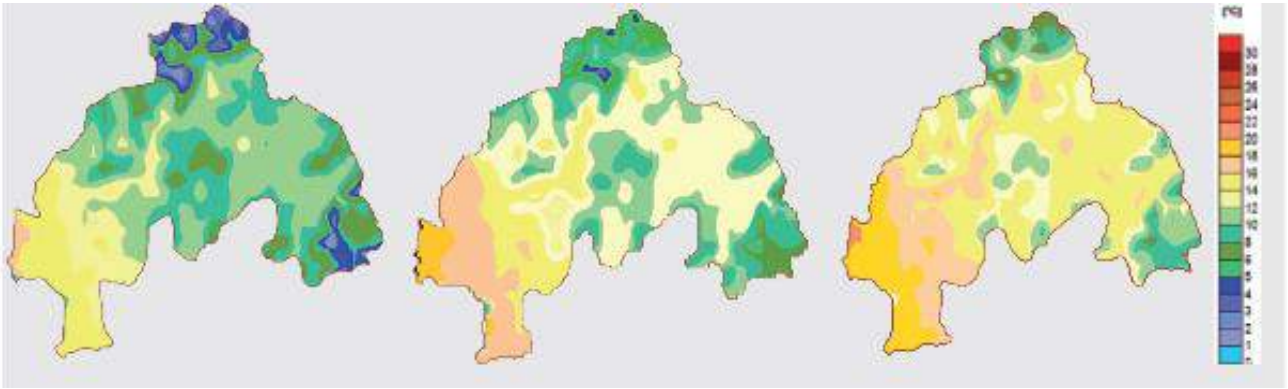

Figure 8. Expected changes in annual temperatures (Shkoder area part of Drini Basin) [17]

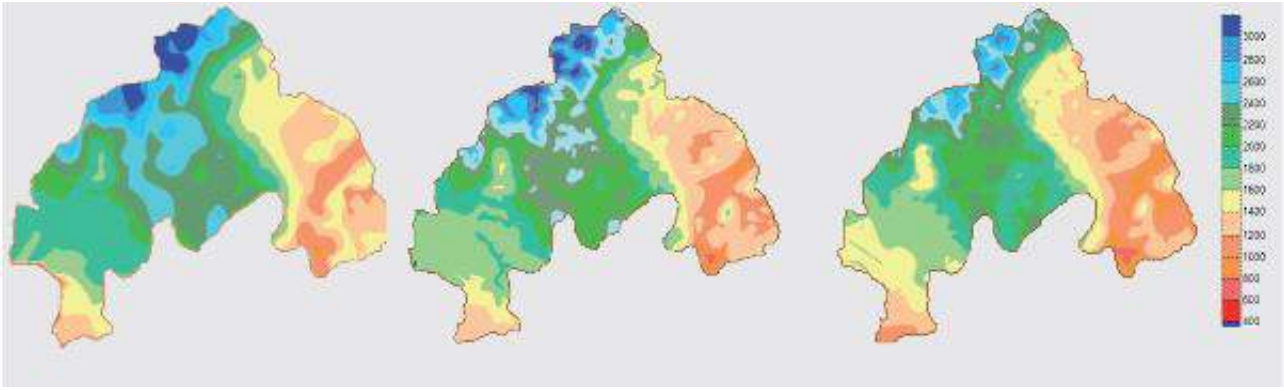

Figure 9. Expected changes in annual precipitation (Shkoder area part of Drini Basin) [18]

On the albania areafor theassessmentof climatechange scenarios severalclimate models are used. The most common isclimate modelregcm, developed in*international centre for theoretical physics* in trieste [19], which was used for climate predictionsfor the period 2011-2040. Gfdl-esm2m it is a global climate model which, for climate change simulations, takes initial and boundary conditions from joint global climate model echam5/mpi-om[20],[21]. For climate change assessment for the period up to the year 2100 inthe framework of project ccwaters[22], withmentionedgfdl-esm2mmodelwhere climate change projections are made until the year 2100.

From dynamical downscaling of gfdl-esm2m is performed several scenarios by considering different periodes as below:

1. 2025-2049 vs1980-2004
2. 2050-2074vs1980-2004
3. 2071-2095 vs1980-2004

In the first period of future climate (2025-2049 vs1980-2004) in albania (figure 3) during winter a temperature increase of 3 °c is expected, and 4°c during summer.

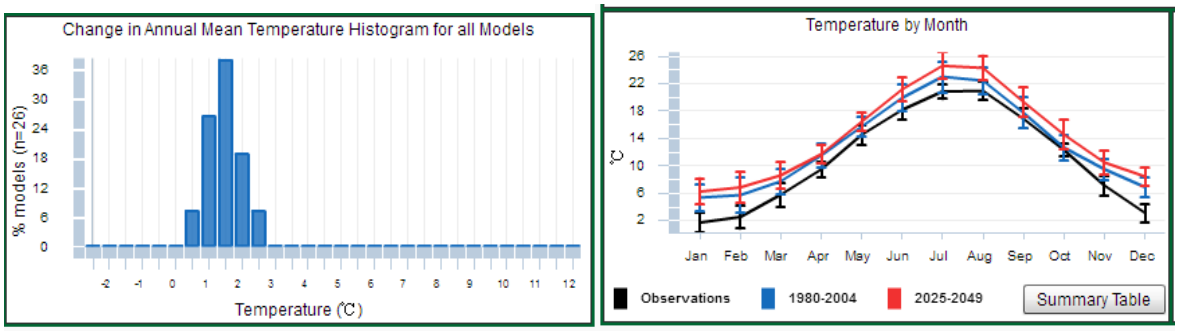

Figure 10. Change in ground air temperature (in °c) in Albania in the period 2025-2049 in respect of the period 1980-2004 according to the results of the ensemble mean of global climate model gfdl-esm2m

In the second period of future climate (2050-2074vs1980-2004) the expected increase amplitude in albania (figure 4) during winter is up to 4 °c and during summer up to 4.5 °c.

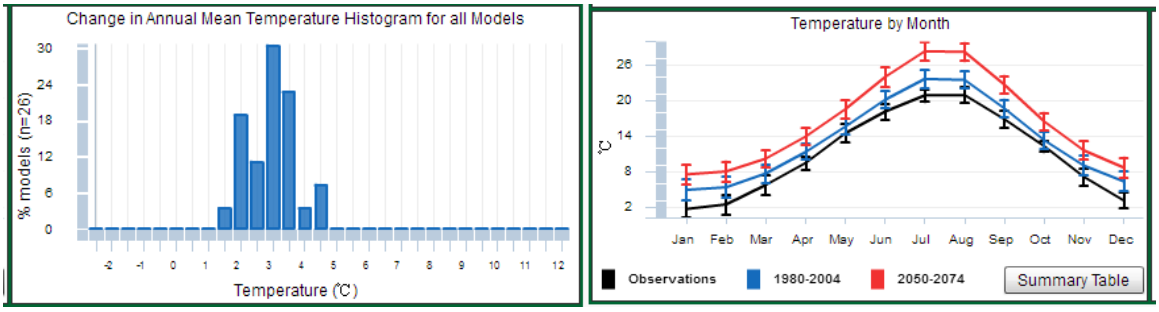

Figure 11. Change in ground air temperature (in °c) in Albania in the period 2050-2074 in respect of the period 1980-2004 according to the results of the ensemble mean of global climate model gfdl-esm2m.

In the third period of future climate (2071-2095 vs 1980-2004) the expected increase amplitude in albania (figure 4) during winter is up to 6 °c and during summer up to 6.4 °c.

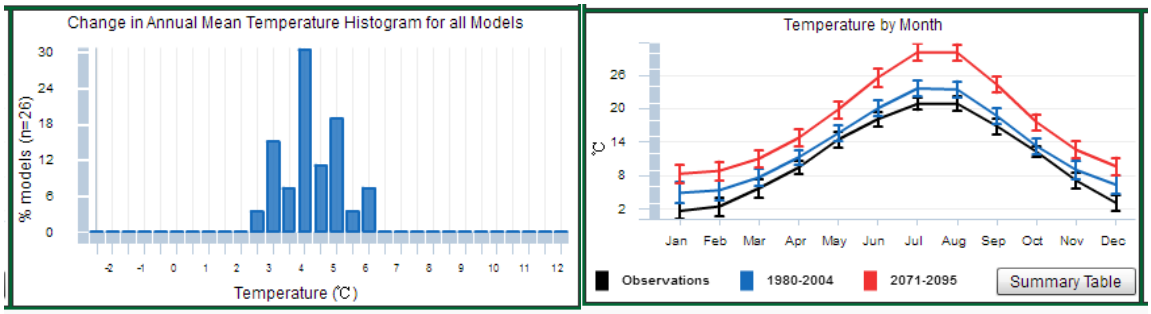

Figure 12. Change in ground air temperature (in °c) in Albania in the period 2071-2095 in respect of the period 1980-2004 according to the results of the ensemble mean of global climate model gfdl-esm2m.

In addition a long term scanirio is presented in figure 6, it is abvious that there is a significiant increase of temperature specially in coming years.

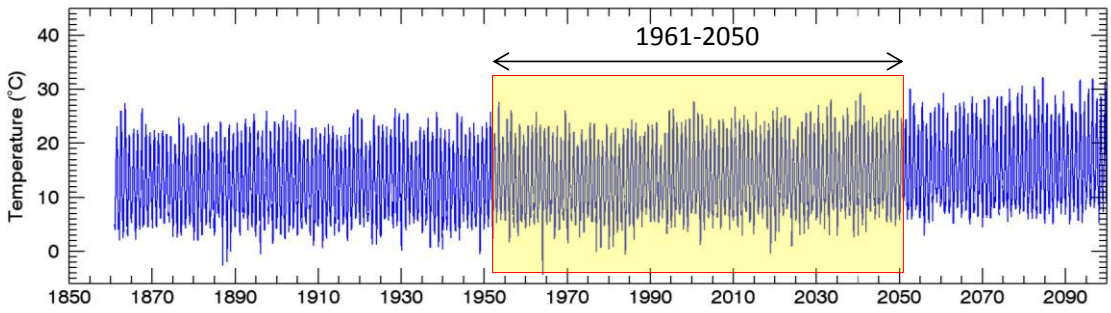

Figure 13. Change in ground air temperature (in °c) in Albania in the period 1850-2095 according to the results of the ensemble mean of global climate model gfdl-esm2m

Changes in precipitation amounts in the near future (2025-2049) are significiant small but they vary in the sign depending ofthe season (figure 7). The biggest change in precipitation, according to first scenario, can be expected in the adriatic inautumn when gfdl-esm2m indicates adecrease ofprecipitation with a maximumofapproximately5-6mmin the southern adriatic. However, this reduction of autumnprecipitation amountis notstatisticallysignificant.

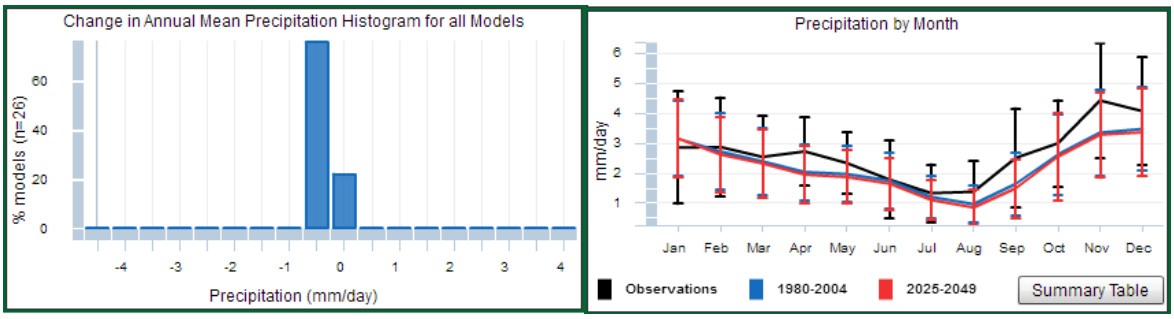

Figure 14. Change in precipitation in Albania (in mm/day) in the period 2025-2049 in respect of the period 1980-2004 according to the results of the ensemble mean of regional climate model gfdl-esm2m[3]

In the second period of future climate (2041-2070) precipitation changes in albania are somewhatmore expressed (figure 8). During summer in the mountainous albania and inthe coastal area a decrease inprecipitation is expected. Reductionsreachvalue of5-6 mm and they are statisticallysignificant. During winter an increase inprecipitationinnorth-western albania and on the adriatic can be expected, however that increaseis notstatisticallysignificant

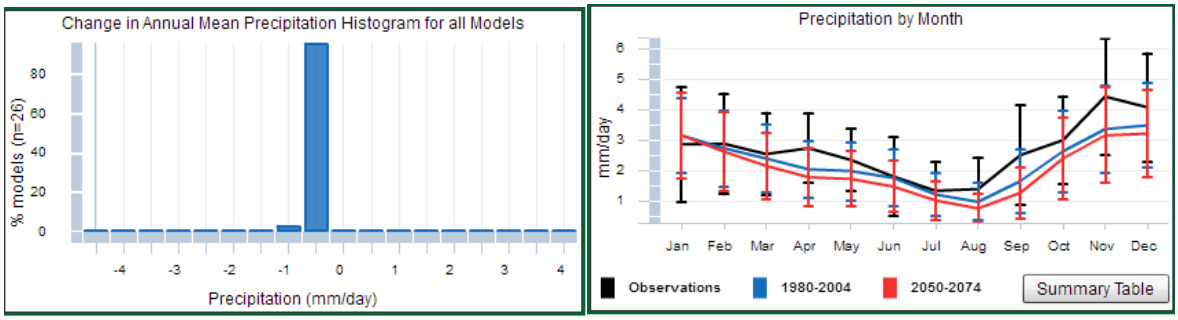

Figure 15. Change in precipitation in Albania (in mm/day) in the period 2050-2074 in respect of the period 1980-2004 according to the results of the ensemble mean of regional climate model gfdl-esm2m [3]

In the third period of future climate (205-2095) precipitation changes in albania are somewhatmore expressed (figure 9). During summer in the mountainous albania and inthe coastal area a decrease inprecipitation is expected. Reductionsreachvalue of5-6mm and they are statisticallysignificant. During winter an increase inprecipitationinnorth-western albaniaand on the adriatic can be expected, however that increaseis notstatisticallysignificant

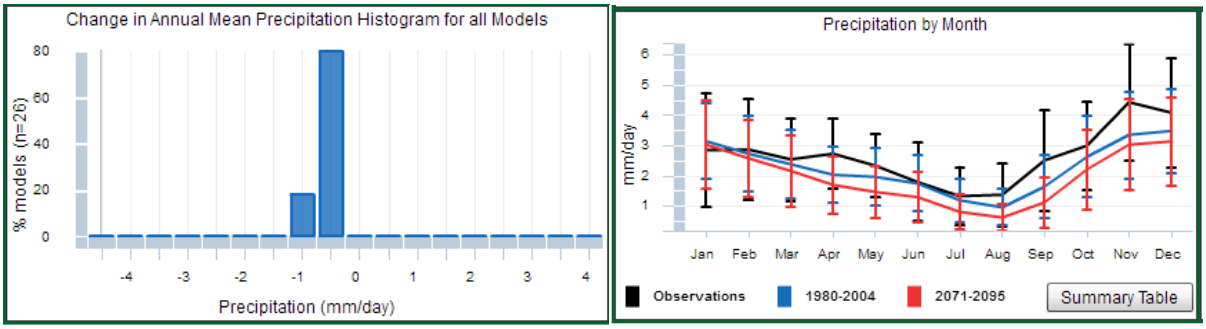

Figure 16. Change in precipitation in Albania (in mm/day) in the period 2071-2095 in respect of the period 1980-2004 according to the results of the ensemble mean of regional climate model gfdl-esm2m

In addition a long term scanirio is presented in figure 10; it is abvious that there is a significiant decrease of precipitation especially in coming years.

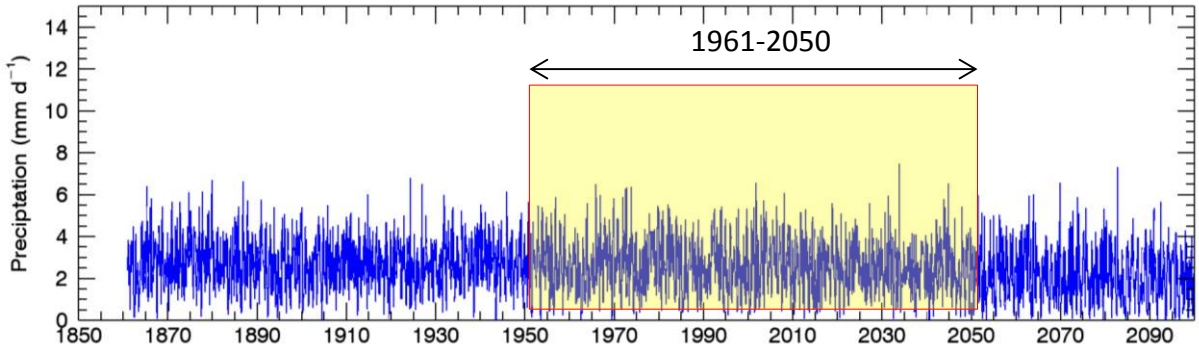

Figure 17. Change in precipitation in Albania (in mm/day) in the period 1850-2095 according to the results of the ensemble mean of regional climate model gfdl-esm2m

According to second national communication, drought is expected during summer due to increased temperature (likely increase up to 5.6 °c) and potential evaporation, not balanced by precipitation (reduction by 41%).increasing temperatures will raise the probability of extreme events and higher intra-annual variability of minimum temperatures. Higher increase of daily minimum than maximum temperatures is likely to occur. More frequent and severe droughts with greater fire risk are likely. Decreased number of frost days (temperatures ≤–5°c) in high altitudes is likely to occur. Expected decrease is 4–5 days, 9 days and 15 days by 2025, 2050 and 2100 respectively. Owing to higher average temperatures in winter more precipitation is likely to fall in the form of rain rather than snow, which will increase both soil moisture and run-off. Increase in total precipitation rate may induce greater risks of soil erosion, depending on the intensity of rain episodes. Increase in summer temperature is likely to result in increase in frequency and intensity of extreme weather events (heat waves). The number of days with the mtemperature ≥35 °c is likely to increase by 1–2 days by 2025 and by 3–4 days by 2050 compared to 1951–2000 average [23].

REFERENCES

[1]http://aea-al.org/climate-characteristics-of-albania/

[2]pano, niko. Burimet ujore te shqiperise. Tirane: akademia e shkencave, 2008.

[3]european environment agency

[4]undp albania

[5]bogdani-ndini, m., demiraj-bruci, e., &lushaj, b. M. Climate changes and the expected impact to the transboundary water resources in albania.

[6]islami, b., kamberi, m., demirajbruci, e., &fida, e. (2009). Albania's second national communication to the conference of parties under the united nation's framework convention on climate change.

[7] alder, j.r., hostetler, s.w., williams, d., 2013. An interactive web application for visualizing climate data. Eos trans. Agu 94, 197–198. Doi: 10.1002/2013eo220001.

[8] pal, j.s. et all. (2007): the ictp regcm3 and regcnet: regional climate modeling for the developing world, bull. Amer. Meteor. Soc., 88, 1395–1409.

[9]roeckner, e., bäuml, g., bonaventura, l., brokopf, r., esch, m., giorgetta, m., hagemann, s., kirchner, i., kornblueh, l., manzini, e., rhodin, a., schlese, u., schulzweida, u., tompkins, a. (2003): the atmospheric general circulation model echam5. Part i: model description. Max-planck institute for meteorology rep. 349, hamburg, pp 127.

[10]marsland, g.a., haak, h., jungclaus, j.h., latif, m., röske, f. (2003): the max planck institute global/sea-ice model with orthogonal curvilinear coordinates. Ocean model 5, 91-127.

[11]belmecheri, soumaya, et al. "climate controlled ostracod preservation in lake ohrid (albania, macedonia)." *palaeogeography, palaeoclimatology, palaeoecology* 277.3 (2009): 236-245.

[12]hughes, philip d. "twenty-first century glaciers and climate in the prokletije mountains, albania." *arctic, antarctic, and alpine research* 41.4 (2009): 455-459.

[13]aufgebauer, anne, et al. "climate and environmental change in the balkans over the last 17 ka recorded in sediments from lake prespa (albania/fyr of macedonia/greece)." *quaternary international* 274 (2012): 122-135.

[14]seim, andrea, et al. "climate sensitivity of a millennium-long pine chronology from albania." *climate research* 51.3 (2012): 217.

[15]wagner, bernd, et al. "a 40,000-year record of environmental change from ancient lake ohrid (albania and macedonia)." *journal of paleolimnology* 41.3 (2009): 407-430.

[16]frasheri, alfred, and n. Pano. "outlook on paleoclimate changes in albania."*international conference" the earth thermal field and related research methods" moscow*. 2002.

[17]seim, a., et al. "exploring the potential of pinusheldreichii christ for long-term climate reconstruction in albania." *trace* 8 (2010): 75-82.

[18]bordon, amandine, et al. "pollen-inferred late-glacial and holocene climate in southern balkans (lake maliq)." *quaternary international* 200.1 (2009): 19-30.

[19]jaho, s., et al. "climate of albania." *hidmet, tiranë* (1975).

[20]ellwood, brooks b., et al. "paleoclimate characterization and intra-site correlation using magnetic susceptibility measurements: an example from konispol cave, albania." *journal of field archaeology* 23.3 (1996): 263-271.

[21]purse, bethan v., et al. "climate change and the recent emergence of bluetongue in europe." *nature reviews microbiology* 3.2 (2005): 171-181.

[22]bruci, e. "climate variability and trends in albania." *university of polytechnics–institute for energy, water and environment, tirana* (2008).

[22]bruci, eglantinademiraj. "climate variability and expected changes in albania."*presentation at world bank workshop on climate risks and vulnerabilities of albania's energy sector*.vol. 10. 2009.

Let's grow up together

DRINK ADRIA

Adriatic IPA
Cross Border Cooperation 2007-2013

The project is co-funded by the European Union,
Instrument for Pre-Accession Assistance

WP4.1 Report:

Climate and climate change data for Greece

Civil Engineering Department
University of Thessaly
On behalf of
Region of Ionian Islands - Directorate of Developmental Programming
(FB15)

Volos, 2014

Lead Author/s	Assoc. Prof. Vasilis Kanakoudis
Lead Authors Coordinator	Assoc. Prof. Vasilis Kanakoudis
Contributor/s	Dr. S. Tsitsifli, A. Papadopoulou, I. Argyriadou, A. Rouva, I. Hitiri
Date last release	22/9/2014
State of document	Final

Let's grow up together

DRINK ADRIA

Adriatic IPA
Cross Border Cooperation 2007-2013

The project is co-funded by the European Union, Instrument for Pre-Accession Assistance

CONTENT

1. INTRODUCTION

Greece has a total surface area of 131,957 km^2 occupying the southernmost extension of the Balkan Peninsula *[1]*. The mainland accounts for 80% of the land area, with the remaining 20% divided among nearly 3,000 islands *[1]*. According to the 6th national communication to the United Nations FCC *[1]* Greece has a Mediterranean climate, with mild and wet winters in the southern lowland and island regions and cold winters with strong snowfalls in the mountainous areas in the central and northern regions and hot, dry summers. The mean temperature during summer (April to September) is approximately 24°C in Athens and southern Greece, while lower in the north. Generally, temperatures are higher in the southern part of the country. Except for a few thunderstorms, rainfall is rare from June to August, where sunny and dry days are mainly observed *[1]*. The dry, hot weather is often relieved by a system of seasonal breezes. The mean annual temperature for the period 2001 – 2013, as measured at selected meteorological stations of the country, is higher in most of the stations compared to the mean annual temperature of the period 1991 – 2000 while the mean annual temperature for the period 1991 – 2000 is higher compared to these of the period 1961 – 1990 *[1]*.

According to the same National Communication *[1]*, since the '90s Greece is experiencing an annual increase of temperature of about 0.4-0.6^{0}C, as to the mean values of 1961-1990. This increase is mostly due to a steady rise of temperature during summer period (from April to September). Winter temperatures seem to overcome the declining trend that has been observed in the past, showing a lot of fluctuations in the recent years *[1]*. Various studies converge that in the recent years there is a significant reduction of the precipitation in the Greek Territory, especially during the 2nd half of the 20th century. This trend seems to be confirmed also in the recent years. Precipitation is decreasing more abruptly in the islands of the Ionian and Aegean Sea (Corfu, Rhodes, Mytilini, Irakleio) as well as in the Peloponnese (Kalamata) *[1]*. However, this trend becomes smoother in the cities of the mainland (Athens, Thessaloniki, Aleksandroupoli) and the decrease could be even characterised as insignificant in Larissa, where the precipitation height shows a lot of fluctuations in the period under examination. As regards to the sea level increase in some stations the sea level shows intense fluctuations (Irakleio, Pireus, Rhodes), in a way that no safe conclusion could be conducted. On the contrary, the trend of the time series in Thessaloniki, Aleksandroupoli and Kalamata is much smoother, indicating an overall rise of the sea level in the recent years. The frequency of extreme events has significantly increased in the last two decades. Heat waves are happening every single year since 1997, although duration days are not as high as in the years 1997-2001 *[1]*. In particular in summer of 2007 Greece experienced an all record hot summer which, in combination with a prolonged dry period, led to the catastrophic forest fires causing the death of 70 people and the destruction of properties. Almost quite as interesting is the trend of the cold waves duration index: although there has been a period of almost 30 years from the mid '50s, since 1987 extreme cold waves seem to be more frequent than in the beginning of the century, causing problems in transportation, communication and electric power provision *[1]*.

Figure 1-1 Map of Greece - supplemented with pilot areas of project DRINK ADRIA [2]

The focus of this report are temperature and precipitation data for the Greek republic, existing as well as estimated for some of the most likely climate change scenarios, which are determined by the application of several standard methodological procedures, which are referenced. Figure 1-1 shows the map of Greece with marked pilot area of project DRINK ADRIA.

2. EXISTING CLIMATE FEATURES IN GREECE

2.1. In Greece (national)

The 5th national report to the UNFCCC states that the climate in Greece is typical of the Mediterranean climate: mild and rainy winters, relatively warm and dry summers with, generally, long sunshine duration almost all the year *[1]*. A great variety of climate subtypes, always in the Mediterranean climate frame, are encountered in several regions, due to the influence of topography (great mountain chains along the central part and other mountainous bodies) on the air coming from the moisture sources of the central Mediterranean Sea. As a result, the dry climate of Attiki (the great area of capital, Athens) and of the east part of Greece in general, changes significantly towards a wet one in North and West Greece *[1]*.

In terms of climatology, the year can be broadly divided mainly into two seasons. The cold and rainy period lasting from the mid of October until the end of March, and the warm and non -rain season lasting from April until September *[1]*. During the first period the coldest months are January and February, with a mean minimum temperature ranging between 5 to 10^0C near the coasts and 0 – 5^0C over mainland areas, with lower values (generally below freezing) over the northern part of the country. As regards to the summer period, the warmest days usually include the last days of July up to the first week of August, when the typical mean maximum temperature lies in the range of 29 and 35^0C. During the warm period the high temperatures are dampened from the fresh sea breezes in the coastal areas of the country and from the north winds blowing mainly in Aegean, well known as 'Etesian' *[1]*.
The deviation of the average annual mean temperature from the normal values of the period 1961-1990 in selected stations of the Hellenic National Meteorological Service (http://www.hnms.gr) is presented *[1]*.

According to the 5th National Report to the UNFCC, various studies converge that in the recent years there is a significant reduction of the precipitation in the Greek Territory, especially during the 2nd half of the 20th century *[1]*. This trend seems to be confirmed also in the recent years. It is found that precipitation is decreasing more abruptly in the islands of the Ionian and Aegean Sea (Corfu, Rhodes, Mytilini, Irakleio).

The frequency of extreme events has significantly increased in the last two decades. It is noted that heat waves are happening every single year since 1997, although duration days are not as high as in the years 1997-2001 *[1]*. In particular in summer of 2007 Greece experienced an all record hot summer which, in combination with a prolonged dry period, led to the catastrophic forest fires causing the death of 70 people and the destruction of properties. Almost quite as interesting is the trend of the cold waves duration index: although there has been a period of almost 30 years from the mid '50s, since 1987 extreme cold waves seem to be more frequent than in the beginning of the century, causing problems in transportation, communication and electric power provision. Also, according to extreme events reports of the Hellenic National Meteorological Service, floods have been reported (due to heavy storms) in many cities of the mainland and the islands, having destructive effects on agriculture, infrastructure and transportation *[1]*.

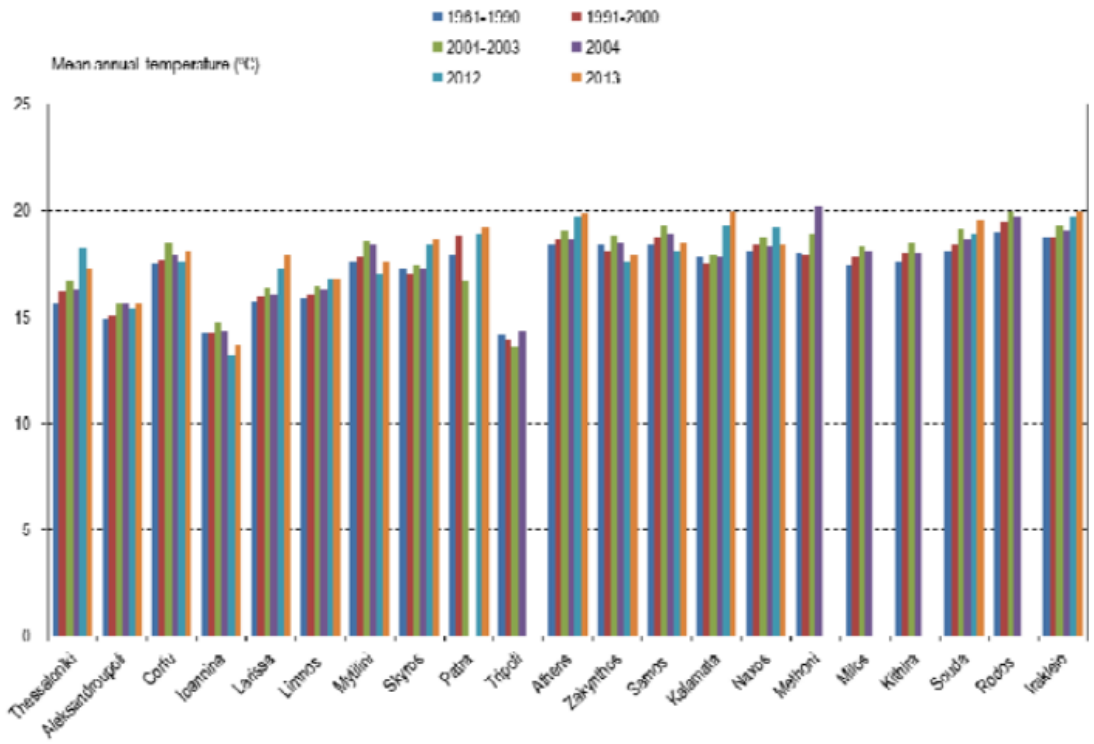

Figure 2-1. Mean annual temperature at selected meteorological stations for the periods 1961 – 1990 and 1991 – 2000, 2001-2003 and for the years 2004, 2012 & 2013 [1]

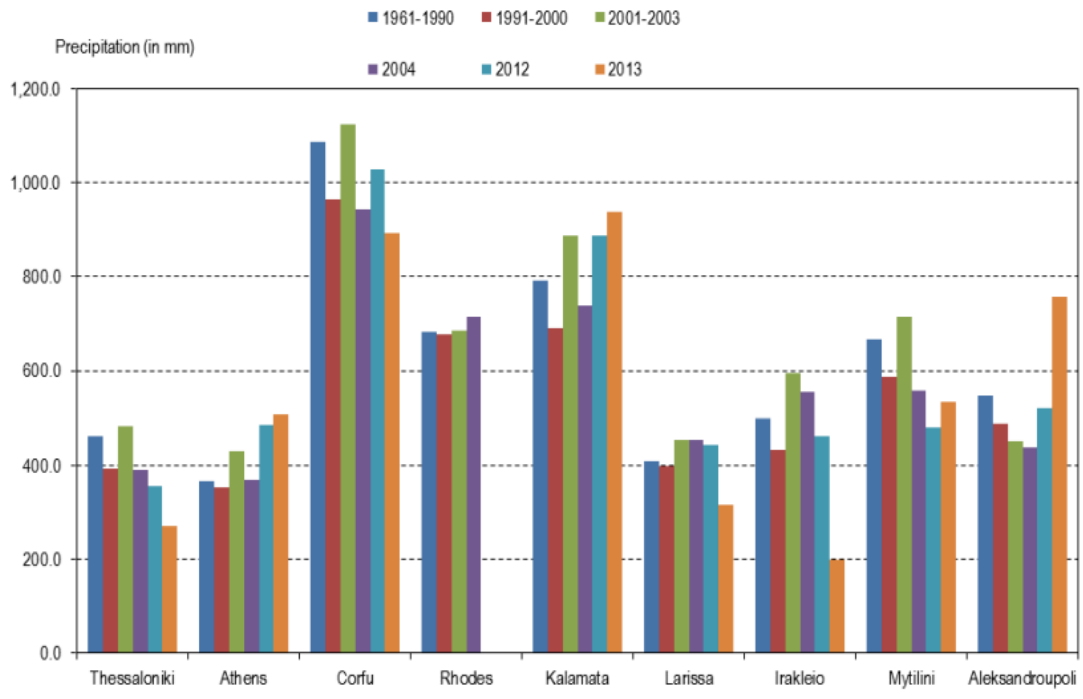

Figure 2-2. Precipitation height (in mm) at selected meteorological stations for the periods 1961 – 1990 and 1991 – 2000, 2001-2003 and for the yearw 2004, 2012 & 2013 [1]

Another study contected by the National Technical University of Greece *[3]* provided data regarding the mean annual precipitation in the country (Figure 2-3).

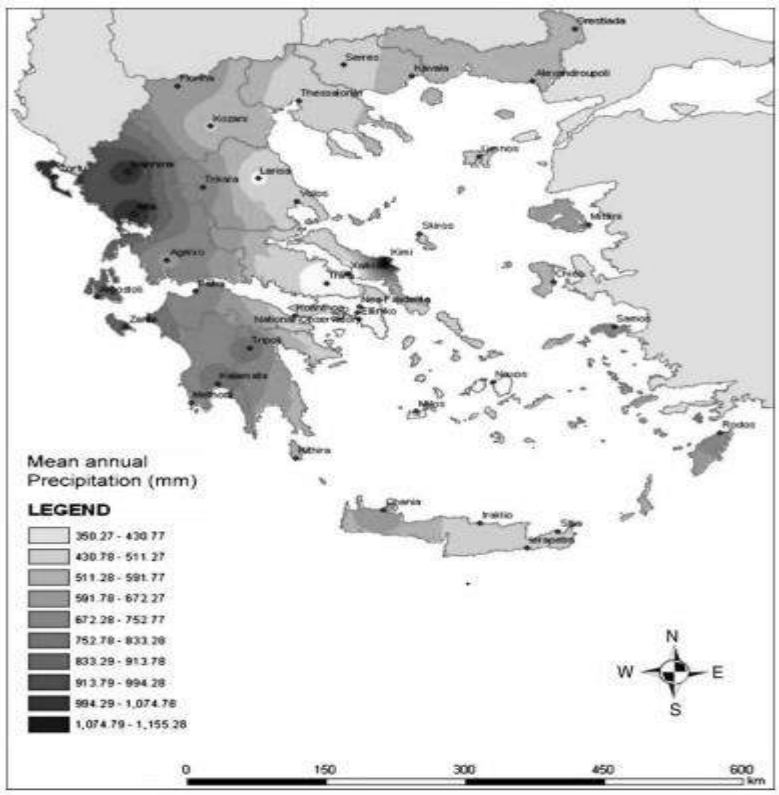

Figure 2-3. Mean annual precipitation (mm) [3]

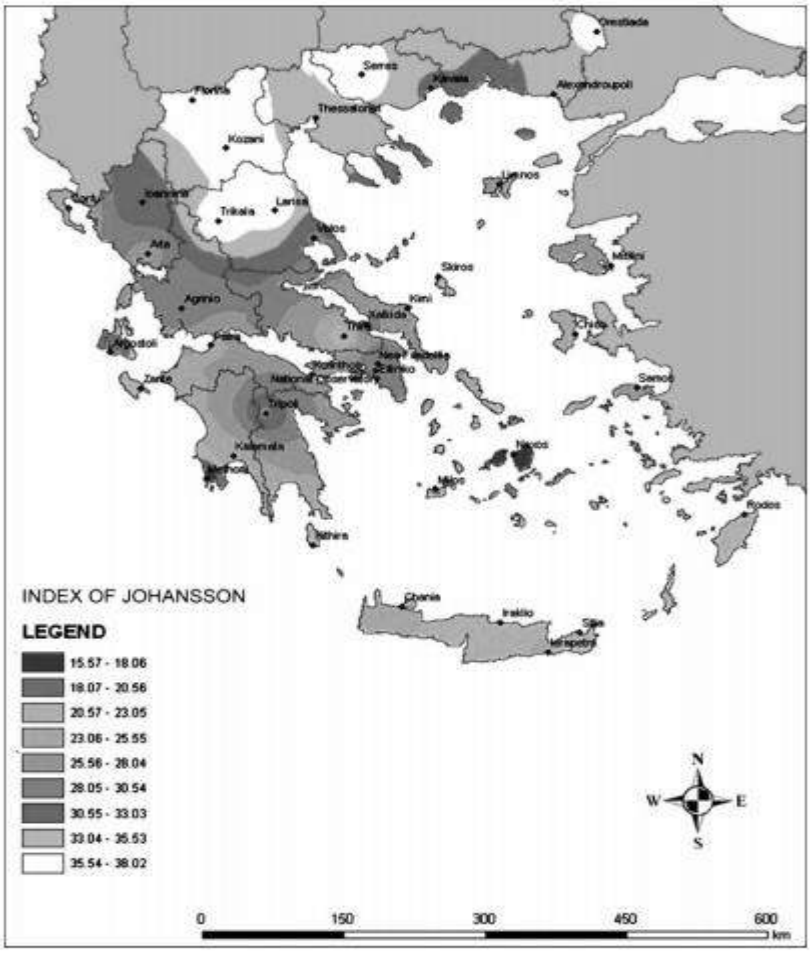

Figure 2-4. The Johansson continentality index [3]

The same study used two climatic indices: the Johansson Continentality Index and the De Martonne Aridity Index *[3].* The index of De Martonne belongs in the category of aridity-humidity indices and was selected for the derivation of the aridity map of the country. The Johansson Continentality Index was selected for the basic distinction between continentality and oceanity of a region *[3]*. The spatial distribution of Johansson Continentality Index is shown in Figure 2-4. At 11 of the 40 stations the index value was higher than or equal to 33 (limit), denoting continental climate *[3]*. These stations are mainly located in the northern part of the country, while a marine climate type characterizes the rest of the country *[3]*. The De Martonne Aridity Index is given in Figure 2-5. The index values range from 12.59 (Xalkida), denoting a semi-dry climate to 45.43 (Kimi), denoting a very humid climate *[3]*. The values of the index gradually increase from the eastern to the western parts of Greece, covering almost the entire range of the classification's climate categories, from dry to very humid. At the stations in Kimi, Ioannina, Arta and Corfu, the values of the index were higher than 35, implying very humid conditions. These stations, except for Kimi, are located in the north-western part of Greece, where the mean annual precipitation is the highest in the country and exceeds 1000 mm. On the eastern coast, including the region of Attica where the majority of the country's population lives, the index values range from 12.6 to 19, implying semi-dry conditions *[3]*.

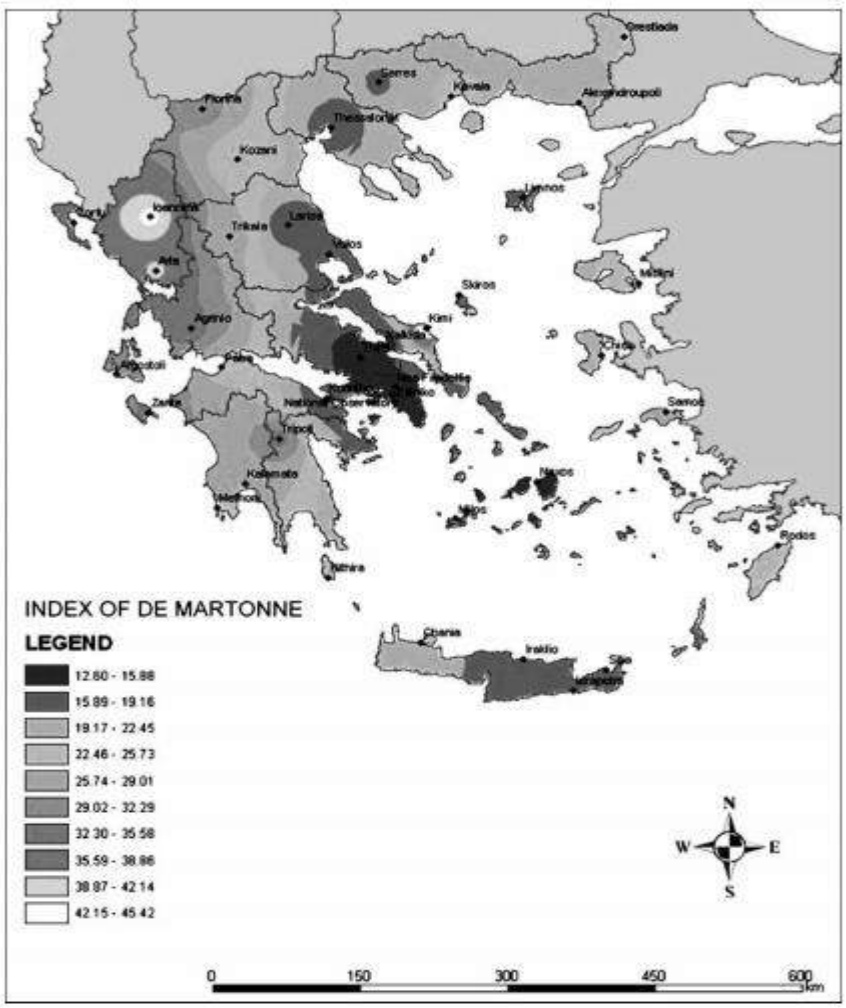

Figure 2-5. The De Martonne aridity index [3]

2.2. In Ionian Islands region

The region of Ionian Islands is situated in the Western part of Greece (Figure 2-6) and constitutes one of the 13 Greek regions. The Ionian Islands include the following main islands: Corfu, Kefallonia, Zakynthos, Lefkada. As Greece implements the Water Framework Directive 2000/60/EC, the country is divided in 14 Water Districts (Figure 2-7). The Ionian islands belong to different Water Districts (Table 2-1). The island of Corfu belongs to the Water District of Ipiros (GR05).

Table 2-1. List of the Ionian islands and their Water Districts

Island	**Water District**
Corfu; Paxi	Ipiros - GR05
Lefkada	Western Sterea Ellada - GR04
Kefallonia; Zakynthos; Ithaki	Northern Peloponissos - GR02

Figure 2-6. The Ionian islands region [4]

Figure 2-7. The 14 Greek Water Districts [5]

Corfu

According to the River Basin Management Plan (RBMP) of Ipiros, the climate in Corfu is the maritime Mediterranean one *[6]*. The average annual temperature ranges from 10 to 18^{o}C (in the coastal and island areas). The warmest month is August and the coldest ones are January and February. The average precipitation level of the water district ranges from 1,000 to 1,200 mm in the coastal areas *[6]*. The number of rainy days annualy range from 70 to 120 and it gets greater in the coastal areas compared to the water district continental areas *[6]*.

To describe analytically the climatic characteristics of the area, the data from 1980 to 2001 from the Hellenic National Meteorological Service are used *[1]*. The meteorological station elevation level in Corfu is 2m. The following graphs show data on the annual precipitation and temperature in the study area. During 20 years (1980-2001) the precipitation shows an unstable fluctuation and there is an increase during 1985-86, 1990-91, 1994-95 και 1997-99 *[1]*.

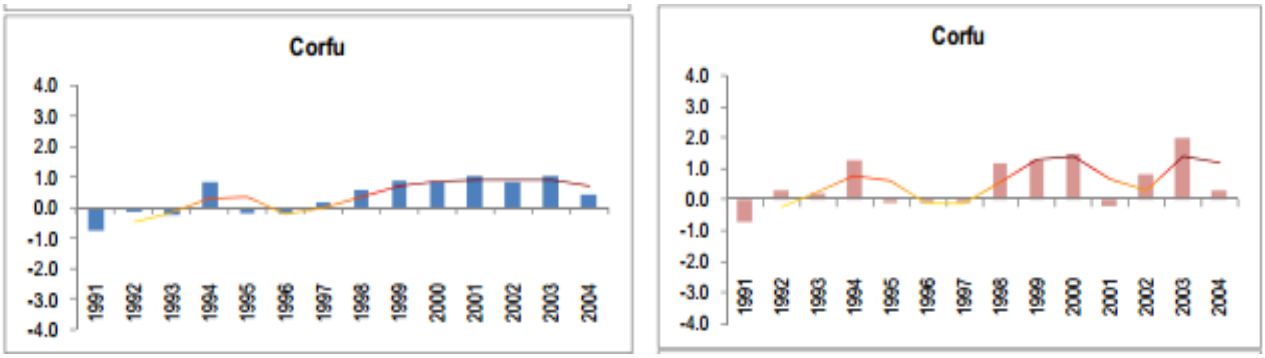

Figure 2-8. (a) Deviation of the average annual temperature from the average period 1961-1990; (b) Deviation of the average summer temperature from the average rates in Corfu [1]

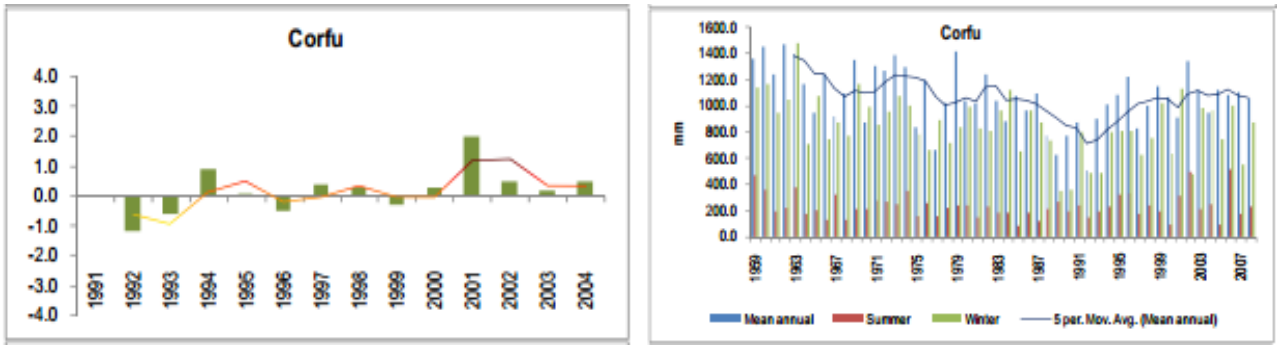

Figure 2-9. (a) Deviation of the average winter temperature from the average rates of the period 1961-1990; (b) Annual and seasonal (summer/winter) precipitation height and 5-year moving average in Corfu [1]

Additional data are provided by the meteorological station in Corfu (Kerkyra) for 1955-1997 *[7].* These data include mean monthly temperature (Figure 2-10), mean monthly humidity (Figure 2-11) and mean monthly precipitation level (Figure 2-12).

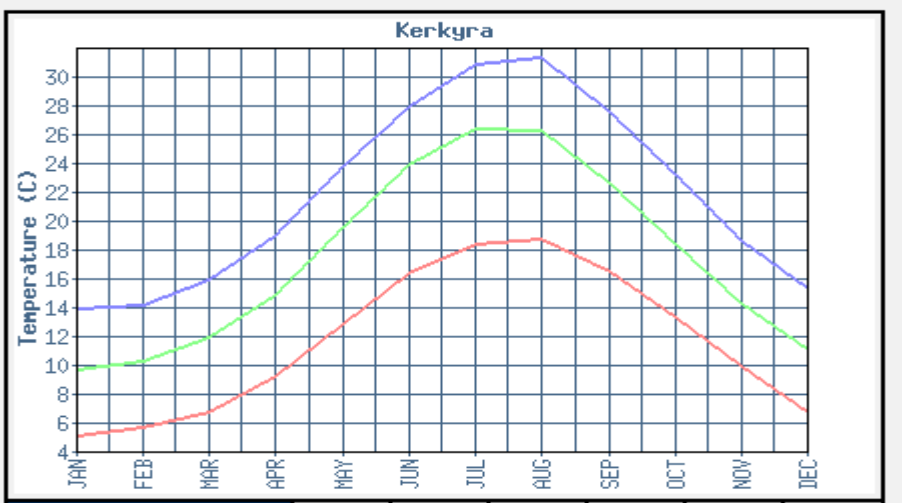

1º Semester	JAN	FEB	MAR	APR	MAY	JUN
Monthly Min Temperature	5.1	5.7	6.8	9.2	12.9	16.4
Monthly Average Temperature	9.7	10.3	12.0	14.9	19.6	23.9
Monthly Max Temperature	13.9	14.2	16.0	19.0	23.8	28.0
2º Semester	JUL	AUG	SEP	OCT	NOV	DEC
Monthly Min Temperature	18.4	18.8	16.5	13.4	9.9	6.8
Monthly Average Temperature	26.4	26.3	22.7	18.4	14.3	11.1
Monthly Max Temperature	30.9	31.3	27.6	23.2	18.7	15.3

Figure 2-10. Average monthly temperature 1955-1997 Corfu [7]

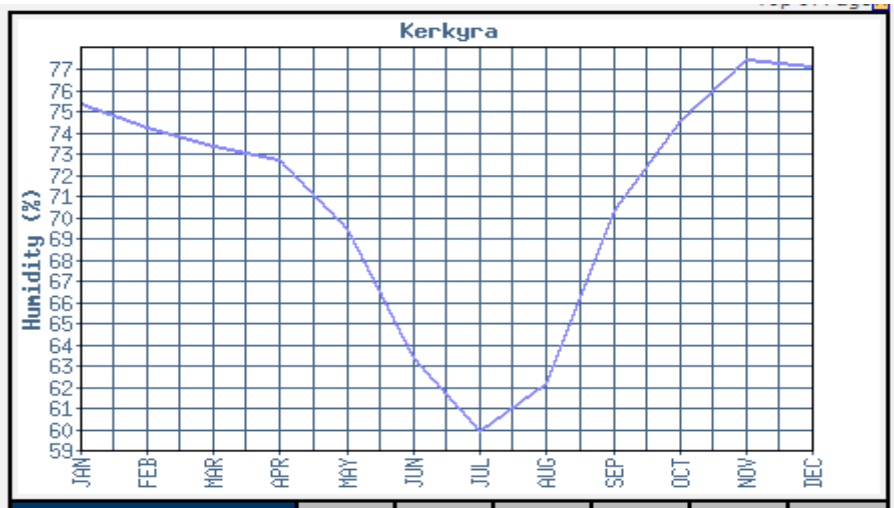

1º Semester	JAN	FEB	MAR	APR	MAY	JUN
Monthly Average Humidity	75.4	74.3	73.4	72.8	69.5	63.4
2º Semester	JUL	AUG	SEP	OCT	NOV	DEC
Monthly Average Humidity	60.0	62.2	70.4	74.6	77.5	77.2

Figure 2-11. Average monthly humidity 1955-1997 Corfu [7]

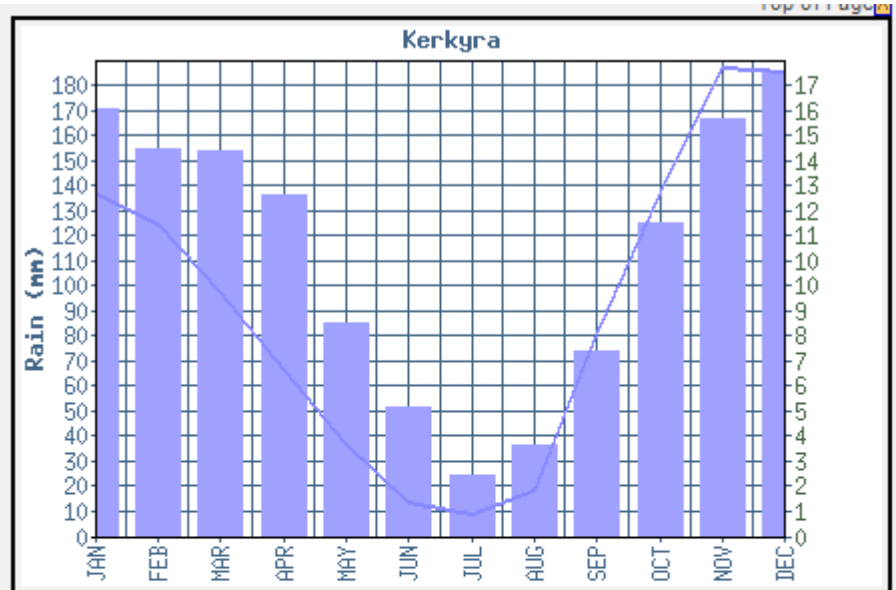

1º Semester	JAN	FEB	MAR	APR	MAY	JUN
Monthly Average Rainfall	136.6	124.6	98.1	66.7	37.0	14.1
Total days of Rain	16.1	14.6	14.5	12.9	8.0	4.9
2º Semester	JUL	AUG	SEP	OCT	NOV	DEC
Monthly Average Rainfall	9.2	19.0	81.3	137.7	187.4	185.6
Total days of Rain	2.3	3.4	7.0	11.8	15.7	17.5

Figure 2-12. Average monthly rain level 1955-1997 Corfu [7]

Kefalonia

Data are provided by the meteorological station in Argostoli (Kefalonia) for 1955-1997 *[8]*. These data include mean monthly temperature (Figure 2-13), mean monthly humidity (Figure 2-14) and mean monthly precipitation level (Figure 2-15). According to the RBMP of Northern Peloponnisos the precipitation in the basin are almost 800mm annualy in Kefalonia *[9].*

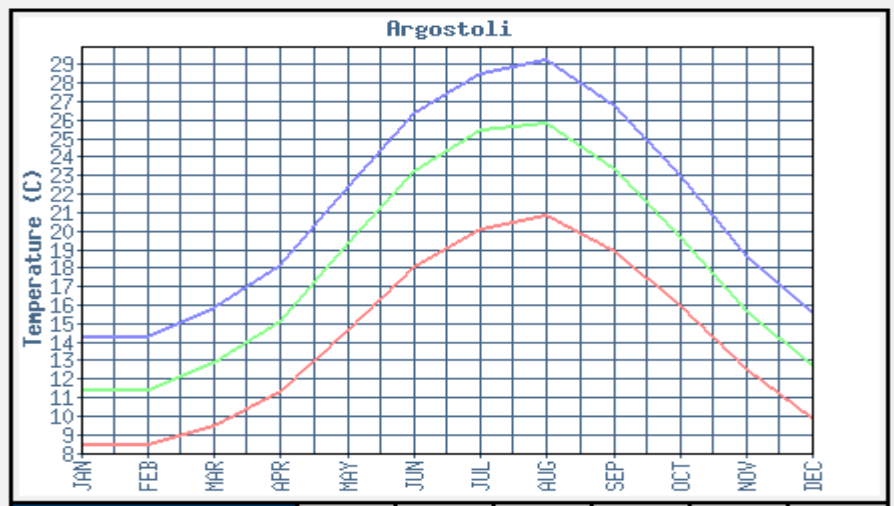

1º Semester	JAN	FEB	MAR	APR	MAY	JUN
Monthly Min Temperature	8.5	8.5	9.5	11.4	14.7	18.1
Monthly Average Temperature	11.5	11.5	12.9	15.2	19.4	23.3
Monthly Max Temperature	14.3	14.3	15.9	18.2	22.5	26.4
2º Semester	JUL	AUG	SEP	OCT	NOV	DEC
Monthly Min Temperature	20.2	20.9	19.0	16.0	12.6	9.9
Monthly Average Temperature	25.5	25.9	23.4	19.7	15.7	12.8
Monthly Max Temperature	28.6	29.3	26.8	23.0	18.7	15.6

Figure 2-13. Average monthly rain level 1955-1997 Kefalonia [8]

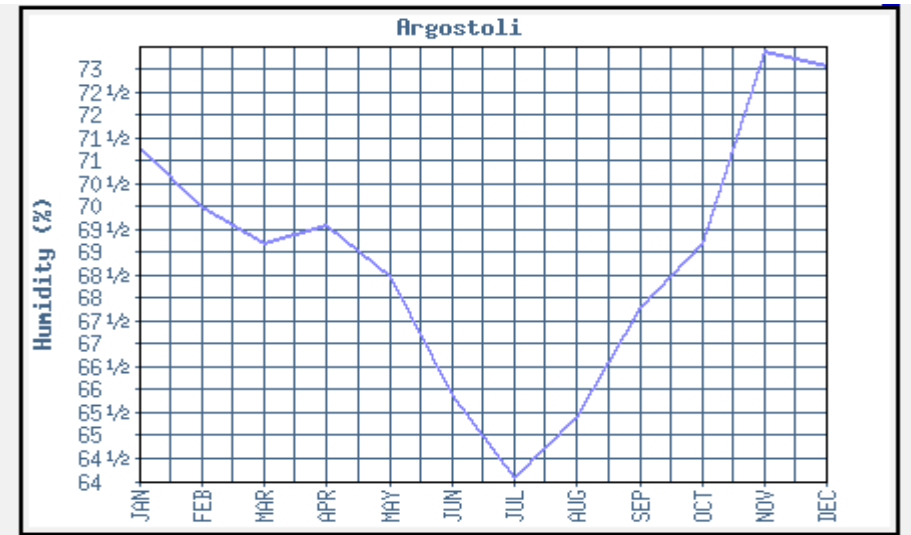

1º Semester	JAN	FEB	MAR	APR	MAY	JUN
Monthly Average Humidity	71.3	70.0	69.2	69.6	68.5	65.9
2º Semester	JUL	AUG	SEP	OCT	NOV	DEC
Monthly Average Humidity	64.1	65.4	67.8	69.2	73.4	73.1

Figure 2-14. Average monthly rain level 1955-1997 Kefalonia [8]

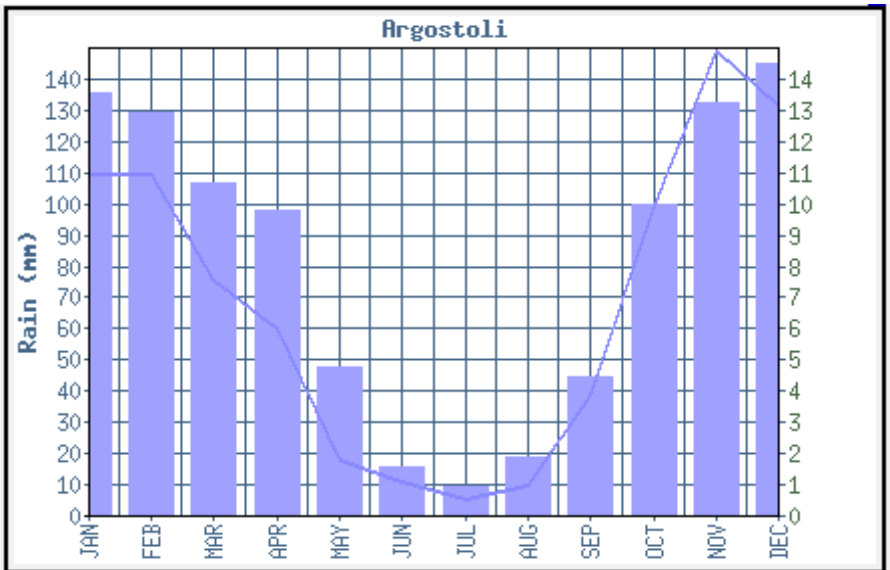

1º Semester	JAN	FEB	MAR	APR	MAY	JUN
Monthly Average Rainfall	109.7	110.0	75.7	60.4	17.9	10.8
Total days of Rain	13.2	12.6	10.4	9.5	4.6	1.5
2º Semester	JUL	AUG	SEP	OCT	NOV	DEC
Monthly Average Rainfall	5.3	9.8	38.5	100.2	149.5	132.2
Total days of Rain	0.9	1.8	4.3	9.7	12.9	14.1

Figure 2-15. Average monthly rain level 1955-1997 Kefalonia [8]

Zakynthos

The precipitation in the basin is 700mm in Zakynthos *[9].* The more wet period is October to March and the most wet month is December. The most dry month is June. The average annual evaporotransiration is estimated in 489mm *[9]*.

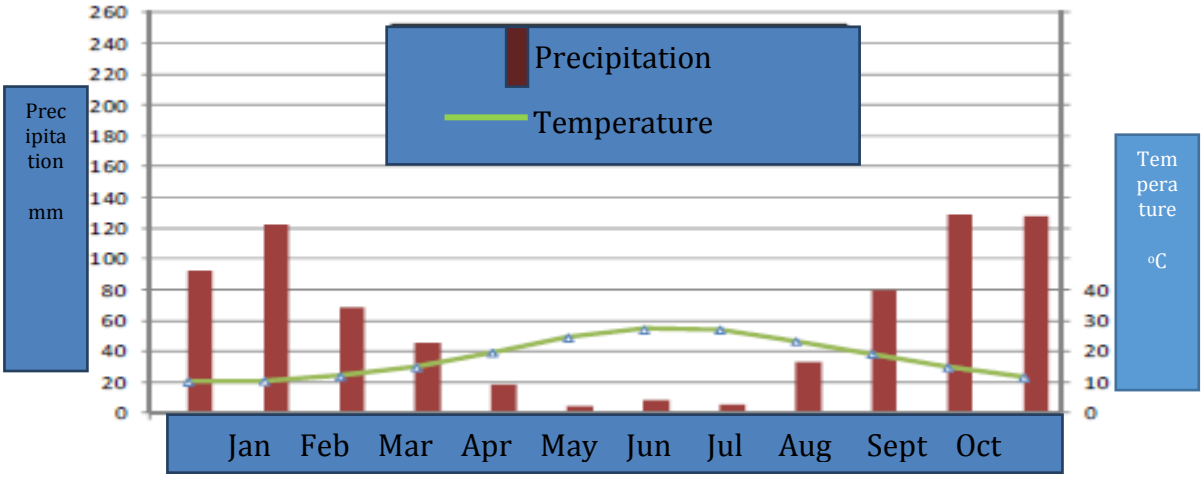

Figure 2-16. Average monthly precipitation and average monthly temperature in Zakynthos [9]

3. CLIMATE CHANGE SCENARIOS

According to the 6th National Communication to the UNFCCC *[1]*, current climate change has been estimated to account for a temperature increase of about 1ºC (ground surface temperature) in the last 500 years *[10;11]* and of 0.76ºC in the last 100 years *[12]*. Temperatures in the second half of the 20th century were, as estimated, very likely to have been higher than during any other 50- year period in the last 500 years, and likely the highest in the past 1,300 years *[12]*. Figures 3-1 and 3-2 show model projections of daytime maximum (TX) and nighttime maximum (TN) temperature during summer by the middle and the end of the twenty-first century, concerning the Eastern Mediterranean and Middle East region (EMME) *[1]*. They also show the 95-percentile confidence ranges obtained by bootstrapping *[1]*. The ranges in the lower panels are the differences between the upper and lower confidence limits. Furthermore, Figure 3-3 indicates that the regional warming will be gradual, both of daytime maximum (TX) and nighttime maximum (TN), ranging from 1°C to 3°C in the near-future (2010–2039), to 3–5°C in the mid-century period (2040–2069) and 3.5–7°C by the end of the century (2070–2099) *[1]*. In each period, this warming is more spatially uniform for winter TN, while for TX it is most pronounced at latitudes north of 36°–38°N (reaching 6–7°C in the Balkans, Turkey and the Caucasus by 2070–2099) and weaker in the southern EMME (~3.5°C) *[1]*.

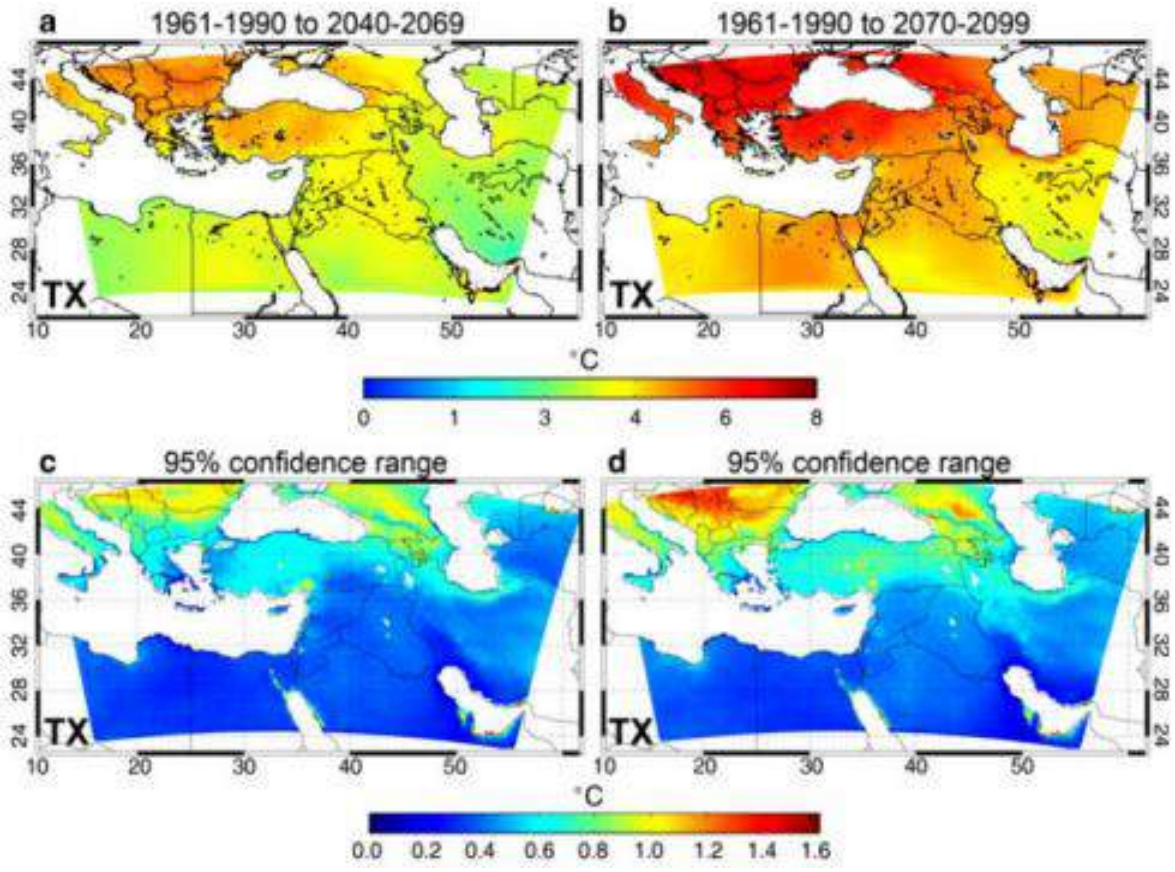

Figure 3-1. Changing daytime maximum temperature TX (a, b) and the 95 percentile confidence ranges (c, d) averaged over June–July– August, for the periods 2040–2069 (a, c) and 2070–2099 (b, d) relative to the period 1961–1990. Model calculations are for the A1B scenario [13]

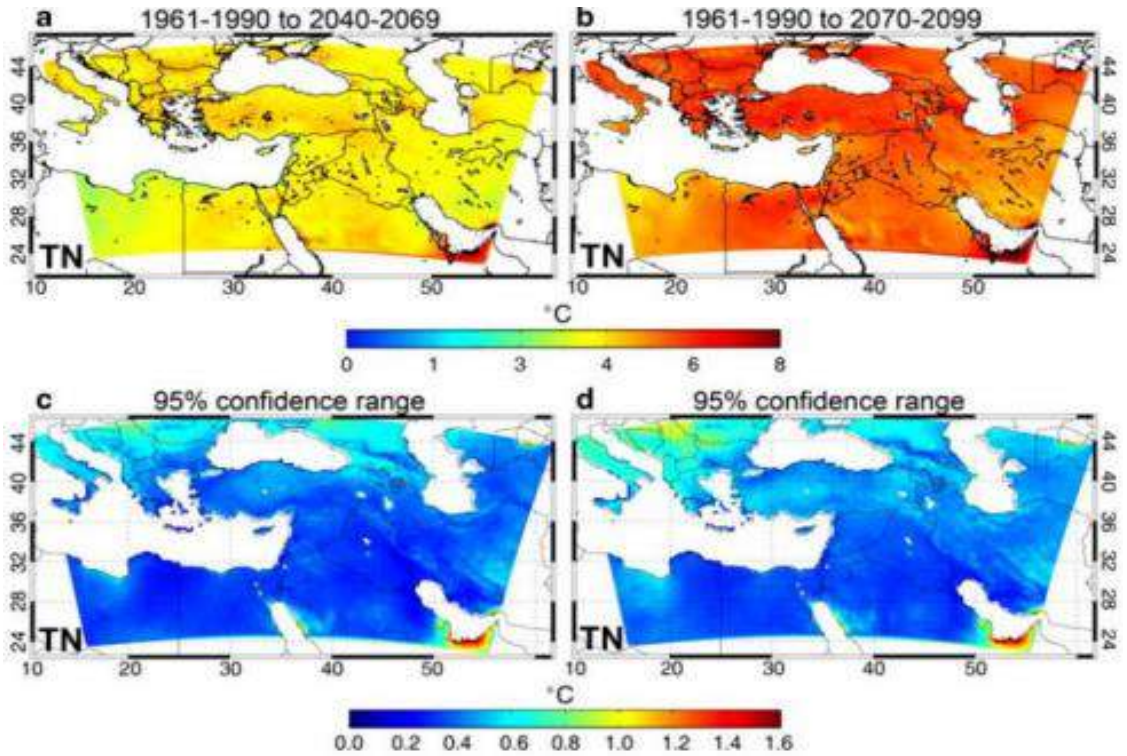

Figure 3-2. Changing nighttime maximum temperature TN (a, b) and the 95 percentile confidence ranges (c, d) averaged over June–July– August, for the periods 2040–2069 (a, c) and 2070–2099 (b, d) relative to the period 1961–1990. Model calculations are for the A1B scenario [13]

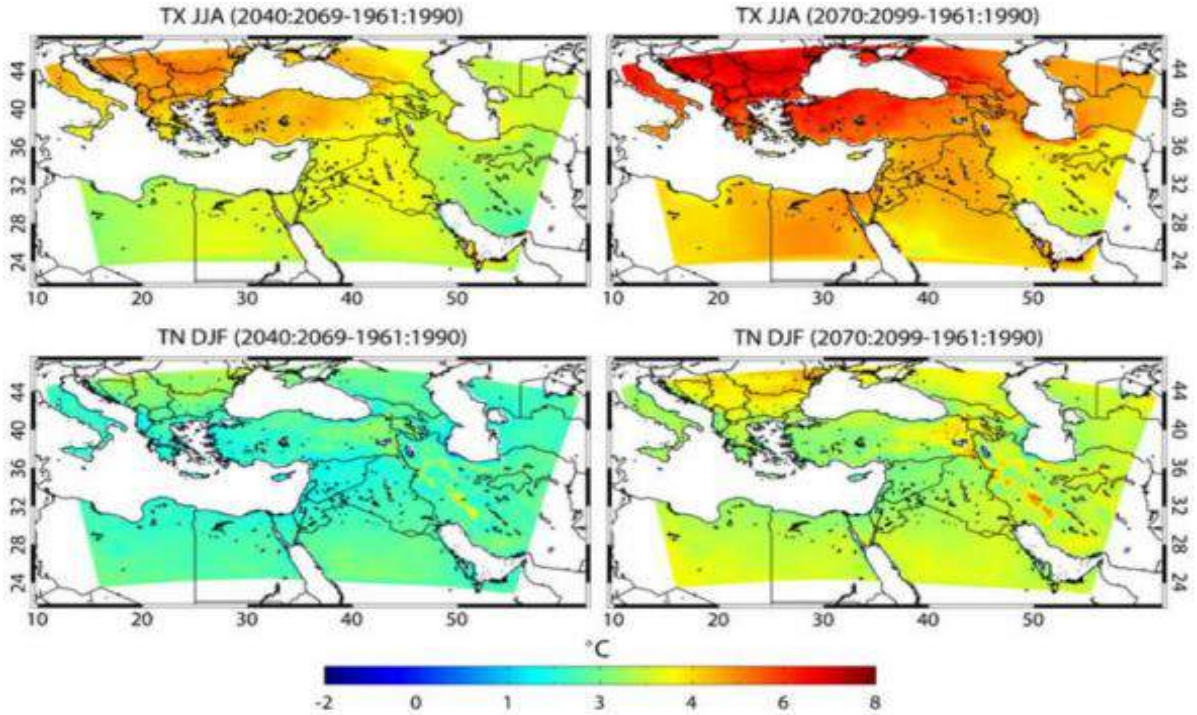

Figure 3-3. Patterns of changing mean summer maximum (JJA) and mean winter minimum (DJF) temperatures, TX (top) and TN (bottom), respectively, calculated from PRECIS output. The left panels show the mean changes for 2040–2069 and the right panels for 2070–2099 relative to the 1961–1990 control period. [13]

The 6th National Communication to UNFCCC reports that the severity of the climate change impact is more likely to be associated with changes in the frequency of extreme weather events than with a drawn-out 'average' climate evolution, given that, in the case of extreme events, a simple change in mean value above a critical threshold can bring about a disproportionate, non-linear impact *[1]*.

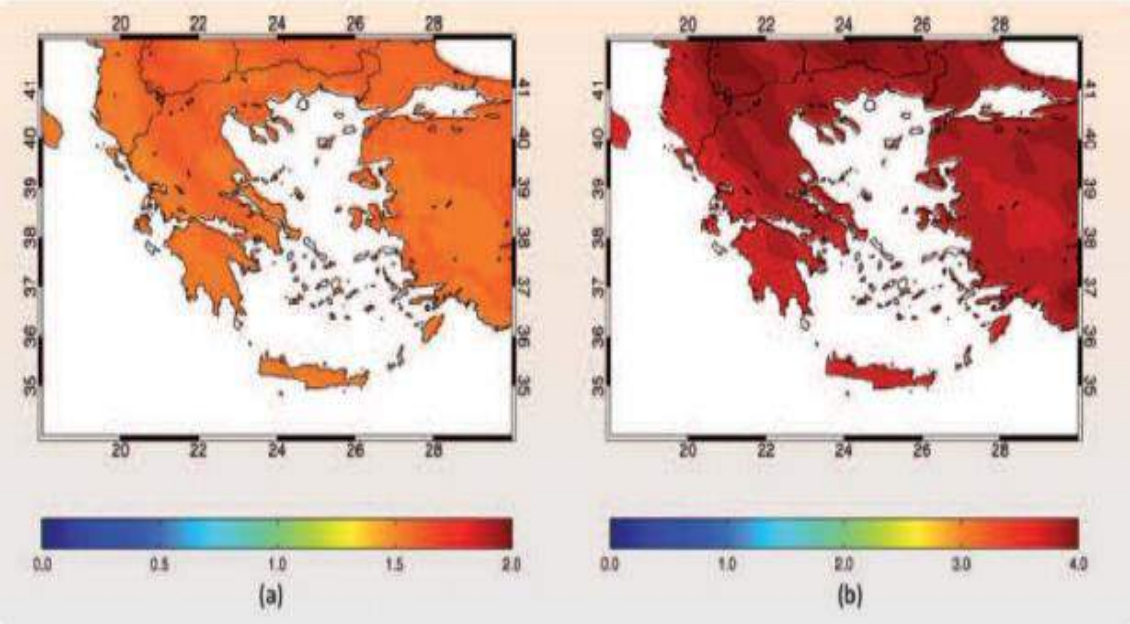

Figure 3-4. Variation in the mean minimum winter temperature in (a) 2021-2050 and (b) 2071-2100, relative to 1961-1990 (in ºC) [1;14]

According to the "Environmental, Economic and Social impacts of climate change in Greece" report performed by the Bank of Greece *[14]*, the climate model RACMO2, developed by the Royal Meteorological Institute of the Netherlands (KNMI), was used with a horizontal resolution of 0.25° (~25 km). These datasets cover a 30-year reference period, 1961-1990, for the current climate, and two future periods, 2021-2050 and 2071-2100, for the study of climate change using Scenario A1B of the IPCC. For each of Greece's 13 climate zones, the change in the relevant climate indices was computed between each future period (2021-2050 and 2071-2100) and the reference period (1961-1990). Scenario A1B is a mid-line scenario in terms of carbon dioxide emissions and economic growth. The first future period, 2021-2050, was chosen with the specific needs of policy-makers in mind, in order to assist them with nearer-term planning, whereas the second period, 2071-2100, serves to underscore the extent of the changes toward the end of the 21st century. Using the data from this model, it was possible to study the variation in climate parameters and indices between the reference period and each one of the two future periods, and to determine climate change for each of Greece's 13 climate zones *[1]*.
As can be seen from the projected changes in mean minimum winter temperature represented in Figure 3-4, minimum winter temperatures in all of Greece's regions will be ~1.5ºC higher in 2021-2050 and ~3.5ºC higher in 2071-2100, than in the reference period 1961-1990. These results concur with large-scale findings, which have recorded a significant upward trend in minimum temperatures over the past few decades *[1]*.

The warming trend will be more pronounced in the more mountainous areas, especially in the mountain ranges of Pindos and of Northern Greece, where it is projected to reach 2ºC in 2021-2050 and 4ºC in 2071-2100 *[14]*). The increase in this parameter is likely to have an impact on forests, presently adapted to colder weather conditions. If the conditions become prohibitive, certain categories of forests (e.g. fir) would have to shift to higher altitudes.

The projected changes in mean maximum summer temperatures are represented in Figure 3-5 *[1;14]*. The increase in mean maximum summer temperatures in the period 2021-2050 will be greater than that of the winter minimums and will exceed 1.5ºC and in some cases reach as much as 2.5ºC. In the period 2071-2100, the increase in mean maximum summer temperatures may be as much as 5ºC. Most affected will be the continental inland regions, situated far from the cooling effects of the sea, whereas regions with strong sea breezes (Crete, Aegean islands) will experience a significantly smaller variation in maximum summer temperatures *[1]*.

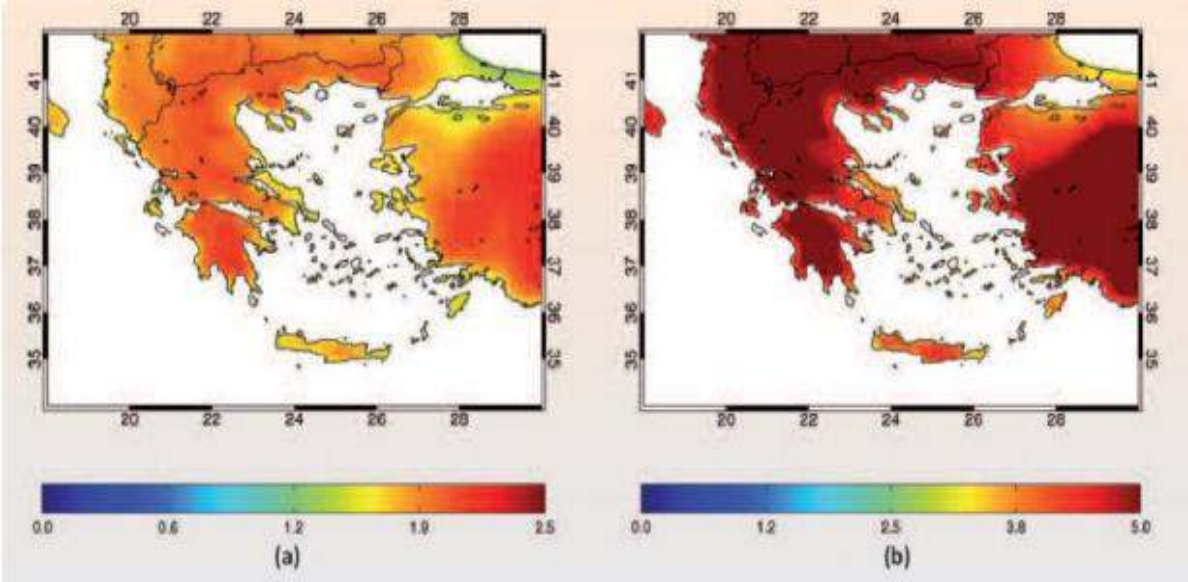

Figure 3-5. Variation in the mean maximum summer temperature in (a) 2021-2050 and(b) 2071-2100, relative to 1961-1990 (in ºC) [1;14]

The projected variation in the number of days with maximum temperatures above 35ºC, as represented in Figure 3-6, is expected to have a significant impact on human discomfort, especially in urban areas, as the number of hot days countrywide is clearly projected to increase *[1;14].*

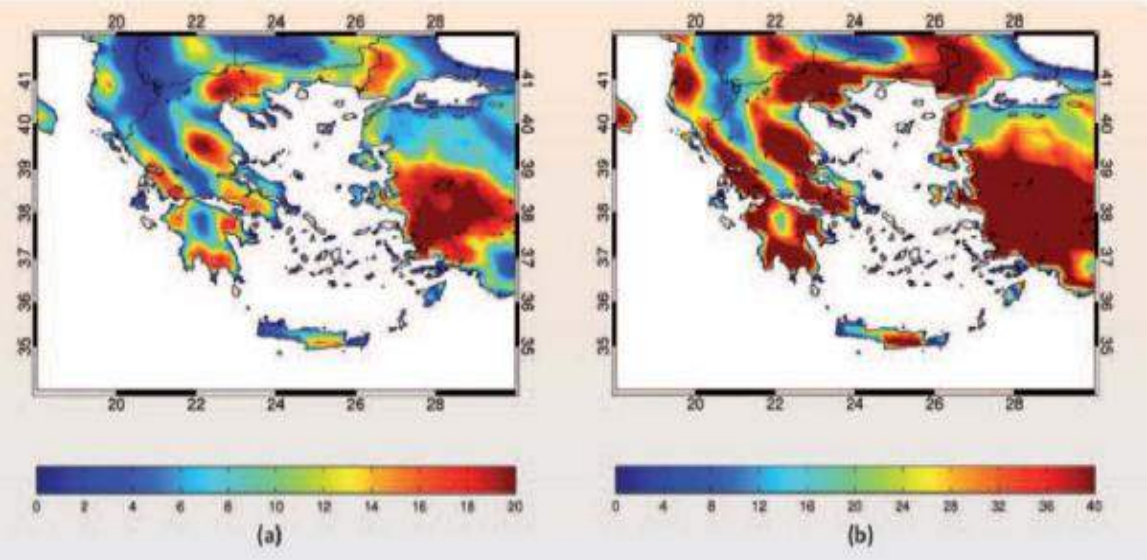

Figure 3-6. Variation in the number of days with maximum temperature > 35ºC in (a) 2021-2050 and (b) 2071-2100, relative to 1961-1990 [1;14]

According to the same report and the same study *[1;14]* the most noticeable changes are projected for the low-lying inland regions of Central Greece, Thessaly, the Southern Peloponnese as well as Central Macedonia, where up to 20 additional very warm days are expected per year in 2021-2050 and up to 40 in 2071-2100, relative to the reference period 1961-1990. The change is expected to be somewhat milder in Crete and Attica, where the number of additional very warm days per year should not exceed 15 in 2021-2050 and 30 in 2071-2100, and milder yet in the Aegean and the Ionian islands, which will count 10 additional very warm days per year in 2021-2050 and 15 additional ones in 2071-2100, due to the proximity of the sea and the tempering effect of sea breezes *[1]*. Another temperature-related and significant parameter is the change in the annual number of warm nights. Nights are defined as warm (or tropical) when the minimum temperature does not fall below 20ºC *[1]*. This parameter is closely associated with human health, as a tropical night following an extremely hot day can increase human discomfort. As can be seen from Figure 3-7, the annual number of tropical nights is projected to increase almost everywhere in Greece, but substantially more so in the coastal and island regions than in the continental mainland regions *[1]*. Crete, the coastal regions of Eastern Greece and the Aegean islands are expected to have 40 additional warm nights per year in 2021-2050 and 80 additional warm nights per year in 2071-2100. In Western Greece and Eastern Macedonia-Thrace, however, the increase in the annual number of warm nights will be less than 30 in 2021-2050 and 70 in 2071-2100, with even smaller increases projected for Western Macedonia (15 or less additional warm nights per year in 2021-2050 and 30 or less in 2071-2100) *[1;14]* .

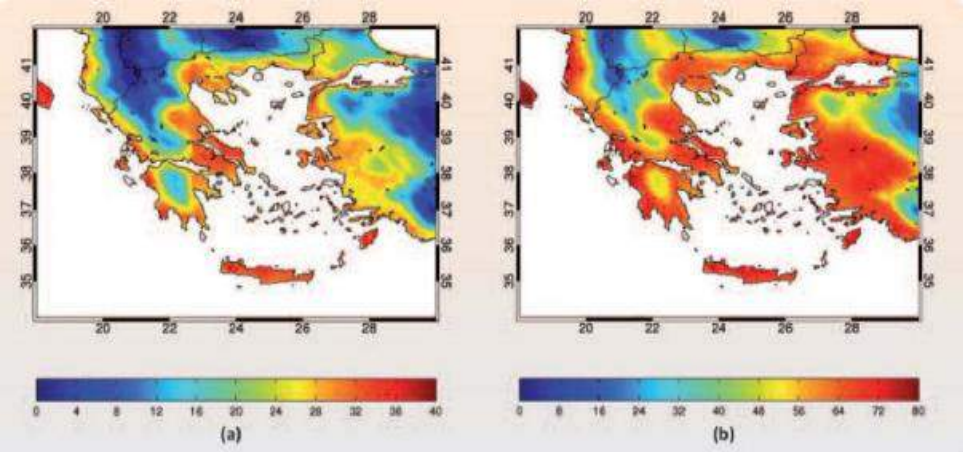

Figure 3-7. Variation in the number of days with minimum temperature > 20ºC in (a) 2021-2050 and (b) 2071-2100, relative to 1961-1990 [1;14]

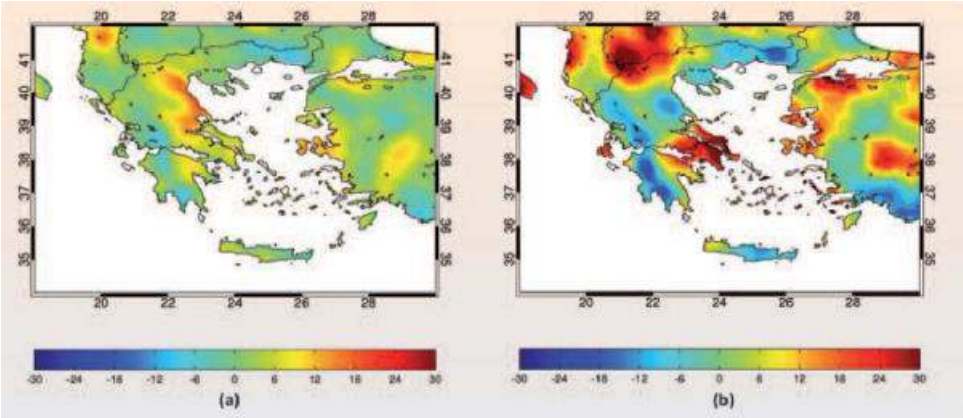

Figure 3-8. Percentage change in annual maximum consecutive 3-day precipitation in (a) 2021-2050 and (b) 2071-2100, relative to 1961-1990 [1;14]

Figure 3-8 shows the percentage variation in annual maximum consecutive 3-day precipitation which is projected to increase *[1;14]*. Together with the projected decrease in total annual rainfall, this means that extreme precipitation events will increase in intensity, thereby raising the flood risk. As can be seen from the left panel of Figure 3-8, maximum consecutive 3-day precipitation period during 2021-2050 will remain essentially unchanged, relative to the reference period 1961-1990, in regions like Western Greece, Eastern Macedonia-Thrace and Crete, but will increase significantly in others *[1]*. In the eastern continental regions, in particular, maximum consecutive 3-day precipitation is projected to increase by 20%. These contrasts become even more pronounced toward the end of the 21st century, with the amount of extreme rainfall projected to decrease by 10-20% in regions of Western Greece and Thrace, but to increase by 30% in the Eastern Central Greece and the NW Macedonia. Small variations are projected for the rest of the country *[1]*.

Projections were also made regarding the variation in the maximum duration of dry spells, i.e. consecutive dry days, defined as days with no or less than 1 mm precipitation *[1]*. As can be seen from Figure 3-9, the length of dry spells will clearly increase *[1]*. The smallest variations in dry spell length are projected for Greece's western regions in 2021-2050 (less than 10 more consecutive dry days) and for Western and Northern Greece in 2071-2100 (less than 20 more consecutive dry days). The largest increases in dry spell length are projected for the eastern continental regions (Eastern Central Greece, the Eastern Peloponnese and Euboia) and Northern Crete, which will have more than 20 additional consecutive dry days in 2021-2050 and as many as 40 more consecutive dry days in 2071-2100 *[1]*.

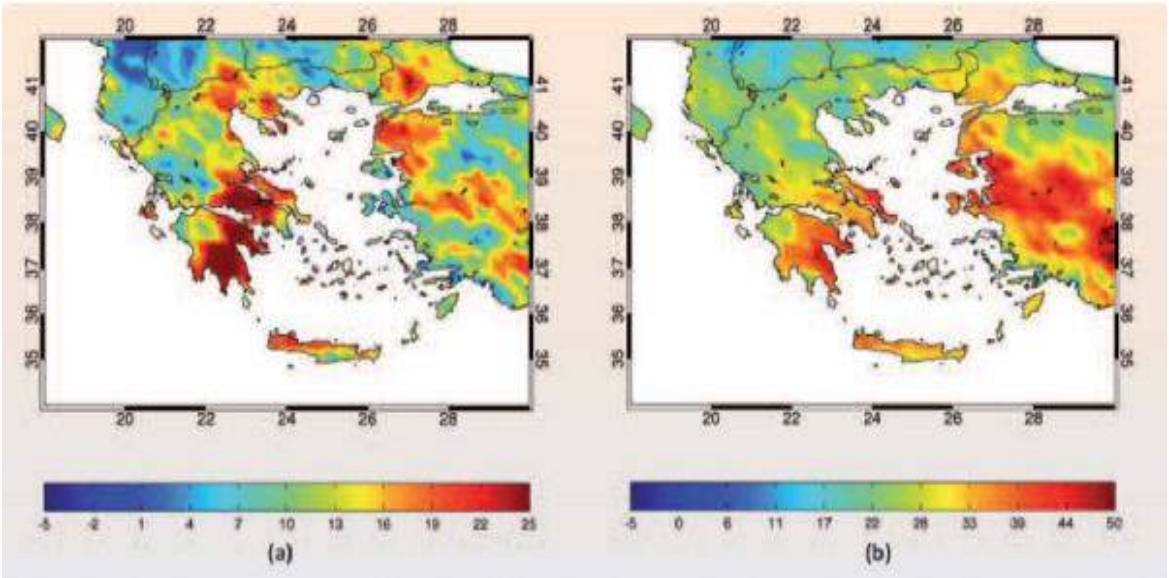

Figure 3-9. Variation in maximum length of dry spell (in consecutive dry days) in (a) 2021-2050 and (b) 2071-2100, relative to 1961-1990 [1;14]

The projected changes in the number of frost days per year are represented in Figure 3-10 *[1]*. This is an important parameter for agricultural regions, especially those where frost-sensitive crops, like citrus fruit, are grown. The number of frost days per year is projected to decrease in Macedonia and Thrace by 15 in 2021-2050 and by 40 in 2071-2100, and in the continental regions of Thessaly and the Peloponnese by 10 to 15 in 2021-2050 and by 25 in 2071-2100 *[1]*. Smaller decreases are projected for the rest of Greece, mainly because of the small number of frost days that these regions have even today *[1]*.

In addition to the number of frost days, the length of the growing season was also examined, defined as the period favorable to plant and crop growth between the last spring frost and the first autumn frost *[1]*. The projected changes in the length of the growing season are represented in Figure 3-11. The observable lengthening can be attributed to the earlier occurrence of the last spring frost and to the later occurrence of the first autumn frost. The largest increases in growth season length (in the order of 25 days for 2021-2050 and 45 days for 2071-2100) are projected for the country's continental mountain regions *[1]*. Length increases of 10-15 days for 2021-2050 and 15-25 days for 2071-2100 are projected for the rest of the country *[1;14]*.

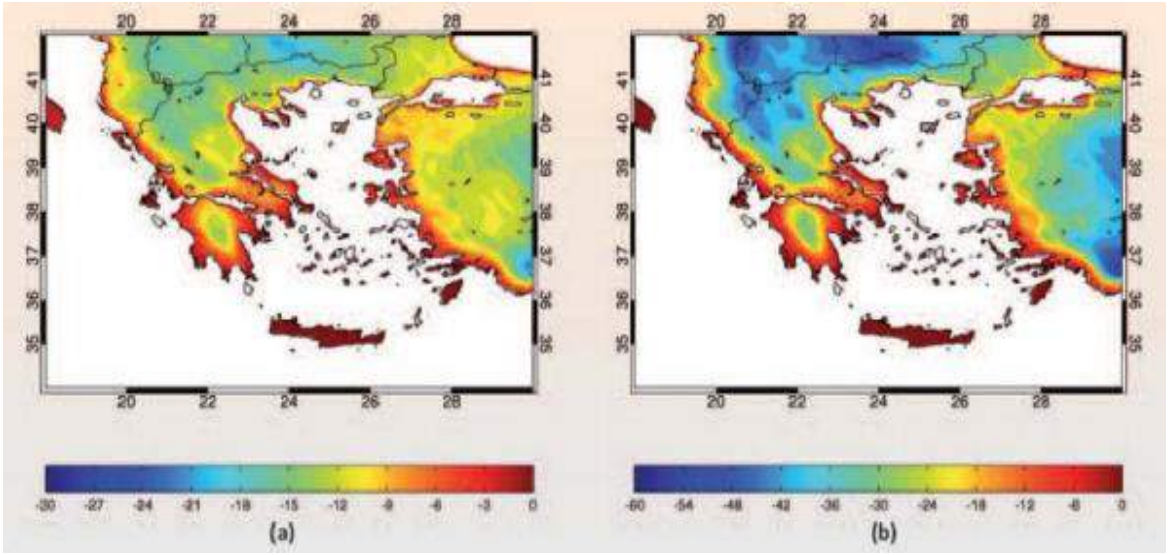

Figure 3-10. Variation in number of night frosts in (a) 2021-2050 and (b) 2071-2100, relative to 1961-1990 [1;14]

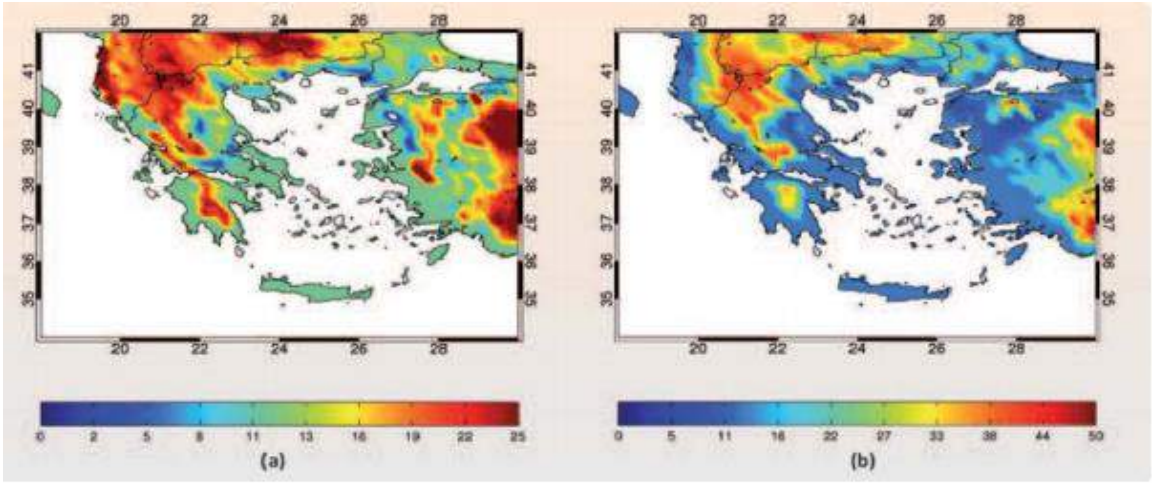

Figure 3-11. Variation in growing season length (in days) in (a) 2021-2050 and (b) 2071-2100, relative to 1961-1990 [1;14]

For the purpose of project CCWaterS *[15]* two pilot areas in Greece are examined: one in Northern Greece and the other one in Peloponnisos. From the analysis of the results of the three regional climate models under study it was found that generally all models agree that the domain of study would exhibit a general reduction of precipitation mainly during the second future period. So the models indicate generally dryer conditions in the testy sites especially by the end of the 21st century *[15]*.

According to the 6th National Report to the UNFCCC, the impacts of climatic change on water systems can be summarised as follows *[1]*:

1. An overall decrease in aquifer infiltration and recharge, as a result of decreased rainfall;
2. Increased salinity of coastal and subsea aquifers;

3. Higher pollutant load concentrations in coastal water bodies and the sea;
4. Faster degradation of deltaic regions, in cases where degradation has already begun as a result of transversal dam construction upstream;
5. Contamination or drainage of coastal wetlands;
6. Amplification of the desertification phenomenon as a result of water deficits;
7. Droughts determined by social factors such as population changes, population shifts, demographic characteristics, technology, government policies, environmental awareness, water use trends, social behaviour, level of water development and/or exploitation, and water availability.

4. LITERATURE:

[1] Ministry of Environment, Energy and Climate Change (2014): 6th National Communication and 1st Biennial Report under the united Nations Framework Convention on Climate Change.

[2] http://www.globaltrade.net/map/Greece.html [acccessed June 18 2014]

[3] Batlas E.A. (2008): Climatic Conditions and Availability of Water Resources in Greece. Water Resources Development, Vol. 24, No. 4:635–649.

[4] http://en.wikipedia.org/wiki/Ionian_Islands_(region)#mediaviewer/File:Periferia_Ionion_Nision [acccessed June 18 2014]

[5] http://wfd.opengov.gr/index.php?option=com_content&task=section&id=2&Itemid=12 [acccessed June 18 2014]

[6] Special Secretariat For Water (2013): River Basin Management Plan of GR05 – Ipiros, http://dl.dropboxusercontent.com/u/50953375/RBMP_GR05.pdf

[7]http://www.hnms.gr/hnms/english/climatology/climatology_region_diagrams_html?dr_city=Kerkyra&dr_region=ClimIonian_Islands [accessed June 20, 2014]

[8]http://www.hnms.gr/hnms/english/climatology/climatology_region_diagrams_html?dr_city=Argostoli&dr_region=ClimIonian_Islands [accessed June 20, 2014]

[9] Special Secretariat For Water (2013): River Basin Management Plan of GR02 – Northern Peloponnisos, https://dl.dropboxusercontent.com/u/52514924/GR02_RBMP.pdf

[10] Huang, S., H. N. Pollack, et al. (2000): Temperature trends over the past five centuries reconstructed from borehole temperatures. Nature 403(6771): 756-758.

[11] Pollack, H. N. and J. E. Smerdon (2004): Borehole climate reconstructions: Spatial structure and hemispheric averages." Journal of Geophysical Research D: Atmospheres 109(11): D11106 1-9

[12] IPCC (2007). Climate change 2007: The physical science basis. Contribution of Working Group I to the Fourth Assessment Report of the Intergovernmental Panel on Climate Change S. Solomon, D. Qin, M. Manning, Z. Chen, M. Marquis, K.B. Averyt, M. Tignor, H.L. Miller. Cambridge, New York, Cambridge University Press: 996.

[13] Lelieveld, J., P. Hadjinicolaou, et al. (2013): Climate change and impacts in the Eastern Mediterranean and the Middle East. Climatic Change 114(3-4): 667-687.

[14] Bank of Greece (2011): The Environmental, Economic and Social Impacts of Climate Change in Greece, Climate Change Impacts Study Committee.

[15] *http://www.ccwaters.eu/*

Let's grow up together

DRINK ADRIA

Adriatic IPA
Cross Border Cooperation 2007-2013

The project is co-funded by the European Union,
Instrument for Pre-Accession Assistance

ANNEX 2

Let's grow up together

The project is co-funded by the European Union,
Instrument for Pre-Accession Assistance

Annex 2:

2.1. Report: Climate and climate change data for test area Isonzo Plain (Italy, Friuli Venezia Giulia Region)
2.2. Report: Climate and climate change data for ATO 3 test area (Marche Region, Italy)
2.3. Report: Climate and climate change data for the Ostuni test area (Italy, Apulia Region)
2.4. Report: Analysis of observed and simulated climate and climate change for Slovenian test areas (Kobariški stol, Mia, Matajur and Mirna River catchments)
2.5. Report: Climate and climate change data for test areas in Croatia (with data from Bosnia and Herzegovina)
2.6. Report: Climate and climate change data for test areas in Nikšić, Montenegro
2.7. Report: Climate change for Drini Basin (test area in Albania)
2.8. Report: Climate and climate change data for test area in Greece

Report:

Climate and climate change data for pilot area in Italy

AcegasApsAmga

jointly with DMG - UNITS

(LP)

Trieste, 2014

Let's grow up together

DRINK ADRIA

Adriatic IPA
Cross Border Cooperation 2007-2013

The project is co-funded by the European Union,
Instrument for Pre-Accession Assistance

Table of contents

1. INTRODUCTION

The pilot area corresponds to the **Isonzo Plain** located in the northeastern side of the Friuli Venezia Giulia Region at the border with Slovenia. Its extend approximately between latitude 45° 58' 00" and 45° 49' 00" and longitude 13° 20' 00" and 13° 40' 00", WGS1984, UTM ZONE 33N.
The elevation ranges between 10 and 131 m a.s.l., with an average altitude of 35 m a.s.l.

Figure 1: The Pilot area "Isonzo Plain" (in red).

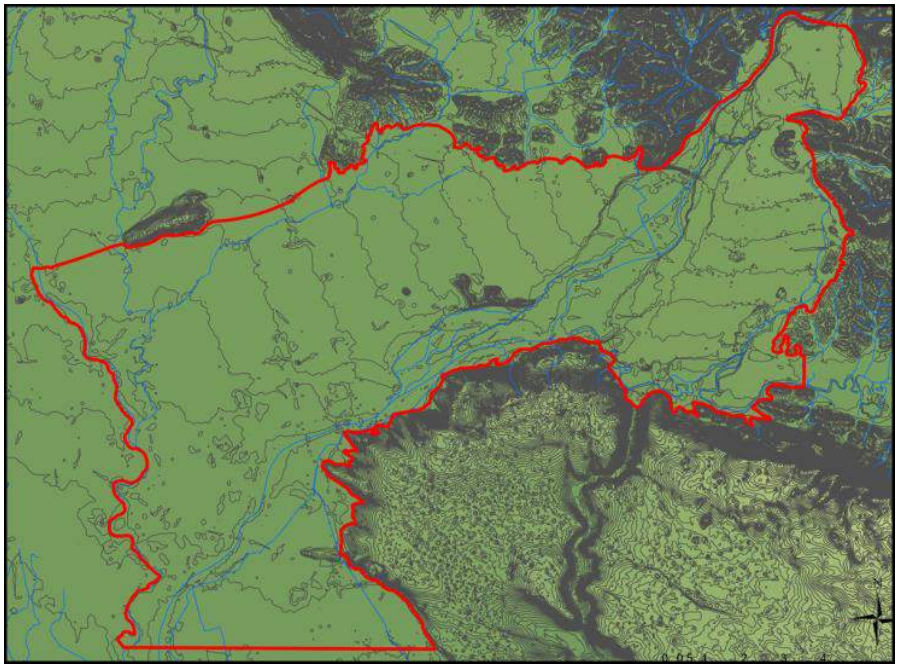

Figure 2: The Digital Terrain Model (DTM) of the "Isonzo Plain" pilot area.

The water quantity present in the alluvial deposits is significant, but the ever-increasing demand requires careful withdrawal planning to maintain the sustainability. At the moment the water quality

is good, however, the intense withdrawals jointed with the wrong land use might lead to a gradual quality decrease.
Cross-border contamination could occur more or less quickly and more or less concentrated reaching, through the riverbed losses the water table and consequently the phreatic and later the artesian aquifers. In addition, contamination could easily reach other sites of water supply in Slovenia (Klarici pumping station) and Italy (Moschenizze Nord, Sardos and Timavo springs) through the karst aquifer.

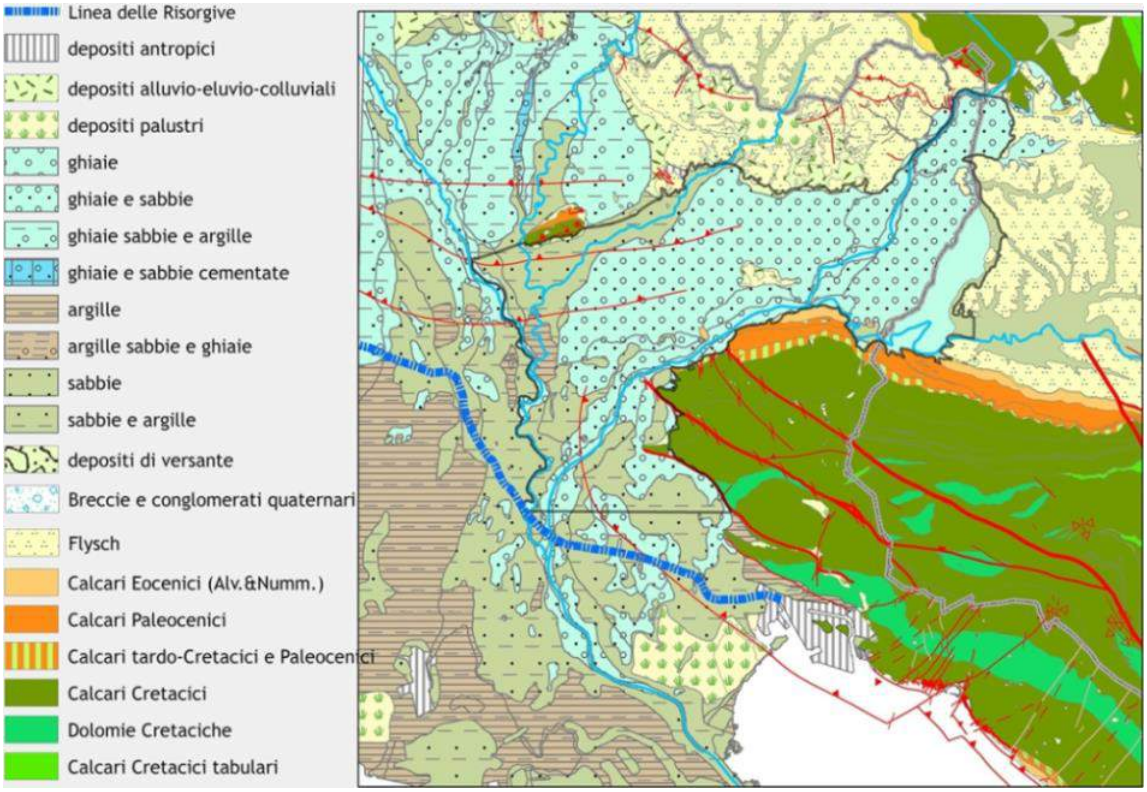

Figure 3 Sketch of the geological Map (from 1:10.000 scale data) of the Pilot area.

The system of aquifer that supply waters to the Trieste aqueduct is located at San Pier d' Isonzo. It is confined in the alluvial deposits of the Isonzo/Soca River. The Isonzo Plain is the eastern end of the Friuli Plain and has genetic and hydrogeological characteristics typical of lowland areas, facing the sea and sited at the foot of hills. It is an areal arched as the course of the Isonzo River, which extends from the outlet at the italian-slovenian border into the plain to the sea and the lagoon of Grado (about 35 km long 10 wide). It is flowing between the hills of Collio to the north, the Carso to the SE, the Corno River to the W. The plain is the result of the combined actions among the alluvial deposits from E transported by Vipacco and Soca rivers and those from the N brought by the streams of Judrio, Versa, Torre and Natisone rivers. The fluvial deposits, interacting with the ones from the Adriatic sea, took to the construction of the plain, often giving rise to furniture lagoons.
Deposits fill what we might call the paleovalley of Vipacco, Isonzo Torre and Natisone rivers: bedrock is partially made up by cretaceous limestones, in part by terrigenous facies of flysch (Tertiary) and deepening hundred meters from E to W and from N to S. The bedrock morphology is complicated by the corrugations related to the main tectonic lines approximately E-W oriented (sometimes partially broken by transcurrent N-S) and some probably related to the karst depressions.

2. EXISTING CLIMATE FEATURES IN THE ISONZO RIVER PLAIN

The local climate characteristics are described here for the 1961-1990 period, recommended by the World Meteorological Organization as the reference time-period for the present climate conditions and for the DRINKADRIA Project.
Seasonality is described in terms of annual cycle of the mean annual precipitation and temperature, their standard deviation (of monthly mean) and the coefficient of variations.

Trends are calculated for the whole span of available data, i.e. 1941 – 2011 for temperature and 1919 – 2012 for precipitation. Data is presented on monthly, seasonal (winter – December to February; spring – March to May; summer – June to August; autumn – September to November) and annual average basis.

The discussion of the extremes is based on percentiles calculated starting from the empirical values expressed as cumulative distribution function (CFD). We analyzed, for the present research, good quality rainfall and temperature time-series.

In Friuli Venezia Giulia are active several meteorological stations, some of which record since dozens of years. In fact, there have been numerous different manager over time:

-the Magistrato alle acque di Venezia,
-the Regione autonoma Friuli Venezia Giulia (FVG),
-the Osservatorio Meteorologico Regionale (OSMER),
-the Agenzia Regionale Per l'Ambiente (ARPA-FVG),
-the Consiglio Nazionale delle Ricerche (CNR)
-the Protezione civile del FVG.

The web site http://www.osmer.fvg.it/ offers information, forecasts, data, publications, models continually updated and free.

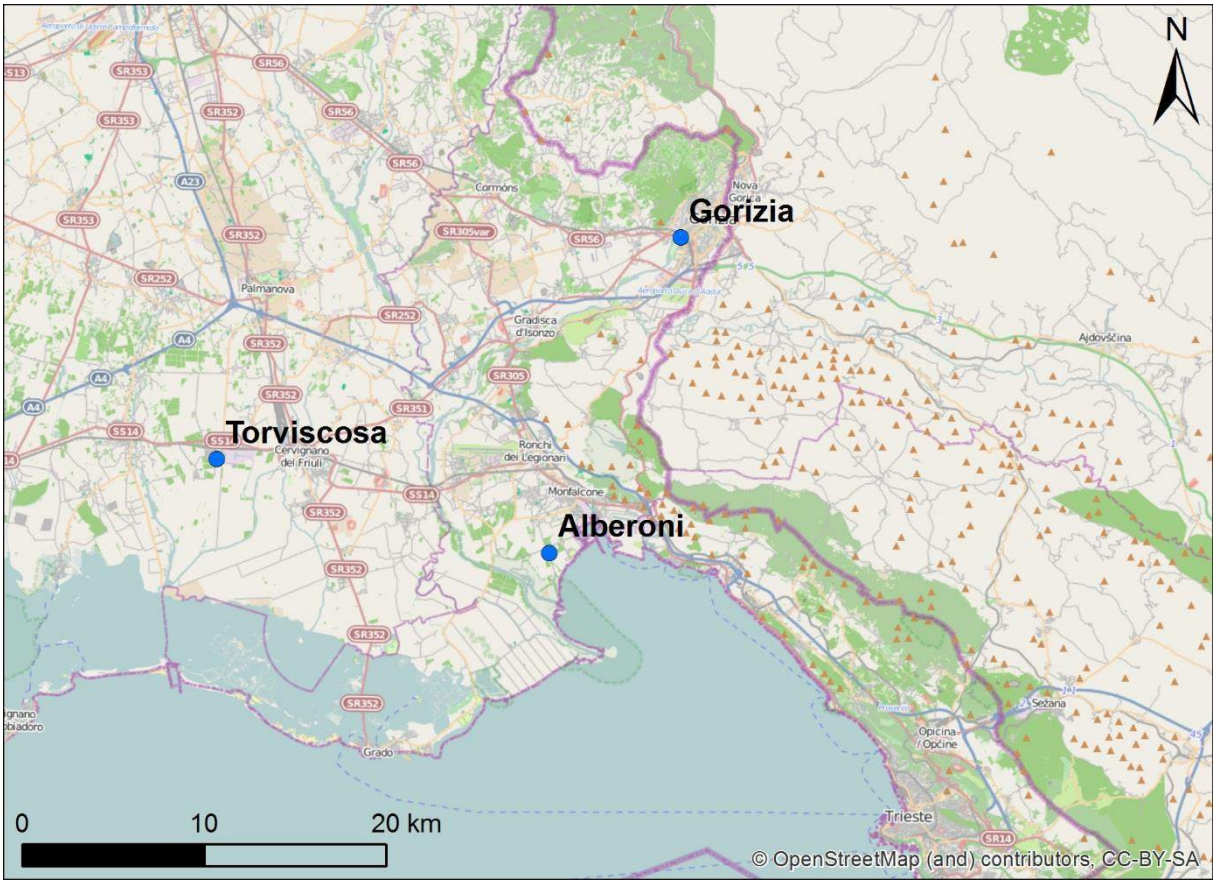

Figure 4 Spatial distribution of the hydro-meteorological monitoring stations with good quality time-series in the surrounding of the pilot area.

ID Station	Place	P data [mm]	P period	T data [°C]	T period
P005	Monfalcone - Piscina comunale	daily	31/07/2009 - 02/01/2012	daily	2010 - 2012
P001	Monfalcone	daily	01/01/1919 - 31/12/1991	daily	1972 - 1991
P002	Alberoni, Idrovora Sacchetti	daily	01/01/1925 - 02/01/2012		
J209	Torviscosa	daily	01/01/1951 - 02/01/2012	daily	1942 - 2010
J211	Belvat	daily	01/01/1969 - 30/09/1996		
J212	Cervignano	daily	01/01/1917 - 02/01/2012		
N022	Gorizia, Presa C.B.P.I.	daily	01/10/1919 - 02/01/2012	daily	1941 - 2011
N701	Gorizia, Aeroporto di Merna	daily	01/01/1995 - 02/01/2012	daily	2001 - 2011
N024	Farra d'Isonzo, M.Fortin	daily	01/01/1994 - 02/01/2012		
N025	Farra d'Isonzo, Acquedotto IRIS	daily	15/10/1991 - 15/12/2002		
N026	Gradisca d'Isonzo	daily	01/01/1919 - 31/07/1991		
P003	Ronchi dei Legionari	daily	01/05/1925 - 31/12/1934		

Table 1: Stations data and available measurement time periods for temperature (T) and precipitation (P) data within the study area. For the analysis, it has been decided to use the Gorizia prese CBPI station due to the excellent data quality.

3. TEMPERATURE ANALYSIS

Temperatures were analyzed in three meteorological stations: Gorizia prese CBPI, Torviscosa and Alberoni (Monfalcone). Data are initially presented and later analyzed.

Temperature analysis for the reference period 1961-1990					
Gorizia, prese CBPI	**DJF**	**MAM**	**JJA**	**SON**	**Year**
mean [°C]	4,2	12,7	21,6	13,5	13,1
stdev [°C]	1,9	3,8	1,7	4,6	0,6
max [°C]	22,0	32,0	39,0	34,0	39,0
min [°C]	-11,0	-9,0	6,0	-7,0	-11,0

Table 2: Basic statistics (mean, standard deviation, maximum and minimum) for annual and seasonal mean air temperature from the reference time period 1961-1990 for the analyzed climatological station in the Isonzo catchment.

Percentiles	**DJF**	**MAM**	**JJA**	**SON**	**Year**
1%	-0,1	4,9	18,4	5,8	12,0
2%	0,4	5,4	18,5	6,4	12,0
5%	1,0	6,2	19,0	6,7	12,1
10%	2,0	7,5	19,5	7,5	12,2
90%	6,5	17,5	24,0	19,5	13,8
95%	7,5	18,5	24,5	20,5	13,9
98%	8,2	19,0	25,1	21,6	14,1
99%	9,2	19,2	25,5	22,0	14,1

Table 3: The percentiles calculated for seasonal and annual mean air temperature empirical distribution for the reference time period 1961-1990 1990 for the analyzed climatological station in the Isonzo catchment.

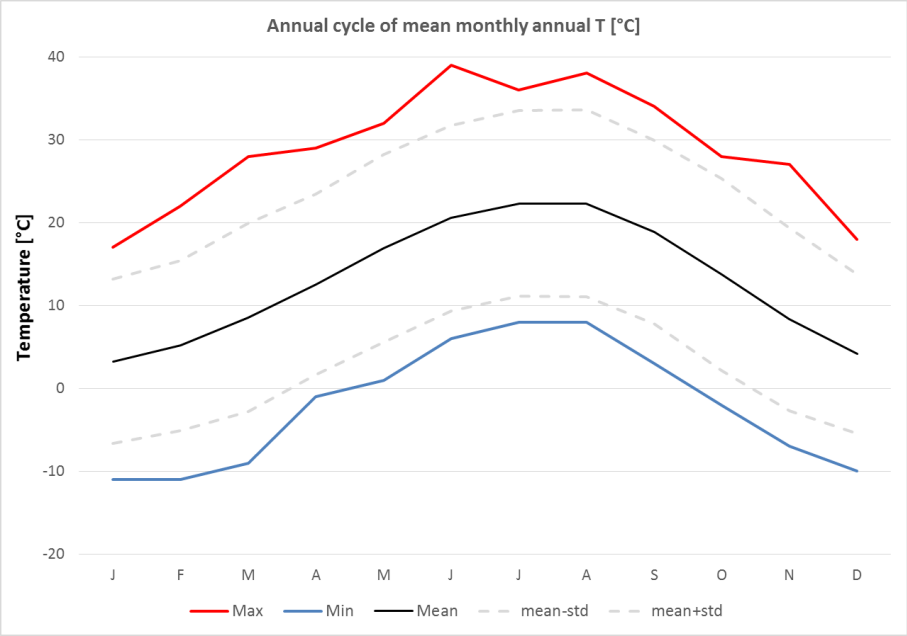

Figure 5: Annual cycle for the mean monthly air temperature [°C].

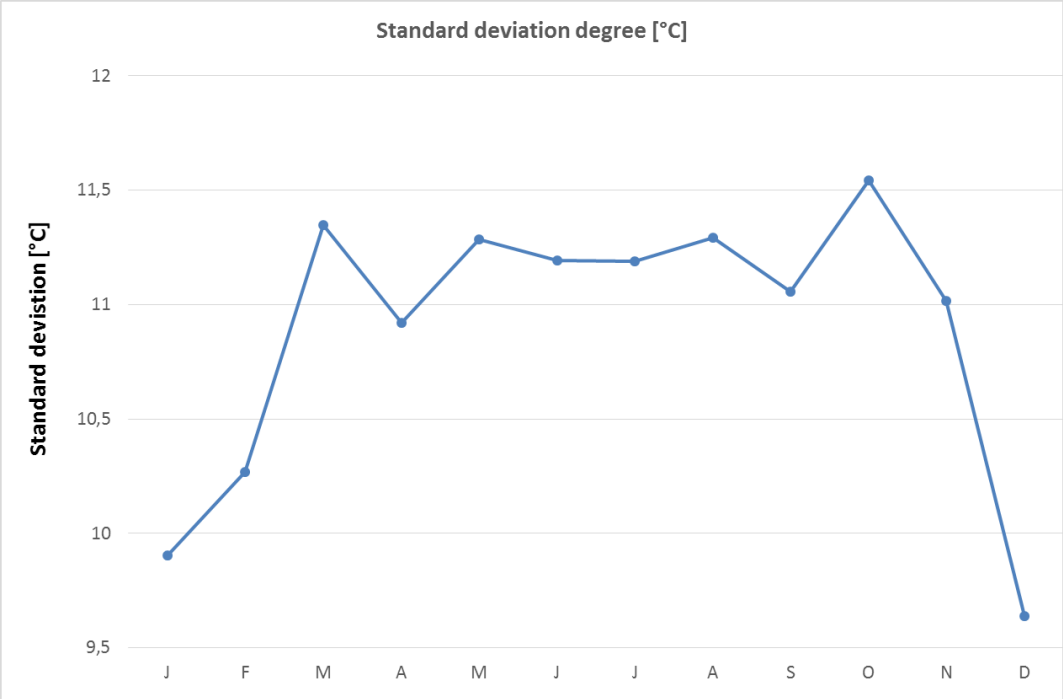

Figure 6: Standard deviation calculated on the annual cycle.

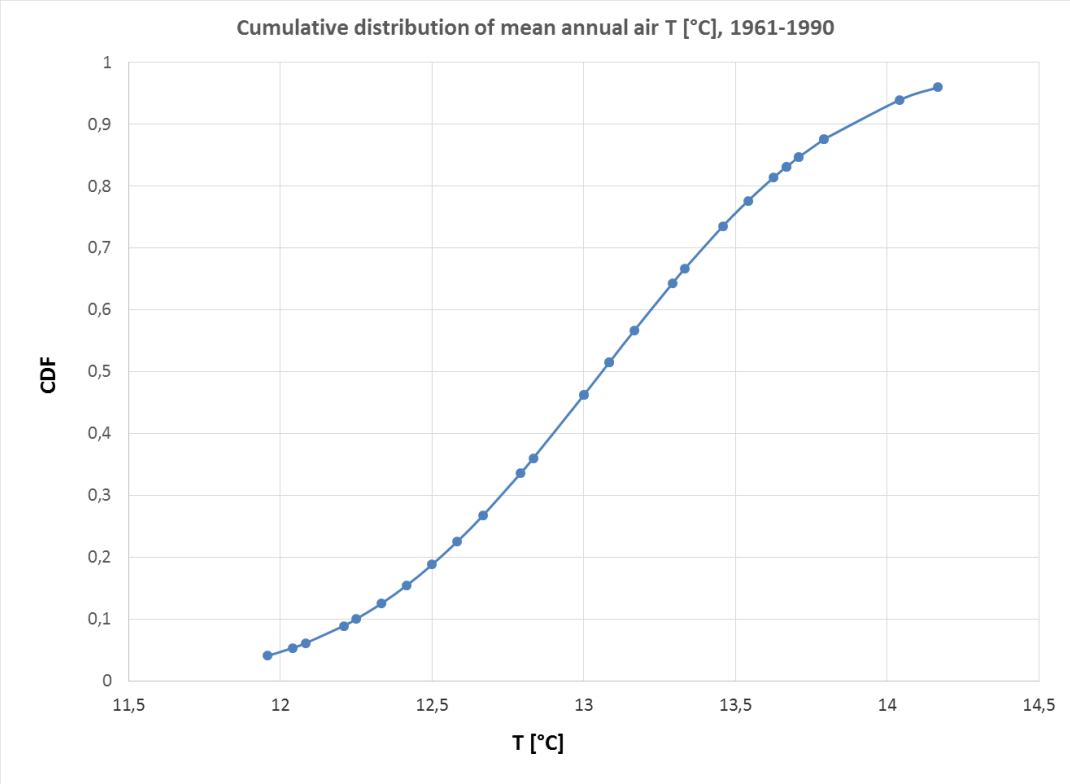

Figure 7: Cumulative distribution of mean annual air temperature for the period 1961-1990.

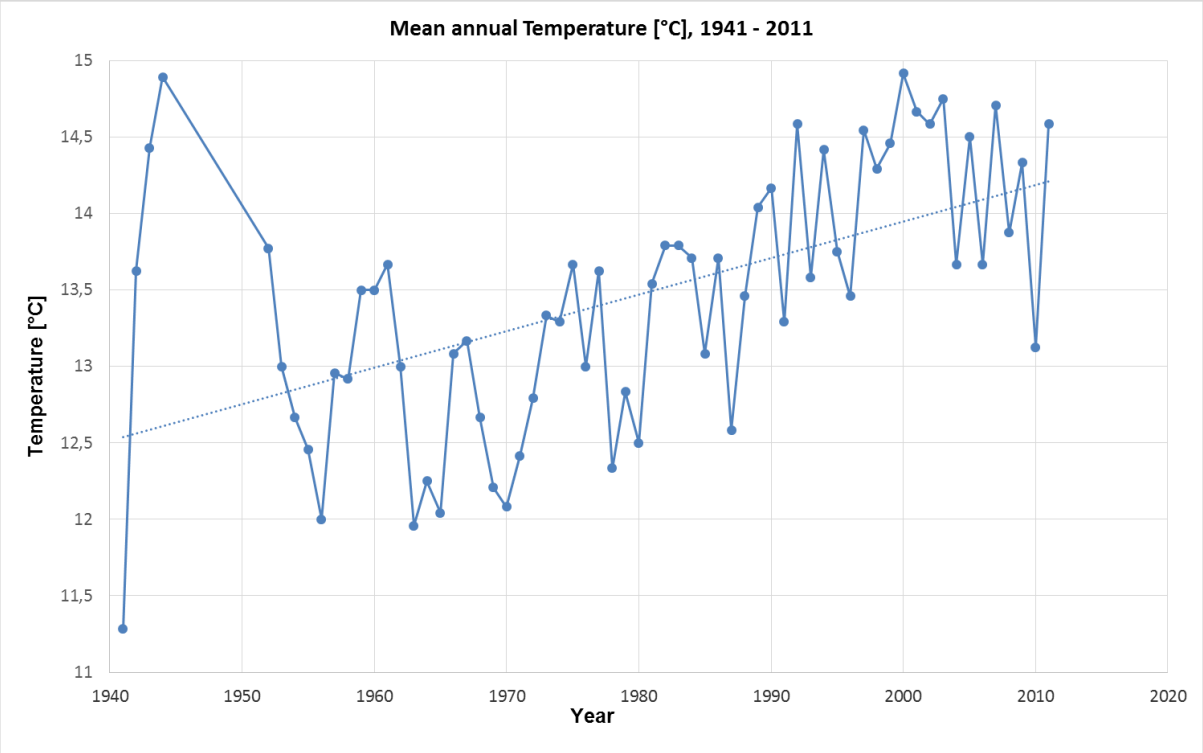

Figure 8: Time series of mean annual air temperature with the fitted trend for the period 1941-2011 for the meteorological station of Gorizia (prese CBPI). Trend=0,2°C/10y, t(1941-2011)=13,4°C.

Temperature analysis for the reference period 1942-2010					
Torviscosa	**DJF**	**MAM**	**JJA**	**SON**	**Year**
mean [°C]	4,7	13,4	22,1	13,8	13,5
stdev [°C]	2,2	4,3	2,4	4,6	1,9
max [°C]	25,0	37,0	37,0	34,1	37,0
min [°C]	-12,8	-8,0	-6,9	-6,0	-12,8

Table 4: Basic statistics (mean, standard deviation, maximum and minimum) for annual and seasonal mean air temperature from the available time period 1942-2010 for the analyzed climatological TORVISCOSA station in the Isonzo catchment.

Percentiles	**DJF**	**MAM**	**JJA**	**SON**	**Year**
1%	-0,7	5,2	16,8	4,9	4,3
2%	-0,5	5,7	17,4	5,8	6,7
5%	0,7	6,4	18,0	7,0	9,8
10%	2,4	7,5	19,0	8,0	11,0
90%	7,5	18,9	24,5	19,5	15,5
95%	8,0	20,1	25,0	21,3	17,1
98%	8,8	20,7	26,0	22,0	17,9
99%	9,4	21,7	26,6	22,0	18,1

Table 5: The percentiles calculated for seasonal and annual mean air temperature empirical distribution for the reference time period 1942-2010 for the analyzed TORVISCOSA climatological station in the Isonzo catchment.

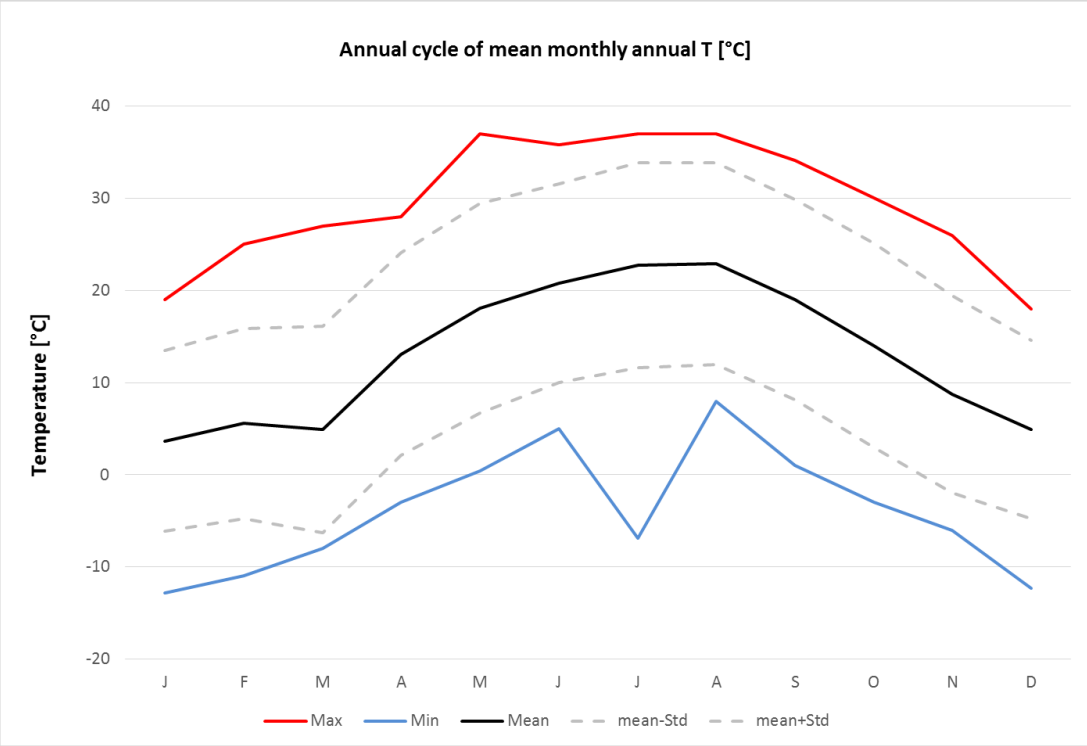

Figure 9: Annual cycle for the mean monthly air temperature [°C] for the TORVISCOSA station.

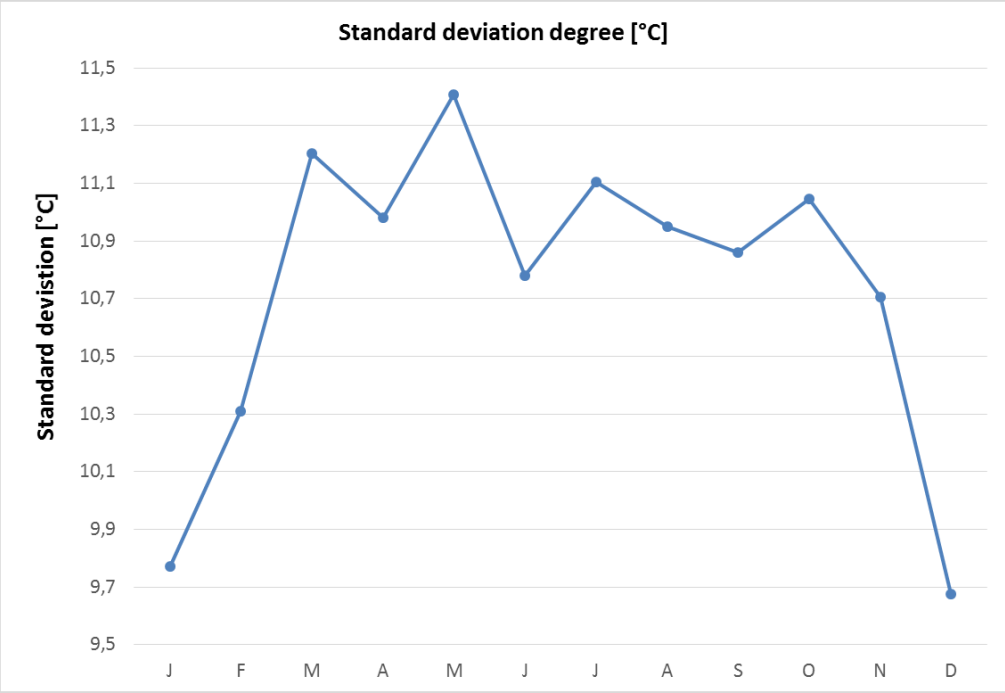

Figure 10: Standard deviation calculated on the annual cycle.

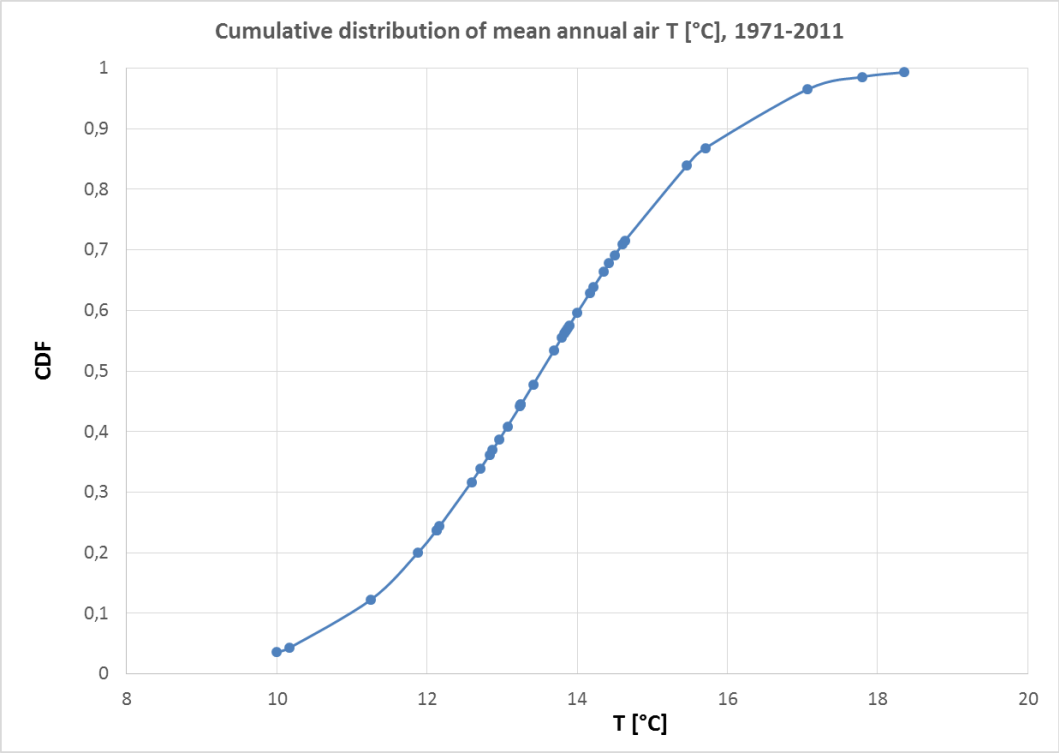

Figure 11: Cumulative distribution of mean annual air temperature for the period 1971-2011 for TORVISCOSA climatic station.

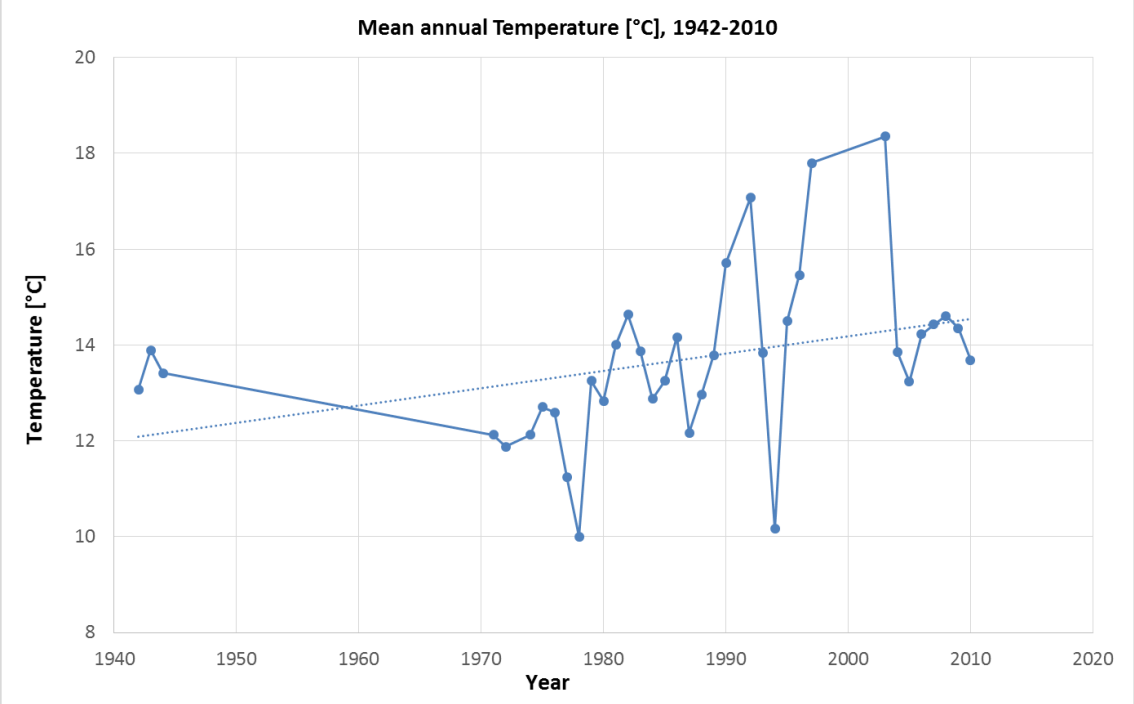

Figure 12: Time series of mean annual air temperature with the fitted trend for the period 1942-2010 for the meteorological station of TORVISCOSA. Trend=0,6°C/10y, t(1941-2011)=13,5°C.

Temperature analysis for the reference period 1972-2011					
Monfalcone	**DJF**	**MAM**	**JJA**	**SON**	**Year**
mean [°C]	5,7	14,1	22,8	14,8	14,2
stdev [°C]	8,6	10,4	9,6	10,1	11,4
max [°C]	22,0	32,6	36,0	34,0	36,0
min [°C]	-10,6	-5,0	9,0	-3,0	-10,6

Table 6: Basic statistics (mean, standard deviation, maximum and minimum) for annual and seasonal mean air temperature from the available time period 1972-2011 for the analyzed climatological ALBERONI station in the Isonzo catchment.

Percentiles	DJF	MAM	JJA	SON	Year
1%	1,2	6,6	9,6	-3,0	10,2
2%	1,8	7,7	10,0	-2,7	10,7
5%	3,0	8,4	11,0	-1,8	11,9
10%	3,4	9,0	11,1	0,0	13,5
90%	8,0	19,0	16,0	12,0	15,1
95%	8,4	19,2	16,0	12,8	15,1
98%	9,5	20,5	17,0	14,7	15,2
99%	10,4	20,7	17,4	15,4	15,2

Table 7: The percentiles calculated for seasonal and annual mean air temperature empirical distribution for the reference time period 1972-2011 for the analyzed Alberoni climatological station in the Isonzo catchment.

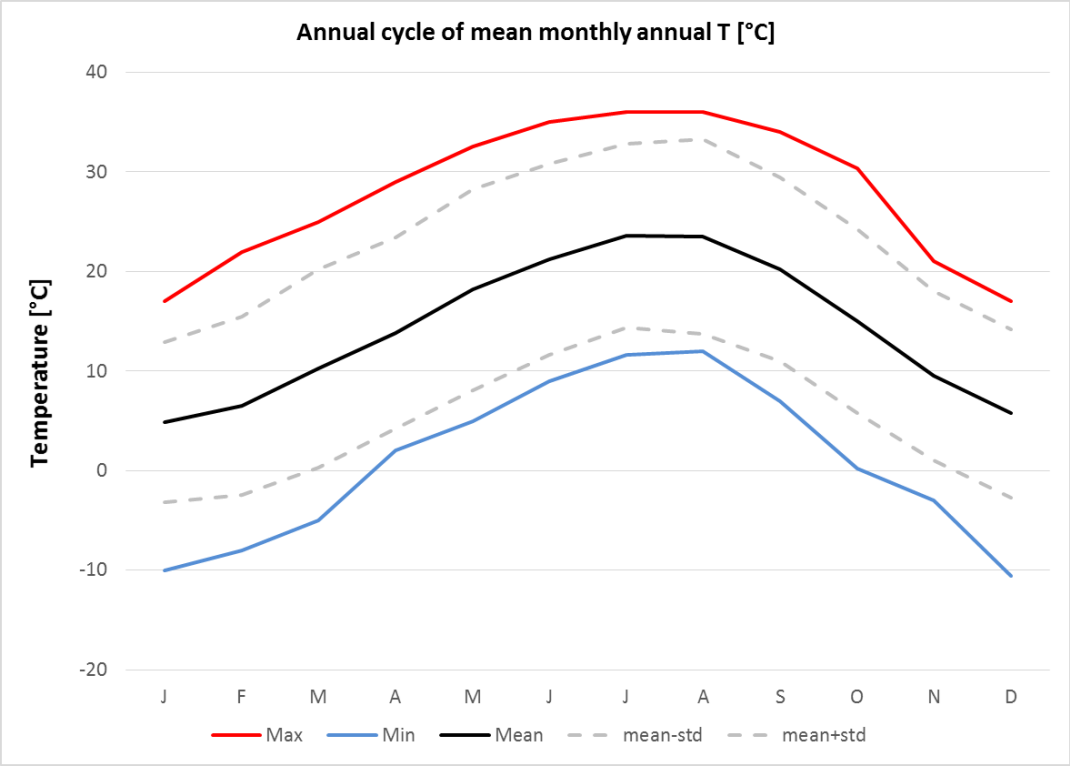

Figure 13: Annual cycle for the mean monthly air temperature [°C] for the MONFALCONE station.

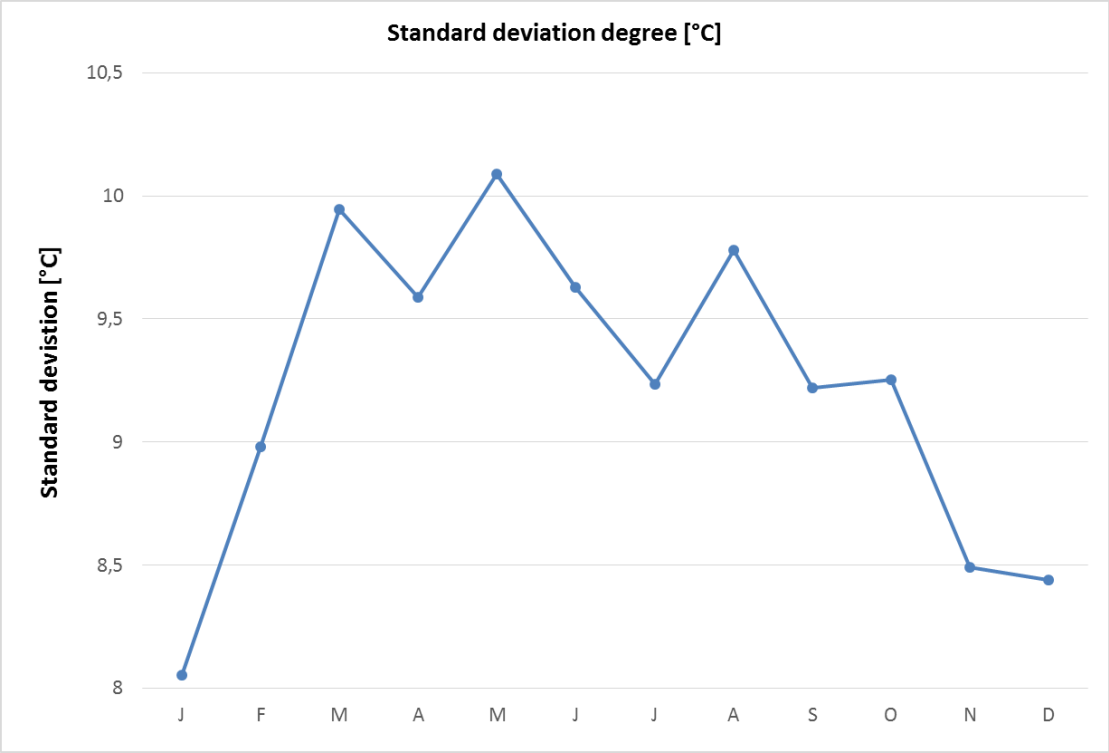

Figure 14: Standard deviation calculated on the annual cycle.

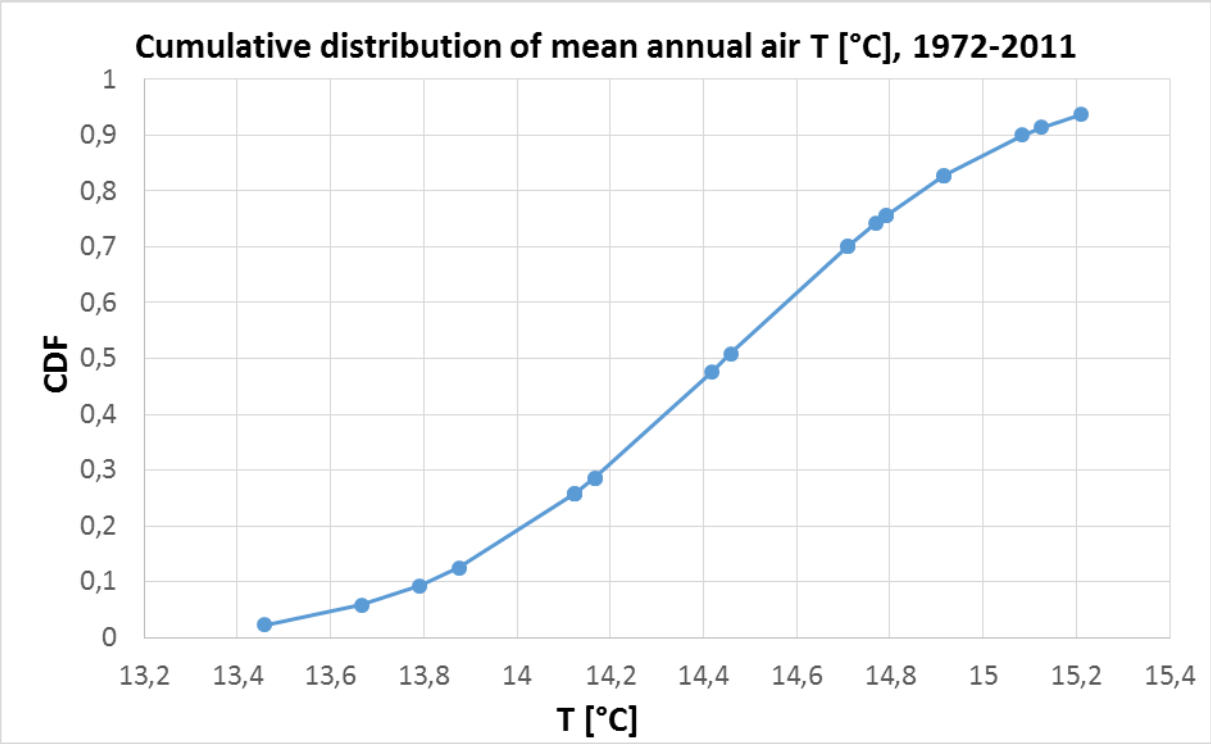

Figure 15: Cumulative distribution of mean annual air temperature for the period 1971-2011 for MONFALCONE climatic station.

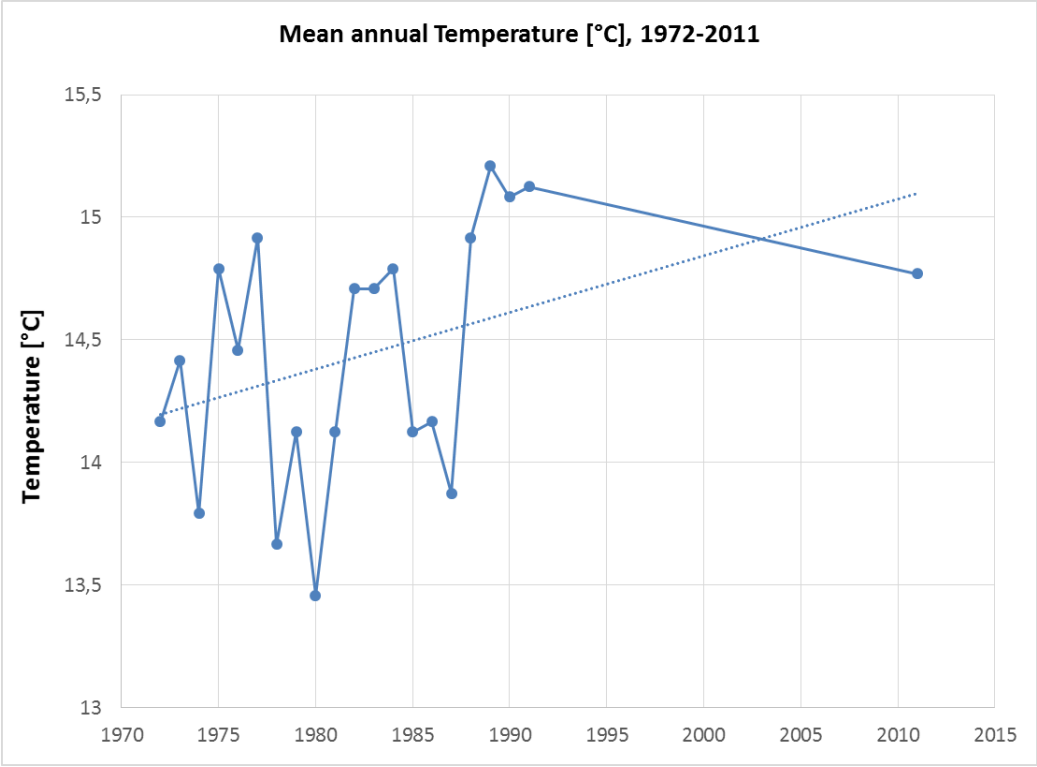

Figure 16: Time series of mean annual air temperature with the fitted trend for the period 1972-2011 for the meteorological station of Alberoni. Trend=0,4°C/10y, t(1972-2011)=14,4°C.

Temperatures in the catchment area of the Isonzo River vary greatly. Three meteorological stations were analyzed: Gorizia prese, Torviscosa and Alberoni, close to Monfalcone.
For all the three stations, the annual cycle of air temperatures is well defined, with a maximum of 36°-39°C and a minimum of -10,6 – -12°C indicating a passage by a temperate marine climate to a continental alpine ones, but with a maritime prevalence where autumn (SON) are slightly warmer than springs (MAM).
The standard deviation of mean monthly air temperatures indicate the highest variability in autumn for two of the three stations. The situation is different for Alberoni where the marine influence is higher and the variability for a 0,3°C is wider during springtime than in autumn (10,1).
The monthly values of the Sdev range between 1.7 and 4.6 for Gorizia station, 8.6 and 10.4 at Alberoni and 2.2 and 4.6 at Torviscosa indicating a quite high inter-annual variability with a higher variability while leaving the sea.
The calculated percentiles represent the extreme values of annual and seasonal mean temperatures. In the annual cycle of the percentiles of the mean daily air temperature, the difference between the 98th percentile and the 2nd, for the Gorizia station, is highest in spring and autumn due to the highest variability of the temperature values. At Torviscosa and Alberoni stations, even if with different values, the situation is similar, with higher variability in springtime and autumn.

3.1 Temperature trends

Temperature trends are similar for the analyzed stations: **Gorizia** is clearly indicating a positive trend with increasing temperatures from 12,5°C recorded during the 40s, till the 14,3°C of the actual measures. **Torviscosa** is going from 12,2 to 14,3°C even if data are affected by a not so good quality time-series (some annual values are interpreted due to the data scarcity). Also **Alberoni** station indicates an increase in the temperature during the last period, with values that goes from 14,2°C to 15,1°C (Figure 16). Here temperatures are always higher than the other examined stations due to the sea influence. As consequence, for Gorizia the Trend is of 0,2°C/10y, with a mean temperature value in the analyze period (1941-2011) of 13,4°C; for Torviscosa the Trend is of

0,6°C/10y, with a mean temperature value in the analyze period (1941-2011) of 13,5°C. For Alberoni station the Trend is of 0,4°C/10y, with a mean temperature value in the analyze period (1972-2011) of 14,4°C.

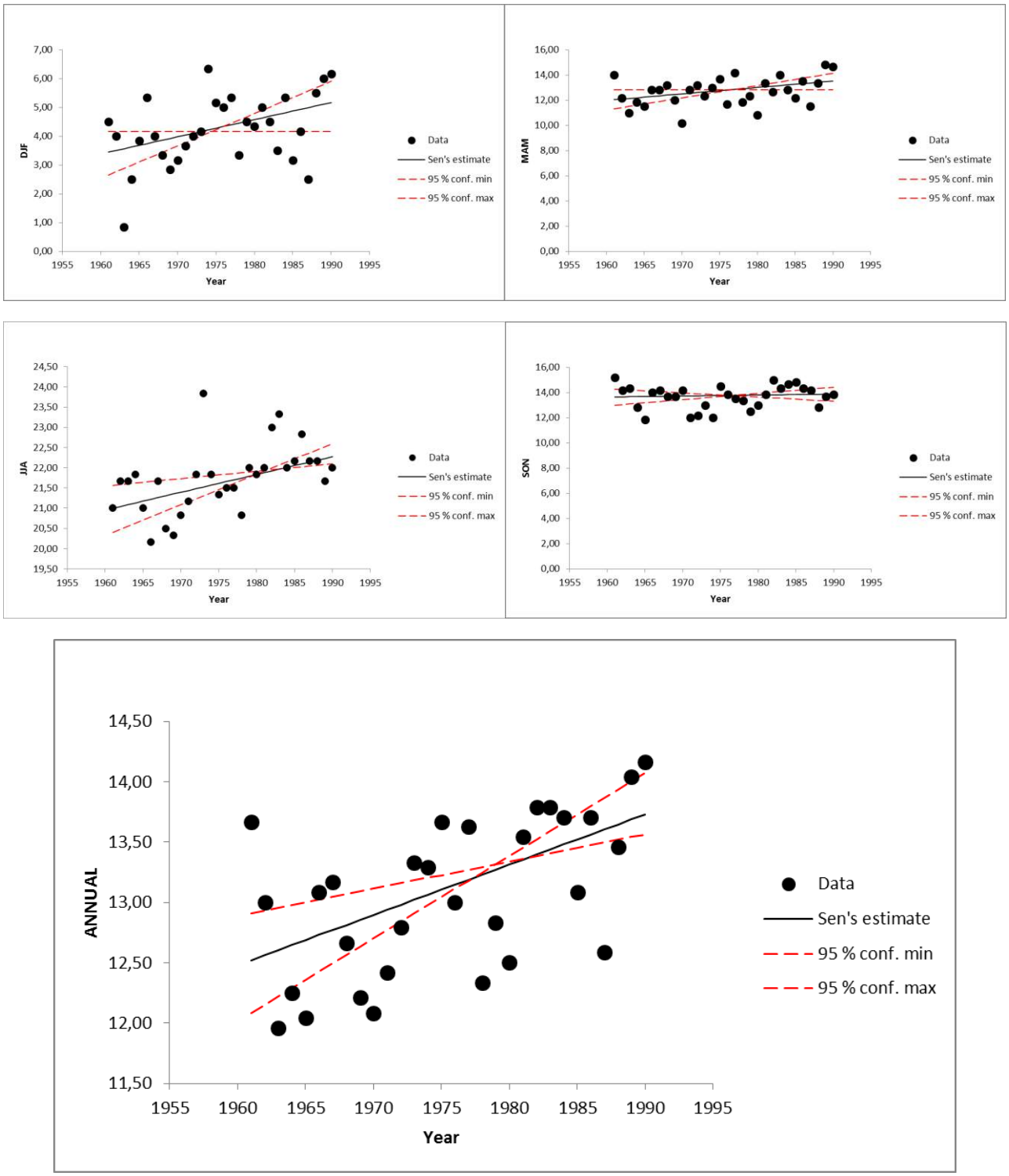

Figure 177: Mean month and annual air temperature Trend statistics for the time-reference period 1961-1990 for the ***Gorizia prese CBPI station****. The trend has been realized using the Sen's estimator and has been validated using the Mann-Kendall test. The time-series has been primarily subjected to a linear trend analysis (linear regression analysis) and later to the Sen's estimator and to the Mann-Kendall test (Sen, 1968; ISPRA, 2012).*

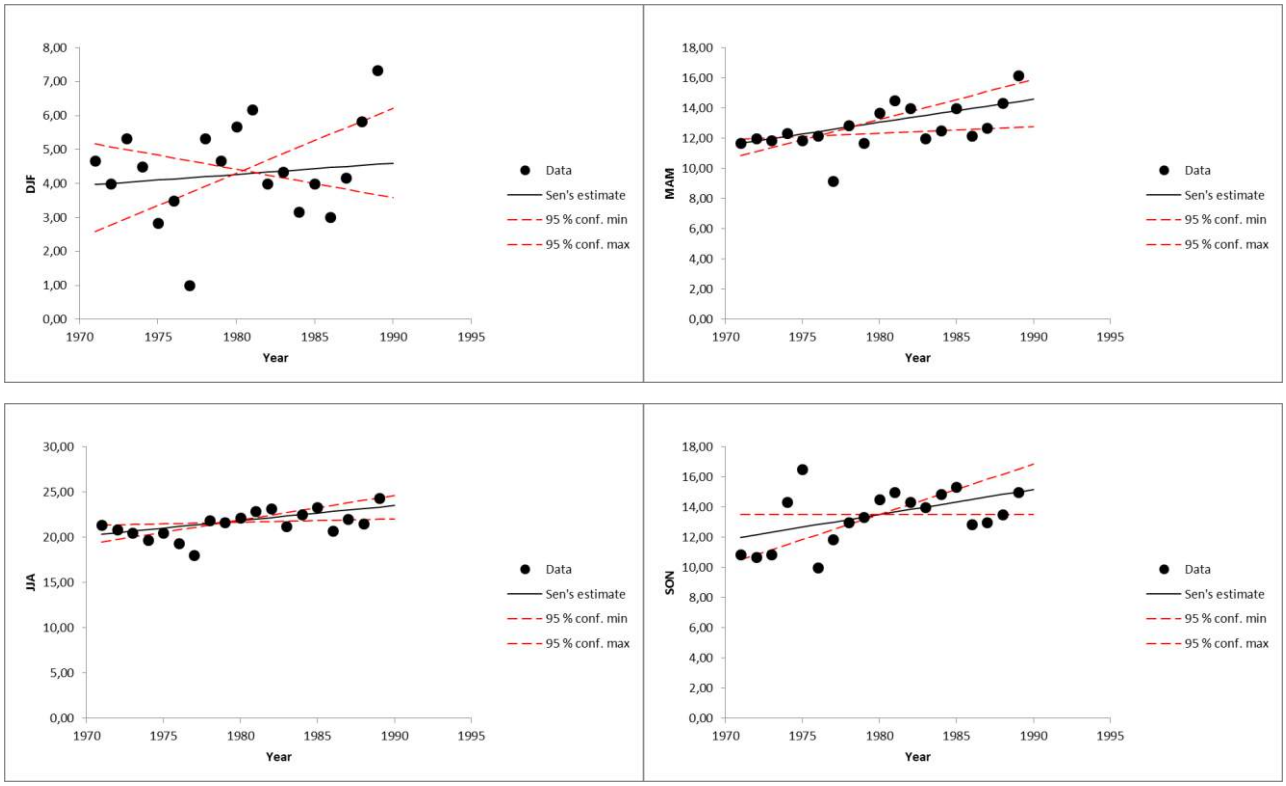

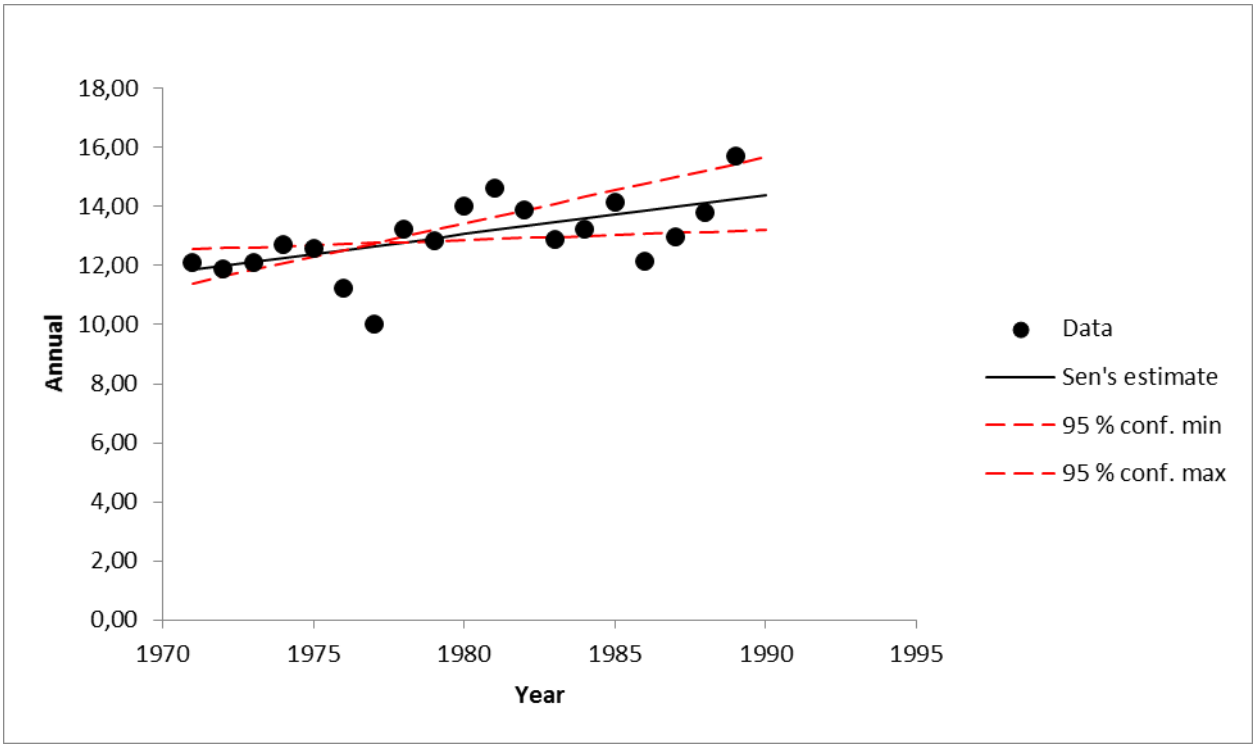

Figure 188: Mean month and annual air temperature Trend statistics for the time-reference period 1971-1990 for the ***Torviscosa station****. The trend has been realized using the Sen's estimator and has been validated using the Mann-Kendall test. The time-series has been primarily subjected to a linear trend analysis (linear regression analysis) and later to the Sen's estimator and to the Mann-Kendall test.*

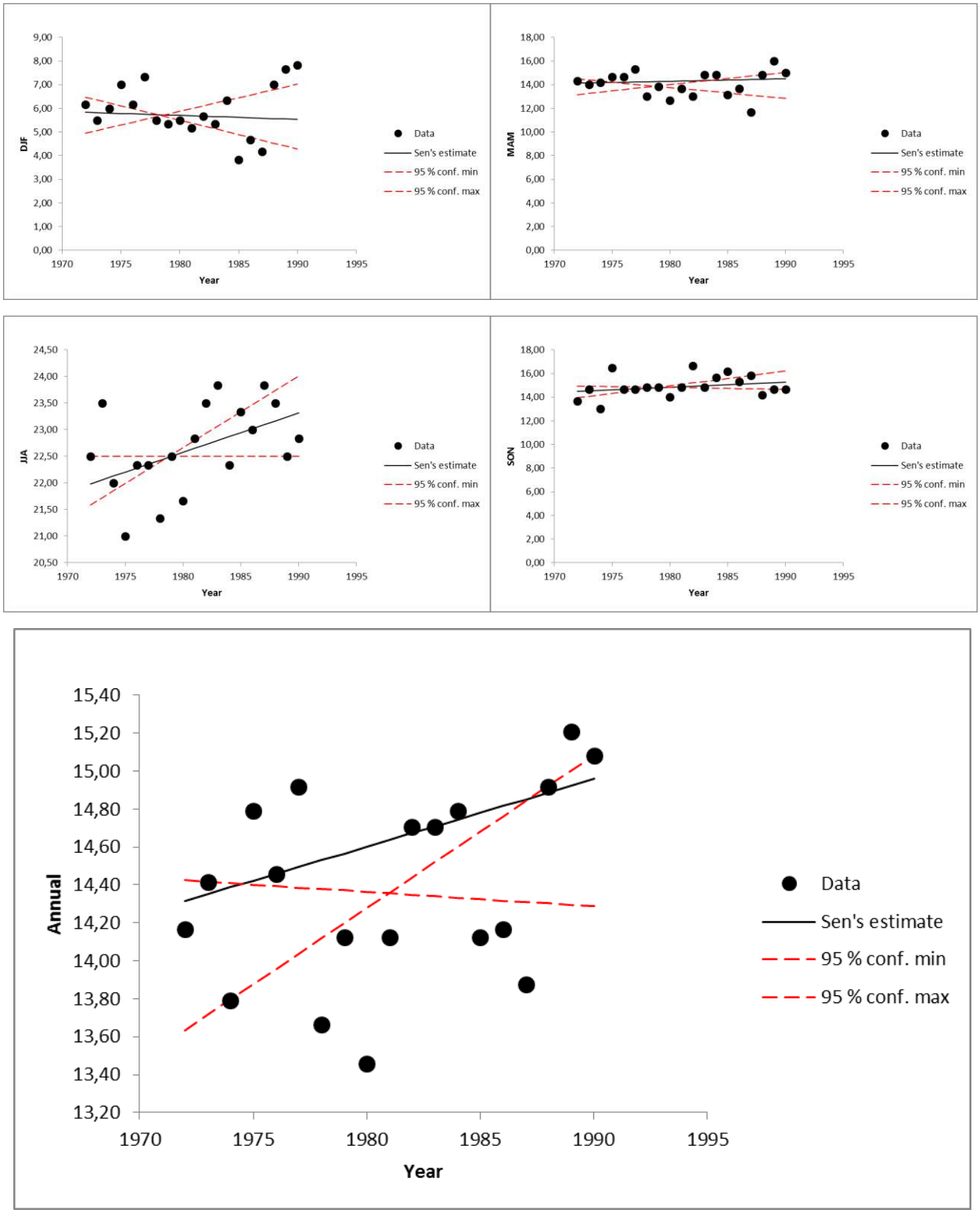

Figure 199: Mean month and annual air temperature Trend statistics for the time-reference period 1972-1990 for the ***Monfalcone station****. The trend has been realized using the Sen's estimator and has been validated using the Mann-Kendall test. The time-series has been primarily subjected to a linear trend analysis (linear regression analysis) and later to the Sen's estimator and to the Mann-Kendall test.*

°C/10y	DJF		MAM		JJA		SON		Year	
Gorizia prese CBPI	0.7	0.5	0.4	0.5	0.5	0.4	0.1	0.0	0.4	0.4
Torviscosa	0.5	0.3	1.5	1.4	1.5	1.5	1.6	1.5	1.2	1.2
Monfalcone	0.0	-0.1	0.0	0.0	0.6	0.7	0.4	0.2	0.3	0.3

Table 8: Temperature trends for the analyzed stations (°C/10y) based on the reference period 1961-1990 time series. For each season, two trend values are given, according to different methods: linear regression method (left value) and Sen's estimator (right value).

As summarized in Table 8, the trend results indicate a significant increase in the annual mean air temperatures with values ranging between 0.3 and 1.2 °C/10y. It is important to say that the time-series are quite short, especially for Torviscosa and Monfalcone stations, 1971-1990 and 1972-1990 respectively with some missing data. Torviscosa station is the one presenting the wider increase, not in the wintertimes but during the rest of the year reaching also values of 1.6°C /10y.

4. PRECIPITATION ANALYSIS

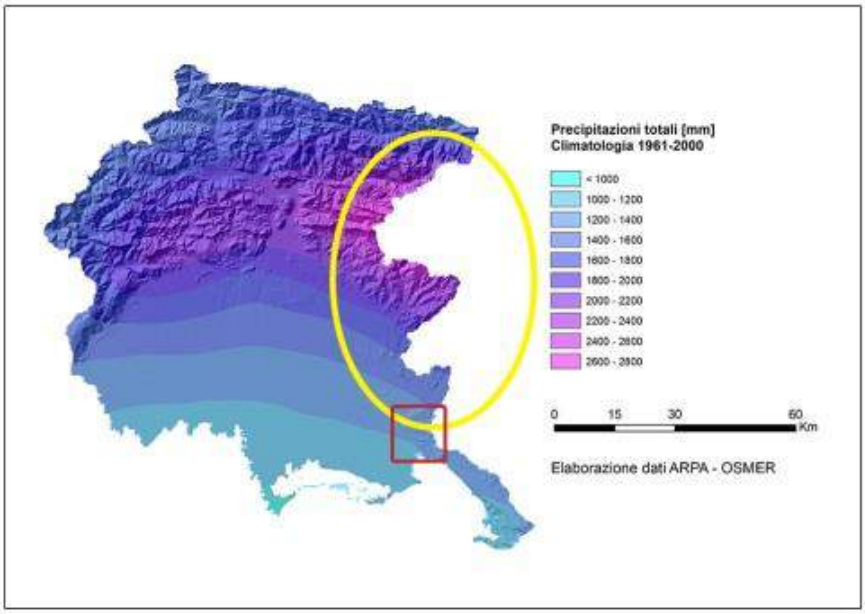

Figure 20 Average annual rainfall in the basin of the river Soča (Italian sector) http://www.osmer.fvg.it/clima.php

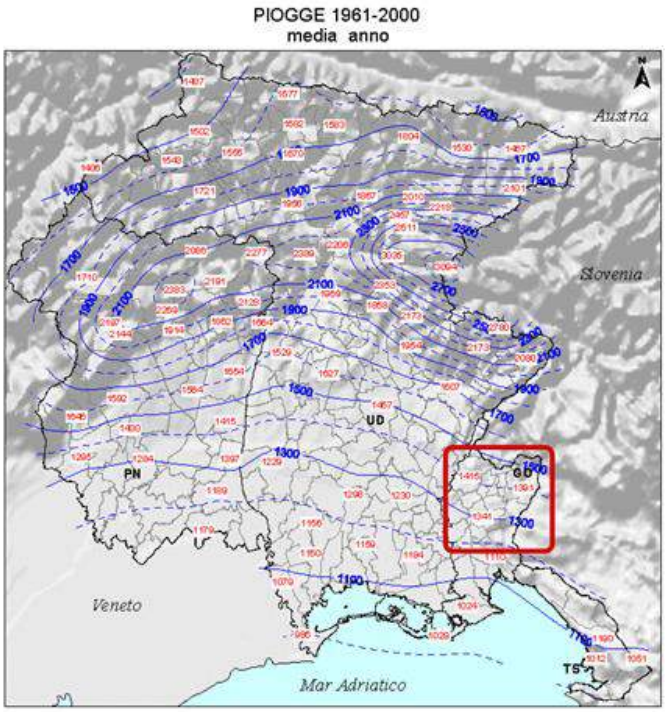

Figure 21 Mean annual rainfall in the pilot area (http://www.osmer.fvg.it/clima.php).

For the test site area, precipitations recorded by three different stations were analyzed. Below are presented the analyzed data for Gorizia prese (CBPI), Torviscosa and Alberoni (Monfalcone) stations. Firstly are shown the basic statistics, than the percentiles, then the annual cycle with its mean, max and min values, later the standard deviation and the coefficient of variation and, finally, the annual precipitation trend over the years, for the available dataset.

Precipitation analysis for the reference period 1961-1990					
Gorizia prese (CBPI)	**DJF**	**MAM**	**JJA**	**SON**	**Year**
mean [mm]	102,0	110,1	123,6	136,7	116,5
stdev [mm]	34,0	35,6	38,3	50,5	14,6
cv	0,33	0,32	0,31	0,37	0,13
max [mm]	286	255	275	430	430
min [mm]	1	1	12	0	0

Table 9: Basic statistics (mean, standard deviation, maximum and minimum) for annual and seasonal precipitations from the reference time-period 1961-1990 for the analyzed climatological station Gorizia prese (CBPI) in the Isonzo catchment.

Percentiles	DJF	MAM	JJA	SON	Year
1%	71,4	73,6	92,4	93,4	93,2
2%	79,8	76,2	98,8	97,7	94,5
5%	92,9	87,2	108,5	106,3	96,5
10%	96,7	102,3	116,2	124,3	97,0
90%	239,2	218,9	246,6	294,3	130,6
95%	262,9	237,7	254,2	334,6	137,3
98%	274,4	245,7	264,0	388,2	149,6
99%	280,2	250,4	269,5	409,1	156,2

Table 10: The percentiles calculated for seasonal and annual mean rainfall empirical distribution for the reference time-period 1961-1990 1990 for the analyzed climatological station Gorizia prese (CBPI) in the Isonzo catchment.

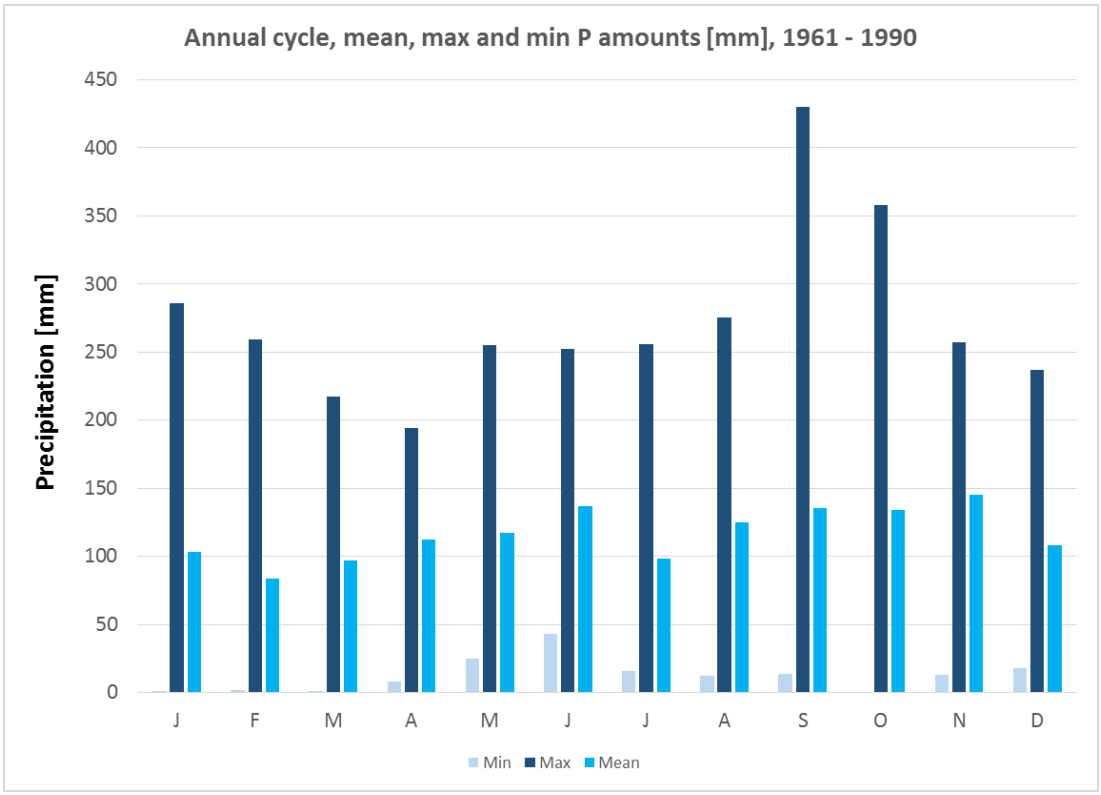

Figure 22: Annual cycle, min, max and mean annual precipitation amounts in mm calculated for the selected time-period 1961-1990 for the Gorizia prese (CBPI) station.

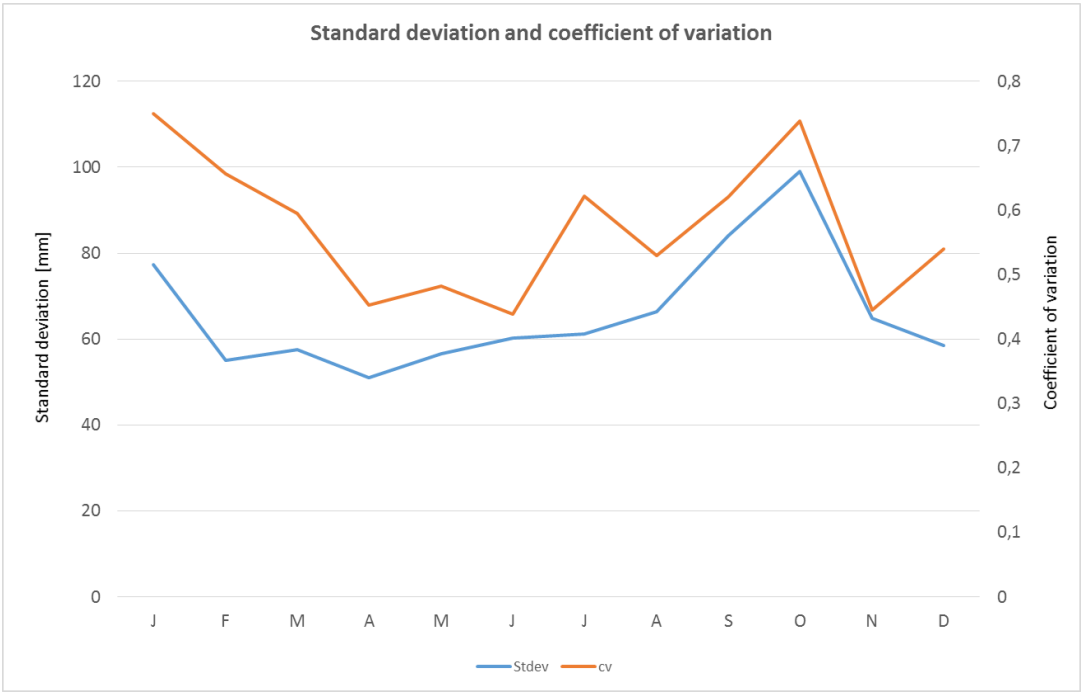

Figure 203: Standard deviation calculated on the annual cycle for the Gorizia prese (CBPI) station.

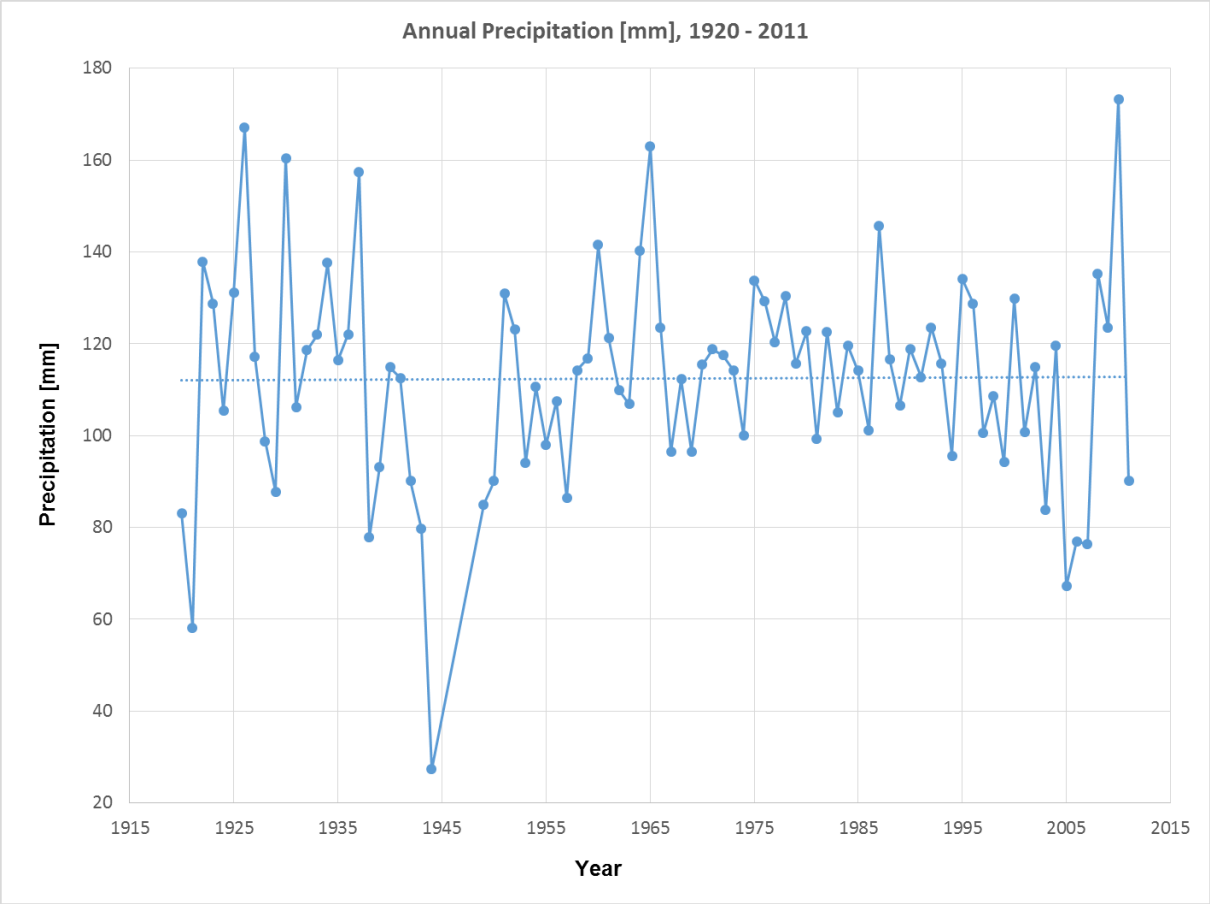

Figure 214: Time series of mean annual precipitations with the fitted trend for the period 1920-2011 for the meteorological station of Gorizia (prese CBPI). Trend=0,1mm/10y; R(1961-1990)=1397,5 mm.

Precipitation analysis for the reference period 1951-2011					
TORVISCOSA	**DJF**	**MAM**	**JJA**	**SON**	**Year**
mean [mm]	88,4	91,4	95,6	118,9	96,4
stdev [mm]	61,4	61,9	57,0	82,7	19,8
cv	0,69	0,68	0,60	0,70	0,21
max [mm]	252,8	267,6	290,1	317	317
min [mm]	2,2	0	2	8,6	0

Table 11: Basic statistics (mean, standard deviation, maximum and minimum) for annual and seasonal precipitations from the reference time-period 1951-2011 for the analyzed TORVISCOSA climatological station in the Isonzo catchment.

Percentiles	DJF	MAM	JJA	SON	Year
1%	47,2	35,0	51,6	71,2	58,0
2%	51,2	45,4	64,8	75,5	58,5
5%	53,7	58,9	73,9	82,6	65,7
10%	68,7	75,0	84,8	103,1	69,0
90%	196,8	199,7	198,7	282,8	117,7
95%	204,6	252,8	231,0	314,5	119,3
98%	239,8	267,6	290,1	317,0	132,0
99%	246,3	267,6	290,1	317,0	139,1

Table 12: The percentiles calculated for seasonal and annual mean rainfall empirical distribution for the reference time period 1951-2011 for the analyzed TORVISCOSA climatological station in the Isonzo catchment.

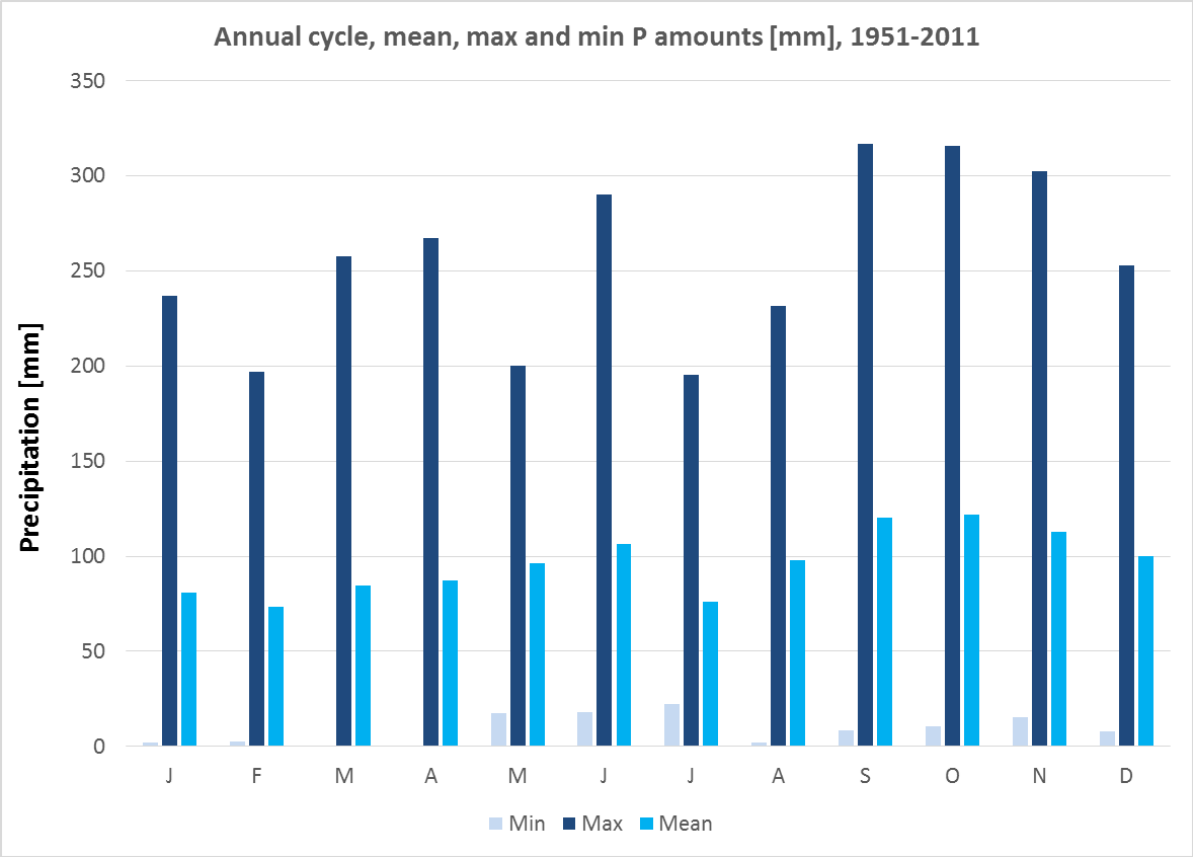

Figure 225: Annual cycle, min, max and mean annual precipitation amounts in mm calculated for the selected time period 1951-2010 for the TORVISCOSA station.

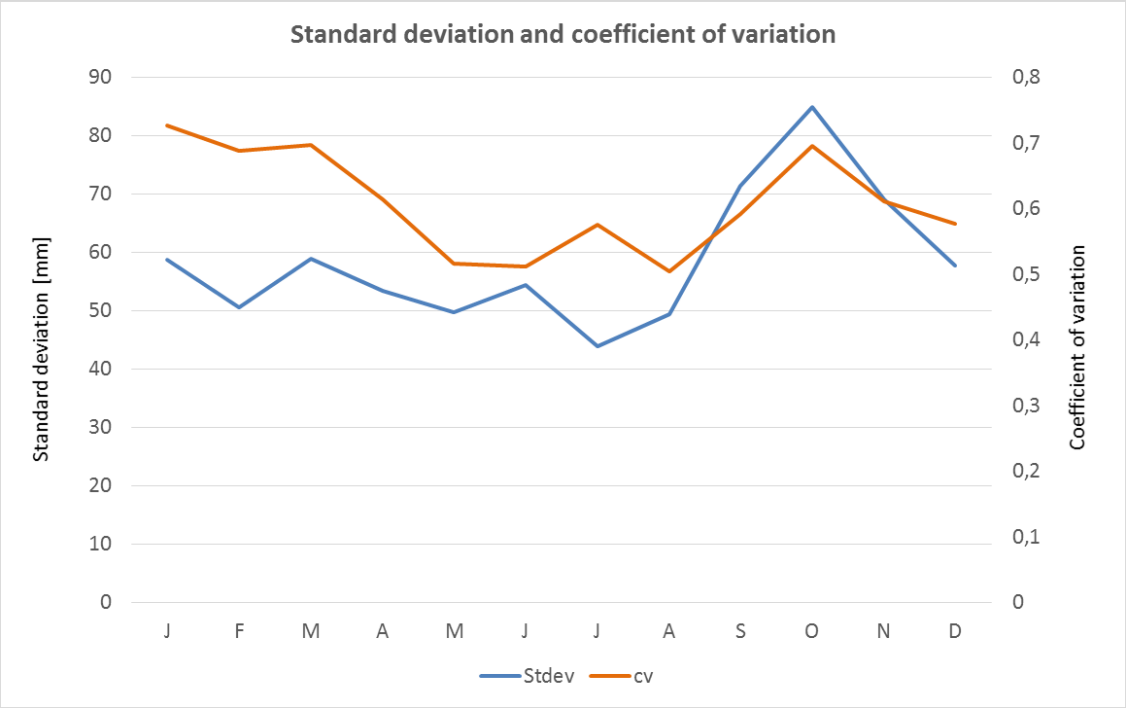

Figure 236: Standard deviation calculated on the annual cycle for the Torviscosa station.

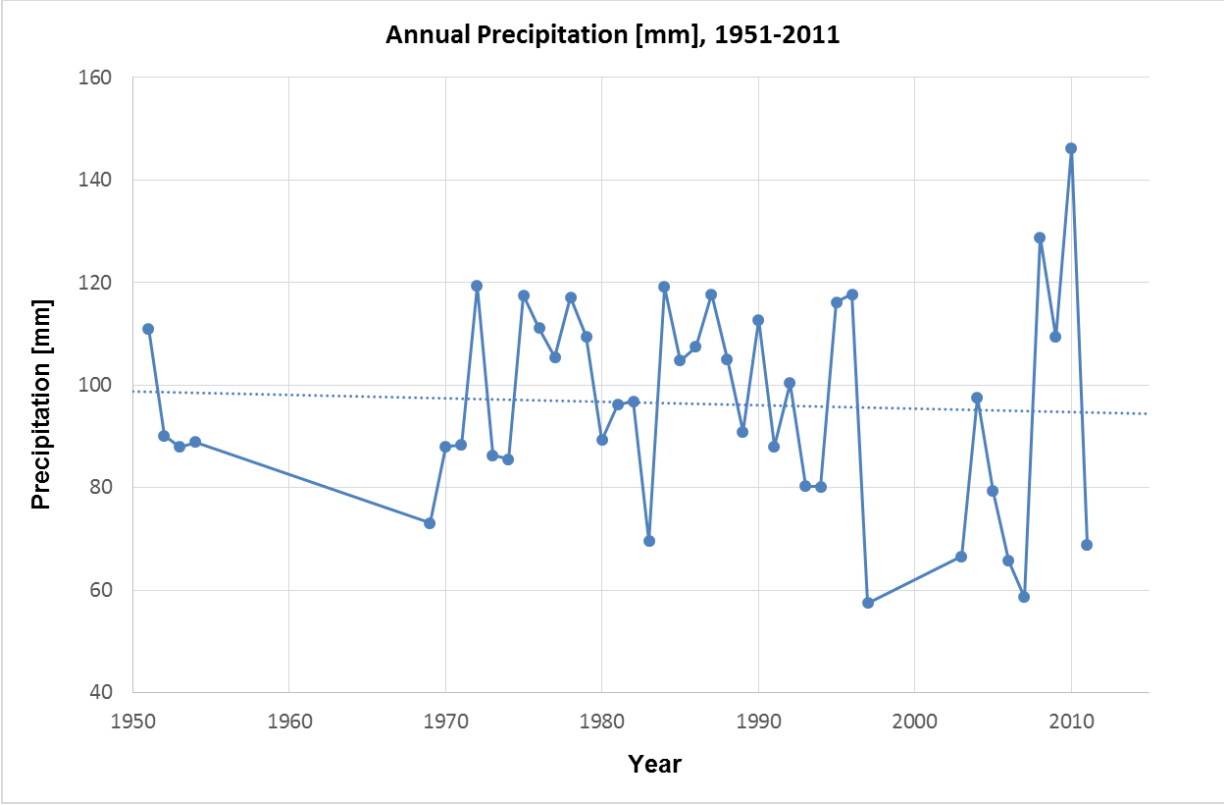

Figure 247: Time series of mean annual precipitations with the fitted trend for the period 1951-2011 for the meteorological station of Torviscosa. Trend= -1,2 mm/10y; R(1951-2000)=1184,3 mm.

Precipitation analysis for the reference period 1919-2011					
Alberoni (Monflacone)	DJF	MAM	JJA	SON	Year
mean [mm]	71,9	77,1	85,2	112,8	85,9
stdev [mm]	56,5	53,2	55,9	81,7	17,7
cv	0,79	0,69	0,66	0,72	0,21
max [mm]	268,6	241,3	277,1	422,8	422,8
min [mm]	0,4	0	2,4	12	0

Table 13: Basic statistics (mean, standard deviation, maximum and minimum) for annual and seasonal precipitations from the reference time-period 1919-2011 for the analyzed Alberoni (Monfalcone) climatological station in the Isonzo catchment.

Percentiles	DJF	MAM	JJA	SON	Year
1%	14,9	36,9	20,6	50,7	43,7
2%	32,5	47,5	30,1	60,9	49,6
5%	44,5	55,7	49,1	69,3	56,3
10%	52,8	64,5	65,5	87,1	63,9
90%	192,9	173,7	193,5	258,7	105,7
95%	198,8	183,2	204,6	332,1	110,1
98%	232,9	214,6	231,7	392,4	120,4
99%	268,6	241,3	277,1	422,8	129,9

Table 14: The percentiles calculated for seasonal and annual mean rainfall empirical distribution for the reference time period 1919-2011 for the analyzed Alberoni (Monfalcone) climatological station in the Isonzo catchment.

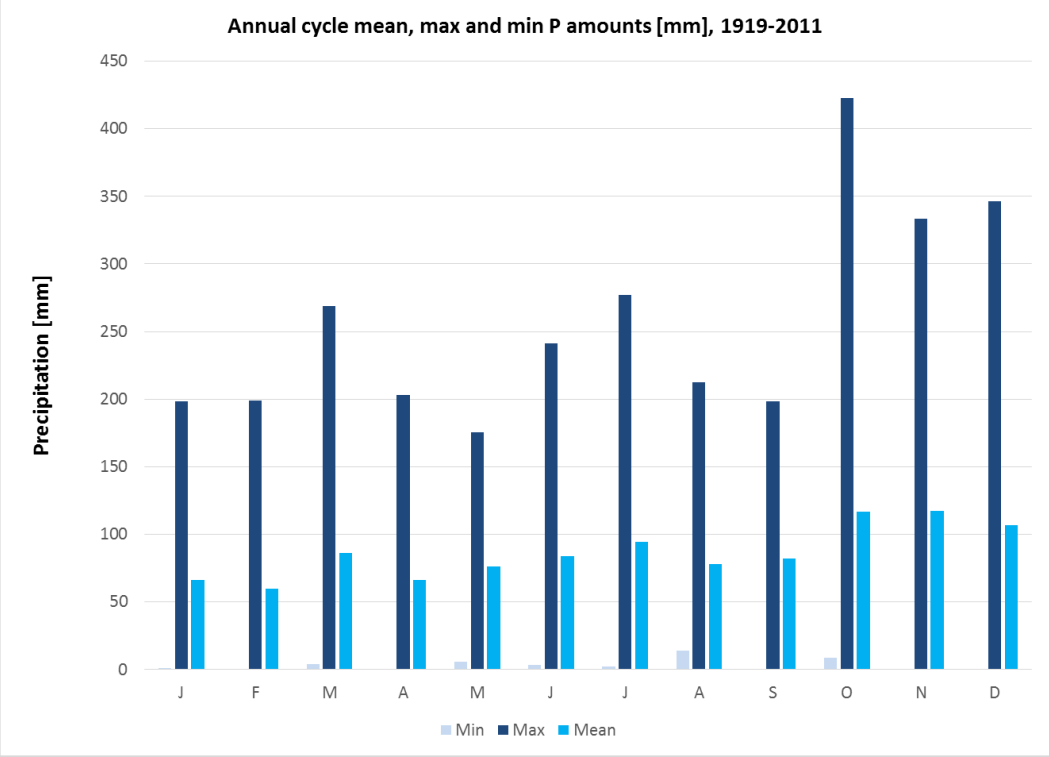

Figure 258: Annual cycle, min, max and mean annual precipitation amounts in mm calculated for the selected time period 1919-2011 for the Alberoni (Monfalcone) station.

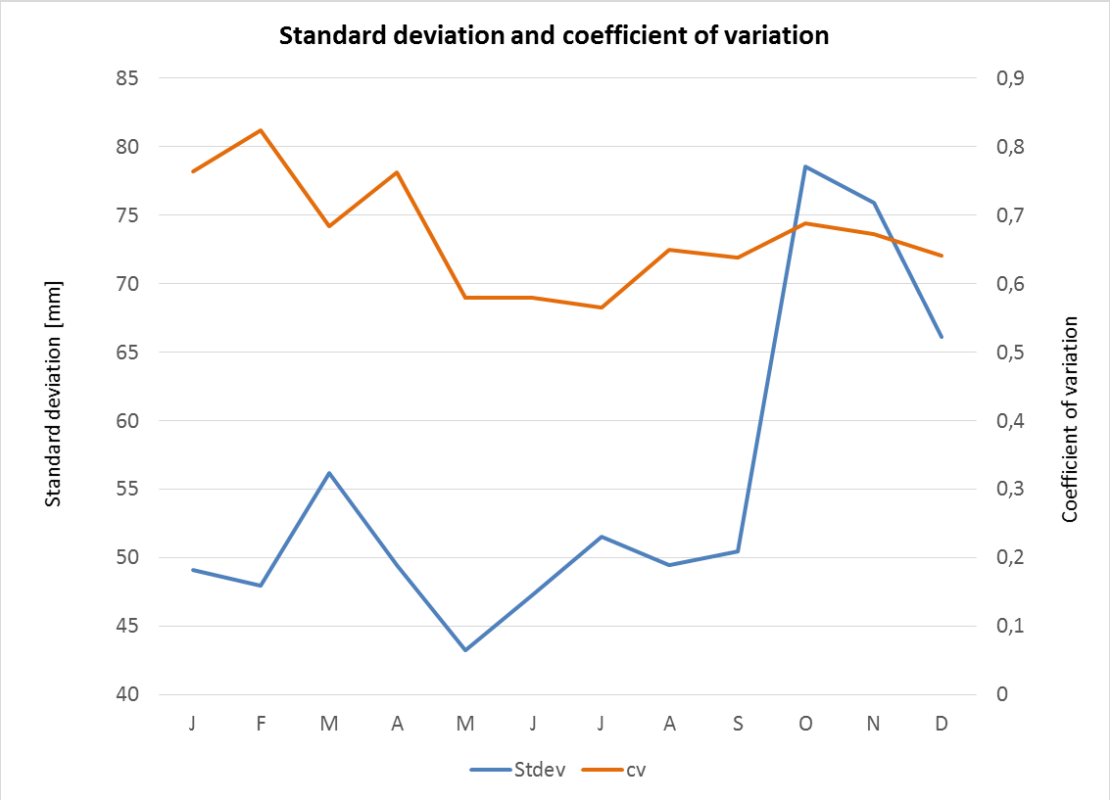

Figure 269: Standard deviation calculated on the annual cycle for the Alberoni (Monfalcone) station.

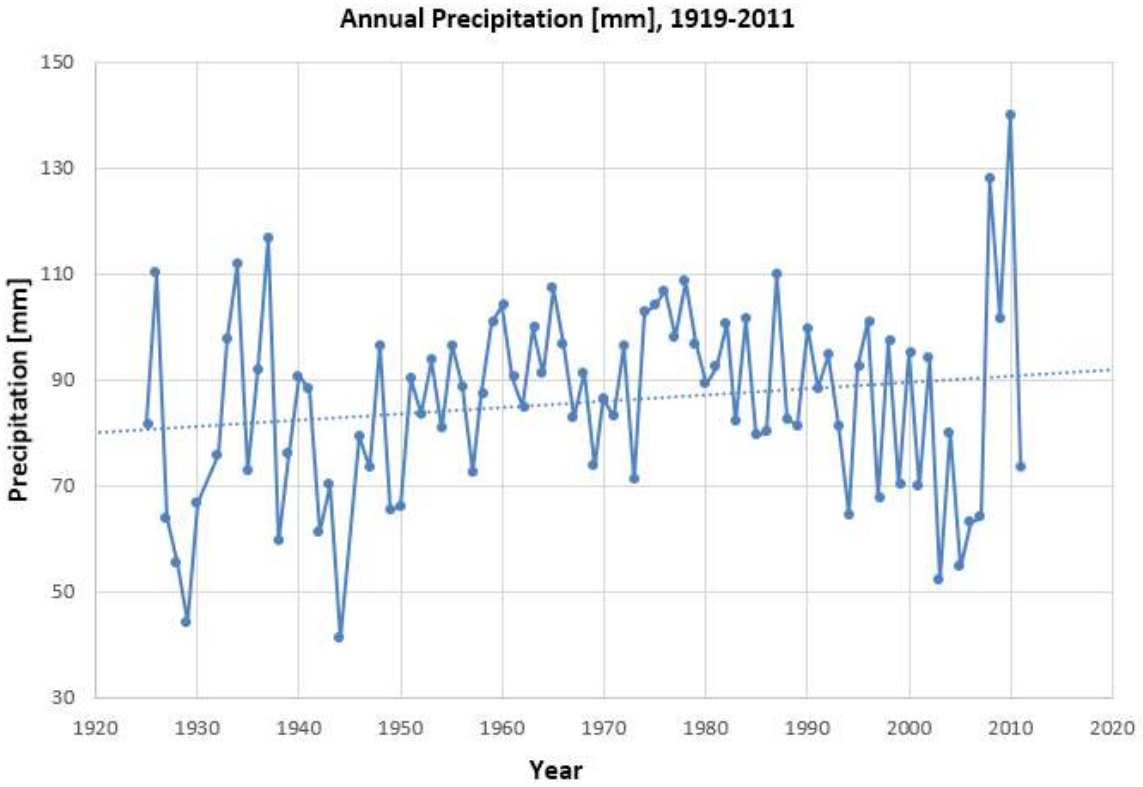

Figure 30: Time series of mean annual precipitations with the fitted trend for the period 1919-2011 for the meteorological station of Alberoni (Monfalcone). Trend= 1,4 mm/10y; R(1925-2011)=1014,3 mm.

In the pilot area, the average annual rainfall is calculated for the period of 1961-1990 for the Gorizia CPBI station, for the period 1951-2011 for Torviscosa station and for the period 1919-2011 for Alberoni station.
At Gorizia, seasonality, the highest precipitation amount usually occur during autumn with maximum recorded values of 430 mm and min values of 0 mm. This generate a high variability and a std of 50.5. DJF, MAM and JJA have very similar values: the maximum ranges between 255 and 286 mm and the min values are between 1 and 12 mm.
Also at Torviscosa the highest precipitations are recorded in autumn with average values of 118.9 mm and maximum values up to 317 mm. Also the minimum precipitations recorded in autumn are higher (8.6 mm) than during the other periods.
The same trend is visible for the Alberoni station where the higher mean values belong to autumn with values of 112.8 mm. Here the max recorded values are of 422.8 mm and the min values are of 12 mm.

4.1 Precipitation trends

The trends in the study area have been calculated for the available periods 1925-2011 respectively using the Kendall's tau method (Sen, 1968).
Looking at the stations, the situation is completely different. There is no homogeneity in the behavior.

From Figure 22, related to **Gorizia station**, emerges that there is an increase in the minimum precipitations in the month of June, while on the maximum precipitations, September is leading. These values are anyway not so meaningful on the overall trend that indicates an almost constant behavior with no increasing or decreasing (0.5 and -0.5 are the mm/10y computed). In this case the total amount can be considered the same, but what is changing is the fluctuation and distribution within the months with the increasing, as previously noticed, in June and September and decreasing in January and April. If we look at the trimester SON, the decreasing trend over 10y is important. The calculated Trend is of 0,1mm/10y with a mean value of 1397,5 mm computed for the reference period 1961-1990 (R).

Figure 25 and 27 concern instead the situation recorded at **Torviscosa**. Here the general trend is negative, with a decreasing of the precipitations since 1950. The only positive time of the year is the autumn with estimated values of 6.8-5.7 mm/10y. March, April and August are the dryer months, while September and October are the rainier. The calculated Trend is of -1,2 mm/10y with a R value (1961-1990) of 1194,0 mm.

Different is the situation while analyzing the data recorded by **Alberoni station**. Figure 28 highlights a positive trend of the precipitations indicating an increasing value with very wet periods during October, November and December. Due to the inconsistency of the recorded min data, it is not always possible to define the min precipitation values that seems to show a very small amount in the winter times. The Trend is of 1,4 mm/10y with a R value (1961-1990) of 1108,23 mm.

mm/10y	DJF		MAM		JJA		SON		Year	
Gorizia prese CBPI (1961-1990)	0.3	-1.8	-2.5	-3.4	0.6	1.7	-11.6	-12.2	0.5	-0.5
Torviscosa (1970-2011)	-3.00	-0.3	-7.2	-8.3	-5.9	-6.4	6.8	5.7	-3.9	-2.9
Alberoni (1925-2011)	2.1	1.2	1.0	-0.1	0.7	0.4	4.1	3.4	1.2	1.2

Table 85: Decadal precipitation trends (mm/10y) for the analyzed stations of Gorizia prese CBPI, Torviscosa and Alberoni (Monfalcone). The analyzed periods are different according to the data availability. Foe each season two trend are given: the Sen's slope on the left and the linear regression on the right.

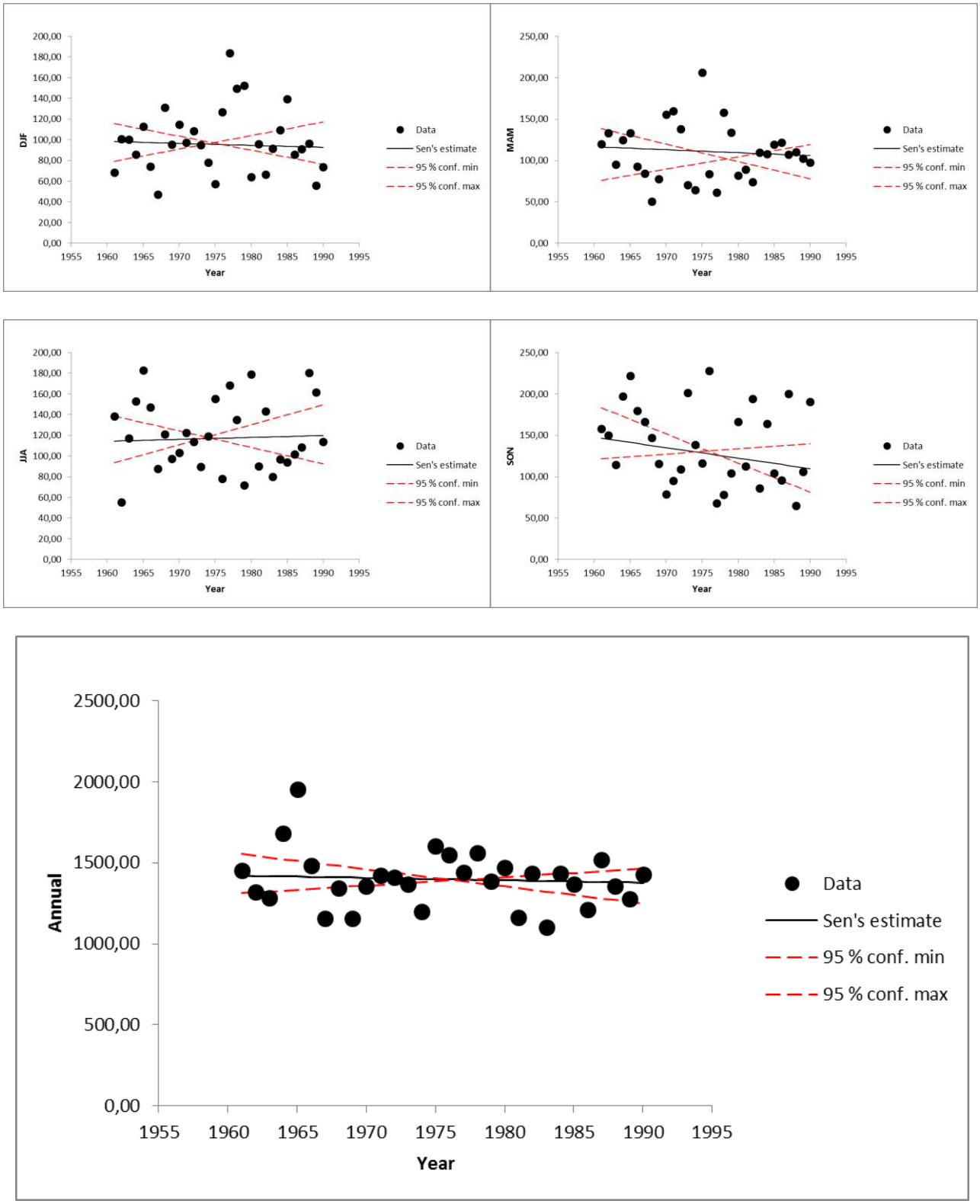

Figure 31: Mean month and annual precipitation trends for the time-reference period 1961-1990 for the ***Gorizia prese CBPI station****. The trend has been realized using the Sen's estimator and has been validated using the Mann-Kendall test. The time-series has been primarily subjected to a linear trend analysis (linear regression analysis) and later to the Sen's estimator and to the Mann-Kendall test.*

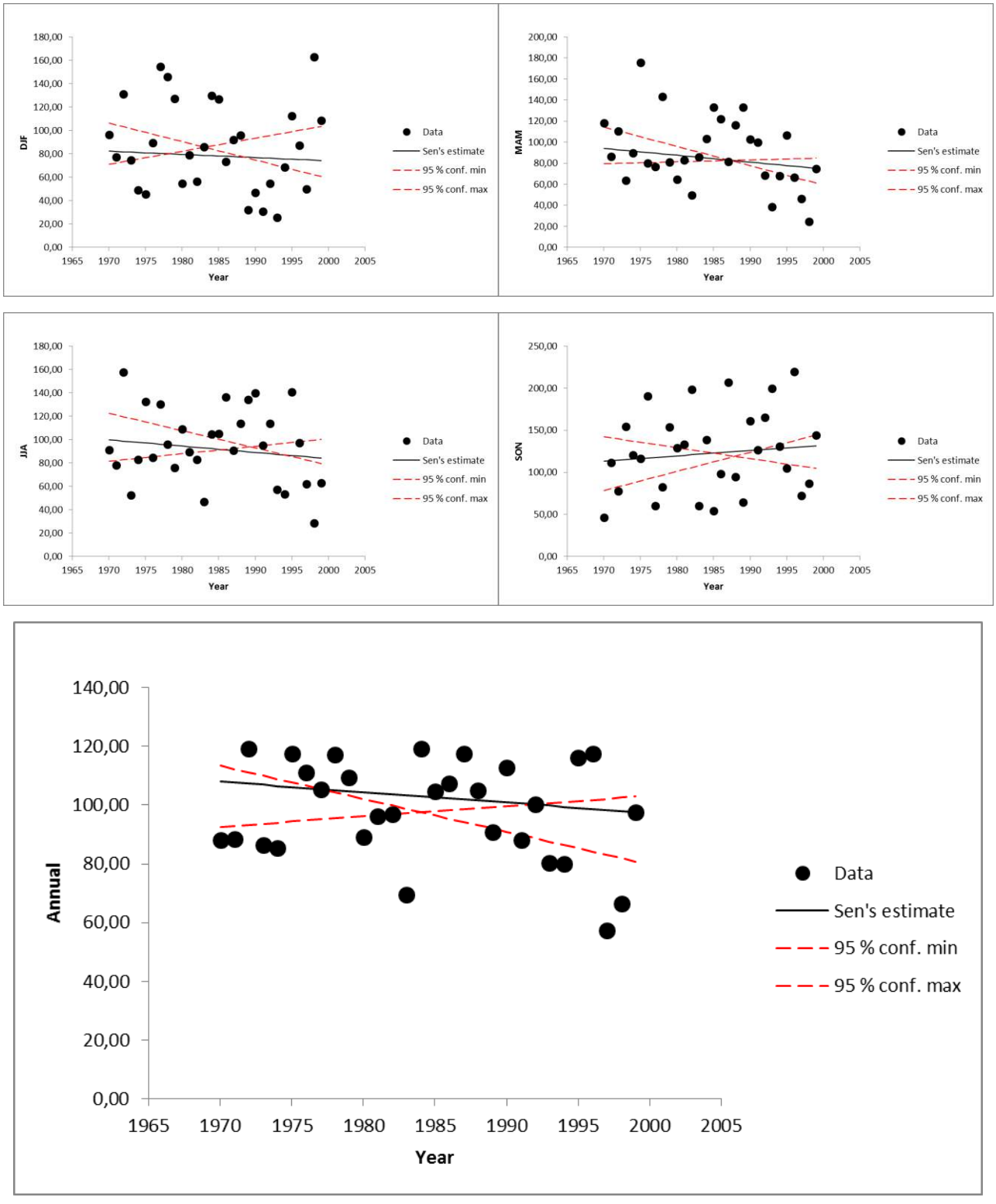

Figure 32: Mean month and annual precipitation trends for the time-reference period 1970-2011 for the ***Torviscosa station****. The trend has been realized using the Sen's estimator and has been validated using the Mann-Kendall test. The time-series has been primarily subjected to a linear trend analysis (linear regression analysis) and later to the Sen's estimator and to the Mann-Kendall test.*

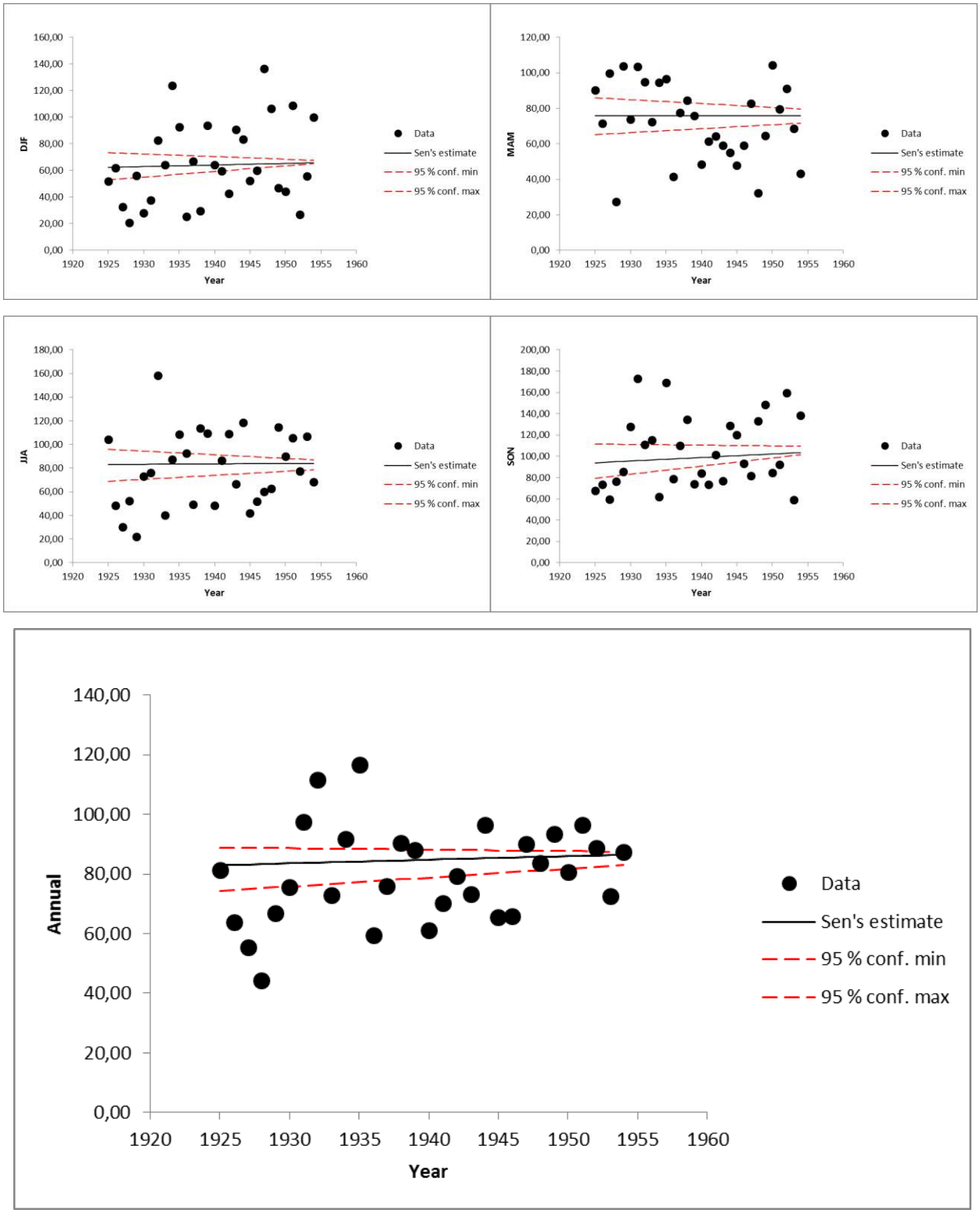

Figure 33: Mean month and annual precipitation trends for the time-reference period 1925-2011 for the ***Monfalcone station.*** *The trend has been realized using the Sen's estimator and has been validated using the Mann-Kendall test. The time-series has been primarily subjected to a linear trend analysis (linear regression analysis) and later to the Sen's estimator and to the Mann-Kendall test.*

5. REGIONAL CLIMATE MODEL SIMULATIONS

The regional climate models (RCMs) used are the Aladin (Bubnova et al. 1995), Promes (Castro et al. 1993) and RegCM3 models (Pal et al. 2007). The initial and boundary data for each RCM were provided from different global climate models (GCMs): the ECHAM5 GCM data were used to force RegCM3, Aladin was forced by the Arpege GCM and Promes was forced by the HadCM3Q GCM. For the present climate, models are compared with the local observations (Observations - obs). RCM corr is further adjusted model time series due to the differences between the CCmodels data and local observations.

5.1. Gorizia CBPI station, temperature

Data recorded by the Gorizia CBPI prese meteorological station initially refers to the reference period 1961-1990. For this period were evaluated, not only the observed data temperatures, but also the three RCM bias corrected models available thanks to the CCWATER project.

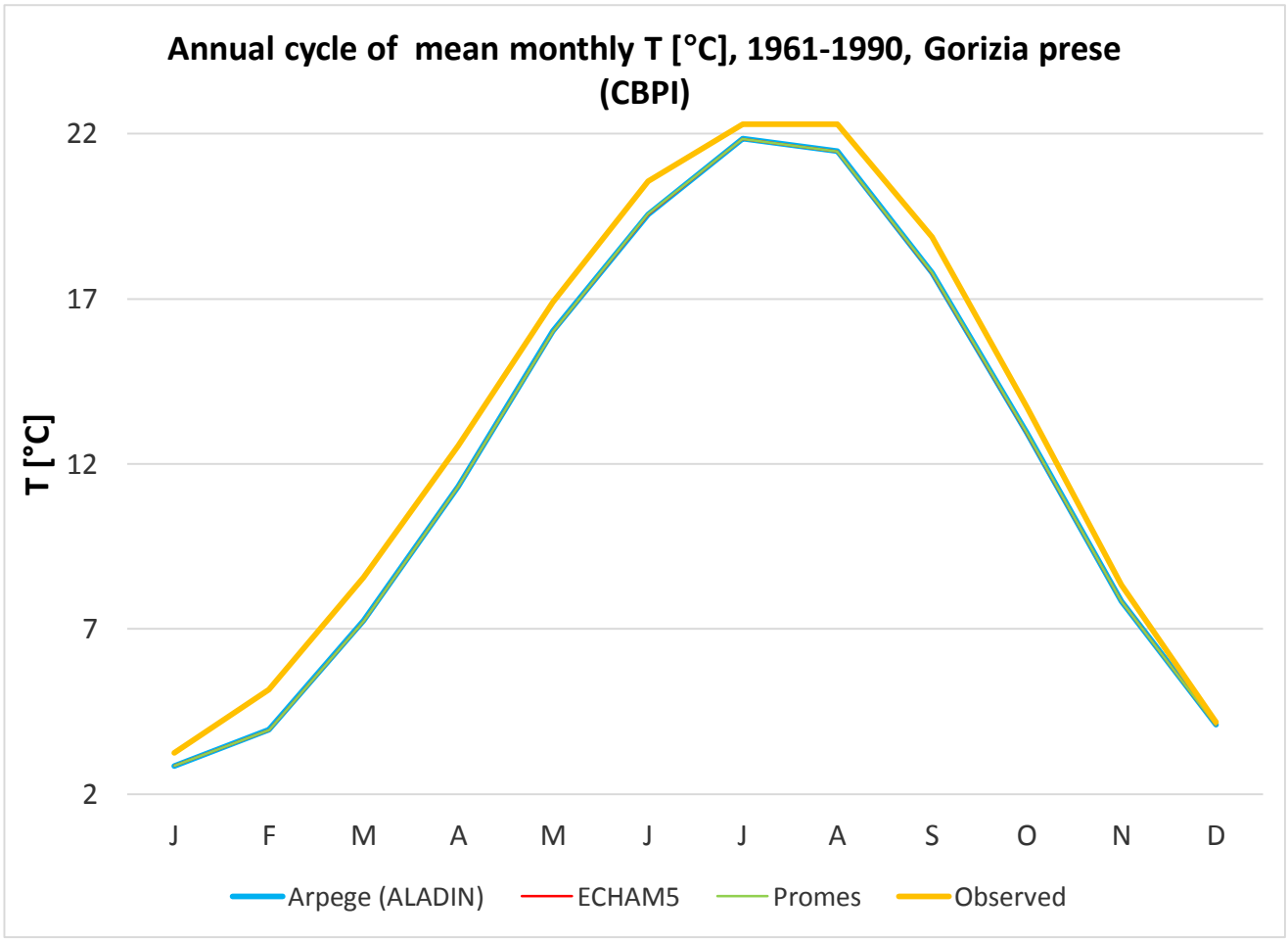

Figure 34: Gorizia prese CBPI, annual cycle of mean monthly temperature.

All the three models perfectly fits but the observed data instead are always higher than the models in a range that vary between 2 and 18%. The Standard deviation calculated on the monthly mean temperature for the annual cycle indicate a small variability in the three models, while it increase when considering the observed values (Figure 34).

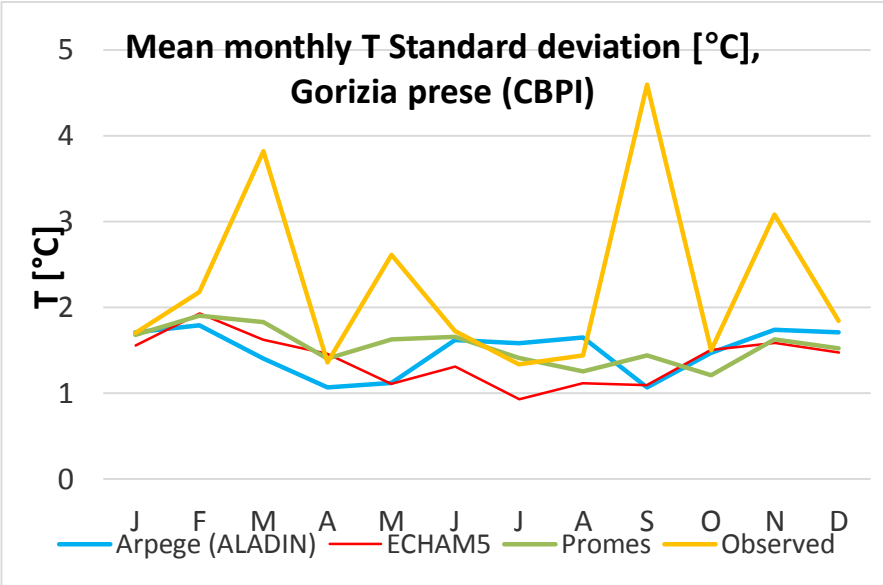

Figure 35: Gorizia prese CBPI, mean monthly temperature standard deviation on annual cycle.

Figure 35 represents the fluctuations of the mean annual temperatures within the studied time series from 1951 until 2000 for the observed data and the three models. What is noticeable is that if observed data and the models are initially partially fitting, with observed values always higher than the models, in the last years of analysis, there is a disagreement in the behavior with an increase in the observed temperature higher than in the models. Anyway all data are confirming a general positive trend in the temperatures reaching max values of 14,9°C (observed data).

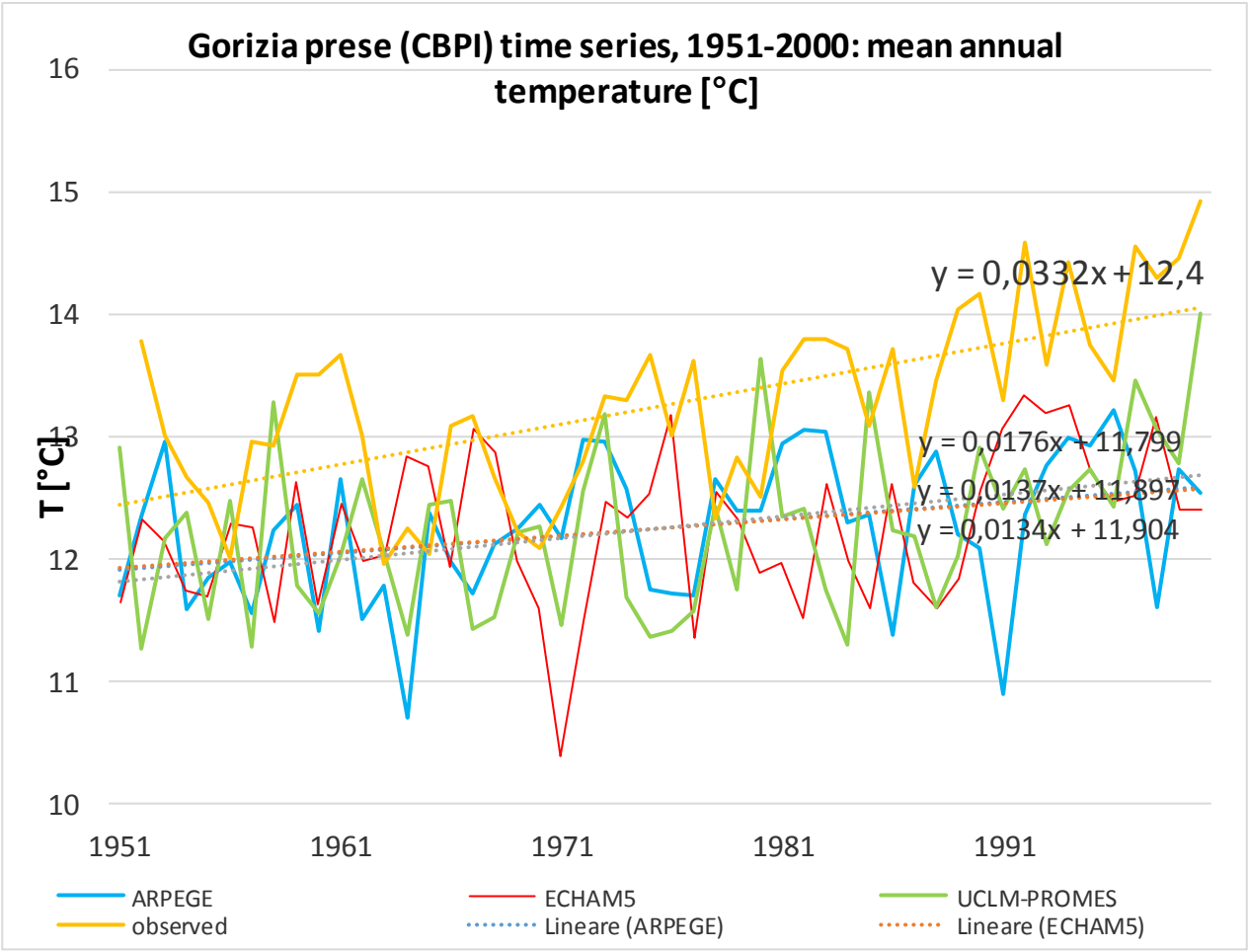

Figure 276: Gorizia prese (CBPI) meteorological station time series 1951-2000: mean annual temperature fluctuation.

Analyzing the data over a provisional trend, all the three models are admitting an increasing tendency. To define the future scenarios it is important to correct the model data on the observed ones. The following table shows the obtained mean monthly and corrected values.

	RCMs from CCWaters				Corrected values for RCMs		
	Arpege (ALADIN)	ECHAM5	Promes	Observed	Obs-Arpege	Obs-ECHam5	Obs-Promes
J	2,901978033	2,440913767	2,6930998	3,25	0,348021967	0,809086233	0,5569002
F	3,973709933	3,916943767	3,777733	5,166667	1,192956733	1,2497229	1,388933667
M	7,202677	7,168515333	7,010644333	8,566667	1,363989667	1,398151333	1,556022333
A	11,29706433	11,315011	11,36005767	12,55	1,252935667	1,234989	1,189942333
M	16,01011667	16,02698	15,89905	16,9	0,889883333	0,87302	1,00095
J	19,67023	19,48611	19,33954667	20,56667	0,896436667	1,080556667	1,22712
J	21,68917667	21,81457	21,54771667	22,3	0,610823333	0,48543	0,752283333
A	21,50426667	21,28164	21,13251	22,3	0,795733333	1,01836	1,16749
S	17,86528333	17,87079333	17,71686	18,86667	1,001383333	0,995873333	1,149806667
O	12,97032333	12,57168567	12,97682333	13,73333	0,76301	1,161647667	0,75651
N	7,791076667	7,778757333	7,849403	8,333333	0,542256667	0,554576	0,483930333
D	4,1693441	3,937504833	4,118967567	4,183333	0,013989233	0,2458285	0,064365767

Table 16: corrections realized on the RCMs models.

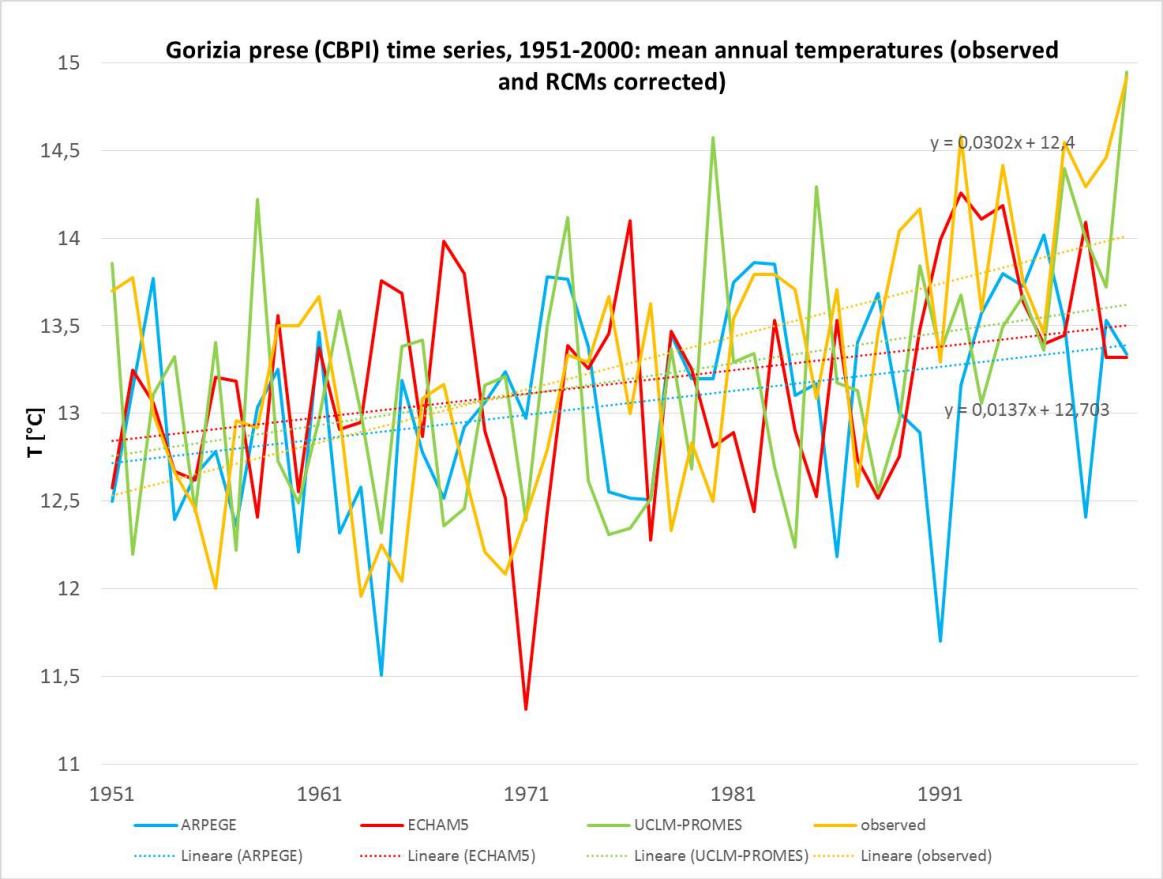

Figure 287: Gorizia prese (CBPI) meteorological station time series 1951-2000: mean annual temperature fluctuation. RCMs corrected, according to the table 16 and observed data.

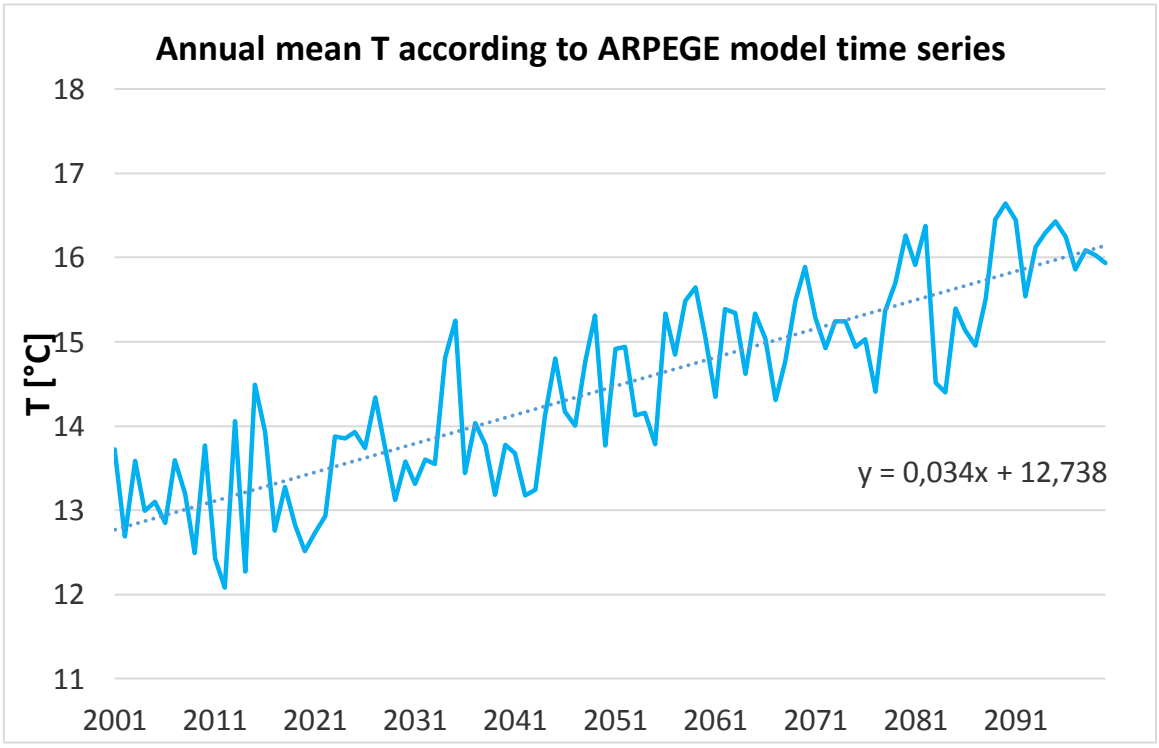

Figure 298: Annual mean temperature and the relative fitted linear trend of Gorizia prese (CBPI) according CNRM-RM5.1 (or ALADIN) forced by ARPEGE.

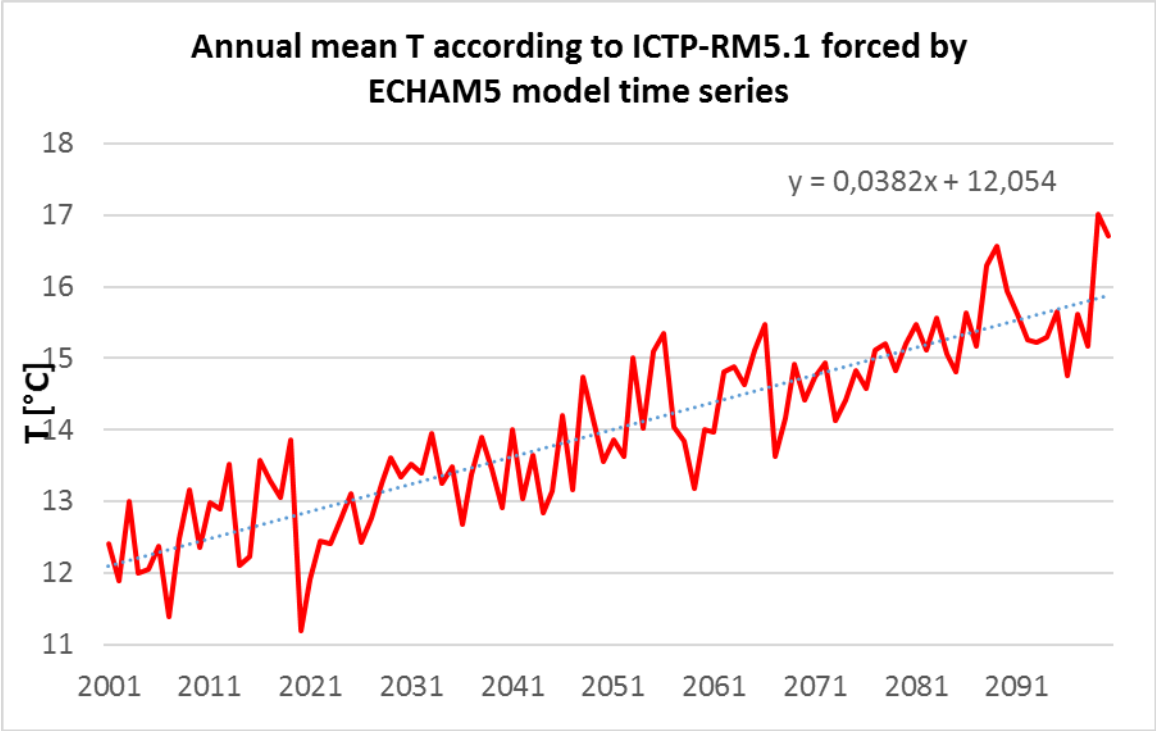

Figure 309: Annual mean temperature and the relative fitted linear trend of Gorizia prese (CBPI) according ICTP-REGCM forced by ECHAM5.

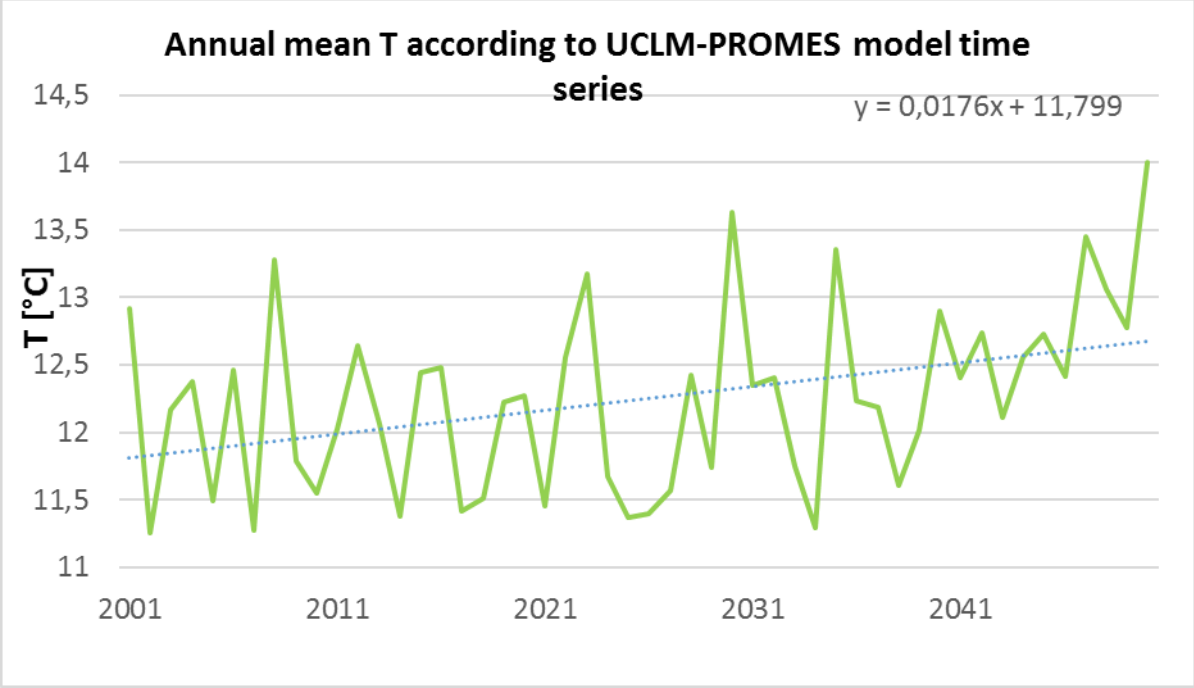

Figure 40: Annual mean temperature and the relative fitted linear trend of Gorizia prese (CBPI) according UCLM-PROMES forced by HadCM3Q0.

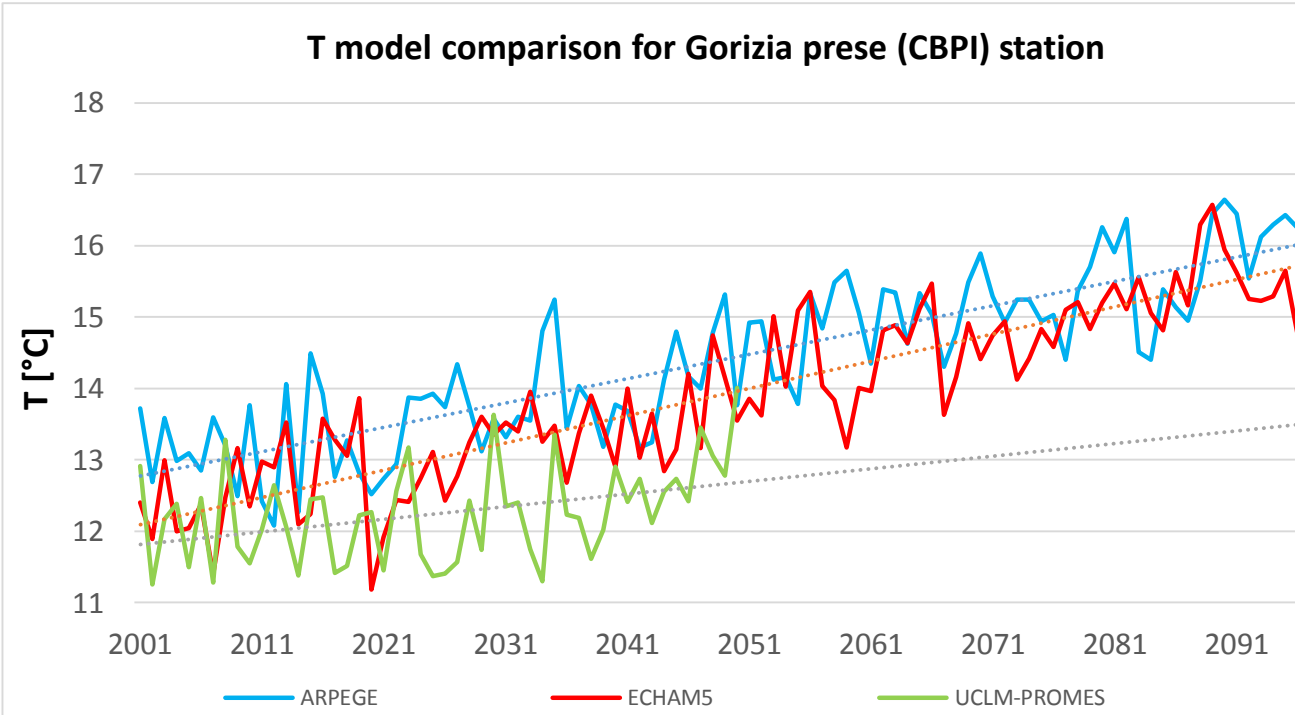

Figure 41: Annual mean temperature and the relative fitted linear trend of Gorizia prese (CBPI) comparison between the three available models: CNRM-RM5.1 (or ALADIN) forced by ARPEGE, ICTP-REGCM forced by ECHAM5 and UCLM-PROMES forced by HadCM3Q0.

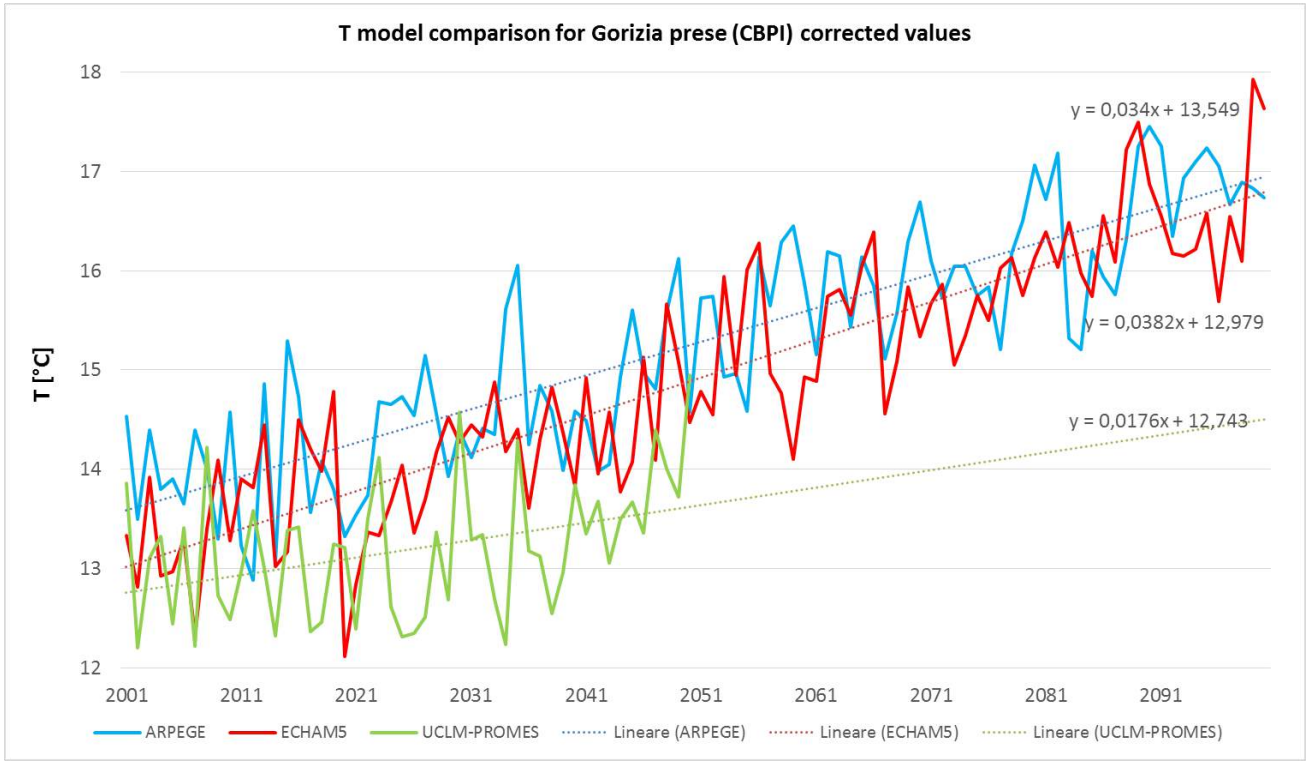

Figure 42: Annual mean temperature and the relative fitted linear trend of Gorizia prese (CBPI) comparison between the three available models. All the three models are showing a huge increase of about 3,5°C. With respect to the previous figure, the models have been corrected. All the three models are showing a huge increase of about 0.34°C/10y (ARPEGE), 0.38°C/10y (ECHAM5) and 0.17°C/10y (Promes) respectively.

5.3 Gorizia CBPI station, precipitation

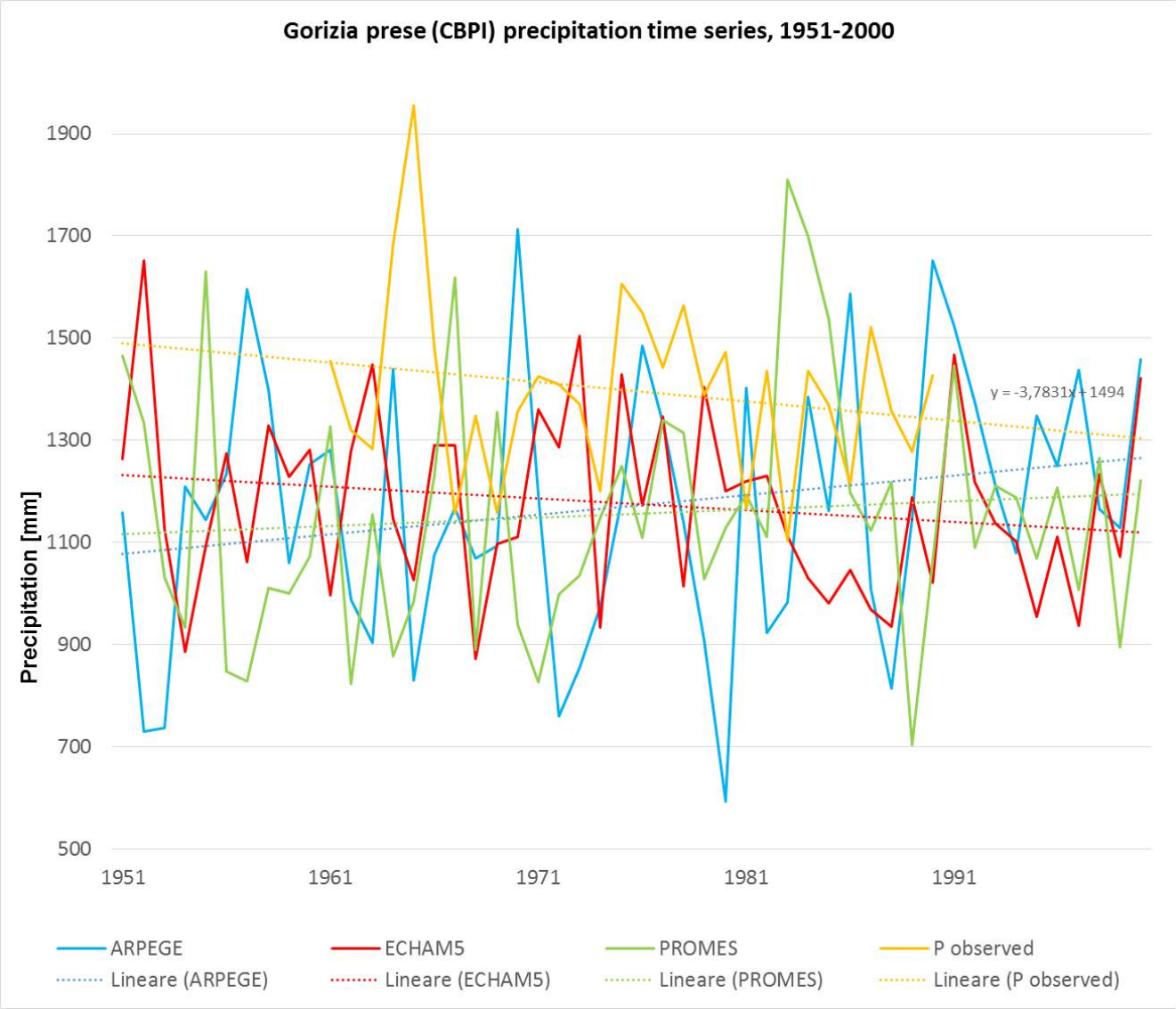

Figure 43: Gorizia prese (CBPI) station time series 1951-2000, annual precipitation amount.

For Gorizia prese (CBPI) station, the available observed precipitation time series were firstly analyzed and later compared with the three model time series CNRM-RM5.1 (or ALADIN) forced by ARPEGE, ICTP-REGCM forced by ECHAM5 and UCLM-PROMES forced by HadCM3Q0 for the period 1951-2000. Figure 43 is showing the obtained results. The observed precipitation dataset has a decreasing constant behavior while the three models are not in agreement one with the other highlighting a slight decrease (ECHAM5) or increase(ARPEGE and PROMES) in the total annual cycle precipitation amount. On average, the models underestimate the total annual amount of rainfall of a value of about 200 mm. For this reason, a correction has been applied according to the corrected values available in the table 17.

	RCMs from CC Waters				Corrected values for RCMS		
	ARPEGE	ECHAM5	PROMES	obs	obs/ARPEGE	Obs/ECHAM5	Obs/PROMES
J	97,01448	97,44499	96,24516	102,9667	1,061353567	1,056664535	1,069837333
F	97,01209	97,70815	96,22309	83,76667	0,86344497	0,857315047	0,870546422
M	96,98866	97,77725	96,35789	96,83333	0,998132765	0,990346259	1,004934091
A	97,02299	97,76655	96,04194	112,4667	1,159277091	1,150359327	1,171016245
M	97,27523	97,482	95,96689	117,2667	1,20875424	1,202957085	1,221949184
J	97,4862	97,49015	95,92564	137,1667	1,413878254	1,406979707	1,429927092
J	97,57049	97,51341	95,88523	98,36667	1,013937965	1,00875012	1,025879246
A	97,65182	97,52903	95,78404	125,2333	1,290872564	1,284062093	1,307455108
S	97,7701	97,55671	95,80934	135,5667	1,397385871	1,389619144	1,414962985
O	97,54701	97,48404	95,66214	134,2333	1,383642218	1,376977527	1,403202295
N	97,82065	97,65212	95,70068	145,5667	1,500463265	1,490665674	1,521062003
D	97,86102	97,83345	95,68879	108,2333	1,115640994	1,106301957	1,13109726

Table 17: Mean monthly and corrected values (quotients here are considered) are here presented for the Gorizia prese (CBPI) station.

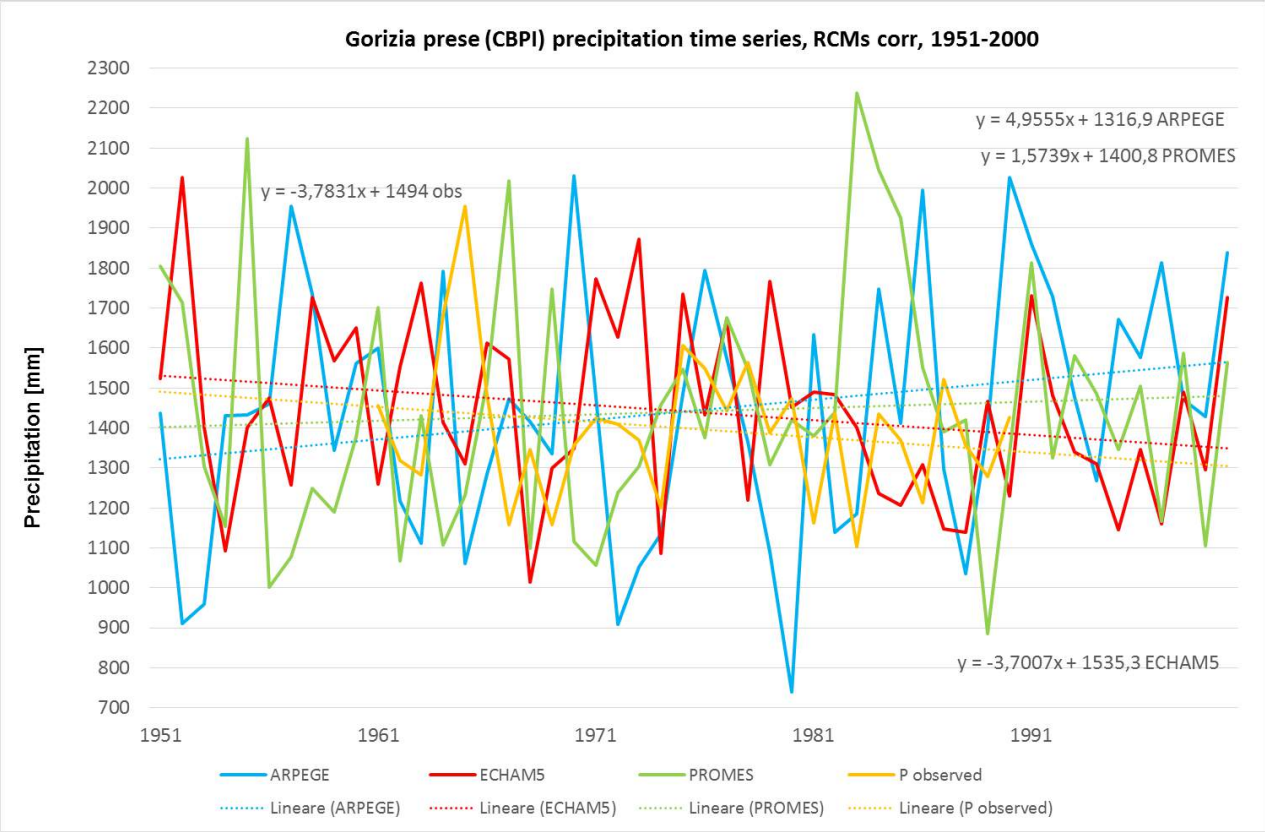

Figure 44: Gorizia prese (CBPI) station time series 1951-2000, annual precipitation amount corrected. The trend for the ARPEGE values is of 25 mm/10y, for PROMES is of 9 mm/10y. The trend is instead decreasing for ECHAM5 with values of -19 mm/10y as for the observed values: -20 mm/10y.

If we have a look at the future projection (Figure 45), using the three model time series CNRM-RM5.1 (or ALADIN) forced by ARPEGE, ICTP-REGCM forced by ECHAM5 and UCLM-PROMES forced by HadCM3Q0 for the period 2001-2100, one realize that, all the models evidence

a slight decrease in the annual precipitation amount passing from value of 1300 mm to values of 1100, with a decreasing of approximately 2 mm/1y.

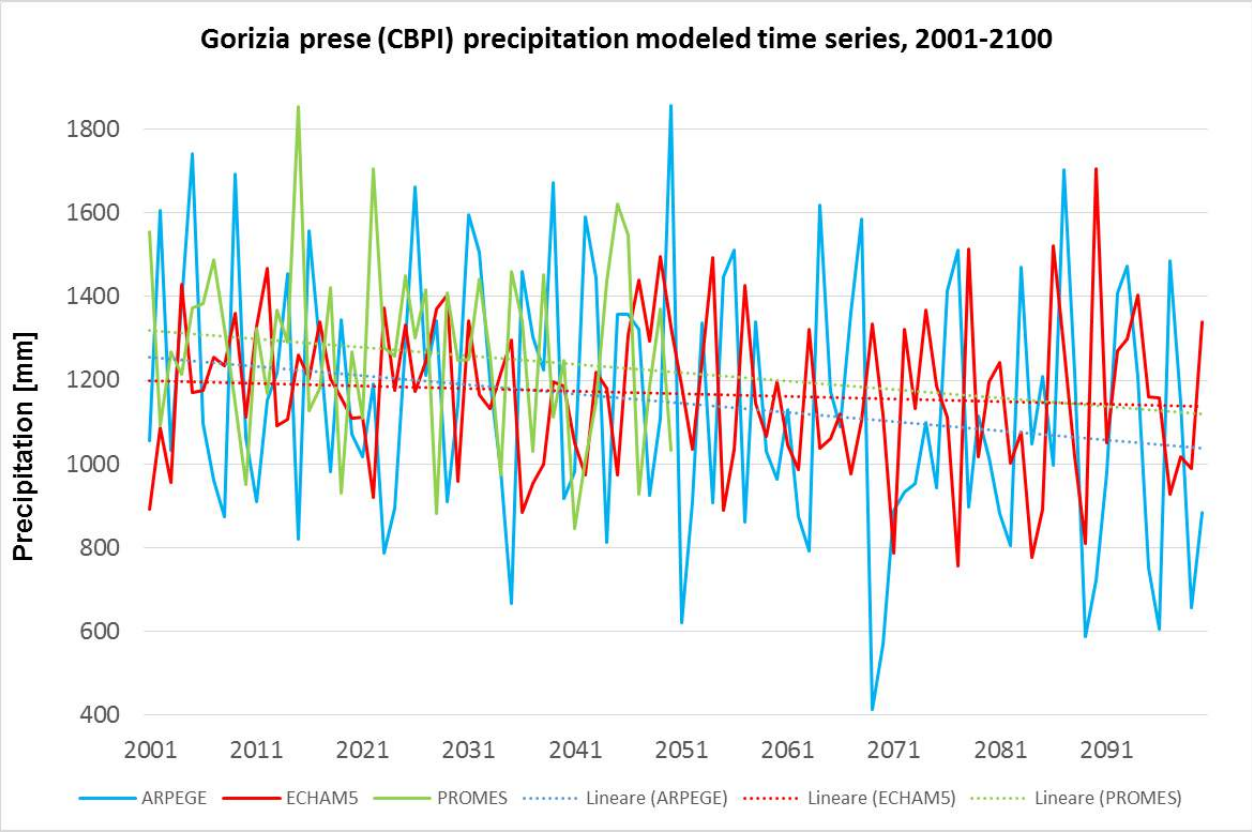

Figure 45: Model comparison for the Gorizia prese (CBPI) station in the period between 2001-2100.

Applying the corrections to the future scenarios, it emerges that there is a difference between the 50years scenarios and the 100years. This can be seen in figure 46, where, for the Gorizia prese CBPI station, it emerges that there is a clear decreasing trend in the precipitation amount.

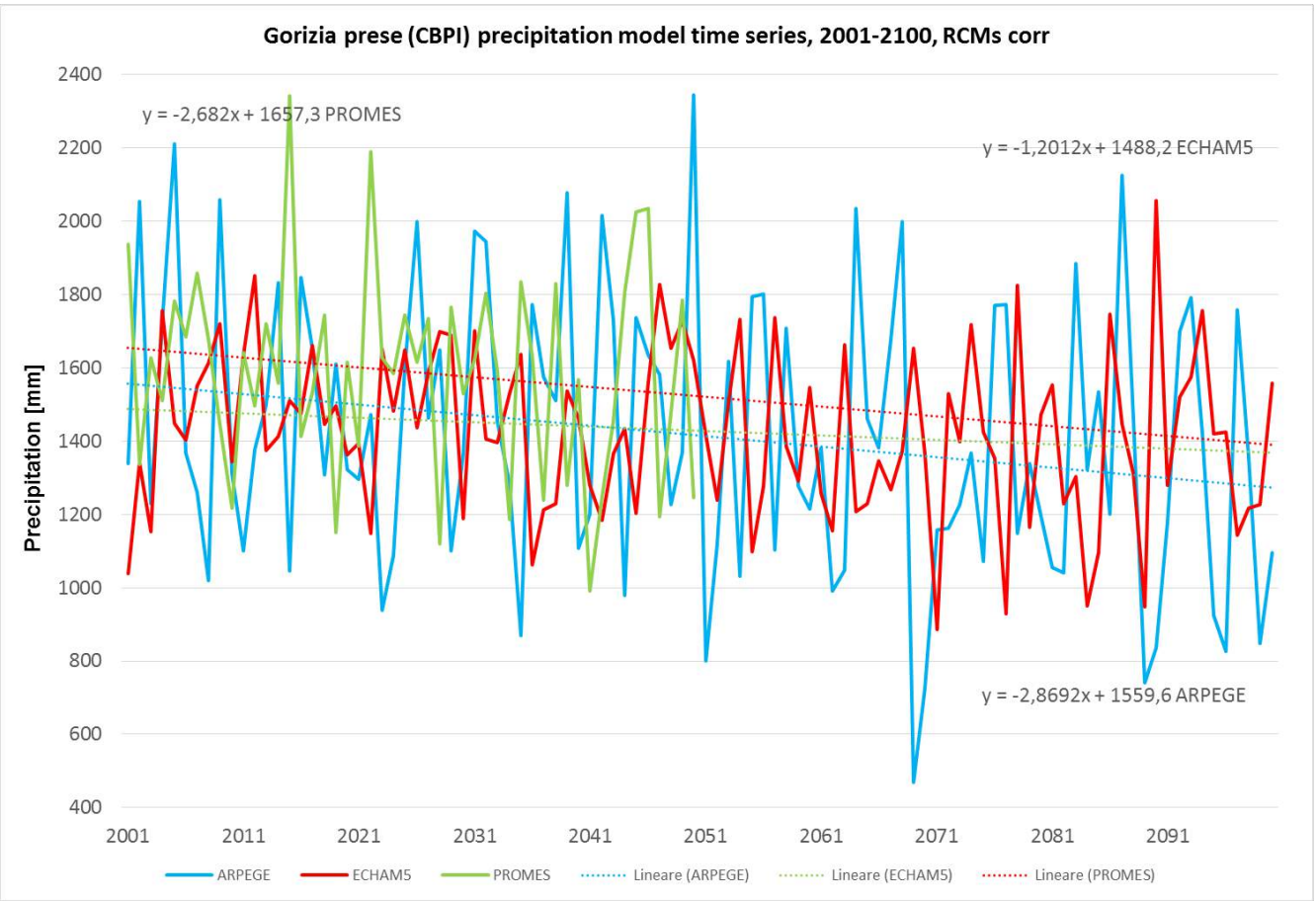

Figure 46: Gorizia prese (CBPI) station time series 2001-2100, annual precipitation amount corrected. The trend for the ARPEGE values is of -28 mm/10y, for PROMES is of -12 mm/10y and for ECHAM5 is of -26 mm/10y. All the three models are indicating a decreasing trend.

Gorizia prese CBPI	ARPEGE	PROMES	ECHAM5	Observed
Temperature [°C/10y] 50y	0.18	0,19	0,14	0,28
Temperature [°C/10y] 100y	0,34	0,17	0,38	
P (50y) [mm/10y]	25	9	-19	-20
P (100y) [mm/10y]	-28	-12	-26	

Table 18: Summary of the results calculated for the Gorizia prese CBPI station.

5.3 Torviscosa station, temperature

Data time series for Torviscosa station were analyzed for two different period: the first one considering the data from 1951 until 2000 and comparing the observed time serie with the three different model available after the end of the CC Water Project; the second one is between 2001 and 2100 proposing a prediction witinn the following 90 yeasrs of the temperature changes. Observed data time series show an increase from a minimum of 10°C reaching vlues of 18°C. In this time period the models are more cautelative, showing a very slight increase of less than 1°C. The situation is different and more worrying for the future where the comparison among the three models highlight, for this station, a very large temperature increase (Figure 50).

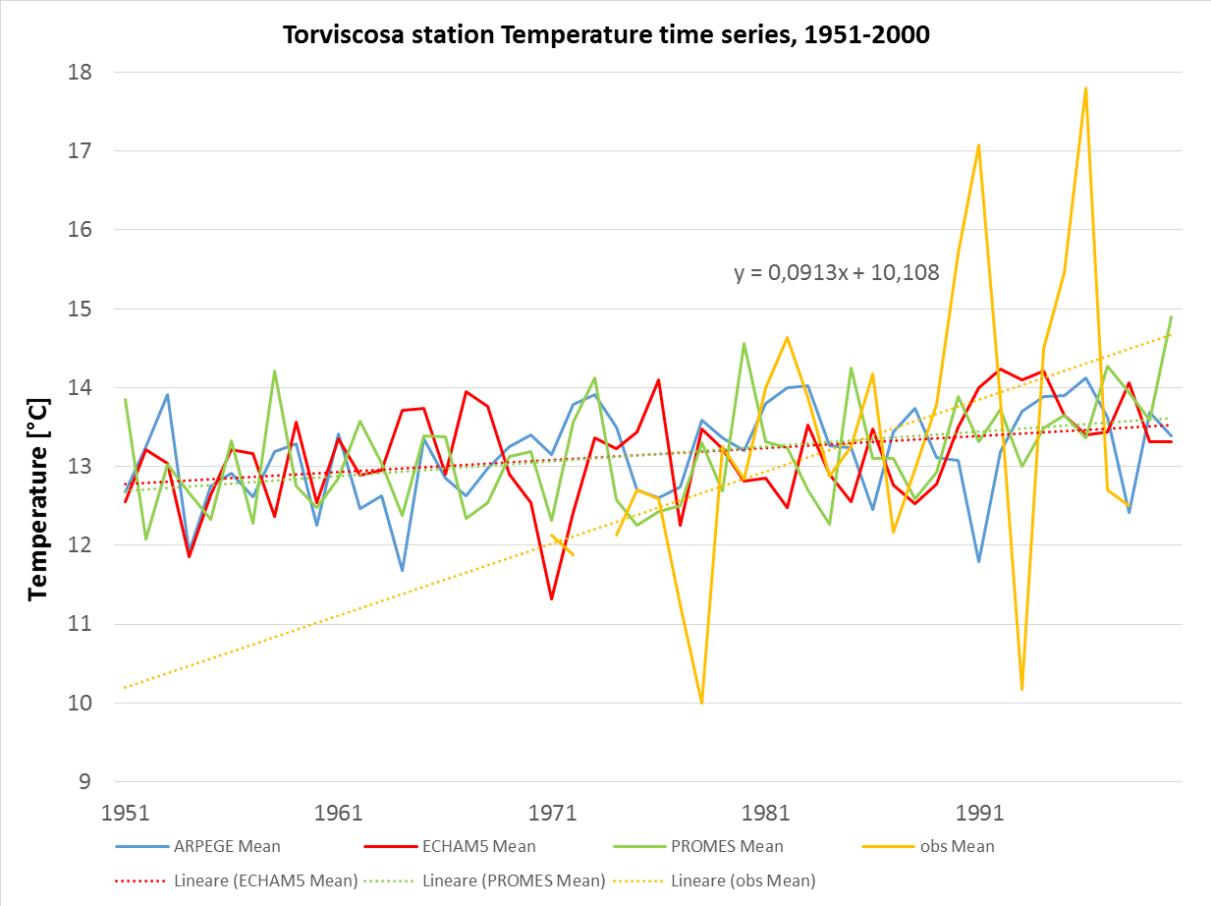

Figure 31: Torviscosa station time series 1951-2000, mean annual temperature.

	RCMs from CCWaters				Corrected values for RCMs		
	Arpege (ALADIN)	ECHAM5	Promes	Observed	Obs-Arpege	Obs-ECHam5	Obs-Promes
J	3,534922806	3,529735	3,533207	3,679412	0,144488959	0,149676345	0,146204565
F	4,78789668	4,787722	4,789627	5,575	0,78710332	0,78727848	0,785372734
M	8,2183978	8,220676	8,217436	4,941176	-3,277221329	-3,27949993	-3,276259129
A	12,295502	12,29779	12,29875	13,08939	0,793891939	0,791600539	0,790643339
M	17,006524	16,9998	17,00029	18,07059	1,064064235	1,070788235	1,070302235
J	20,592966	20,59153	20,59143	20,78429	0,191319714	0,192755714	0,192851714
J	22,867446	22,86714	22,86441	22,75	-0,117446	-0,11714	-0,114412
A	22,531144	22,53093	22,52962	22,90143	0,370284571	0,370500571	0,371808571
S	18,90854	18,90285	18,90915	19,03286	0,124317143	0,130005143	0,123707143
O	13,950304	13,95249	13,95493	14,03194	0,081640444	0,079452444	0,077014444
N	8,6239312	8,622536	8,617613	8,748571	0,124640229	0,126035629	0,130958629
D	4,70607658	4,703967	4,70516	4,912857	0,206780563	0,208889743	0,207696943

Table 19: corrections realized on the RCMs models for Torviscosa stations.

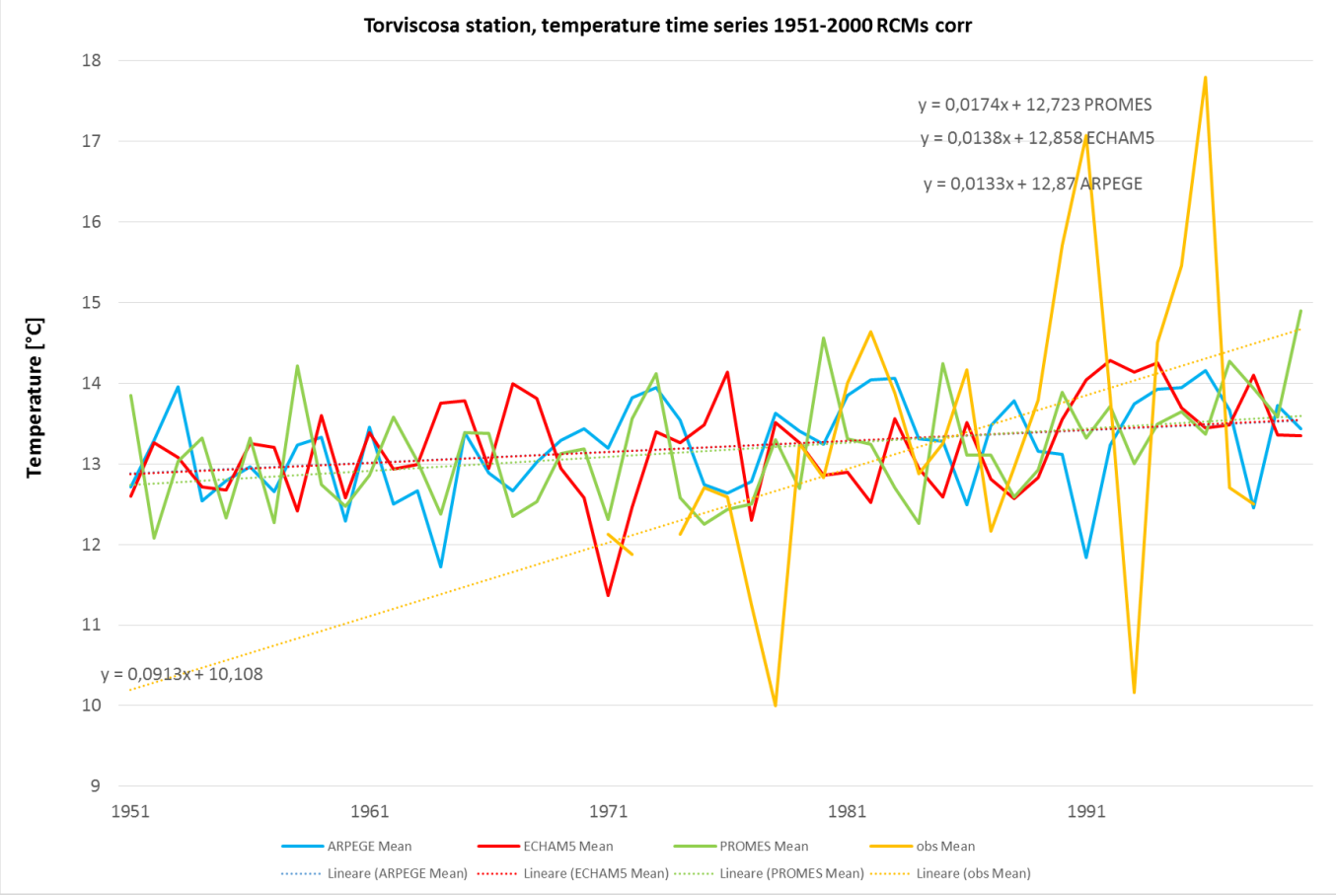

Figure 48: Torviscosa station time series 1951-2000, annual precipitation amount corrected. The temperature value is slighting increasing with a trend for the ARPEGE model of 0.06°C/10y, for PROMES of 0.11°C/10y, for ECHAM5 with values of 0.06°C/10y. For the observed data, the increasing trend has a value of 0.9 °C/10y.

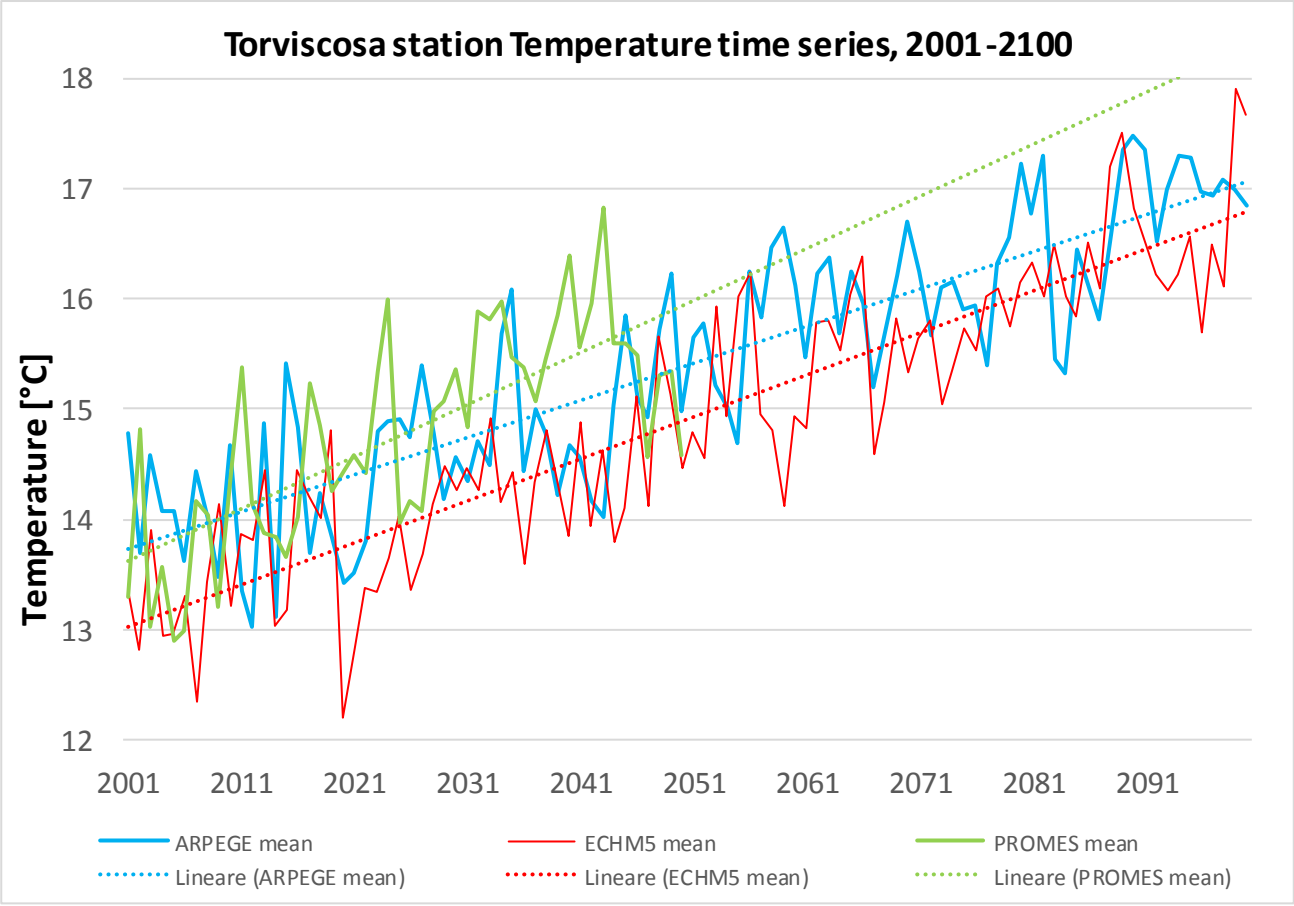

Figure 49: Temperature model comparison for the Torviscosa station in the period between 2001-2100.

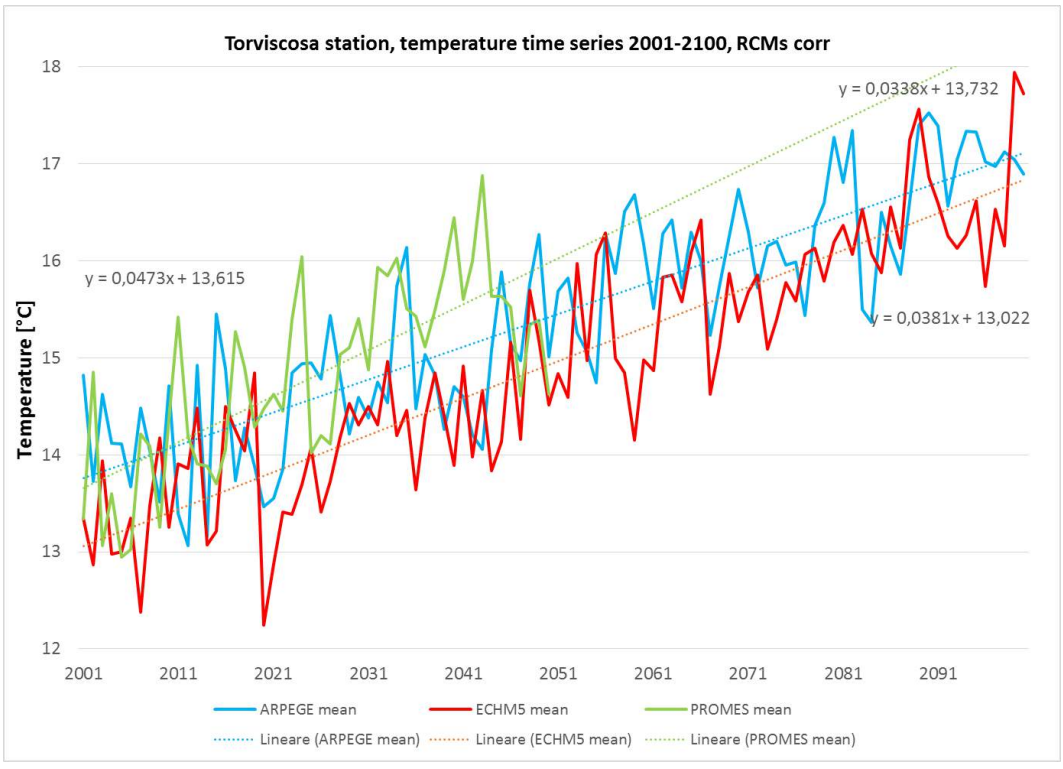

Figure 50: Torviscosa station time series 2001-2100, annual precipitation amount corrected. The temperature value is slighting increasing with a trend for the ARPEGE model of 0.3°C/10y, for PROMES of 0.5°C/10y, for ECHAM5 with values of 0.4°C/10y.

5.4 Torviscosa station, precipitation

For Torviscosa station, the available observed precipitation time series were firstly analyzed and later compared with the three model time series CNRM-RM5.1 (or ALADIN) forced by ARPEGE, ICTP-REGCM forced by ECHAM5 and UCLM-PROMES forced by HadCM3Q0 for the period 1951-2000. Figure 51 is showing the obtained results. The observed precipitation dataset has a linear decreasing behavior while the three models are not in agreement one with the other highlighting a slight decrease (ECHAM5) or increase (ARPEGE and PROMES) in the total annual cycle precipitation amount, as for the Gorizia prese (CBPI) station. On average the models underestimate the total annual amount of rainfall of a value of 200 mm (1100-1300 mm). If we have a look at the future projection (Figure 54), using the three model time series CNRM-RM5.1 (or ALADIN) forced by ARPEGE, ICTP-REGCM forced by ECHAM5 and UCLM-PROMES forced by HadCM3Q0 for the period 2001-2100, it is possible to realize that, all the models evidence a slight decrease in the annual precipitation amount passing from value of 1300 mm to values of 1100, with a decreasing of 2 mm/1y.

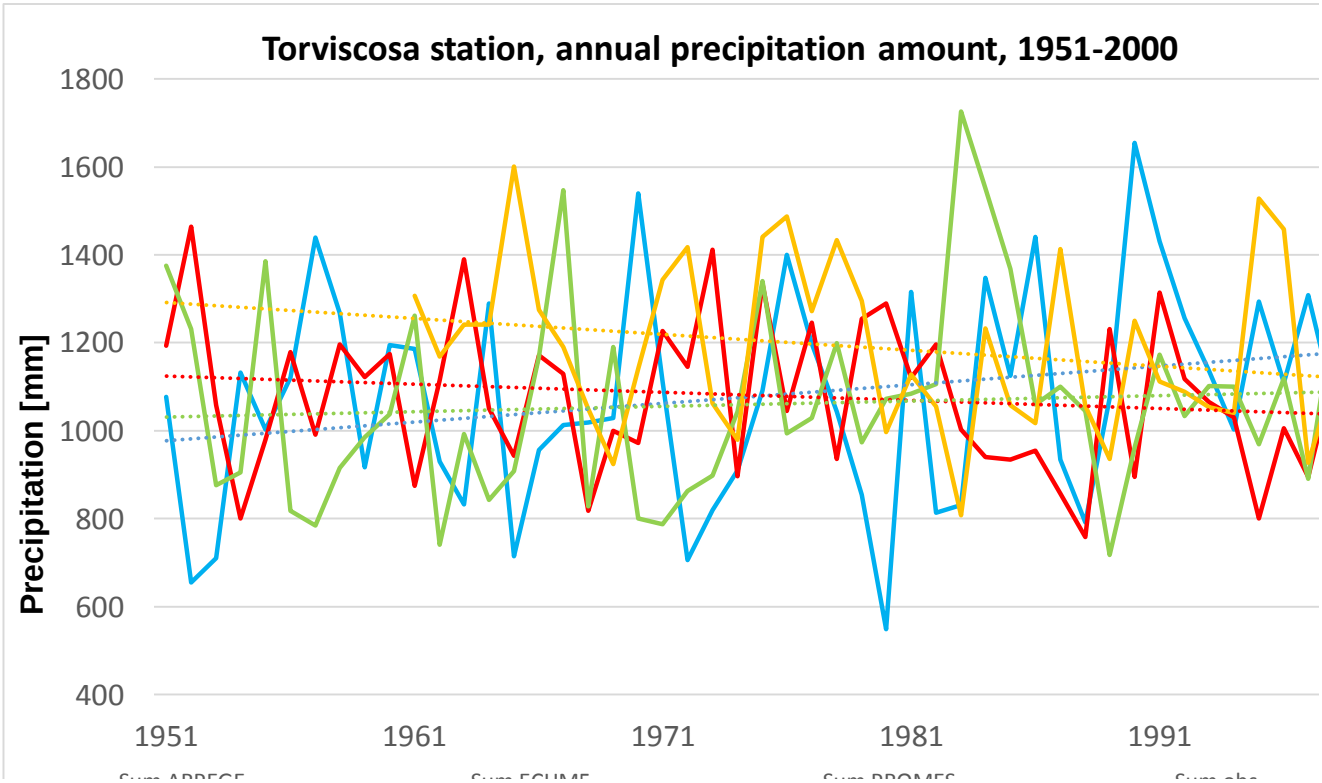

Figure 51: Torviscosa station time series 1951-2000, annual precipitation amount.

	RCMs from CC Waters				Corrected values for RCMS		
	ARPEGE	ECHAM5	PROMES	obs	bs/ARPEG	bs/ECHAM	Obs/PROMES
J	89,57404	89,5798	88,49253	80,87073	0,902837	0,902779	0,913870718
F	89,56903	89,80866	88,46401	73,54634	0,821068	0,818923	0,831370228
M	89,57492	89,86791	88,5674	84,37561	0,941965	0,938885	0,952671158
A	89,60705	89,83905	88,2438	87,17073	0,97317	0,970299	0,987839697
M	89,84598	89,54635	88,09949	96,27381	1,074796	1,075128	1,092785086
J	90,09467	89,54856	88,10136	106,3381	1,187153	1,187491	1,206997229
J	90,10772	89,57301	88,02733	76,3119	0,851942	0,851952	0,866911457
A	90,17997	89,56723	87,99728	98,06905	1,094838	1,094921	1,114455398
S	90,2983	89,56401	87,98947	120,5214	1,345495	1,345646	1,369725531
O	90,06121	89,41511	87,81868	122,0976	1,363092	1,365514	1,390337739
N	90,31837	89,53582	87,8163	113,1071	1,262722	1,263261	1,287997153
D	90,35876	89,72683	87,79559	100,0238	1,116661	1,114759	1,139280622

Table 20: Mean monthly and corrected values (quotients here are considered) are here presented for the Torviscosa station.

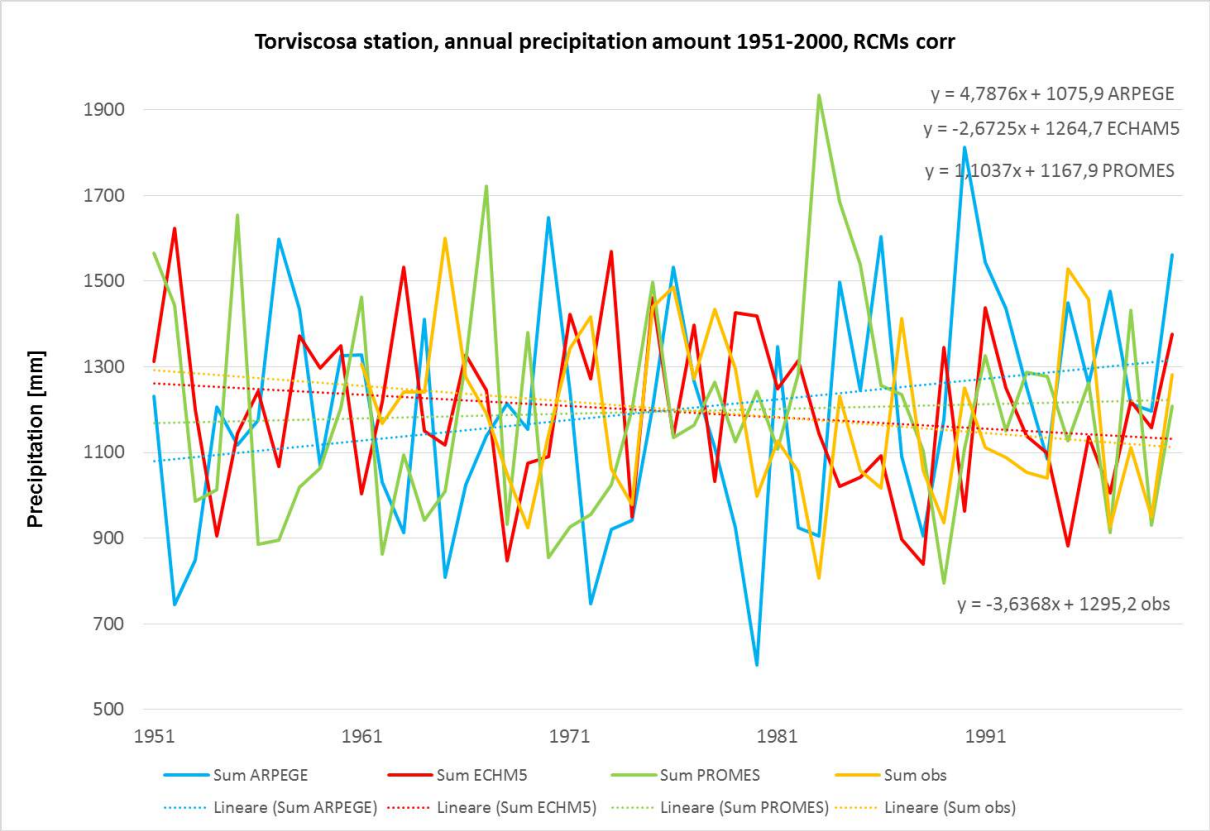

Figure 52: Torviscosa station time series 1951-2000, annual precipitation amount corrected. The precipitation value is slighting increasing with a trend for the ARPEGE model of 47 mm/10y, for PROMES of 4 mm/10y, for ECHAM5 with values of – 30 mm/10y. For the observed data, the decreasing trend has a value of -36 mm/10y.

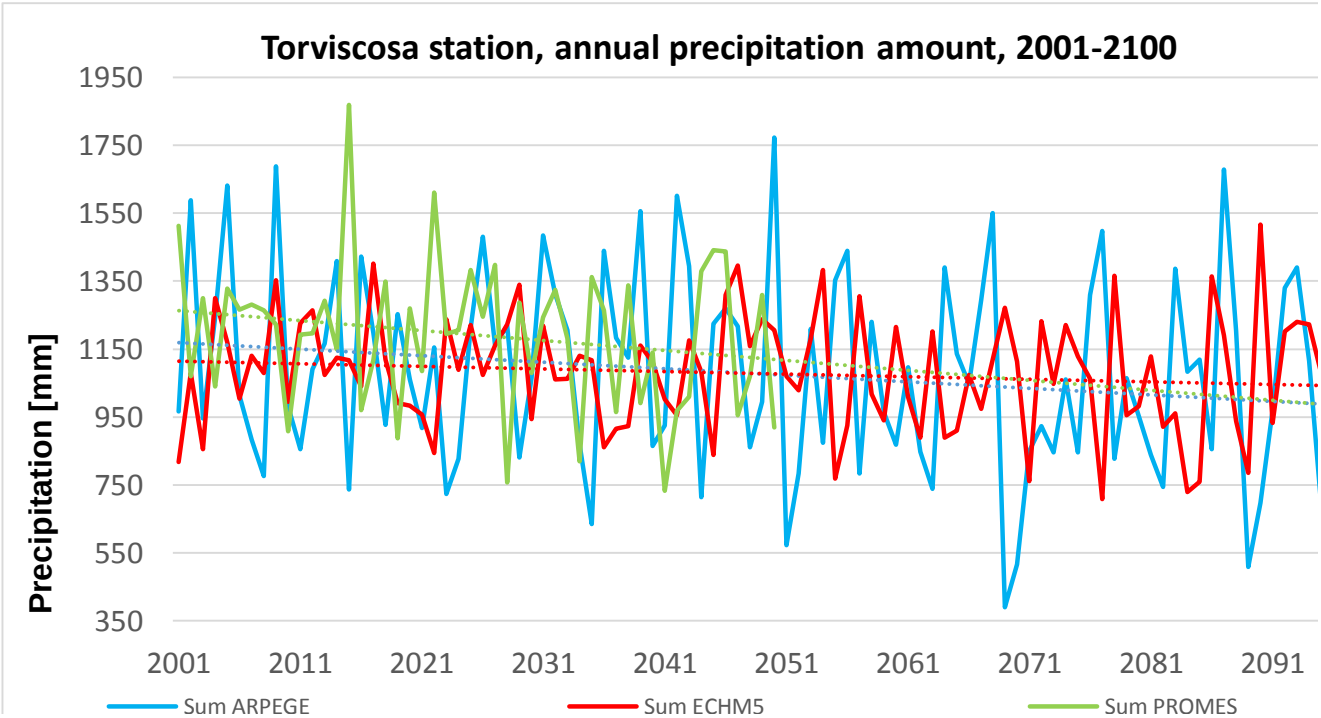

Figure 53: Precipitation model comparison for the Torviscosa station in the period between 2001-2100.

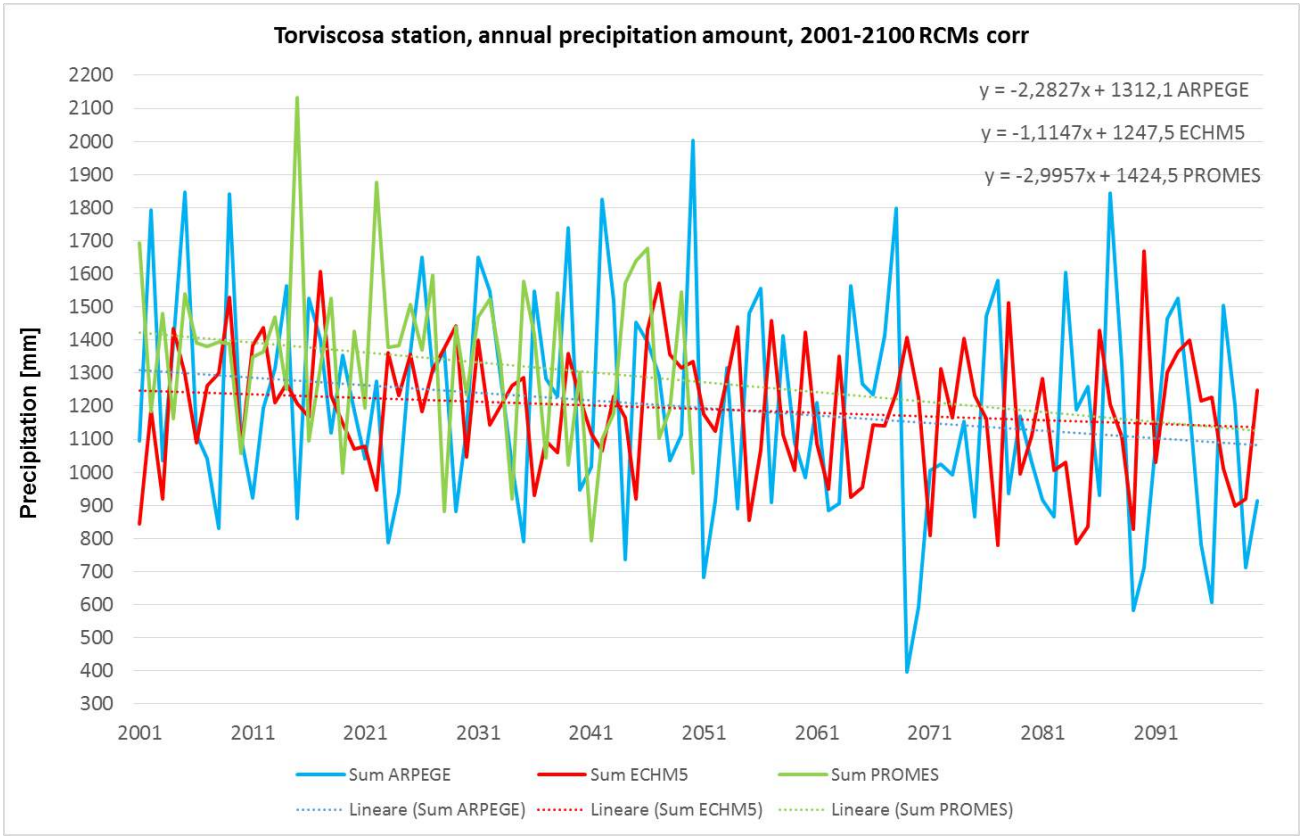

Figure 54: Torviscosa station time series 2001-2100, annual precipitation amount corrected. The trend for the ARPEGE values is of -22 mm/10y, for PROMES is of -30 mm/10y and for ECHAM5 is of -11 mm/10y. All the three models are indicating a decreasing trend.

Torviscosa	ARPEGE	PROMES	ECHAM5	Observed
Temperature [°C/10y] 50y	0,06	0,11	0,06	0,9
Temperature [°C/10y] 100y	0,34	0,47	0,38	
P (50y) [mm/10y]	47	4	-30	-36
P (100y) [mm/10y]	-22	-30	-11	

Table 21: Summary of the results calculated for the Torviscosa station.

5.5 Alberoni station, temperature

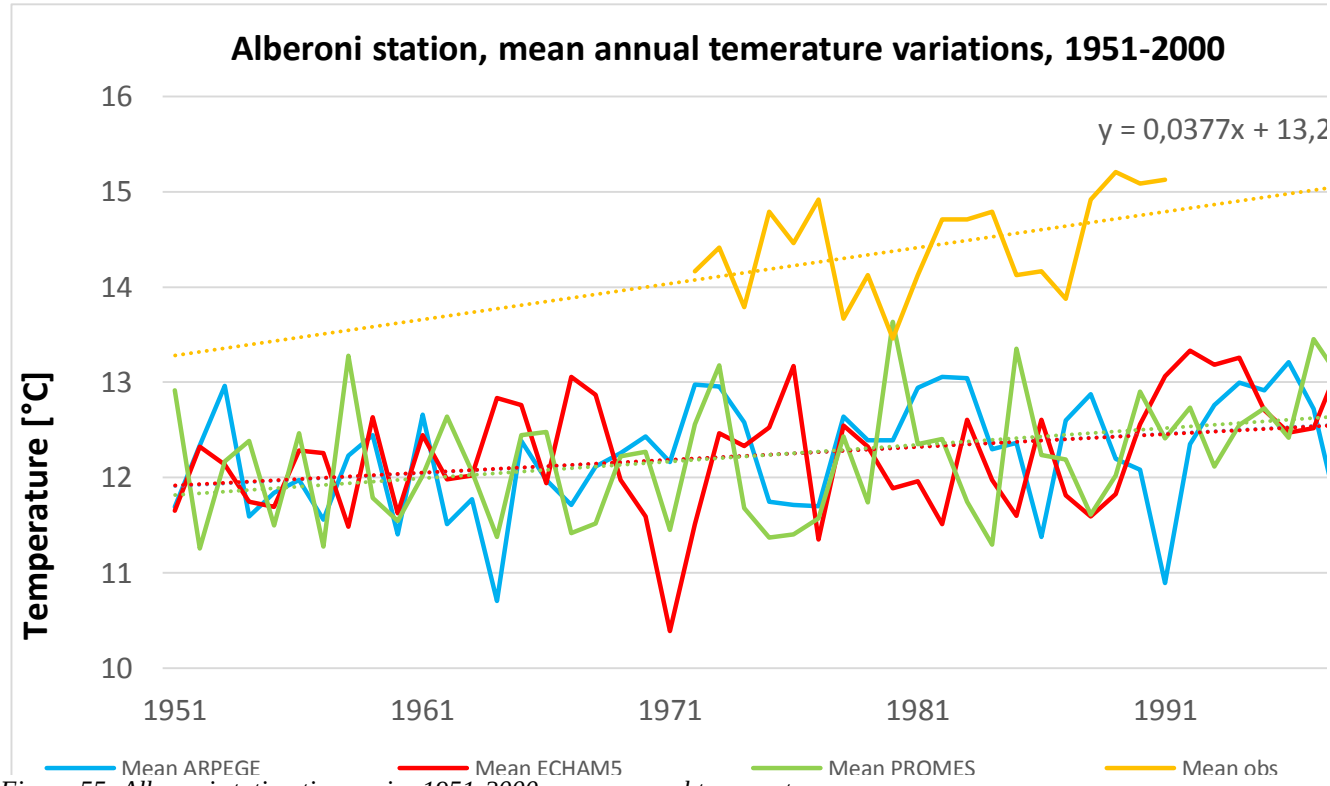

Figure 55: Alberoni station time series 1951-2000, mean annual temperature.

Data time series for Alberoni station were analyzed for two different period: the first one considering the data from 1951 till 2000 later comparing the observed time serie with the three different model available after the end of the CC Water Project; the second one is between 2001 and 2100 proposing a prediction witin the following 100 yeasrs of the temperature changes. Observed data time series show an increase from a minimum of about 13,2°C reaching vlues of 15,3°C. In this analyzed time period the models are definitively more cautelative, showing a very slight increase of about 1°C. The gap between the models and the observed data is of about 1,7°C.

The situation, as for the other meteorological stations analyzed, is different and more worrying for the future because the comparison among the three models highlight, a very large temperature increase of more than 3°C with values ranging from 12,2°C to 15,8°C.

	RCMs from CCWaters				Corrected values for RCMs		
	Arpege (ALADIN)	ECHAM5	Promes	Observed	Obs-Arpege	Obs-ECHam5	Obs-Promes
J	2,85592188	2,852464	2,85566	4,875	2,01907812	2,02253568	2,01933998
F	3,94336418	3,939928	3,938027	6,525	2,58163582	2,58507188	2,58697346
M	7,2512578	7,251425	7,250286	10,25682	3,005560382	3,005393582	3,006532182
A	11,3222518	11,32827	11,32503	13,80909	2,486839109	2,480817709	2,484058309
M	16,022678	16,01935	16,02323	18,19318	2,170503818	2,173831818	2,169951818
J	19,553088	19,55646	19,56035	21,21905	1,665959619	1,662589619	1,658697619
J	21,852276	21,85446	21,8533	23,58333	1,731057333	1,728873333	1,730029333
A	21,468114	21,47168	21,46665	23,46667	1,998552667	1,994990667	2,000012667
S	17,79938	17,79148	17,79747	20,22381	2,424429524	2,432325524	2,426341524
O	12,949984	12,95018	12,9573	15,00238	2,052396952	2,052200952	2,045076952
N	7,8481866	7,848574	7,846315	9,495238	1,647051495	1,646664495	1,648923495
D	4,10007106	4,099135	4,101234	5,759524	1,65945275	1,66038851	1,65829001

Table 22: corrections realized on the RCMs models for Alberoni station.

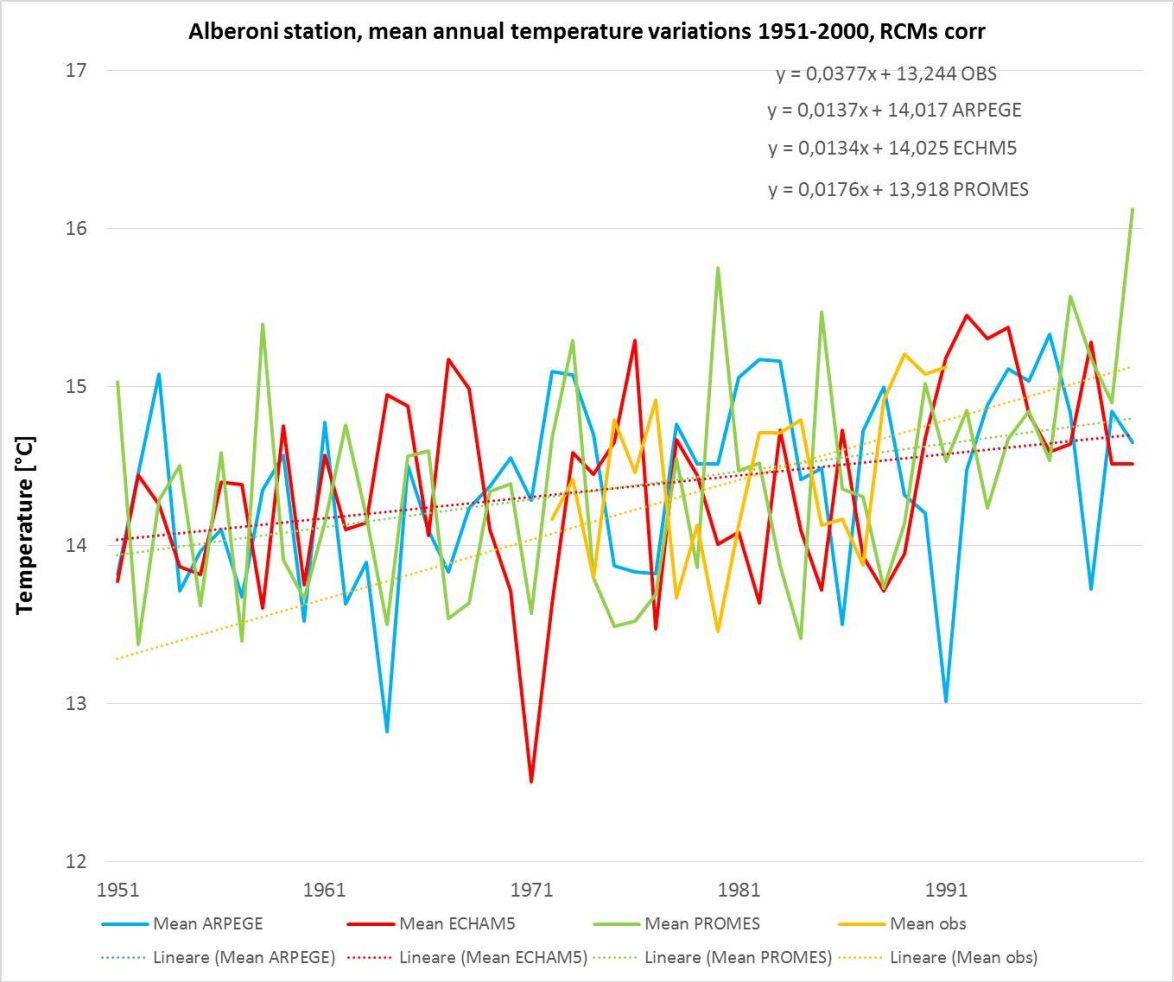

Figure 56: Alberoni station time series 1951-2000, annual precipitation amount corrected. The temperature value is slighting increasing with a trend for the ARPEGE model of 0.13°C/10y, for PROMES of 0.17 °C/10y, for ECHAM5 with values of 0.13°C/10y. For the observed data, the increasing trend has a value of 0.37 °C/10y.

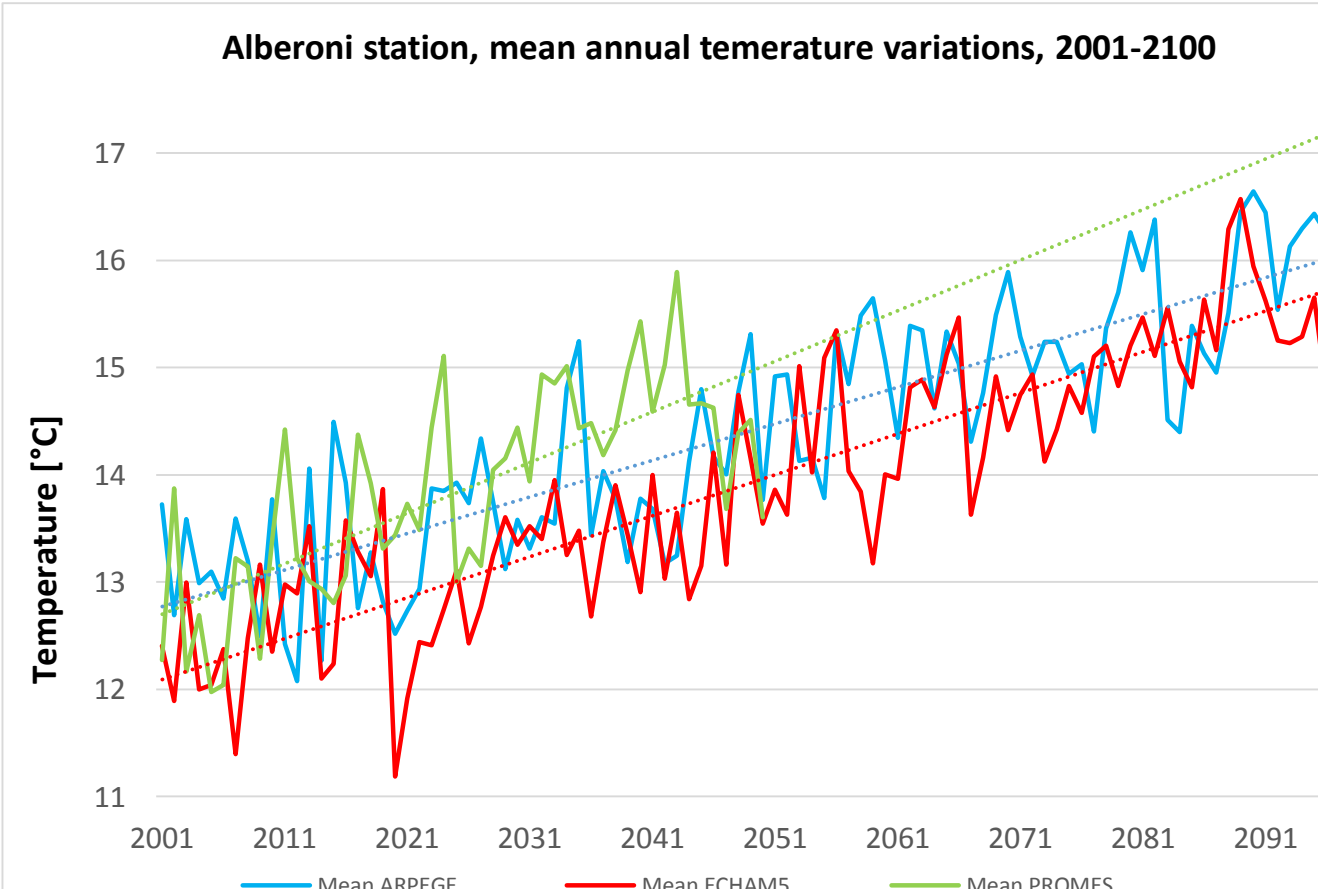

Figure 57: Temperature model comparison for the Alberoni station in the period between 2001-2100.

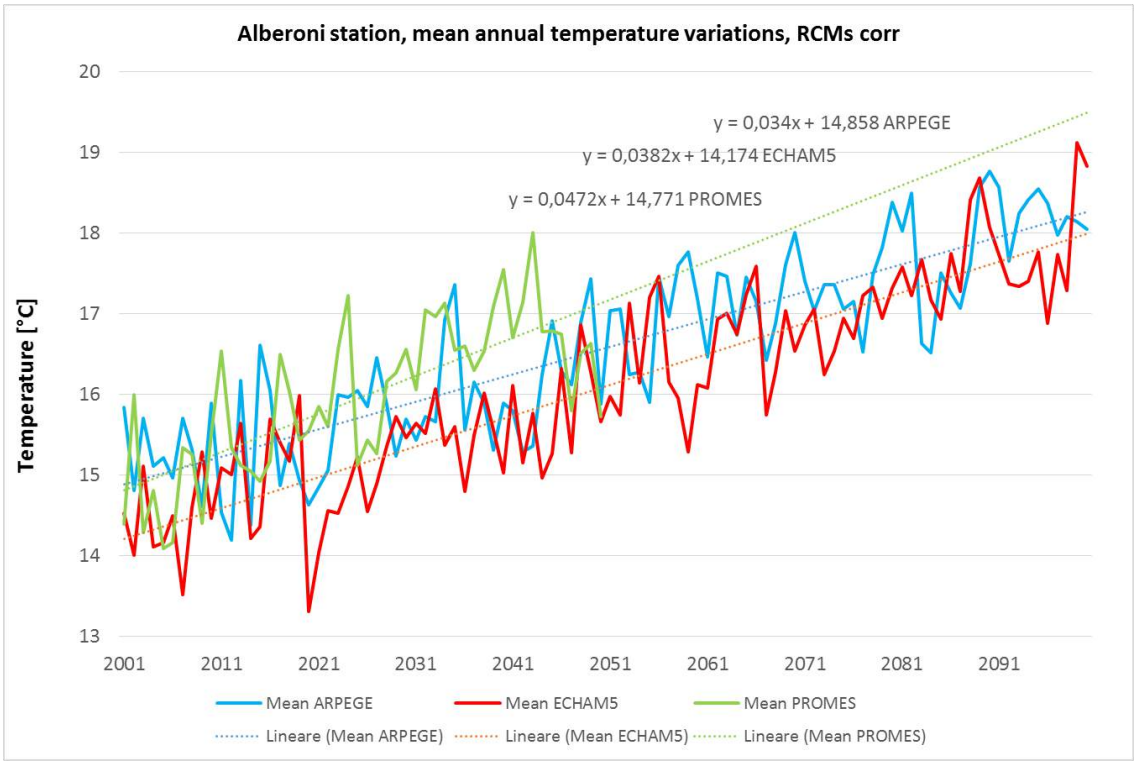

Figure 58: Alberoni station time series 2001-2100, annual precipitation amount corrected. The temperature value is slighting increasing with a trend for the ARPEGE model of 0.3°C/10y, for PROMES of 0.5°C/10y, for ECHAM5 with values of 0.4°C/10y.

5.6 Alberoni station, precipitation

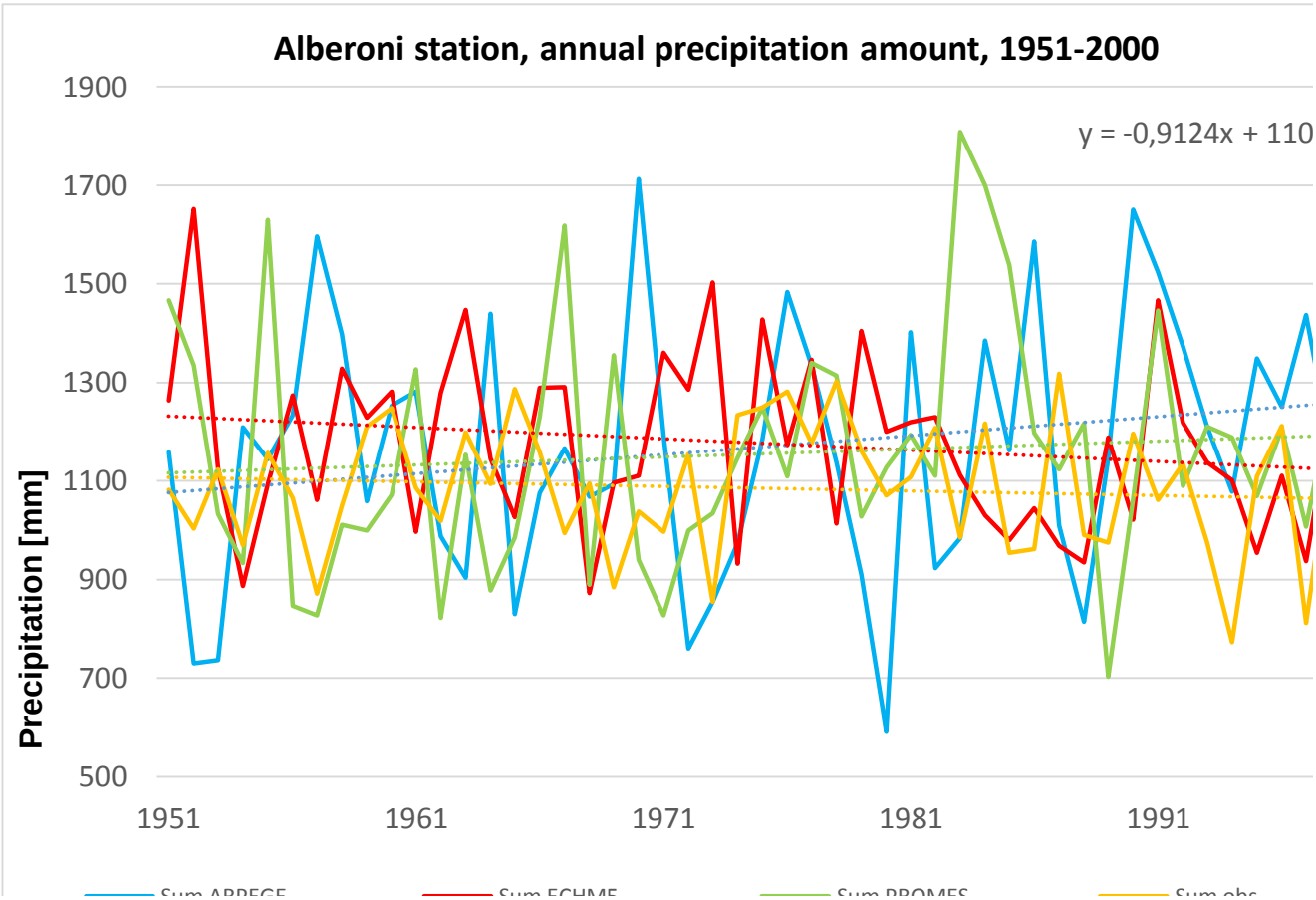

Figure 59: Alberoni station time series 1951-2000, annual precipitation amount.

	RCMs from CC Waters				Corrected values for RCMS		
	ARPEGE	ECHAM5	PROMES	obs	obs/ARPEGE	Obs/ECHAM5	Obs/PROMES
J	97,01448	97,44499	96,24516	66,54819	0,685961428	0,682930869	0,691444556
F	97,01209	97,70815	96,22309	59,57381	0,614071303	0,609711778	0,619121767
M	96,98866	97,77725	96,35789	86,15244	0,88803689	0,88110925	0,894088017
A	97,02299	97,76655	96,04194	66,49286	0,685391043	0,680118658	0,692331499
M	97,27523	97,482	95,96689	76,325	0,786738209	0,782965033	0,795326363
J	97,4862	97,49015	95,92564	83,62143	0,861947894	0,857742307	0,871731807
J	97,57049	97,51341	95,88523	94,36747	0,972715287	0,967738359	0,984171083
A	97,65182	97,52903	95,78404	78,06905	0,804715398	0,800469827	0,815052769
S	97,7701	97,55671	95,80934	81,96145	0,844837224	0,840141584	0,855464067
O	97,54701	97,48404	95,66214	116,9571	1,205563749	1,199756821	1,222606392
N	97,82065	97,65212	95,70068	117,0651	1,206676133	1,198796888	1,223241688
D	97,86102	97,83345	95,68879	106,9096	1,101996693	1,092771873	1,117263929

Table 23: Mean monthly and corrected values (quotients here are considered) are here presented for the Alberoni station.

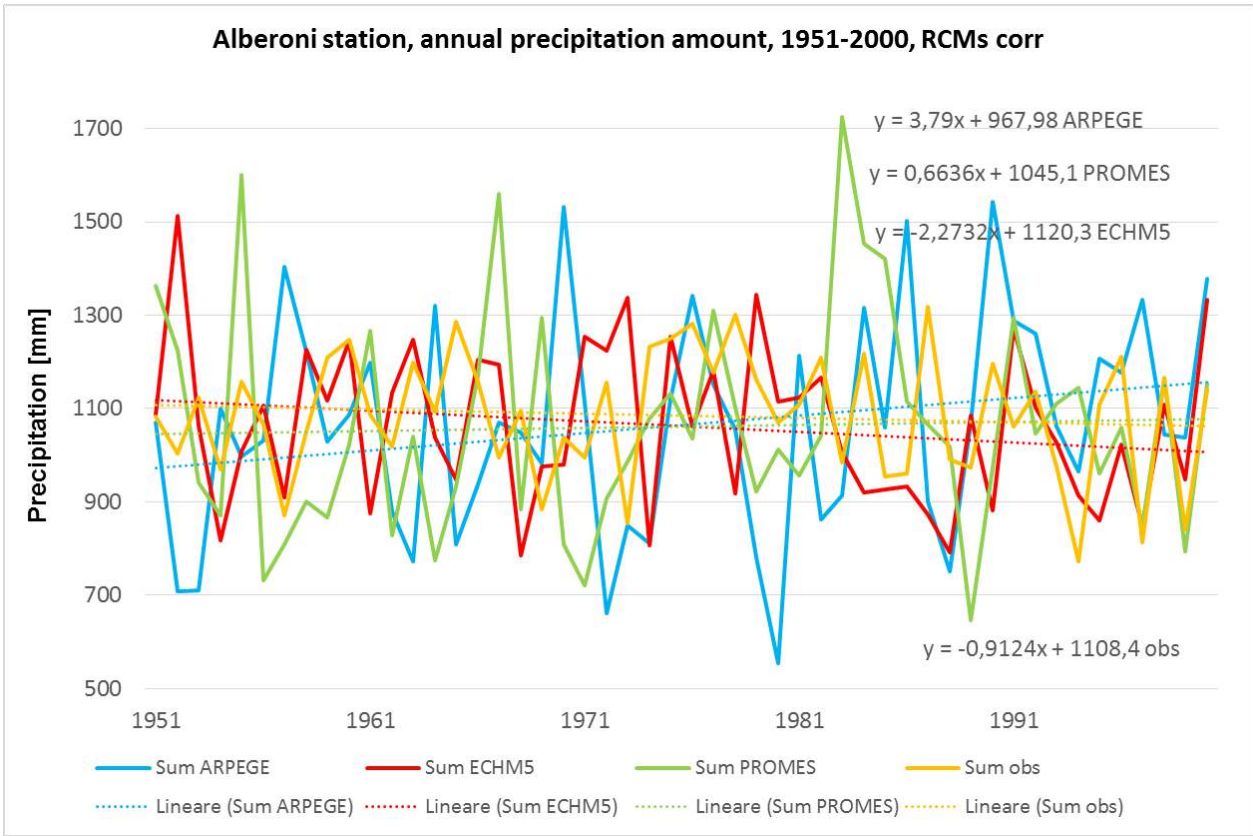

Figure 60: Alberoni station time series 1951-2000, annual precipitation amount corrected. The precipitation value is slighting increasing with a trend for the ARPEGE model of 38 mm/10y, for PROMES of 6,6 mm/10y. For ECHAM5 a decreasing value of –22 mm/10y. For the observed data, the decreasing trend has a value of -9 mm/10y.

For Alberoni station, the available observed precipitation time series were firstly analyzed and later compared with the three model time series CNRM-RM5.1 (or ALADIN) forced by ARPEGE, ICTP-REGCM forced by ECHAM5 and UCLM-PROMES forced by HadCM3Q0 for the period 1951-2000. Figure 60 is showing the obtained results. Also for this station the three models are not in agreement one with the other highlighting a slight decrease (ECHAM5) or increase (ARPEGE and PROMES) in the total annual cycle precipitation amount. On average the models are in agreement with the total annual amount of rainfall. If we have a look at the future projection (Figure 62), using the three model time series CNRM-RM5.1 (or ALADIN) forced by ARPEGE, ICTP-REGCM forced by ECHAM5 and UCLM-PROMES forced by HadCM3Q0 for the period 2001-2100, it is possible to realize that, all the models evidence a slight decrease in the annual precipitation amount.

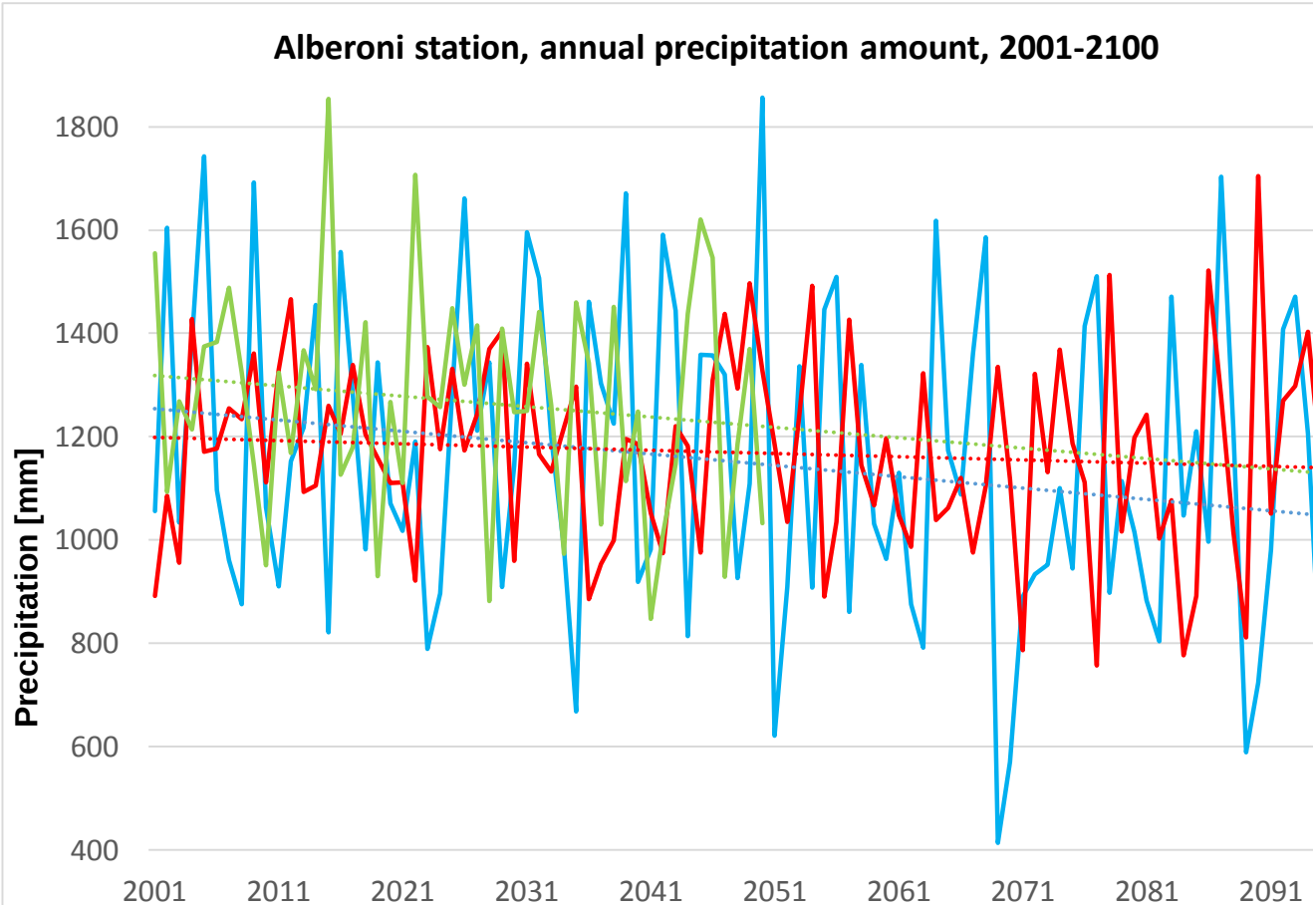

Figure 61: Precipitation model comparison for the Alberoni station in the period between 2001-2100.

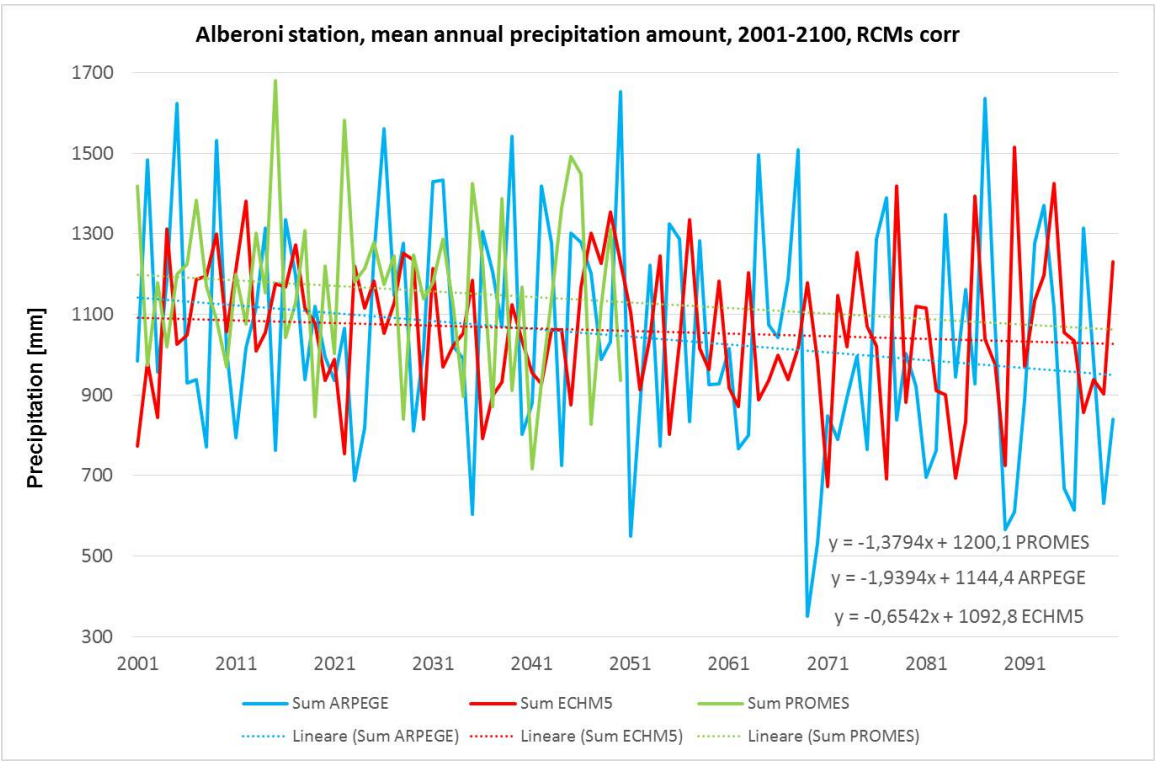

Figure 62: Torviscosa station time series 2001-2100, annual precipitation amount corrected. The trend for the ARPEGE values is of -19 mm/10y, for PROMES is of -13 mm/10y and for ECHAM5 is of -6 mm/10y. All the three models are indicating a decreasing trend.

Alberoni	ARPEGE	PROMES	ECHAM5	Observed
Temperature [°C/10y] 50y	0,13	0,13	0,17	0,37
Temperature [°C/10y] 100y	0,34	0,47	0,38	
P (50y) [mm/10y]	38	6,6	-22	-9
P (100y) [mm/10y]	-19	-13	-6	

Table 24: Summary of the results calculated for the Alberoni station.

Short references

Bubnova, R., Hello, G., Bénard, P., Geleyn, J-F., 1995. Integration of the fully elastic equations cast in hydrostatic pressure terrain-following coordinate in the framework of the ARPEGE/Aladin NWP system. Mon.Wea.Rev.,123:515–535.

Castro, M., Fernández C., Gaertner M.A., 1993. Description of a meso-scale atmospheric numerical model. In:J.I. Díaz, J.L. Lions (eds), Mathematic, climate and environment, Masson.

Desiato, F., Fioravanti, G., Fraschetti, P., Perconti, W., Piervitali, E. (2012) Elaborazione delle serie temporali per la stima delle tendenze climatiche. ISPRA, ISBN 978-88-448-0559-3. pp.37

Pal, J.S., and Coauthors, 2007. Regional climate modeling for the developing world: The ICTP RegCM3 and RegCNET. Bull. Amer. Meteor. Soc., 88:1395–1409.

Sen, P.K. (1968) Estimates of the regression coefficient based on Kendall's tau. J.Am.Stat. Assoc. 63:1379-1389.

Let's grow up together

DRINK ADRIA

Adriatic IPA
Cross Border Cooperation 2007-2013

The project is co-funded by the European Union,
Instrument for Pre-Accession Assistance

REPORT:

Climate and Climate Change data

for ATO 3 Test Area, Italy

Lead Author/s	Daniele Nardi
Lead Authors Coordinator	
Contributor/s	Marco Materazzi, Simona Mercuri
Date last release	30/09/2014
State of document	Final

Let's grow up together

DRINK ADRIA

Adriatic IPA
Cross Border Cooperation 2007-2013

The project is co-funded by the European Union,
Instrument for Pre-Accession Assistance

Table of contents

Introduction

In this report you'll find a summary of the results of the activities implemented by A.ATO 3 Organization in order to contribute to the DRINKADRIA Project objective to develop an analysis of observed and simulated data on climate and climate change concerning ATO 3 Pilot Area, including Musone, Chienti, Potenza (and upper part of Tevere) River basins.

Available data, models and main limitations of the applied methodology are presented in Chapter 1.

Analysis of observed and simulated climate and climate change data, concerning ATO 3 Pilot Area, are shown and discussed in Chapter 2.

Supplement files containing observed and simulated time series are attached, as Appendices 1 and 2.

1. Methodology

General climate characteristics, climate variability and trends in ATO 3 Pilot Area are analysed based on available climatological data. They include measurements of air temperature and precipitation amounts from the reference climate period 1961-1990. Observed trends are estimated from a longer period: 1951-2008 as far as concerns precipitations and 1957-2008 for temperatures, with only few data missing.

The analysis is based on monthly, seasonal and annual averages derived from daily data on the most representative climatological stations of existing Regional observational network.

An assessment of the present and future climates is based on the results from numerical simulations of the three regional climate models that were also analysed for the purpose of the CC-WaterS (www.ccwaters.eu) project. These models also participated in the ENSEMBLES (www.ensambles-eu.org) project, with downscaling simulations at a 25-km horizontal resolution. In this report, analysis of the model data is carried out for those model grid cells which are the closest to the locations of the chosen climatological station (thus representing simulated climatological characteristics for ATO 3 Pilot Area).

The regional climate models (RCMs) used are the Aladin (Bubnova et al. 1995), Promes (Castro et al. 1993) and RegCM3 models (Pal et al. 2007). The RCMs were forced by the observed concentrations of the greenhouse gases (GHGs) from 1951 to 2000; from 2001 onwards the IPCC4 A1B scenario of the GHGs emissions is applied. The initial and boundary data for each RCM were provided from different global climate models (GCMs):

the ECHAM5 GCM data were used to force RegCM3, Aladin was forced by the Arpege GCM and Promes was forced by the HadCM3Q GCM. For the present climate, models are compared with the local DHMZ observations and with the EOBS gridded temperature and precipitation data (Haylock et al. 2008). The following two abbreviations are used in the report:

1. RCMcorr: the RCMs' output was bias corrected by EOBS data, see e.g. Déqué (2007) and Formayer and Haas (2010) for the description of the bias correcting methodology. The RCMcorr data are available from the CC-WaterS database http://climdat.boku.ac.at/opendap/ccwaters;

2. RCMcorr_adj: this is further adjusted model time series due to the differences between EOBS data and local stations observations. The adjustment procedure is described in detail in Chapter 2.

The purpose of this report is to provide an input for further hydrological analyses. However, due to experimental nature of the regional climate simulations, several limitations should be emphasised:

1. Spatial resolution of the regional climate model simulations (RCMs) used here is 25 km. At this resolution the main orographic features and the land-sea boundary of the Adriatic coast are resolved reasonably well. However, at the same resolution local characteristics for specific station or catchment may not be fully resolved.

2. For the period 1951-2000 all the RCMs in this report are forced by historical (observed) concentrations of the GHGs. From 2001 onwards, however, the IPCC A1B scenario is applied, meaning that only one assumption of the GHG concentration is evaluated. This must be taken into consideration when evaluating the amplitude of projected climate changes (e.g. the higher GHGs emission scenarios are usually associated with the higher temperature increase).

3. The three RCMs models used here account only for a part of possible modelling uncertainties. The use of the multi-model ensemble approach in climate projection studies is strongly recommended in order to avoid projection dependence on specific model assumptions.

4. In the analysed RCM simulations of the reference climate, the RCMs are not reproducing the actual variability observed in the real climate system. Since RCMs are forced at the boundaries by different global climate models (each having its own internal variability, e.g. the sequence of warm and cold years over Europe), the RCMs simulate different variability, e.g. their own sequence of warm and cold years (or dry and wet years). Specific values indicated in the time series presented in this report do not signify a specific prediction for a specific year.

The models can be compared with observations and with each other in terms of the reference and projected mean climate and overall variability. Models simulations of the

future climate should be interpreted as projections of possible state(s) of the climate system which is sensitive to applied initial and boundary conditions, GHGs scenarios and a model internal configuration. Projections are expected to represent future trends and changes over longer time period as realistic as possible.

2. Results and discussion

This chapter provides an overview of climate characteristics of the observed climate variability and trends for ATO 3 Pilot Area, in Marche Region, Central Italy (Adriatic coast). It may serve as a basis for hydrological analysis relevant for water supply estimates as well as for validation of simulated climate changes. The analysis is based on monthly, seasonal and annual averages of air temperature and precipitation amounts over the reference climate period 1961-1990. The catchment includes several climatological stations providing both temperature and precipitation data concerning the period 1951-2008. Geographical location data and available time periods of meteorological measurements are given in Table 2.1.

***Table 2.1**. Geographical station data (elevation h, longitude* l*, latitude* f*) and the available measurement time periods for temperature (t) and precipitation (P) data for 2 stations in ATO 3 Pilot Area.*

	Station	*h* (m	f	l	t	P
1.	Lornano	232	43° 17’	13° 25’	1957-2008 (1)	1951-2008 (2)
2.	Montemonaco	987	42° 53’	13° 19’	1957-2007	1951-2007 (3)

(1) *the whole year 1977 is missing.*
(2) *some data of 1989 are missing.*
(3) *the whole years 1988 and 1989 are missing.*

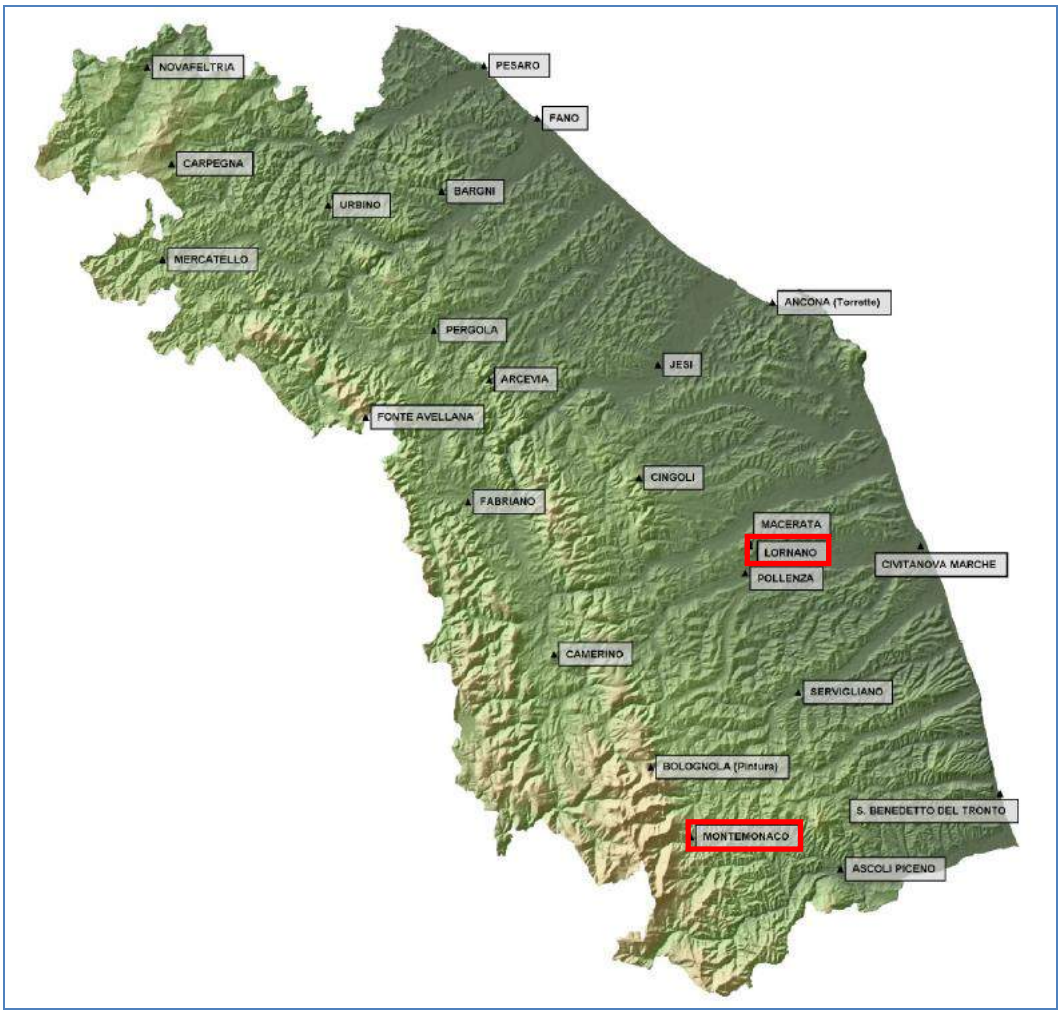

Fig. 2.1 – Geographical distribution of climatological stations (24) in Marche Region, with localization of those relevant for ATO 3 Pilot Area

Air temperature

The annual cycle of air temperature monthly averages in ATO 3 Pilot Area is well defined: the maximum occurs in summer (JJA) and the minimum in winter (DJF), with significant differences between the mountains (Appennines), internal area and the medium-low hill area (see Table 2.2), but generally indicating a typical maritime annual cycle with autumn (SON) being warmer than spring (MAM).

The annual course of standard deviations (stdev) of mean monthly air temperatures indicates a higher variability in the central, medium-low hill area, especially in autumn (SON), while the monthly values of stdev, fo the mountain meteorological station taken into account range between 0.9°C (JJA) and 1.8°C (DJF) indicating that interannual variability is generally small.

Table 2.2 *Basic statistics (mean, standard deviation, maximum and minimum) for annual and seasonal mean air temperature from the reference period 1961-1990 for the two climatological stations in ATO 3 Pilot Area.*

	DJF	MAM	JJA	SON	Year
			Lornano		
mean (°C)	6,5	13,3	23,4	15,7	14,7
stdev (°C)	1,8	3,8	2,3	4,3	1,0
max (°C)	10,7	22,7	31,5	26,3	17,3
min (°C)	2,1	5,4	19,1	7,8	13,4
			Montemonaco		
mean (°C)	3,4	9,5	19,3	12,2	11,1
stdev (°C)	1,8	1,7	0,9	1,1	0,7
max (°C)	8,9	15,8	21,0	14,5	13,0
min (°C)	-0,3	6,6	17,0	10,0	9,8

The percentiles that determine extreme values of annual and seasonal mean temperatures, according to the empirical cumulative distributions of the mean annual air temperature for Lornano and Montemonaco stations in the reference period 1961-1990 are given in Table 2.3.

Table 2.3 *The percentiles for annual and seasonal mean air temperature according to the empirical distribution from the reference period 1961-1990 for the two climatological stations in ATO 3 Pilot Area.*

Perc.	DJF	MAM	JJA	SON	Year
Lornano					
1	2,3	5,5	19,3	8,2	13,5
2	2,5	6,3	19,3	8,4	13,5
5	3,2	7,4	19,6	9,5	13,6
10	3,7	7,9	20,3	9,7	13,7
90	8,5	17,7	25,8	21,2	15,8
95	9,3	18,1	26,2	21,7	16,1
98	9,7	18,9	26,9	22,7	16,4
99	10,1	19,5	27,0	24,3	16,4
Montemonaco					
1	0,0	6,8	17,1	10,2	9,9
2	0,3	7,0	17,2	10,3	9,9
5	0,7	7,4	17,7	10,6	10,1
10	1,2	7,5	18,2	10,8	10,4
90	5,1	11,1	20,5	13,3	11,8
95	5,9	11,3	20,6	13,6	12,3
98	7,4	13,3	20,8	14,1	12,7
99	8,2	14,6	20,9	14,3	12,8

Precipitations

The ATO 3 Pilot Area has a mix of the maritime and continental types of annual precipitation cycle. The basic statistics for annual and seasonal precipitation amounts are given in Table 2.4.

In some years there is a significant deviation in monthly amounts from the average precipitation conditions. Coefficient of variation indicates a high interannual variation in mean monthly precipitation, especially on the Appennines.

Table 2.4 *Basic statistics (mean, standard deviation, coefficient of variation, maximum and minimum) for annual and seasonal precipitation amounts from the reference period 1961-1990 for the two climatological stations in ATO 3 Pilot Area.*

	DJF	MAM	JJA	SON	Year
Lornano					
mean	178,2	178,7	187,2	210,2	748,7
stdev (mm)	71,5	49,2	79,5	67,9	159,3
c_v	0,4	0,3	0,4	0,3	0,2
max (mm)	330,8	252,0	463,6	379,0	1163,0
min (mm)	33,8	76,2	47,4	83,0	483,2
Montemonaco					
mean	340,8	303,1	236,0	337,9	1217,7
stdev (mm)	94,9	89,3	122,5	81,8	204,9
c_v	0,3	0,3	0,5	0,2	0,2
max (mm)	579,0	541,9	683,4	494,0	1781,0
min (mm)	190,4	173,6	76,6	165,6	965,5

The percentiles that determine extreme values in the cumulative distribution (CDF) of annual precipitation are given for annual and also for seasonal precipitation in Table 2.5. The empirical CDF gives the general insight into the precipitation amount distribution shape providing the expecting probabilities of the observed amounts. The differences in the CDFs across a small region such as the ATO 3 Pilot Area reveal the overall large spatial variability of precipitation amounts.

Table 2.5 *The percentiles for annual and seasonal precipitation according to the empirical distribution from the reference period 1961-1990 for the two climatological stations in ATO 3 Pilot Area.*

Perc.	DJF	MAM	JJA	SON	Year
Lornano					
1	39,0	81,0	52,3	87,3	501,1
2	44,1	85,8	57,1	91,6	518,9
5	66,8	95,9	80,7	105,0	548,4
10	91,7	115,8	107,1	129,6	567,2
90	271,8	240,7	263,1	292,5	890,5
95	304,6	245,8	290,8	318,0	1028,0
98	322,1	249,7	364,3	352,2	1129,8
99	326,4	250,8	414,0	365,6	1146,4
Montemonaco					
1	191,8	181,9	78,7	180,9	965,7
2	193,1	190,2	80,7	196,3	965,9
5	199,1	205,2	97,0	225,6	966,6
10	215,9	212,5	124,6	232,7	991,6
90	212,1	210,2	123,1	232,3	982,2
95	504,4	486,5	405,5	471,1	1584,9
98	545,1	529,2	534,8	482,3	1710,3
99	562,0	535,6	609,1	488,2	1745,6

Trends

Trends in seasonal and annual mean monthly air temperature and precipitation amounts are calculated for the available period. They have been estimated by the Kendall's tau method (or Sen's slope; Sen 1968), which is statistically more robust estimator of the trend than the least squares estimator. However, a linear trend is also calculated and given for comparison. The trends are expressed as decadal values for both variables. Additionally, the trends in precipitation amounts are given as the percentage of the corresponding seasonal and annual means from 1961-1990 period.

The trend results reveal the statistically significant increase in annual mean air temperature (0.3°C/10yrs) since 1961 in the ATO 3 Pilot Area (see Table 2.6). The annual

mean temperature increase is predominantly due to the significant increase in spring (0.2-0.4°C/10yrs) and summer (0.2-0.5°C/10yrs) mean air temperature. Changes observed in the cold half-year are very weak. These results are in line with the observed regional and global warming.

Table 2.6 *Decadal air temperature trends (°C/10 yrs) for Lornano and Montemonaco climatological stations based on the 1957-2007 (or 2008) data series.*

°C/10yrs	DJF	MAM	JJA	SON	Year
Lornano	0,10	0,20	0,20	0,06	0,30
Montemonac	0,28	0,41	0,49	0,16	0,33

The trends in precipitation amounts show the significant decrease in annual totals (2-5%/10yrs) over the ATO 3 Pilot Area. There is a consistent decrease of precipitation amounts in all seasons (see Table 2.7).

Table 2.7 *Decadal precipitation trends (mm/10 yrs and %/10 yrs) for Lornano and Montemonaco climatological stations based on the 1951-2007 (or 2008) data series.*

	DJF	MAM	JJA	SON	Year
Lornano					
mm/10yrs	-11,2	-4,8	-14,9	-10,9	-36,3
%/10yrs	-6,3	-2,7	-8,0	-5,2	-4,8
Montemonaco					
mm/10yrs	-8,0	-7,3	-0,7	-10,6	-26,6
%/10yrs	-2,4	-2,4	-0,3	-3,1	-2,2

3. Regional climate model simulations

Lornano

Air temperature and precipitation from local observations at the Lornano climatological station, EOBS data and bias corrected simulations of the three regional climate models in the historical period P0 (1961-1990) are compared in Fig. 3.1. The EOBS air temperature is lower than the local observations throughout the annual cycle (Fig. 3.1a). Since EOBS data made the basis for calculation of RCM biases, the bias-corrected modelling data, RCMcorr, are therefore constrained to be closer to EOBS than to the observations. This restriction makes the RCMcorr annual cycles also colder than the local observations; the RCMcorr graphs overlap exactly with the EOBS curve and could be hardly distinguished from each other on Fig. 3.1a. The underestimation of the observed air temperature seen in Fig. 3.1a) may seem small, but it becomes substantial in the annual mean.

The mean monthly precipitation deviates in most months only slightly from local observations. Annual cycles of both mean air temperature and mean total precipitation are, during the P0 (1961-1990) period, generally similar in all datasets considered (Fig. 3.1a,b).

Only for air temperature the variation of the local observation data is, in most months, slightly underestimated by EOBS (Fig. 3.1c,d). This underestimation is likely due to the interpolation method applied to derive the EOBS gridded data.

Time series of the mean annual air temperature in the period 1951-2000 (Fig. 3.1e) indicates that the EOBS and RCMcorr values are lower than the local observations, further confirming the underestimations of the local annual cycle shown in Fig 3.1a. A large year-to-year variation of the air temperature annual means differs among various data sources (Fig. 3.1e). This difference in the representation of interannual variability does not signify that a particular model failed to correctly simulate observed natural variability. It may be attributed to a different external forcing of the RCMs by different global circulation models, but also to a different internal variability inherent to each single RCM (see Methodology). Standard deviation of the annual mean air temperature time series in all data sources are quite similar indicating that the RCMs are close to observations in representing atmospheric natural variability.

For annual precipitation amounts, the EOBS and the local observation datasets are relatively close to each other (Fig. 3.1f). The model values in some years tend to differ from the observations; however, no clear signal (overestimation or underestimation) is obvious.

The empirical cumulative distribution functions (CDFs) does not show a close correspondence of EOBS and RCMcorr data from the local observations in the P0 through all annual air temperature ranges (Fig. 3.1g). For the annual total precipitation, a shift of the of EOBS and the RCMcorr data from the local observations is seen for all data sources (Fig. 3.1h).

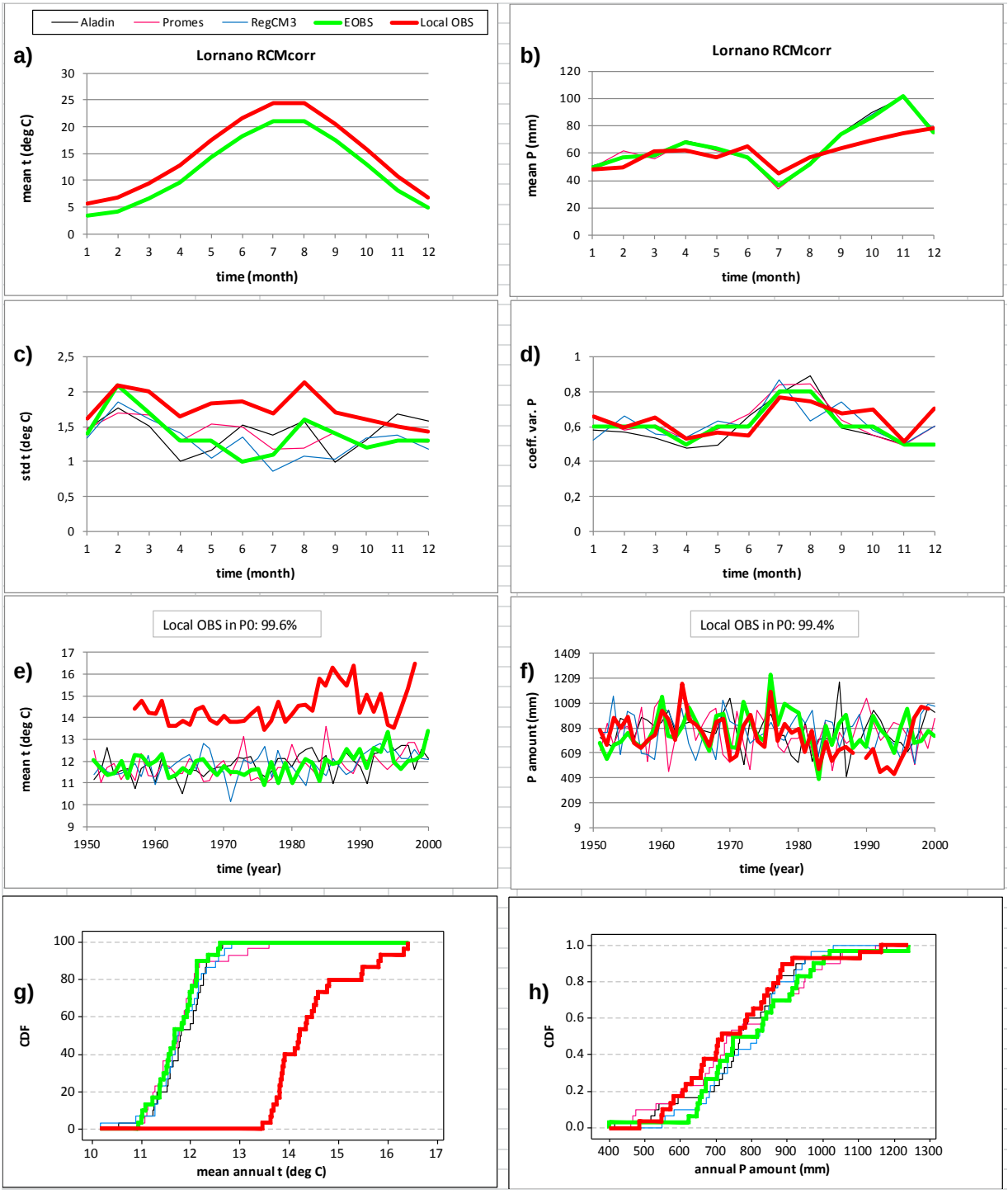

Figure 3.1 *Lornano station: annual cycle a) mean monthly temperature, b) monthly precipitation amount, c) mean monthly temperature standard deviation, d) coefficient of variation of monthly precipitation amount; time series e) mean annual temperature, f) annual precipitation amount; empirical cumulative distribution functions CDFs g) mean annual temperature, h) annual precipitation amount. Model time series are RCMcorr. Period of analysis: P0 (1961-1990).*

For the period 1951-2050, all three bias corrected models simulate statistically significant increasing trends in the mean annual temperature from 0.16 °C/10yr in RegCM to 0.30 °C/10yr in Promes (Fig. 3.2). It should be emphasised here that, in the model simulations for the period 1951-2000, the observed concentrations of the greenhouse gases (GHGs) is used, and in the period 2001-2050, the models were forced by the GHGs concentrations for the IPCC A1B scenario. In the period 1961-2007, when the local observations were available, all three models agree with the observations in the simulated sign of trend, with a magnitude of trend similar to that of the local observations (0.33 °C/10yr; Table 2.6).

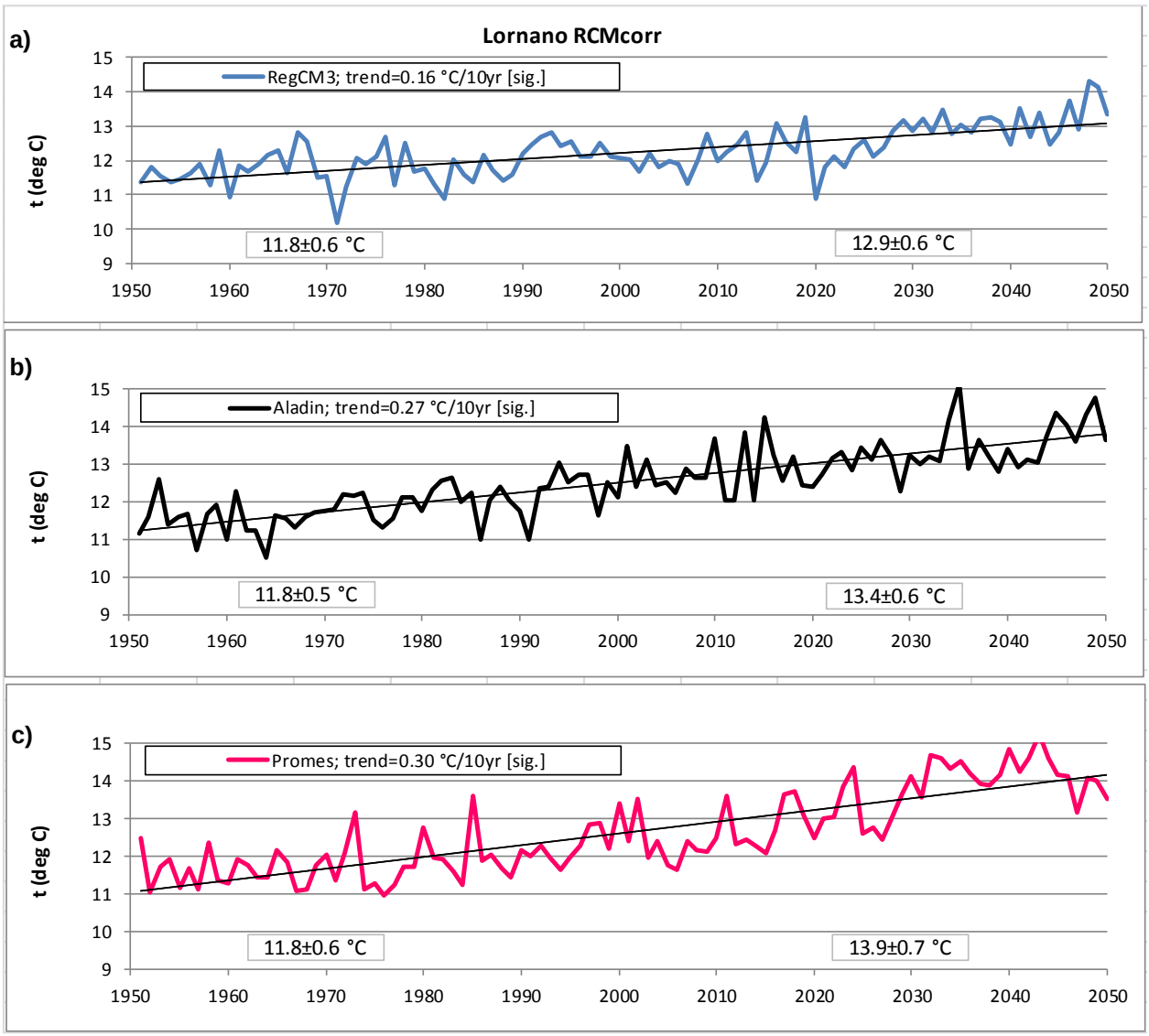

Figure 3.2 *Lornano station: annual mean temperature and associated linear trend in a) RegCM3, b) Aladin, c) Promes. Decadal trend based on the entire time series is shown in panel legends. The statistical significance of the trend is assessed using the Mann-Kendall test and 5% significance level. Additional numbers at the bottom of each panel are mean values and standard deviations during P0 (1961-1990) and P1 (2021-2050). Model time series are RCMcorr.*

Two of the three bias-corrected models (RegCM3, Aladin) simulate decreasing trend in the annual precipitation amount for the period 1951-2050 (Fig. 3.3), while the third one (Promes) simulates opposite sign of the trend. However, in all the models, these trends are not statistically significant. For the period 1951-2008, when local observations at the Lornano station show decreasing trend in annual precipitation amount (-36.3mm/10yr; Table 2.7), RegCM3 and Aladin simulates the same sign of the trend as observed, but with greatly reduced amplitude and no statistical significance. This implies that, according to the CC-WaterS bias corrected RCMcorr simulations presented here, no robust estimates of significant precipitation change could be made for the first part of the 21st century.

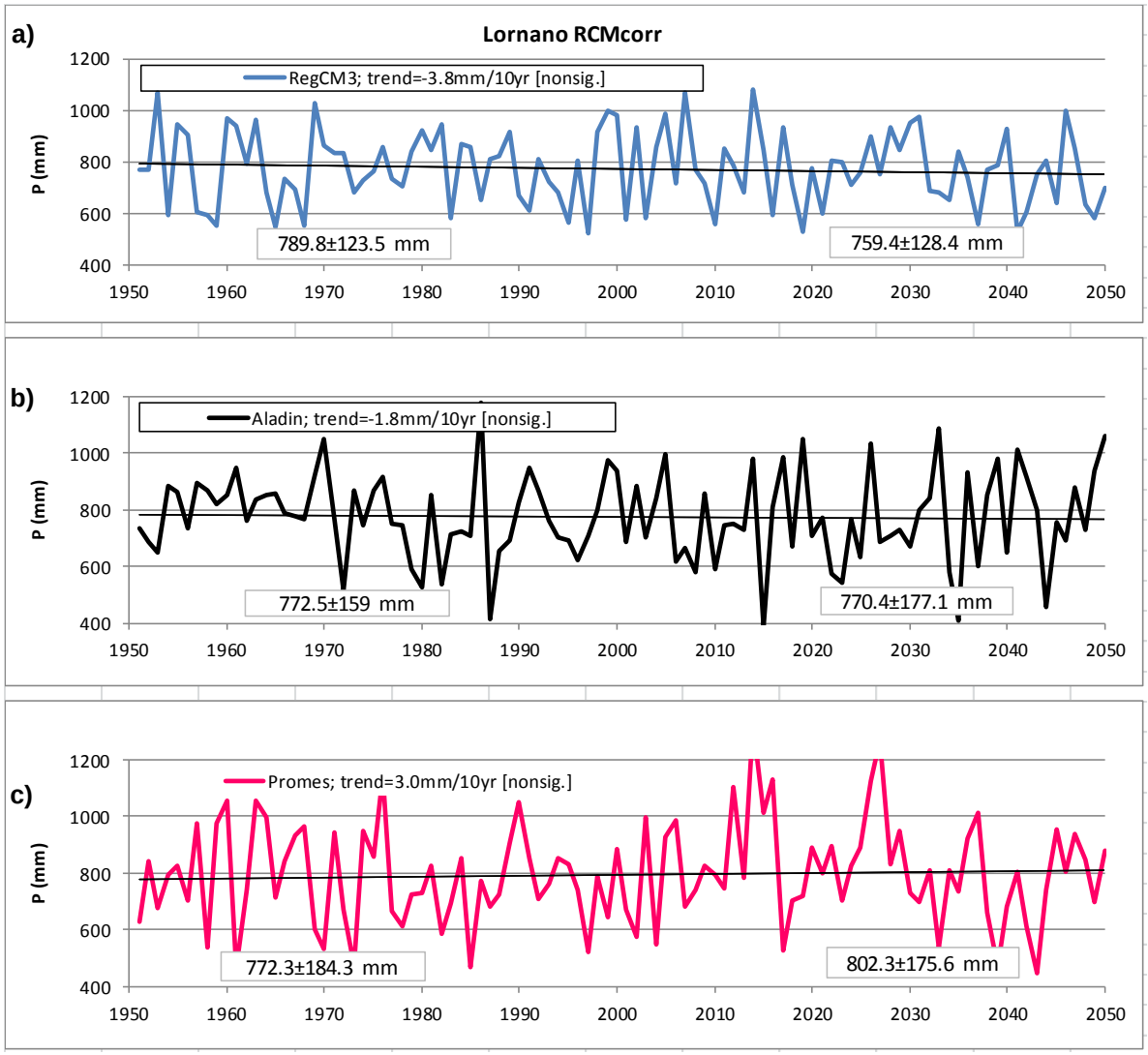

Figure 3.3 *Lornano station: annual precipitation amount and associated linear trend in a) RegCM3, b) Aladin, c) Promes. Decadal trend based on the entire time series is shown in panel legends. The statistical significance of the trend is assessed using the Mann-Kendall test and 5% significance level. Additional numbers at the bottom of each panel are mean values and standard deviations during P0 (1961-1990) and P1 (2021-2050). Model time series are RCMcorr.*

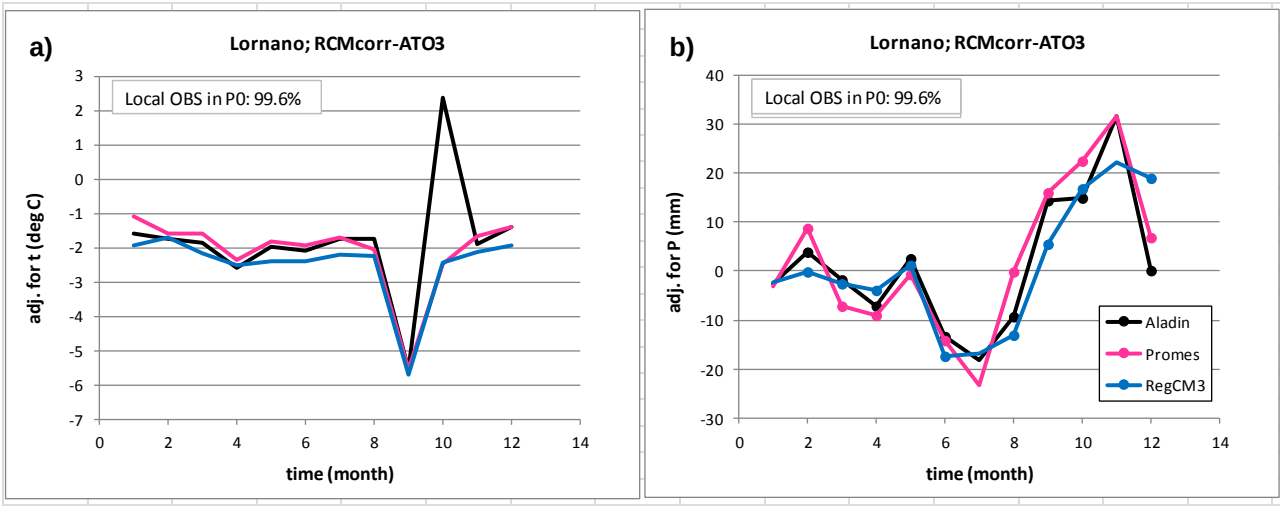

Figure 3.4 *Lornano station: adjustment differences a) mean monthly temperature b) monthly precipitation amount. Differences are based on 1961-1990 period and the availability of local observations in this period is almost 100%. Statistically significant differences according to the Wilcoxon-Mann-Whitney nonparameteric rank-sum test and 5% significance level are marked by the filled circles.*

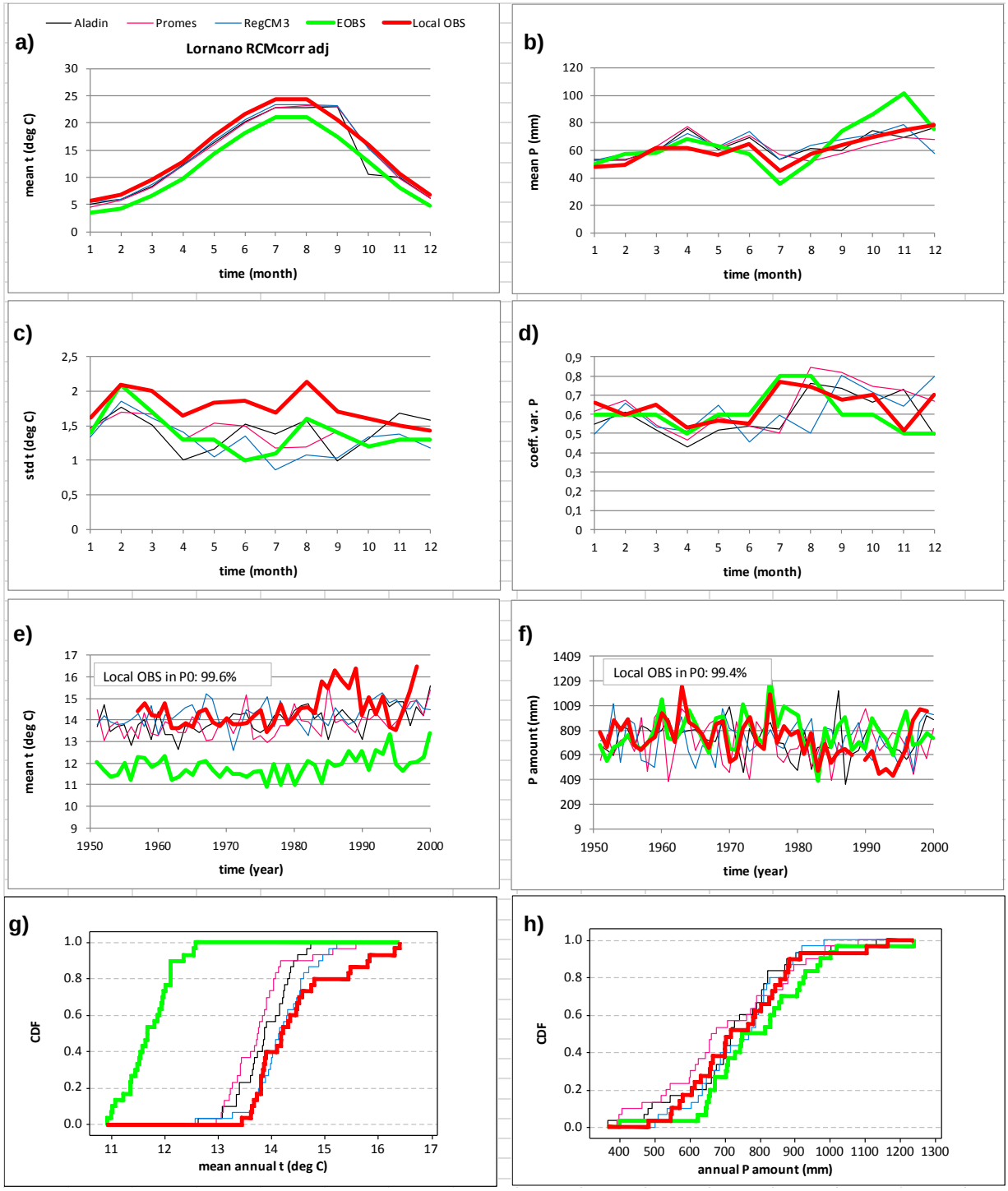

Figure 3.5 *Lornano station: annual cycle a) mean monthly temperature, b) monthly precipitation amount, c) mean monthly temperature standard deviation, d) coefficient of variation of monthly precipitation amount; time series e) mean annual temperature, f) annual precipitation amount; empirical cumulative distribution functions CDFs g) mean annual temperature, h) annual precipitation amount. Model time series are RCMcorr_adj. Period of analysis: P0 (1961-1990).*

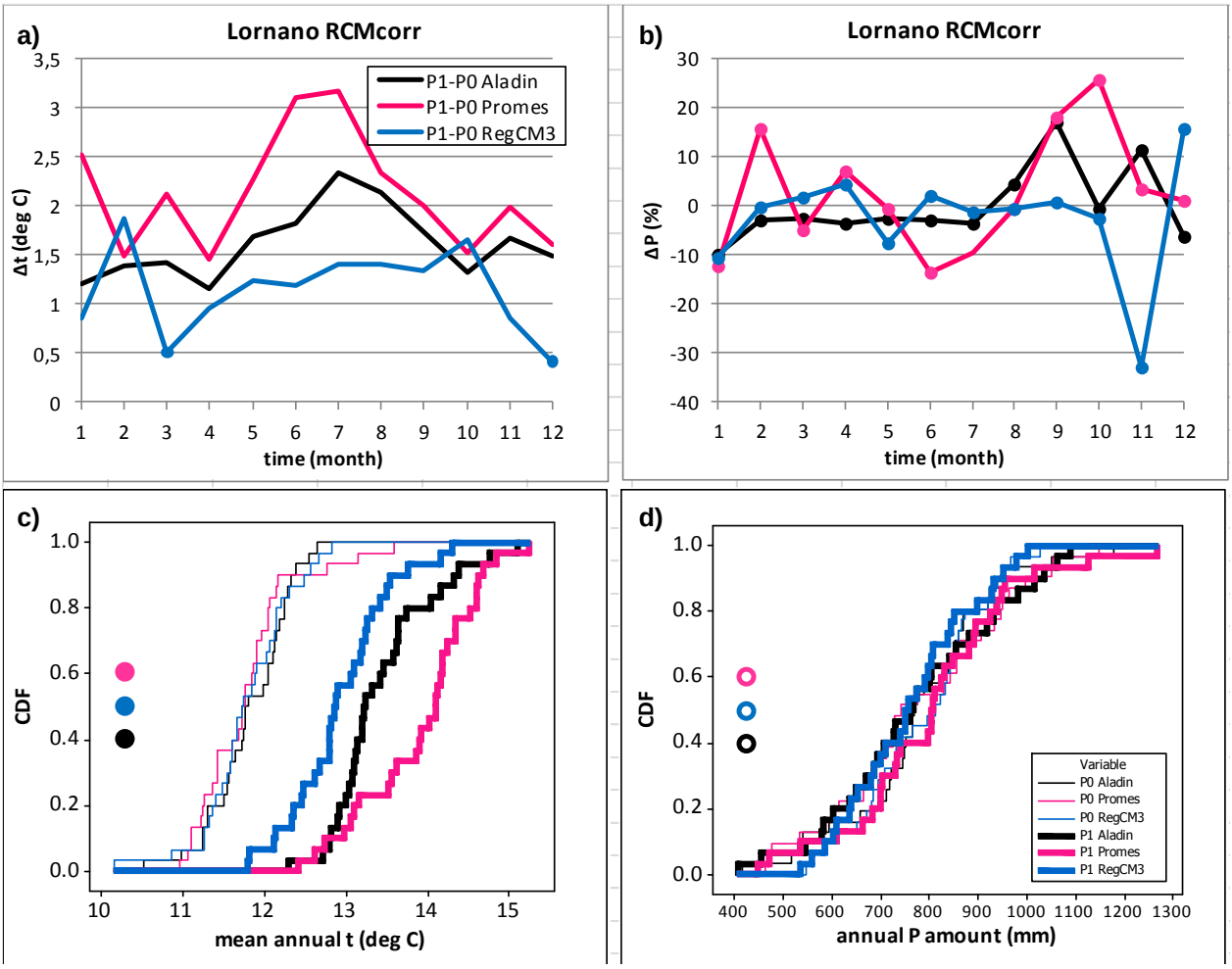

Figure 3.6 *Lornano station: a) monthly mean temperature P1 vs. P0 change; b) relative monthly precipitation P1 vs. P0 change; c) empirical cumulative distribution functions CDFs of mean annual temperature in P0 and P1; d) same as c) but for annual precipitation amount. Time periods are: P0 1961-1990 and P1 2021-2050. Statistically significant differences in a) and b) according to the Wilcoxon-Mann-Whitney nonparameteric rank-sum test and 5% significance level are marked by the filled circles. Statistically significant differences according to the Kolmogorov-Smirnov test and 5% significance level between CDFs in two periods for every model in panels c) and d) are marked by the filled circles. Model time series are RCMcorr.*

Montemonaco

Air temperature and precipitation from local observations at the Montemonaco climatological station, EOBS data and bias corrected simulations of the three regional climate models in the historical period P0 (1961-1990) are compared in Fig. 3.7. The EOBS air temperature is lower than the local observations throughout the annual cycle (Fig. 3.7a). Since EOBS data made the basis for calculation of RCM biases, the bias-corrected modelling data, RCMcorr, are therefore constrained to be closer to EOBS than to the observations. This restriction makes the RCMcorr annual cycles also colder than the local observations; the RCMcorr graphs overlap exactly with the EOBS curve and could be hardly distinguished from each other on Fig. 3.7a. The underestimation of the observed air temperature seen in Fig. 3.7a) may seem small, but it becomes substantial in the annual mean. The same as for temperature can be also observed for precipitation (Fig. 3.7b).

Annual cycles of both mean air temperature and mean total precipitation are, during the P0 (1961-1990) period, generally similar in all datasets considered (Fig. 3.7a,b).

Time series of the mean annual air temperature/precipitation amount in the period 1951-2000 (Fig. 3.7e,f) indicates that the EOBS and RCMcorr values are lower than the local observations, further confirming the underestimations of the local annual cycle shown in Fig 3.7 a) and b). A large year-to-year variation of the air temperature annual means /annual precipitation amount differs among various data sources (Fig. 3.2e,f). This difference in the representation of interannual variability does not signify that a particular model failed to correctly simulate observed natural variability. It may be attributed to a different external forcing of the RCMs by different global circulation models, but also to a different internal variability inherent to each single RCM (see Methodology). Standard deviation of the annual mean air temperature/annual precipitation amount time series in all data sources are quite similar indicating that the RCMs are close to observations in representing atmospheric natural variability.

The empirical cumulative distribution functions (CDFs) does not show a close correspondence of EOBS and RCMcorr data from the local observations in the P0 through all annual air temperature/annual total precipitation ranges (Fig. 3.7g,h).

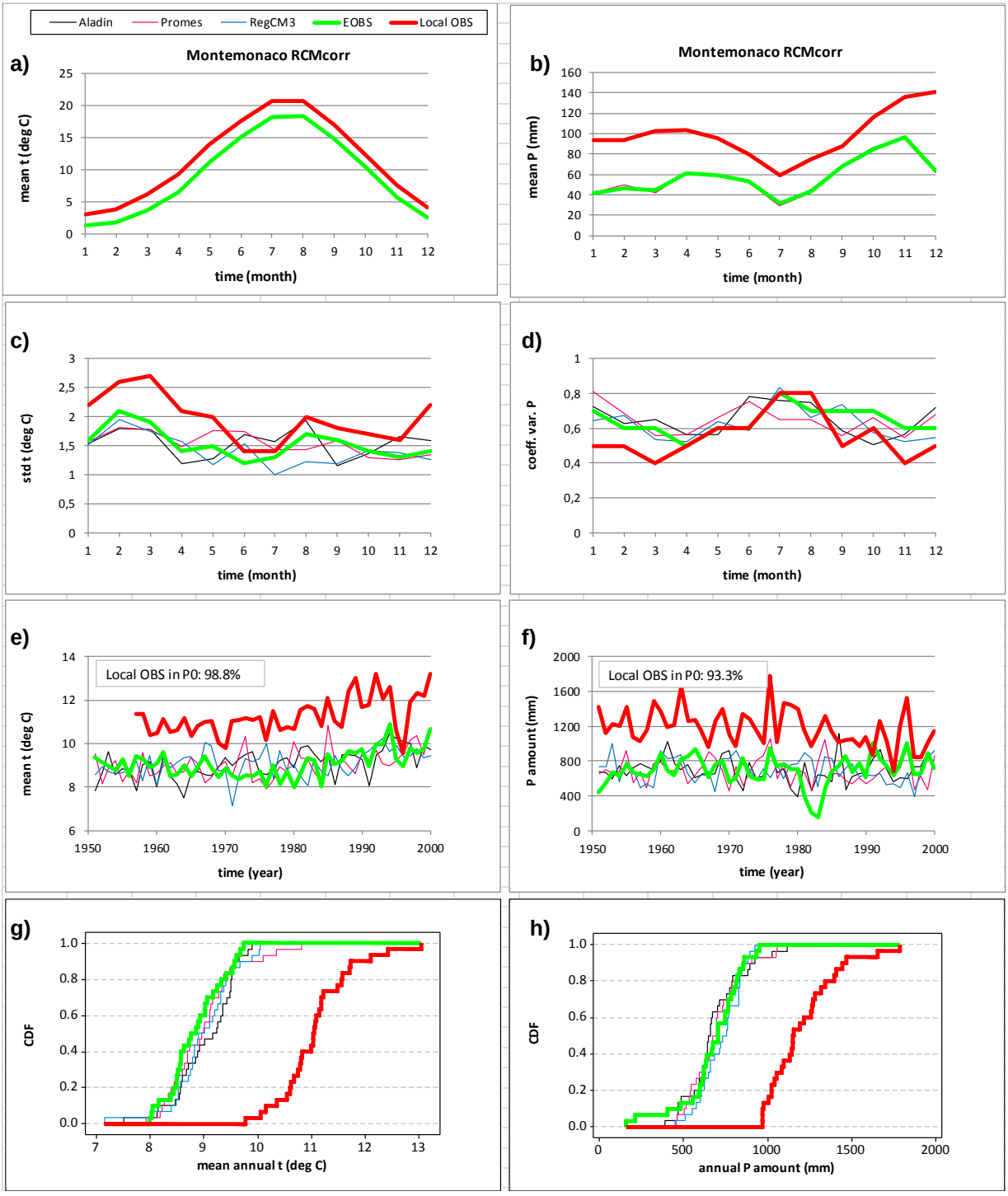

Figure 3.7 *Montemonaco station: annual cycle a) mean monthly temperature, b) monthly precipitation amount, c) mean monthly temperature standard deviation, d) coefficient of variation of monthly precipitation amount; time series e) mean annual temperature, f) annual precipitation amount; empirical cumulative distribution functions CDFs g) mean annual temperature, h) annual precipitation amount. Model time series are RCMcorr. Period of analysis: P0 (1961-1990).*

For the period 1951-2050, all three bias corrected models simulate statistically significant increasing trends in the mean annual temperature from 0.17 °C/10yr in RegCM to 0.32 °C/10yr in Promes (Fig. 3.8). It should be emphasised here that, in the model simulations for the period 1951-2000, the observed concentrations of the greenhouse gases (GHGs) is used, and in the period 2001-2050, the models were forced by the GHGs concentrations for the IPCC A1B scenario. In the period 1961-2008, when the local observations were available, all three models agree with the observations in the simulated sign of trend, with a magnitude of trend similar to that of the local observations (0.3 °C/10yr; Table 2.6).

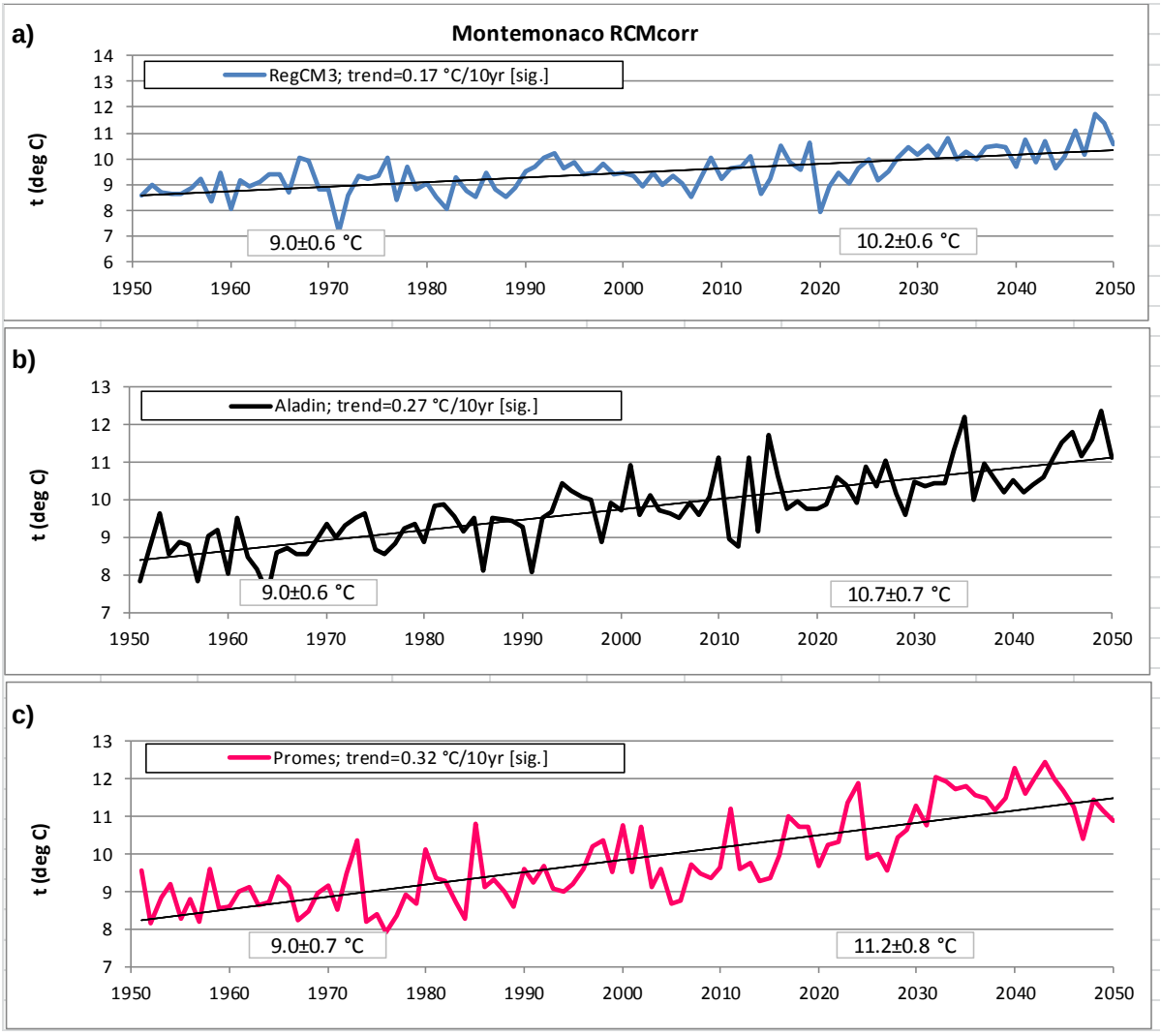

Figure 3.8 *Montemonaco station: annual mean temperature and associated linear trend in a) RegCM3, b) Aladin, c) Promes. Decadal trend based on the entire time series is shown in panel legends. The statistical significance of the trend is assessed using the Mann-Kendall test and 5% significance level. Additional numbers at the bottom of each panel are mean values and standard deviations during P0 (1961-1990) and P1 (2021-2050). Model time series are RCMcorr.*

All three bias-corrected models simulate decreasing trend in the annual precipitation amount for the period 1951-2050 (Fig. 3.9), even if, for all the models, these trends are not statistically significant. For the period 1951-2008, when local observations at the Montemonaco station show decreasing trend in annual precipitation amount (-26.6mm/10yr; Table 2.7), the models simulates the same sign of the trend as observed, but with greatly reduced amplitude and no statistical significance. This implies that, according to the CC-WaterS bias corrected RCMcorr simulations presented here, no robust estimates of significant precipitation change could be made for the first part of the 21st century.

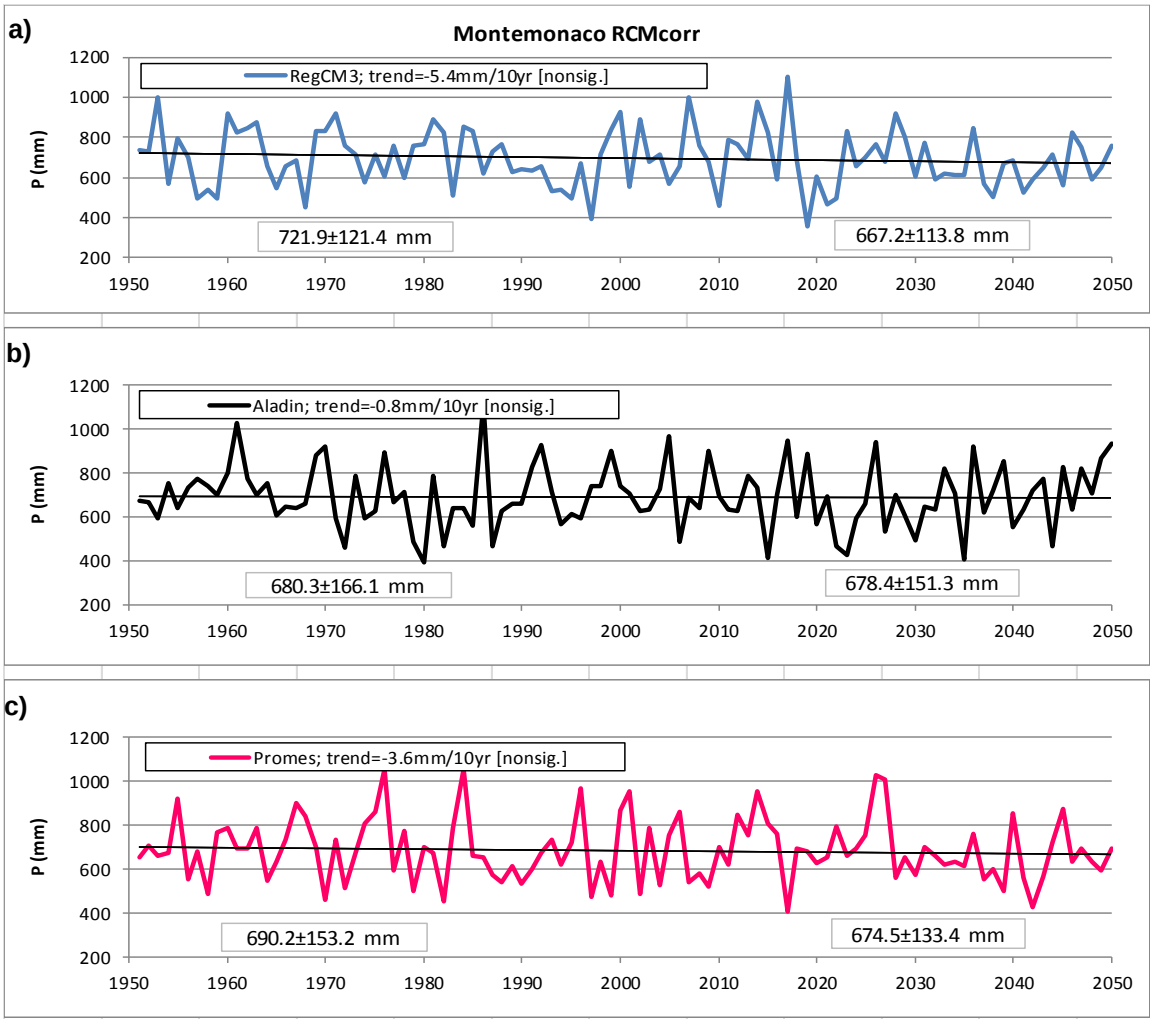

Figure 3.9 *Montemonaco station: annual precipitation amount and associated linear trend in a) RegCM3, b) Aladin, c) Promes. Decadal trend based on the entire time series is shown in panel legends. The statistical significance of the trend is assessed using the Mann-Kendall test and 5% significance level. Additional numbers at the bottom of each panel are mean values and standard deviations during P0 (1961-1990) and P1 (2021-2050). Model time series are RCMcorr.*

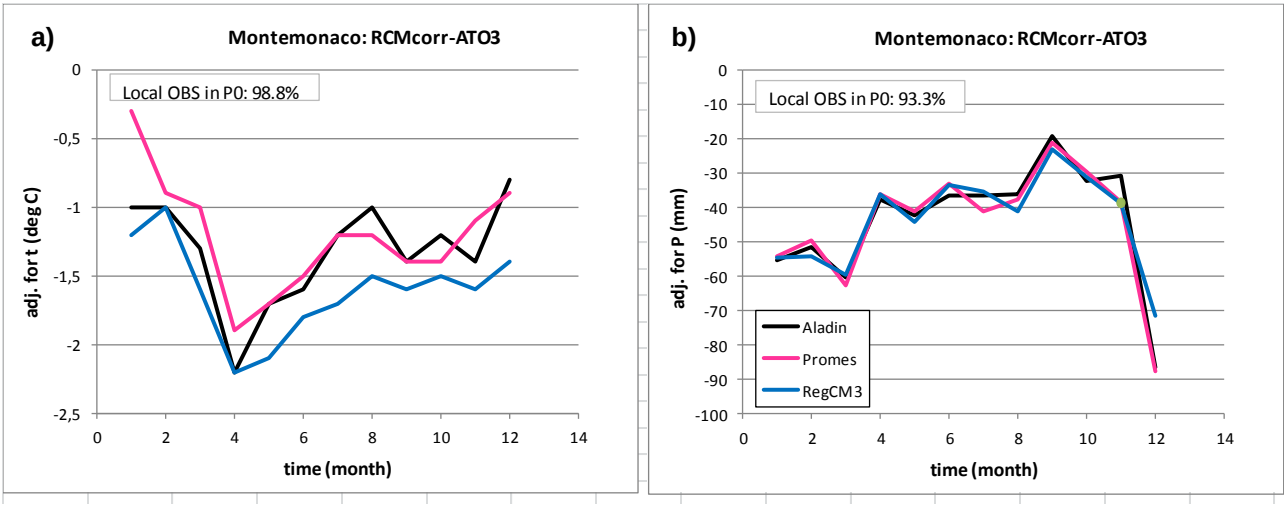

Figure 3.10 *Montemonaco station: adjustment differences a) mean monthly temperature b) monthly precipitation amount. Differences are based on 1961-1990 period and the availability of local observations in this period is almost 100%. Statistically significant differences according to the Wilcoxon-Mann-Whitney nonparameteric rank-sum test and 5% significance level are marked by the filled circles.*

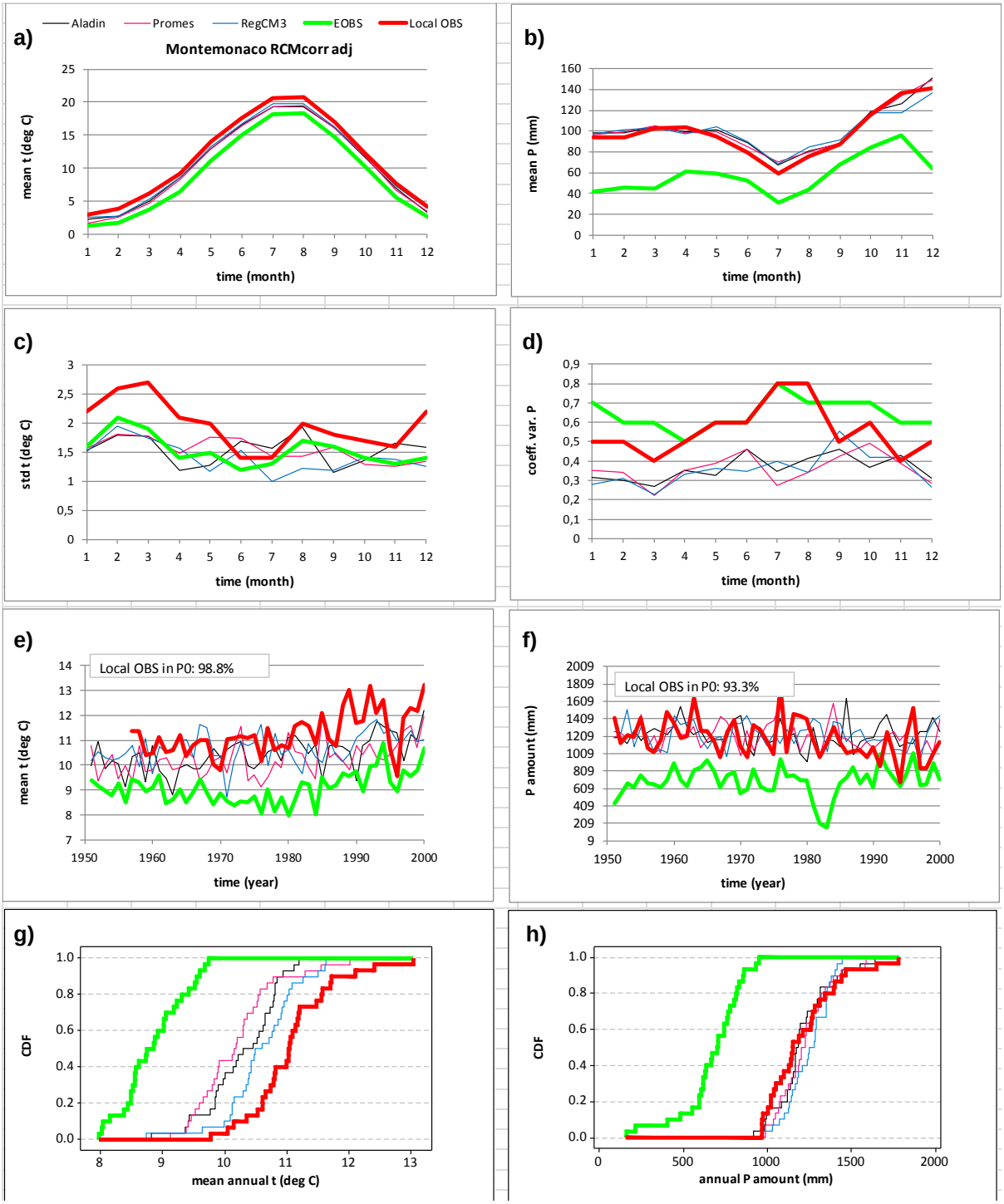

Figure 3.11 *Montemonaco station: annual cycle a) mean monthly temperature, b) monthly precipitation amount, c) mean monthly temperature standard deviation, d) coefficient of variation of monthly precipitation amount; time series e) mean annual temperature, f) annual precipitation amount; empirical cumulative distribution functions CDFs g) mean annual temperature, h) annual precipitation amount. Model time series are RCMcorr_adj. Period of analysis: P0 (1961-1990).*

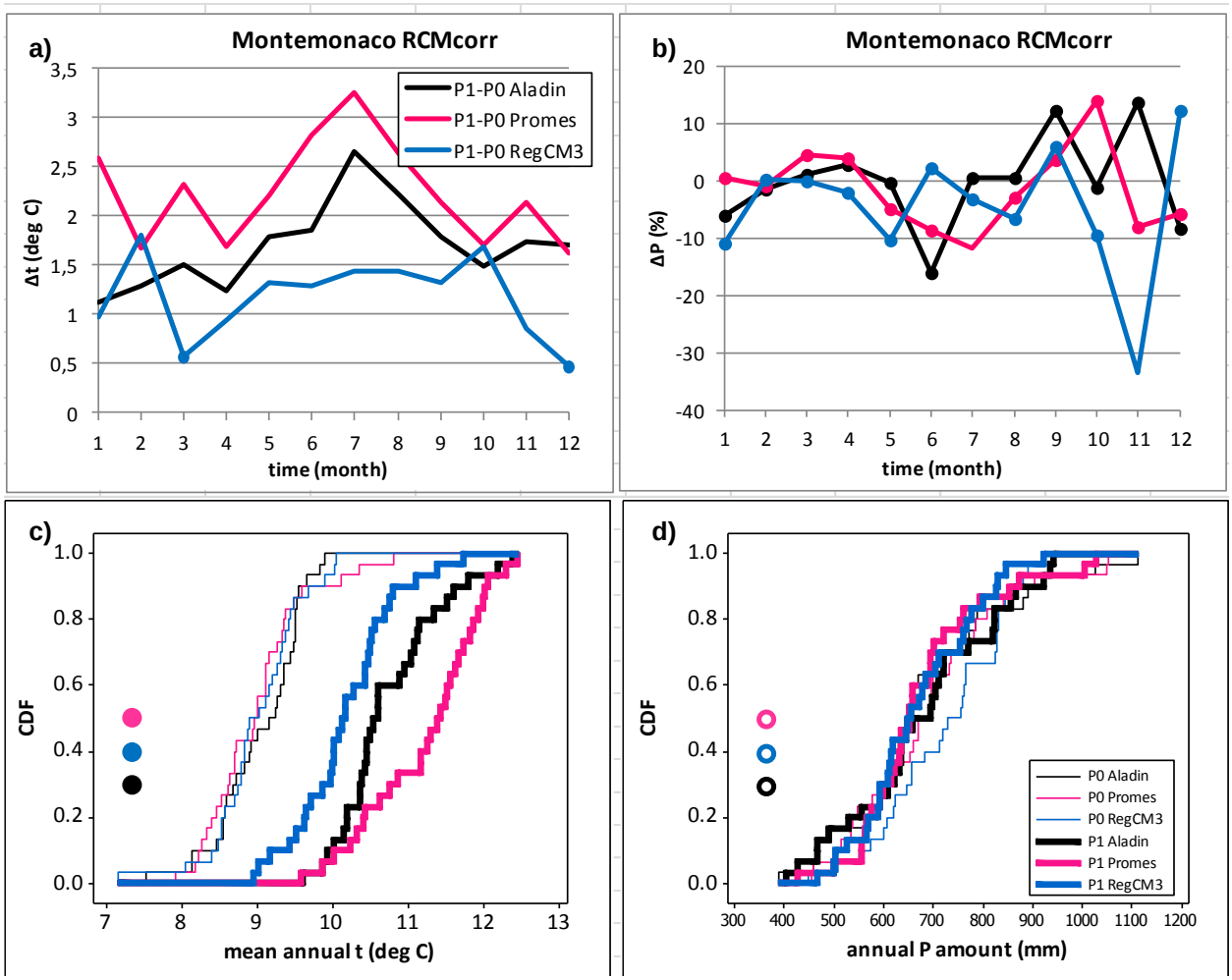

Figure 3.12 *Montemonaco station: a) monthly mean temperature P1 vs. P0 change; b) relative monthly precipitation P1 vs. P0 change; c) empirical cumulative distribution functions CDFs of mean annual temperature in P0 and P1; d) same as c) but for annual precipitation amount. Time periods are: P0 1961-1990 and P1 2021-2050. Statistically significant differences in a) and b) according to the Wilcoxon-Mann-Whitney nonparameteric rank-sum test and 5% significance level are marked by the filled circles. Statistically significant differences according to the Kolmogorov-Smirnov test and 5% significance level between CDFs in two periods for every model in panels c) and d) are marked by the filled circles. Model time series are RCMcorr.*

Appendix 1: Description of the supplement files containing observed data

Two files in the xls format containing time series of the observed data are prepared:

1. ATO3_general_Lornano.xls: contains monthly, seasonal (MAM – spring, JJA- summer, SON- autumn, DJF –winter) and annual precipitation amounts for the available period from 1951 to 2008 and mean monthly, seasonal (MAM – spring, JJA- summer, SON- autumn, DJF –winter) and annual 2m air temperature for the available period from 1957 to 2008 for Lornano station;

2. ATO3_general_Montemonaco.xls: contains monthly, seasonal (MAM – spring, JJA- summer, SON- autumn, DJF –winter) and annual precipitation amounts for the available period from 1951 to 2008 and mean monthly, seasonal (MAM – spring, JJA- summer, SON- autumn, DJF –winter) and annual 2m air temperature for the available period from 1957 to 2008 for Lornano station

Appendix 2: Description of the supplement files containing simulated data

Three files in the xls format containing simulated time series are prepared:

1. ATO3_RCM_MM_Sept2014.xls: contains monthly mean 2m air temperature and monthly total precipitation sum. Data for each location are in the separate sheet. Columns B and C contain specific year and month. Columns from D to F contain RCMcorr air temperature from the three models, columns from G to I contain RCMcorr precipitation from the same models. Remaining columns have the same description but are based on the RCMcorr_adj time series.

2. ATO3_RCM_SM_Sept2014.xls: contains seasonal mean 2m air temperature and seasonal total precipitation sum. The structure of the file is similar to 1. Data are presented first for the MAM season, and then in the same manner for the JJA, SON and DJF seasons.

3. ATO3_RCM_YM_Sept2014.xls: contains annual mean 2m air temperature and annual total precipitation sum. The structure of the file is similar to 1. and 2.

Table A List of abbreviations in xls files:

Variables	temp	2m air temperature
	precip	Total precipitation amount
Average/sum interval	MM	Monthly mean/sum
	SM	Seasonal mean/sum
	YM	Annual mean/sum
CC-WaterS regional climate models (RCM)	MOD1	Aladin
	MOD2	RegCM3
	MOD3	Promes
Types of RCM time series	corr	CC-WaterS regional climate simulations bias-corrected using E-OBS data (i.e. RCMcorr)
	corr_adj	Adjusted RCMcorr time series using local data for stations and variables when more than 90% of local data are available in the period 1961-1990 (i.e. RCMcorr_adj)
Seasons	MAM	climatological spring (March, April, May)
	JJA	climatological summer (June, July, August)
	SON	climatological autumn (September, October, November)
	DJF	climatological winter (December, January, February)

References

Bubnova, R., Hello, G., Bénard, P., Geleyn, J-F., 1995. Integration of the fully elastic equations cast in hydrostatic pressure terrain-following coordinate in the framework of the ARPEGE/Aladin NWP system. *Mon.Wea.Rev.*,123:515–535.

Castro, M., Fernández C., Gaertner M.A., 1993. Description of a meso-scale atmospheric numerical model. In:J.I. Díaz, J.L. Lions (eds), Mathematic, climate and environment, Masson.

Déqué, M., 2007. Frequency of precipitation and temperature extremes over France in an anthropogenic scenario: Model results and statistical correction according to observed values. *Global and Planetary Change*, 57:16–26.

Formayer, H., Haas P., 2010. Correction of RegCM3 model output dana using a rank matching approach applied on various meteorological parameters. In Deliverable D3.2 RCM output localization methods (BOKU-contribution of the FP6 CECILIA project on http://www.cecilia-eu.org/).

Haylock, M.R., Hofstra N., Klein Tank A.M.G., Klok E.J., Jones P.D., New M., 2008. A European daily high-resolution gridded dataset of surface temperature and precipitation for 1950-2006. J. Geophys. Res.,113, D20119, doi:10.1029/2008JD010201.

Pal, J.S., and Coauthors, 2007. Regional climate modeling for the developing world: The ICTP RegCM3 and RegCNET. *Bull. Amer. Meteor. Soc.*, 88:1395–1409.

CC on ATO 3 Test Area – Macerata 30.09.2014

Let's grow up together

DRINK ADRIA

Adriatic IPA
Cross Border Cooperation 2007-2013

The project is co-funded by the European Union,
Instrument for Pre-Accession Assistance

Report:

Climate and climate change change data for the Ostuni pilot area (Italy, Apulia region)

Water Research Institute –
National Research Council

(FB3)

Bari, September 2014

Let's grow up together

DRINK ADRIA

Adriatic IPA
Cross Border Cooperation 2007-2013

The project is co-funded by the European Union,
Instrument for Pre-Accession Assistance

Table of contents

1. INTRODUCTION

This report is a contribution to the DRINKADRIA Work Package 4 on regional characteristics of climate and climate change which is the base for water resources availability analyses. An analysis of the observed and simulated climate and climate changes is presented for the pilot area of Ostuni (Apulia region).

An assessment of the present and future climates is based on the results from numerical simulations of the three regional climate models that were also analysed for the purpose of the CC-WaterS[1] project. These models participated in the ENSEMBLES[2] project, with downscaling simulations at a 25-km horizontal resolution. In this report, analysis of the model data is carried out for those model grid cells which were the closest to the locations of the Ostuni meteorological station.

The regional climate models (RCMs) used are the Aladin (Bubnova et al. 1995), Promes (Castro et al. 1993) and RegCM3 models (Pal et al. 2007). The RCMs were forced by the observed concentrations of the greenhouse gases (GHGs) from 1951 to 2000; from 2001 onwards the IPCC[3] A1B scenario of the GHGs emissions is applied. The initial and boundary data for each RCM were provided from different global climate models (GCMs): the ECHAM5 GCM data were used to force RegCM3, Aladin was forced by the Arpege GCM and Promes was forced by the HadCM3Q GCM. For the present climate, models are compared with the local DHMZ observations and with the EOBS gridded temperature and precipitation data (Haylock et al. 2008). The following two abbreviations are used in the report:

1. RCMcorr: the RCMs' output was bias corrected by EOBS data, see e.g. Déqué (2007) and Formayer and Haas (2010) for the description of the bias correcting methodology. The RCMcorr data are available from the CC-WaterS database http://climdat.boku.ac.at/opendap/ccwaters.

   Additional details regarding bias correction procedure are available from http://climdat.boku.ac.at/opendap/ccwaters/Documentations/RCM_explanator_report.pdf .

2. RCMcorr_adj: this is further adjusted model time series due to the differences between EOBS data and local observations. The adjustment procedure is described in detail in subsection 3.2.

The purpose of this report is to provide an input for further hydrological analyses. However, due to experimental nature of the regional climate simulations, several limitations should be emphasised:

1. Spatial resolution of the regional climate model simulations (RCMs) used here is 25 km. At this resolution the main orographic features and the land-sea boundary of the Croatian coast are resolved reasonably well. However, at the same

[1] www.ccwaters.eu

[2] www.ensembles-eu.org

[3] Intergovernmental Panel on Climate Change, www.ipcc.ch

resolution local characteristics for specific station or catchment may not be fully resolved.

2. For the period 1951-2000 all the RCMs in this report are forced by historical (observed) concentrations of the GHGs. From 2001 onwards, however, the IPCC A1B scenario is applied, meaning that only one assumption of the GHG concentration is evaluated. This must be taken into consideration when evaluating the amplitude of projected climate changes (e.g. the higher GHGs emission scenarios are usually associated with the higher temperature increase).

3. The three RCMs models used here account only for a part of possible modelling uncertainties. The use of the multi-model ensemble approach in climate projection studies is strongly recommended in order to avoid projection dependence on specific model assumptions.

4. In the analysed RCM simulations of the reference climate, the RCMs are not reproducing the actual variability observed in the real climate system. Since RCMs are forced at the boundaries by different global climate models (each having its own internal variability, e.g. the sequence of warm and cold years over Europe), the RCMs simulate different variability, e.g. their own sequence of warm and cold years (or dry and wet years). Specific values indicated in the time series presented in this report do not signify a specific prediction for a specific year.

   The models can be compared with observations and with each other in terms of the reference and projected mean climate and overall variability. Models simulations of the future climate should be interpreted as projections of possible state(s) of the climate system which is sensitive to applied initial and boundary conditions, GHGs scenarios and a model internal configuration. Projections are expected to represent future trends and changes over longer time period as realistic as possible.

A detailed discussion on the modelling limitations emphasized in this subsection see e.g. Hawkins and Sutton (2009) and Jacob et al. (2014).

2. PRESENT CLIMATE ANALYSIS

2.1 Meteorological database and analysis of local observations: the Ostuni pilot area (Italy, Apulia Region)

The Ostuni pilot area is located in the Apulia region (south of Italy); the climate is tipically Mediterranean, with hot and dry summer and wet and temperate winter.
The current climate analysis presented in this report has been performed considering 9 temperature stations and 9 rainfall stations, whose location within the study area is shown in figure 1.
In table 1 and 2 a comprehensive list of the available meteorological stations is presented for temperature and precipitation, respectively.

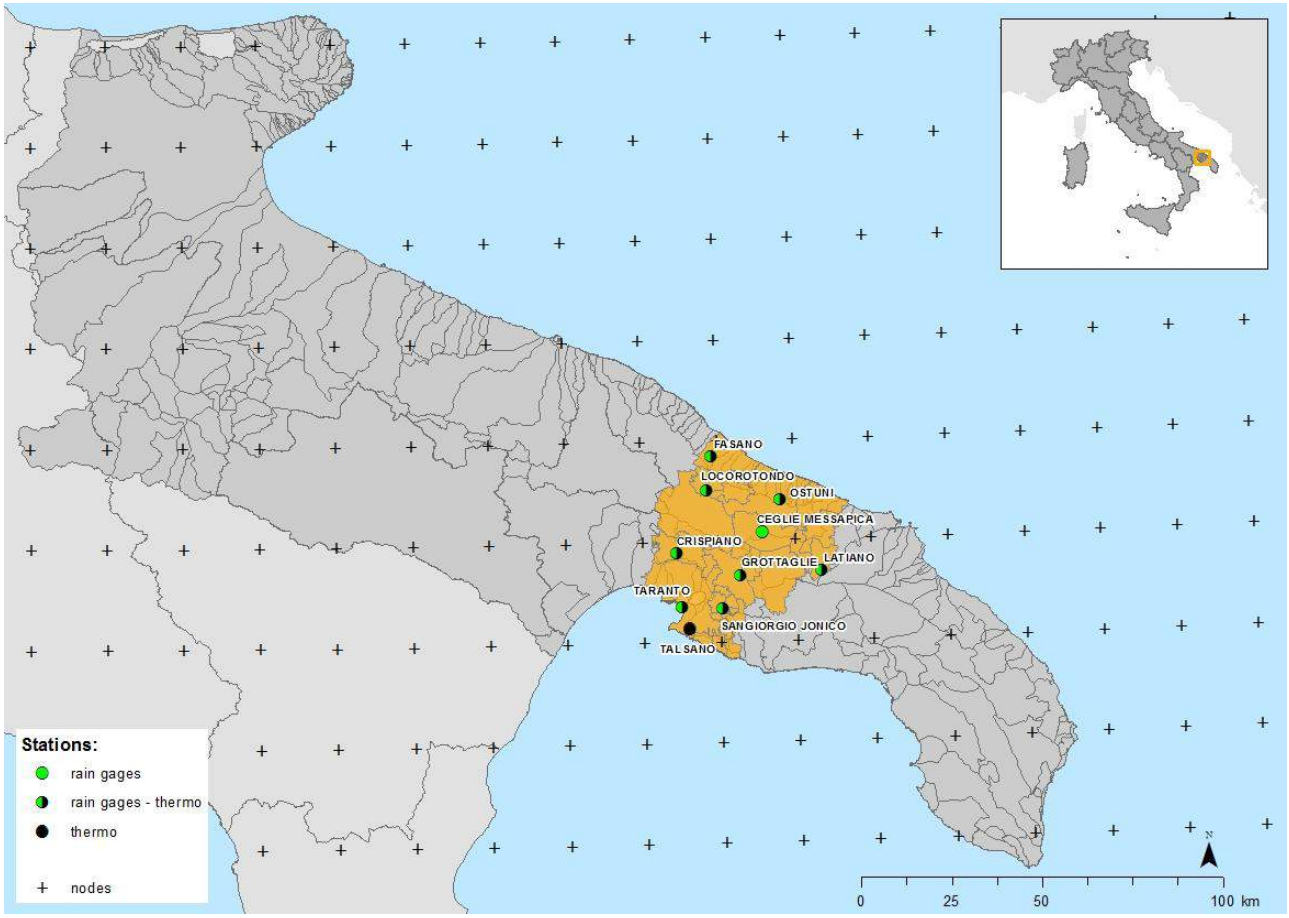

Figure 1 Ostuni area, Apulia Region, Italy

TEMPERATURE						
	Station	**h (m)**	**ϕ(°)**	**λ (°)**	**t**	**%**
1	CRISPIANO	264	17.2	40.6	1950-2007	86.8%

2	FASANO	121	17.4	40.8	1950-2007	76.0%
3	GROTTAGLIE	140	17.4	40.5	1950-2007	91.5%
4	LATIANO	107	17.7	40.5	1950-2007	87.2%
5	LOCOROTONDO	404	17.3	40.8	1950-2007	93.8%
6	OSTUNI	234	17.6	40.7	1950-2007	75.7%
7	SANGIORGIO JONICO	86	17.4	40.5	1950-2007	67.0%
8	TALSANO	37	17.3	40.4	1950-2007	52.9%
9	TARANTO	27	17.3	40.5	1950-2007	90.5%

Table 1 Geographical station (elevation *h* (m), longitude λ, latitude φ) and available measurement time periods for temperature data.

PRECIPITATION						
	Station	**h (m)**	**ϕ(°)**	**λ (°)**	**R**	**%**
1	CEGLIE MESSAPICA		17.5	40.6	1950-2007	99.7%
2	CRISPIANO	264	17.2	40.6	1950-2007	96.4%
3	FASANO	121	17.4	40.8	1950-2007	92.7%
4	GROTTAGLIE	140	17.4	40.5	1950-2007	97.3%
5	LATIANO	107	17.7	40.5	1950-2007	99.1%
6	LOCOROTONDO	404	17.3	40.8	1950-2007	100.0%
7	OSTUNI	234	17.6	40.7	1950-2007	100.0%
8	SANGIORGIO JONICO	86	17.4	40.5	1950-2007	86.2%
9	TARANTO	27	17.3	40.5	1950-2007	99.7%

Table 2 Geographical station (elevation *h* (m), longitude λ, latitude φ) and available measurement time periods for precipitation data

2.2 Air temperature analysis

The available air temperature time series have been analysed in terms of the basic statistics (mean, standard deviation, maximum and minimum) at annual and seasonal time scale for the reference period 1961-1990 (*P0*) and for the whole observation period 1950-2007 (P_{obs}) (table 3).
In table 4 the percentiles for annual and seasonal mean air temperature according to the empirical distribution from the reference period 1961-1990 P0 and for the whole

observation period 1950-2007 P_{obs} of the nine climatological stations in the Ostuni pilot area are shown

Moreover, air temperature decadal trends (°C/10year) based on the reference period *P0* and the whole observation period P_{obs} are shown (table 5).

	DJF		MAM		JJA		SON		Year	
	CRISPIANO									
	P0	**P_{obs}**	**P0**	**P_{obs}**	**P0**	**P_{obs}**	**P0**	**P_{obs}**	**P0**	**P_{obs}**
mean (°C)	8.4	8.4	14.0	14.1	24.0	24.4	17.1	17.0	15.8	15.9
stdev (°C)	0.9	0.9	0.8	0.9	0.8	1.0	1.0	1.1	0.5	0.7
max (°C)	10.1	10.1	15.5	15.7	25.2	27.3	18.5	18.7	17.1	17.4
min (°C)	7.0	7.0	12.6	12.3	22.2	22.2	14.9	14.3	15.2	14.5
	FASANO									
	P0	**P_{obs}**	**P0**	**P_{obs}**	**P0**	**P_{obs}**	**P0**	**P_{obs}**	**P0**	**P_{obs}**
mean (°C)	9.7	9.9	14.3	14.8	23.6	24.3	17.2	17.7	15.7	16.6
stdev (°C)	1.8	1.5	1.6	1.8	1.3	1.8	1.5	1.7	1.6	1.8
max (°C)	12.4	12.6	16.7	17.8	25.8	28.3	19.5	20.4	17.7	18.9
min (°C)	4.5	4.5	9.9	9.9	20.1	19.8	14.1	13.7	12.5	12.5
	GROTTAGLIE									
	P0	**P_{obs}**	**P0**	**P_{obs}**	**P0**	**P_{obs}**	**P0**	**P_{obs}**	**P0**	**P_{obs}**
mean (°C)	9.3	9.3	14.8	15.0	24.7	25.4	17.9	17.9	16.8	17.0
stdev (°C)	0.7	0.9	1.0	1.2	0.8	1.2	1.1	1.1	0.4	0.8
max (°C)	10.6	11.9	16.6	18.0	26.0	28.2	19.7	19.7	17.3	18.5
min (°C)	7.5	7.3	12.1	12.1	23.0	22.8	15.6	14.3	15.8	14.5
	LATIANO									
	P0	**P_{obs}**	**P0**	**P_{obs}**	**P0**	**P_{obs}**	**P0**	**P_{obs}**	**P0**	**P_{obs}**
mean (°C)	8.5	8.6	14.4	14.4	23.9	24.5	17.0	17.2	16.0	16.3
stdev (°C)	0.9	0.9	1.2	1.1	0.9	1.2	1.2	1.0	0.6	0.6
max (°C)	10.0	10.6	17.2	17.2	25.4	28.0	18.7	18.7	17.0	17.5
min (°C)	6.6	6.6	11.8	11.8	22.4	22.4	14.2	14.2	15.1	15.1
	LOCOROTONDO									

	P0	P_{obs}	P0	P_{obs}	P0	P_{obs}	P0	P_{obs}	P0	P_{obs}
mean (°C)	7.5	7.4	12.7	12.8	22.3	22.8	15.7	15.6	14.6	14.7
stdev (°C)	1.2	1.2	1.4	1.3	0.8	1.1	1.5	1.2	0.9	0.9
max (°C)	10.3	10.3	15.1	15.1	23.8	26.0	18.5	18.5	16.4	16.4
min (°C)	5.3	4.7	9.7	9.7	21.0	20.2	13.0	13.0	13.4	12.8
	OSTUNI									
	P0	P_{obs}	P0	P_{obs}	P0	P_{obs}	P0	P_{obs}	P0	P_{obs}
mean (°C)	8.4	8.6	13.7	14.0	23.3	23.9	16.7	16.9	15.7	16.0
stdev (°C)	0.6	0.8	0.9	1.1	0.8	1.2	1.1	1.1	0.4	0.7
max (°C)	9.5	11.1	15.3	16.3	24.6	27.0	18.2	18.8	16.4	17.5
min (°C)	7.3	6.8	11.7	11.7	21.0	21.0	14.4	14.4	14.9	14.7
	SANGIORGIOJONICO									
	P0	P_{obs}	P0	P_{obs}	P0	P_{obs}	P0	P_{obs}	P0	P_{obs}
mean (°C)	9.5	9.5	14.7	15.0	24.2	25.0	18.0	17.9	16.5	16.9
stdev (°C)	1.0	0.9	1.0	1.1	0.9	1.4	1.3	1.2	0.7	1.0
max (°C)	10.9	11.7	16.2	17.3	25.6	28.8	20.5	20.5	17.7	18.4
min (°C)	7.0	7.0	13.0	13.0	22.6	22.6	15.8	15.8	15.7	14.9
	TALSANO									
	P0	P_{obs}	P0	P_{obs}	P0	P_{obs}	P0	P_{obs}	P0	P_{obs}
mean (°C)	9.3	9.5	13.9	14.4	23.8	24.6	17.6	17.9	16.3	16.7
stdev (°C)	0.7	0.9	0.8	1.2	0.8	1.2	1.0	1.0	0.4	0.8
max (°C)	10.2	11.7	15.0	16.8	25.2	27.9	19.9	19.9	16.8	18.1
min (°C)	7.8	7.8	12.2	12.2	23.1	23.1	16.1	15.9	15.7	15.4
	TARANTO									
	P0	P_{obs}	P0	P_{obs}	P0	P_{obs}	P0	P_{obs}	P0	P_{obs}
mean (°C)	10.2	10.4	14.9	15.3	24.8	25.5	18.4	18.6	17.1	17.5
stdev (°C)	0.8	1.0	0.8	1.0	0.6	1.3	1.1	1.1	0.2	0.8
max (°C)	11.4	13.1	16.9	18.1	25.9	29.4	20.0	21.0	17.4	19.3
min (°C)	8.6	8.0	13.2	13.2	23.7	23.7	16.1	15.7	16.7	16.1

Table 3 Basic statistics (mean, standard deviation, maximum and minimum) for annual and seasonal mean air temperature for the reference period *P0* 1961-1990 and for the whole observation period P_{obs} 1950-2007 for the nine climatological stations in the Ostuni pilot area.

	DJF		MAM		JJA		SON		Year	
	CRISPIANO									
Percentile	P0	P_{obs}	P0	P_{obs}	P0	P_{obs}	P0	P_{obs}	P0	P_{obs}
1	6.98	6.98	12.57	12.30	22.20	22.20	14.90	14.25	15.20	14.55
2	6.98	7.01	12.57	12.42	22.20	22.35	14.90	14.48	15.20	14.63
5	7.01	7.09	12.74	12.65	22.42	22.55	15.06	15.11	15.21	15.00
10	7.08	7.23	12.97	12.79	22.55	23.32	15.38	15.37	15.22	15.09
90	9.56	9.73	15.17	15.42	25.07	25.76	18.10	18.20	16.33	16.76
95	9.94	9.84	15.42	15.60	25.18	26.37	18.30	18.38	16.89	17.14
98	10.10	10.03	15.53	15.67	25.20	26.94	18.47	18.63	17.05	17.32
99	10.10	10.10	15.53	15.70	25.20	27.30	18.47	18.72	17.05	17.36
	FASANO									
Percentile	P0	P_{obs}	P0	P_{obs}	P0	P_{obs}	P0	P_{obs}	P0	P_{obs}
1	4.53	4.53	9.87	9.87	20.13	19.75	14.12	13.65	12.45	12.45
2	4.53	4.93	9.87	10.14	20.13	19.87	14.12	13.79	12.45	12.45
5	5.45	6.77	10.42	11.38	21.29	20.92	14.22	14.20	12.49	13.01
10	7.29	8.37	12.25	12.45	21.98	21.96	14.59	15.38	12.94	13.26
90	11.61	11.51	15.93	16.73	25.10	26.52	19.03	19.50	17.25	18.59
95	12.04	12.16	16.46	17.52	25.69	27.15	19.25	20.01	17.67	18.68
98	12.40	12.57	16.67	17.71	25.82	28.08	19.48	20.33	17.71	18.85
99	12.40	12.63	16.67	17.75	25.82	28.30	19.48	20.35	17.71	18.85
	GROTTAGLIE									
Percentile	P0	P_{obs}	P0	P_{obs}	P0	P_{obs}	P0	P_{obs}	P0	P_{obs}

1	7.47	7.33	12.08	12.08	23.00	22.83	15.58	14.27	15.83	14.53
2	7.47	7.39	12.08	12.40	23.00	22.91	15.58	14.93	15.83	14.81
5	7.95	7.54	12.94	12.84	23.25	23.45	15.80	15.92	15.92	15.63
10	8.44	8.29	13.75	13.47	23.68	24.06	16.04	16.38	16.21	15.87
90	9.98	10.25	16.18	16.45	25.54	27.30	19.11	19.15	17.33	17.87
95	10.26	10.73	16.51	16.75	25.78	27.62	19.52	19.42	17.33	18.35
98	10.57	11.53	16.58	17.98	26.02	28.00	19.70	19.58	17.33	18.46
99	10.57	11.93	16.58	18.00	26.02	28.18	19.70	19.70	17.33	18.51
	LATIANO									
Percentile	**P0**	**P_{obs}**	**P0**	**P_{obs}**	**P0**	**P_{obs}**	**P0**	**P_{obs}**	**P0**	**P_{obs}**
1	6.60	6.60	11.77	11.77	22.40	22.40	14.20	14.20	15.12	15.12
2	6.60	6.61	11.77	12.03	22.40	22.51	14.20	14.57	15.12	15.12
5	6.61	6.93	12.09	12.47	22.55	22.74	14.72	15.30	15.12	15.13
10	6.84	7.53	12.68	12.83	22.72	22.99	15.46	16.04	15.28	15.38
90	9.36	9.83	15.68	15.48	24.98	26.21	18.50	18.49	16.89	17.02
95	9.76	10.24	16.54	16.01	25.30	26.70	18.64	18.55	17.00	17.41
98	10.02	10.49	17.20	16.75	25.40	27.57	18.73	18.69	17.00	17.45
99	10.02	10.55	17.20	17.20	25.40	28.02	18.73	18.73	17.00	17.45
	LOCOROTONDO									
Percentile	**P0**	**P_{obs}**	**P0**	**P_{obs}**	**P0**	**P_{obs}**	**P0**	**P_{obs}**	**P0**	**P_{obs}**
1	5.27	4.73	9.72	9.73	20.97	20.25	12.95	12.95	13.44	12.83
2	5.27	4.91	9.72	10.03	20.97	20.65	12.95	13.14	13.44	12.90
5	5.77	5.26	10.32	10.61	21.25	21.33	13.24	13.36	13.47	13.37
10	6.19	5.79	11.13	11.31	21.47	21.50	13.83	13.91	13.64	13.61
90	9.06	8.90	14.70	14.71	23.39	24.47	17.50	17.36	16.09	15.94
95	9.64	9.34	15.09	14.97	23.67	24.92	18.00	17.53	16.39	16.29
98	10.28	10.18	15.10	15.09	23.76	25.53	18.47	18.15	16.44	16.40
99	10.28	10.28	15.10	15.10	23.77	25.92	18.47	18.46	16.44	16.44

	OSTUNI									
Percentile	**P0**	**P_{obs}**	**P0**	**P_{obs}**	**P0**	**P_{obs}**	**P0**	**P_{obs}**	**P0**	**P_{obs}**
1	7.32	6.83	11.65	11.65	20.97	20.97	14.38	14.38	14.94	14.75
2	7.32	6.93	11.65	11.79	20.97	21.29	14.38	14.59	14.94	14.75
5	7.50	7.33	11.99	12.20	21.60	22.21	14.82	15.12	14.97	14.91
10	7.78	7.68	12.31	12.33	22.25	22.82	15.13	15.30	15.08	15.14
90	9.08	9.42	14.67	15.25	24.08	25.37	18.17	18.14	15.99	17.12
95	9.34	9.83	15.12	16.20	24.33	26.13	18.21	18.22	16.32	17.42
98	9.52	10.87	15.27	16.27	24.55	26.86	18.23	18.63	16.41	17.47
99	9.52	11.10	15.27	16.28	24.55	27.00	18.23	18.78	16.41	17.47
	SANGIORGIO JONICO									
Percentile	**P0**	**P_{obs}**	**P0**	**P_{obs}**	**P0**	**P_{obs}**	**P0**	**P_{obs}**	**P0**	**P_{obs}**
1	7.03	7.03	13.03	13.03	22.58	22.58	15.77	15.77	15.65	14.94
2	7.03	7.09	13.03	13.05	22.58	22.63	15.77	15.78	15.65	14.94
5	7.32	7.75	13.06	13.11	22.67	23.03	15.90	15.89	15.65	15.36
10	8.32	8.55	13.30	13.71	23.04	23.22	16.49	16.26	15.68	15.64
90	10.73	10.65	16.12	16.22	25.34	26.76	19.95	19.66	17.44	18.20
95	10.84	10.91	16.19	16.91	25.52	27.57	20.42	19.80	17.66	18.26
98	10.87	11.65	16.20	17.29	25.57	28.65	20.53	20.43	17.66	18.35
99	10.87	11.72	16.20	17.35	25.57	28.77	20.53	20.53	17.66	18.35
	TALSANO									
Percentile	**P0**	**P_{obs}**	**P0**	**P_{obs}**	**P0**	**P_{obs}**	**P0**	**P_{obs}**	**P0**	**P_{obs}**
1	7.83	7.83	12.18	12.18	23.07	23.07	16.08	15.88	15.70	15.40
2	7.83	7.86	12.18	12.22	23.07	23.07	16.08	15.90	15.70	15.40
5	7.90	8.15	12.26	12.60	23.07	23.11	16.11	16.08	15.70	15.50
10	8.19	8.35	12.70	12.98	23.10	23.19	16.24	16.28	15.72	15.55
90	9.99	10.36	14.72	16.15	25.06	26.05	18.77	18.87	16.72	17.99
95	10.16	11.32	14.99	16.74	25.21	26.56	19.70	19.38	16.76	18.03
98	10.20	11.70	15.03	16.81	25.23	27.80	19.92	19.86	16.76	18.09

99	10.20	11.73	15.03	16.81	25.23	27.92	19.92	19.92	16.76	18.10
	TARANTO									
Percentile	**P0**	**P_{obs}**	**P0**	**P_{obs}**	**P0**	**P_{obs}**	**P0**	**P_{obs}**	**P0**	**P_{obs}**
1	8.57	7.95	13.20	13.20	23.65	23.65	16.12	15.73	16.67	16.08
2	8.57	8.20	13.20	13.51	23.65	23.72	16.12	15.91	16.67	16.18
5	8.68	8.65	13.58	14.00	23.77	23.92	16.41	16.64	16.70	16.48
10	9.02	9.23	14.05	14.23	24.00	24.22	16.84	17.29	16.81	16.69
90	11.21	11.40	15.87	16.95	25.51	27.42	19.47	19.88	17.37	19.11
95	11.30	11.57	16.35	17.26	25.75	27.88	19.82	20.31	17.40	19.30
98	11.35	12.59	16.87	17.81	25.90	28.83	20.03	20.79	17.41	19.32
99	11.35	13.10	16.87	18.12	25.90	29.42	20.03	20.97	17.41	19.32

Table 4 Percentiles for annual and seasonal mean air temperature according to the empirical distribution from the reference period *P0* 1961-1990 and for the whole observation period P_{obs} 1950-2007 for the nine climatological stations in the Ostuni pilot area.

	AIR TEMPERATURE DECADAL TREND (°C/10yrs)									
	DJF		**MAM**		**JJA**		**SON**		**Year**	
°C/10yrs	P0	P_{obs}	P0	P_{obs}	P0	P_{obs}	P0	P_{obs}	P0	P_{obs}
CRISPIANO	0.5	0.1	0.4	**0.2**	0.2	**0.2**	-0.1	0.1	0.2	0.1
FASANO	**1.5**	**0.6**	**0.8**	**0.8**	0.7	**1**	**0.8**	**0.7**	1.1	**1**
GROTTAGLIE	0.1	**-0.2**	-0.3	-0.2	**-0.4**	-0.1	-0.3	**-0.2**	-0.2	**-0.2**
LATIANO	0	0	-0.4	0	-0.3	-0.1	-0.5	-0.1	-0.4	0
LOCOROTONDO	-0.6	-0.1	-0.5	0.1	-0.1	**0.2**	-0.6	0	-0.4	0.1
OSTUNI	-0.2	0.1	-0.4	0.2	0	**0.4**	**-0.4**	0.1	**-0.3**	0.2
SANGIORGIO JONICO	**0.6**	0.2	0.1	**0.4**	**0.7**	**0.7**	0.3	**0.3**	**0.6**	**0.4**

TALSANO	-0.1	0.4	-0.2	**0.8**	0.1	**1**	**1.2**	**0.4**	0	**0.6**
TARANTO	0.1	0.1	-0.2	**0.3**	0.1	**0.4**	-0.3	0.1	-0.2	0.2

Table 5 Air temperature decadal trends (°C/10year) for the nine climatological stations based on the reference period *P0* 1961-1990 and the whole observation period P_{obs} 1950-2007 data series. Trends significant at the 5% level are bolded.

On the ground of the results shown in the previous tables, some remarks on possible trends of temperature can be done:

1. A significant variability among stations exist, mostly in terms of trends. It is hard to infer a common tendency for all the stations, both for the sign, and for the statistical significance. However, at annual scale considering the whole observation period P_{obs} (last column of table 5) the majority of the stations present a tendency to increase (7 out of 9, 3 of them statistically significant); only for 1 out of 9 there is a slight but significant tendency to decrease. Different results can be inferred considering the base-line period *P0* during which 5 stations out of 9 indicate a decrease of temperature (although statistically significant in only 1 case) and 4 out of 9 indicate an increase (statistically significant in only 1 case). In general, at annual scale can be observed a general increase of the temperature if one considers the whole observation period, and a stationarity if one consider the base line period 1961-1990

2. Such an increasing temperature tendency appears to be mostly related to an increase of the summer temperature (June, July, August): 7 stations out of 9 indicate a significant increasing temperature for the whole observation period. Similar increase, but not statistically significant, is observed also if one considers the *P0* period.

3. Also the other seasons present a general tendency to increase temperatures during the period of observation, but the number of stations for which such a tendency is statistically significant are less (2 in winter, 5 in spring and 3 in autumn).

4. We can conclude that a general increase of annual temperature is observed for the whole observation period (1960-2007), due to an increase of temperature (particularly during summer) during the last two decades (1991-2007). This climatic signal is not observed in all the stations, suggesting that local climate can be superimposed to the regional and/or global climatic trend

In the following, the annual cycle of mean monthly air temperature (a) and standard deviation (b), cumulative distribution of mean annual air temperature (c) and time series of mean annual air temperature with fitted trend line for the period 1950-2007 (d) are shown for all the analysed stations.

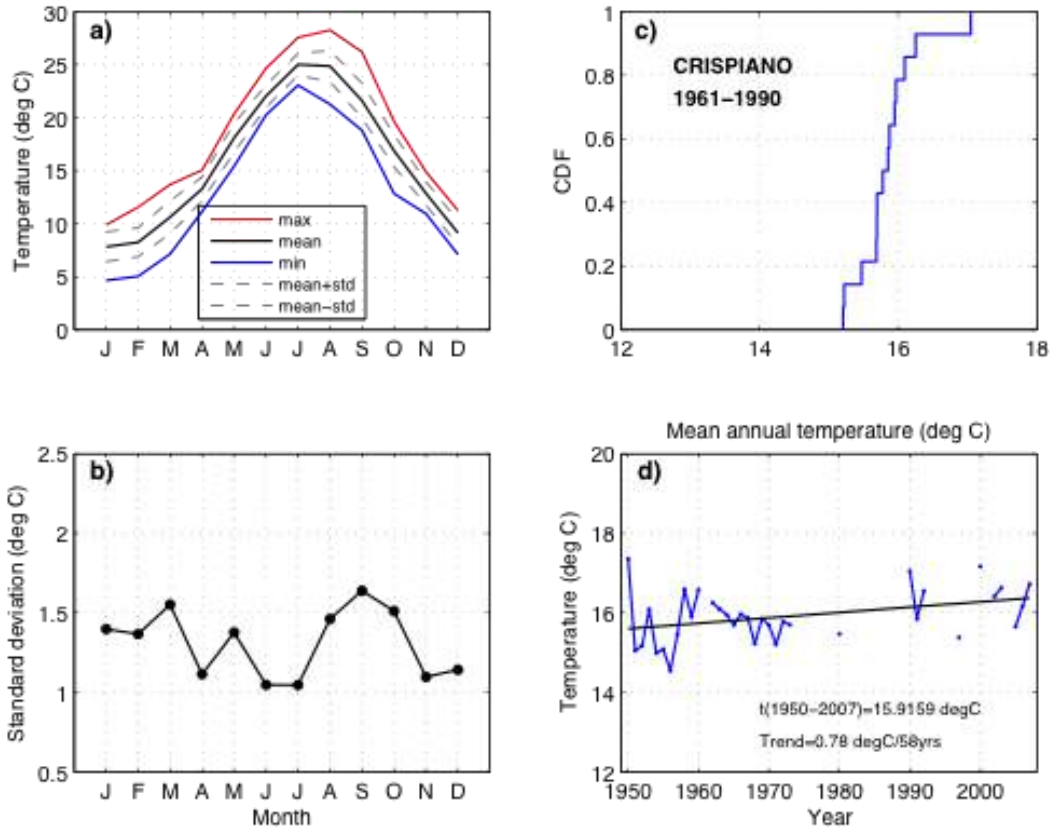

Figure 2 Annual cycle of mean monthly air temperature (a) and standard deviation (b), cumulative distribution of mean annual air temperature (c) and time series of mean annual air temperature with fitted trend line for the period 1950-2007 (d) for Crispiano climatological station.

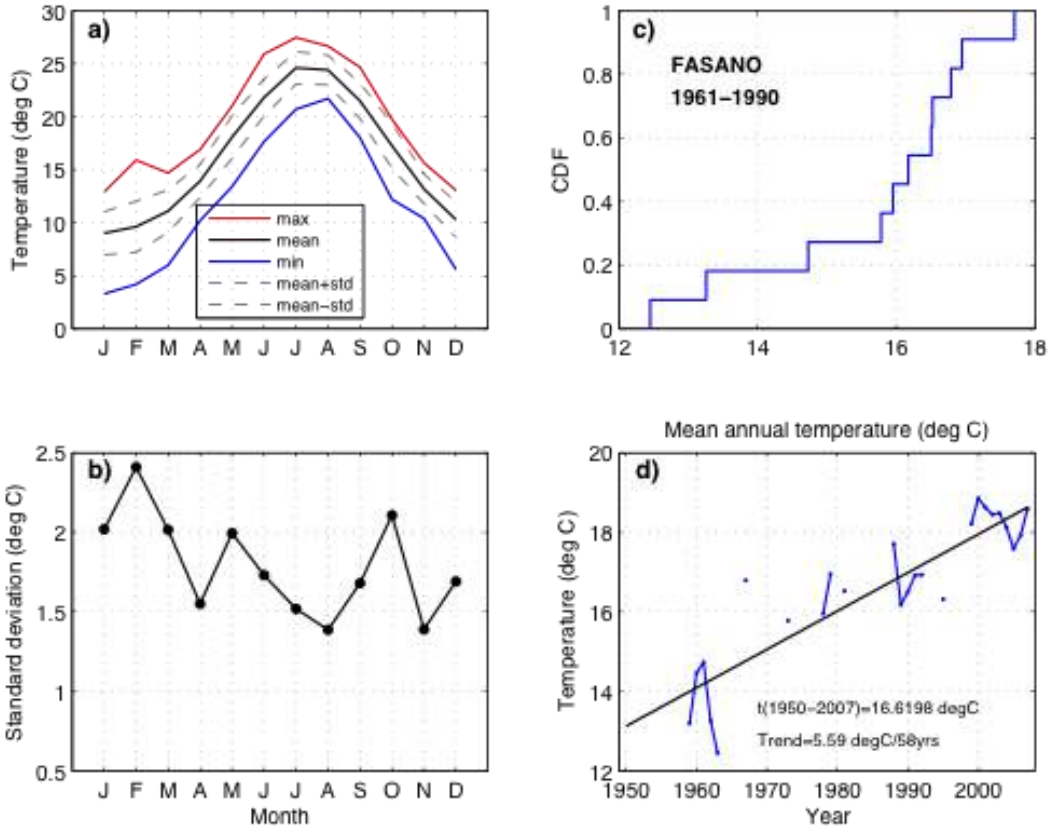

Figure 3 Annual cycle of mean monthly air temperature (a) and standard deviation (b), cumulative distribution of mean annual air temperature (c) and time series of mean annual air temperature with fitted trend line for the period 1950-2007 (d) for Fasano climatological station.

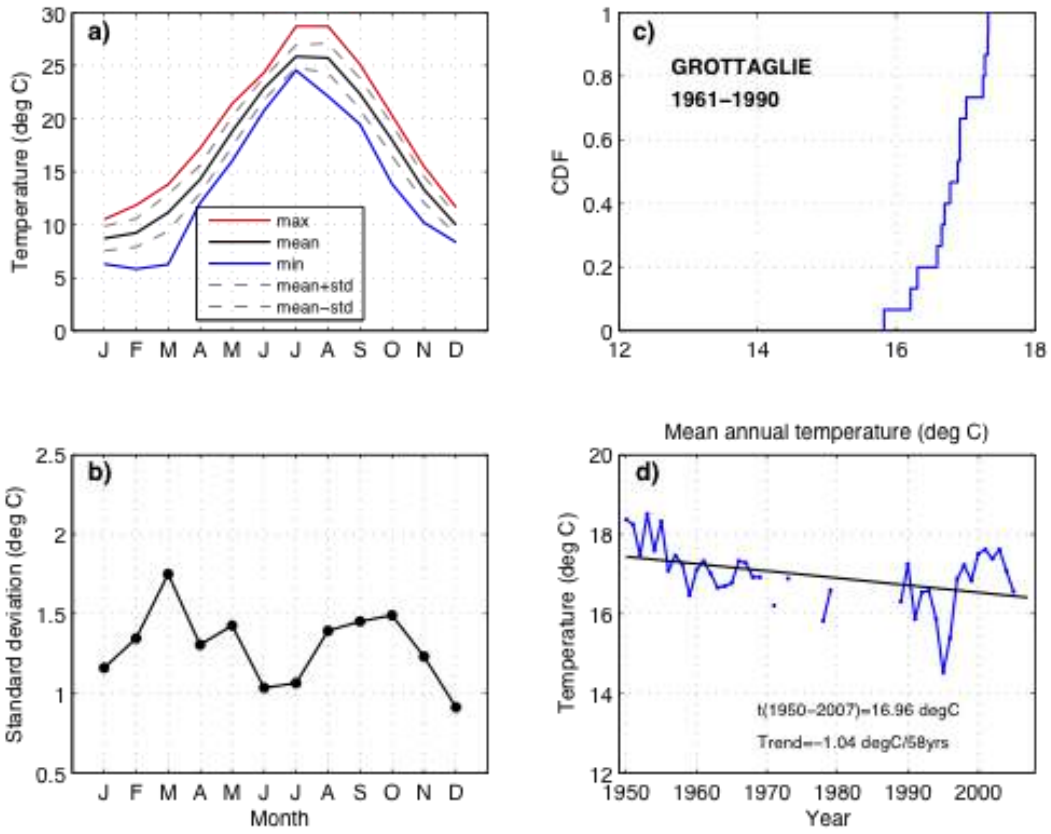

Figure 4 Annual cycle of mean monthly air temperature (a) and standard deviation (b), cumulative distribution of mean annual air temperature (c) and time series of mean annual air temperature with fitted trend line for the period 1950-2007 (d) for Grottaglie climatological station.

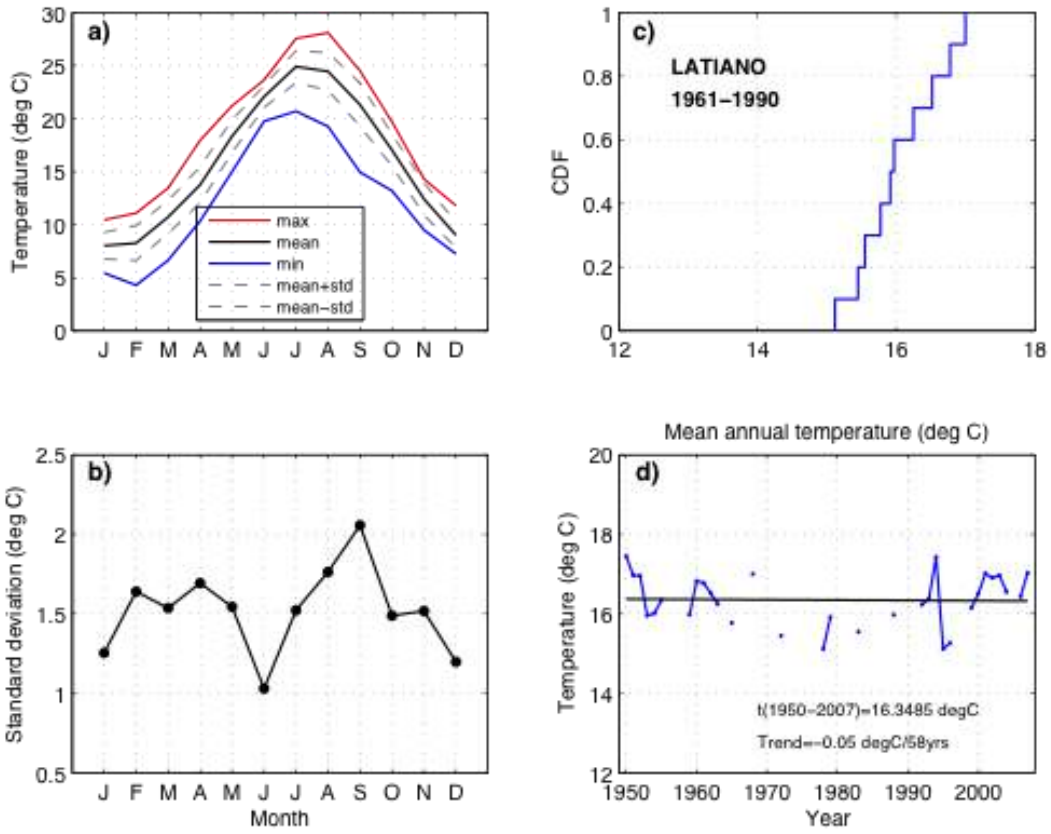

Figure 5 Annual cycle of mean monthly air temperature (a) and standard deviation (b), cumulative distribution of mean annual air temperature (c) and time series of mean annual air temperature with fitted trend line for the period 1950-2007 (d) for Latiano climatological station.

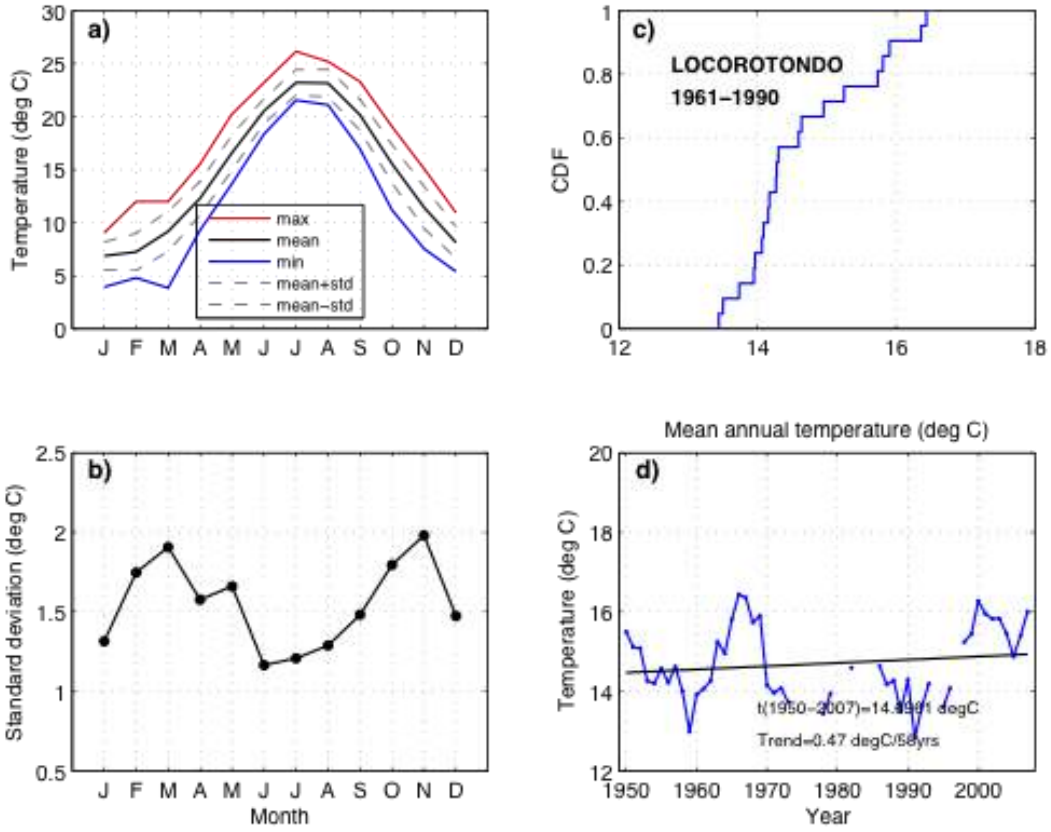

Figure 6 Annual cycle of mean monthly air temperature (a) and standard deviation (b), cumulative distribution of mean annual air temperature (c) and time series of mean annual air temperature with fitted trend line for the period 1950-2007 (d) for Locorotondo climatological station.

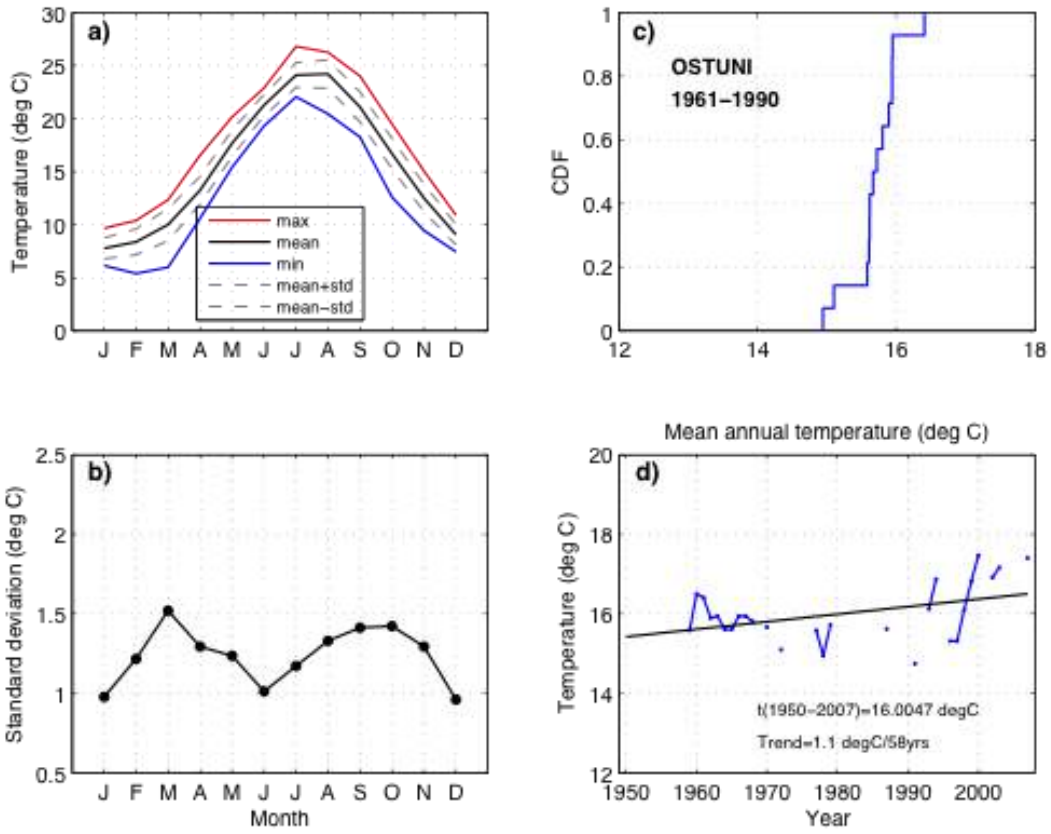

Figure 7 Annual cycle of mean monthly air temperature (a) and standard deviation (b), cumulative distribution of mean annual air temperature (c) and time series of mean annual air temperature with fitted trend line for the period 1950-2007 (d) for Ostuni climatological station.

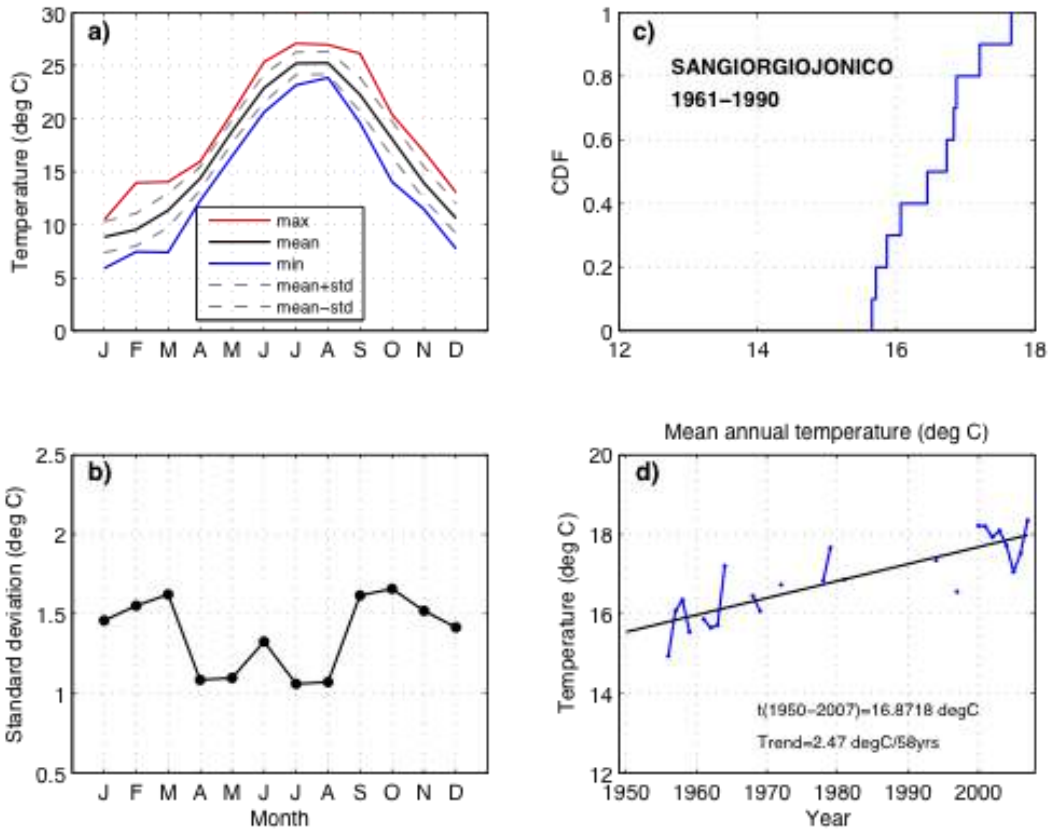

Figure 8 Annual cycle of mean monthly air temperature (a) and standard deviation (b), cumulative distribution of mean annual air temperature (c) and time series of mean annual air temperature with fitted trend line for the period 1950-2007 (d) for SanGiorgio Jonico climatological station.

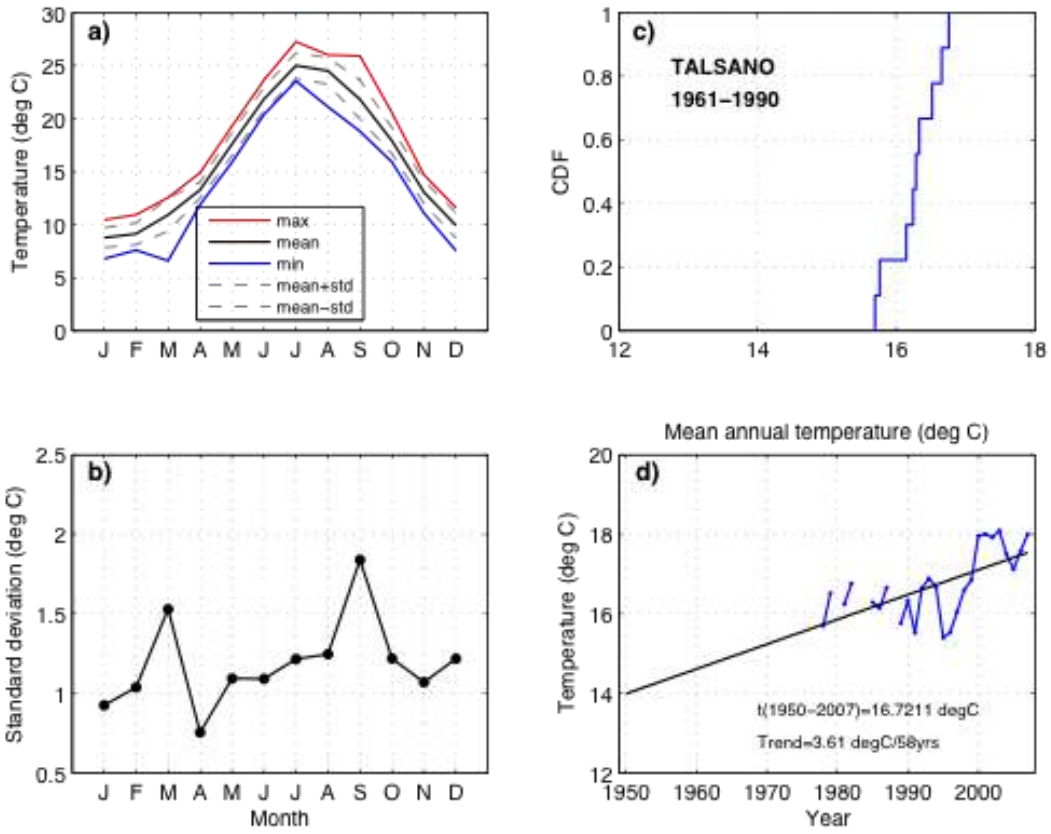

Figure 9 Annual cycle of mean monthly air temperature (a) and standard deviation (b), cumulative distribution of mean annual air temperature (c) and time series of mean annual air temperature with fitted trend line for the period 1950-2007 (d) for Talsano climatological station.

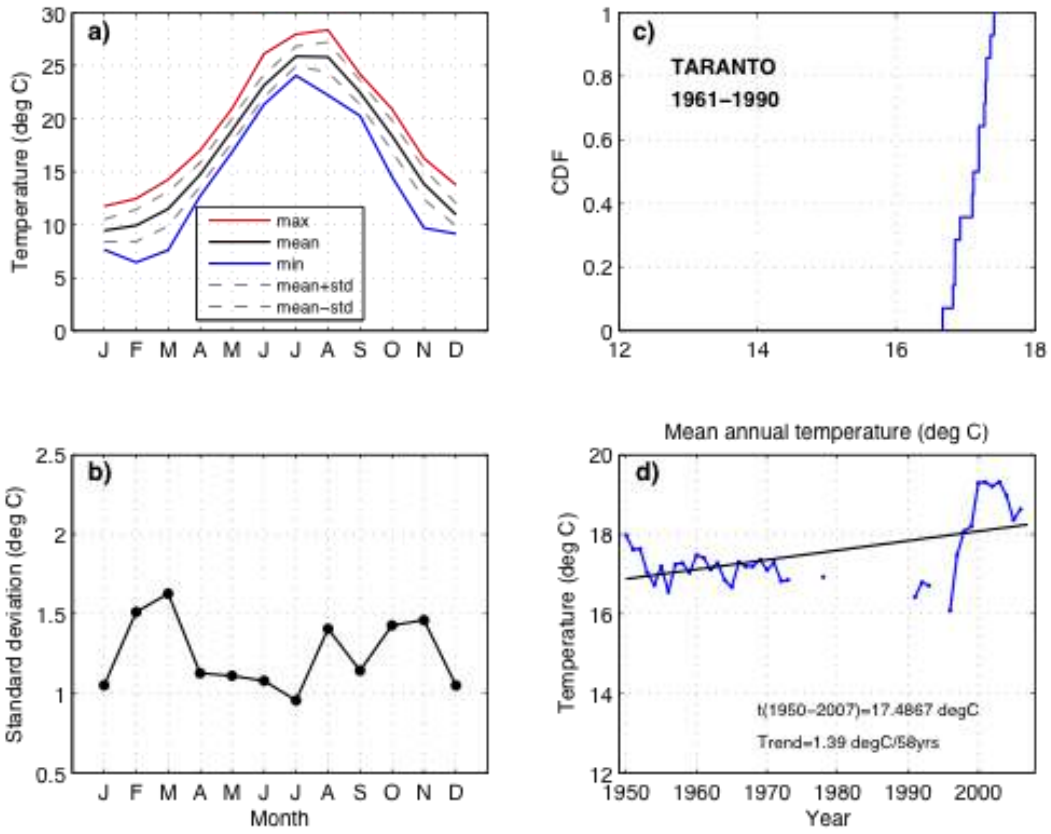

Figure 10 Annual cycle of mean monthly air temperature (a) and standard deviation (b), cumulative distribution of mean annual air temperature (c) and time series of mean annual air temperature with fitted trend line for the period 1950-2007 (d) for Taranto climatological station.

2.3 Precipitation analysis

The available precipitation time series have been analysed in terms of the basic statistics (mean, standard deviation, maximum and minimum) at annual and seasonal time scale for the reference period 1961-1990 (*P0*) and for the whole observation period 1950-2007 (P_{obs}) (table 6).

In table 7 the percentiles for annual and seasonal precipitation according to the empirical distribution from the reference period *P0* 1961-1990 and for the whole observation period P_{obs} 1950-2007 of the nine climatological stations in the Ostuni pilot area are shown

Moreover, precipitation decadal trends (mm/10year) based on the reference period *P0* and the whole observation period P_{obs} are shown (table 8).

	DJF		MAM		JJA		SON		Year	
	CEGLIE MESSIANICA									
	P0	**P_{obs}**	**P0**	**P_{obs}**	**P0**	**P_{obs}**	**P0**	**P_{obs}**	**P0**	**P_{obs}**
mean (mm)	215.0	238.3	139.3	153.2	75.4	76.2	200.0	206.1	634.9	674.7
stdev (mm)	81.0	94.8	53.1	64.7	47.8	51.1	77.9	74.0	156.3	161.0
c_v	0.4	0.4	0.4	0.4	0.6	0.7	0.4	0.4	0.2	0.2
max (mm)	441.0	520.2	262.0	310.0	179.0	196.0	345.0	349.0	961.0	984.0
min (mm)	73.0	73.0	66.0	64.0	9.0	7.0	72.0	63.0	374.0	374.0
	CRISPIANO									
	P0	**P_{obs}**	**P0**	**P_{obs}**	**P0**	**P_{obs}**	**P0**	**P_{obs}**	**P0**	**P_{obs}**
mean (mm)	180.1	185.4	122.4	128.1	78.3	75.8	166.1	174.6	547.5	563.7
stdev (mm)	72.1	89.5	42.7	49.6	50.8	52.0	86.4	81.1	165.6	155.7
c_v	0.4	0.5	0.3	0.4	0.6	0.7	0.5	0.5	0.3	0.3
max (mm)	361.0	573.0	214.0	236.0	222.0	222.0	438.0	438.0	1020	1020
min (mm)	46.0	46.0	43.0	43.0	13.0	7.8	71.0	64.0	334.0	334.0
	FASANO									
	P0	**P_{obs}**	**P0**	**P_{obs}**	**P0**	**P_{obs}**	**P0**	**P_{obs}**	**P0**	**P_{obs}**
mean (mm)	196.3	212.4	123.3	128.2	68.9	69.4	183.6	192.1	576.8	606.3
stdev (mm)	65.8	81.9	57.3	54.2	46.6	49.9	67.6	78.1	114.0	133.7
c_v	0.3	0.4	0.5	0.4	0.7	0.7	0.4	0.4	0.2	0.2

max (mm)	393.0	468.2	242.0	242.0	231.0	231.0	373.0	391.4	862.0	982.0
min (mm)	64.0	64.0	39.0	39.0	4.0	4.0	77.0	77.0	364.0	364.0
	GROTTAGLIE									
	P0	**P_{obs}**	**P0**	**P_{obs}**	**P0**	**P_{obs}**	**P0**	**P_{obs}**	**P0**	**P_{obs}**
mean (mm)	153.5	169.5	114.2	123.9	77.9	76.3	159.1	168.9	506.9	542.2
stdev (mm)	55.5	71.6	41.4	52.7	54.9	53.5	72.8	70.4	145.9	144.8
c_v	0.4	0.4	0.4	0.4	0.7	0.7	0.5	0.4	0.3	0.3
max (mm)	272.0	405.4	203.0	249.0	206.0	258.4	391.0	391.0	927.0	948.6
min (mm)	52.0	52.0	34.0	34.0	9.0	9.0	58.0	47.8	332.0	332.0
	LATIANO									
	P0	**P_{obs}**	**P0**	**P_{obs}**	**P0**	**P_{obs}**	**P0**	**P_{obs}**	**P0**	**P_{obs}**
mean (mm)	195.0	218.0	134.9	142.3	69.0	73.0	201.2	204.3	599.8	636.5
stdev (mm)	72.7	93.9	52.6	62.5	51.3	49.0	74.5	82.6	149.3	155.8
c_v	0.4	0.4	0.4	0.4	0.7	0.7	0.4	0.4	0.2	0.2
max (mm)	364.0	547.0	256.0	285.0	163.0	182.4	415.0	415.0	958.0	961.0
min (mm)	63.0	63.0	37.0	37.0	3.0	3.0	74.0	74.0	331.0	331.0
	LOCOROTONDO									
	P0	**P_{obs}**	**P0**	**P_{obs}**	**P0**	**P_{obs}**	**P0**	**P_{obs}**	**P0**	**P_{obs}**
mean (mm)	240.5	239.7	148.1	152.2	85.2	77.9	216.5	213.0	692.0	682.0
stdev (mm)	83.8	88.4	56.9	56.2	55.7	55.3	92.2	88.3	179.7	160.0
c_v	0.3	0.4	0.4	0.4	0.7	0.7	0.4	0.4	0.3	0.2
max (mm)	413.0	549.0	262.0	274.0	275.0	275.0	497.0	497.0	1247.0	1247.0
min (mm)	52.0	52.0	38.0	38.0	9.0	9.0	87.0	76.2	335.0	335.0
	OSTUNI									
	P0	**P_{obs}**	**P0**	**P_{obs}**	**P0**	**P_{obs}**	**P0**	**P_{obs}**	**P0**	**P_{obs}**
mean (mm)	224.7	251.0	149.0	159.9	69.2	76.8	218.6	231.7	663.6	716.6

stdev (mm)	79.5	93.8	59.1	68.6	45.3	63.3	83.5	92.8	142.6	171.6
c_v	0.4	0.4	0.4	0.4	0.7	0.8	0.4	0.4	0.2	0.2
max (mm)	492.0	623.8	283.0	315.0	165.0	310.6	404.0	457.2	948.0	1146
min (mm)	78.0	78.0	38.0	38.0	5.0	5.0	73.0	73.0	376.0	376.0
	SANGIORGIOJONICO									
	P0	**P_{obs}**	**P0**	**P_{obs}**	**P0**	**P_{obs}**	**P0**	**P_{obs}**	**P0**	**P_{obs}**
mean (mm)	173.4	176.9	123.8	126.7	71.6	72.5	178.0	180.8	551.1	558.1
stdev (mm)	67.7	76.7	57.5	60.2	50.4	47.9	87.8	83.2	175.1	151.0
c_v	0.4	0.4	0.5	0.5	0.7	0.7	0.5	0.5	0.3	0.3
max (mm)	339.0	460.4	243.0	295.0	214.0	214.0	513.0	513.0	1083.0	1083.0
min (mm)	55.0	55.0	35.0	35.0	10.0	5.2	75.0	43.0	282.0	282.0
	TARANTO									
	P0	**P_{obs}**	**P0**	**P_{obs}**	**P0**	**P_{obs}**	**P0**	**P_{obs}**	**P0**	**P_{obs}**
mean (mm)	165.7	166.1	111.1	110.9	54.6	57.1	155.2	152.5	486.5	486.1
stdev (mm)	67.3	77.7	52.6	51.8	42.3	41.7	75.9	74.3	152.9	138.6
c_v	0.4	0.5	0.5	0.5	0.8	0.7	0.5	0.5	0.3	0.3
max (mm)	305	493	216	253	146	193	439	439	965	965
min (mm)	35	35	31	31	8	2.8	58	33.8	261	261

Table 6 Basic statistics (mean, standard deviation, coefficient of variation, maximum and minimum) for annual and seasonal precipitation amounts for the reference period 1961-1990 P0 and for the whole observation period 1950-2007 P_{obs} for the nine climatological stations in the Ostuni pilot area.

	DJF		**MAM**		**JJA**		**SON**		**Year**	
	CEGLIE MESSAPICA									
Percentile	**P0**	**P_{obs}**	**P0**	**P_{obs}**	**P0**	**P_{obs}**	**P0**	**P_{obs}**	**P0**	**P_{obs}**
1	73.0	73.6	66.0	64.1	9.0	7.2	72.0	63.6	374.0	376.1

2	74.0	79.2	66.0	65.3	10.3	8.3	72.9	68.8	377.4	393.3
5	83.0	92.4	66.0	66.7	22.0	10.8	82.5	88.3	413.9	416.0
10	110.5	123.0	78.0	77.0	24.5	22.3	100.0	111.0	450.4	464.0
90	323.5	349.4	231.2	257.1	141.5	152.8	316.6	322.3	887.2	911.8
95	339.0	419.7	238.3	270.9	170.0	175.4	344.1	344.7	938.2	965.6
98	430.8	503.3	260.0	308.7	178.1	195.6	344.9	346.4	959.1	981.8
99	441.0	518.6	262.0	309.9	179.0	196.0	345.0	348.7	961.0	983.8
	CRISPIANO									
Percentile	**P0**	**P_{obs}**	**P0**	**P_{obs}**	**P0**	**P_{obs}**	**P0**	**P_{obs}**	**P0**	**P_{obs}**
1	46.0	46.1	43.0	43.3	13.0	8.2	71.0	64.4	334.0	334.5
2	46.6	51.2	43.7	46.6	14.1	11.1	71.5	68.2	337.6	341.3
5	55.0	57.2	51.6	52.8	24.0	15.5	76.7	78.0	376.8	381.2
10	57.9	71.4	67.4	65.0	35.0	25.0	89.4	90.0	392.8	397.0
90	263.9	286.4	175.0	205.0	153.5	153.4	260.8	272.8	769.2	759.7
95	313.3	307.4	194.1	217.5	192.0	182.9	374.4	349.6	939.3	903.2
98	357.8	462.8	212.3	232.4	219.0	217.5	432.6	417.1	1013.2	1002.8
99	361.0	570.9	214.0	235.7	222.0	221.5	438.0	436.3	1020.0	1018.8
	FASANO									
Percentile	**P0**	**P_{obs}**	**P0**	**P_{obs}**	**P0**	**P_{obs}**	**P0**	**P_{obs}**	**P0**	**P_{obs}**
1	64.0	64.0	39.0	39.4	4.0	4.1	77.0	77.2	364.0	365.4
2	68.2	73.6	40.0	44.8	5.2	6.0	77.4	79.8	368.6	389.8
5	113.4	108.1	49.0	49.2	16.0	12.2	81.8	82.1	419.1	422.3
10	123.0	123.0	55.5	62.0	27.0	19.6	111.4	95.0	435.2	432.1
90	276.0	330.2	212.0	210.4	124.0	133.1	268.6	317.8	705.0	763.5
95	329.4	391.1	215.0	221.9	133.0	172.1	316.0	368.4	768.0	850.5
98	387.6	432.1	239.3	239.7	221.2	203.0	368.2	381.1	854.1	944.1
99	393.0	468.2	242.0	241.8	231.0	229.1	373.0	390.8	862.0	980.0
	GROTTAGLIE									

Percentile	P0	P_{obs}	P0	P_{obs}	P0	P_{obs}	P0	P_{obs}	P0	P_{obs}
1	52.0	52.6	34.0	35.1	9.0	9.1	58.0	48.4	332.0	332.7
2	53.5	60.4	37.0	44.9	9.1	9.6	58.6	54.1	333.4	340.4
5	67.0	67.2	64.0	60.3	10.0	11.0	64.0	63.6	346.0	353.1
10	75.0	78.2	65.5	64.1	16.5	17.2	83.0	75.8	358.0	387.0
90	230.5	262.9	177.0	202.5	165.0	139.8	234.5	244.7	699.5	699.2
95	255.0	276.6	183.0	232.5	189.0	186.2	308.0	292.1	820.0	839.5
98	270.3	348.3	201.0	248.9	204.3	224.9	382.7	349.8	916.3	935.6
99	272.0	401.5	203.0	249.0	206.0	254.7	391.0	387.0	927.0	947.5
	LATIANO									
Percentile	P0	P_{obs}	P0	P_{obs}	P0	P_{obs}	P0	P_{obs}	P0	P_{obs}
1	63.0	63.8	37.0	37.2	3.0	3.1	74.0	74.2	331.0	331.2
2	64.4	71.7	39.5	38.3	3.1	3.6	75.6	75.9	336.2	333.0
5	77.0	88.3	62.0	57.2	4.0	6.7	90.0	90.4	383.0	393.9
10	99.5	110.5	78.5	78.3	7.0	14.0	113.0	107.4	428.0	442.6
90	289.5	320.6	204.0	234.3	146.0	146.0	293.0	334.6	763.0	871.0
95	321.0	360.7	224.0	266.6	148.0	164.2	337.0	362.7	909.0	935.4
98	359.7	526.4	252.8	276.0	161.5	173.6	407.2	392.6	953.1	959.1
99	364.0	545.0	256.0	283.9	163.0	181.4	415.0	412.6	958.0	960.8
	LOCOROTONDO									
Percentile	P0	P_{obs}	P0	P_{obs}	P0	P_{obs}	P0	P_{obs}	P0	P_{obs}
1	52.0	54.3	38.0	39.2	9.0	9.0	87.0	77.1	335.0	342.8
2	55.9	76.2	39.5	47.9	10.5	9.0	88.4	83.3	351.7	399.7
5	91.0	107.5	53.0	67.8	24.0	10.2	101.0	98.0	502.0	447.8
10	141.5	135.1	90.0	87.1	31.5	24.0	135.0	114.2	550.5	535.0
90	350.5	352.5	232.5	235.1	130.5	146.3	346.0	323.3	899.0	859.2
95	399.0	395.1	251.0	257.6	225.0	205.5	417.0	411.8	1120.0	986.2
98	411.6	464.7	260.9	272.0	270.0	242.0	489.0	455.0	1234.3	1163.2
99	413.0	540.8	262.0	273.8	275.0	271.0	497.0	491.9	1247.0	1236.8

	OSTUNI									
Percentile	**P0**	**P_{obs}**	**P0**	**P_{obs}**	**P0**	**P_{obs}**	**P0**	**P_{obs}**	**P0**	**P_{obs}**
1	78.0	79.0	38.0	40.6	5.0	5.3	73.0	73.0	376.0	377.0
2	80.6	88.5	41.4	59.8	5.9	7.6	73.0	73.0	379.3	383.9
5	104.0	114.2	72.0	73.6	14.0	11.1	73.0	87.8	409.0	423.8
10	150.5	153.3	86.0	84.7	19.5	19.0	116.0	122.7	467.5	492.6
90	316.5	354.0	229.5	262.9	145.5	151.0	331.5	371.4	849.5	945.0
95	342.0	370.2	265.0	281.4	151.0	212.3	349.0	393.0	930.0	1018.3
98	477.0	542.1	281.2	309.1	163.6	279.8	398.5	422.1	946.2	1118.3
99	492.0	615.9	283.0	314.3	165.0	306.9	404.0	452.9	948.0	1142.6

	SANGIORGIO JONICO									
Percentile	**P0**	**P_{obs}**	**P0**	**P_{obs}**	**P0**	**P_{obs}**	**P0**	**P_{obs}**	**P0**	**P_{obs}**
1	55.0	55.0	35.0	35.0	10.0	5.2	75.0	43.0	282.0	282.0
2	55.4	57.5	35.2	36.0	10.1	7.6	75.4	48.0	288.5	285.2
5	60.4	64.5	36.9	48.0	11.0	11.0	79.8	67.0	359.0	363.0
10	73.5	72.3	50.8	56.2	17.6	24.3	91.4	82.5	375.0	387.5
90	250.3	252.1	201.2	206.5	146.6	142.7	264.2	285.6	724.6	724.0
95	324.6	326.2	212.6	226.8	160.8	158.0	343.9	311.0	925.3	772.0
98	338.0	409.4	240.4	269.0	209.5	191.5	498.8	424.0	1069.7	1000.0
99	339.0	460.4	243.0	295.0	214.0	214.0	513.0	513.0	1083.0	1083.0

	TARANTO									
Percentile	**P0**	**P_{obs}**	**P0**	**P_{obs}**	**P0**	**P_{obs}**	**P0**	**P_{obs}**	**P0**	**P_{obs}**
1	35.0	36.1	31.0	31.1	8.0	3.2	58.0	34.0	261.0	263.4
2	36.9	46.8	31.2	32.3	8.0	6.2	59.0	35.3	264.8	283.1
5	54.0	56.4	33.0	38.8	8.0	9.2	68.0	62.0	299.0	303.9
10	65.5	68.8	40.0	56.4	13.0	15.0	79.0	71.8	318.0	329.6
90	262.5	255.4	180.5	175.4	120.0	114.6	225.5	223.7	644.5	641.0
95	295.0	299.9	195.0	208.7	142.0	144.4	281.0	263.6	752.0	751.9

98	304.0	376.4	213.9	238.9	145.6	164.8	423.2	414.3	943.7	896.5
99	305.0	481.7	216.0	251.5	146.0	189.6	439.0	436.0	965.0	957.5

Table 7 The percentiles for annual and seasonal precipitation according to the empirical distribution for the reference period 1961-1990 P0 and for the whole observation period 1950-2007 P_{obs} for the nine climatological stations in the Ostuni pilot area.

	DJF		MAM		JJA		SON		Year	
	CEGLIE MESSAPICA									
TREND	**P0**	**P_{obs}**	**P0**	**P_{obs}**	**P0**	**P_{obs}**	**P0**	**P_{obs}**	**P0**	**P_{obs}**
mm/10yr	**-37.9**	-12	4.8	-0.2	-2.6	-0.2	-1.3	-5	-27.1	-16.8
%/10yr	**-17.6**	-5	3.4	-0.1	-3.4	-0.3	-0.6	-2.4	-4.3	-2.5
	CRISPIANO									
TREND	**P0**	**P_{obs}**	**P0**	**P_{obs}**	**P0**	**P_{obs}**	**P0**	**P_{obs}**	**P0**	**P_{obs}**
mm/10yr	-38.1	-1.5	0.3	-1.3	-4.1	1.4	-20.5	3.8	-58.4	2.8
%/10yr	-21.1	-0.8	0.2	-1	-5.2	1.8	-12.3	2.2	-10.7	0.5
	FASANO									
TREND	**P0**	**P_{obs}**	**P0**	**P_{obs}**	**P0**	**P_{obs}**	**P0**	**P_{obs}**	**P0**	**P_{obs}**
mm/10yr	-16.9	-5.9	0.1	3	-6.5	1.5	11	0.7	-14.1	-3.7
%/10yr	-8.6	-2.8	0.1	2.3	-9.4	2.2	6	0.4	-2.4	-0.6
	GROTTAGLIE									
TREND	**P0**	**P_{obs}**	**P0**	**P_{obs}**	**P0**	**P_{obs}**	**P0**	**P_{obs}**	**P0**	**P_{obs}**
mm/10yr	**-25.2**	-0.1	3.3	-4.5	-4.7	5	-12	-0.8	-30.3	-4.9
%/10yr	**-16.4**	-0.1	2.9	-3.6	-6	6.5	-7.5	-0.5	-6	-0.9
	LATIANO									
TREND	**P0**	**P_{obs}**	**P0**	**P_{obs}**	**P0**	**P_{obs}**	**P0**	**P_{obs}**	**P0**	**P_{obs}**

mm/10yr	**-33.5**	**-15**	-4	1	-4.1	2.4	-2.8	-8.2	-36.7	-19.6
%/10yr	**-17.2**	**-6.9**	-3	0.7	-5.9	3.3	-1.4	-4	-6.1	-3.1
	LOCOROTONDO									
TREND	**P0**	**P_{obs}**	**P0**	**P_{obs}**	**P0**	**P_{obs}**	**P0**	**P_{obs}**	**P0**	**P_{obs}**
mm/10yr	**-47.9**	-5.2	6.6	-0.5	-4.6	0.6	-16.4	-6.5	-59.1	-12.1
%/10yr	**-19.9**	-2.2	4.5	-0.3	-5.4	0.8	-7.6	-3.1	-8.5	-1.8
	OSTUNI									
TREND	**P0**	**P_{obs}**	**P0**	**P_{obs}**	**P0**	**P_{obs}**	**P0**	**P_{obs}**	**P0**	**P_{obs}**
mm/10yr	**-27.2**	-5.3	4.1	-0.6	1.5	4.3	17.2	3	5.4	2.3
%/10yr	**-12.1**	-2.1	2.8	-0.4	2.2	5.6	7.9	1.3	0.8	0.3
	SANGIORGIO JONICO									
TREND	**P0**	**P_{obs}**	**P0**	**P_{obs}**	**P0**	**P_{obs}**	**P0**	**P_{obs}**	**P0**	**P_{obs}**
mm/10yr	-25.6	-6.1	3.4	-3.4	-6.9	-0.5	-7.1	-7.3	-31.8	-20.7
%/10yr	-14.8	-3.4	2.7	-2.7	-9.6	-0.7	-4	-4	-5.8	-3.7
	TARANTO									
TREND	**P0**	**P_{obs}**	**P0**	**P_{obs}**	**P0**	**P_{obs}**	**P0**	**P_{obs}**	**P0**	**P_{obs}**
mm/10yr	-27.4	0.8	5.2	0.8	6	3.8	0.8	3.6	-14.5	9.8
%/10yr	-16.5	0.5	4.7	0.7	11	6.7	0.5	2.4	-3	2

Table 8 Precipitation trends for the nine climatological stations based on the reference period 1961-1990 P0 and the whole observation period 1950-2007 P_{obs} data series. Trends are expressed as differences considering the whole period of analysis (P0 or P_{obs})Trends significant at the 5% level are bolded.

On the ground of the results shown in the previous tables, some remarks on possible trends of precipitation can be done:

1. In terms of annual mean, the precipitation regime appears to be uniform over the study area (this value ranges from 486 mm/year to 716 mm/year, if one considers the P_{obs} period).

2. A very high interannual variability can be observed, both considering the min and max values, and considering the percentile. For example, concerning the Ostuni station (the most rainy), the 5th percentile is equal to 424 mm/year, while the 95th is equal to 1018 mm/year; similarly, concerning the Taranto station (the less rainy), the 5th percentile is equal to 263 mm/year, while the 95th percentile is equal to 957 mm/year. As a consequence, it is possible to infer that the mean values of precipitation cannot be representative of the transient regime of recharge to the aquifer.

3. Concerning the trends, it is possible to observe a general decrease of annual precipitation, both for the base line period *P0* and for the whole observation period P_{obs}. However, such a decrease, although observed in all the rain gauges, it is never statistically significant. This is probably due to the high interannual variability, as suggested by the first point.

4. The analysis of the seasonal trends suggests that the decrease of precipitation observed at annual scale (although not significant) is mainly due to a decrease of the winter precipitation, which is observed in all the stations (and statistically significant for 5 out of 9) for the period P0. A similar decreasing trend is observed also if the whole observation period considered (8 stations out of 9): however, such a trend is generally not significant from a statistical point of view. The last observation lead to two important consequences: a) concerning precipitation, at least for the Ostuni pilot area, the base line 1961-1990 (which is usually considered stationary from a climatic point of view) is not stationary; b) the impact of a decreasing in precipitation on the Ostuni aquifer and on the possible salt intrusion is currently ongoing

5. The observed winter precipitation trend ranges for the period P0 between -16.9 mm/10yrs (Fasano) and -47.9 mm/yrs (Locorotondo)

In the following, the annual cycle of mean monthly precipitation amounts (a), standard deviation and coefficient of variation (b), cumulative distribution (c) and time series of annual precipitation with fitted trend line for the period 1950-2007 (d) for all the analysed stations.

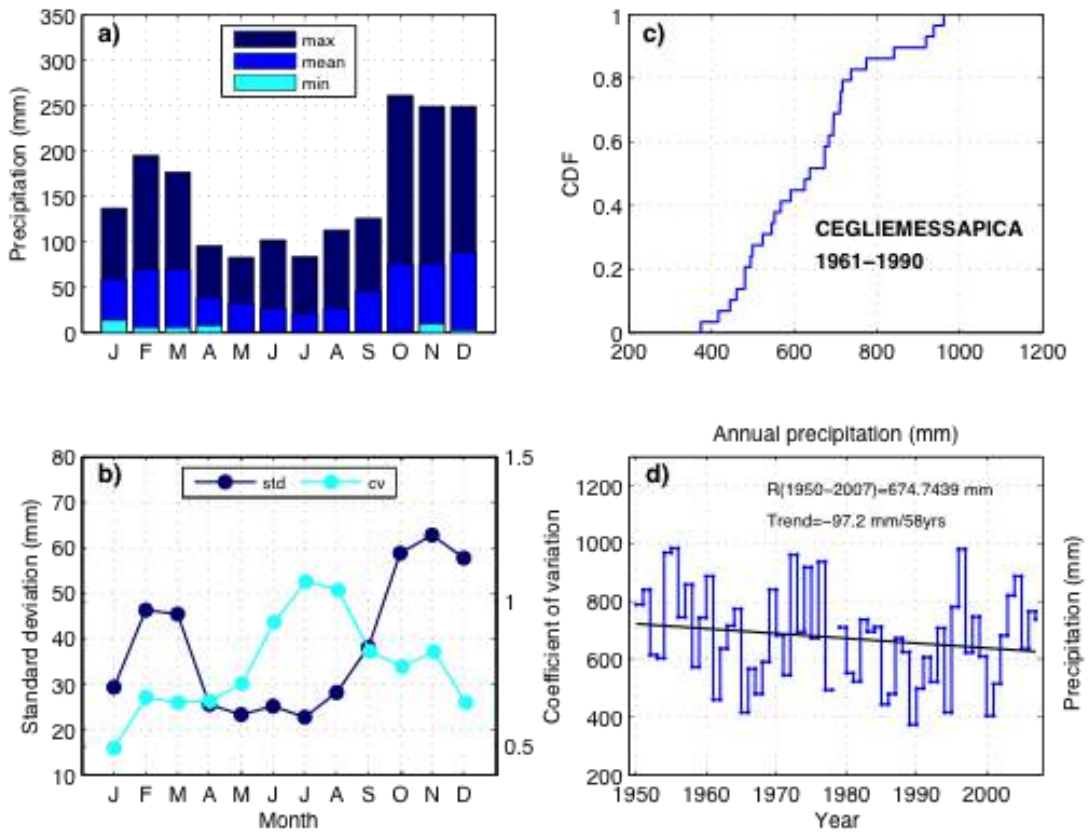

Figure 11 Annual cycle of mean monthly precipitation amounts (a), standard deviation and coefficient of variation (b), cumulative distribution (c) and time series of annual precipitation with fitted trend line for the period 1950-2007 (d) for Ceglie Messapica climatological station.

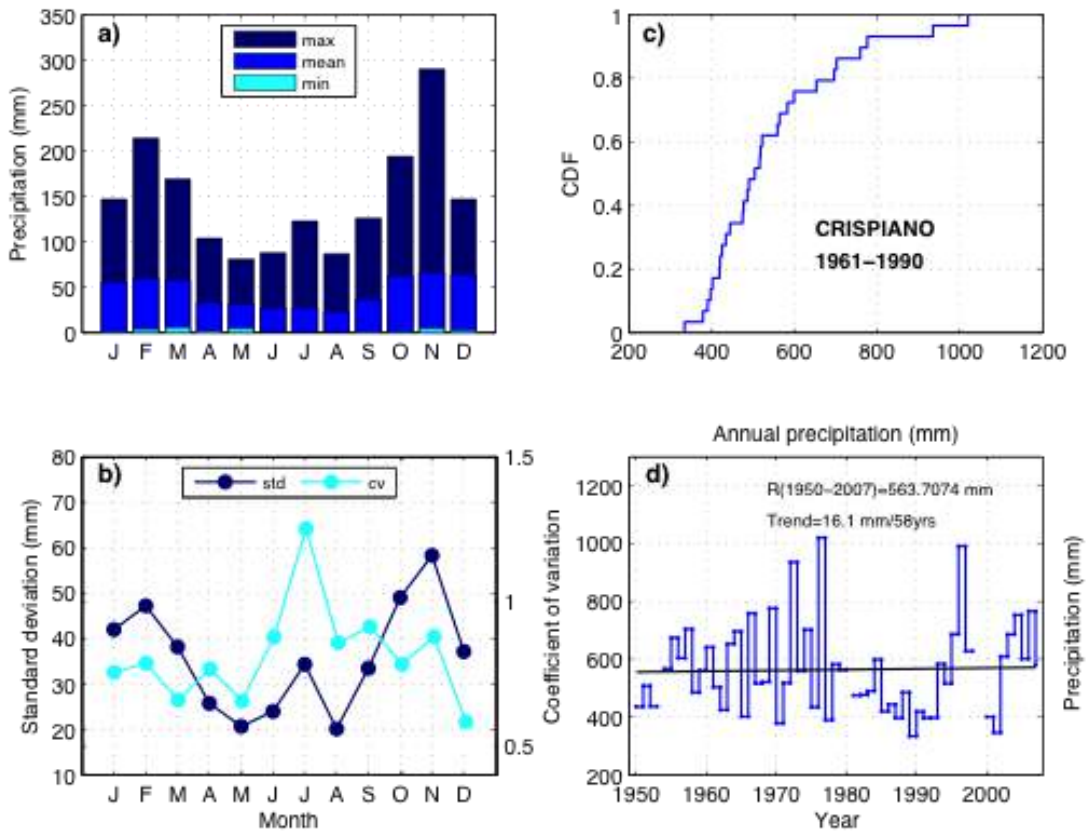

Figure 12 Annual cycle of mean monthly precipitation amounts (a), standard deviation and coefficient of variation (b), cumulative distribution (c) and time series of annual precipitation with fitted trend line for the period 1950-2007 (d) for Crispiano climatological station.

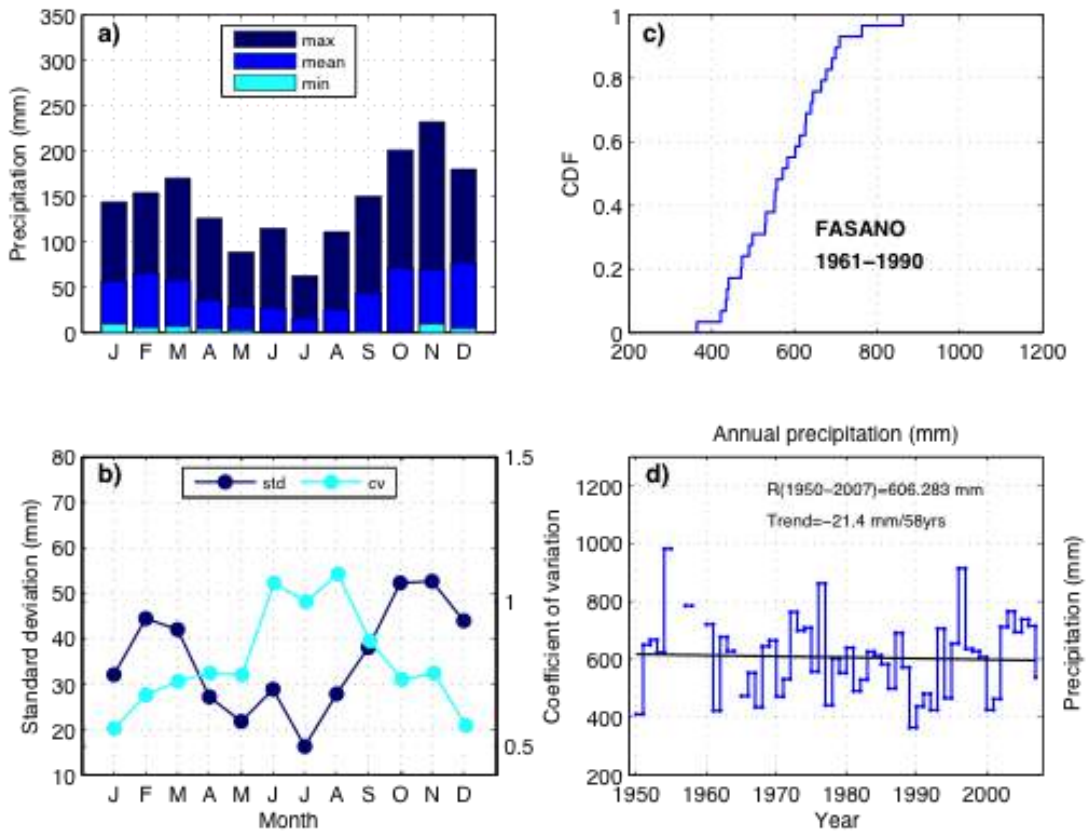

Figure 13 Annual cycle of mean monthly precipitation amounts (a), standard deviation and coefficient of variation (b), cumulative distribution (c) and time series of annual precipitation with fitted trend line for the period 1950-2007 (d) for Fasano climatological station.

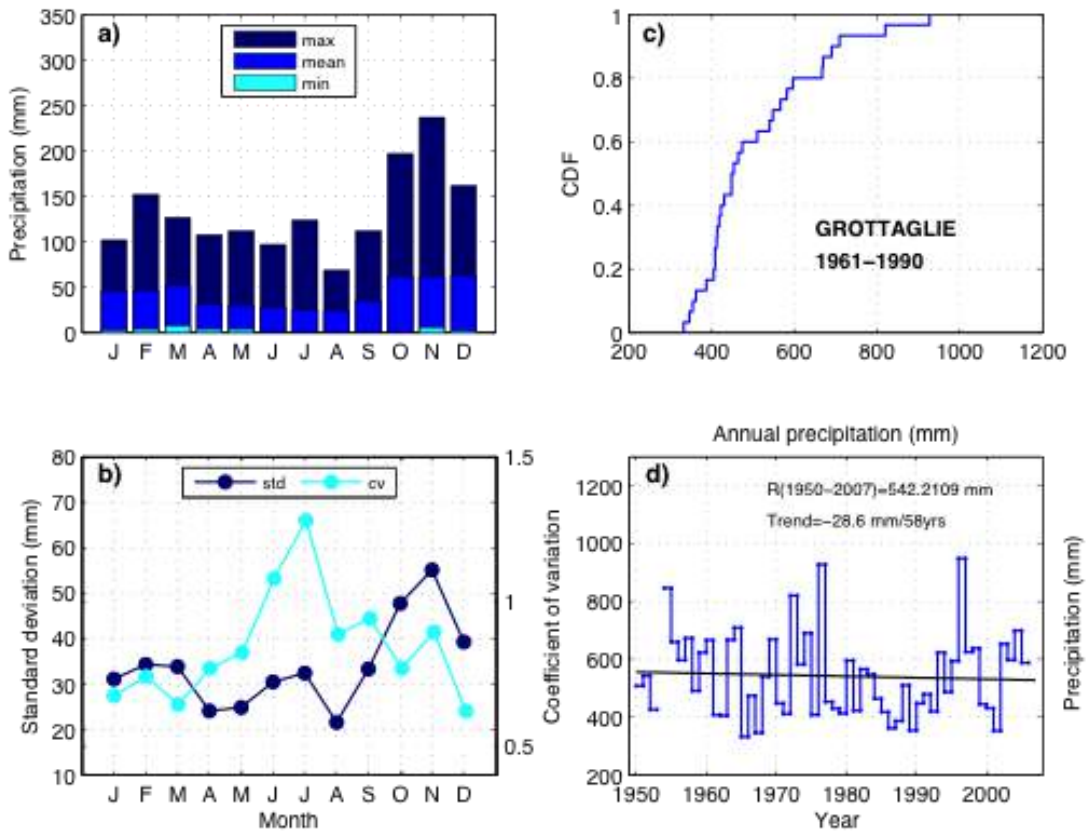

Figure 14 Annual cycle of mean monthly precipitation amounts (a), standard deviation and coefficient of variation (b), cumulative distribution (c) and time series of annual precipitation with fitted trend line for the period 1950-2007 (d) for Grottaglie climatological station.

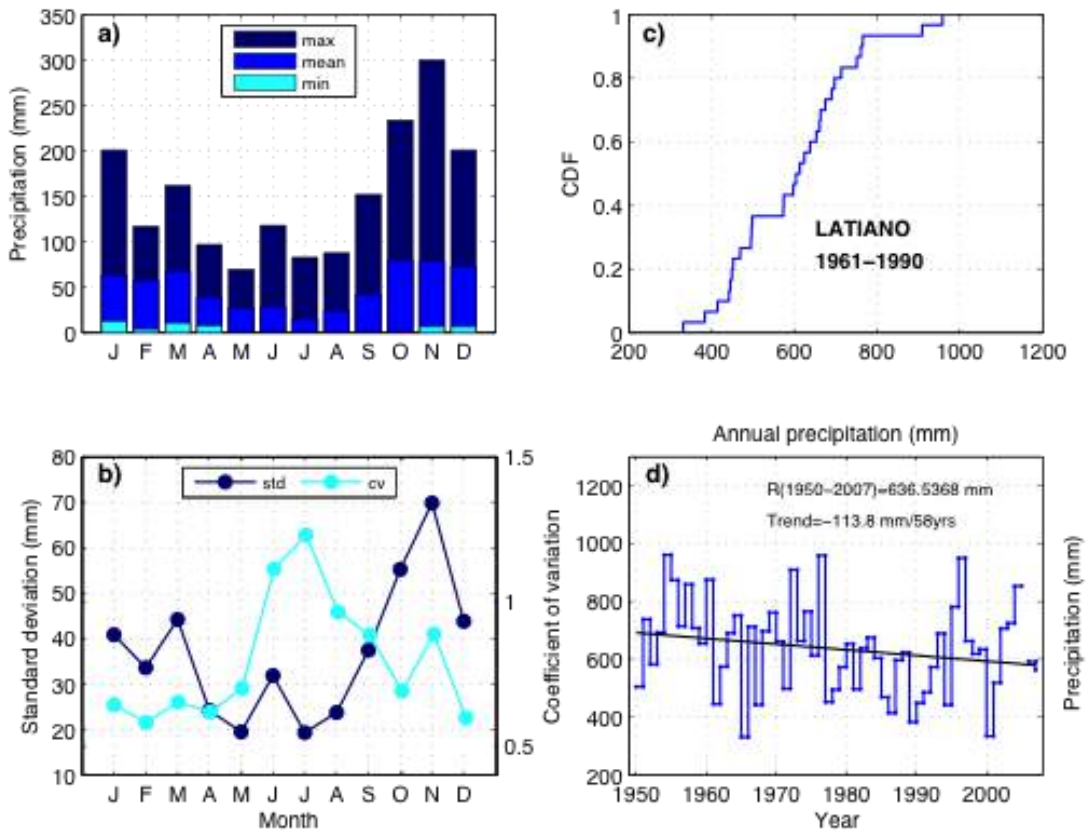

Figure 15 Annual cycle of mean monthly precipitation amounts (a), standard deviation and coefficient of variation (b), cumulative distribution (c) and time series of annual precipitation with fitted trend line for the period 1950-2007 (d) for Latiano climatological station.

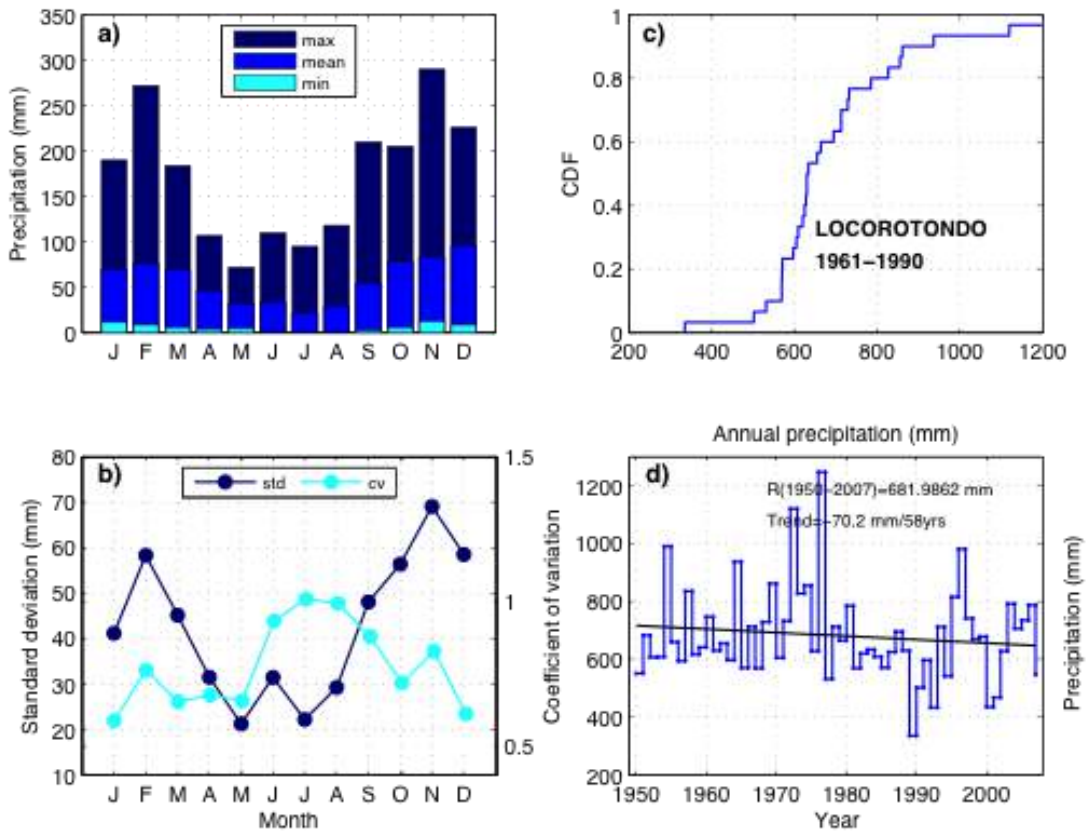

Figure 16 Annual cycle of mean monthly precipitation amounts (a), standard deviation and coefficient of variation (b), cumulative distribution (c) and time series of annual precipitation with fitted trend line for the period 1950-2007 (d) for Locorotondo climatological station.

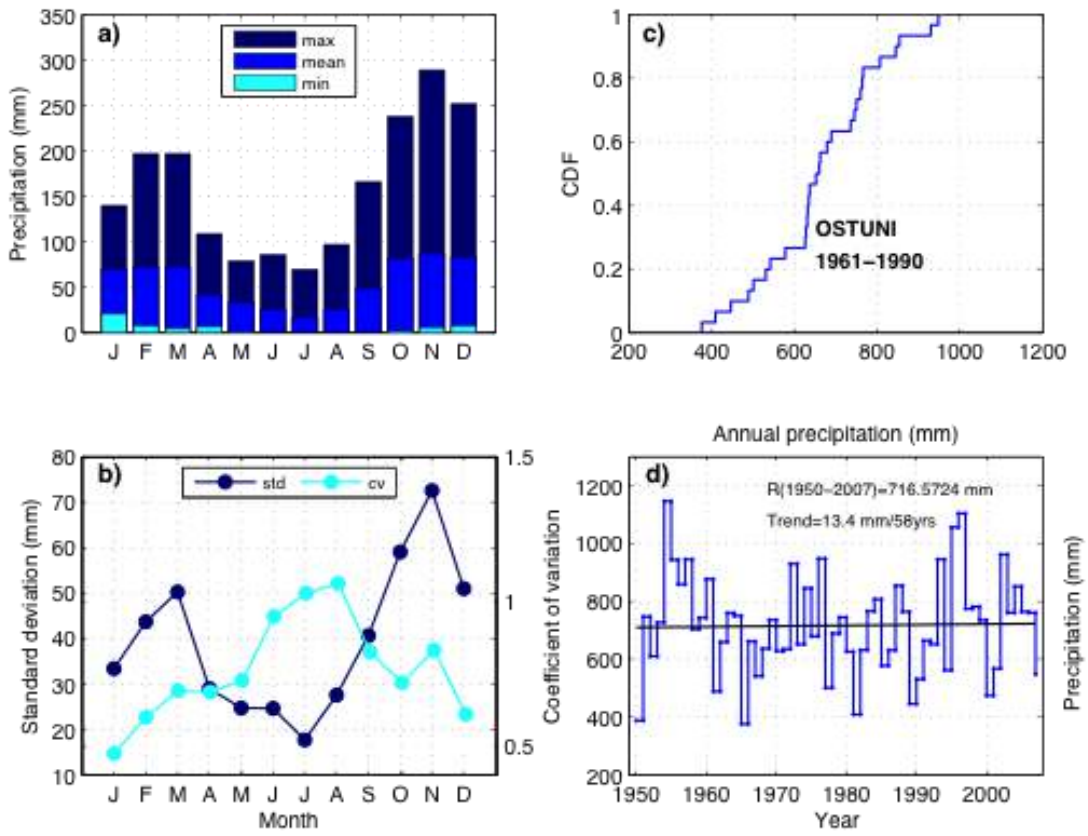

Figure 17 Annual cycle of mean monthly precipitation amounts (a), standard deviation and coefficient of variation (b), cumulative distribution (c) and time series of annual precipitation with fitted trend line for the period 1950-2007 (d) for Ostuni climatological station.

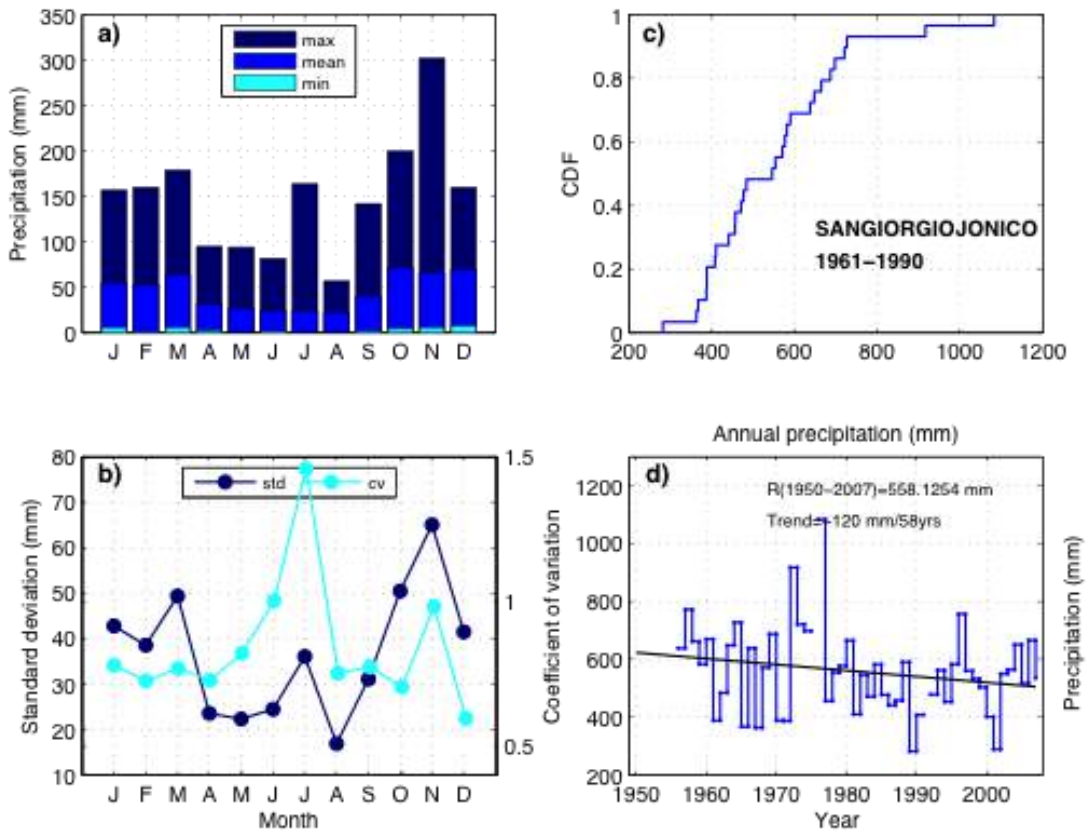

Figure 18 Annual cycle of mean monthly precipitation amounts (a), standard deviation and coefficient of variation (b), cumulative distribution (c) and time series of annual precipitation with fitted trend line for the period 1950-2007 (d) for SanGiorgio Jonico climatological station.

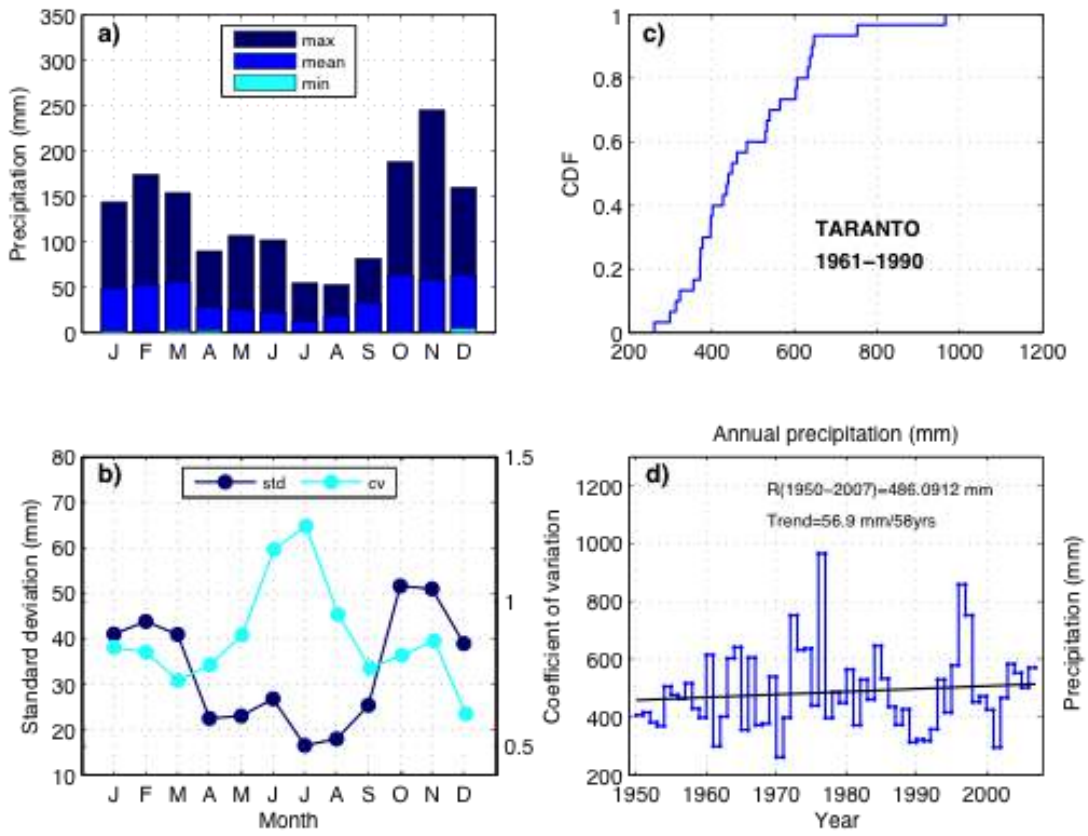

Figure 19 Annual cycle of mean monthly precipitation amounts (a), standard deviation and coefficient of variation (b), cumulative distribution (c) and time series of annual precipitation with fitted trend line for the period 1950-2007 (d) for Taranto climatological station.

3. REGIONAL CLIMATE AND MODEL SCENARIOS

In the following, results from the Regional Climate Models are compared to the observations and the model scenarios are analyzed, mainly in terms of trend.

As already explained in the introduction we used two different types of time series:

1. **RCMcorr**: bias corrected model output by EOBS data (Déqué 2007, Formayer and Haas 2010), available from http://climdat.boku.ac.at/opendap/ccwaters
2. **RCMcorr_adj**: RCM model output downscaled to the observed time series through a q-q plot procedure.

Basically, in the first time series only the bias are corrected, while through the second procedure all the cumulative density function is corrected.

The figures show for all the stations, the mean monthly precipitation observed (red line) and computed through the two downscaling procedure cited above

CEGLIE MESSAPICA STATION

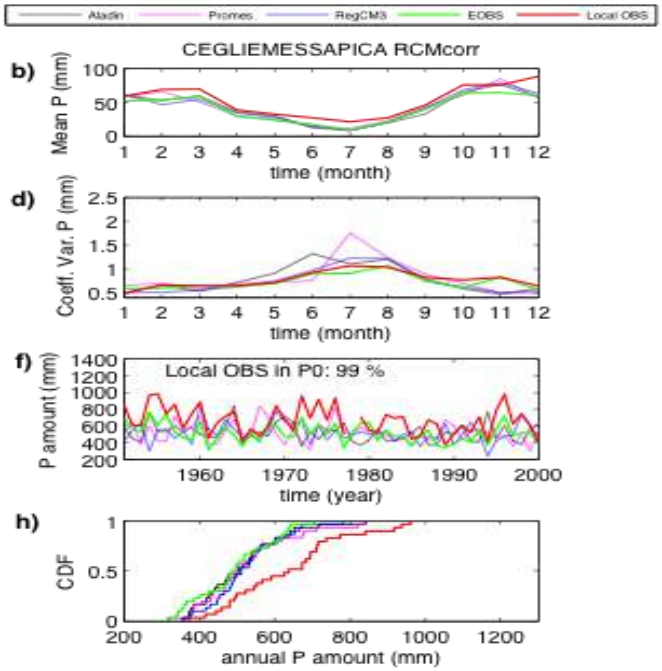

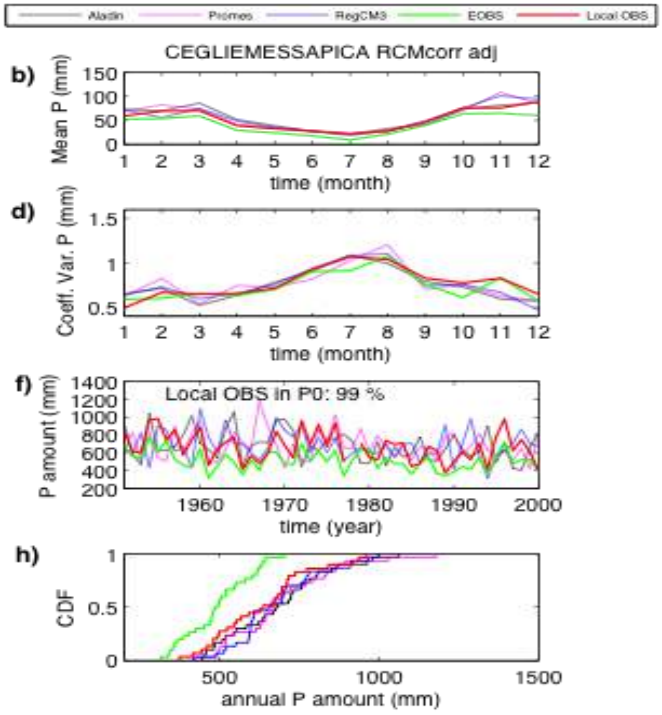

Figure 20 Ceglie Messapica station: annual cycle b) monthly precipitation amount, d) coefficient of variation of monthly precipitation amount; f) time series annual precipitation amount; h) empirical cumulative distribution functions CDFs annual precipitation amount. Model time series are RCMcorr (above); RCM_adj (below). Period of analysis:P0(1961-1900)

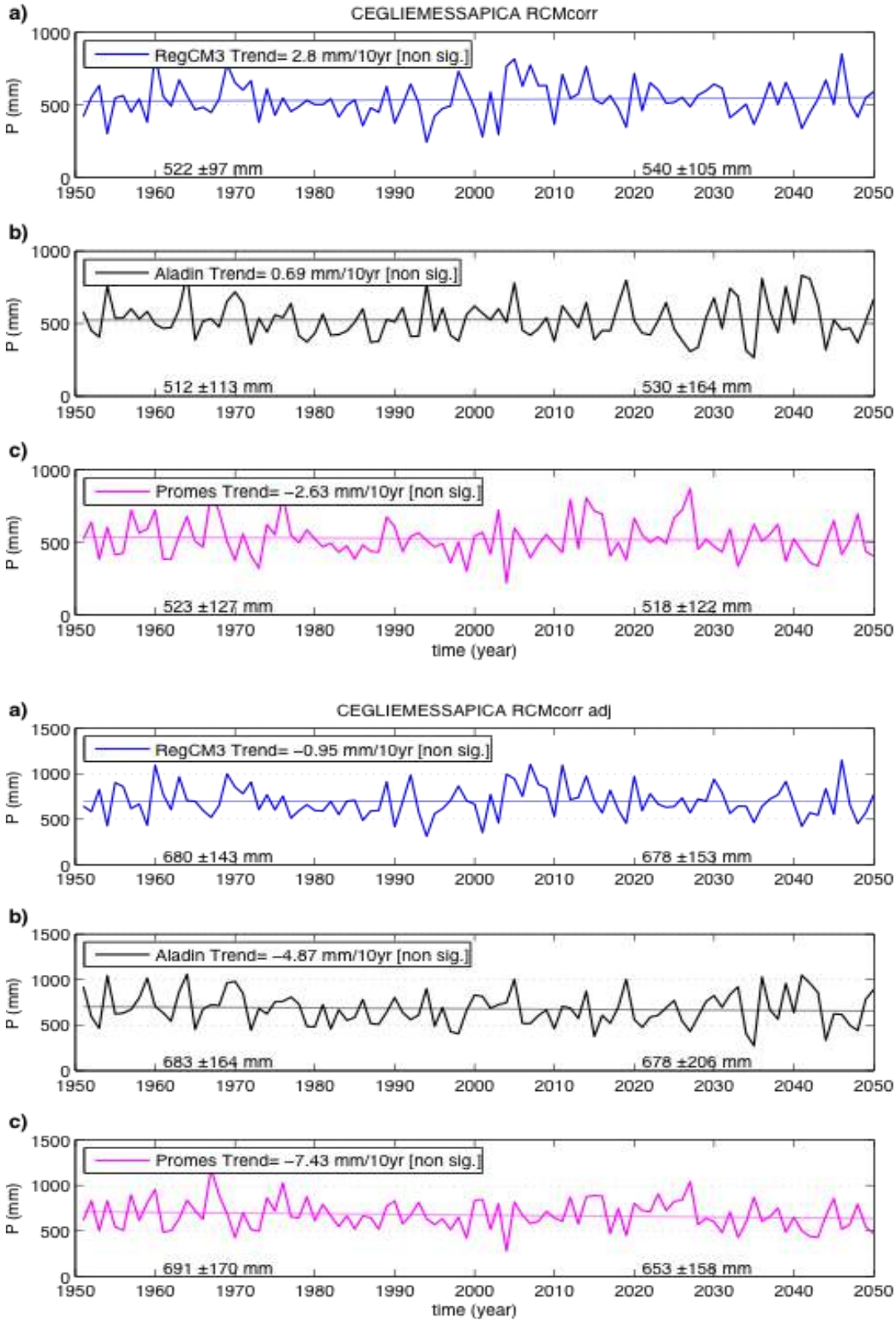

Figure 21 Ceglie Messapica station: annual precipitation amount and associated linear trend in a) RegCM3, b) Aladin, c) Promes. Decadal trend based on the entire time series is shown in panel legends. The statistical significance of the trend is assessed using the Mann-Kendall test and 5% significance level. Additional numbers at the bottom of each panel are mean

values and standard deviations during P0 (1961-1990) and P1 (2021-2050). Model time series: RCMcorr (above); RMcorr_adj (below).

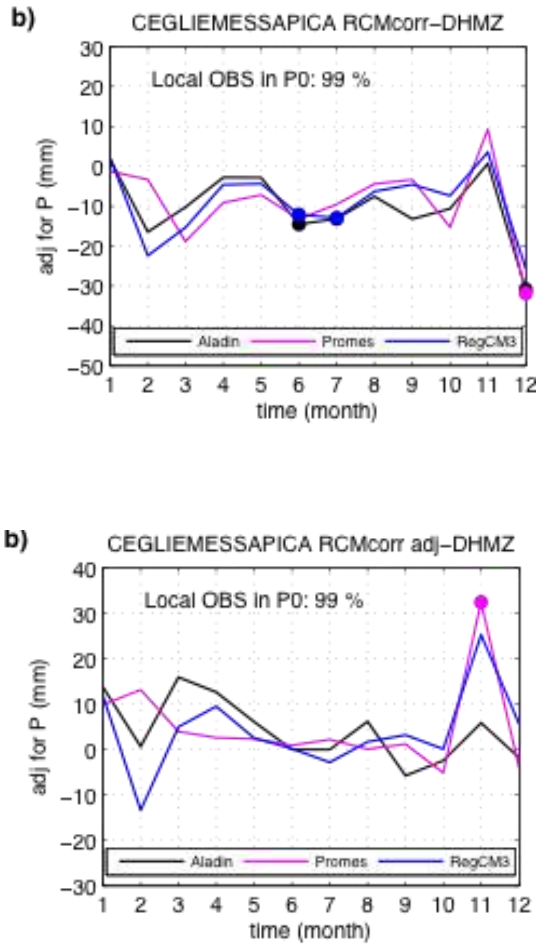

Figure 22 Ceglie Messapica station: b) adjustment differences monthly precipitation amount. Differences are based on 1961-1990 period and the availability of DHMZ observations. Statistically significant differences according to the Wilcoxon-Mann-Whitney non parameteric rank-sum test and 5% significance level are marked by the filled circles. Model time series: RCMcorr (above); RMcorr_adj (below).

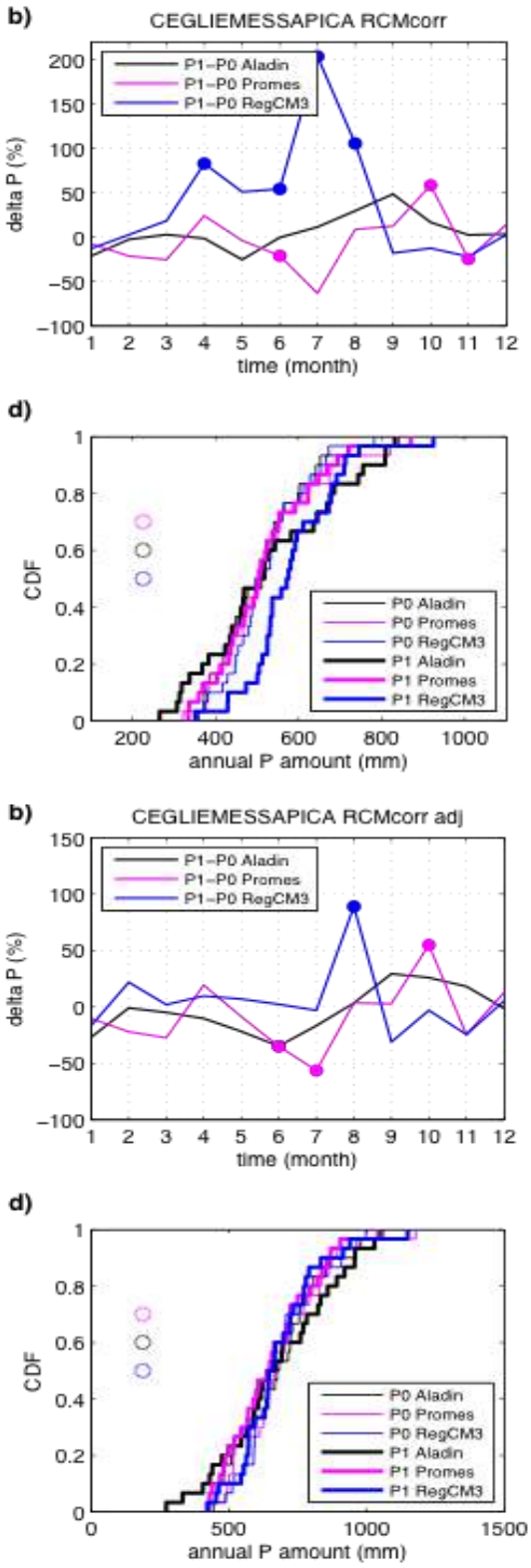

Figure 23 Ceglie Messapica station: b) relative monthly precipitation P1 vs. P0 change; d) empirical cumulative distribution functions CDFs of annual precipitation amount in P0 and P1. Time periods are: P0 1961-1990 and P1 2021-2050. Statistically significant differences in b) according to the Wilcoxon-Mann-Whitney non parameteric rank-sum test and 5% significance level are marked by the filled circles. Statistically significant differences according to the

Kolmogorov-Smirnov test and 5% significance level between CDFs in two periods for every model in panel d) are marked by the filled circles. Model time series: RCMcorr (above); RMcorr_adj (below).

CRISPIANO STATION

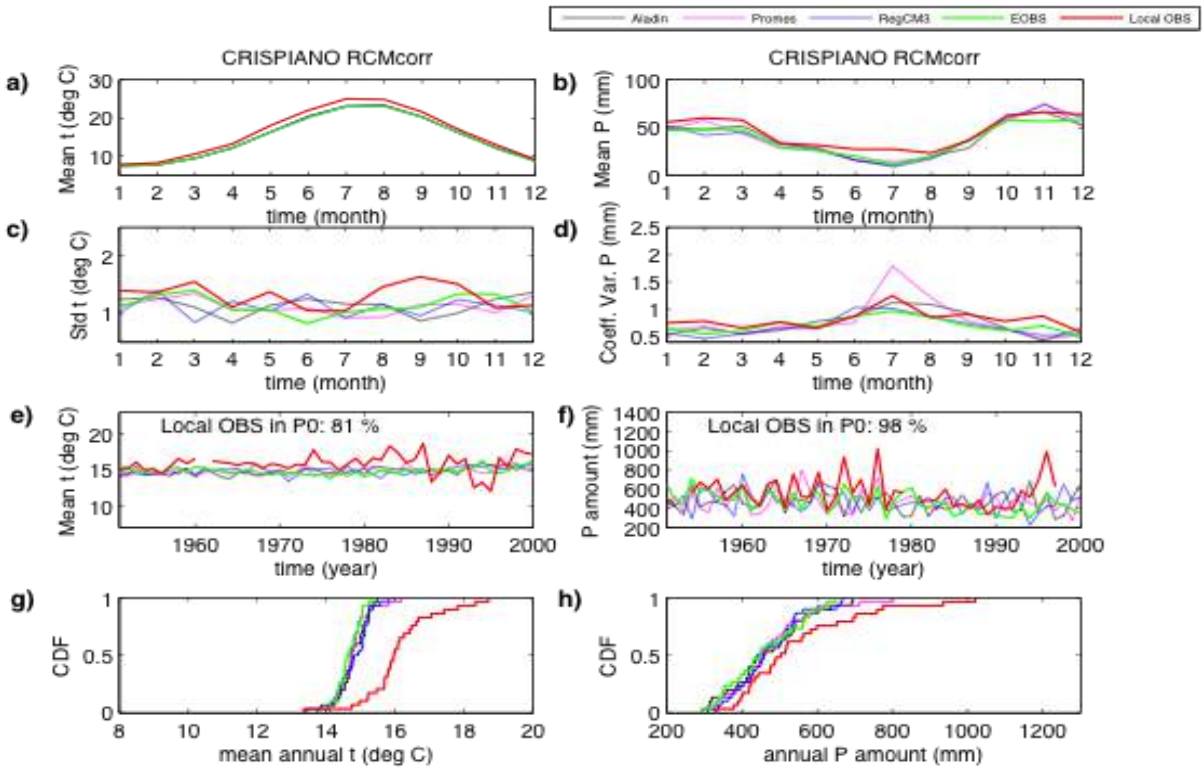

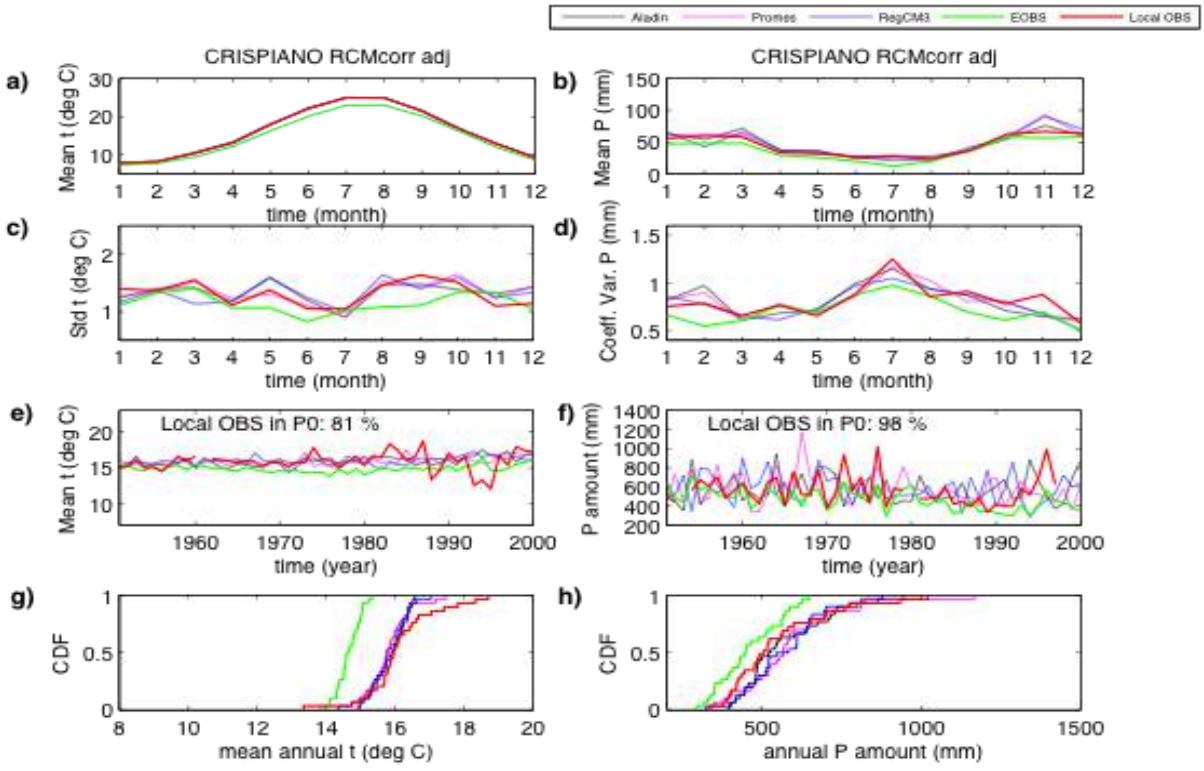

Figure 24 Crispiano station: annual cycle a) mean monthly temperature, b) monthly precipitation amount, c) mean monthly temperature standard deviation, d) coefficient of variation of monthly precipitation amount; time series e) mean annual temperature, f) annual precipitation amount; empirical cumulative distribution functions CDFs g) mean annual temperature, h) annual precipitation amount. Model time series are RCMcorr (above); RCM_adj (below). Period of analysis:P0(1961-1900)

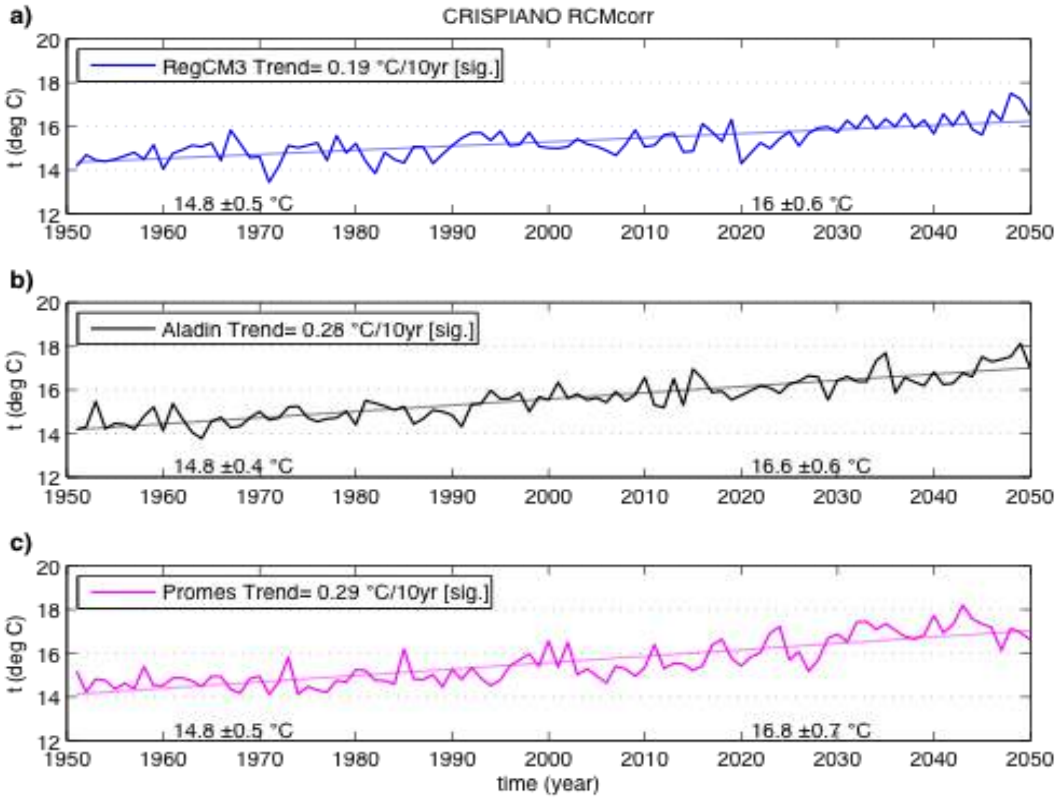

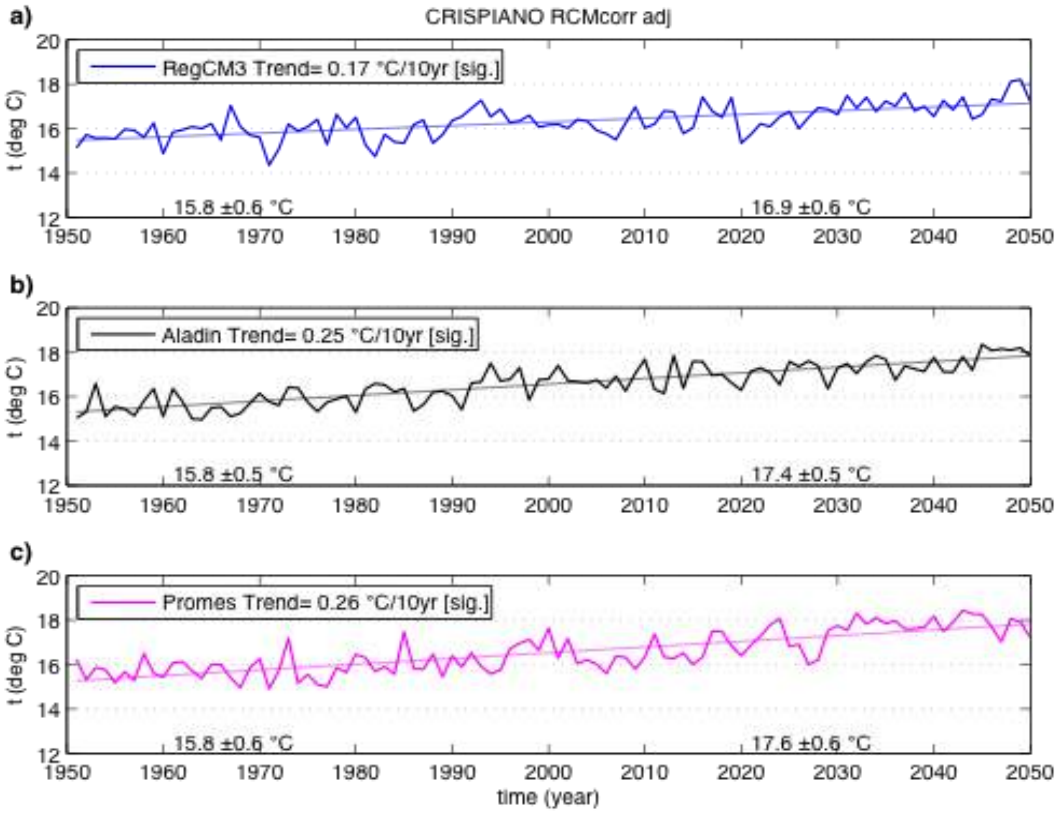

Figure 25 Crispiano station: annual mean temperature and associated linear trend in a) RegCM3, b) Aladin, c) Promes. Decadal trend based on the entire time series is shown in panel legends. The statistical significance of the trend is assessed using the Mann-Kendall test and 5% significance level. Additional numbers at the bottom of each panel are mean values and standard deviations during P0 (1961-1990) and P1 (2021-2050). Model time series: RCMcorr (above); RCMcorr_adj (below).

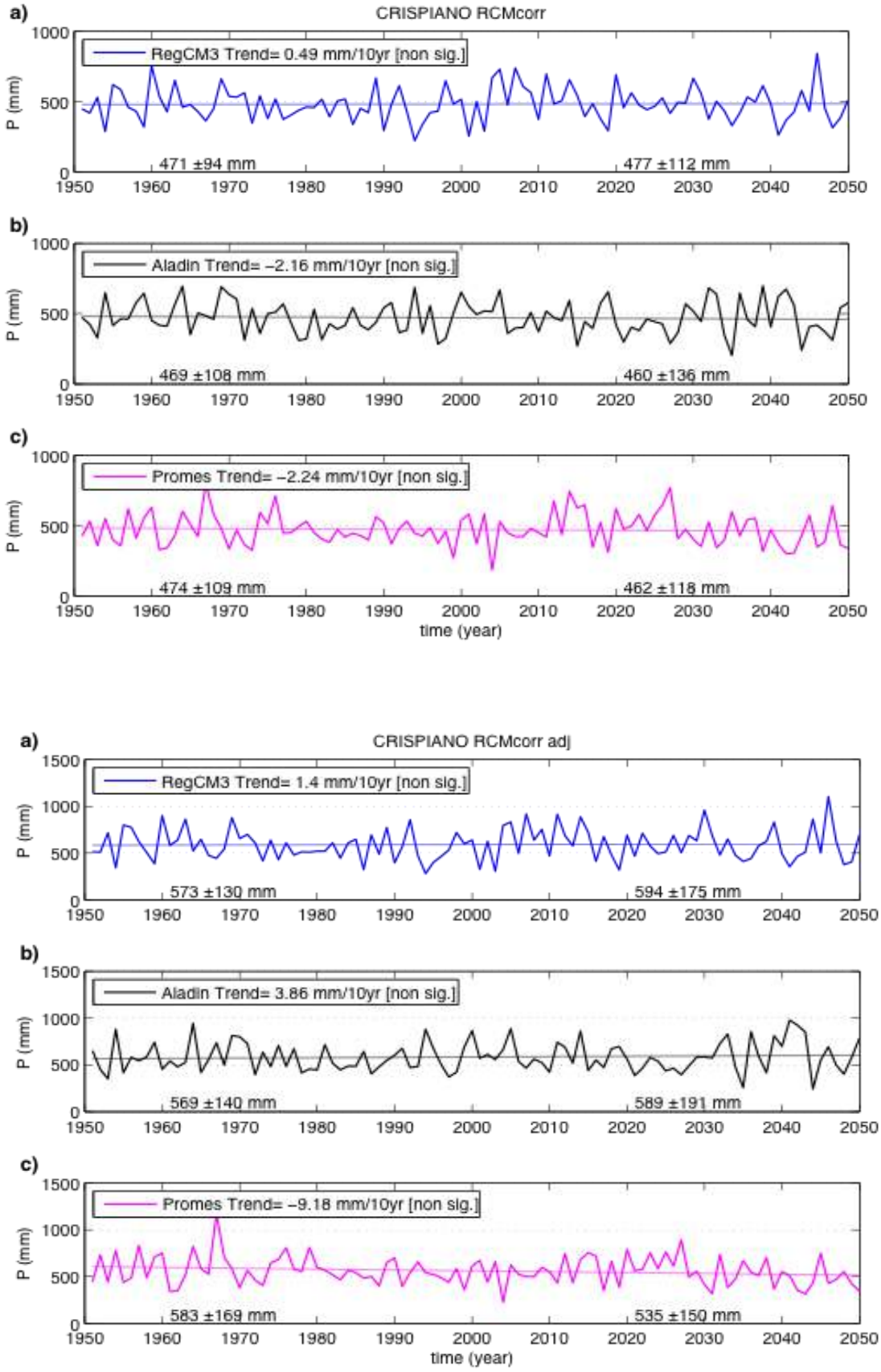

Figure 26 Crispiano station: annual precipitation amount and associated linear trend in a) RegCM3, b) Aladin, c) Promes. Decadal trend based on the entire time series is shown in panel legends. The statistical significance of the trend

is assessed using the Mann-Kendall test and 5% significance level. Additional numbers at the bottom of each panel are mean values and standard deviations during P0 (1961-1990) and P1 (2021-2050). Model time series: RCMcorr (above); RMcorr_adj (below).

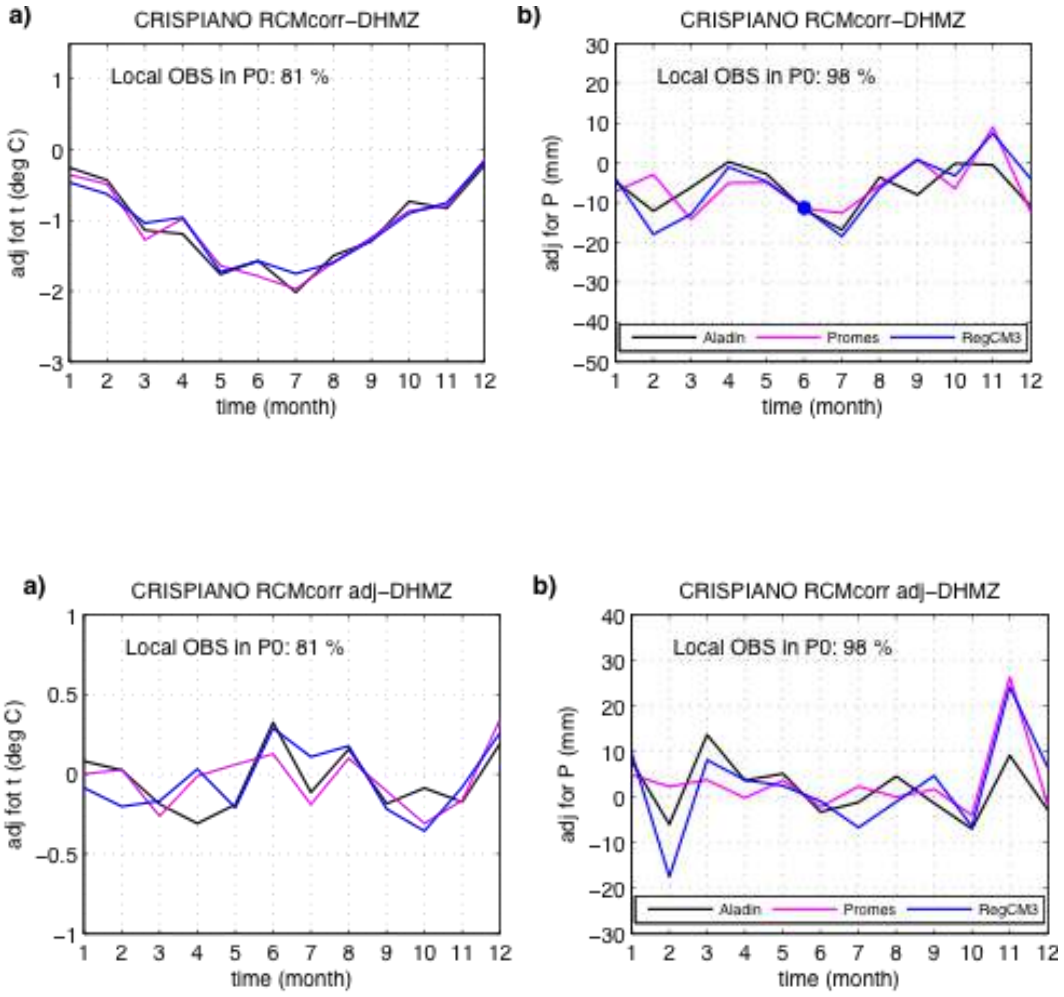

Figure 27 Crispiano station: adjustment differences a) mean monthly temperature b) monthly precipitation amount. Differences are based on 1961-1990 period and the availability of DHMZ observations. Statistically significant differences according to the Wilcoxon-Mann-Whitney nonparameteric rank-sum test and 5% significance level are marked by the filled circles. Model time series: RCMcorr (above); RMcorr_adj (below).

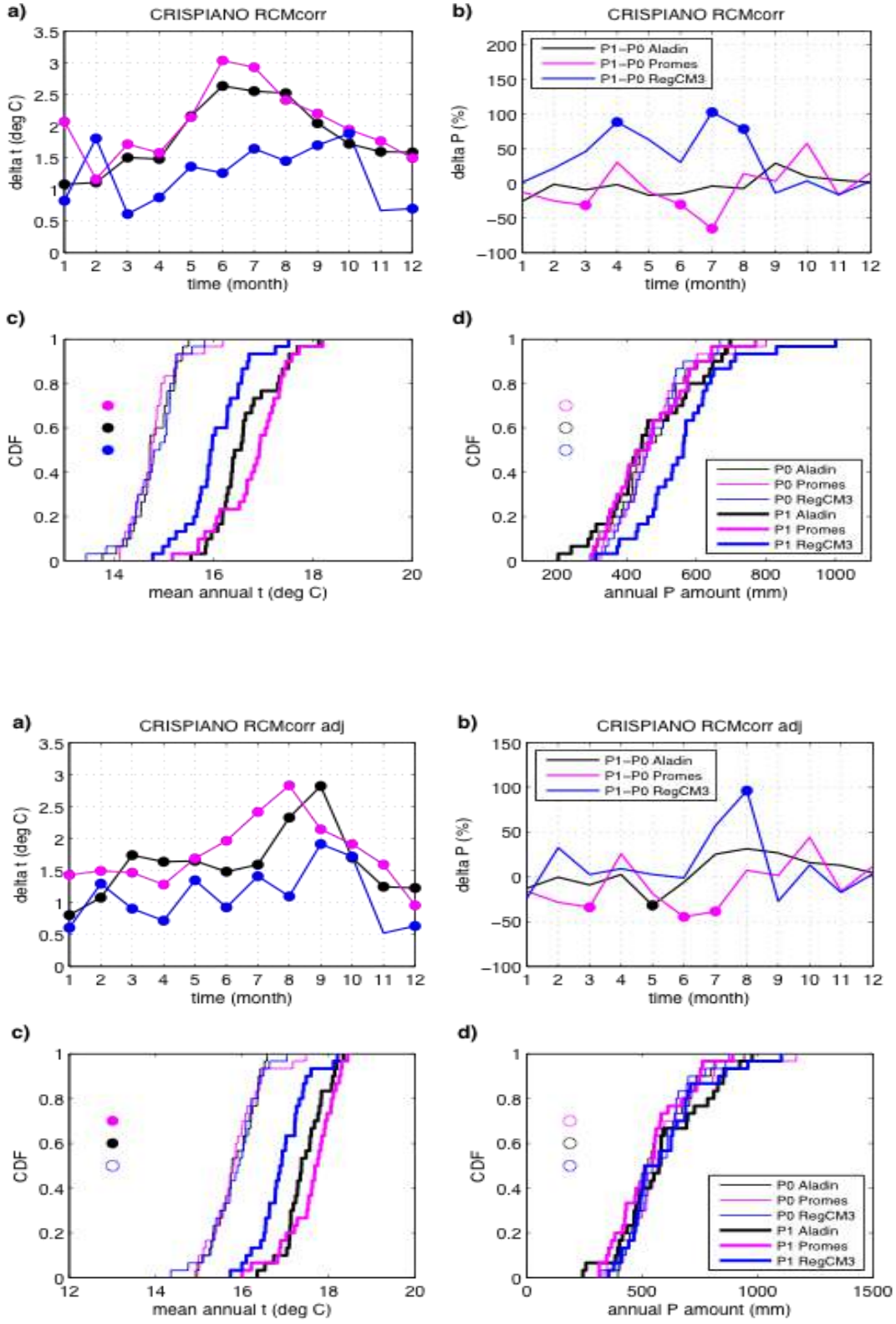

Figure 28 Crispiano station: a) monthly mean temperature P1 vs. P0 change; b) relative monthly precipitation P1 vs. P0 change; c) empirical cumulative distribution functions CDFs of mean annual temperature in P0 and P1; d) same as c) but for annual precipitation amount. Time periods are: P0 1961-1990 and P1 2021-2050. Statistically significant differences in a) and b) according to the Wilcoxon-Mann-Whitney nonparameteric rank-sum test and 5% significance level are marked by the filled circles. Statistically significant

differences according to the Kolmogorov-Smirnov test and 5% significance level between CDFs in two periods for every model in panels c) and d) are marked by the filled circles. Model time series: RCMcorr (above); RMcorr_adj (below).

FASANO STATION

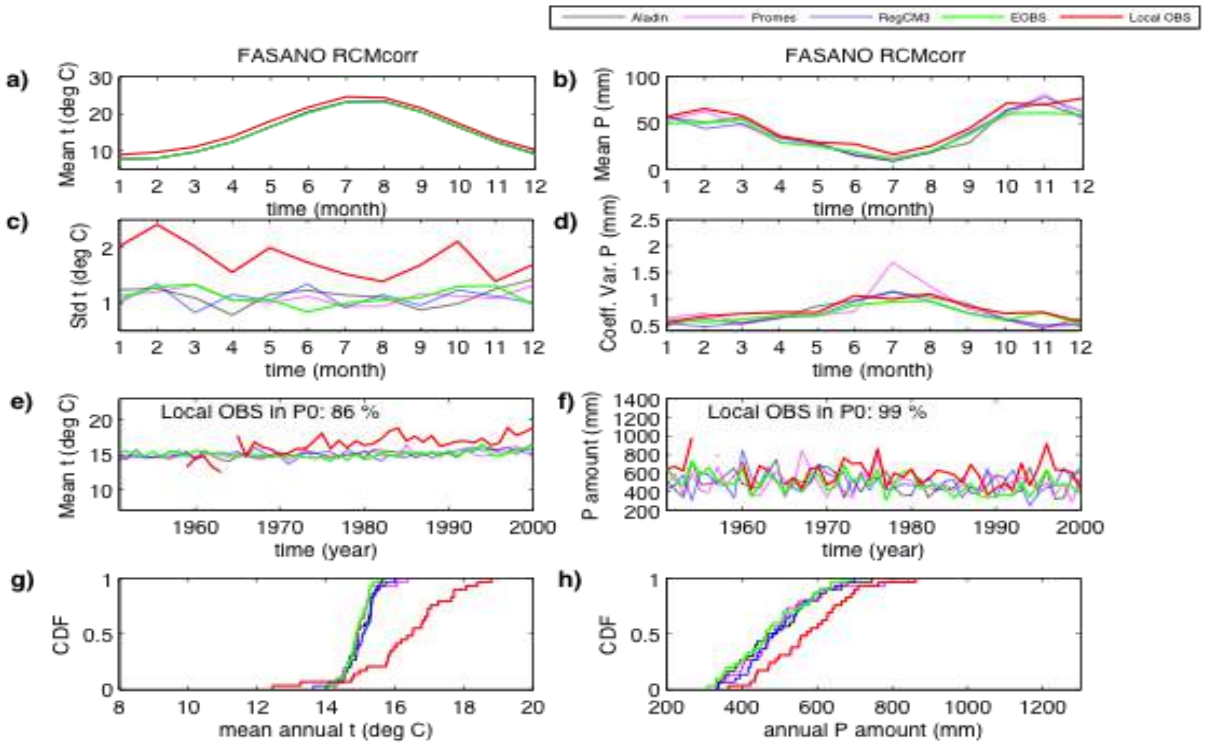

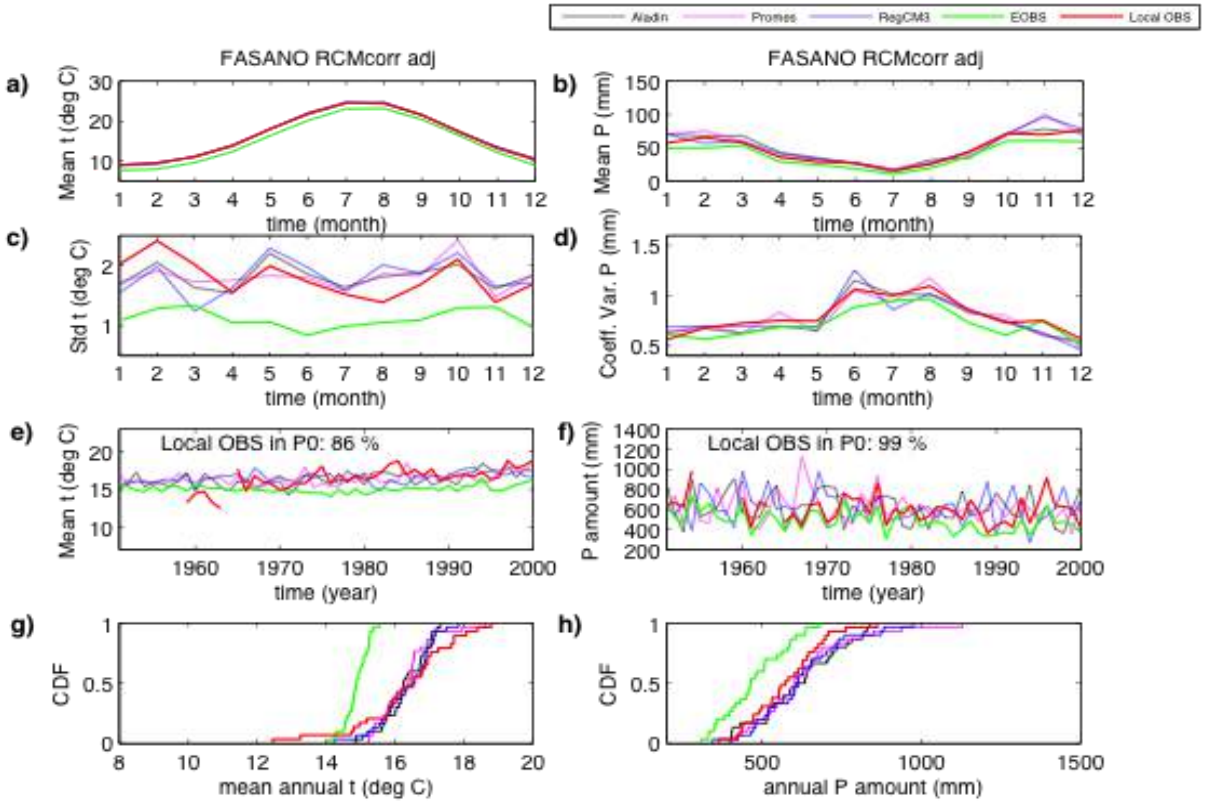

Figure 29 Fasano station: annual cycle a) mean monthly temperature, b) monthly precipitation amount, c) mean monthly temperature standard deviation, d) coefficient of variation of monthly precipitation amount; time series e) mean annual temperature, f) annual precipitation amount; empirical cumulative distribution functions CDFs g) mean annual temperature, h) annual precipitation amount. Model time series are RCMcorr (above); RCM_adj (below). Period of analysis:P0(1961-1900)

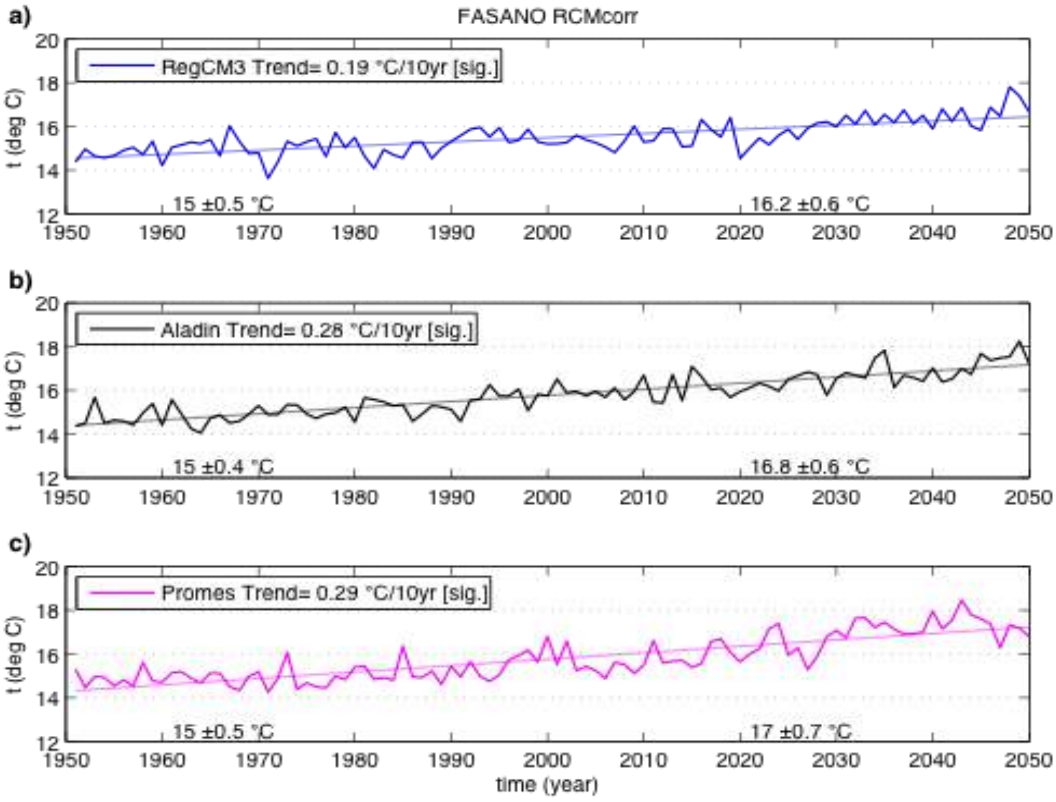

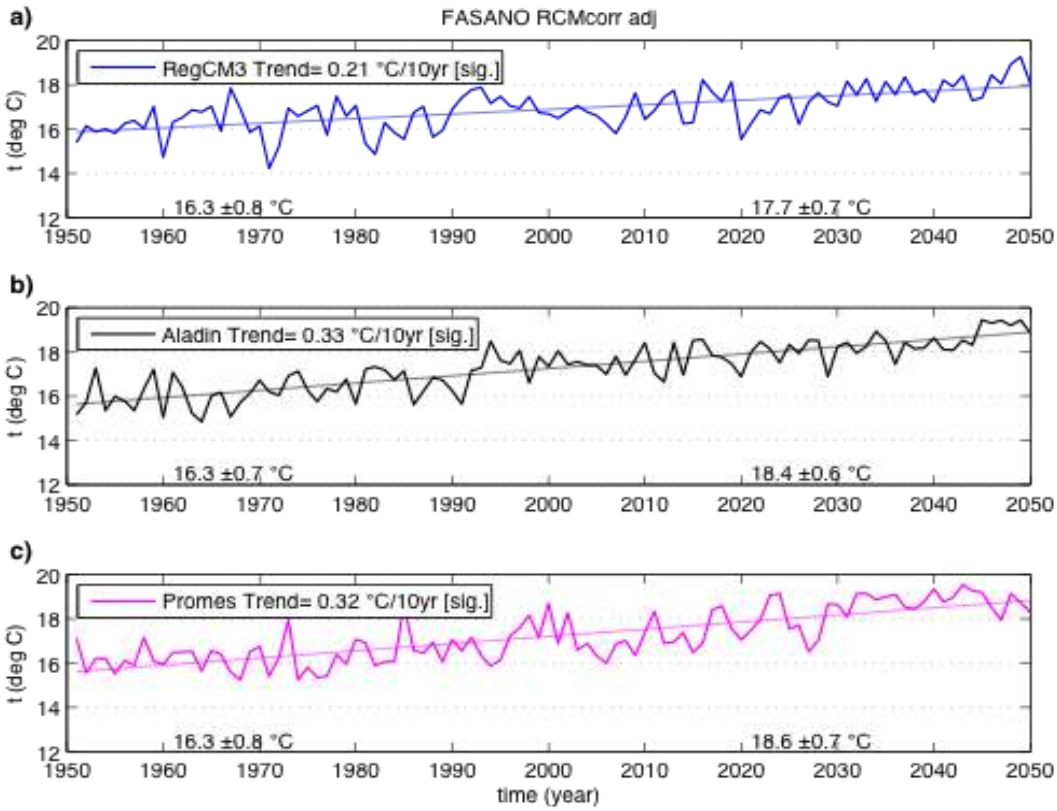

Figure 30 Fasano station: annual mean temperature and associated linear trend in a) RegCM3, b) Aladin, c) Promes. Decadal trend based on the entire time series is shown in panel legends. The statistical significance of the trend

is assessed using the Mann-Kendall test and 5% significance level. Additional numbers at the bottom of each panel are mean values and standard deviations during P0 (1961-1990) and P1 (2021-2050). Model time series: RCMcorr (above); RCMcorr_adj (below).

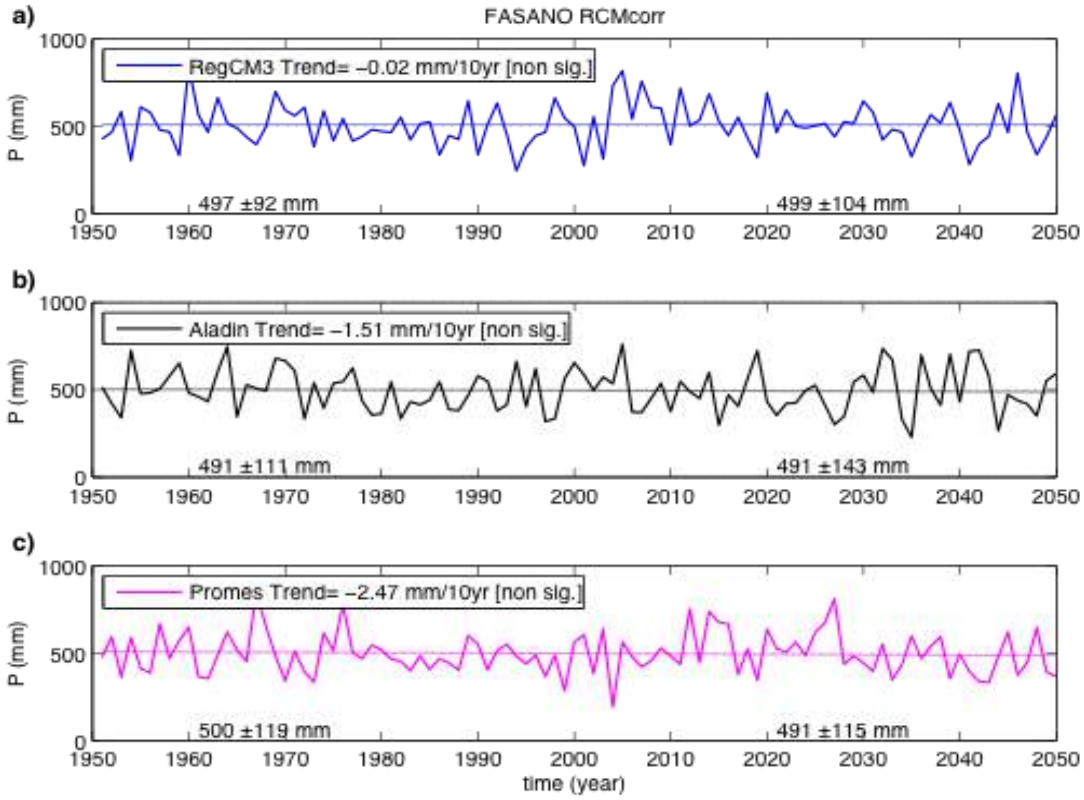

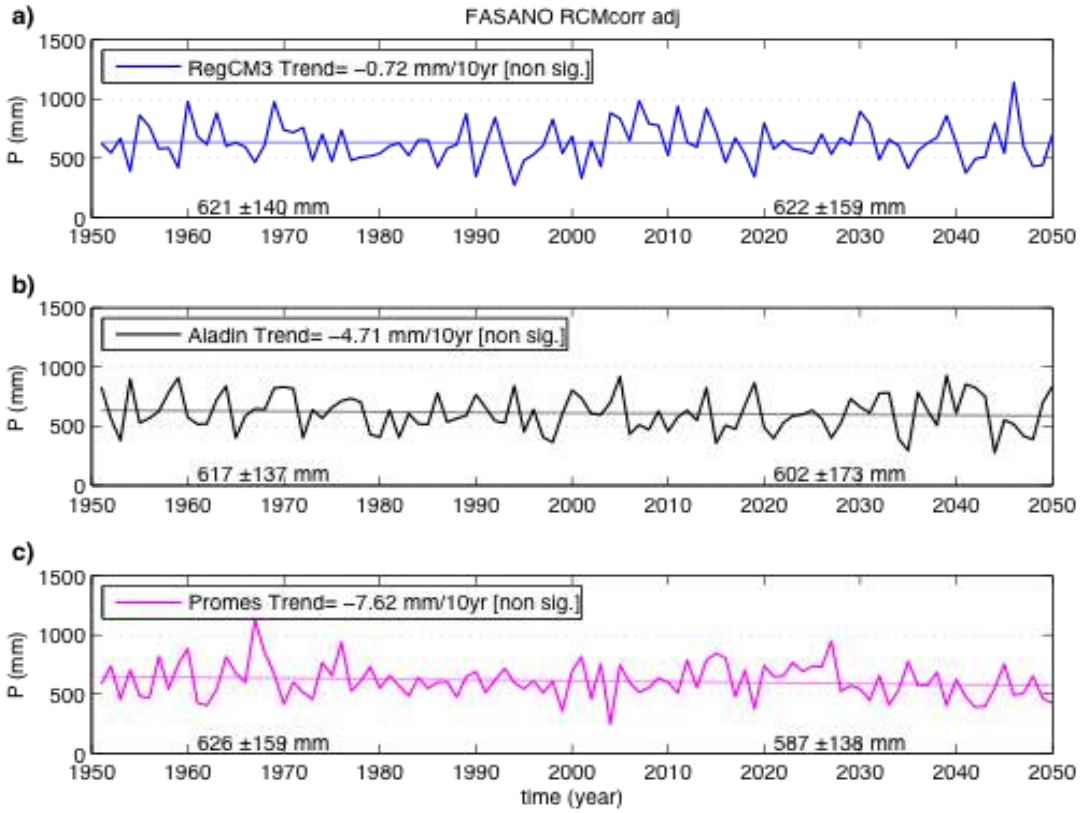

Figure 31 Fasano station: annual precipitation amount and associated linear trend in a) RegCM3, b) Aladin, c) Promes. Decadal trend based on the entire time series is shown in panel legends. The statistical significance of the trend is assessed using the Mann-Kendall test and 5% significance level. Additional numbers at the bottom of each panel are mean values and standard deviations during P0 (1961-1990) and P1 (2021-2050). Model time series: RCMcorr (above); RMcorr_adj (below).

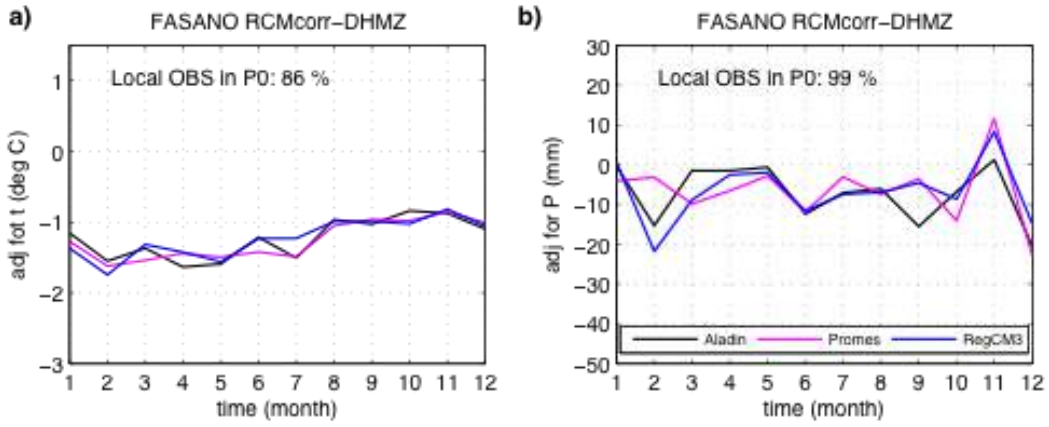

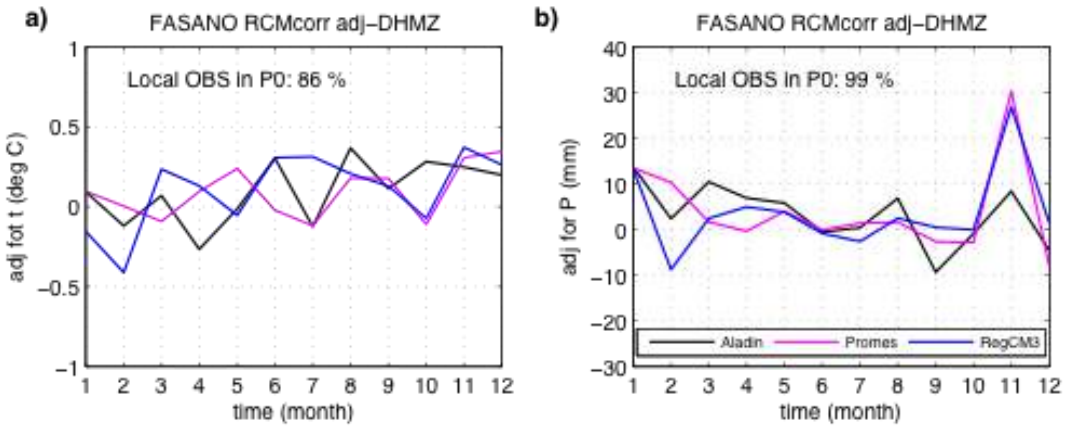

Figure 32 Fasano station: adjustment differences a) mean monthly temperature b) monthly precipitation amount. Differences are based on 1961-1990 period and the availability of DHMZ observations. Statistically significant differences according to the Wilcoxon-Mann-Whitney nonparameteric rank-sum test and 5% significance level are marked by the filled circles. Model time series: RCMcorr (above); RMcorr_adj (below).

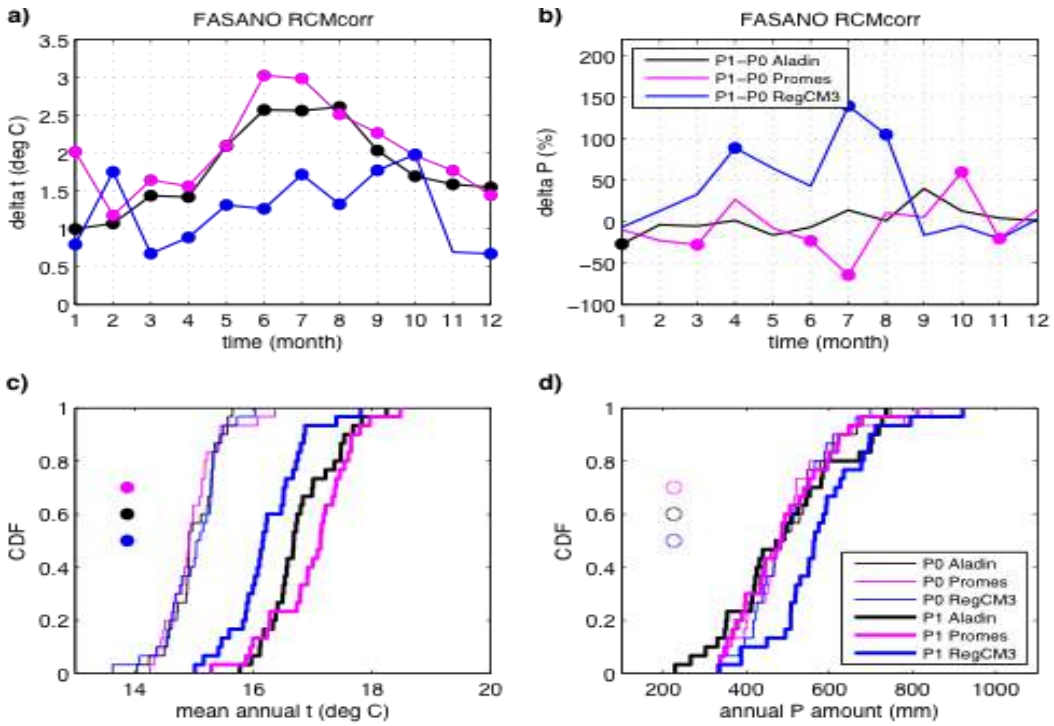

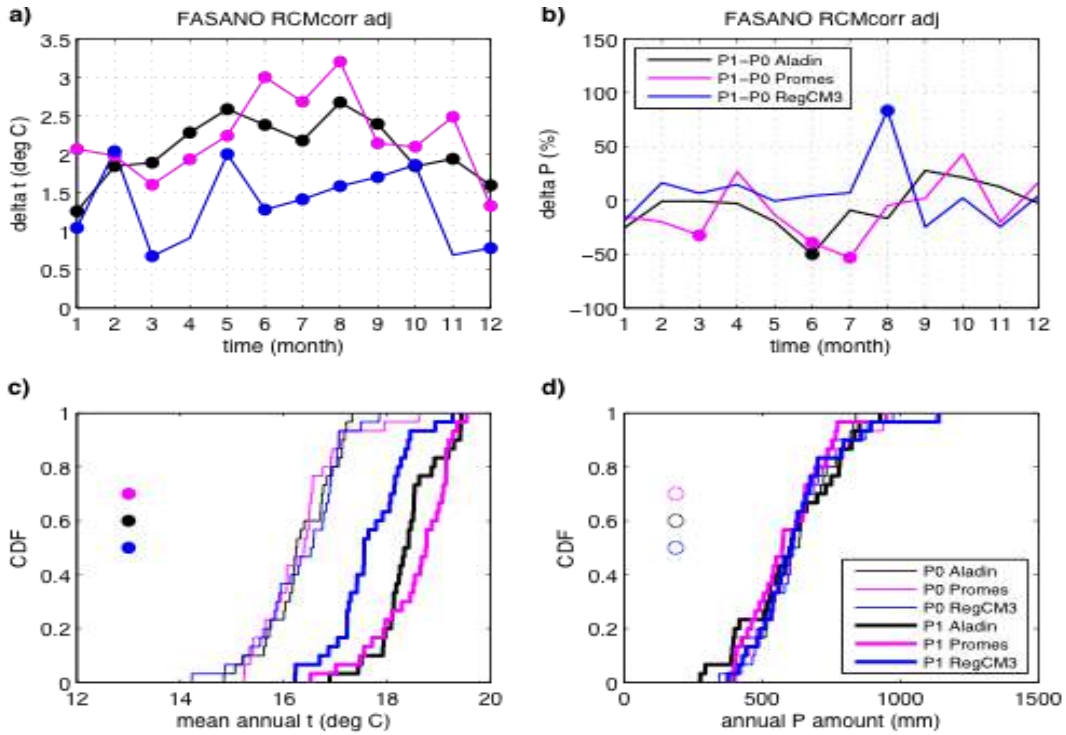

Figure 33 Fasano station: a) monthly mean temperature P1 vs. P0 change; b) relative monthly precipitation P1 vs. P0 change; c) empirical cumulative distribution functions CDFs of mean annual temperature in P0 and P1; d) same as c) but for annual precipitation amount. Time periods are: P0 1961-1990 and P1 2021-2050. Statistically significant differences in a) and b) according to the Wilcoxon-Mann-Whitney nonparameteric rank-sum test and 5% significance level are marked by the filled circles. Statistically significant differences according to the Kolmogorov-Smirnov test and 5% significance level between CDFs in two periods for every model in panels c) and d) are marked by the filled circles. Model time series: RCMcorr (above); RMcorr_adj (below).

GROTTAGLIE STATION

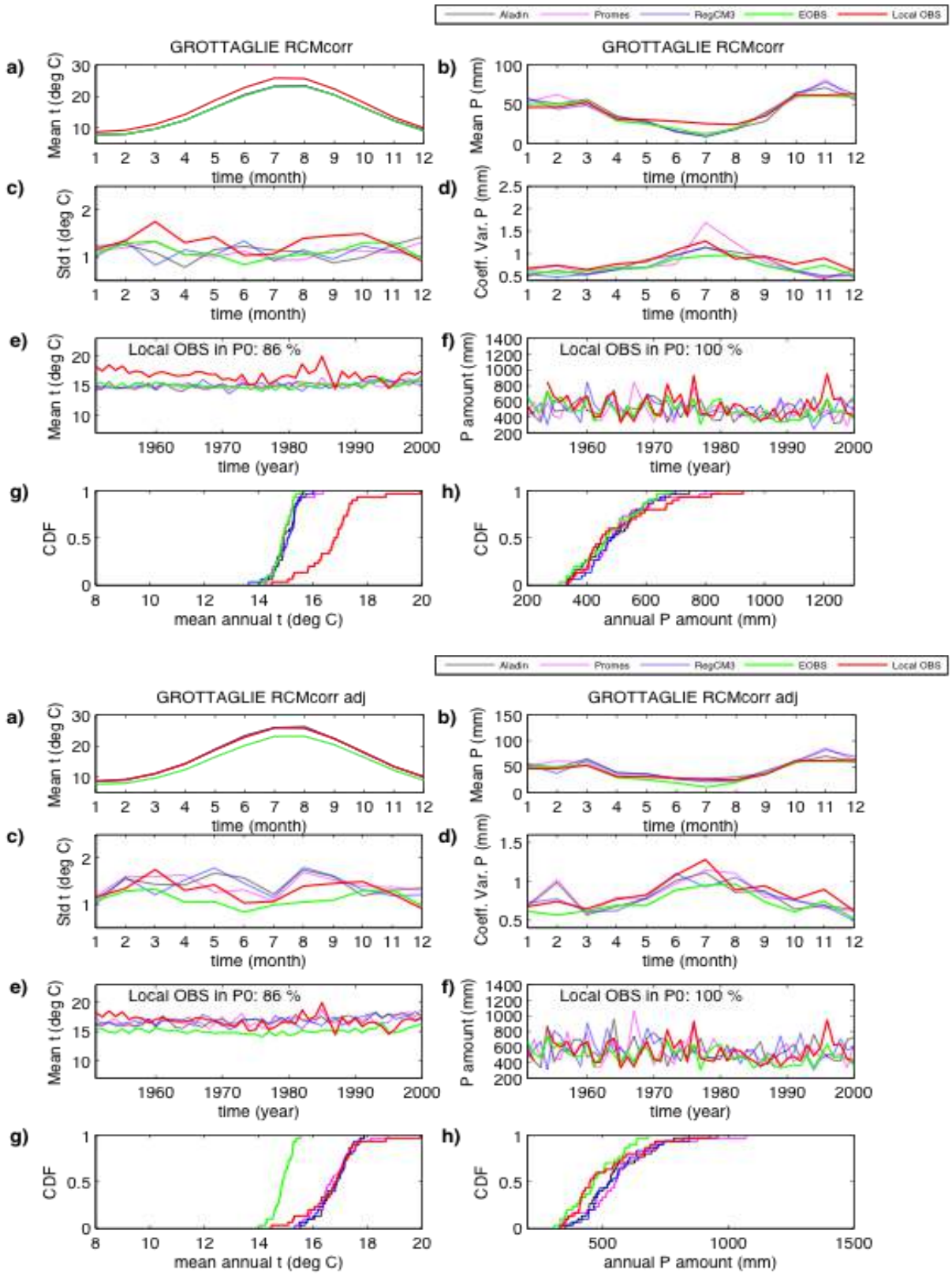

Figure 34 Grottaglie station: annual cycle a) mean monthly temperature, b) monthly precipitation amount, c) mean monthly temperature standard deviation, d) coefficient of variation of monthly precipitation amount; time series e) mean annual temperature, f) annual precipitation amount; empirical cumulative distribution functions CDFs g) mean annual temperature, h) annual

precipitation amount. Model time series are RCMcorr (above); RCM_adj (below). Period of analysis:P0(1961-1900)

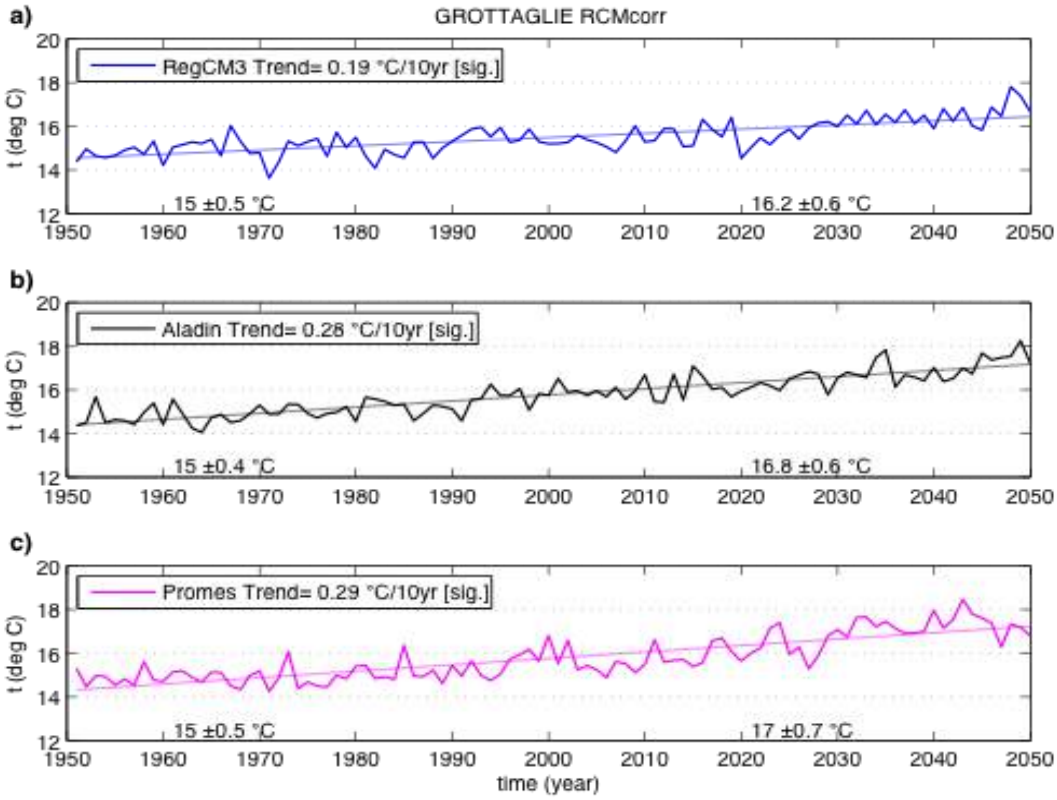

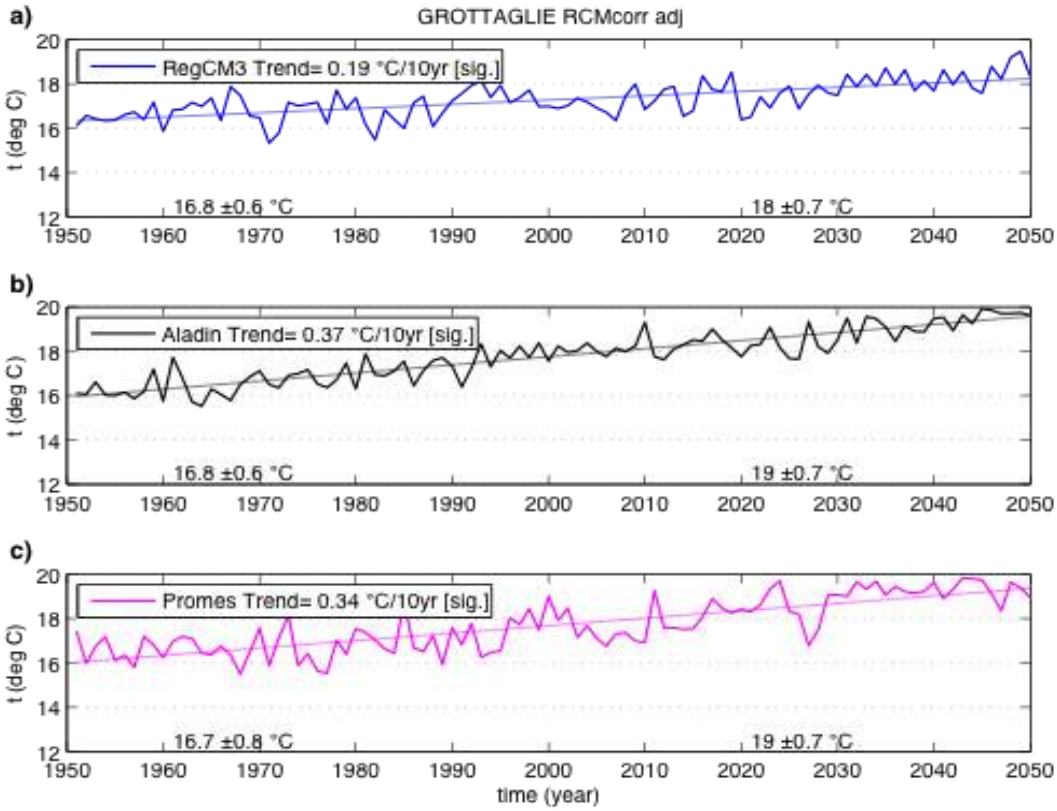

Figure 35 Grottaglie station: annual mean temperature and associated linear trend in a) RegCM3, b) Aladin, c) Promes. Decadal trend based on the entire time series is shown in panel legends. The statistical significance of the trend is assessed using the Mann-Kendall test and 5% significance level. Additional numbers at the bottom of each panel are mean values and standard deviations during P0 (1961-1990) and P1 (2021-2050). Model time series: RCMcorr (above); RCMcorr_adj (below).

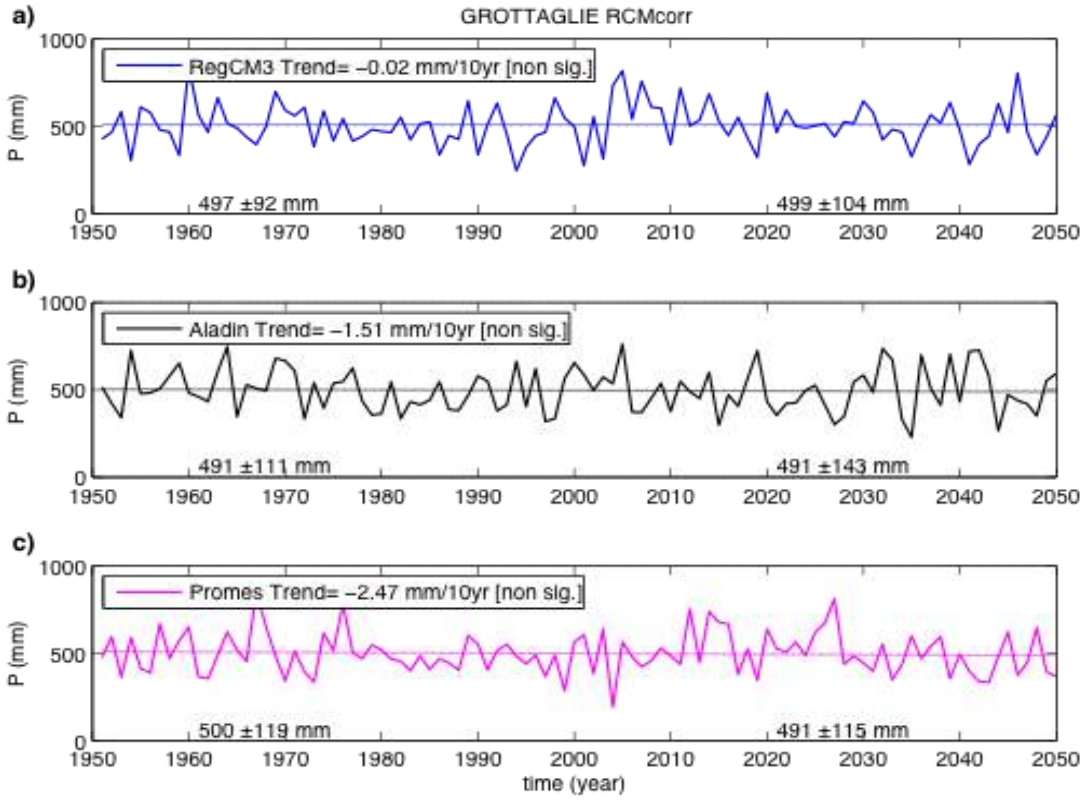

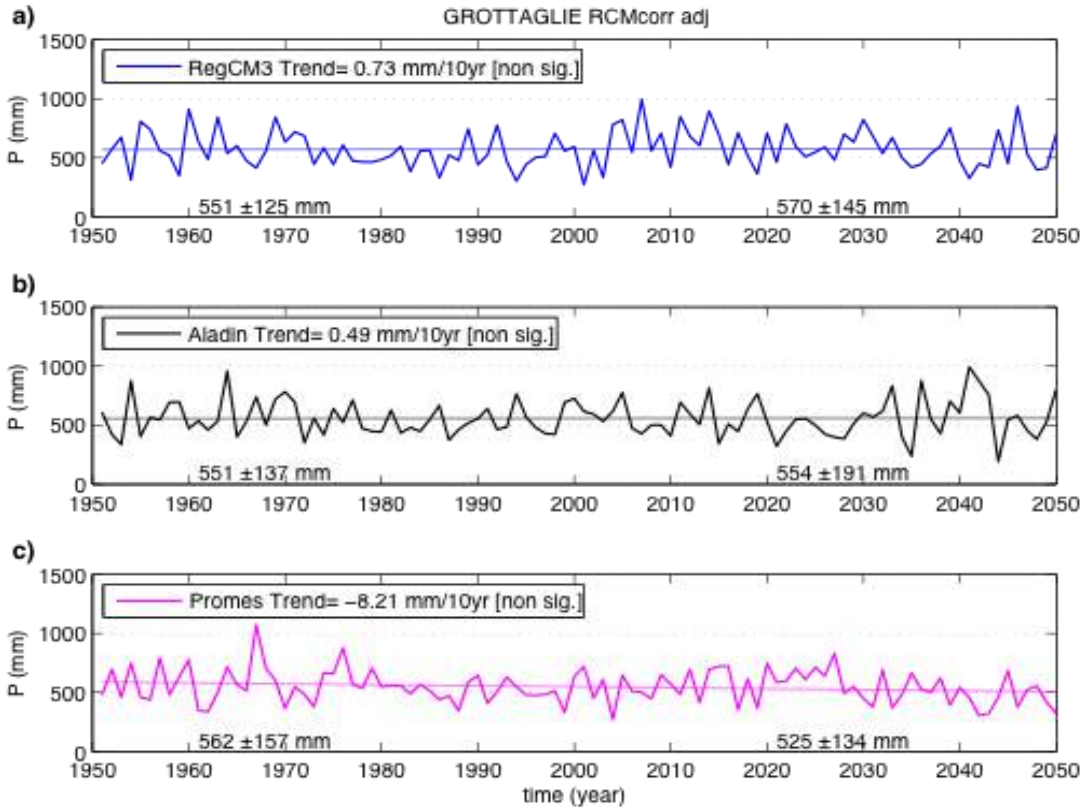

Figure 36 Grottaglie station: annual precipitation amount and associated linear trend in a) RegCM3, b) Aladin, c) Promes. Decadal trend based on the entire time series is shown in panel legends. The statistical significance of the trend is assessed using the Mann-Kendall test and 5% significance level. Additional numbers at the bottom of each panel are mean values and standard deviations during P0 (1961-1990) and P1 (2021-2050). Model time series: RCMcorr (above); RMcorr_adj (below).

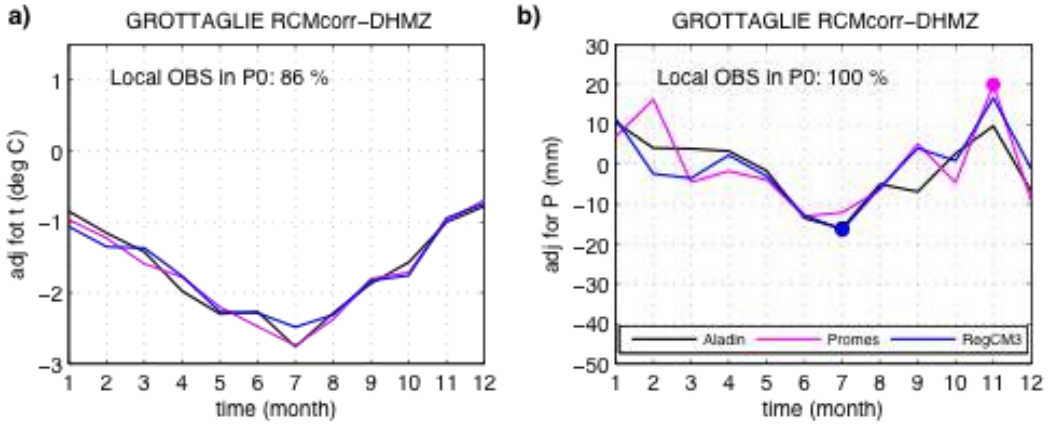

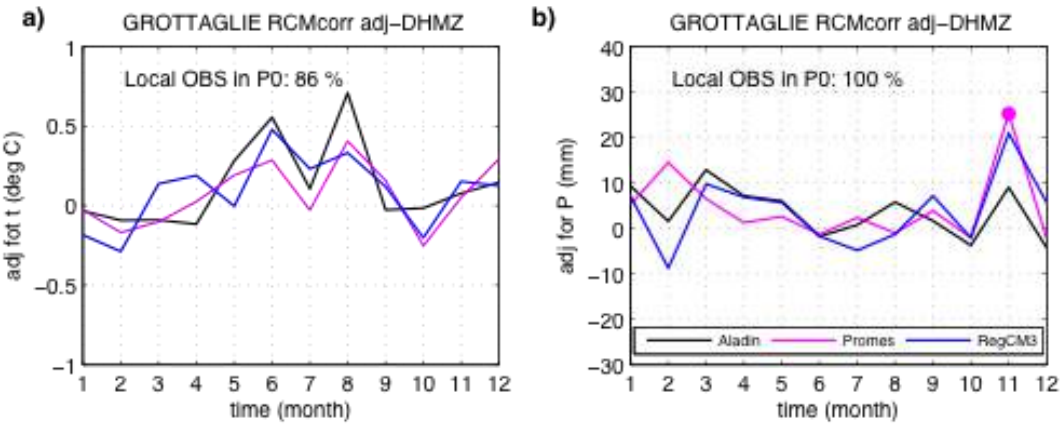

Figure 37 Grottaglie station: adjustment differences a) mean monthly temperature b) monthly precipitation amount. Differences are based on 1961-1990 period and the availability of DHMZ observations. Statistically significant differences according to the Wilcoxon-Mann-Whitney nonparameteric rank-sum test and 5% significance level are marked by the filled circles. Model time series: RCMcorr (above); RMcorr_adj (below).

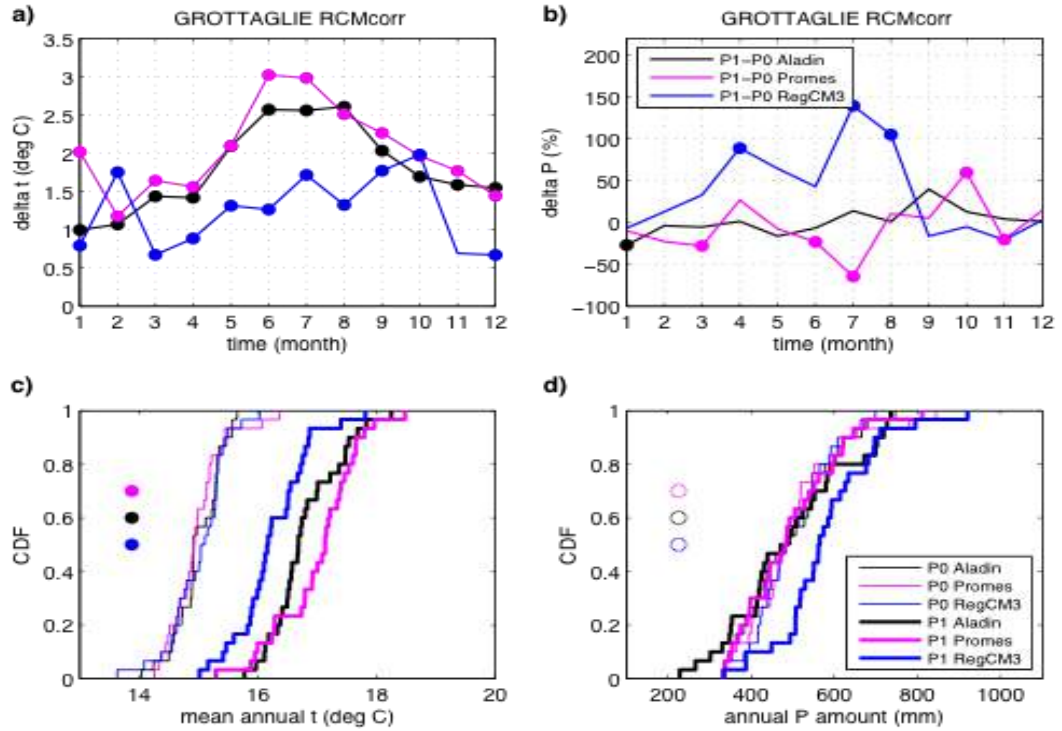

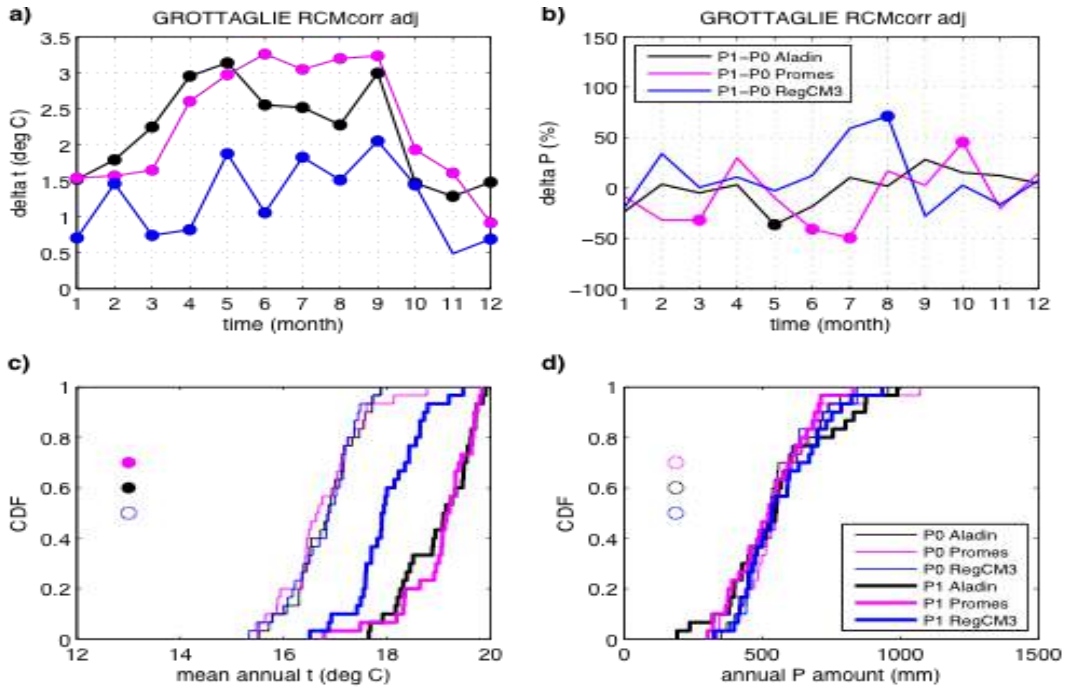

Figure 38 Grottaglie station: a) monthly mean temperature P1 vs. P0 change; b) relative monthly precipitation P1 vs. P0 change; c) empirical cumulative distribution functions CDFs of mean annual temperature in P0 and P1; d) same as c) but for annual precipitation amount. Time periods are: P0 1961-1990 and P1 2021-2050. Statistically significant differences in a) and b) according to the Wilcoxon-Mann-Whitney nonparameteric rank-sum test and 5% significance level are marked by the filled circles. Statistically significant differences according to the Kolmogorov-Smirnov test and 5% significance level between CDFs in two periods for every model in panels c) and d) are marked by the filled circles. Model time series: RCMcorr (above); RMcorr_adj (below).

LATIANO STATION

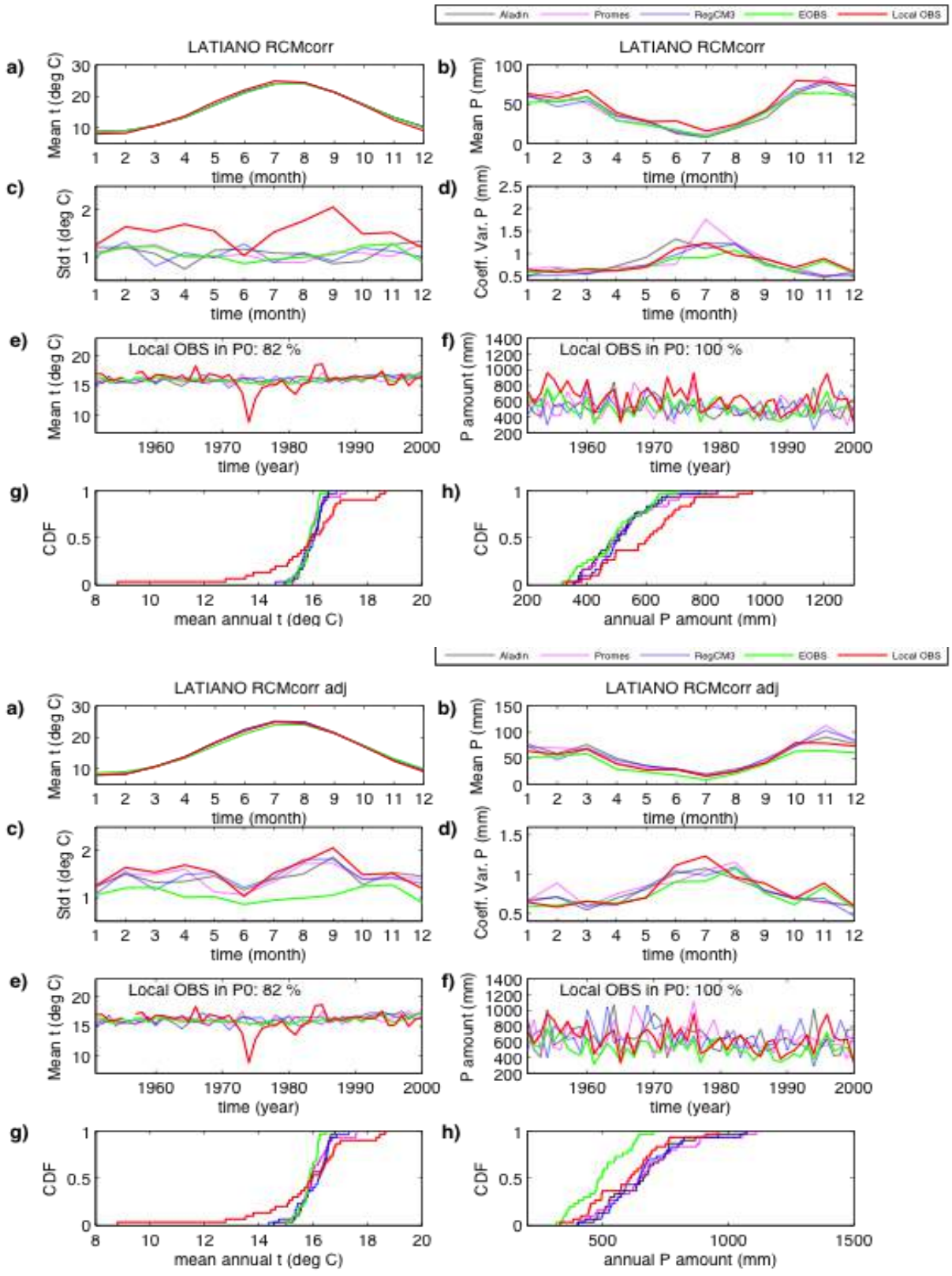

Figure 39 Latiano station: annual cycle a) mean monthly temperature, b) monthly precipitation amount, c) mean monthly temperature standard deviation, d) coefficient of variation of monthly precipitation amount; time series e) mean annual temperature, f) annual precipitation amount; empirical cumulative distribution functions CDFs g) mean annual temperature, h) annual

precipitation amount. Model time series are RCMcorr (above); RCM_adj (below). Period of analysis:P0(1961-1900)

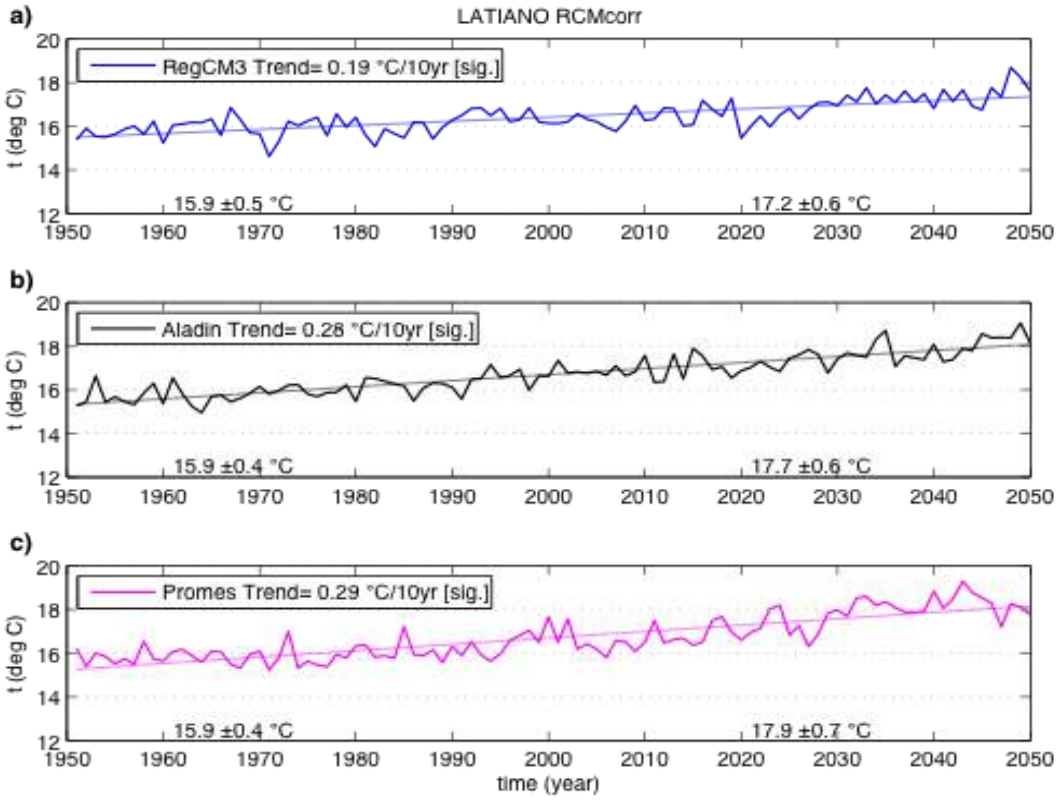

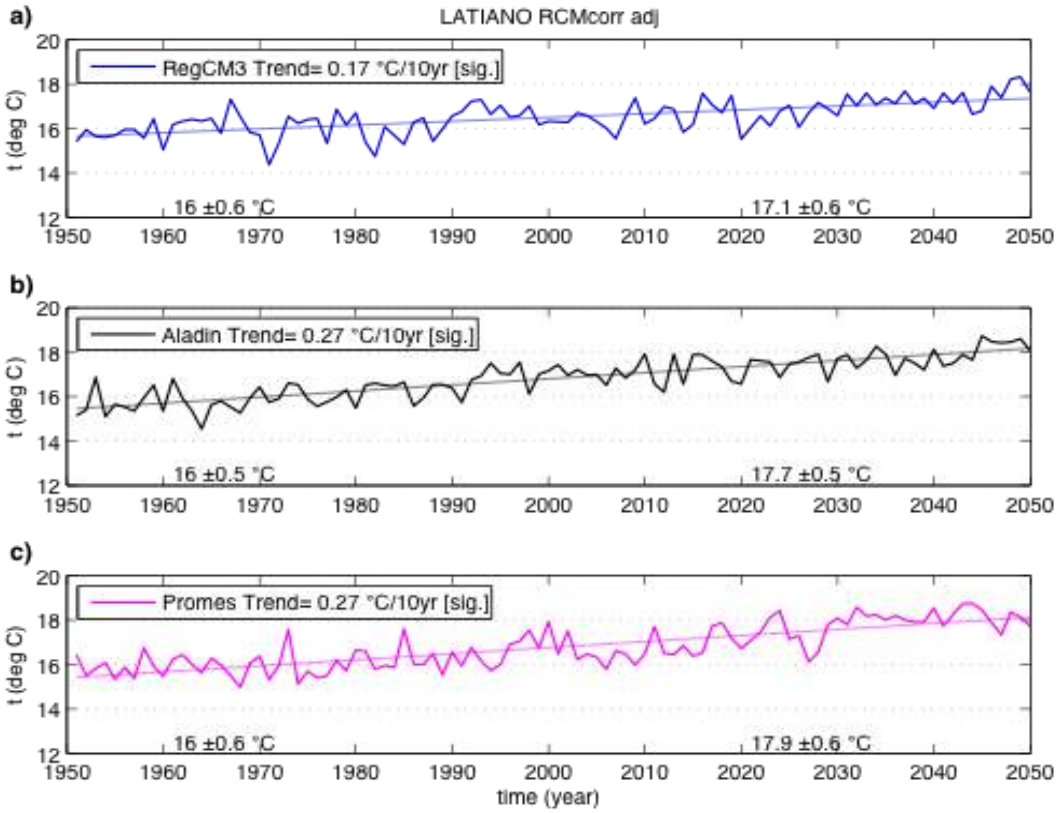

Figure 40 Latiano station: annual mean temperature and associated linear trend in a) RegCM3, b) Aladin, c) Promes. Decadal trend based on the entire time series is shown in panel legends. The statistical significance of the trend is assessed using the Mann-Kendall test and 5% significance level. Additional numbers at the bottom of each panel are mean values and standard deviations during P0 (1961-1990) and P1 (2021-2050). Model time series: RCMcorr (above); RCMcorr_adj (below).

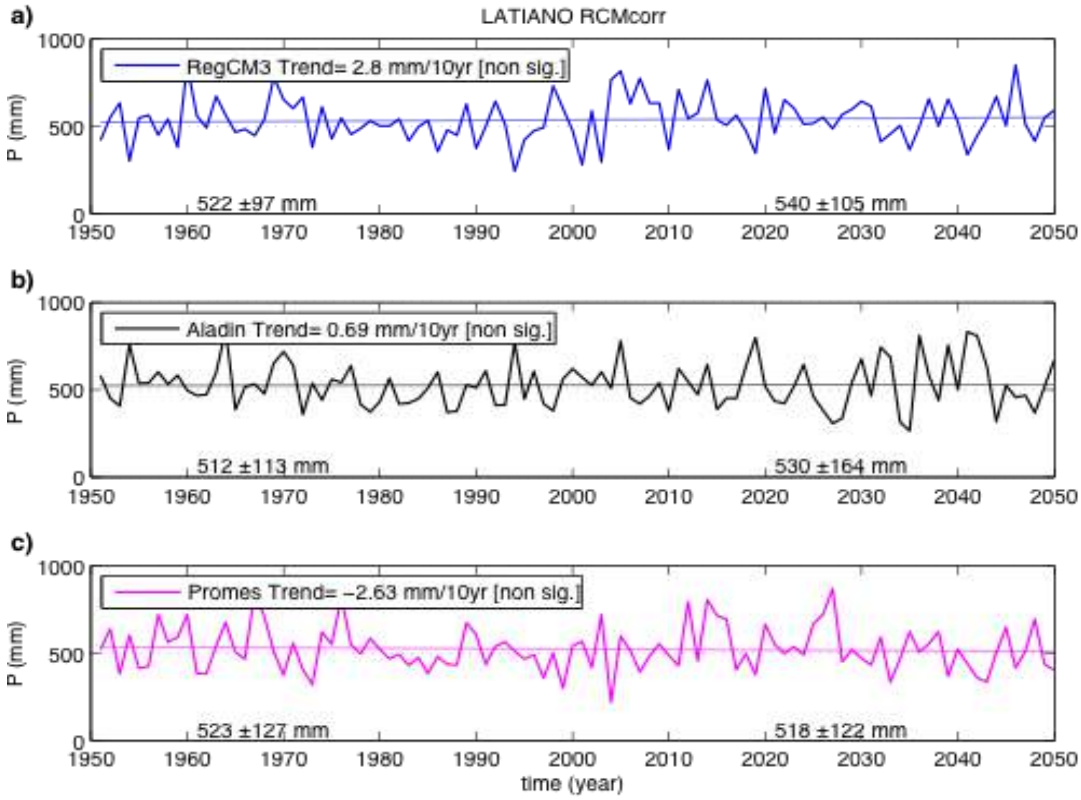

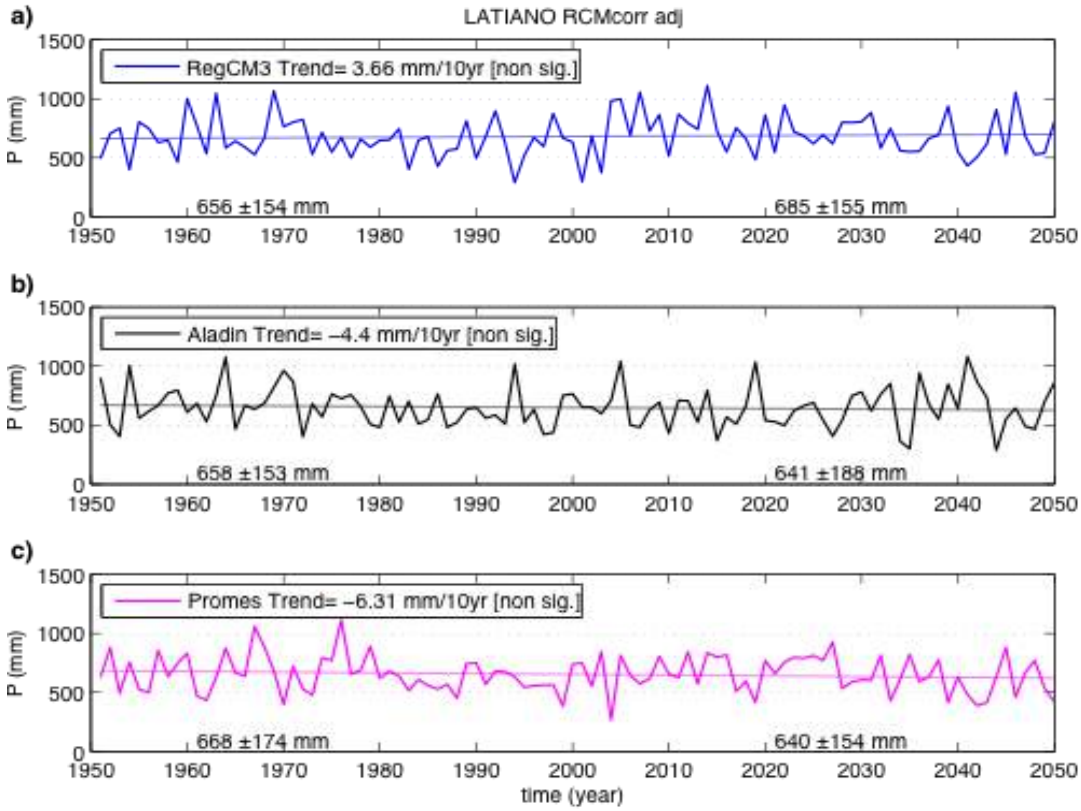

Figure 41 Latiano station: annual precipitation amount and associated linear trend in a) RegCM3, b) Aladin, c) Promes. Decadal trend based on the entire time series is shown in panel legends. The statistical significance of the trend is assessed using the Mann-Kendall test and 5% significance level. Additional numbers at the bottom of each panel are mean values and standard deviations during P0 (1961-1990) and P1 (2021-2050). Model time series: RCMcorr (above); RMcorr_adj (below).

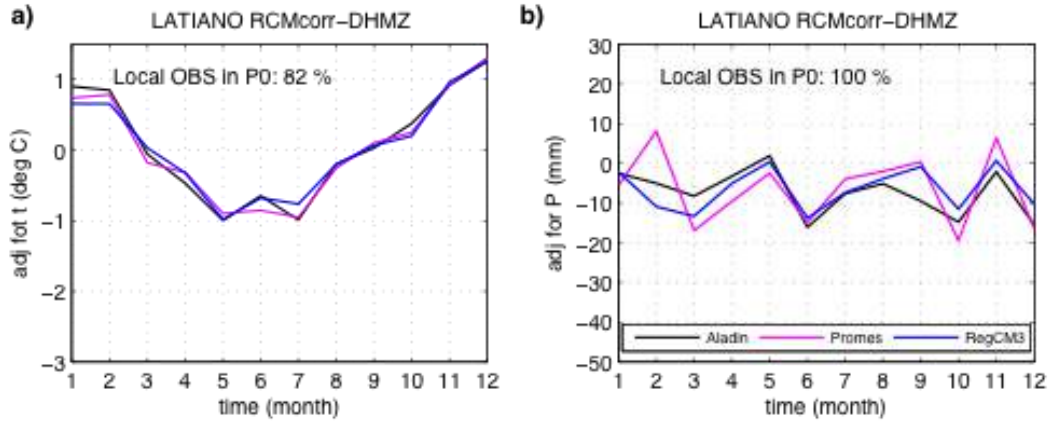

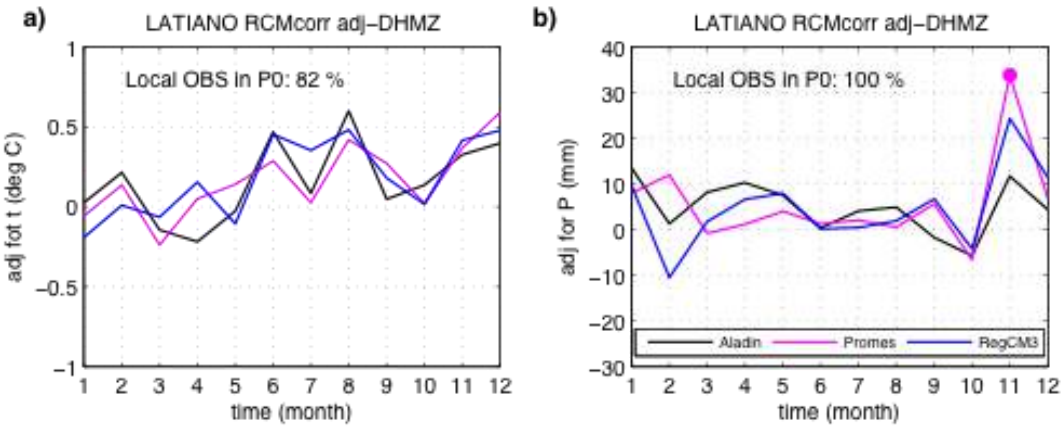

Figure 42 Latiano station: adjustment differences a) mean monthly temperature b) monthly precipitation amount. Differences are based on 1961-1990 period and the availability of DHMZ observations. Statistically significant differences according to the Wilcoxon-Mann-Whitney nonparameteric rank-sum test and 5% significance level are marked by the filled circles. Model time series: RCMcorr (above); RMcorr_adj (below).

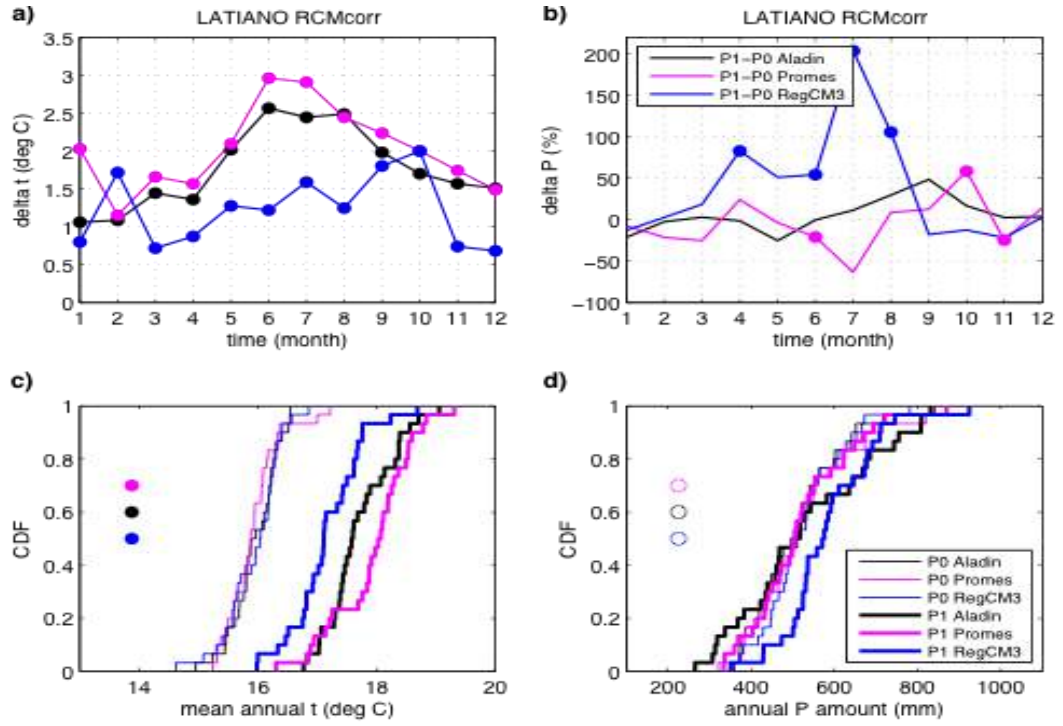

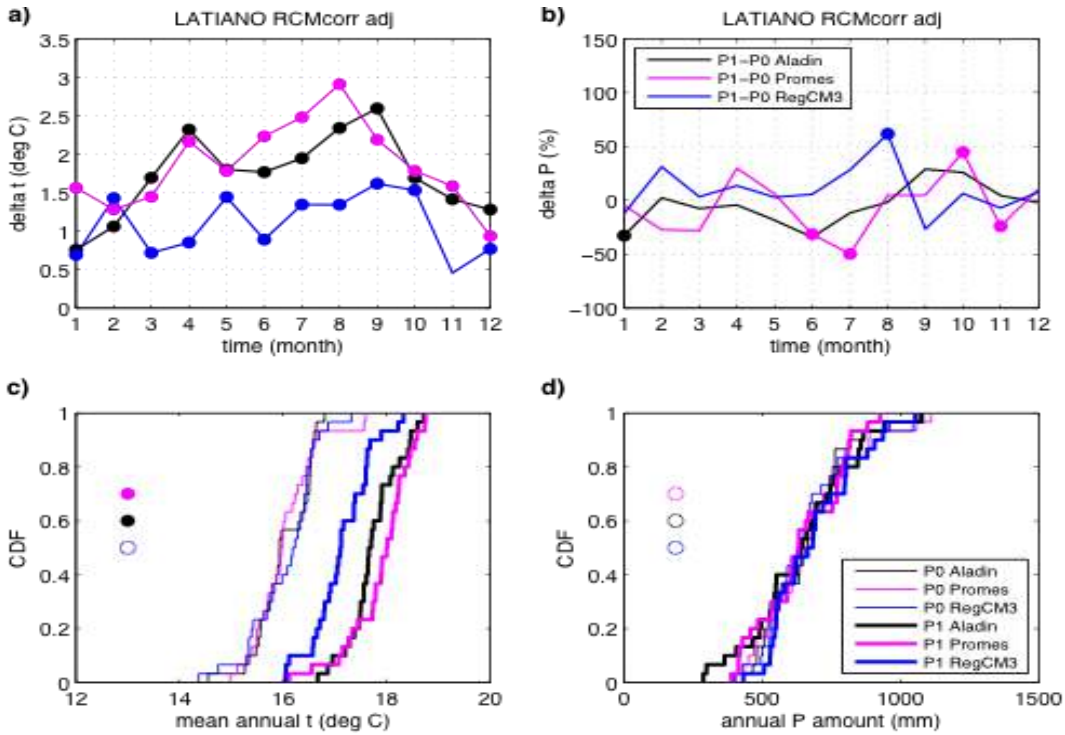

Figure 43 Latiano station: a) monthly mean temperature P1 vs. P0 change; b) relative monthly precipitation P1 vs. P0 change; c) empirical cumulative distribution functions CDFs of mean annual temperature in P0 and P1; d) same as c) but for annual precipitation amount. Time periods are: P0 1961-1990 and P1 2021-2050. Statistically significant differences in a) and b) according to the Wilcoxon-Mann-Whitney nonparameteric rank-sum test and 5% significance level are marked by the filled circles. Statistically significant differences according to the Kolmogorov-Smirnov test and 5% significance level between CDFs in two periods for every model in panels c) and d) are marked by the filled circles. Model time series: RCMcorr (above); RMcorr_adj (below).

LOCOROTONDO STATION

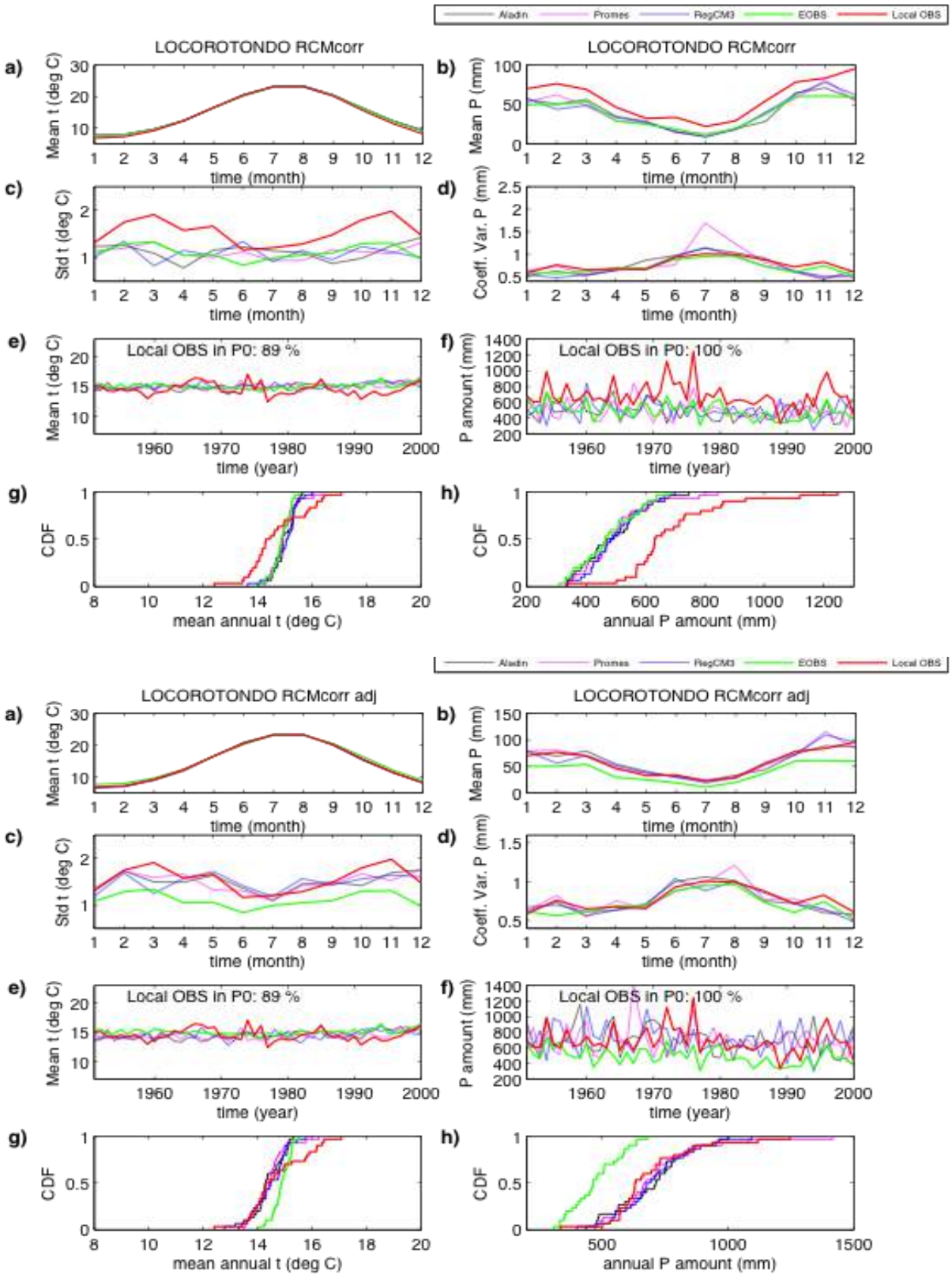

Figure 44 Locorotondo station: annual cycle a) mean monthly temperature, b) monthly precipitation amount, c) mean monthly temperature standard deviation, d) coefficient of variation of monthly precipitation amount; time series e) mean annual temperature, f) annual precipitation amount; empirical cumulative distribution functions CDFs g) mean annual temperature, h) annual

precipitation amount. Model time series are RCMcorr (above); RCM_adj (below). Period of analysis:P0(1961-1900)

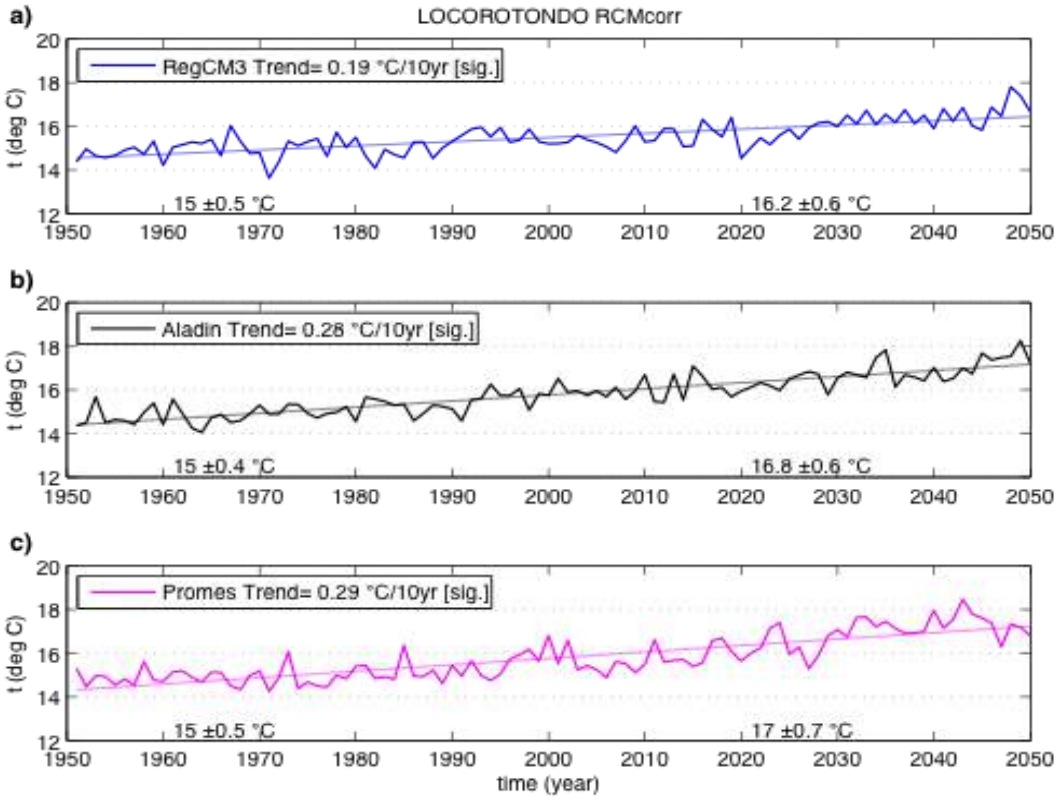

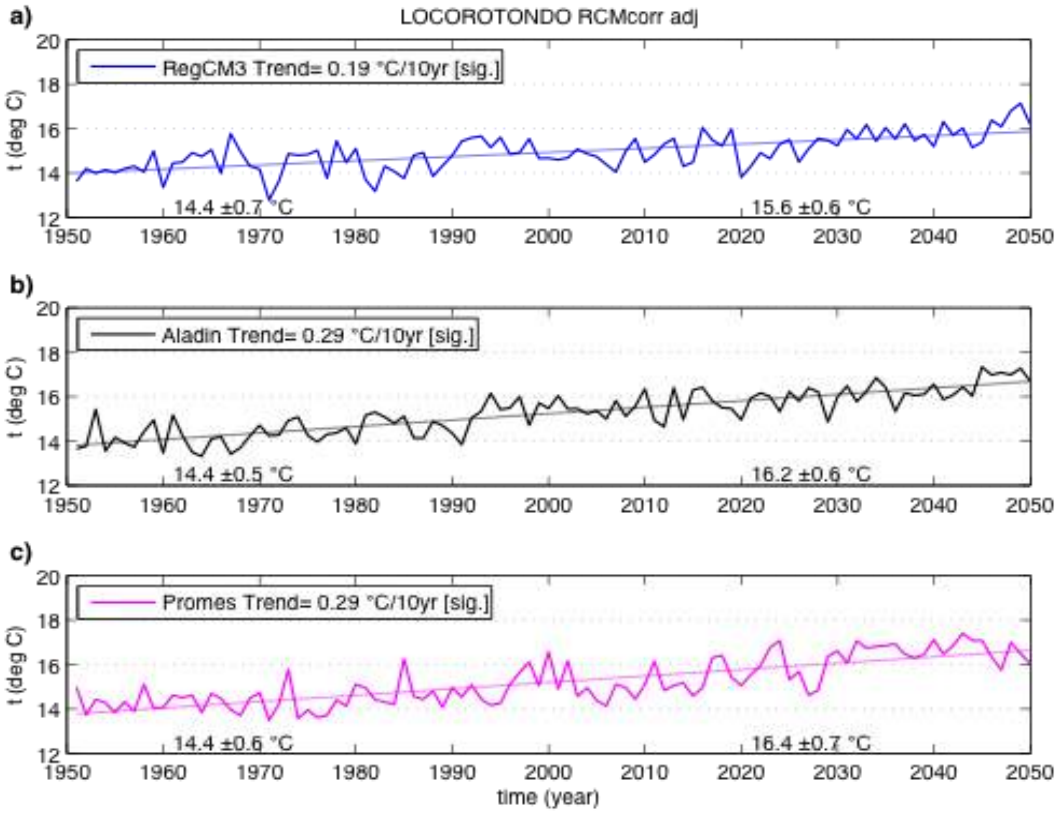

Figure 45 Locorotondo station: annual mean temperature and associated linear trend in a) RegCM3, b) Aladin, c) Promes. Decadal trend based on the entire time series is shown in panel legends. The statistical significance of the trend is assessed using the Mann-Kendall test and 5% significance level. Additional numbers at the bottom of each panel are mean values and standard deviations during P0 (1961-1990) and P1 (2021-2050). Model time series: RCMcorr (above); RCMcorr_adj (below).

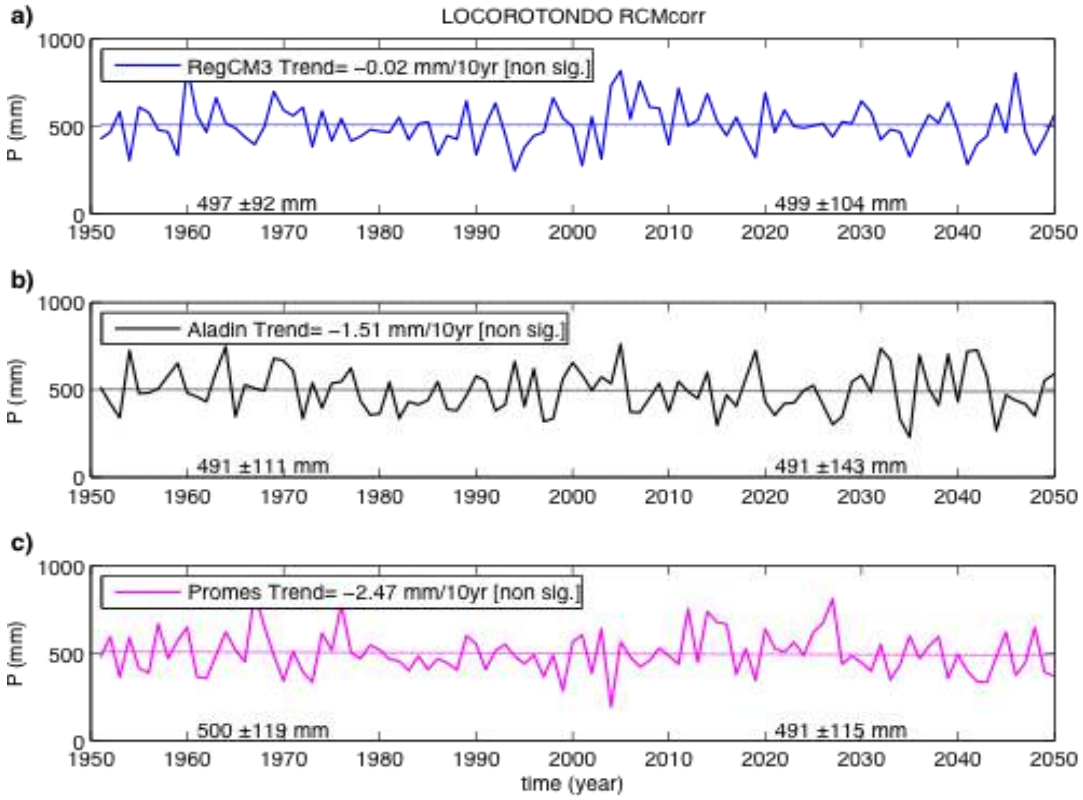

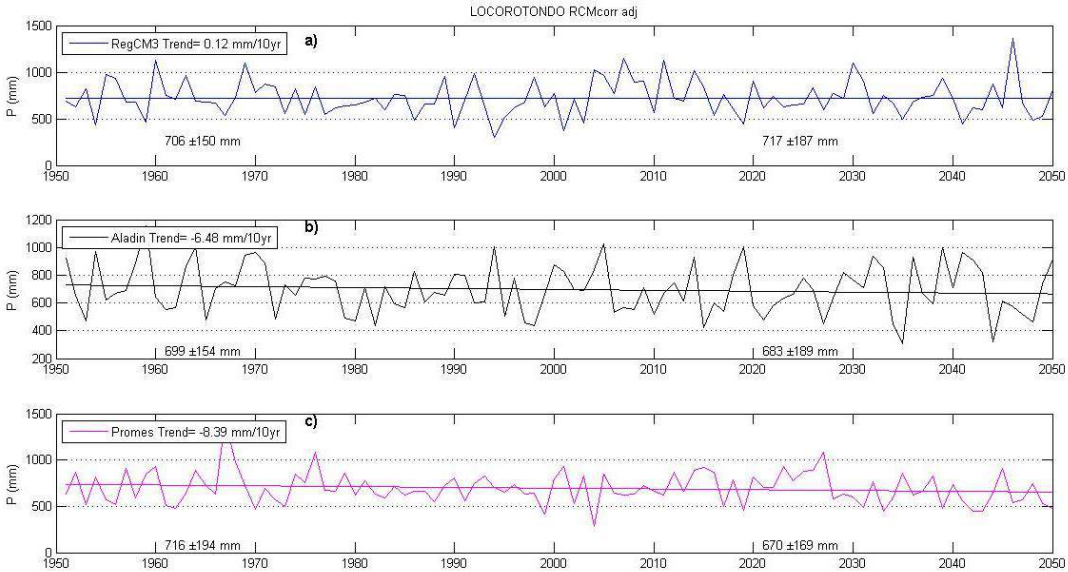

Figure 46 Locorotondo station: annual precipitation amount and associated linear trend in a) RegCM3, b) Aladin, c) Promes. Decadal trend based on the entire time series is shown in panel legends. The statistical significance of the trend is assessed using the Mann-Kendall test and 5% significance level. Additional numbers at the bottom of each panel are mean values and standard deviations during P0 (1961-1990) and P1 (2021-2050). Model time series: RCMcorr (above); RMcorr_adj (below).

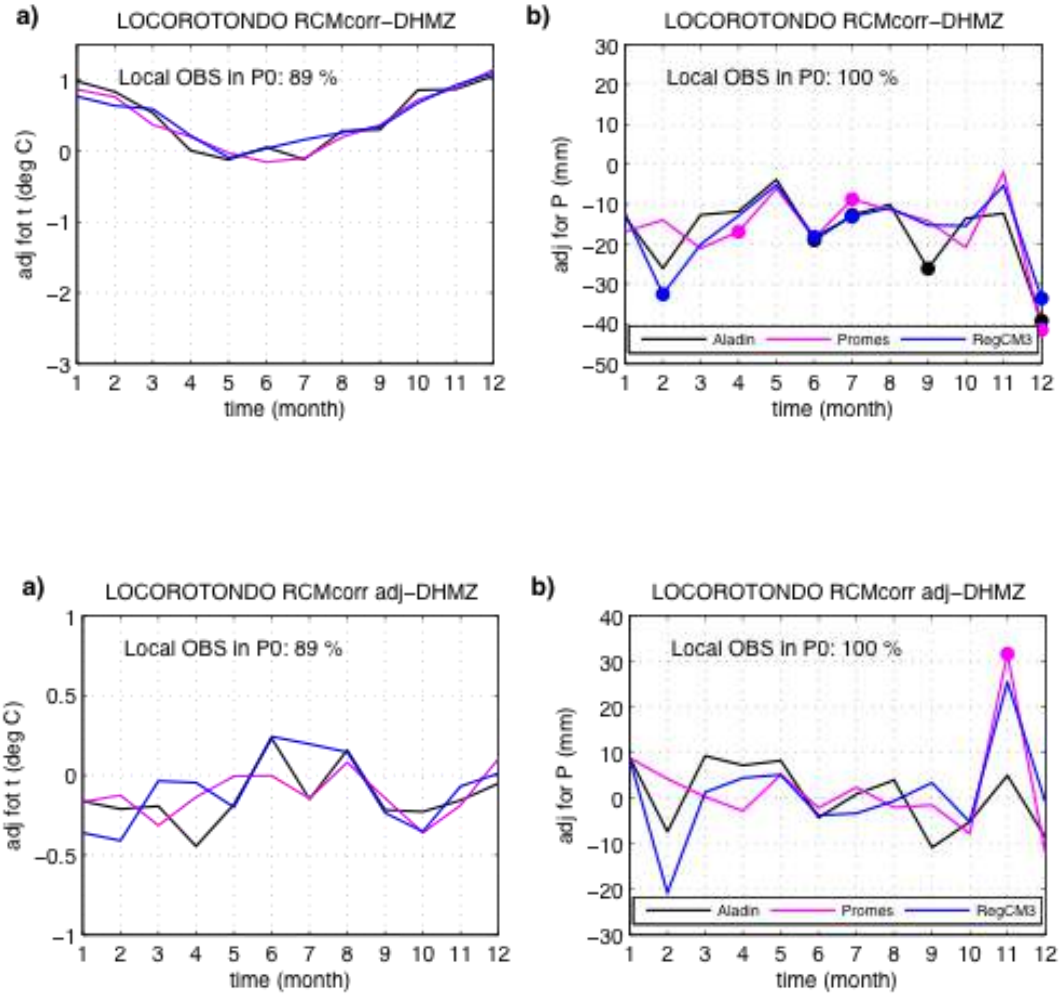

Figure 47 Locorotondo station: adjustment differences a) mean monthly temperature b) monthly precipitation amount. Differences are based on 1961-1990 period and the availability of DHMZ observations. Statistically significant differences according to the Wilcoxon-Mann-Whitney nonparameteric rank-sum test and 5% significance level are marked by the filled circles. Model time series: RCMcorr (above); RMcorr_adj (below).

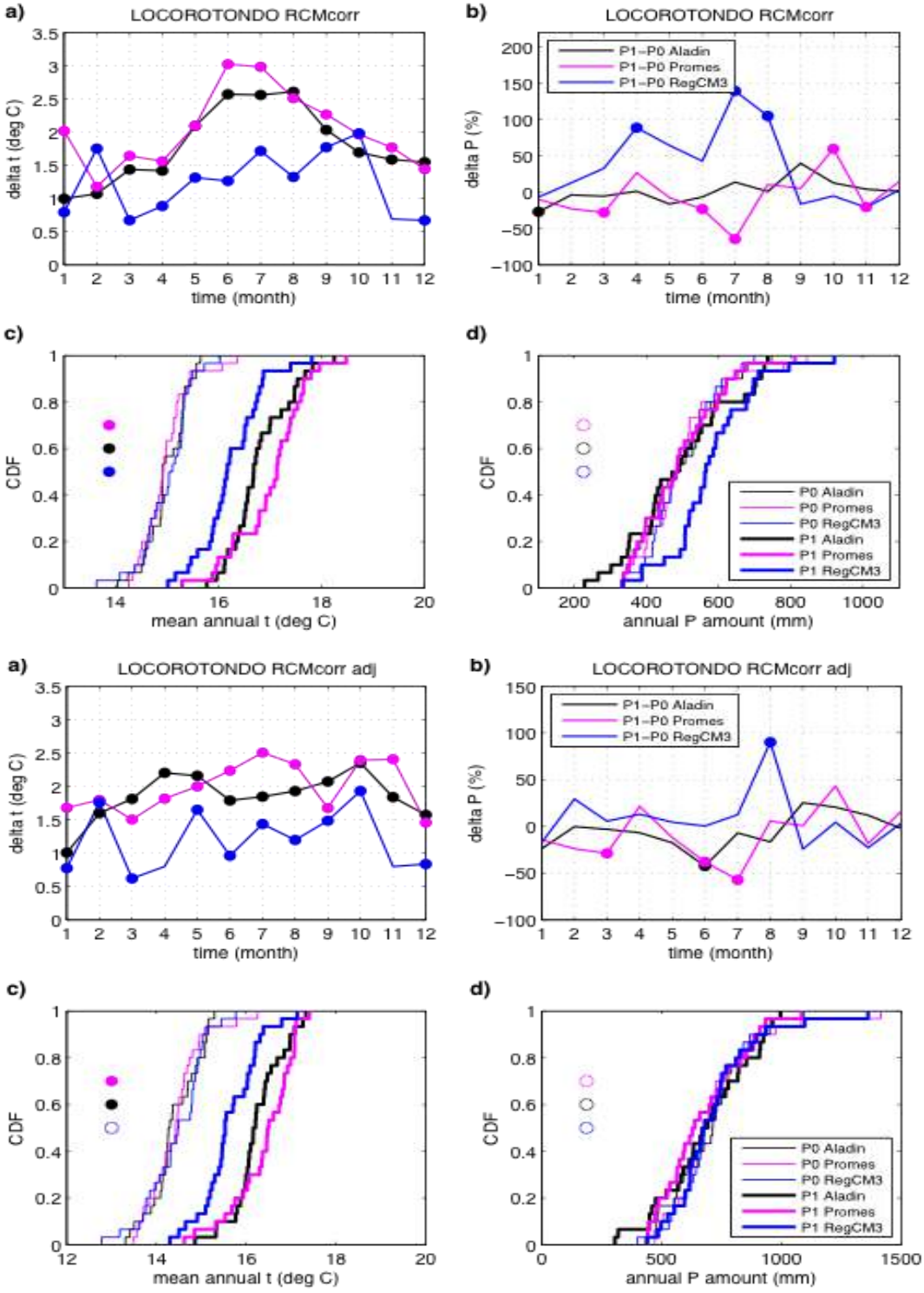

Figure 48 Locorotondo station: a) monthly mean temperature P1 vs. P0 change; b) relative monthly precipitation P1 vs. P0 change; c) empirical cumulative distribution functions CDFs of mean annual temperature in P0 and P1; d) same as c) but for annual precipitation amount. Time periods are: P0 1961-1990 and P1 2021-2050. Statistically significant differences in a) and b) according to the Wilcoxon-Mann-Whitney nonparameteric rank-sum test and 5% significance level are marked by the filled circles. Statistically significant differences according to the Kolmogorov-Smirnov test and 5% significance level between CDFs in two periods for every model in panels c) and d) are

marked by the filled circles. Model time series: RCMcorr (above); RMcorr_adj (below).

OSTUNI STATION

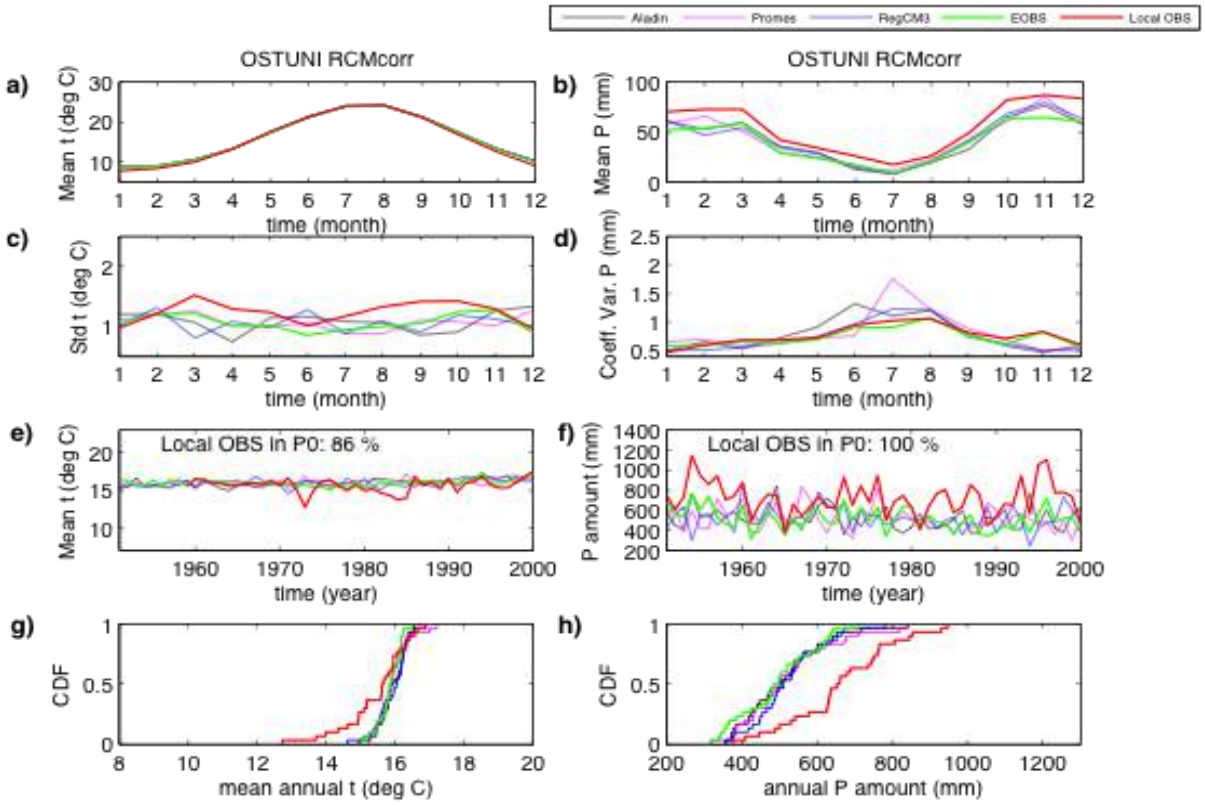

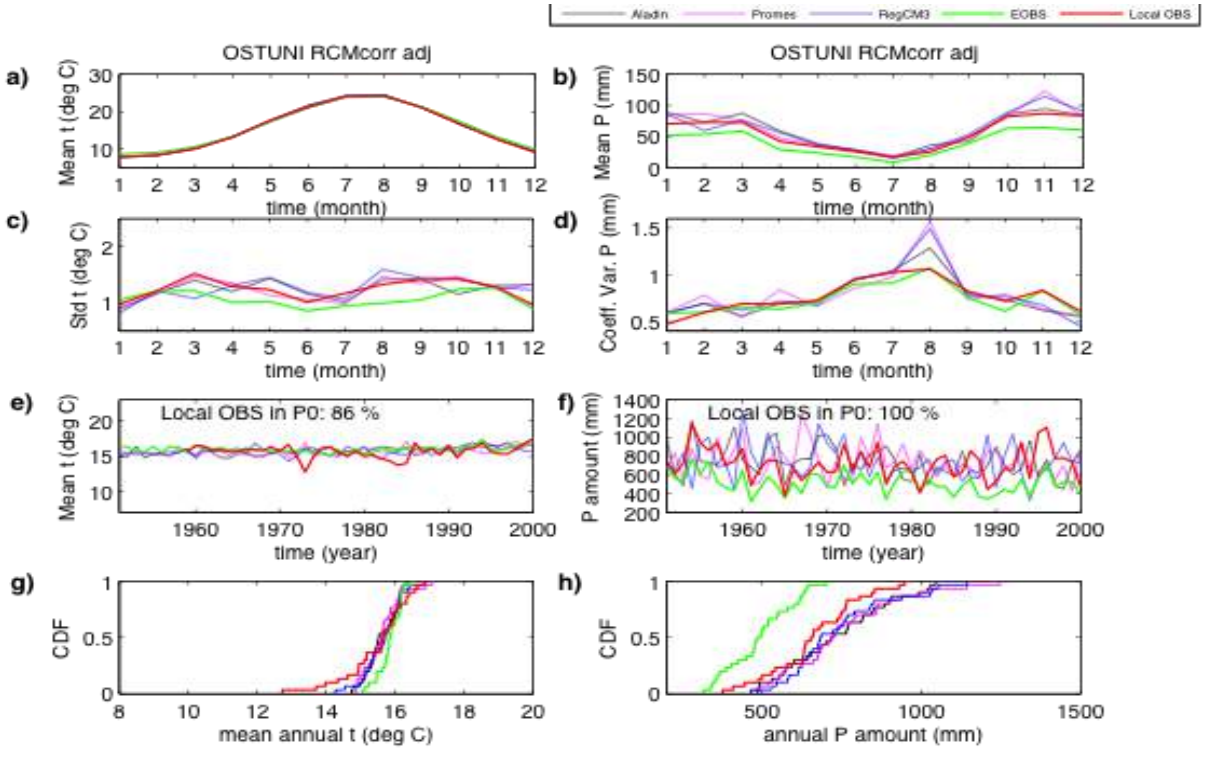

Figure 49 Ostuni station: annual cycle a) mean monthly temperature, b) monthly precipitation amount, c) mean monthly temperature standard deviation, d) coefficient of variation of monthly precipitation amount; time series e) mean annual temperature, f) annual precipitation amount; empirical cumulative distribution functions CDFs g) mean annual temperature, h) annual precipitation amount. Model time series are RCMcorr (above); RCM_adj (below). Period of analysis:P0(1961-1900)

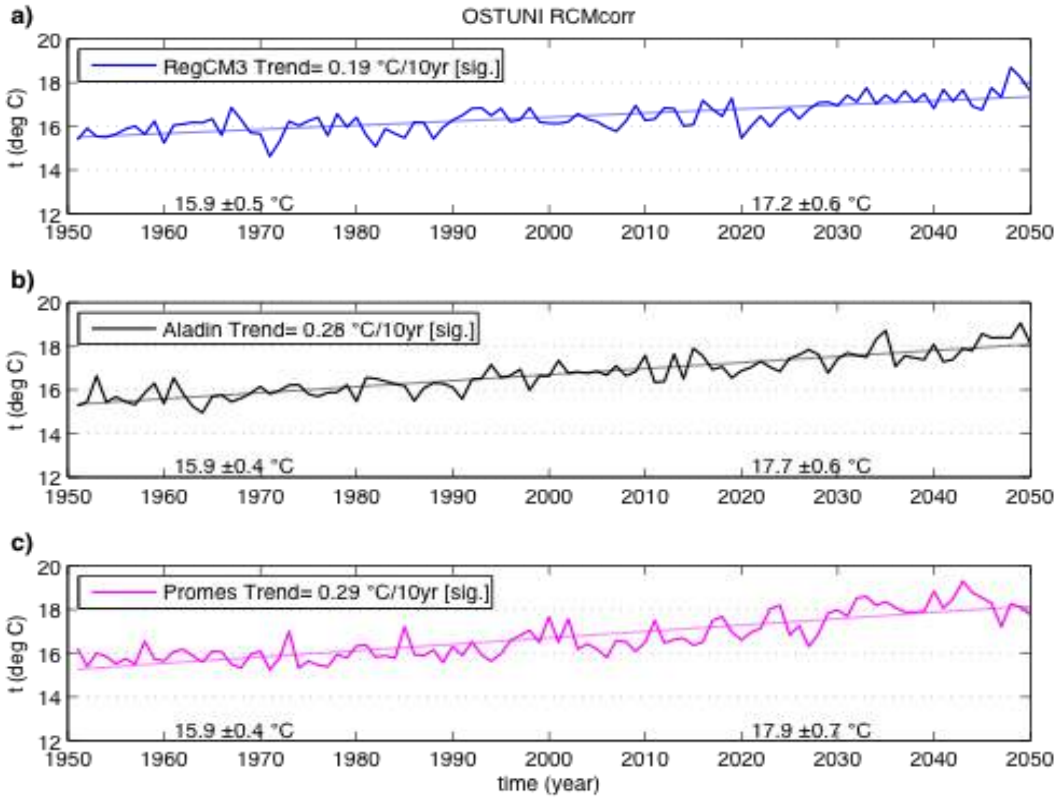

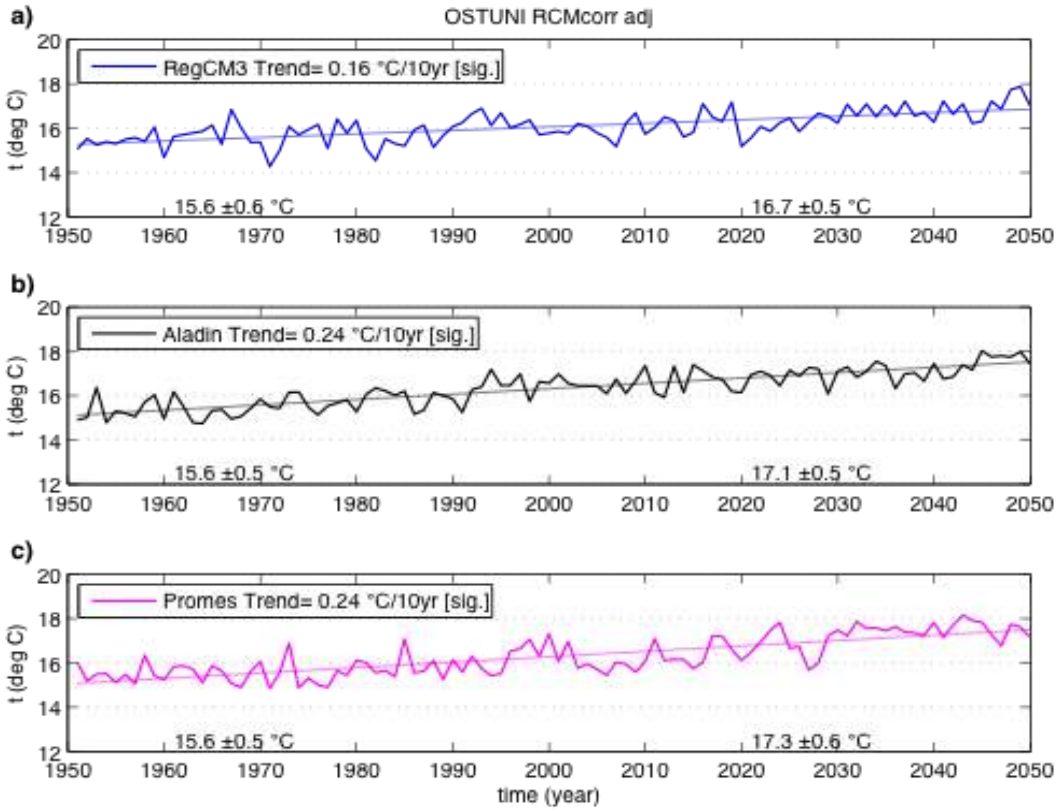

Figure 50 Ostuni station: annual mean temperature and associated linear trend in a) RegCM3, b) Aladin, c) Promes. Decadal trend based on the entire time series is shown in panel legends. The statistical significance of the trend is assessed using the Mann-Kendall test and 5% significance level. Additional numbers at the bottom of each panel are mean values and standard deviations during P0 (1961-1990) and P1 (2021-2050). Model time series: RCMcorr (above); RCMcorr_adj (below).

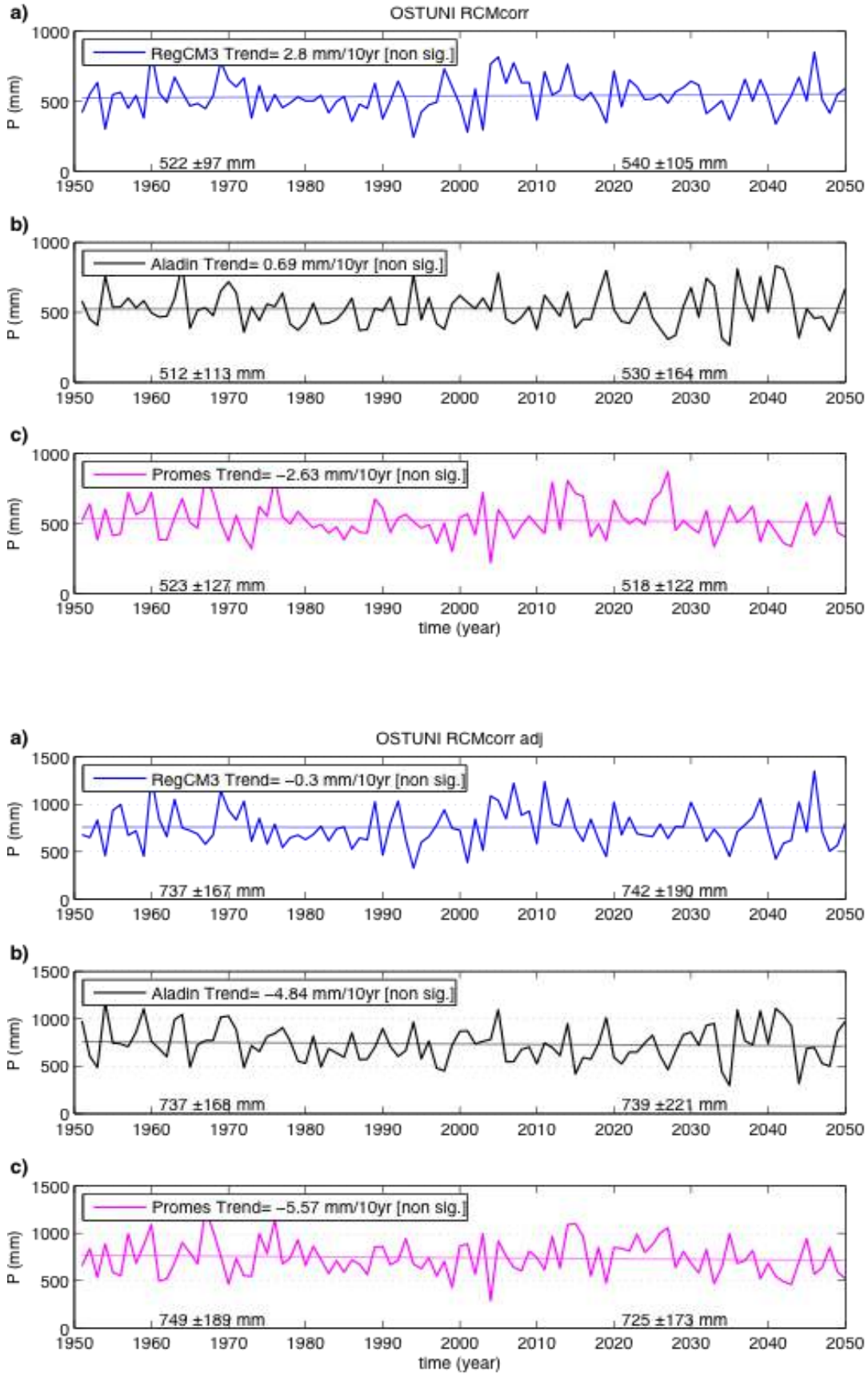

Figure 51 Ostuni station: annual precipitation amount and associated linear trend in a) RegCM3, b) Aladin, c) Promes. Decadal trend based on the entire time series is shown in panel legends. The statistical significance of the trend

is assessed using the Mann-Kendall test and 5% significance level. Additional numbers at the bottom of each panel are mean values and standard deviations during P0 (1961-1990) and P1 (2021-2050). Model time series: RCMcorr (above); RMcorr_adj (below).

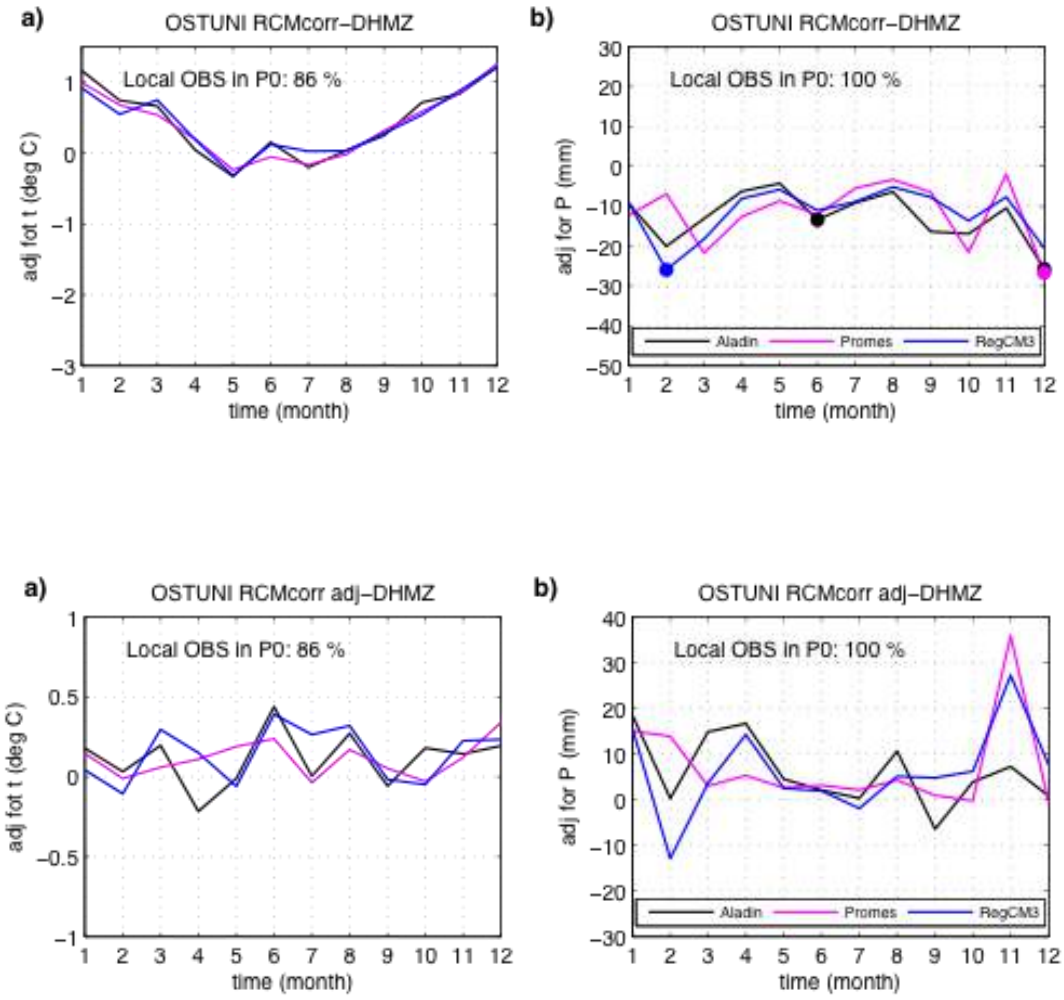

Figure 52 Ostuni station: adjustment differences a) mean monthly temperature b) monthly precipitation amount. Differences are based on 1961-1990 period and the availability of DHMZ observations. Statistically significant differences according to the Wilcoxon-Mann-Whitney nonparameteric rank-sum test and 5% significance level are marked by the filled circles. Model time series: RCMcorr (above); RMcorr_adj (below).

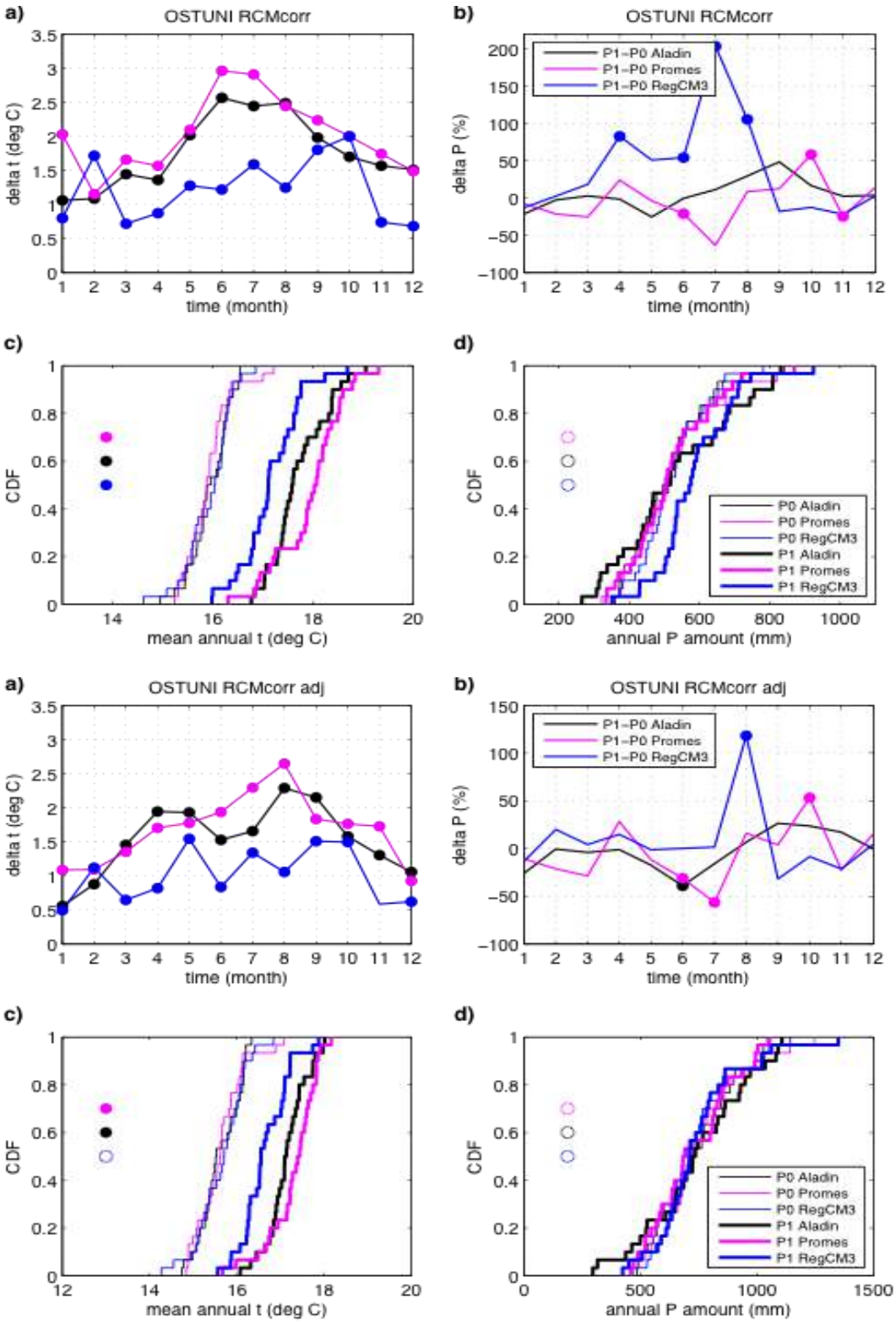

Figure 53 Ostuni station: a) monthly mean temperature P1 vs. P0 change; b) relative monthly precipitation P1 vs. P0 change; c) empirical cumulative distribution functions CDFs of mean annual temperature in P0 and P1; d) same as c) but for annual precipitation amount. Time periods are: P0 1961-1990 and P1 2021-2050. Statistically significant differences in a) and b) according to the Wilcoxon-Mann-Whitney nonparameteric rank-sum test and 5% significance level are marked by the filled circles. Statistically significant differences according to the Kolmogorov-Smirnov test and 5% significance

level between CDFs in two periods for every model in panels c) and d) are marked by the filled circles. Model time series: RCMcorr (above); RMcorr_adj (below).

SANGIORGIO JONICO STATION

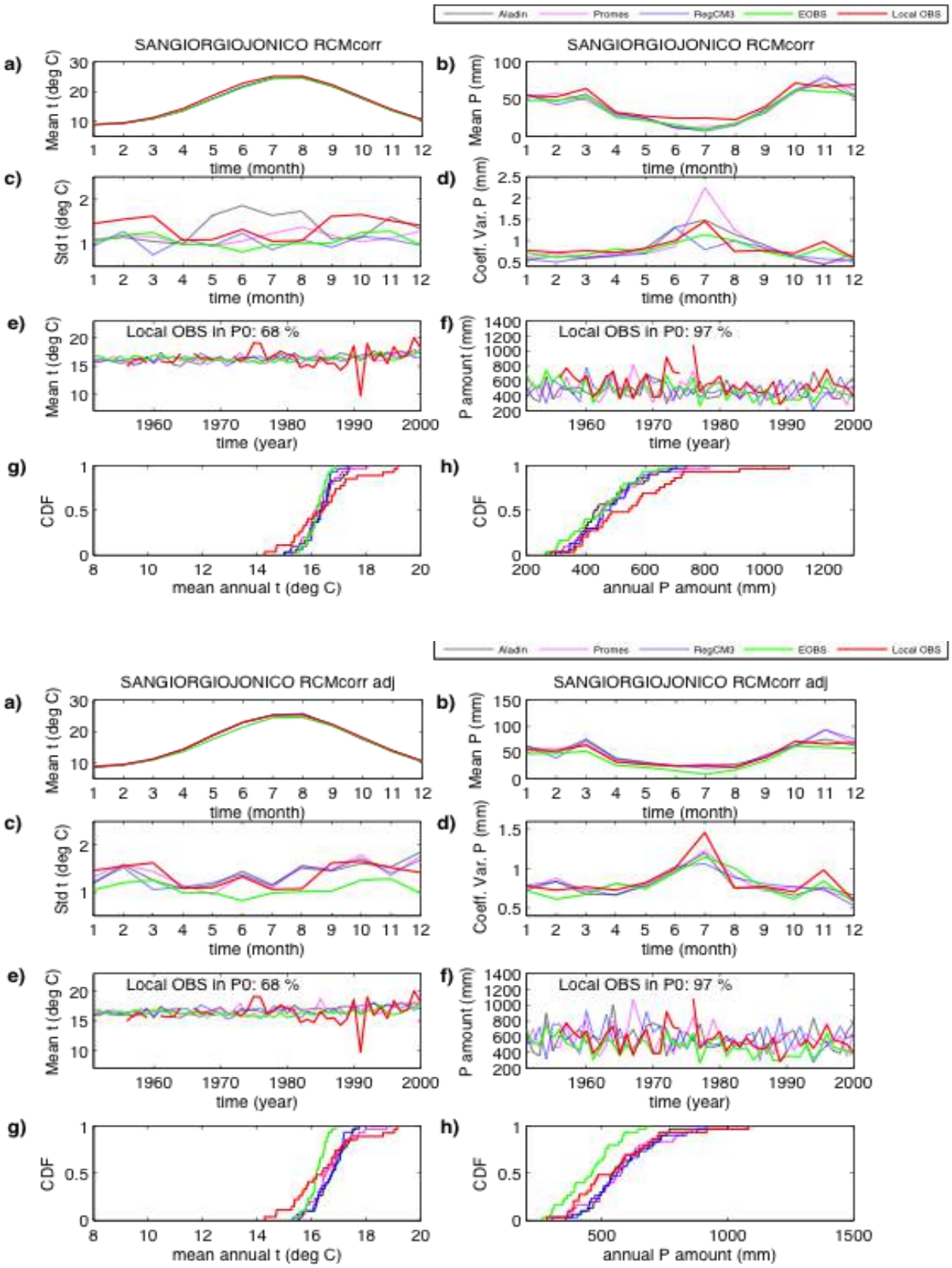

Figure 54 SanGiorgio Jonico station: annual cycle a) mean monthly temperature, b) monthly precipitation amount, c) mean monthly temperature standard deviation, d) coefficient of variation of monthly precipitation amount; time series e) mean annual temperature, f) annual precipitation amount; empirical cumulative distribution functions CDFs g) mean annual temperature, h) annual precipitation amount. Model time series are RCMcorr (above); RCM_adj (below). Period of analysis:P0(1961-1900)

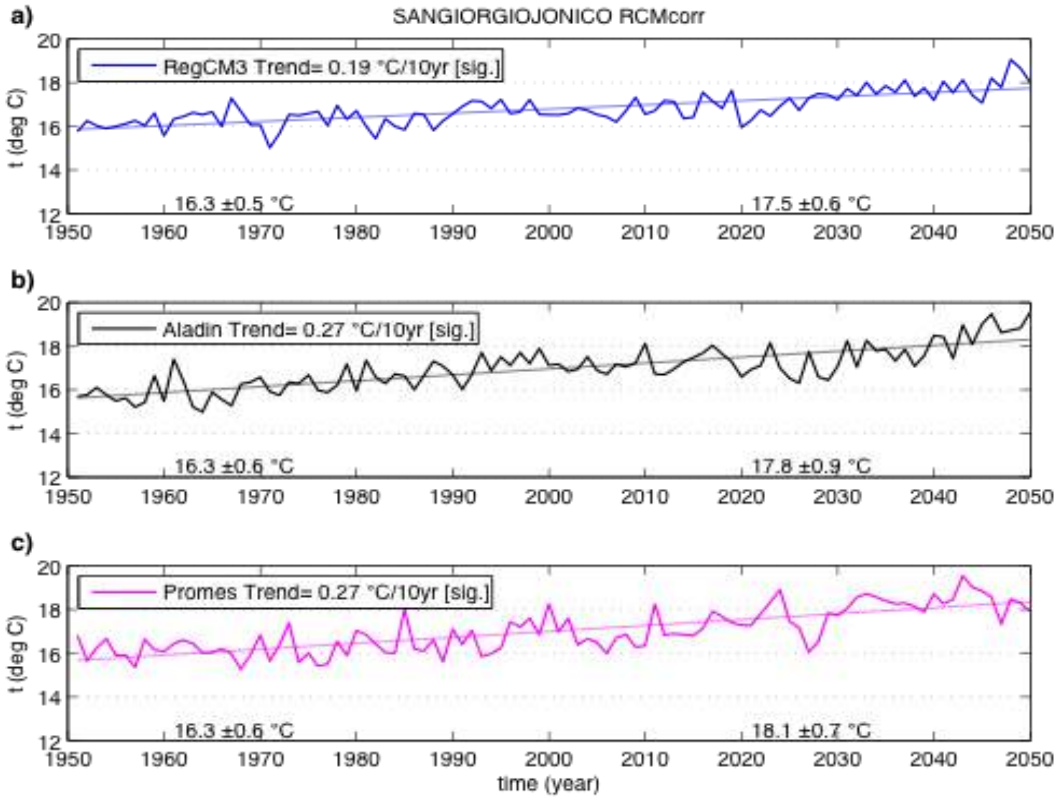

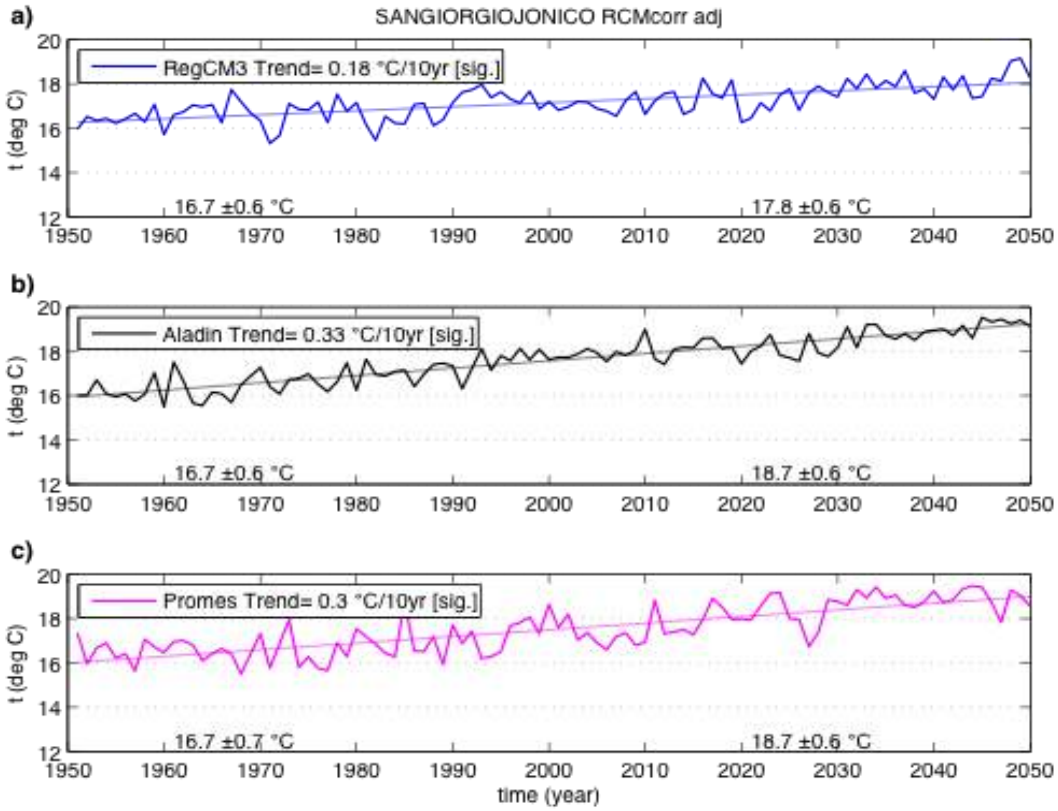

Figure 55 SanGiorgio Jonico station: annual mean temperature and associated linear trend in a) RegCM3, b) Aladin, c) Promes. Decadal trend based on the entire time series is shown in panel legends. The statistical significance of the trend is assessed using the Mann-Kendall test and 5% significance level. Additional numbers at the bottom of each panel are mean values and standard deviations during P0 (1961-1990) and P1 (2021-2050). Model time series: RCMcorr (above); RCMcorr_adj (below).

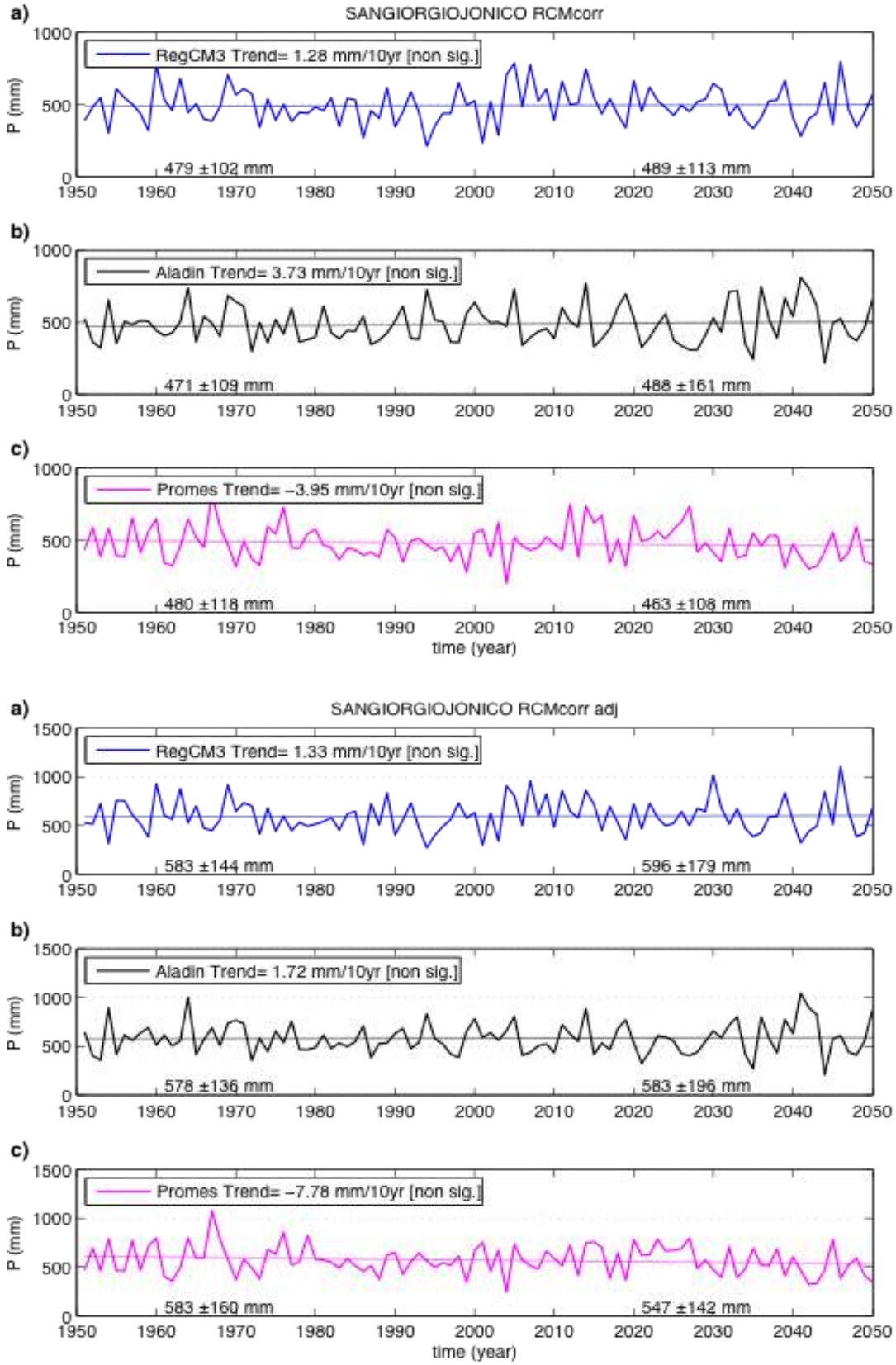

Figure 56 SanGiorgio Jonico station: annual precipitation amount and associated linear trend in a) RegCM3, b) Aladin, c) Promes. Decadal trend based on the entire time series is shown in panel legends. The statistical significance of the trend is assessed using the Mann-Kendall test and 5% significance level. Additional numbers at the bottom of each panel are mean

values and standard deviations during P0 (1961-1990) and P1 (2021-2050). Model time series: RCMcorr (above); RMcorr_adj (below).

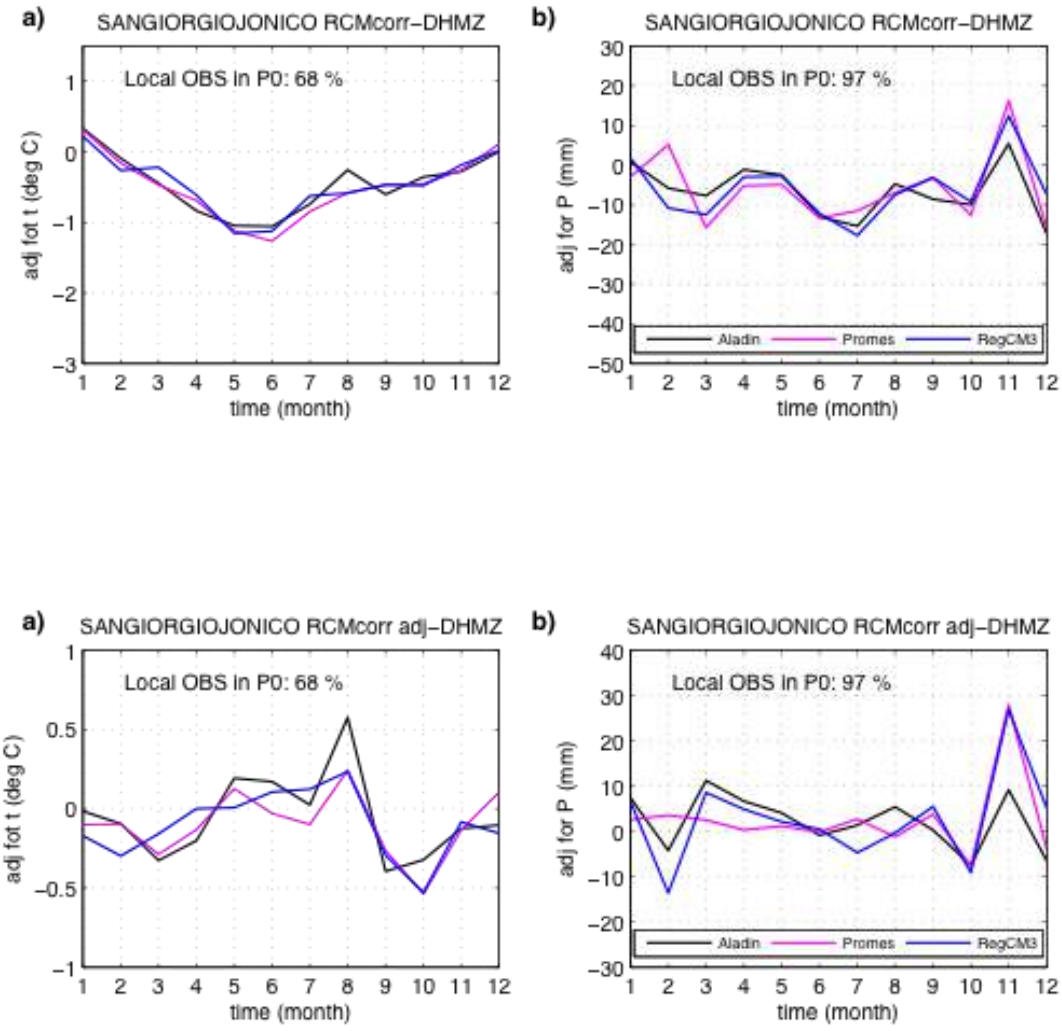

Figure 57 SanGiorgio Jonico station: adjustment differences a) mean monthly temperature b) monthly precipitation amount. Differences are based on 1961-1990 period and the availability of DHMZ observations. Statistically significant differences according to the Wilcoxon-Mann-Whitney nonparameteric rank-sum test and 5% significance level are marked by the filled circles. Model time series: RCMcorr (above); RMcorr_adj (below).

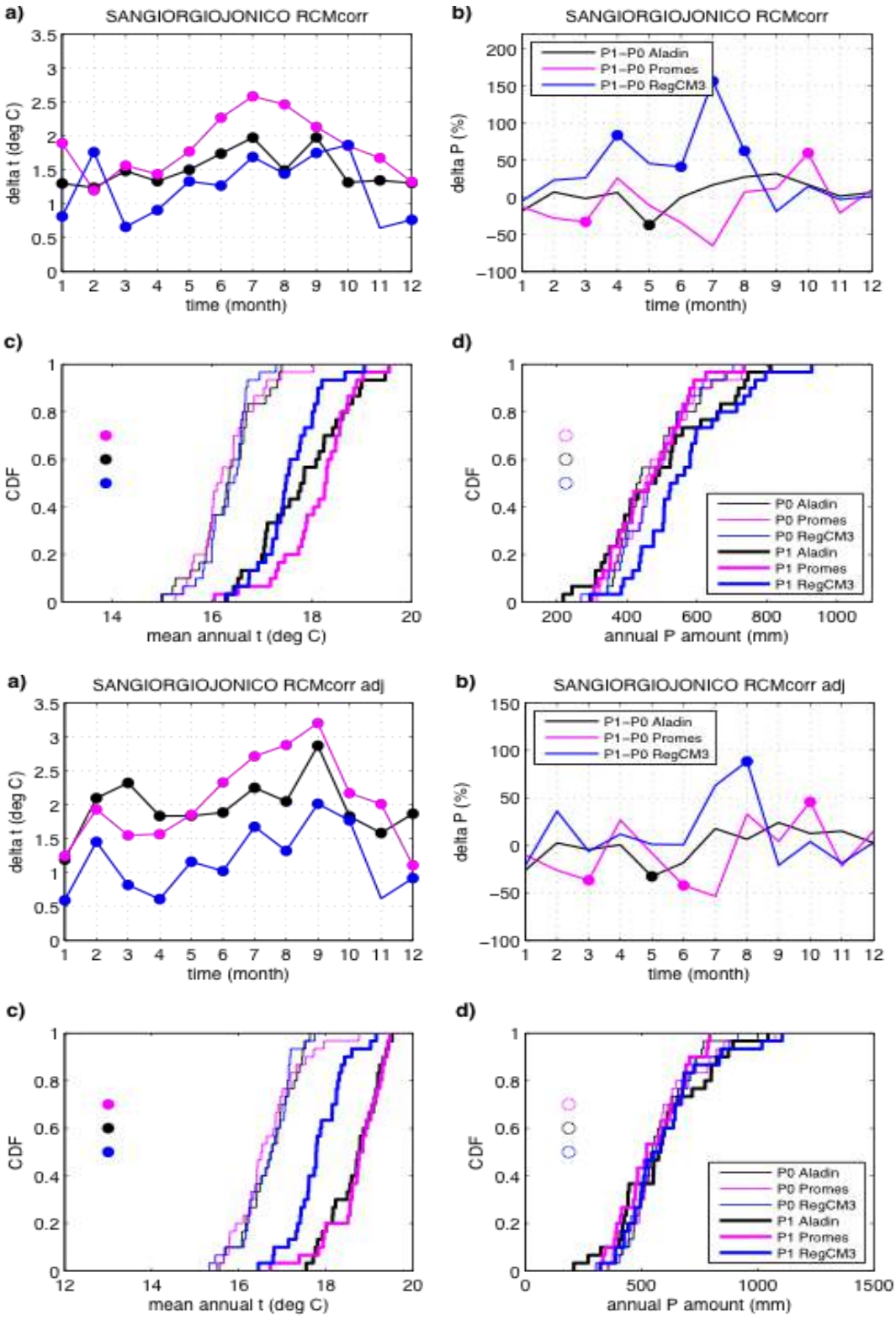

Figure 58 SanGiorgio Jonico station: a) monthly mean temperature P1 vs. P0 change; b) relative monthly precipitation P1 vs. P0 change; c) empirical cumulative distribution functions CDFs of mean annual temperature in P0 and P1; d) same as c) but for annual precipitation amount. Time periods are: P0 1961-1990 and P1 2021-2050. Statistically significant differences in a) and b) according to the Wilcoxon-Mann-Whitney nonparameteric rank-sum test and 5% significance level are marked by the filled circles. Statistically significant differences according to the Kolmogorov-Smirnov test and 5% significance

level between CDFs in two periods for every model in panels c) and d) are marked by the filled circles. Model time series: RCMcorr (above); RMcorr_adj (below).

TALSANO STATION

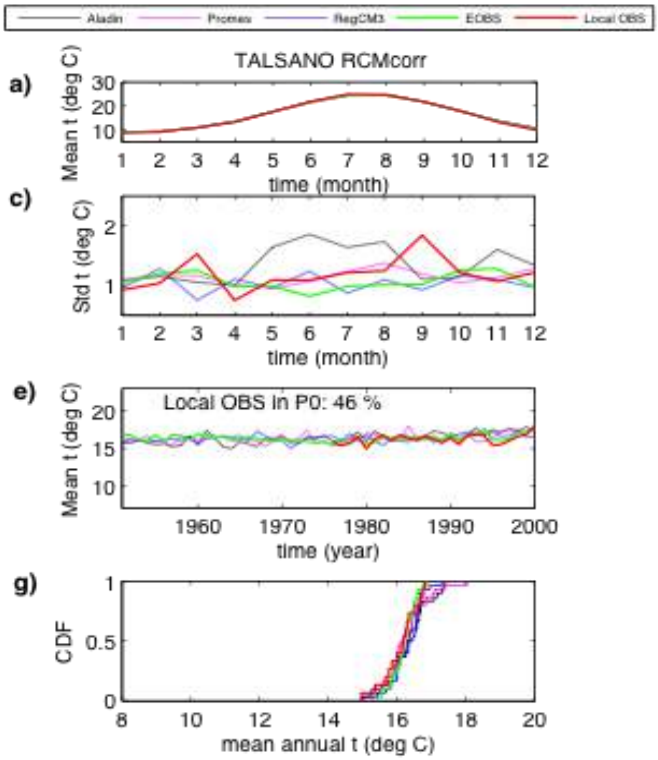

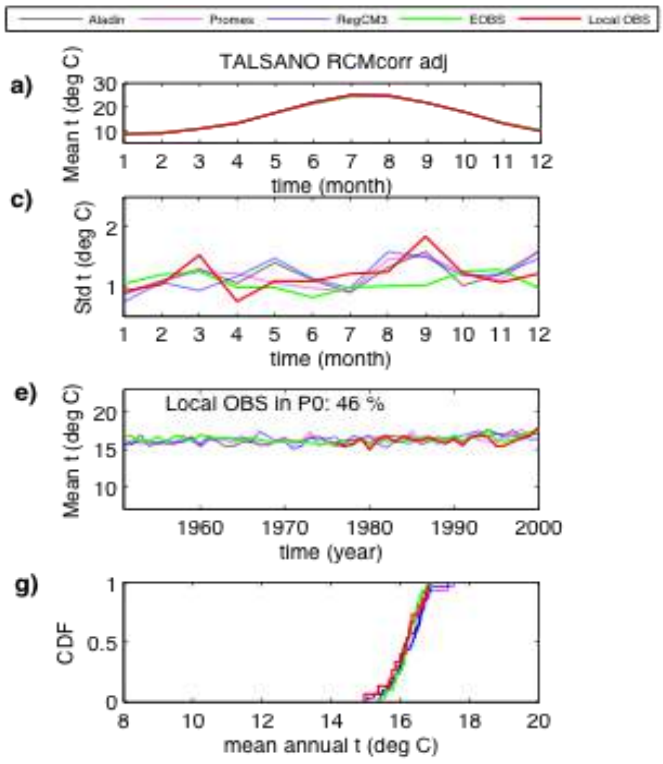

Figure 59 Talsano station: annual cycle a) mean monthly temperature, c) mean monthly temperature standard deviation; e) time series mean annual temperature; g) empirical cumulative distribution functions CDFs mean annual temperature. Model time series are RCMcorr (above); RCM_adj (below). Period of analysis:P0(1961-1900)

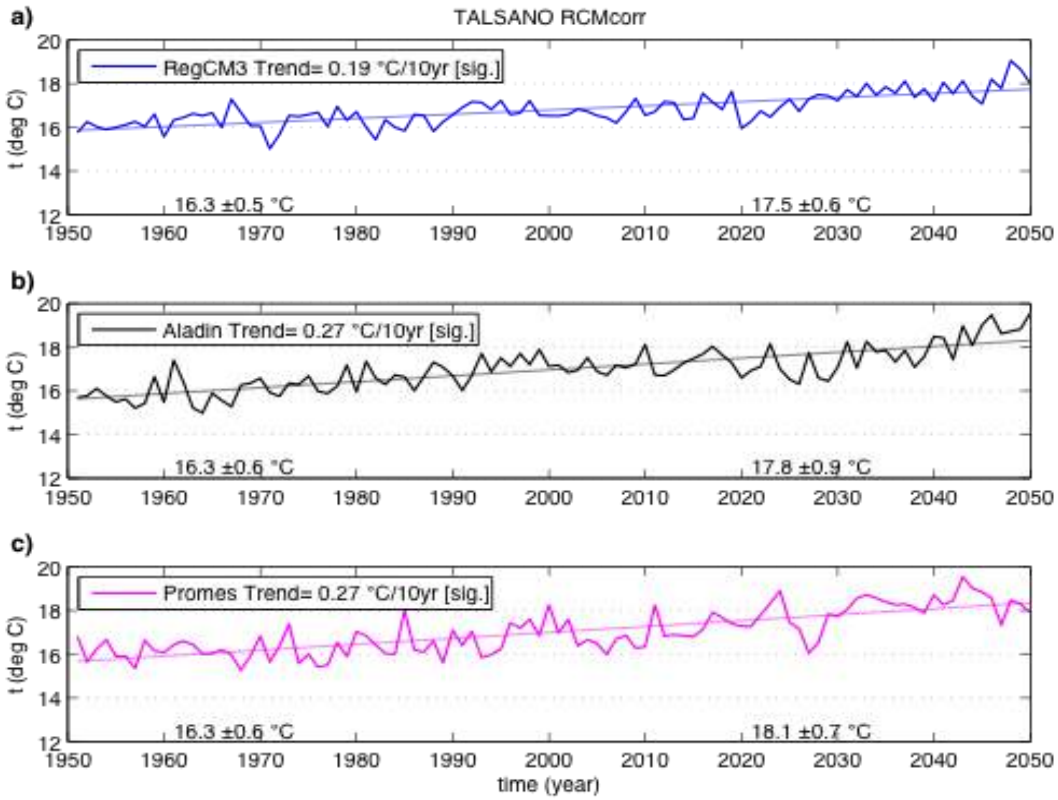

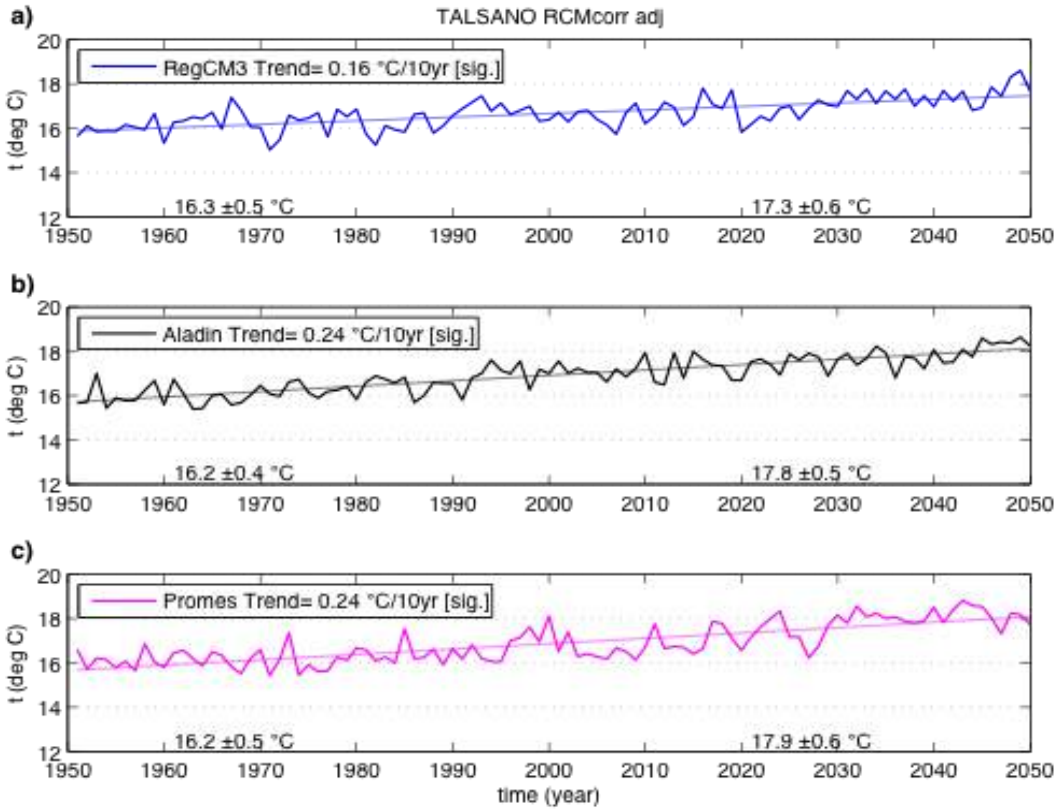

Figure 60 Talsano station: annual mean temperature and associated linear trend in a) RegCM3, b) Aladin, c) Promes. Decadal trend based on the entire time series is shown in panel legends. The statistical significance of the trend is assessed using the Mann-Kendall test and 5% significance level. Additional numbers at the bottom of each panel are mean values and standard deviations during P0 (1961-1990) and P1 (2021-2050). Model time series: RCMcorr (above); RCMcorr_adj (below).

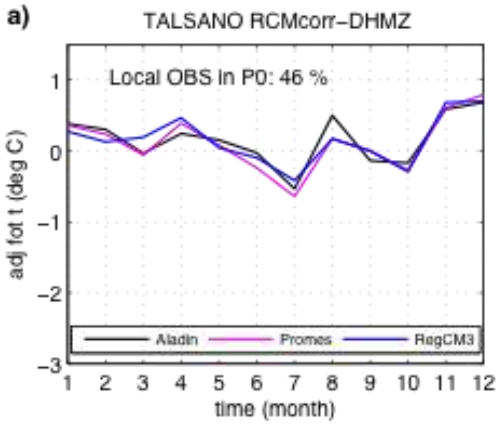

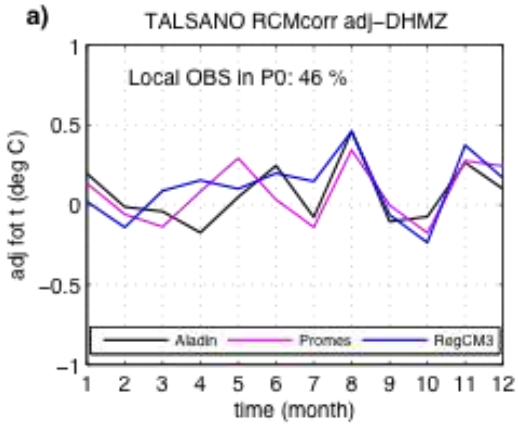

Figure 61 Talsano station: adjustment differences a) mean monthly temperature. Differences are based on 1961-1990 period and the availability of DHMZ observations. Statistically significant differences according to the Wilcoxon-Mann-Whitney nonparameteric rank-sum test and 5% significance level are marked by the filled circles. Model time series: RCMcorr (above); RMcorr_adj (below).

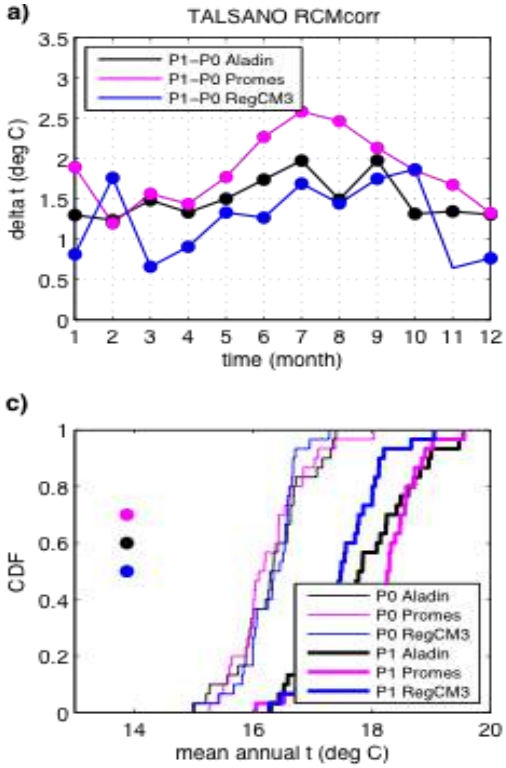

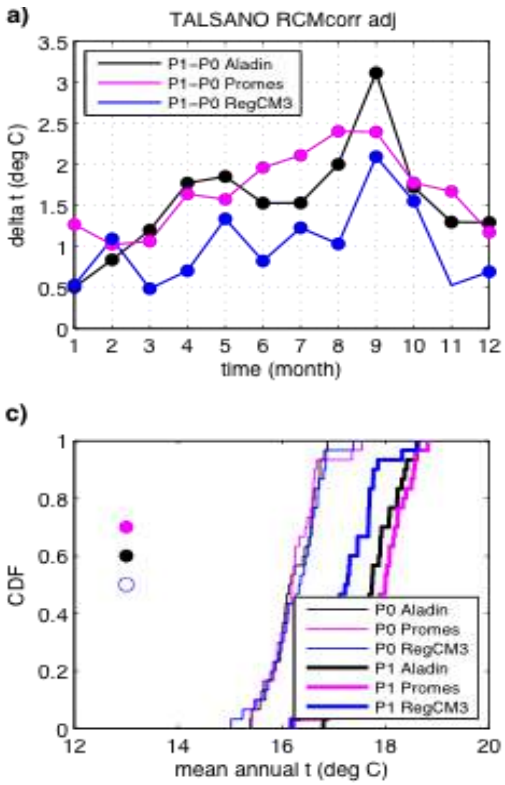

Figure 62 Talsano station: a) monthly mean temperature P1 vs. P0 change; c) empirical cumulative distribution functions CDFs of mean annual temperature in P0 and P1. Time periods are: P0 1961-1990 and P1 2021-2050. Statistically significant differences in a) and b) according to the Wilcoxon-Mann-Whitney nonparameteric rank-sum test and 5% significance level are marked by the filled circles. Statistically significant differences according to the Kolmogorov-Smirnov test and 5% significance level between CDFs in two periods for every model in panels c) and d) are marked by the filled circles. Model time series: RCMcorr (above); RMcorr_adj (below).

TARANTO STATION

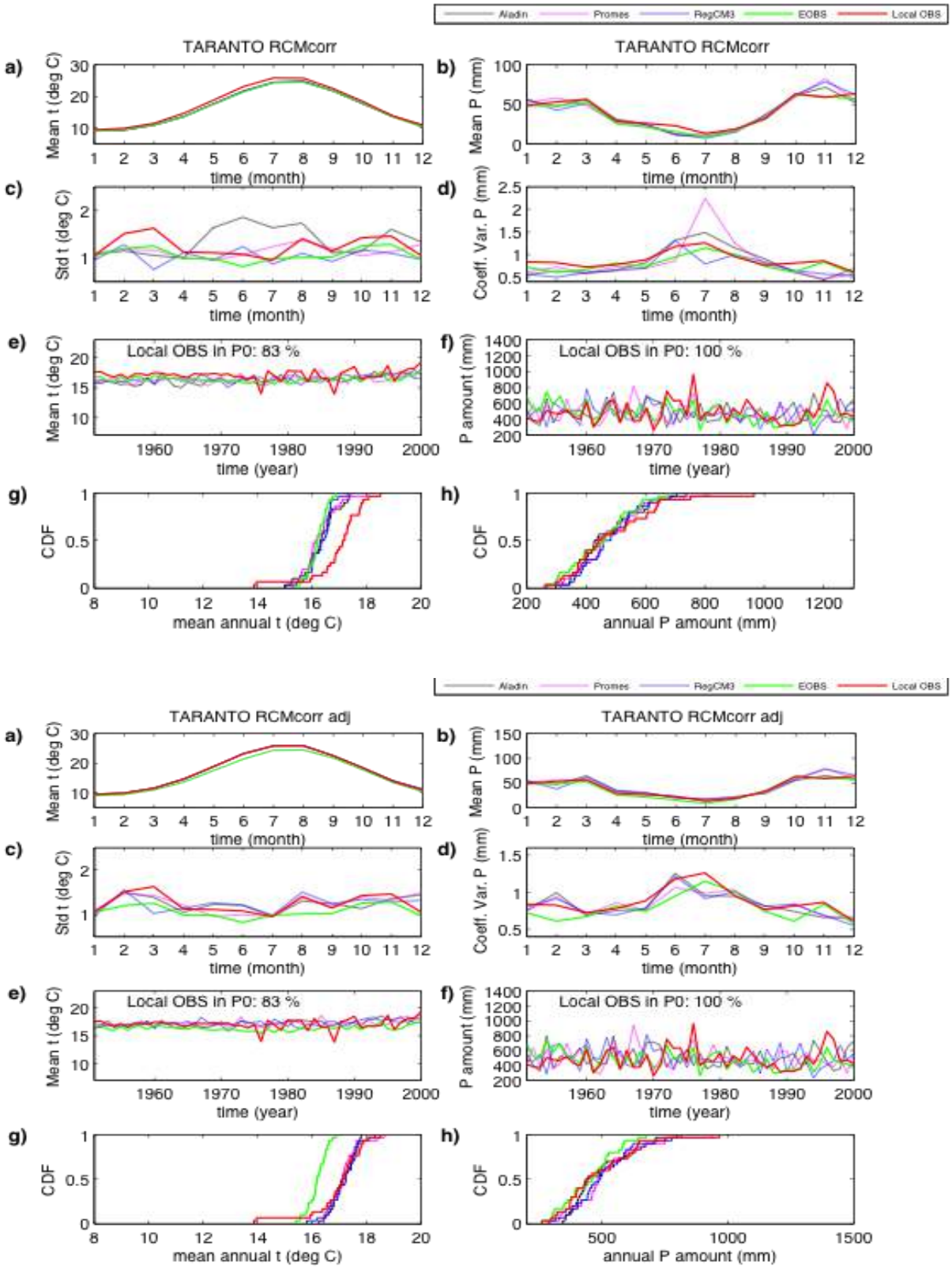

Figure 63 Taranto station: annual cycle a) mean monthly temperature, b) monthly precipitation amount, c) mean monthly temperature standard deviation, d) coefficient of variation of monthly precipitation amount; time series e) mean annual temperature, f) annual precipitation amount; empirical cumulative distribution functions CDFs g) mean annual temperature, h) annual

precipitation amount. Model time series are RCMcorr (above); RCM_adj (below). Period of analysis:P0(1961-1900)

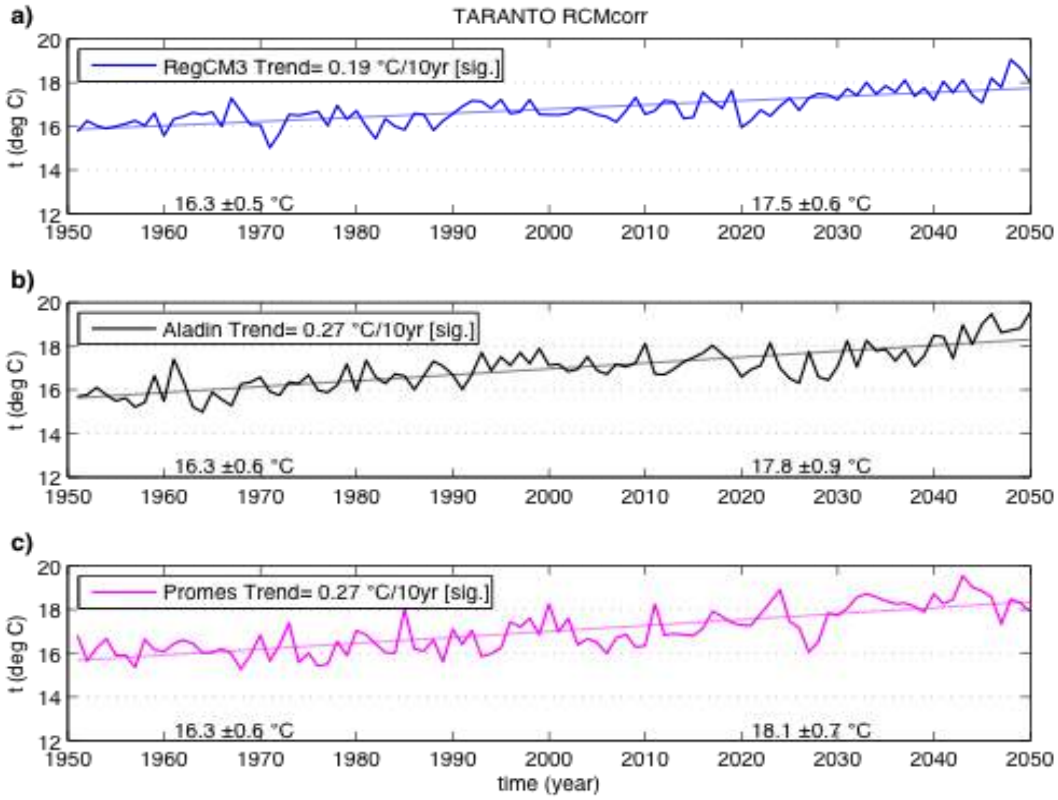

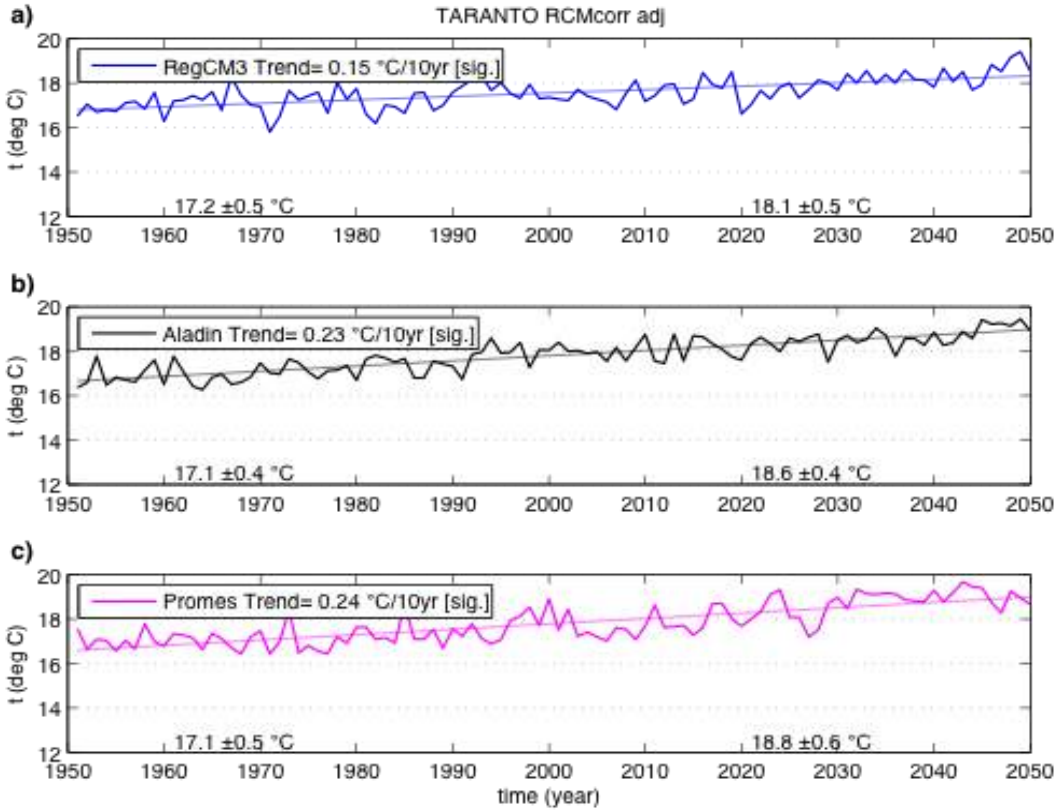

Figure 64 Taranto station: annual mean temperature and associated linear trend in a) RegCM3, b) Aladin, c) Promes. Decadal trend based on the entire time series is shown in panel legends. The statistical significance of the trend is assessed using the Mann-Kendall test and 5% significance level. Additional numbers at the bottom of each panel are mean values and standard deviations during P0 (1961-1990) and P1 (2021-2050). Model time series: RCMcorr (above); RCMcorr_adj (below).

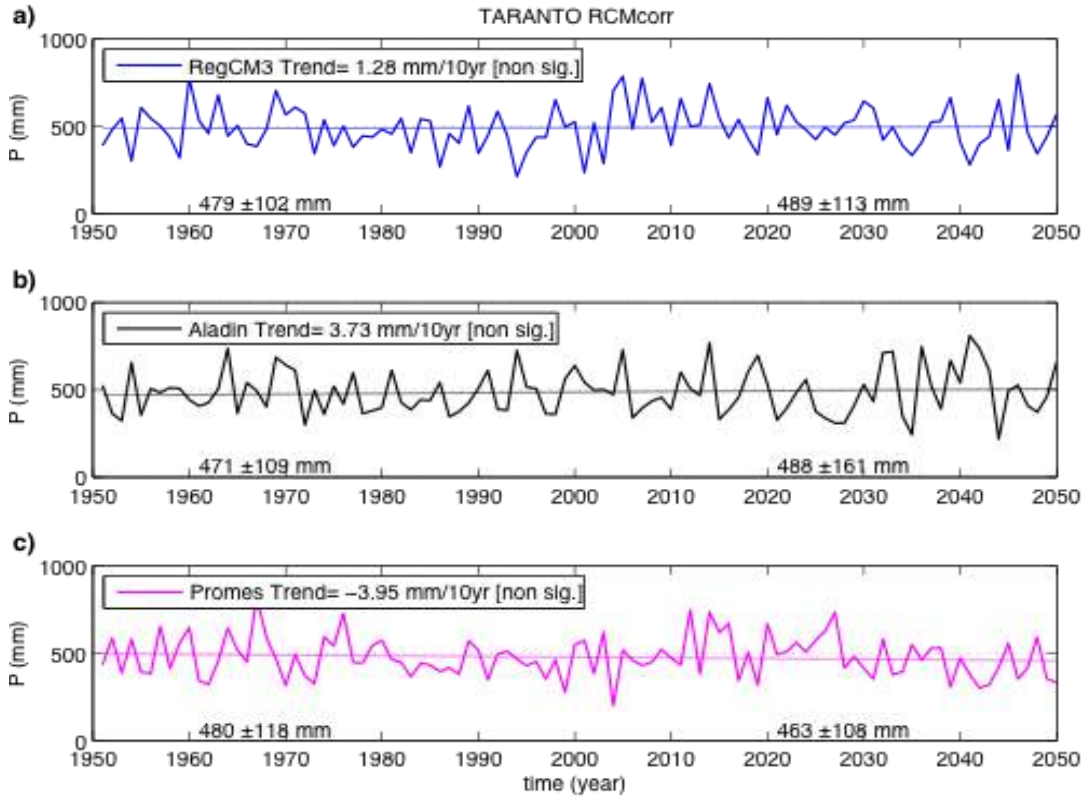

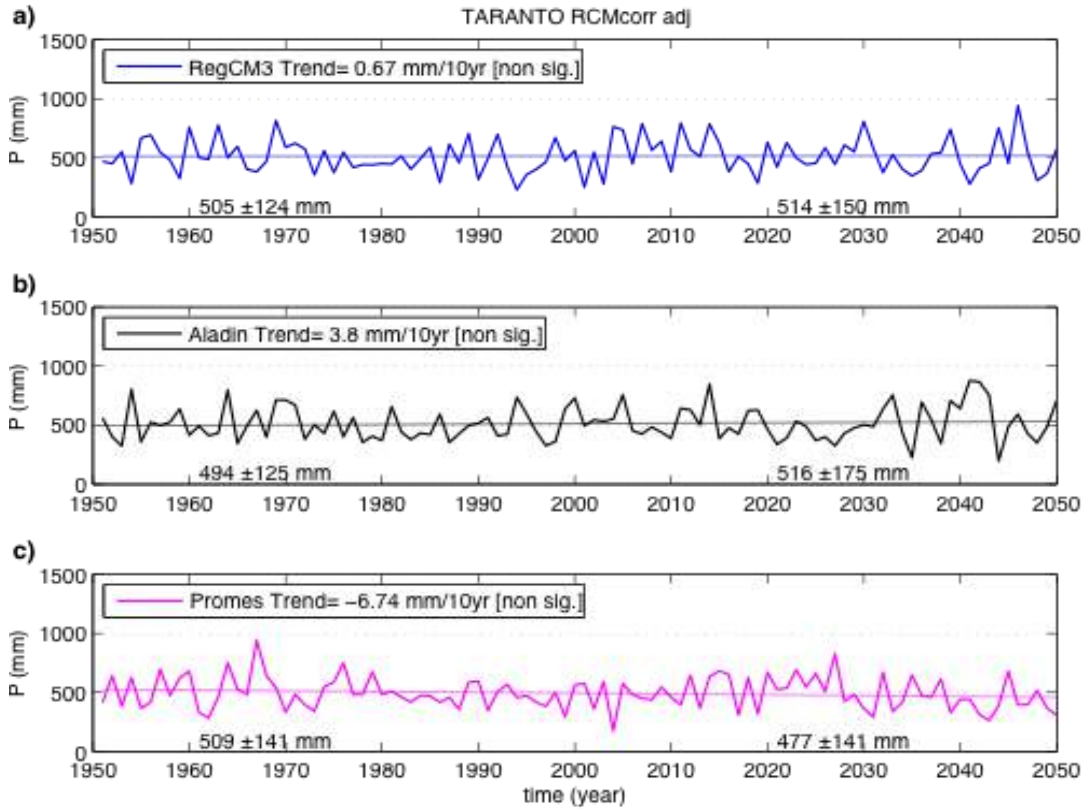

Figure 65 Taranto station: annual precipitation amount and associated linear trend in a) RegCM3, b) Aladin, c) Promes. Decadal trend based on the entire time series is shown in panel legends. The statistical significance of the trend is assessed using the Mann-Kendall test and 5% significance level. Additional numbers at the bottom of each panel are mean values and standard deviations during P0 (1961-1990) and P1 (2021-2050). Model time series: RCMcorr (above); RMcorr_adj (below).

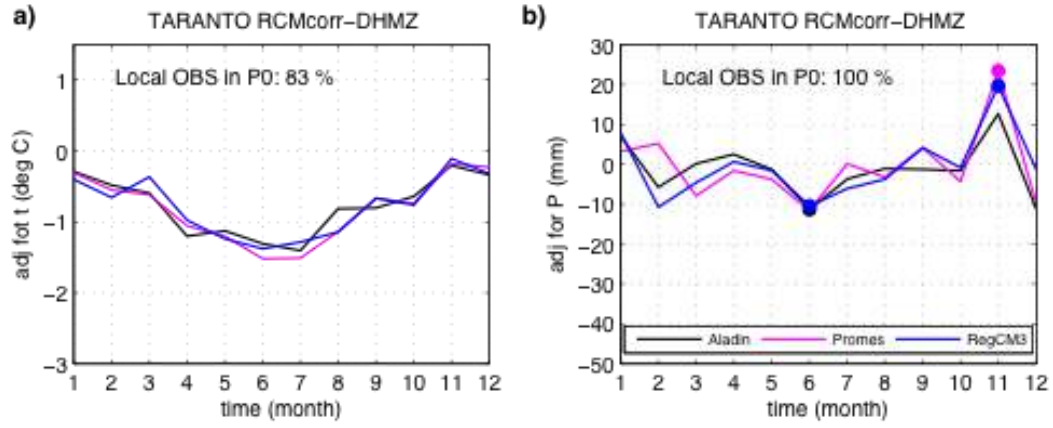

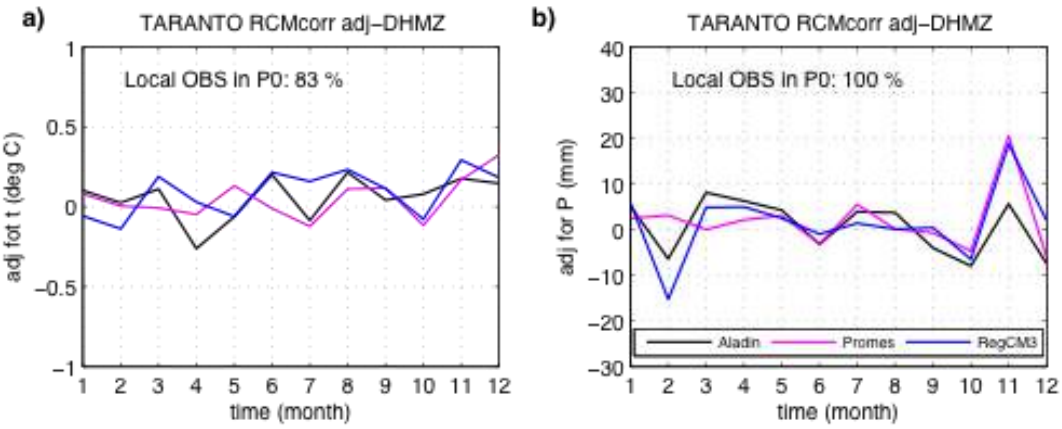

Figure 66 Taranto station: adjustment differences a) mean monthly temperature b) monthly precipitation amount. Differences are based on 1961-1990 period and the availability of DHMZ observations. Statistically significant differences according to the Wilcoxon-Mann-Whitney nonparameteric rank-sum test and 5% significance level are marked by the filled circles. Model time series: RCMcorr (above); RMcorr_adj (below).

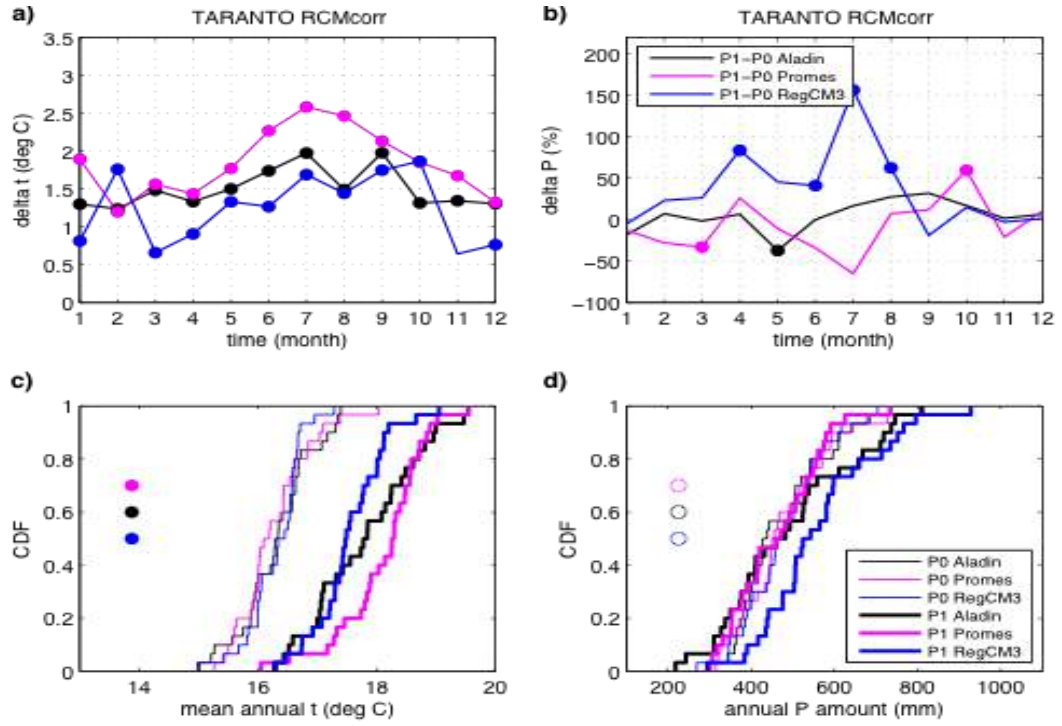

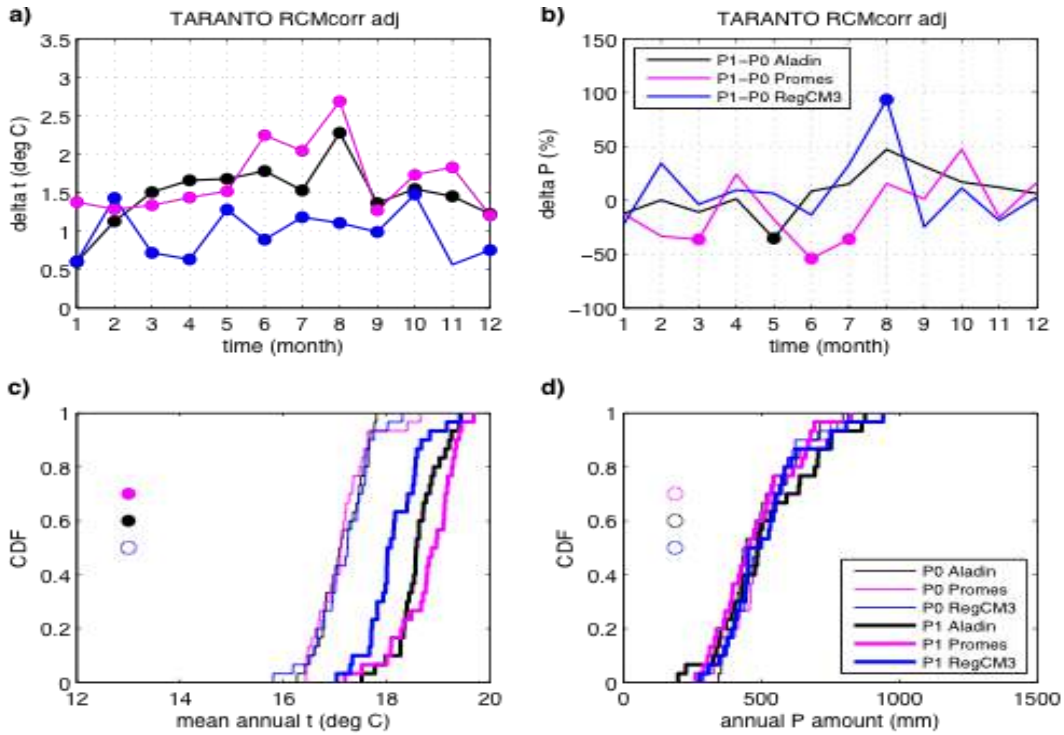

Figure 67 Taranto station: a) monthly mean temperature P1 vs. P0 change; b) relative monthly precipitation P1 vs. P0 change; c) empirical cumulative distribution functions CDFs of mean annual temperature in P0 and P1; d) same as c) but for annual precipitation amount. Time periods are: P0 1961-1990 and P1 2021-2050. Statistically significant differences in a) and b) according to the Wilcoxon-Mann-Whitney nonparameteric rank-sum test and 5% significance level are marked by the filled circles. Statistically significant differences according to the Kolmogorov-Smirnov test and 5% significance level between CDFs in two periods for every model in panels c) and d) are marked by the filled circles. Model time series: RCMcorr (above); RMcorr_adj (below).

The following tables show a comparison among stations and among RCM for temperature and precipitation trends.

- Tables 9 and 11 focus the attention on the RegCM3 forcing, analyzing the trend computed for each available station both for RCMcorr and RCMcorr_adj. The goal is to verify whether the downscaled signal is uniform over the study area or not and if the trends computed through the two adopted methods of downscaling are comparable, evaluating the possible gain arising from the q-q plot adjustment.
- Table 10 and 12 permit to analyze the differences among the adopted RCM, for both the dowscaling methods. The trends (computed as linear regression) are expressed in °C/10yrs for temperature and mm/10yrs for precipitation

	TEMPERATURE TREND 1955-2050 RegCM3

	TREND [°C/10yrs]		MEAN 1961-1990		MEAN 2021-2050	
	corr	corr_adj	corr	corr_adj	corr	corr_adj
CRISPIANO	0.19	0.17	14.8±0.5	15.8±0.6	16.0±0.6	16.9±0.6
FASANO	0.19	0.21	15.0±0.5	16.3±0.8	16.2±0.6	17.7±0.7
GROTTAGLIE	0.19	0.19	15.0±0.5	16.8±0.6	16.2±0.6	18.0±0.7
LATIANO	0.19	0.17	15.9±0.5	16.0±0.6	17.2±0.6	17.1±0.6
LOCOROTONDO	0.19	0.19	15.0±0.5	14.4±0.7	16.2±0.6	15.6±0.6
OSTUNI	0.19	0.16	15.9±0.5	15.6±0.6	17.2±0.6	16.7±0.5
SANGIORGIO JONICO	0.19	0.18	16.3±0.5	16.7±0.6	17.5±0.6	17.8±0.6
TALSANO	0.19	0.16	16.3±0.5	16.3±0.5	17.5±0.6	17.3±0.6
TARANTO	0.19	0.15	16.3±0.5	17.2±0.5	17.5±0.6	18.1±0.5

Table 9 Temperature trends computed from RegCM3 downscaled using the bias correction (*corr*) and the q-q plot methods (*corr_adj*)

	PRECIPITATION TREND 1955-2050 RegCM3					
	TREND [mm/10yrs]		MEAN 1961-1990		MEAN 2021-2050	
%	corr	corr_adj	corr	corr_adj	corr	corr_adj
CRISPIANO	0.49	1.4	471±94	573±130	477±112	594±175
FASANO	-0.02	-0.72	497±92	621±140	499±104	622±159
GROTTAGLIE	-0.02	0.73	497±92	551±125	499±104	570±145
LATIANO	2.8	3.66	522±97	656±154	540±105	685±145
LOCOROTONDO	-0.02	0.12	497±92	706±150	499±104	727±187
OSTUNI	2.8	-0.30	522±97	737±167	499±104	742±190
SANGIORGIO JONICO	1.28	1.33	479±102	583±144	489±113	596±196
TARANTO	1.28	0.67	497±102	505±124	489±113	514±150

Table 10 Precipitation trends computed from RegCM3 downscaled using the bias correction (*corr*) and the q-q plot methods (*corr_adj*)

	TEMPERATURE TREND 1955-2050					
	RegCM3		ALADIN		PROMES	
%	corr	corr_adj	corr	corr_adj	corr	corr_adj
CRISPIANO	0.19	0.17	0.28	0.25	0.29	0.26
FASANO	0.19	0.21	0.28	0.33	0.29	0.32
GROTTAGLIE	0.19	0.19	0.28	0.37	0.29	0.34
LATIANO	0.19	0.17	0.28	0.27	0.29	0.27
LOCOROTONDO	0.19	0.19	0.28	0.29	0.29	0.29
OSTUNI	0.19	0.16	0.28	0.24	0.29	0.24

SANGIORGIO JONICO	0.19	0.18	0.27	0.33	0.27	0.30
TALSANO	0.19	0.16	0.27	0.24	0.27	0.24
TARANTO	0.19	0.15	0.27	0.23	0.27	0.24

Table 11 Temperature trends computed considering different RCM (RegCM3, Aladin and Promes) and different downscaling methodologies (bias correction: *corr*; q-q plot: *corr_adj*)

	PRECIPITATION TREND 1955-2050					
	RegCM3		ALADIN		PROMES	
mm/10yrs	**corr**	**corr_adj**	**corr**	**corr_adj**	**corr**	**corr_adj**
CELLE MESSAPICA	2.8	-0.95	0.69	-4.87	-2.63	-7.43
CRISPIANO	0.49	1.4	-2.16	3.66	-2.24	-9.18
FASANO	-0.02	-0.72	-1.51	-4.71	-2.47	-7.62
GROTTAGLIE	-0.02	0.73	-1.51	0.49	-2.47	-8.21
LATIANO	2.8	3.66	0.69	-4.4	-2.63	-6.31
LOCOROTONDO	-0.02	0.12	-1.51	-6.48	-2.47	-8.39
OSTUNI	2.8	-0.3	0.69	-4.84	-2.63	-5.57
SANGIORGIO JONICO	1.28	1.33	3.73	1.72	-3.95	-7.78
TARANTO	1.28	0.67	3.73	3.8	-3.95	-6.74

Table 12 Precipitation trends computed considering different RCM (RegCM3, Aladin and Promes) and different downscaling methodologies (bias correction: *corr*; q-q plot: *corr_adj*)

From tables 9 to 12 it is possible to infer that:

1. Concerning the temperature, the climatic signal over the area is uniform (table 9). In other words, the correction due to the downscaling does not affect the tendency to the increasing temperature forecast by all the RCMs. It is approximately +0.2 °C/10yrs over the period 1955-2050 and it ranges between +0.15 °C/10yrs and +0.21 °C/10yrs (for the RegCM3corr_adj time series). The trends computed without the q-q plot correction are similar

2. Similar results (space uniformity of the temperature signal and substantial invariance with respect to the adopted downscaling method) are obtained considering the two other RCMs (Aladin and Promes)

3. Concerning the precipitation, the climatic signal over the area, once chosen the RCM, is strongly not uniform, both adopting only the bias correction (*corr*) and adopting the q-q plot correction (corr_adj). This is mainly due to the fact that the forcing from the RCM is strongly not uniform in space: in fact, as one can argue from table 10, if the only bias correction is applied, the sign and intensity of the trend are equal for the stations that belong to the same RCM

grid (i.e. Fasano, Grottaglie and Locorotondo; Latiano and Ostuni; Sangiorgio Jonico and Taranto; Crispiano). The signs of such trends are not equal for all the stations stations: in other words, at some nodes RegCM3 forecast an increase of precipitation and in some other nodes RegCM3 forecast a decrease.

4. Applying a q-q plot correction (*corr_adj* time series) the trends significantly change both in sign and modulus (for example, for the Ostuni station, the trend is +2.8 mm/10yrs considering the *corr* time series and -0.30 mm/10yrs considering the *corr_adj* time series). This indirectly means that the correction of the tails of the distributions strongly affect the assessment of the trend

5. A comparison among RCMs temperature scenarios (table 11) shows that the Aladin and Promes RCM forecast a higher increase with respect to RegCM3. As a consequence, for developing impact scenarios of climate change on the Ostuni area, it appears more suitable to adopt the worst temperature scenarios from Promes and Aladin, neglecting the RegCM3 RCM. Similar results, both in time and modulus, are obtained after q-q plot

6. Precipitation scenarios from Promes (table 12) indicate a uniform in space decrease of precipitation, both for *corr* and *corr_adj* time series; such a decrease is in the order of 2.5 mm/10yrs if the only bias correction is applied, while a correction of the tail distribution lead to a higher decrease, in the order of 8 mm/10yrs.

7. Also Aladin RCM forecast a tendency to reduction of precipitation, although less significant than Promes and not uniform in space. Similar results are obtained from RegCM3.

8. As a conclusion the worst scenarios, in terms of possible water shortage and salt intrusion in the Ostuni area, are obtained from Promes RCM. We suggest to use this model for the next impact studies on the pilot area aquifer.

4. CONCLUSIONS

Some general conclusions can be drawn from our analysis on the present climate:

1. Concerning temperatures, a general increase is observed for the whole observation period (1960-2007), due to an increase of temperature (particularly during summer) during the last two decades (1991-2007). This climatic signal is not observed in all the stations, suggesting that local climate can be superimposed to the regional and/or global climate.

2. In terms annual mean, the present precipitation regime appears to be uniform over the study area; differences among stations are mostly related to the altitude

3. A very high interannual variability in the precipitation regime can be observed, both considering the min and max values, and considering the percentiles of the probability distributions: as a consequence, the mean values of precipitation cannot be representative of the transient regime of recharge to the aquifer.

4. Concerning the trends, it is possible to observe a general decrease of annual precipitation, both for the base line period P0 and for the whole observation period P_{obs}. However, such a decrease, although observed in all the rain gauges, it is never statistically significant. This is probably due to the high interannual variability.

5. The analysis of the seasonal trends suggest that the decrease of precipitation observed at annual scale is mainly due to a decrease of the winter precipitation, which is observed in all the stations during the period P0. A similar decreasing trend is observed also if the whole observation period is considered (8 stations out of 9): however such a trend is generally not significant from a statistical point of view. The last remark lead to two important consequences: a) concerning precipitation, at least for the Ostuni pilot area, the base line 1961-1990 (which is usually considered stationary from a climatic point of view) is not stationary; b) the impact of a decreasing in precipitation on the Ostuni aquifer and on the possible salt intrusion is currently ongoing

General conclusions on the climate scenarios can be summarized as follows:

6. Concerning the temperature, the forecast downscaled climatic signal over the area is uniform in space. In other words, the correction due to the downscaling does not affect the tendency to the increasing temperature forecast by all the RCMs.

7. Concerning the precipitation, the climatic signal over the area, once chosen the RCM, is strongly not uniform, both adopting only the bias correction (*corr*) and adopting the q-q plot correction (corr_adj). This is mainly due to the fact that the forcing from the RCM is strongly not uniform in space.

8. Applying a q-q plot correction (*corr_adj* time series) the trends significantly change both in sign and modulus with respect to the bias correction (*corr* time

series). This indirectly indicates that the correction of the tails of the distributions strongly affects the estimate of the trend

9. A comparison among RCMs temperature scenarios (table 11) shows that the Aladin and Promes RCM forecast a higher increase with respect to RegCM3. As a consequence, for developing impact scenarios of climate change on the Ostuni area, it appears more suitable to adopt the worst temperature scenarios from Promes and Aladin, neglecting the RegCM3 RCM. Similar results, both in time and modulus, are obtained after q-q plot

10. Precipitation scenarios from Promes (table 12) indicate a uniform in space decrease of precipitation, both for *corr* and *corr_adj* time series; such a decrease is in the order of 2.5 mm/10yrs if the only bias correction is applied, while a correction of the tail distribution lead to a higher decrease, in the order of 8 mm/10yrs. Also Aladin RCM forecast a tendency to reduction of precipitation, although less significant than Promes and not uniform in space. Similar results are obtained from RegCM3.

11. The worst scenarios, in terms of possible water shortage and salt intrusion in the Ostuni area, are obtained from Promes RCM. We suggest to use this model for the next impact studies on the pilot area aquifer.

5. REFERENCES

Bubnova, R., Hello, G., Bénard, P., Geleyn, J-F., 1995. Integration of the fully elastic equations cast in hydrostatic pressure terrain-following coordinate in the framework of the ARPEGE/Aladin NWP system. *Mon.Wea.Rev.*,123:515-535.

Castro, M., Fernández C., Gaertner M.A.,1993. Description of a meso-scale atmospheric numerical model. In:J.I.Díaz, J.L.Lions (eds), Mathematic, climate and environment, Masson.

Déqué, M., 2007. Frequency of precipitation and temperature extremes over France in an anthropogenic scenario: Model results and statistical correction according to observed values. *Global and PlanetaryChange*, 57:16–26.

Formayer, H., Haas P., 2010. Correction of RegCM3 model output dana using a rank matching approach applied on various meteorological parameters. In Deliverable D3.2 RCM output localization methods (BOKU-contribution of the FP6 CECILIA project on http://www.cecilia-eu.org/).

Haylock, M.R., Hofstra N., Klein Tank A.M.G., Klok E.J., Jones P.D., New M., 2008. A European daily high-resolution gridded dataset of surface temperature and precipitation for 1950-2006. *J. Geophys. Res.*,113, D20119, doi:10.1029/2008JD010201.

Pal, J.S., and Coauthors, 2007. Regional climate modeling for the developing world: The ICTP RegCM3 and RegCNET. *Bull.Amer.Meteor.Soc.*, 88:1395-1409.

Let's grow up together

DRINK ADRIA

Adriatic IPA
Cross Border Cooperation 2007-2013

The project is co-funded by the European Union,
Instrument for Pre-Accession Assistance

Analysis of observed and simulated climate and climate change for Slovenian pilot areas (Kobariški stol, Mia, Matajur and Mirna River catchments)

Faculty of Natural Sciences and Engineering
University of Ljubljana
(FB5)

Ljubljana, 2014

Lead Author/s	Nina Zupančič, Petra Vrhovnik, Petra Žvab Rožič. Barbara Čenčur Curk
Lead Authors Coordinator	Name and Surname
Contributor/s	Name and Surname
Date last release	28.8.2014
State of document	Final

Let's grow up together

DRINK ADRIA

Adriatic IPA
Cross Border Cooperation 2007-2013

The project is co-funded by the European Union, Instrument for Pre-Accession Assistance

Table of content

1 Introduction

This report present the contribution to DRINKADRIA WP4 dealing with the regional characteristics of climate and climate change in a wider range of Slovenian pilot areas.
In the first part we analyse observed air temperature and precipitation from two meteorological stations (Bilje and Portorož) positioned on the west of Slovenia. Climate characteristics and variability are presented for 1961 – 1990 reference time period and trends are calculated for the whole span of available data, i.e. 1956 – 2011 for temperature and 1961 – 2011 for precipitation. Data is presented on monthly, seasonal (winter – December to February; spring – March to May; summer – June to August; autumn – September to November) and annual average basis.
The second part of the report comprises simulation of present and future climate based on three different regional climate models; Aladin (Bubnova et al., 1995), Promes (Castro et al., 1993) and RegCM3 (Pal et al., 2007). The analyses were performed with RCM corrected and RCM corrected & adjusted data.

2 Pilot areas observations

Slovenian pilot areas are positioned along the western Slovenian border with Italy (Kobariški stol, Mia and Matajur) and south-western border with Croatia (supply area of Mirna river). On this area two main meteorological station were selected to present climate and climate change characteristics (temperature, precipitation) of this area.

2.1 Meteorological database and statistics of local observations

In the Slovenian Adriatic area there are two meteorological stations situated approximately 35 km apart (Table 1, Figure 1). Meteorological station Bilje is positioned close to Nova Gorica near the western Slovenian border with Italy, while Portorž station lies just on the SW corner of Slovenia. Portorož meteorological station is positioned directly on the seacoast, while Bilje is inland station, situated in Vipava Valley, between Karst plateau on the south and Trnovski gozd plateau on the north.

Table 1: Geographical station data and available time spans of data sets for Bilje and Portorož meteorological stations. φ – longitude, λ – latitude, h – elevation, T – temperature data range, P – precipitation data range.

Station	*φ (°)*	*λ (°)*	*H (m)*	*T*	*P*
Bilje	45° 53'45''	13° 37' 44''	55	1956 - 2011	1961 - 2011
Portorož	45° 28' 32''	13° 37' 14''	2	1956 - 2011	1961 - 2011

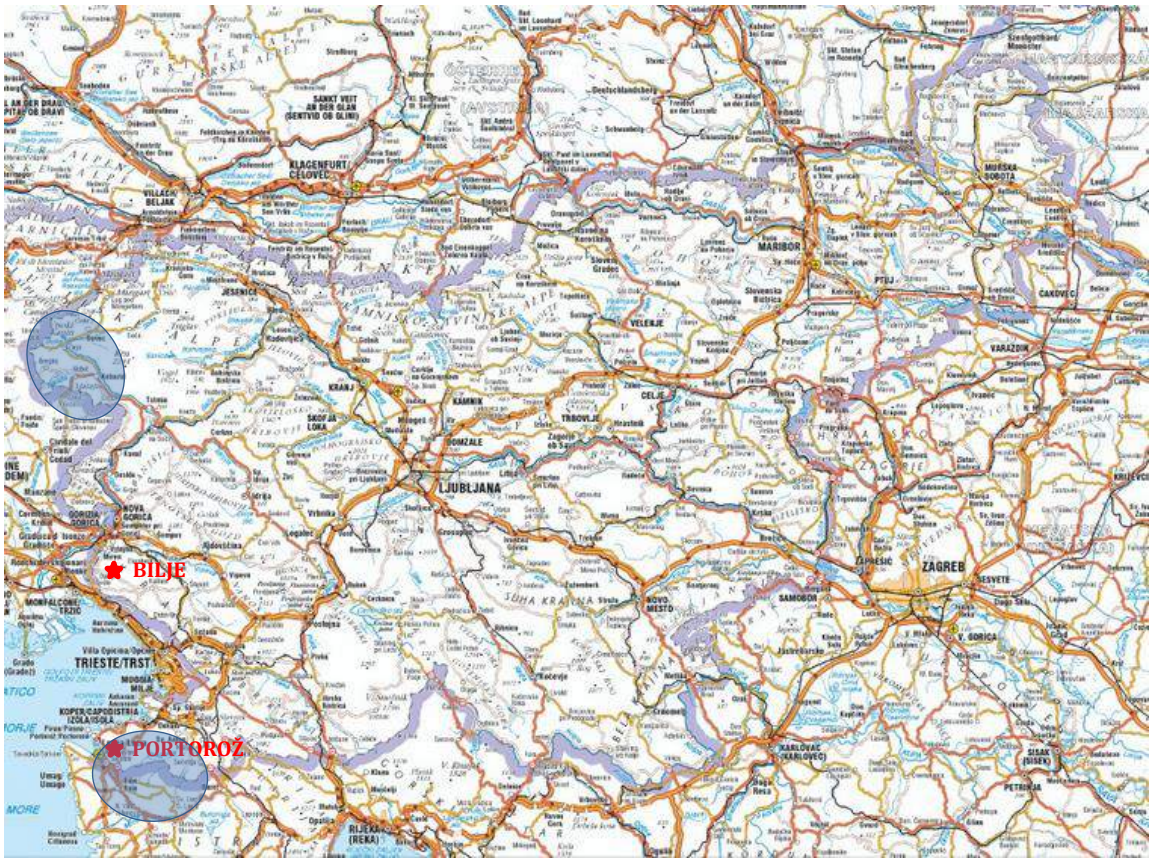

Figure 1: Geographical position of Bilje and Portorož meteorological stations (red stars) and locations of pilot areas (blue fields) (Geopedia, 2014).

DRINK ADRIA

2.2 Bilje meteorological station

2.2.1 Temperature

InBilje station the coldest month is January and the warmest July (Table 2, Figure 2). According to standard deviation and coefficient of variation the temperature is most variable in the winter months and quite uniform in summer (Table 2, Figure 3). The percentiles for seasonal mean air temperature based on empirical distribution from the reference period 1961 – 1990 for Bilje station is presented in Table 3.

Annual air temperature exhibits slight increase of temperature during observed period (Figure 3), but the trend is statistically significant at 5 % level for winter, spring and summer season. For spring and summer also the highest increase of temperature is predicted by regression analysis. Table 4 shows decadal air temperature trends (°C/10 years) for Bilje station based on 1956 – 2011 data series.

Table 2: Basic statistics (Mean, Std – standard deviation, Max – maximum, Min – minimum and CV – coefficient of variation) for monthly, seasonal and annual mean air temperature (°C) for the reference period 1961-1990 from Bilje meteorological station.

Month	*Mean*	*Std*	*Min*	*Max*	*CV*
1 January	2.2	1.84	-2.3	6.2	0.83
2 February	3.7	2.04	-0.2	7.9	0.55
3 March	6.7	1.7	3	9.3	0.25
4 April	11.1	1.19	9.2	14.2	0.11
5 May	15.5	1.25	13.3	18.2	0.08
6 June	19.2	1.06	17.6	21.5	0.06
7 July	21.5	1.13	19.8	24.3	0.05
8 August	20.7	1.13	18	22.9	0.05
9 September	17.1	1.36	13.8	20.1	0.08
10 October	12.6	1.38	8.1	15.4	0.11
11 November	7.3	1.44	4.5	11.1	0.2
12 December	3.3	1.4	0.4	5.6	0.43
Winter	3.1	1.87	-2.3	7.9	0.61
Spring	12.3	4.22	4.5	20.1	0.34
Summer	20.5	1.45	17.6	24.3	0.07
Autumn	11.1	3.87	3	18.2	0.35
Year	11.8	6.91	-2.3	24.3	0.59

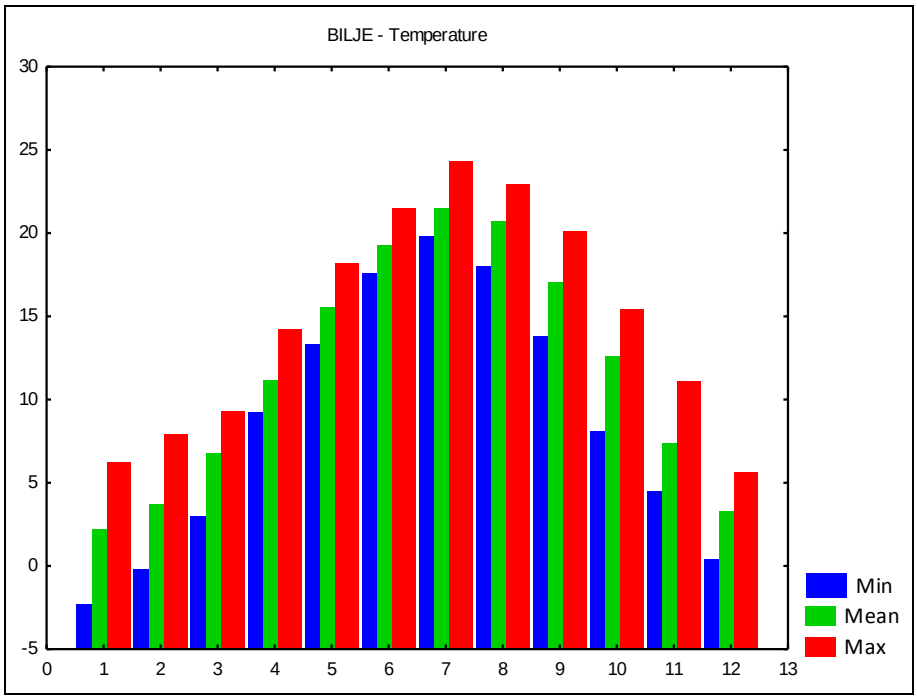

Figure 2: Annual cycle of minimum, mean and maximum monthly temperature (^{o}C) for the reference period 1961-1990 for Bilje meteorological station.

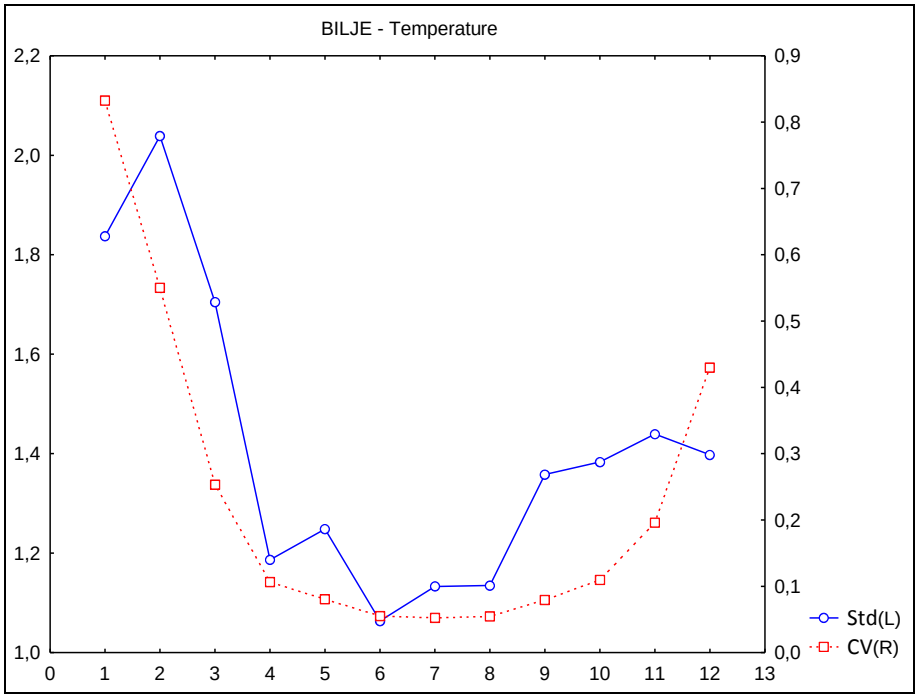

Figure 3: Annual cycle of temperature standard deviation and coefficient of variation for the reference period 1961-1990 for Bilje meteorological station.

Table 3: The percentiles for seasonal mean air temperature based on empirical distribution for the reference period 1961 – 1990 for Bilje meteorological station.

Percentile	*Winter*	*Spring*	*Summer*	*Autumn*
0.01	0.15	9.34	19.14	10.8
0.02	0.77	9.42	19.25	10.82
0.025	1.08	9.45	19.3	10.84
0.05	1.71	9.64	19.55	11.03
0.1	1.83	9.93	19.88	11.26
0.25	2.42	10.67	20.13	11.62
0.5	3.08	11.2	20.42	12.37
0.75	3.82	11.6	20.89	12.76
0.9	4.5	12.04	21.15	13.7
0.95	4.59	12.22	21.5	13.86
0.97	4.73	12.24	21.68	13.97
0.98	4.94	12.26	21.71	13.98
0.99	5.15	12.28	21.74	13.99

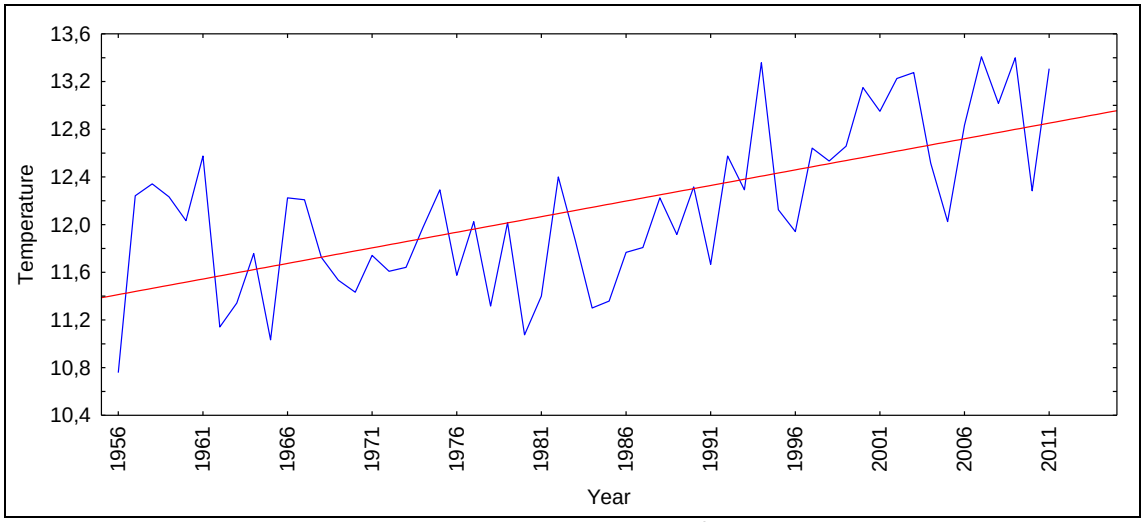

Figure 4: Time series of annual mean temperature (°C) with fitted trend line for the period 1956-2011 for the meteorological station Bilje.

*Table 4: Decadal air temperature trends (°C/10 years) based on 1956 – 2011 data series for Bilje meteorological station. * – statistically significant trend at 95 % probability.*

Winter	*Spring*	*Summer*	*Autumn*	*Year*
0.23*	0.34*	0.35*	0.13	0.26

2.2.2 Precipitation

In Bilje station the driest month is on average February and the wettest November, although the precipitation maximum is observed September (Table 5, Figure 5). On average spring is the wettest and winter is the driest season. According to standard deviation and coefficient of variation, annual precipitation is the most variable in October and the least in April and May (Table 5, Figure 6). Figure 7 presents cumulative distribution of annual precipitation amounts for Bilje station for the reference period 1961-1990. The percentiles for seasonal precipitation based on empirical distribution from the reference period 1961 – 1990 for Bilje station are shown in Table 6.

Time series of annual precipitation for the period 1961-2011 is shown in Figure 8. Annual, winter, spring and summer precipitations seem to decrease and autumn precipitation to increase during the observed period, but the annual and seasonal trends are not statistically significant at 5 % level (Table 7). For spring and summer the highest decrease is predicted by regression analysis. In Table 7 decadal precipitation trends (mm/10 years) for Bilje station based on 1961 – 2011 data series are presented.

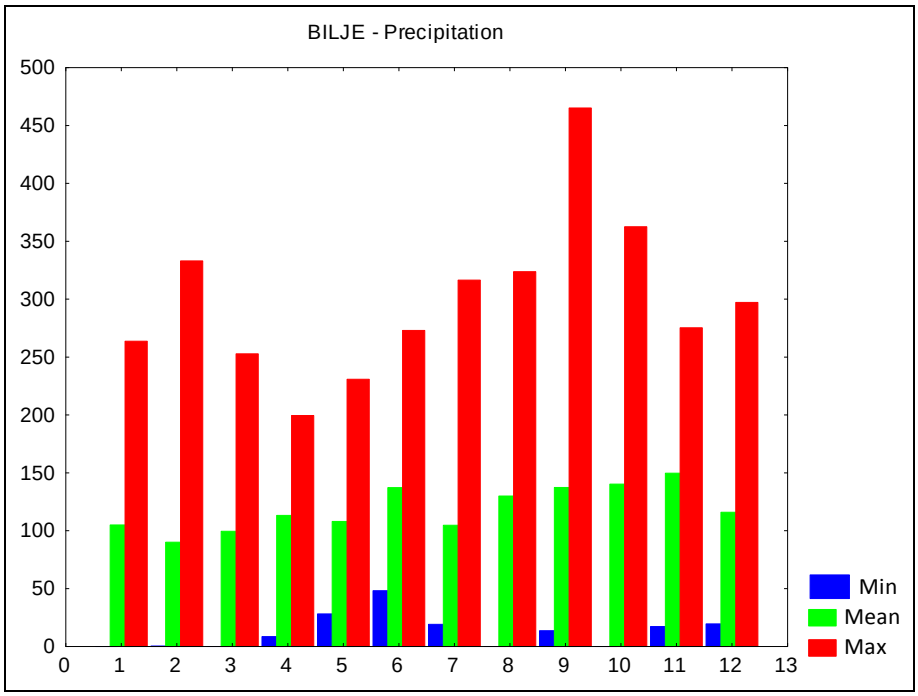

Figure 5: Annual cycle of minimum, mean and monthly precipitation amounts for Bilje station for the reference period 1961-1990.

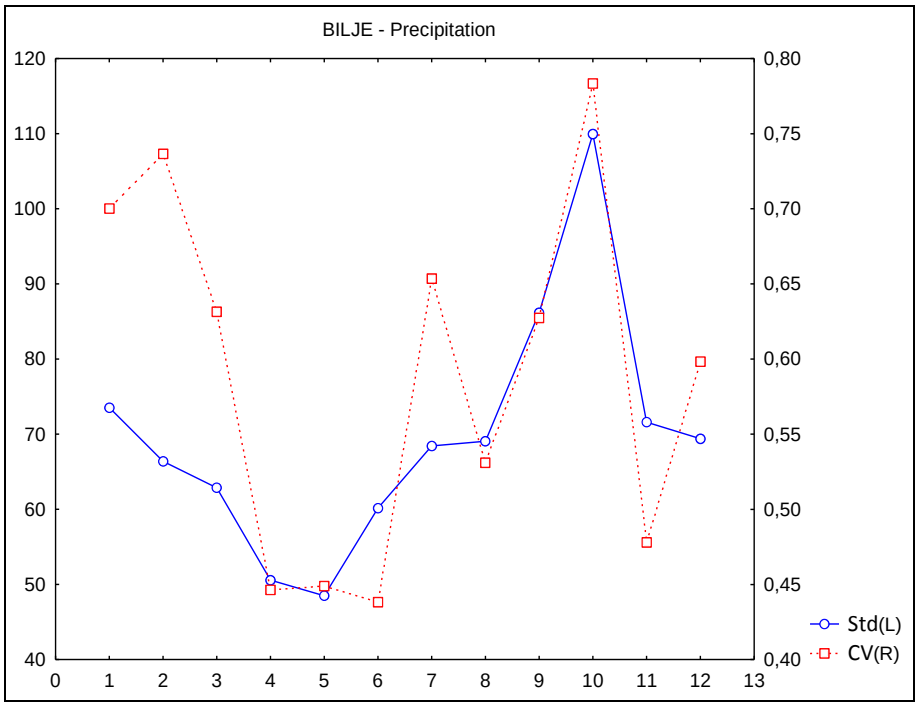

Figure 6: Annual cycle of precipitation standard deviation and coefficient of variation for Bilje station for the reference period 1961-1990.

Table 5: Basic statistics (Mean, Std – standard deviation, Max – maximum, Min – minimum and CV – coefficient of variation) for monthly, seasonal and annual mean precipitation for the reference period 1961-1990 for the Bilje meteorological station.

Month	*Mean*	*Std*	*Min*	*Max*	*CV*
1 January	105.0	73.55	0.0	263.8	0.70
2 February	90.1	66.40	0.5	333.0	0.74
3 March	99.6	62.88	0.0	252.8	0.63
4.apr	113.3	50.58	8.6	199.5	0.45
5 May	108.0	48.50	28.2	230.9	0.45
6 June	137.3	60.16	48.2	273.1	0.44
7 July	104.7	68.44	19.2	316.5	0.65
8 August	130.0	69.06	0.0	323.7	0.53
9 September	137.3	86.18	13.7	465.1	0.63
10 October	140.4	109.98	0.0	362.6	0.78
11 November	149.8	71.60	17.2	275.3	0.48
12 December	116.0	69.39	19.5	297.3	0.60
Winter	103.7	69.87	0.0	333.0	0.67
Spring	142.5	89.78	0.0	465.1	0.63
Summer	107.0	54.05	0.0	252.8	0.51
Autumn	124.0	66.76	0.0	323.7	0.54
Year	119.3	72.64	0.0	465.1	0.61

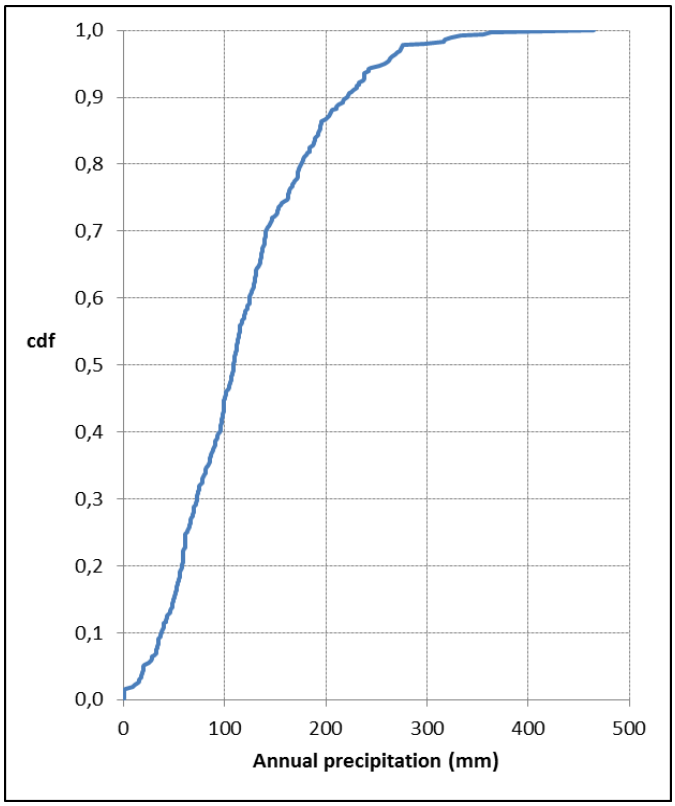

Figure 7: Cumulative distribution of annual precipitation amounts for the reference period 1961-1990 for Bilje meteorological station.

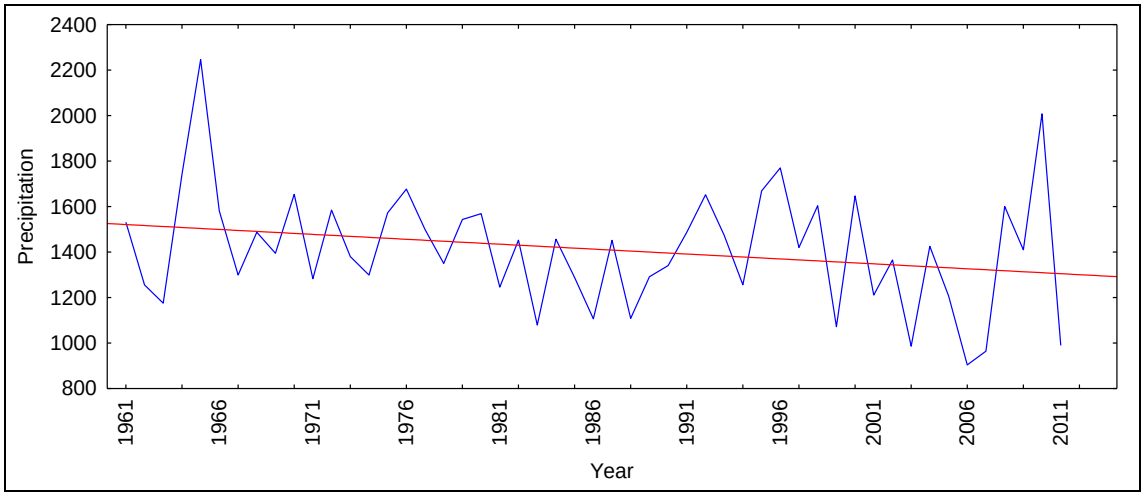

Figure 8: Time series of annual precipitation (mm) with fitted trend line for the period 1961-2011 for Bilje meteorological station.

Table 6: The percentiles for seasonal precipitation based on empirical distribution from the reference period 1961 – 1990 for Bilje meteorological station.

Percentile	*Winter*	*Spring*	*Summer*	*Autumn*
0.010	55.0	56.8	54.8	65.6
0.020	55.6	57.0	67.2	66.4
0.025	55.9	57.1	73.5	66.7
0.050	57.8	60.8	87.1	69.3
0.100	60.0	70.6	89.4	73.4
0.250	80.7	80.2	101.2	96.6
0.500	97.0	97.3	118.0	139.6
0.750	122.3	124.7	136.2	189.5
0.900	152.4	158.7	177.0	201.9
0.950	160.5	181.2	198.5	219.2
0.970	162.6	186.0	202.0	230.3
0.980	164.8	187.0	202.4	234.7
0.990	167.0	187.9	202.8	239.1

*Table 7: Decadal precipitation trends (mm/10 years) based on reference time period 1961 – 2011 for Bilje meteorological station. * - statistically significant trend at 95 % probability (not observed).*

Winter	*Spring*	*Summer*	*Autumn*	*Year*
-3.5	-4.8	-6.4	0.3	-3.6

2. 3 Portorož meteorological station

2.3.1 Temperature

In Portorož station the coldest month is January and the warmest July (Table 8, Figure 9). According to standard deviation and coefficient of variation, the temperature is most variable in the winter months and quite uniform in summer (Table 8, Figure 10). In Table 9 the percentiles for seasonal mean air temperature based on empirical distribution from the reference period 1961 – 1990 are presented.

Figure 11 shows time series of annual mean temperature (°C) with fitted trend line for the period 1956-2011. Annual air temperature exhibits slight increase of temperature during observed period, but the trend is statistically significant at 5 % level for winter and summer season (Table 10). For spring and summer the highest increase of temperature is predicted by regression analysis. Decadal air temperature trends (°C/10 years) are shown in Table 10.

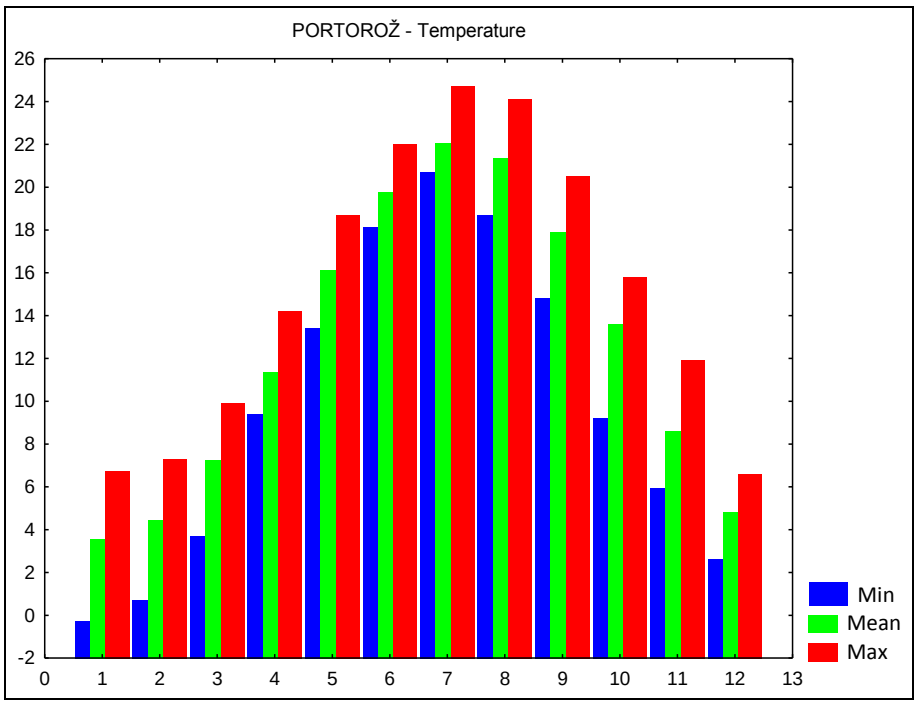

Figure 9: Annual cycle of minimum, mean and maximum monthly temperature (°C) for the reference period 1961-1990 for Portorož meteorological station.

Table 8: Basic statistics (Mean, Std – standard deviation, Max – maximum, Min –minimum and CV – coefficient) of variation for monthly, seasonal and annual mean air temperature for reference period 1961-1990 for Portorož meteorological station.

Month	*Mean*	*Std*	*Min*	*Max*	*CV*
1 January	3.5	1.62	-0.3	6.7	0.46
2 February	4.4	1.80	0.7	7.3	0.40
3 March	7.3	1.62	3.7	9.9	0.22
4 April	11.3	1.11	9.4	14.2	0.10
5 May	16.1	1.22	13.4	18.7	0.08
6 June	19.7	0.98	18.1	22.0	0.05
7 July	22.0	1.00	20.7	24.7	0.05
8 August	21.3	1.15	18.7	24.1	0.05
9 September	17.9	1.35	14.8	20.5	0.08
10 October	13.6	1.25	9.2	15.8	0.09
11 November	8.6	1.29	5.9	11.9	0.15
12 December	4.8	1.07	2.6	6.6	0.22
Winter	4.2	1.60	-0.3	7.3	0.38
Spring	13.3	4.03	5.9	20.5	0.30
Summer	21.0	1.41	18.1	24.7	0.07
Autumn	11.6	3.88	3.7	18.7	0.34
Year	12.5	6.68	-0.3	24.7	0.53

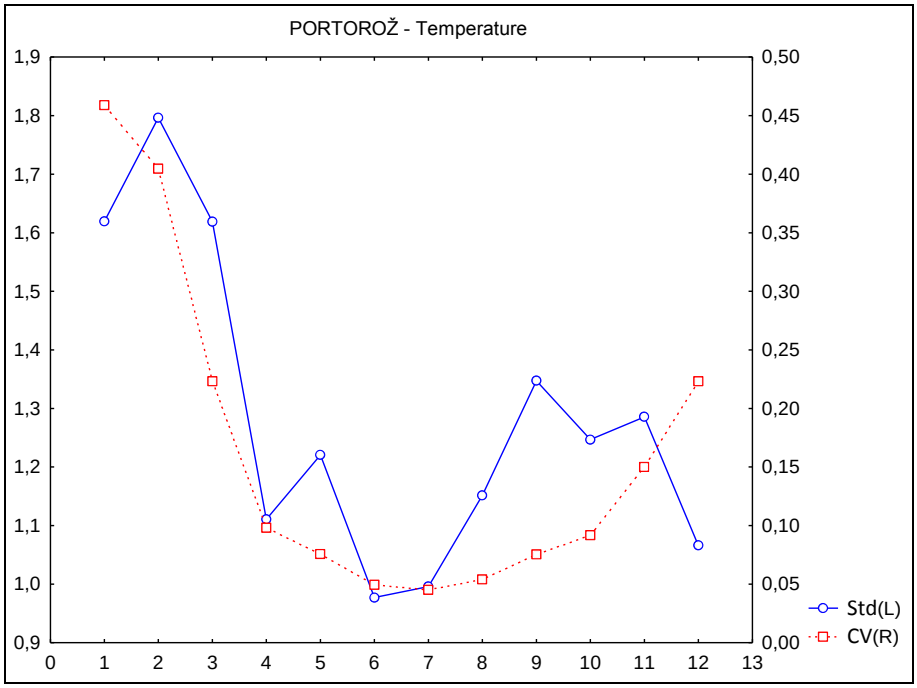

Figure 10: Annual cycle of temperature standard deviation and coefficient of variation for the reference period 1961-1990 for Portorož meteorological station.

Table 9: The percentiles for seasonal mean air temperature based on empirical distribution from the reference period 1961 – 1990 for Portorož meteorological station.

Percentile	*Winter*	*Spring*	*Summer*	*Autumn*
0.010	1.75	9.97	19.97	11.69
0.020	2.26	10.01	19.97	11.77
0.025	2.51	10.03	19.97	11.82
0.050	3.03	10.16	20.06	12.02
0.100	3.19	10.30	20.35	12.44
0.250	3.73	10.87	20.61	12.77
0.500	4.32	11.63	21.07	13.35
0.750	4.71	12.10	21.40	13.74
0.900	5.48	12.47	21.80	14.39
0.950	5.69	12.68	21.87	14.65
0.970	5.76	12.74	21.98	14.69
0.980	5.82	12.75	22.07	14.75
0.990	5.88	12.76	22.17	14.81

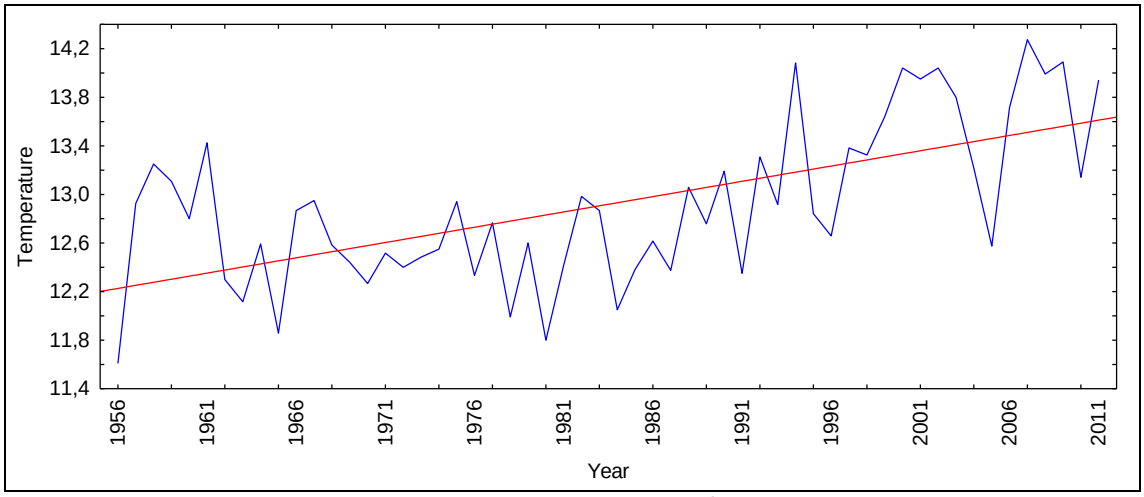

Figure 11: Time series of annual mean temperature (°C) with fitted trend line for the period 1956-2011 for Portorož meteorological station.

*Table 10: Decadal air temperature trends (°C/10 years) based on 1956 – 2011 data series for Portorož meteorological station. * - statistically significant trend at 95 % probability.*

Winter	*Spring*	*Summer*	*Autumn*	*Year*
0.28*	0.29	0.31*	0.13	0.25

2.3.2 Precipitation

In Portorož the driest month is on average February and the wettest September, where also the precipitation minimum and maximum are observed (Table 11, Figure 12). On average autumn is the wettest and winter the driest season. According to standard deviation and coefficient of variation, annual precipitation is most variable in October and least variable in April, May and June (Table 11, Figure 13). Cumulative distribution of annual precipitation amounts for Portorož station for the reference period 1961-1990 is presented in Figure 14. Table 12 summarises the percentiles for seasonal precipitation based on empirical distribution from the reference period 1961 – 1990 for Portorož station.

Time series of annual precipitation (mm) with fitted trend line for the period 1961-2011 is shown in Figure 15. Annual, winter, spring and summer precipitation seem to decrease and autumn precipitation to increase in the observed period, but the only statistically significant trend at 5 % level is observed for spring (Table 13). For spring and summer the highest decrease is predicted by regression analysis. Table 13 shows decadal precipitation trends (mm/10 years) for Portorož station based on 1961 – 2011 data series.

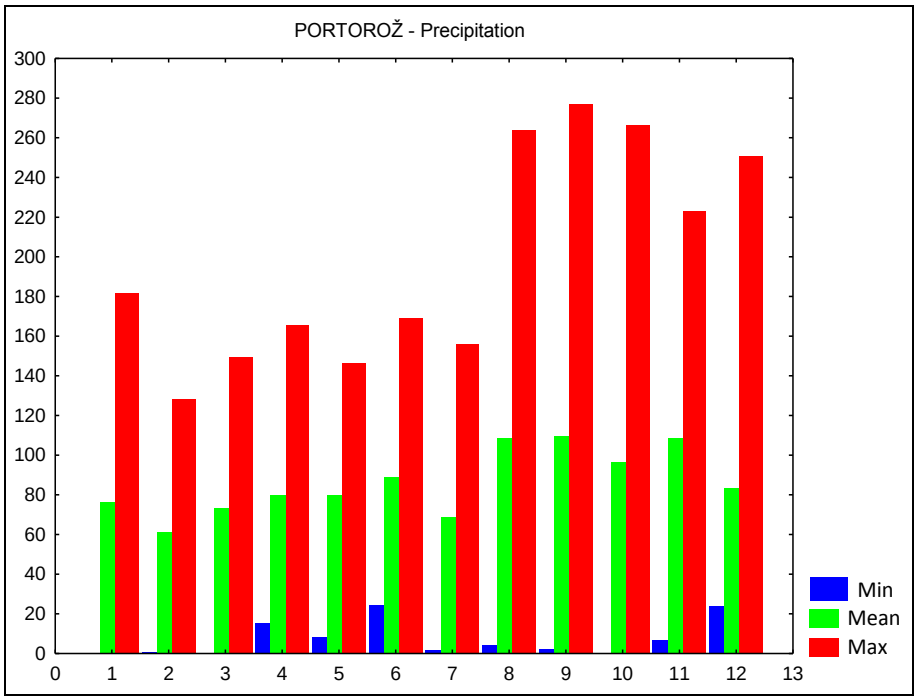

Figure 12: Annual cycle of minimum, mean and monthly precipitation amounts for the reference period 1961-1990 for Portorož meteorological station.

Table 11: Basic statistics (Mean, Std – standard deviation, Max – maximum, Min – minimum and CV – coefficient of variation) for monthly, seasonal and annual mean precipitation for reference period 1961-1990 for Portorož meteorological station.

Month	Mean	Std	Min	Max	CV
1 January	76.4	50.63	0.0	181.7	0.66
2 February	60.8	36.08	0.5	128.3	0.59
3 March	73.1	41.53	0.0	149.3	0.57
4 April	79.5	33.04	15.0	165.3	0.42
5 May	79.7	35.50	8.0	146.4	0.45
6 June	88.8	32.96	24.4	168.9	0.37
7 July	68.8	43.09	1.5	155.7	0.63
8 August	108.6	64.16	4.3	263.8	0.59
9 September	109.5	62.71	2.3	276.7	0.57
10 October	96.5	80.65	0.0	266.0	0.84
11 november	108.5	57.07	6.6	223.0	0.53
12 December	83.5	49.80	23.6	250.7	0.60
Winter	73.6	46.46	0.0	250.7	0.63
Spring	77.5	36.57	0.0	165.3	0.47
Summer	88.7	50.67	1.5	263.8	0.57
Autumn	104.8	67.06	0.0	276.7	0.64
Year	86.1	52.59	0.0	276.7	0.61

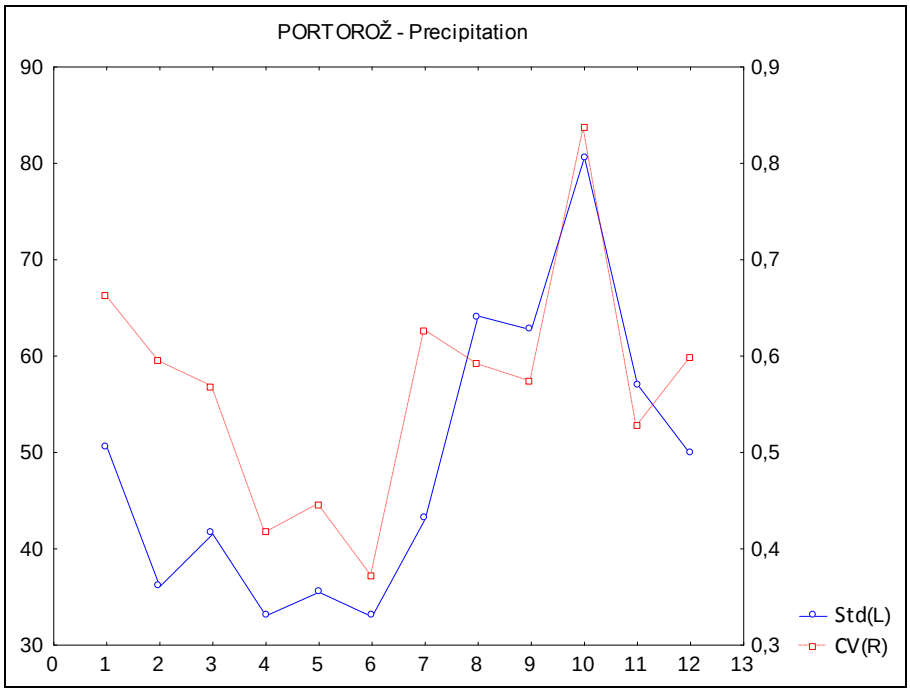

Figure 13: Annual cycle of precipitation standard deviation and coefficient of variation for the period 1961-1990 for Portorž meteorological station.

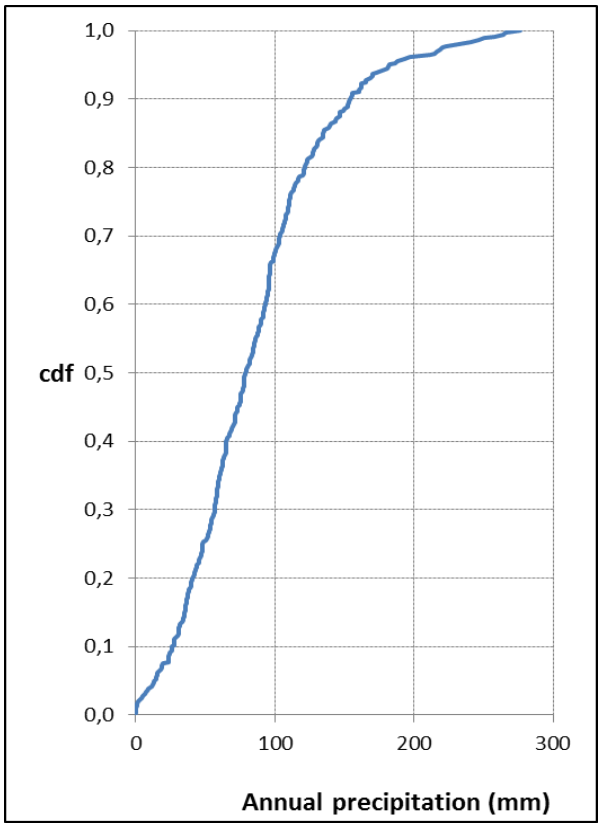

Figure 14: Cumulative distribution of annual precipitation amounts for the reference period 1961-1990 for Portorož meteorological station.

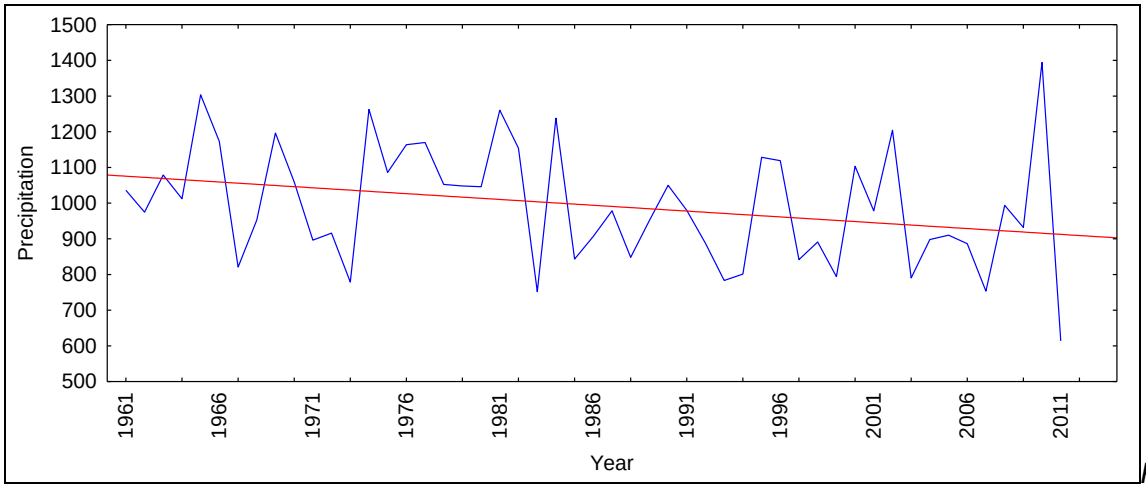

Figure 15: Time series of annual precipitation (mm) with fitted trend line for the period 1961-2011 for the meteorological amounts station Bilje.

Table 12: The percentiles for seasonal precipitation based on empirical distribution from the reference period 1961 – 1990 for Portorož meteorological station.

Percentile	*Winter*	*Spring*	*Summer*	*Autumn*
0.010	24.8	44.0	35.3	45.6
0.020	30.0	45.4	39.0	46.0
0.025	32.6	46.0	40.9	46.2
0.050	41.0	50.6	46.5	48.7
0.100	48.0	56.8	54.1	54.7
0.250	55.3	63.9	65.6	78.9
0.500	72.7	77.1	86.0	101.2
0.750	86.6	86.6	101.3	130.6
0.900	108.7	97.3	134.7	154.0
0.950	109.4	117.3	139.9	169.8
0.970	112.8	126.5	146.2	174.1
0.980	119.5	128.1	154.4	179.1
0.990	126.2	129.7	162.5	184.1

*Table 13: Decadal precipitation trends (mm/10 years) based on 1961 – 2011 data series for Portorož meteorological station. * - statistically significant trend at 95 % probability.*

Winter	*Spring*	*Summer*	*Autumn*	*Year*
-1.6	-4.7*	-4.9	0.3	-2.7

2. 4 Comparison of Bilje and Portorož meteorological stations

Bilje and Portorož meteorological stations show some differences in climatic patterns. Although they are not very distant (app. 35 km), their geomorphological position is quite different. The annual, seasonal and monthly differences in air temperatures and precipitation between both stations were checked by parametric t-test and non-parametric Mann-Whitney test. Both approaches gave nearly the same results, with the only difference of statistical significance in February precipitation and May temperature (Table 14).

*Table 14: Parametric (Student t) and non-parametric (Mann-Whitney Z) test of equality of population temperature and precipitation means/medians of Bilje and Portorož meteorological station data. * - statistically significant differences at 95% probability.*

		Temperature	*Precipitation*
Annual	Student t	-1.6	7.0*
	Mann-Whitney Z	-1.7	6.5*
January	Student t	-2.9*	1.7
	Mann-Whitney Z	-2.9*	1.4
February	Student t	-1.5	2.1*
	Mann-Whitney Z	-1.3	1.8
March	Student t	-1.2	1.9
	Mann-Whitney Z	-1.2	1.5
April	Student t	-0.6	3.1*
	Mann-Whitney Z	-0.7	2.8*
May	Student t	-1.8	2.6*
	Mann-Whitney Z	-2.0*	2.4*
June	Student t	-1.9	3.9*
	Mann-Whitney Z	-1.9	3.3*
July	Student t	-1.8	2.4*
	Mann-Whitney Z	-1.7	2.1*
August	Student t	-2.1*	1.2
	Mann-Whitney Z	-2.1*	1.1
September	Student t	-2.3*	1.4
	Mann-Whitney Z	-2.5*	1.5
October	Student t	-2.8*	1.8
	Mann-Whitney Z	-3.2*	1.7
November	Student t	-3.5*	2.5*
	Mann-Whitney Z	-3.2*	2.4*

December	Student t	-4.7*	2.1*
	Mann-Whitney Z	-4.1*	2.0*
Winter	Student t	-4.6*	3.4*
	Mann-Whitney Z	-4.4*	2.9*
Spring	Student t	-0.7	4.3*
	Mann-Whitney Z	-0.8	3.8*
Summer	Student t	-2.6*	4.0*
	Mann-Whitney Z	-2.5*	3.7*
Autumn	Student t	-1.6	3.2*
	Mann-Whitney Z	-1.8	2.8*

Generally, we could conclude that both station differ in mean January, August, September, October, November, December, winter and summer temperatures, with Bilje being a bit colder than Portorož (Table 14, Figure 16). The annual precipitation is on the contrary higher in Bilje and the differences are statistically significant at 5 % level for annual, April, May, June, July, November, December and all four seasons. Bilje exhibits also higher variability of the data than Portorož (Table 14, Figures 17).

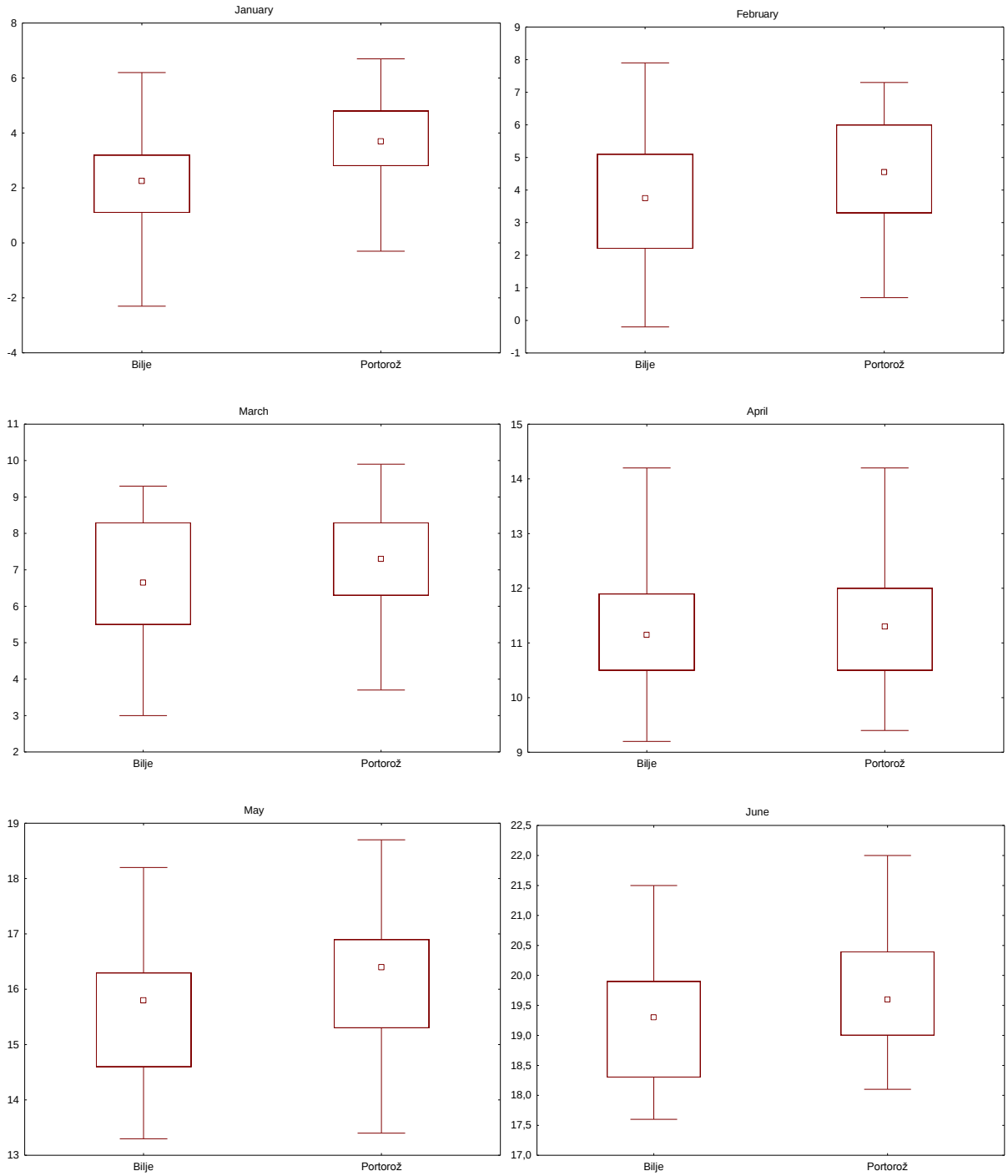

Figure 16: Box-whisker plots representing median (point), 25 – 75% quartiles (box), and minimum – maximum values (whiskers) of temperatures (^{o}C) for both meteorological stations (Bilje and Portorož).

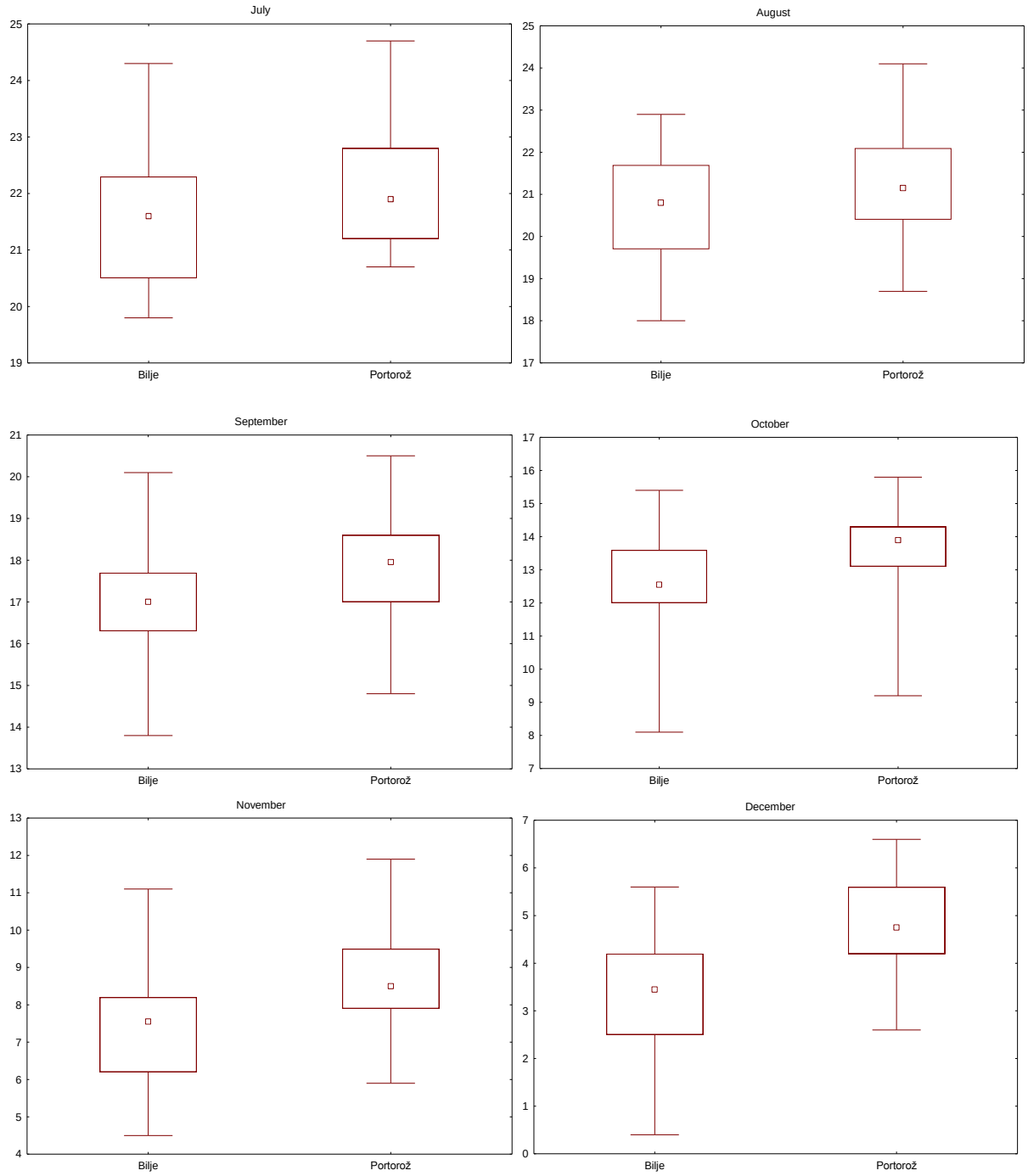

Figure 16: Continued.

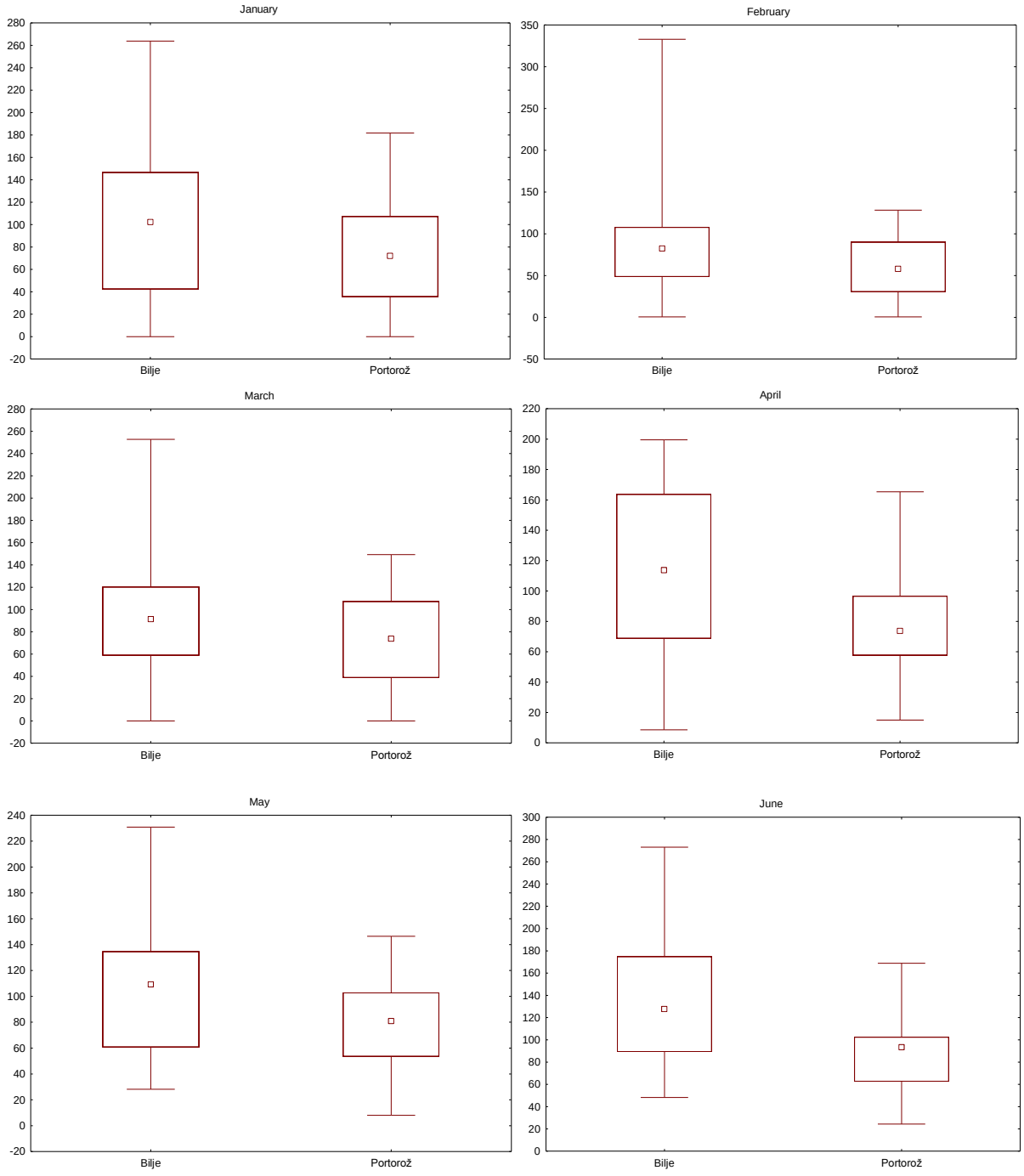

Figure 17: Box-whisker plots representing median (point), 25 – 75% quartiles (box), minimum – maximum values (whiskers) precipitation (mm) for both meteorological stations (Bilje and Portorož).

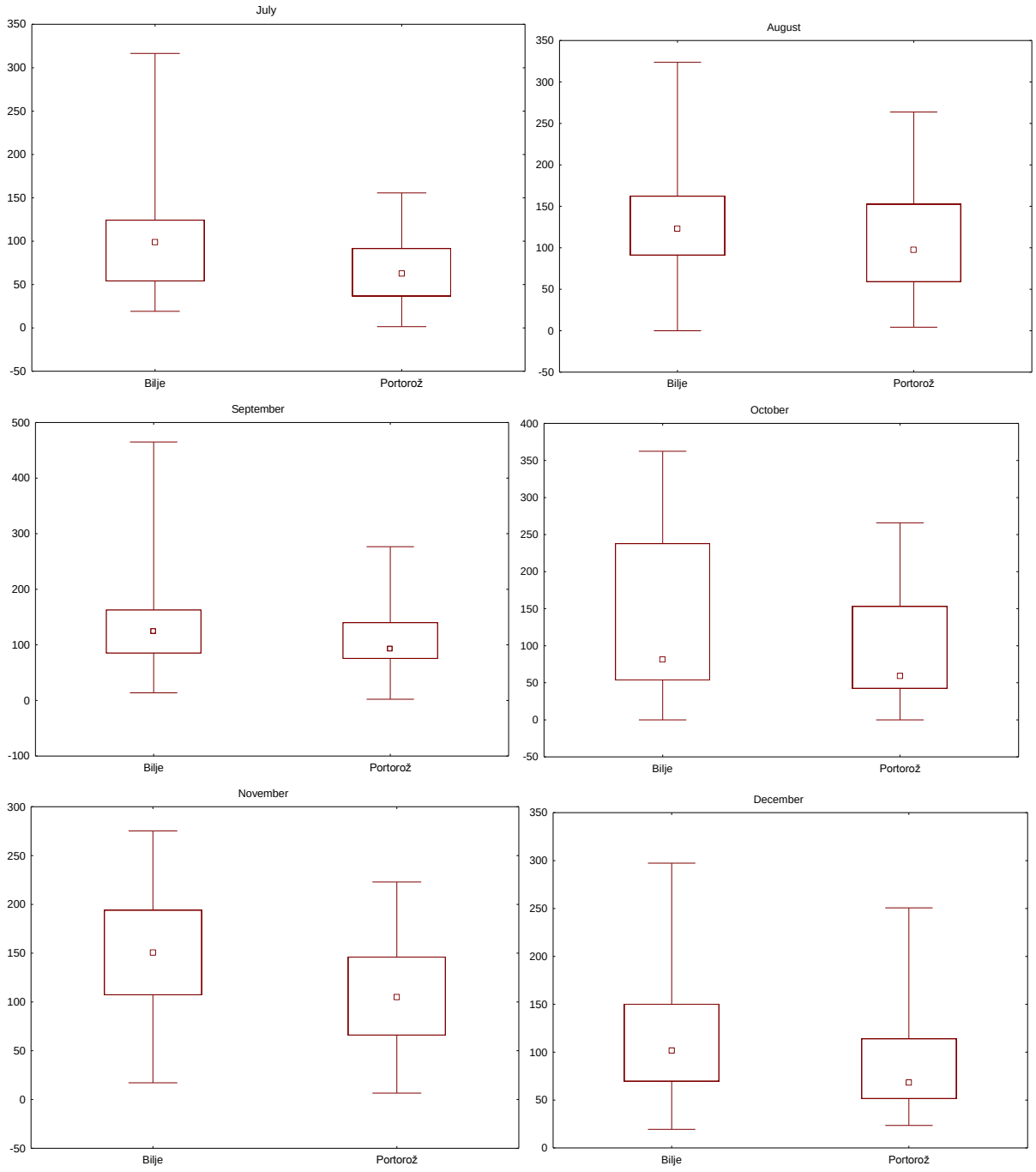

Figure 17: Continued.

3 Regional climate model simulations

3.1 Bilje meteorological station

3.1.1 RCM bias corrected models

3.1.1.1 Temperature

Mean monthly temperatures for the reference period 1961 –1990 of all three RCM bias corrected models fit very well between themselves, but observed temperatures, are a bit lower than predicted by any of the models (Figure 18). There are more discrepancies among the models and observations in the case of extremes – minimum and maximum of temperature, especially in the coldest and hottest months (Figure 18). Mean annual temperature fluctuations are presented in Figure 19 and their empirical cumulative distribution function (CDF) in Figure 20. They were calculated for the period of all available observed data, i.e. 1961 – 1990 and confirm a good fit between all models and observations.

For the all three models, time series of annual mean temperatures with fitted linear trend is shown on Figure 21. Trends for all three models are statistically significant at 5 % significance level. Table 15 summarises decadal temperature trend based on entire time series, and mean and standard deviations during periods P0 (1961-1990) and P1 (2021-2050) calculated from monthly averages.

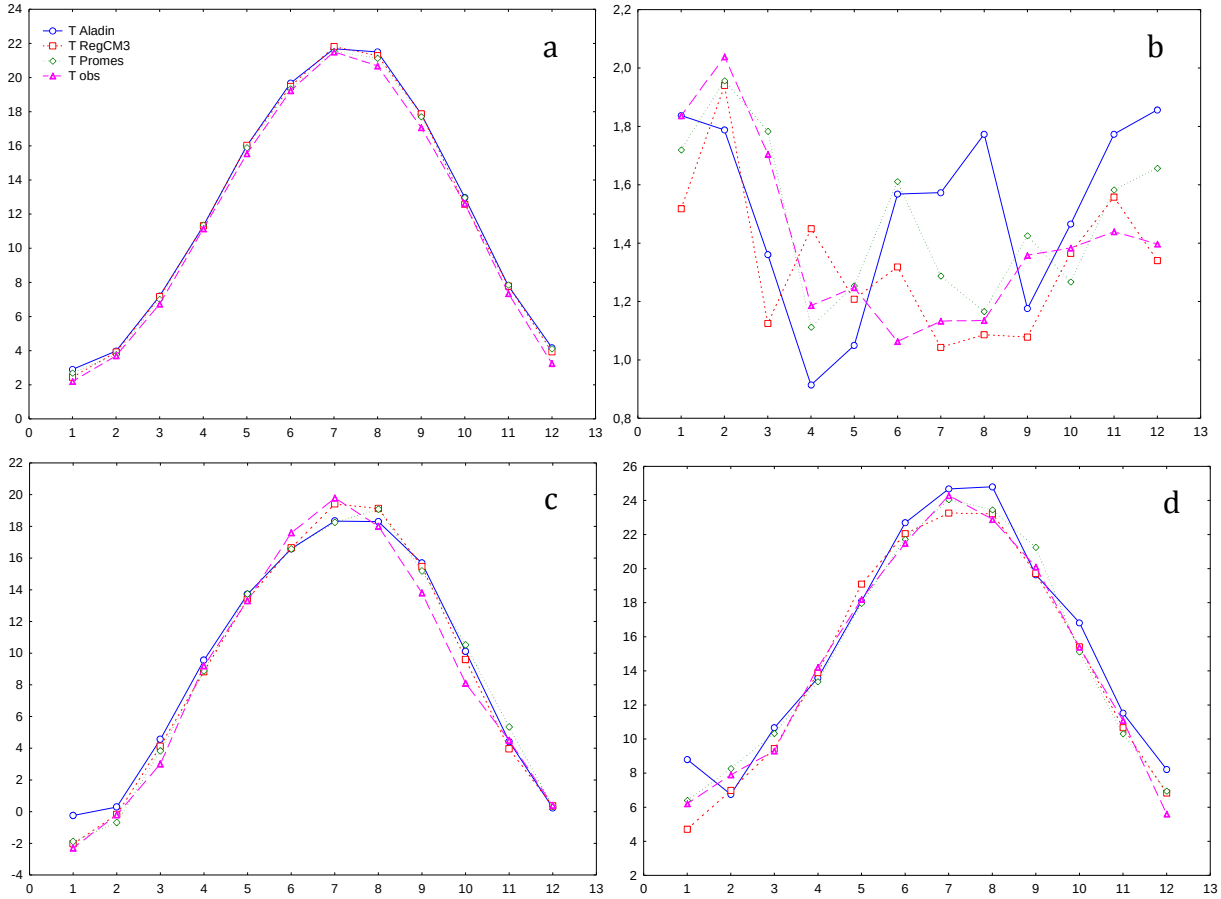

Figure 18: Bilje meteorological station: annual cycle of a) mean monthly temperature, b) mean monthly temperature standard deviation, c) minimum monthly temperature, and d) maximum monthly temperature for observed and three regional climate models. Model time series are RCMcorr. Period of analysis is P0 (1961-1990).

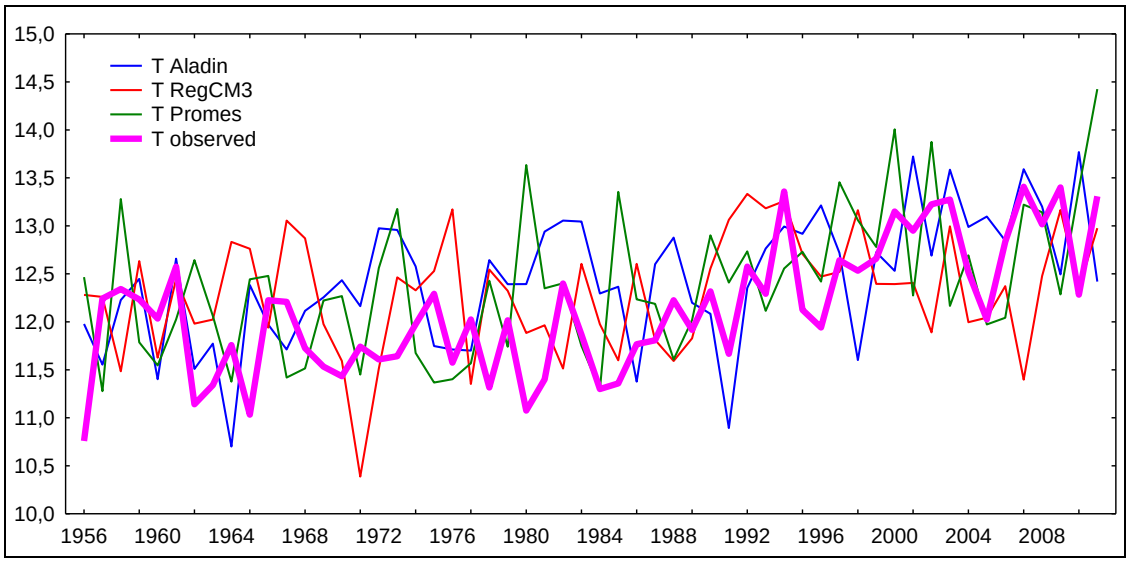

Figure 19: Bilje meteorological station time series 1956 – 2011: mean annual temperature fluctuation. Model time series are RCMcorr.

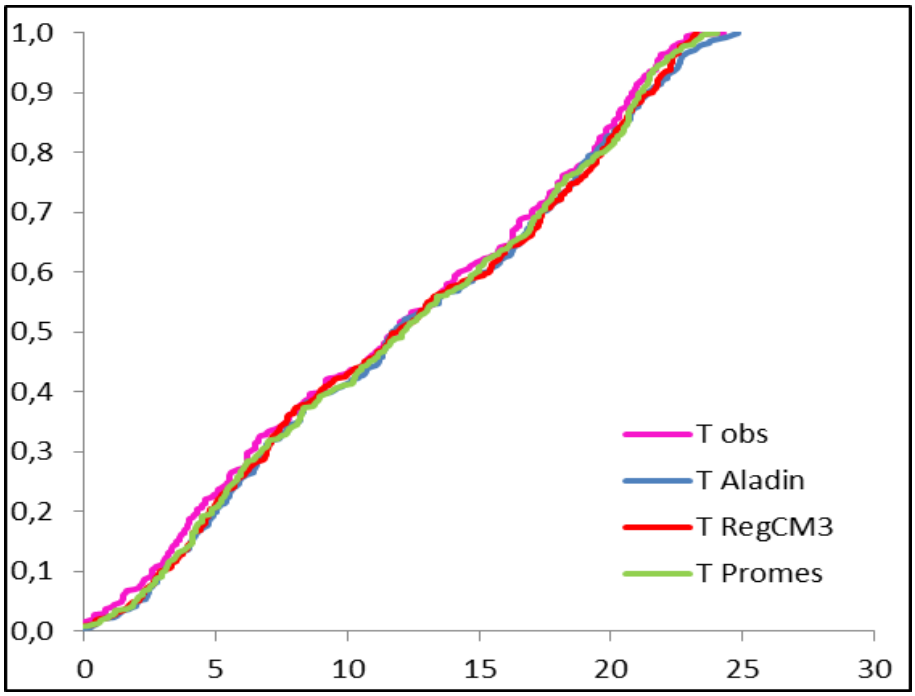

Figure 20: Bilje station empirical cumulative distribution function (CDF) for mean annual temperature for reference period 1961 – 1990. Model time series are RCMcorr.

Table 15: Decadal temperature trend of Bilje station based on entire time series, and mean and standard deviations during timr period P0 (1961-1990) and P1 (2021-2050) calculated from monthly averages. Model time series are RCMcorr.

Model	*Decadal trend*	*P0 mean*	*P0 std*	*P1 mean*	*P1 std*
Aladin	0.25	12.3	6.9	13.9	7.1
RegCM3	0.17	12.1	6.9	13.3	7.1
Promes	0.32	12.1	6.9	14.4	6.9

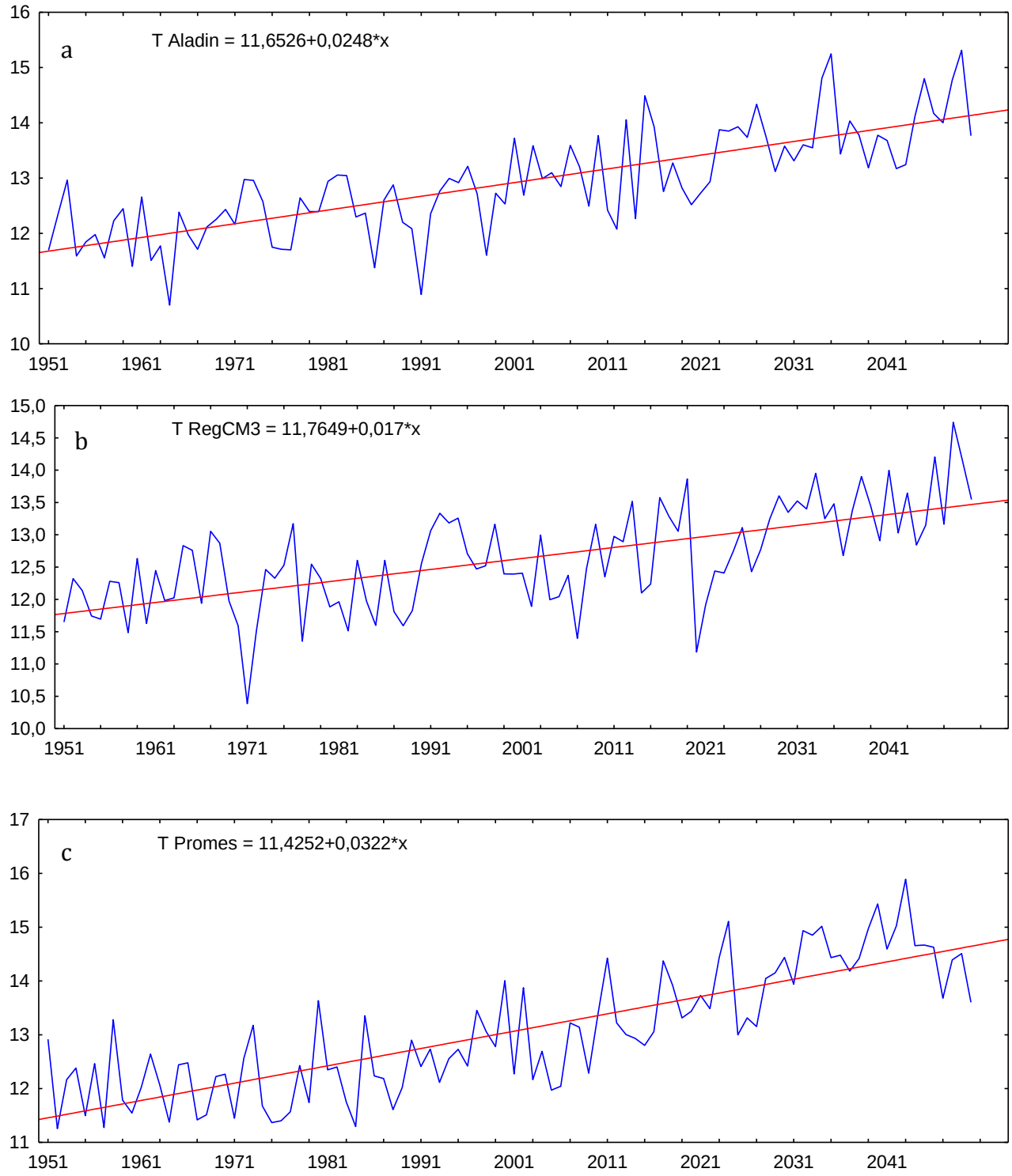

Figure 21: Annual mean temperature and fitted linear trend of Bilje meteorological station after a) Aladin, b) RegCM3 and c) Promes model. Trends for all three models have statistically significant regression at 5 % significance level. Model time series are RCMcorr.

3.1.1.2 Precipitation

Figure 22 shows that there is more differences between the climate models and observations regarding monthly precipitation amount, although the differences are not statistically significant. Observed values are higher (except for April, where they fit well with the RegCM3 and Promes models) than proposed by the models and have wider range of values, as demonstrated also from standard deviations (Figure 22). Mean annual precipitation amount variability is shown in Figure 23 and empirical cumulative distribution function (CDF) in Figure 24. They were calculated for the period of all available observed data, i.e. 1961 – 1990 and confirm a good fit between all models and observations.

For all three models, time series of annual precipitation amount with fitted statistically non-significant linear trend for Aladin and RegCM3 models, and statistically significant for Promes model, is shown on Figure 25. Table 16 summarises decadal precipitation amount trend based on entire time series, and mean and standard deviations during periods P0 (1961-1990) and P1 (2021-2050) calculated from monthly averages.

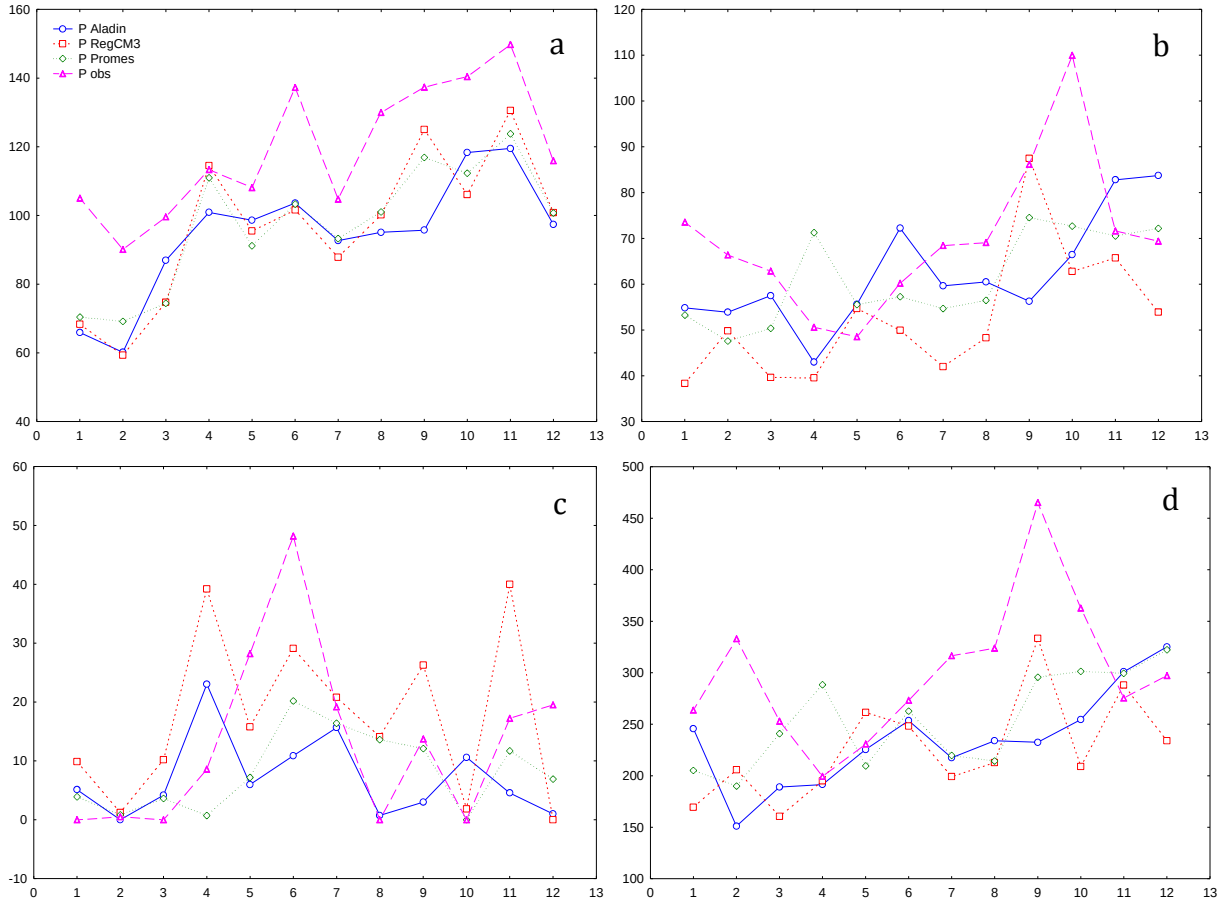

Figure 22: Bilje meteorological station: annual cycle of a) monthly precipitation amount, b) monthly precipitation amount standard deviation, c) minimum monthly precipitation amount, and d) maximum monthly precipitation amount. Model time series are RCMcorr. Period of analysis is P0 (1961-1990).

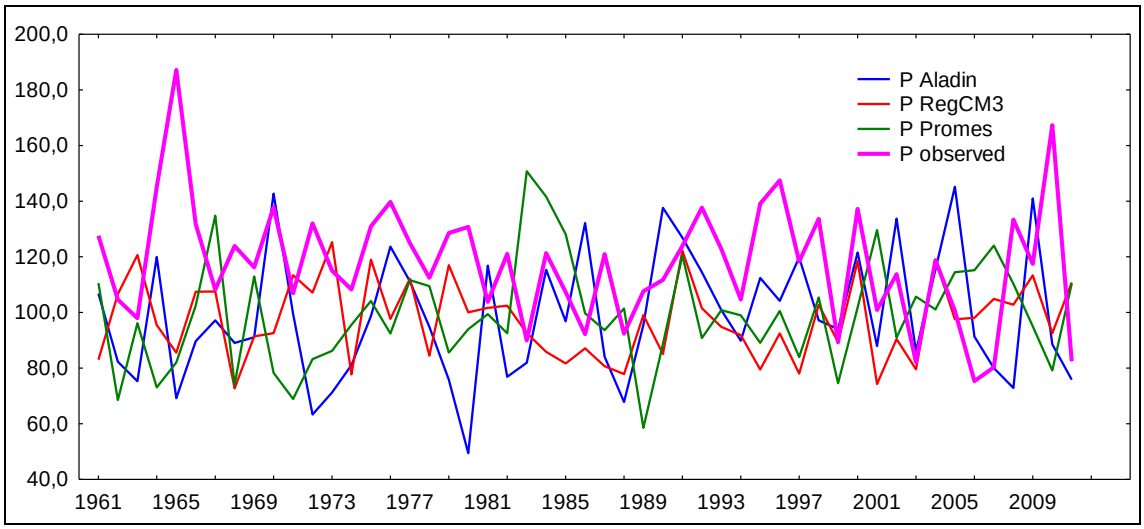

Figure 23: Bilje station time series 1961 – 2011: annual precipitation amount. Model time series are RCMcorr.

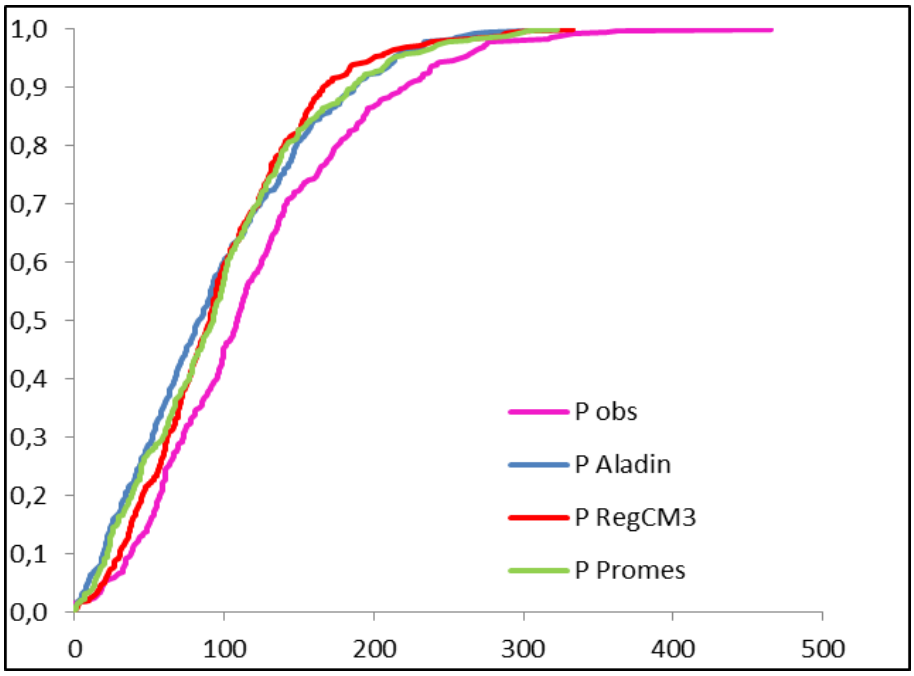

Figure 24: Bilje meteorological station empirical cumulative distribution function (CDF) for annual precipitation amount (1961 – 1990). Model time series are RCMcorr.

Table 16: Decadal precipitation amount trend of Bilje meteorological station based on entire time series, and mean and standard deviations during periods P0 (1961-1990) and P1 (2021-2050) calculated from monthly averages. Model time series are RCMcorr.

Model	*Decadal trend*	*P0 mean*	*P0 std*	*P1 mean*	*P1 std*
Aladin	1.17	94.6	64.5	102.1	70.7
RegCM3	0.04	97.0	57.4	99.2	65.4
Promes	1.38	97.3	63.6	104.8	68.0

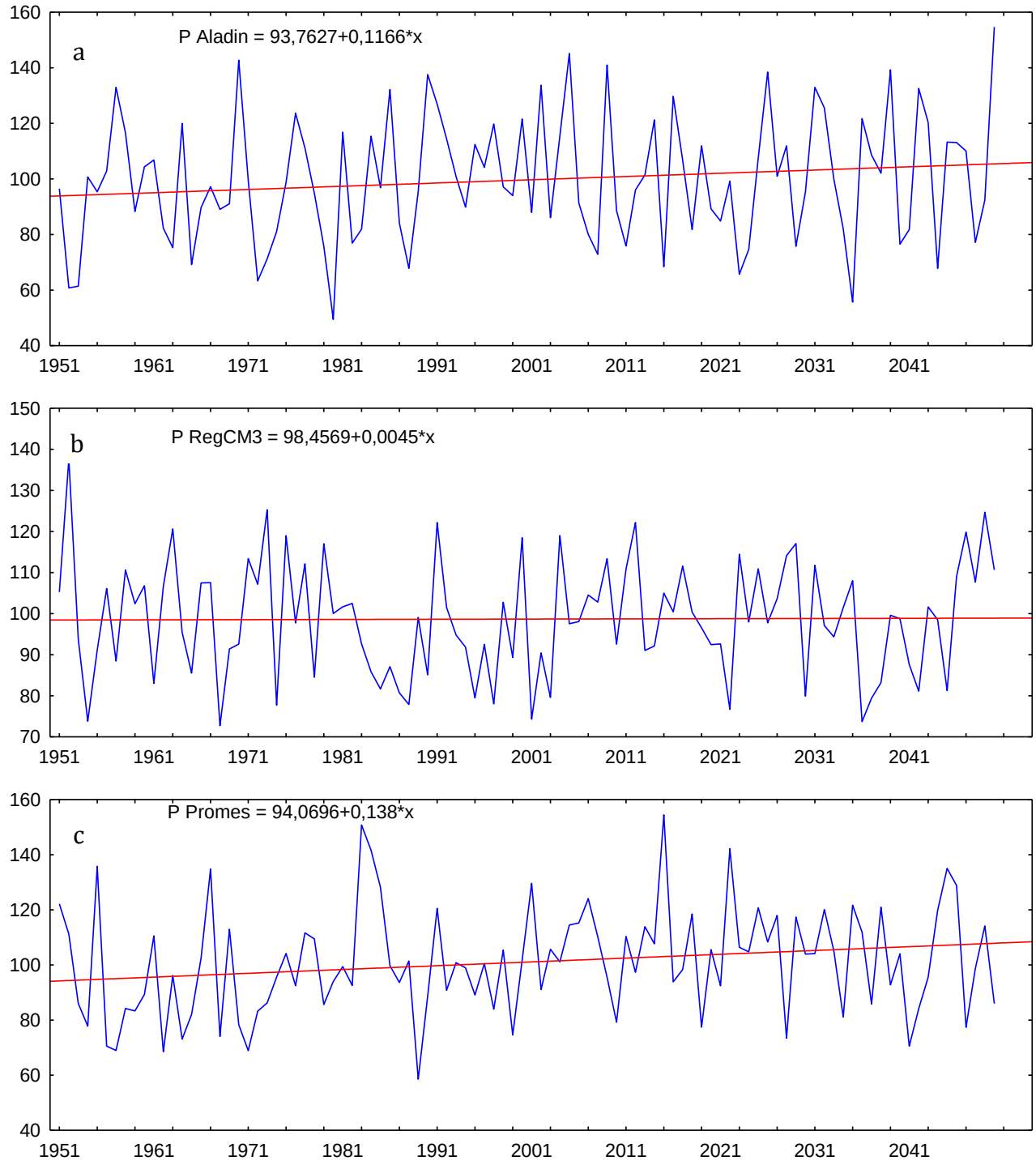

Figure 25: Annual precipation amount and fitted linear trend of Bilje meteorological station after a) Aladin, b) RegCM3 and c) Promes model. Aladin and RegCM3 models have statistically non-significant trend at 5 % significance level, and for Promes the trend is statistically significant. Model time series are RCMcorr.

3.1.2 RCM bias corrected and adjusted models

3.1.2.1 Temperature

Figure 26 shows adjustment differences, based on 1961-1990 reference period, for all three climate models (Aladin, RegCM3 and Promes). According to Mann-Whitney test differences between corrected and adjusted values are statistically significant at 5 % significance level for September and December for Aladin model, and for the same two months plus August for RegCM3 model.

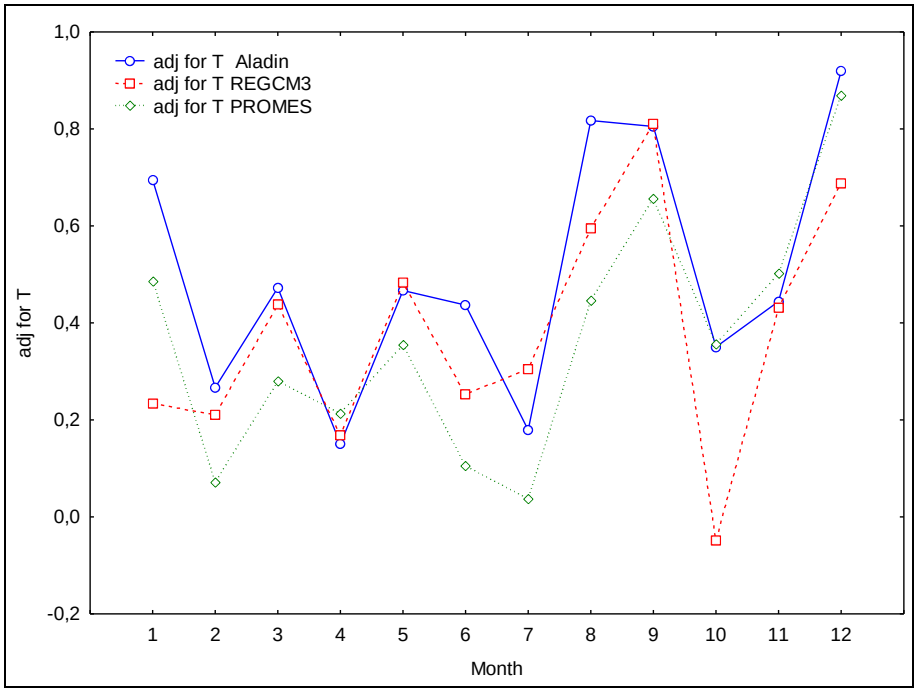

Figure 26: Bilje meteorological station: adjustment differences for mean monthly temperature.

Mean monthly temperatures for the 1961 –1990 of all three RCM bias corrected and adjusted models fit perfectly between them and observed temperatures, the only exception is RegCM3, where all monthly averages are higher in comparison to other two models and observations (Figure 27). There is more discrepancies among the models and observations in the case of extremes (minimum and maximum temperature), especially in the coldest and hottest months (Figure 27). Mean annual temperature fluctuations are presented in Figure 28 and their empirical cumulative distribution function (CDF) in Figure

29. They were calculated for the period of all available observed data, i.e. 1961 – 1990 and confirm an excellent fit between all models and observations.

For the all three models Figure 30 shows time series of annual mean temperatures with fitted linear trend. Trends for all three models are statistically significant at 5 % significance level. Table 17 summarises decadal temperature trend based on entire time series, and mean and standard deviations during periods P0 (1961-1990) and P1 (2021-2050) calculated from monthly averages.

According to Mann-Whitney test comparisons of monthly mean temperatures between P0 (1961-1990) vs. P1 (2021-2050), statistically significant differences at 5 % significance level were found for all models and months, except for RegCM3 in December (Figure 31). The increase of temperatures in future is proven also by Kolmogorov-Smirnov test (Figure 32).

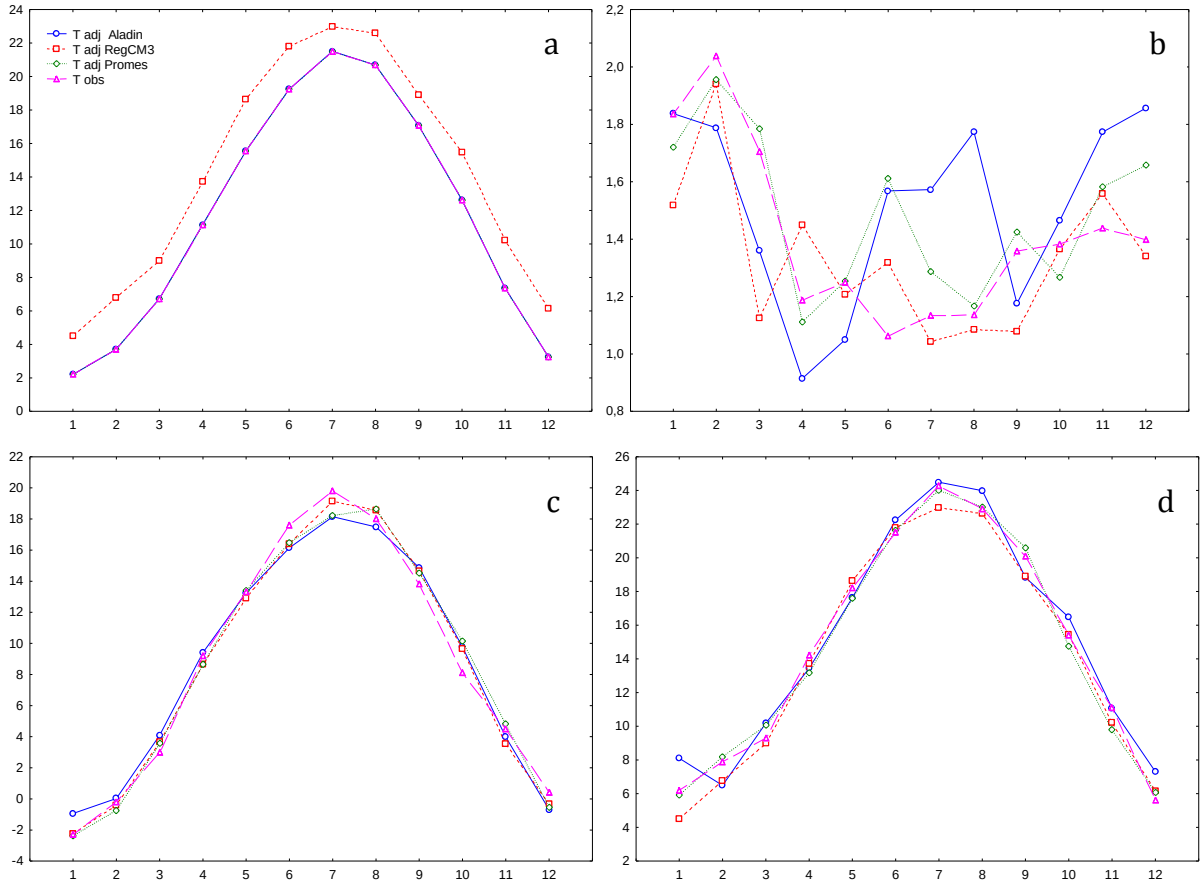

Figure 27: Bilje meteorological station: annual cycle of a) mean monthly temperature, b) mean monthly temperature standard deviation, c) minimum monthly temperature, and d) maximum monthly temperature. Model time series are RCMcorr_adj. Period of analysis is P0 (1961-1990).

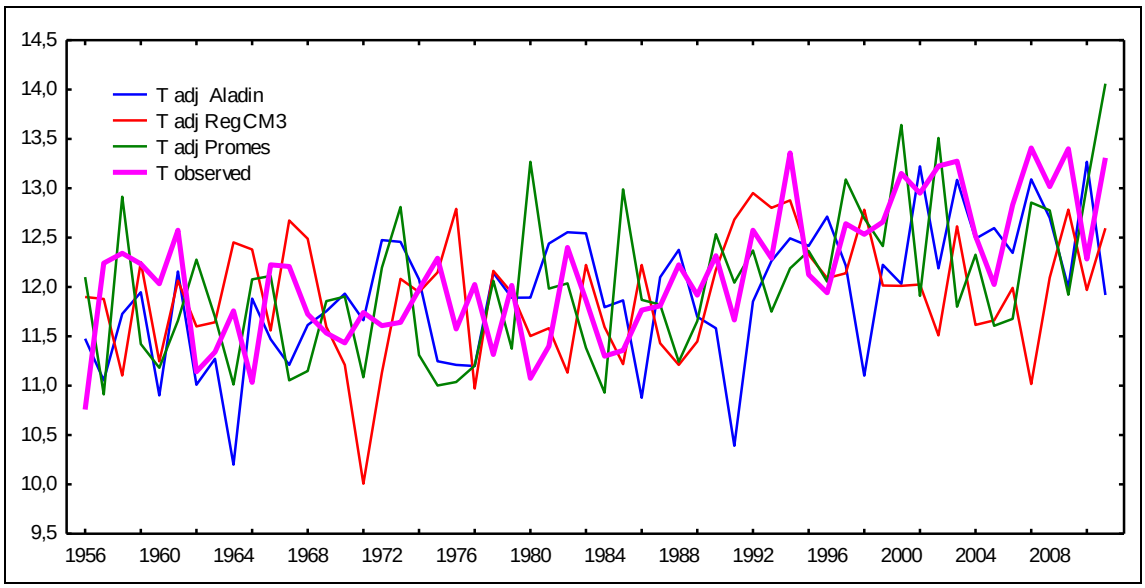

Figure 28: Bilje station time series 1956 – 2011: mean annual temperature. Model time series are RCMcorr_adj.

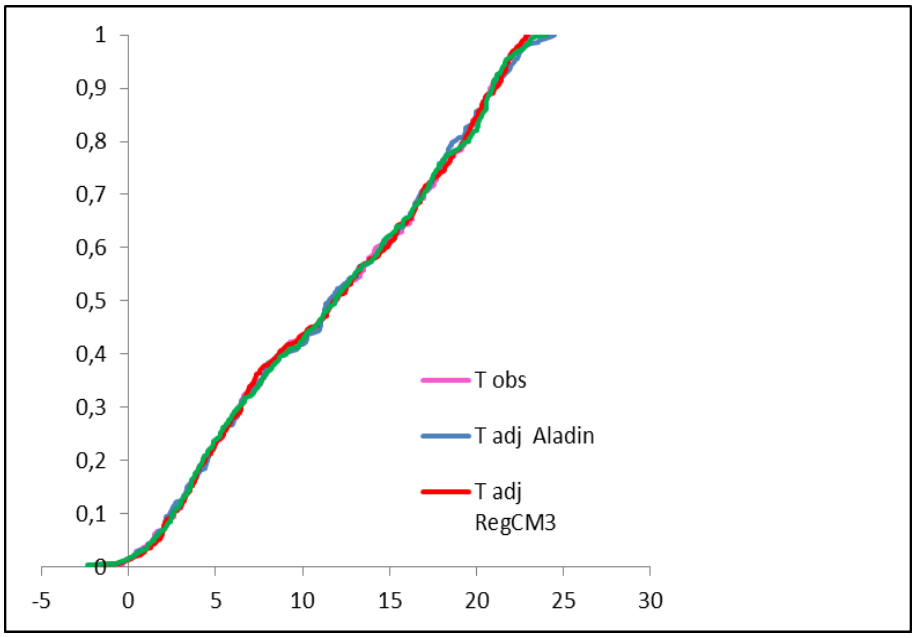

Figure 29: Bilje station empirical cumulative distribution function (CDF) for mean annual temperature (1961 – 1990). Model time series are RCMcorr_adj.

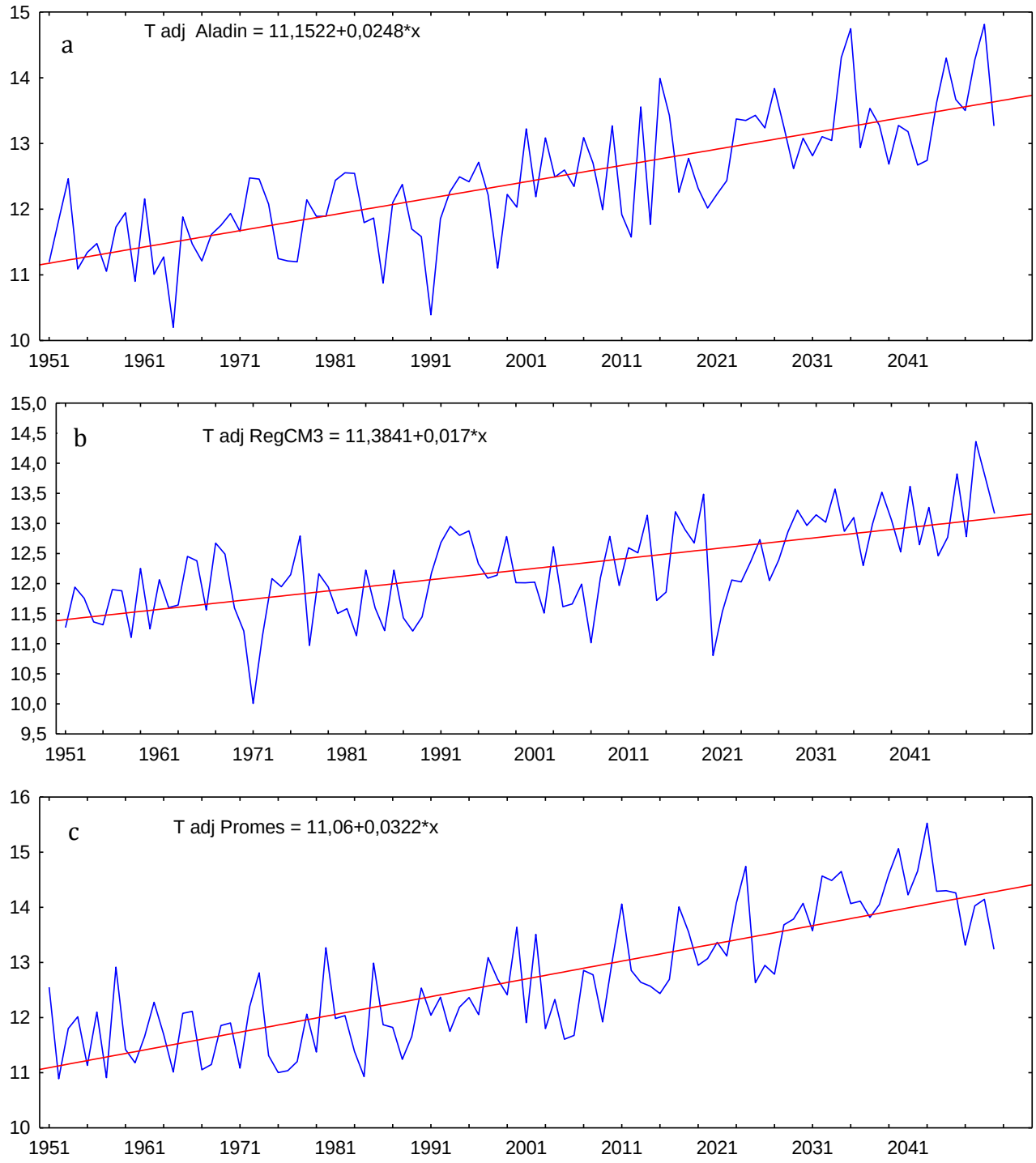

Figure 30: Annual mean temperature and fitted linear trend of Bilje meteorological station after a) Aladin, b) RegCM3 and c) Promes model. Trends for all three models have statistically significant regression at 5 % significance level. Model time series are RCMcorr_adj.

Table 17: Decadal temperature trend of Bilje meteorological station based on entire time series, and mean and standard deviations during P0 (1961-1990) and P1 (2021-2050) calculated from monthly averages. Model time series are RCMcorr_adj.

T	*decadal trend*	*P0 mean*	*P0 std*	*P1 mean*	*P1 std*
Aladin	0.25	11.8	6.9	13.4	7.1
RegCM3	0.17	11.8	6.9	12.9	7.0
Promes	0.32	11.8	6.9	14	7.0

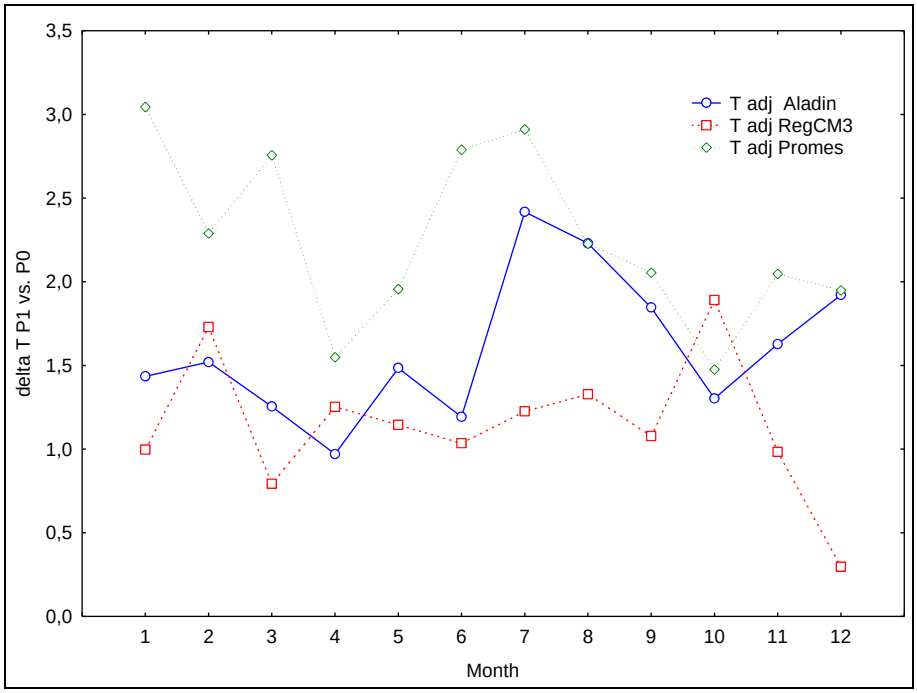

Figure 31: Monthly mean temperature P0 (1961-1990) vs. P1 (2021-2050) change for Bilje meteorological station. Differences are statistically significant for all models and months, except for RegCM3 in December, according to Mann-Whitney test at 5 % significance level.

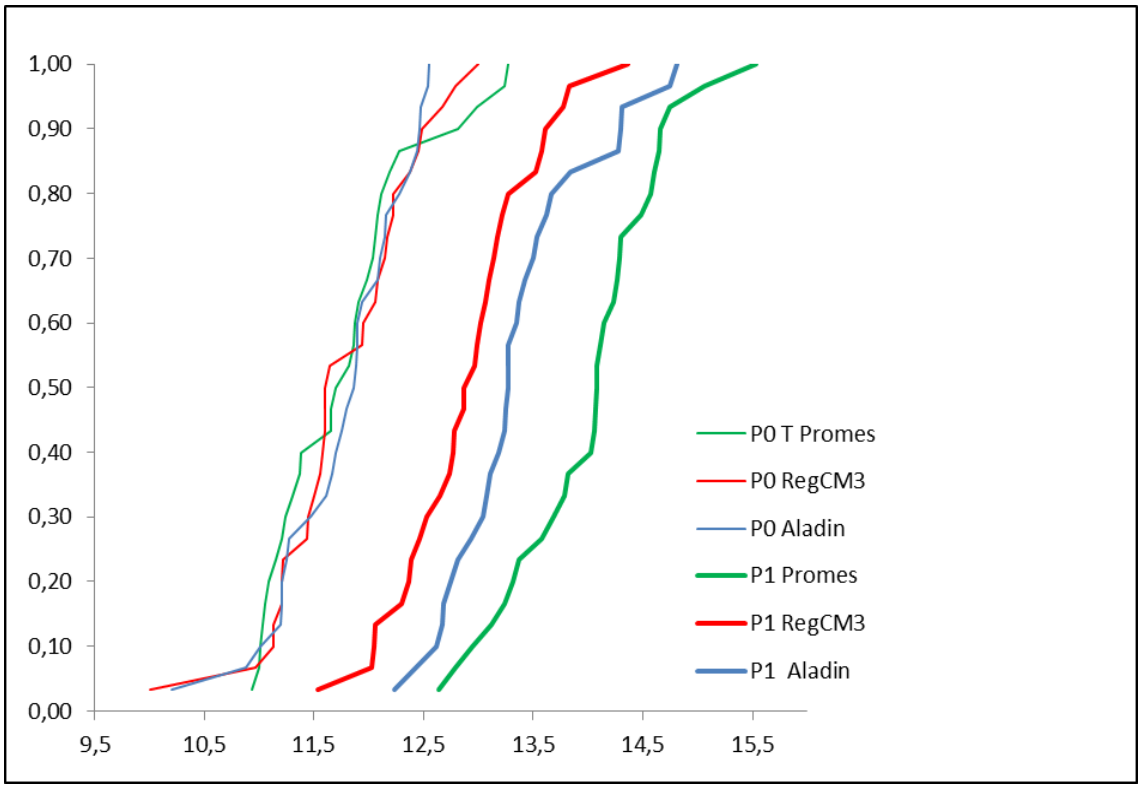

Figure 32: Empirical cumulative distribution functions CDFs of mean annual temperature of Bilje meteorological station in P0 and P1. Differences between periods P0 and P1 are according to Kolmogorov-Smirnov test statistically significant at 5 % significance level, for all three models.

3.1.2.2 Precipitation

Figure 33 shows adjustment differences, based on 1961-1990 period, for all three climate models. According to Mann-Whitney test differences between corrected and adjusted values statistically differences at 5 % significance level were found for Aladin model for January, February, June, August and September, for RegCM3 for January, February, March, June, September and October, and for Promes for Janaury, March and June.

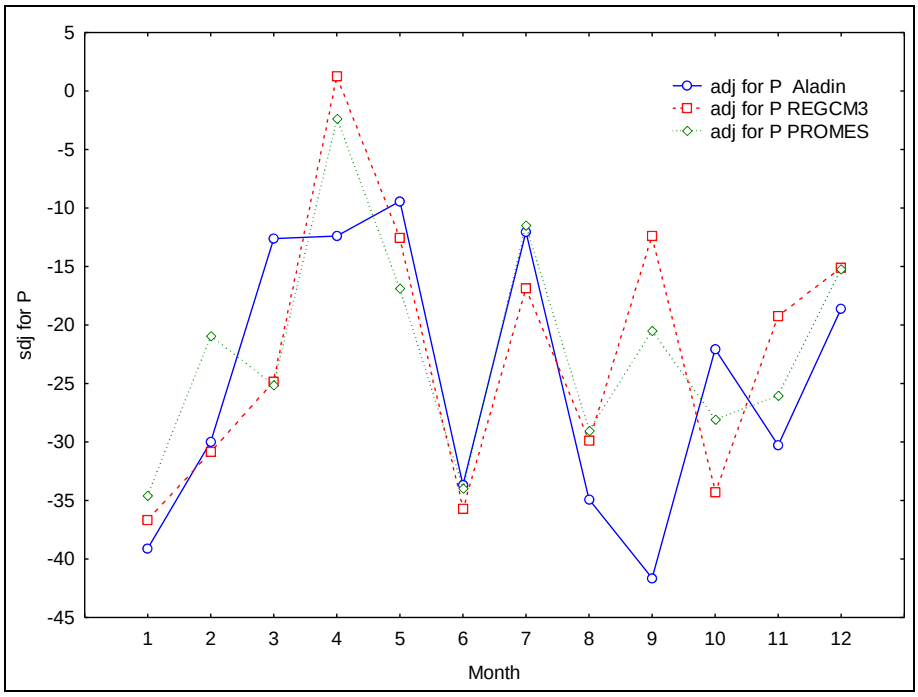

Figure 33: Adjustment differences for monthly precipitation amount of Bilje meteorological station.

Figure 34 shows that there is practically no difference between the observations and models regarding monthly precipitation amount, but differences exist in the extreme (minimum and maximum) monthly precipitations. Generally, observed minimum values are lower than predicted by any of models and maximum observed values are higher (except for April). Mean annual precipitation amount variability is shown in Figure 35 and empirical cumulative distribution function (CDF) in Figure 36. They were calculated for the period of

all available observed data, i.e. 1961 – 1990 and confirm a good fit between all climate models and observations.

For the all three models, time series of annual precipitation amount with fitted statistically non-significant linear trend for Aladin and RegCM3 models, and statistically significant for Promes model, is shown on Figure 37. Table 17 summarises decadal precipitation amount trend based on entire time series, and mean and standard deviations during periods P0 (1961-1990) and P1 (2021-2050) calculated from monthly averages.

According to Mann-Whitney test comparisons of monthly mean temperatures between P0 (1961-1990) vs. P1 (2021-2050) doesn't prove statistically significant differences at 5 % significance level for any of models and months, except for Aladin in September and RegCM3 in August (Figure 38). The differences in annual precipitation amount are statistically non-significant at 5 % significance levels, as indicated by Kolmogorov-Smirnov test (Figure 39).

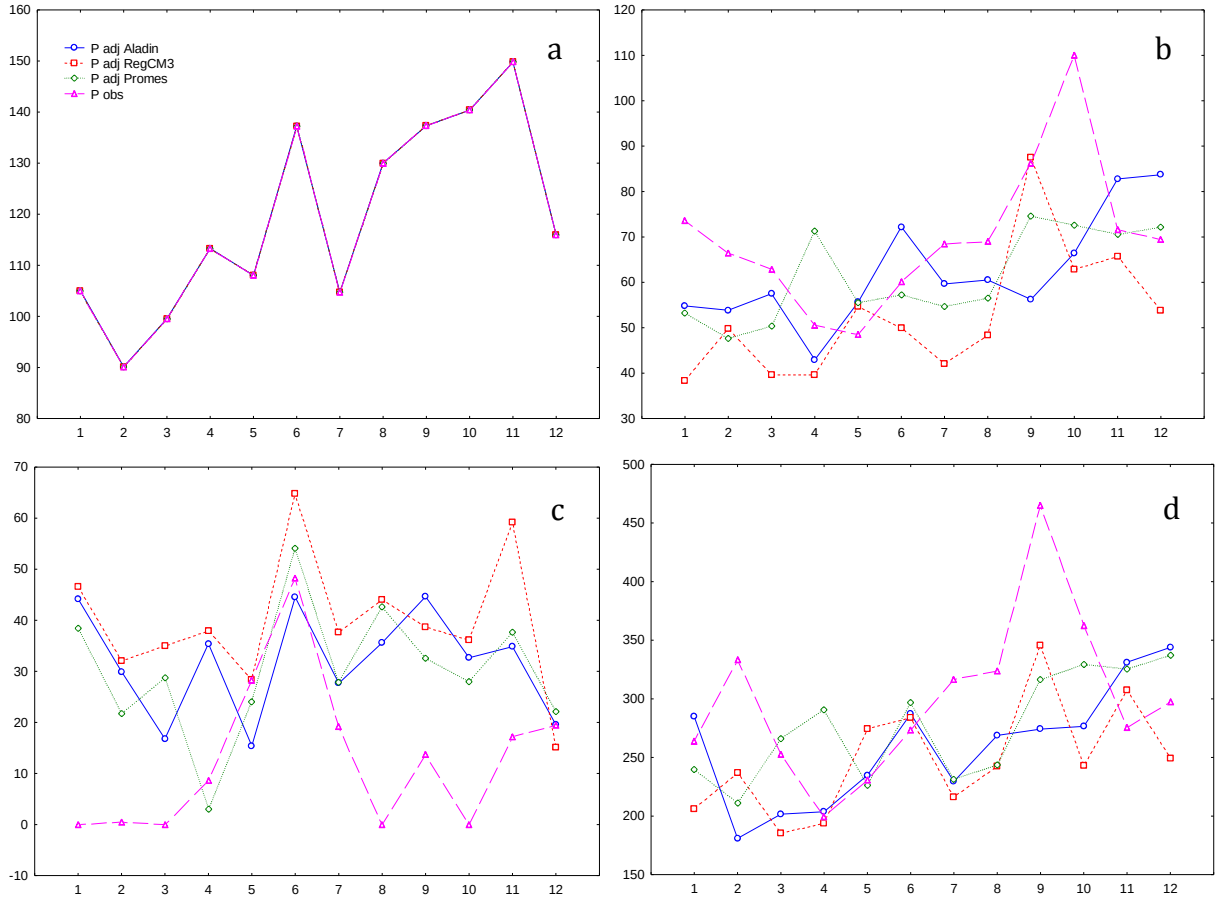

Figure 34: Bilje station: annual cycle of a) monthly precipitation amount, b) monthly precipitation amount standard deviation, c) minimum monthly precipitation amount, and d) maximum monthly precipitation amount. Model time series are RCMcorr. Period of analysis is P0 (1961-1990).

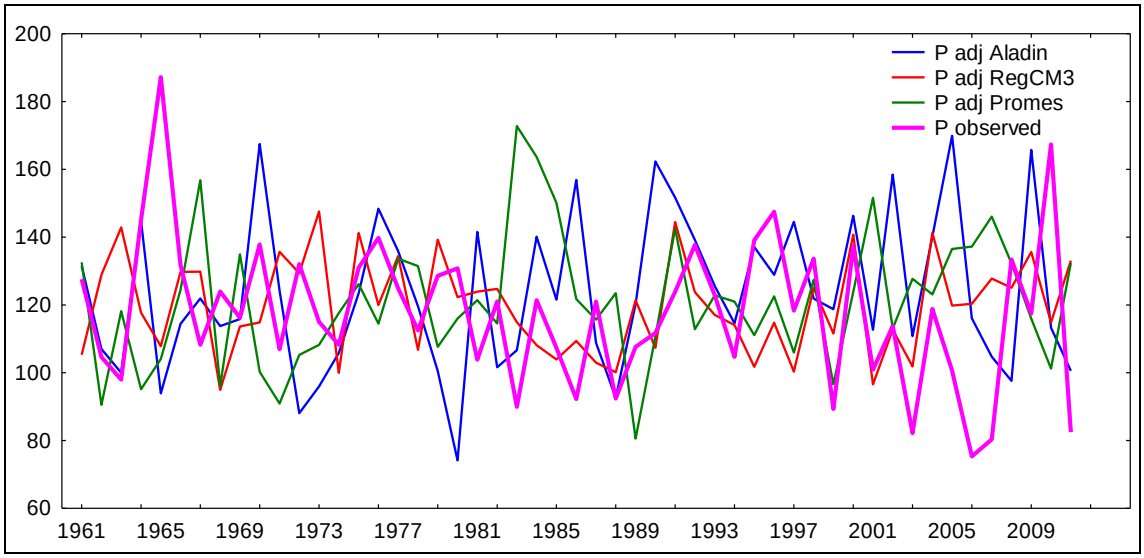

Figure 35: Bilje station time series 1961 – 2011: annual precipitation amount. Model time series are RCMcorr_adj.

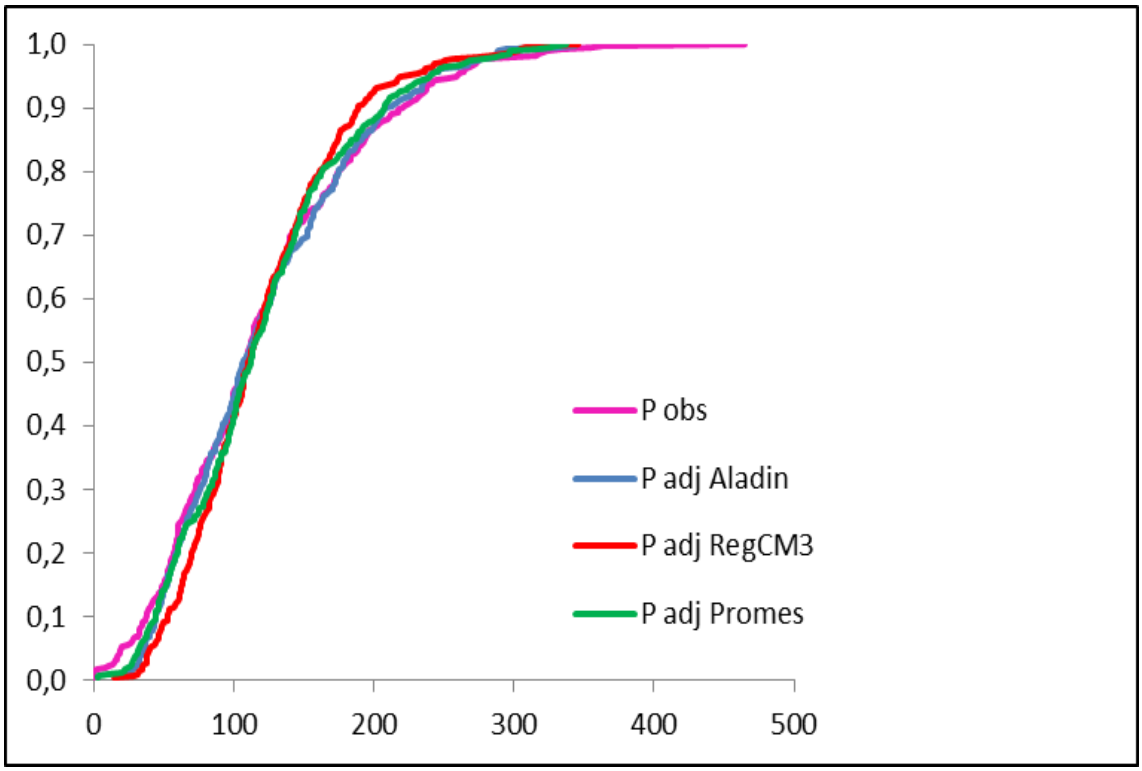

Figure 36: Bilje station empirical cumulative distribution function (CDF) for annual precipitation amount (1961 – 1990). Model time series are RCMcorr_adj.

Table 17: Decadal precipitation amount trend based on entire time series, and mean and standard deviations during periods P0 (1961-1990) and P1 (2021-2050) calculated from monthly averages. Model time series are RCMcorr_adj.

Model	*Decadal trend*	*P0 mean*	*P0 std*	*P1 mean*	*P1 std*
Aladin	1.17	119.3	64.9	126.8	72.1
RegCM3	0.05	119.3	56.5	121.4	65.7
Promes	1.14	119.3	63.8	126.8	68.9

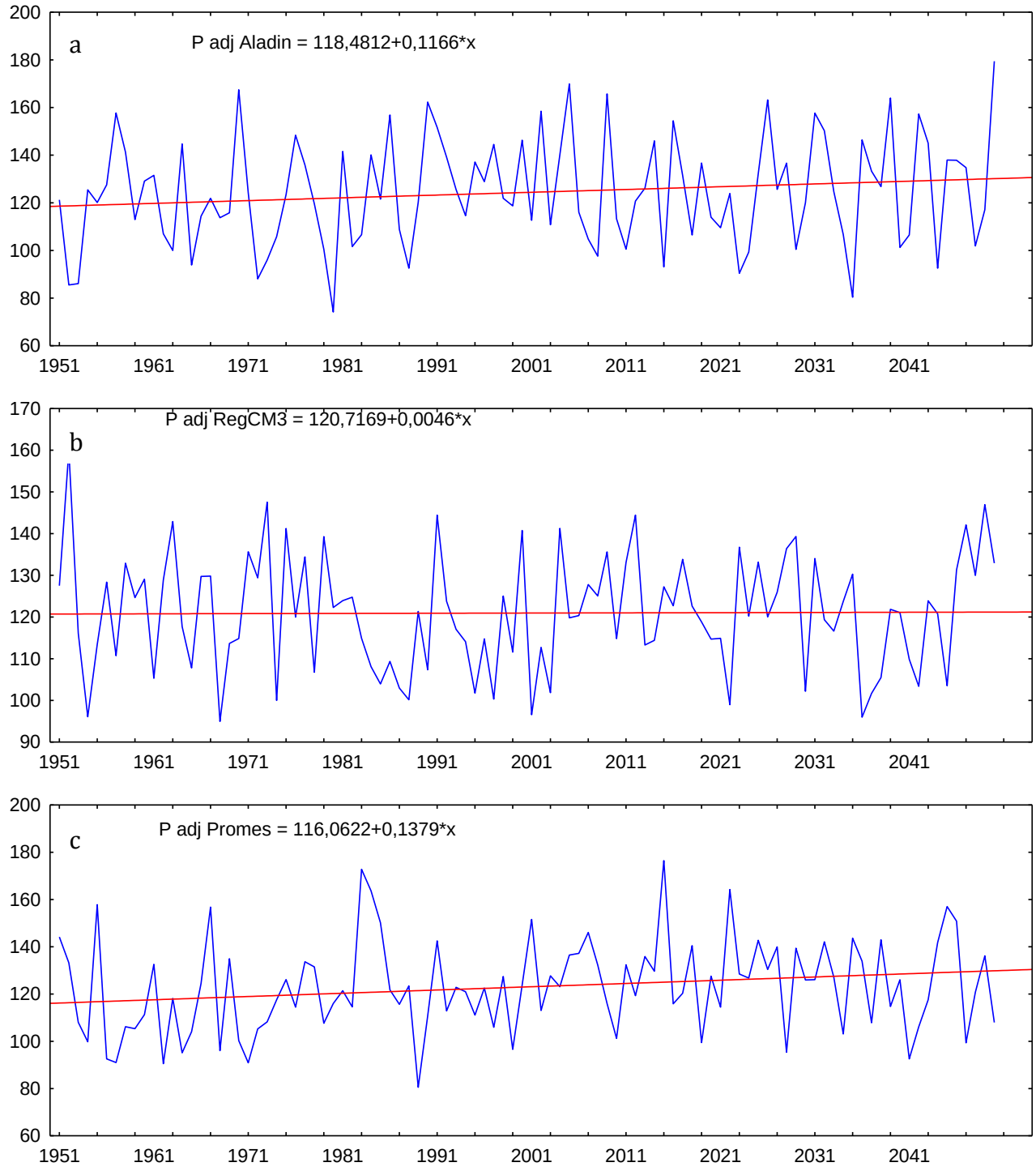

Figure 37: Annual precipation amount and fitted linear trend of Bilje station after a) Aladin, b) RegCM3 and c) Promes. Aladin and RegCM3 have statistically non-significant trend at 5 % significance level, and for Promes the trend is statistically significant. Model time series are RCMcorr.

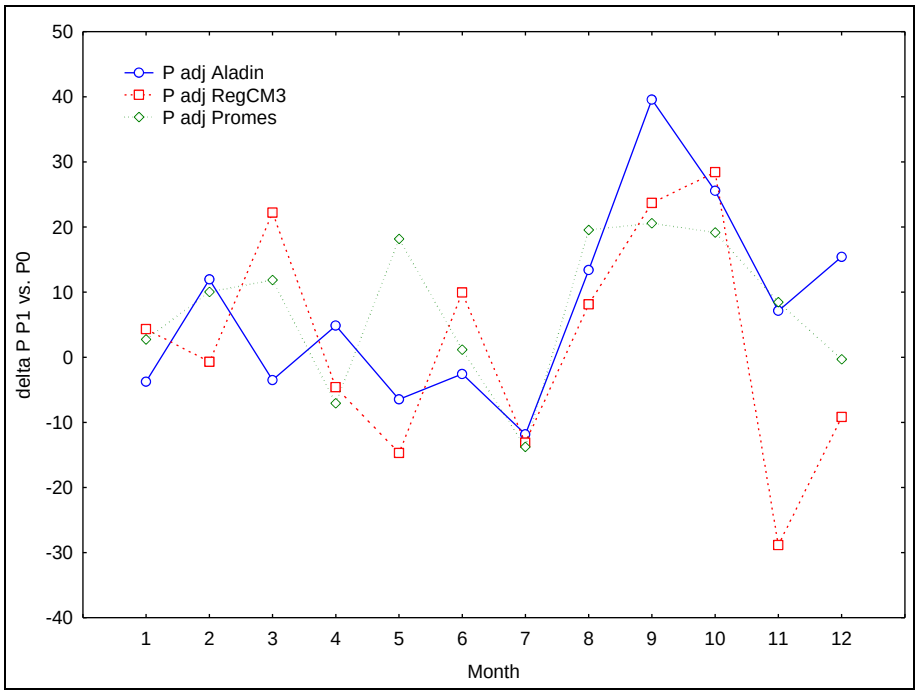

Figure 38: Relative monthly precipitation of Bilje meteorological station for P0 (1961-1990) vs. P1 (2021-2050) change. Differences are statistically non-significant for all stations and months according to Mann-Whitney test at 5 % significance level.

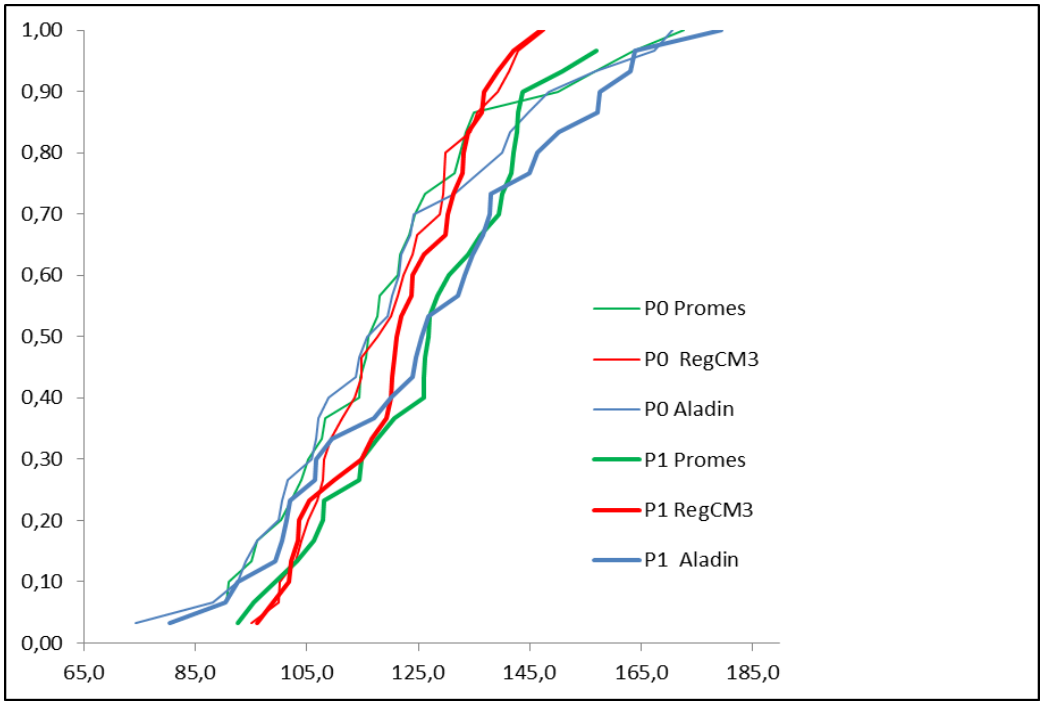

Figure 39: Empirical cumulative distribution functions CDFs of mean annual precipitation amount in P0 and P1 for Bilje meteorological station. Differences between periods P0 and P1 are according to Kolmogorov-Smirnov test statistically non-significant at 5 % significance level, for all three models.

3.2 Portorož meteorological station

3.2.1 RCM bias corrected models

3.2.1.1 Temperature

Mean monthly temperatures for the time period 1961 –1990 of all three RCM bias corrected models fit very well between themselves, but observed temperatures, are a bit lower than predicted by any of the models (Figure 40). There are more discrepancies among the models and observations in the case of extremes (minimum and maximum) of temperature, especially in the coldest and hottest months (Figure 40). Mean annual temperature fluctuations are presented in Figure 41 and their empirical cumulative distribution function (CDF) in Figure 42. They were calculated for the period of all available observed data, i.e. 1961 – 1990 and confirm a good fit between all models and observations.

For all three models, time series of annual mean temperatures with fitted linear trend is shown on Figure 43. Trends for all three models are statistically significant at 5 % significance level. Table 18 summarises decadal temperature trend based on entire time series, and mean and standard deviations during periods P0 (1961-1990) and P1 (2021-2050) calculated from monthly averages.

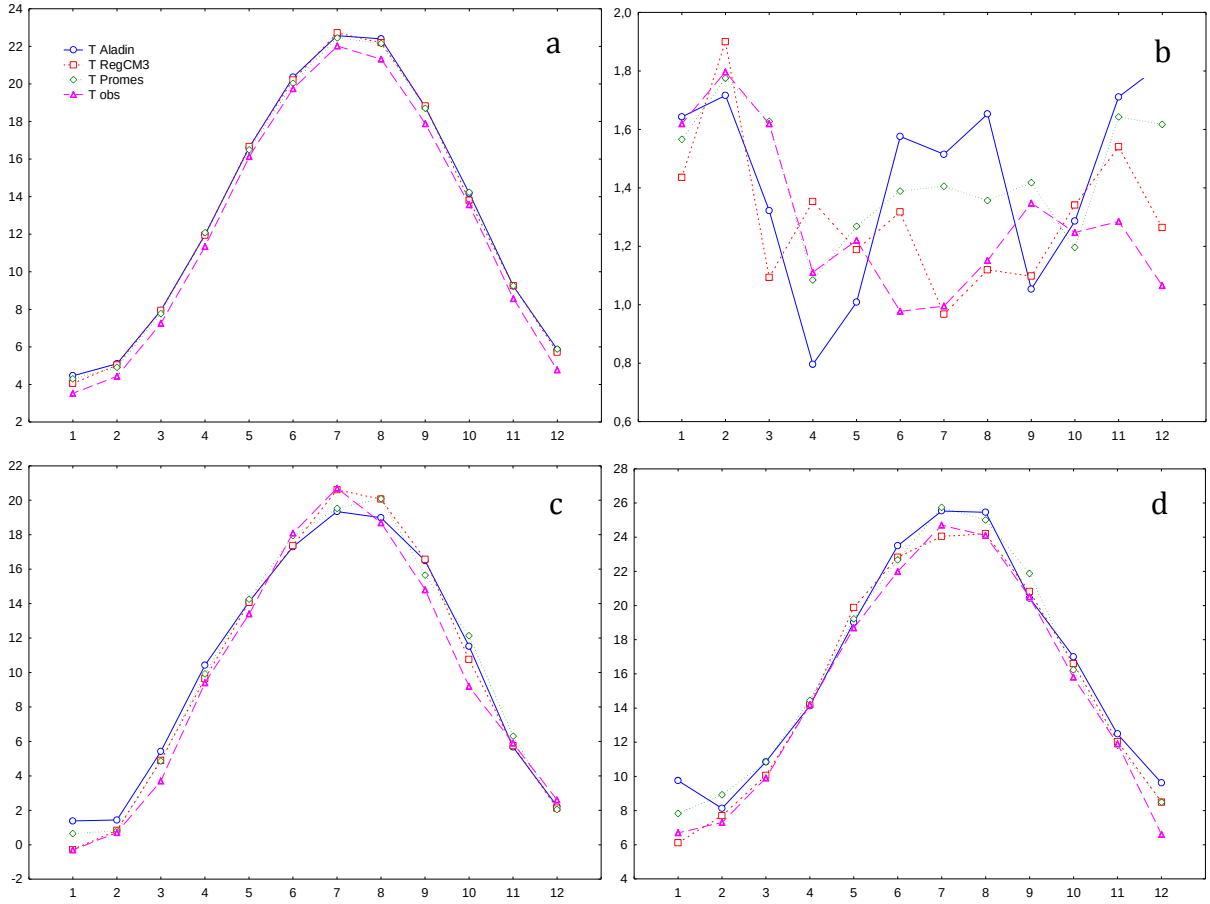

Figure 40: Portorož station: annual cycle of a) mean monthly temperature, b) mean monthly temperature standard deviation, c) minimum monthly temperature, and d) maximum monthly temperature. Model time series are RCMcorr. Period of analysis is P0 (1961-1990).

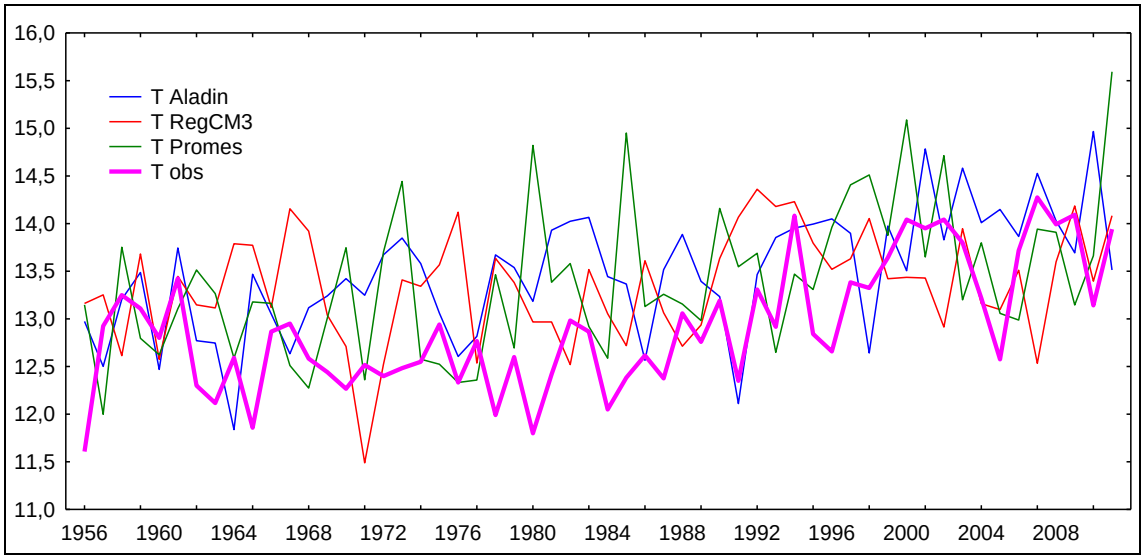

Figure 41: Portorož station time series 1956 – 2011: mean annual temperature. Model time series are RCMcorr.

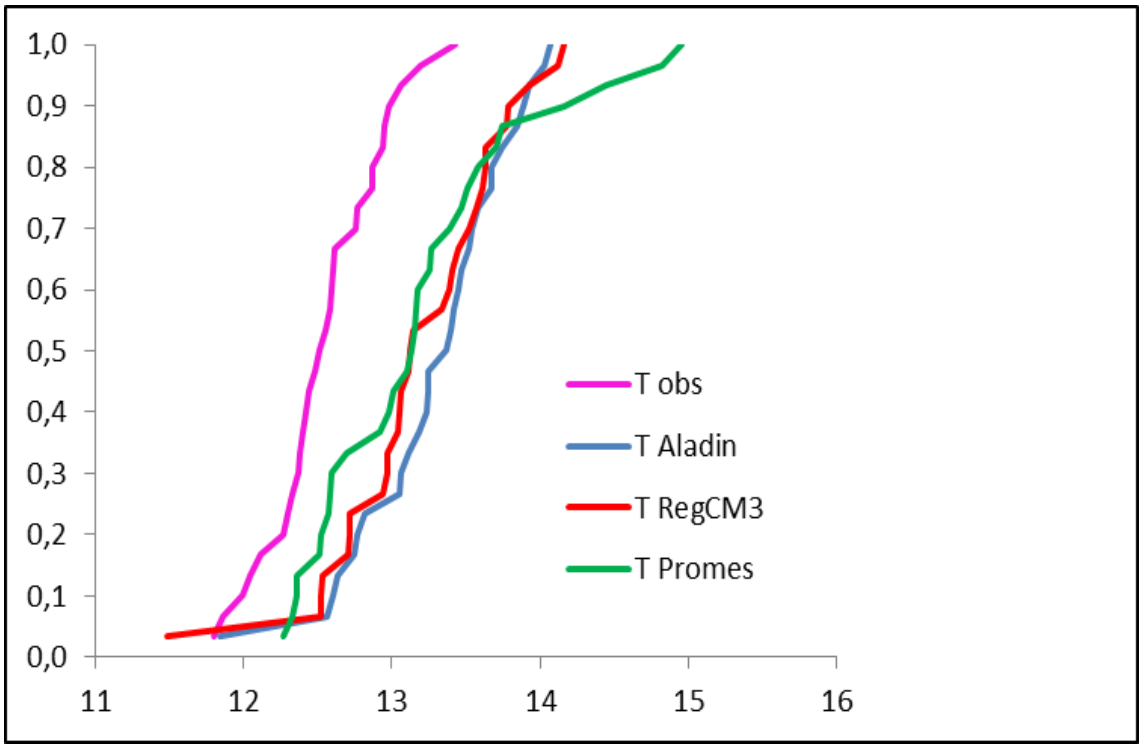

Figure 42: Portorož station empirical cumulative distribution function (CDF) for mean annual temperature (1961 – 1990). Model time series are RCMcorr.

Table 18: Decadal temperature trend of Portorož meteorological station based on entire time series, and mean and standard deviations during P0 (1961-1990) and P1 (2021-2050) calculated from monthly averages. Model time series are RCMcorr.

Model	*decadal trend*	*P0 mean*	*P0 std*	*P1 mean*	*P1 std*
Aladin	0.25	13.3	6.7	14.9	6.9
RegCM3	0.17	13.2	6.7	14.3	6.8
Promes	0.3	13.2	6.6	15.2	6.7

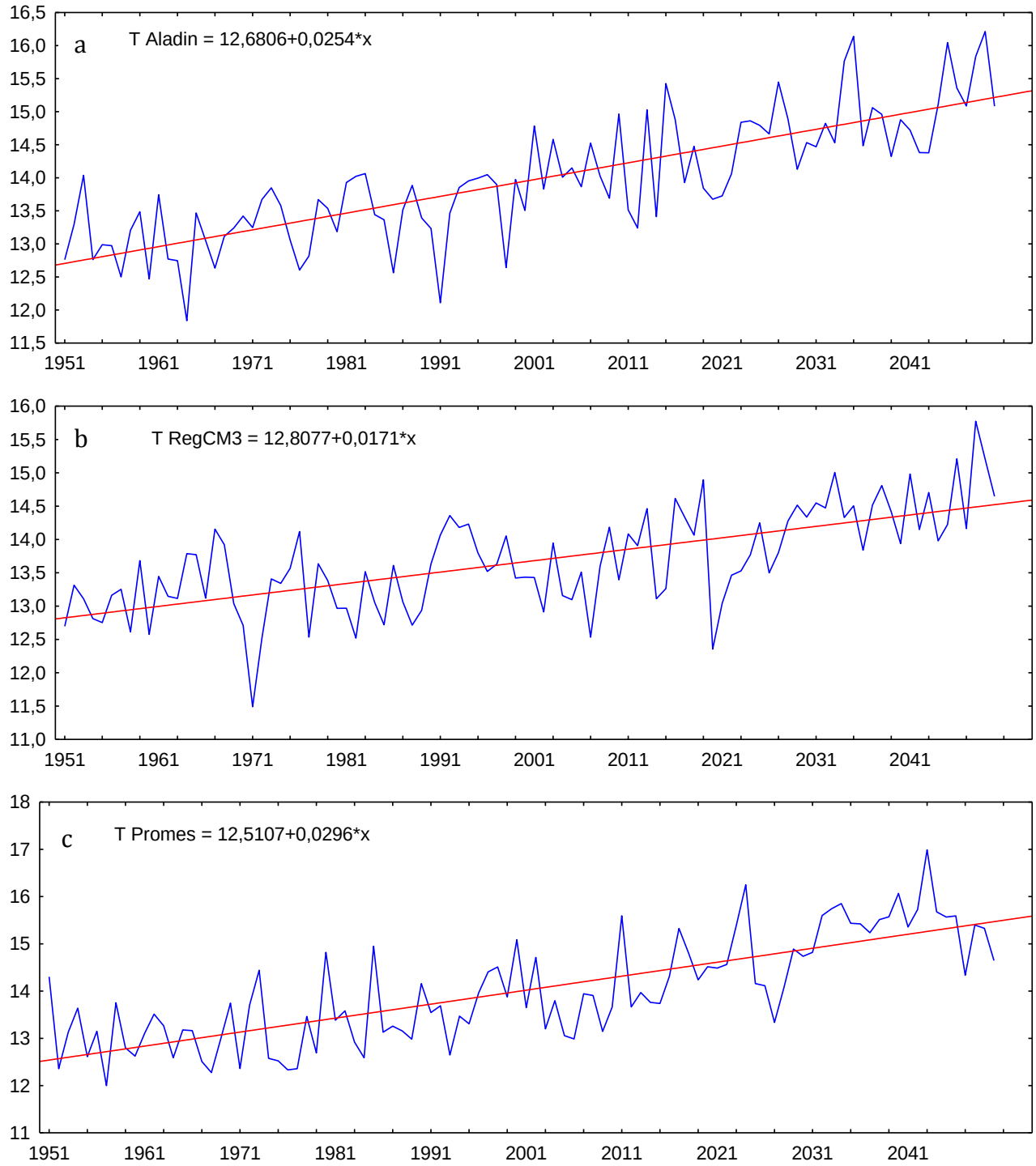

Figure 43: Annual mean temperature and fitted linear trend of Portorož meteorological station after a) Aladin. b) RegCM3 and c) Promes. Trends for all three models have statistically significant regression at 5 % significance level. Model time series are RCMcorr.

3.2.1.2 Precipitation

Figure 44 shows some differences between the models and observations regarding monthly precipitation amount, although the differences are not statistically significant. Mean annual precipitation amount variability is shown in Figure 45 and empirical cumulative distribution function (CDF) in Figure 46. They were calculated for the period of all available observed data, i.e. 1961 – 1990 and confirm a good fit between all models and observations.

For all three models, time series of annual precipitation amount with fitted statistically non-significant linear trend is shown on Figure 47. Table 19 summarises decadal precipitation amount trend based on entire time series, and mean and standard deviations during periods P0 (1961-1990) and P1 (2021-2050) calculated from monthly averages.

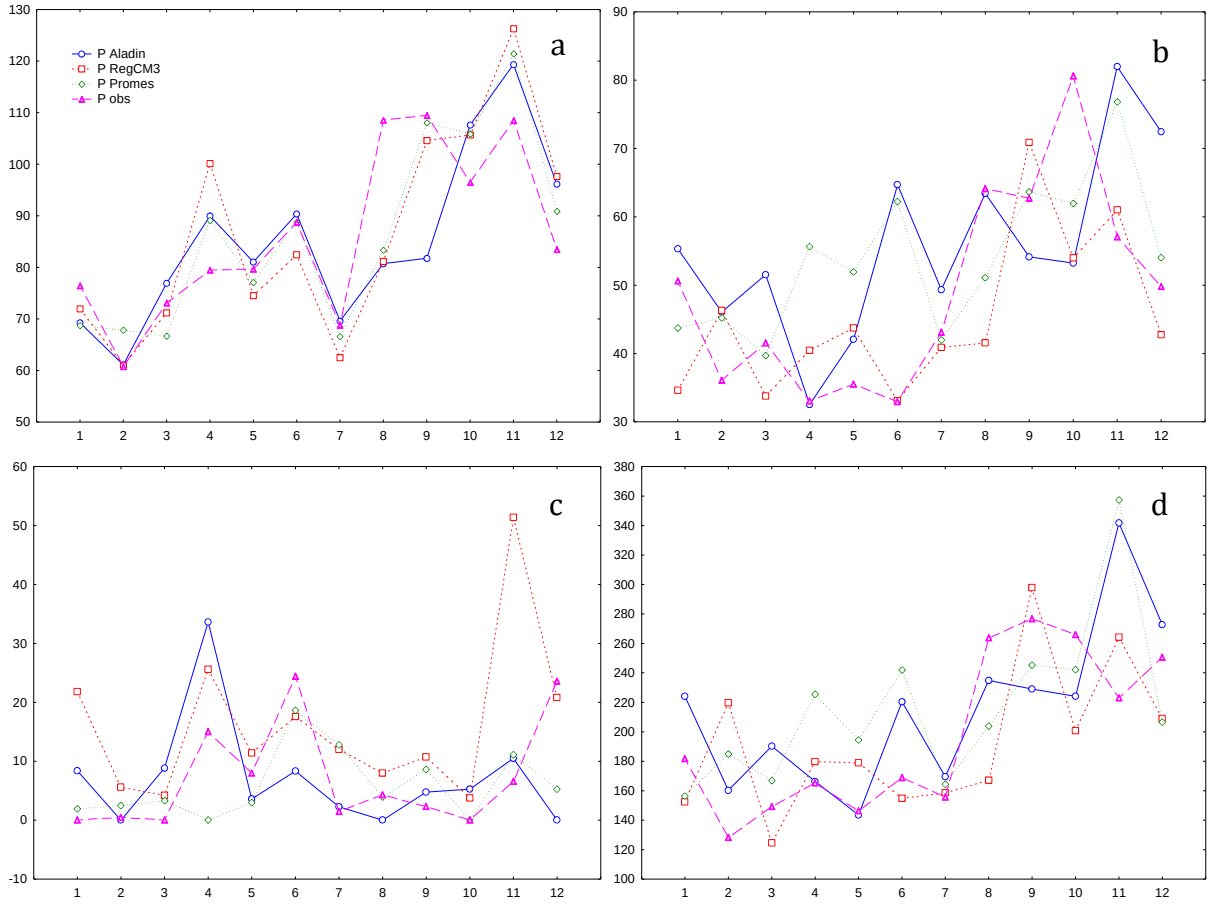

Figure 44: Portorož meteorological station: annual cycle of a) monthly precipitation amount, b) monthly precipitation amount standard deviation, c) minimum monthly precipitation amount, and d) maximum monthly precipitation amount. Model time series are RCMcorr. Period of analysis is P0 (1961-1990).

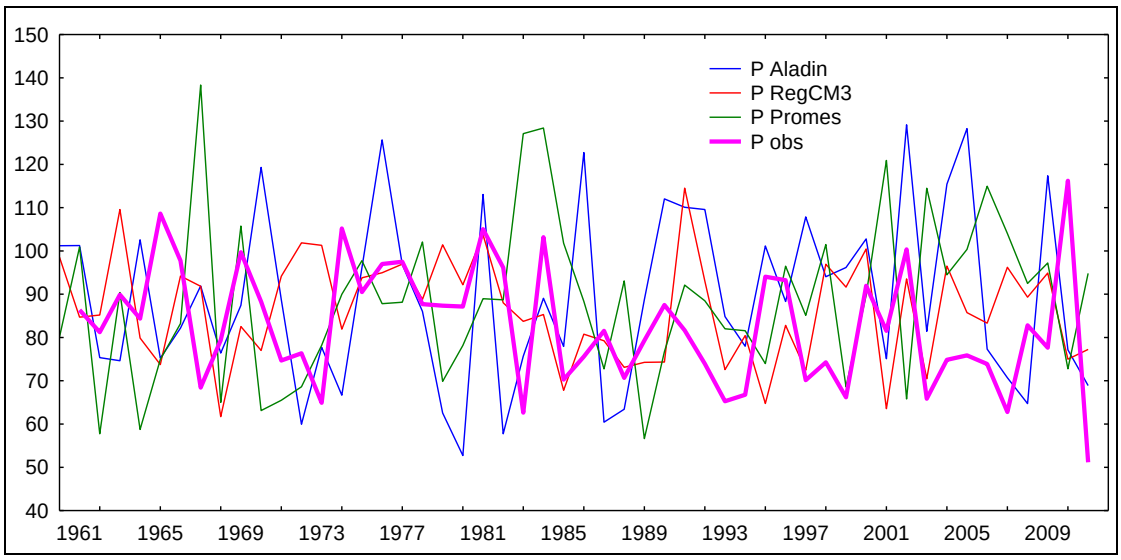

Figure 45: Portorož station time series 1961 – 2011: annual precipitation amount. Model time series are RCMcorr.

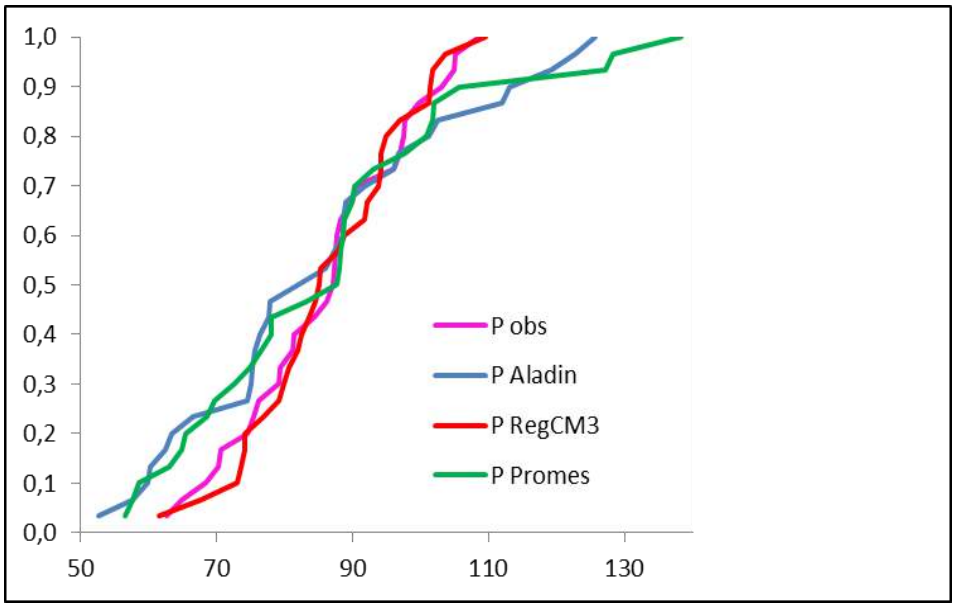

Figure 46: Portorož station empirical cumulative distribution function (CDF) for annual precipitation amount (1961 – 1990). Model time series are RCMcorr.

Table 19: Decadal precipitation amount trend of Portorož meteorological station based on entire time series, and mean and standard deviations during periods P0 (1961-1990) and P1 (2021-2050) calculated from monthly averages. Model time series are RCMcorr.

Model	*decadal trend*	*P0 mean*	*P0 std*	*P1 mean*	*P1 std*
Aladin	0.85	85.3	58.4	90.9	65.9
RegCM3	0.56	86.6	49.7	92.8	58.0
Promes	1.13	86.2	56.9	93.3	62.3

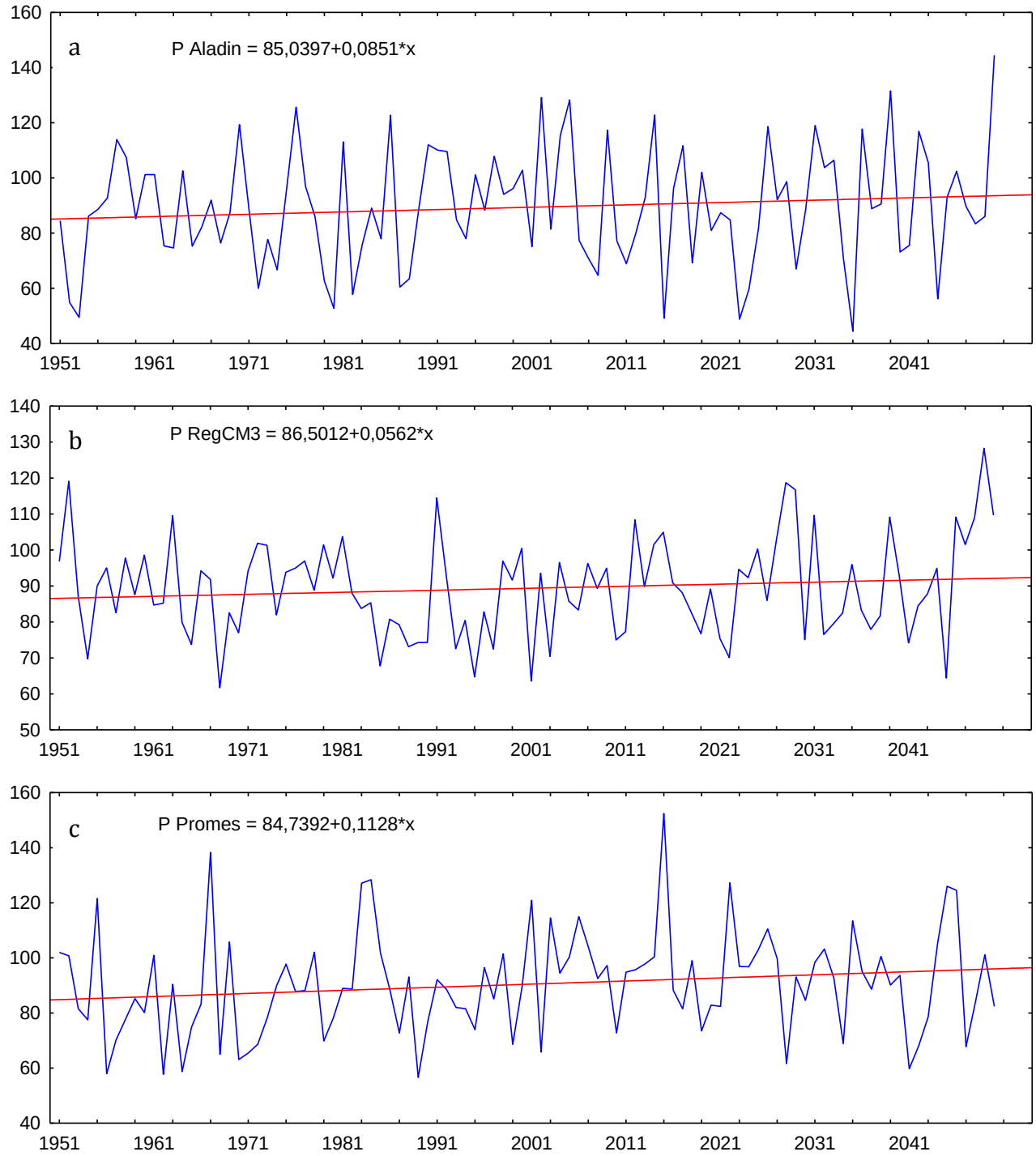

Figure 47: Annual precipitation amount and fitted linear trend of Portorož meteorological station after a) Aladin, b) RegCM3 and c) Promes model. All three trends have statistically non-significant regression at 5 % significance level. Model time series are RCMcorr.

3.2.2. RCM bias corrected and adjusted models

3.2.2.1 Temperature

Figure 48 shows adjustment differences, based on 1961-1990 period, for all three climate models. According to Mann-Whitney test differences between corrected and adjusted values are statistically significant at 5 % significance level for January, March, April, May, August, September and December for Aladin model, for March, July, August, September and December for RegCM3 model, and for April, August, September and December for Promes model.

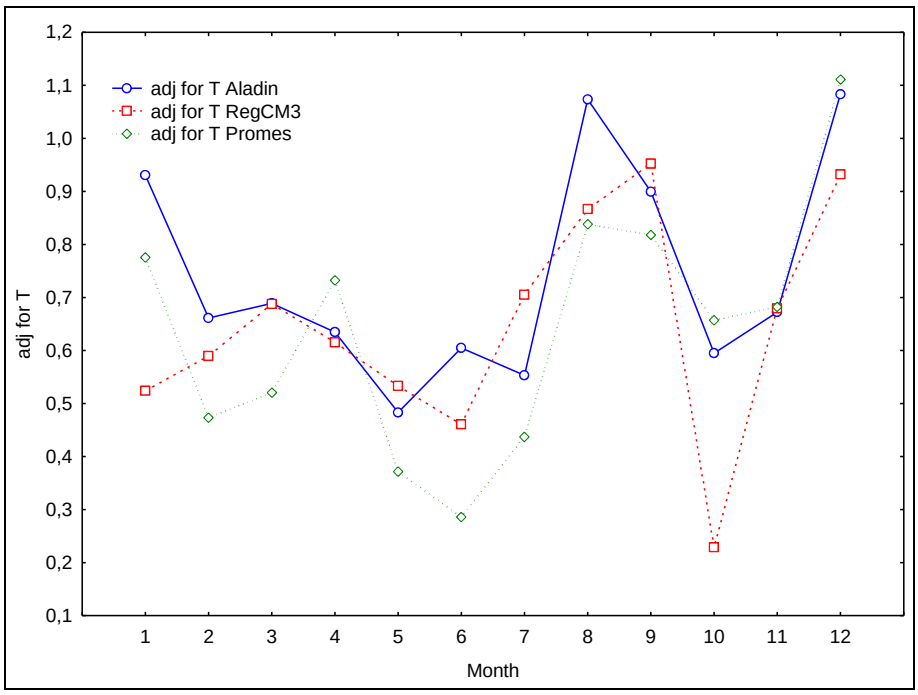

Figure 48: Portorož meteorological station: adjustment differences for mean monthly temperature.

Mean monthly temperatures for the time period 1961 –1990 of all three RCM bias corrected and adjusted models fit perfectly between themselves and observed temperatures (Figure 49). There are more discrepancies among the models and observations in the case of extremes (minimum and maximum) of temperature, especially in the coldest and hottest months (Figure 49). Mean annual temperature fluctuations are presented in Figure 50 and their empirical cumulative distribution function (CDF) in Figure

51. They were calculated for the period of all available observed data, i.e. 1961 – 1990 and confirm an excellent fit between all models and observations.

For the all three models Figure 52 shows time series of annual mean temperatures with fitted linear trend. Trends for all three models are statistically significant at 5 % significance level. Table 20 summarises decadal temperature trend based on entire time series, and mean and standard deviations during periods P0 (1956-1990) and P1 (2021-2050) calculated from monthly averages.

According to Mann-Whitney test comparisons of monthly mean temperatures between P0 (1961-1990) vs. P1 (2021-2050) show statistically significant differences at 5 % significance level for all models and months, except for RegCM3 in March and December (Figure 53). The increase of temperatures in future is proven also by Kolmogorov-Smirnov test for Aladin and Promes models (Figure 54).

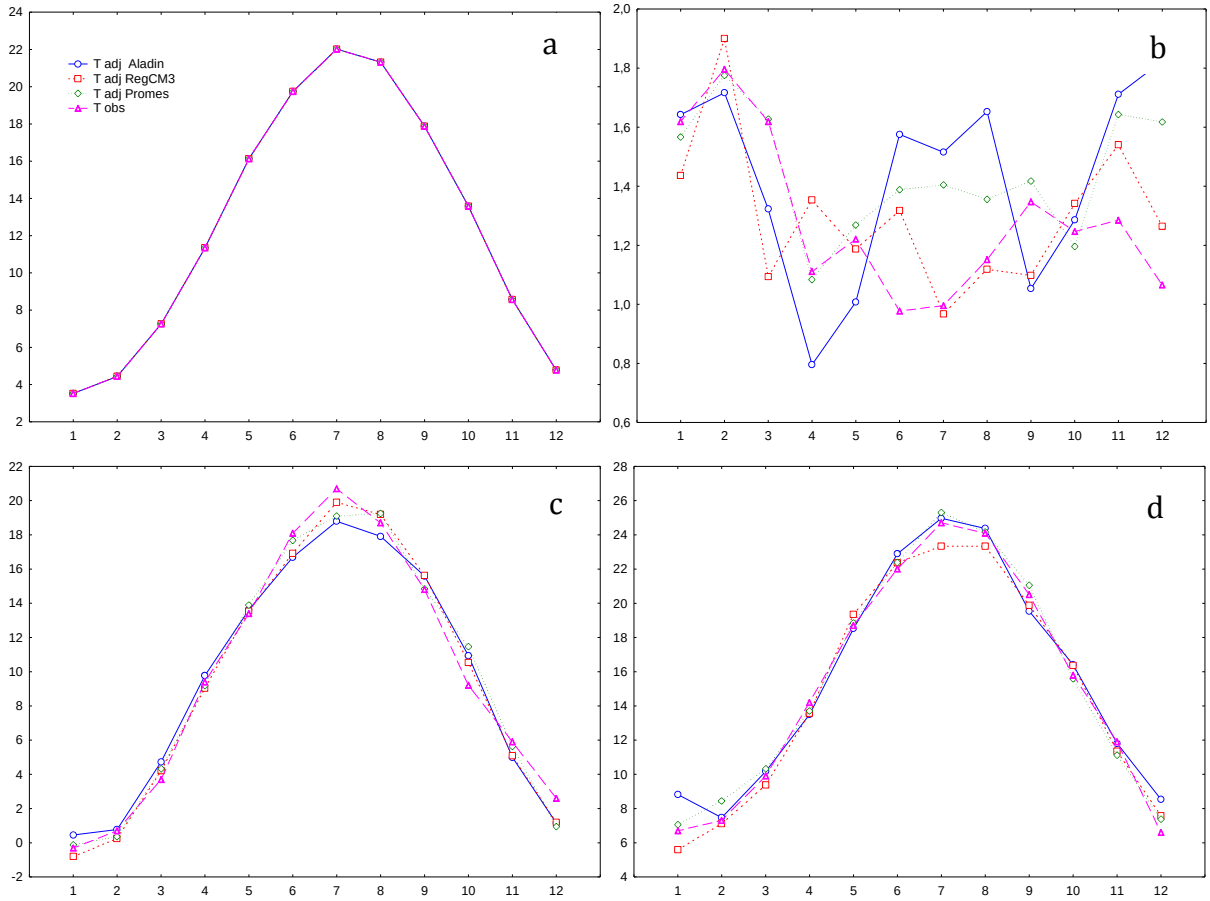

Figure49: Portorož meteorological station: annual cycle of a) mean monthly temperature, b) mean monthly temperature standard deviation, c) minimum monthly temperature, and d) maximum monthly temperature. Model time series are RCMcorr_adj. Period of analysis is P0 (1961-1990).

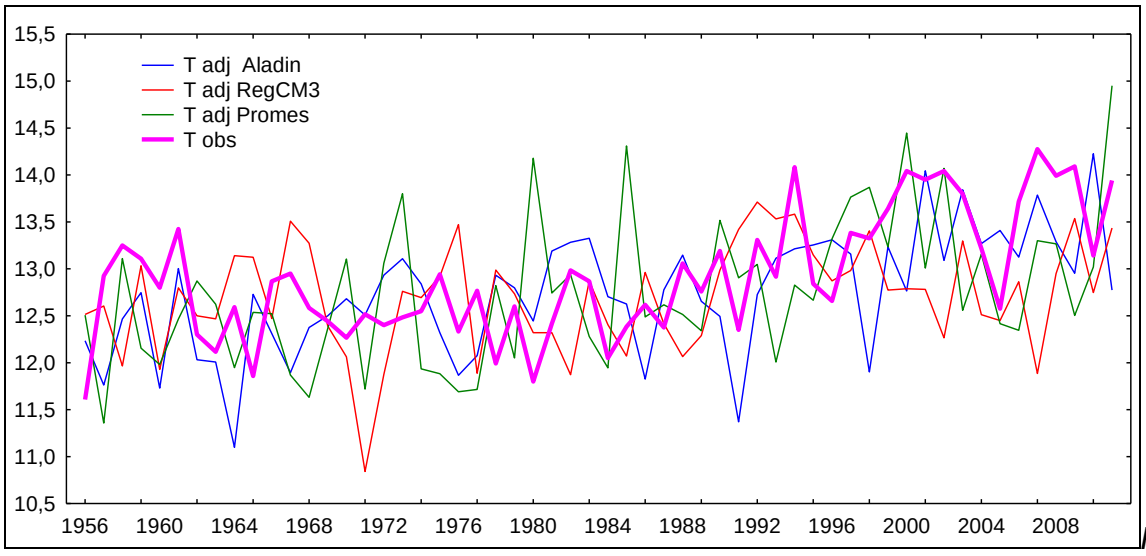

Figure 50: Portorož station time series 1956 – 2011: mean annual temperature. Model time series are RCMcorr_adj.

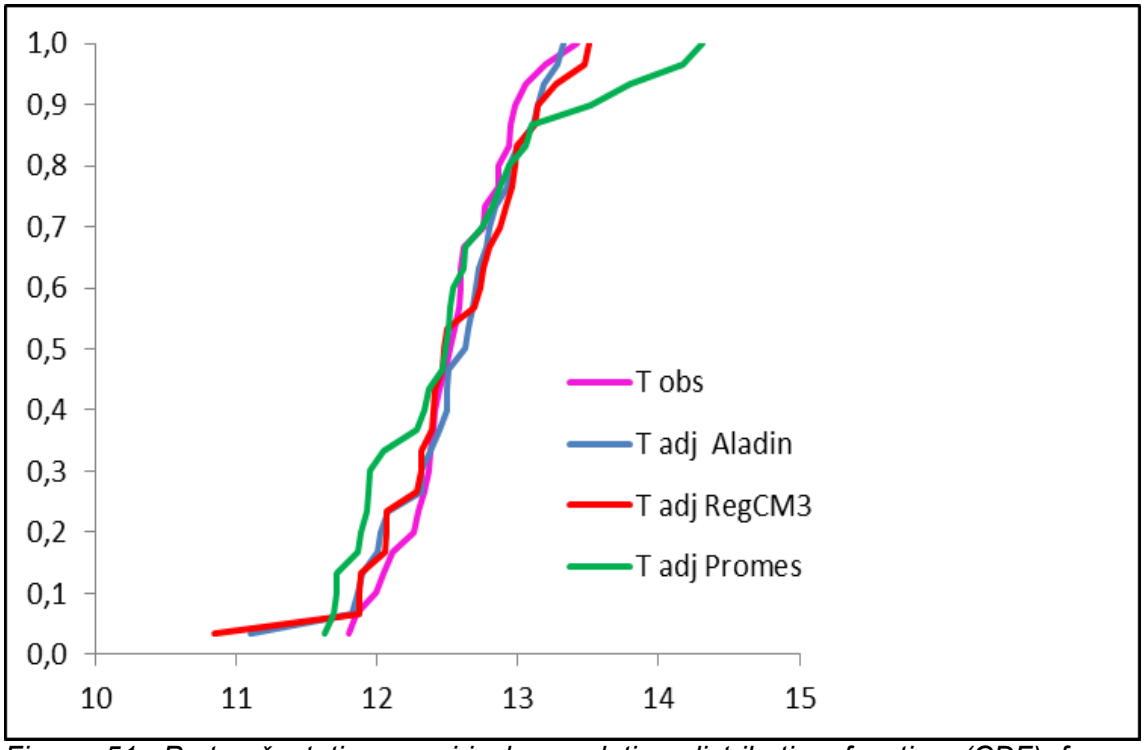

Figure 51: Portorož station empirical cumulative distribution function (CDF) for mean annual temperature (1961 – 1990). Model time series are RCMcorr_adj.

Table 20: Decadal temperature trend of Portorož meteorological station based on entire time series, and mean and standard deviations during P0 (1961-1990) and P1 (2021-2050) calculated from monthly averages. Model time series are RCMcorr_adj.

Model	*decadal trend*	*P0 mean*	*P0 std*	*P1 mean*	*P1 std*
Aladin	0.25	12.5	6.7	14.2	7.0
RegCM3	0.17	12.5	6.7	13.7	6.8
Promes	0.30	12.5	6.7	14.6	6.8

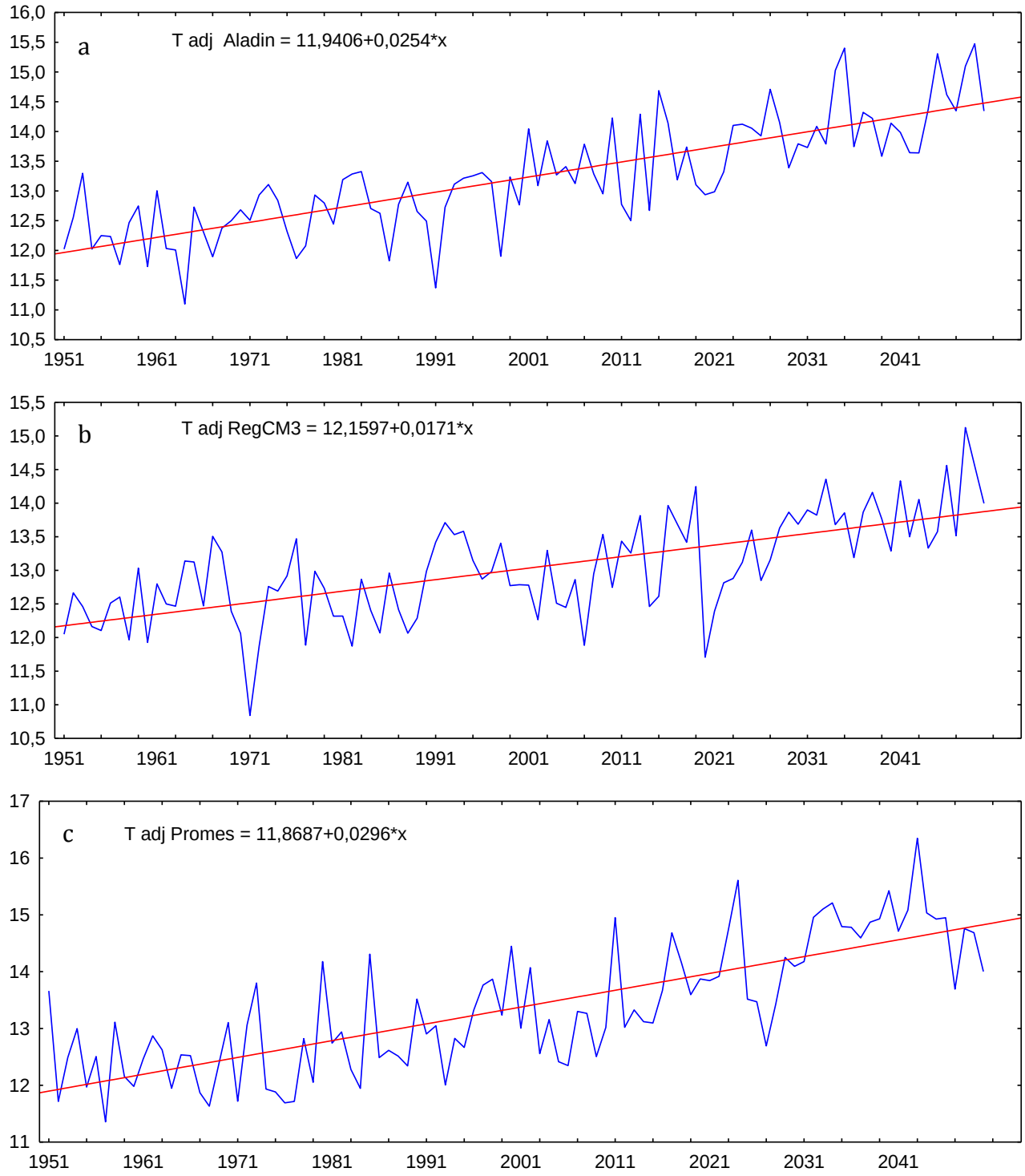

Figure 52: Annual mean temperature and fitted linear trend of Portorož meteorological station after a) Aladin. b) RegCM3 c) Promes. Trends for all three models have statistically significant regression at 5 % significance level. Model time series are RCMcorr_adj.

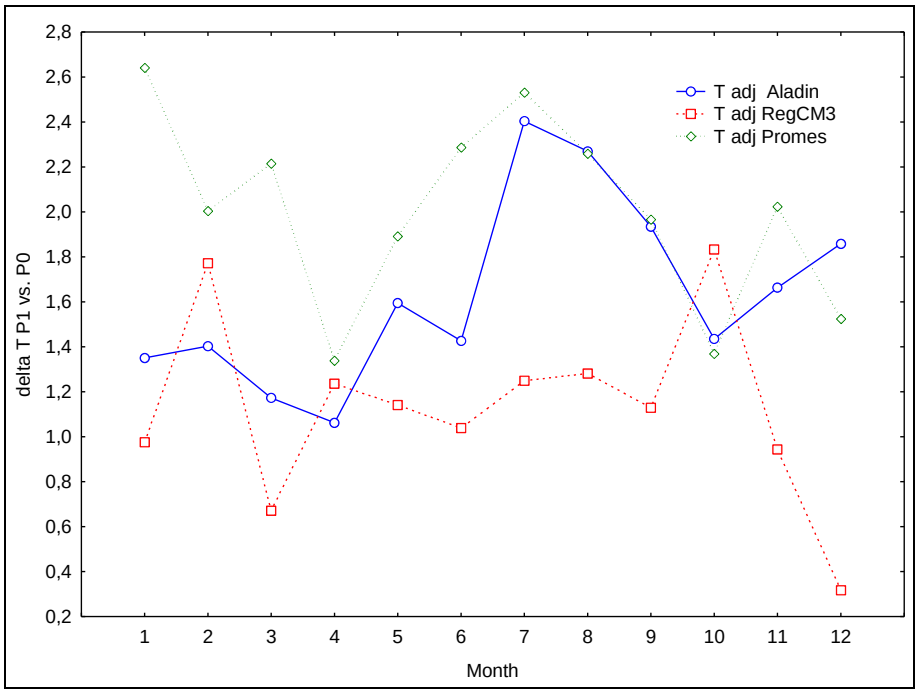

Figure 53: Monthly mean temperature of Portorož meteorological station for P0 (1961-1990) vs. P1 (2021-2050) change.

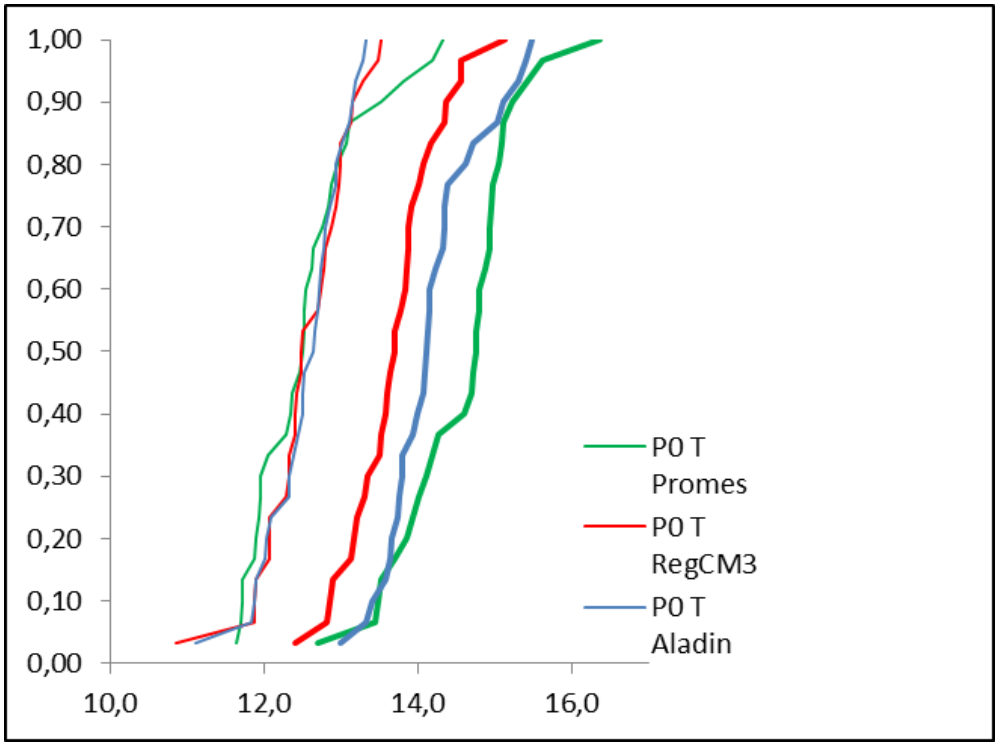

Figure 54: Portorož station empirical cumulative distribution functions CDFs of mean annual temperature in P0 (1961-1990) and P1 (2021-2050).

DRINK ADRIA

3.2.2.2 Precipitation

Figure 55 shows adjustment differences, based on 1961-1990 time period, for all three models. According to Mann-Whitney test differences between corrected and adjusted values are statistically significant at 5 % significance level for Aladin model for September and for RegCM3 for August.

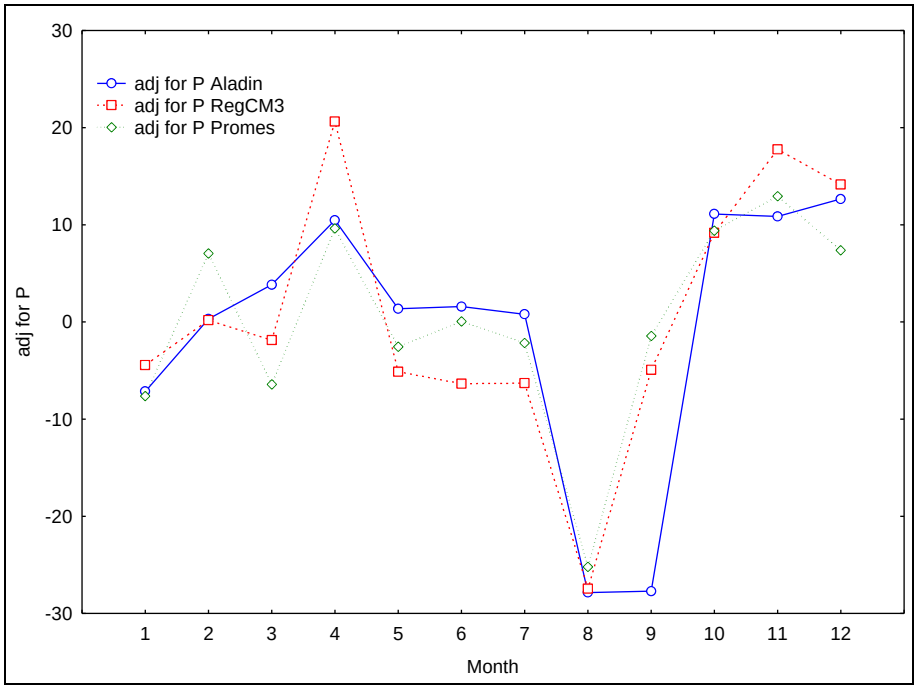

Figure 55: Portorož meteorological station: adjustment differences for monthly precipitation amount.

Figure 56 shows that there are no differences between the models and observations regarding monthly precipitation amount. Differences exist in the extreme (minimum and maximum) monthly precipitations between the models and observations. Mean annual precipitation amount variability is shown in Figure 57 and empirical cumulative distribution function (CDF) in Figure 58. They were calculated for the period of all available observed data, i.e. 1961 – 1990 and confirm a good fit between all models and observations.

For all three models, time series of annual precipitation amount with fitted statistically non-significant linear trend is shown on Figure 59. Table 21 summarises decadal precipitation amount trend based on entire time series, and mean and standard deviations during periods P0 (1961-1990) and P1 (2021-2050) calculated from monthly averages.

According to Mann-Whitney test comparisons of monthly mean temperatures between P0 (1961-1990) vs. P1 (2021-2050) doesn't prove statistically significant differences at 5 % significance level for any of stations and months (Figure 60). The differences in annual precipitation amount are statistically non-significant at 5 % significance levels, as indicated by Kolmogorov-Smirnov test (Figure 61).

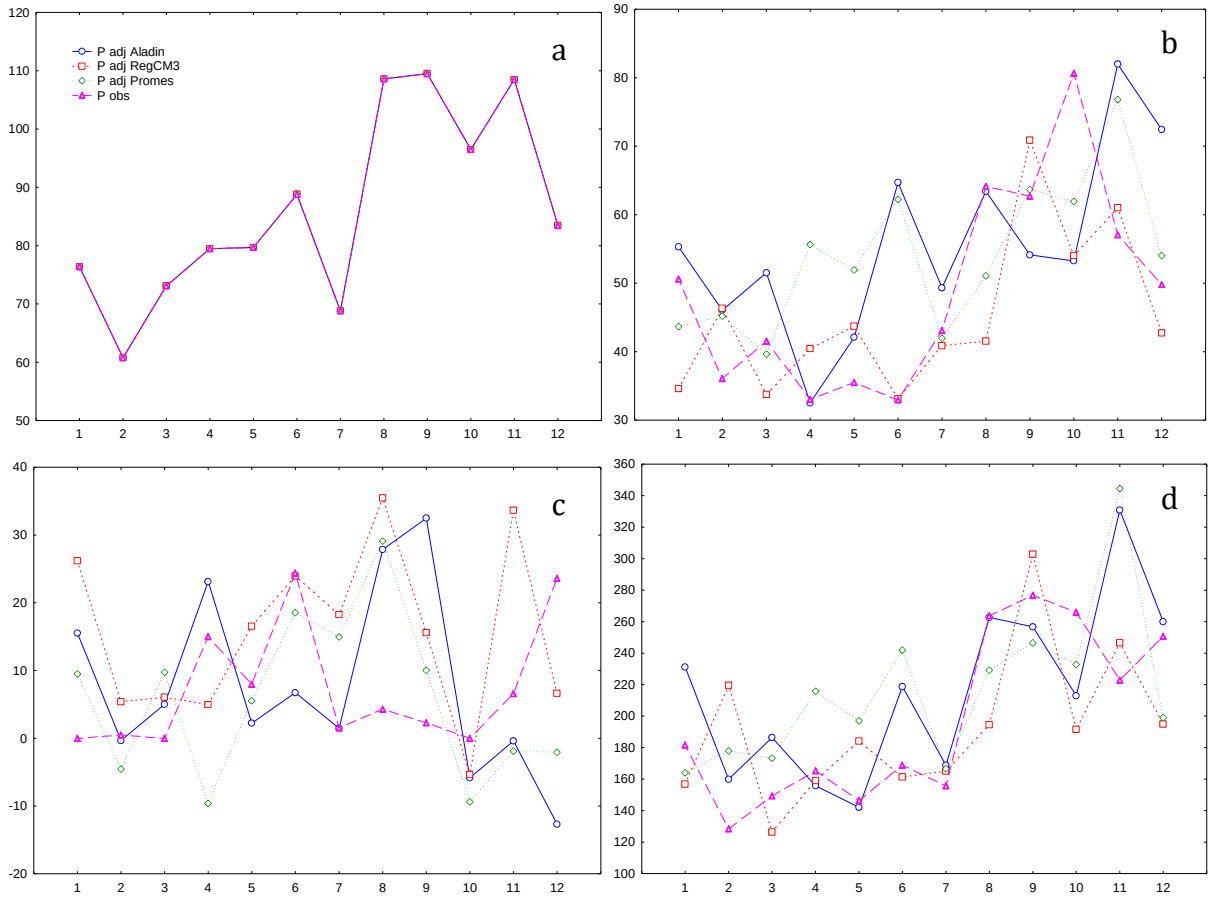

Figure 56: Portorož meteorological station: annual cycle of a) monthly precipitation amount, b) monthly precipitation amount standard deviation, c) minimum monthly precipitation amount, and d) maximum monthly precipitation amount. Model time series are RCMcorr. Period of analysis is P0 (1961-1990).

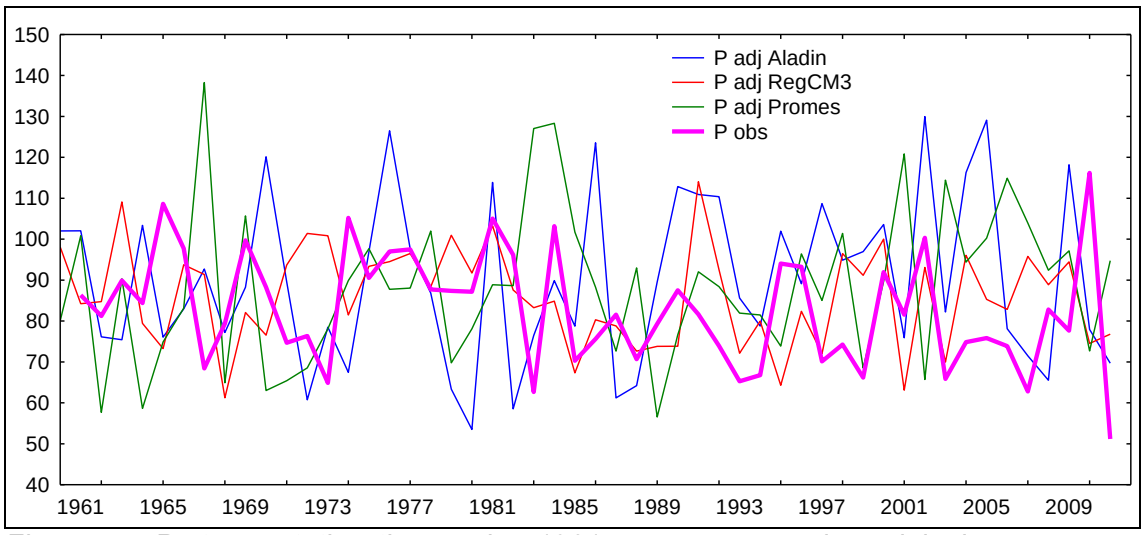

Figure 57: Portorož station time series 1961 – 2011: annual precipitation amount. Model time series are RCMcorr_adj.

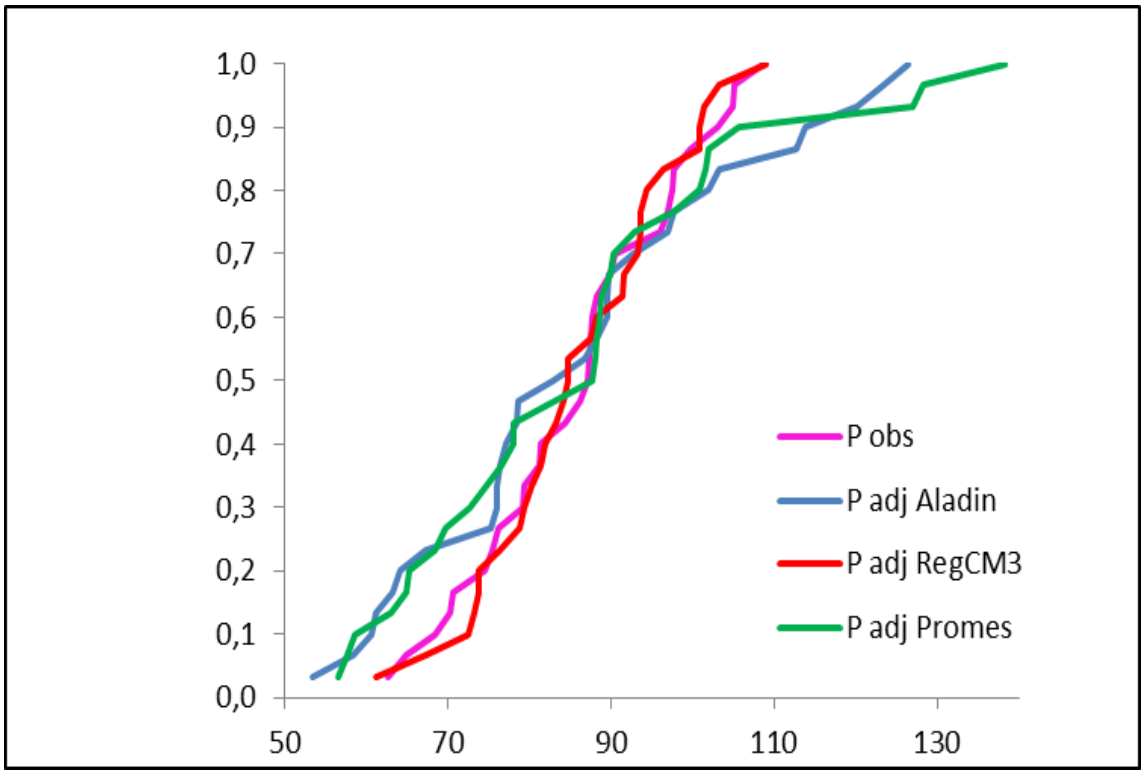

Figure 58: Portorož station empirical cumulative distribution function (CDF) for annual precipitation amount (1961 – 1990). Model time series are RCMcorr_adj.

Table 21: Decadal precipitation amount trend of Portorož meteorological station based on entire time series, and mean and standard deviations during periods P0 (1961-1990) and P1 (2021-2050) calculated from monthly averages. Model time series are RCMcorr_adj.

Model	*decadal trend*	*P0 mean*	*P0 std*	*P1 mean*	*P1 std*
Aladin	0.85	86.1	58.3	91.7	66.8
RegCM3	0.56	86.1	48.5	92.4	57.9
Promes	1.13	86.1	56.4	93.2	61.8

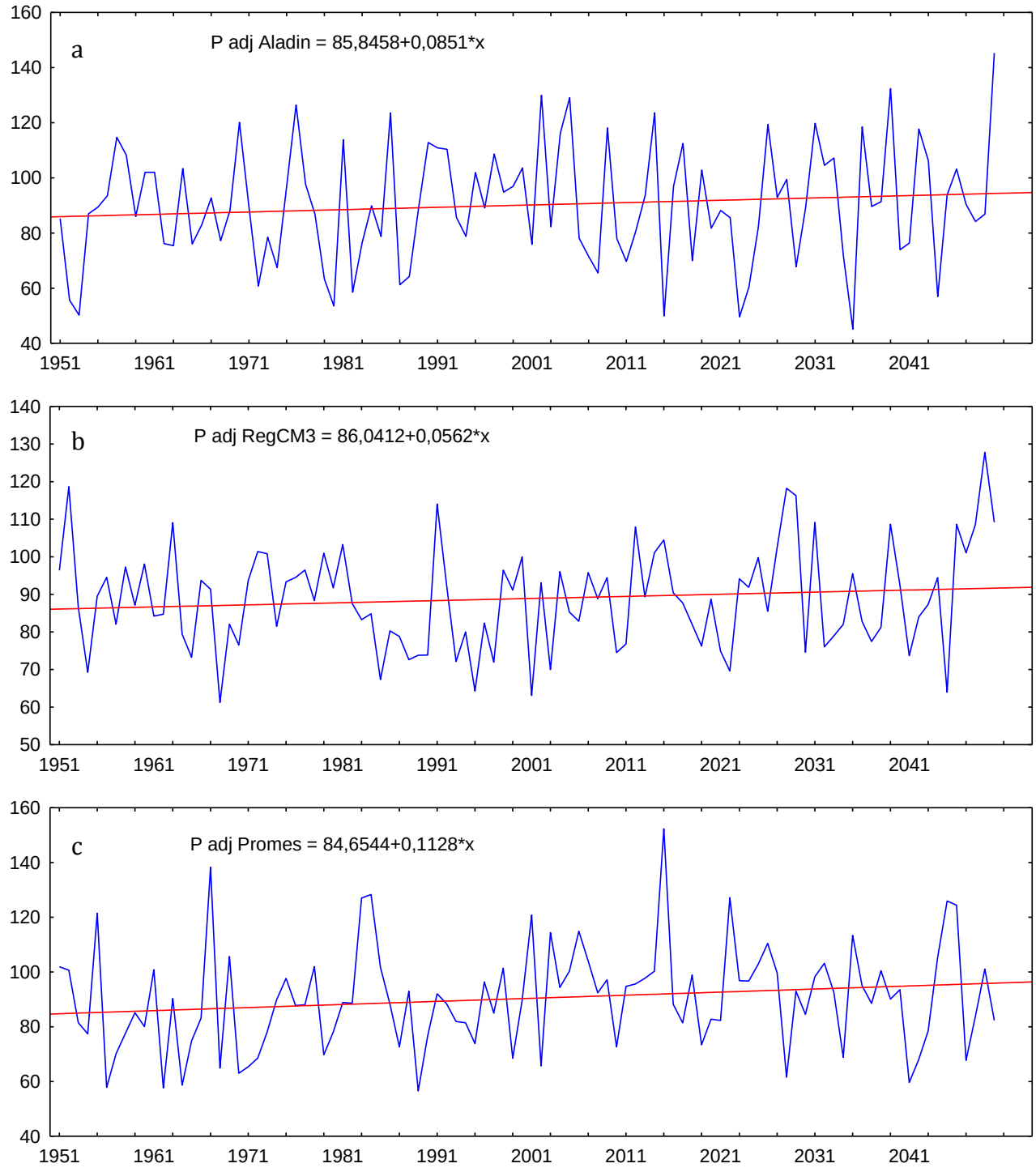

Figure 59: Annual precipitation amount and fitted linear trend of Portorož meteorological station after a) Aladin, b) RegCM3 and c) Promes model. All three trends have statistically non-significant regression at 5 % significance level. Model time series are RCMcorr_adj.

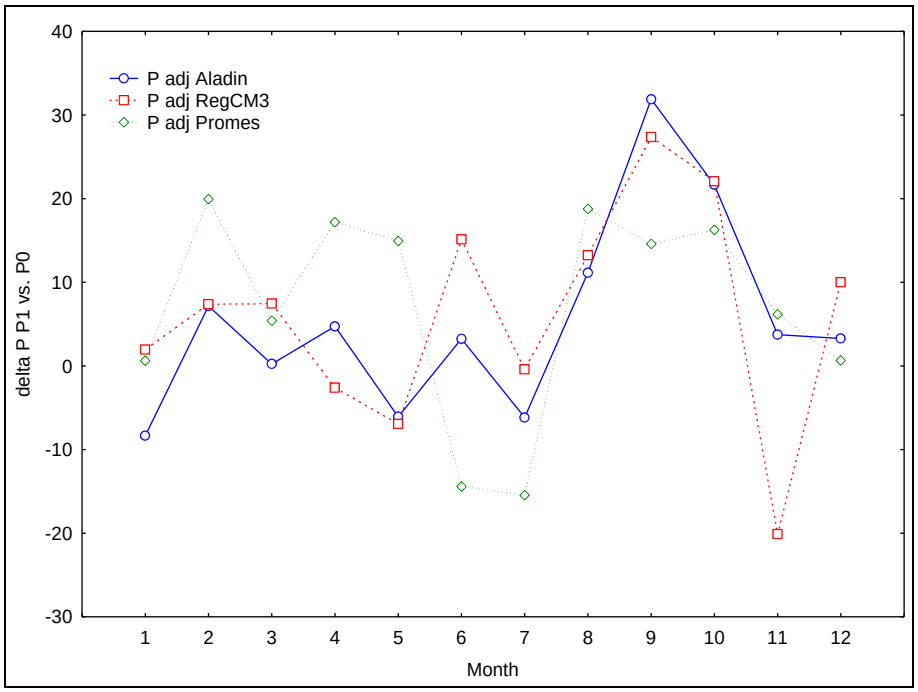

Figure 60: Relative monthly precipitation of Portorož meteorological station for P0 (1961-1990) vs. P1 (2021-2050) change.

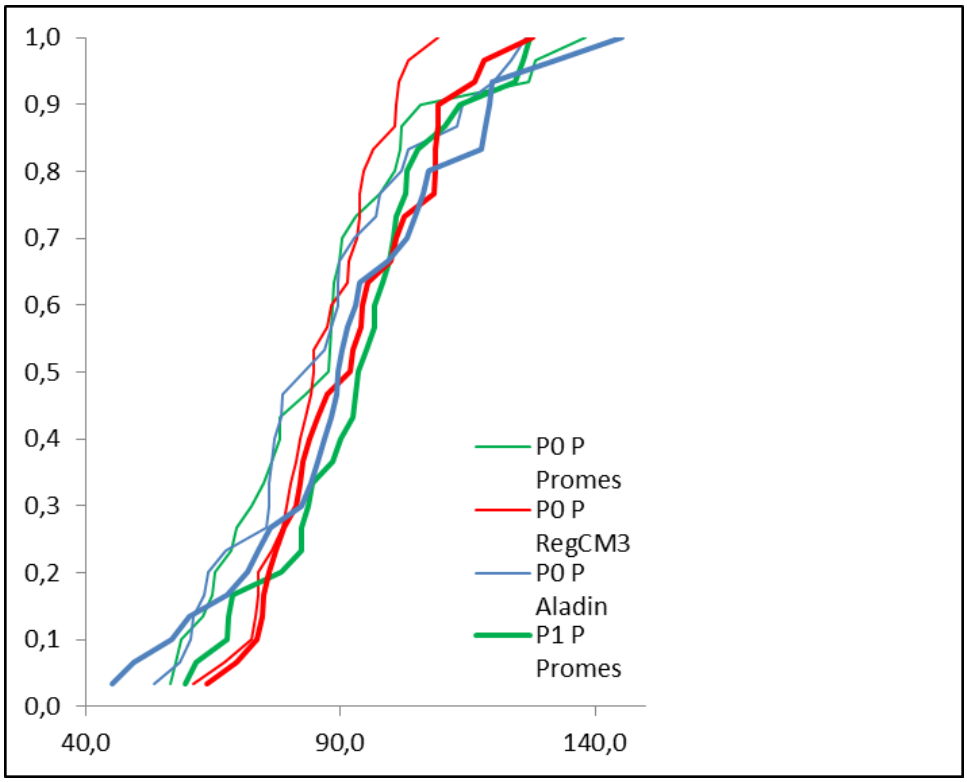

Figure 61: Portorož station empirical cumulative distribution functions CDFs of mean annual precipitation amount in P0 and P1 time periods.

DRINK ADRIA

4 References

Bubnova, R., Hello, G., Bénard, P., Geleyn, J-F., 1995. Integration of the fully elastic equations cast in hydrostatic pressure terrain-following coordinate in the framework of the ARPEGE/Aladin NWP system. *Mon.Wea.Rev.*,123:515-535.

Castro, M., Fernández C., Gaertner M.A.,1993. Description of a meso-scale atmospheric numerical model. In:J.I.Díaz, J.L.Lions (eds), Mathematic, climate and environment, Masson.

Pal, J.S., and Coauthors, 2007. Regional climate modeling for the developing world: The ICTP RegCM3 and RegCNET. *Bull.Amer.Meteor.Soc.*, 88:1395-1409.

Analysis of observed and simulated climate and climate change for Slovenian pilot areas (Kobariški stol, Mia, Matajur and Mirna River catchments) - Ljubljana, August 2014

Let's grow up together

DRINK ADRIA

Adriatic IPA
Cross Border Cooperation 2007-2013

The project is co-funded by the European Union,
Instrument for Pre-Accession Assistance

Report:

Climate and climate change data for pilot areas in Croatia

Faculty of Civil Engineering
University of Rijeka
(FB8)

Rijeka, 2014

Lead Author/s	Ivan Güttler, Marjana Gajić-Čapka, Ksenija Cindrić
Lead Authors Coordinator	Barbara Karleuša
Contributor/s	FB12
Date last release	15.09.2014.
State of document	FINAL

Let's grow up together

The project is co-funded by the European Union,
Instrument for Pre-Accession Assistance

Table of contents

1. Introduction

This report is a contribution to the DRINKADRIA Work Package 4 on regional characteristics of climate and climate change which is the base for water resources availability analyses, and is based on reports by Gajić-Čapka (2014), Cindrić (2014) and Güttler (2014). An analysis of the observed and simulated climate and climate changes is presented for the two catchments in Croatia: the river Mirna (pilot area 1: Northern Istria) and the spring Prud (pilot area 2: Prud catchment and Korčula). The report is structured as follows. In Section 2, data, models and main limitations of the applied methodology are presented. In Section 3, analysis of observed and simulated climate and climate changes are shown and discussed first for the Mirna catchment and then for the Prud catchment. In Appendices 1 and 2, supplement files containing observed and simulated time series are described; these files came out of an initial analysis presented in the DHMZ[1] (2014). In Appendix 3, the results of an additional climatological analysis of observations from the four locations in the river Neretva catchment (Bosnia and Herzegovina) are presented.

2. Methodology

2.1. Data

General climate characteristics, climate variability and trends in the Mirna River and in the Prud wellspring catchment are analysed from the available DHMZ climatological data. They include measurements of air temperature and precipitation amounts from the reference climate period 1961-1990. Observed trends are estimated from a longer period: 1961-2012. The analysis is based on monthly, seasonal and annual averages derived from daily data on climatological stations from the DHMZ observational network. All the DHMZ data are continuously monitored and a routine quality control is applied.

2.2. Models

An assessment of the present and future climates is based on the results from numerical simulations of the three regional climate models that were also analysed for the purpose of the CC-WaterS[2] project. These models participated in the ENSEMBLES[3] project, with downscaling simulations at a 25-km horizontal resolution. In this report, analysis of the model data is carried out for those model grid cells which were the closest to the locations of the Pazin climatological station (thus representing simulated climatological characteristics for the Mirna River catchment) and the Opuzen climatological station (representing the Prud spring catchment).

The regional climate models (RCMs) used are the Aladin (Bubnova et al. 1995), Promes (Castro et al. 1993) and RegCM3 models (Pal et al. 2007). The RCMs were forced by the observed concentrations of the greenhouse gases (GHGs) from 1951 to 2000; from 2001

[1] Meteorological and Hydrological Service of Croatia (Državni hidrometeorološki zavod, DHMZ)

[2] www.ccwaters.eu

[3] www.ensembles-eu.org

onwards the IPCC[4] A1B scenario of the GHGs emissions is applied. The initial and boundary data for each RCM were provided from different global climate models (GCMs): the ECHAM5 GCM data were used to force RegCM3, Aladin was forced by the Arpege GCM and Promes was forced by the HadCM3Q GCM. For the present climate, models are compared with the local DHMZ observations and with the EOBS gridded temperature and precipitation data (Haylock et al. 2008). The following two abbreviations are used in the report:

1. RCMcorr: the RCMs' output was bias corrected by EOBS data, see e.g. Déqué (2007) and Formayer and Haas (2010) for the description of the bias correcting methodology. The RCMcorr data are available from the CC-WaterS database http://climdat.boku.ac.at/opendap/ccwaters.

   Additional details regarding bias correction procedure are available from http://climdat.boku.ac.at/opendap/ccwaters/Documentations/RCM_explanator_report.pdf .

2. RCMcorr_adj: this is further adjusted model time series due to the differences between EOBS data and local DHMZ observations. The adjustment procedure is described in detail in subsection 3.2.

2.3. Limitations of the methodology

The purpose of this report is to provide an input for further hydrological analyses. However, due to experimental nature of the regional climate simulations, several limitations should be emphasised:

1. Spatial resolution of the regional climate model simulations (RCMs) used here is 25 km. At this resolution the main orographic features and the land-sea boundary of the Croatian coast are resolved reasonably well. However, at the same resolution local characteristics for specific station or catchment may not be fully resolved.

2. For the period 1951-2000 all the RCMs in this report are forced by historical (observed) concentrations of the GHGs. From 2001 onwards, however, the IPCC A1B scenario is applied, meaning that only one assumption of the GHG concentration is evaluated. This must be taken into consideration when evaluating the amplitude of projected climate changes (e.g. the higher GHGs emission scenarios are usually associated with the higher temperature increase).

3. The three RCMs models used here account only for a part of possible modelling uncertainties. The use of the multi-model ensemble approach in climate projection studies is strongly recommended in order to avoid projection dependence on specific model assumptions.

4. In the analysed RCM simulations of the reference climate, the RCMs are not reproducing the actual variability observed in the real climate system. Since RCMs are forced at the boundaries by different global climate models (each having its own internal variability, e.g. the sequence of warm and cold years over Europe), the RCMs simulate different variability, e.g. their own sequence of warm

[4] Intergovernmental Panel on Climate Change, www.ipcc.ch

and cold years (or dry and wet years). Specific values indicated in the time series presented in this report do not signify a specific prediction for a specific year.

The models can be compared with observations and with each other in terms of the reference and projected mean climate and overall variability. Models simulations of the future climate should be interpreted as projections of possible state(s) of the climate system which is sensitive to applied initial and boundary conditions, GHGs scenarios and a model internal configuration. Projections are expected to represent future trends and changes over longer time period as realistic as possible.

A detailed discussion on the modelling limitations emphasized in this subsection see e.g. Hawkins and Sutton (2009) and Jacob et al. (2014).

3. Results and discussion

3.1. Meteorological database and analysis of local observations: the Mirna River catchment (pilot area 1: Northern Istria)

This chapter provides an overview of climate characteristics of the observed climate variability and trends for the Mirna catchment (pilot area 1: Northern Istria) in the Istrian peninsula, the northern Croatian Adriatic coast. It will serve as a basis for hydrological analysis relevant for water resources estimates as well as for validation of simulated climate changes. The analysis is based on monthly, seasonal and annual averages of air temperature and precipitation amounts over the reference climate period 1961-1990. The catchment includes 4 climatological stations providing both temperature and precipitation data and 8 rain-gauge stations from the period 1961-2012. In Table 3.1.1, geographical data and available time periods of meteorological measurements are given.

Table 3.1.1 Geographical station data (elevation *h* (m), longitude λ, latitude φ) and the available measurement time periods for temperature (t) and precipitation (P) data for 12 stations in the Mirna catchment.

	Station	*h*	φ	λ	t	P
1.	Pazin	291	45° 14' 27"	13° 56' 43"	1961-2012	1961-2012
2.	Celega	20	45° 19' 43"	13° 33' 48"	1982-2012	1982-2012
3.	Abrami	85	45° 25' 51"	13° 55' 48	1963-2012	1963-2012
4.	Poreč	15	45° 13' 19"	13° 36' 13"	1961-2012	1961-2012
5.	Baderna	260	45° 13'	13° 46'		1961-2012
6.	Umag	2	45° 26'	13° 32'		1961-2012
7.	Kloštar Istra	120	45° 10'	13° 42'		1961-2012
8.	Sv. Petar u Šumi	341	45° 11'	13° 52'		1961-2012
9.	Lupoglav Istra	390	45° 21'	14° 07'		1964-2012
10.	Vodice Istra	661	45° 29'	14° 03'		1961-1991; 1997-2012
11.	Lanišće	542	45° 24’ 31”	14° 6’ 53”		1961-2012
12.	Momjan	275	45° 26'	13° 43'		1961-2012

3.1.1 Climate

The climate of the Istrian peninsula is determined by the mid-latitude air circulation and it is modified by the influence of the sea. The maritime impact penetrates the lowland of the peninsula, in particular the valley of the Mirna River. In addition to the direct cyclogenetic effects of the northern Adriatic Sea, the climate of the area is strongly modified by orography of the Učka and Ćićarija mountains, the mountainous region of Gorski Kotar and the Dinaric Alps. The latitude determines primarily the amount of sunshine and radiation that this area receives during the year and the mid-latitude circulation systems impact local weather and climate. In the summer (JJA), the area is at the northern edge of the subtropical high pressure zone. Therefore, stable, clear and dry summer weather, typical of the Azorean high, is interrupted by frequent occurrences of instabilities and local storms. In the cold part of the year and during the night time, the local turbulence is weak and the impact of local conditions (e.g. orography and land-sea contrast) become dominant. In anticyclonic situations during the night and in winter (DJF), an increased, locally specific, cooling may occur. For anticyclones of the cold part of the year, especially in winter, the bora wind is typical for the northern Adriatic. It blows from the northeast quadrant and is known for its gusts and high speeds. In Istria, the bora dominates on the coast, but it is weaker and relatively infrequent in the inland area. The cyclonic activity, typical for the winter, early spring and late autumn, is important for the precipitation regime and cloudiness over the region.
The local climate characteristics are described for the 1961-1990 period recommended by

the World Meteorological Organization as the referent period for the present climate conditions. Seasonality is described in terms of annual cycle of the mean monthly air temperature and precipitation, and their interannual variability by standard deviation of monthly means and coefficient of variation for precipitation (i.e. standard deviation divided by the mean). The discussion of extremes in the annual and seasonal air temperature and precipitation averages is based on percentiles calculated from the empirical cumulative distribution function (CDF).

Air temperature

The annual cycle of air temperature monthly averages over the Mirna River catchment is well defined: the maximum occurs in July (from 20.4°C to 22.2 °C) and the minimum in January (from 2.5 °C to 4.6 °C; see Table 3.1.1.1 and Figs 3.1.1.1a-3.1.1.3a), indicating a typical maritime annual cycle with autumn (SON) being warmer than spring (MAM).
The annual course of standard deviations (std) of mean monthly air temperatures indicates the highest variability in the cold part of year, especially in February. However, the monthly values of std range between 0.9°C (June or July) and 2.0°C (February) indicating that interannual variability is generally small due to a strong influence of the sea, which moderates temperature extremes (Figs. 3.1.1.1b-3.1.1.3b).
Empirical cumulative distributions of the mean annual air temperature for Pazin, Abrami and Poreč are given in Figs. 3.1.1.1c-3.1.1.3c. The percentiles that determine extreme values of annual and seasonal mean temperatures are given in Table 3.1.1.2. In the annual cycle of the percentiles of mean daily air temperature, the difference between the 98th percentile and the 2nd percentile is the largest in winter due to the highest variability in winter months, particularly in February.

Table 3.1.1.1 Basic statistics (mean, standard deviation, maximum and minimum) for annual and seasonal mean air temperature from the reference period 1961-1990 for the three climatological stations in the Mirna River catchment.

	DJF	MAM	JJA	SON	Year
Pazin					
mean	3.1	10.2	19.3	11.6	11.1
stdev	1.1	0.8	0.7	0.9	0.4
max (°C)	5.3	11.6	20.7	13.5	11.7
min (°C)	-0.1	8.7	18.2	10.0	10.3
Abrami					
mean	4.2	11.3	20.3	12.5	12.1
stdev	0.9	0.7	0.7	0.9	0.4
max (°C)	5.9	12.5	21.5	14.3	12.9
min (°C)	2.4	9.6	18.8	10.8	11.2
Poreč					
mean	5.2	11.7	21.2	13.8	13.0
stdev	1.0	0.8	0.5	1.0	0.3
max (°C)	7.2	13.3	22.0	15.3	13.8
min (°C)	2.4	9.8	20.0	11.1	12.3

Table 3.1.1.2 The percentiles for annual and seasonal mean air temperature empirical distribution from the reference period 1961-1990 for the three climatological stations in the Mirna River catchment.

	DJF	MAM	JJA	SON	Year
Pazin					
1	-0.1	8.7	18.2	10.0	10.3
2	0.1	8.7	18.2	10.0	10.3
5	1.2	8.8	18.3	10.1	10.5
10	1.7	9.0	18.4	10.3	10.5
90	4.5	11.2	20.4	12.7	11.5
95	5.0	11.3	20.6	13.3	11.7
98	5.3	11.6	20.7	13.4	11.7
99	5.3	11.6	20.7	13.5	11.7
Abrami					
1	2.4	9.6	18.8	10.8	11.2
2	2.4	9.6	18.8	10.8	11.2
5	2.8	9.9	19.0	11.0	11.2
10	2.8	10.2	19.3	11.2	11.5
90	5.4	12.3	21.1	13.7	12.5
95	5.6	12.4	21.5	14.2	12.8
98	5.8	12.5	21.5	14.3	12.9
99	5.9	12.5	21.5	14.3	12.9
Poreč					
1	2.4	9.8	20.0	11.1	12.3
2	2.5	9.8	20.0	11.2	12.3
5	3.1	10.6	20.1	12.3	12.3
10	4.1	10.6	20.5	12.4	12.6
90	6.6	12.5	21.9	15.1	13.4
95	6.7	12.7	21.9	15.3	13.6
98	7.2	13.2	22.0	15.3	13.8
99	7.2	13.3	22.0	15.3	13.8

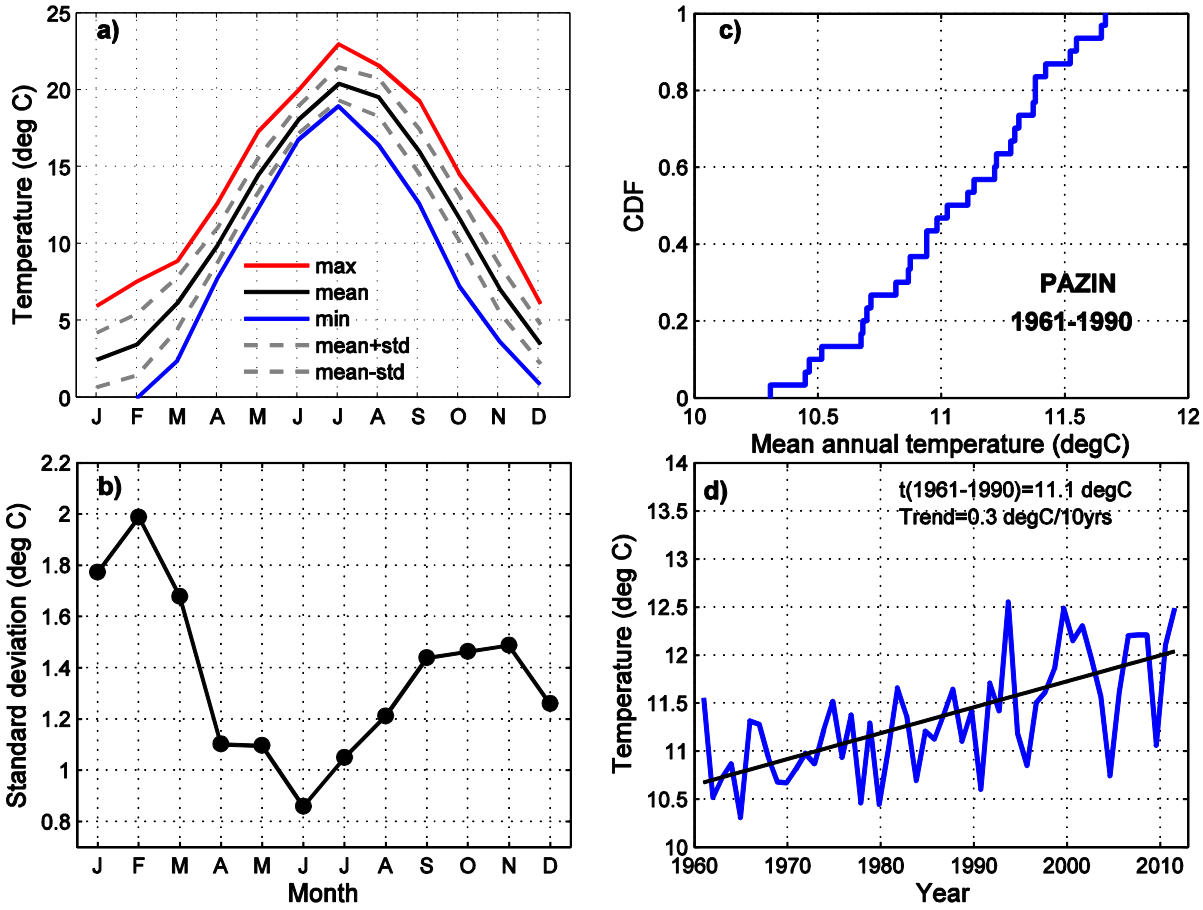

Figure 3.1.1.1 Annual cycle of (a) mean monthly air temperature, (b) its standard deviation, (c), cumulative distribution of mean annual air temperature for the period 1961-1990 and (d) time series of mean annual air temperature with fitted trend line for the period 1961-2012 for the meteorological station Pazin.

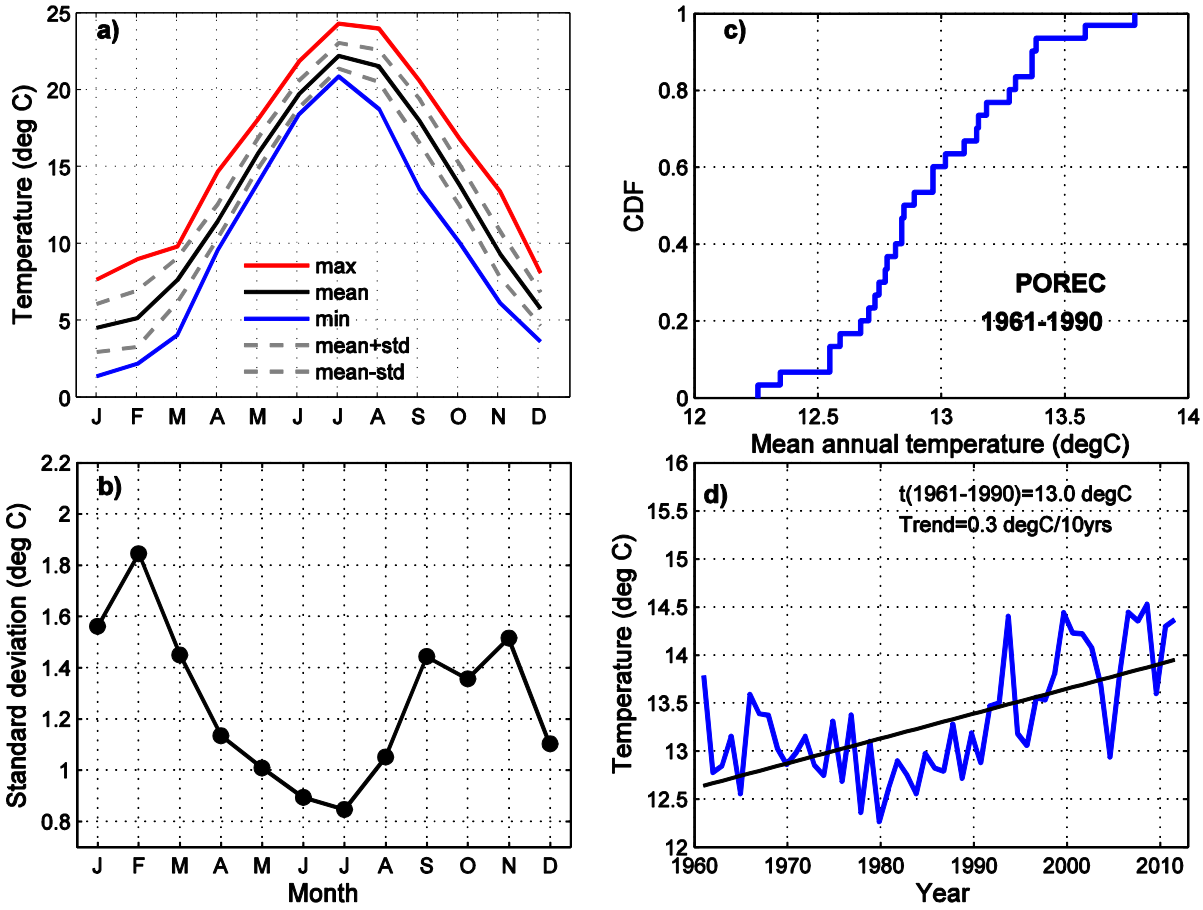

Figure 3.1.1.2 Annual cycle of (a) mean monthly air temperature, (b) its standard deviation, (c) cumulative distribution of mean annual air temperature for the period 1961-1990 and (d) time series of mean annual air temperature with fitted trend line for the period 1961-2012 for the meteorological station Poreč.

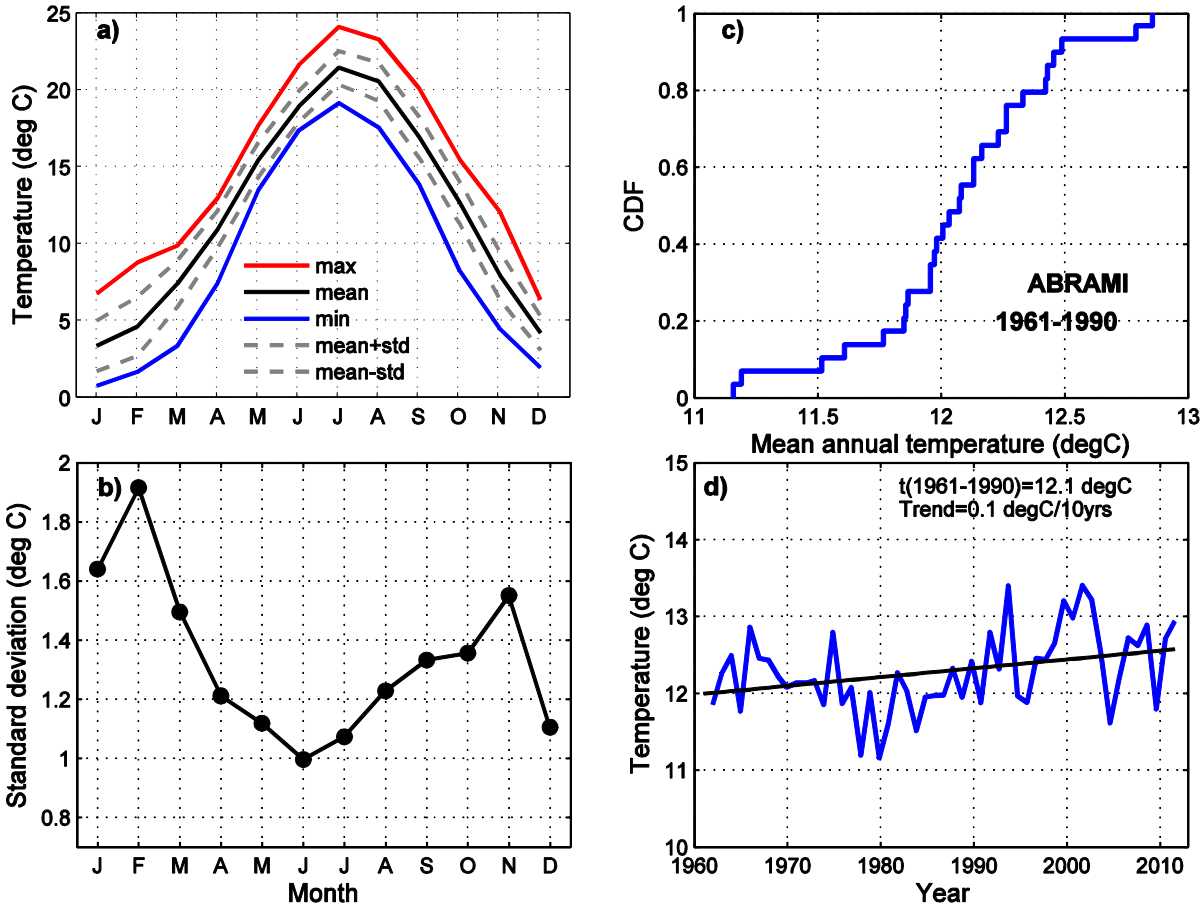

Figure 3.1.1.3 Annual cycle of (a) mean monthly air temperature, (b) its standard deviation, (c) cumulative distribution of mean annual air temperature for the period 1961-1990 and (d) time series of mean annual air temperature with fitted trend line for the period 1961-2012 for the meteorological station Abrami.

Precipitation

Precipitation in Croatia is the consequence of passing cyclones and related atmospheric fronts, within the general circulation of the atmosphere (Zaninović et al. 2008). Their variation during a year influences the seasonality of precipitation. The Mirna River catchment has a mix of the maritime and continental types of annual cycle which is characteristic for the inland Istrian peninsula. The lowest precipitation amount generally occurs during the warm period of year (Fig. 3.1.1.4a-3.1.1.6a); the minimum in annual cycle appears in July (between 54 mm near the coast and 80 mm in the inland of Istria), while the maximum occurs in November (105 mm - 134 mm). However, there is a second minimum that occurs in February (59 mm – 80 mm) thus resulting in the similar proportion (49% to 51%) of the cold (October to March) and warm (April to September) half-year in total annual precipitation amount. Seasonally, the highest precipitation amounts (295 mm – 336 mm) are received during autumn months (September-October-November); while in

other seasons the precipitation amounts are quite similar (Table 3.1.1.3). In the inland of Istria at some locations the minimum precipitation amounts can also be found in winter. The dominant cold southeast advection over the Istrian peninsula contributes to the persistent, stable inversion conditions in winter which are characterised by long periods without precipitation (Lončar and Bajić 1994; Cindrić et al. 2010).

Table 3.1.1.3 Basic statistics (mean, standard deviation, coefficient of variation, maximum and minimum) for annual and seasonal precipitation amount from the reference period 1961-1990, for the three climatological stations in the Mirna River catchment.

	DJF	MAM	JJA	SON	Year
Pazin					
mean	251.4	269.1	252.0	335.8	1115.5
stdev (mm)	108.1	63.5	96.2	129.9	179.8
cv (mm)	0.43	0.24	0.38	0.39	0.16
max (mm)	503.2	385.0	517.5	555.7	1470.2
min (mm)	64.9	137.9	69.3	87.0	731.1
Abrami					
mean	203.2	209.5	243.3	294.5	946.8
stdev (mm)	88.9	66.1	95.4	103.6	148.8
cv (mm)	0.44	0.32	0.39	0.35	0.16
max (mm)	411.4	363.1	443.1	546.6	1289.8
min (mm)	39.9	117.6	92.4	129.7	621.1
Poreč					
mean	225.1	208.1	200.8	298.8	934.8
stdev (mm)	98.2	52.7	67.5	110.4	152.3
cv (mm)	0.44	0.25	0.34	0.37	0.16
max (mm)	455.0	309.5	361.2	515.8	1183.4
min (mm)	40.5	111.5	80.1	71.8	573.8

In some years there is a significant deviation in monthly amounts from the average precipitation conditions. Coefficient of variation indicates a higher interannual variation in mean monthly precipitation during the cold half-year, particularly in October ranging from 80% to 90% (Figs 3.1.1.4b-3.1.1.6b).

Cumulative distribution (CDF) of annual precipitation is shown in Figs. 3.1.1.4c-3.1.1.6c. The percentiles that determine extreme values are given for annual and also for seasonal precipitation in Table 3.1.1.4. The empirical CDF gives the general insight into the precipitation amount distribution shape providing the expecting probabilities of the observed amounts. For example, for the Poreč meteorological station the annual precipitation amount of over 1151 mm can be expected on average once in ten years (90^{th} percentile), and over 1316 mm once in 50 years (98^{th} percentile). For all the given return levels in the right tail of the distribution (90^{th} to 99^{th} percentile), the highest values of precipitation amounts can be found in the autumn months. On the other hand, extremely dry seasons are those with precipitation amount lower than the 2^{nd} percentile. The lowest value of the 2^{nd} percentile is generally found in the summer months; however, in the

northern part of the catchment (Abrami) the minimum value is obtained during the winter. The differences in the CDFs across a small region such as the Mirna River catchment reveal the overall large spatial variability of precipitation amounts.

Table 3.1.1.4 The percentiles for annual and seasonal precipitation empirical distribution from the reference period 1961-1990, for the three climatological stations in the Mirna catchment.

	DJF	MAM	JJA	SON	Year
Pazin					
1	64.9	107.5	32.7	87.0	671.4
2	68.3	110.5	52.1	89.2	679.0
5	72.8	135.5	85.1	127.2	726.8
10	91.1	143.3	128.9	180.8	813.4
90	415.1	341.4	361.9	551.0	1373.0
95	487.3	354.4	418.1	570.9	1478.5
98	497.3	369.7	497.7	637.4	1611.3
99	503.2	384.7	516.8	691.1	1661.2
Abrami					
1	40.1	82.6	76.0	129.9	621.3
2	51.2	90.5	84.4	134.5	629.7
5	66.8	115.3	96.6	139.6	669.6
10	79.9	126.2	122.8	157.8	711.7
90	330.6	294.7	356.6	473.4	1088.9
95	352.1	319.6	399.9	544.5	1176.0
98	400.4	359.0	423.2	598.9	1425.3
99	411.2	362.9	442.7	621.0	1569.3
Poreč					
1	40.7	98.4	38.5	71.8	543.7
2	50.6	99.6	40.5	74.3	559.2
5	61.5	111.7	80.4	131.9	583.7
10	78.4	133.7	89.8	178.5	723.3
90	353.7	264.6	285.5	490.9	1151.4
95	387.8	293.5	356.6	504.1	1183.1
98	438.9	303.0	424.3	524.4	1316.2
99	454.7	309.3	438.9	533.5	1385.0

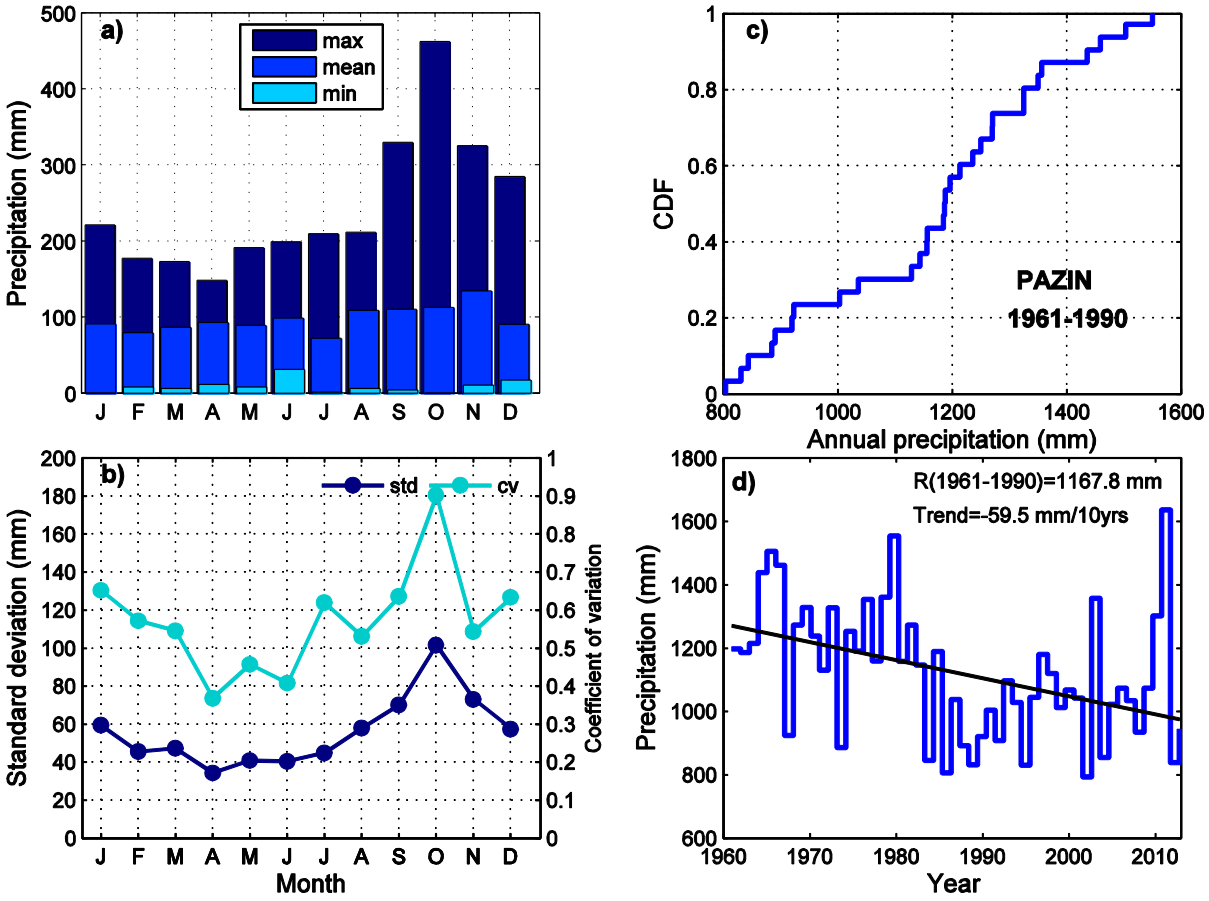

Figure 3.1.1.4 Annual cycle of (a) mean monthly precipitation amounts, (b) standard deviation and coefficient of variation, (c) cumulative distribution of annual precipitation amounts for the period 1961-1990 and (d) time series of annual precipitation amounts with fitted trend line for the period 1961-2012 for the meteorological station Pazin.

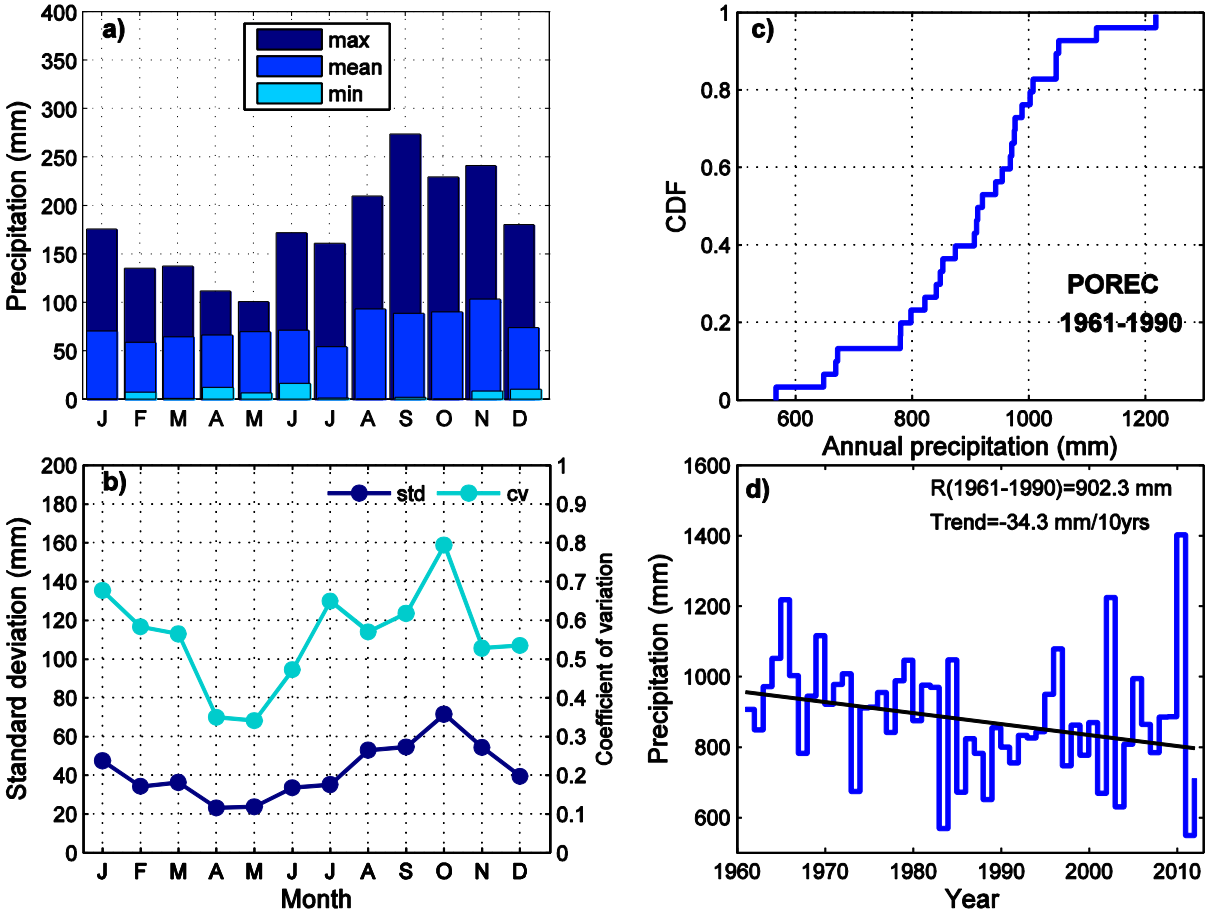

Figure 3.1.1.5 Annual cycle of (a) mean monthly precipitation amounts, (b) standard deviation and coefficient of variation, (c) cumulative distribution of annual precipitation amounts for the period 1961-1990 and (d) time series of annual precipitation amounts with fitted trend line for the period 1961-2012 for the meteorological station Poreč.

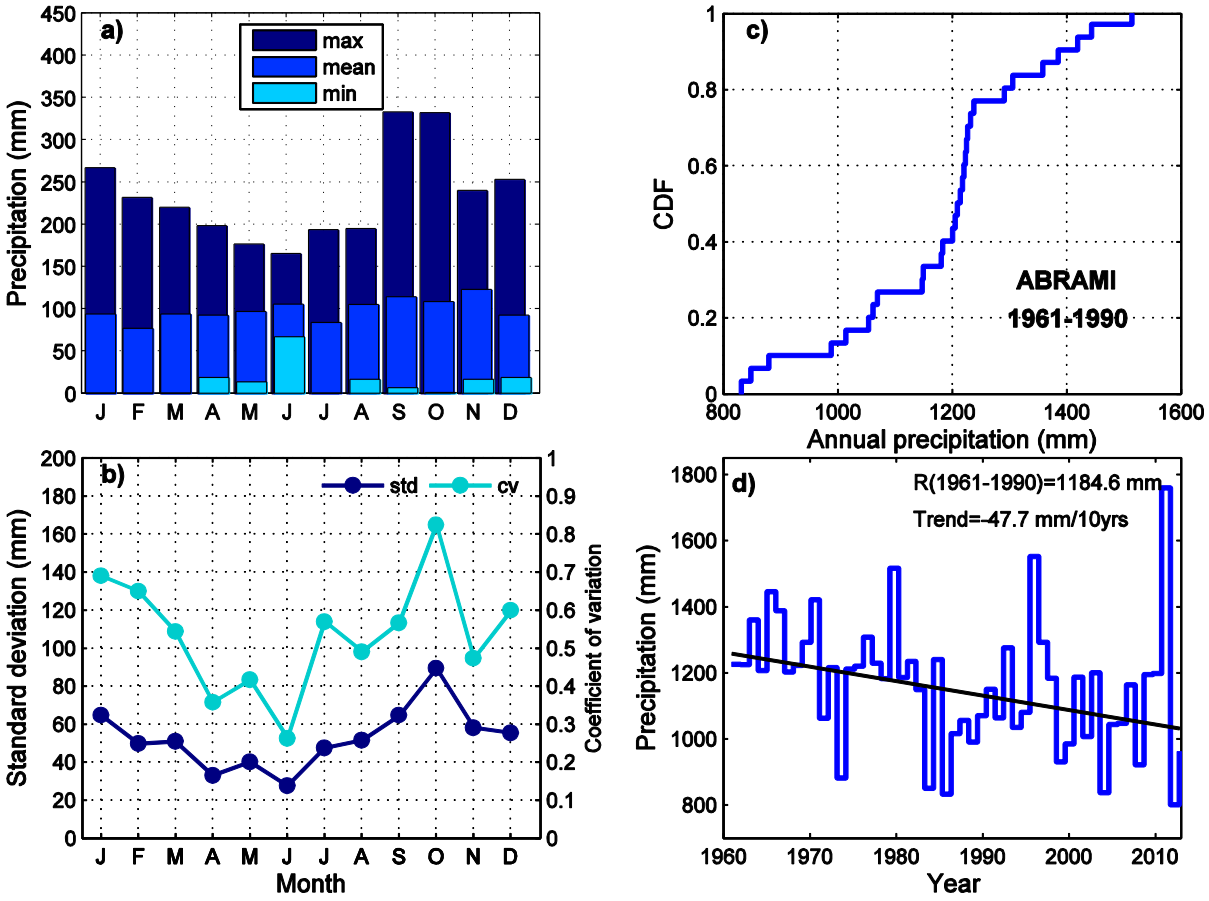

Figure 3.1.1.6 Annual cycle of (a) mean monthly precipitation amounts, (b) standard deviation and coefficient of variation, (c) cumulative distribution of annual precipitation amounts for the period 1961-1990 and (d) time series of annual precipitation amounts with fitted trend line for the period 1961-2012 for the meteorological station Abrami.

3.1.2 Trends

Trends in seasonal and annual mean monthly air temperature and precipitation amounts are calculated for the available period 1961-2012. They have been estimated by the Kendall's tau method (or Sen's slope; Sen 1968), which is statistically more robust estimator of the trend than the least squares estimator. However, a linear trend is also calculated and given for comparison. The trends are expressed as decadal values for both variables. Additionally, the trends in precipitation amounts are given as the percentage of the corresponding seasonal and annual means from 1961-1990 period. The statistical significance of the trend is estimated using the non-parametric Mann–Kendall test (Gilbert 1987).
The examples of time series of mean annual temperature and precipitation amounts are given in Figs 3.1.1.1d-3.1.1.6d with the associated trend lines and with the given mean values from the reference period 1961-1990.
The trend results reveal the statistically significant increase in annual mean *air temperature* (0.1-0.3°C/10yrs) since 1961 in the Mirna catchment (Table 3.1.2.1). The annual mean temperature increase is predominantly due to the significant increase in spring (0.2-0.3°C/10yrs) and summer (0.3-0.5°C/10yrs) mean air temperature. Changes observed in the cold half-year are very weak. These results are in line with the observed regional and global warming.

Table 3.1.2.1 Decadal air temperature trends (°C/10 yrs) for Pazin, Abrami and Poreč stations based on the 1961-2012 data series. Trends significant at the 5% level are bolded. For each season two trend values are given, according to different methods: Sen's slope (left value) and least square estimator (right value).

°C/10yr	DJF		MAM		JJA		SON		Year	
Pazin	0.1	0.1	**0.3**	**0.3**	**0.4**	**0.5**	0.1	0.1	**0.3**	**0.3**
Abrami	-0.1	0.0	**0.2**	**0.2**	**0.3**	**0.3**	0.0	0.0	**0.1**	**0.1**
Poreč	0.1	0.1	**0.3**	**0.3**	**0.5**	**0.5**	0.1	0.1	**0.3**	**0.3**

The trends in *precipitaiton* amounts show the significant decrease in annual totals (4-5%/10yrs) over the Mirna River catchment. There is a consistent decrease of precipitation amounts in all seasons (Table 3.1.2.2), nevertheless decrease in annual amount is mainly forced by a decrease in the warm seasons (spring and summer).

Table 3.1.2.2 Decadal precipitation trends (mm/10 yrs and %/10 yrs) for Pazin, Abrami and Poreč stations based on the 1961-2012 data series. Trends significant at the 5% level are bolded. For each season two trend values are given according to different methods: Sen's slope (left value) and least square estimator (right value).

	DJF		MAM		JJA		SON		Year	
Pazin										
mm/10	-12.7	-8.4	**-14.8**	**-13.6**	-17.6	-14.4	-17.4	-13.2	**-59.5**	**-52.5**
%/10yr	-4.9	-3.3	**-5.5**	**-5.0**	-6.3	-5.1	-4.9	-3.7	**-5.1**	**-4.5**
Abrami										
mm/10	-3.3	-1.9	-10.2	-10.1	-18.0	-16.6	-12.4	-7.4	**-47.7**	**-38.3**
%/10yr	-1.3	-0.7	-3.6	-3.6	-6.1	-5.7	-3.6	-2.2	**-4.0**	**-3.2**
Poreč										
mm/10	-5.3	-2.4	**-11.8**	**-9.3**	**-15.4**	**-13.9**	-1.1	2.7	**-34.3**	**-25.0**
%/10yr	-2.6	-1.2	**-5.9**	**-4.7**	**-7.1**	**-6.4**	-0.4	1.0	**-3.8**	**-2.8**

3.2. Regional climate model simulations: Pazin climatological station

For the Pazin climatological station, air temperature and precipitation from DHMZ observations, EOBS data and bias corrected simulations of the three regional climate models in the historical period P0 (1961-1990) are compared in Fig. 3.2.1. The EOBS air temperature is higher than DHMZ observations throughout the annual cycle (Fig. 3.2.1a). Since EOBS data made the basis for calculation of RCM biases, the bias-corrected modelling data, RCMcorr, are therefore constrained to be closer to EOBS than to DHMZ observations. This restriction makes the RCMcorr annual cycles also warmer than the DHMZ observations; the RCMcorr graphs overlap exactly with the EOBS curve and could be hardly distinguished from each other on Fig. 3.2.1a. The overestimation of the observed air temperature seen in Fig. 3.2.1a may seem small, but it becomes substantial in the annual mean (see the discussion below). The mean monthly precipitation deviates in most months only slightly from observations (DHMZ and EOBS) and annual cycles of both mean air temperature and mean total precipitation are, during the P0 (1961-1990) period, generally similar in all datasets considered (Fig. 3.2.1 a,b). A shortcoming of the EOBS data (Haylock et al. 2008) to correctly represent points (areas) at or near the coast for the reason that they were derived from the land points only was indicated by Patarčić et al. (2014).

Variation of both air temperature and precipitation in the DHMZ data is, in most months, slightly underestimated by EOBS (Fig. 3.2.1 c,d). This underestimation is likely due to the interpolation method applied to derive the EOBS gridded data. However, when the RCMcorr data are compared with the two observational datasets, much large differences in monthly variability become evident. For example, in the summer months, the Aladin RCMcorr largely overestimates both precipitation and particularly air temperature variability. For this geographic location, the bias corrected RegCM3 model (blue curve in Fig. 3.2.1 c,d) is reproducing reasonably well interannual variability. However, neither

model captures successfully the October maximum in the total precipitation coefficient of variation (i.e. standard deviation divided by the mean; Fig. 3.2.1 d).
Time series of the mean annual air temperature in the period 1951-2000 (Fig. 3.2.1e) indicates that the EOBS and RCMcorr values are higher than DHMZ observations, further confirming the overestimations of the DHMZ annual cycle shown in Fig 3.2.1a. A large year-to-year variation of the air temperature annual means differs among various data sources (Fig. 3.2.1e). This difference in the representation of interannual variability does not signify that a particular model failed to correctly simulate observed natural variability. It may be attributed to a different external forcing of the RCMs by different global circulation models, but also to a different internal variability inherent to each single RCM (see Methodology). Standard deviation of the annual mean air temperature time series in all data sources are quite similar (Table 3.2.1) indicating that the RCMs are close to observations in representing atmospheric natural variability.

Table 3.2.1: Pazin: mean and standard deviation of time series shown in Fig. 3.2.1 e) and f).

	t (°C)		P (mm)	
	1951-2000	1961-2000	1951-2000	1961-2000
RegCM3	12.5±0.6	12.6±0.6	1134±161	1127±155
Aladin	12.5±0.5	12.6±0.6	1136±231	1147±227
Promes	12.5±0.7	12.6±0.7	1117±216	1123±219
DHMZ		11.2±0.5		1133±193
EOBS	12.5±0.5	12.4±0.4	1129±175	1158±149

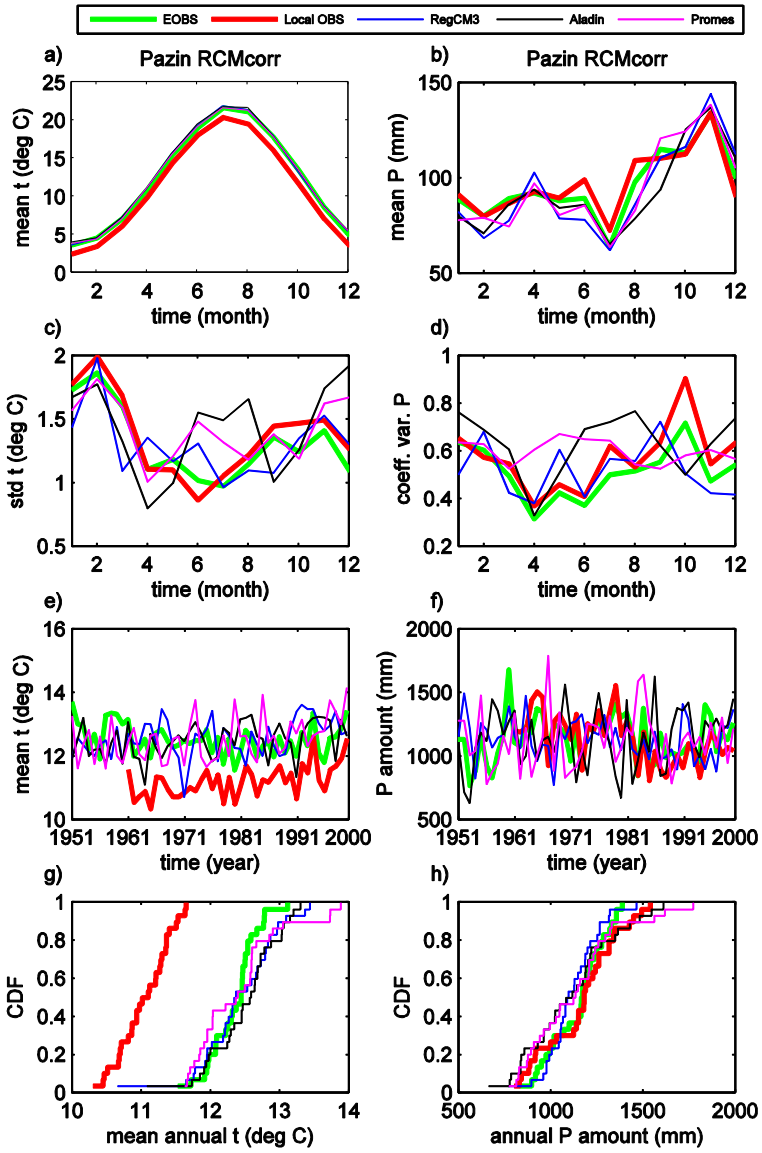

Figure 3.2.1 Pazin station: annual cycles a) mean monthly temperature, b) mean monthly precipitation amount, c) mean monthly temperature standard deviation, d) coefficient of variation of monthly precipitation amount; time series e) mean annual temperature, f) annual precipitation amount; empirical cumulative distribution functions CDFs g) mean annual temperature, h) annual precipitation amount. Model time series are RCMcorr. The analysis period is 1951-2000 in panels e) and f) and P0 (1961-1990) in all other panels.

For annual precipitation amounts, the EOBS and DHMZ datasets are relatively close to each other (Fig. 3.2.1f). The model values in some years tend to differ from the observations; however, no clear signal (overestimation or underestimation) is obvious. Standard deviations of the modelled annual precipitation vary between 14% and 20% and in effect agree with the standard deviation value of 17% for DHMZ data (Table 3.2.1).
In the empirical cumulative distribution functions (CDFs) a constant shift of the EOBS and RCMcorr data from the DHMZ observations in the P0 period is seen through all annual air

temperature ranges (Fig. 3.2.1g). For the annual total precipitation, however, a close correspondence is seen for all data sources (Fig. 3.2.1h). In the Promes model (cyan curve in Fig. 3.2.1 g,h), higher air temperature and precipitation amounts than in the other two models are simulated in that part of the CDFs associated with the highest mean annual values.

For the period 1951-2050, all three bias corrected models simulate statistically significant increasing trends in the mean annual temperature from 0.17 °C/10yr in RegCM to 0.31 °C/10yr in Promes (Fig. 3.2.2). It should be emphasised here that, in the model simulations for the period 1951-2000, the observed concentrations of the greenhouse gases (GHGs) is used, and in the period 2001-2050, the models were forced by the GHGs concentrations for the IPCC A1B scenario. In the period 1961-2012, when the DHMZ observations were available, all three models agree with the observations in the simulated sign of trend, but with a lower than DHMZ observed magnitude of trend (0.3 °C/10yr; Table 3.1.2.1). For the two periods analysed (1951-2050 and 1961-2012), linear trends of the simulated mean seasonal temperature are generally highest in the summer and in the Promes model (Table 3.2.2), and most of seasonal trends are statistically significant.

All three bias-corrected models simulate increasing trend in the annual precipitation amount for the period 1951-2050 (Fig. 3.2.3). However, in all the models, these trends are not statistically significant. For the period 1961-2012, when DHMZ observations at the Pazin station show statistically significant decreasing trend in annual precipitation amount (-52.5 mm/10yr; Table 3.1.2.2), only RegCM3 simulates the same sign of the trend as observed, but with greatly reduced amplitude and no statistical significance. Even for seasonal precipitation, trends are rarely statistically significant and are model dependent in terms of both the amplitude and sign (Table 3.2.3). This implies that, according to the CC-WaterS bias corrected RCMcorr simulations presented here, no robust estimates of significant precipitation change could be made for the first part of the 21st century.

Table 3.2.2 Pazin: decadal trends of seasonal and annual means of temperature. Statistically significant trends at the 5% level according to Mann-Kendall test are in bold. Units are °C/10 yrs.

	DJF		MAM		JJA		SON		Annual	
	1951-2050	1961-2012	1951-2050	1961-2012	1951-2050	1961-2012	1951-2050	1961-2012	1951-2050	1961-2012
RegCM3	**0.13**	0.06	**0.17**	0.03	**0.20**	0.14	**0.18**	**0.18**	**0.17**	0.09
Aladin	**0.23**	**0.24**	**0.20**	**0.21**	**0.31**	0.21	**0.25**	**0.26**	**0.25**	**0.22**
Promes	**0.34**	**0.37**	**0.31**	**0.31**	**0.37**	0.20	**0.25**	0.04	**0.31**	**0.23**

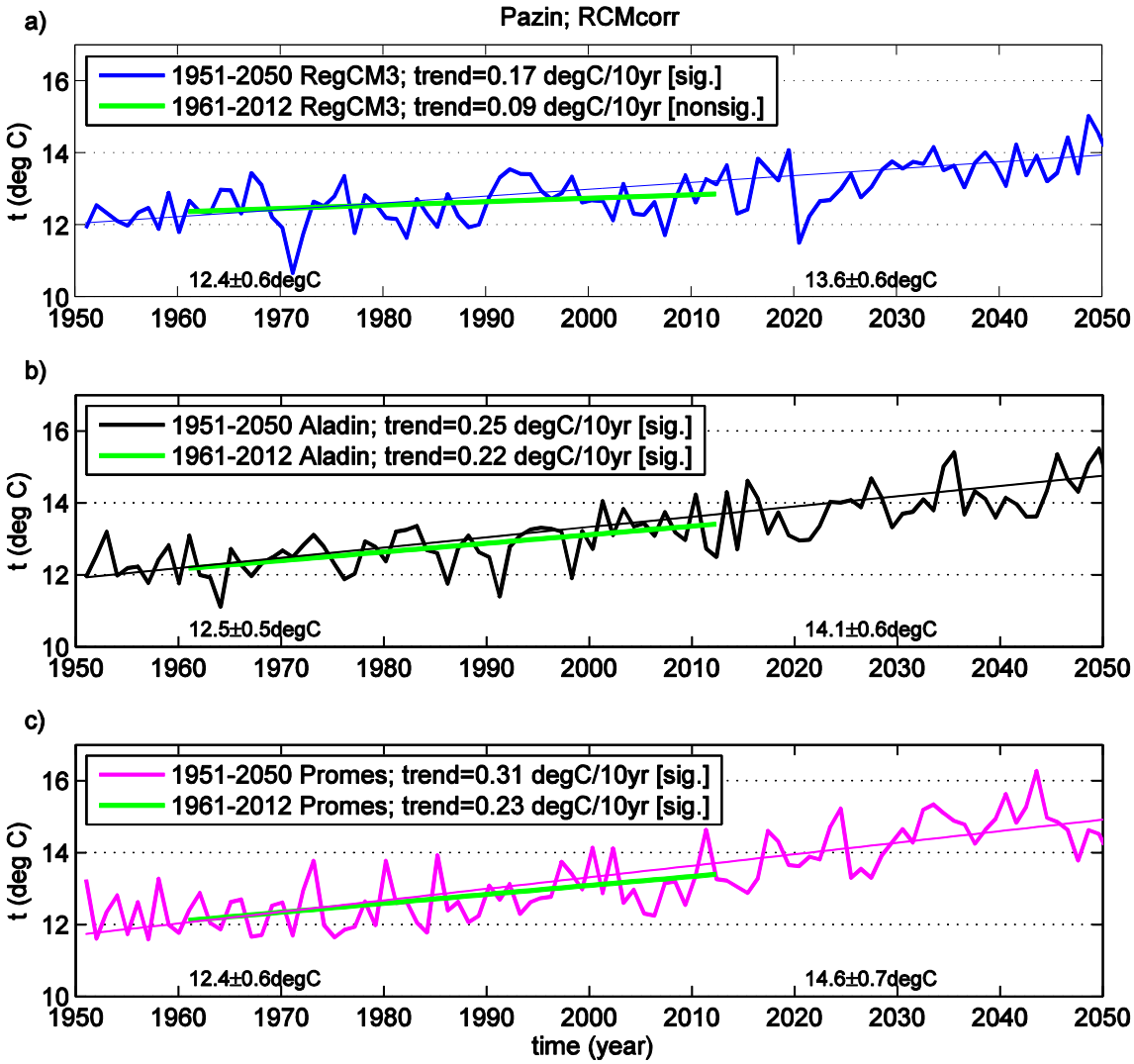

Figure 3.2.2 Pazin station: annual mean temperature and associated linear trend in a) RegCM3, b) Aladin, c) Promes. Trend based on the entire time series (1951-2050) is in the same colour as the corresponding time series and trend based on the 1961-2012 period is in green in every panel. The numbers at the bottom of each panel are mean values and standard deviations for the periods P0 (1961-1990) and P1 (2021-2050). The model time series are for RCMcorr.

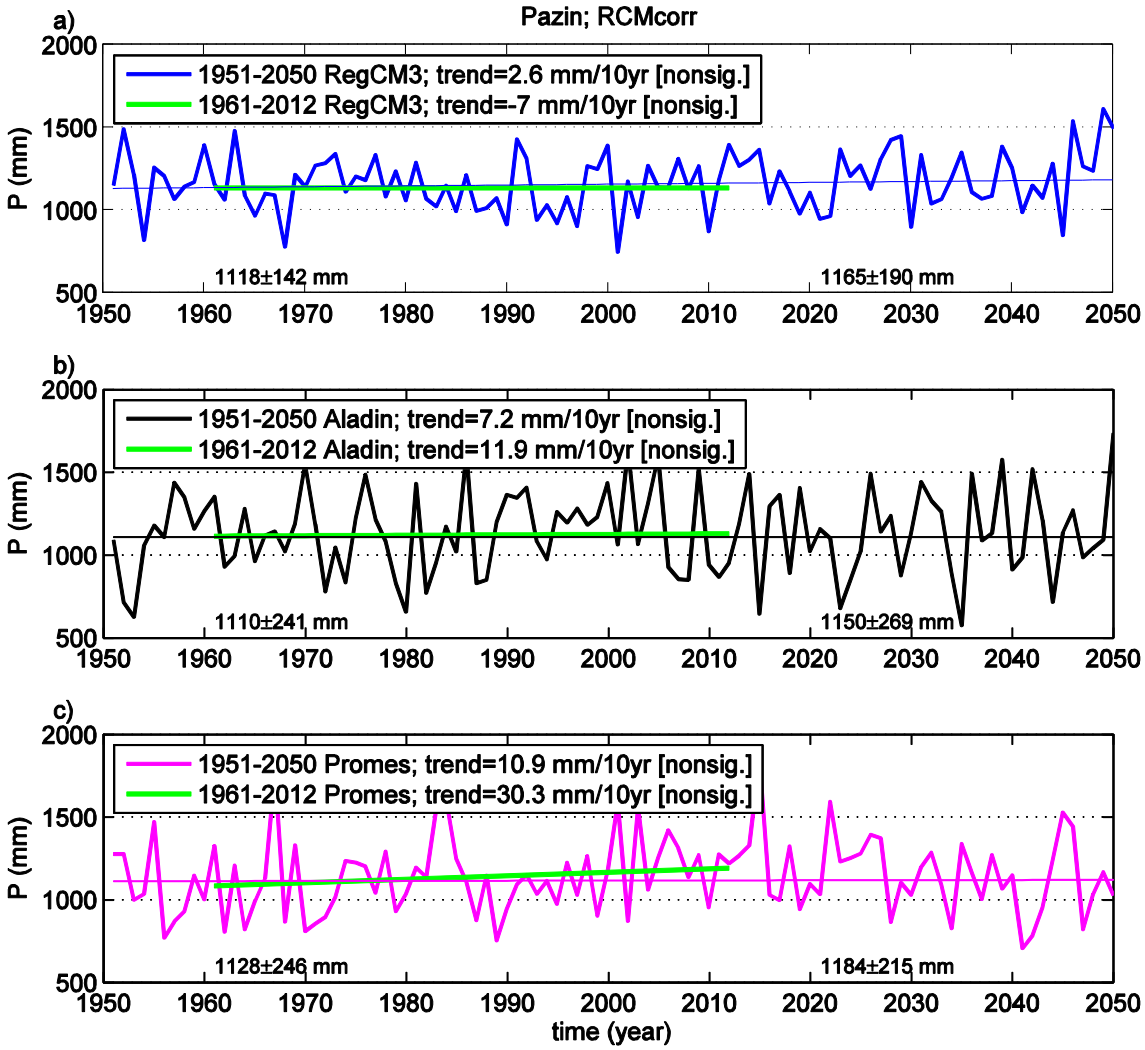

Figure 3.2.3 As Fig. 3.2.2 but for annual precipitation amounts.

Table 3.2.3 As Table 3.2.2 but for seasonal and annual precipitation amounts. Units are mm/10 yrs.

	DJF		MAM		JJA		SON		Annual	
	1951-2050	1961-2012	1951-2050	1961-2012	1951-2050	1961-2012	1951-2050	1961-2012	1951-2050	1961-2012
RegCM3	4.2	2.4	-0.5	-2.8	-2.2	-7.7	-0.2	-0.4	2.6	-7.0
Aladin	-4.2	-4.4	2.4	-7.4	1.9	8.2	7.5	18.4	7.2	11.9
Promes	3.6	19.0	**5.5**	-6.9	-1.1	**21.4**	2.8	-6.5	10.9	30.3

Since bias correction of the RCM values (RCMcorr) is based on the EOBS data, the differences between EOBS and DHMZ observations, clearly seen in Fig. 3.2.1, require an additional adjustment of the RCMcorr values to be comparable with the DHMZ data. Thus, the adjustment differences are computed for RCMcorr from DHMZ values for each month *i* (*i*=1,…,12) in the P0 period as adj(*i*)=RCMcorr(*i*)-DHMZ(*i*), where RCMcorr(*i*) and DHMZ(*i*) are monthly temperature averages (or precipitation sums) from a RCM and observations, respectively. These adjustment differences are then applied on the RCMcorr time series for the whole analysed period (1951-2050) to obtain RCMcorr_adj in the following manner: RCMcorr_adj(*i,j*)=RCMcorr(*i,j*)-adj(*i*); *i*=1,…12; *j*=1951, …, 2050.

The adjustment differences between RCMcorr and DHMZ in the P0 for air temperature are between 0.8 °C in the spring and 2.1 °C during the late summer (i.e. the bias corrected models RCMcorr are warmer than the DHMZ observations) and, in most cases, are statistically significant (Fig. 3.2.4 a). For precipitation, differences are generally between -30 mm and +20 mm, but are statistically significant only in few cases (Fig. 3.2.4 b). The magnitude of the adjustment differences is similar for all three models, which is expected since the adjustment is applied on the RCMcorr (not on the raw RCM output). An analysis of the raw RCM output is not made in this study; however, generally, for different models, different amplitude and sign of the systematic errors can be expected.

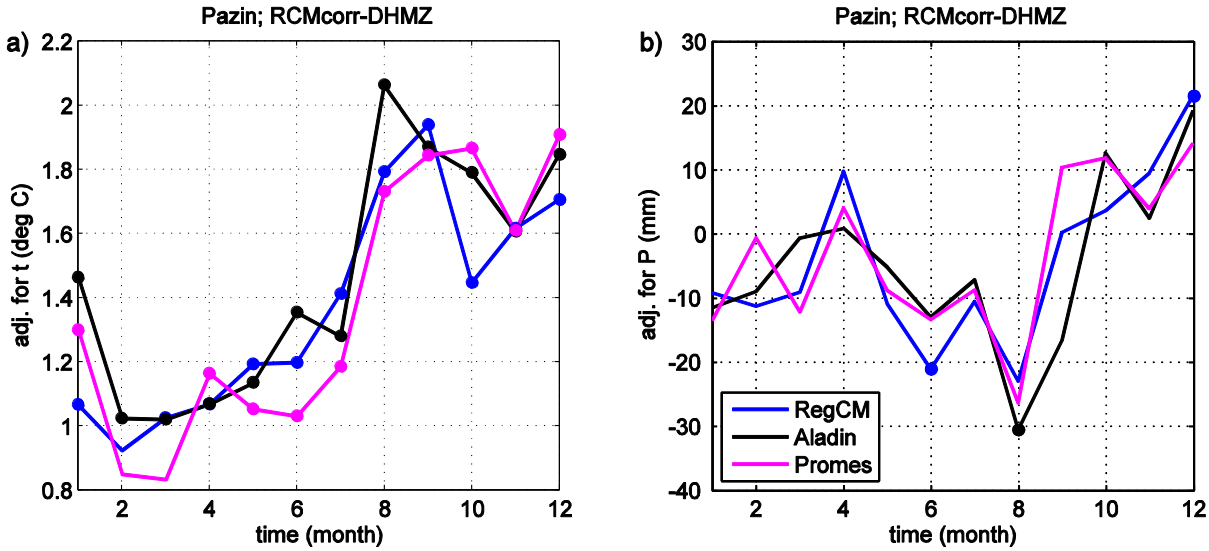

Figure 3.2.4 Pazin station: adjustment differences a) mean monthly temperature b) mean monthly precipitation amounts. Differences are based on the 1961-1990 period. The availability of DHMZ observations in this period was 100%. Statistically significant differences according to the Wilcoxon-Mann-Whitney non-parametric rank-sum test at the 5% significance level are marked by the solid circles.

For air temperature, the impact of the adjustment procedure is seen as a shift of the model annual cycles towards the DHMZ observations: they coincide now exactly with that for DHMZ (Fig. 3.2.5 a). Similar is the case for precipitation (Fig. 3.2.5 b), where mean annual cycles of all models now overlap with DHMZ observations in the P0 period.

For air temperature standard deviation, no changes are seen (Fig. 3.2.5c) since the additive nature of the adjustment does not affect variations in the annual cycle. For the total precipitation coefficient of variation, a general improvement is seen, in particular for the Aladin model (Fig. 3.2.5d) where in the summer RCMcorr_adj is now much closer to observational datasets than RCM_corr in Fig. 3.2.1d.

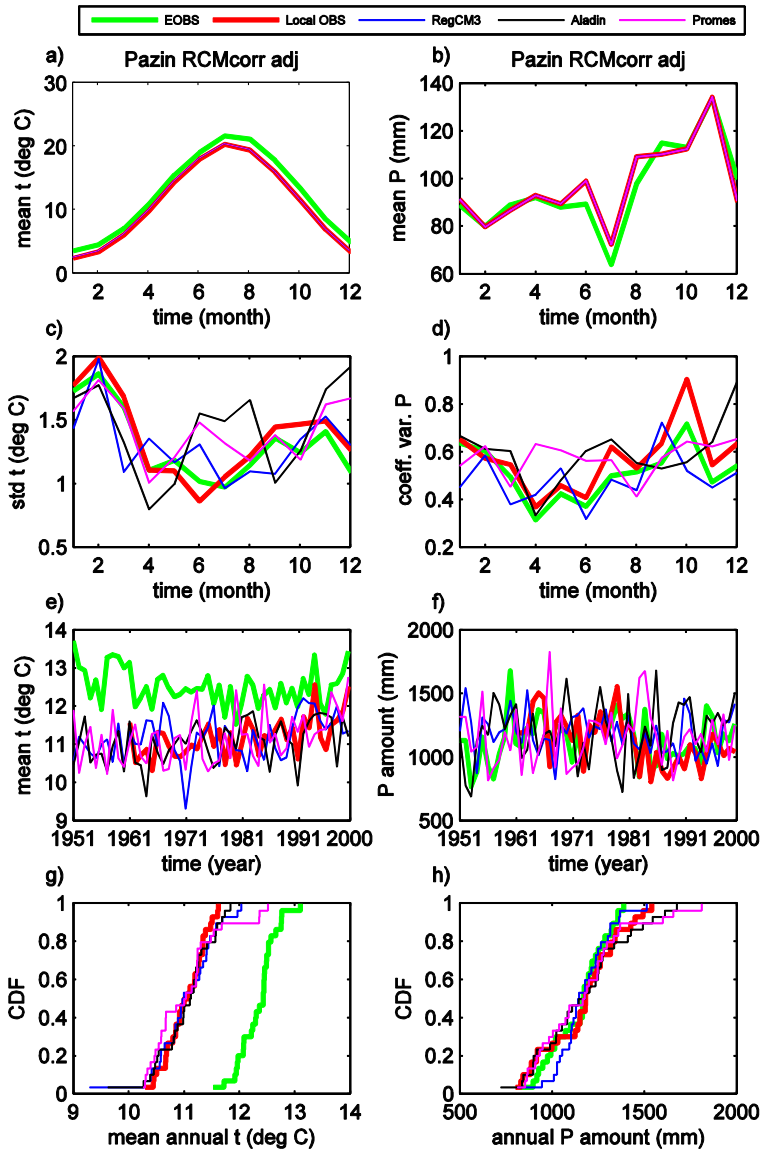

Figure 3.2.5 As Figure 3.2.1 but for the adjusted model data RCMcorr_adj.

The only change in the annual precipitation time series after the adjustment (Fig. 3.2.5f) is a slight, almost negligible reduction of precipitation amounts in comparison with Fig. 3.2.1f. For air temperature (Fig. 3.2.5e), a clear shift of the model data towards DHMZ observations is seen. A similar shift is also seen in the model CDFs for temperature (Fig. 3.2.5g), whereas for precipitation no major differences between RCMcorr and RCMcorr_adj can be noticed.

Lastly, we analyse projected climate changes for the RCMcorr data; similar results are obtained for the RCMcorr_adj data because of the additive nature of the applied adjustment. All three regional climate models simulate an increase in mean monthly air temperature from the reference period 1961-1990 to the future period 2021-2050. The projected warming is in most cases statistically significant and ranges between 0.5 °C in RegCM3 for December and 3 °C in Promes for July (Fig. 3.2.6 a). The Promes model tends to simulate a larger temperature increases for most months in the year than the other two models. As for precipitation, the projected changes between P0 and P1 are statistically significant only in two cases although the models are relatively close to each other. It appears that the prevalent sign of changes indicates an increase in precipitation (i.e. most changes are positive); however, they vary in amplitude generally between -20% and 20% (Fig. 3.2.6 b).

The warming signal in all three models is also present in the empirical cumulative distribution functions CDFs of the mean annual temperature (Fig. 3.2.6 c). For all three models, CDF in the P1 period is, according to the Kolmogorov-Smirnov test. For all three models, CDFs of annual precipitation amounts in the P0 and P1 periods are not significantly different (Fig. 3.2.6 d).

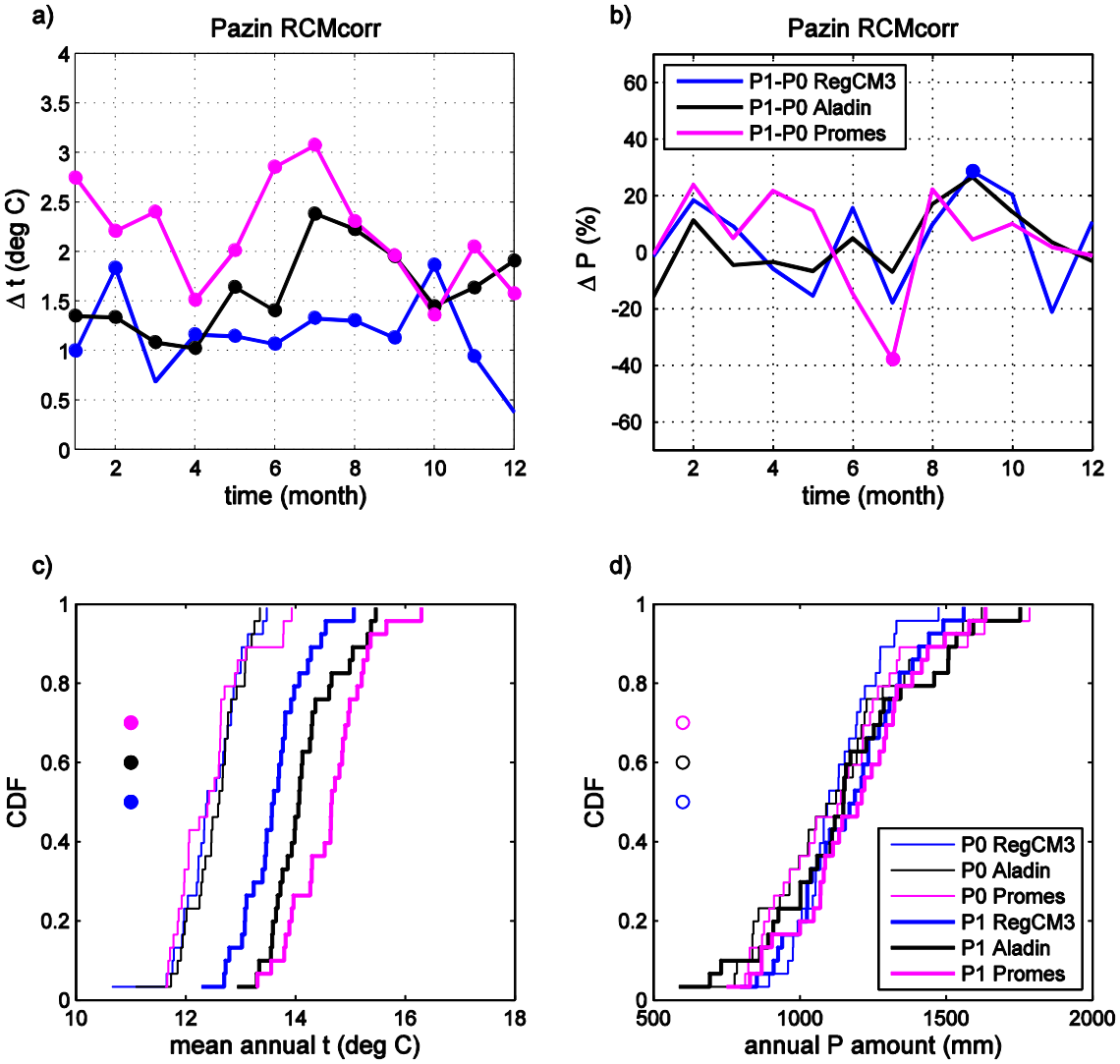

Figure 3.2.6 Pazin station: P1 vs. P0 change for a) monthly mean temperature (in °C); b) relative monthly precipitation change (in %); c) empirical cumulative distribution functions CDFs of mean annual temperature in P0 and P1; d) same as c) but for annual precipitation amount. Time periods are: P0 1961-1990 and P1 2021-2050. Statistically significant differences in a) and b) according to the Wilcoxon-Mann-Whitney nonparameteric rank-sum test at the 5% significance level are marked by solid circles. Statistically significant differences according to the Kolmogorov-Smirnov test at the 5% significance level between CDFs in the two periods for every model in panels c) and d) are marked by solid circles. Model time series are RCMcorr.

3.3. Meteorological database and analysis of local observations for Prud Spring catchment (pilot area 2: Prud catchment and Korčula)

This chapter provides the general climate characteristics and the observed climate variability and trends in the lower Neretva river catchment (pilot area 2: Prud catchment and Korčula). Over the spring Prud catchment, that belongs to the Neretva river catchment, there is no active meteorological station. Therefore, the climatological analysis for the air temperature and precipitation data series is deduced from the meteorological station Opuzen (altitude h = 3ma.s.l., φ = 43° 1' 3", λ = 17° 33' 31") located at the mouth of the Neretva river in the southern Croatian Adriatic coastal region. The analysis is based on monthly, seasonal and annual averages of air temperature and precipitation amounts over the reference climate period 1961-1990. The results may serve as the basis for a hydrological analysis relevant for water supply estimates as well as to the validation of the simulated possible climate changes.

3.3.1 Climate

The climate characteristics of the spring Prud catchment are determined by the mid-latitude air circulation and modified by the influence of the sea that reaches deep into the mainland through the valley of the Neretva River, to a lesser extent they are governed by the altitude, relief configuration, soil type, etc. The geographical latitude determines primarily the amount of sunshine and radiation that the area receives during the year, and, on the other hand, it determines the general atmospheric circulation systems which form the weather and the climate. It is under the influence of the subtropical high pressure zone during summer , with dry and warm weather. The sea, with its large thermal capacity, moderates air temperature extremes: it has cooling effect in summer and reduces the cold in winter . In contrast to the Neretva River valley, the climate of the Prud area is also largely determined by local orography that prevents a direct influence of the sea. The carstic soil type of the neighbouring hills contributes to warming in the summer. During the cold part of the year the area is within the zone of the main western winds that dominate mid-latitudes, with a constant change of low and high pressure systems.
The local climate characteristics are described for the years 1961-1990, the period recommended by the World Meteorological Organization as the referent period for the present climate conditions. Seasonality is described in terms of annual cycle of the mean monthly air temperature and precipitation, and their interannual variability by standard deviation of monthly means and coefficient of variation for precipitation. The discussion of extremes in the annual and seasonal air temperature and precipitation averages is based on percentiles calculated from the empirical cumulative distribution function (CDF).

Air temperature

Air temperature depends mainly on the length and intensity of solar radiation, and partly on the composition of land surface (e.g. soil type, vegetation) and on topography.

The annual cycle of air temperature monthly averages over the spring Prud catchment within the lower Neretva river catchment has maritime characteristics with autumn being warmer than spring by 1.8°C on average (Table 3.3.1.1). The winters are mild with average air temperature of 7.4°C and the summers are moderately warm (23.8°C). On average, July is the warmest month with an average air temperature of 24.9°C, followed by August (24.2°C). In some years, the coldest month may be with equal probability January, February or December, and on average the coldest month is January (6.5°C).
Standard deviation of mean monthly air temperature ranges between 0.8°C (July) to 1.9°C (February) indicating that interannual variability is small due to a strong influence of the sea, which moderates the air temperature extremes (Fig. 3.3.1.11b). July is the least likely to change its thermal character and February is the most unstable month.
Empirical cumulative distribution of the mean annual air temperature for Opuzen is shown in Fig.3.3.1.1c. The percentiles that determine extreme values of annual and seasonal mean temperatures are given in Table 3.3.1.2. In the annual cycle of the percentiles for mean daily air temperature, the difference between the 98th percentile and the 2nd percentile is the largest in February (6.8°C) and November (6.6°C) and the smallest in July (2.6°C). These differences are reflected in seasonal differences: the largest are in the autumn (3.7°C) and winter (3.4°C).

Table 3.3.1.1 Basic statistics (mean, standard deviation, maximum and minimum) for annual and seasonal mean air temperature from the reference period 1961-1990 for the Opuzen meteorological station.

	DJF	MAM	JJA	SON	Year
mean	7.4	14.5	23.8	16.3	15.5
stdev (°C)	1.0	0.9	0.5	0.9	0.4
max (°C)	9.1	15.9	24.9	18.0	16.2
min (°C)	5.4	12.3	22.6	13.9	14.6

Table 3.3.1.2 The percentiles for annual and seasonal mean air temperature empirical distribution from the reference period 1961-1990 for the Opuzen meteorological station.

	DJF	MAM	JJA	SON	Year
1	5.4	12.3	22.6	13.9	14.6
2	5.5	12.4	22.6	13.9	14.6
5	5.7	12.9	22.8	14.4	14.8
10	5.8	13.3	23.1	15.1	14.8
90	8.5	15.7	24.5	17.4	16.1
95	8.8	15.8	24.7	17.8	16.2
98	9.1	15.9	24.9	18.0	16.2
99	9.1	15.9	24.9	18.0	16.2

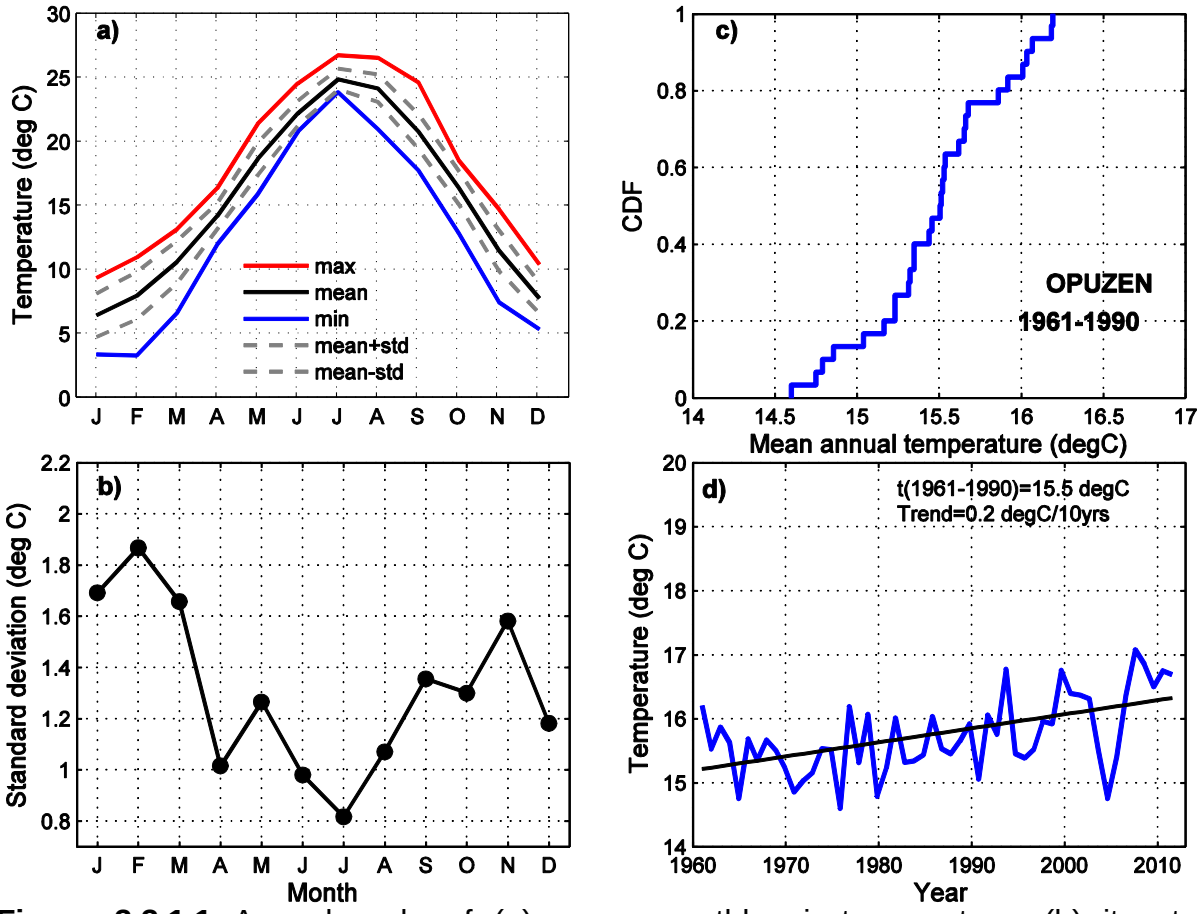

Figure 3.3.1.1 Annual cycle of (a) mean monthly air temperature, (b) its standard deviation, (c) cumulative distribution of mean annual air temperature for the period 1961-1990 and (d) time series of mean annual air temperature with fitted trend line for the period 1961-2012 for the meteorological station Opuzen.

Precipitation

Precipitation is mainly dependent on the air circulation and moisture content, and their variation during the year influences precipitation seasonality. The spring Prud catchment within the lower Neretva river catchment has the maritime annual cycle. The differences in annual total precipitation between the locations at low altitudes (e.g. Opuzen 3 m) and parts of the basin at about 400 m a.s.l. (e.g. Veliki Prolog 433 m) are higher in the cold part of the year (21% to 38%) than in the warm part (up to 14%). During the cold half-year (October to March) this area receives more precipitation than in the warm half year (on average 66% of the annual total in Opuzen and 70% in Veliki Prolog). Monthly amounts are above 150 mm from October to December in Opuzen (the Neretva River delta) and at the higher altitudes distant from the sea (Veliki Prolog) they occur from October to March

having maximum in November (180 mm in Opuzen and 221 mm in Veliki Prolog). The lowest monthly precipitation amounts occur in the warm period of the year (April to September). The summer precipitation amounts slightly over 13% of the annual precipitation (Table 3.3.1.3), and the monthly minimum is in July (36 mm).
In some years a significant deviation in monthly amounts from the average precipitation conditions is observed (Fig. 3.3.1.2b). There were years when in the autumn and winter months, with normally abundant precipitation, less than half of the monthly average precipitation was recorded. In the summer months there were occurrences of very little or no rain, or on the other hand, that the average monthly amount was exceeded several times over. Coefficient of variation indicates such a high interannual variation in the mean monthly precipitation amounts that are higher than 50% (April).
Cumulative distribution function (CDF) of annual precipitation is shown in Fig. 3.3.1.2c. The percentiles that determine extreme values are given for annual and also for seasonal precipitation in Table. 3.3.1.4. The empirical CDF gives an insight into the shape of the precipitation distribution indicating the expecting probabilities of the observed amounts. According to the Opuzen data, the annual precipitation amount over 1637 mm can be expected once in 10 years (90th percentile), and over 1727 mm once in 50 years (98th percentile). For all observed return levels at the right tail of the distribution (90th to 99th percentile) the highest seasonal values of precipitation amounts can be found for the winter and autumn. Differences between these two seasons decrease for higher percentiles (Table 3.3.1.4). On the other hand, extremely dry seasons are those with precipitation amounts lower than the 2nd percentile. This value is the lowest for summer (21 mm) and the highest for autumn (182 mm). On monthly scale, there may be no precipitation at all from July to October and in January, while for other months the 2nd percentile values range between 11 mm and 34 mm (not shown).

Table 3.3.1.3 Basic statistics (mean, standard deviation, coefficient of variation, maximum and minimum) for annual and seasonal precipitation amount from the reference period 1961-1990 for Opuzen meteorological station.

	DJF	MAM	JJA	SON	Year
mean	416.3	281.9	170.4	436.2	1308.
stdev (mm)	184.0	100.5	82.1	156.2	223.4
cv (mm)	0.4	0.4	0.5	0.4	0.2
max (mm)	851.4	549.7	342.1	739.5	1734.
min (mm)	69.5	95.0	33.8	173.0	710.3

Table 3.3.1.4 The percentiles for annual and seasonal precipitation empirical distribution from the reference period 1961-1990 for Opuzen meteorological station.

	DJF	MAM	JJA	SON	Year
1	69.5	95.0	33.8	173.0	710.3
2	72.6	97.3	35.4	174.7	725.9
5	100.1	117.8	49.5	189.5	866.5
10	128.9	159.0	61.3	227.6	1047.0
90	659.3	417.6	296.3	667.1	1636.5
95	768.7	492.7	331.1	694.3	1661.0
98	843.1	544.0	341.0	735.0	1727.2
99	851.4	549.7	342.1	739.5	1734.6

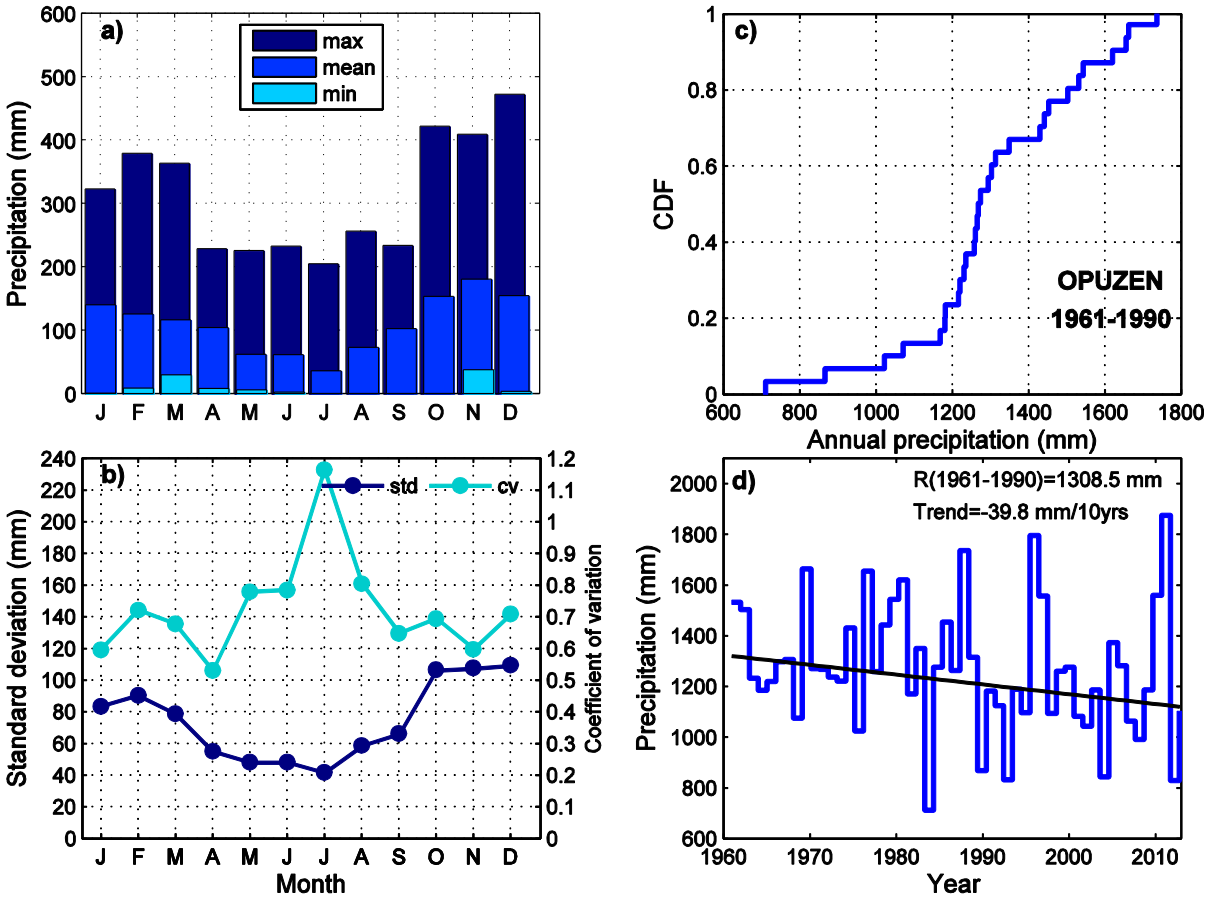

Figure 3.3.1.2 Annual cycle of (a) mean monthly precipitation amounts, (b) standard deviation and coefficient of variation, (c) cumulative distribution of annual precipitation amounts for the period 1961-1990 and (d) time series of annual precipitation amounts with fitted trend line for the period 1961-2012 for the meteorological station Opuzen.

3.3.2 Trends

Trends in seasonal and annual mean monthly air temperature and precipitation amounts are calculated for the period 1961-2012. They have been estimated by means of Kendall's tau method (or Sen's slope; Sen 1968). The trends are expressed as decadal values for both variables. Additionally, trends in precipitation amounts are given as the percentage of corresponding seasonal and annual means from the 1961-1990 period. The statistical significance of trends is estimated by the non-parametric Mann–Kendall test (Gilbert 1987).
Time series of the mean annual air temperature and precipitation amounts, with associated trend lines and their mean values from the reference period 1961-1990 are shown in Fig 3.3.1.1d and Fig. 3.3.1.2d, respectively.
During the period 1961-2012, the mean annual air temperature anomalies are mainly positive. During the recent 20 years air temperature trend is amplified. The consequence of such temperature fluctuations is that eight out of ten warmest years in the observed 52-years period were recorded in the first decade of the 21st century. This amplification in the temperature trend(s) is in accordance with observed regional and global warming (IPCC 2007). The annual trend reveals the statistically significant increase in the mean air temperature of 0.2°C/10yrs since 1961 according to the Opuzen data (Table 3.3.2.1). The annual temperature increase is predominantly due to a significant increase in the summer (0.3°C/10yrs) and spring (0.2°C/10yrs) mean air temperature.

Table 3.3.2.1 Decadal air temperature trends (°C/10yrs) trends for Opuzen meteorological station based on the 1961-2012 data series. Trends significant at the 5% level are bolded. For each season two trend values are given, according to different methods: Sen's slope (left value) and least square estimator (right value).

	DJF		MAM		JJA		SON		Year	
°C/10yrs	0.2	0.1	**0.2**	**0.2**	**0.3**	**0.4**	0.1	0.1	**0.2**	**0.2**

The trends in precipitation amounts reveal drying in the annual (-3.0 %/10yrs) and seasonal amounts according to Opuzen data, although they are not statistically significant. The main contribution to annual drying primarily comes from the reduction in summer precipitation totals (-8.2%/10yrs).

Table 3.3.2.2 Decadal precipitation trends (mm/10yrs and %/10yrs) for Opuzen meteorological station based on the 1961-2012 data series. For each season two trend values are given, according to different methods: Sen's slope (left value) and least square estimator (right value).

	DJF		MAM		JJA		SON		Year	
mm/10y	-6.5	-0.9	-0.3	-1.3	-	-	-9.3	-	-	-
%/10yrs	-1.6	0.1	-0.1	-0.4	-8.2	-6.2	-2.1	-2.3	-3.0	-2.4

The combined influence of observed meteorological parameters, air temperature and precipitation, effects water balance components. The detected increase in air temperature in spring and summer causes an increase in evapotranspiration. When associated with a decreasing tendency in precipitation in all seasons, but especially in summer, the precipitation deficit is expected to increase in the warm season. At the same time runoff and the filling of aquifers in autumn and winter could be reduced due to negative precipitation trends in these seasons, and could have impact on water supply.

3.4. Regional climate model simulations: Opuzen climatological station

Bias corrected simulations, RCMcorr, of the three regional climate models, DHMZ observations and EOBS data in the historical period 1961-1990 for the Opuzen climatological station are compared in Fig. 3.4.1. The EOBS annual cycle shows a lower air temperature when compared to DHMZ observations, which is the opposite of the DHMZ and EOBS annual cycles for the Pazin station shown in Fig. 3.2.1. Due to the nature of the bias correction applied to regional climate models, this makes RCMcorr also colder than the DHMZ observations; all RCM graphs overlap with that of EOBS (Fig. 3.4.1 a). For precipitation, an underestimation of DHMZ observation by EOBS and RCMs is seen, which is particularly large in the colder part of the year (Fig. 3.4.1 b).

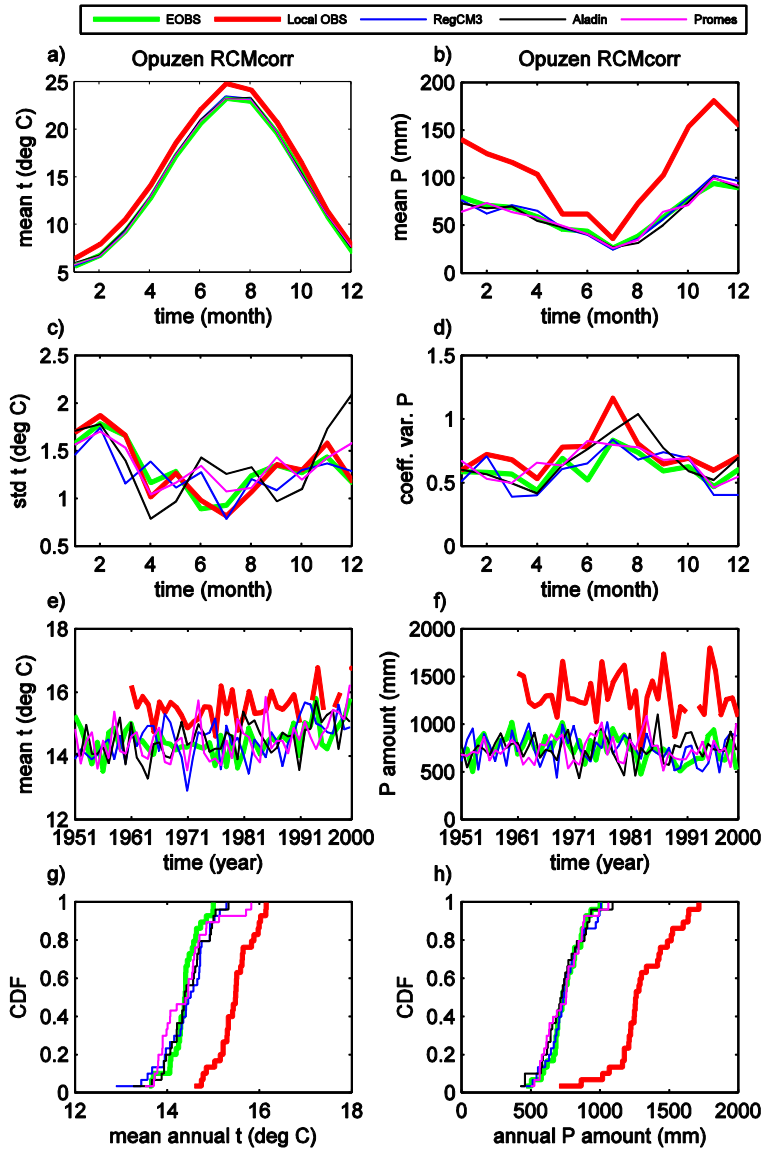

Figure 3.4.1 Same as Fig. 3.2.1 but for the Opuzen station.

For the air temperature standard deviation and total precipitation coefficient of variation some differences between RCMcorr and the two observational datasets are seen (Fig. 3.4.1 c,d). Whereas for this location Aladin RCMcorr overestimates air temperature variability in the summer and at the end of the year, bias corrected RegCM3 and Promes reproduce reasonably well interannual variability of both temperature and precipitation (Fig. 3.4.1 c,d). However, the models were not successful in capturing the July maximum in total precipitation coefficient of variation found in DHMZ observations (Fig. 3.4.1d). This maximum is also underestimated in the EOBS data.
Time series of the mean annual air temperature and annual precipitation amounts in the 1951-2000 period confirm the above-discussed relationship among the five datasets: EOBS and RCMcorr air temperature and annual precipitation are lower than DHMZ

observations (Fig. 3.4.1 e,f; Table 3.4.1). The empirical cumulative distribution functions CDFs of the annual data in the P0 period again show a constant shift of the EOBS and RCMcorr air temperature and precipitation amount from DHMZ observations (Fig. 3.4.1 g,h). Additionally, there is a tendency of the Promes model, similar to the result for the Pazin location, to simulate higher air temperature than the other two models in the part of CDFs which is associated with the highest mean annual air temperatures in the P0 period.

Table 3.4.1: Opuzen: mean and standard deviation of time series shown in Figs. 3.4.1 e) and f).

	t (°C)		P (mm)	
	1951-2000	1961-2000	1951-2000	1961-2000
RegCM3	14.5±0.6	14.6±0.6	743±150	745±148
Aladin	14.5±0.5	14.5±0.5	743±134	744±144
Promes	14.5±0.6	14.5±0.6	733±129	738±139
DHMZ		15.6±0.5		1300±226
EOBS	14.5±0.5	14.5±0.5	742±132	740±130

All three bias corrected models simulate statistically significant increasing trends in the mean annual temperature for the period 1951-2050 amounting to 0.19 °C/10yrs in RegCM, 0.27 °C/10yrs in Aladin and 0.31 °C/10yr in Promes (Fig. 3.4.2). For the period corresponding to the available DHMZ observations (1961-2012), all three models agree with observations in the sign of trend, and simulated trend slopes, except for RegCM3, are close to the observed slope (i.e. 0.2 °C/10yrs in DHMZ observations for Opuzen;Table 3.3.2.1). Similar to the Pazin climatological station, trends of the mean seasonal temperature are highest for the summer season and when using the Promes model, and are statistically significant in most cases (Table 3.4.2).
For annual precipitation in the period 1951-2050, RegCM3 and Aladin simulate an increasing trend while Promes simulates a decreasing trend (Fig. 3.4.3); however, these trends are not statistically significant. For the period 1961-2012, when the DHMZ annual precipitation amounts show a non-significant decreasing trend (i.e. -31.8 mm/10yr;Table 3.3.2.2), all models simulate trend of the opposite sign with increasing trends slopes smaller than 5 mm/10 yrs. Again, the climate change signal of the CC-WaterS simulations is weak for the first part of the 21st century and no significant trends in seasonal precipitation are found (Table 3.4.3).

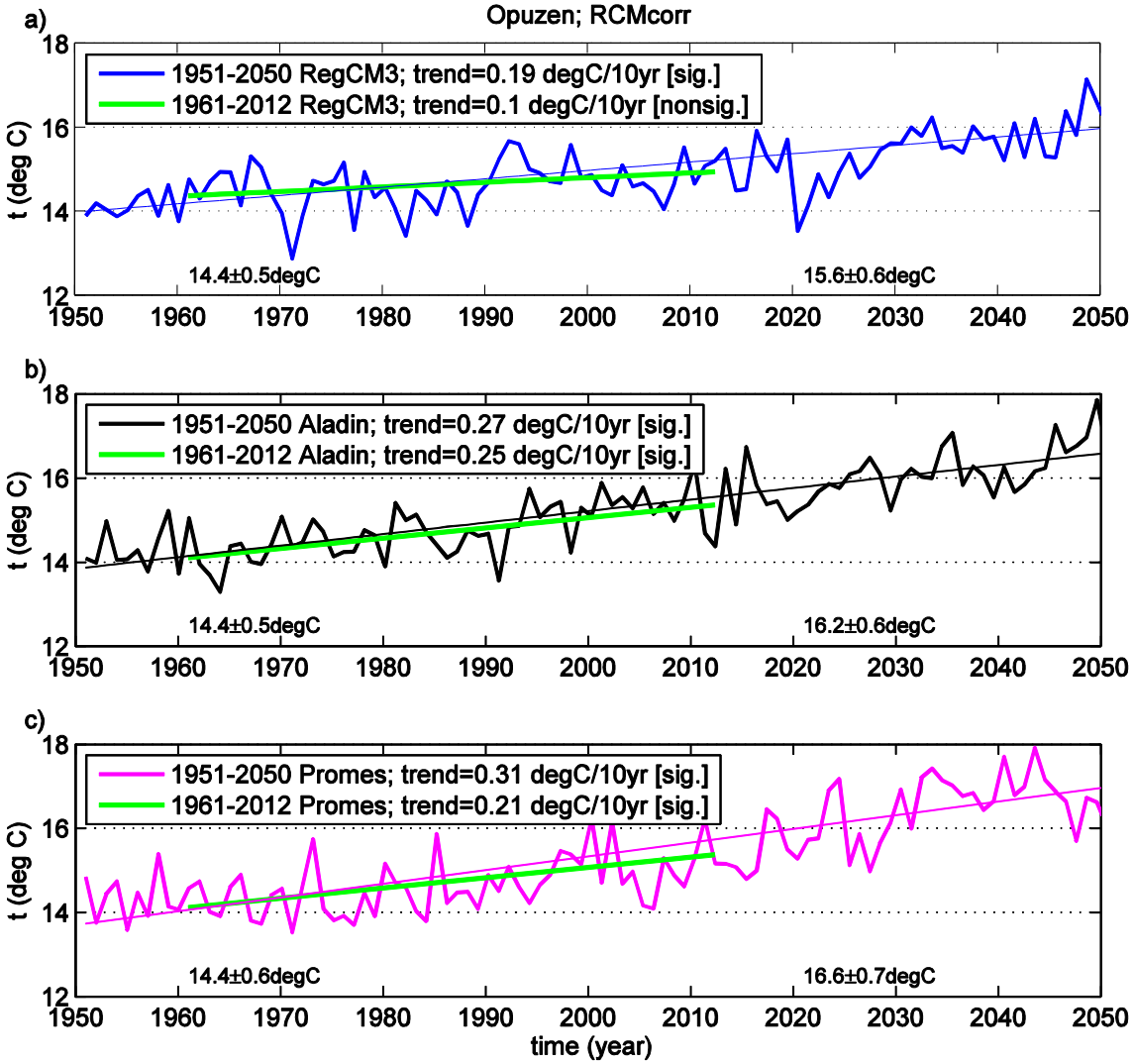

Figure 3.4.2 Same as Fig. 3.2.2 but for the Opuzen location.

Table 3.4.2 Opuzen: decadal trends of seasonal and annual means of temperature. Statistically significant trends at the 5% level according to Mann-Kendall test are in bold. Units are °C/10 yrs.

	DJF		MAM		JJA		SON		Annual	
	1951-2050	1961-2012	1951-2050	1961-2012	1951-2050	1961-2012	1951-2050	1961-2012	1951-2050	1961-2012
RegCM3	**0.15**	0.09	**0.18**	0.05	**0.21**	0.13	**0.20**	**0.18**	**0.19**	0.10
Aladin	**0.19**	0.18	**0.24**	**0.26**	**0.37**	**0.34**	**0.28**	**0.25**	**0.27**	**0.25**
Promes	**0.27**	**0.30**	**0.31**	**0.34**	**0.39**	**0.20**	**0.27**	0.03	**0.31**	**0.21**

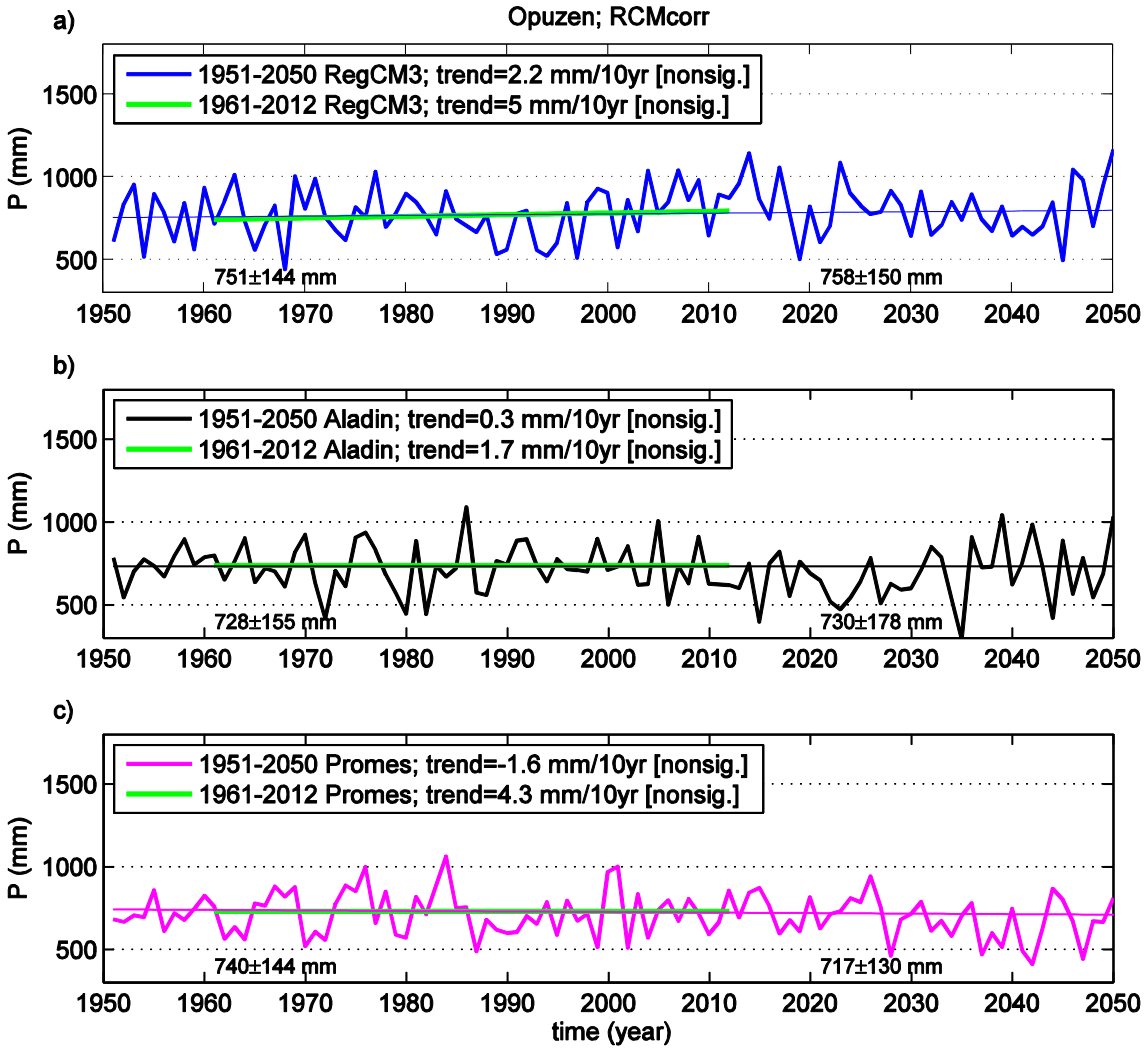

Figure 3.4.3 Same as Fig. 3.2.3 but for the Opuzen location.

Table 3.4.3 Opuzen: decadal trends of seasonal and annual precipitation amounts. Statistically significant trends at the 5% level according to Mann-Kendall test are in bold. Units are mm/10 yrs.

	DJF		MAM		JJA		SON		Annual	
	1951-2050	1961-2012	1951-2050	1961-2012	1951-2050	1961-2012	1951-2050	1961-2012	1951-2050	1961-2012
RegCM3	3.5	3.6	-0.3	-3.7	1.7	0.5	-3.3	4.6	2.2	5.0
Aladin	**-6.1**	-6.2	0.9	-2.5	-0.6	-1.5	6.9	13.1	0.3	1.7
Promes	-3.0	6.7	3.6	-7.9	-1.9	6.8	-0.5	-4.5	-1.6	4.3

RCMcorr_adj time series for the Opuzen station are prepared in the same manner as described for the Pazin station in section 3.2. The adjustment differences between RCMcorr and DHMZ in P0 are negative throughout the year. They range between -1.8 in the summer and -0.2 °C in December, i.e. the bias corrected models, RCMcorr, are colder than the DHMZ observations and the differences are statistically significant for all three models in most of the year except in winter (Fig. 3.4.4 a). For precipitation, the adjustment differences for all three models are also negative, i.e., the bias-corrected models are between -80 mm and -10 mm wetter than observations. The differences are statistically significant in the most of the year except from May to July (Fig. 3.4.4 b). The magnitude of adjustment differences is similar in all three models, which is expected since the adjustment is applied on the already corrected time series (RCMcorr) and not on the raw RCM output.

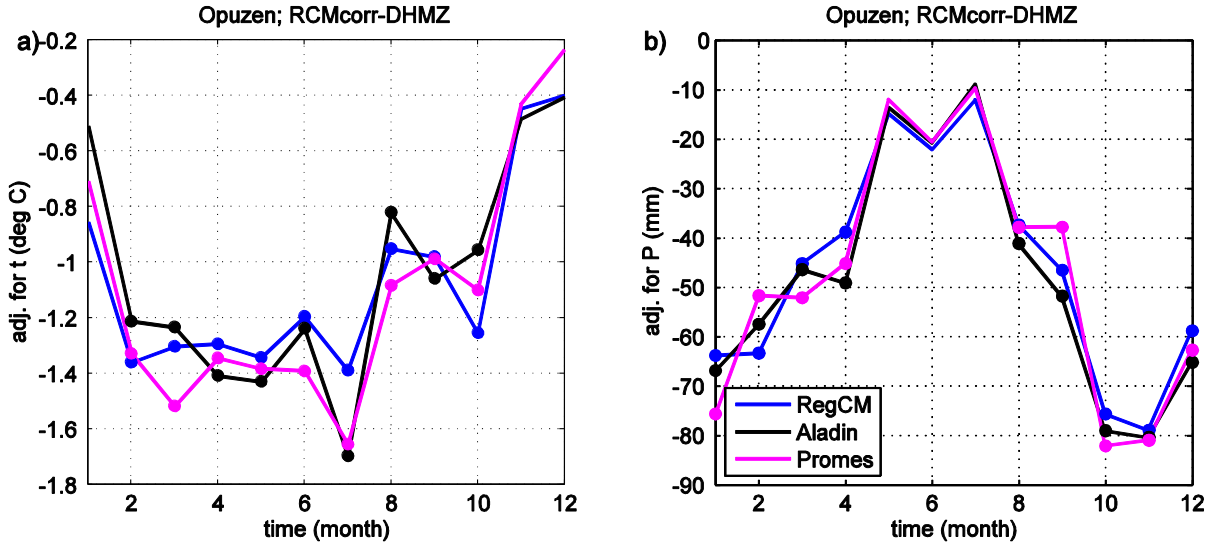

Figure 3.4.4 Same as Fig. 3.2.4 but for the Opuzen location.

The impact of the adjustment procedure is seen, similar to what was discussed for the Pazin station, as a shift in the model annual cycles and time series towards the DHMZ observations (Fig. 3.4.5 a, b, e, f); for precipitation, the model adjusted annual cycles now fully overlap with observations. However, the precipitation coefficient of variation is reduced in all three models, which may be interpreted as deterioration in the RCMcorr_adj data.

For the projected climate changes of the RCMcorr data an increase in the mean air temperature by mid-21st century, i.e. in P1 relative to P0, is simulated by all three RCMs (RCMcorr; Fig. 3.4.6a). The projected warming in the 2021-2050 period ranges between 0.5 °C and nearly 3.5 °C and in most cases is statistically significant. The Promes model tends to simulate a larger temperature increase than the other two models (similar as in the case of the Pazin station). On the other hand, the amplitude of projected precipitation change varies greatly throughout the year from one model to the other (between -60% and +60% in P1 relative to P0), but even so it is almost insignificant (Fig. 3.4.6 b). The range of precipitation changes is larger than for the Pazin station.

The warming signal is also present in the empirical cumulative distribution functions, CDFs, of the mean annual temperature (Fig. 3.4.6 c), and for all three models, CDFs in P1 and P0 periods are significantly different according to the Kolmogorov-Smirnov test at the 5% significance level. Corresponding CDFs for the annual precipitation are not significantly different (Fig. 3.4.6 d). In terms of CDFs, the results for both Opuzen and Pazin stations are similar.

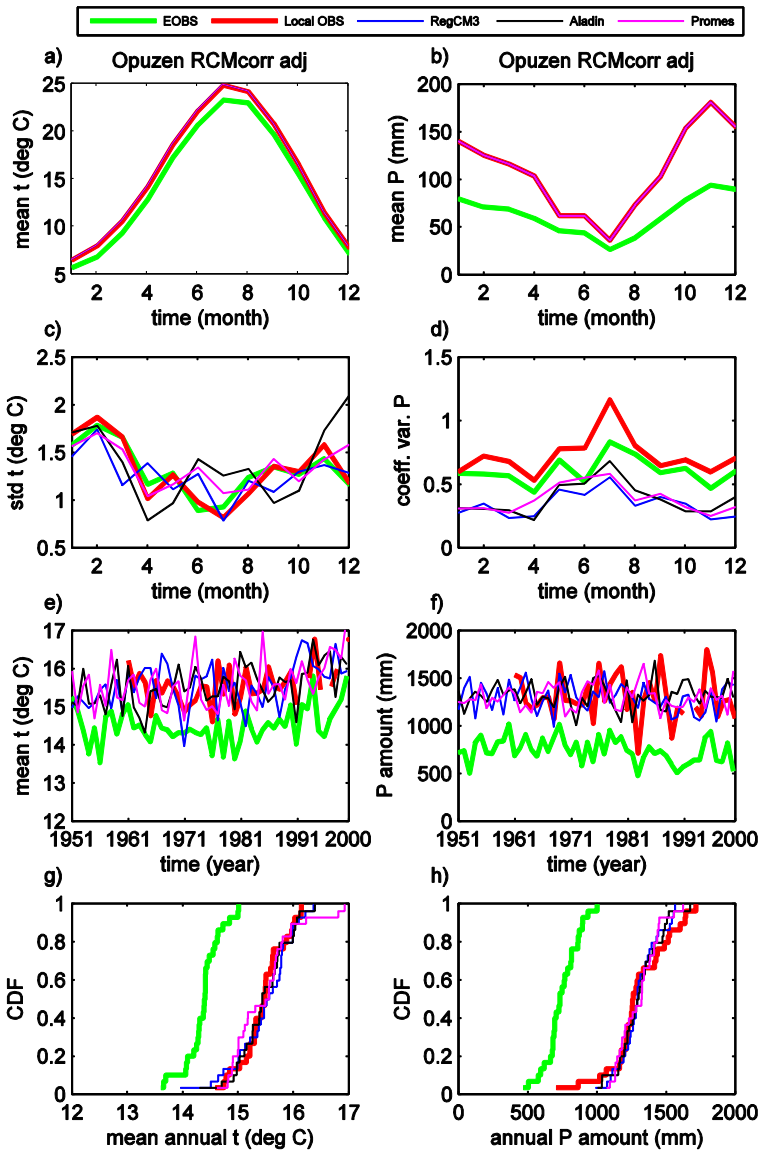

Figure 3.4.5 Same as Fig. 3.2.5 but for the Opuzen location.

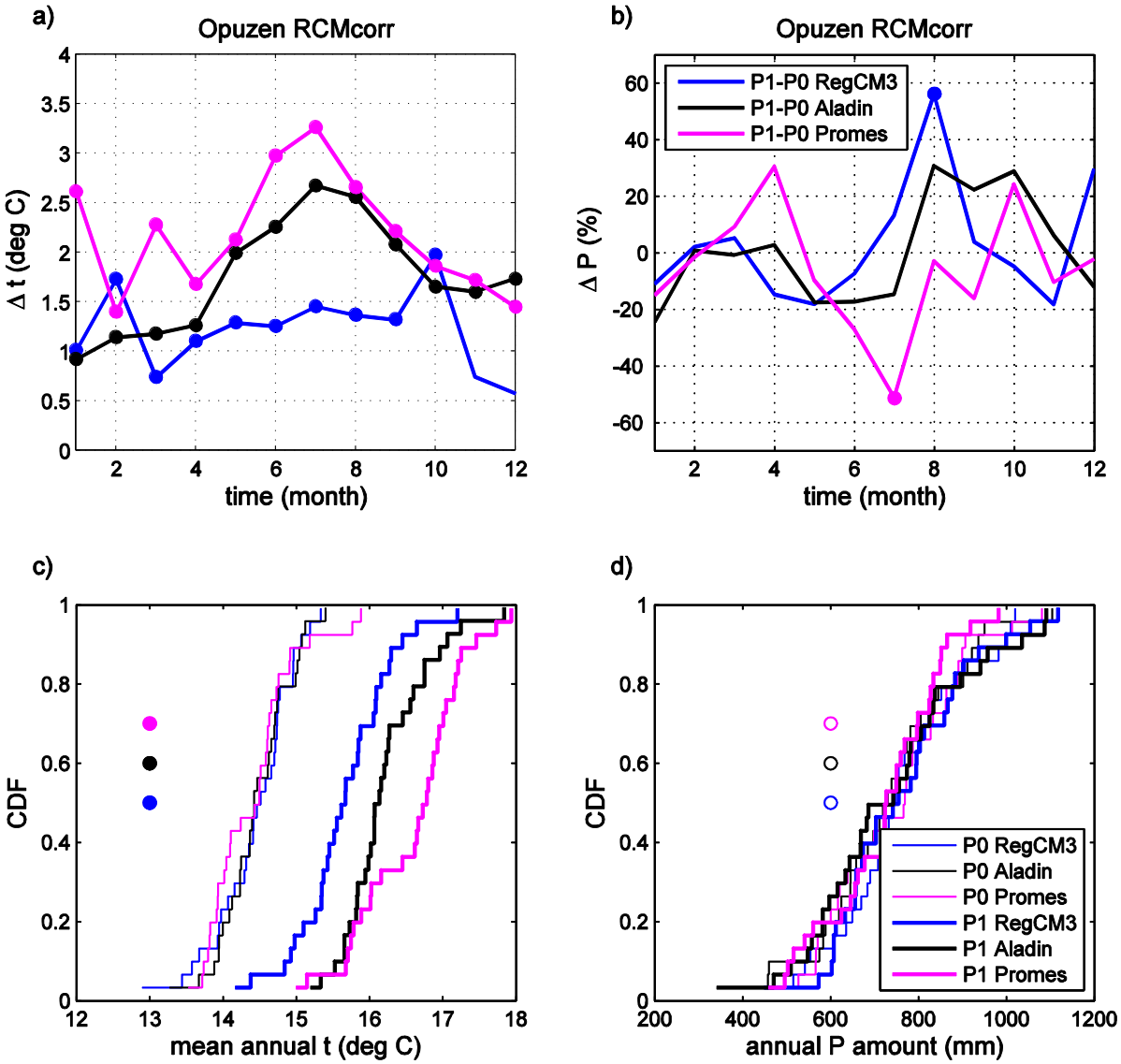

Figure 3.4.6 Same as Fig. 3.2.6 but for the Opuzen location.

Appendix 1: Description of the supplement files containing observed data

Two files in the xls format containing time series of the observed data are prepared:

1. Oborina_podaci.xls: contains monthly, seasonal (MAM – spring, JJA – summer, SON – autumn, DJF – winter) and annual precipitation amounts for the available period from 1961 to 2012. Each sheet corresponds to one station from Tables 2.1 and 3.1.
2. Temperatura_podaci.xls: contains mean monthly, seasonal (MAM – spring, JJA – summer, SON – autumn, DJF – winter) and annual 2m air temperature for the available period from 1961 to 2012. Each sheet corresponds to one station from Tables 2.1 and 3.1.

Appendix 2: Description of the supplement files containing simulated data

Three files in the xls format containing simulated time series are prepared:

1. DHMZ_RCM_MM_May2014.xls: contains monthly mean 2m air temperature and monthly total precipitation sum. Data for each location are in the separate sheet. Columns B and C contain specific year and month. Columns from D to F contain RCMcorr air temperature from the three models, columns from G to I contain RCMcorr precipitation from the same models. Remaining columns have the same description but are based on the RCMcorr_adj time series.
2. DHMZ_RCM_SM_May2014.xls: contains seasonal mean 2m air temperature and seasonal total precipitation sum. The structure of the file is similar to 1. Data are presented first for the MAM season, and then in the same manner for the JJA, SON and DJF seasons.
3. DHMZ_RCM_YM_May2014.xls: contains annual mean 2m air temperature and annual total precipitation sum. The structure of the file is similar to 1. and 2.

Table A2.1 List of abbreviations in xls files:

Variables	tas	2m air temperature
	pr	Total precipitation amount
Average/sum interval	MM	Monthly mean/sum
	SM	Seasonal mean/sum
	YM	Annual mean/sum
CC-WaterS regional climate models (RCM)	MOD1	Aladin
	MOD2	RegCM3
	MOD3	Promes
Types of RCM time series	corr	CC-WaterS regional climate simulations bias-corrected using E-OBS data (i.e. RCMcorr)
	corr_adj	Adjusted RCMcorr time series using DHMZ data for stations and variables when more than 90% of DHMZ data are available in the period 1961-1990 (i.e. RCMcorr_adj)
Seasons	MAM	climatological spring (March, April, May)
	JJA	climatological summer (June, July, August)
	SON	climatological autumn (September, October, November)
	DJF	climatological winter (December, January, February)

Table A2.2 Details for specific DHMZ station and corresponding closest land grid-cell in regional climate models:

Station	Additional comments
Pazin	Availability of DHMZ observations during the period 1961-1990 is 100% and RCMcorr_adj are prepared for both tas and pr.
Abrami	Availability of DHMZ observations during the period 1961-1990 is >90% and RCMcorr_adj are prepared for both tas and pr.
Poreč	Availability of DHMZ observations during the period 1961-1990 is >90% and RCMcorr_adj are prepared for both tas and pr.
Celega	Availability of DHMZ observations during the period 1961-1990 is 30% and RCMcorr_adj are not prepared for tas and pr. Monthly RCMcorr are retrieved from the CC-WaterS databes and seasonal and annual time series are prepared.
Metković	Availability of DHMZ observations during the period 1961-1990 is 100% for pr and 0% for tas. Files contain both RCMcorr and RCMcorr_adj precipitation time series and RCMcorr tas time series.
Ploče	Availability of DHMZ observations during the period 1961-1990 is 43% and RCMcorr_adj are not prepared for tas and pr. Monthly RCMcorr are retrieved from the CC-WaterS databes and seasonal and annual time series are prepared.
Opuzen	Availability of DHMZ observations during the period 1961-1990 is 100% and RCMcorr_adj are prepared for both tas and pr.

Appendix 3: Tables and figure for the Neretva River catchment (meteorological stations in Bosnia and Herzegovina)

Table A3.1 Basic statistics (mean, standard deviation, maximum and minimum) for annual and seasonal mean air temperature from the reference period 1961-1990 for the Neretva River catchment (meteorological stations in Bosnia and Herzegovina).

	DJF	MAM	JJA	SON	Year
Mostar					
mean (°C)	5.9	13.6	23.5	15.2	14.5
stdev (°C)	1.1	1.0	0.8	1.0	0.5
max (°C)	7.6	15.2	25.0	17.2	15.6
min (°C)	3.3	11.4	21.7	13.0	13.6
Široki brijeg					
mean (°C)	4.3	12.1	21.5	13.3	12.8
stdev (°C)	1.0	0.9	0.9	1.3	0.6
max (°C)	5.9	13.6	23.3	15.4	14.0
min (°C)	2.2	9.8	19.8	9.4	11.4
Rakitno					
mean (°C)	1.0	8.0	17.4	10.1	9.1
stdev (°C)	1.1	1.1	0.9	1.0	0.5
max (°C)	3.4	9.5	19.0	11.7	10.1
min (°C)	-1.2	5.3	15.2	8.4	8.2
Čapljina					
mean (°C)	5.9	13.4	22.4	14.2	14.0
stdev (°C)	1.2	1.2	1.0	1.5	0.5
max (°C)	9.9	15.3	24.5	16.2	15.2
min (°C)	3.6	10.6	20.2	9.3	12.8

Table A3.2 The percentiles for annual and seasonal mean air temperature empirical distribution from the reference period 1961-1990 for the Neretva River catchment (meteorological stations in Bosnia and Herzegovina).

	DJF	MAM	JJA	SON	Year
Mostar					
1	3.3	11.4	21.7	13.0	13.6
2	3.4	11.4	21.7	13.0	13.6
5	4.2	11.5	22.1	13.3	13.7
10	4.4	12.6	22.4	13.9	14.1
90	7.2	14.9	24.8	16.5	15.1
95	7.5	14.9	24.8	16.8	15.5
98	7.6	15.1	25.0	17.2	15.6
99	7.6	15.2	25.0	17.2	15.6
Široki brijeg					
1	2.2	9.8	19.8	9.4	11.4
2	2.2	9.8	19.8	9.6	11.4
5	2.4	10.1	20.0	11.3	11.9
10	3.2	11.0	20.4	11.8	12.2
90	5.6	13.1	22.5	15.0	13.6
95	5.8	13.4	23.3	15.2	13.8
98	5.9	13.6	23.3	15.4	14.0
99	5.9	13.6	23.3	15.4	14.0
Rakitno					
1	-1.2	5.3	15.2	8.4	8.2
2	-1.2	5.3	15.3	8.4	8.2
5	-0.9	5.9	16.0	8.6	8.3
10	-0.6	6.7	16.4	8.8	8.5
90	2.4	9.3	18.5	11.5	9.6
95	2.6	9.5	18.6	11.5	9.9
98	3.4	9.5	18.9	11.7	10.1
99	3.4	9.5	19.0	11.7	10.1
Čapljina					
1	3.6	10.6	20.2	9.3	12.8
2	3.6	10.6	20.3	9.6	12.8
5	4.2	11.2	20.6	12.0	13.2
10	4.2	11.7	21.1	12.5	13.3

90	7.1	14.6	23.6	16.0	14.7
95	7.9	15.2	24.1	16.1	15.1
98	9.7	15.3	24.4	16.2	15.2
99	9.9	15.3	24.5	16.2	15.2

Table A3.3 Basic statistics (mean, standard deviation, coefficient of variation, maximum and minimum) for annual and seasonal precipitation amount from the reference period 1961-1990 for the Neretva River catchment (meteorological stations in Bosnia and Herzegovina).

	DJF	MAM	JJA	SON	Year
Mostar					
mean	487.5	374.5	197.8	444.6	1501.2
stdev (mm)	184.7	118.8	77.0	163.2	294.1
cv (mm)	0.38	0.32	0.39	0.37	0.20
max (mm)	845.0	748.0	385.0	748.0	1987.0
min (mm)	114.0	213.0	76.0	172.0	840.0
Široki brijeg					
mean	556.1	409.9	196.7	513.6	1672.3
stdev (mm)	217.8	133.0	69.8	185.6	305.3
cv (mm)	0.39	0.32	0.35	0.36	0.18
max (mm)	909.0	797.0	370.0	867.0	2224.0
min (mm)	108.0	199.0	72.0	236.0	954.0
Rakitno					
mean	583.8	424.3	235.8	540.8	1779.2
stdev (mm)	282.4	135.8	93.0	202.7	429.3
cv (mm)	0.48	0.32	0.39	0.37	0.24
max (mm)	1152.3	807.0	450.0	913.0	2675.7
min (mm)	114.0	219.0	77.0	168.0	1130.0
Čapljina					
mean	331.8	228.1	161.4	363.8	1084.0
stdev (mm)	151.8	71.2	82.4	130.4	228.6
cv (mm)	0.46	0.31	0.51	0.36	0.21
max (mm)	655.0	383.0	381.7	641.0	1482.0
min (mm)	57.6	104.0	38.0	126.0	525.0

Table A3.4 The percentiles for annual and seasonal precipitation empirical distribution from the reference period 1961-1990 for the Neretva River catchment (meteorological stations in Bosnia and Herzegovina).

	DJF	MAM	JJA	SON	Year
Mostar					
1	114.0	213.0	76.0	172.0	840.0
2	115.4	213.3	78.1	174.5	840.6
5	131.1	216.0	97.0	197.0	846.0
10	204.2	251.0	113.0	233.5	1105.0
90	730.8	525.0	324.0	670.5	1864.0
95	770.8	612.6	374.0	729.0	1901.0
98	838.8	734.5	383.9	746.1	1978.4
99	845.0	748.0	385.0	748.0	1987.0
Široki brijeg					
1	108.0	199.0	72.0	236.0	954.0
2	110.4	203.1	73.2	238.3	975.3
5	136.5	240.0	84.2	259.0	1167.0
10	248.8	249.5	111.5	284.0	1302.0
90	871.2	561.5	288.0	776.0	2095.0
95	891.0	673.0	352.0	848.0	2139.0
98	907.5	784.6	368.2	865.1	2215.5
99	909.0	797.0	370.0	867.0	2224.0
Rakitno					
1	114.0	219.0	77.0	168.0	1130.0
2	115.8	221.2	77.6	180.7	1134.0
5	134.9	241.0	82.6	294.6	1170.0
10	194.2	262.0	130.0	313.0	1300.9
90	939.8	570.0	370.5	883.5	2451.3
95	1027.	747.0	427.0	910.0	2544.0
98	1141.	801.0	447.7	912.7	2662.5
99	1152.	807.0	450.0	913.0	2675.7
Čapljina					
1	57.6	104.0	38.0	126.0	525.0
2	58.4	104.4	38.1	126.5	535.5
5	67.5	108.0	39.0	131.0	630.3
10	124.0	133.5	64.7	213.5	840.3
90	554.0	330.5	277.5	536.0	1378.9

95	589.5	366.0	302.0	563.6	1447.0
98	649.5	381.3	373.7	633.3	1478.5
99	655.0	383.0	381.7	641.0	1482.0

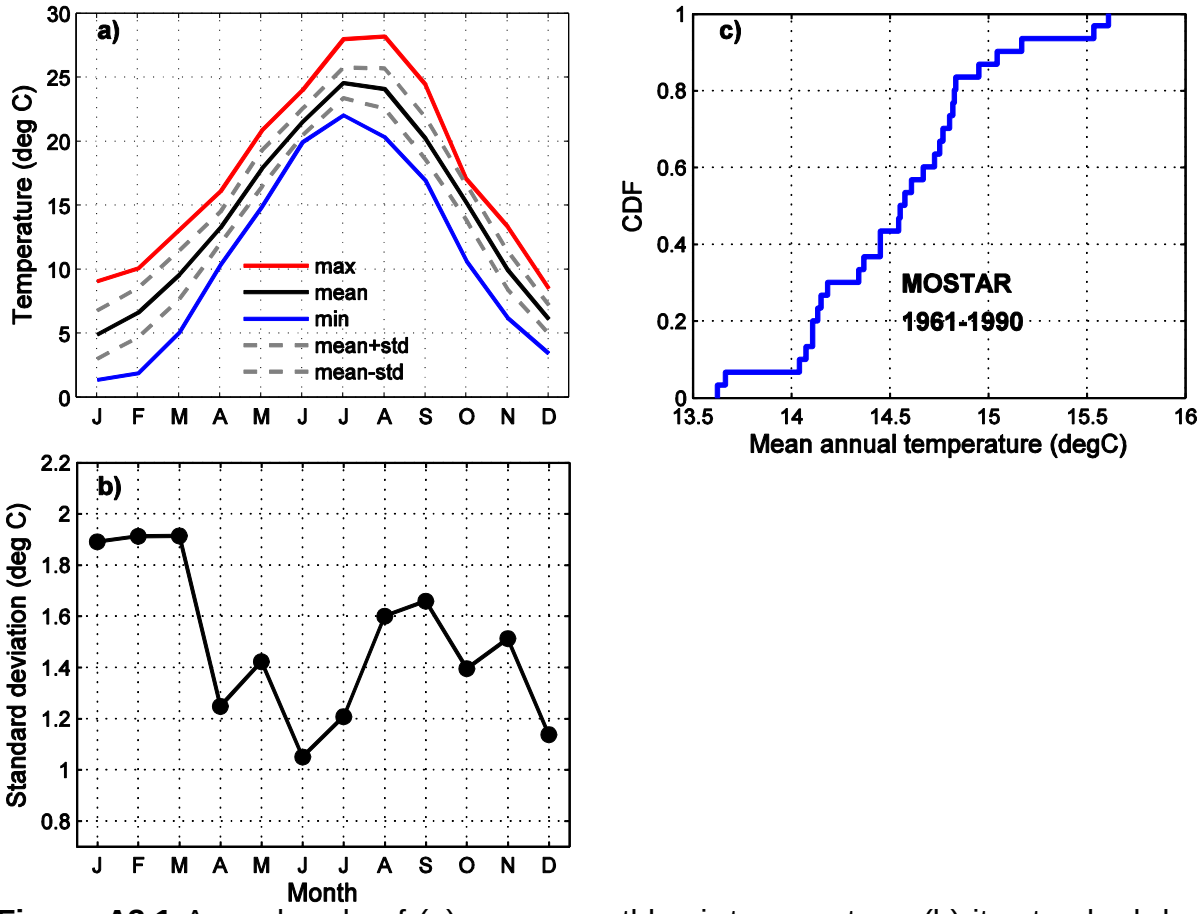

Figure A3.1 Annual cycle of (a) mean monthly air temperature, (b) its standard deviation and (c) cumulative distribution of mean annual air temperature for the period 1961-1990 for the meteorological station Mostar.

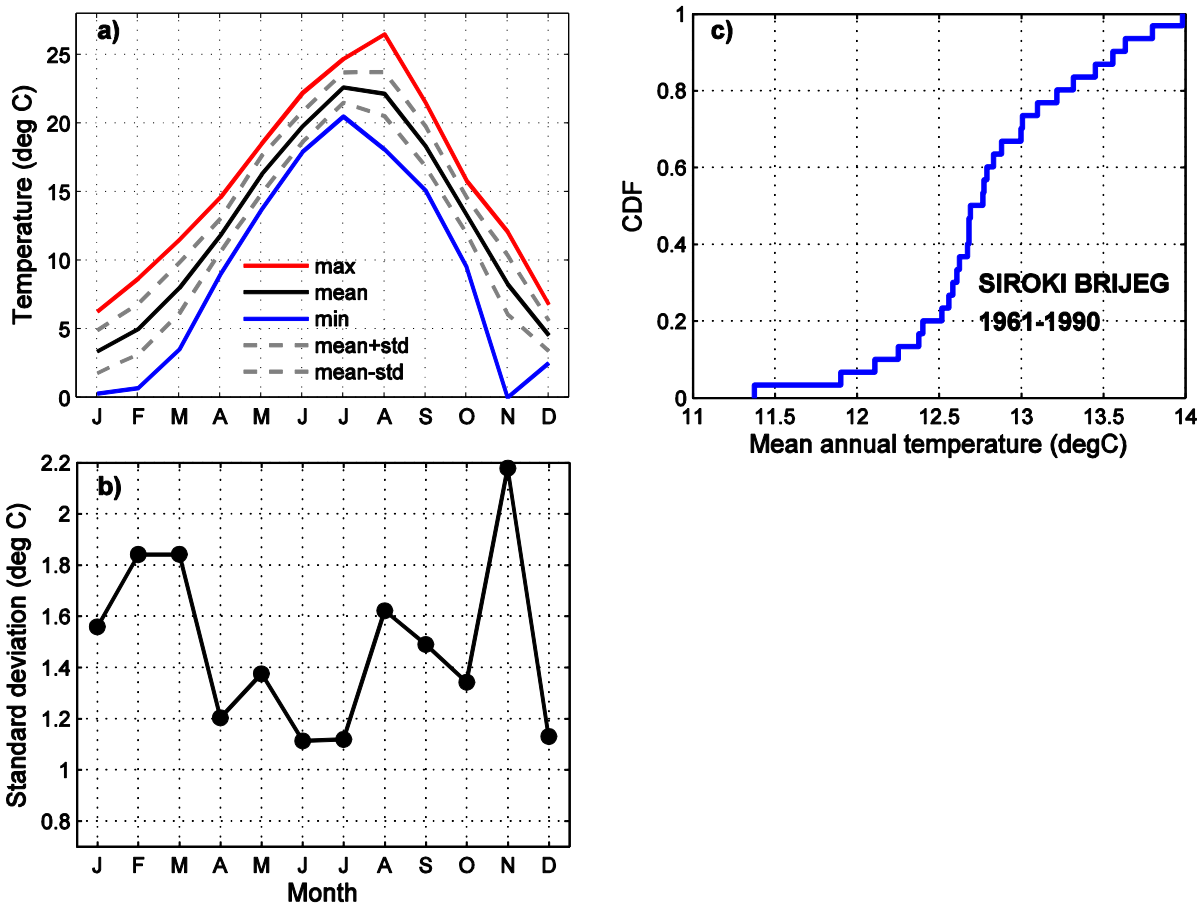

Figure A3.2 Annual cycle of (a) mean monthly air temperature, (b) its standard deviation and (c) cumulative distribution of mean annual air temperature for the period 1961-1990 for the meteorological station Široki Brijeg.

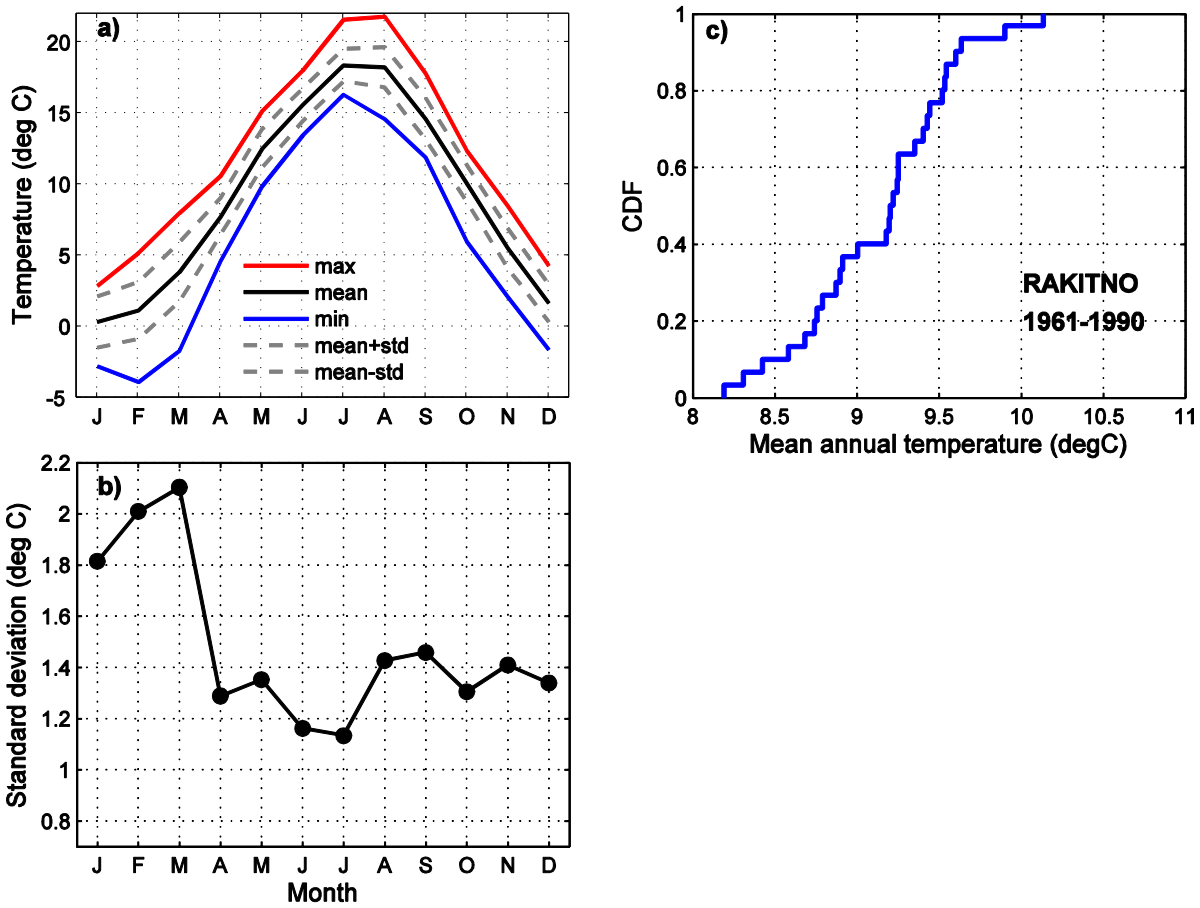

Figure A3.3 Annual cycle of (a) mean monthly air temperature, (b) its standard deviation and (c) cumulative distribution of mean annual air temperature for the period 1961-1990 for the meteorological station Rakitno.

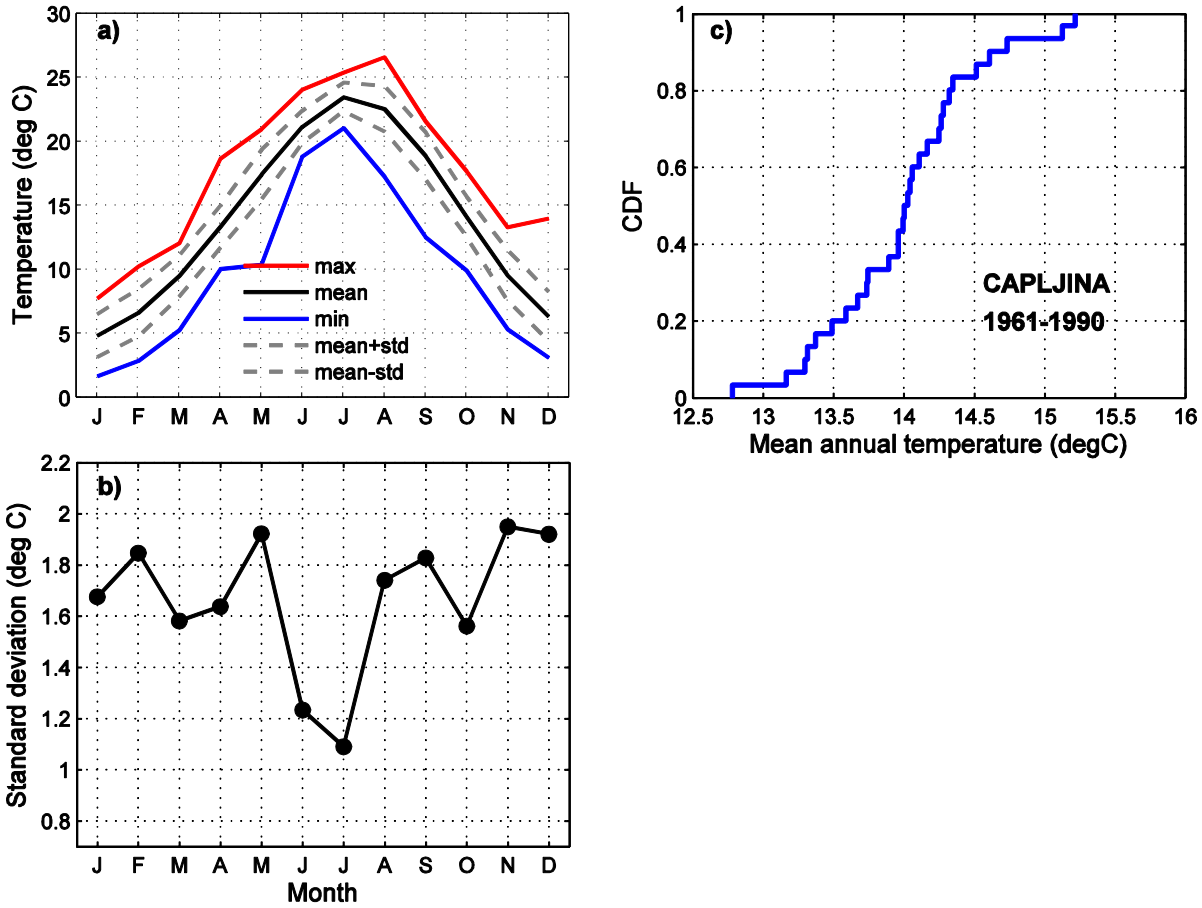

Figure A3.4 Annual cycle of (a) mean monthly air temperature, (b) its standard deviation and (c) cumulative distribution of mean annual air temperature for the period 1961-1990 for the meteorological station Čapljina.

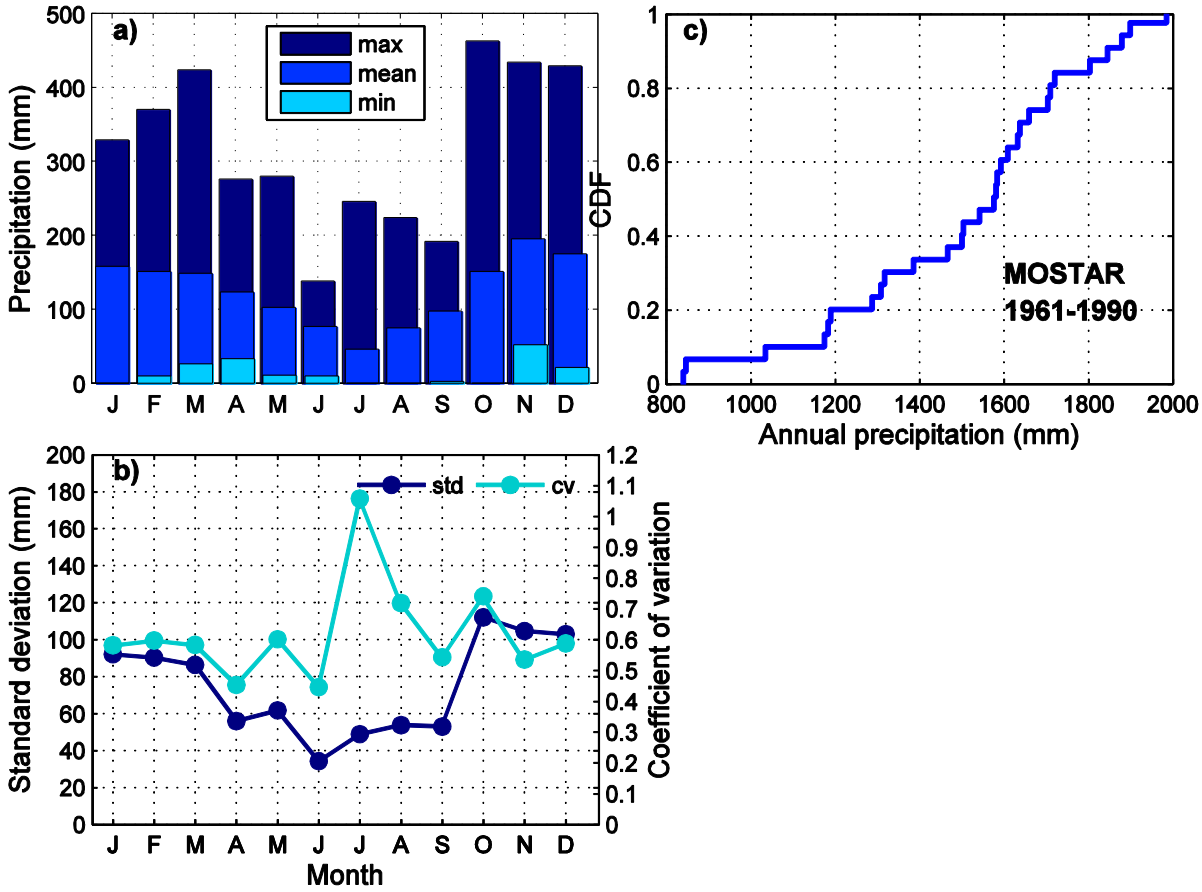

Figure A3.5 Annual cycle of (a) mean monthly precipitation amounts, (b) standard deviation and coefficient of variation and (c) cumulative distribution of annual precipitation amounts for the period 1961-1990 for the meteorological station Mostar.

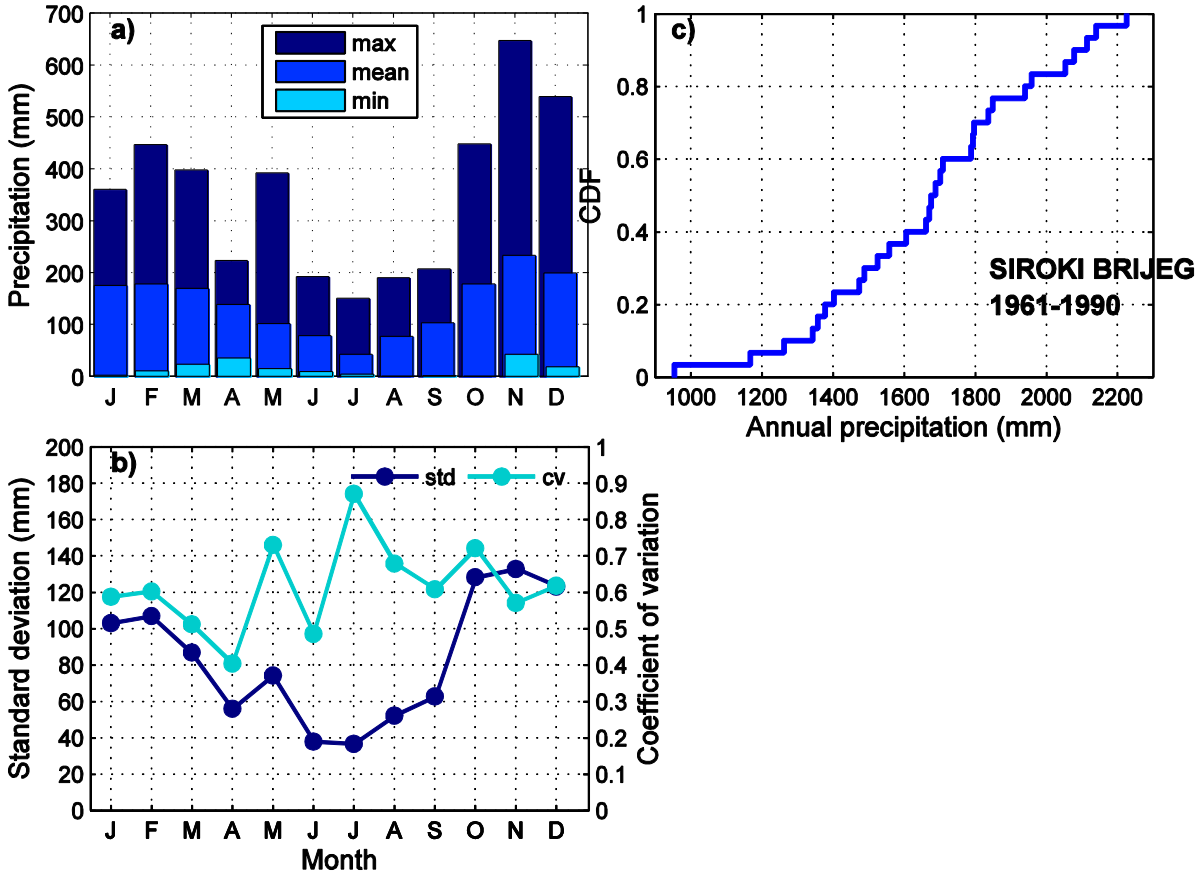

Figure A3.6 Annual cycle of (a) mean monthly precipitation amounts, (b) standard deviation and coefficient of variation and (c) cumulative distribution of annual precipitation amounts for the period 1961-1990 for the meteorological station Široki Brijeg.

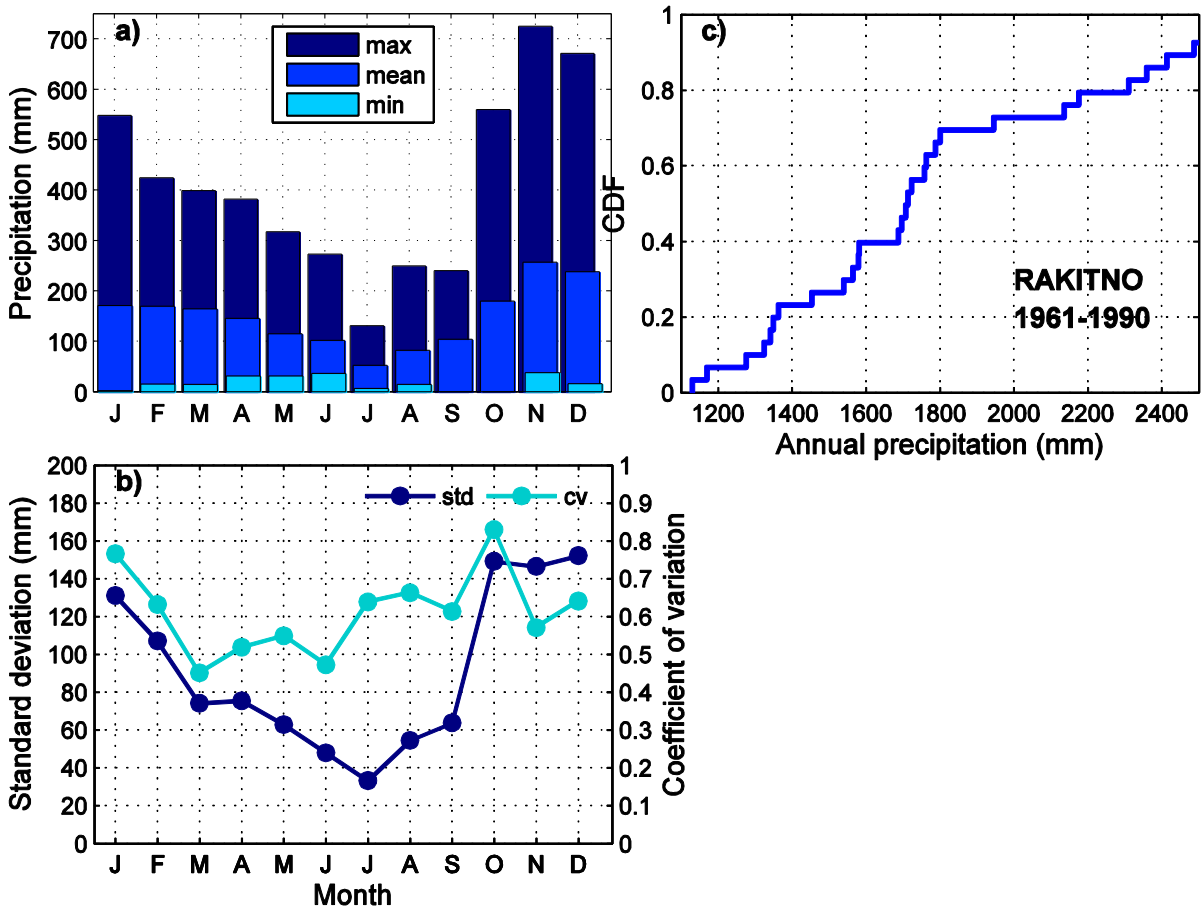

Figure A3.7 Annual cycle of (a) mean monthly precipitation amounts, (b) standard deviation and coefficient of variation and (c) cumulative distribution of annual precipitation amounts for the period 1961-1990 for the meteorological station Rakitno.

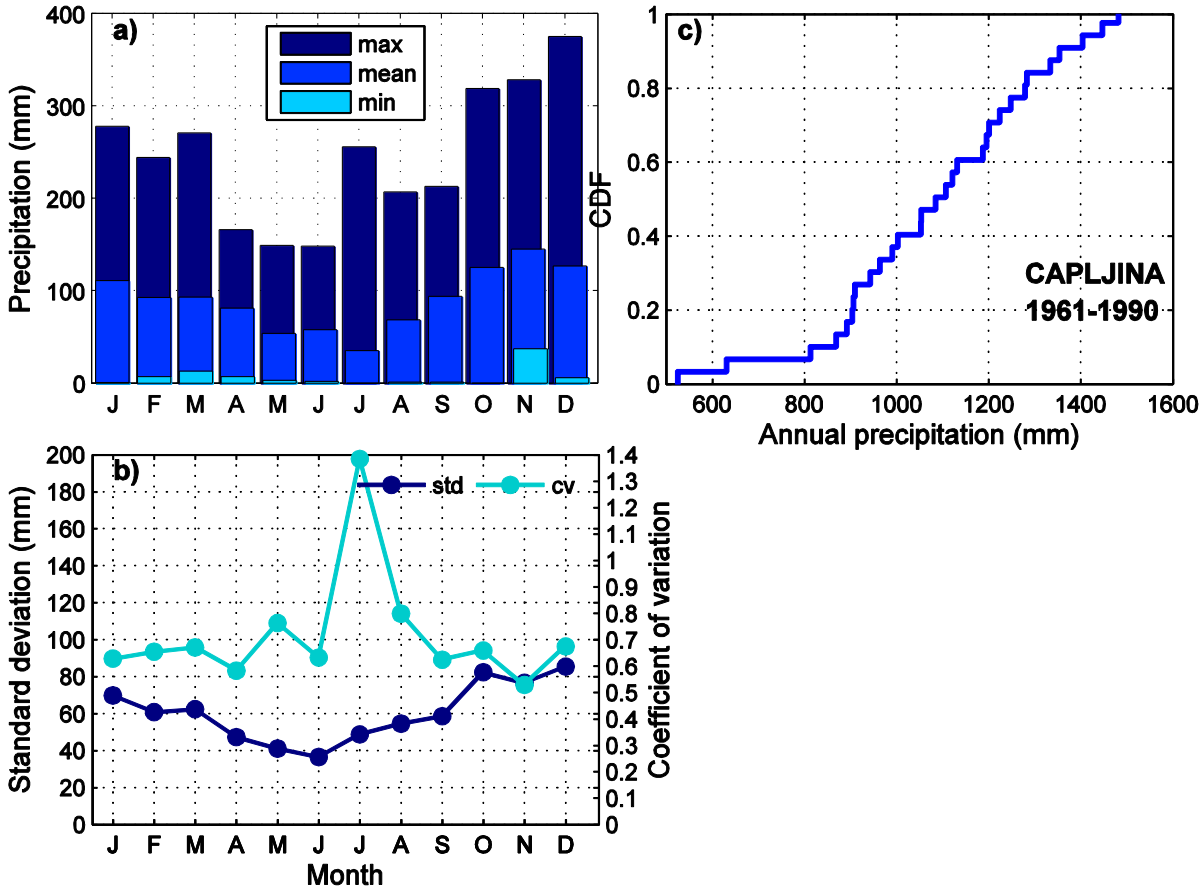

Figure A3.8 Annual cycle of (a) mean monthly precipitation amounts, (b) standard deviation and coefficient of variation and (c) cumulative distribution of annual precipitation amounts for the period 1961-1990 for the meteorological station Čapljina.

References

Bubnova, R., Hello, G., Bénard, P., Geleyn, J-F., 1995. Integration of the fully elastic equations cast in hydrostatic pressure terrain-following coordinate in the framework of the ARPEGE/Aladin NWP system. *Mon.Wea.Rev.*,123:515–535.

Castro, M., Fernández C., Gaertner M.A., 1993. Description of a meso-scale atmospheric numerical model. In:J.I. Díaz, J.L. Lions (eds), Mathematic, climate and environment, Masson.

Cindrić, K., 2014. Analysis of observed climate for the Mirna River catchments (report)

Cindrić, K., Z. Pasarić, and M. Gajić-Čapka, 2010. Spatial and temporal analysis of dry spells in Croatia. *Theor. Appl. Climatol.*, 102:171–184.

Déqué, M., 2007. Frequency of precipitation and temperature extremes over France in an anthropogenic scenario: Model results and statistical correction according to observed values. *Global and Planetary Change*, 57:16–26.

DHMZ, 2014. Klimatske podloge za dva pilot područja u Hrvatskoj u okviru EU projekta DRINK-ADRIA. Državni hidrometeorološki zavod, pp 34.

Gilbert, R.O., 1987. Statistical methods for environment pollution monitoring. Wiley, New York

Formayer, H., Haas P., 2010. Correction of RegCM3 model output dana using a rank matching approach applied on various meteorological parameters. In Deliverable D3.2 RCM output localization methods (BOKU-contribution of the FP6 CECILIA project on http://www.cecilia-eu.org/).

Hawkins, E., and R. Sutton, 2009. The potential to narrow uncertainty in regional climate predictions. *Bull. Amer. Meteor. Soc.*, 90:1095–1107.

Haylock, M.R., Hofstra N., Klein Tank A.M.G., Klok E.J., Jones P.D., New M., 2008. A European daily high-resolution gridded dataset of surface temperature and precipitation for 1950-2006. J. Geophys. Res.,113, D20119, doi:10.1029/2008JD010201.

Gajić-Čapka, M., 2014. Analysis of observed climate for the Prud wellspring catchment (report).

Güttler, I., 2014. Analysis of simulated climate for the Mirna River and Prud wellspring catchments (report)

IPCC, 2007. Climate change 2007: The Physical Science Basis, Contribution of Working Group I to the Fourth Assessment Report of the Intergovernmental Panel on Climate Change. Solomon S., Qin D., Manning M., Chen Z., Marquis M., Averyt K., Tignor M., Miller H.L. (eds). Cambrige University Press, UK

Jacob, D., and Coauthors, 2014. EURO-CORDEX: new high-resolution climate change projections for European impact research. *Reg. Environ. Change*, 14(2):563–578,.

Lončar, E., A. Bajić, 1994. Tipovi vremena u Hrvatskoj. *Hrvatski meteorološki časopis,* 29:31–41.

Pal, J.S., and Coauthors, 2007. Regional climate modeling for the developing world: The ICTP RegCM3 and RegCNET. *Bull. Amer. Meteor. Soc.*, 88:1395–1409.

Patarčić, M., M. Gajić-Čapka, K. Cindrić and Č. Branković, 2014: Recent and near-future changes in indices of precipitation extremes at the Croatian Adriatic coast. *Climate Research* (submitted, in revision).

Sen, P.K., 1968. Estimates of the regression coefficient based on Kedall's tau. *J. Am. Stat. Assoc.* 63:1379–1389.
Zaninović, K., M. Gajić-Čapka, M. Perčec Tadić, and Coauthors, 2008. *Climate atlas of Croatia 1961–1990, 1971–2000*. Meteorological and Hydrologic

Climate and CC data for pilot areas in Croatia – Rijeka 15.09.2014

Let's grow up together

DRINK ADRIA

Adriatic IPA
Cross Border Cooperation 2007-2013

The project is co-funded by the European Union,
Instrument for Pre-Accession Assistance

Report:

Climate and climate change data for pilot areas in Nikšić, Montenegro

Institute for Development of Water Resources
“Jaroslav Černi”
(FB10)

Belgrade, 2014

Let’s grow up together

The project is co-funded by the European Union, Instrument for Pre-Accession Assistance

VODOVOD I KANALIZACIJA NIKŠIĆ - MONTENEGRO

Climate data for pilot area Nikšić in Montenegro in the framework of DRINK-ADRIA EU project

Institute for development of Water Resources "Jaroslav Černi"

Beograd, June 2014

Studija “Klimatske podloge za pilot područje Nikšić u Crnoj Gori u okviru EU projekta DRINK-ADRIA” izrađen je u Institutu za vodoprivredu “Jaroslav Černi” u Beogradu.

Study „Climate data for pilot area Nikšić in Montenegro in the framework of DRINK-ADRIA EU project” is done in Institute for development of Water Resources “Jaroslav Černi” from Belgrade.

Responsible:

Dejan Dimkić

Table of Contents

1. Introduction

In this study the climatological data presenting general climate characteristics, climate variability and trends at the Temperature station Nikšić and Precipitation stations Nikšić and Lukovo, The Zeta River catchment. The present climate characteristics include measurements of air temperature and precipitation amounts from the reference climate period 1961-1990; while the future characteristics are estimated from the simulations of the regional climate models from the CC-WaterS[1] project (based on the ENSEMBLES[2] project). The whole overview is based on monthly and annual average values from climate stations. Data sets from all climate and raingauge stations listed in Study are prepared separately in Excel tables, and they are available on request.

The regional climate models are Aladin (Bubnova et al. 1995), Promes (Castro et al. 1993) and RegCM3 (Pal et al. 2007). For 2m temperature and precipitation, time series for each model were considered and for present climate they are compared with local observations.

[1] www.ccwaters.eu

[2] www.ensembles-eu.org

2. PILOT AREA : Nikšić waterworks company, Zeta River catchment, T and P station Nikšić, P station Lukovo

2.1. Meteorological data base and statistics of local observations

Table 2.1. Geographical station data (elevation *h,* longitude □, latitude □) and the available measurement time periods for temperature (T) and precipitation (P) data for 2 stations near Nikšić.

	Station	*h* (m.a.s.)	□(°)	□ (°)	T	P
1.	Nikšić	627	42,78° N	18,94° E	1949-2012	1949-2012
2.	Lukovo	838	42,81° N	19,02° E	No data	1960-2012

Air temperature

Table 2.2 Basic statistics (mean, standard deviation, maximum and minimum) for annual and monthly mean air temperature from the reference period 1961-1990 for the Temperature station Nikšić.

	Dec	Jan	Feb	Mar	Apr	May	Jun	Jul	Aug	Sep	Oct	Nov	Year
	Winter			Spring			Summer			Autumn			
	Temperature station **Nikšić**												
mean (°C)	1,3	2,6	5,7	9,6	14,2	17,5	20,5	20,1	16,3	11,4	6,6	2,9	10,7
stdev (°C)	1,8	2,0	2,1	1,3	1,5	1,0	1,1	1,6	1,6	1,2	1,4	1,2	0,4
max (°C)	4,2	5,9	8,9	12,4	16,8	19,6	24,2	23,6	20,1	13,5	9,3	4,9	11,5
min (°C)	-2,3	-3,0	0,3	7,0	10,3	15,8	19,2	15,9	13,1	7,7	2,5	0,5	9,9

Observed period for T station Nikšić is 1949-2012. For Serbia period which exhibit a close similarity to estimated longterm temperature and precipitation trends is from 1949 to 2006 (JČI 2011; HMSS 2011). We can not be sure that this period is also convenient for Montenegro (we didn't analyze other relevant Montenegrian climatological stations), but we present, where available, the trends for this period also.

Table 2.3. Decadal air temperature trends (°C/10 yrs) for Nikšić Temperature station for 1949-2012 and 1949-2006 data series.

	Dec	Jan	Feb	Mar	Apr	May	Jun	Jul	Aug	Sep	Oct	Nov	Year
	Winter			Spring			Summer			Autumn			
	Temperature station **Nikšić**												
°C/10yrs 1949-2012	-0.14	0.21	0.08	0.16	0.05	0.20	0.29	0.28	0.25	-0.04	0.08	-0.02	0.12
	0.05 *			0.13 *			0.27 *			0.01 *			
°C/10yrs 1949-2006	-0.16	0.21	0.07	0.11	-0.11	0.17	0.21	0.19	0.07	-0.17	0.11	-0.11	0.05
	0.04 *			0.06 *			0.15 *			-0.06 *			

* As average of trends in three months

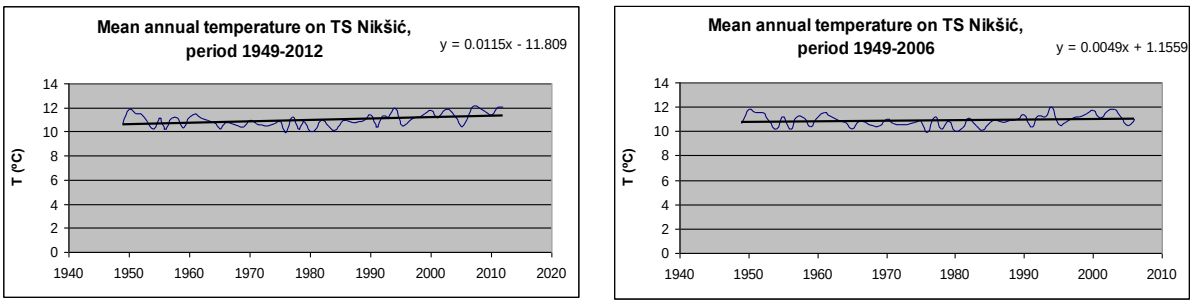

Figure 2.1 Observed Mean annual temperature data with trends on TS Nikšić, periods 1949-2012 and 1949-2006

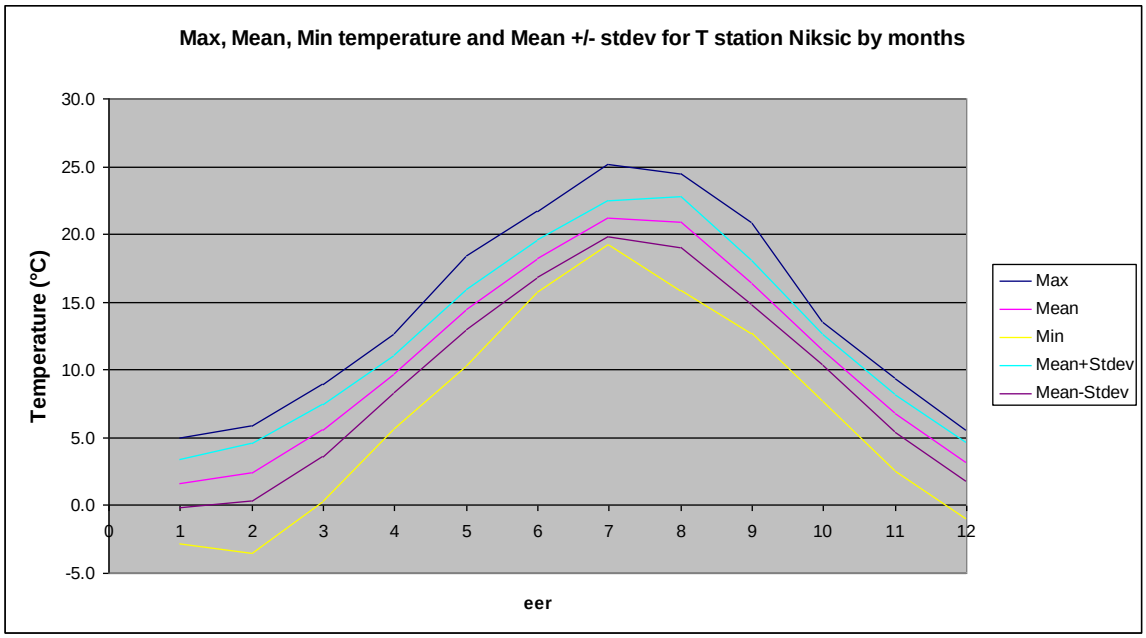

Figure 2.2 TS Nikšić, period 1949-2012 : Observed temperature values by months: Max, Mean, Min, Mean+stdev and Mean-stdev

Precipitation

Table 2.4 Basic statistics (mean, standard deviation, maximum and minimum) for annual and monthly mean precipitation from the reference period 1961-1990 for the Precipitation stations Nikšić and Lukovo.

	Dec	Jan	Feb	Mar	Apr	May	Jun	Jul	Aug	Sep	Oct	Nov	Year
	Winter			Spring			Summer			Autumn			
	Precipitation station **Nikšić**												
mean (mm)	239	208	194	186	170	108	93	63	86	138	202	298	1986
stdev (mm)	134	130	122	83	108	67	54	47	64	116	175	170	374
max (mm)	555	454	511	389	460	338	232	182	254	489	710	806	2994
min (mm)	39.3	3.3	15.6	41.9	15.7	22.3	19.1	0.6	10.8	3.6	0.0	56.7	1270
	Precipitation station **Lukovo**												
mean (mm)	204	191	171	166	165	110	95	58	90	125	189	287	1851
stdev (mm)	109	113	94	74	89	59	43	43	76	93	163	140	331
max (mm)	461	419	367	388	443	271	193	182	399	324	649	697	2740
min (mm)	26.6	2.1	17.5	37.5	29.9	15.5	27.6	0.0	21.1	5.7	0.0	59.2	1247

Table 2.5. Decadal trends (mm/10years and %/10years) for Nikšić and Lukovo Precipitation stations for available data series (PS Nikšić: 1949-2012 and PS Lukovo: 1960-2012), and additionally for PS Nikšić periods 1949-2006 and 1960-2012.

	Dec	Jan	Feb	Mar	Apr	May	Jun	Jul	Aug	Sep	Oct	Nov	Year
	Winter			Spring			Summer			Autumn			
	Precipitation station **Nikšić**												
mm/10yrs 1949-2012	-3.2	-2.6	-2.3	1.5	8.3	-0.8	-3.7	-2.2	1.5	5.3	2.4	-1.3	2.6
	-2.74 *			2.98 *			-1.47 *			2.11 *			
mm/10yrs 1949-2006	-11.8	-8.7	-7.4	-1.0	12.8	-0.9	-5.9	-1.6	6.8	9.7	2.8	-2.0	-7.2
	-9.32 *			3.63 *			-0.23 *			3.52 *			
mm/10yrs 1960-2012	5.3	-3.5	-1.6	-10.1	-2.8	3.1	-3.1	-9.3	-2.9	3.6	0.1	-12.3	-33.7
	0.04 *			-3.27 *			-5.12 *			-2.88 *			
%/10yrs 1949-2012	-1.2	-1.4	-1.2	0.9	5.2	-0.7	-4.2	-4.3	2.1	3.8	1.2	-0.5	0.14
	-1.26 *			1.80 *			-2.11 *			1.50 *			
%/10yrs 1949-2006	-4.5	-4.6	-3.9	-0.6	7.9	-0.9	-6.7	-3.0	8.9	6.9	1.4	-0.7	-0.38
	-4.34 *			2.15 *			-0.27 *			2.53 *			
%/10yrs 1960-2012	2.0	-1.8	-0.9	-6.0	-1.6	2.9	-3.6	-16.7	-3.8	2.5	0.0	-4.2	-1.72
	-0.21 *			-1.58 *			-8.06 *			-0.54 *			
	Precipitation station **Lukovo**												
mm/10yrs 1960-2012	-10.1	-14.1	-6.5	-14.5	-12.1	-0.4	-6.2	-8.1	-8.2	1.4	-5.9	-21.6	-104.2
	-10.19 *			-9.00 *			-7.48 *			-8.68 *			
%/10yrs 1960-2012	-5.0	-8.8	-4.1	-9.9	-8.1	-0.4	-7.2	-15.3	-10.6	1.1	-3.1	-8.2	-6.1
	-5.96 *			-6.11 *			-11.05 *			-3.38 *			

* As average of trends in three months

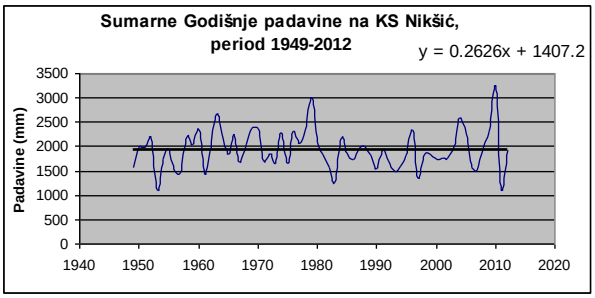

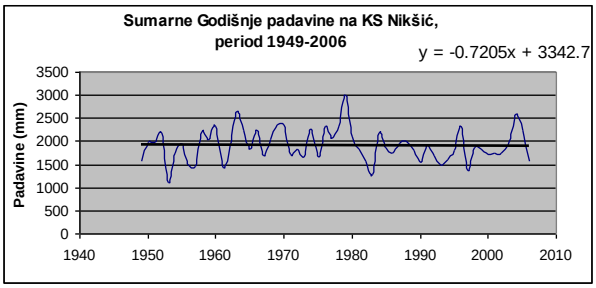

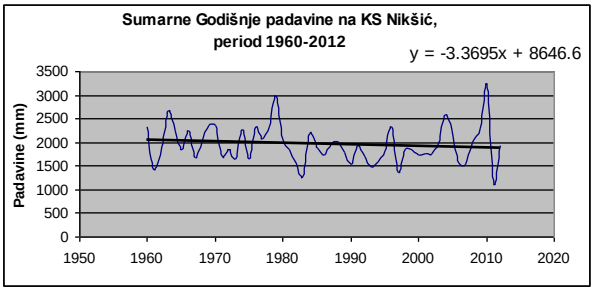

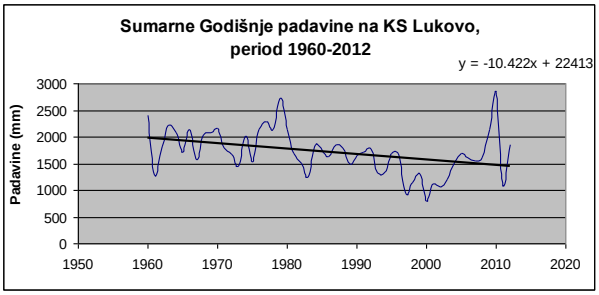

Figure 2.3 Observed Sum annual precipitation data with trends on PS Nikšić, periods 1949-2012, 1949-2006 and 1960-2012, and PS Lukovo 1960-2012

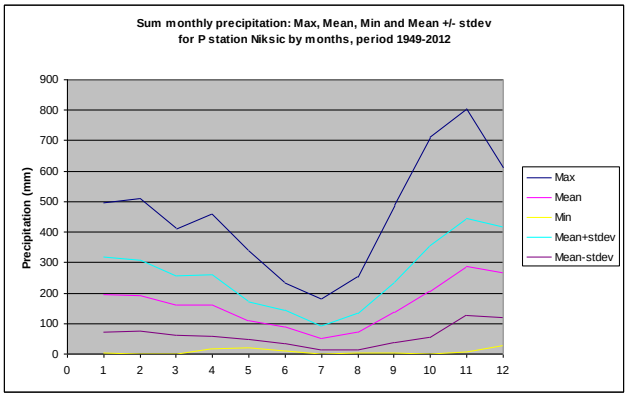

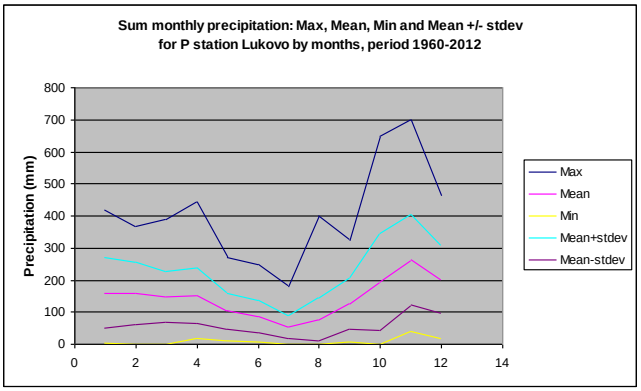

Figure 2.4 PS Nikšić, period 1949-2012 and PS Lukovo, period 1960-2012: Observed precipitation values by months: Max, Mean, Min, Mean+stdev and Mean-stdev

2.2. Regional climate model simulations

We have download temperature and precipitation data from CCWaterS project (grid points). Nikšić temperature and precipitation station and Lukovo precipitation station have follows latitude and longitude and they are inside these four grid points:

	STATION			Grid point (GP)			
	Nikšić - T	**Nikšić - P**	**Lukovo - P**	1	2	3	4
Latitude (8 N)	42.78	42.78	42.81	42.625	42.625	42.875	42.875
Longitude (8 E)	18.94	18.94	19.02	18.875	19.125	18.875	19.125

T and P data for two stations for RCMs we have calculated according to distance from grid points. The respective coefficients are:

T and P Nikšić: GP1 0.28 ; GP2 0.16 ; GP3 0.34 ; GP4 0.22 ; Total 1.00

P Lukovo: GP1 0.17 ; GP2 0.21 ; GP3 0.29 ; GP4 0.33 ; Total 1.00

Temperature

After calculated **Nikšić-T** in RCMs (appendixes 4, 5 and 6) for both periods (1961-1990 and 2021-2050), obtained mean monthly and corrected values are as follows (table 2.6):

Table 2.6	RCMs from CCWaterS				Temperature Nikšić (°C)	Corrected values for RCMs		
month	Aladin	Promes	RegCM3	Observed		Aladin	Promes	RegCM3
JAN	-1.3	-1.6	-1.8	1.3		2.5	2.8	3.0
FEB	-0.4	-0.6	-0.5	2.6		3.0	3.2	3.1
MAR	2.7	2.4	2.6	5.7		3.0	3.3	3.1
APR	6.6	6.6	6.8	9.6		3.1	3.0	2.8
MAY	11.3	11.4	11.4	14.2		2.9	2.8	2.8
JUN	14.8	14.6	14.9	17.5		2.7	2.9	2.6
JUL	16.8	16.9	17.2	20.5		3.7	3.6	3.3
AUG	17.1	16.9	17.1	20.1		2.9	3.1	3.0
SEP	13.6	13.7	13.6	16.3		2.7	2.6	2.6
OCT	9.1	8.9	8.8	11.4		2.2	2.5	2.6
NOV	4.4	4.5	4.5	6.6		2.2	2.1	2.1
DEC	0.4	0.5	0.3	2.9		2.5	2.5	2.7
Year	**7.9**	**7.8**	**7.9**	**10.7**		**2.78**	**2.87**	**2.82**

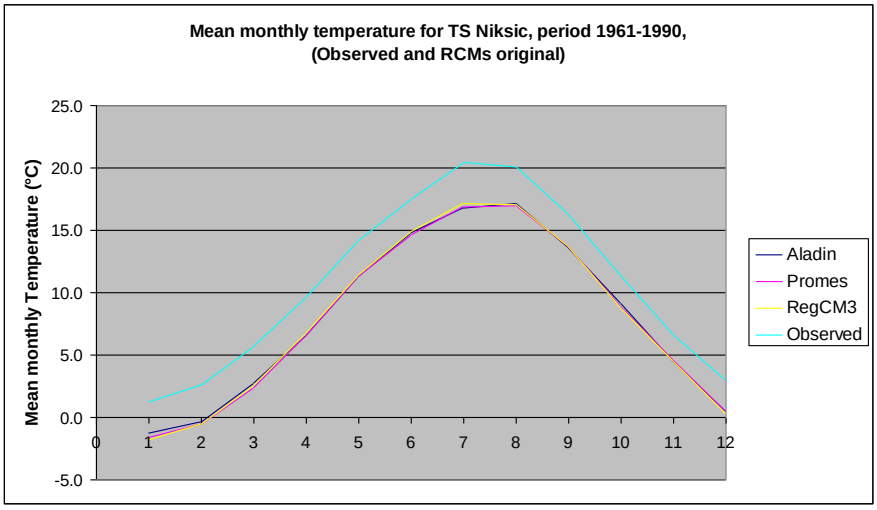

Figure 2.5 TS Nikšić, mean monthly temperature, period 1961-1990: RCMs original and Observed data

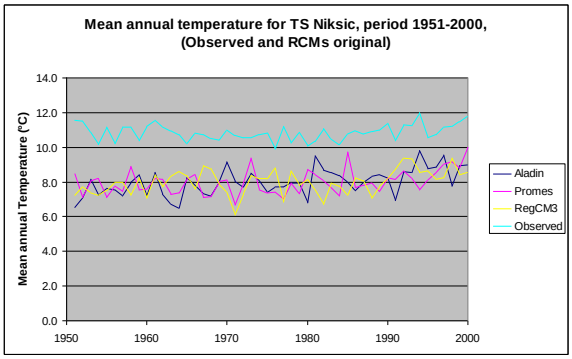

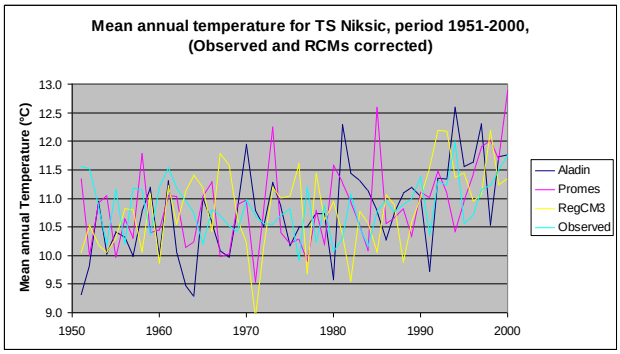

Figure 2.6 TS Nikšić, mean annual temperature, period 1951-2000: RCMs original and Observed data (first graph) and RCMs corrected and Observed data (second graph)

For future period (2021-2050), corrected monthly data for TS Nikšić for all three models (Aladin, Promes, RegCM3) are available on Appendix 13.

Figure 2.7a-c shows mean annual corrected temperatures with trend for TS Nikšić for all three models (period 1951-2050).

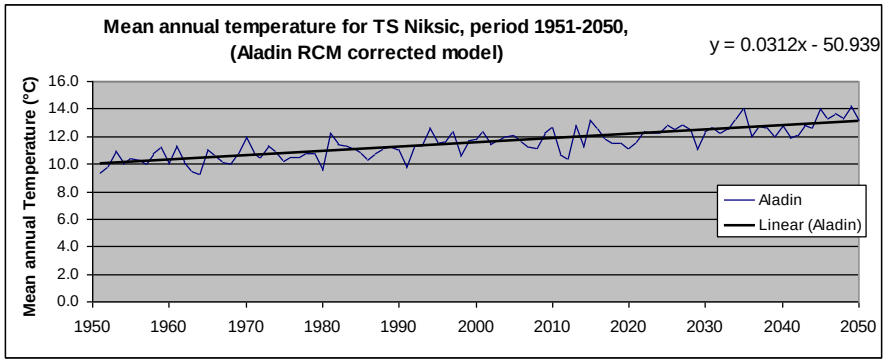

Figure 2.7a RCM Aladin

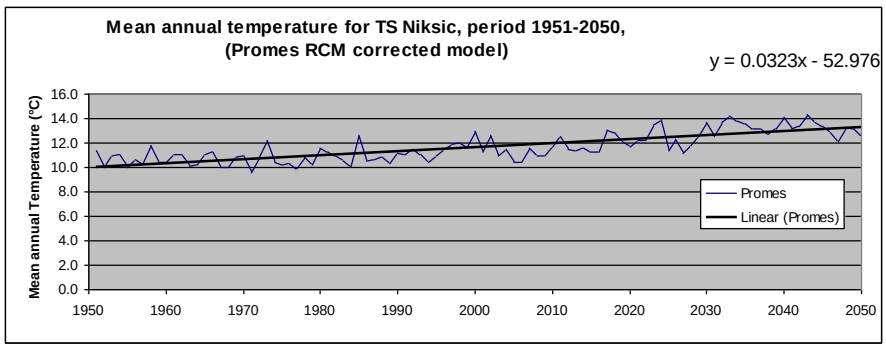

Figure 2.7b RCM Promes

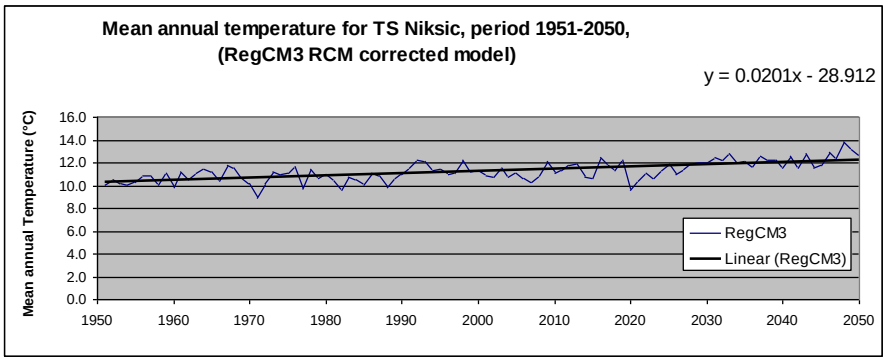

Figure 2.7c RCM RegCM3

Precipitation

After calculated **Nikšić-P** in RCMs (appendixes 7, 8 and 9) for both periods (1961-1990 and 2021-2050), obtained mean monthly and corrected values (instead differences, quotients here are more suitable) are as follows (table 2.7):

Table 2.7	RCMs from CCWaterS				Precipitation Nikšić (mm)	Corrected values for RCMs		
month	Aladin	Promes	RegCM3	Observed		Aladin	Promes	RegCM3
JAN	76	68	83	208		2.75	3.06	2.52
FEB	71	74	63	194		2.72	2.62	3.07
MAR	74	69	73	186		2.52	2.68	2.55
APR	65	67	74	170		2.61	2.55	2.29
MAY	69	69	66	108		1.56	1.56	1.64
JUN	61	58	55	93		1.53	1.59	1.70
JUL	42	43	43	63		1.51	1.48	1.48
AUG	43	47	53	86		2.02	1.84	1.64
SEP	66	83	70	138		2.10	1.66	1.96
OCT	92	80	88	202		2.19	2.51	2.29
NOV	108	111	112	298		2.76	2.69	2.67
DEC	97	99	97	239		2.46	2.42	2.46
Year	863	869	877	1986				

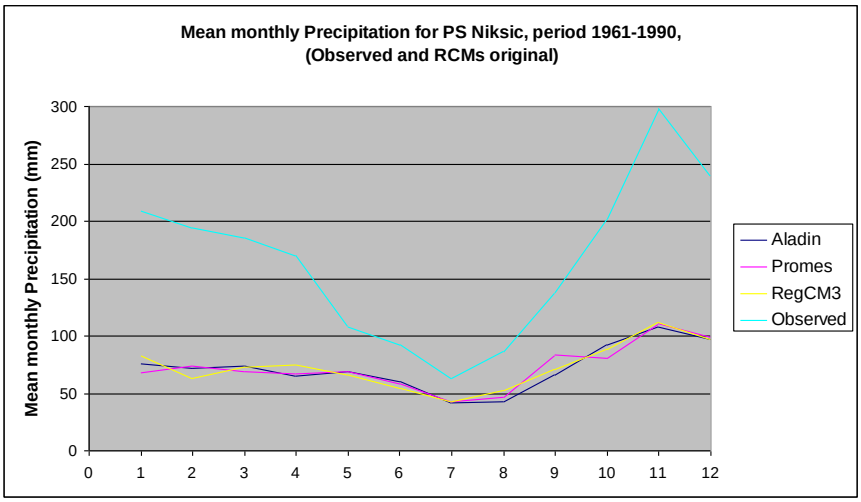

Figure 2.8 PS Nikšić, mean monthly precipitation, period 1961-1990: RCMs original and Observed data

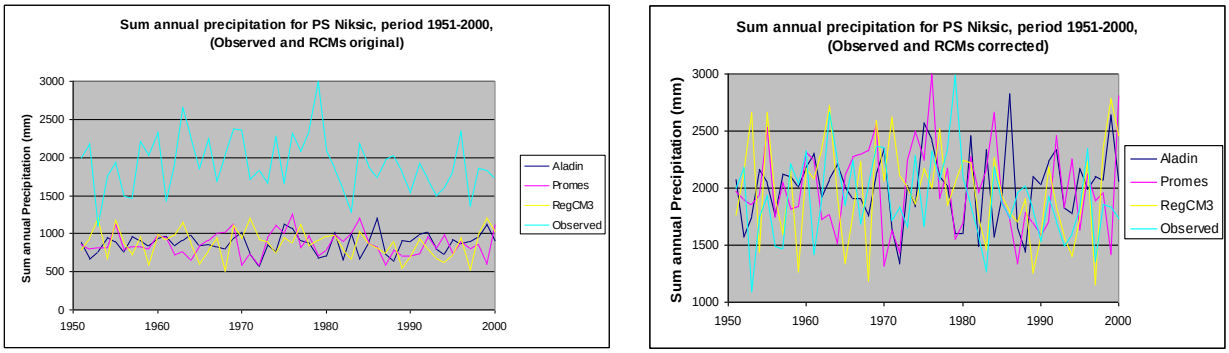

Figure 2.9 PS Nikšić, sum annual precipitation, period 1951-2000:
RCMs original and Observed data (first graph) and RCMs corrected and Observed data (second graph)

For future period (2021-2050), corrected monthly data for PS Nikšić for all three models (Aladin, Promes, RegCM3) are available on Appendix 14.

Figure 2.10a-c shows mean annual corrected precipitations with trends for PS Nikšić for all three models (period 1951-2050).

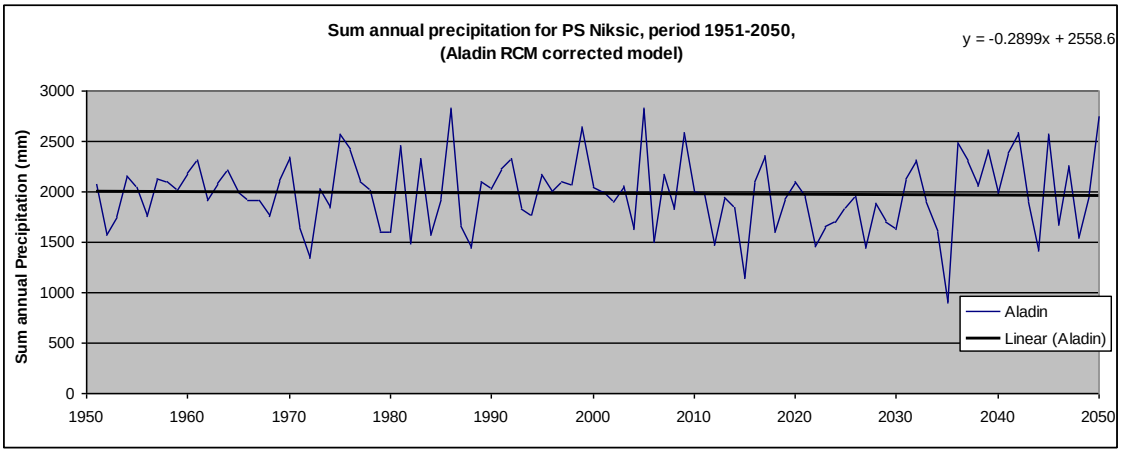

Figure 2.10a RCM Aladin

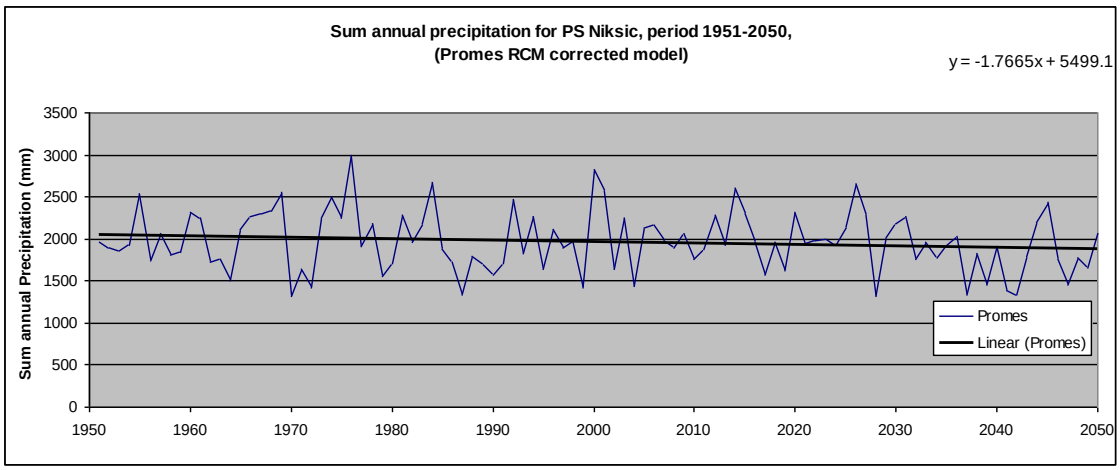

Figure 2.10b RCM Promes

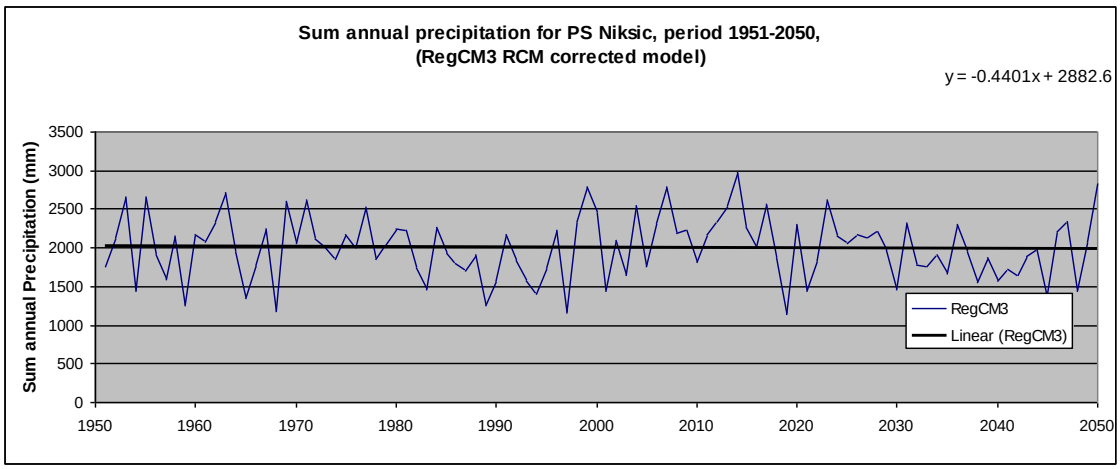

Figure 2.10c RCM RegCM3

After calculated **Lukovo-P** in RCMs (appendixes 10, 11 and 12) for both periods (1961-1990 and 2021-2050), obtained mean monthly and corrected values (instead differences, quotients here are more suitable) are as follows (table 2.8):

Table 2.8	RCMs from CCWaterS				Precipitation Lukovo (mm)	Corrected values for RCMs		
month	Aladin	Promes	RegCM3	Observed		Aladin	Promes	RegCM3
JAN	74	66	81	191		2.59	2.88	2.36
FEB	70	72	62	171		2.45	2.36	2.76
MAR	72	68	72	166		2.29	2.44	2.32
APR	65	66	73	165		2.56	2.50	2.25
MAY	70	70	66	110		1.57	1.57	1.65
JUN	62	59	56	95		1.54	1.60	1.71
JUL	43	44	44	58		1.37	1.33	1.33
AUG	43	47	53	90		2.09	1.91	1.69
SEP	65	82	70	125		1.92	1.52	1.80
OCT	91	79	87	189		2.08	2.39	2.18
NOV	106	109	110	287		2.71	2.64	2.61
DEC	95	97	95	204		2.14	2.11	2.15
Year	855	860	868	1851				

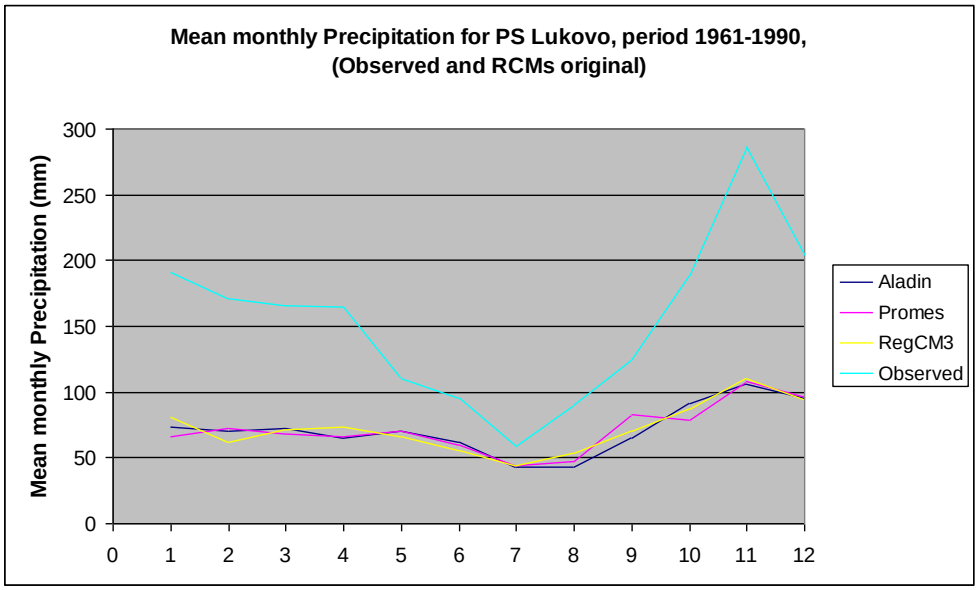

Figure 2.11 PS Lukovo, mean monthly precipitation, period 1961-1990: RCMs original and Observed data

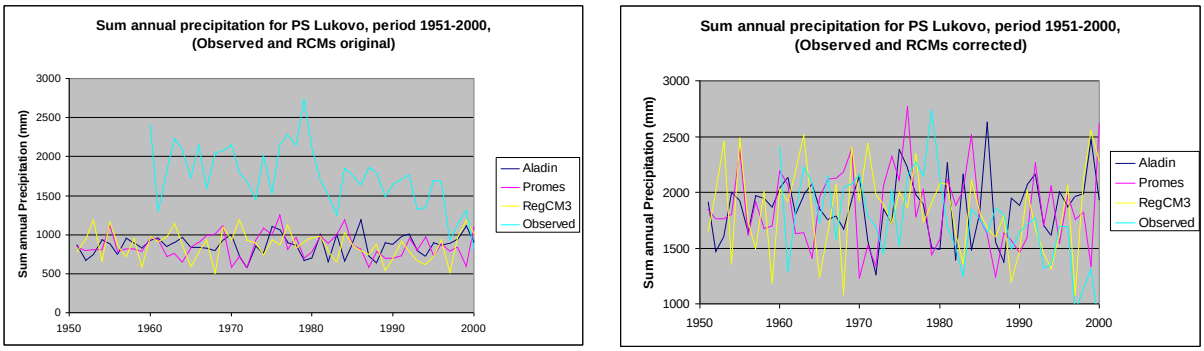

Figure 2.12 PS Lukovo, sum annual precipitation, period 1951-2000:
RCMs original and Observed data (first graph) and RCMs corrected and Observed data (second graph)

For future period (2021-2050), corrected monthly data for PS Lukovo for all three models (Aladin, Promes, RegCM3) are available on Appendix 15.

Figure 2.13a-c shows mean annual corrected precipitations with trends for PS Lukovo for all three models (period 1951-2050).

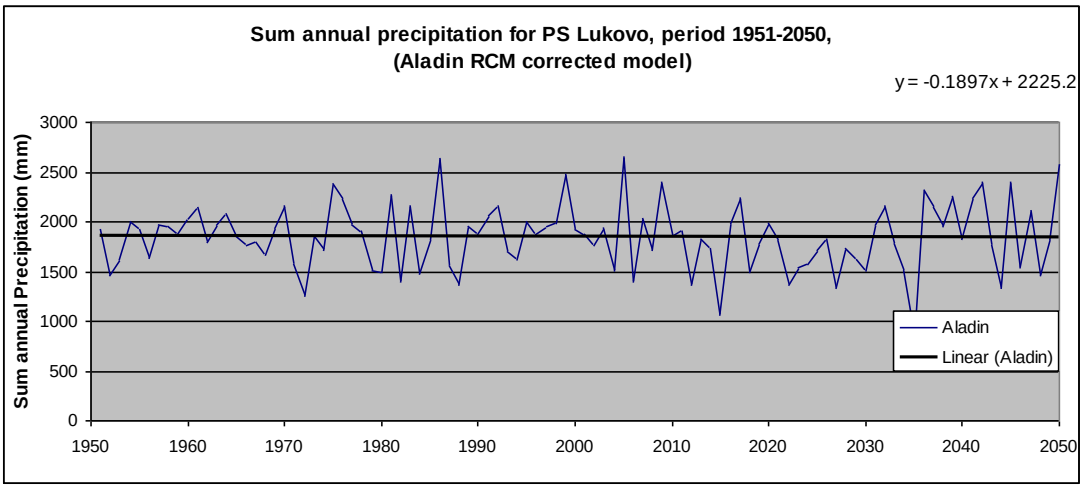

Figure 2.13a RCM Aladin

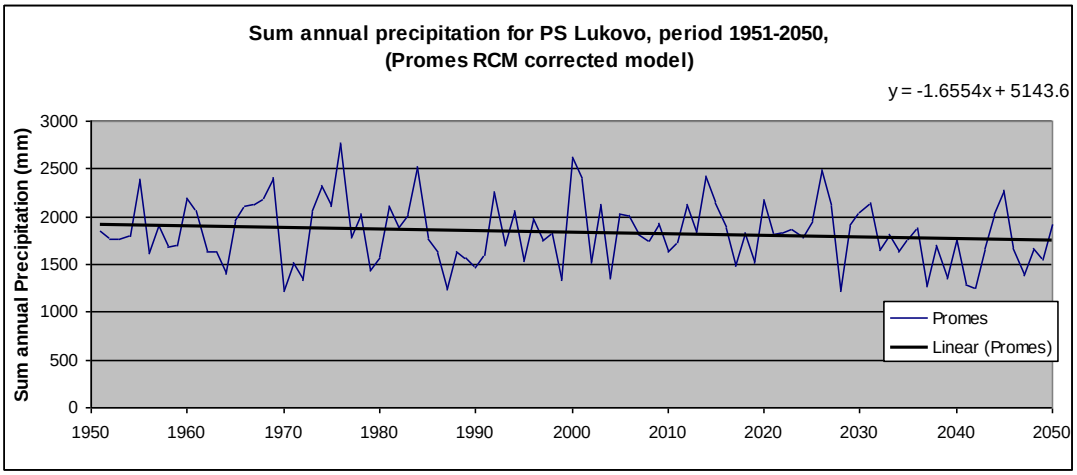

Figure 2.13b RCM Promes

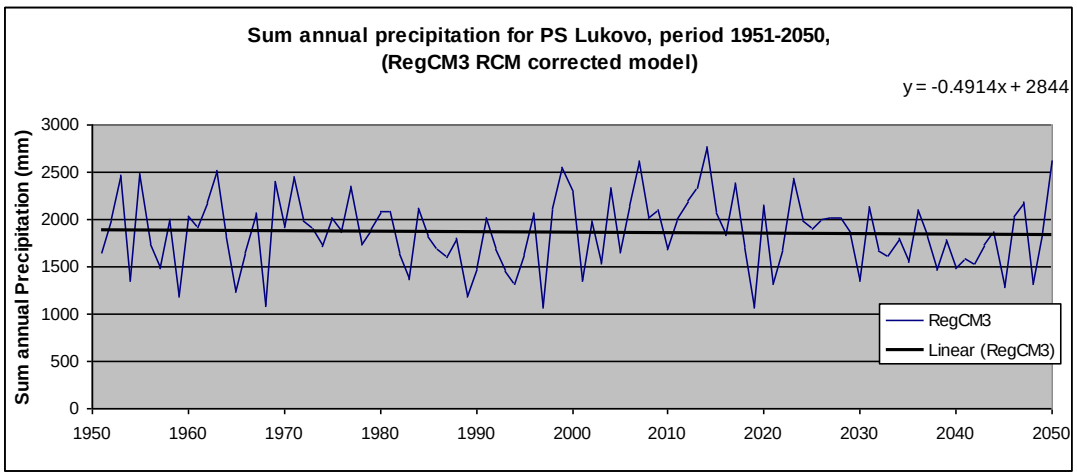

Figure 2.13c RCM RegCM3

3. Conclusion remarks

Observed temperature trend for TS Niksic are in the range 0.5 – 1.0 °C / 100 years, which is similar to region and whole world average. Seasonal increasing trends have been observed in winter, spring and particularly summer, while decreasing trend is observed for autumn. That's very much in line with observed trend results of other central part of Balkan peninsula (Serbia).

Observed precipitation trends for PS Niksic and PS Lukovo differ a lot. It seems that a slightly decreasing P trend is observed at annual level, but reliability of this claim is not high. Regarding seasonal P trends, even results indicate possibility that decreasing trend have been observed in winter, spring and particularly summer, while slightly increasing trend could be present for autumn, uncertainties is very high.

Analyzed RCMs models, a cause the extremely big differences between observed and projected values (especially for P) didn’t help us a lot.

One T and two P stations are too low number to make some more precise conclusion. The results of these T and P stations just indicate possible climate change of this part of Montenegro. The reliability of T trends could be assess as relativelly high, while for P is much lower. As known, future prediction is much more uncertaint, especially for precipitation.

Appendix 1: Observed data for Temperature station Nikšić (period 1949-2012)

T	Jan	Feb	Mar	Apr	May	Jun	Jul	Aug	Sep	Oct	Nov	Dec	Year
1949	3.2	1.8	2.2	11.2	14.7	15.9	19.6	19	16.4	12.2	8	3.6	10.65
1950	-0.1	3.7	7.1	10.6	15.5	19.3	24	22.6	17.3	10.6	6.7	5.2	11.88
1951	2.9	4.7	6.1	9.5	14	18.7	20.8	22.2	17.8	10.3	7.7	3.9	11.55
1952	1	1.3	4.1	12.3	12.9	19.4	23.3	23.9	17.7	11	6.6	4.9	11.53
1953	1.6	0.6	4.5	10.7	13.9	18.3	22.2	21.1	17.2	12.7	5.3	2.3	10.87
1954	-2.8	-2.3	6	8.6	12.7	19.3	20.8	21.2	18.5	10.8	6.4	3	10.18
1955	5	4.5	5.2	7.9	15.4	18.8	20.1	18.6	15.6	11.9	6.1	4.9	11.17
1956	2.8	-3.5	1.5	9.1	14.3	16.4	21.3	23.5	18.8	10.3	6	1.9	10.2
1957	0.1	3.8	6.6	10.3	13	19.6	21.6	20.8	16.3	12.4	7.3	2.3	11.18
1958	2.1	4.3	2.1	7.4	17	17.5	21.3	21.9	16.1	10.8	7.9	5.4	11.15
1959	-0.8	2.4	8.2	9.7	13.8	16.1	20.8	18.6	14.3	9.4	6.6	5.2	10.36
1960	1.6	3.2	6.1	9.8	13.4	18.3	19.2	21.2	15.4	12.4	8.3	5.5	11.2
1961	1.9	4.2	7.3	12.1	12.8	17.9	19.4	21	18.3	12.3	8	3.3	11.54
1962	3.7	1.3	3.4	10.2	15	17.1	20.8	23.6	17.4	12.9	7.4	1.3	11.18
1963	-1.5	0.8	3.8	10.7	14.6	18.3	21	21.5	17.4	11.3	9.3	4.3	10.96
1964	-0.2	2.5	5.7	9.8	13.9	19	19.9	19.2	15.6	11.6	7.7	4.1	10.73
1965	2.1	-3	5.3	8	13.2	17.8	21.9	19.2	15.9	11	6.9	4	10.19
1966	-1.6	4.8	4.4	11	13.7	17.8	19.4	20.4	16.9	13.5	6.3	3	10.8
1967	-1.4	1	6	9	14.7	16.4	21	21.8	16.4	13.1	8.2	2.3	10.71
1968	-2.3	3	4.8	12.4	16.3	17.7	20.5	17.3	14.9	11.4	7.8	2.4	10.52
1969	0.6	2	5.2	9	16.8	15.8	19.2	19.3	16.6	11.6	7.8	1.3	10.43
1970	1	4.9	8.9	11.8	10.3	17.8	20	19.7	17.1	10.1	6.9	3.3	10.98
1971	4.1	2.4	2.1	10	16	17.8	20.3	22	13.8	9.8	6	4	10.69
1972	2.4	4.5	8.2	10.3	13.9	19.6	19.4	18.7	13.1	7.7	6.5	2.4	10.56
1973	2.3	2.5	3.9	7.4	15.2	18	20.4	20.3	17.8	11.8	4.9	2	10.54
1974	3.2	4.5	7.6	8.2	12.5	16.6	20.3	21.8	16.8	8.6	5.5	2.9	10.71
1975	2.1	1.9	6.1	10	15.1	17.5	20.6	19	17.8	11.3	5.3	3.2	10.83
1976	0.6	3.2	3.9	9.2	14.8	17.1	19.6	15.9	13.8	12	6.4	2.5	9.917
1977	3	5.7	8.4	9.4	14.4	17.2	21.1	19	15.3	10.9	7.5	2.5	11.2
1978	1.5	2.9	6.4	8.7	12.2	17.6	19.8	19.5	13.7	10.9	5.3	4.3	10.23
1979	0.3	4.3	6.9	7.8	15.3	18.8	19.2	18.2	15.6	11.5	7.7	4.9	10.88
1980	-0.2	3.3	5	7	11.6	16.9	19.6	20.6	16.8	11.7	7.5	1	10.07
1981	-0.9	1.8	7.8	10.1	13.4	18.9	19.3	19.9	15.6	12	3.9	2	10.32
1982	2.1	1.1	4.9	8.9	15.2	19.5	20.5	20.1	18.5	11.5	6.4	4.3	11.08
1983	3.1	-0.2	6.4	10.4	14.8	16.5	21.7	18.9	15.6	10.4	4.9	3.3	10.48
1984	2.1	1.6	4.2	8.9	13	16.7	19.9	18.8	14.6	12.6	6.8	2.7	10.16
1985	-1.1	-0.9	5.4	10.1	15.5	16.7	21.7	21.3	17.8	11.2	6.8	4.8	10.78
1986	1.3	1.5	6.9	10.4	16.3	17	19.6	21.8	17.7	11.9	6.7	0.5	10.97
1987	0.6	3.3	0.3	9.1	12	17.3	22.6	20	20.1	12.3	7.5	4	10.76
1988	4.2	2.9	3.8	9.4	14.8	16.7	24.2	22.4	16.1	11.2	2.5	2.5	10.89
1989	3.2	4.6	8.8	10.7	13.2	15.8	20.4	19.9	16	10.7	5.5	3.1	10.99
1990	1.8	5.9	8.9	8.8	14.5	17.7	21.1	20.8	15.1	12.6	8	1.4	11.38
1991	1.9	1.2	8.4	8.4	10.7	18.9	20.7	20.5	16.37	10.7	6.8	-0.2	10.36
1992	1.5	2.2	5.5	9.1	15.4	17.1	20.4	24.5	17.4	12.4	7.7	2.3	11.29
1993	2.5	1.6	3.9	9.9	15.7	19.3	21	22	15.4	12.7	5.9	5	11.24
1994	3.6	3	8.3	9.5	15	18.3	22.2	22.8	18.3	12.3	7.5	3.1	11.99
1995	0.7	5.3	4	8.6	13.8	17.9	22.7	18.7	13.7	11.8	4	5.5	10.56
1996	3.2	1.2	2.9	9.4	15.2	20.2	21.5	20.9	12.7	10.3	7.5	3.5	10.71
1997	4.5	3.3	6.7	5.7	15.1	20	21	19.7	17.3	9.3	7.6	3.6	11.15
1998	3.7	5.9	3.5	9.8	14	19.5	22.6	22.4	15.1	12	5.4	0.8	11.23
1999	2.7	0.3	6	9.6	15.9	19.2	21.8	22.4	17.6	12.5	6.6	3.3	11.49
2000	-0.6	2.2	4.8	11.8	16.4	20.6	21.3	23.4	16	12.3	9	4	11.77
2001	3.7	3.8	5.568	8.9	16	18	22.1	23.2	14.2	13.2	5.6	-0.9	11.11
2002	1	5.5	8.2	10.3	15.1	20.1	21.15	20.93	14.5	10.9	8.3	4.3	11.69
2003	3.4	-1.2	5.4	8.8	18.4	21.6	23.2	24.2	15.7	10.5	8.8	3.3	11.84
2004	0.6	2.7	5.6	11	12.3	18.9	22	20.2	17.1	13.4	6	4.9	11.23
2005	1.4	-0.8	4.2	9.7	15.5	18.5	21.4	19.3	16.4	11.2	6	2.6	10.45
2006	0.7	1.6	4.6	10.9	14.8	18.5	22.6	19.4	17.3	13.2	5.5	3.6	11.06
2007	4	5.4	7.2	12.7	15.9	20.5	24.4	22.6	14.5	11.4	4.7	2.4	12.14
2008	3.1	4	6.2	10.1	15.7	19.9	22.1	23	16	12.1	7.7	3.7	11.97
2009	2.5	1.5	4.9	12.3	17	18.2	21.8	22.3	17.5	10.6	7.5	4.5	11.72
2010	1.6	2.9	5.568	11.1	14	18.6	22	23.3	16.1	10.4	9	2.5	11.42
2011	2.3	4	6.1	11.5	14.8	19.6	21.3	23.4	20.8	10.9	6.6	3.7	12.08
2012	0.2	-0.7	8.4	9.7	14.48	21.7	25.2	23.9	18.5	13	9.2	0.7	12.02
average	1.6	2.5	5.6	9.8	14.5	18.3	21.2	20.9	16.4	11.5	6.8	3.2	11.0
stdev	1.8	2.1	1.9	1.4	1.5	1.4	1.4	1.9	1.6	1.2	1.3	1.4	0.6
max	5.0	5.9	8.9	12.7	18.4	21.7	25.2	24.5	20.8	13.5	9.3	5.5	12.1
min	-2.8	-3.5	0.3	5.7	10.3	15.8	19.2	15.9	12.7	7.7	2.5	-0.9	9.9

Appendix 2: Observed data for Precipitation station Nikšić (period 1949-2012)

P	Jan	Feb	Mar	Apr	May	Jun	Jul	Aug	Sep	Oct	Nov	Dec	Year
1949	172.8	6.9	58.6	25.7	178.8	87.5	12.8	65.7	89.8	78.7	566.5	238.2	1582
1950	161.1	228.8	16.5	109.5	48.7	100.9	33.2	21.2	109	392.5	226.1	545.7	1993
1951	164.9	309.8	262.1	110.4	138.1	82.3	25.2	70.2	202.2	175.2	284.6	169.9	1995
1952	275.4	170.9	51.4	40.1	117.2	18.6	21	9.7	239.8	309.4	325.4	609.4	2188
1953	202.8	207.1	0.2	160.1	118.3	169	17.3	51.7	81.1	23.1	6	59.7	1096
1954	221.5	172.1	318	117	230.8	76.6	24.2	16.4	54.6	163.4	125.4	226.1	1746
1955	278.5	366.6	126.2	20.9	21	51.1	73.7	70.2	255.4	358.9	140.6	180.3	1943
1956	123.8	275.9	81	86	124.9	164	12.1	9.2	21.8	145.2	322.6	125.4	1492
1957	172.8	188.9	29.9	82.6	128.2	37.1	51	55.3	42	180.1	207.4	293.3	1469
1958	173.7	237.3	261	255.9	94.3	175.1	34.1	46.6	76.4	150.9	305	401.8	2212
1959	257.1	46.6	69.6	98.2	175.8	178.1	71.9	186.1	103.2	102.5	198.8	540.7	2029
1960	142.7	309	253.5	144.4	63.5	27.7	56.2	31.7	175.7	250.6	458.7	415.8	2330
1961	139.3	37.1	41.9	128.5	125.3	149.5	70.8	17.8	17.3	193.9	397.6	101.7	1421
1962	107.3	93.6	388.6	264.2	22.3	40.6	79.7	11.4	82.3	96.6	464.8	259.4	1911
1963	358.6	381	161.1	83.5	97.2	188.3	181.8	88.6	125.8	118.2	429.1	449.6	2663
1964	4.1	150.6	258	148.4	68.8	141.8	87.1	62.6	51.2	581.8	137.5	555	2247
1965	145.2	101.3	249	294.5	92.6	87.2	6.5	71.5	128.7	0	401	272.8	1850
1966	290.1	273.1	111.8	85.4	82.9	54.2	166.4	10.8	108.8	426.1	441.6	198.3	2250
1967	301	50	140.9	211.9	77	168.2	51.9	23.3	144.7	44.6	177.4	290.6	1682
1968	255.5	128.7	210.7	32	142.9	109.6	40.9	165.8	161.4	50.7	382.3	351	2032
1969	234.2	511	116	159.3	78.9	231.5	45.7	173.9	146.3	0	326.3	346.3	2369
1970	449.6	266.2	304.1	434.2	102.7	70.8	53.9	56.2	10.6	122.8	211.8	277.6	2361
1971	454.4	115.4	179.2	15.7	39.1	27.5	33.7	34.2	175.4	89	374.3	177.1	1715
1972	261.7	239	70.6	248.4	84.2	23	132.4	135.7	314.6	103.3	185.6	39.3	1838
1973	179.1	339.4	98.8	155.4	39.3	58.5	90.4	67.2	129.3	64.9	179.8	253.1	1655
1974	43.8	280.9	86.1	161.9	210.7	74.7	21.6	80.2	332.9	710.2	190.3	92.8	2286
1975	36.6	15.6	227	165.7	76.3	39.6	92	147.7	50.3	494.9	205.7	109.9	1661
1976	169	104.6	195	233.5	93.3	144.4	91.1	133.2	141.1	263.9	336.7	418.9	2325
1977	288.3	220.5	258.4	150	77.5	40.4	36.7	158	192.1	156.2	313.5	180.9	2073
1978	182.6	282.7	219.7	321.4	337.6	64.6	35.9	31.3	301.5	187.2	132.7	246	2343
1979	383.1	272.6	155.4	460	38.5	149.2	144.9	253.7	89.2	324.7	496.1	226.3	2994
1980	227.2	62.5	228.7	107.2	182.5	81.4	36.1	17.5	31.5	366.7	538.5	207.2	2087
1981	175.4	136.2	153.5	113.2	110.3	72.3	46.7	43.7	118.5	288.6	56.7	530.3	1845
1982	50.3	91.2	200.3	60.3	55.4	53.5	99.4	104.6	52.9	268.2	159.7	381.4	1577
1983	40.4	249.3	87.2	87.2	92	74.5	23.8	96	147.5	50.9	98.1	223.3	1270
1984	356.8	179.2	141.7	108.6	232.4	19.1	28.6	90.7	488.6	209.5	233.6	97.5	2186
1985	215.3	131.9	236.4	73.3	91.1	77.8	2.8	21.8	3.6	23.9	805.8	186.1	1870
1986	254.4	417.2	246.3	99.9	115.3	153.8	49.3	18.7	45.3	181.1	66.9	89.3	1738
1987	386.5	163.2	284	69.5	210.6	100.7	12.6	45.8	23	69.6	471.6	125.2	1962
1988	183	313.6	272.4	194.8	115.9	106.1	0.6	155.6	354.4	64.5	75.7	187.7	2024
1989	3.3	178.1	201.6	160.4	102	135.2	75.2	204.2	116.1	250.1	339.9	39.3	1805
1990	75.1	44.9	42.7	281.6	51.9	42.9	50.2	66.7	57.6	258.2	303.4	258	1533
1991	18.4	294.2	53.9	174.5	138	72.2	129.3	16.6	138.3	265.9	598.9	27.2	1927
1992	78.6	37.3	113.7	255.1	33.8	142	78.8	4	34	619.4	138.9	169.9	1706
1993	7.5	0	140	96.3	107.2	24.5	61.2	66.8	121.9	223.2	299.3	345.5	1493
1994	132.1	154	12.9	410.7	99	61.1	52.8	41.9	132.4	319.4	114.5	68.9	1600
1995	161.3	238.8	234.6	118.3	126.7	78	49.6	218.4	215.3	0.2	131.1	249.3	1822
1996	226.3	204.6	139.8	274.7	208.2	36.7	1.7	82.7	377	184.5	398.1	208.1	2342
1997	98.7	92.9	76.2	138.1	102.8	18.8	20.9	74.9	28.5	103.5	315.9	288.3	1360
1998	111.5	64.2	6.4	209.9	177.7	152.3	38.5	124	233.3	348	178.5	215	1859
1999	154.2	210	132.3	156.6	59.4	83.1	57.2	45	56.2	112	259.7	513.3	1839
2000	58	96.1	109.2	198.6	41.5	11.3	54	5	130.5	236.4	307.1	475.5	1723
2001	323.2	95	183.8	192.7	55	31.1	24.1	42.9	242.1	43.6	413.6	104.3	1751
2002	69	112.1	35.8	185.7	139.5	40.2	87	171.9	278.3	228.7	136.9	269	1754
2003	397	121.1	2.3	123.1	33.6	157.6	5.1	26.9	134.9	442.1	416.8	144.9	2005
2004	392.5	239	255.5	204	223.7	117	30.4	54	150.8	127.1	273.2	519.1	2586
2005	128.1	380.7	220	126.8	42.8	84	57.9	124.2	186.3	155.7	368.2	381.3	2256
2006	111.9	220.8	238.3	121.5	71.7	75.8	26.8	129.1	101.5	127.8	126.4	218	1570
2007	209.3	292.4	246.9	16.4	92.8	30.2	5.4	13.8	129.9	146.2	220.4	122.7	1526
2008	185.6	65.9	411.9	123.1	75.8	105.6	17.6	39.9	102.1	220.9	218.2	433.1	2000
2009	495.1	143	193	45.1	73.3	157.6	80.7	51.3	48.2	279.8	337.4	403.3	2308
2010	441.4	447.3	170.2	186	157.4	220	39.4	23.1	209.6	195.9	620	501	3211
2011	58.1	132.8	116.4	74	146.4	35.1	69.2	17.4	63	106.4	33.9	278	1131
2012	64.9	280.3	0	394	98.5	35.7	26.3	46.8	141.4	300.7	293.5	246	1928
average	196	192	159	159	109	89	52	73	138	206	286	268	1927
stdev	123	115	98	100	61	55	39	60	99	151	158	149	398
max	495	511	412	460	338	232	182	254	489	710	806	609	3211
min	3.3	0.0	0.0	15.7	21.0	11.3	0.6	4.0	3.6	0.0	6.0	27.2	1096

Appendix 3: Observed data for Precipitation station Lukovo (period 1960-2012)

P	Jan	Feb	Mar	Apr	May	Jun	Jul	Aug	Sep	Oct	Nov	Dec	Year
1960	140.7	337.9	237.8	137.4	67.3		72.2	32.6	164.9	345.1	500	368.9	2405
1961	103.1	22.1	45.1	86.5	160.4	100.6	56.9	22.7	23.4	226.2	360.3	83.9	1291
1962	94.7	82.4	387.7	227.7	15.5	67.4	73.8	22.5	76.6	100	444.9	221.2	1814
1963	320.1	331.3	128.5	70.8	87.3	162.5	107.1	111.7	112.1	97.2	328	372.9	2230
1964	4.6	97.8	238.7	169.2	95.6	120.5	69.3	76.5	41.6	550.1	153.2	461	2078
1965	116.4	102.2	199.6	270	103.7	96.7	5.5	96	132	0	347.1	251.7	1721
1966	252.6	204.9	99.5	85.4	182.9	60	181.3	47.5	78.4	416.9	362	179.2	2151
1967	263.9	30.6	144.8	190.1	59.1	151.8	80.2	56.8	134.3	54.2	163.8	251.4	1581
1968	307.2	98.1	219.8	29.9	130.1	119.2	21.6	174.4	153.7	38.1	325.2	425.2	2043
1969	157.5	366.9	107.9	151.5	89.3	193.1	51.9	184.3	151.4	0	259.5	363.9	2077
1970	331.9	238.5	252.4	443.1	123.7	54.1	69.1	66.9	13	113.2	245	206.8	2158
1971	419	106.8	211.3	170.3	60.7	50.6	40.1	36.1	144.8	64.6	358.2	127.8	1790
1972	237.4	160.5	53.4	213.5	78.1	30.1	181.6	165.8	263	94.3	176.6	26.6	1681
1973	146.1	221.8	96.8	173.5	34.8	49.1	89	60.3	122.2	73.4	159.7	219.1	1446
1974	25.4	199.9	69.1	164	181.5	81.1	14.5	66.7	314.1	648.5	191	67.9	2024
1975	25.8	17.5	187.8	124	76.4	78.3	83.5	64.4	42.5	399.9	302.3	118.1	1521
1976	164.9	115.9	147.7	223.4	83.5	141.2	69.2	92.9	107.6	271.4	372.2	355.5	2145
1977	241.6	225.1	183.7	122.3	71.3	117.1	41.9	398.5	204.8	201.1	297.4	172.7	2278
1978	234.7	287.7	202	288.1	270.7	65.8	20.7	37.5	287.7	161.5	84.7	203.1	2144
1979	337.3	242.2	177.7	362.1	41.2	191	94.7	217.9	84.2	357.9	439.6	193.9	2740
1980	220.7	79.9	223.1	131.6	183.5	69.6	50.2	30.6	38.4	380.3	493.3	234.6	2136
1981	150.2	129.6	157	149.7	103.2	85.9	52.8	76.7	127.7	193.1	263.1	201.3	1690
1982	159.8	158.1	147.1	69.3	36.9	89	60.4	57.8	74.4	252.8	137.7	259.1	1502
1983	53.8	225.5	89.1	108.1	99.8	91.5	46.5	79.7	111.3	53.2	98.2	190.4	1247
1984	275.6	163.7	159.1	88.2	230	27.6	13.3	88.8	315.8	146.8	254.6	87.8	1851
1985	186.9	115.3	202.1	80.1	106.7	79.7	19	53.6	5.7	27.1	697.4	190.2	1764
1986	259.6	364.1	202.8	151.4	98.9	158.1	45.1	21.1	38.9	143.1	59.2	91.3	1634
1987	388.3	129.2	249.2	104.8	190.1	65.4	7.7	56.4	38.8	67.8	452	111.5	1861
1988	132.4	275.8	174.6	209	94.4	87.1	0	89.4	324.4	62.9	140.7	207.1	1798
1989	2.1	178	188.2	147.9	97.6	85.9	52.8	76.7	127.7	200	302.3	28.8	1488
1990	112.8	158.1	37.5	149.7	103.2	85.9	52.8	76.7	66.9	271.3	328.8	201.3	1645
1991	18.1	254.9	56	129	157.1	81	52.8	76.7	127.7	339	398.1	18	1708
1992	41.8	30.3	147.1	250.7	48.8	139.5	63.7	3.4	29.4	606.3	263.1	144.7	1769
1993	3.1	1.2	147.1	84.2	85.7	20.7	76.6	98.4	139.4	201.4	263.1	201.3	1322
1994	123.4	114.3	18.2	335.8	62.9	55.1		23.3	187.7	241.7	113.8	71.7	1348
1995	159.8	182.7	203.1	137.3	118.9	121.2	42.7	175.8	210	0	97	250.4	1699
1996	60.8	158.1	120.6	77.3	185.8	34.2	59.3	75.2	290.7	233.1	263.8	127.3	1686
1997	73.8	22.6	89.6	85.1	53.3	18.6	32.9	51.1	127.73	81.5	193.6	101.8	932
1998	49.5	31.6	5.3	128.9	103.17	85.92	38.2	76.67	205.1	191.1	128	97.6	1141
1999	77.2	127.9	147.1	157.2	103.17	85.92	31.1	59.6	32.9	74.8	145.8	271	1314
2000	43.8	62.9	57	57.4	9.7	7.3	43.4	33.1	62.4	120.4	147	148.5	793
2001	121	74.6	147.1	99.5	39.9	26.9	18.1	20.1	142.5	11.9	219.5	201.3	1122
2002	38	51.5	25.8	104.5	106.5	39	60.3	91.8	157	127.3	96.2	155.7	1054
2003	207.4	158.1	0.5	70.5	19.7	57.6	7.5	1.6	75.1	341.7	182.9	79.4	1202
2004	210	176.3	170.3	130.9	163.7	61.7	19.6	30.9	68.4	77.3	161.2	257.1	1527
2005	49.8	274.4	165.5	60.7	51.6	41.3	52.8	76.7	127.7	193.1	221	369.9	1685
2006	120.2	180.6	205.6	122.6	71.6	61.8	45.4	153.3	70.3	109.9	263.1	201.3	1606
2007	236.2	198.2	147.1	17.7	164.4	51.3	3.2	76.7	189.1	209.1	172.3	83.8	1549
2008	148.7	60.4	284.6	112.6	89.8	69.3	72.6	23	149.1	150.2	184.9	263.3	1609
2009	346.8	119.1	147.1	119.3	37.4	213.9	45.5	141.1	48.7	221.9	347.9	358	2147
2010	341.6	352.8	169.5	149.3	216.3	247.4	58.8	13.8	183.8	152.8	618.4	325.9	2830
2011	51.6	99.3	119.4	66.1	114	67.4	79.9	5.1	84.2	132	38.5	241.8	1099
2012	78.5	179.3	0	342.8	107	24.9	18.4	16.9	138.1	406.6	327.5	223.1	1863
average	160	158	147	150	103	86	53	77	128	193	263	201	1716
stdev	111	96	78	86	57	52	36	67	82	152	139	105	426
max	419	367	388	443	271	247	182	399	324	649	697	461	2830
min	2.1	1.2	0.0	17.7	9.7	7.3	0.0	1.6	5.7	0.0	38.5	18.0	793

Appendix 4: CCWaterS original RCM data for Temperature station Nikšić (Aladin, periods 1961-1990 and 2021-2050)

	Jan	Feb	Mar	Apr	May	Jun	Jul	Aug	Sep	Oct	Nov	Dec	Year
1961	-1.27	-0.30	1.91	7.56	10.60	14.12	18.69	17.11	12.48	8.50	6.95	5.97	**8.53**
1962	1.08	-2.94	0.67	6.49	10.88	15.88	17.77	16.26	14.61	8.58	-0.30	-1.43	**7.30**
1963	-1.07	-0.64	2.82	6.11	8.93	14.96	16.20	14.68	11.74	8.59	1.72	-3.67	**6.70**
1964	-1.39	-4.54	-0.23	5.42	8.78	11.78	14.10	14.54	12.66	9.21	6.30	1.56	**6.52**
1965	-3.26	-1.48	4.49	7.12	10.79	16.02	18.52	20.36	13.45	7.18	6.40	-0.75	**8.24**
1966	-3.50	0.91	2.49	7.66	10.16	15.38	16.32	17.30	12.55	8.28	4.05	1.86	**7.79**
1967	2.17	-1.58	1.85	5.63	10.95	13.56	17.28	17.84	13.27	5.83	4.20	-3.27	**7.31**
1968	-2.28	-0.76	1.65	3.77	10.69	13.10	15.97	16.13	11.22	10.56	7.54	-1.34	**7.19**
1969	-0.77	-0.23	-1.79	5.86	11.89	13.68	17.87	18.89	13.90	9.83	2.97	4.24	**8.03**
1970	-0.27	4.53	3.65	8.42	11.59	14.64	17.83	15.67	15.63	11.21	4.44	2.62	**9.16**
1971	-1.69	-0.72	4.13	7.65	12.45	12.94	16.15	16.90	13.82	9.00	5.33	0.27	**8.02**
1972	-3.05	1.41	3.74	6.79	11.81	16.06	17.34	15.70	13.92	5.73	5.49	-2.30	**7.72**
1973	-3.76	2.25	0.72	6.85	9.72	15.30	18.84	20.17	13.02	9.63	5.53	3.82	**8.51**
1974	-0.02	1.31	2.60	5.99	12.20	14.31	15.46	17.90	16.27	11.49	2.00	-2.69	**8.07**
1975	-1.92	-0.20	3.19	6.18	11.30	15.15	14.79	15.60	13.62	9.80	1.70	-0.50	**7.39**
1976	-2.19	1.40	3.68	5.71	11.53	15.33	15.76	13.57	11.79	8.76	2.74	4.61	**7.72**
1977	-0.82	-0.55	3.26	5.86	11.77	16.35	15.45	16.92	14.91	7.95	2.76	-1.21	**7.72**
1978	-1.94	0.67	4.07	6.74	11.66	15.82	14.94	16.41	12.70	9.60	5.28	-0.43	**7.96**
1979	-2.54	1.10	2.30	5.86	13.06	15.85	14.99	16.86	14.02	9.12	5.95	-1.06	**7.96**
1980	-4.05	-4.91	-0.52	5.52	9.02	16.68	16.63	18.02	12.69	9.56	1.94	0.97	**6.80**
1981	5.90	3.92	8.18	7.29	11.90	15.02	16.69	20.14	12.88	9.03	2.85	0.38	**9.52**
1982	-0.32	-3.52	3.97	7.59	13.29	17.51	19.40	18.61	13.17	10.71	2.04	1.49	**8.66**
1983	-0.58	-3.07	4.49	6.06	11.67	15.52	17.56	19.68	13.59	9.92	6.16	1.36	**8.53**
1984	-0.45	-2.95	2.82	7.26	12.63	15.68	20.24	15.06	15.73	7.78	6.09	0.51	**8.37**
1985	-2.95	1.37	4.19	7.78	11.44	12.24	16.97	18.31	14.55	10.23	3.65	-1.76	**8.00**
1986	-4.37	-0.73	4.42	3.54	10.26	13.31	15.18	14.58	13.23	9.39	8.38	2.69	**7.49**
1987	2.35	0.30	3.01	6.95	11.02	14.28	17.82	17.00	13.56	9.24	1.58	-1.51	**7.97**
1988	-1.99	-0.58	0.54	8.03	13.24	14.14	17.74	20.05	13.11	10.40	7.06	-1.97	**8.31**
1989	-1.98	0.09	4.26	7.45	13.15	15.37	15.78	17.87	13.77	7.91	4.11	3.18	**8.41**
1990	-1.41	-0.35	1.48	7.90	10.65	14.02	14.76	16.35	15.57	11.36	7.92	0.80	**8.25**
Average	**-1.28**	**-0.36**	**2.73**	**6.57**	**11.30**	**14.80**	**16.77**	**17.15**	**13.58**	**9.15**	**4.43**	**0.41**	**7.94**
	Jan	**Feb**	**Mar**	**Apr**	**May**	**Jun**	**Jul**	**Aug**	**Sep**	**Oct**	**Nov**	**Dec**	**Year**
2021	-2.22	1.02	3.88	8.18	12.81	13.45	18.26	20.47	15.66	10.97	4.93	-1.65	**8.82**
2022	-1.02	2.16	4.41	8.87	11.37	17.71	20.14	19.47	15.64	9.67	5.27	1.58	**9.61**
2023	-2.01	3.28	2.22	9.75	12.94	15.88	18.87	20.40	14.95	10.02	4.73	2.98	**9.50**
2024	-0.78	-0.48	4.58	9.37	14.92	19.29	20.01	18.11	13.84	8.90	2.19	3.31	**9.44**
2025	0.26	2.13	6.87	6.67	14.07	16.66	17.94	17.35	14.77	11.07	8.23	4.00	**10.00**
2026	2.28	0.23	6.84	6.99	11.93	13.79	19.24	20.31	16.37	12.02	5.04	2.52	**9.80**
2027	1.37	1.79	4.66	9.98	18.29	16.83	16.72	19.95	16.28	11.12	2.90	0.68	**10.05**
2028	0.04	2.45	2.51	9.01	11.93	16.77	19.72	20.43	14.67	11.72	4.84	2.23	**9.69**
2029	-1.84	-0.15	2.24	7.11	10.35	17.64	17.63	17.98	15.32	5.56	4.08	2.98	**8.24**
2030	-2.63	0.83	6.91	9.33	12.46	17.59	16.76	21.17	16.27	10.73	5.23	0.45	**9.59**
2031	1.97	2.11	3.35	6.67	13.83	15.80	17.54	19.41	15.70	11.30	6.71	4.35	**9.89**
2032	-0.13	-2.82	2.31	7.08	12.65	17.81	20.91	22.12	12.88	10.74	8.52	1.80	**9.49**
2033	-0.40	1.92	5.72	10.17	12.52	15.53	20.71	19.59	16.29	9.74	4.23	0.60	**9.72**
2034	-0.01	1.99	2.70	7.68	13.98	20.85	21.35	21.05	16.36	11.38	6.66	1.76	**10.48**
2035	0.31	-1.18	1.96	6.61	16.68	23.04	25.11	23.71	18.70	12.91	5.37	1.58	**11.23**
2036	0.24	2.78	7.17	6.06	12.44	15.46	19.10	16.01	12.22	8.40	7.75	2.69	**9.19**
2037	0.35	0.70	5.00	6.19	12.06	18.48	19.88	19.49	16.70	12.07	8.48	0.08	**9.96**
2038	0.08	1.33	5.02	9.22	14.86	18.22	21.86	17.25	15.00	11.80	3.31	0.39	**9.86**
2039	-1.53	4.13	4.66	7.19	12.07	16.63	17.48	15.11	11.90	11.53	6.90	3.81	**9.16**
2040	-0.26	-2.09	3.65	8.81	14.59	16.64	21.48	20.47	15.58	9.95	5.49	6.29	**10.05**
2041	2.88	2.38	3.47	7.18	13.11	16.60	17.25	18.67	14.31	9.25	3.10	1.61	**9.15**
2042	-0.24	0.80	2.15	8.22	11.40	14.33	20.81	18.34	14.32	11.60	8.21	1.84	**9.32**
2043	-1.01	1.54	7.44	9.63	12.50	17.35	21.74	18.07	16.77	10.53	3.55	2.24	**10.03**
2044	1.07	0.22	2.25	8.57	13.48	17.45	20.54	23.00	16.35	7.88	5.45	1.87	**9.85**
2045	1.66	1.02	5.44	9.23	14.58	18.83	22.37	21.03	16.88	11.91	8.18	4.43	**11.30**
2046	0.88	1.35	5.70	8.00	16.51	18.43	19.20	20.65	15.98	9.33	6.26	3.32	**10.47**
2047	-0.21	3.65	7.00	10.91	14.98	19.74	17.66	22.18	14.94	11.11	7.51	0.69	**10.85**
2048	-2.11	-0.56	4.15	9.54	14.26	19.35	21.67	22.01	16.70	12.83	8.26	0.33	**10.54**
2049	-0.61	2.44	3.53	8.86	15.16	19.14	23.04	23.03	16.95	11.43	8.08	6.52	**11.46**
2050	5.35	2.37	1.85	9.30	12.85	15.21	18.89	18.99	17.83	12.91	8.07	0.61	**10.35**
Average	**0.06**	**1.25**	**4.32**	**8.35**	**13.52**	**17.35**	**19.80**	**19.86**	**15.54**	**10.68**	**5.92**	**2.20**	**9.90**

Appendix 5: CCWaterS original RCM data for Temperature station Nikšić (Promes, periods 1961-1990 and 2021-2050)

	Jan	Feb	Mar	Apr	May	Jun	Jul	Aug	Sep	Oct	Nov	Dec	Year
1961	0.4	2.2	-0.2	4.7	10.3	14.4	15.7	18.4	14.5	9.4	5.1	3.3	**8.2**
1962	-1.9	-1.1	3.0	8.0	9.9	15.7	17.4	17.6	16.2	8.8	5.0	-0.6	**8.2**
1963	-5.5	0.1	3.5	7.6	10.9	14.9	15.1	17.3	15.1	7.6	3.9	-3.3	**7.3**
1964	-5.0	-1.6	-0.5	6.4	12.9	17.0	19.5	17.8	13.9	6.8	3.7	-2.5	**7.4**
1965	-2.7	-1.1	1.6	5.5	10.9	16.4	18.9	16.5	14.9	11.6	5.5	0.1	**8.2**
1966	1.4	-2.6	2.3	4.9	11.1	16.7	16.2	15.9	17.0	9.3	5.9	3.0	**8.4**
1967	-1.2	-3.5	-1.0	5.7	10.0	12.7	16.3	16.7	11.7	9.7	7.2	1.2	**7.1**
1968	-2.9	-2.2	0.8	6.6	10.0	15.9	17.0	15.1	9.8	7.2	5.2	3.4	**7.2**
1969	-0.3	-2.6	2.7	5.5	13.7	12.8	16.7	17.6	13.6	11.1	5.1	0.4	**8.0**
1970	-3.9	-1.6	5.3	9.1	11.4	14.5	17.1	16.9	14.7	10.9	2.0	0.7	**8.1**
1971	-2.2	1.2	3.2	4.9	9.2	13.9	17.9	16.4	11.4	8.0	0.4	-4.4	**6.7**
1972	-3.2	-0.8	4.9	8.2	11.6	13.4	17.5	16.1	17.1	9.7	3.6	-2.9	**7.9**
1973	-0.2	1.9	6.2	9.5	13.1	17.4	17.6	18.7	14.0	7.2	6.5	0.7	**9.4**
1974	1.2	-0.6	2.6	5.2	11.3	13.4	17.8	14.1	12.0	8.1	6.4	-1.2	**7.5**
1975	-1.5	-0.5	1.0	5.6	10.8	13.3	17.4	16.0	12.3	8.7	3.2	1.9	**7.4**
1976	-3.5	-1.8	1.5	5.3	11.1	15.1	16.7	16.0	11.5	7.4	7.2	2.5	**7.4**
1977	-3.4	-4.6	0.3	5.6	9.4	14.8	16.9	17.8	12.3	7.1	4.9	3.3	**7.0**
1978	0.6	1.0	2.1	7.2	9.8	13.4	16.6	18.7	14.6	6.9	2.8	1.5	**7.9**
1979	-3.1	-2.0	1.1	7.3	10.7	15.4	15.3	16.8	15.5	8.0	0.9	1.9	**7.3**
1980	1.0	1.0	3.1	7.9	12.9	13.4	16.1	17.8	15.2	9.7	4.6	1.9	**8.7**
1981	2.3	0.6	2.7	5.7	13.1	15.0	17.1	15.3	12.9	10.2	5.8	0.2	**8.4**
1982	-1.7	1.8	2.4	5.8	13.6	12.2	16.4	15.6	13.7	7.8	7.5	1.6	**8.1**
1983	-4.0	0.7	4.1	7.6	9.6	12.8	13.1	16.6	13.6	10.0	6.2	1.5	**7.7**
1984	-1.3	-0.3	2.0	7.9	10.6	12.7	15.2	15.6	12.6	8.2	4.3	-1.1	**7.2**
1985	-0.1	4.5	5.6	9.0	12.6	16.5	17.7	18.6	14.8	9.0	6.5	1.9	**9.7**
1986	-0.5	-0.2	2.3	7.1	11.0	12.7	17.0	16.5	12.8	10.0	3.2	0.4	**7.7**
1987	-1.9	1.3	4.0	4.8	10.9	15.1	17.5	17.8	12.3	10.7	2.7	-1.8	**7.8**
1988	-0.5	0.6	0.1	6.4	12.9	16.7	18.2	19.5	12.5	10.1	1.6	-2.6	**8.0**
1989	-1.0	-3.3	-0.1	5.9	12.3	14.9	17.1	18.2	13.9	7.2	3.7	0.7	**7.5**
1990	-2.9	-3.9	5.3	7.3	13.6	15.3	16.6	16.2	14.2	9.7	5.5	1.8	**8.2**
Average	**-1.6**	**-0.6**	**2.4**	**6.6**	**11.4**	**14.6**	**16.9**	**16.9**	**13.7**	**8.9**	**4.5**	**0.5**	**7.8**
	Jan	**Feb**	**Mar**	**Apr**	**May**	**Jun**	**Jul**	**Aug**	**Sep**	**Oct**	**Nov**	**Dec**	**Year**
2021	0.4	3.1	4.6	9.0	13.4	16.2	19.8	19.1	12.7	6.2	5.9	1.3	**9.3**
2022	2.5	1.6	4.3	6.8	13.4	14.4	19.1	17.9	15.5	8.5	6.8	1.8	**9.4**
2023	2.6	3.8	4.3	7.2	14.1	16.9	22.8	20.5	16.8	10.8	5.8	1.9	**10.6**
2024	1.0	2.2	7.8	9.2	15.2	16.8	22.0	19.1	15.5	12.4	6.1	5.0	**11.0**
2025	-1.9	-1.3	2.3	7.3	12.6	17.1	17.9	17.9	15.3	9.8	3.4	1.4	**8.5**
2026	0.6	-0.2	4.6	9.7	14.6	15.2	19.0	18.2	14.3	8.9	7.4	0.6	**9.4**
2027	0.3	0.5	-0.9	6.3	11.6	17.6	16.7	17.8	16.2	9.7	2.5	0.8	**8.3**
2028	1.1	-1.7	1.4	5.7	14.0	20.8	17.4	17.2	16.8	10.0	3.1	1.9	**9.0**
2029	0.6	2.7	8.3	6.4	13.2	17.6	18.3	17.5	15.0	10.7	5.5	-0.1	**9.6**
2030	-1.8	2.5	3.7	9.6	12.0	19.4	22.9	21.2	17.2	11.7	7.1	4.3	**10.8**
2031	-2.5	-0.2	5.4	8.7	14.5	15.4	20.1	19.1	16.6	12.5	4.2	1.8	**9.6**
2032	2.8	2.7	3.7	9.3	13.8	19.9	19.6	18.6	17.9	12.2	5.9	3.4	**10.8**
2033	4.8	3.4	8.0	12.1	16.2	18.7	22.7	18.6	11.9	8.5	8.4	2.2	**11.3**
2034	2.7	1.7	5.6	7.8	14.8	17.2	20.0	19.4	17.4	10.9	9.5	4.3	**10.9**
2035	2.3	3.2	6.1	6.6	11.8	21.2	20.2	19.2	14.7	13.4	6.4	3.1	**10.7**
2036	0.8	-0.3	8.4	9.7	13.5	16.8	18.8	19.4	16.0	11.7	6.1	2.6	**10.3**
2037	1.9	0.6	7.3	9.9	14.4	18.8	19.8	20.9	14.5	12.7	4.0	-1.2	**10.3**
2038	2.9	-1.6	6.4	9.3	14.4	16.9	19.5	20.8	15.5	11.4	6.4	-3.2	**9.9**
2039	2.3	2.9	3.4	9.6	15.2	17.5	20.1	21.4	15.6	9.3	5.2	0.8	**10.3**
2040	2.1	3.3	5.6	8.4	15.2	21.7	23.0	19.2	17.4	12.6	3.9	2.4	**11.2**
2041	2.1	3.2	4.0	6.5	10.9	18.5	22.1	22.6	15.3	12.0	6.0	0.2	**10.3**
2042	2.7	-3.3	4.5	8.4	14.4	18.9	21.4	20.1	17.3	12.9	5.6	2.6	**10.5**
2043	0.5	-0.7	5.8	12.5	15.7	20.6	19.5	21.3	18.4	12.0	7.1	5.2	**11.5**
2044	3.4	1.9	5.8	8.8	12.6	17.5	20.3	17.8	16.0	12.8	9.4	3.7	**10.8**
2045	3.8	1.7	4.8	8.2	13.5	17.8	20.7	19.6	16.6	10.6	6.7	2.3	**10.5**
2046	0.2	-1.8	3.6	9.5	11.1	17.3	21.3	17.9	17.0	8.0	9.8	5.9	**10.0**
2047	3.3	-3.0	3.6	9.9	13.2	17.4	18.5	19.6	14.3	9.2	5.4	-0.4	**9.3**
2048	-0.3	2.5	6.1	10.7	14.0	16.2	19.6	19.8	15.4	11.7	7.3	1.7	**10.4**
2049	1.0	-0.5	4.8	9.7	12.6	16.0	19.0	21.7	17.3	11.3	8.6	1.5	**10.3**
2050	-3.9	0.7	4.1	9.6	11.1	19.5	21.1	21.9	14.6	9.5	6.2	1.4	**9.7**
Average	**1.3**	**1.0**	**4.9**	**8.7**	**13.6**	**17.9**	**20.1**	**19.5**	**15.8**	**10.8**	**6.2**	**2.0**	**10.1**

Appendix 6: CCWaterS original RCM data for Temperature station Nikšić (RegCM3, periods 1961-1990 and 2021-2050)

	Jan	Feb	Mar	Apr	May	Jun	Jul	Aug	Sep	Oct	Nov	Dec	Year
1961	-1.6	3.4	5.7	7.6	12.4	14.6	18.2	16.7	12.9	7.3	3.9	-0.2	**8.4**
1962	-3.6	0.9	0.8	7.9	12.3	15.2	17.8	16.4	12.6	9.7	4.2	-1.5	**7.7**
1963	0.1	2.4	1.5	5.8	12.1	14.5	17.6	17.6	14.2	7.8	5.3	0.8	**8.3**
1964	0.9	-2.8	3.8	9.9	11.8	15.3	16.9	16.3	15.0	10.5	6.0	-0.4	**8.6**
1965	-4.2	-0.8	1.9	6.8	14.7	15.2	17.8	19.0	13.0	7.6	5.0	4.7	**8.4**
1966	0.3	-4.1	2.0	5.8	11.0	15.0	16.6	18.8	11.9	8.2	4.0	1.5	**7.6**
1967	-1.8	0.6	4.8	8.3	13.0	14.8	17.4	16.8	14.4	12.6	4.2	2.4	**9.0**
1968	-0.4	2.6	4.8	6.0	11.5	14.8	18.6	19.1	16.2	6.5	5.2	0.3	**8.8**
1969	-0.8	2.6	1.9	5.3	12.3	11.4	15.5	15.2	15.7	10.7	2.7	1.4	**7.8**
1970	-2.9	-0.2	3.0	7.9	11.8	14.3	16.6	15.3	13.0	8.2	1.5	0.2	**7.4**
1971	-6.7	-3.2	0.2	4.4	10.5	13.3	14.3	16.0	11.6	9.4	2.6	0.6	**6.1**
1972	-4.5	-1.0	3.1	8.1	10.0	15.5	16.4	16.0	13.7	6.7	4.8	-1.0	**7.3**
1973	-1.7	1.2	3.2	4.6	11.7	16.4	17.2	15.7	14.5	10.7	8.2	-1.3	**8.4**
1974	-3.4	2.2	2.7	8.4	10.9	15.7	18.5	17.6	14.3	7.9	4.1	-0.7	**8.2**
1975	-2.8	2.2	4.1	9.3	12.3	13.4	17.0	18.2	12.2	9.3	4.7	-1.2	**8.2**
1976	-0.5	-1.1	3.5	9.2	12.5	14.2	18.5	18.9	12.7	10.3	5.6	1.6	**8.8**
1977	-1.0	-2.9	0.3	4.3	8.7	16.4	16.7	16.8	11.9	6.3	5.9	-1.2	**6.9**
1978	0.8	-1.1	4.0	8.4	11.7	17.8	17.5	14.3	12.5	11.7	4.0	1.9	**8.6**
1979	-2.2	-1.3	1.4	6.3	12.4	13.1	17.6	17.4	15.0	7.6	7.5	-1.3	**7.8**
1980	0.5	-0.8	3.0	9.8	10.8	14.7	17.0	18.7	14.4	7.1	2.2	-0.1	**8.1**
1981	-2.2	-2.9	1.0	7.3	12.5	14.1	17.6	15.8	11.9	7.3	5.5	2.6	**7.5**
1982	-1.6	-3.0	-0.5	3.1	9.1	13.1	16.5	16.1	12.9	9.9	3.5	1.5	**6.7**
1983	0.0	-0.3	2.5	7.9	12.0	13.9	16.6	17.1	15.4	8.5	4.6	-2.6	**8.0**
1984	-0.4	1.7	4.1	6.0	9.6	12.5	16.9	17.7	14.3	7.9	3.2	-0.4	**7.8**
1985	-4.1	-2.5	1.0	5.9	10.3	16.6	16.0	16.8	11.7	9.0	5.7	0.6	**7.2**
1986	1.3	-0.8	2.0	5.3	11.4	15.9	15.5	17.9	15.2	10.8	2.8	1.7	**8.3**
1987	-3.8	-1.4	3.6	6.0	11.4	17.0	17.2	17.1	15.4	9.0	4.1	1.3	**8.1**
1988	-3.1	-0.1	2.2	4.4	9.3	15.2	18.5	14.8	13.2	8.6	0.8	1.1	**7.1**
1989	-3.0	-4.7	2.0	7.8	11.3	17.6	18.7	18.5	13.2	7.6	7.3	-3.1	**7.8**
1990	-0.8	-0.1	4.0	6.1	10.7	15.2	18.0	19.3	14.0	8.3	5.5	-1.6	**8.2**
Average	**-1.8**	**-0.5**	**2.6**	**6.8**	**11.4**	**14.9**	**17.2**	**17.1**	**13.6**	**8.8**	**4.5**	**0.3**	**7.9**
	Jan	**Feb**	**Mar**	**Apr**	**May**	**Jun**	**Jul**	**Aug**	**Sep**	**Oct**	**Nov**	**Dec**	**Year**
2021	-2.4	-2.3	-0.8	5.5	11.3	15.4	18.6	17.6	13.8	9.7	7.4	-3.0	**7.6**
2022	0.4	-0.1	-0.5	5.8	14.9	16.8	18.7	18.6	14.1	10.8	2.5	-2.4	**8.3**
2023	-0.7	-2.0	4.3	8.8	12.0	13.5	15.5	18.1	13.3	8.5	2.5	-0.4	**7.8**
2024	-2.5	0.8	3.2	6.0	11.5	16.6	18.2	17.1	13.9	9.5	5.7	1.9	**8.5**
2025	-1.4	1.8	-0.2	9.3	11.5	17.6	18.7	19.4	14.2	11.8	4.6	2.1	**9.1**
2026	-1.2	2.1	4.9	9.0	12.4	14.5	15.1	17.4	11.2	6.5	4.0	1.5	**8.1**
2027	-1.7	-0.4	5.1	5.2	11.2	15.1	20.3	16.7	14.6	10.7	5.7	0.9	**8.6**
2028	0.3	0.6	4.6	7.8	13.8	14.7	17.0	17.1	15.1	10.5	5.9	1.4	**9.1**
2029	-2.3	2.5	7.0	8.4	12.9	13.4	16.1	18.7	15.0	14.2	4.5	-0.2	**9.2**
2030	-1.3	3.2	0.7	7.1	11.1	17.7	16.9	18.6	17.2	13.2	4.9	0.3	**9.1**
2031	-0.9	0.8	5.1	7.3	13.8	16.2	18.8	21.2	16.7	9.2	5.1	2.6	**9.7**
2032	0.8	1.6	4.5	5.4	13.1	16.7	17.6	18.2	16.6	11.2	4.0	3.0	**9.4**
2033	1.5	1.9	2.1	8.1	12.9	15.6	18.5	20.7	14.9	14.5	7.6	1.3	**10.0**
2034	-0.2	2.5	6.6	8.5	11.3	16.3	20.2	18.3	13.8	7.8	3.0	1.8	**9.2**
2035	-3.6	4.0	4.6	10.0	13.9	18.0	17.1	18.7	15.2	9.9	3.2	0.4	**9.3**
2036	-3.7	-0.3	3.2	7.8	11.7	17.1	19.4	17.8	16.7	9.0	4.9	2.0	**8.8**
2037	-1.0	0.2	5.2	7.9	13.1	16.3	19.0	20.4	16.9	10.4	7.9	0.4	**9.7**
2038	-0.7	3.5	5.8	8.7	11.6	14.7	18.4	16.7	14.6	11.3	5.4	2.7	**9.4**
2039	1.0	0.3	3.2	9.0	10.9	18.2	19.4	16.7	18.6	11.4	5.3	-1.2	**9.4**
2040	1.5	2.2	3.2	7.2	12.7	14.2	19.8	17.6	15.5	10.8	3.4	-3.0	**8.8**
2041	-2.2	2.3	3.4	9.5	15.2	15.6	19.8	18.2	14.3	10.3	8.0	2.9	**9.8**
2042	-1.1	-4.1	3.7	6.8	13.3	18.8	19.1	17.9	14.7	9.7	4.6	1.5	**8.7**
2043	1.2	5.7	4.1	7.3	14.4	16.5	19.1	22.0	15.9	11.0	3.4	-0.9	**10.0**
2044	-4.2	2.7	0.6	7.7	12.6	18.3	21.3	18.0	15.1	10.2	4.3	-1.4	**8.8**
2045	1.5	1.5	0.1	7.0	11.9	14.5	19.4	18.8	14.2	11.5	4.1	2.3	**8.9**
2046	4.3	2.3	4.7	9.8	14.5	18.9	16.5	19.3	12.1	11.9	6.6	0.2	**10.1**
2047	0.7	1.7	1.9	9.3	12.0	16.6	20.0	17.9	13.3	10.6	6.0	4.4	**9.5**
2048	0.2	1.6	6.8	8.2	14.9	16.4	22.5	20.4	17.4	14.1	8.7	1.1	**11.0**
2049	0.2	3.1	4.3	9.2	13.1	16.0	19.4	18.1	18.0	11.3	6.4	4.4	**10.3**
2050	0.3	2.2	3.9	8.9	11.1	14.8	19.3	18.6	15.1	12.2	9.4	2.1	**9.8**
Average	**-0.6**	**1.4**	**3.5**	**7.9**	**12.7**	**16.2**	**18.6**	**18.5**	**15.1**	**10.8**	**5.3**	**1.0**	**9.2**

Appendix 7: CCWaterS original RCM data for Precipitation station Nikšić (Aladin, periods 1961-1990 and 2021-2050)

	Jan	Feb	Mar	Apr	May	Jun	Jul	Aug	Sep	Oct	Nov	Dec	Year
1961	89.5	64.5	69.3	58.1	48.1	57.1	35.8	58.9	40.7	25.1	182.8	236.4	**966**
1962	68.6	85.0	90.5	50.3	103.0	44.8	42.0	66.4	7.2	116.6	54.0	120.1	**848**
1963	153.1	86.6	56.7	96.3	123.1	31.3	18.0	165.6	46.6	44.0	76.8	10.3	**908**
1964	73.8	24.2	54.3	107.3	131.0	64.4	83.4	37.4	11.9	79.6	194.5	117.8	**980**
1965	29.9	4.5	89.8	15.9	36.3	27.6	9.2	12.9	171.7	107.4	220.5	122.4	**848**
1966	49.6	132.8	70.4	31.7	143.0	28.8	35.7	36.8	109.0	66.7	61.7	85.4	**852**
1967	140.2	61.8	98.6	54.3	76.3	66.2	43.0	21.8	62.5	98.2	72.5	36.4	**832**
1968	68.3	25.6	88.5	68.6	58.2	128.5	58.8	53.3	20.4	123.4	72.9	39.5	**806**
1969	34.8	39.3	14.4	73.7	78.0	64.2	15.5	12.0	88.1	194.4	58.1	264.5	**937**
1970	125.8	111.6	103.2	59.7	75.7	95.5	34.3	43.5	46.1	101.8	59.6	159.0	**1016**
1971	37.7	37.0	55.6	105.2	73.2	49.1	0.8	89.2	51.4	111.6	53.5	64.7	**729**
1972	49.8	135.6	31.4	44.0	56.5	28.1	44.2	40.7	38.8	11.4	71.0	23.8	**575**
1973	50.7	150.8	19.6	22.3	70.9	63.9	12.5	4.8	48.7	89.4	85.5	242.2	**861**
1974	143.2	85.2	78.6	77.2	24.6	75.4	32.5	56.0	19.6	6.0	128.2	35.7	**762**
1975	101.6	30.4	72.3	118.0	87.6	22.9	103.8	4.1	199.8	100.2	172.6	109.6	**1123**
1976	29.9	142.1	92.0	45.9	73.7	94.0	76.9	38.6	154.6	59.4	86.7	182.4	**1076**
1977	129.8	57.9	43.3	100.1	80.3	60.1	39.6	43.4	48.5	93.1	120.8	87.1	**904**
1978	37.4	79.4	46.0	87.8	45.2	61.3	90.9	55.1	11.1	118.4	197.0	47.1	**877**
1979	94.6	117.2	33.6	81.0	29.7	57.3	61.2	23.4	0.3	40.9	98.7	36.7	**675**
1980	76.2	37.9	95.4	47.5	81.1	35.2	77.6	9.4	65.8	19.2	97.4	63.7	**706**
1981	220.4	126.0	104.3	48.2	43.9	84.8	16.5	0.8	134.2	59.6	116.5	66.6	**1022**
1982	83.8	7.6	67.9	98.0	14.5	46.2	16.5	31.3	146.1	48.7	9.0	77.6	**647**
1983	96.4	73.1	94.5	29.9	64.7	66.4	52.2	39.1	82.3	71.7	120.9	215.6	**1007**
1984	64.2	84.5	101.7	54.3	64.7	21.6	7.9	64.2	7.1	76.2	90.6	25.5	**662**
1985	24.1	48.5	103.3	43.3	128.8	137.1	32.9	67.5	24.0	85.2	95.8	105.1	**896**
1986	25.1	122.5	113.5	61.4	71.4	106.5	72.0	15.0	49.4	155.3	280.1	139.9	**1212**
1987	63.7	37.7	54.4	92.5	72.2	38.6	16.2	40.6	74.6	201.7	40.1	5.1	**738**
1988	25.3	16.5	97.4	32.7	29.7	91.1	14.7	47.7	85.9	55.9	132.4	8.4	**638**
1989	62.5	45.1	91.1	80.6	47.2	26.0	36.6	62.0	85.9	201.2	83.8	89.2	**911**
1990	21.0	71.5	81.5	70.9	47.8	42.6	70.4	37.8	43.5	201.6	102.9	99.6	**891**
Average	**75.7**	**71.4**	**73.8**	**65.2**	**69.4**	**60.5**	**41.7**	**42.6**	**65.9**	**92.1**	**107.9**	**97.2**	**863**
	Jan	**Feb**	**Mar**	**Apr**	**May**	**Jun**	**Jul**	**Aug**	**Sep**	**Oct**	**Nov**	**Dec**	**Year**
2021	27.9	88.4	106.6	52.7	33.3	58.5	25.4	30.0	133.1	136.0	123.5	26.6	**842**
2022	28.3	73.4	117.4	61.8	86.8	16.5	0.0	16.8	41.0	89.3	57.9	37.0	**626**
2023	13.5	162.9	102.3	106.5	109.1	29.7	41.1	17.7	8.3	20.1	54.9	48.1	**714**
2024	30.4	33.9	60.2	35.5	38.2	20.5	61.6	108.8	164.1	153.5	15.9	62.9	**785**
2025	20.2	31.0	54.2	95.0	57.3	46.5	17.9	26.0	56.6	80.9	126.3	173.9	**786**
2026	73.8	85.8	61.0	132.9	83.0	69.5	41.3	11.8	9.3	88.9	46.7	144.9	**849**
2027	81.2	97.9	32.6	34.1	27.0	76.8	103.9	13.2	56.2	104.7	0.1	34.1	**662**
2028	40.6	110.9	139.7	50.7	62.2	25.2	41.6	16.5	31.5	109.9	72.0	99.6	**800**
2029	61.2	20.5	78.9	50.9	62.9	58.3	64.5	101.1	49.3	20.9	123.3	67.2	**759**
2030	4.0	53.8	80.1	96.1	71.4	28.9	162.7	13.5	62.0	50.9	29.6	109.6	**763**
2031	162.2	83.2	61.6	39.5	70.0	129.1	69.1	47.6	63.0	36.4	41.6	149.9	**953**
2032	50.9	46.9	44.5	112.7	69.8	31.7	40.5	10.9	145.9	126.2	210.4	97.6	**988**
2033	62.0	80.4	44.1	65.4	81.6	74.0	32.4	20.7	107.4	93.9	131.0	39.8	**833**
2034	24.8	5.9	101.8	132.5	53.6	12.4	47.8	44.1	73.9	89.1	90.6	19.4	**696**
2035	28.3	51.6	42.5	38.8	13.1	11.4	4.0	0.0	46.3	28.6	72.0	29.3	**366**
2036	62.8	113.3	193.0	76.8	56.0	41.6	17.5	116.5	40.2	106.0	117.8	104.4	**1046**
2037	86.6	93.6	65.1	98.4	54.0	11.3	44.1	25.7	22.8	290.4	130.1	51.2	**973**
2038	64.4	97.2	116.3	72.1	40.1	24.4	19.1	166.2	86.0	63.0	96.9	36.7	**882**
2039	9.8	166.9	71.4	67.0	73.2	20.9	46.9	141.7	109.9	116.9	142.7	79.0	**1046**
2040	95.0	59.4	64.7	21.1	26.8	39.1	30.1	49.9	181.8	64.5	84.9	137.8	**855**
2041	62.1	66.7	39.7	134.1	67.2	88.6	63.8	72.3	187.3	96.7	108.4	78.7	**1065**
2042	165.0	109.7	76.2	61.5	99.1	85.0	19.1	79.5	213.0	66.8	104.4	51.8	**1131**
2043	1.7	80.3	155.0	20.8	88.2	36.1	13.0	115.9	71.7	96.4	42.0	128.1	**849**
2044	85.3	50.0	17.4	76.9	47.7	29.2	0.2	11.5	76.6	72.6	91.3	37.0	**596**
2045	77.9	73.7	93.6	63.6	84.0	10.3	5.1	26.3	124.5	247.4	137.1	148.5	**1092**
2046	41.2	26.5	93.1	22.2	13.8	78.8	62.1	61.5	122.7	58.9	85.3	85.5	**751**
2047	34.6	78.9	60.2	81.1	56.6	48.7	34.9	49.8	140.1	160.6	190.6	36.4	**973**
2048	64.8	12.3	84.3	31.1	62.0	20.5	10.1	14.5	13.1	184.6	146.4	14.6	**658**
2049	44.8	15.3	16.6	129.5	31.6	50.0	18.4	31.7	59.1	69.6	186.8	162.1	**816**
2050	220.4	65.7	55.2	105.6	66.8	93.5	64.6	77.9	57.2	168.2	184.2	20.5	**1180**
Average	**60.9**	**71.2**	**77.6**	**72.2**	**59.5**	**45.6**	**40.1**	**50.7**	**85.1**	**103.1**	**101.5**	**77.1**	**845**

Appendix 8: CCWaterS original RCM data for Precipitation station Nikšić (Promes, periods 1961-1990 and 2021-2050)

	Jan	Feb	Mar	Apr	May	Jun	Jul	Aug	Sep	Oct	Nov	Dec	Year
1961	75.4	12.1	96.2	37.1	71.1	54.6	40.4	4.3	30.3	166.2	81.6	281.1	**950**
1962	53.1	74.8	64.5	6.7	102.6	28.1	10.4	39.7	2.5	121.5	169.6	47.6	**721**
1963	69.5	60.9	100.5	96.9	65.6	22.4	76.8	5.5	84.1	33.0	111.4	36.6	**763**
1964	25.7	62.3	41.7	98.8	69.2	9.0	17.4	3.7	102.4	46.7	119.1	57.3	**653**
1965	170.0	61.2	34.1	88.7	50.5	27.9	20.3	37.8	26.4	71.9	137.6	121.3	**848**
1966	197.2	60.1	77.4	2.2	69.4	25.0	20.5	30.5	44.7	92.2	203.0	87.7	**910**
1967	114.5	87.0	77.2	50.7	52.6	75.3	83.4	43.2	105.5	100.8	139.7	72.7	**1003**
1968	64.2	50.8	101.8	18.9	35.2	81.2	57.6	151.0	45.6	40.5	213.9	157.9	**1018**
1969	65.7	73.1	54.1	99.4	12.1	126.6	41.8	24.6	182.7	254.8	147.6	41.4	**1124**
1970	4.2	72.1	107.5	82.4	95.2	51.4	16.9	11.3	23.3	0.0	58.4	58.3	**581**
1971	43.2	106.4	67.3	22.2	39.6	46.3	19.9	99.4	94.9	87.2	46.0	56.5	**729**
1972	9.3	23.7	84.7	69.6	32.6	18.9	18.8	39.4	0.0	82.9	163.6	41.8	**585**
1973	37.6	90.2	24.3	49.4	33.0	23.6	84.1	22.5	16.2	169.5	166.4	227.6	**944**
1974	47.5	78.6	161.3	78.1	55.6	57.9	29.7	98.8	182.0	61.3	150.3	106.6	**1108**
1975	38.5	94.4	81.4	64.0	77.6	151.5	8.7	92.9	41.5	179.4	60.6	111.9	**1002**
1976	149.7	81.0	80.3	43.1	41.7	28.9	46.6	50.3	174.7	213.1	155.7	200.4	**1266**
1977	59.8	60.9	27.0	115.2	86.8	46.6	7.8	26.1	48.2	66.2	120.4	150.2	**815**
1978	63.8	183.4	63.7	124.3	141.7	124.3	47.0	24.4	30.0	17.0	43.7	112.6	**976**
1979	41.1	117.4	63.2	63.4	109.6	38.2	25.7	17.0	104.4	55.2	19.1	52.5	**707**
1980	81.0	78.0	17.9	54.3	51.6	69.9	61.0	24.5	149.7	46.5	46.2	102.6	**783**
1981	103.6	141.2	27.7	109.1	61.2	19.3	95.9	55.8	132.0	0.0	152.7	98.0	**997**
1982	14.2	28.9	88.1	74.2	42.9	151.0	7.7	121.0	82.1	86.5	149.9	48.1	**895**
1983	3.0	86.7	106.5	59.1	149.2	82.0	124.6	24.6	21.9	138.8	83.1	124.3	**1004**
1984	94.9	118.8	95.9	149.7	157.8	99.7	74.8	107.0	96.3	40.3	135.1	36.5	**1207**
1985	23.0	36.0	62.2	78.6	105.8	31.4	87.7	44.8	120.7	62.9	152.2	60.9	**866**
1986	50.4	41.8	36.0	10.3	101.8	139.7	25.3	78.2	98.3	65.4	62.8	114.7	**825**
1987	16.9	61.3	72.3	7.9	63.0	46.1	19.1	28.5	39.5	93.5	67.7	72.4	**588**
1988	114.6	129.0	70.1	47.2	38.7	25.7	8.5	25.0	253.1	9.4	34.4	37.5	**793**
1989	130.6	28.7	57.2	159.5	32.2	22.7	44.0	3.7	84.9	7.7	56.1	79.5	**707**
1990	79.4	25.6	39.0	45.8	35.9	27.4	57.5	72.0	75.7	2.2	71.2	168.0	**700**
Average	**68.0**	**74.2**	**69.4**	**66.9**	**69.4**	**58.4**	**42.7**	**46.9**	**83.1**	**80.4**	**110.6**	**98.8**	**869**
	Jan	**Feb**	**Mar**	**Apr**	**May**	**Jun**	**Jul**	**Aug**	**Sep**	**Oct**	**Nov**	**Dec**	**Year**
2021	37.1	79.5	96.6	138.4	8.9	31.7	34.1	28.3	65.1	55.4	143.6	89.7	**808**
2022	131.9	98.1	68.7	47.0	57.9	65.6	12.0	32.0	164.3	65.1	49.7	73.7	**866**
2023	67.4	68.7	43.7	192.0	40.0	26.3	4.7	3.4	38.4	120.3	121.7	79.8	**807**
2024	34.0	44.8	56.7	37.8	68.6	83.0	0.4	48.4	49.1	210.3	40.9	171.2	**845**
2025	67.3	142.1	122.7	83.5	99.1	47.9	100.3	3.9	62.2	41.6	43.7	130.1	**944**
2026	135.3	92.9	108.2	78.8	30.6	119.3	19.6	88.3	138.8	56.7	176.6	97.8	**1143**
2027	138.9	118.8	57.0	119.9	105.3	51.3	11.9	43.4	125.4	112.4	19.0	83.8	**987**
2028	30.6	44.0	49.0	37.7	43.0	10.4	37.2	48.0	52.7	8.0	74.3	143.6	**579**
2029	23.0	44.9	30.4	129.8	41.1	34.6	79.2	185.5	25.6	58.9	154.2	94.2	**901**
2030	72.8	134.2	23.7	80.9	60.9	17.7	7.9	37.8	77.2	211.2	90.8	98.0	**913**
2031	80.1	48.5	24.0	145.9	50.2	98.3	11.1	41.9	86.7	243.1	106.3	35.6	**972**
2032	54.8	63.5	82.1	86.7	48.2	16.8	15.4	63.6	101.8	20.6	147.3	52.4	**753**
2033	119.0	87.6	59.9	5.8	8.0	15.7	2.5	14.4	122.2	170.4	134.8	50.6	**791**
2034	49.0	96.8	88.4	42.3	36.2	66.5	16.7	24.8	57.3	55.8	68.6	154.9	**757**
2035	7.6	48.9	80.4	59.8	52.5	2.8	6.6	49.8	57.7	173.4	80.0	194.4	**814**
2036	79.3	117.3	56.6	24.9	99.5	32.9	16.7	41.3	96.9	214.9	56.5	38.9	**876**
2037	42.6	90.5	36.6	68.0	157.3	35.0	36.6	0.8	21.8	31.8	51.3	37.5	**610**
2038	96.5	21.1	68.1	27.5	50.5	33.1	17.8	17.7	9.6	150.0	138.7	112.9	**743**
2039	107.7	90.9	69.2	87.2	28.2	55.9	9.1	36.4	70.3	18.2	16.3	25.3	**615**
2040	13.0	22.0	53.5	153.6	77.1	10.1	9.6	106.6	49.6	84.6	63.6	190.1	**834**
2041	60.3	90.0	37.8	61.5	77.1	29.5	8.6	50.6	29.4	18.2	61.1	74.9	**599**
2042	57.5	23.9	76.2	59.0	39.8	30.4	15.2	7.8	20.1	92.1	61.5	69.5	**553**
2043	104.0	39.8	119.6	60.4	32.8	31.5	48.6	0.6	20.5	138.3	60.2	74.6	**731**
2044	34.5	86.6	153.7	13.8	74.6	26.7	11.9	58.7	92.7	147.6	109.8	131.9	**943**
2045	69.7	73.7	87.8	113.5	71.7	27.8	37.0	42.8	82.9	136.1	155.3	130.8	**1029**
2046	34.0	62.9	62.4	23.1	121.7	59.8	15.8	116.5	70.4	37.9	96.2	108.9	**810**
2047	53.7	15.0	19.8	123.7	69.1	43.1	47.0	37.1	69.0	179.1	1.2	2.8	**661**
2048	33.0	19.1	110.2	52.6	57.5	98.0	18.2	12.4	67.0	123.6	89.4	95.1	**776**
2049	2.6	34.1	122.8	50.7	87.2	56.5	24.0	15.6	61.2	86.2	131.9	56.7	**729**
2050	14.5	130.9	56.5	72.7	90.6	7.7	13.2	29.9	75.6	118.0	143.2	130.0	**883**
Average	**61.7**	**71.0**	**70.7**	**75.9**	**62.8**	**42.2**	**23.0**	**42.9**	**68.7**	**106.0**	**89.6**	**94.3**	**809**

Appendix 9: CCWaterS original RCM data for Precipitation station Nikšić (RegCM3, periods 1961-1990 and 2021-2050)

	Jan	Feb	Mar	Apr	May	Jun	Jul	Aug	Sep	Oct	Nov	Dec	Year
1961	56.9	8.5	39.0	130.9	34.3	46.0	9.1	1.9	182.5	114.6	104.5	188.7	**917**
1962	72.0	144.9	89.9	110.2	27.7	59.7	21.1	70.5	7.0	94.9	168.9	106.1	**973**
1963	113.8	151.8	76.9	60.5	70.6	59.0	83.2	26.4	89.6	121.4	201.5	106.0	**1161**
1964	114.0	49.2	66.7	60.5	43.2	19.9	72.3	71.9	57.1	188.4	81.3	43.4	**868**
1965	50.2	3.4	51.5	7.1	12.7	51.4	5.4	17.7	154.1	64.9	119.0	57.7	**595**
1966	29.8	59.3	79.6	120.4	44.8	75.6	58.5	12.4	98.9	32.5	95.4	85.3	**793**
1967	147.6	96.5	59.1	53.4	32.8	31.8	41.3	44.0	65.7	132.1	119.4	125.0	**949**
1968	29.2	55.4	93.1	51.2	16.0	20.3	35.3	19.5	35.8	24.7	26.7	99.5	**507**
1969	172.3	181.3	105.9	98.7	64.1	90.0	60.1	76.8	2.1	92.9	91.5	70.7	**1106**
1970	42.6	68.2	110.7	50.4	55.5	65.2	65.2	126.1	37.8	117.0	84.3	113.2	**936**
1971	66.7	58.7	85.1	103.0	64.8	116.8	102.3	62.6	156.7	208.8	87.5	99.2	**1212**
1972	87.5	22.1	72.9	82.0	78.4	38.4	21.2	48.0	82.3	132.0	152.1	111.6	**928**
1973	32.2	42.5	137.7	88.6	89.0	58.7	36.2	105.8	67.3	22.4	157.6	62.6	**901**
1974	10.1	164.5	98.6	30.3	60.3	27.2	0.3	50.0	15.5	44.5	171.2	79.1	**751**
1975	44.3	95.2	142.5	90.0	60.7	95.9	32.2	50.2	52.9	74.1	96.5	111.5	**946**
1976	81.6	56.7	100.7	35.1	63.4	96.9	18.6	92.5	39.8	38.6	162.8	93.9	**881**
1977	101.6	83.1	31.5	60.9	152.7	6.0	77.4	90.9	127.7	50.6	181.6	169.4	**1133**
1978	105.0	20.7	48.5	91.1	116.8	11.8	12.4	76.4	97.9	71.9	106.0	78.1	**837**
1979	90.3	38.9	84.5	84.9	74.0	112.3	35.9	33.8	59.5	15.4	109.3	173.7	**912**
1980	70.2	95.1	26.7	33.7	81.1	62.2	37.5	8.4	67.4	189.9	148.0	146.9	**967**
1981	155.5	65.3	56.4	70.6	41.3	65.1	29.7	110.5	90.9	39.0	107.4	152.3	**984**
1982	90.1	53.6	49.8	74.6	45.8	60.8	53.1	56.3	79.9	148.8	34.8	46.0	**794**
1983	71.6	50.9	20.0	56.9	30.8	70.6	51.5	40.4	15.5	210.3	28.8	14.7	**662**
1984	155.7	34.2	58.7	80.4	168.5	64.9	35.6	19.3	99.1	118.3	54.7	145.2	**1035**
1985	83.2	19.0	56.7	76.1	68.0	34.3	76.2	51.0	21.3	154.7	118.7	108.1	**867**
1986	134.1	36.7	58.0	67.5	81.2	55.7	23.6	69.0	78.2	75.8	69.3	60.2	**809**
1987	71.9	29.3	110.7	64.2	32.9	3.7	121.2	28.2	27.4	1.1	183.2	71.4	**745**
1988	44.3	40.9	54.8	138.9	139.7	46.3	16.8	62.7	173.2	2.3	83.7	86.3	**890**
1989	34.3	45.0	19.6	96.0	76.4	18.5	24.0	12.7	7.8	25.7	152.2	29.2	**542**
1990	126.4	27.1	100.6	66.2	46.8	72.7	21.3	44.5	21.2	38.2	50.1	81.5	**697**
Average	**82.8**	**63.3**	**72.9**	**74.5**	**65.8**	**54.6**	**42.6**	**52.7**	**70.4**	**88.2**	**111.6**	**97.2**	**877**
	Jan	**Feb**	**Mar**	**Apr**	**May**	**Jun**	**Jul**	**Aug**	**Sep**	**Oct**	**Nov**	**Dec**	**Year**
2021	60.3	138.5	27.5	44.0	60.3	9.9	27.1	24.7	43.7	65.7	46.9	53.1	**602**
2022	57.4	66.7	55.2	72.1	20.5	24.0	41.4	46.4	86.7	66.1	176.5	67.9	**781**
2023	103.0	41.1	193.4	43.0	53.8	106.9	21.5	115.9	165.2	122.7	86.7	130.7	**1184**
2024	39.3	25.5	100.1	31.5	65.6	44.4	25.5	114.0	139.0	36.8	131.9	215.8	**969**
2025	44.2	100.7	121.0	59.2	126.6	37.7	49.1	28.0	64.8	44.1	79.7	148.1	**903**
2026	105.1	94.6	121.5	9.8	55.4	95.2	39.2	35.5	143.8	88.2	65.3	105.6	**959**
2027	51.0	68.3	55.9	114.2	61.0	68.4	13.1	50.4	127.6	151.7	164.0	18.1	**944**
2028	77.1	75.0	66.5	37.3	61.2	33.5	6.3	44.2	39.3	121.8	145.3	220.2	**928**
2029	41.3	59.7	53.0	47.5	97.1	209.0	65.5	70.1	31.7	50.3	70.9	137.3	**933**
2030	36.6	17.0	104.4	127.8	41.8	35.7	36.8	4.7	8.1	35.5	55.6	127.7	**632**
2031	41.4	69.8	79.6	67.9	84.5	97.8	11.7	20.8	184.7	39.4	130.7	194.2	**1023**
2032	40.1	61.3	67.1	155.3	53.2	30.0	43.4	43.5	44.6	82.3	79.1	85.3	**785**
2033	39.1	44.4	46.9	25.8	71.9	49.4	96.0	7.8	100.3	10.0	136.1	163.6	**791**
2034	109.0	67.3	51.5	44.4	157.5	79.1	32.1	61.4	54.6	114.4	52.8	60.8	**885**
2035	15.4	36.6	42.4	24.2	96.3	79.7	88.4	52.2	85.0	118.8	20.8	139.6	**799**
2036	95.5	76.8	119.8	78.1	33.1	12.1	4.7	84.8	20.6	103.0	57.3	285.0	**971**
2037	17.7	78.5	43.4	17.4	118.1	30.7	14.2	10.7	91.0	204.0	108.7	121.5	**856**
2038	79.3	35.5	34.9	47.4	137.5	110.0	39.3	75.7	17.1	65.1	9.1	102.5	**754**
2039	91.7	34.7	61.5	102.7	65.3	5.3	13.5	204.1	24.2	107.1	101.8	44.2	**856**
2040	90.8	26.3	6.8	117.3	31.9	61.6	55.9	92.1	46.0	54.7	39.4	106.2	**729**
2041	71.8	29.8	83.8	25.8	13.1	67.1	42.3	94.4	90.2	88.9	12.7	163.3	**783**
2042	48.6	71.9	47.2	52.2	23.4	21.2	32.3	34.2	1.0	125.2	99.0	136.7	**693**
2043	104.4	158.9	121.4	44.2	17.8	18.9	8.4	29.8	7.3	93.3	28.1	125.2	**758**
2044	79.1	81.6	49.9	98.6	37.2	10.5	41.6	84.5	85.2	118.5	149.5	28.2	**864**
2045	135.1	10.6	12.2	77.8	40.9	68.4	36.7	46.7	73.9	61.5	58.1	10.0	**632**
2046	120.4	29.7	82.8	96.9	34.9	62.6	36.3	96.4	63.9	93.1	102.9	156.4	**976**
2047	66.5	90.6	128.7	93.1	95.8	75.2	18.7	97.8	160.5	96.4	109.8	18.7	**1052**
2048	29.8	43.4	68.4	46.4	13.4	53.8	20.3	15.5	23.6	39.8	117.2	132.2	**604**
2049	97.2	99.2	149.2	67.1	35.7	25.4	26.4	47.1	29.3	2.7	28.0	257.0	**864**
2050	102.4	116.0	136.2	55.8	151.2	77.5	84.6	49.7	97.9	96.4	130.2	166.3	**1264**
Average	**69.7**	**65.0**	**77.7**	**64.2**	**65.2**	**56.7**	**35.7**	**59.4**	**71.7**	**83.3**	**86.5**	**124.0**	**859**

Appendix 10: CCWaterS original RCM data for Precipitation station Lukovo (Aladin, periods 1961-1990 and 2021-2050)

	Jan	Feb	Mar	Apr	May	Jun	Jul	Aug	Sep	Oct	Nov	Dec	Year
1961	87.7	63.5	68.5	57.3	47.5	60.4	38.3	60.4	39.7	24.2	176.7	232.5	**957**
1962	67.0	84.3	88.9	49.9	104.0	45.3	43.7	70.8	6.9	113.6	52.8	117.6	**845**
1963	148.6	84.4	56.0	93.1	124.1	34.5	17.0	162.8	47.2	43.2	75.0	10.2	**896**
1964	71.4	23.3	53.4	106.6	131.4	64.0	83.0	36.3	11.4	77.4	190.6	114.3	**963**
1965	28.5	4.9	87.7	15.5	35.7	27.9	10.5	13.3	169.5	105.6	216.7	119.2	**835**
1966	48.1	131.4	68.7	30.0	144.8	28.6	37.0	36.2	107.2	66.0	59.3	82.1	**840**
1967	136.5	59.8	96.5	52.9	77.0	68.8	43.9	23.5	62.5	97.3	72.6	35.7	**827**
1968	66.6	24.8	88.9	67.6	58.0	127.9	62.4	53.0	19.9	123.2	71.6	38.3	**802**
1969	33.7	37.5	14.0	72.5	79.2	64.1	16.3	12.8	87.4	191.3	57.2	258.0	**924**
1970	122.4	109.4	99.8	60.1	76.3	95.2	36.1	44.2	45.1	100.3	58.1	154.3	**1001**
1971	36.3	36.5	55.5	104.0	75.2	51.5	0.7	90.8	52.3	109.8	51.4	62.4	**726**
1972	48.9	133.1	30.7	43.2	56.2	30.3	46.0	41.7	39.0	11.5	70.4	23.4	**574**
1973	50.1	148.8	19.8	22.7	71.7	63.6	14.1	5.6	48.3	88.8	83.6	239.1	**856**
1974	138.1	82.8	77.0	76.3	25.4	78.6	35.9	54.5	19.9	5.7	125.8	34.7	**755**
1975	100.4	29.5	71.7	116.2	89.2	22.9	105.2	3.4	197.7	97.6	167.9	107.0	**1109**
1976	29.5	139.0	89.4	46.3	73.8	96.9	77.6	37.2	153.3	59.4	84.8	178.6	**1066**
1977	126.1	55.6	43.8	98.7	80.0	63.9	40.7	43.2	48.7	92.8	118.3	85.2	**897**
1978	35.8	77.0	44.8	87.7	45.3	64.0	92.4	53.7	11.2	115.6	191.8	46.2	**866**
1979	91.9	116.1	33.1	79.5	29.6	60.6	61.6	23.0	0.2	40.2	97.8	36.0	**670**
1980	76.3	37.1	94.1	46.7	81.3	36.1	77.5	10.3	65.5	19.6	95.5	61.7	**702**
1981	214.6	122.1	101.7	47.9	45.2	84.7	17.5	1.1	135.2	58.8	114.5	65.3	**1008**
1982	82.4	7.7	66.8	96.9	15.0	49.8	18.9	34.0	144.6	48.4	8.7	76.3	**649**
1983	93.6	71.0	92.3	31.1	65.1	68.8	52.8	41.3	82.2	70.9	120.2	213.4	**1003**
1984	62.3	83.1	99.2	53.8	66.0	22.3	8.2	64.0	9.0	75.6	88.6	24.9	**657**
1985	23.2	46.4	100.8	43.1	130.6	136.6	34.8	72.4	23.8	83.0	93.1	102.7	**890**
1986	24.4	119.3	111.2	61.5	71.0	105.1	72.7	16.4	49.0	152.7	276.4	137.1	**1197**
1987	62.3	36.5	54.4	92.0	73.6	37.7	16.6	40.7	71.9	197.2	39.2	5.0	**727**
1988	24.6	16.0	96.1	32.9	30.4	92.5	16.1	47.5	86.8	54.0	129.6	8.1	**635**
1989	60.3	44.1	88.7	80.8	46.5	25.7	36.2	60.7	83.7	200.8	83.1	86.3	**897**
1990	20.6	70.2	78.8	69.9	48.3	42.0	68.7	38.1	43.0	199.3	100.1	98.8	**878**
Average	**73.7**	**69.8**	**72.4**	**64.6**	**69.9**	**61.7**	**42.8**	**43.1**	**65.4**	**90.8**	**105.7**	**95.2**	**855**
	Jan	**Feb**	**Mar**	**Apr**	**May**	**Jun**	**Jul**	**Aug**	**Sep**	**Oct**	**Nov**	**Dec**	**Year**
2021	27.5	87.8	103.8	52.8	35.2	57.7	24.8	33.4	131.4	131.8	121.1	25.0	**832**
2022	28.0	70.8	114.8	61.9	86.4	17.9	0.0	16.7	41.6	88.5	56.9	35.7	**619**
2023	13.8	160.3	100.5	104.1	111.3	31.1	41.6	17.6	9.1	19.8	53.6	47.7	**710**
2024	29.5	33.4	60.5	34.8	38.0	20.7	63.8	106.1	159.0	149.7	15.8	60.5	**772**
2025	19.6	30.2	52.9	93.3	59.3	47.3	18.1	28.4	57.8	80.9	121.2	170.6	**780**
2026	72.3	84.3	60.0	131.7	84.4	72.8	44.9	13.9	8.5	87.3	45.7	140.9	**847**
2027	80.3	95.6	31.7	34.6	28.8	77.3	102.9	15.3	55.5	102.5	0.1	33.2	**658**
2028	40.2	109.8	135.8	50.3	63.6	27.6	43.6	17.6	31.2	108.5	68.7	97.4	**794**
2029	60.4	19.9	78.7	51.6	63.1	58.8	67.8	99.9	49.9	20.0	121.0	65.5	**757**
2030	3.8	53.1	77.8	95.4	71.9	31.0	164.0	15.0	60.8	49.7	28.9	107.6	**759**
2031	158.4	81.8	60.3	38.9	69.9	129.1	68.7	47.1	63.0	35.0	40.0	147.7	**940**
2032	49.8	45.7	43.4	111.0	69.3	32.8	39.2	12.9	142.8	122.3	206.4	96.1	**972**
2033	60.5	77.5	42.9	65.7	80.5	73.7	32.0	21.1	106.7	93.2	129.6	38.0	**822**
2034	23.7	5.6	101.2	130.7	53.6	13.9	48.1	44.5	73.4	86.7	88.6	19.1	**689**
2035	28.0	51.1	42.5	37.9	14.3	12.7	5.2	0.0	45.4	27.4	70.7	28.7	**364**
2036	62.1	111.3	190.8	75.7	54.5	42.6	16.4	119.5	40.0	102.6	115.2	102.8	**1033**
2037	83.8	91.8	64.0	98.4	55.0	11.6	46.9	23.0	24.0	282.7	127.0	50.1	**958**
2038	63.5	96.0	115.3	71.2	41.0	26.4	19.0	164.3	86.0	61.0	96.0	35.5	**875**
2039	9.9	164.0	68.6	65.6	75.3	21.3	46.2	140.1	108.9	114.7	138.1	77.6	**1030**
2040	93.0	59.1	64.2	19.6	27.9	39.5	30.0	47.8	178.5	63.3	83.3	135.8	**842**
2041	60.7	65.7	38.6	134.5	67.4	88.0	65.3	72.6	185.6	94.1	106.6	77.3	**1056**
2042	160.2	106.6	74.9	60.3	100.4	83.4	19.8	81.0	209.7	65.2	100.0	50.1	**1111**
2043	1.8	78.1	152.4	21.0	88.1	37.9	13.9	114.2	70.8	94.2	41.8	124.6	**839**
2044	84.2	49.2	17.6	76.2	48.0	29.7	0.1	11.7	76.4	72.4	89.2	36.5	**591**
2045	75.8	72.7	92.9	63.4	87.0	10.7	6.1	26.1	123.8	245.4	134.4	147.4	**1086**
2046	40.9	25.8	92.1	22.7	13.9	80.8	61.8	59.9	119.2	58.6	83.4	82.6	**742**
2047	34.3	77.4	58.3	79.3	55.5	47.2	33.3	52.1	137.5	157.3	188.8	35.8	**957**
2048	63.4	12.1	82.1	31.3	64.0	20.9	9.5	16.6	13.1	179.6	144.6	14.6	**652**
2049	44.0	14.8	16.1	126.2	32.6	52.4	19.8	31.3	60.7	66.8	182.5	159.3	**807**
2050	218.4	63.5	55.1	104.7	67.8	92.5	65.8	76.9	55.0	161.4	180.4	20.2	**1162**
Average	**59.7**	**69.8**	**76.3**	**71.5**	**60.3**	**46.3**	**40.6**	**50.9**	**84.2**	**100.8**	**99.3**	**75.5**	**835**

Appendix 11: CCWaterS original RCM data for Precipitation station Lukovo (Promes, periods 1961-1990 and 2021-2050)

	Jan	Feb	Mar	Apr	May	Jun	Jul	Aug	Sep	Oct	Nov	Dec	Year
1961	73.0	11.8	94.0	37.5	72.0	55.1	41.9	4.3	29.9	163.6	80.5	275.9	**939**
1962	52.0	73.8	63.6	6.7	103.5	29.3	11.1	38.9	2.9	121.3	167.4	46.7	**717**
1963	67.4	60.3	98.7	95.5	65.8	22.9	78.9	5.8	83.4	31.7	109.8	35.3	**756**
1964	25.3	60.8	41.1	97.2	69.7	9.3	18.0	3.9	101.5	45.9	116.4	56.1	**645**
1965	164.7	60.0	33.4	87.7	50.9	28.7	21.2	38.5	25.5	70.1	135.1	118.7	**834**
1966	192.5	58.4	75.9	2.4	69.6	25.1	21.9	30.9	45.1	91.8	200.4	85.0	**899**
1967	110.4	84.1	75.9	49.8	53.1	74.2	85.0	43.3	104.8	98.2	136.5	71.1	**986**
1968	63.1	50.0	100.0	18.6	37.5	81.1	59.8	151.2	45.8	39.4	209.5	154.4	**1010**
1969	63.7	71.9	53.6	99.0	12.8	128.3	43.5	26.0	182.3	249.0	144.2	40.3	**1115**
1970	4.0	70.9	105.8	80.7	95.2	53.2	17.5	11.7	23.3	0.0	58.2	56.6	**577**
1971	42.2	103.7	65.9	21.6	40.1	47.7	20.1	100.7	94.1	86.5	45.0	55.3	**723**
1972	9.0	22.9	82.9	67.2	32.7	19.3	19.5	39.4	0.0	82.0	159.6	40.6	**575**
1973	37.0	88.4	23.9	48.1	32.9	24.2	85.6	23.6	16.2	165.3	163.6	222.3	**931**
1974	46.2	76.1	158.8	76.9	55.8	57.9	30.4	99.0	178.4	59.2	148.4	104.2	**1091**
1975	37.1	92.1	80.1	63.5	77.9	154.1	9.4	93.8	41.1	175.5	59.0	109.5	**993**
1976	147.0	78.5	78.8	43.0	42.8	29.6	48.6	51.5	172.8	211.4	152.1	195.8	**1252**
1977	58.7	59.7	27.1	113.4	88.5	46.8	8.2	27.4	47.9	64.6	117.2	146.3	**806**
1978	62.2	178.4	62.8	123.4	142.1	125.4	49.2	25.2	29.3	16.9	43.0	110.2	**968**
1979	40.7	114.5	61.9	62.8	111.4	39.2	26.7	16.3	102.4	53.9	18.7	50.9	**699**
1980	79.6	76.6	17.9	53.8	51.6	72.0	63.1	24.4	150.6	46.1	44.9	100.6	**781**
1981	100.3	137.7	27.3	108.0	61.4	20.1	99.4	56.5	130.1	0.0	151.2	96.5	**988**
1982	13.9	28.2	87.2	73.7	43.6	152.3	7.6	122.3	81.0	86.9	147.3	47.0	**891**
1983	3.2	85.0	104.7	58.9	149.4	85.1	126.2	24.9	21.3	136.1	80.7	121.7	**997**
1984	92.2	115.6	93.5	147.3	157.4	101.5	76.7	107.1	96.7	39.4	132.6	35.7	**1196**
1985	22.8	35.4	61.0	76.9	106.0	32.7	92.4	44.9	120.3	61.1	148.8	59.8	**862**
1986	48.5	40.8	35.1	10.1	102.1	141.5	26.5	79.4	97.9	64.7	62.1	111.3	**820**
1987	15.9	59.5	71.6	8.0	62.8	46.5	20.0	28.5	40.4	91.0	66.6	70.4	**581**
1988	113.0	125.4	67.3	46.5	40.4	26.6	8.7	24.8	250.4	9.2	34.3	36.8	**783**
1989	128.1	28.0	56.3	157.8	32.1	23.7	44.6	4.0	83.3	7.8	54.1	76.6	**696**
1990	77.4	24.9	38.4	46.4	37.7	28.6	59.0	72.4	75.4	2.2	69.8	163.7	**696**
Average	**66.4**	**72.4**	**68.1**	**66.1**	**70.0**	**59.4**	**44.0**	**47.3**	**82.5**	**79.0**	**108.6**	**96.5**	**860**
	Jan	**Feb**	**Mar**	**Apr**	**May**	**Jun**	**Jul**	**Aug**	**Sep**	**Oct**	**Nov**	**Dec**	**Year**
2021	36.5	77.7	94.6	136.7	8.8	33.7	33.8	27.1	64.4	54.9	141.1	88.3	**798**
2022	128.0	95.8	68.1	46.8	58.1	67.5	13.3	32.6	162.5	64.8	48.2	72.4	**858**
2023	66.1	67.3	43.3	189.7	40.8	26.6	5.1	4.0	37.4	117.9	119.3	77.5	**795**
2024	33.1	43.5	55.7	37.6	67.2	84.2	0.5	49.2	48.6	205.8	39.8	166.7	**832**
2025	65.7	138.6	120.0	83.1	99.8	49.5	102.5	4.2	61.2	39.2	43.3	126.6	**934**
2026	131.6	90.5	105.7	78.1	31.5	122.0	20.3	90.1	137.2	55.5	172.4	95.4	**1130**
2027	136.0	116.5	55.0	117.9	106.6	52.0	13.0	43.1	122.7	110.1	18.1	81.7	**973**
2028	29.9	42.6	47.5	37.4	44.5	11.2	37.5	48.9	52.5	7.6	73.4	140.7	**574**
2029	22.2	43.4	29.6	128.3	41.1	36.1	82.0	183.8	25.9	57.7	152.2	92.8	**895**
2030	71.1	132.3	23.1	80.5	61.9	19.0	8.3	38.6	77.3	206.6	90.0	95.5	**904**
2031	79.8	47.7	23.8	143.5	49.5	99.5	12.1	41.5	86.6	239.6	104.9	34.6	**963**
2032	53.8	62.4	81.0	86.3	48.5	17.2	16.3	62.0	101.7	19.5	145.0	51.0	**744**
2033	116.3	85.7	58.9	5.9	7.9	16.0	2.8	15.2	121.5	169.4	132.3	49.1	**781**
2034	47.7	94.2	87.3	41.5	35.8	67.2	16.6	25.9	56.9	54.5	67.7	151.6	**747**
2035	7.6	48.0	78.3	58.6	54.4	3.3	7.0	49.4	56.6	169.7	78.2	190.2	**801**
2036	78.1	113.8	55.6	24.7	99.3	34.0	18.5	41.4	95.4	211.5	55.2	37.9	**865**
2037	41.3	88.5	35.7	67.7	159.4	35.6	38.7	1.1	21.7	31.2	50.0	37.6	**608**
2038	94.1	20.9	67.4	27.5	50.5	33.2	18.6	17.8	9.2	146.6	136.0	110.5	**732**
2039	105.2	88.9	68.5	85.7	28.6	56.7	9.8	38.2	69.7	17.8	15.7	24.6	**610**
2040	12.7	21.8	52.6	150.6	78.4	10.3	10.4	105.0	47.7	83.4	62.4	184.0	**819**
2041	58.6	88.2	36.8	60.8	76.8	30.3	9.0	49.7	29.1	18.3	59.5	73.2	**590**
2042	56.2	23.6	75.5	58.5	40.0	30.6	16.1	8.3	20.4	90.4	60.6	67.8	**548**
2043	100.8	38.7	118.2	59.3	33.5	32.5	50.8	0.6	20.6	136.2	59.1	72.7	**723**
2044	33.2	84.5	150.9	13.9	75.9	28.1	12.7	58.6	92.3	146.4	107.7	128.0	**932**
2045	67.8	72.0	85.9	112.1	73.0	28.1	37.5	42.4	83.0	134.3	153.0	128.7	**1018**
2046	33.8	61.5	61.7	22.9	122.3	60.9	16.0	118.3	71.3	38.6	94.5	106.8	**809**
2047	51.6	15.0	19.3	122.2	70.4	44.0	49.6	38.2	70.5	175.1	1.2	2.9	**660**
2048	32.5	18.8	107.8	53.4	57.7	100.0	18.7	12.9	68.2	121.1	88.6	92.7	**772**
2049	2.5	33.4	120.8	49.9	88.4	57.1	24.6	15.2	59.9	85.0	129.4	55.6	**722**
2050	14.5	127.9	55.2	71.7	92.2	7.7	14.5	30.3	74.8	118.5	139.5	127.1	**874**
Average	**60.3**	**69.5**	**69.5**	**75.1**	**63.4**	**43.1**	**23.9**	**43.1**	**68.2**	**104.2**	**87.9**	**92.1**	**800**

Appendix 12: CCWaterS original RCM data for Precipitation station Lukovo (RegCM3, periods 1961-1990 and 2021-2050)

	Jan	Feb	Mar	Apr	May	Jun	Jul	Aug	Sep	Oct	Nov	Dec	Year
1961	55.7	8.4	38.7	131.0	34.6	46.9	10.3	1.5	178.1	112.6	103.0	183.6	**904**
1962	69.3	142.6	88.6	109.9	27.3	61.0	22.7	70.9	7.1	93.8	168.4	102.3	**964**
1963	110.7	149.2	75.3	59.0	71.4	60.7	82.7	26.6	88.9	118.8	198.0	103.9	**1145**
1964	111.9	48.2	64.9	60.2	44.8	19.7	74.0	72.8	56.9	186.1	80.4	42.6	**862**
1965	49.3	3.3	50.9	6.9	13.1	51.8	6.1	18.2	152.1	63.1	115.3	56.1	**586**
1966	28.6	58.2	78.0	117.3	44.7	77.6	60.6	12.5	96.6	31.5	92.5	83.9	**782**
1967	144.9	96.2	56.5	53.7	32.8	33.0	42.6	43.3	66.2	131.1	118.1	122.1	**940**
1968	28.6	54.1	91.0	51.4	17.1	21.3	36.3	18.7	36.1	24.8	26.2	96.7	**502**
1969	169.2	177.0	103.4	96.9	65.4	91.7	62.5	76.7	2.2	91.2	90.0	67.5	**1094**
1970	41.9	65.3	108.2	50.2	56.6	64.6	68.2	126.4	37.2	113.7	82.9	109.5	**925**
1971	64.6	57.2	83.1	99.9	65.4	115.9	106.9	62.1	155.3	206.2	86.6	97.2	**1200**
1972	85.3	21.6	70.3	80.0	79.4	41.0	22.6	48.8	80.9	132.7	148.9	111.2	**922**
1973	30.9	41.9	138.0	86.4	89.2	60.1	36.9	106.2	66.1	22.2	158.3	61.1	**897**
1974	9.8	161.0	97.2	30.5	59.6	26.9	0.3	51.9	15.7	44.3	166.2	77.9	**741**
1975	42.6	93.7	140.3	89.1	62.3	96.2	32.8	49.8	52.8	72.4	93.8	108.5	**934**
1976	79.4	55.4	97.1	34.6	63.4	95.5	18.7	92.8	40.2	36.6	160.8	91.6	**866**
1977	99.2	81.1	31.5	59.6	150.5	7.1	78.8	93.4	126.3	50.7	177.9	165.4	**1121**
1978	101.8	19.9	47.9	89.9	118.5	11.5	12.4	79.4	97.4	70.1	102.1	76.0	**827**
1979	89.3	37.8	83.5	83.4	74.1	112.7	37.6	32.1	59.4	15.1	106.9	170.7	**903**
1980	68.8	93.6	25.0	33.5	82.7	65.3	38.6	8.5	66.9	186.0	146.7	142.7	**958**
1981	152.0	63.6	55.5	69.8	42.6	66.9	30.1	109.9	90.8	38.7	106.0	149.1	**975**
1982	87.0	52.5	48.8	73.7	45.1	63.7	53.1	60.5	80.8	144.8	34.1	45.1	**789**
1983	68.9	49.7	20.1	55.7	31.7	70.7	53.3	40.9	15.0	204.3	27.5	13.8	**652**
1984	152.0	33.7	56.5	79.7	170.8	65.9	37.4	18.3	98.4	117.4	53.1	142.7	**1026**
1985	81.4	18.3	55.6	74.7	69.4	35.7	80.6	52.8	21.2	152.3	117.6	104.7	**864**
1986	130.2	35.6	56.9	65.1	83.1	57.7	24.7	68.7	77.3	75.4	68.4	59.0	**802**
1987	70.1	28.3	110.3	65.3	33.8	3.8	123.0	29.9	27.5	1.4	181.6	69.8	**745**
1988	43.8	39.9	54.1	137.6	140.2	46.4	17.0	63.4	171.1	2.3	82.6	82.9	**881**
1989	34.3	43.6	19.0	94.5	76.2	19.5	23.3	13.5	7.7	25.9	148.4	28.9	**535**
1990	124.4	26.7	101.6	65.0	48.1	76.1	21.6	46.5	20.9	37.8	48.4	79.8	**697**
Average	**80.9**	**61.9**	**71.6**	**73.5**	**66.5**	**55.6**	**43.9**	**53.2**	**69.8**	**86.8**	**109.7**	**94.9**	**868**
	Jan	**Feb**	**Mar**	**Apr**	**May**	**Jun**	**Jul**	**Aug**	**Sep**	**Oct**	**Nov**	**Dec**	**Year**
2021	58.7	136.7	26.6	44.0	60.2	10.9	28.4	24.6	44.0	63.3	45.6	52.4	**595**
2022	55.7	64.4	53.5	70.9	20.8	25.0	42.6	46.3	84.7	63.0	174.1	65.9	**767**
2023	98.8	40.2	190.6	44.5	55.2	109.1	22.7	114.3	166.9	118.3	85.0	127.3	**1173**
2024	38.2	24.8	97.8	31.3	65.8	44.4	26.8	112.4	138.8	36.9	127.5	208.9	**954**
2025	43.6	97.7	119.4	58.3	130.4	38.5	50.6	28.5	64.1	44.2	78.4	145.5	**899**
2026	102.8	91.5	118.3	9.6	56.3	97.2	41.8	34.6	143.1	88.3	65.0	103.8	**952**
2027	49.3	67.1	55.0	112.8	61.5	70.5	13.5	49.4	127.7	149.6	161.2	17.5	**935**
2028	75.5	72.5	65.0	36.8	62.4	35.4	6.5	44.6	39.0	120.4	143.3	213.6	**915**
2029	39.9	58.3	51.7	46.8	98.6	209.5	66.8	69.9	31.4	50.9	70.7	132.0	**926**
2030	35.6	16.9	103.1	126.1	43.1	36.8	37.0	5.1	7.8	34.6	54.2	124.7	**625**
2031	40.3	67.1	78.5	65.5	84.3	103.3	12.6	21.1	181.2	38.1	128.9	189.1	**1010**
2032	38.7	61.6	66.7	153.9	53.0	31.0	44.2	43.5	44.3	81.4	77.3	83.9	**779**
2033	38.3	44.2	45.9	26.6	72.0	50.2	100.9	7.7	99.5	10.0	132.2	161.1	**789**
2034	107.1	66.3	49.6	44.3	154.6	77.9	32.5	60.9	53.5	113.4	52.2	59.4	**872**
2035	15.3	35.9	43.0	24.1	98.1	79.7	89.3	51.9	83.5	118.3	20.4	136.9	**796**
2036	93.0	73.6	119.0	77.3	33.3	11.6	4.9	86.0	19.7	102.9	56.6	277.3	**955**
2037	17.9	76.5	43.3	17.5	120.7	31.3	16.2	10.8	89.7	200.4	108.9	118.7	**852**
2038	78.3	34.9	33.9	47.5	134.7	110.0	39.5	73.2	16.9	63.8	8.9	99.4	**741**
2039	90.0	34.9	61.3	102.2	66.2	5.7	13.6	201.1	23.7	105.0	98.4	43.3	**845**
2040	88.0	25.5	6.8	115.9	32.4	62.9	56.6	93.4	45.2	54.0	39.5	104.8	**725**
2041	70.8	29.6	82.3	25.8	13.9	69.2	43.5	94.1	91.4	88.0	12.3	160.7	**782**
2042	47.7	71.1	47.0	51.8	25.2	21.7	33.6	35.6	1.1	123.4	98.0	134.0	**690**
2043	103.0	156.8	119.9	44.8	18.8	20.2	9.2	30.2	7.8	92.3	27.3	122.0	**752**
2044	77.6	78.8	47.9	97.3	37.5	11.4	41.5	85.2	83.8	117.6	147.5	27.3	**853**
2045	130.7	10.8	12.4	76.2	40.8	70.7	36.2	47.0	74.6	60.3	57.8	9.6	**627**
2046	118.3	29.2	80.7	95.4	35.8	63.3	36.7	95.0	62.1	90.8	100.9	153.7	**962**
2047	64.3	88.4	125.1	90.9	98.0	77.8	19.1	96.7	159.6	94.3	108.7	18.3	**1041**
2048	29.3	42.9	67.7	46.4	14.1	54.9	21.3	14.9	23.5	39.8	113.6	128.0	**596**
2049	94.7	96.4	147.1	64.8	35.8	25.2	27.5	45.6	29.0	2.9	27.7	249.8	**846**
2050	99.4	113.7	137.0	54.7	149.3	79.0	84.4	52.2	98.8	94.3	127.9	160.4	**1251**
Average	**68.0**	**63.6**	**76.5**	**63.5**	**65.7**	**57.8**	**36.7**	**59.2**	**71.2**	**82.0**	**85.0**	**121.0**	**850**

Appendix 13: Corrected monthly data for TS Nikšić for all three models (Aladin, Promes, RegCM3), period (2021-2050)

Aladin	Jan	Feb	Mar	Apr	May	Jun	Jul	Aug	Sep	Oct	Nov	Dec	Year
2021	0.33	3.99	6.84	11.24	15.67	16.17	21.97	23.38	18.35	13.21	7.10	0.86	**11.59**
2022	1.53	5.13	7.37	11.92	14.23	20.43	23.85	22.38	18.33	11.91	7.44	4.09	**12.38**
2023	0.54	6.25	5.18	12.81	15.80	18.60	22.58	23.31	17.64	12.26	6.89	5.48	**12.28**
2024	1.76	2.49	7.54	12.42	17.78	22.01	23.72	21.02	16.53	11.13	4.36	5.82	**12.22**
2025	2.81	5.10	9.83	9.73	16.94	19.37	21.66	20.27	17.46	13.31	10.39	6.50	**12.78**
2026	4.82	3.20	9.80	10.05	14.79	16.51	22.95	23.22	19.06	14.25	7.21	5.02	**12.57**
2027	3.91	4.76	7.61	13.03	21.16	19.54	20.43	22.86	18.97	13.36	5.07	3.18	**12.82**
2028	2.59	5.42	5.47	12.06	14.79	19.48	23.43	23.35	17.36	13.95	7.01	4.74	**12.47**
2029	0.70	2.82	5.20	10.17	13.21	20.35	21.34	20.89	18.01	7.80	6.24	5.49	**11.02**
2030	-0.09	3.80	9.87	12.39	15.32	20.31	20.47	24.09	18.96	12.96	7.40	2.96	**12.37**
2031	4.51	5.08	6.31	9.72	16.69	18.51	21.25	22.33	18.39	13.54	8.88	6.85	**12.67**
2032	2.42	0.15	5.27	10.14	15.52	20.53	24.62	25.03	15.57	12.98	10.69	4.31	**12.27**
2033	2.14	4.89	8.68	13.23	15.38	18.25	24.42	22.51	18.98	11.97	6.40	3.11	**12.50**
2034	2.54	4.97	5.65	10.74	16.84	23.56	25.07	23.96	19.05	13.61	8.83	4.26	**13.26**
2035	2.85	1.79	4.91	9.67	19.54	25.76	28.83	26.62	21.39	15.14	7.54	4.09	**14.01**
2036	2.79	5.75	10.13	9.12	15.31	18.18	22.81	18.93	14.91	10.63	9.92	5.20	**11.97**
2037	2.89	3.67	7.96	9.24	14.93	21.19	23.59	22.40	19.39	14.31	10.65	2.59	**12.74**
2038	2.62	4.30	7.98	12.28	17.73	20.93	25.57	20.17	17.69	14.03	5.48	2.90	**12.64**
2039	1.02	7.10	7.62	10.25	14.94	19.34	21.19	18.02	14.59	13.76	9.07	6.32	**11.93**
2040	2.29	0.88	6.61	11.87	17.45	19.36	25.19	23.38	18.27	12.18	7.66	8.79	**12.83**
2041	5.43	5.35	6.43	10.23	15.97	19.31	20.96	21.59	17.00	11.48	5.26	4.12	**11.93**
2042	2.30	3.77	5.11	11.28	14.27	17.04	24.52	21.26	17.01	13.84	10.38	4.35	**12.09**
2043	1.53	4.51	10.39	12.69	15.36	20.07	25.45	20.98	19.46	12.76	5.72	4.74	**12.81**
2044	3.62	3.19	5.21	11.62	16.35	20.17	24.26	25.92	19.04	10.11	7.62	4.38	**12.62**
2045	4.20	3.99	8.40	12.29	17.44	21.55	26.09	23.94	19.57	14.15	10.34	6.93	**14.07**
2046	3.42	4.32	8.65	11.06	19.37	21.15	22.91	23.57	18.67	11.56	8.43	5.83	**13.25**
2047	2.33	6.62	9.95	13.96	17.85	22.45	21.37	25.09	17.63	13.35	9.68	3.19	**13.62**
2048	0.43	2.42	7.11	12.60	17.13	22.06	25.38	24.93	19.39	15.06	10.43	2.83	**13.31**
2049	1.94	5.41	6.48	11.91	18.03	21.86	26.75	25.94	19.64	13.66	10.25	9.02	**14.24**
2050	7.90	5.34	4.81	12.35	15.72	17.93	22.60	21.90	20.52	15.14	10.24	3.12	**13.13**
Average	**2.60**	**4.22**	**7.28**	**11.40**	**16.38**	**20.07**	**23.51**	**22.77**	**18.23**	**12.91**	**8.09**	**4.70**	**12.68**

Promes	Jan	Feb	Mar	Apr	May	Jun	Jul	Aug	Sep	Oct	Nov	Dec	Year
2021	3.27	6.31	7.93	12.00	16.20	19.06	23.38	22.18	15.33	8.69	7.96	3.74	**12.2**
2022	5.36	4.78	7.60	9.77	16.16	17.25	22.76	21.02	18.12	11.00	8.87	4.23	**12.2**
2023	5.44	7.04	7.61	10.26	16.84	19.78	26.42	23.60	19.33	13.28	7.90	4.37	**13.5**
2024	3.84	5.36	11.09	12.21	17.95	19.73	25.66	22.21	18.12	14.94	8.13	7.42	**13.9**
2025	0.97	1.88	5.56	10.28	15.44	19.97	21.56	21.06	17.86	12.31	5.47	3.82	**11.3**
2026	3.44	3.02	7.86	12.71	17.40	18.12	22.65	21.35	16.91	11.42	9.52	3.02	**12.3**
2027	3.14	3.68	2.39	9.30	14.41	20.48	20.28	20.94	18.75	12.22	4.57	3.26	**11.1**
2028	3.98	1.50	4.71	8.71	16.79	23.74	21.03	20.28	19.35	12.49	5.16	4.37	**11.8**
2029	3.41	5.93	11.54	9.37	16.01	20.49	21.96	20.57	17.59	13.19	7.56	2.35	**12.5**
2030	1.06	5.68	7.04	12.64	14.83	22.34	26.54	24.27	19.76	14.20	9.14	6.73	**13.7**
2031	0.34	2.98	8.73	11.67	17.29	18.32	23.74	22.25	19.17	14.99	6.25	4.22	**12.5**
2032	5.62	5.90	7.03	12.35	16.61	22.77	23.27	21.76	20.49	14.71	7.96	5.87	**13.7**
2033	7.68	6.59	11.32	15.10	19.04	21.62	26.33	21.72	14.48	10.97	10.50	4.64	**14.2**
2034	5.51	4.90	8.85	10.77	17.63	20.08	23.59	22.54	19.98	13.38	11.54	6.81	**13.8**
2035	5.12	6.42	9.43	9.64	14.62	24.07	23.83	22.34	17.26	15.91	8.46	5.61	**13.6**
2036	3.64	2.94	11.65	12.69	16.29	19.70	22.40	22.50	18.62	14.17	8.13	5.07	**13.2**
2037	4.73	3.79	10.62	12.91	17.15	21.69	23.42	24.03	17.05	15.23	6.08	1.25	**13.2**
2038	5.79	1.61	9.68	12.36	17.17	19.84	23.14	23.88	18.08	13.87	8.43	-0.77	**12.8**
2039	5.12	6.12	6.68	12.58	17.95	20.40	23.74	24.51	18.17	11.77	7.28	3.29	**13.1**
2040	4.97	6.52	8.86	11.42	17.98	24.62	26.63	22.33	20.00	15.08	5.96	4.86	**14.1**
2041	4.99	6.43	7.26	9.56	13.73	21.35	25.68	25.73	17.91	14.49	8.06	2.70	**13.2**
2042	5.58	-0.06	7.77	11.42	17.19	21.80	25.01	23.27	19.92	15.44	7.67	5.07	**13.3**
2043	3.37	2.44	9.10	15.53	18.50	23.46	23.17	24.43	20.97	14.49	9.15	7.63	**14.4**
2044	6.22	5.04	9.07	11.81	15.40	20.40	23.88	20.89	18.57	15.31	11.44	6.19	**13.7**
2045	6.69	4.89	8.10	11.26	16.33	20.74	24.34	22.70	19.19	13.08	8.77	4.74	**13.4**
2046	3.06	1.42	6.92	12.49	13.86	20.23	24.94	21.05	19.57	10.49	11.86	8.39	**12.9**
2047	6.15	0.18	6.85	12.90	16.02	20.34	22.17	22.69	16.87	11.76	7.49	2.11	**12.1**
2048	2.54	5.65	9.41	13.74	16.83	19.08	23.22	22.92	17.97	14.26	9.37	4.19	**13.3**
2049	3.87	2.67	8.13	12.68	15.39	18.94	22.66	24.78	19.86	13.86	10.70	3.96	**13.1**
2050	-1.01	3.91	7.39	12.57	13.88	22.43	24.69	25.07	17.22	12.02	8.26	3.81	**12.5**
Average	**4.1**	**4.2**	**8.2**	**11.8**	**16.4**	**20.8**	**23.7**	**22.6**	**18.4**	**13.3**	**8.3**	**4.4**	**13.0**

RegCM3	Jan	Feb	Mar	Apr	May	Jun	Jul	Aug	Sep	Oct	Nov	Dec	Year
2021	0.62	0.84	2.33	8.33	14.12	18.00	21.88	20.59	16.39	12.31	9.50	-0.31	**10.4**
2022	3.47	2.98	2.58	8.63	17.63	19.39	22.03	21.63	16.77	13.42	4.62	0.28	**11.1**
2023	2.36	1.07	7.43	11.63	14.80	16.08	18.77	21.06	15.92	11.13	4.64	2.25	**10.6**
2024	0.53	3.89	6.30	8.78	14.27	19.26	21.53	20.12	16.51	12.12	7.80	4.56	**11.3**
2025	1.68	4.91	2.91	12.15	14.27	20.25	21.96	22.41	16.87	14.41	6.68	4.80	**11.9**
2026	1.85	5.19	8.00	11.84	15.19	17.09	18.43	20.46	13.83	9.07	6.14	4.19	**10.9**
2027	1.34	2.67	8.17	8.02	13.98	17.77	23.58	19.69	17.26	13.28	7.78	3.61	**11.4**
2028	3.32	3.74	7.71	10.63	16.54	17.31	20.26	20.12	17.78	13.12	7.97	4.11	**11.9**
2029	0.70	5.66	10.06	11.18	15.71	16.00	19.39	21.73	17.61	16.83	6.60	2.42	**12.0**
2030	1.71	6.28	3.84	9.96	13.91	20.29	20.20	21.66	19.81	15.82	6.96	2.98	**12.0**
2031	2.16	3.90	8.22	10.17	16.57	18.79	22.15	24.17	19.35	11.82	7.24	5.27	**12.5**
2032	3.81	4.69	7.56	8.24	15.88	19.37	20.91	21.18	19.26	13.78	6.07	5.69	**12.2**

2033	4.54	5.00	5.23	10.90	15.65	18.22	21.80	23.73	17.49	17.12	9.74	3.93	**12.8**
2034	2.86	5.65	9.66	11.33	14.11	18.89	23.48	21.29	16.47	10.43	5.12	4.48	**12.0**
2035	-0.60	7.09	7.70	12.86	16.70	20.59	20.39	21.73	17.83	12.51	5.27	3.02	**12.1**
2036	-0.69	2.81	6.33	10.59	14.53	19.77	22.68	20.77	19.36	11.61	7.02	4.63	**11.6**
2037	2.01	3.28	8.27	10.68	15.88	18.88	22.32	23.45	19.50	13.02	9.98	3.11	**12.5**
2038	2.38	6.60	8.86	11.48	14.41	17.34	21.70	19.69	17.21	13.89	7.51	5.33	**12.2**
2039	3.99	3.37	6.27	11.79	13.64	20.79	22.74	19.69	21.24	14.00	7.45	1.49	**12.2**
2040	4.51	5.34	6.26	10.02	15.49	16.86	23.07	20.62	18.18	13.38	5.48	-0.38	**11.6**
2041	0.83	5.37	6.52	12.32	17.96	18.23	23.09	21.21	16.94	12.96	10.14	5.58	**12.6**
2042	1.98	-1.00	6.78	9.64	16.05	21.39	22.44	20.94	17.31	12.33	6.66	4.18	**11.6**
2043	4.23	8.80	7.24	10.09	17.16	19.15	22.38	25.05	18.56	13.59	5.48	1.72	**12.8**
2044	-1.12	5.86	3.75	10.55	15.41	20.90	24.66	21.03	17.69	12.84	6.36	1.27	**11.6**
2045	4.58	4.61	3.22	9.78	14.70	17.15	22.67	21.86	16.82	14.10	6.16	4.93	**11.7**
2046	7.33	5.43	7.77	12.59	17.27	21.52	19.77	22.33	14.71	14.55	8.73	2.82	**12.9**
2047	3.74	4.84	5.04	12.14	14.77	19.23	23.35	20.88	15.99	13.22	8.13	7.06	**12.4**
2048	3.21	4.70	9.86	11.03	17.65	19.03	25.80	23.42	20.06	16.71	10.80	3.80	**13.8**
2049	3.25	6.20	7.36	12.05	15.90	18.61	22.71	21.12	20.63	13.95	8.46	7.08	**13.1**
2050	3.29	5.26	7.04	11.74	13.92	17.48	22.57	21.60	17.69	14.78	11.52	4.74	**12.6**
Average	**2.5**	**4.5**	**6.6**	**10.7**	**15.5**	**18.8**	**22.0**	**21.5**	**17.7**	**13.4**	**7.4**	**3.6**	**12.0**

Appendix 14: Corrected monthly data for PS Nikšić for all three models (Aladin, Promes, RegCM3), period (2021-2050)

Aladin	Jan	Feb	Mar	Apr	May	Jun	Jul	Aug	Sep	Oct	Nov	Dec	Year
2021	76.8	240.6	268.1	137.7	52.0	89.6	38.4	60.7	279.0	298.1	340.8	65.3	**1947**
2022	77.9	199.8	295.4	161.3	135.5	25.3	0.0	34.0	85.9	195.8	159.7	91.1	**1462**
2023	37.2	443.4	257.4	278.0	170.3	45.5	62.0	35.7	17.4	44.1	151.6	118.3	**1661**
2024	83.6	92.2	151.5	92.7	59.5	31.4	93.0	220.1	344.1	336.6	43.8	154.6	**1703**
2025	55.7	84.5	136.2	248.0	89.3	71.1	27.1	52.6	118.7	177.3	348.5	427.4	**1837**
2026	203.0	233.6	153.4	347.1	129.5	106.4	62.3	24.0	19.5	195.0	129.0	356.3	**1959**
2027	223.6	266.3	82.1	89.1	42.1	117.7	156.8	26.7	117.9	229.5	0.2	83.9	**1436**
2028	111.8	301.7	351.5	132.3	97.0	38.5	62.8	33.5	66.0	240.9	198.8	244.8	**1880**
2029	168.4	55.7	198.5	132.9	98.2	89.2	97.4	204.7	103.4	45.9	340.4	165.3	**1700**
2030	11.0	146.5	201.6	250.9	111.4	44.3	245.6	27.3	130.0	111.6	81.6	269.4	**1631**
2031	446.5	226.5	155.0	103.1	109.2	197.7	104.3	96.3	132.1	79.9	114.9	368.4	**2134**
2032	140.0	127.7	111.8	294.2	108.9	48.6	61.1	22.0	305.8	276.7	580.8	239.9	**2318**
2033	170.7	218.8	111.0	170.9	127.3	113.2	48.9	42.0	225.2	205.9	361.5	97.9	**1893**
2034	68.1	15.9	256.1	345.9	83.6	19.0	72.1	89.1	154.8	195.3	250.1	47.6	**1598**
2035	78.0	140.3	106.8	101.2	20.5	17.5	6.0	0.0	97.0	62.7	198.8	72.0	**901**
2036	172.9	308.4	485.5	200.6	87.3	63.7	26.4	235.9	84.3	232.4	325.1	256.7	**2479**
2037	238.3	254.8	163.8	257.1	84.3	17.3	66.6	52.0	47.7	636.8	359.1	126.0	**2304**
2038	177.2	264.5	292.6	188.2	62.6	37.3	28.9	336.3	180.2	138.1	267.3	90.2	**2063**
2039	27.0	454.2	179.5	174.9	114.2	32.0	70.7	286.8	230.3	256.4	393.8	194.3	**2414**
2040	261.4	161.8	162.8	55.1	41.9	59.9	45.5	100.9	381.1	141.5	234.3	338.9	**1985**
2041	170.9	181.7	99.8	350.2	104.8	135.7	96.3	146.3	392.6	211.9	299.2	193.4	**2383**
2042	454.3	298.6	191.6	160.6	154.7	130.1	28.8	160.9	446.5	146.5	288.2	127.3	**2588**
2043	4.8	218.6	389.8	54.3	137.6	55.2	19.7	234.6	150.3	211.4	115.8	314.8	**1907**
2044	234.7	136.1	43.9	200.8	74.4	44.7	0.3	23.2	160.5	159.2	251.9	91.1	**1421**
2045	214.4	200.6	235.4	166.0	131.1	15.8	7.6	53.2	261.0	542.5	378.4	365.0	**2571**
2046	113.4	72.2	234.1	57.9	21.6	120.6	93.7	124.5	257.2	129.1	235.4	210.2	**1670**
2047	95.2	214.8	151.5	211.6	88.3	74.5	52.6	100.9	293.8	352.0	526.2	89.6	**2251**
2048	178.3	33.5	212.1	81.2	96.7	31.3	15.2	29.4	27.4	404.7	404.0	35.9	**1550**
2049	123.4	41.6	41.8	338.3	49.3	76.5	27.7	64.2	124.0	152.6	515.6	398.5	**1954**
2050	606.8	178.8	139.0	275.7	104.2	143.2	97.4	157.7	119.9	368.8	508.3	50.3	**2750**
Average	**167.5**	**193.8**	**195.3**	**188.6**	**92.9**	**69.8**	**60.5**	**102.5**	**178.5**	**226.0**	**280.1**	**189.5**	**1945**
Promes	**Jan**	**Feb**	**Mar**	**Apr**	**May**	**Jun**	**Jul**	**Aug**	**Sep**	**Oct**	**Nov**	**Dec**	**Year**
2021	113.5	208.3	258.5	352.5	13.8	50.3	50.3	52.0	108.2	139.1	386.6	217.0	**1950**
2022	404.1	256.9	183.8	119.7	90.3	104.1	17.8	58.8	273.0	163.5	133.8	178.3	**1984**
2023	206.5	179.9	116.8	489.1	62.4	41.8	7.0	6.3	63.8	302.1	327.7	192.9	**1996**
2024	104.2	117.3	151.6	96.3	107.0	131.7	0.6	89.1	81.6	528.2	110.2	414.1	**1932**
2025	206.0	372.0	328.3	212.7	154.6	76.0	148.0	7.1	103.3	104.5	117.7	314.8	**2145**
2026	414.2	243.4	289.6	200.6	47.7	189.2	29.0	162.3	230.6	142.5	475.3	236.5	**2661**
2027	425.3	311.2	152.4	305.4	164.3	81.5	17.6	79.8	208.3	282.4	51.2	202.8	**2282**
2028	93.8	115.2	131.2	96.0	67.1	16.5	55.0	88.2	87.6	20.2	199.9	347.5	**1318**
2029	70.6	117.5	81.3	330.6	64.1	55.0	116.9	341.2	42.5	147.9	415.0	227.8	**2010**
2030	222.9	351.4	63.5	206.0	95.0	28.1	11.7	69.6	128.2	530.6	244.5	237.0	**2188**
2031	245.5	127.1	64.2	371.7	78.3	156.0	16.4	77.0	144.0	610.7	286.0	86.2	**2263**
2032	167.8	166.2	219.5	220.7	75.2	26.6	22.7	116.9	169.1	51.7	396.4	126.8	**1760**
2033	364.5	229.3	160.3	14.8	12.5	24.9	3.7	26.5	202.9	428.1	362.9	122.5	**1953**
2034	150.1	253.6	236.5	107.7	56.4	105.5	24.6	45.6	95.3	140.3	184.6	374.7	**1775**
2035	23.3	128.0	215.2	152.2	81.9	4.5	9.8	91.7	95.8	435.4	215.4	470.3	**1923**
2036	243.0	307.2	151.5	63.5	155.1	52.3	24.7	76.0	161.0	539.9	152.1	94.2	**2021**
2037	130.6	237.0	98.0	173.1	245.3	55.5	54.1	1.4	36.3	79.8	138.2	90.7	**1340**
2038	295.5	55.2	182.1	69.9	78.7	52.5	26.3	32.6	16.0	376.7	373.3	273.1	**1832**
2039	329.9	238.1	185.1	222.1	43.9	88.6	13.5	66.9	116.9	45.6	43.8	61.3	**1456**
2040	39.9	57.5	143.1	391.2	120.3	16.1	14.1	196.1	82.4	212.5	171.3	460.0	**1905**
2041	184.6	235.6	101.0	156.5	120.2	46.8	12.8	93.0	48.9	45.6	164.4	181.1	**1391**
2042	176.0	62.5	203.9	150.1	62.1	48.2	22.5	14.4	33.3	231.3	165.5	168.2	**1338**
2043	318.6	104.1	319.9	153.8	51.1	49.9	71.7	1.1	34.1	347.4	162.0	180.5	**1794**
2044	105.7	226.8	411.2	35.1	116.4	42.4	17.6	107.9	154.0	370.7	295.6	319.1	**2203**
2045	213.4	193.1	234.8	289.1	111.8	44.1	54.6	78.7	137.7	341.9	418.0	316.5	**2434**
2046	104.1	164.8	167.0	58.8	189.7	94.8	23.2	214.3	117.0	95.2	259.0	263.5	**1751**
2047	164.5	39.4	52.8	315.1	107.8	68.4	69.3	68.2	114.6	449.9	3.2	6.8	**1460**
2048	101.2	50.0	294.8	133.9	89.6	155.5	26.9	22.9	111.3	310.5	240.7	230.2	**1767**
2049	7.8	89.4	328.6	129.0	136.0	89.7	35.4	28.6	101.7	216.6	355.1	137.1	**1655**
2050	44.5	342.7	151.2	185.2	141.2	12.2	19.5	55.0	125.6	296.5	385.6	314.5	**2074**
Average	**189.0**	**186.0**	**189.3**	**193.4**	**98.0**	**67.0**	**33.9**	**79.0**	**114.2**	**266.2**	**241.2**	**228.2**	**1885**
RegCM3	**Jan**	**Feb**	**Mar**	**Apr**	**May**	**Jun**	**Jul**	**Aug**	**Sep**	**Oct**	**Nov**	**Dec**	**Year**
2021	151.7	425.4	70.1	100.7	99.2	16.8	40.0	40.4	85.7	150.6	125.1	130.7	**1436**
2022	144.3	205.0	140.5	164.9	33.7	40.8	61.1	76.0	170.1	151.3	471.1	167.0	**1826**
2023	259.1	126.2	492.4	98.3	88.5	181.5	31.7	189.9	324.0	281.1	231.3	321.3	**2625**
2024	98.8	78.5	254.9	72.0	107.9	75.3	37.6	186.7	272.5	84.4	351.9	530.7	**2151**
2025	111.2	309.4	308.1	135.3	208.2	64.0	72.6	45.8	127.1	101.0	212.8	364.2	**2059**
2026	264.4	290.6	309.4	22.4	91.2	161.6	57.9	58.1	282.0	202.0	174.3	259.7	**2173**
2027	128.4	209.7	142.4	261.2	100.3	116.2	19.3	82.5	250.3	347.5	437.6	44.5	**2140**
2028	194.0	230.5	169.2	85.3	100.7	56.8	9.2	72.4	77.1	278.9	387.7	541.6	**2203**
2029	103.8	183.5	134.9	108.6	159.7	354.9	96.7	114.8	62.2	115.1	189.2	337.7	**1961**
2030	92.1	52.2	265.9	292.4	68.7	60.6	54.3	7.7	15.8	81.3	148.4	314.0	**1453**
2031	104.3	214.4	202.7	155.4	139.0	166.1	17.3	34.1	362.3	90.3	348.8	477.4	**2312**
2032	100.8	188.2	170.8	355.2	87.4	51.0	64.1	71.3	87.5	188.4	211.0	209.8	**1786**

2033	98.3	136.4	119.5	58.9	118.3	83.8	141.9	12.8	196.7	23.0	363.3	402.2	**1755**
2034	274.1	206.6	131.2	101.6	259.1	134.2	47.5	100.5	107.2	262.0	141.0	149.4	**1914**
2035	38.7	112.4	107.8	55.3	158.3	135.4	130.6	85.5	166.7	272.1	55.5	343.2	**1662**
2036	240.1	235.9	305.1	178.5	54.5	20.5	6.9	138.9	40.5	236.0	153.0	700.9	**2311**
2037	44.4	241.0	110.5	39.8	194.2	52.1	21.0	17.6	178.6	467.2	290.1	298.7	**1955**
2038	199.6	109.2	88.9	108.4	226.2	186.8	58.1	124.0	33.6	149.1	24.3	252.0	**1560**
2039	230.6	106.5	156.7	234.9	107.4	9.0	20.0	334.3	47.5	245.3	271.6	108.7	**1872**
2040	228.4	80.7	17.2	268.4	52.5	104.6	82.5	150.8	90.2	125.2	105.1	261.2	**1567**
2041	180.5	91.4	213.5	59.0	21.5	113.9	62.5	154.6	176.8	203.5	33.8	401.6	**1713**
2042	122.2	220.8	120.2	119.4	38.4	36.0	47.7	56.0	1.9	286.8	264.3	336.1	**1650**
2043	262.7	488.1	309.2	101.1	29.2	32.0	12.4	48.8	14.3	213.7	75.0	307.8	**1894**
2044	198.9	250.5	126.9	225.5	61.2	17.8	61.5	138.4	167.0	271.3	399.0	69.4	**1987**
2045	339.9	32.4	31.1	178.0	67.3	116.1	54.2	76.5	145.0	140.9	155.1	24.5	**1361**
2046	302.9	91.2	210.8	221.7	57.3	106.4	53.6	157.9	125.4	213.1	274.5	384.6	**2199**
2047	167.3	278.3	327.6	213.0	157.5	127.8	27.6	160.2	314.9	220.8	293.1	46.0	**2334**
2048	75.1	133.3	174.1	106.2	22.1	91.3	29.9	25.4	46.3	91.1	312.8	325.0	**1433**
2049	244.5	304.7	379.8	153.5	58.7	43.1	39.1	77.1	57.5	6.2	74.7	631.8	**2071**
2050	257.6	356.4	346.7	127.6	248.7	131.7	125.0	81.4	192.1	220.8	347.4	408.9	**2844**
Average	**175.3**	**199.7**	**197.9**	**146.7**	**107.2**	**96.3**	**52.8**	**97.3**	**140.6**	**190.7**	**230.8**	**305.0**	**1940**

Appendix 15: Corrected monthly data for PS Lukovo for all three models (Aladin, Promes, RegCM3), period (2021-2050)

Aladin	Jan	Feb	Mar	Apr	May	Jun	Jul	Aug	Sep	Oct	Nov	Dec	Year
2021	71.2	215.0	238.1	135.1	55.2	89.1	33.9	70.0	251.6	274.2	328.4	53.4	**1815**
2022	72.3	173.3	263.3	158.4	135.5	27.7	0.0	34.9	79.7	184.1	154.3	76.4	**1360**
2023	35.7	392.5	230.6	266.3	174.6	47.9	56.8	36.8	17.4	41.2	145.4	102.1	**1547**
2024	76.5	81.8	138.8	89.1	59.5	31.9	87.1	222.2	304.4	311.5	42.8	129.4	**1575**
2025	50.6	73.9	121.3	238.8	93.0	73.0	24.8	59.4	110.7	168.3	328.7	364.9	**1708**
2026	187.2	206.3	137.6	337.0	132.4	112.4	61.3	29.1	16.3	181.6	123.9	301.3	**1826**
2027	207.8	234.0	72.6	88.6	45.1	119.3	140.6	32.0	106.4	213.2	0.3	71.0	**1331**
2028	104.0	268.8	311.6	128.6	99.7	42.6	59.6	36.9	59.8	225.7	186.3	208.3	**1732**
2029	156.4	48.7	180.5	131.9	99.0	90.8	92.7	209.1	95.5	41.7	328.2	140.1	**1615**
2030	9.8	129.9	178.4	244.0	112.9	47.9	224.2	31.4	116.5	103.3	78.5	230.2	**1507**
2031	409.9	200.2	138.2	99.6	109.6	199.3	93.8	98.6	120.7	72.8	108.4	315.8	**1967**
2032	129.0	111.9	99.6	283.9	108.6	50.6	53.6	26.9	273.5	254.5	559.5	205.5	**2157**
2033	156.6	189.8	98.5	168.1	126.3	113.8	43.7	44.1	204.3	194.0	351.4	81.4	**1772**
2034	61.5	13.8	232.1	334.4	84.1	21.5	65.7	93.2	140.5	180.5	240.2	40.9	**1508**
2035	72.5	125.1	97.5	96.9	22.5	19.6	7.2	0.0	87.0	57.0	191.6	61.4	**838**
2036	160.7	272.3	437.6	193.6	85.5	65.7	22.5	250.2	76.5	213.5	312.4	219.9	**2310**
2037	216.9	224.7	146.7	251.7	86.3	17.9	64.1	48.2	45.9	588.2	344.2	107.1	**2142**
2038	164.4	234.9	264.5	182.0	64.3	40.7	25.9	344.0	164.6	127.0	260.4	76.0	**1949**
2039	25.5	401.4	157.3	167.8	118.1	32.9	63.2	293.4	208.5	238.6	374.4	165.9	**2247**
2040	240.8	144.7	147.3	50.2	43.8	61.0	41.0	100.1	341.9	131.8	225.8	290.4	**1819**
2041	157.0	160.9	88.6	344.0	105.7	135.9	89.2	151.9	355.4	195.8	288.9	165.3	**2239**
2042	414.6	261.0	171.7	154.2	157.5	128.8	27.0	169.6	401.6	135.6	271.1	107.1	**2400**
2043	4.7	191.3	349.7	53.7	138.1	58.6	19.0	239.0	135.6	196.0	113.3	266.4	**1765**
2044	217.8	120.5	40.3	195.0	75.4	45.8	0.1	24.4	146.3	150.6	241.8	78.1	**1336**
2045	196.2	178.0	213.0	162.3	136.5	16.5	8.3	54.5	237.1	510.6	364.3	315.3	**2393**
2046	105.8	63.0	211.2	58.2	21.7	124.8	84.5	125.4	228.2	121.8	226.2	176.7	**1548**
2047	88.8	189.4	133.7	202.9	87.0	72.8	45.5	109.1	263.4	327.2	511.9	76.6	**2108**
2048	164.0	29.5	188.4	80.1	100.4	32.2	13.0	34.7	25.1	373.6	392.1	31.2	**1464**
2049	114.0	36.2	36.9	322.9	51.2	80.8	27.1	65.5	116.3	139.0	494.7	340.7	**1825**
2050	565.4	155.5	126.5	268.0	106.4	142.8	89.9	161.1	105.4	335.9	489.1	43.3	**2589**
Average	**154.6**	**171.0**	**175.1**	**182.9**	**94.5**	**71.5**	**55.5**	**106.5**	**161.2**	**209.6**	**269.3**	**161.4**	1813
Promes	**Jan**	**Feb**	**Mar**	**Apr**	**May**	**Jun**	**Jul**	**Aug**	**Sep**	**Oct**	**Nov**	**Dec**	**Year**
2021	104.8	183.4	230.6	341.6	13.8	54.1	44.9	51.7	97.8	131.2	372.5	186.3	**1813**
2022	368.1	226.2	166.0	117.0	91.1	108.2	17.6	62.1	246.7	154.9	127.2	152.6	**1838**
2023	190.2	158.7	105.6	474.1	64.0	42.7	6.7	7.7	56.7	281.8	314.8	163.4	**1866**
2024	95.1	102.7	135.8	93.9	105.3	134.9	0.7	93.8	73.8	491.8	105.0	351.4	**1784**
2025	188.8	327.1	292.6	207.7	156.4	79.3	136.0	8.0	93.0	93.6	114.4	267.0	**1964**
2026	378.4	213.5	257.7	195.2	49.4	195.5	27.0	171.6	208.4	132.6	455.1	201.2	**2486**
2027	391.1	275.0	134.1	294.7	167.1	83.3	17.3	82.1	186.4	263.2	47.7	172.3	**2114**
2028	85.9	100.5	115.8	93.5	69.8	18.0	49.8	93.2	79.7	18.1	193.9	296.6	**1215**
2029	64.0	102.4	72.2	320.7	64.5	57.8	108.8	350.2	39.3	137.9	401.9	195.7	**1915**
2030	204.4	312.1	56.4	201.2	97.1	30.5	11.1	73.6	117.3	493.7	237.6	201.4	**2037**
2031	229.5	112.5	58.1	358.7	77.6	159.4	16.1	79.1	131.6	572.7	277.0	73.0	**2145**
2032	154.6	147.3	197.5	215.6	76.1	27.5	21.6	118.1	154.4	46.6	382.7	107.5	**1649**
2033	334.4	202.3	143.6	14.8	12.4	25.6	3.8	28.9	184.5	404.8	349.3	103.6	**1808**
2034	137.2	222.4	212.7	103.7	56.2	107.7	22.1	49.3	86.4	130.2	178.7	319.6	**1626**
2035	21.8	113.2	190.8	146.4	85.3	5.3	9.3	94.1	85.9	405.7	206.4	401.1	**1765**
2036	224.6	268.7	135.5	61.8	155.7	54.5	24.6	78.9	144.8	505.4	145.8	80.0	**1880**
2037	118.7	208.8	87.1	169.2	249.9	57.0	51.3	2.1	33.0	74.5	131.9	79.3	**1263**
2038	270.5	49.4	164.4	68.8	79.2	53.2	24.7	33.9	14.0	350.5	358.9	232.9	**1700**
2039	302.6	209.9	167.0	214.2	44.9	90.9	13.0	72.8	105.8	42.6	41.6	51.8	**1357**
2040	36.5	51.4	128.1	376.4	123.0	16.4	13.7	200.2	72.4	199.3	164.6	387.9	**1770**
2041	168.6	208.2	89.7	152.0	120.3	48.6	11.9	94.7	44.1	43.8	157.0	154.4	**1293**
2042	161.6	55.7	184.0	146.3	62.8	49.1	21.4	15.8	31.0	216.2	160.0	142.9	**1247**
2043	290.0	91.3	288.1	148.3	52.5	52.0	67.5	1.1	31.2	325.6	156.0	153.3	**1657**
2044	95.6	199.5	367.7	34.9	119.0	45.0	16.8	111.7	140.1	349.9	284.4	269.8	**2035**
2045	194.9	169.9	209.5	280.1	114.4	45.1	49.7	80.7	126.1	321.0	403.9	271.5	**2267**
2046	97.3	145.2	150.4	57.2	191.8	97.6	21.2	225.5	108.2	92.3	249.5	225.1	**1661**
2047	148.4	35.4	47.0	305.6	110.4	70.5	65.8	72.7	107.1	418.6	3.1	6.0	**1391**
2048	93.5	44.5	262.7	133.4	90.5	160.2	24.8	24.6	103.6	289.5	233.9	195.4	**1657**
2049	7.1	78.9	294.5	124.7	138.5	91.6	32.6	29.0	90.9	203.3	341.5	117.1	**1550**
2050	41.7	302.0	134.5	179.2	144.6	12.4	19.3	57.8	113.6	283.2	368.2	268.0	**1924**
Average	**173.3**	**163.9**	**169.3**	**187.7**	**99.4**	**69.1**	**31.7**	**82.2**	**103.6**	**249.2**	**232.2**	**194.3**	1756
RegCM3	**Jan**	**Feb**	**Mar**	**Apr**	**May**	**Jun**	**Jul**	**Aug**	**Sep**	**Oct**	**Nov**	**Dec**	**Year**
2021	138.5	377.5	61.7	99.0	99.4	18.7	37.8	41.7	78.9	137.7	119.2	112.4	**1322**
2022	131.4	178.0	124.2	159.4	34.3	42.9	56.7	78.4	152.0	137.3	455.0	141.3	**1691**
2023	233.3	111.0	442.1	100.0	91.1	186.8	30.3	193.7	299.6	257.5	222.2	273.1	**2441**
2024	90.1	68.6	226.8	70.5	108.5	76.1	35.7	190.5	249.2	80.3	333.1	448.1	**1977**
2025	102.8	269.8	277.0	131.1	215.1	66.0	67.4	48.3	115.0	96.3	204.9	312.2	**1906**
2026	242.7	252.7	274.5	21.6	92.8	166.5	55.7	58.7	257.0	192.3	169.7	222.7	**2007**
2027	116.4	185.4	127.6	253.5	101.4	120.7	18.0	83.7	229.3	325.7	421.3	37.5	**2021**
2028	178.2	200.2	150.8	82.8	102.9	60.7	8.7	75.7	70.0	262.2	374.4	458.1	**2025**
2029	94.1	160.9	120.0	105.2	162.6	359.0	88.9	118.4	56.3	110.8	184.7	283.2	**1844**
2030	83.9	46.7	239.3	283.4	71.0	63.1	49.3	8.6	14.0	75.4	141.7	267.4	**1344**
2031	95.0	185.2	182.2	147.3	139.1	176.9	16.7	35.7	325.3	82.9	336.7	405.7	**2129**
2032	91.4	170.1	154.8	346.0	87.5	53.1	58.8	73.8	79.5	177.2	201.9	179.9	**1674**

2033	90.4	122.2	106.4	59.8	118.7	86.0	134.5	13.0	178.6	21.7	345.6	345.6	**1622**
2034	252.8	183.2	115.2	99.6	255.1	133.4	43.3	103.3	96.0	246.9	136.4	127.4	**1793**
2035	36.0	99.0	99.7	54.2	161.8	136.6	118.9	88.0	149.9	257.6	53.2	293.7	**1549**
2036	219.4	203.2	276.0	173.7	55.0	19.9	6.5	145.7	35.4	224.0	147.9	594.9	**2102**
2037	42.2	211.2	100.4	39.4	199.1	53.6	21.5	18.3	161.0	436.3	284.5	254.7	**1822**
2038	184.8	96.5	78.7	106.7	222.2	188.4	52.6	124.0	30.4	138.8	23.2	213.1	**1459**
2039	212.5	96.4	142.2	229.6	109.3	9.7	18.1	340.9	42.6	228.5	257.1	92.8	**1780**
2040	207.7	70.5	15.9	260.5	53.4	107.7	75.4	158.3	81.2	117.5	103.2	224.8	**1476**
2041	167.1	81.8	191.0	57.9	23.0	118.5	58.0	159.4	164.1	191.6	32.3	344.6	**1589**
2042	112.6	196.3	109.0	116.4	41.5	37.2	44.7	60.3	1.9	268.7	256.0	287.5	**1532**
2043	243.2	433.1	278.1	100.8	31.0	34.5	12.2	51.2	14.1	201.0	71.4	261.6	**1732**
2044	183.3	217.6	111.1	218.6	61.8	19.6	55.3	144.5	150.5	255.9	385.3	58.5	**1862**
2045	308.5	29.8	28.7	171.3	67.4	121.1	48.3	79.6	133.9	131.3	151.1	20.5	**1292**
2046	279.1	80.7	187.3	214.4	59.1	108.4	48.8	160.9	111.4	197.6	263.6	329.7	**2041**
2047	151.8	244.2	290.3	204.3	161.7	133.2	25.5	163.9	286.5	205.2	284.0	39.1	**2190**
2048	69.1	118.6	157.0	104.2	23.2	94.0	28.3	25.2	42.2	86.6	296.8	274.6	**1320**
2049	223.6	266.2	341.3	145.7	59.0	43.3	36.6	77.2	52.1	6.3	72.3	535.8	**1859**
2050	234.7	313.8	317.9	123.0	246.4	135.3	112.5	88.4	177.4	205.2	334.2	344.1	**2633**
Average	**160.6**	**175.7**	**177.6**	**142.7**	**108.5**	**99.0**	**48.8**	**100.3**	**127.8**	**178.5**	**222.1**	**259.5**	**1801**

References

Arnell, N. W., 2003: Effects of IPCC SRES emissions scenarios on river runoff: A global perspective. *Hydrol. Earth Syst. Sci*., **7**, 619–641.

Climate Change and Impacts on Water Supply (CC-WaterS) - International Study for SE Europe, 18 Institutions from SE Europe, May 2009 – May 2012, [Available online at http://www.ccwaters.eu/index.php?option=com_content&view=article&id=48&Itemid=54&56b00064c3e6beb26da3b96d1578b92a=caac98a9a4248cd115a194c70c97a142].

Dimkić, D., and J. Despotović, 167-180, Climate Change - anthology, Inferences from Paleoclimate and Regional aspects, 2012, (Eds.) A. Berger, F. Mesinger, Dj. Šijački, ISBN 978-3-7091-0972-4

Fowler, H. J., C. G. Kilsby, and J. Stunell, 2007: Modelling the impacts of projected future climate change on water resources in north-west England. *Hydrol. Earth Syst. Sci*., **11**, 1115–1126.

Fujihara, Y., K. Tanaka, T. Watanabe, T. Nagano, and T. Kojiri, 2008: Assessing the impacts of climate change on the water resources of the Seyhan River Basin in Turkey: Use of dynamically downscaled data for hydrologic simulations. *J. Hydrol*., **353**, 33–48.

Hydro-Meteorological Service of Serbia (HMSS), 2011, [Available online at http://www.hidmet.gov.rs].

International project SINTA (Mediterranean project, participants: Euro-Mediterranean Center for Climate Change from Bologna, University of Belgrade Institute of Meteorology, and the Hydro-Meteorological Service of Serbia), 2007-2008, [Available online at http://www.earth-prints.org/handle/2122/4675].

IPCC, 2007: Climate Change 2007: Synthesis Report. Contribution of Working Groups I, II and III to the Fourth Assessment Report of the Intergovernmental Panel on Climate Change. Core Writing Team, Pachauri, R. K. and Reisinger, A. (Eds.) IPCC, Geneva, Switzerland. 104 pp. [Available online at http://www.ipcc.ch/publications_and_data/publications_ipcc_fourth_assessment_report_synthesis_report.htm.]

Jaroslav Černi Institute for the Development of Water Resources (JČI), 2010-2012, Climate Change Impacts on River Hydrology in Serbia – National Study, in Serbian.

Juckem, P. F., R. J. Hunt, M. P. Anderson, and D. M. Robertson, 2008: Effects of climate and land management change on stream flow in the driftless area of Wisconsin. *J. Hydrol*., **355**, 123– 130.

Ma, Z., S. Kang, L. Zhang, L. Tong, and X. Su, 2008: Analysis of impacts of climate variability and human activity on stream flow for a river basin in arid region of northwest China. *J. Hydrol*., **352**, 239–249.

Novotny, E. V., and H. G. Stefan, 2007: Stream flow in Minnesota: Indicator of climate change. *J. Hydrol.,* **334**, 319–333.

Smailagić, J., Climate change in Serbia, Monograph: In Memory of Milutin Milanković, 2009, ISBN 978-86-910313-1-2.

South East Europe Climate Outlook Forums (SEECOFs), 2008-2010., [Available online at http://www.google.rs/search?hl=sr&source=hp&q=climate+change+seecof&btnG=Google+%D0%BF%D1%80%D0%B5%D1%82%D1%80%D0%B0%D0%B3%D0%B0&meta=&gbv=2&oq=climate+change+seecof&aq=f&aqi=&aql=&gs_sm=s&gs_upl=1280l13231l0l17334l23l23l1l5l3l0l297l3464l0.9.8l17l0].

Let's grow up together

DRINK ADRIA

Adriatic IPA
Cross Border Cooperation 2007-2013

The project is co-funded by the European Union,
Instrument for Pre-Accession Assistance

Climate change for Drini Basin

SHUKALB: Water Supply and Sewerage Utility of Albania (FB11)

Tirane, 2014

Lead Author/s	Alban Kuriqi
Lead Authors Coordinator	Arlinda Ibrahimllari
Contributor/s	Anisa Aliaj
Date last release	17.10.2014
State of document	Final report

Let's grow up together

DRINK ADRIA

Adriatic IPA
Cross Border Cooperation 2007-2013

The project is co-funded by the European Union, Instrument for Pre-Accession Assistance

Table of Contents

List of Figures

List of tables

1. INTRODUCTION

One of the most significant impacts of climate changes will be on hydrological processes and consequently on water resources. The long-term planning of water resources should take account of the potential impacts of future change, which requires an understanding of both sensitivities to change and current variability over time. Changes in climate are not the only changes that may be experienced in a catchment's over the next few decades. Land use has an influence on river flow regimes and changes in vegetation cover, for example, it could have a significant effects on both annual yields and the distribution of flow over time. Catchment's vegetation cover can be expected to change as climate evolves, but changes in land use and agricultural policy may possibly be as important in an intensively-exploited landscape, such as this area is. These changes may be independent from climate change, but could be responses to changing climatic conditions. Demand for water from all sectors can also be expected to change over the next decades. On the other hand, this change in demand may be climatically-influenced. It is important to remember that climate is not the only driver that controls the flow regimes and water resources that may change in the future. The infiltration of rainfall and snowmelt into soil is dependent not just on rainfall and vegetation characteristics but also on soil structure properties [1]. These too may change perhaps slowly with a changing climate and vegetation cover. Increased temperatures might lead summer cracking, for example, whilst longer periods of water-logging in winter could lead to increased soil degradation.

Soil structure has an important influence on the rate at which storm rainfall reaches channels, and changes in soil structure would therefore alter hydrograph shape. If for example, storm rainfall were to be directed to river channels more rapidly, less water would be available for maintaining flows during dry periods. Finally, the processes by which stream runoff is generated may be altered by climate change.Global warming will also result in sea-level rise, and as oceans expand, storm patterns will become more energetic [2]. Consequently, sea level rise will affect most of the world's coastlines through inundation and increased erosion. Sound predictions of the development of these hazards over the next century are needed in order to manage the resulting risks. Coastal flooding is somewhat easier to predict than erosion since inundation can be estimated using coastal contours. However its prediction is not trivial since inundation may be followed by rapid reshaping of the shoreline by, amongst other things, waves, tidal currents and human interventions. In addition to submergence, seawater intrusion into freshwater aquifers in deltaic areas is an increasing problem associated with rising of sea level [3].

2. INPUT DATA

The Drin River Basin is located in the Western Balkans and it is shared between Albania, Greece, Kosovo, Macedonia and Montenegro. The basin represents a very complex water system where Rivers, lakes, wetlands, groundwater interact with each other and create a very rich ecosystem in terms of natural resources [4].

The total catchment area of the basin is around 19,600 km2 and it includes the Black Drin, White Drin and Buna River, as well as the Shkodra, Ohrid and Prespa lakes.

The Black Drin originates from Lake Ohrid and flows up north crossing the border between Macedonia and Albania and meets the White Drin which rises in Kosovo. They flow together as Drin River through the territory of Albania until they meet the Buna River and discharge finally to Adriatic Sea. On the other hand, the water from Prespa Lakes, which are shared between Albania, Greece and Macedonia, flows to Lake Ohrid through the porous underground karstic formations. The basin represents great importance in terms of natural resources not only on national level for the riparian countries but also in the global level. Shkodra Lake, which is the largest lake in the Balkan Peninsula, is one of the largest bird reserves in Europe and therefore has been.

Included in the Ramsar list of wetlands of international importance. Prespa Lakes are the highest tectonic lakes in the Balkans and they are especially important for water birds, notably the largest breeding colony of Dalmatian pelicans in the world and they are also part of Ramsar List of Wetlands of International Importance [5]. Ohrid Lake is one of Europe's deepest and oldest lakes and the deepest lake in the Balkans.

Figure 1. River basins map of Albania [6]

There are consider 5 meteorological stations to perform climate change study. The meteorological study consider in this study are as following: Theth, Shkoder A, Shishtavec, Peshkopi, Shupenze (Figure 2).

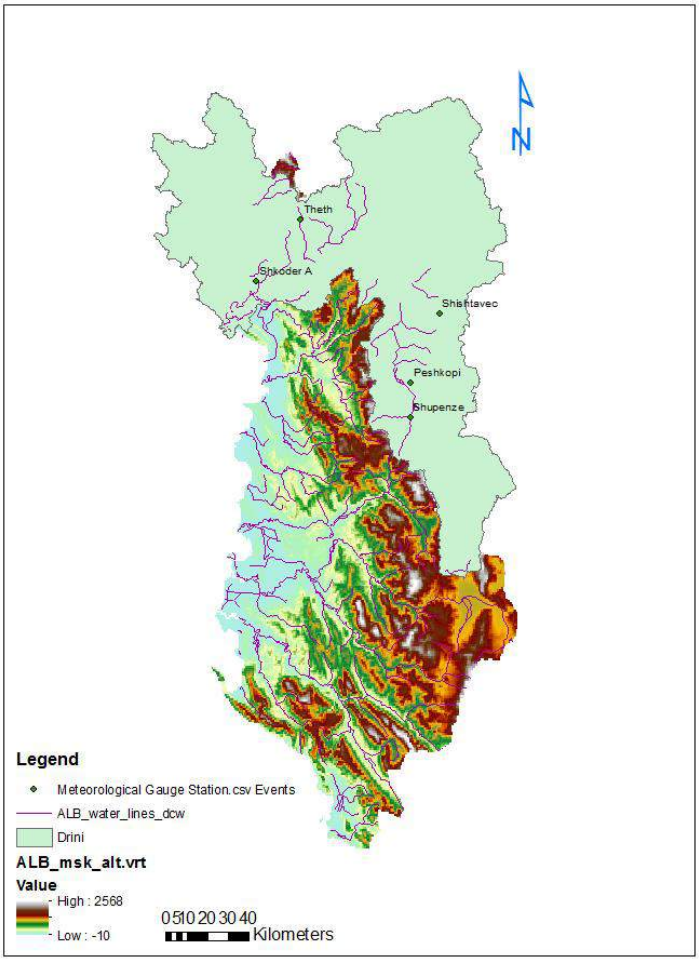

Figure 2. Meteorological stations location

3. THE MODELS USED

Three basic approaches are adopted in this report: (a) a regionalized approach based on empirical relationships developed nationally and then transferring the information to the selected catchments, (b) an empirical relationship developed across the catchment's and (c) a modeling approach applied at a range of the catchment's. The main objective of this study is to develop climate change scenarios in order to assess the potential changes in flow regimes in this particular catchment's. There are a range of empirical approaches to estimating impacts, based on the analysis of regional hydrological data. Empirical approaches do not require the local calibration of a model, and can provide very quick estimates of sensitivities to change in catchments.

The study presents results from the application of rainfall-runoff models to estimate changes and sensitivities in selected catchments, and contains a comparison of the 'generalized' and 'modeling' approaches. Other studies have used simple relationships between average annual runoff, rainfall and evapotranspiration or temperature to determine the possible effects of changes in input on runoff [7], for example, constructed rainfall-runoff models to estimate average annual runoff from average annual precipitation and temperatures developed across all the country.

3.1 Empirical Approaches

This section attempts to use regional relationships between average annual runoff, rainfall and potential evapotranspiration to determine the sensitivity of average annual runoff in the catchment to change. Most of the investigations are based on regional regression relationships developed between average annual runoff and climatic indices. The following assumptions are made:

(i) A model that is developed using average data from different catchments can be assumed to apply to annual data from an individual catchment.

(ii) The coefficients of the model do not change over time (changes in land use, for example, which may influence evaporative losses, are ignored);

(iii) Changes in precipitation and evapotranspiration apply equally throughout the year.

Four models to estimate average annual runoff were considered:

(i) The regional regression model, to estimate average annual runoff from average annual precipitation that is:

$$R = 0.2415*P^{1.21} \quad (1)$$

$$R^2 = 0.75$$

(ii) A simple linear regression relationship between average annual runoff-R, Precipitation-P and Potential Evapotranspiration-PE, where average annual runoff is calculated over the entire period of flow record available:

$$R = a + b*P + c*EPI \quad (2)$$

(iii) A simple linear regression derived in the FREND from 214 catchments with basin area up to 500 km2:

$$R = 0.97\ P - 0.55\ PE - 147 \quad (3)$$

$$R2 = 0.98$$

(iv) The procedure recommended in the Low Flow Studies Report (Institute of Hydrology, United Kingdom, 1980):

$$R = P - E \quad (4)$$

E is estimated from potential evapotranspiration using a ratio which is dependent on P:

$$E = r\,PE$$

$$r = 0.0002\,P + 0.78$$

$$r < 1.0$$

The sensitivity of average annual runoff to changes in average annual rainfall and potential evapotranspiration was assessed using data from the gauging stations in Drini river Basin.The first regression model, (1), is based and derived only on the relation rainfall-runoff from the data of the Drini catchment's area. According to the climate change scenarios the precipitation for the four time horizons will decrease as shown in the (Table 1, 2) and in (Figure 3). This decrease in annual precipitation produces a decrease in annual runoff. Using the regression found for this basin the sensitivity of average annual runoff to changes in average rainfall is as follows:

$$\frac{R_1}{R_0} = \left(\frac{P_1}{P_0}\right)^{1.44} \quad (5)$$

Where; the subscripts 0 and 1 refer to current and future conditions respectively. A 10% increase in average annual rainfall would increase average annual runoff by 17%.

Table 1. Scenarios of mean annual runoff change after the regional regression model

Year	2030		2050		2080		2100	
	Precip.	Runoff	Precip.	Runoff	Precip.	Runoff	Precip.	Runoff
A1BAIM -aver	-3.9	-5.7	-8.1	-12.9	-12.9	-22.0	-15.5	-27.4
A2ASF -min	-2.6	-3.6	-5.5	-8.5	-8.4	-13.5	-9.0	-14.5
A1FIMI -max	-5.4	-7.6	-11.0	-18.3	-21.0	-30.4	-26.1	-40.6

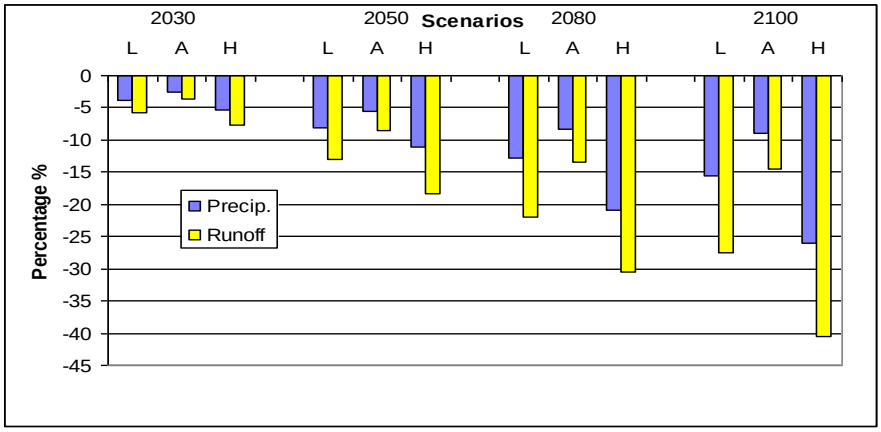

Figure 3. Graphical presentation of the precipitation and runoff change

The assessments of runoff for all the other empirical models are summarized in the (Table 2) below.

Table 2. Percent change in runoff

Equation	Scenarios	2030	2050	2080	2100
		Values in %			
R = 0.97 P - 0.55 PE - 147	A	7.33	14.3	22.3	27.0
A1FIMI	H	8.9	17.7	25.1	41.0
E = (0.0002 P + 0.78) PE	A	12.3	15.0	20.8	36.8
Low flow UK	L	10.7	13.4	19.0	33.8
A1FIMI	H	13.2	17.2	23.4	43.7
R = 482 + 1.06*P – 1.7*EPI	A	11.8	21.4	27.2	40.0
FNC	L	10.1	19.9	25.3	38.1
A1FIMI	H	12.4	23.8	30.2	53.1

A- A1BAIM scenario (Average values)
L- B1IMA scenario (Low values)
H- A1FIMI scenario (High values)

3.2. Impact assessment using hydrological models

The previous chapter considered the application of a range of generalized procedures for the estimation of the impacts of climate change on some aspects of flow regime. The objective of this chapter is to use a simple hydrological model applied in the basin to further explore the sensitivities of the flow, to changes. A monthly water-balance model is used. This model, referred as the Thornthwaite monthly water-balance program, is used to examine changes in monthly flow regimes, in average seasonal and annual runoff [8]. As it is shown above, simple empirical procedures can give some insights into the sensitivity of average annual runoff in climate changes, but more sophisticated analyses can be based on hydrological models. Such models allow the investigation of the effect of different seasonal distributions of change and the importance of catchment's characteristics.

In the most general terms, the determination of the effects of climate change on flow regimes and water resources involves the following stages:

(i) Develop a hydrological model that converts climatic inputs into hydrological response, and calibrate under the current climatic conditions;

(ii) Create a 'climatic time series', representing the climate under the scenario;

(iii) Run the model with the climate inputs, and compare indices of flow regime (such as mean monthly runoff) under the future climate with those under the current climate.

This section presents results from the application of the monthly model described above to estimate average annual runoff under a range of scenarios. Results are compared with those obtained from the generalized procedures developed in the previous chapter.

3.2.1. Watbal model

The WatBal model is an integrated water balance model developed for assessing the impact of climate change on river basin runoff. The water-balance model analyses the allocation of water among various components of the hydrologic system using a monthly accounting procedure based on the methodology originally presented by Thorn Thwaite [9]. Inputs to the model are mean monthly temperature (*T*, in degrees Celsius), monthly total precipitation (*P*, in millimeters), runoff factor, direct runoff factor, soil-moisture storage capacity, latitude of location, rain temperature threshold, snow temperature threshold, and maximum snow-melt rate of the snow storage that are modified through the graphical user interface.

The output components are: effective precipitation, potential evapotranspiration, total modeled runoff (direct, surface, subsurface runoff and base flow). Monthly data series of 7 meteorological stations and 2 runoff gauging-stations covering the period from 1961 till 1990 have been used for calibration of the WatBal model in the local conditions of this area [10]. The values of the modification of the air temperature and precipitation in the catchments, for the reference year of 2030, 2050, 2080 and 2100 were determined after the climate change scenarios prepared.

4. RESULTS

4.1. Past situation of precipitation (1961-1990)

In order to have an idea about rainfall and temperature regime on the Drini River basin there consider 5 meteorological stations. Respectively meteorological stations consider for this purpose are as following: Theth, Shkoder A, Shupenze, Shishtavec, Peshkopi. The reason why are consider these stations is to have an accurate overview of climate variability over entire basin. Monthly and yearly average are estimated for all considered stations. Concerning to the rainfall regime below (Figure 4, 5) are shown respectively variability of monthly and yearly average rainfall.

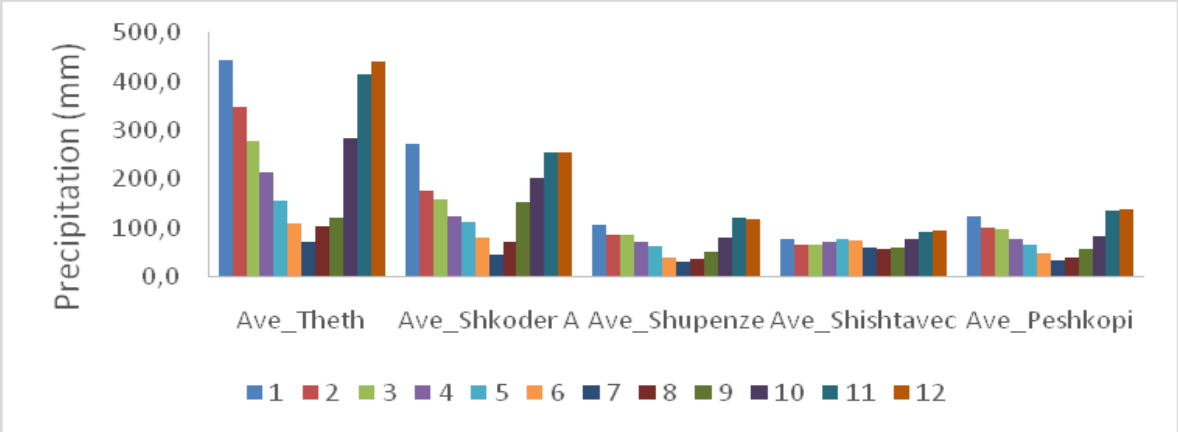

Figure 4. Monthly average precipitation variability

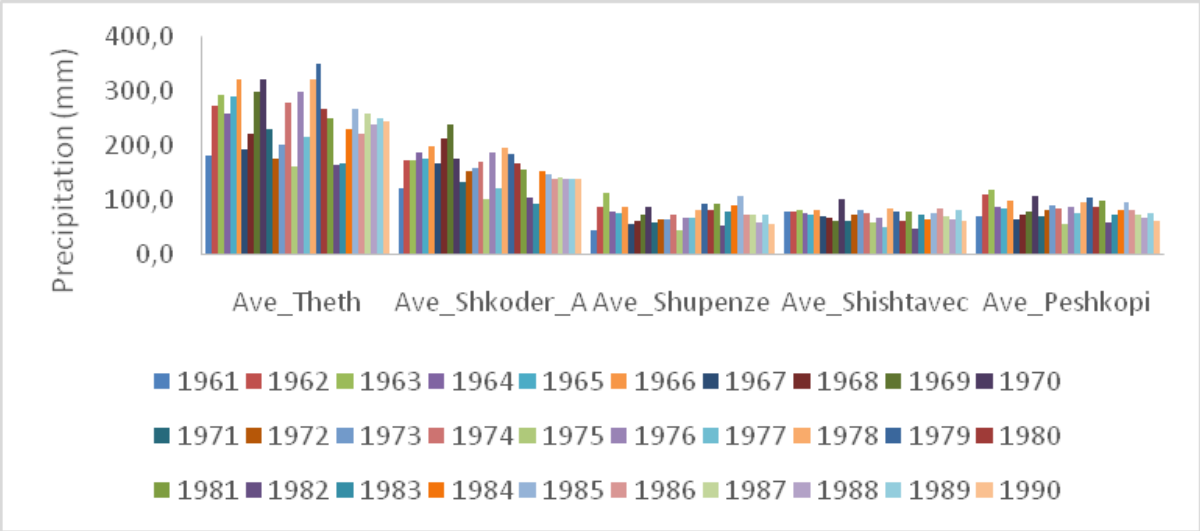

Figure 5. Yearly average precipitation variability

As it is shown in both scenarios (i.e. monthly and yearly average rainfall variability), among 5 stations 2 of them, respectively Theth and Shkoder A are characterized from rainfall intensity, in mean time from high variability through the months and years. This high variability for 2 stations mostly is due to geomorphology and positioning of these stations. While 3 other stations almost they have the same variability through the months and years also with each other. In addition a summary of statistical computation are shown below (Table 3, 4).

Table 3. Summary statistic monthly average precipitation

Variable	Observations	Obs. with missing data	Obs. without missing data	Minimum	Maximum	Mean	Std. deviation
1	5	0	5	75.548	445.650	204.502	154.649
2	5	0	5	65.490	347.685	154.418	115.987
3	5	0	5	63.130	276.448	136.056	85.984
4	5	0	5	69.445	213.608	110.222	61.739
5	5	0	5	61.553	154.137	93.925	39.090
6	5	0	5	38.210	108.489	68.968	27.869
7	5	0	5	29.897	71.049	46.902	17.361
8	5	0	5	35.967	102.153	60.379	27.292
9	5	0	5	49.150	153.089	87.599	46.594
10	5	0	5	75.103	284.535	143.782	94.972
11	5	0	5	89.800	415.044	202.487	134.208
12	5	0	5	93.425	440.403	208.697	143.678

Table 4. Summary statistic yearly average precipitation

Variable	Observations	Obs. with missing data	Obs. without missing data	Minimum	Maximum	Mean	Std. deviation
Series1	30	0	30	1961.000	1990.000	1975.500	8.803
Ave_Theth	30	0	30	160.183	350.042	248.369	51.808
Ave_Shkoder_A	30	0	30	93.167	240.025	157.958	33.422
Ave_Shupenze	30	0	30	42.358	112.317	72.898	16.852
Ave_Shishtavec	30	0	30	45.692	99.792	71.082	11.312
Ave_Peshkopi	30	0	30	55.717	118.467	82.207	15.818

Cross-correlation through the years between 5 considered stations are shown below (Figure 6). From this statistical study we see that there 2 group's (Theth and Shkoder A, Shupenze, Shishtavec and Peshkopi) which are representing a weak Cross-correlation between each other, while between stations that are representing each group there is a good Cross-correlation.

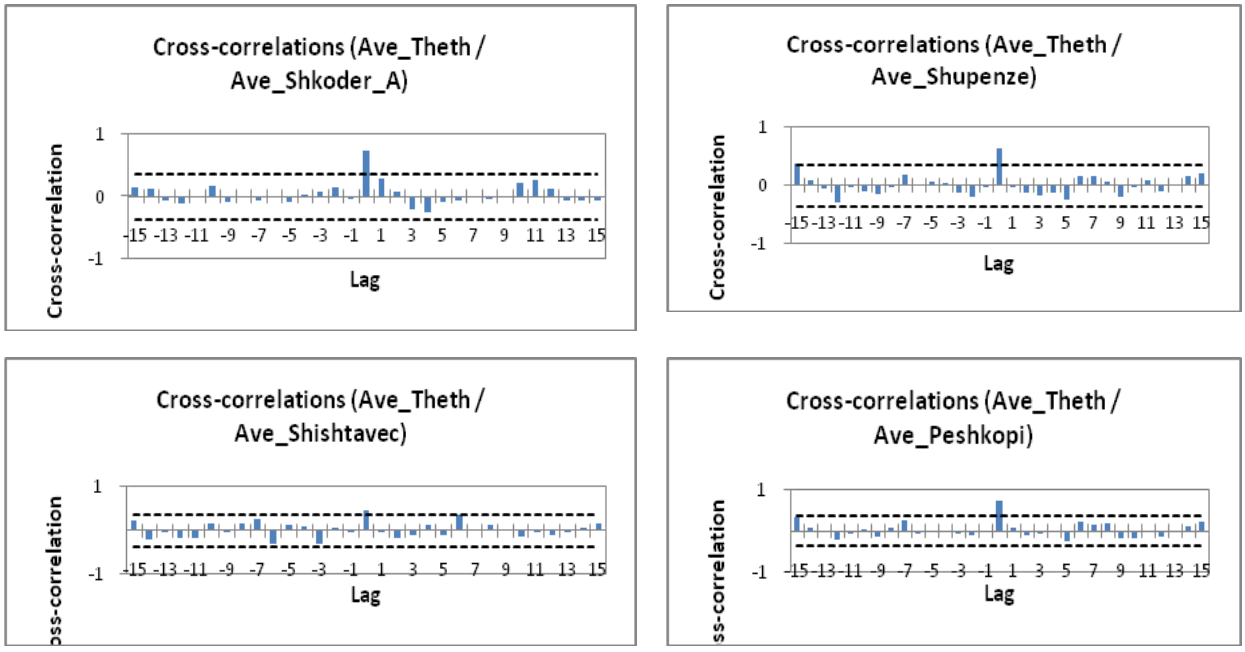

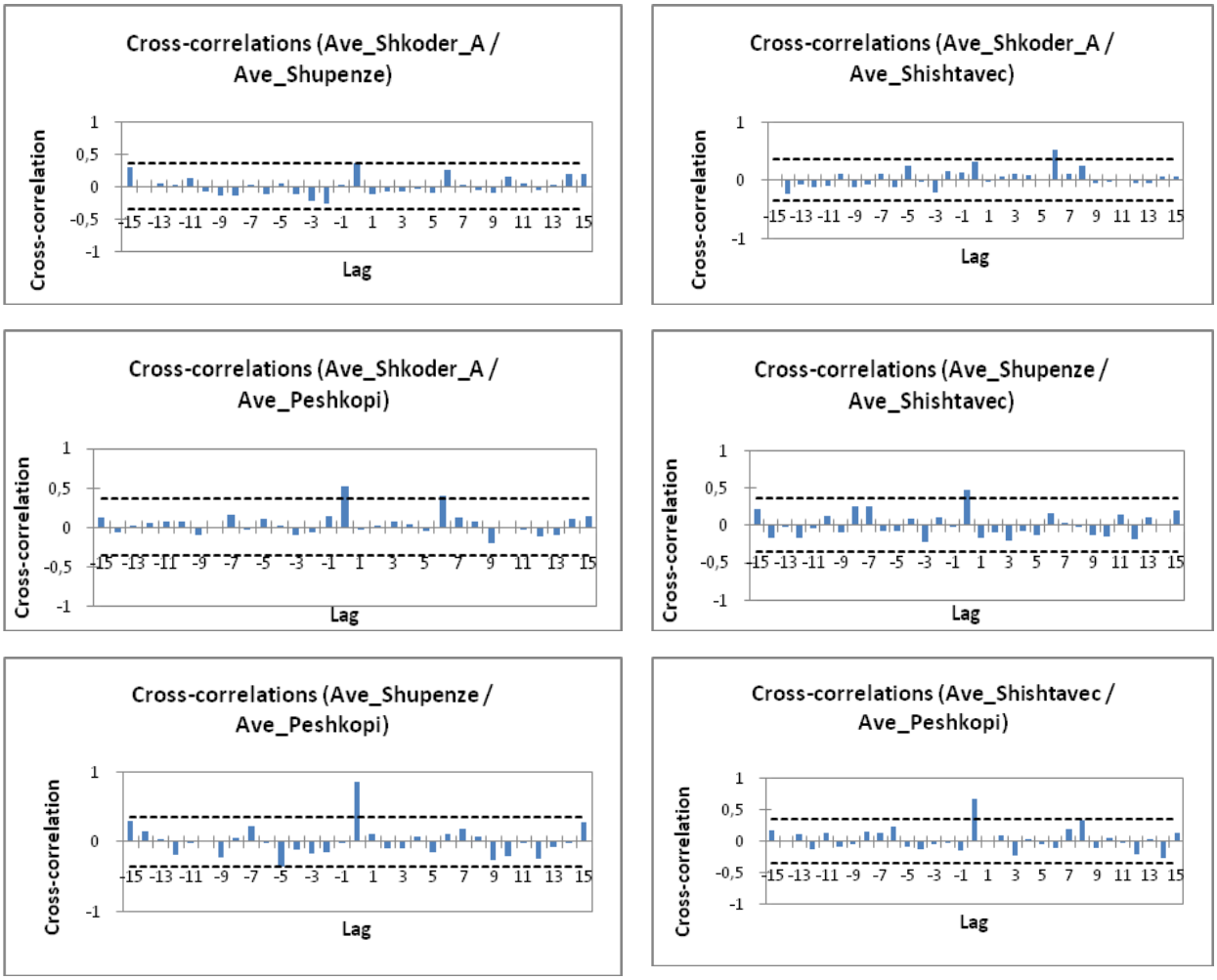

Figure 6. Precipitation Cross-correlation between stations

4.2. Past situation of temperatures (1961-1990)

Concerning to the variability of temperatures for all 5 stations considered for analyzing of climate change over entire Drini River basin below (Figure 7, 8), are shown monthly and yearly average variability for each respective station. Station"Shkodra A" is representing the highest temperature compare with other stations. While lowest temperature is noticed at "Shishtave". Diversely from variability of monthly and yearly average precipitation, variability of temperature through all the stations is almost the same (i.e. not big differences). This happened because temperature depends on the average velocity of the air molecules and their mass, and so temperature generally increases with air density.

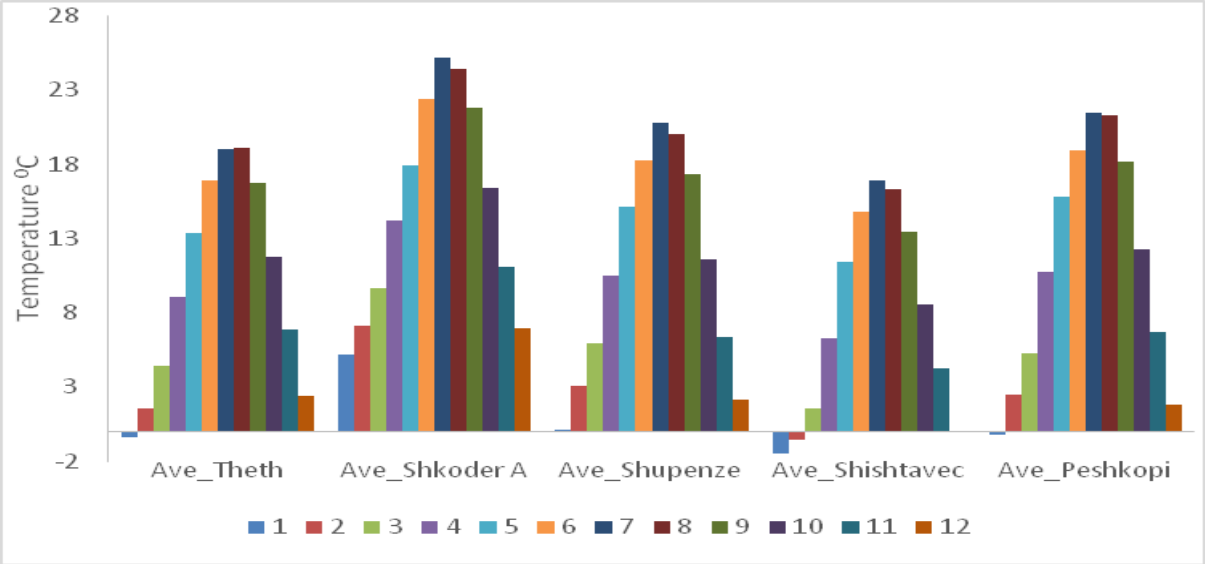

Figure 7. Monthly average temperatures variability

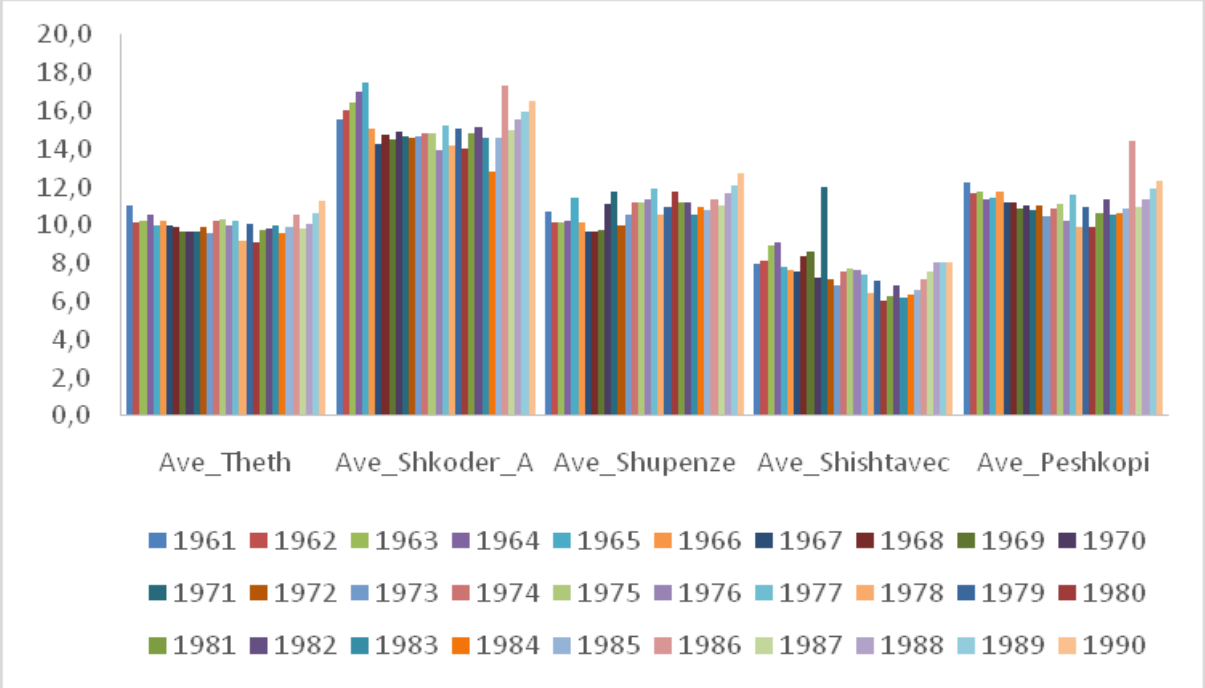

Figure 8. Yearly average temperatures variability

In addition a summary of statistical computation concerning to the temperatures regime are shown below (Table 5, 6).

Table 5. Summary statistic monthly average precipitation

Variable	Observations	Obs. with missing data	Obs. without missing data	Minimum	Maximum	Mean	Std. deviation
1	5	0	5	-1.457	5.170	0.642	2.600
2	5	0	5	-0.532	7.083	2.725	2.793
3	5	0	5	1.501	9.652	5.336	2.941
4	5	0	5	6.218	14.221	10.138	2.901
5	5	0	5	11.392	17.874	14.699	2.462
6	5	0	5	14.732	22.330	18.221	2.797
7	5	0	5	16.861	25.109	20.629	3.068
8	5	0	5	16.325	24.361	20.200	2.950
9	5	0	5	13.451	21.782	17.483	2.990
10	5	0	5	8.565	16.335	12.082	2.780
11	5	0	5	4.272	11.083	7.055	2.481
12	5	0	5	-0.004	6.917	2.654	2.562

Table 6. Summary statistic yearly average precipitation

Variable	Observations	Obs. with missing data	Obs. without missing data	Minimum	Maximum	Mean	Std. deviation
Series1	30	0	30	1961.000	1990.000	1975.500	8.803
Ave_Theth	30	0	30	9.117	11.253	10.055	0.463
Ave_Shkoder_A	30	0	30	12.807	17.498	15.149	1.035
Ave_Shupenze	30	0	30	9.642	12.703	10.935	0.754
Ave_Shishtavec	30	0	30	6.058	12.025	7.631	1.146
Ave_Peshkopi	30	0	30	9.950	14.433	11.227	0.849

Cross-correlation through the years between 5 considered stations are shown below (Figure 9). Different from cross-correlation between stations concerning to the precipitations variability where a significant differences is noticed, while concerning to the temperatures variability there is a good cross-correlation between all stations. Sure that if we compare variability of temperatures linked to Theth and Shkoder A with three other stations there are some differences but not significiant.

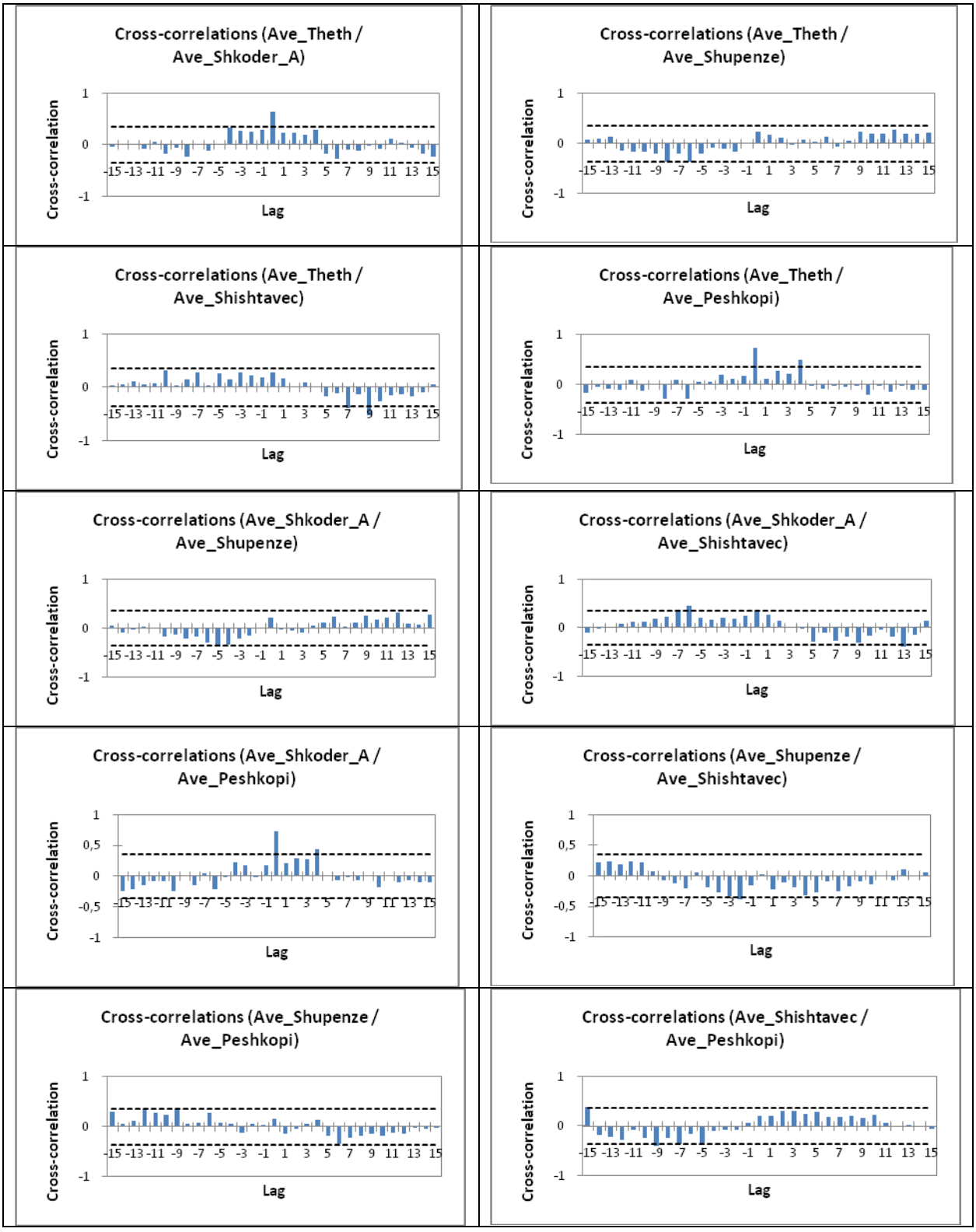

Figure 9. Temperature Cross-correlation between stations

4.3. Projections for precipitation

The precipitation total during winter, related to 1990, is likely to decrease an average of -8.0% (-4.3 to -12.4%) by 2050; 11.9% (-5.7 to -23.7%) by 2080 and 13.7% (- 4.7 to -29.4%) by 2100; during spring this is likely to decrease up to 6.9% (-5.9 to - 8.1%°C) by 2050; 12.3% (-9.0 to -17.7%°C) by 2080 and 15.0% (-10.1 to - 22.2%°C) by 2100 (Table 4 and Figure 4).

Table 7. Projections of annual precipitation changes (%) related to 1990

Years	2030	2050	2080	2100
A1BAIM	-	-	-12.9	-15.5
A2ASF (min)	-	-	-8.4	-9.0
A1FIMI (max)	-	-11.0	-21.0	-26.1

The highest decrease in average precipitation is likely during summer, up to -24.6% (-16.5 to -33.9%) by 2050; -45.7% (-36.0 to -58.8%) by 2080 and -54.8% (-44.2 to -71.8%°C) by 2100 (Figure 26).

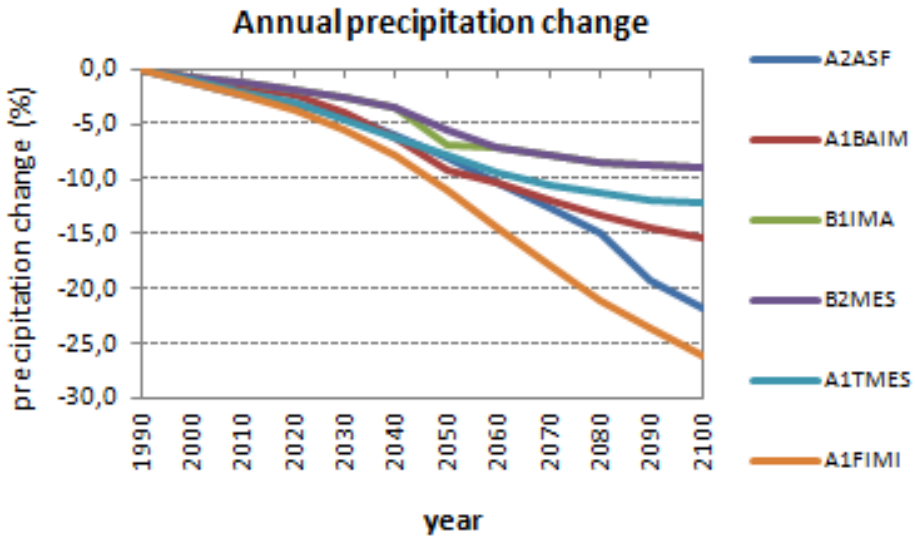

Figure 10. Projections of annual precipitation (%) [11]

The high decrease in precipitation, combined with the high increase in temperature, might lead to prolonged summer droughts over the area. The demand for water could increase, especially in summer. Decrease in total precipitation combined with higher evaporative demand would probably result in less river flow (run-off). Water resources are likely to be further stressed due to a projected growth in demand and climate-driven changes in supply for irrigation, cities, industry and environmental flows. The increased temperatures expected in summer could lead to higher local precipitation extremes and associated flood risks in project area.

4.4. Temperature projections

The likely changes (averages) in annual temperature for different scenarios and time horizons reveal a likely increase in seasonal and annual temperatures related to 1990 for all time horizons. The annual temperature is likely to increase up to 1.8°C (1.3 - 2.4°C) by 2050; 2.8°C (2.1 - 4.1°C) by 2080 and 3.2°C (2.3 - 5.0°C) by 2100 (Table 3, Figure 3).

Table 8. The likely changes in annual temperature (°C)

Years	2030	2050	2080	2100
A1BAIM	1.2	1.8	2.8	3.2
A1FIMI	1.3	2.4	4.1	5.0
A2ASF	0.8	1.3	2.1	2.3

The scenarios project the lowest increase in temperature for winter compared to other seasons with higher increases in absolute values likely for spring temperatures related to 1990 for the same scenarios - increases up to 1.6°C (1.3 - 2.2°C) by 2050; 2.5°C (1.7 - 3.6°C) by 2080 and 3.0°C (1.9 - 4.4°C) by 2100 (Figure 3). Increasing spring temperatures will accelerate soil temperature warming after the winter period and extend zones suitable for summer crops as well as lengthening their growth season. Summer projections indicate increases in annual temperature up to 2.7°C (2.4 - 3.6°C) by 2050; 4.3°C (3.1 - 6.3°C) by 2080 and 5.1°C (3.4 - 7.7°C) by 2100 (Figure 3). Such a situation is likely to result in increases to the frequency and/or intensity of extreme weather events. It is known that the relationship between averages and extremes is often non-linear. For example, a shift in average temperature is likely to be associated with much more significant changes in very hot days. The disproportionate increase in the frequency of extreme events is not limited to the frequency of very hot days but could occur with many other climate extremes that could have significant consequences on all socio-economic systems.

The average autumn temperature is likely to increase up to 1.8°C (1.5 - 2.3°C) by 2050; 2.9°C (2.2 - 4.1°C) by 2080 and 3.5°C (2.4 - 5.0°C) by 2100 (Figure 3). The expected changes in surface air temperatures will lead to changes in air humidity. This combination is likely to influence the increases in the heat index (which is a measure of the combined effects of temperature and moisture). Recent investigations show that increasing temperatures will be followed by an increase in the probabilities of extreme events and a higher intra-annual variability of minimum temperatures (IPCC, 1997). More frequent and severe droughts with a consequent greater fire risk are likely. An increase in daily minimum temperatures means that frost days and cold waves are very likely to become fewer.

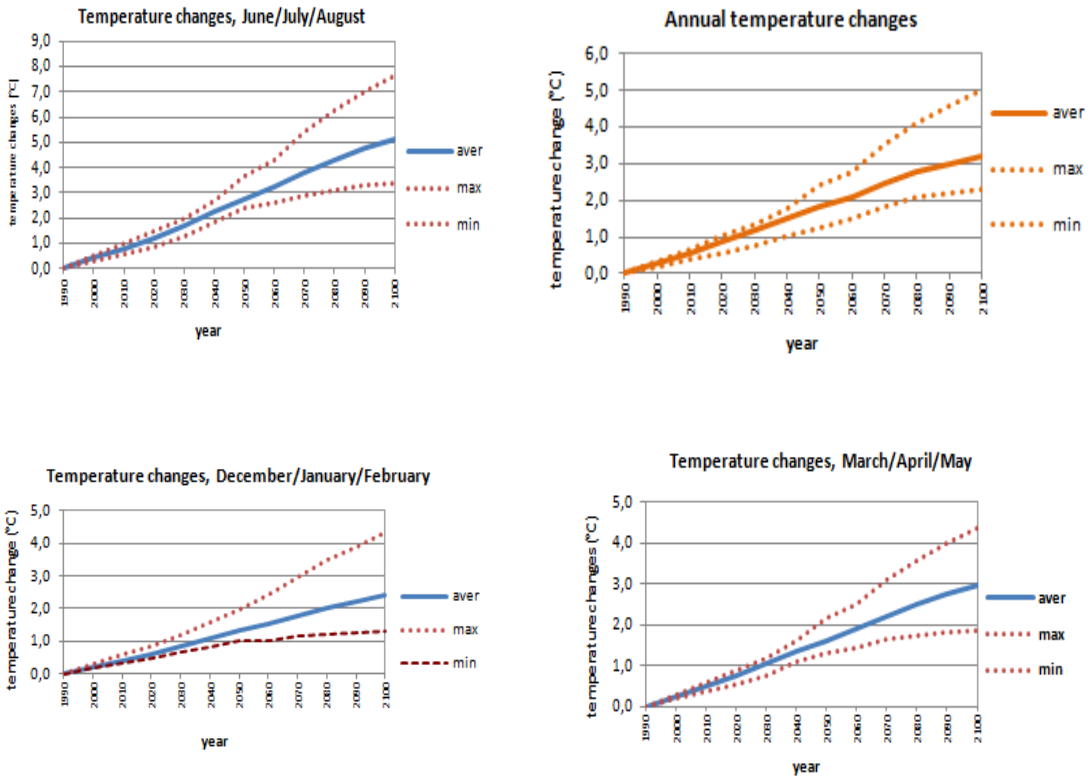

Figure 11. Annual temperature projections. From top left, average, winter, spring and summer (bottom right) [11]

4.5. Expected effects of climate change

Due to the expected changes in temperature, precipitation, mean sea level pressure and sea level the following effects to climate indicators are expected.

4.5.1. Effects of expected changes in temperature

Increasing temperatures will be followed by an increased probability of extreme events and a higher intra-annual variability of minimum temperatures. More frequent and severe droughts with greater fire risk are likely. A reduced temperature range, resulting from a higher rate of increase in minimum versus maximum temperatures, is likely to occur over nearly all land areas. Frost days and cold waves are very likely to become fewer. The number of days with temperatures in excess of 35°C will become more frequent and is expected to increase by about 10 days by 2100 compared to present. As a consequence of this, the number of heat wave days are expected to increase too with about 80, 95, and 120 days with a heat wave likely to be registered by the years 2050, 2080 and 2100 respectively. Cold wave days are also expected to increase to approximately 10 days by 2030, 7 days by 2050 and 5 days for 2080. Warmer winters would reduce “heating degree days” and the demand for heating energy.

Increases in air temperature are also projected to lead to an increase in “cooling degree days” (which is a measure of the amount of cooling required on any given day once the temperature exceeds a threshold of 17.5°C). Taking into account the projections for summer temperature, the number of cooling degree days may reach about 550, 670, 840 and 930 by the years 2030, 2050, 2080 and 2010 respectively. Warming and population growth will increase annual heat-related deaths in those aged over 65 and contribute to the spread of vector-borne, water-borne and food-borne diseases. Warmer average and extreme temperatures will enhance the demand for freshwater and water for irrigation purposes, especially for soils with low water-storage capacities. If precipitation declines, the project area would face substantially increased risks of summer water shortages.

Maximum Temperatures ≥ 35°C

Based on correlation existing between the numbers of days with heat wave (temperature >35°C) and the average temperature for summer (during the period 1961-2008), the number of heat wave days up to the year 2100 is calculated as 80, 95, and 120 days, by the years 2050, 2080 and 2100 respectively. More frequent and severe droughts with greater fire risk are expected. More hot days and heat waves are very likely over the study area. The drought in Europe in 2003 combined unusually high temperatures with water stress and reduced primary productivity by 30% .If temperature increases too much, faster respiration may tip the balance towards plants becoming a CO2 source. Temperature rise will also effect habitat composition, since generally C3 plants are more sensitive to heat stress than C4 plants and CAM plants.

Across the globe, climate change velocity and temperature extremes are projected to exceed the capacity of many species and communities to keep up with their climate niche space (Malcolm et al. 2005). However, the more frequent occurrence of climatic extremes is likely to make salt-marsh plant species more vulnerable and sensitive to other pressures and this increases the need for careful management. Additionally, whilst land management practices have decreased the incidence of wildfires, increased temperatures and decreased water availability are likely to lead to an increase of fires with associated carbon release.

Minimum Temperatures <-5°C

Cold days are currently an infrequent phenomenon and likely to become even more in-frequent under climate change scenarios for the area. Based on the correlation between the numbers of days with a cold wave and the average temperature for winter months (period 1961 - 2008), it is calculated that the number of days with cold waves will be approximately 10 days by 2030, 7 days by 2050 and 5 days by 2080.

4.6. Effect of hazardous precipitation

An increase of the number of rainy days with hazardous rainfalls is expected to increase by approximately 4 - 5 days by 2100 time horizons. The occurrence of severe, moderate and dry drought is expected to increase by 2100. An increase of SPI3, (cases of moderate, severe and extremely dry weather) to approximately 18 cases by 2030, and 20, 22 and 24 cases by 2050, 2080 and 2100 respectively is expected. Increasing spring temperatures will accelerate soil temperature increases from winter minima and extend suitable zones for summer crops and lengthening of their growth season.

The length of the growing season is projected to increase from 263 days in 1990 to potentially 289 days in 2100 (26 days longer).

5. CONCLUSIONS

River flow regimes reflect the climate conditions and, naturally respond to these climatic changes. To asses this impact, in this study, two approaches were considered: the empirical and hydrological model. In the first approach four different models were used and in the last one the water balance model was used. As it was expected, for all the time horizons, all the models gave a reduction of the runoff. Comparing the result in all the case, the lower value, belongs to the Regional Regression Model used (-5.7; -12.9;-22; and -27%) and the highest to the Linear Regression derived in the First National Communication (-11.8;-21.4; -27.2 and -40.0%).Even between the two approaches, the Regional Regression Model result with lower values and the same Linear Regression has the highest values. The Mean annual flow decreases as the time horizon is larger, so from the values of -3.9% in the year 2030, it decreases to -27% by the 2100 time horizon. In general, it was found that changes in flow regimes are very sensitive to the assumed change scenario. Changes in catchment water balance were found to be more sensitive to changes in catchment rainfall than changes in evapotranspiration. Rainfall changes are amplified in changes in runoff, by factors ranging from 1.2 to 1.7.

References

[1] Parry, M. L., Rosenzweig, C., Iglesias, A., Livermore, M., & Fischer, G. (2004). Effects of climate change on global food production under SRES emissions and socio-economic scenarios. Global Environmental Change, 14(1), 53-67.

[2] Purse, B. V., Mellor, P. S., Rogers, D. J., Samuel, A. R., Mertens, P. P., &Baylis, M. (2005). Climate change and the recent emergence of bluetongue in Europe. Nature Reviews Microbiology, 3(2), 171-181.

[3] Araújo, M. B., Alagador, D., Cabeza, M., Nogués-Bravo, D., &Thuiller, W. (2011). Climate change threatens European conservation areas. Ecology letters, 14(5), 484-492.

[4] Rakaj, M. (2009). New aquatic macrophytes for the flora of Albania from the Lake Shkodra, Drini and Buna basins. J. Int. Environmental Application & Science, 4(3), 278-284.

[5] Skarbøvik, E., Perovic, A., Shumka, S., &Nagothu, U. S. Nutrient Inputs, Trophic Status and Water Management Challenges intheTransboundary Lake Skadar/Shkodra, Western Balkans.

[6] Wikipedia online

[7] FNC (2002) The First National Communication Of Albania To The United Nations Framework Convention On Climate Change. ALB/96/G32/A/1G/99.Tirana, July, 2002.

[8] O.G.CH -Office of Global Change. Effects of Climate Variability and Change on Groundwater Resources of the United States. 2008.

[9] Rao, K. D., Rao, V. V., &Dadhwal, V. K. (2014). Improvement to the Thornthwaite Method to Study the Runoff at a Basin Scale Using Temporal Remote Sensing Data. Water Resources Management, 28(6), 1567-1578.

[10] Mic, R. P., &Corbus, C. (2014, May). Analysis of potential climate change impact on mean flow in Somes, river basin, Romania. In EGU General Assembly Conference Abstracts (Vol. 16, p. 10053).

[11] UNDP, Identification and Implementation of Adaptation Response Measures in the Drini–Mati River Deltas"

[12] Muçaj, L. (2010). Climate Change Scenarios for Drini-Mati River Deltas area.UNDP Climate Change Program, Project "Identification and implementation of adaptation response measures to Drini-Mati River Deltas". Tirana.

Let's grow up together

DRINK ADRIA

Adriatic IPA
Cross Border Cooperation 2007-2013

The project is co-funded by the European Union,
Instrument for Pre-Accession Assistance

WP4.1 Report:

Climate and climate change data for test area in Greece

Civil Engineering Department
University of Thessaly - Greece

Volos, 2015

Lead Author/s	Assoc. Prof. Vasilis Kanakoudis
Lead Authors Coordinator	Assoc. Prof. Vasilis Kanakoudis
Contributor/s	Dr. S. Tsitsifli, A. Papadopoulou, I. Argyriadou, A. Rouva, I. Hitiri
Date last release	14/4/2015
State of document	Final

Let's grow up together

DRINK ADRIA

Adriatic IPA
Cross Border Cooperation 2007-2013

The project is co-funded by the European Union,
Instrument for Pre-Accession Assistance

Table of contents

1.

INTRODUCTION

The test area is the **Corfu island** located in the northwestern side of Greece belonging to the Ionian Islands Region. It extends approximately between latitude 39° 21' 00" and 39° 49' 00" and longitude 19° 37' 00" and 20° 06' 00". The island's surface is 588 Km^2, its length is 64 Km and its width 32 Km (in its wider part). The coastline reaches 217 Km and its altitude is about 914 m (Pantokratoras mountain).

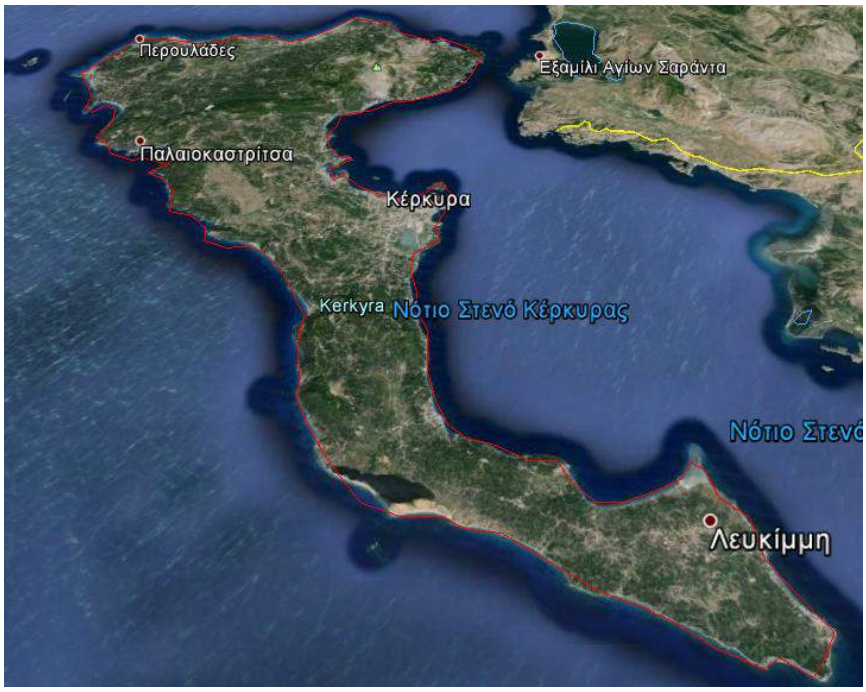

Figure 1: The Test area "Corfu island" (in red) (from Google Earth).

Figure 2: Soil formations in Corfu [1]

showing the soil formations in Corfu shows the following kinds of soil [1]:

2. Calcaric Leptosol (LPca);
17. Calcaric Regosol (RGca);
19. Calcaric Fluvisol (FLca);
22. Calcaric Fluvisol (FLca);
27. Calcaric Cambisol (CMca);

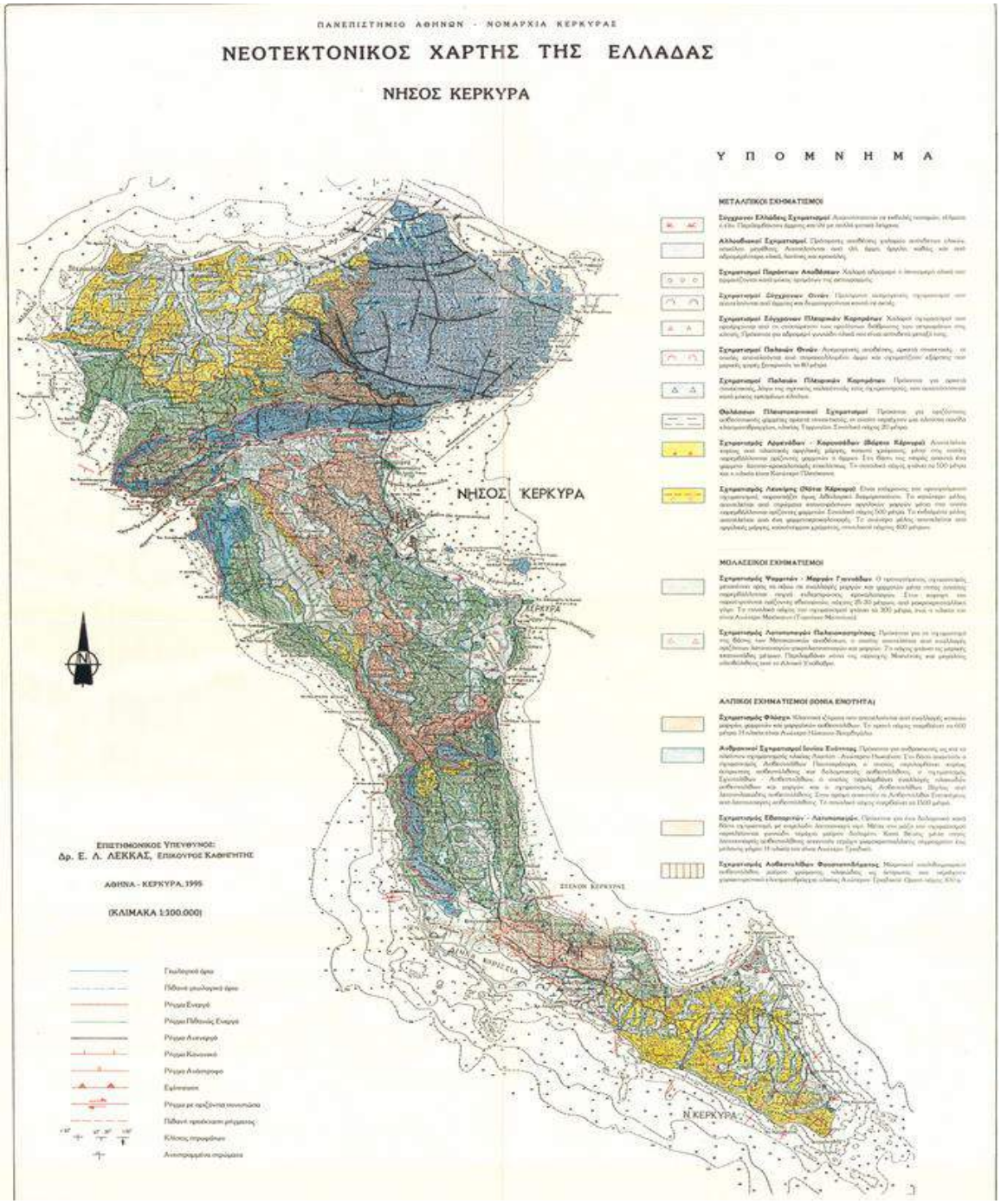

Figure 2 Sketch of the geological Map (from 1:100.000 scale data) of the Test area – Corfu [2].

The River Basin Management Plan of Epirus identify surface waters including three small rivers, 3 lagoons and 3 groundwater bodies in Corfu [3]. There are no river water bodies with a significant abstraction pressure in the river basin of Corfu-Paxi [3]. The main aquifers are developed in the carbonate formations of the Ionian zone containing high sulfates concentrations because of the presence of evaporites. Aquifers of local importance are developed in the granular formations. High concentrations of sulfates are met locally because of the natural background (gypsum presence). In the groundwater bodies there are increased concentrations of nitrates and ammonium of local importance due to the point and diffuse sources of pollution [3]. Locally there are high concentrations of chlorides in the coastal zones because of the sea intrusions due to excessive pumping and natural causes. In general there are no problems of groundwater exlpoitation . The water abstractiona from the groundwater bodies constitute a small percentage of their average annual natural recharge. Locally in the two main hydrosystems of Corfu (limestone system (GR0500010) and granular aquifer system(GR0500030)) there are local excessive pumping resulting in local salination in the coastal zones [3]. Another issue connected to the cover of the water needs of the islands is that there is salination in the carstic systems connected to mainly natural causes and not to excessive pumping of water.

Table 1: Total Annual water abstraction and annual water demand for each water use (Year:2007) [3]

Total annual water abstraction (million m^3)	
Surface Water	0.5
Groundwater	29

Water Use	**Annual demand (millions m^3)**
Demand for irrigation for the total irrigated lands	125
Demand for drinking water (water supply and tourism)	16

According to the RBMP of Epirus [3] the groundwater systems in the hydrologic basin of Corfu – Paxi are sourrounded by the sea and this is the reason of some sea water intrusion. The karstic limestone system of the island of Corfu (GR500010) includes the carbonates presence in the island excluding the tertiary breccia system [3]. In the northern sub-system of the Pantokratoras mountain there are noted increased concentrations of chlorides locally due to geological natural causes (open karstic system to the sea) and in local over-abstractions. Locally the chlorides cpncentrations excedd 2,000 mg/l with average values in the respective zones about 800-900 mg/l [3]. In the granular aquifers system of the island of Corfu (GR500030) some local salination is noted due to over-abstractions in the coastal zone in the northwestern part and in teh southern part of Lefkimi. The chlorides concentrations are about 1,900 mg/l [3].

2. EXISTING CLIMATE FEATURES IN THE CORFU ISLAND

The local climate characteristics are provided for the 2013 and 2014 in detail [4] while the temperature's and the precipiation average values are given from 1955-1997 from the Hellenic National Meteorological Service [5].
Seasonality is described in terms of annual cycle of the mean annual precipitation and temperature, their standard deviation (of monthly mean) and the coefficient of variations. The discussion of the extremes is based on percentiles calculated starting from the empirical values expressed as cumulative distribution function (CFD). For the present research, were analyzed the data for the rainfall and temperature stations present in the study area with good quality time-series.

In the island of Corfu there is an active meteorological station in Gouvia at an elevation of 1.13m, latitude 39o36'0'' and longitude 19o54'0''(Figure 4) [6].

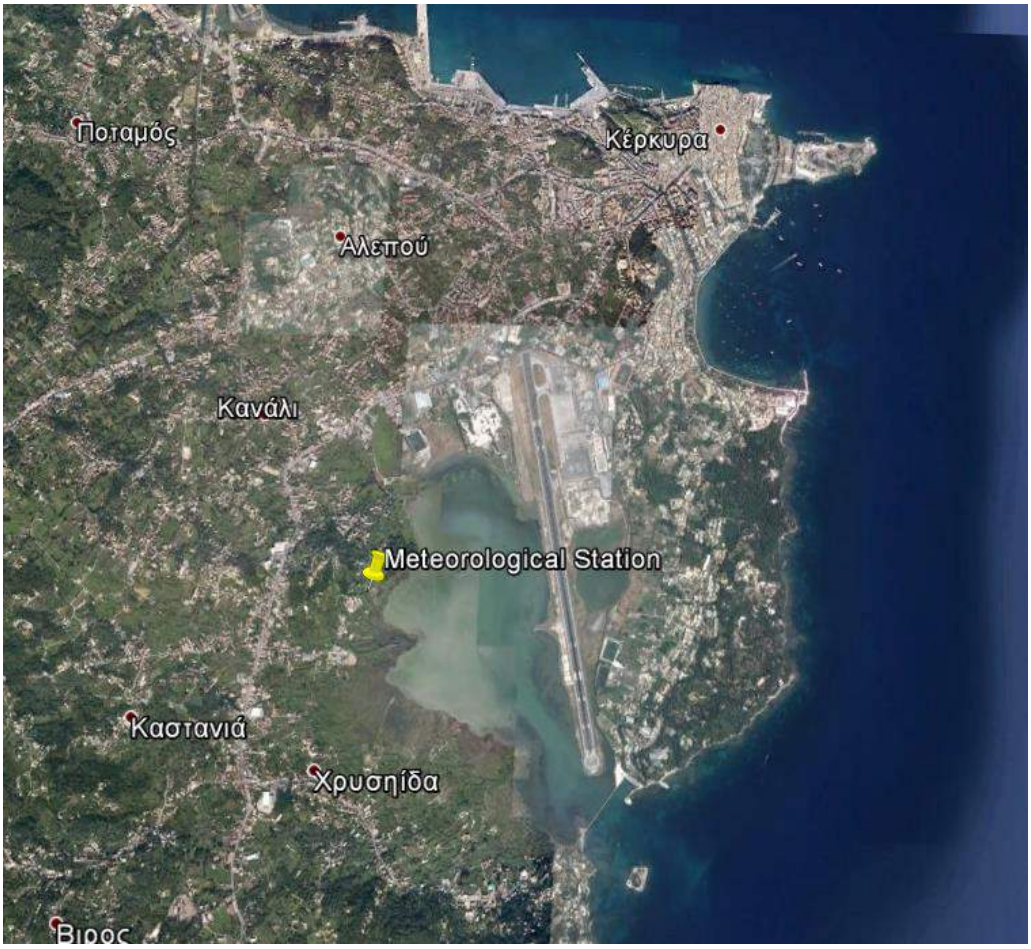

Figure 3 The meteorological monitoring stations of the pilot area (Google earth).

3. TEMPERATURE ANALYSIS

3.1 Years 2013 and 2014

Temperature is analyzed in the meteorological station in Corfu and it is given in Table 2. The seasonality of the temperature is checked (DJF=December;January;February – MAM=March;April;May – JJA=June;July;August – SON=September;October;November).

	DJF	MAM	JJA	SON	Year
Mean (ºC)	11.6	16.0	25.2	19.0	22.4
Standard Deviation (ºC)	1.5	2.1	1.2	2.7	5.4
MAX (ºC)	22.0	29.2	36.2	31.7	36.2
MIN (ºC)	6.4	8.3	18.3	12.1	6.4

Table 2: Basic statistics (mean, standard deviation, maximum and minimum) for annual and seasonal mean air temperature from the time period 2013-2014 for Corfu island.

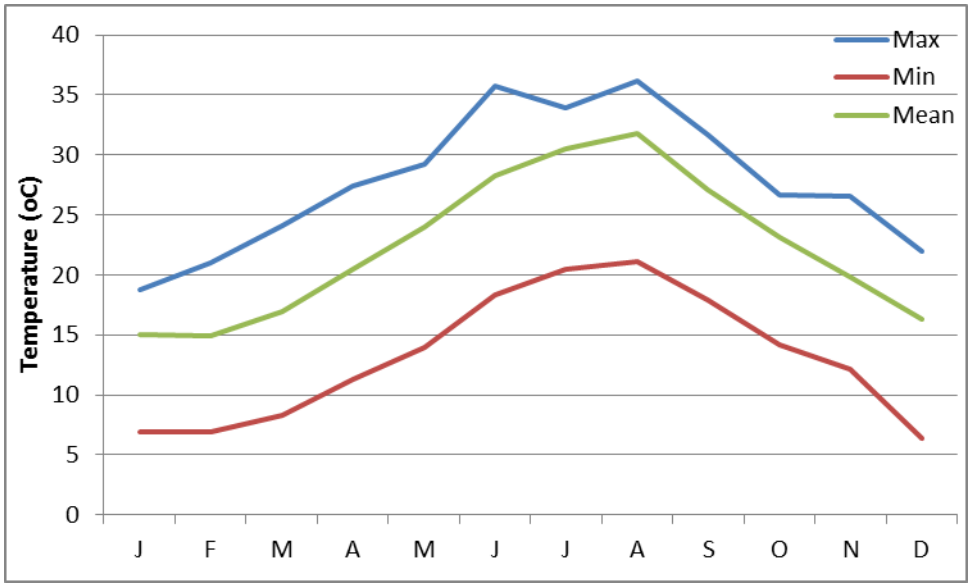

Figure 4: Annual cycle for the mean monthly air temperature [°C] (2013-2014).

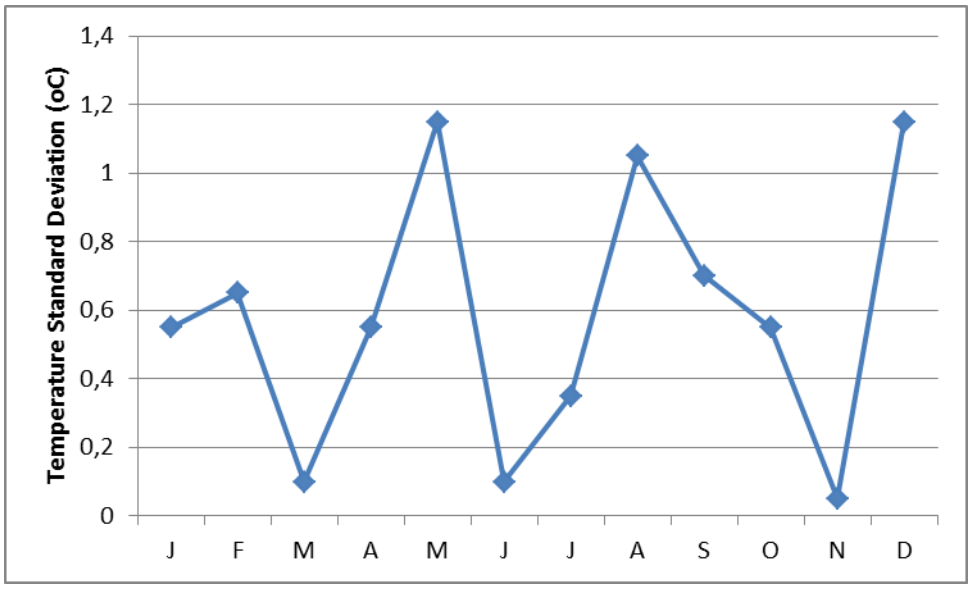

Figure 5: Standard deviation calculated on the annual cycle (2013-2014).

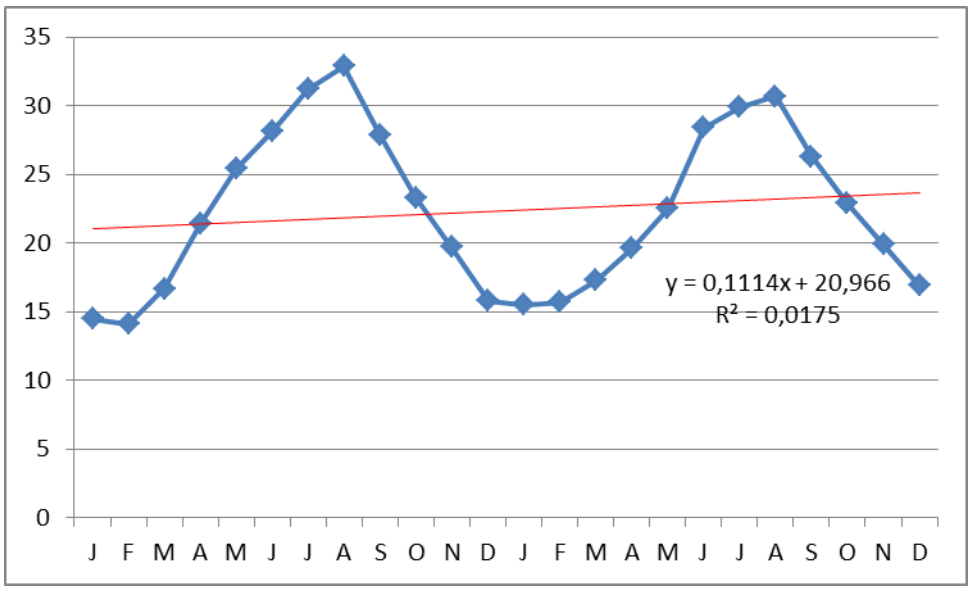

Figure 7: Time series of mean annual air temperature with the fitted trend for the period 2013-2014 for the meteorological station of Corfu.

The temperature in Corfu varies greatly. The data include only 2013 and 2014 (Figures 5-7). The maximum temperature is about 36 ºC and the minimum 6 ºC. The standard deviation of the mean monthly temperature varies a lot (0.05-1.15ºC) but there is no safe conclusion drawn since the study period is only 2 years. The temperature trend is positive.

3.2 Period 1955-1997

Figure 8 shows the mean, max and min temperatures from 1955-1997 in Corfu. In general the climate is the Mediterranean one.

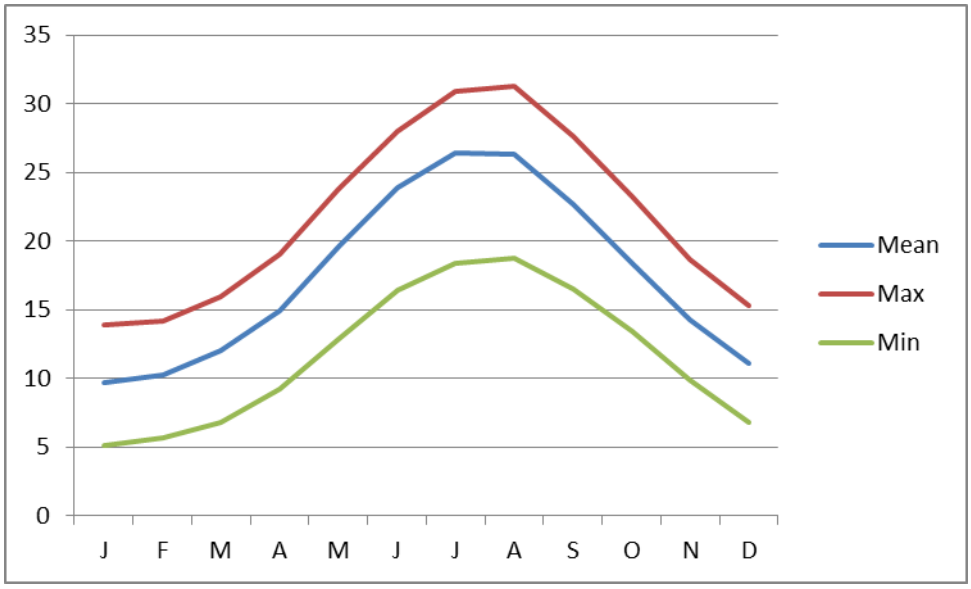

Figure 8: Annual cycle for the mean monthly air temperature [°C] (1955-1997).

3.3 Period 1975-2004

Additional data for the period 1975-2004 provide the average temperature (oC) values for Corfu Island (Figures 9 & 10) monthly and seasonal [7].

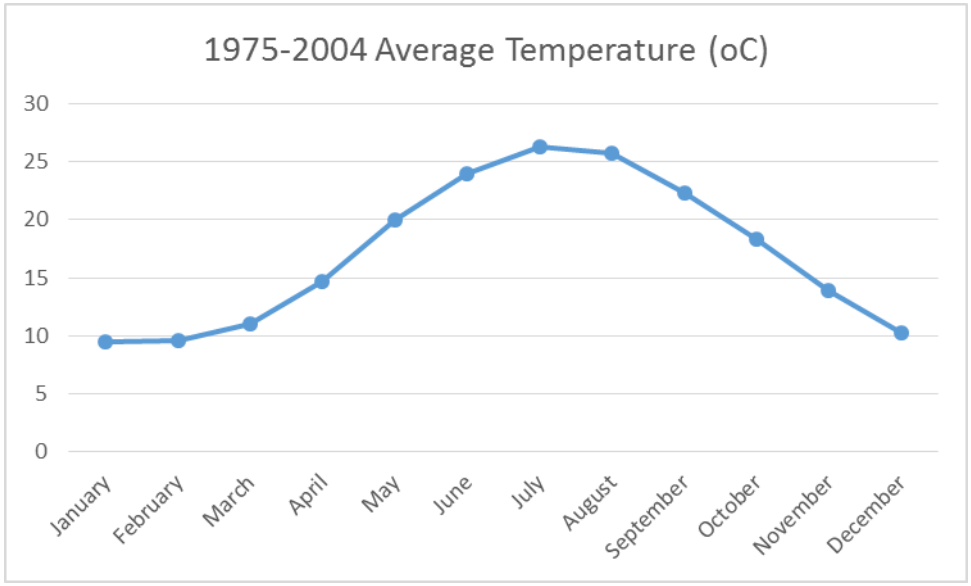

Figure 9: Annual cycle for the mean monthly air temperature [°C] (1975-2004) [7].

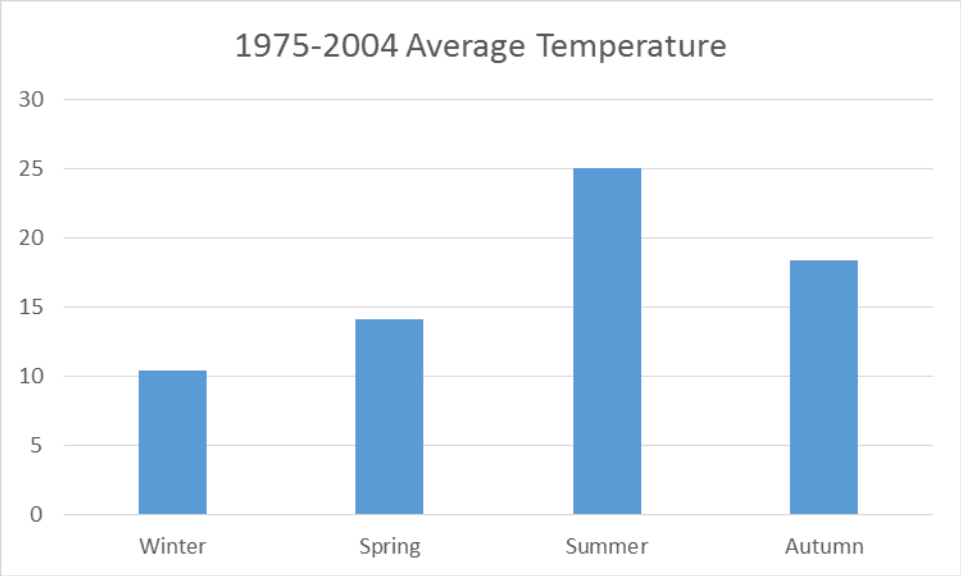

Figure 10: Annual cycle for the mean seasonal air temperature [°C] (1975-2004) [7].

It is worth noting that when the 4 different temperature datasets are compared (Figure 11), the temperature values are increased in January, February, March, November and December in more recent years. During spring and summer the mean temperature remains more or less the same. It seems that climate change makes autumn and winter less cold.

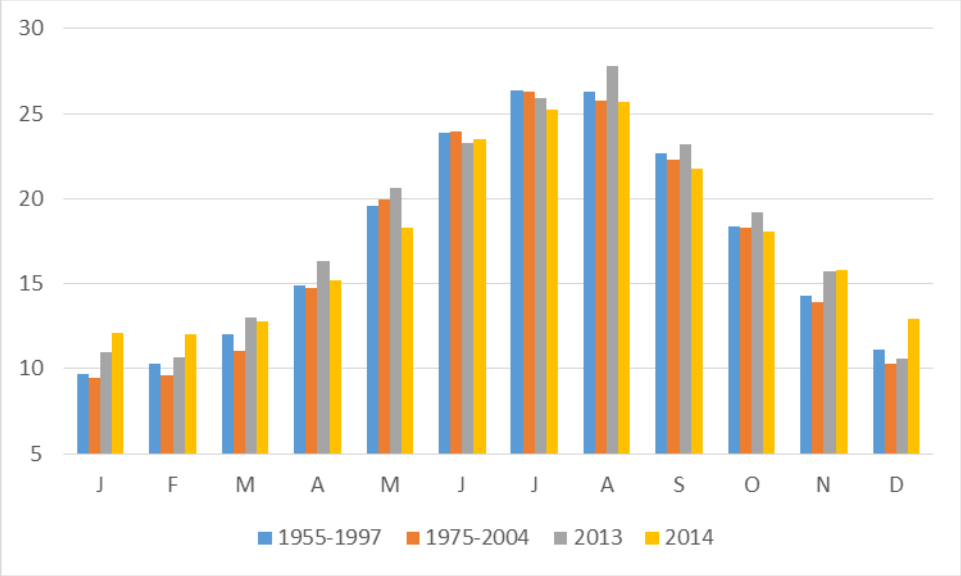

Figure 11: Annual cycle for the mean seasonal air temperature [°C] compared for the periods: 1955-1997; 1975-2004; 2013; 2014.

Data gathered from the meteorological station of Corfu from 1956-2010 show that the mean temperature tends to increase with a trend of +0.089 and significance 0.131 [7] (Figure 12).

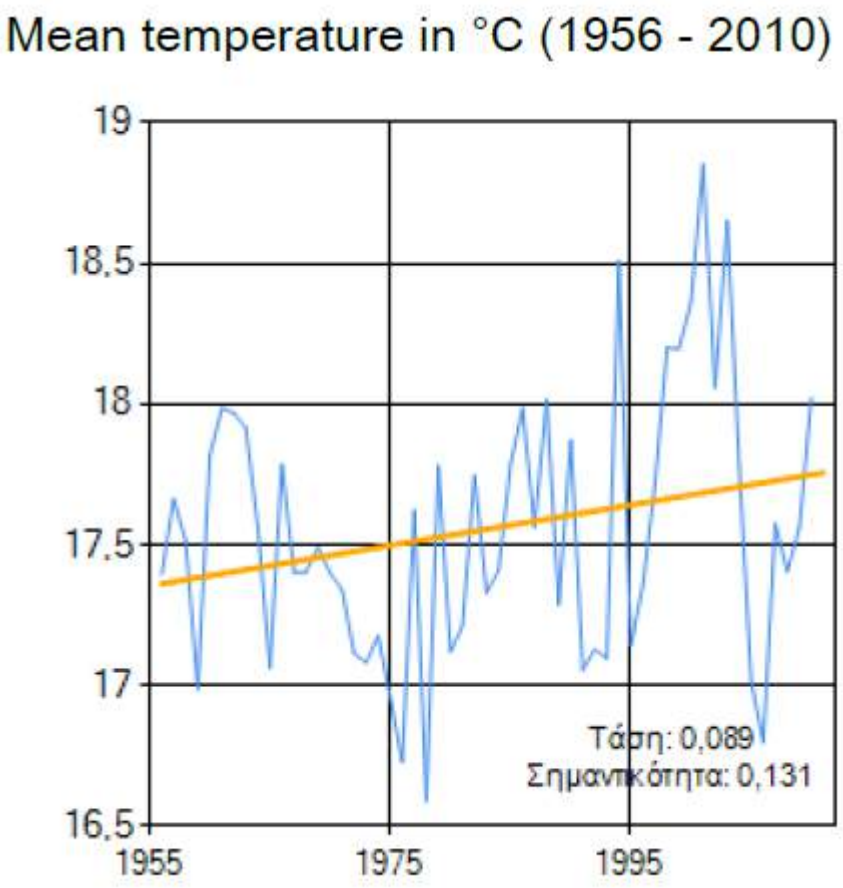

Figure 12: Annual cycle for the mean air temperature [°C] for 1956-2010

4. PRECIPITATION ANALYSIS

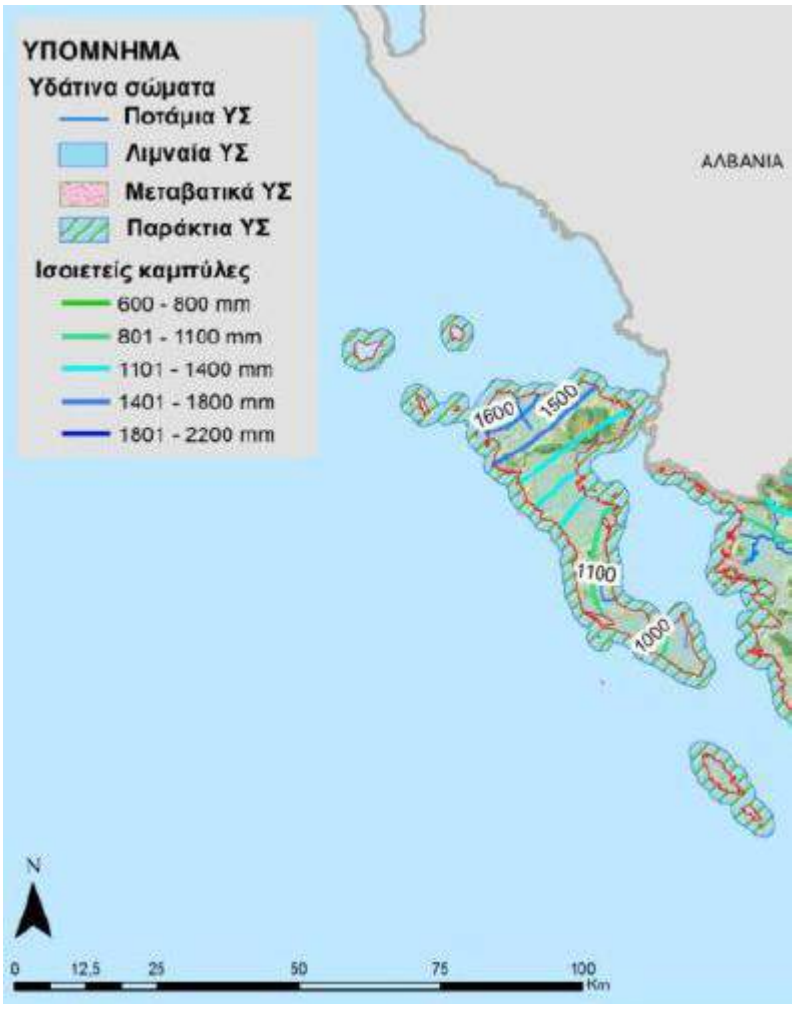

Figure 13 Average annual rainfall in Corfu Island [1]

4.1 Years 2013 & 2014

For the test site area, the precipitation recorded in 2013-2014 and the average precipitation (1955-1997) is analyzed. The basic statistics and the annual cycle are provided (Table 3; Figures 13-15).

	DJF	MAM	JJA	SON	Year
Mean (mm)	147.1	60.6	30.6	137.7	94
MAX (mm)	238.2	121.6	127.8	245.2	245.2
MIN (mm)	63.6	15.2	0.2	13	0.2
Standard Deviation (mm)	54.1	41.8	46.1	73.8	74.3

Table 3: Basic statistics (mean, standard deviation, maximum and minimum) for annual and seasonal precipitations from the period 2013-2014 for Corfu.

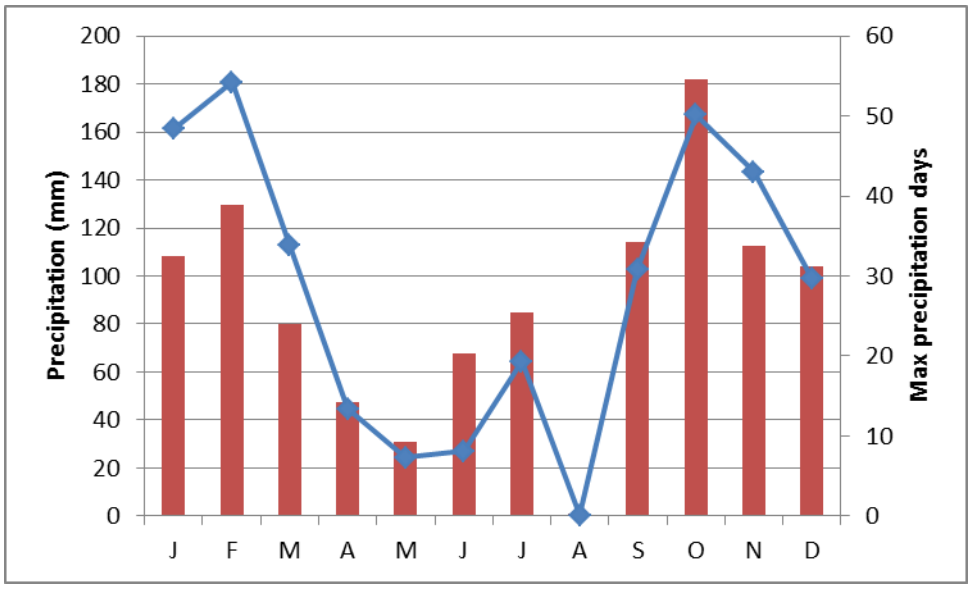

Figure 14: Annual cycle mean precipitation amounts in mm and maximum raining days for the period 2013-2014 for Corfu.

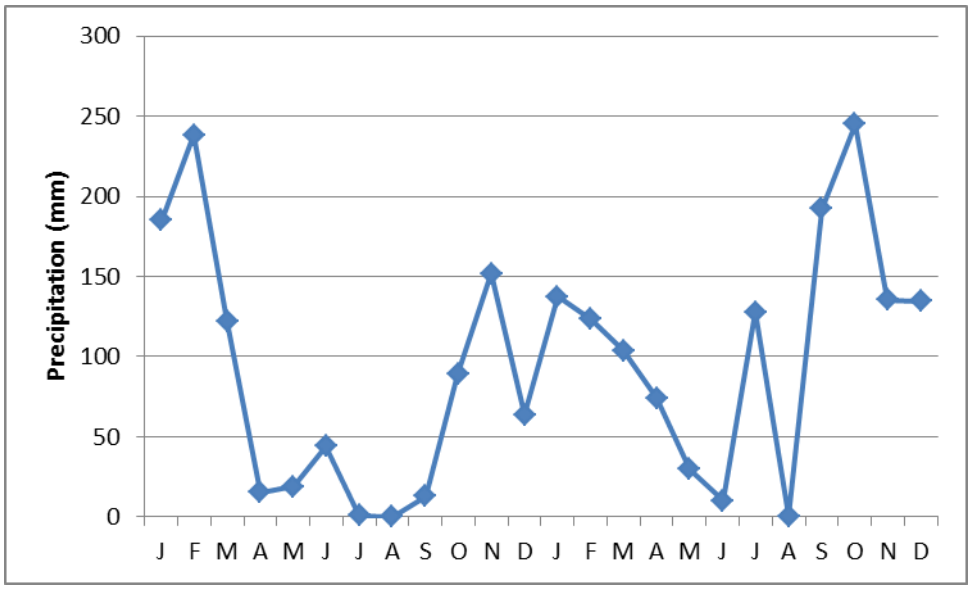

Figure 15: Time series of mean annual precipitations for the period 2013-2014 for Corfu.

4.2 Period 1955-1997

In the pilot area, the average annual rainfall is calculated for the period of 1955-1997 for Corfu station. The highest precipitation occurs in autumn and winter (also in total raining days) and the lowest in the summer months. There is variability in precipitation (Figure 16).

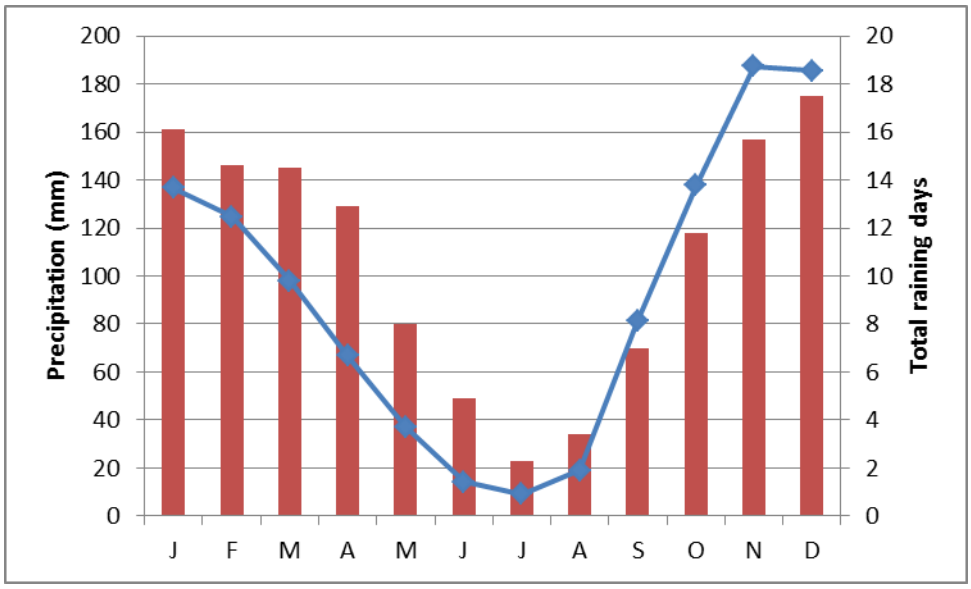

Figure 16: Annual cycle mean annual precipitation amounts in mm and maximum raining days for the period 1955-1997 for Corfu.

It is generally concluded from the Strategic Environmental Impacts Assessment of Epirus that the precipitation varies from one year to the other.

4.3 Period 1975-2004

Additional data for the period 1975-2004 provide mean precipitation values for the test area monthly and seasonally (Figures 17 & 18) [7].

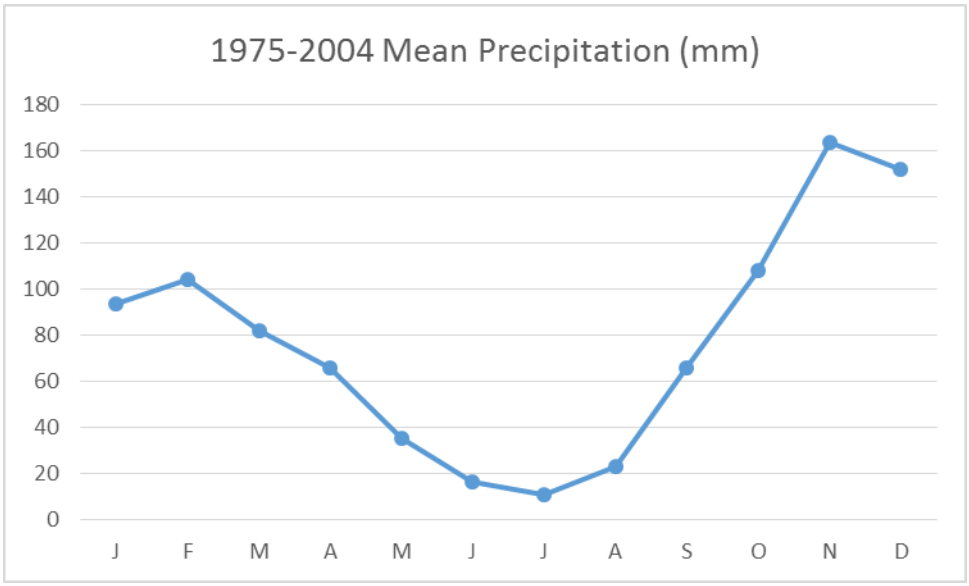

Figure 17: Annual cycle mean monthly precipitation amounts in mm for the period 1975-2004 for Corfu [7].

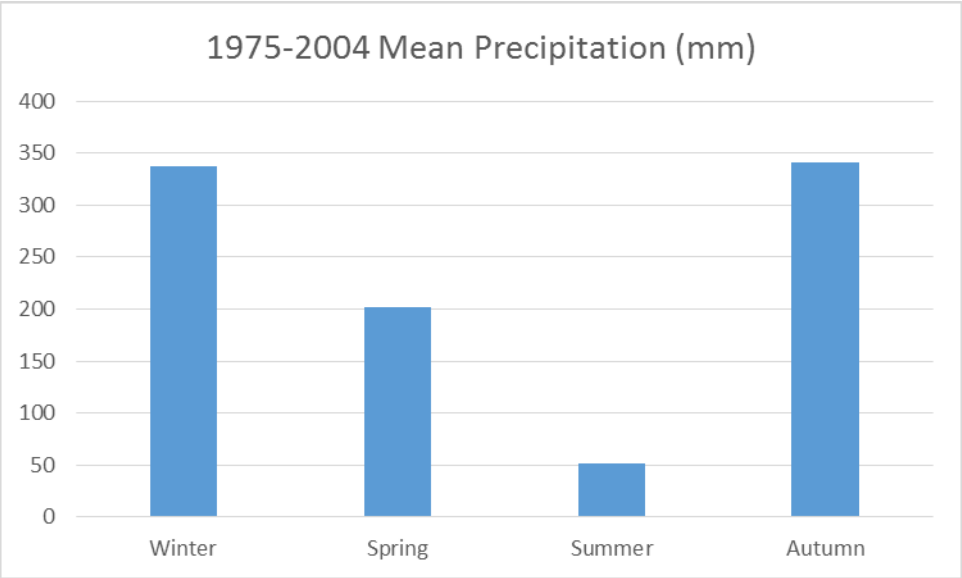

Figure 18: Annual cycle mean seasonal precipitation amounts in mm for the period 1975-2004 for Corfu [7].

The results from the comparison of the mean precipitation values for the 4 time periods show that in general there is a reduction in precipitation values but there are big variations (Figure 19).

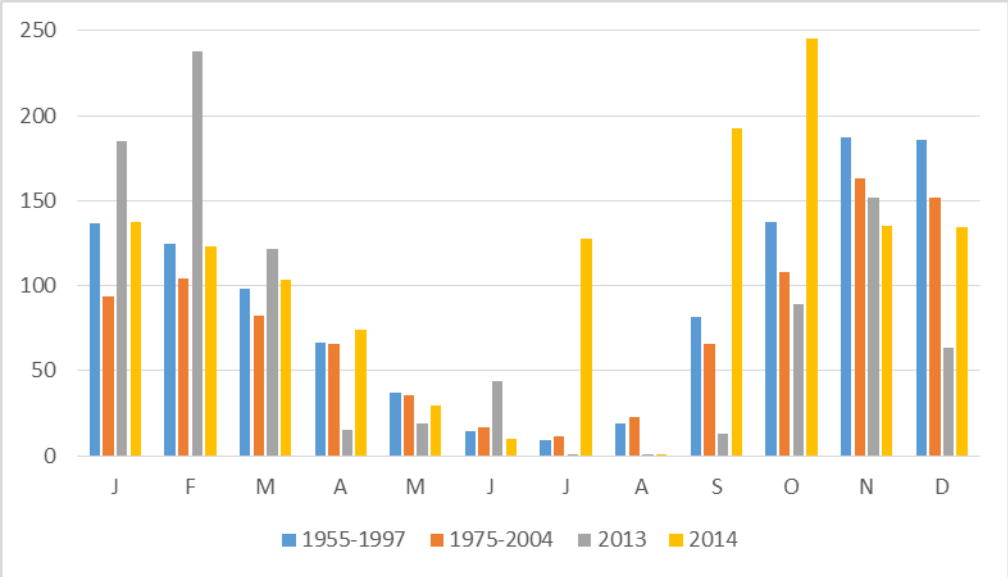

Figure 19: Annual cycle mean monthly precipitation amounts in mm for the periods: 1955-1997; 1975-2004; 2013; 2014.

Data gathered from the meteorological station of Corfu from 1956-2010 show that the precipitation tends to decrease with a trend of -3.628 and significance 0.033 [7] (Figure 20).

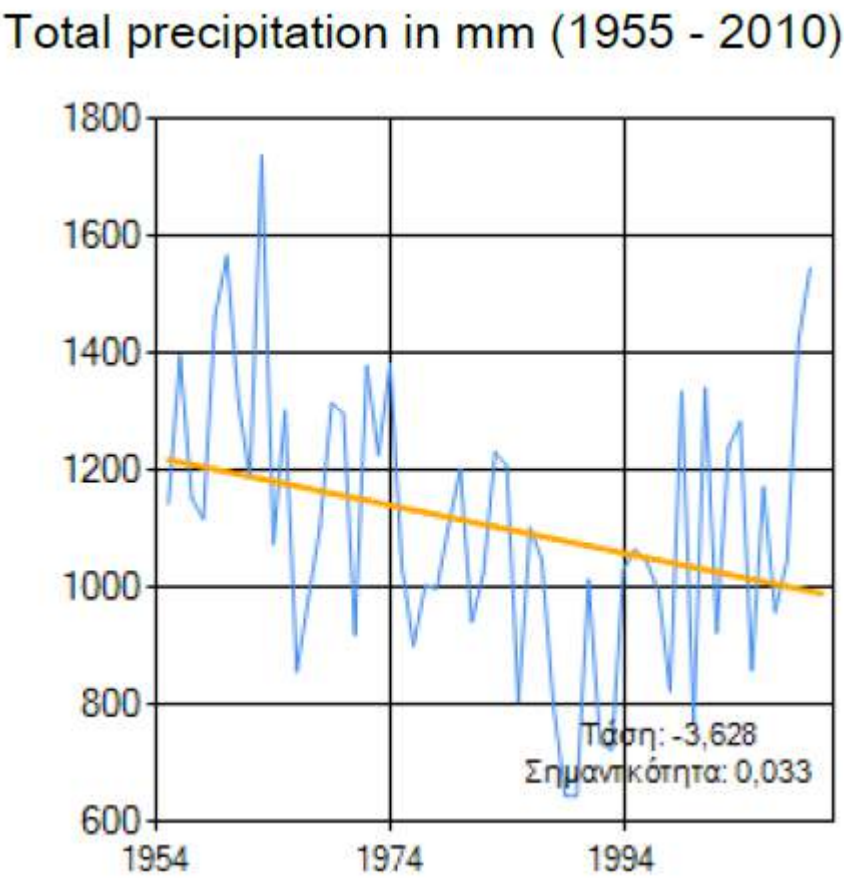

Figure 20: Annual cycle precipitation amounts in mm for the period 1955-2010 [7]

5. CLIMATE MODELS SIMULATION

Four models are used to simulate climate conditions in the test area of Corfu: Ensemble (scenario A1B); Prudence (scenario A2); Prudence (scenario B2); and REGCM (scenario A1B) [7]. The work has been elaborated by the project Geoklima [7]. The simulation models results for the Corfu test area are presented in Table 4 for the period 1961-1990 and 2021-2050.

The results show that temperature is expected to increase (minimum, maximum and average values) during all the seasons and annually. The model showing the highest temperature increase is Prudence scenario A2, followed by Prudence scenario B2, while Ensemble and REGCM models provide comparative values [7] (Figures 21-24). The average annual mean temperature is expected to increase from 1.23ºC to 4.27ºC. The total precipitation is expected to decrease especially in the summer months (Figure 24). In the winter months two out of four models predict a slight increase in total precipitation values. Total annual precipitation values are expected to decrease from 3.93% to 25.4% depending on the model.

	Ensemble (A1B)					Prudence (A2)					Prudence (B2)					REGCM (A1B)				
Change in	Winter	Spring	Summer	Autumn	Year	Winter	Spring	Summer	Autumn	Year	Winter	Spring	Summer	Autumn	Year	Winter	Spring	Summer	Autumn	Year
minimum air temperature (ºC)	1,04	0,89	1,52	1,51	1,24	3,58	3,29	5,55	4,26	4,17	2,46	2,39	4,43	3,12	3,1	1,14	0,77	1,52	1,36	1,19
maximum air temperature (ºC)	0,98	0,93	1,5	1,51	1,23	3,81	3,77	6,19	4,68	4,61	2,43	2,48	4,78	3,4	3,27	1,15	0,9	1,53	1,47	1,26
average air temperature (ºC)	1,01	0,91	1,51	1,49	1,23	3,58	3,44	5,76	4,32	4,27	2,37	2,42	4,51	3,2	3,12	1,15	0,87	1,53	1,15	1,25
total precipitation (%)	2,29	-13,9	-11,13	-5,31	-3,9	-1,47	-15,1	-60,01	-24,88	-25,4	5,94	-1,19	-44,54	-3,15	-10,7	-16,56	-6,3	-44,01	-9,19	-7,9

Table 4: Changes in minimum, maximum, average temperature and total precipitation values predicted by climatic simulation models for Corfu area (period 2021-2015)

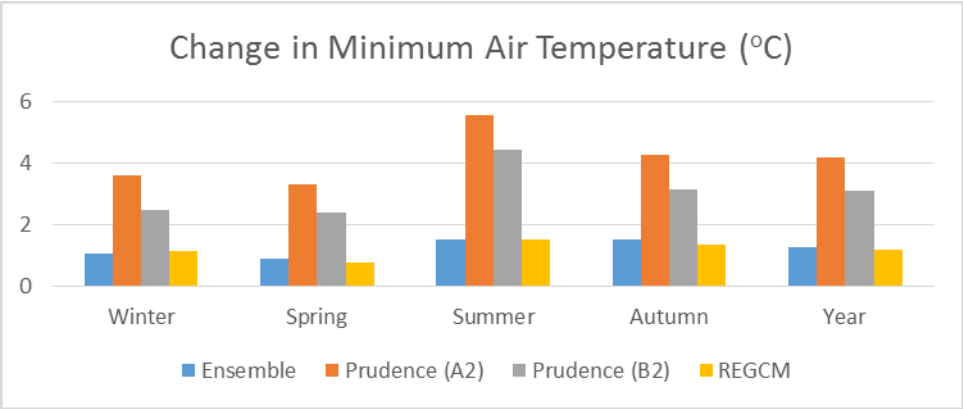

Figure 21: Change in minimum air temperature values (°C) [7]

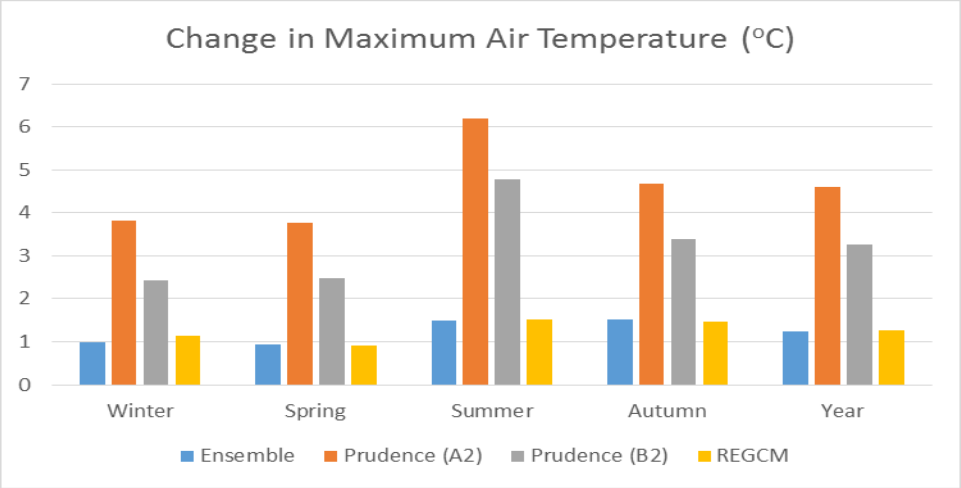

Figure 22: Change in maximum air temperature values (°C) [7]

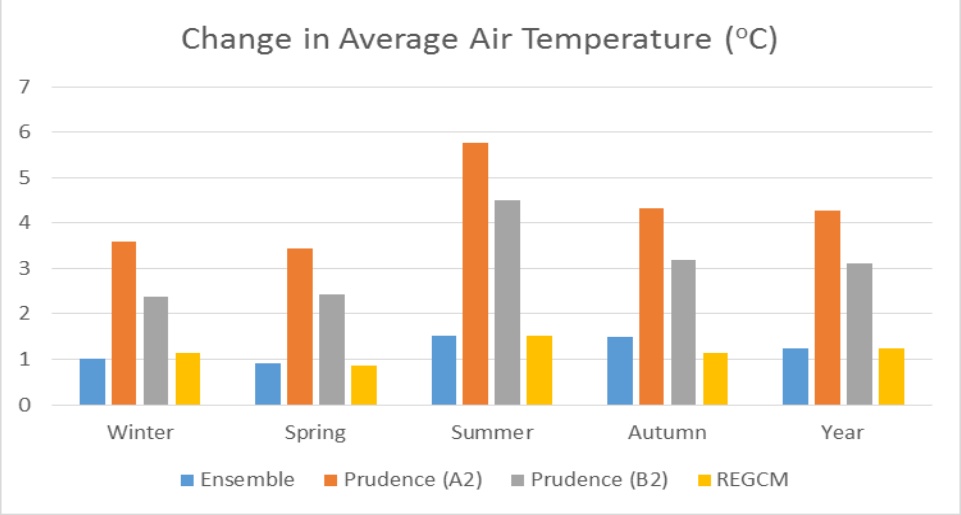

Figure 23: Change in average air temperature values (°C) [7]

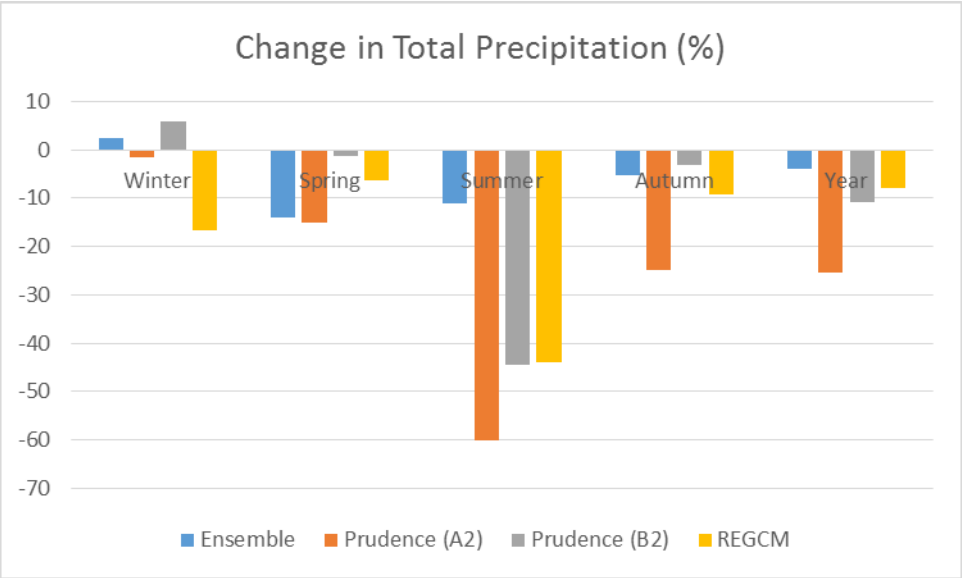

Figure 24: Change total precipitation values (%) [7]

REFERENCES

1. Strategic Environmental Impact Assessment for Epirus Water District (GR05),
2. http://www.elekkas.gr/images/stories/photos/Xartes/KERKYRA_Neotek.jpg
3. River Basin Management Plan of the Water District of Epirus, https://dl.dropboxusercontent.com/u/50953375/RBMP_GR05.pdf
4. http://penteli.meteo.gr/stations/kerkyra/NOAAPRYR.TXT
5. http://www.hnms.gr/hnms/greek/climatology/climatology_region_diagrams_html?dr_city=Kerkyra
6. http://penteli.meteo.gr/stations/kerkyra/
7. http://www.geoclima.eu/ http://geo-ellanikos.aegean.gr:88/geoclima/

Climate and Climate change data for Corfu, Greece – Volos 14.04.2015

Let's grow up together

DRINK ADRIA

Adriatic IPA
Cross Border Cooperation 2007-2013

The project is co-funded by the European Union,
Instrument for Pre-Accession Assistance